RIKEN Accelerator Progress Report

2015

vol. 49

理化学研究所　仁科加速器研究センター
RIKEN Nishina Center for Accelerator-Based Science

RIKEN Accelerator Progress Report 2015

vol. **49**

理化学研究所　仁科加速器研究センター
RIKEN Nishina Center for Accelerator-Based Science
Wako, Saitama, 351-0198 JAPAN

RIKEN Accelerator Progress Report 2015 vol.49

This is an unabridged version of the 49th volume of RIKEN Accelerator Progress Report (hereinafter referred to as APR), the official annual report of the Nishina Center for Accelerator-Based Science.

A PDF version of APR can be downloaded from our website.
http://www.nishina.riken.jp/researcher/APR/index_e.html

Published by
RIKEN Nishina Center for Accelerator-Based Science
2-1 Hirosawa, Wako-shi, Saitama 351-0198 JAPAN

Director of RIKEN Nishina Center for Acclerator-Based Science
Hideto En'yo

Contact
Progress@ribf.riken.jp

RIKEN Nishina Center for Accelerator-Based Science, March 2017

PREFACE

New Year's Eve 2015 turned out to be a historical moment for the Nishina Center. In the early morning on the same day, Kosuke Morita received an email from IUPAC notifying that the experiment team of RIKEN has been certified as the discoverer of the 113th element, and that the team will be granted the naming right for the element. At 17:00, we held a press conference at the RIKEN RIBF building for a large number of media. Immediately following the conference, the news was featured in a variety of media.

In Japan, there is a very popular TV singing-contest program shown on the Sylvester night every year from 19:00 to 24:00 with a high audience rating of more than 40%. Midway through the show, a national news program featured the groundbreaking news that RIKEN has clinched the naming rights for element 113. This means 40-50% of the Japanese watched our press conference and saw a joyful face of Morita-san. The news that we have been waiting for so long could not have come at a better timing. We extend our heartiest congratulations to everyone who contributed to this superb accomplishment, especially to Morita's group and the accelerator group, and would like to share the joy with all the members of the Nishina Center.

At the collaboration meeting held in March 2016, the name and the symbol of the 113th element were decided as Nihonium and Nh, which are currently undergoing a public review by IUPAC until November 2016. "Japan" is written in Japanese with two Chinese characters "日本" meaning "the land of the rising sun". They can be read as Nihon or Nippon, with both pronunciations officially accepted in Japan. "Japan" is a European dialect for pronouncing Nippon. Thus we call our country Japan, Nippon or Nihon. This is similar to Genève, Geneva or Genf, all of which are from the same verbal origin and officially allowed in Swiss.

In 1908, Ogawa discovered element 43 and named it "nipponium" (Np), the name which was added to the old periodic tables. He was wrong. Tecnetium (Z=43) is unstable, and what he actually discovered was rhenium (Z=75, in the same family). In 1940, Nishina discovered element 93, but was unable to perform purified isolation. Element 93 was named Neptunium (Np) by McMillan. Now our earnest wish spanning100 years finally came true. Morita and his collaborator chose the name Nihonium *to pay homage to their predecessors*.

Another big news of the year was Dr. Tohru Motobayashi and Dr. Hiroyoshi Sakurai, our fellow researchers at the Nishina Center, being jointly awarded the 2015 Nishina Memorial Prize for their research on "Discovery of anomalies in magic numbers of neutron-rich nuclei". The award signifies a true recognition of the research accomplishments obtained at RIKEN RIBF. The fact that they were given the award not only for their latest papers but also for the one written two decades ago shows that the quintessence of the long, sustained effort required for research in the field of nuclear physics has been properly acknowledged and appreciated. Together with the 2005 Nishina Memorial Prize recipient Morita, the 2011 Prize recipient Dr. Yasuyuki Akiba and the 2012 Prize recipient Dr. Tetsuo Hatsuda, there are now five recipients of the Award affiliated with the Nishina Center. Since 3% of the Nishina Memorial Award recipients have received the Nobel Prize in Physics in the past, I believe we are finally beginning to see the next higher goal.

There were many surprises and joyous moments shared at the Nishina Center in 2015. The scientific highlights are compiled in this volume of Accelerator Progress Report including: the first data from SEASTAR collaboration, polarized RI purified with BigRIPS, Multi-Reflection TOF measurements for superheavy elements, discovery of ideal charge stripper, successful commissioning of PALIS/Rare-RI-Ring/SAMURAI-TPC, discovery of tetra neutron, gluon polarization in polarized proton determined at RHIC, hint for bound K^-pp states discovered in J-PARC, and more. I was in awe to see many prominent researchers in the field of nuclear physics from research institutions abroad participate in the experiment not as a commander but as a mere soldier. Such is the "magnetism" of the experiment that can only be conducted at RIBF.

Another event worthy of special mention is the official inauguration of the KEK Wako Nuclear Science Center. With the closing of the Institute for Nuclear Study (INS) located in Tanashi in 1997, the "troops" of nuclear physicists have gone their separate ways to either KEK or CNS, U-Tokyo. After 18 years, they are again reunited at RIKEN RIBF.

In April 2015, RIKEN was reborn as a National Research and Development Institution. The year 2016 will see RIKEN evolve even further under the new initiatives and management.

Hideto En'yo

Director,
RIKEN Nishina Center for Accelerator-Based Science

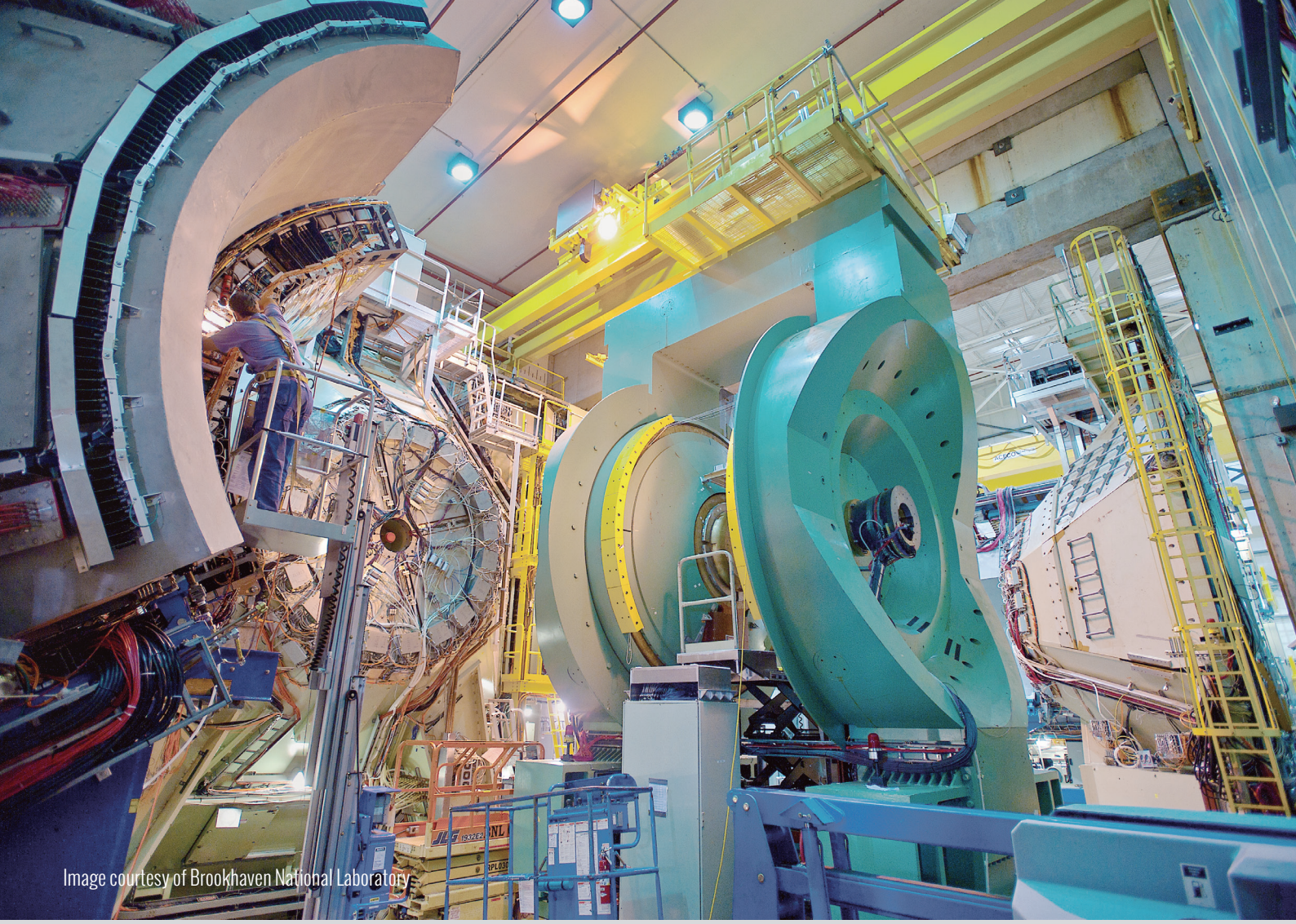

Image courtesy of Brookhaven National Laboratory

PHENIX

- looking at hot and cold nuclear matter and resurrecting itself again and again

The Relativistic Heavy Ion Collider, RHIC, at Brookhaven National Laboratory on Long Island, NY, was built to study the conditions in an early universe shortly after the Big Bang. In that epoch the temperature of the universe was so hot, that quarks and gluons, mediators of the strong interaction, were not yet condensated into hadrons such as protons and neutrons. This phase of the universe is known as the quark-gluon plasma (QGP). Its existence was predicted and RHIC was set to discover it which it eventually did.

At the same time also the internal structure of the most fundamental building blocks of the visible world today, protons and neutrons was not understood well and particularly the spin composition between quarks, gluons and their orbital angular momenta were at odds with earlier nucleon models. RHIC was also set to understand the role of gluon spins and sea quarks. The spin program was realized at the initiative and with substantial support of RIKEN and greatly improved our understanding of cold nuclear matter and brought in turn new surprises.

PHENIX

- looking at hot and cold nuclear matter
and resurrecting itself again and again

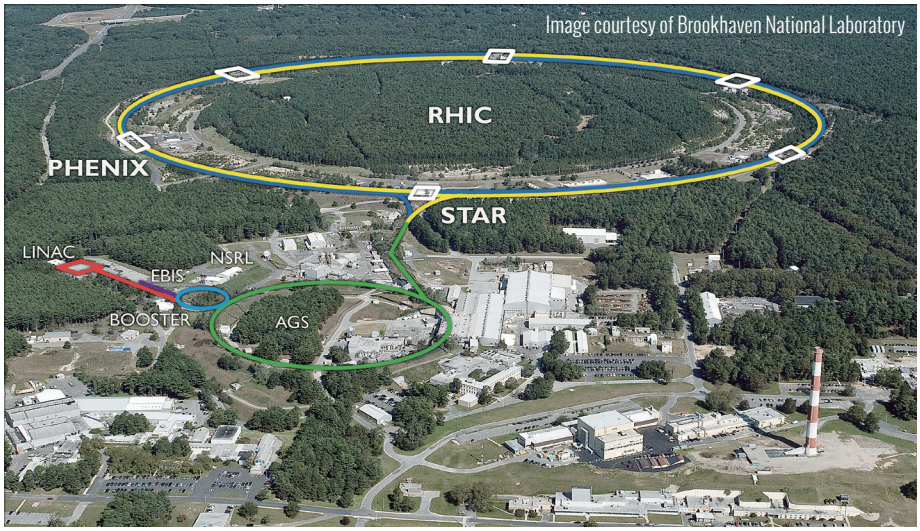

Figure 1: Aerial view of the RHIC accelerator complex including pre-accelerators and locations of currently operating detectors.

While at the beginning of RHIC one typical collider detector was already approved to be built, several other proposals for more dedicated detectors were initially rejected out of funding constraints. As a result these rejected proposals worked together and, like the fabled bird, rose from the ashes being appropriately named PHENIX (though the official name stands for Pioneering High Energy Nuclear Interaction eXperiment). PHENIX's strong points were the rather precise central detectors, especially electromagnetic calorimetry, forward muon detectors and high rate data taking capabilities at the expense of coverage. Currently about 400 collaborators from 78 institutions (including 11 Japanese) in 14 countries are participating in the PHENIX experiment.

With this initial detector configuration, it was possible to both find the QGP [1] and learn about its properties. One telltale sign of the QGP was the suppression of hadrons and jets at higher energies due to the additional interactions within the hot, dense QGP medium. In contrast, high energetic photons were not suppressed as they are only interacting electromagnetically. These features are summarized in Figure 2.

One of the main surprises was that this QGP does not behave like a gas but more like a perfect liquid with a very small viscosity. With the help of light emitted inside the plasma it was even possible to roughly determine the temperature of the QGP [2] within models which led to the 2011 Nishina

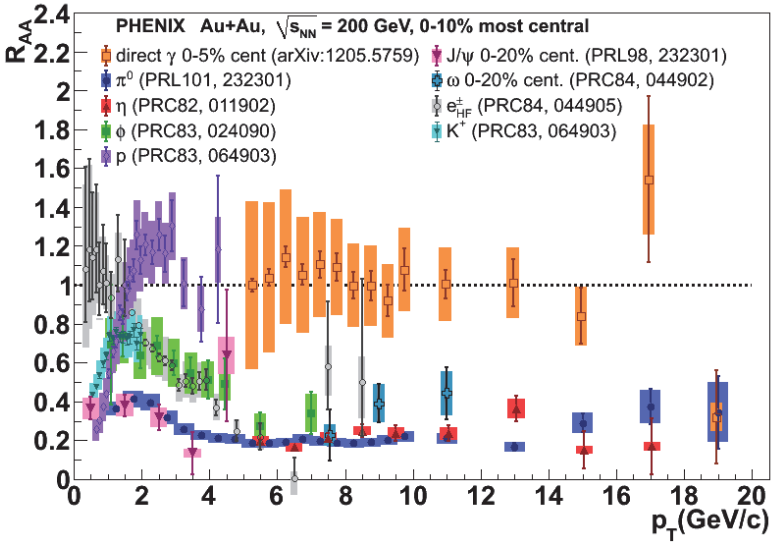

Figure 2: Summary of cross section ratios between most central AuAu collisions and proton proton collisions. All hadrons seem to be suppressed at high transverse momenta as expected when traversing the Quark-gluon plasma.

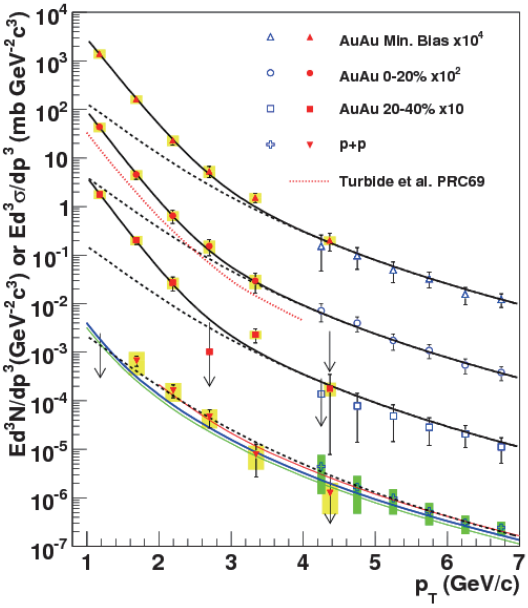

Figure 3: Photon cross sections in AuAu and proton proton collisions. An enhancement indicates the thermal radiation of the Quark-gluon plasma and allows estimating its temperature.

Memorial Prize [3]. The low-energetic photon spectra are shown in Figure 3 for Au-Au collisions at various centralities in comparison to "cold" proton-proton collisions and display an additional contribution due to the thermal radiation within the QGP.

In recent years the focus moved towards studying QGP properties using heavy quarks which required the installation of a silicon vertex tracker. A large part of this upgrade was performed by RIKEN.

For the study of the spin structure of the nucleon for a long time spin double spin asymmetries in polarized proton-proton collisions were small, ruling out extreme gluon spin contributions to the spin of the nucleon as suggested by early models (i.e., contributing several units of ħ to be mostly compensated by opposite orbital angular momentum). With the high statistics data sets in the years 2009 [4] at a collision energy of 200GeV and 2012/2013 [5] for energies of 510GeV it is now established that the gluon spin plays a substantial and potentially even dominant role [6] in the proton spin. Figure 4 displays the current knowledge of the total gluon spin contribution as a function of the minimum Bjorken variable x. To extend our knowledge to even lower x, more forward measurements are ongoing at RHIC while eventually an electron-ion collider will reach the lowest fractional momenta similar to HERA in the unpolarized case.

To evaluate the contribution of sea quarks the parity violation of the weak interaction was used in proton-proton collisions to select their contribution in real W boson production. Their contributions appear to be nonzero and not symmetric between up- and down-type flavors.

Furthermore, many transverse spin effects, originally expected to be low-energy phenomena, continue to surprise to the highest collisions energies available at RHIC with the RHIC experiments slowly unraveling its origins.

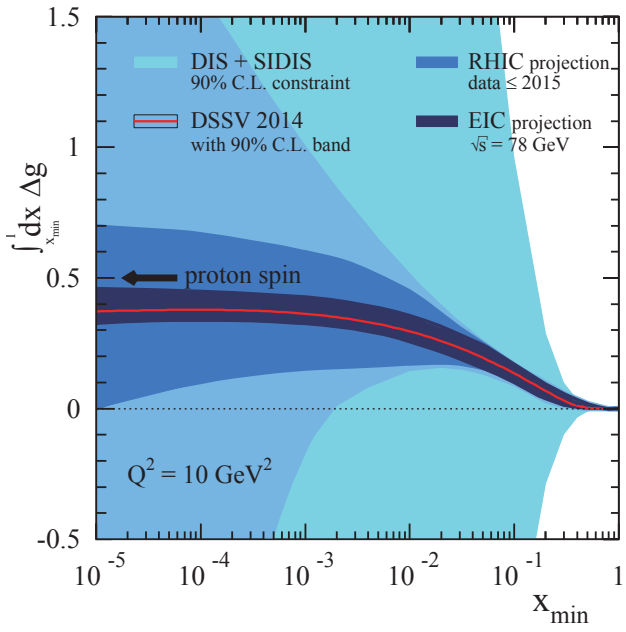

Figure 4: Running integral of the gluon spin contribution to the proton spin from non RHIC data (light blue), including published RHIC data, expected improvements and an eventual electron ion collider (in successively darker shades of blue). The RHIC data first showed a rather substantial contribution. [7]

PHENIX

- looking at hot and cold nuclear matter
and resurrecting itself again and again

As the name suggests, PHENIX has re-emerged already once and it is bound to do the same once more right now. The Heavy Ion physics interest at RHIC moves towards jets, and heavy quark-antiquark states to provide complementary measurements to the LHC heavy ion program. Also the study of the spin structure is interested to look at forward rapidities which allows to access transverse spin effects unique to RHIC at higher momentum fractions while also looking at lower momentum fractions to pin down the gluon spin in regions not covered yet.

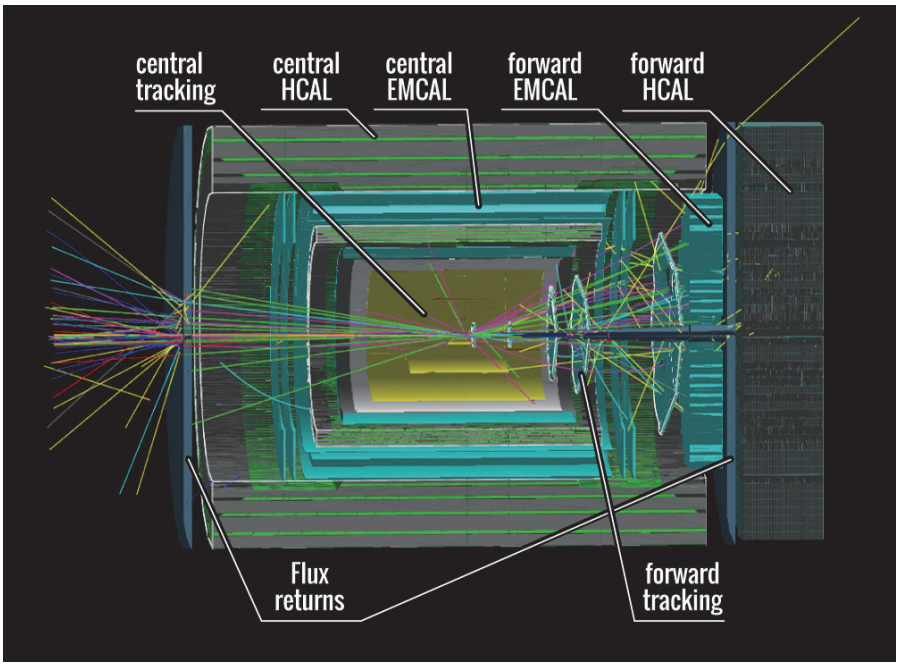

Figure 5: GEANT4 Rendering of the sPHENIX detector including forward upgrades currently under consideration in a 500 GeV proton-proton collision event.

As such, PHENIX is currently re-inventing itself as sPHENIX and forward sPHENIX concentrating on jet detection at central and forward rapidities with electromagnetic and hadronic calorimetry, tracking and the former BABAR 1.5 Tesla solenoid magnet being already transferred to BNL. These mostly new systems could then even re-rise yet again in the case the electron ion collider (EIC) is built at BNL as a zero-day EIC detector currently dubbed as ePHENIX.

References:

[1] K. Adcox et al.[PHENIX Collaboration], “Formation of dense partonic matter in relativistic nucleus-nucleus collisions at RHIC: Experimental evaluation by the PHENIX collaboration”, Nucl. Phys. A757, 184 (2005)

[2] A. Adare et al. [PHENIX Collaboration], ”Enhanced production of direct photons in Au+Au collisions at √sNN=200 GeV and implications for the initial temperature”, Phys. Rev. Lett. 104, 132301 (2010)

[3] www.nishina-m.or.jp/NishinaMemorialPrize-E.html

[4] A. Adare et al. [PHENIX Collaboration], “Inclusive double-helicity asymmetries in neutral-pion and eta-meson production in p+p collisions at √s=200 GeV”, Phys. Rev. D91, 012007, (2014)

[5] A. Adare et al. [PHENIX Collaboration], ”Inclusive cross section and double-helicity asymmetry for π^0 production at midrapidity in p+p collisions at √s=510 GeV,” Phys. Rev. D93, 011501 (2016)

[6] D. de Florian, R. Sassot, M. Stratmann and W. Vogelsang, “Evidence for polarization of gluons in the proton”, Phys. Rev. Lett. 113 , 012001 (2014)

[7] E. Aschenauer, R. Sassot, M. Stratmann, "Unveiling the Proton Spin Decomposition at a Future Electron-Ion Collider" Phys.Rev. D92 (2015) 094030

C O N T E N T S

Page

2. Nuclear Physics (Theory)

3. Nuclear Data

4. Hadron Physics

5. Hadron Physics (Theory)

6. Particle Physics

7. Astrophysics and Astro-Glaciology

8. Accelerator

9. Instrumentation

3. Radiochemistry and Nuclear Chemistry

4. Radiation Chemistry and Biology

Ⅳ. OPERATION RECORDS

I. HIGHLIGHTS OF THE YEAR

<< Selection process of highlights >>

Highlights are selected by a two-step process. In the first step, a referee who reviews a manuscript decides whether she/he would recommend it as one of the highlights.
Members of the editorial board then make additional recommendations if they think an important contribution has not been recommended by the referee.

The second step involves the editor-in-chief proposing a list of highlights based on the recommendation given above to the editorial board. After discussing the scientific merits and uniqueness of the manuscripts from viewpoints of experts/non-experts, the editorial board makes the final decision.

Extension of the N=40 island of inversion to neutron-rich Cr and Fe isotopes†

C. Santamaria,[*1,*2] C. Louchart ,[*3] A. Obertelli,[*1,*2] V. Werner ,[*3] P. Doornenbal ,[*2] F. Nowacki ,[*4] G. Authelet ,[*1,*2] H. Baba,[*2] D. Calvet,[*1,*2] F. Château,[*1] A. Corsi,[*1,*2] A. Delbart ,[*1,*2] J.-M. Gheller,[*1,*2] A. Gillibert,[*1,*2] T. Isobe ,[*2] V. Lapoux,[*1,*2] M. Matsushita ,[*5] S. Momiyama ,[*2,*6] T. Motobayashi ,[*2] M. Niikura,[*6] H. Otsu,[*2] C. Péron,[*1,*2] A. Peyaud,[*1,*2] E.C. Pollacco,[*1] J.-Y. Roussé ,[*1,*2] H. Sakurai ,[*2,*6] M. Sasano ,[*2] Y. Shiga ,[*2,*7] S. Takeuchi,[*2] R. Taniuchi ,[*2,*6] T. Uesaka,[*2] H. Wang,[*2] K. Yoneda,[*2] and the SEASTAR collaboration

The N = 40 island of inversion has been further explored towards the N = 50 shell closure. The 2_1^+ and 4_1^+ states in the ^{66}Cr and ^{70,72}Fe neutron-rich isotopes have been measured from in-beam γ spectroscopy at the RIBF. The measurements were part of the first campaign of the SEASTAR program [1]. The SEASTAR setup is composed of the DALI2 high-efficiency gamma spectrometer[2] and the MINOS device[3] composed of a 100-mm thick liquid hydrogen target and a vertex tracker. Low-energy states in ^{66}Cr and ^{70,72}Fe were populated via $(p, 2p)$ reactions induced by ^{67}Mn and ^{71,73}Co.

A ^{238}U beam was accelerated to 345 MeV/nucleon and impinged on a 3-mm thick ^{9}Be primary target at the entrance of the BigRIPS separator with a mean intensity of 12 pnA. Two beam settings were tuned for ^{67}Mn and ^{71,73}Co, respectively. The identification of beam particles and secondary residues were performed event by event from the BigRIPS and ZeroDegree spectrometers, respectively. The incident energies at the entrance (exit) of the secondary target were ∼260 (∼200) MeV/nucleon for ^{67}Mn and ^{71,73}Co. Their intensities were measured to be 12 s^{-1}, 45 s^{-1} and 6 s^{-1}, respectively. The total beam intensity on target for the two settings was about 6 kHz.

A plateau in the 2^+ and 4^+ energy systematics is observed for Cr and Fe isotopes beyond N=38 and N=40, respectively. Fig. 1 shows the spectrum of ^{66}Cr (top) and the systematics of the first 2^+ and 4^+ states for Cr isotopes (bottom). The data are well reproduced by state-of-the-art shell model calculations with a modified version of the LNPS interaction[4]. This plateau was interpreted within the shell model as an extension of the N=40 island of inversion towards N=50. Whereas quadrupole collectivity is maximum at N=40, the evolution of pairing correlations slightly shifts the minimum of 2_1^+ and 4_1^+ energies.

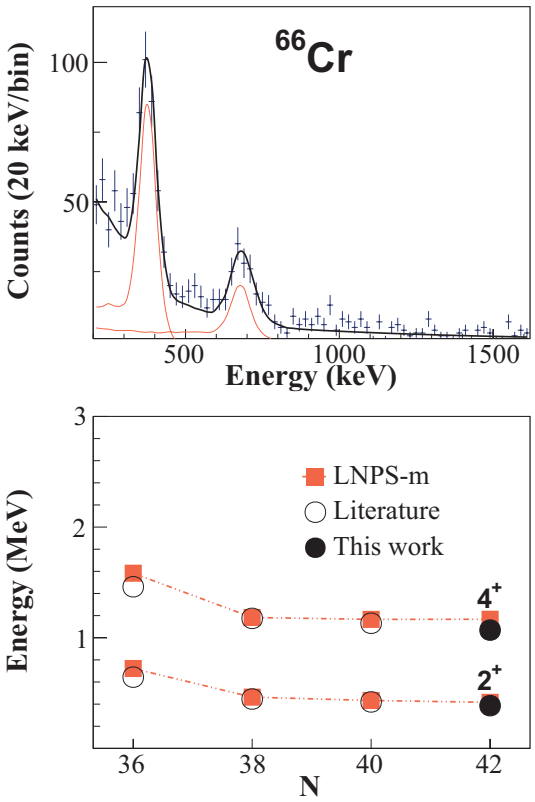

Fig. 1. (Top) Spectrum of ^{66}Cr. (Bottom) Systematics of low-lying 2_1^+ and 4_1^+ states in Cr isotopes.

This study has been partly supported by JSPS through the long-term fellowship L-13520 at the RIKEN Nishina center, by the ERC through the grant MINOS-258567, and by the IPA program of RIKEN.

References

1) Shell Evolution And Search for Two-plus states At the RIBF, RIKEN Proposal for Scientific Program (2013).
2) S. Takeuchi *et al.*, Nucl. Instr. Meth. A **763**, 596 (2014).
3) A. Obertelli *et al.*, Eur. Phys. J. A **50**, 8 (2014).
4) S. Lenzi *et al.*, Phys. Rev. C **82**, 054301 (2010).

† Condensed from the article:
C. Santamaria *et al.*, Phys. Rev. Lett. **115**, 192501 (2015).

*1 CEA, Centre de Saclay
*2 RIKEN Nishina Center
*3 Institut für Kernphysik, Technische Universität Darmstadt
*4 IPHC, CNRS/IN2P3, Université de Strasbourg
*5 Center for Nuclear Study, University of Tokyo
*6 Department of Physics, University of Tokyo
*7 Department of Physics, Rikkyo University

Low-lying structure of ^{50}Ar and the $N = 32$ subshell closure†

D. Steppenbeck,[*1] S. Takeuchi,[*2] N. Aoi,[*3] P. Doornenbal,[*1] M. Matsushita,[*4] H. Wang,[*1] Y. Utsuno,[*5] H. Baba,[*1] S. Go,[*6] J. Lee,[*7] K. Matsui,[*8] S. Michimasa,[*4] T. Motobayashi,[*1] D. Nishimura,[*9] T. Otsuka,[*4,*8] H. Sakurai,[*1,*8] Y. Shiga,[*10] N. Shimizu,[*4] P.-A. Söderström,[*1] T. Sumikama,[*1] R. Taniuchi,[*8] J. J. Valiente-Dobón,[*11] and K. Yoneda[*1]

It is now well known that far from the line of β stability the nuclear magic numbers can change from their standard values. For example, in the pf shell, the onset of a new magic number at $N = 32$ has been reported along the Cr, Ti, and Ca isotopic chains, while a sizable gap at $N = 34$ was deduced from the structure of ^{54}Ca[1]. Very recently, the persistence of the $N = 32$ subshell closure was established in systems below the $Z = 20$ core[2]. In the present work, the low-lying structure of ^{50}Ar has been investigated to shed light on the character of the $N = 32$ magic number at more extreme neutron-to-proton ratios. Preliminary results are discussed in Ref.[3].

A primary beam of ^{70}Zn^{30+} ions with a typical intensity of ~ 60 pnA was used to generate a fast radioactive beam containing ^{54}Ca, ^{55}Sc, and ^{56}Ti, amongst other products. The constituents were identified using the BigRIPS separator and focused on a 10-mm-thick ^{9}Be reaction target at the eighth focal plane. Reaction products emerging from the target were identified by the ZeroDegree spectrometer (ZDS); despite the fact that the ZDS was optimized for the transmission of ^{54}Ca[1], a sufficient number of ^{50}Ar ions fell within the acceptance of the spectrometer to extract structural information. The reaction target was surrounded by the DALI2 γ-ray detector array to measure transitions emitted from nuclear excited states.

The γ-ray energy spectra—corrected for the Doppler effect—are presented in Fig. 1 using the sum of the ^{9}Be(^{54}Ca, ^{50}Ar)X, ^{9}Be(^{55}Sc, ^{50}Ar)X, and ^{9}Be(^{56}Ti, ^{50}Ar)X multinucleon removal reactions. The line at 1178(18) keV, which is the most intense peak in the spectra, is assigned as the transition from the yrast 2^+ state to the 0^+ ground state in ^{50}Ar. A weaker, tentative peak is present at 1582(38) keV, and is suggested as the transition between the 4_1^+ and 2_1^+ levels. Statistics were insufficient to confirm the proposed decay scheme using $\gamma\gamma$ coincidence relationships.

The 2_1^+ state in ^{50}Ar indicates an increase in energy relative to its even-even neighbour ^{48}Ar and, therefore, naively suggests the presence of a sizable subshell closure at $N = 32$ in Ar isotopes. In order to investigate the nature of the increase in energy in more detail, large-scale shell-model calculations employing a modified version of the SDPF-MU Hamiltonian[4] were performed; the modifications were based on recent experimental data from exotic Ca[1] and K[5] isotopes. The predictions reproduce the experimental energy levels in lighter Ar isotopes, and the results of the present work, in a satisfactory manner. Moreover, the calculations indicate that the magnitude of the $N = 32$ subshell closure in ^{50}Ar is equally as significant as the gaps in ^{52}Ca and ^{54}Ti, where the experimental evidence for this magic number is well documented. The calculations also indicate a rather high 2_1^+ energy in ^{52}Ar and, therefore, experimental input on this nucleus is encouraged to investigate the significance of the $N = 34$ subshell closure in more exotic systems.

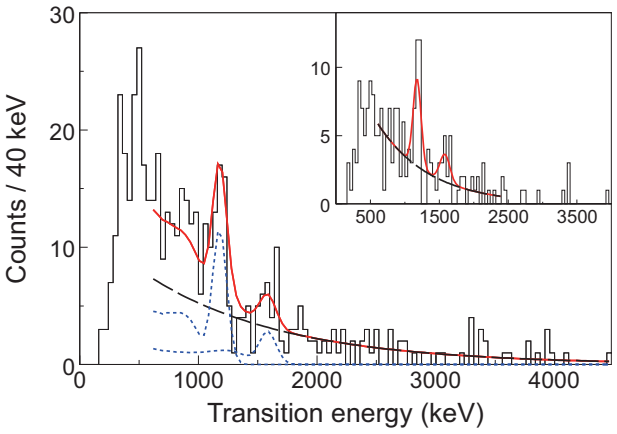

Fig. 1. (colour) Doppler-corrected γ-ray energy spectra for ^{50}Ar. The main and inset panels display $M_\gamma \geq 1$ and $M_\gamma \leq 3$ data, respectively. The black dashed lines are exponential fits to the backgrounds and the blue dashed lines are GEANT4 simulations; the solid red lines are total (sum) fits.

† Condensed from the article in Phys. Rev. Lett. **114**, 252501 (2015).

*1 RIKEN Nishina Center
*2 Dept of Physics, Tokyo Institute of Technology
*3 RCNP, University of Osaka
*4 Center for Nuclear Study, University of Tokyo
*5 Japan Atomic Energy Agency
*6 Dept of Science and Engineering, University of Tennessee
*7 Dept of Physics, University of Hong Kong
*8 Dept of Physics, University of Tokyo
*9 Dept of Physics, Tokyo University of Science
*10 Dept of Physics, Rikkyo University
*11 Laboratori Nazionali di Legnaro

References

1) D. Steppenbeck *et al.* Nature **502**, 207 (2013).
2) M. Rosenbusch *et al.* Phys. Rev. Lett. **114**, 202501 (2015).
3) D. Steppenbeck *et al.* JPS Conf. Proc. **6**, 020019 (2015).
4) Y. Utsuno *et al.* Phys. Rev. C **86**, 051301(R) (2012).
5) J. Papuga *et al.* Phys. Rev. Lett. **110**, 172503 (2013).

Candidate resonant tetraneutron state populated by the ^{4}He(^{8}He,^{8}Be) reaction

K. Kisamori,[*1] S. Shimoura,[*2] H. Miya,[*1,2] M. Assie,[*3] H. Baba,[*1] T. Baba,[*4] D. Beaumel,[*1,3] M. Dozono,[*1] T. Fujii,[*1,2] N. Fukuda,[*1] S. Go,[*1,2] F. Hammache,[*3] E. Ideguchi,[*4] N. Inabe,[*1] M. Itoh,[*6] D. Kameda,[*1] S. Kawase,[*2] T. Kawabata,[*4] M. Kobayashi,[*2] Y. Kondo,[*1,7] T. Kubo,[*1] Y. Kubota,[*1,2] M. Kurata-Nishimura,[*1] C. S. Lee,[*1,2] Y. Maeda,[*8] H. Matsubara,[*1] S. Michimasa,[*2] K. Miki,[*5] T. Nishi,[*1,9] S. Noji,[*10] S. Ota,[*2] S. Sakaguchi,[*1,11] H. Sakai,[*1] Y. Sasamoto,[*2] M. Sasano,[*1] H. Sato,[*1] Y. Shimizu,[*1] A. Stolz,[*10] H. Suzuki,[*1] M. Takaki,[*2] H. Takeda,[*1] S. Takeuchi,[*1] A. Tamii,[*5] L.T. Tang,[*2] H. Tokieda,[*2] M. Tsumura,[*4] T. Uesaka,[*1] K. Yako,[*2] Y. Yanagisawa,[*1] and R. Yokoyama[*2]

The possible existence of a tetraneutron system forming a resonance state is still an open and fascinating question; however, theoretical and experimental studies suggest that the tetraneutron does not exist as a bound state[1,2]. An experiment to search for the tetraneutron state has been performed by measuring the double-charge exchange (DCX) reaction ^{4}He(^{8}He,^{8}Be) at 186 MeV/u at RIBF using the SHARAQ spectrometer. Utilizing the large positive Q-value of the (^{8}He,^{8}Be) reaction, an almost recoil-less condition of the four-neutron system was achieved in order to populate weakly interacting four-neutron systems efficiently. The detail of the experiment and data-analysis have been described in previous reports[3,4].

We obtained the missing-mass spectrum of a tetraneutron system, as shown in Fig. 1 (a). To interpret this spectrum, we assumed two different states: (1) direct decay contributing to the continuum with a final-state interaction between the two correlated neutron pairs; (2) a possible resonant state of the tetraneutron system near the threshold. To demonstrate the significance of the yields near the threshold, we fitted the experimental data with a trial function assuming the absence of the resonant state and estimated the goodness-of-fit with the likelihood ratio test (Fig. 1 (b)). Because of the small contribution from the continuum and experimental background, the significance level of the peak is 4.9 with the analysis of the look elsewhere effect.

In conclusion, the four events in the $0 < E_{4n} < 2$ MeV region are candidates for the resonant state of the tetraneutron system. The mean energy of the events is evaluated to be 0.83±0.65 MeV with an additional systematic uncertainty of 1.25 MeV due to uncertainty in the calibration of the missing-mass energy. These results suggest a possible resonant state of the tetraneutron system, although the possibility of a bound state is not experimentally excluded. The upper limit of the width of the peak is estimated to be 2.6 MeV (FWHM), which is mainly determined by experimental missing-mass resolution. The rather narrow width may be understood by considering a small phase space for the four-body decay.

The result indicating the resonant state may suggest necessity of strong many-body forces, such as isospin T =3/2 three-body force and/or $T = 2$ four-body force, which are incompatible with the present understanding of nuclear interactions[5]. Our results should serve as a basis for further investigations.

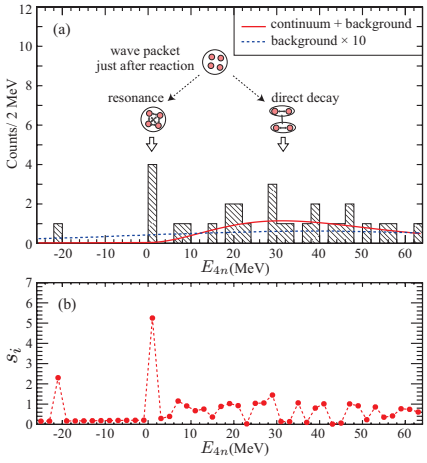

Fig. 1. (a) Missing-mass spectrum of the tetraneutron system. The solid (red) line represents the sum of the direct decay of the correlated two-neutron pairs and the estimated background. The dashed (blue) line represents the estimated background multiplied by a factor of 10. (b) Evaluation of the goodness of fit for each bin.

References

1) F. Marques et al.: Phys. Rev. C 65, 044006 (2002).
2) S. Pieper: Phys. Rev. Lett. 90, 252501 (2003).
3) K. Kisamori et. al.: Accelerator Progress Rep. Vol. 45 (2012).
4) K. Kisamori et. al.: Accelerator Progress Rep. Vol. 46 (2013).
5) R. Lazauskas et. al.: Phys. Rev. C 71, 044004 (2005).

† Condensed from the article in Phys. Rev. Lett. **116**, 052501 (2016)

*1 RIKEN Nishina Center
*2 Center for Nuclear Study, the University of Tokyo
*3 IPN, Orsay
*4 Department of Physics, Kyoto University
*5 Research Center Nuclear Physics, Osaka University
*6 Cyclotron and Radioisotope Center, Tohoku University
*7 Department of Physics, Tokyo Institute of Technology
*8 Faculty of Engineering, University of Miyazaki
*9 Department of Physics, the University of Tokyo
*10 NSCL, Michigan State University
*11 Faculty of Science, Kyushu University

Magnetic moment measurement of isomeric state in ^{75}Cu

Y. Ichikawa,[*1] A. Takamine,[*1] H. Nishibata,[*2] K. Imamura,[*1,*3] T. Fujita,[*1,*2] T. Sato,[*4] S. Momiyama,[*5] Y. Shimizu,[*1] D. S. Ahn,[*1] K. Asahi,[*4] H. Baba,[*1] D. L. Balabanski,[*1,*6] F. Boulay,[*1,*7,*8] J. M. Daugas,[*1,*8] T. Egami,[*9] N. Fukuda,[*1] C. Funayama,[*4] T. Furukawa,[*10] G. Georgiev,[*11] A. Gladkov,[1,*12] N. Inabe,[*1] Y. Ishibashi,[*1,*13] Y. Kobayashi,[*14] S. Kojima,[*4] A. Kusoglu,[*11,*15] T. Kawaguchi,[*9] T. Kawamura,[*2] I. Mukul,[*16] M. Niikura,[*5] T. Nishizaka,[*9] A. Odahara,[*2] Y. Ohtomo,[*1,*4] D. Ralet,[*11] T. Shimoda,[*2] G. S. Simpson,[*17] T. Sumikama,[*1] H. Suzuki,[*1] H. Takeda,[*1] L. C. Tao,[*1,*18] Y. Togano,[*4] D. Tominaga,[*9] H. Ueno,[*1] H. Yamazaki,[*1] and X. F. Yang[*19]

The ^{75}Cu nucleus has attracted much attention because the ground-state spin parity changes from $3/2^-$ to $5/2^-$[1] as a result of the migration of the $5/2^-$ levels along the Cu isotopic chain[2]. The ^{75}Cu nucleus has two isomeric states[3] at 62-keV and 66-keV levels directly decaying to the ground state[4], one of which is expected to have a spin parity of $3/2^-$ inherited from the ground state of ^{73}Cu. In order to investigate the wave function of the $3/2^-$ state and to compare it with the $5/2^-$ ground state[1], the magnetic moment of the isomeric state of ^{75}Cu was measured.

The experiment was carried out at the BigRIPS at the RIBF. The two-step fragmentation scheme with momentum-dispersion matching[5] was employed to produce highly spin-aligned ^{75}Cu. In the reaction at F0, ^{76}Zn was produced by a fission reaction of a 345-MeV/nucleon ^{238}U beam on a ^{9}Be target with a thickness of 1.29 g/cm^2. The secondary ^{76}Zn beam was introduced to a second target of wedge-shaped aluminum with a mean thickness of 0.81 g/cm^2, placed at the momentum-dispersive focal plane F5. The ^{75}Cu nuclei including those in isomeric state ^{75m}Cu were produced through one-proton removal from ^{76}Zn. The ^{75}Cu beam was subsequently transported to F7 under the condition that the momentum dispersion between F5 and F7 was matched to that between F3 and F5.

The g-factor of ^{75m}Cu was determined by means of the time-differential perturbed angular distribution (TDPAD) methods. The TDPAD apparatus, placed at F8, consists of a dipole magnet, a Cu crystal stopper, Ge detectors, and a plastic scintillator. The dipole magnet provided a static magnetic field of $B_0 = 0.200$ T. ^{75m}Cu was implanted into the Cu stopper, and γ rays were detected with four Ge detectors located perpendicular to B_0 at a distance of 7.0 cm from the stopper and at angles of ±45 and ±135 degrees with respect to the beam axis. The plastic scintillator of 0.1 mm in thick was placed upstream of the stopper, the signal from which provided the time-zero trigger.

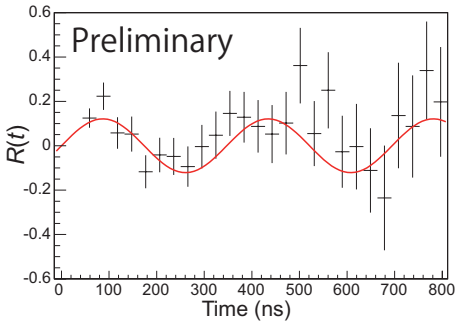

Fig. 1. Preliminary result of $R(t)$ ratio for the 66-keV γ ray. The solid line represents the sine function after fitting to the the experimental $R(t)$ ratio.

The $R(t)$ ratio representing the change of anisotropy of γ rays synchronized with the spin precession was obtained according to

$$R(t) = \{N_{13}(t) - \epsilon N_{24}(t)\}/\{N_{13}(t) + \epsilon N_{24}(t)\}, \quad (1)$$

where $N_{13}(t)$ and $N_{24}(t)$ are the sums of the photopeak count rates at the two pairs of Ge detectors placed diagonally to each other, and ϵ denotes a correction factor for the difference in the detection efficiency. In this experiment we observed an oscillation pattern only for the 66-keV γ ray with over 5σ significance, as shown in Fig. 1. The magnitude of spin alignment was found to be larger than 50%. The detailed analysis and the deduction of the g-factor is in progress.

*1 RIKEN Nishina Center
*2 Department of Physics, Osaka University
*3 Department of Physics, Meiji University
*4 Department of Physics, Tokyo Institute of Technology
*5 Department of Physics, University of Tokyo
*6 ELI-NP, IFIN-HH
*7 GANIL, CEA/DSM-CNRS/IN2P3
*8 CEA, DAM, DIF
*9 Department of Advanced Sciences, Hosei University
*10 Department of Physics, Tokyo Metropolitan University
*11 CSNSM, CNRS/IN2P3, Université Pris-Sud
*12 Department of Physics, Kyungpook National University
*13 Department of Physics, University of Tsukuba
*14 Department of Informatics and Engineering, University of Electro-Communications
*15 Department of Physics, Istanbul University
*16 Department of Particle Physics, Weizmann Institute
*17 LPSC, Université Joseph Fourier Grenoble 1, CNRS/IN2P3
*18 School of Physics, Peking University
*19 Intsituut voor Kern-en Srralingsfysica, K. U. Leuven

References

1) K. T. Flanagan et al.: Phys. Rev. Lett. **103**, 142501 (2009).
2) S. Franchoo et al.: Phys. Rev. Lett. **81**, 3100 (1998).
3) J. M. Daugas et al.: Phys. Rev. C **81**, 034304 (2010).
4) C. Petrone et al.: Acta. Phys. Pol. B **44**, 637 (2013).
5) Y. Ichikawa et al.: Nature Phys. **8**, 918 (2012).

Deuteron Analyzing Powers for *d*–*p* elastic scattering at 190 MeV/nucleon and three–nucleon force effects

K. Sekiguchi,[*1*2] T. Akieda,[*1] Y. Wada,[*1] D. Eto,[*1] A. Watanabe,[*1] H. Kon,[*1] N. Sakamoto,[*2] H. Sakai,[*2] M. Sasano,[*2] H. Suzuki,[*2] T. Uesaka,[*2] Y. Yanagisawa,[*2] M. Dozono,[*3] Y. Kubota,[*3] K. Yako,[*3] Y. Maeda,[*4] S. Kawakami,[*4] T. Yamamoto,[*4] S. Sakaguchi,[*5] T. Wakasa,[*5] J. Yasuda,[*5] A. Ohkura,[*5] Y. Shindo,[*5] M. Tabata,[*5] E. Milman,[*2*6] and S. Chebotaryov[*2*6]

Study of three-nucleon forces (3NFs) is essentially important in clarifying nuclear phenomena, e.g. discrete states of nuclei and equation of state of nuclear matter. Nucleon–deuteron (Nd) scattering, for which a rigorous formulation in terms of Faddeev equations exists and exact solutions of these equations for any dynamical input can be obtained, offers a good opportunity for the dynamical aspects of 3NFs, such as momentum, spin and/or iso-spin dependences. With the aim of clarifying properties of the 3NFs the study of energy dependent deuteron–proton (d–p) scattering with polarized deuteron beams at intermediate energies ($E \sim 200$ MeV/nucleon(MeV/N)) are in progress at RIBF. Here we report a measurement of all the deuteron analyzing powers (iT_{11}, T_{20}, T_{21}, and T_{22}) in d–p elastic scattering at 190 MeV/N performed in May 2015.

A schematic diagram of the experimental setup is provided in Ref.[1]. Vector- and tensor- polarized deuteron beams were accelerated by the injector cyclotrons AVF and RRC up to 70 MeV/N; subsequently, they were accelerated up to 190 MeV/N by the SRC. The measurement of the d–p elastic scattering was performed using a detector system, BigDpol, which was installed at the extraction beam line of the SRC. Polyethylene (CH_2) with a thickness of 330 mg/cm^2 was used as hydrogen target. In BigDpol, four pairs of plastic scintillators coupled with photo-multiplier tubes were placed symmetrically in the directions of azimuthal angles to the left, right, up and down. Scattered deuterons and recoil protons were detected in the kinematical coincidence condition by each pair of the detectors. The measured angular range is 39°–165° in the center-of-mass system. In the experiment, the deuteron beams were stopped in the Faraday cup, which was installed at the focal plane F0 of the BigRIPS spectrometer. The beam polarizations were monitored continuously with a beam line polarimeter Dpol prior to the acceleration by the SRC using the reaction of elastic d–p scattering at 70 MeV/nucleon. The analyzing powers for this reaction have been calibrated in the previous measurement by using the ^{12}C$(d,\alpha)^{10}$B* [2$^+$] reaction[2]. In the measurement typical values of the beam polarizations were 80% of the theoretical maximum values.

Preliminary results are shown with open circles in Fig. 1. Only the statistical uncertainties are shown. The data are compared with the Faddeev calculations with (without) Tucson–Melbourne'99 3NF[3] based on the modern NN potentials, namely CDBonn[4], AV18[5], Nijmegen I and II[6]. The solid lines are the calculations with the Urbana IX 3NF[7] based on the AV18 potential. Generally data for the backward angles $\theta_{\rm c.m.} \gtrsim 120°$ are well explained by the calculations with the 3NFs except for T_{20}.

Detailed analysis is now in progress. Discussions on the energy-dependence of the deuteron analyzing powers for d–p elastic scattering at 70–300 MeV/N will be performed.

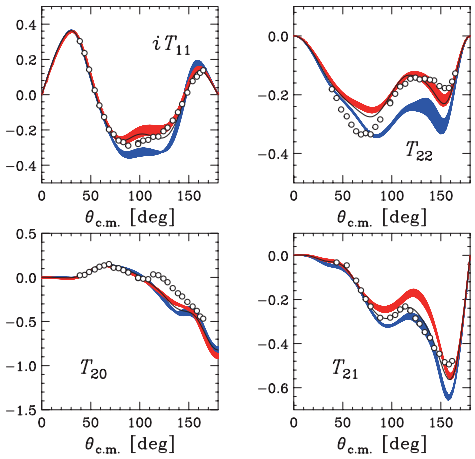

Fig. 1. Preliminary results of the vector and tensor analyzing powers for the d-p elastic scattering at 190 MeV/N.

*1 Department of Physics, Tohoku University
*2 RIKEN Nishina Center
*3 CNS, University of Tokyo
*4 Faculty of Engineering, University of Miyazaki
*5 Department of Physics, Kyushu University
*6 Department of Physics, Kyungpook National University

References
1) K. Sekiguchi et al., Phys. Rev. C **89**, 064007 (2014).
2) K. Suda et al., Nucl. Instrum. Methods Phys. Res. A. **572**, 745 (2007).
3) S. A. Coon, H. K. Han, Few Body Syst. **30**, 131 (2001).
4) R. Machleidt, Phys. Rev. C **63**, 024001 (2001).
5) R. B. Wiringa et al., Phys. Rev. C **51**, 38 (1995).
6) V. G. J. Stoks et al., Phys. Rev. C **49**, 2950 (1994).
7) B. S. Pudliner et al., Phys. Rev. C**56**, 1720 (1997).

Measurement of multiple isobar chains as a first step toward SHE identification via mass spectrometry†

P. Schury,[*1] M. Wada,[*1,*2] Y. Ito,[*2] D. Kaji,[*2] P.-A. Söderström,[*2] A. Takamine,[*2] F. Arai,[*2,*3] H. Haba,[*2] S. Jeong,[*1] S. Kimura,[*1,*2,*3] H. Koura,[*4] H. Miyatake,[*1] K. Morimoto,[*2] K. Morita,[*2,*5] A. Ozawa,[*3] M. Reponen,[*2] T. Sonoda,[*2] T. Tanaka,[*2,*5] and H. Wollnik[*6]

In the search for the long-predicted "island of stability", the use of so-called hot-fusion reactions has allowed for extending the table of isotopes up to element-118 in recent years. A dearth of projectile-target combinations available for cross-bombardment reactions and α-decay chains terminating in spontaneous fission before reaching well-known nuclei were bottlenecks to acceptance of element-113, -115, -117 and -118[1]. As we push ever closer to the island of stability, whether by use of more exotic projectile-target combinations or use of multi-nucleon transfer reactions[2], this problem will become ever more severe; we can expect many spontaneously fissioning nuclei, longer α-decay half-lives, and a recurrence of β-decay[3].

As the first step toward mass spectrographic identification of SHE, we have installed a gas cell connected to an MRTOF-MS[4] after the gas-filled recoil ion separator GARIS-II[5]. We have used this system to initially perform mass measurements with fusion-evaporation reaction products lighter than uranium, the masses of some of which have not previously been directly measured. In these measurements we demonstrate the ability of the MRTOF-MS to simultaneously measure the masses of atomic (and molecular) ions across multiple isobar chains. With reasonable statistics a high-precision can be achieved, while with less than 10 detected ions the mass can be determined with sufficient precision to identify an ion species.

A 1.5 pμA beam of $^{40}Ar^{11+}$ at 4.825 MeV/u was provided by the RIKEN heavy-ion linear accelerator RILAC. The beam impinged upon a rotating target wheel with 16 target windows. The target wheel comprised 4 windows of $^{165}_{67}$Ho with a thickness of ∼0.14 mg/cm^2 and 12 windows of $^{169}_{69}$Tm with a thickness of ∼0.29 mg/cm^2. The ^{165}Ho and ^{169}Tm targets were prepared using sputtering and electro-deposition methods, respectively, on 3 μm Ti backing foil. A rotating shadow wheel ensured the beam could only impinge on one type of target at a time[6].

Figure 1 shows the spectrum seen when bombarding the $^{169}_{69}$Tm target. We were able to simultaneously observe the 3n and 4n evaporation channels, $^{205,205}Fr^+$, in a single time-of-flight spectrum. At the same time we could observe lighter isobars, although whether they were decays or $xpyn$ evaporation channels could not be definitively determined.

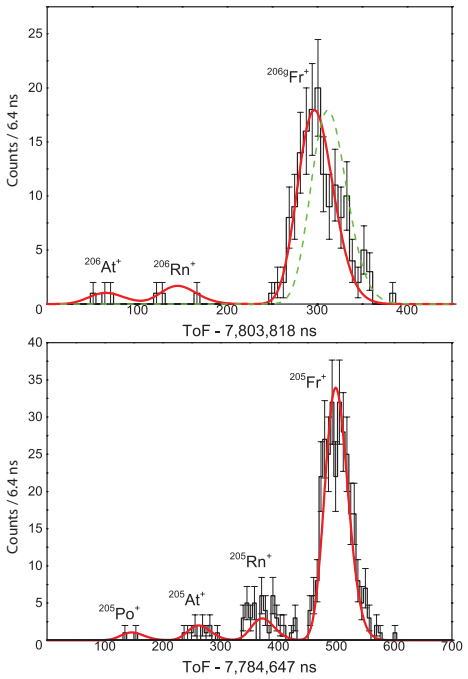

Fig. 1. Spectrum observed for A/q=201, 205, and 206 species at n=148 laps.

References

1) Robert C. Barber, Paul J. Karol, Horimichi Nakahara, Emanuele Vardaci, and Erich W. Vogt, Pure and Applied Chemistry, Vol. 83, No. 7, pp. 1485-1498 (2011)
2) J. V. Kratz, M. Schädel, and H. W. Gäggeler, Phys. Rev. C 88 (2013) 054615
3) A. V. Karpov, V. I. Zagrebaev, Y. Martinez Palenzuela, L. Felipe Ruiz, Walter Greiner, Int. J. Mod. Phys. E 21 (2012) 1250013
4) P.Schury et al., EMIS2015 proceeding, submitted to NIMB
5) D. Kaji, K. Morimoto, N. Sato, A. Yoneda, K. Morita, Nuclear Instruments and Methods in Physics Research Section B: Beam Interactions with Materials and Atoms, 317B (2013) 311-314
6) D. Kaji, K. Morimoto, Nuclear Instruments and Methods in Physics Research Section A: Accelerators, Spectrometers, Detectors and Associated Equipment 792 (2015) 11-14

† Condensed from article submitted to Phys. Rev. C http://arxiv.org/abs/1512.00141

*1 Institute of Particle and Nuclear Studies (IPNS), High Energy Accelerator Research Organization (KEK)
*2 RIKEN Nishina Center
*3 Institute of Physics, University of Tsukuba
*4 Advanced Science Research Center, Japan Atomic Energy Agency
*5 Kyushu University
*6 New Mexico State University

Gauge symmetry in the large-amplitude collective motion of superfluid nuclei†

K. Sato *1

The adiabatic self-consistent collective coordinate (ASCC) method[2] is a practical method for describing large-amplitude collective motion in atomic nuclei with superfluidity and an advanced version of the adiabatic time-dependent Hartree–Fock–Bogoliubov theory. In the application of the one-dimensional ASCC method, Hinohara et al.[3] encountered numerical instability and found that it was caused by the symmetry of the basic equations of the ASCC method under a certain continuous transformation. This transformation involves the gauge angle φ and changes the phase of the state vector. In this sense, Hinohara et al. called it the "gauge" symmetry. They proposed a gauge-fixing prescription to remove redundancy associated with the gauge symmetry and successfully applied it to the shape coexistence phenomena in proton-rich Se and Kr isotopes.

We investigated this symmetry on the basis of the Dirac–Bergmann theory of constrained systems[4,5]. As is well known, the gauge symmetry is associated with constraints originating from the singularity of the Lagrangian. In the ASCC method, the linear term of the particle number n in the collective Hamiltonian can be regarded as a constraint, and it leads to the gauge symmetry.

In the ASCC method, we assume the following form of the state vector.

$$|\phi(q,p,\varphi,n)\rangle = e^{-i\varphi\tilde{N}}|\phi(q,p,n)\rangle = e^{-i\varphi\tilde{N}}e^{i\hat{G}}|\phi(q)\rangle,$$

with $\hat{G}(q,p,n) = p\hat{Q}(q) + n\hat{\Theta}(q)$ and $\tilde{N} = \hat{N} - N_0$. φ is the gauge angle conjugate to the particle number $n = N - N_0$ measured from a reference value N_0. The collective Hamiltonian is defined and expanded up to $O(n)$ as below.

$$\begin{aligned}\mathcal{H}(q,p,n) &:= \langle\phi(q,p,\varphi,n)|\hat{H}|\phi(q,p,\varphi,n)\rangle \\ &= V(q) + \frac{1}{2}B(q)p^2 + \lambda n. \end{aligned} \tag{1}$$

This can be regarded as a system with the constraint $n = 0$, and λ is a Lagrange multiplier.

In Lagrange formalism, the Lagrangian corresponding to this (total) Hamiltonian is given by

$$L = \frac{1}{2B(q^1)}(\dot{q}^1)^2 - V(q^1,q^2), \tag{2}$$

with $(q^1,q^2) := (q,\varphi)$, and the rank of the Hessian $(\partial^2 L/\partial\dot{q}^i\partial\dot{q}^j)$ is one. (We allowed the potential V to depend on $q^2 = \varphi$ in order to make it easy to observe the number of the degrees of freedom.) Hence, this Lagrangian leads to one constraint, $p_2 = \frac{\partial L}{\partial\dot{q}^2} = n = 0$. The time derivative of the constraint is given by $\dot{n} = \{n,\mathcal{H}\} = -\partial_\varphi V$. Thus, the constraint is preserved in time if $V(q,\varphi) = V(q)$. Then, we have only one constraint $n = 0$, and it is a first-class constraint. From the above, it is clear that our system has one gauge degree of freedom.

It is known that a generator of a gauge transformation can always be written as a "linear combination" of the first-class constraints. We can write the generator G as $G = \epsilon(q,p,\varphi,n,t)n$ with an infinitesimal function ϵ. This generator gives the gauge transformation of collective variables.

$$\delta q = n\partial_p\epsilon \approx 0, \quad \delta p = -n\partial_q\epsilon \approx 0, \tag{3}$$

$$\delta\varphi = \epsilon + n\partial_n\epsilon \approx \epsilon, \quad \delta n = -n\partial_\varphi\epsilon \approx 0. \tag{4}$$

Here, the symbol $\approx$ denotes weak equality. As ϵ is an arbitrary function of (q,p,φ,n,t), in particular, of p, the linear and higher-order terms of p are mixed only into φ by this gauge transformation. This is important for the adiabatic expansion in the ASCC method to make sense.

With the choice $\epsilon = \alpha pn$, we obtain

$$\delta q = \alpha n, \quad \delta p = 0, \quad \delta\varphi = \alpha p, \quad \delta n = 0, \tag{5}$$

which leads to the transformation of operators,

$$\hat{Q} \to \hat{Q} + \alpha\tilde{N}, \quad \hat{\Theta} \to \hat{\Theta} + \alpha\hat{P}. \tag{6}$$

This is exactly the transformation found in Ref. 3), and thus, we confirmed that the symmetry discussed in Ref. 3) is a gauge symmetry.

In Ref. 1), the most general gauge transformation is discussed. While the equation of collective submanifold, from which the basic equations of the ASCC method (the moving-frame HFB & QRPA equations) are derived, is invariant under the most general gauge transformation, the gauge symmetry is partially broken by the adiabatic expansion at the level of the moving-frame HFB & QRPA equations. Above, we have considered the expansion of the collective Hamiltonian up to $O(n)$. In Ref. 1), it is also shown that there is no gauge symmetry in the case where the collective Hamiltonian is expanded up to $O(n^2)$.

† Condensed from the article in Ref. 1)

*1 RIKEN Nishina Center

References

1) K. Sato, Prog. Theor. Exp. Phys. **2015**, 123D01
2) M. Matsuo, T. Nakatsukasa, and K. Matsuyanagi, Prog. Theor. Phys. **103**, 959 (2000).
3) N. Hinohara, T. Nakatsukasa, M. Matsuo, and K. Matsuyanagi, Prog. Theor. Phys. **117**, 27 (2007).
4) P. A. M. Dirac, Can. J. Math. **2**, 129 (1950).
5) J. L. Anderson, P. G. Bergmann, Phys. Rev. **83**, 1018 (1951).

Cross section measurement for the spallation reaction of long-lived fission products

H. Wang,[*1] H. Otsu,[*1] H. Sakurai,[*1] D. Ahn,[*1] M. Aikawa,[*2] T. Ando,[*3] S. Araki,[*4,*1] H. Baba,[*1] S. Chen,[*1] N. Chiga,[*1] P. Doornenbal,[*1] N. Fukuda,[*1] T. Isobe,[*1] T. Ichihara,[*1] S. Kawakami,[*5,*1] S. Kawase,[*6,*4] T. Kin,[*4] Y. Kondo,[*7,*1] S. Koyama,[*3] S. Kubono,[*1] Y. Maeda,[*5] A. Makinaga,[*8] M. Matsushita,[*6] T. Matsuzaki,[*1] S. Michimasa,[*6] S. Momiyama,[*3] S. Nagamine,[*3] T. Nakamura,[*7,*1] K. Nakano,[*4,*1] M. Niikura,[*3] Y. Ozaki,[*7,*1] A. T. Saito,[*7,*1] T. Saito,[*3] H. Sato,[*1] Y. Shiga,[*1,*9] M. Shikata,[*7,*1] Y. Shimizu,[*1] S. Shimoura,[*6] T. Sumikama,[*1] P.-A. Söderström,[*1] H. Suzuki,[*1] H. Takeda,[*1] S. Takeuchi,[*7,*1] R. Taniuchi,[*1,*3] Y. Togano,[*7,*1] J. Tsubota,[*7,*1] M. Uesaka,[*1] Ya. Watanabe,[*1] Yu. Watanabe,[*4] K. Wimmer,[*3,*1] T. Yamamoto,[*5,*1] and K. Yoshida[*1]

Long-lived fission products (LLFPs) are one of the major components in the nuclear waste from nuclear reactor systems. LLFP nuclei are highly radioactive and have long half lives. In order to reduce the quantity of high-level radioactive waste, partitioning and transmutation technology has been introduced in recent years[1]. For LLFP transmutation, the possibility of proton-induced spallation reaction has been discussed[2]; however, experimental data are insufficient. For a systematic study on LLFP transmutation, we report on the spallation reactions for ^{90}Sr, ^{93}Zr, ^{107}Pd, and ^{135}Cs with protons and deuterons at different reaction energies, following the study for ^{90}Sr and ^{137}Cs in 2014[3].

Secondary beams were produced by the in-flight fission of a ^{238}U primary beam at 345 MeV/nucleon on a beryllium target with a thickness of 1 mm. The momentum acceptance of BigRIPS was set as 0.1%. Several secondary beam settings were applied in BigRIPS and optimized for ^{90}Sr, ^{93}Zr, ^{107}Pd, and ^{135}Cs. Note that the secondary ^{90}Sr and ^{93}Zr beams were produced with the same BigRIPS setting. The beam energies for ^{90}Sr, ^{93}Zr, ^{107}Pd, and ^{135}Cs were approximately 115 MeV/nucleon in front of the secondary targets. In addition, another setting was used for ^{107}Pd to study the reaction at a high reaction energy of 220 MeV/nucleon. Secondary cocktail beams were identified event-by-event via the TOF – $B\rho-\Delta E$ method by using standard BigRIPS diagnosis detectors[4].

To induce the secondary reactions, CH_2, CD_2[5], and ^{12}C targets were used. Their thicknesses were 179.2, 217.8, and 226.0 mg/cm^2, respectively. In order to obtain the background contribution, data were accumulated using the target holder with no target inserted.

Reaction residues were identified by measuring TOF, $B\rho$, ΔE, and the total kinetic energy in the ZeroDegree spectrometer[6] with the large acceptance mode. In order to cover a broad range of spallation products, several different $B\rho$ settings were applied in the ZeroDegree spectrometer. An example of the particle identification (PID) for the reaction residues detected by the ZeroDegree spectrometer is shown in Fig. 1. The PID plot was obtained in the ^{107}Pd setting at 220 MeV/nucleon with the CD_2 target.

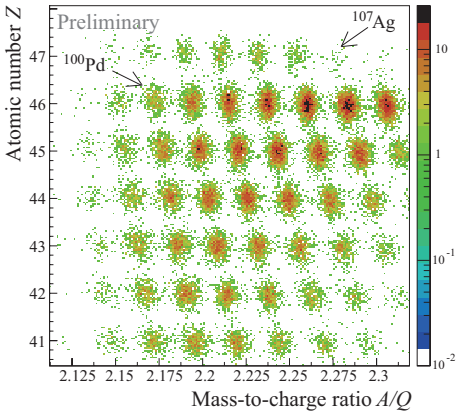

Fig. 1. Particle identification plot of Z versus A/Q in the ZeroDegree spectrometer for the reaction residues produced from the ^{107}Pd beam at 220 MeV/nucleon.

The analysis of the proton- and deuteron-induced cross sections for the LLFP nuclei is currently in progress. This work was supported by ImPACT program of Council for Science, Technology and Innovation (Cabinet Office, Government of Japan).

References

1) IAEA Technical Reports Series No. 435 (2004).
2) A. Hermanne, J. Nucl. Sci. Technol. 39, Suppl. 2, 1202 (2002).
3) H. Wang et al. RIKEN Accel. Prog. Rep. 48, 6 (2015).
4) N. Fukuda et al. Nucl. Instrum. Methods B 317, 323 (2013).
5) Y. Maeda et al. Nucl. Instr. Meth. A 490, 518 (2002).
6) T. Kubo et al. Prog. Theor. Exp. Phys. 2012, 03C003 (2012).

*1 RIKEN Nishina Center
*2 Faculty of Science, Hokkaido University
*3 Department of Physics, University of Tokyo
*4 Kyushu University
*5 University of Miyazaki
*6 CNS, University of Tokyo
*7 Tokyo Institute of Technology
*8 JEin institute for fundamental science, NPO Einstein
*9 Department of Physics, Rikkyo University

Final results of $A_{LL}^{\pi^0}$ measurement at $\sqrt{s} = 510$ GeV at mid-rapidity through a PHENIX experiment†

I. Yoon*1,*2 for the PHENIX collaboration

One of the important functions of the relativistic heavy ion collider (RHIC) longitudinally polarized proton program is to constrain the gluon-spin component of proton (ΔG) by measuring the double helicity asymmetry (A_{LL}) of π^0 production ($A_{LL}^{\pi^0}$) and jet production (A_{LL}^{Jet}). Based on the results of deep inelastic scattering experiments, the quark-spin component of the proton is only $0.330 \pm 0.011(Theo.) \pm 0.025(Exp.) \pm 0.028(Evol.)$[1]. The remaining spin might be carried by gluons or orbital momentum.

Studies on the measurement of $A_{LL}^{\pi^0}$ and A_{LL}^{Jet} at $\sqrt{s} = 200$ GeV have been successfully published, and they have contributed to constrain ΔG[2,3]. Consequently, a positive $\Delta g(x)$ has been observed in the measured x region[4]. However, the uncertainty of ΔG is still significant owing to the uncertainty at lower the Bjorken x region, which has not been accessed so far[4].

To explore the lower x region, where uncertainty is dominant, longitudinally polarized proton-proton collisions with increased energy, i.e., $\sqrt{s} = 510$ GeV, were successfully carried out in 2012 (Run12) and 2013 (Run13). With the data, $A_{LL}^{\pi^0}$ at $\sqrt{s} = 510$ GeV was measured and published recently. Because of the increased energy, the measurement of $A_{LL}^{\pi^0}$ at $\sqrt{s} = 510$ GeV could reach a lower x range, $0.01 < x$, while the previous measurement of $A_{LL}^{\pi^0}$ and A_{LL}^{Jet} at $\sqrt{s} = 200$ GeV could reach $0.02 < x$ and $0.05 < x$, respectively.

$A_{LL}^{\pi^0}$ can be defined in terms of differences in cross-sections as

$$A_{LL}^{\pi^0} = \frac{d\Delta\sigma^{\pi^0}}{d\sigma^{\pi^0}} = \frac{d\sigma_{++}^{\pi^0} - d\sigma_{+-}^{\pi^0}}{d\sigma_{++}^{\pi^0} + d\sigma_{+-}^{\pi^0}} \quad (1)$$

where $\sigma_{++(+-)}$ denotes the π^0 cross-section for proton collisions with the same(opposite) helicity. The π^0 cross-section can be decomposed into parton distribution functions, partonic reaction cross-sections, and fragmentation functions. Because most of π^0s are from quark-gluon or gluon-gluon scattering at mid-rapidity region, $\Delta g(x)$ is accessible by measuring $A_{LL}^{\pi^0}$. This description is verified by comparing the π^0 cross-section between theoretical and experimental data. Equation 1 can be rewritten in terms of experimental observables as

$$A_{LL} = \frac{1}{P_B P_Y} \frac{N_{++} - RN_{+-}}{N_{++} + RN_{+-}}, R = \frac{L_{++}}{L_{+-}} \quad (2)$$

where $P_{B(Y)}$ is the polarization of RHIC's "Blue (Yellow)" beam, $N_{++(+-)}$ is the yield of the π^0 candidate from the same (opposite) helicity collisions, and R is the relative luminosity of same and opposite helicity collisions.

π^0s are reconstructed by photon pairs detected by PHENIX mid-rapidity electromagnetic calorimeters. Sophisticated cuts are applied to suppress combinatorial background. The relative luminosity is fully corrected for multiple collisions and detector resolution effects.

Fig. 1 shows the result of $A_{LL}^{\pi^0}$ measurement at $\sqrt{s} = 510$ GeV. The world's first non-zero A_{LL} in hadron production is observed. The results agree with DSSV14 calculation based on a global fit of world A_{LL} data and supports positive ΔG. It thus supports positive ΔG in the previously accessed x region and extends the probed x region down to $x \sim 0.01$. Therefore it provides an additional constraint on ΔG[5,6] This is a crucial step toward world-wide efforts to extract ΔG.

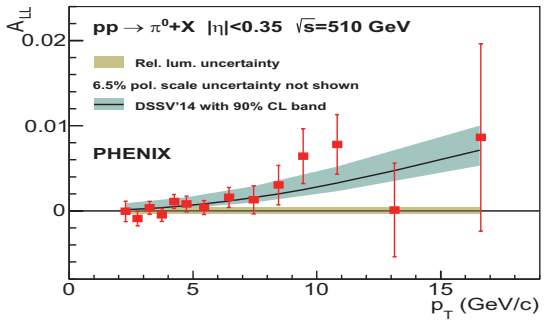

Fig. 1. Result of $A_{LL}^{\pi^0}$ measurement at $\sqrt{s} = 510$ GeV. The red error bars represent combined statistical and point-to-point systematic uncertainties. The yellow box represents systematic uncertainty from the relative luminosity. The theoretical curve with 90% C.L. band is obtained from the DSSV14 calculation[4].

References
1) A. Airapetian et al., Phys. Rev. D **75**, 012007 (2007).
2) A. Adare et al., Phys. Rev. D **90**, 012007 (2014).
3) L. Adamczyk et al., Phys. Rev. Lett. **115**, 092002 (2015).
4) D. de Florian, R. Sassot, M. Stratmann and W. Vogelsang: Phys. Rev. Lett. **113**. 012001 (2014)
5) R. Sassot (DSSV Group), private communication.
6) E. Nocera (NNPDF Group), private communication.

† Condensed from the article in Phys. Rev. D. **93**, 011501 (2016)

*1 RIKEN Nishina Center
*2 The Research Institute of Basic Science, Seoul National University

A_N of forward neutron production in $\sqrt{s}$=200 GeV polarized proton-nucleus collisions in the PHENIX expermient

M. Kim[*1,*2] for the PHENIX collaboration

The first attempt to collide a polarized proton and a nucleus was executed at RHIC in Run15. This provides a unique opportunity to study the totally unexplored reaction mechanism of $p^{\uparrow}+A$ at high energy. We report the first asymmetry measurement of forward ($6.8 < \eta < 8.8$) neutron results from $p + Al$, and $p + Au$. The observed asymmetries showed unexpectedly large values and strong A-dependence.

The single transverse spin asymmetry, A_N, is written as

$$A_N = \frac{d\sigma^{\uparrow} - d\sigma^{\downarrow}}{d\sigma^{\uparrow} + d\sigma^{\downarrow}} \quad (1)$$

where $\uparrow$ and $\downarrow$ represent the spin directions of incident protons. In terms of scattering amplitudes, the condition for nonzero A_N is

$$A_N \propto Im\{\phi^{*}_{\rm filp}\phi_{\rm nonfilp}\sin\delta\} \neq 0 \quad (2)$$

where $\phi^{*}_{\rm filp}(\phi_{\rm nonfilp})$ is the spin flip (nonfilp) amplitude, and δ is a relative phase between the two amplitudes.

In 2011, a one pion exchange (OPE) model that well describes the cross section and A_N of forward neutron production from the PHENIX data[1)] for $\sqrt{s}$=200 GeV p+p collision was published[2)]. The model describes the spin flip amplitude by pion exchange and the non-spin flip amplitude mainly by the a1-Reggeon exchange. As a consequence, the model satisfactory reproduced the experimental A_N data.

Fig. 1 shows a preliminary plot of the Run15 forward neutron A_N results.The red points are A_N of ZDC (zero degree calorimeter, a neutron detector) inclusive measurements. They show unexpectedly strong mass number (A) dependence; $A_N^{p^{\uparrow}+Au}$ is 3 times larger than $A_N^{p^{\uparrow}+p}$, and they have opposite sign.

The observed A dependence immediately eliminates naive expectations such as isospin symmetric effects, which do not change the sign of A_N with increasing number of protons and neutrons.

Although electromagnetic interaction was not even considered in p+p, it may not be ignorable in p+A because of the smallness of the $-t$ range ($< 0.5\mathrm{GeV/c}^2$) of the measurements. Without full description, equation 2 is thus modified as

$$\begin{aligned} A_N \propto\ & \phi^{\rm EM*}_{\rm filp}\phi^{\rm EM}_{\rm nonfilp}\sin\delta_1 + \phi^{\rm EM*}_{\rm filp}\phi^{\rm had}_{\rm nonfilp}\sin\delta_2 \\ & + \phi^{\rm had*}_{\rm filp}\phi^{\rm EM}_{\rm nonfilp}\sin\delta_3 + \phi^{\rm had*}_{\rm filp}\phi^{\rm had}_{\rm nonfilp}\sin\delta_4 \end{aligned} \quad (3)$$

where "EM" stands for electromagnetic interactions,

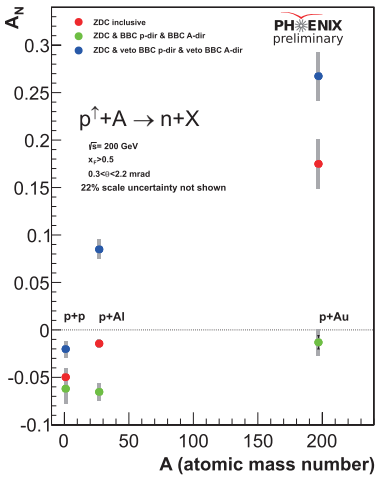

Fig. 1. Forward neutron A_N ploted as a function of atomic mass number with BBC correlations in $\sqrt{s}$ = 200 GeV $p + p$, $p + Al$, and $p + Au$ collisions.

"had" stands for strong interaction, and from δ_1 to δ_4 are relative phases. The majority of the elecromagnetic process should be given by $\gamma^{*}p \to \Delta^{+} \to n + \pi^{+}$ where γ^{*} is supplied from the EM field of the nucleus. The second and third terms are known as Coulomb nuclear interference (CNI), which is observed to cause $\lesssim 5\%$ asymmetry in the elastic scattering in p+p, and $p + C$ processes[3)]. According to an MC simulation, Δ^{+} decay products are predicted to be more forward boosted as compared to hadronic interactions[4)]. In order to suppress competing effects, a correlation study was carried out using beam beam counters (BBCs, $3.1 < \eta < 3.9$). Since the most of neutron and pion pairs decayed from Δ^{+} via the EM process events pass through the BBC hole, requiring/vetoing activities in BBC can suppress/enhance contributions from the EM terms in equation 3. The green points in Fig. 1 denote A_N with BBC activities, and the blue points denote A_N without BBC activity. We can see a clear correlation between the A_N and BBC activities.

There can be other processes that are not discussed here. Theoretical development is underway to explain this interesting discovery.

*1 RIKEN Nishina Center
*2 Department of Physics and Astronomy, Seoul National University

References

1) A. Adare et al., Phys. Rev. D **88**, 032006 (2013).
2) B. Z. Kopeliovich, I. K. Potashnikova, Ivan Schmidt, Phys. Rev. D **84**, 114012 (2011).
3) I. G. Alekseev et al., Phys. Rev. D **79**, 094014 (2009).
4) G. Mitsuka, Eur. Phys. J. C **75**:614 (2015).

Search for the deeply bound K^-pp state from the semi-inclusive forward-neutron spectrum in the in-flight K^- reaction on helium-3†

T. Hashimoto,[*1] K. Itahashi,[*1] M. Iwasaki,[*1] Y. Ma,[*1]H. Ohnishi,[*1] S. Okada,[*1] H. Outa,[*1] F. Sakuma,[*1] M. Sato,[*1] M. Tokuda,[*1] and Q. Zhang,[*1] for the J-PARC E15 collaboration

The existence of a strongly attractive force between antikaons ($\bar{K}$) and nucleons in isospin 0 channels leads to the prediction of the formation of deeply bound kaonic-nuclei.[1)] The investigation of these exotic states will provide unique information that will reveal the sub-threshold $\bar{K}N$ interaction. However, their existence has not been conclusively established to date.

The simplest kaonic nucleus is theoretically considered to be the so-called K^-pp state, consisting of a negative kaon and two protons.[a)] We searched for this state by using an in-flight K^- reaction in the J-PARC E15 experiment at the K1.8BR beam line.[2)] The first physics data acquisition was performed in May 2013, with 5×10^9 kaons at 1 GeV/c on a liquid ^{3}He target.

Figure 1 shows the semi-inclusive neutron spectrum at $\theta_n^{lab} = 0°$. Forward neutrons were detected with a plastic scintillation counter array placed $\sim$ 15 m away from the target and their momenta were reconstructed by the time-of-flight method. At least one charged particle was tagged in a cylindrical detector system (CDS) surrounding the target to determine the reaction vertex. The K^0-tagged spectrum, shown in the inset of Fig. 1, is attributed to the quasi-free charge-exchange reaction, and demonstrates that the detector resolution and the missing-mass scale are well understood.

The observed yield in the deeply bound region, corresponding to K^-pp binding energies greater than 80 MeV, was in good agreement with the evaluated backgrounds originating from 1) accidental hits and neutral particles other than neutrons, 2) reactions on the target cell, and 3) neutrons produced via charged Σ decay. Therefore, mass-dependent upper limits on the production cross section were determined in the missing-mass range from 2.06 to 2.29 GeV/c^2 for a $K^-pp \to \Lambda p$ isotropic decay. They were determined to be 30–180, 70–250, and 100–270 μb/sr, for natural widths of 20, 60, and 100 MeV, respectively, at 95% confidence levels. The upper limits obtained were one-order-of-magnitude smaller than the theoretical calculation performed by Koike and Harada for the deeply bound K^-pp case.[3)] The ratios of the upper limits to the cross sections of the quasi-elastic channels are (0.5–5)% ($K^-n \to K^-n$) and (0.3–3)% ($K^-p \to K^0n$). These ratios are rather small compared to the sticking probability of the usual hypernucleus formation.

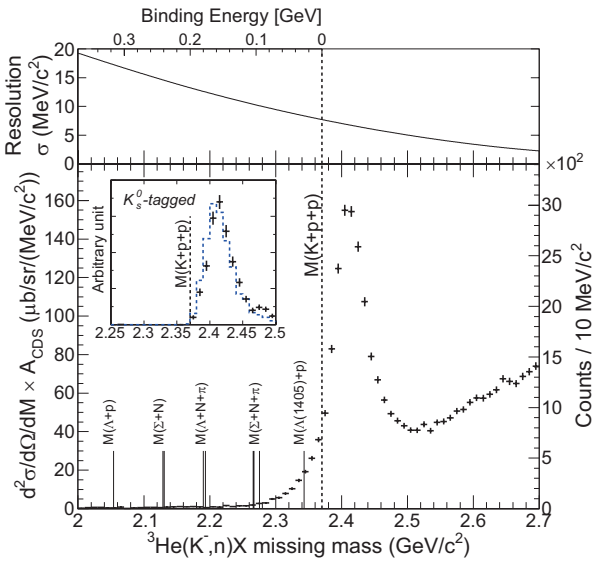

Fig. 1. ^{3}He$(K^-, n)X$ semi-inclusive missing-mass distribution (below) and experimental resolution (above). The CDS tagging acceptance (A_{CDS}) is not corrected. The K^-pp binding threshold is indicated by a dotted line and other related mass thresholds are indicated by solid lines. The inset shows the K^0_s-tagged spectrum compared with the simulation (blue dotted line).

In the loosely bound region, we observed a large yield which cannot be explained elementally processes. The cross section of this excess above the background is $\sim$ 1 mb/sr, assuming loosely bound K^-pp formation. This is about the same yield as that given by Koike and Harada,[3)] but much greater than the value given by Yamagata-Sekihara *et al.*[4)] In spite of the observed large yield, the structure near the threshold suggested in the theoretical spectral functions cannot be identified from only this semi-inclusive measurement. For further investigation of the origin of the sub-threshold structure, an exclusive analysis of the forthcoming dataset is required.

References
1) T. Yamazaki, Y. Akaishi, Phys. Lett. B **535** (2002) 70.
2) M. Iwasaki et al., J-PARC proposal P15, (2005).
K. Agari et al., Prog. Theor. Exp. Phys. 2012, 02B011.
3) T. Koike, T. Harada, Phys. Rev. C **80** (2009) 055208.
4) J. Yamagata-Sekihara, D. Jido, H. Nagahiro, S. Hirenzaki, Phys. Rev. C **80** (2009) 045204.

† Condensed from the article in Prog. Theor. Exp. Phys. (2015) 061D01

*1 RIKEN Nishina Center

a) More generally, it is expressed as $[\bar{K} \otimes \{NN\}_{I=1,S=0}]_{I=1/2}$ with J^π=0$^-$.

Phase-space distributions in QGP and thermal photons†

A. Monnai*1

The discovery of collective dynamics of QCD media in the BNL Relativistic Heavy Ion Collider (RHIC) and the CERN Large Hadron Collider (LHC) implies early equilibration of low-momentum partons and materialization of a quark-gluon plasma (QGP). The azimuthal momentum anisotropy v_2 of hadrons is well-explained in the framework of hydrodynamics, but that of direct photons, whose anisotropy is inherited from the medium during thermal emission, is underestimated roughly by a factor of 2. This apparent discrepancy is recognized as a "photon puzzle".

Thermal photon emission in the QGP phase is calculated using phase-space distribution functions. They are conventionally assumed to be ideal Fermi-Dirac and Bose-Einstein distributions, but as the lattice QCD calculations indicate, the system is a strongly interacting one and thus, non-ideal corrections have to be taken into account. The reduction of the effective degrees of freedom at high temperatures could suppress early-time photons with underdeveloped anisotropy and could enhance v_2.

I discuss the effects of the interaction corrections in the parton phase-space distributions on heavy-ion photons based on a quasi-particle parametrization, as the QGP photon emission rate is often given as a functional of distribution functions. The effective one-particle distribution can be expressed as

$$f^i_{\rm eff} = (e^{\omega_i/T} \pm 1)^{-1}, \tag{1}$$

and the partition function, in the logarithmic form as,

$$\ln Z_i = \pm V \int \frac{g_i d^3p}{(2\pi)^3} \ln\left(1 \pm e^{-\omega_i/T}\right) - \frac{V}{T}\Phi_i(T), \tag{2}$$

where $\omega_i = \sqrt{p^2 + m_i^2} + W^i_{\rm eff}$ is the effective energy and Φ_i is the background contribution required for and determined by the thermodynamic consistency condition[1]. Then the standard thermodynamic relations yield the energy density and pressure as $e = (T^2/V)\sum_i(\partial \ln Z_i/\partial T)$ and $P = (1/V)\sum_i T \ln Z_i$, respectively.

Here, I determine the effective interaction contribution $W^i_{\rm eff}$ for the quasi-particle model to reproduce the thermodynamic quantities calculated by lattice QCD[2] assuming it is temperature dependent. For simplicity and for the lack of constraints, $W_{\rm eff}$ is assumed to be common for all partons.

The QGP photon emission rate is expressed as[3],

$$E\frac{dR}{d^3p} = \frac{5\alpha\alpha_s}{9\pi^2} T^2 e^{-E/T} \lambda^2 \left\{ \left[\log\left(\frac{4ET}{k_c^2}\right) + \frac{1}{2} - \gamma \right] \right.$$

† Condensed from the article in Phys. Rev. C **92**, 014905 (2015)

*1 RIKEN Nishina Center

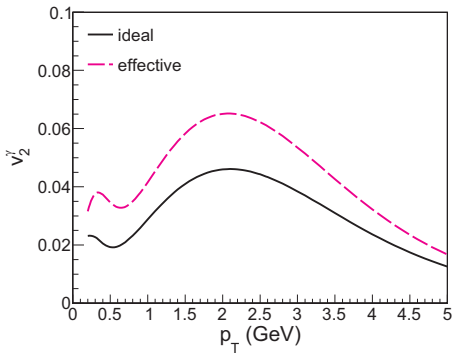

Fig. 1. (Color online) Thermal photon v_2 with ideal (solid line) and effective distributions (dashed line).

$$\left. + \left[\log\left(\frac{4ET}{k_c^2}\right) - 1 - \gamma \right] \right\}, \tag{3}$$

where $\lambda = e^{-W_{\rm eff}/T}$ is the effective fugacity, γ is Euler's constant, and k_c is the infra-red cut-off.

I estimate thermal photon elliptic flow numerically by using the same equation of state in the quasi-particle and hydrodynamic models. A Monte Carlo Glauber model is employed to simulate the initial conditions. The elliptic flow is defined as

$$v_2^\gamma(p_T, y) = \frac{\int_0^{2\pi} d\phi_p \cos(2\phi_p - \Psi) \frac{dN^\gamma}{d\phi_p p_T dp_T dy}}{\int_0^{2\pi} d\phi_p \frac{dN^\gamma}{d\phi_p p_T dp_T dy}}. \tag{4}$$

Figure 1 shows the thermal photon v_2 with ideal and effective distributions for Au-Au collisions at $\sqrt{s_{NN}} =$ 200 GeV with the impact parameter $b = 6$ fm. One can see that v_2 is enhanced in the presence of the effective interactions. This is owing to the suppression of the photons emitted from the medium with underdeveloped momentum anisotropy. This mechanism also leads to reduction in the photon yields and enhancement of higher order flow harmonics.

To conclude, effective parton distributions are constructed so that the thermal emission is consistent with the lattice QCD equation of state. The decreased degrees of freedom in the QGP phase lead to enhancement of thermal photon v_2, which contributes positively to the resolution of the photon puzzle. Future prospects include application of the effective distribution to the derivation of hydrodynamic equations.

References

1) T. S. Biro, A. A. Shanenko, V. D. Toneev, Phys. Atom. Nucl. **66**, 982 (2003).
2) S. Borsanyi *et al.*,Phys. Lett. B **730**, 99 (2014).
3) M. Strickland, Phys. Lett. B **331**, 245 (1994).

$\Lambda_b \to p\,\ell^-\,\bar{\nu}_\ell$ and $\Lambda_b \to \Lambda_c\,\ell^-\,\bar{\nu}_\ell$ form factors from lattice QCD with relativistic heavy quarks†

S. Meinel,[*1,*2] W. Detmold,[*3] and C. Lehner[*4]

The smallest and most uncertain element of the Cabibbo-Kobayashi-Maskawa (CKM) quark mixing matrix is V_{ub}. Improved measurements of $|V_{ub}|$ are important because they constrain the length of the left side of the $(\bar{\rho}, \bar{\eta})$ unitarity triangle, which lies opposite the precisely known angle β[1]. The matrix element $|V_{cb}|$ also plays a central role in flavor physics, as it normalizes the unitarity triangle and is the dominant source of uncertainty in Standard-Model predictions of the kaon CP-violation parameter ε_K[2].

Until recently, all direct determinations of $|V_{ub}|$ and $|V_{cb}|$ were performed using measurements of B meson semileptonic or leptonic decays at e^+e^- colliders. For both $|V_{ub}|$ and $|V_{cb}|$, there are tensions between the most precise extractions from exclusive and inclusive semileptonic B decays; the 2014 Review of Particle Physics lists[1]

$$\begin{aligned} |V_{ub}|_{\text{excl.}} &= (3.28 \pm 0.29) \times 10^{-3}, \\ |V_{ub}|_{\text{incl.}} &= (4.41 \pm 0.15^{+0.15}_{-0.17}) \times 10^{-3}, \\ |V_{cb}|_{\text{excl.}} &= (39.5 \pm 0.8) \times 10^{-3}, \\ |V_{cb}|_{\text{incl.}} &= (42.2 \pm 0.7) \times 10^{-3}. \end{aligned}$$

The Large Hadron Collider allows new determinations of $|V_{ub}|$ and $|V_{cb}|$ using the baryonic decays $\Lambda_b \to p\,\mu^-\bar{\nu}_\mu$ and $\Lambda_b \to \Lambda_c\,\mu^-\bar{\nu}_\mu$, provided that the relevant $\Lambda_b \to p$ and $\Lambda_b \to \Lambda_c$ hadronic form factors can be calculated. In this work, we performed a precise lattice QCD calculation of these form factors, utilizing lattice gauge-field ensembles generated by the RBC and UKQCD Collaborations. Using our form factor results, we can predict the $\Lambda_b \to p\,\mu^-\bar{\nu}_\mu$ and $\Lambda_b \to \Lambda_c\,\mu^-\bar{\nu}_\mu$ differential decay rates as functions of $|V_{ub}|^2$ and $|V_{cb}|^2$, as shown in Fig. 1. The LHCb Collaboration has recently measured the following ratio of the partially integrated decay rates[3],

$$\frac{\int_{15\ \text{GeV}^2}^{q^2_{\max}} \frac{\mathrm{d}\Gamma(\Lambda_b \to p\,\mu^-\bar{\nu}_\mu)}{\mathrm{d}q^2}\mathrm{d}q^2}{\int_{7\ \text{GeV}^2}^{q^2_{\max}} \frac{\mathrm{d}\Gamma(\Lambda_b \to \Lambda_c\,\mu^-\bar{\nu}_\mu)}{\mathrm{d}q^2}\mathrm{d}q^2} = (1.00 \pm 0.09) \times 10^{-2},$$

where the q^2-ranges were chosen to cover the region of the smallest uncertainties in our lattice QCD predictions. The combination of the LHCb measurement with our calculation gives

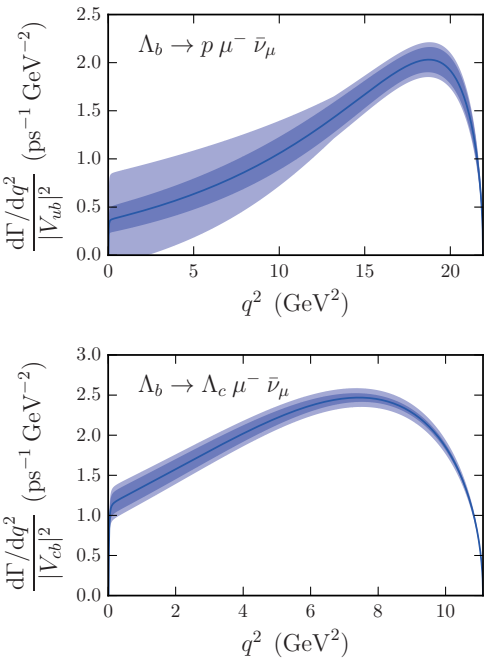

Fig. 1. Lattice QCD predictions for the $\Lambda_b \to p\,\mu^-\bar{\nu}_\mu$ and $\Lambda_b \to \Lambda_c\,\mu^-\bar{\nu}_\mu$ differential decay rates. The bands indicate the statistical-only and the total uncertainties.

$$\frac{|V_{ub}|}{|V_{cb}|} = 0.083 \pm 0.004(\text{expt}) \pm 0.004(\text{lattice}),$$

and, taking the 2014 PDG value for $|V_{cb}|$ from exclusive B decays,

$$|V_{ub}| = (3.27 \pm 0.23) \times 10^{-3}.$$

Because of the nonzero spin of the baryons, this analysis also provides important new constraints on possible right-handed currents beyond the Standard Model, whose existence had been suggested as an explanation of the exclusive-inclusive tension in $|V_{ub}|$[4]. The new measurement strongly disfavors this explanation [3], demonstrating that powerful complementary constraints on physics beyond the Standard Model can be derived from baryonic b decays.

References
1) K. A. Olive *et al.* [Particle Data Group], Chin. Phys. C **38**, 090001 (2014).
2) J. A. Bailey *et al.* [SWME Collaboration], Phys. Rev. D **92**, 034510 (2015).
3) R. Aaij *et al.* [LHCb Collaboration], Nature Phys. **11**, 743 (2015).
4) A. Crivellin, Phys. Rev. D **81**, 031301 (2010).

† Condensed from the article in Phys. Rev. D **92**, 034503 (2015)

*1 RIKEN Nishina Center
*2 Department of Physics, University of Arizona
*3 Center for Theoretical Physics, Massachusetts Institute of Technology
*4 Physics Department, Brookhaven National Laboratory

Development of carbon disk at the final stripping section

H. Hasebe,[*1] H. Okuno,[*1] H. Kuboki,[*1] H. Imao,[*1] N. Fukunishi,[*1] M. Kase,[*1] and O. Kamigaito[*1]

The rotating disk stripper at the final stripping section has played a significant role especially in providing a high-intensity and stable U beam since 2012, owing to the discovery of the Be disk[1,2,3,4]. However, the heat load caused by the increasing beam intensity led to the deformation of the Be disk after a short irradiation period. We needed to look for other candidates to replace the Be disk.

In the autumn of 2014, we attempted to polish a glassy carbon (GC) disk using the polishing technology applied for the Be disk. The GC disk has good properties of high heat resistance, high mechanical strength, and fine-grained structure. This GC disk (model number F-22) had a density of 1.93 g·cm^{-3}. The thickness of the disk for operation was 0.085 mm, which was reduced from a 1-mm-thick disk by diamond polishing. Tanken Seal Seiko Co. LTD[5] provided the disk material and machining was carried out by Crystal Optics Inc[6].

Around the same time, a highly oriented graphite sheet (GS) fabricated by Kaneka Corporation[7] was tested as a stripping material. They provided a sample of GS with a thickness of 0.035 mm (7.1 mg·cm^{-2}) with a density of 2.0 g·cm^{-3}. This GS was made from a polymer sheet under high-temperature and high-pressurized conditions. A prominent feature was the high thermal conductivity of 1500 W·m^{-1}·K^{-1} in the plane direction. In addition, the GS had a high thermal diffusivity of 9.0 cm^{2}·s^{-1}, which was greater than copper or aluminum. Therefore, the rise in temperature at the beam spot position was suppressed. Besides that, the non uniformity in the thickness was half of the Be disk. The GS was mechanically strong and could be handled easily using scissors or a cutter knife. The GS was stacked as two layers to make a 0.07-mm-thick disk and was cut with an outer diameter of 110 mm.

In October 2014, we tested these two new disks (GC and GS) with the U beam. The charge distributions of the GC and GS disks were almost the same as the Be disk (Fig. 1.). The beam profiles downstream of the stripping section were also the same as the Be disk, which indicated that both disks were applicable for beam operation instead of the Be disk.

We successfully obtained two types of carbon disks, and the GS disk was used for the U beam from March to May[8], and it was used again from October to November in 2015. A total of 2.19×10^{18} U particles with a maximum intensity of 17.5 eμA were irradiated on the GS disk. The heat load maximally became 240 W. This total amount of the irradiated U particles was twice the amount of the Be disk when its lifetime was over. Nevertheless, the GS disk was still usable. Figure 2 shows the photograph of (a) the new GS disk and (b) the disk after usage. No change in the appearance was observed except for a slight color change and deformation. It is evident that the GS disk has high durability.

The GS disk has shown the greatest performance and longest lifetime compared to all disks so far. The GS can be applied for multilayer disks with variable thickness. It is useful for the acceleration of other ion beams. The three-layer GS disk was already used for the krypton beam operation, and it successfully worked. The problem in the final stripping section was solved.

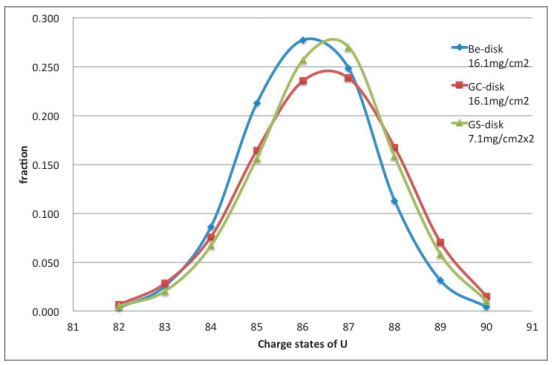

Fig. 1. Charge distributions of Be-, GC-, and GS-disks.

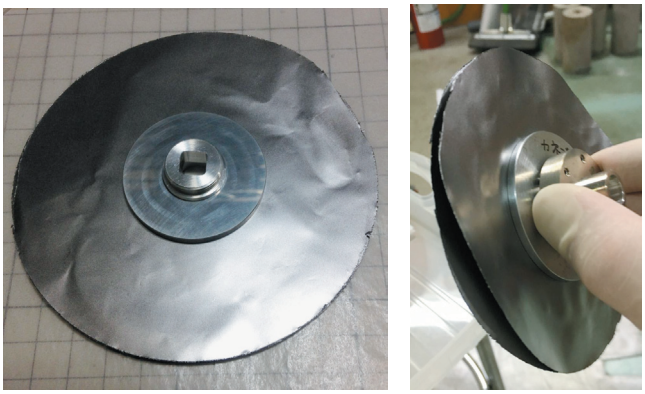

(a) (b)

Fig. 2. (a) New GS disk and (b) the disk after usage (slightly deformed).

References

1) H. Ryuto et al., Nucl. Instr. Meth. A **569**, 697 (2008).
2) H. Hasebe et al., RIKEN Accel. Prog. Rep. **46**, 133 (2013).
3) H. Hasebe et al., RIKEN Accel. Prog. Rep. **47**, 144 (2014).
4) H. Hasebe et al., RIKEN Accel. Prog. Rep. **48**, 190 (2015).
5) Kaneka Corporation
http://www.elecdiv.kaneka.co.jp/english/index.html
6) Tanken Seal Seiko Co. LTD
http://www.tankenseal.co.jp/other/english.html
7) Crystal Optics Inc
http://www.crystal-opt.co.jp/global/
8) H. Hasebe et al., HIAT2015. MOA1C01 (2015).

*1 RIKEN Nishina Center

Development of Particle identification method of high-intensity secondary beams at BigRIPS

S. Ota,[*1] J. Zenihiro,[*2] H. Takeda,[*2] S. Michimasa,[*1] M. Dozono,[*1] M. Matsushita,[*1] K. Kisamori,[*1] M. Kobayashi,[*1] Y.N. Watanabe,[*3] Y. Kiyokawa,[*1] Y. Yamaguchi,[*1] S. Masuoka,[*1] S. Shimoura,[*1] K. Yako,[*1] N. Imai,[*1] H. Baba,[*2] T. Kubo,[*2] K. Yoshida,[*2] N. Inabe,[*2] N. Fukuda,[*2] H. Suzuki,[*2] D.S. Ahn,[*2] D. Murai,[*2] H. Sato,[*2] Y. Sato,[*2] H. Otsu,[*2] and T. Uesaka[*2]

Recent development of accelerators enables us to utilize high-intensity primary beams and resultant high-intensity secondary beams at RIBF. Available intensity of the secondary beam becomes more than 10^5 cps at BigRIPS. However, when we apply the standard particle identification method of TOF-$B\rho$-ΔE for such high-intensity beams, in particular around Z=50 beams, two problems arise.

One serious problem is that the resolution of ΔE becomes worse due to the pile up of the slow signal from the ionization chamber, thereby reducing the resolution of atomic number. The other problem is the radiation damage of plastic scintillators that are used to measure the TOF. In addition to these problems, the PPAC had larger discharge probability with the high-intensity beams than that with the low-intensity beams. In this paper, we report a new particle identification method using detectors with high radiation hardness and fast time response at BigRIPS, in order to resolve this problem and identify the high-intensity secondary beams.

We propose the new particle identification method of TOF-$B\rho$-$B\rho$, where ΔE is not measured directly. An energy degrader is placed at the dispersive second focus (F5) and the energy loss at the degrader is indirectly used for the extraction of atomic number. Assuming that mass number and charge do not change at the degrader, the energy loss at F5 is expressed by $\Delta E = (\gamma_{35}-1)Am_u - (\gamma_{57}-1)Am_u = cZ(\frac{B\rho_{35}}{\beta_{35}} - \frac{B\rho_{57}}{\beta_{57}})$. Combining this expression with the Bethe-Bloch formula for the energy loss, $\Delta E \sim d\frac{Z^2}{\beta_{35}^2}$, where d is the thickness of the degrader, and assuming that the ion is fully stripped, namely $Q = Z$, the atomic number can be obtained as,

$$Z = C(\frac{B\rho_{35}}{\beta_{35}} - \frac{B\rho_{57}}{\beta_{57}})\frac{\beta_{35}^2}{d}. \quad (1)$$

In order to overcome the difficulty of radiation damage and discharge, plastic scintillators and PPACs are replaced with diamond detectors[1] and low-pressure multi-wire drift chambers[2] (LP-MWDC), respectively.

The test experiment was performed using a ^{132}Sn beam at incident energies of 100 and 200 MeV/u. The typical intensity was 1×10^6 cps and the maximum intensity was 3.4×10^6 cps. Figure 1 shows the correlation between the atomic numbers deduced using the new method and the standard method, which are shown by the horizontal and vertical axes, respectively. There is a clear correspondence of two values, which validates that the new method extracts the correct atomic number. Figure 2(a) shows the plot for particle identification with a low-intensity beam (less than 10^3 cps). Vertical and horizontal axes show the atomic number and mass-to-charge ratio, respectively. Figure 2(b) shows the same plot with the high-intensity beams (about 10^6 cps). Efficiency seems worse for the high-intensity beams, which may be caused by wrong position deduction of LP-MWDC, which will be recovered by further analysis.

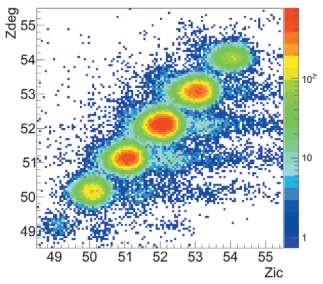

Fig. 1.: Correlation between the atomic numbers deduced using the new method (Zdeg) and the standard method (Zic).

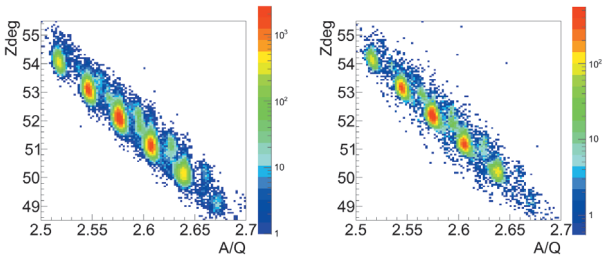

(a) 10^4 cps. (b) 10^6 cps.

Fig. 2.: Correlation between the atomic number and the mass-to-charge ratio.

[*1] Center for Nuclear Study, The University of Tokyo
[*2] RIKEN Nishina Center
[*3] Department of Physics, The University of Tokyo

References
1) S. Michimasa *et al.*, Nucl. Instrum. Meth. **B**317 (2013) 710.
2) H. Miya *et al.*, Nucl. Instrum. Meth. **B**317 (2013) 701.

The first on-line commissioning study on parasitic production of low-energy RI-beam system(PALIS) at BigRIPS

T. Sonoda,[*1] M. Wada,[*1] M. Reponen,[*1] I. Katayama,[*1] T.M. Kojima,[*1] H. Iimura,[*2] A. Deuk Soon,[*1] N. Fukuda,[*1] T. Kubo,[*1] K. Kusaka,[*1] N. Inabe,[*1] Y. Shimizu,[*1] T. Sumikama,[*1] H. Suzuki,[*1] H. Takeda,[*1] M. Wakasugi,[*1] Y. Yanagisawa,[*1] K. Yoshida,[*1] Y. Hirayama,[*3] D. Matsui,[*4] H. Miyatake,[*3] V. Sonnenschein,[*4] S. Takamatsu,[*4] H. Tomita,[*4] Y.X. Watanabe,[*3] F. Arai,[*1] S. Arai,[*1] N. Imai,[*5] Y. Ito,[*1] K. Okada,[*6] P. Schury,[*3] H. Wollnik,[*7] and ImPACT Collaboration

The first on-line commissioning study for the parasitic production of low-energy RI-beam system(PALIS) [1,2] was performed. The beam time was dedicated for 0.5 day and also in a parasitic manner during ImPACT experiment. We confirmed the feasibility of the parasitic experiment in actual BigRIPS beam time. We observed the beta-rays from radioactive decay of RIs, which were extracted from the gas cell after deceleration and thermalization in a gas.

By installing a small gas cell immediately in front of the second focal plane (F2) slit in BigRIPS, the restoration of unused RI-beams is implemented. Thus unused beams in flight with a main beam consist of isotonic chains of nuclei arrived at the right and left slit plates in F2, which are symmetrical with respect to the main beam. The PALIS gas cell can move on the bilateral side by crossing the main beam. We investigated the interference on the transmission of the main beam by varying the gas cell position as shown in Fig. 1. The main beam was ^{79}Se with 200 MeV/u and the yield was counted at the downstream plastic scintillator located in the third focal plane chamber (F3) in BigRIPS. We confirmed that there is no interruption on the main beam passage, unless the gas cell stays in the beam central axis within ± 15 mm.

A simple RIs extraction test was also done. The Cu isotope beams, which are mainly $^{66-69}$Cu, produced by in-flight fission were implanted into the gas cell. The beams were first decelerated by a degrader, where the energy was reduced from around 280 MeV/u to 10 MeV/u, and then thermalized in the gas cell. The stopped RIs were transported by a gas flow to the exit hole. A small plastic scintillator installed at the outlet of the gas cell exit hole detected the radiation by decay of extracted RIs. In order to avoid background, the BigRIPS beam was stopped during the measurement. Through the obtained decay curve as shown in Fig. 2, we confirmed that 10% of ^{66,68,69}Cu isotopes were extracted against the total number of those implanted isotopes.

In the next on-line commissioning study, we plan to produce single charged low-energy RI-beams by the resonant laser ionization/IGISOL method and to identify as the individual isotopic beam.

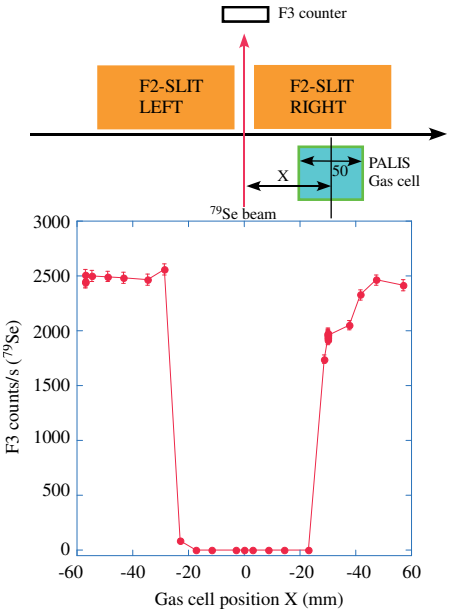

Fig. 1. Interference on the transmission of main beam by varying the gas cell position.

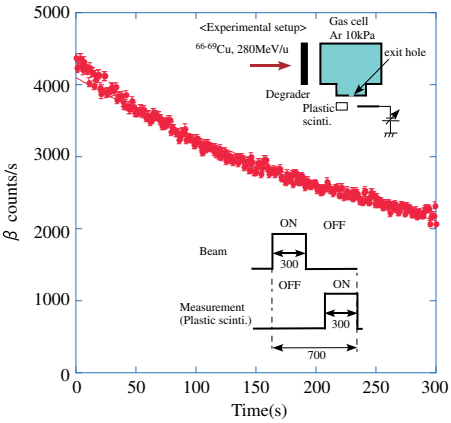

Fig. 2. Beta ray counts of the extracted RIs.

*1 RIKEN Nishina Center
*2 Japan Atomic Energy Agency
*3 High Energy Accelerator Research Organization (KEK)
*4 Faculty of Engering, Nagoya University
*5 Center for Nuclear Study, the University of Tokyo
*6 Department of Physics, Sophia University
*7 New Mexico State University

References

1) T. Sonoda *et al.*, AIP Conf. Proc. **1104** (2009) 132.
2) T. Sonoda *et al.*, Nucl. Inst. and Meth. B**295** (2013)1.

NeuLAND demonstrator at SAMURAI: commissioning and efficiency studies

J. Kahlbow,[*1,*2] T. Aumann,[*1] K. Boretzky,[*3,*2] I. Gašparić,[*4,*2] Y. Kondo,[*5,*2] T. Nakamura,[*5,*2] H. Otsu,[*2] H. Simon,[*3] Y. Togano,[*5,*2] H. Törnqvist,[*1,*2] T. Uesaka,[*2] and the NeuLAND-SAMURAI Collaboration

NeuLAND (New Large-Area Neutron Detector) is the new neutron detector being developed for the R^{3}B setup (Reactions with Relativistic Radioactive Beams) at FAIR, Germany. This time-of-flight spectrometer is designed to have an invariant-mass resolution of $\Delta E < 20$ keV at 100 keV above the neutron threshold[1)] and identify six coincident neutrons.

This high-granularity detector will consist of 3000 single plastic-scintillator bars organised in 30 modular double-planes, each assembled out of 50 horizontal and 50 vertical scintillator bars of $5 \times 5 \times 250$ cm^3.

In January 2015, the first four double-planes of NeuLAND – the so-called demonstrator – were shipped from GSI in Germany to the RIBF in Japan. By adding NeuLAND to the neutron detection system NEBULA at SAMURAI, the multi-neutron detection efficiency and position resolution of the system are improved significantly. This allows for measurement of 3- and 4-neutron-unbound nuclear systems with good statistics, as conducted in autumn 2015 with the spectroscopy of unbound neutron-rich oxygen isotopes[2)].

During the autumn campaign, the performance of the 400 single NeuLAND modules for fast neutrons at SAMURAI was studied in a one-day machine-study experiment using quasi-monoenergetic neutrons from the ^{7}Li(p,n)^{7}Be reaction. The aim was to extract the one-neutron detection efficiency, study the detector response of NeuLAND and NEBULA at 110 MeV and 250 MeV, and establish a method to separate multi-neutron events with the help of simulations.

In this experiment, NeuLAND was placed 10.87 m downstream from the target at zero degrees. The two NEBULA sub-detectors were located behind it. In front of NeuLAND, a layer of eight 1 cm thin plastic scintillators was placed to veto charged-particle events. The 800 NeuLAND PMT channels were read out with TacQuila electronics developed at GSI, which include QDC, TDC, and trigger multiplexer boards.

To determine the one-neutron detection efficiency of the NeuLAND demonstrator at 110 MeV and 250 MeV, the neutrons from ^{7}Li(p,n)^{7}Be(g. s. + 430 keV) were measured. In this charge-exchange reaction, almost monoenergetic neutrons were produced, as either the ^{7}Be ground state or excited state at 430 keV is directly populated. These neutrons were emitted in the forward direction and detected by NeuLAND, whereas the unreacted protons were bent in the SAMURAI dipole magnet.

The secondary proton beam was produced by the fragmentation of a ^{48}Ca primary beam at 345 MeV/nucleon and impinged on the 1.05 g/cm^2 thick natural Li target. The incident proton-beam rate was about 1 MHz and the reaction trigger rate (NeuLAND×Beam) about 1.5 kHz. The beam spot was determined by two plastic-scintillator veto-counters with a hole diameter of 3 cm.

In order to identify one-neutron events in NeuLAND, the neutron velocity spectrum, shown in Fig. 1, is considered. The peak marked by the fitted curve is associated with the response to quasi-monoenergetic neutrons; the continuum is mainly caused by neutrons from other break-up reactions.
The mean time resolution obtained from cosmic-ray data for horizontal bars is $\sigma_t = 118(18)$ ps with an energy cut $E > 5$ MeVee, a high multiplicity condition, and a horizontal position $|x| < 50$ cm.

The final results from this calibration measurement with high-energy monoenergetic neutrons will allow the precise determination of cross sections in measurements using NeuLAND at SAMURAI.

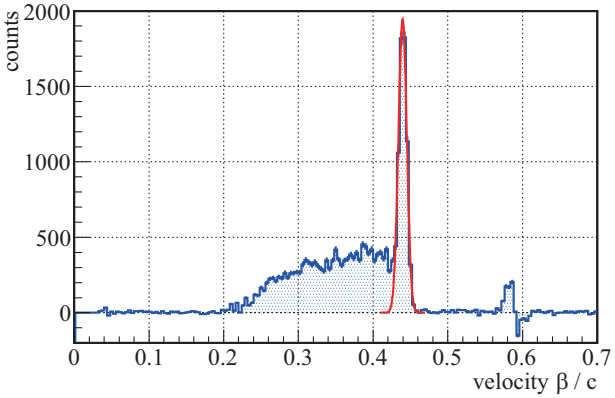

Fig. 1. Preliminary experimental velocity spectrum of NeuLAND for ∼ 110 MeV neutrons with veto condition on charged particles, background subtraction, spatial cut, and an energy cut $E > 5$ MeVee. The background was evaluated with an empty-target run. The integral under the red curve indicates the neutron events.

*1 Institut für Kernphysik, TU Darmstadt
*2 RIKEN Nishina Center
*3 GSI Helmholtzzentrum für Schwerionenforschung, Darmstadt
*4 Ruder Bošković Institute, Zagreb
*5 Department of Physics, Tokyo Institute of Technology

References
1) NeuLAND Technical Design Report, http://www.fair-center.eu/fileadmin/fair/experiments/NUSTAR/Pdf/TDRs/NeuLAND-TDR-Web.pdf, accessed: 2016/01/21.
2) Y. Kondo et al., In this report.

Beam commissioning of the rare-RI ring

Y. Yamaguchi,[*1] Y. Abe,[*1] D. Nagae,[*1] F. Suzaki,[*1,*2] H. Miura,[*2] S. Ohmika,[*2] S. Naimi,[*1] Z. Ge,[*2] T. Yamaguchi,[*2] A. Ozawa,[*3] S. Suzuki,[*3] Y. Yanagisawa,[*1] H. Suzuki,[*1] H. Baba,[*1] S. Michimasa,[*4] S. Ota,[*4] T. Uesaka,[*1] M. Wakasugi,[*1] T. Watanabe,[*1] Y. Yano,[*1] and Rare-RI Ring Collaborators

We conducted two test experiments of the rare-RI ring in 2015. The first experiment using a ^{78}Kr primary beam with an energy of 168 MeV/u was performed in June. At that time, we succeeded in injecting a particle, which was randomly produced from a DC beam from cyclotrons, into the ring individually with a fast kicker system[1]; we extracted the particle from the ring less than 1 ms after the injection[2]. We also checked the periodic signals of the circulated particle in the ring by using a carbon-foil with an MCP detector[3]. We measured the Time-Of-Flight (TOF) of the particles between the entrance and the exit of the ring to check the isochronism. By adjusting the first-order isochronous magnetic field using trim-coils, which were installed into the dipole magnets of the ring, the isochronism of around 10-ppm was achieved for the momentum spread of $\pm 0.2\%$[4]. In addition, we confirmed that a resonance-type Schottky pick-up successfully acquired the revolution frequency information of one particle with a resolution of approximately 1.3×10^{-6} in a storage mode[5].

The second experiment was performed in December by using a secondary beam to verify the principle of mass determination using the following equation.

$$\frac{m_1}{q} = (\frac{m_0}{q})\frac{T_1}{T_0}\sqrt{\frac{1-\beta_1^2}{1-(\frac{T_1}{T_0}\beta_1)^2}}, \quad (1)$$

where $m_{0,1}/q$ is the mass-to-charge ratio of the reference and interested particles, $T_{0,1}$ is revolution time of these particles, $\beta_1 = v/c$, v is the velocity of the interested particles, and c is the light velocity. The secondary beam was produced via the projectile fragmentation of a 345 MeV/u ^{48}Ca primary beam with a ^{9}Be target. We identified the isotopes before the F3 achromatic focus of BigRIPS, and we injected particles to the ring individually with the fast kicker system. Figure 1 (a) shows the timing signal of the detected particles using a plastic scintillation counter, which was installed on the central orbit of the ring at the next straight section of the kicker area. We confirmed that these particles are ^{36}Ar and ^{35}Cl by using the ΔE-TOF information eventually, as shown in Fig. 1 (b). After removing the plastic scintillation counter from the central orbit of the ring, we checked the periodic signals of these two types of particles by using the carbon-foil with the MCP detector[3]. Finally we succeeded in extracting these particles from the ring simultaneously. Figure 2 shows the result of the TOF between the plastic scintillation counter at S0 of SHARAQ and the plastic scintillation counter at the exit area of the ring.

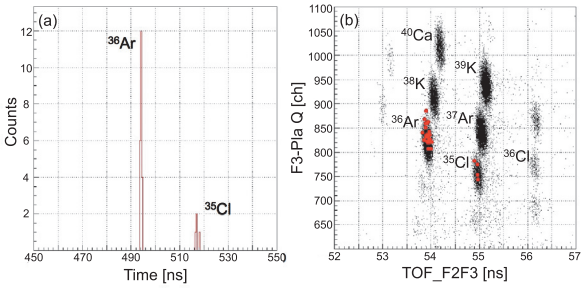

Fig. 1. (a) Timing signal of the detected particles at the plastic scintillation counter after injection by kicker magnets. (b) Two-dimensional for particle identification before the F3 of BigRIPS. The red circle indicates the injected particles.

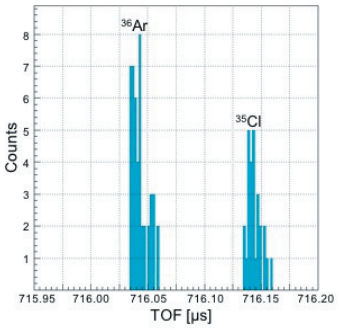

Fig. 2. Spectrum of TOF between the plastic scintillation counter at S0 of SHARAQ and the plastic scintillation counter at the exit area of R3 is shown. The peak on the left side indicates extracted ^{36}Ar, whereas the peak on the right side indicates extracted ^{35}Cl.

Offline analysis is now in progress to determine the revolution time ($T_{0,1}$) and the β_1 values, which will allow the discussion of mass determination using equation (1).

*1 RIKEN Nishina Center
*2 Department of Physics, Saitama University
*3 Institute of Physics, University of Tsukuba
*4 Center for Nuclear Study, University of Tokyo

References
1) Y. Yamaguchi et al.: Phys. Scr. T166 (2015) 014056.
2) H. Miura et al.: In this report.
3) D. Nagae et al.: In this report.
4) Y. Abe et al.: In this report.
5) F. Suzaki et al.: In this report.

Measurement of isochronism using ^{78}Kr beam for the Rare RI Ring

Y. Abe,[*1] Y. Yamaguchi,[*1] M. Wakasugi,[*1] T. Uesaka,[*1] S. Ohmika,[*3] A. Ozawa,[*2] Z. Ge,[*1,*3] F. Suzaki,[*1,*3] S. Naimi,[*1] D. Nagae,[*1] H. Miura,[*3] T. Yamaguchi[*3] and for the Rare RI Ring collaboration

We constructed a new storage ring based on the isochronous mass spectroscopy technique, named the "Rare RI Ring," to measure the masses of rare nuclei with high precision.[1)] An offline machine study using an α-source (^{241}Am) was performed last year. In the offline machine study, we succeeded in tuning the first-order isochronous field using trim coils.[2)]

In June 2015, the first beam commissioning of the Rare RI Ring was performed, where a ^{78}Kr beam at 345 MeV/nucleon was used. To perform an individual injection using a self-trigger signal from F3, the energy of ^{78}Kr beam was degraded to 168 MeV/nucleon by using a degrader.

First, we transported the beam to the ring with a dispersion matching at the center of kicker magnets in accordance with the optical calculations.[3)] After that, we injected ^{78}Kr particles individually using the fast-kicker system.[4)] After the individual injection was successful, we confirmed whether the particle was stored. We confirmed the periodic signals of the circulated particle through a foil detector, which was located on the closed orbit of the ring.[5)] Once the storage was confirmed, the extraction was performed. After removing the foil detector from the closed orbit, we succeeded in extracting the particles from the ring after about 700 μs.

Figure 1 shows the TOF of ^{78}Kr particles as a function of the momentum spread with different values of the radial gradient of the magnetic field $(\partial B/\partial r)/B_0$ and results of fitting with a quadratic function. From the fitting results, we found that the isochronous condition was changed according to the value of $(\partial B/\partial r)/B_0$. Furthermore, to evaluate the isochronism of the ring, the width of the TOF spectrum was extracted. Since the spectrum has a long tail due to higher-order isochronous field contributions in the ring, we fitted the spectrum using a Gaussian function with an exponential tail to evaluate the width that included the tail. Figure 2 shows the TOF spectrum and the result of fitting in the case of $(\partial B/\partial r)/B_0 = 0.279$ m^{-1}. The TOF width of $(\partial B/\partial r)/B_0 = 0.279$ m^{-1} was obtained about 12 ns in FWHM. Therefore, we found that the degree of isochronism achieved is about 1.9×10^{-5}. Thus, we were able to achieve a 10-ppm isochronism by adjusting the first-order isochronous field. Furthermore, we found that the optimum value would be slightly larger than 0.279 m^{-1} from these results.

*1 RIKEN Nishina Center
*2 Institute of Physics, University of Tsukuba
*3 Department of Physics, Saitama University

Since we succeeded in the first beam commissioning using a primary beam, we performed an experiment using a secondary beam in December 2015. In this experiment, we succeeded in extracting two kinds of RI produced from ^{48}Ca.[6)] In the near future, the Rare RI Ring will be able to measure the masses of exotic nuclei, which will have a significant impact on the understanding of the r-process.

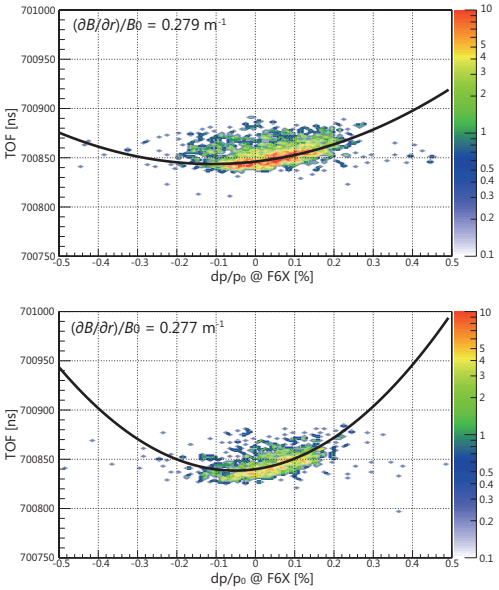

Fig. 1. TOF spectra as a function of the momentum spread with different values of the radial gradient of the magnetic field $(\partial B/\partial r)/B_0$. The solid lines show the results of fitting with a quadratic function.

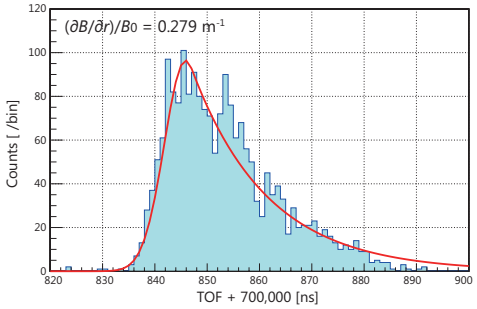

Fig. 2. TOF spectrum and the result of fitting using a Gaussian function with an exponential tail.

References

1) Y. Yamaguchi et al.: RIKEN Accel. Prog. Rep. **46** xiv (2013).
2) Y. Abe et al.: RIKEN Accel. Prog. Rep. **48** 24 (2015).
3) Z. Ge et al.: In this report.
4) H. Miura et al.: In this report.
5) D. Nagae et al.: In this report.
6) Y. Yamaguchi et al.: In this report.

Possible muonic radical formation in cytochrome *c*

Y. Sugawara,[*1] I. Yanagihara,[*1] A. D. Pant,[*2] T. Fujimaki,[*3] I. Shiraki,[*3] M. Kusunoki,[*3] H. Ariga,[*4] W. Higemoto,[*5] K. Shimomura,[*2] K. Ishida,[*6] F. Pratt,[*7] E. Torikai,[*3] and K. Nagamine[*2, *8, *9]

The electron-transfer process plays important roles in the photosynthetic electron transfer chain in chlorophylls and the respiratory chain in mitochondria. Two of the authors of this work (KN and ET) have previously successfully measured μSR spectra of hemoprotein of cytochrome *c* and DNA.[1)] The major parts of μSR spectra were found to follow the Risch-Kehr (R-K) function, $G(t) = \exp(\Gamma t)\mathrm{erfc}(\Gamma t)^{1/2}$, where Γ is the relaxation parameter.[2)] Longitudinal magnetic field dependence of Γ reflects the behavior of the electron brought by the muon.[1-3)] Motivated by these situations, we have been examining μSR spectra of cytochrome *c*, which is one of the members of the respiratory chain in mitochondria.[4)]

It was found that some fractions of the μSR amplitude can be attributed to the muonic radical formation on the basis of an avoided level crossing resonance in the longitudinal field dependence data, the results of which are reported herein.

The μSR measurements of oxidized cytochrome *c* of horse heart (water content was less than 5 % w/w) were carried out at RIKEN-RAL and J-PARC MUSE. The B_{ext} dependence of the relaxation data were analyzed by Lorentzian function.

The longitudinal field dependence of the initial and the baseline asymmetries and relaxation rates (λ) values are shown in Fig. 1a.

The λ became large at around 10 ~ 20 G. Some fractions of the μSR amplitude could be attributed to the muonic radical formation on the basis of an avoided level crossing resonance.

Similar experimental results had been obtained in the case of polyglycine.[5)] Judging from the structural analogy (Fig. 1b), the muonic radical would be formed at a carbonyl moiety of polypeptide bonds, which form the main chain of cytochrome *c*. We should pay attention to the following classification to consider the muon stopping sites and behavior of electrons brought by muons.

1. peptide bonds (-CO-NH-) and side chains of Gln and Asn (-CONH2)
2. side chains of Glu and Asp (-COO-)
3. aromatic side chains *i.e.* phenylalanine, tryptophan, tyrosine, and histidine
4. the porphyrin ring of the heme part.

When a part of the muons stopped at the moieties classified to 1 and 2, muonium radicals would be formed. On the other hand, when muons stopping at the moieties classified to 3 and 4, electrons which were brought by muons would delocalized and diffuse in proteins. Due to the latter contribution, the other fractions of μSR spectra would follow the R-K function.

Improved studies, both experimental and theoretical are in progress.

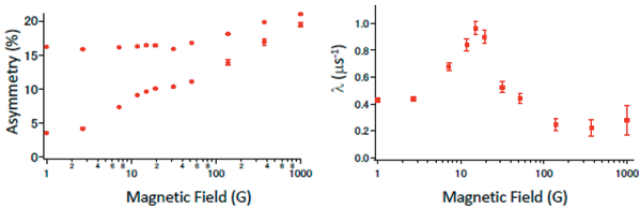

Fig. 1a Longitudinal field dependence of initial asymmetry and baseline asymmetry (left) and relaxation rate (right) of μ^+ in dry cytochrome c.

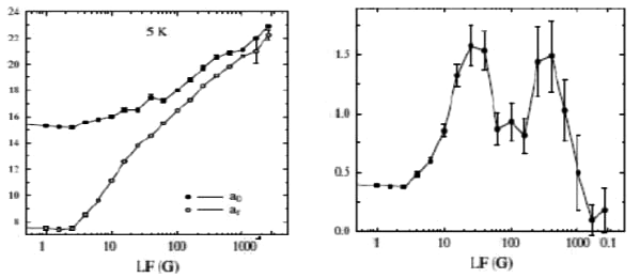

Fig. 1b Longitudinal field dependence of initial asymmetry and baseline asymmetry (left) and relaxation rate (right) of μ^+ in polyglycine.

References

1) K.Nagamine et al., Physica B. **631**, 289-290 (2000).
2) R. Risch and K.W. Kehr, Phys. Rev. B. **46**, 5246 (1992).
3) F.L. Pratt et al., Phys. Rev. Lett. **79**, 2855 (1997).
4) A.D. Pant et al., JPS Conf. Proc. **8**, 033007 (2015).
5) F.L. Pratt et al., (private communication).

*1 Graduate School of Science, Kitasato University
*2 Muon Science Laboratory, KEK-IMSS
*3 Int. Grad. School, University of Yamanashi
*4 Instute for Catalysis, Hokkaido University
*5 ASRC, Japan Atomic Energy Agency
*6 Advanced Meson Science Lab., RIKEN
*7 ISIS, Rutherford Appleton Laboratory
*8 Atomic Physics Laboratory, RIKEN
*9 Physics & Astronmy, UC Riverside

Development of a rapid solvent extraction apparatus for the aqueous chemistry of the heaviest elements

Y. Komori,[*1] H. Haba,[*1] K. Ooe,[*2] A. Toyoshima,[*3] A. Mitsukai,[*3] M. Murakami,[*1,*2] D. Sato,[*2] R. Motoyama,[*2] S. Yano,[*1] K. Watanabe,[*1] A. Sakaguchi,[*4] J. Inagaki,[*4] H. Kikunaga,[*5] and J. P. Omtvedt[*6]

To realize the aqueous chemistry studies of Sg (Z = 106) and heavier elements, we are developing a continuous and rapid solvent extraction apparatus coupled with the GARIS gas-jet system.[1)] This apparatus consists of a continuous dissolution apparatus called as Membrane DeGasser (MDG), Flow Solvent Extractor (FSE), and liquid scintillation detectors. In this work, we developed the MDG and FSE, and conducted online solvent extraction of Tc and Re as homologs of element 107, Bh.

We modified the MDG developed by a research group of Univ. Oslo and JAEA.[2)] Major modifications were to reduce a dead volume of the apparatus from 90 μL to 23 μL and to simplify the structure of the gas/solution-mixing unit to dissolve shorter-lived nuclides with higher efficiencies at a lower flow rate of 1 mL/min. Further, we fabricated the FSE that consisted of a Teflon capillary and a phase separator by referring to a well-known flow injection analysis technique.[3)] The inner diameter of the capillary is 0.5 mm. We can easily change the extraction time by varying the capillary length. In the phase separator, organic and aqueous phases are separated from each other with a PTFE membrane filter (ADVANTEC T300A013A) by applying pressure on the outlet of the capillary of the aqueous phase.

We investigated the performance of the MDG using the AVF cyclotron at RIKEN. Short-lived ^{90m,g}Nb ($T_{1/2}$ = 18.8 s, 14.6 h) and ^{178a}Ta ($T_{1/2}$ = 2.36 h) were simultaneously produced in the ^{nat}Zr(d,xn) and ^{nat}Hf(d,xn) reactions, respectively. The reaction products were transported by the He/KCl gas-jet system to the MDG in the chemistry laboratory. The reaction products were dissolved with 1 M HF at a flow rate of 1 mL/min. The solution from the MDG was collected for 1 min and was then subjected to γ-ray spectrometry with a Ge detector. The dissolution efficiencies were determined by comparing the radioactivity in the solution with that of the direct catch on a glass fiber filter (ADVANTEC GB-100R). Next, we coupled the MDG and the FSE and performed online solvent extraction of Tc and Re. ^{92,94m}Tc ($T_{1/2}$ = 4.25, 293 min) and ^{181}Re ($T_{1/2}$ = 20 h) produced simultaneously in the ^{nat}Mo(d,xn) and ^{nat}W(d,xn) reactions, respectively, were transported by the gas-jet to the MDG. They were continuously dissolved with 0.5 M and 1 M HNO_3, and they were extracted with the FSE into an organic phase of tri-*n*-octylamine (TOA) in toluene. Both aqueous and organic phases from the FSE were then subjected to the γ-ray spectrometry to determine the distribution ratios (D). We measured the D values of Tc and Re by varying the capillary length from 5 cm to 100 cm to change the extraction time. We also varied a concentration of TOA from 0.005 M to 0.1 M to evaluate an applicable D range with the FSE. These D values were compared with those in the batch extraction that were obtained by 3-min shaking.

The dissolution efficiencies of ^{90m}Nb, ^{90g}Nb, and ^{178a}Ta with the MDG were 56 ± 2, 88 ± 6, and 82 ± 7%, respectively. The efficiency of the short-lived ^{90m}Nb is smaller than those of the long-lived ^{90g}Nb and ^{178a}Ta. In the online solvent extraction with the MDG-FSE, a variation of the D values of Tc and Re is shown in Fig. 1 as a function of the capillary length. The extraction equilibrium of Tc and Re was attained with the 40-cm capillary. The time required for the solutions to pass through the 40-cm capillary is calculated as 2.4 s, which is sufficiently short to perform the solvent extraction with ^{265}Sg^{a,b} ($T_{1/2}$ = 8.5 s, 14.4 s)[4)] and ^{266}Bh ($T_{1/2}$ = 10.7 s).[5)] We also found that the D values of Tc and Re increase with increasing the TOA concentration. The D values with the MDG-FSE were consistent with those in the batch extraction except for Tc at a high TOA concentration of > 0.05 M, where the D values obtained for Tc with the MDG-FSE were slightly smaller than those in the batch extraction. The reason of this discrepancy is under consideration.

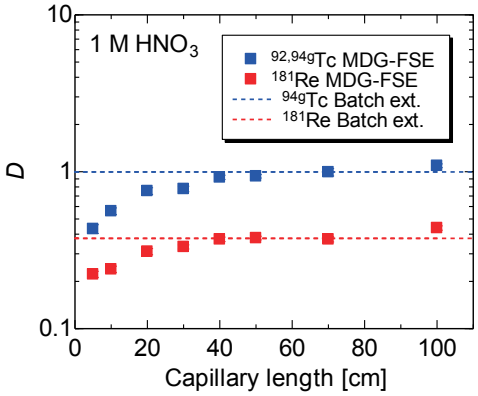

Fig. 1. Variation of the D values of Tc and Re as a function of the capillary length. The concentrations of HNO_3 and TOA are 1 M and 0.01 M, respectively.

*1 RIKEN Nishina Center
*2 Graduate school of Sci. and Technol., Niigata Univ.
*3 JAEA
*4 Univ. Tsukuba
*5 ELPH, Tohoku Univ.
*6 Univ. Oslo

References

1) H. Haba et al.: Chem. Lett. **38**, 426 (2009).
2) K. Ooe et al.: J. Radioanal. Nucl. Chem. **303**, 1317 (2015).
3) S. Motomizu: J. Flow Injection Anal. **5**, 71 (1988).
4) H. Haba et al.: Phys. Rev. C **85**, 024611 (2012).
5) H. Haba et al.: Pacifichem 2015, Honolulu, Hawaii, U.S.A., Dec. INOR 1578, 2015.

Production of ^{67}Cu using the ^{70}Zn(d,an)^{67}Cu reaction

S. Yano,[*1] H. Haba,[*1] S. Shibata,[*1] Y. Komori,[*1] K. Takahashi,[*1] Y. Wakitani,[*2] T. Yamada,[*2] and M. Matsumoto[*2]

Since 2007, we have distributed purified radioisotopes such as ^{65}Zn and ^{109}Cd prepared at the RIKEN AVF cyclotron for the purpose of contribution to society throughout industrial application of accelerator based- science.[1] Copper-67 (half-life $T_{1/2}$ = 61.83 h and β^--decay branch I_β- = 100%) is one of the promising radioisotopes for radiotherapy and radiodiagnosis.[2] Although several routes have been proposed for the production of ^{67}Cu, the high-energy proton-induced reaction of ^{68}Zn(p,$2p$)^{67}Cu has been used most often.[3] In this route, however, a large-scale cyclotron is required to accelerate protons up to ~ 100 MeV, and a large contamination of the radionuclidic impurity of ^{64}Cu is unavoidable in the ^{67}Cu product.[3] Further, the long-lived byproduct of ^{65}Zn ($T_{1/2}$ = 244.06 d) is also undesired in the recycle process of the enriched target material of ^{68}Zn. Thus, we plan to produce ^{67}Cu in the ^{70}Zn(d,αn)^{67}Cu reaction, where small amounts of ^{64}Cu and ^{65}Zn are produced.[4] In this work, for the future distribution of ^{67}Cu, we investigated a procedure to prepare purified ^{67}Cu in the ^{70}Zn(d,αn)^{67}Cu reaction at the AVF cyclotron.

In the ^{70}Zn(d,αn)^{67}Cu route, ^{67}Ga can be produced from Zn isotopes such as ^{66}Zn and ^{67}Zn, which are contained in small amounts in the enriched ^{70}Zn target. The γ-ray energies of ^{67}Ga are identical to those of ^{67}Cu, because ^{67}Ga and ^{67}Cu decay to the same excited levels of ^{67}Zn by EC- and β^--decay, respectively. In addition, the half-life of ^{67}Ga ($T_{1/2}$ = 3.26 d) is almost the same as that of ^{67}Cu. Thus, it is difficult to distinguish between ^{67}Cu and ^{67}Ga by γ-ray spectrometry. Also the expensive enriched isotope of ^{70}Zn should be recovered for reuse. To develop a chemical procedure to remove ^{67}Ga from ^{67}Cu and to recover the rare ^{70}Zn material, we first produced radiotracers of ^{61}Cu, ^{66}Ga, and ^{69m}Zn in the ^{nat}Zn(d,X) reactions by irradiating 24-MeV deuterons on a metallic ^{nat}Zn foil (nat: natural isotopic abundance; chemical purity: >99.99%; thickness: 71.4 mg cm^{-2}). The average beam intensity was 150 nA, and the irradiation time was 26 min. An enriched ^{70}ZnO target (^{70}Zn isotopic abundance: 96.87%; thickness: 327 mg cm^{-2}) was also irradiated with the 24-MeV deuterons in order to evaluate the production yield of ^{67}Cu from ^{70}Zn and the quality of the purified ^{67}Cu product. The average beam intensity was 18 nA, and the irradiation time was 56 min. After the irradiation, as shown in Fig. 1, Cu isotopes were separated from the ^{nat}Zn and ^{70}ZnO targets through a two-step chromatographic separation using the Eichrom Cu resin and the Dowex 1X8 anion-exchange resin.[5] We carried out the chemical procedure using the radiotracers of ^{61}Cu, ^{66}Ga, and ^{69m}Zn produced in the ^{nat}Zn(d,X) reaction. A high chemical yield of 97% was obtained for ^{61}Cu. Decontamination factors of ^{66}Ga and ^{69m}Zn from ^{61}Cu were evaluated to be~10^3 and >10^3,respectively. The recovery of >99% for ^{69m}Zn, was high enough for recycling of the ^{70}Zn target material. Figure 2 shows the γ-ray spectrum of the purified ^{67}Cu from the enriched ^{70}Zn target. Under the present experimental condition, the production yield of ^{67}Cu was 4.0 MBq μA^{-1}h^{-1}. The radioactivity ratio of A(^{67}Cu)/A(^{67}Ga) was about 2×10^4 after the chemical separation. Based on the present results, we estimate that about 1 GBq of ^{67}Cu could be distributed after 3-days irradiation of a metallic ^{70}Zn target of 357-mg cm^{-2} thickness with a 24-MeV and 10-μA deuteron beam, followed by 3 days for chemical separation and shipment.

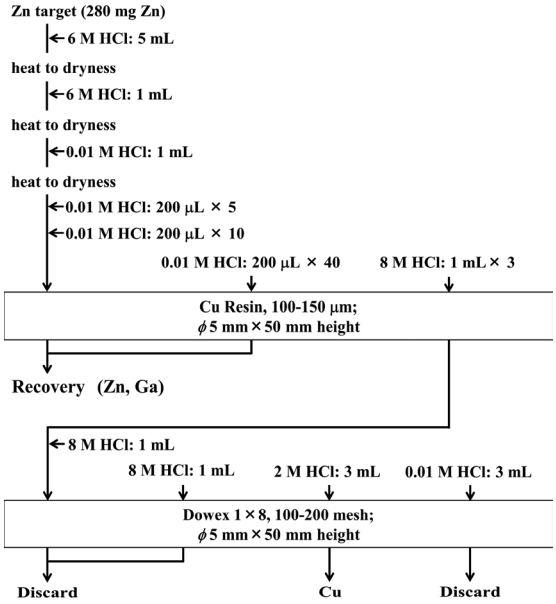

Fig. 1. Chemical separation procedure for ^{67}Cu produced in the ^{70}Zn(d,αn)^{67}Cu reaction.

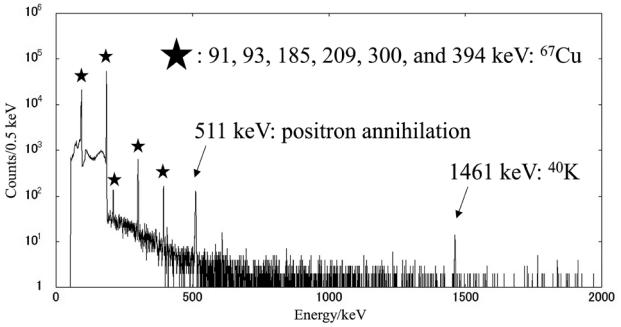

Fig. 2. γ-ray spectrum of the purified ^{67}Cu from the enriched ^{70}Zn target irradiated with the 24-MeV deuteron.

*1 RIKEN Nishina Center
*2 Japan Radioisotope Association

References
1) T. Kambara et al., RIKEN Accel. Prog. Rep. **42**, 295 (2008).
2) I. Novak-Hofer et al., Eur. J. Nucl. Med. **29**, 821 (2002).
3) IAEA Technical Reports Series **473** (2011).
4) J. Kozempel et al., Radiochim. Acta. **100**, 419 (2012).
5) Eichrom technologies' Product Catalog for 2013.

Characteristics of genomic rearrangements induced by heavy-ion beam irradiation in *Arabidopsis thaliana* †

T. Hirano,[*1,*2] Y. Kazama,[*1] K. Ishii,[*1] S. Ohbu,[*1] Y. Shirakawa,[*1] and T. Abe[*1]

Among plants, the molecular nature of mutations induced by heavy-ion beam irradiation has been mainly characterized in *Arabidopsis thaliana*. We previously reported that an Ar-ion or Fe-ion beam with a high LET (≥ 290 keV/μm) often induces large deletion mutations and genomic rearrangements.[1), 2)] However, such genomic rearrangements could not be fully characterized by the conventional method using polymerase chain reaction and sequencing analysis on restricted chromosomal regions or loci. Whole-genome resequencing might help fully detect the rearrangements. In the present study, we characterized the total mutations in the mutant genomes by whole-genome resequencing, and the mutagenic effects of the high-LET heavy-ion beams were evaluated.

Resequencing of three mutant lines of *A. thaliana* ecotype Col-0 was performed at the Takara Dragon Genomics Center (Takara Bio Inc., Mie, Japan) using one lane of the HiSeq 2000 sequencing system (Illumina Inc., CA, USA). Genomic DNAs for the resequencing were isolated from 40 plants of each mutant line (M_3 generation) derived from Ar-ion beam irradiation (290 keV/μm, 50 Gy). The reads obtained from the resequencing were mapped to a reference genome (TAIR10). The total mutations in the mutant genomes were detected by using SAMtools (v0.1.16),[3)] Pindel (v0.2.4.d),[4)] and BreakDancer (v1.1)[5)] algorithms, and the mutations observed at least in two mutants were excluded, being considered as background mutations harbored in ecotype Col-0 in our laboratory.

The three mutant lines selected for the resequencing were prescreened by array-comparative genomic hybridization (CGH), wherein the induced mutations were partially identified. The mutant lines Ar-57-al1, Ar-365-as1, and Ar-443-as1 showed no large deletions (≥ 200 bp), deletions between several hundred bp to several kbp with genomic rearrangements, and a 600-kbp deletion with a genomic rearrangement, respectively. As a result of resequencing followed by mutation detection, total mutations including base substitutions, duplications, in/dels, inversions, and translocations were detected. In mutant line Ar-57-al1, the size range of the detected deletions was from 1 to 75 bp, and these results were in agreement with those from array-CGH. Large deletions and genomic rearrangements were detected by Pindel and BreakDancer, and all of the deleted regions flagged by array-CGH were detected by the resequencing-based method in Ar-365-as1 and Ar-443-as1.

The numbers of homozygous-mutated genes, in which mutations would be expected to affect the mutant phenotypes, were calculated as seven, five, and eleven in the Ar-57-al1, Ar-365-as1, and Ar-443-as1 mutant lines, respectively. The candidate genes responsible for the mutant phenotypes we focused on were found from the homozygous-mutated genes in each mutant line. These results indicate that the mutation detection platform using resequencing data has the appropriate performance standards to detect total mutations induced by radiation treatment.

Resequencing revealed that the three mutants harbored complex genomic rearrangements. In the rearrangements of Ar-365-as1, for example, two inverted fragments were detected in chromosome 2, and one of the fragments translocated in the same chromosome (Fig. 1). In total, 22 DNA fragments were found to have contributed to the complex genomic rearrangements. Of these, 19 fragments were involved in the intra-chromosomal rearrangements. Accelerated Ar ions with high LET lead to dense ionization along the particle path. Therefore, it is suggested that DNA damage induces juxtapositions in the mutant genomes, and that clustered DNA fragments, contributing to the intrachromosomal rearrangements and large deletions, are generated.

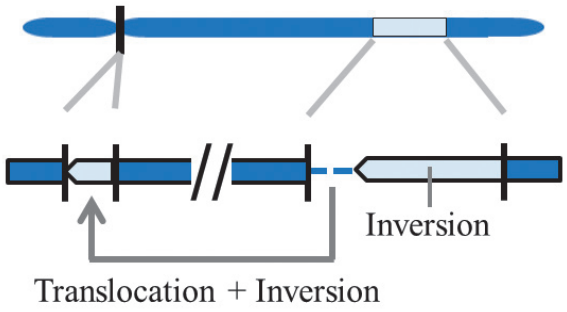

Fig. 1 Schematic representation of genomic rearrangements induced by Ar-ion beam irradiation. The rearrangements were detected in chromosome 2 of mutant line Ar-365-as1.

References
1) T. Hirano et al., Mutat. Res. **735**, 19 (2012).
2) Y. Kazama et al., Genes Genet. Syst. **88**, 189 (2013).
3) H. Li et al., Bioinformatics **25**, 2078 (2009).
4) K. Ye et al., Bioinformatics **25**, 2865 (2009).
5) K. Chen et al., Nature Methods **9**, 677 (2009).

† Condensed from the article in Plant J., **82**, 93 (2015).

*1 RIKEN Nishina Center
*2 Faculty of Agriculture, University of Miyazaki

Breeding of Summer-Autumn Flowering Chrysanthemum cv. Hakuryo with a little generation of malformed flower

A. Hisamura, *1 D. Mine, *2 T. Takeda, *1 T. Abe, *3 Y. Hayashi, *3 and T. Hirano *4

Chrysanthemum is the main element of flowering plant production in Nagasaki Prefecture. Its growing area spreads over 168 hectares and has an output of approximately 3,500 million yen. A summer-autumn flowering Chrysanthemum cv. Iwano-hakusen has come to a main summer-autumn Chrysanthemum cultivar in Nagasaki Prefecture because it is one of the labor-saving cultivars with no lateral shoot and dose not require a shading apparatus controlling the day length for flowering. However, “Iwano-hakusen” has a problem that malformed flowers can be seen significantly among September-flowering type plants (fig. 1-A,B) due to high temperatures in September. This problem is serious because those malformed flowers cannot be commercialized and it directly affects the farmer’s business situation. Thus, developing a new cultivar of summer-autumn Chrysanthemum having minimum generation of malformed flowers had been desired. Therefore, we tried to breed a new cultivar having minimum generation of malformed flowers by using heavy-ion beam irradiation. As a result, we succeeded in breeding a new cultivar known as “Hakuryo” in 2014.

We irradiated C-ion beams (LET: 23keV/μm) of 10 Gy to “Iwano-hakusen” at RIKEN Nishina center in February 2011, and selected a new cultivar “Hakuryo”. We irradiated C-ion beams to 1,440 scions, and obtained 3,702 derivatives from the irradiated scions as a mother stock. Among the 3,702 derivatives, 1,620 showed malformations such as forked or fasciated stems. From the rest of the derivatives, 2,082 were planted and cultured under normal light culturing. After that we selected well-formed flowers on the first selection.The second selection of well-formed flowers in the next generation was performed in 2012. Then on the third selection, “Hakuryo” was isolated. Large-scale experimental production of “Hakuryo” was performed at the agricultural center field and at the local field. We applied for registration of the variety on the March 12, 2015 because the stability of characters was confirmed. “Hakuryo” is a variety of Summer-Autumn Flowering Chrysanthemum and has large white petals (White-group NN115-C on the R.H.S. color chart) (Fig. 1-C, D). It does not need a shading apparatus for flowering, and shipping from July to September is possible using long-day treatment under light culture. Since its neck is short, the balance of upper leaves arrangement is preferred in the market (Fig. 1-C). As compared to “Iwano-hakusen”, “Hakuryo” has these following characteristics. Harvest in natural flowering is from the last ten days of May to the beginning of June, which is about 3 weeks earlier than “Iwano-hakusen”. The flowering days after the end of the long-day treatment is about 45 days. The stem grows faster and is 4 cm – 5 cm longer than “Iwano-hakusen”. The size of the flower at harvest is about the same or little bigger than “Iwano-hakusen”. The number of ray flowers is about the same or little lesser than “Iwano-hakusen”. The occurrence rate of malformed flowers is substantially less than that of “Iwano-hakusen” in September-flowering type plants, which is only about 10% (Fig. 2).

“Hakuryo” is becoming popular gradually because the commercializing rate has been increasing as the generation of malformed flowers decreases, so that farmers can expect financial stability. However, “Hakuryo” has two problems: its weight is slightly lighter because of its longer stem and leaf scorch is often seen. Therefore, we need to select a heavier line and establish a cultivation technique to improve the quality of “Hakuryo”.

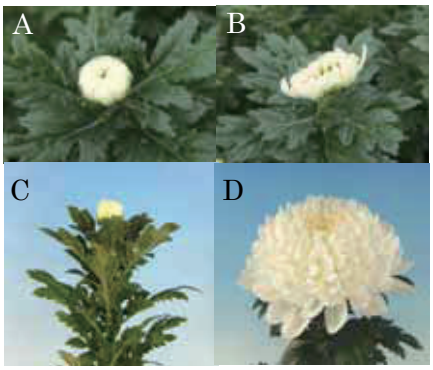

Fig. 1 The normal flower of “Iwano-hakusen” (A) and malformed flower (B). The upper side of “Hakuryo” (C) and in full bloom (D).

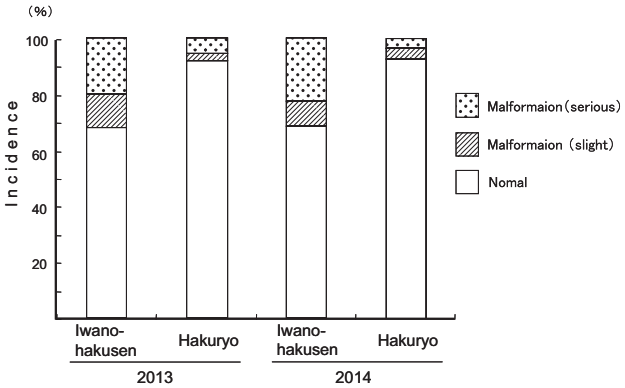

Fig.2 Incidence of Flower malformation in September-flowering type plants

※１） Short diameter/long diameter= 9/10 to 1/1 is nomal, 4/5 to 9/10 is malformaion （slight）, and 7/10 to 4/5 malformaion（serious）

*1 Agriculture and Forestry Technical Development Center, Nagasaki Prefectural Government
*2 Shimabara Development Bureau
*3 RIKEN Nishina Center
*4 Faculty of Agriculture, Miyazaki University

II. RESEARCH ACTIVITIES I
(Nuclear, Particle and Astro-Physics)

1. Nuclear Physics

Decay properties of ^{68,69,70}Mn†

G. Benzoni,[*1] A.I. Morales,[*1,*2] H. Watanabe,[*3,*4] L. Coraggio,[*5] A. Bracco,[*1,*2] P. Doornenbal,[*3] G. Lorusso,[*3] S. Nishimura,[*3] H. Sakurai,[*3] P.A. Söderström,[*3] T. Sumikama,[*6] Z.Y. Xu,[*7] for the RIBF80 and the EURICA collaborations.

In recent years the evolution of magic numbers moving away from the valley of stability has been a hot topic both from experimental and theoretical points of view. In this context, one region in the chart of nuclides that is attracting particular attention lies around ^{78}Ni: this is a key region to study the path toward the N=50 shell closure and its implications on the astrophysical r-process. In particular, the study of the evolution of excited states for the Cr, Fe, Zn, Ge isotopes provides a stringent test for shell model calculations leading to N=50.

The experiment described here was performed at RIKEN in May 2013, as part of the EURICA campaign at the Radioactive-Isotope Beam Factory (RIBF) facility . The nuclear species were produced by means of in-flight fission of a ^{238}U beam at a bombarding energy of 345 MeV/nucleon. The experiment collected data for an equivalent time of 3 days with an average primary beam intensity of 10 pnA. The resulting fragments were transported and separated in the BigRIPS separator and Zero-Degree spectrometer down to the final focal plane. They were implanted in the 5 silicon detectors of the WAS3ABi array[1] which was surrounded by the EURICA spectrometer[2] coupled to 18 small volume $LaBr_3$(Ce) scintillator detectors, for fast-timing measurements[3]. The yields for the mother nuclei, after implantation, were: 6700 ^{68}Mn ions, 4300 ^{69}Mn ions and 400 ^{70}Mn ions.

The experimental data confirm the β-decay spectrum of ^{68}Mn reported previously in Ref.[4] even if we see different relative population of the transitions at 1250 keV and 1514 keV. In addition, γ-ray energies for the decay of ^{69}Fe and ^{70}Fe are extracted for the first time. For the odd isotope, the limited statistics do not allow the extraction of $\gamma - \gamma$ coincidences. Its decay spectrum shows a substantial contribution from the β-delayed neutron channel, which preferentially seems to populate specific low-J states. By systematics and supported by recent shell-model calculations, we assign the γ rays seen in the spectrum of ^{70}Fe to the depopulation of the 2_1^+ and 4_1^+ levels.

The proposed level schemes following the β decay of even-mass isotopes are shown in Fig. 1. The comparison of the decay patterns of ^{68}Mn $\rightarrow$ ^{68}Fe and ^{70}Mn $\rightarrow$ ^{70}Fe shows a sudden change: in the case of ^{70}Mn $\rightarrow$ ^{70}Fe, the feeding seems to preferably go to the proposed 4^+ state, while the 2^+ state is mainly fed by internal decay coming from the higher-lying states. The sudden change of the spin population in the daughter nuclei indicates different spin of the ground state of the mother nuclei.

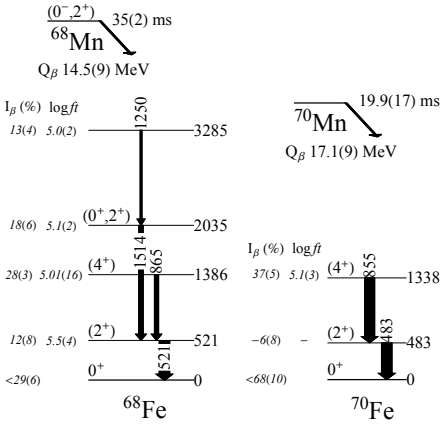

Fig. 1. Partial level schemes following the β decays ^{68}Mn $\rightarrow$ ^{68}Fe (left) and ^{70}Mn $\rightarrow$ ^{70}Fe (right).

The experimental results have been compared to a shell-model calculation performed with the CD-Bonn NN potential in the V_{low-k} approach[5] extended to ^{68,70}Fe isotopes. It is found that the experimental $R_{4/2}$ ratio is properly reproduced by the calculations only with the inclusion of the $1d_{5/2}$ neutron orbital in the valence space. This is interpreted, as for Cr isotopes, in terms of the interplay between the quadrupole correlations of the $\nu 1d_{5/2}$ and $\nu 0g_{9/2}$ orbitals and the monopole component of the $\pi 0f_{7/2}$ - $\nu 0f_{5/2}$ interaction, thus driving the deformation in the neutron-rich Cr-Fe region. Since the maximum of quadrupole deformation has not been reached yet, investigating heavier Fe isotopes is of foremost interest to assess the robustness of the N=50 shell closure below ^{78}Ni.

† Condensed from the article in PLB, Vol.751, 107 (2015)
*1 INFN sezione di Milano, Milano
*2 Dipartimento di Fisica, Universitá degli Studi di Milano, Milano
*3 RIKEN Nishina Center, Riken
*4 IRCNPC, School of Physics and Nuclear Engineering, Beihang University, Beijing
*5 INFN sezione di Napoli, Napoli
*6 Department of Physics, Tohoku University, Sendai
*7 Department of Physics, University of Tokyo, Tokyo

References

1) S. Nishimura, Prog. Theor. Exp. Phys. **2012** (2012) 03C006.
2) P.A. Söderström, Nucl. Instr. Meth. **B317** (2013) 649.
3) Z. Patel et al., RIKEN Accel. Prog. Rep. **47** (2014) 13.
4) S.N. Liddick et al., Phys. Rev. **C87** (2013) 014325.
5) L. Coraggio et al., Phys. Rev. **C89** (2014) 024319.

Excited states of $^{136-138}$Sb from β decay

J. Keatings,[*1] G. Simpson,[*2,*1] A. Jungclaus,[*3] J. Taprogge,[*4] S. Nishimura,[*5] P. Doornenbal,[*5] G. Lorusso,[*5] P. -A. Söderström,[*5] T. Sumikama,[*5] J. Wu,[*5] Z. Y. Xu,[*5] T. Isobe,[*5] H. Sakurai,[*5] and the EURICA RIBF-85 collaboration[*5]

The properties of nuclei close to the doubly magic ^{132}Sn, with $N \geq 82$, have some of the highest impact on the final r-process abundances[1,2]. Studies of the nuclear structure of the nuclei $^{135-139}$Sb can therefore provide important input into r-process calculations, especially as the exact site of this astrophysical reaction is presently unclear. The nucleus ^{135}Sb is the most neutron-rich one currently whose excited states have been studied via β decay[3].

The Sb nuclei have one valence proton with respect to the $Z = 50$ shell closure hence their nuclear structure can provide a sensitive test of the neutron-proton part of the effective interactions used in shell-model calculations. The predicted structure of these nuclei can vary considerably, depending on the effective interaction used. Recently it has been shown that weaker neutron pairing may be necessary to reproduce the features of the Sn nuclei beyond $N = 82$[4]. An interesting consequence of weak pairing is the appearance of low-lying seniority-4 neutron states in ^{137}Sb which has been predicted to cause a rapid compression and considerable mixing, of the low-lying excited states in this nucleus[5]. A consequence of this is that levels with $\pi s_{1/2}$ and $\pi d_{3/2}$ components predicted at energies above 2 MeV in ^{135}Sb may be found at energies below 500 keV in ^{137}Sb.

In order to investigate the structure of the nuclei $^{136-138}$Sb in-flight fission of a 345-MeV/nucleon ^{238}U beam was performed at RIBF. Ions including $^{135-139}$Sn were selected using the BigRIPS spectrometer and implanted in the WAS3ABI stopper, situated at the F11 focal plane. The high segmentation of the WAS3ABI stopper allows detected β decays to be correlated with identified and implanted ions. The EURICA Ge array was used to detect any γ rays emitted following the β decay of $^{135-139}$Sn ions. Use of ion–$\beta-\gamma$ and ion–$\beta-\gamma-\gamma$ coincidences has allowed new level schemes to be established for the nuclei $^{136-138}$Sb.

When adding neutrons beyond the $N = 82$ shell closure the probability for $\beta-n$ emission increases rapidly to values of > 50 %. Therefore performing only an ion–$\beta-\gamma$ coincidences is not sufficient to assign a detected γ ray to a particular nucleus. Common transitions emitted from parent isotopes with masses A and $A+1$ can be assigned to a daugher nucleus with mass A. Gates set on strongly produced transitions along with observed γ decays in grand-daugher nuclei in the same event allow masses to be assigned too. This is thanks to the high granularity and efficiency of the WAS3ABI and EURICA arrays.

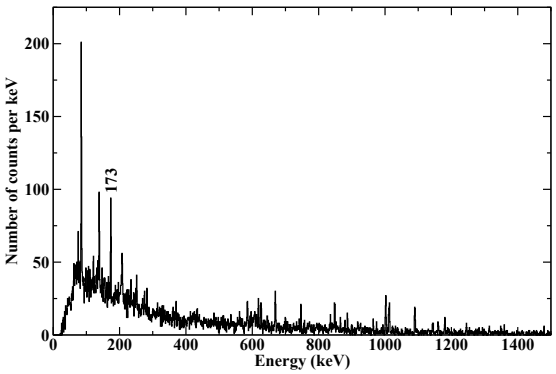

Fig. 1. Spectrum of γ rays obtained from the β and $\beta-n$ decay of ^{137}Sn.

An example of such analysis is shown in Fig. 1, which shows a portion of the γ-rays detected following the β and $\beta-n$ decay of ^{137}Sn. The 173-keV transition has previously been assigned to ^{136}Sb via isomer spectroscopy[6].

Analysis of the decays of the nuclei $^{136-138}$Sn and hence first level schemes for the isotopes $^{136-138}$Sb is nearing completion. Comparisons with the predictions of shell-model calculations will also aid in assigning spins.

*1 University of the West of Scotland
*2 LPSC, Grenoble
*3 IEM, CSIC Madrid
*4 Universidad Autonoma de Madrid
*5 RIKEN Nishina Center

References
1) S. Brett *et al*: Eur. Phys. J. A **48**, 184 (2012).
2) G. Lorusso *et al*: Phys. Rev. Lett. **114**, 192501 (2015).
3) J. Shergur *et al*: Phys. Rev. C **72**, 024305 (2005).
4) G. S. Simpson *et al*: Phys. Rev. Lett. **113**, 132502 (2014).
5) L. Coraggio *et al*: Phys. Rev. C **87**, 034309 (2013).
6) M. Mineva *et al*: Eur. Phys. J. A **11**, 9 (2001).

$T_Z = -1$ and $T_Z = -2$ β-decay studies using ^{78}Kr fragmented beams at BigRIPS, part I

B. Rubio,[*1] J. Agramunt,[*1] A. Algora,[*1] V. Guadilla,[*1] A. Montaner-Piza,[*1] A. I. Morales,[*1] S. E. A. Orrigo,[*1] J. Chiba,[*2] D. Nichimura,[*2] H. Oikawa,[*2] Y. Takei,[*2] S. Yagi,[*2] B. Blank,[*3] P. Ascher,[*3] M. Gerbaux,[*3] T. Goigoux,[*3] J. Giovinazzo,[*3] S. Grévy,[*3] T. Kurtukian Nieto,[*3] C. Magron,[*3] P. Aguilera,[*4] F. Molina,[*4] D. S. Ahn,[*5] P. Doornenbal,[*5] N. Fukuda,[*5] N. Inabe,[*5] G. Kiss,[*5] T. Kubo,[*5] S. Kubono,[*5] S. Nishimura,[*5] Y. Shimizu,[*5] C. Sidong,[*5] P. A. Söderström,[*5] T. Sumikama,[*5] H. Suzuki,[*5] H. Takeda,[*5] P. Vi,[*5] J. Wu,[*5] Y. Fujita,[*6] M. Tanaka,[*6] W. Gelletly,[*1,*7] F. Diel,[*8] D. Lubos,[*9] G. de Angelis,[*10] D. Napoli,[*10] C. Borcea,[*11] A. Boso,[*12] R. B. Cakirli,[*13] E. Ganioglu,[*13] G. de France,[*14] and S. Go[*15]

The study of the beta decay of proton-rich nuclei is interesting for a number of reasons; we can have access to states in the daughter nucleus populated by Fermi (the Isobaric Analogue State, IAS) as well as Gamow-Teller transitions and in some cases the IAS is fragmented (see for instance[1] and[2]); it can also happen that the process goes via the exotic beta-delayed gamma-proton decay, a phenomenon that is the result of a combined effect of the forbidden proton decay of the IAS and the fact that some of the states populated after γ-decay are proton-unbound. Furthermore, spin-isospin excitations can be studied by beta-decay and charge exchange reactions in mirror nuclei, shedding light on mirror symmetry, hence we can compare our results on the beta decay of proton-rich nuclei with the results of charge exchange experiments when appropriate targets for the mirror nuclei are available[3].

Accordingly we have performed experiments at GSI and GANIL to study $T_Z = -1$[4] and $T_Z = -2$[1] nuclei respectively where it became clear that the study of heavier, more exotic systems, demands beam intensities available only at the RIKEN Nishina Center.

The experiment was carried out using the fragmentation of a 345 MeV·A ^{78}Kr beam with unprecedented intensity (up to 300 particle nA) on a Be target. The fragments were separated in flight using the BigRIPS separator[5] and implanted in three 1mm thick WAS3ABi[6] double-sided Si strip detectors (DSSSD) with each of them having an active area of 60 × 40 mm^2 segmented into 60 vertical by 40 horizontal strips. The implantation setup was surrounded by the EUROBALL-RIKEN Cluster Array (EURICA)[7] consisting of 12 HPGe CLUSTER-detectors of Euroball type. Two different settings of BigRIPS were used in this experiment, the first was optimised for the production of ^{58}Zn, ^{60}Ge, ^{62}Ge and ^{64}Se nuclei and overlapped with the experiment planned for the search of new isotopes and two-proton emitters, see the contribution by B. Blank et al. to this volume, and the second for ^{66}Se. Putting conditions on the ToF and ΔE signals of the ions we have produced the identification plot shown in Figure 1 for the first setting. The Y-axis represents the Z of the implanted ion and the X-axis the A/Q. Preliminary results of the analysis are presented in the second contribution to this progress report.

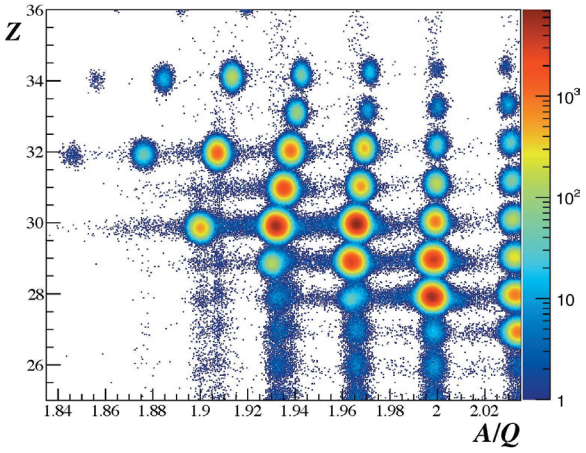

Fig. 1. Particle Identification Plot for isotopes at the first BigRIPS setting, see text.

*1 IFIC, CSIC-Univ. Valencia
*2 Tokyo Univ. Sci
*3 CEN Bordeaux-Gradignan
*4 CCHEN-Chile
*5 RIKEN Nishina Center
*6 Osaka University
*7 Surrey University
*8 Universität zu Köln
*9 Technische Universität München
*10 INFN-Legnaro
*11 IFIN-HH, Bucarest
*12 INFN-Padova
*13 Univ. Istanbul
*14 GANIL-France
*15 Univ. Tenesse

References

1) S.E.A. Orrigo et al., Phys. Rev. Lett. **112**, 222501 (2014).
2) M. MacCormick and G. Audi, Nucl. Phys A **925**, 1151 61 (2014).
3) Y.Fujita, B.Rubio and W.Gelletly, Prog. Part. Nucl. Phys. **66**, 549 (2011).
4) F. Molina et al., Phys. Rev. C **91**, 014301 (2015).
5) T. Kubo et al., Prog. Theor. Exp. Phys. **2012** 03C003 (2012).
6) S. Nishimura et al., RIKEN Accel. Progr. Rep. **46**, 182 (2013)
7) P.-A. Söderström et al., Nuclear Instruments and Methods in Physics Research B **317** (2013) 649652

$T_Z = -1$ and $T_Z = -2$ β-decay studies using ^{78}Kr fragmented beams at BigRIPS, part II

B. Rubio,[*1] J. Agramunt,[*1] A. Algora,[*1] V. Guadilla,[*1] A. Montaner-Piza,[*1] A. I. Morales,[*1] S. E. A. Orrigo,[*1] J. Chiba,[*2] D. Nishimura,[*2] H. Oikawa,[*2] Y. Takei,[*2] S. Yagi,[*2] B. Blank,[*3] P. Ascher,[*3] M. Gerbaux,[*3] T. Goigoux,[*3] J. Giovinazzo,[*3] S. Grévy,[*3] T. Kurtukian Nieto,[*3] C. Magron,[*3] P. Aguilera,[*4] F. Molina,[*4] D. S. Ahn,[*5] P. Doornenbal,[*5] N. Fukuda,[*5] N. Inabe,[*5] G. Kiss,[*5] T. Kubo,[*5] S. Kubono,[*5] S. Nishimura,[*5] Y. Shimizu,[*5] C. Sidong,[*5] P. A. Söderström,[*5] T. Sumikama,[*5] H. Suzuki,[*5] H. Takeda,[*5] P. Vi,[*5] J. Wu,[*5] Y. Fujita,[*6] M. Tanaka,[*6] W. Gelletly,[*1,*7] F. Diel,[*8] D. Lubos,[*9] G. de Angelis,[*10] D. Napoli,[*10] C. Borcea,[*11] A. Boso,[*12] R. B. Cakirli,[*13] E. Ganioglu,[*13] G. de France,[*14] and S. Go[*15]

Spin-isospin excitations can be studied by beta-decay and charge exchange reactions in mirror nuclei, shedding light on mirror symmetry, hence we can compare our results on the beta decay of proton-rich nuclei with the results of charge exchange experiments when appropriate targets for the mirror nuclei are available[1]. Accordingly we have performed experiments at GSI and GANIL to study $T_Z = -1$[2] and $T_Z = -2$[3,4] nuclei respectively where it became clear that the study of heavier, more exotic systems, demands beam intensities available only at the RIKEN Nishina Center. We have performed an experiment using the fragmentation of a 345 MeV·A ^{78}Kr beam with typical intensity of 200 particle nA on a Be target. The fragments were separated in flight using the BigRIPS separator and implanted in three WAS3ABi double-sided Si strip detectors. The implantation setup was surrounded by the EUROBALL-RIKEN Cluster Array (EURICA). The description of the experiment is explained in another contribution to this progress report with the same title called part I. In this contribution the particle identification plot is also presented. Here we present the preliminary analysis of the $t_{1/2}$ values of ^{58}Zn and ^{66}Se with improved accuracy and a new $t_{1/2}$ value for ^{64}Se parent nuclei carried out using correlations between the selected ion (setting conditions on the particle identification plot) and the characteristic γ rays of the daughter nuclei measured with the EURICA array in prompt coincidence with β-signals in the same DSSSD pixel. Preliminary results presented in Figs 1 and 2 give an impression of the quality of the data. Further analysis is in progress.

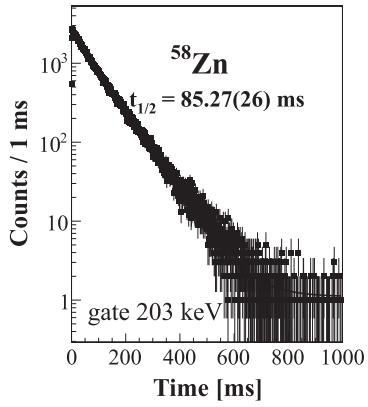

Fig. 1. Time correlations between ^{58}Zn implanted ions in WAS3ABi and the 203 keV γ rays detected in EURICA.The solid line represents the fit to the decay curve.

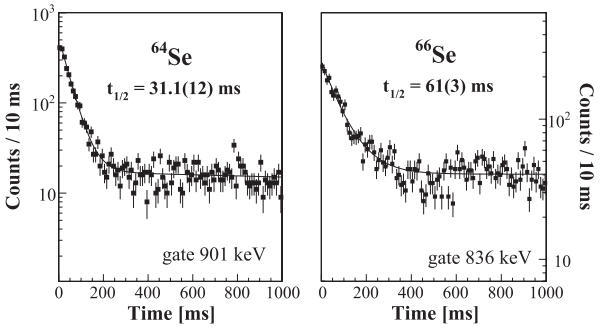

Fig. 2. Time correlations between ^{64}Se (left) and ^{66}Se (right) ions implanted in WAS3ABi and 901 and 836 keV γ rays respectively detected in EURICA. The solid lines represents the fit to the decay curves.

*1 IFIC, CSIC-Univ. Valencia
*2 Tokyo Univ. Sci
*3 CEN Bordeaux-Gradignan
*4 CCHEN-Chile
*5 RIKEN Nishina Center
*6 Osaka University
*7 Surrey University
*8 Universität zu Köln
*9 Technische Universität München
*10 INFN-Legnaro
*11 IFIN-HH, Bucarest
*12 INFN-Padova
*13 Univ. Istanbul
*14 GANIL-France
*15 Univ. Tenesse

References

1) Y.Fujita, B.Rubio and W.Gelletly, Prog. Part. Nucl. Phys. **66**, 549 (2011).
2) F. Molina et al., Phys. Rev. C **91**, 014301 (2015).
3) S.E.A. Orrigo et al., Phys. Rev. Lett. **112**, 222501 (2014).
4) S.E.A. Orrigo et al., Phys. Rev. C **93**, 044336 (2016)

Isospin symmetry studies beyond the $f_{7/2}$ shell: study of the beta decay of ^{70,71}Kr

A. Algora,[*1] A. Morales,[*1] B. Rubio,[*1] J. Agramunt,[*1] V. Guadilla,[*1] A. Montaner-Piza,[*1] S. Orrigo,[*1] G. de Angelis,[*2] D. Napoli,[*2] F. Reccquia,[*3] S. Lenzi,[*3] A. Boso,[*3] S. Nishimura,[*4] G. Kiss,[*4] P. Vi,[*4] J. Wu,[*4] P.-A. Söderström,[*4] T. Sumikama,[*4] H. Suzuki,[*4] H. Takeda,[*4] D.S. Ahn,[*4] H. Baba,[*4] P. Doornebal,[*4] N. Fukuda,[*4] N. Inabe,[*4] T. Isobe,[*4] T. Kubo,[*4] S. Kubono,[*4] Y. Shimizu,[*4] C. Sidong,[*4] B. Blank,[*5] P. Ascher,[*5] M. Gerbaux,[*5] T. Goigoux,[*5] J. Giovinazzo,[*5] S. Grévy,[*5] T. Kurtukian Nieto,[*5] C. Magron,[*5] W. Gelletly,[*6] Zs. Dombrádi,[*7] Y. Fujita,[*8] M. Tanaka,[*8] P. Aguilera,[*9] F. Molina,[*9] J. Eberth,[*10] F. Diel,[*10] D. Lubos,[*11] C. Borcea,[*12] A. Petrovici,[*12] E. Ganioglu,[*13] D. Nishimura,[*14] H. Oikawa,[*14] Y.Takei,[*14] S.Yagi,[*14] W. Korten,[*15] G. de France,[*16] and P. Davies[*17]

Nuclei in the vicinity of the N=Z line around Z=36-38 have been the subject of numerous theoretical and experimental investigations to answer questions about deformation, shape coexistence, shape transitions, np pairing and isospin symmetry. This region is characterized by drastic shape changes depending on the competition in energy between prolate and oblate shapes, which is determined by the occupation of particular single particle orbits. This makes it the ideal playground for our investigations.

The main goal of this experiment was to study isospin related features of the structure of ^{70,71}Kr. One objective of the experiment is the investigation of the isomeric decay of ^{71}Kr, which could answer questions related to isospin symmetry breaking effects in the ^{71}Br/^{71}Kr system. The second goal was the study of the beta decay of ^{70,71}Kr, which may provide information of relevance to our understanding of T=0 np pairing in N=Z nuclei, shape coexistence, isospin symmetry, astrophysics and nuclear structure.

In this report we present some preliminary results from the experiment. A high intensity ^{78}Kr beam provided by the RIKEN Nishina Center Accelerator Complex impinging on a Be target was used to produce the nuclides of interest in fragmentation. In the experiment the EURICA gamma-ray array surrounded the implantation detector WAS3ABI into which the fragments of interest were implanted. The fragments were identified using the BigRIPS separator employing the ΔZ-ToF-Bρ method. Figure 1 shows an identification plot of the fragments using this technique for the ^{70}Kr setting. Several gamma transitions emitted from states populated in the beta decay of ^{70,71}Kr have been observed for the first time. Figure 2 shows the preliminary analysis of the beta decay half-life of ^{70}Kr based on coincidences with two of the newly identified gamma transitions. The value obtained is in agreement with the results from Ref. 1. The determination of beta decay half-lives in this region is of relevance for a better understanding of the rp-process (Ref. 2). The analysis of the experimental data on the ^{70,71}Kr decays and the decay of the ^{71}Kr isomer decay is in progress.

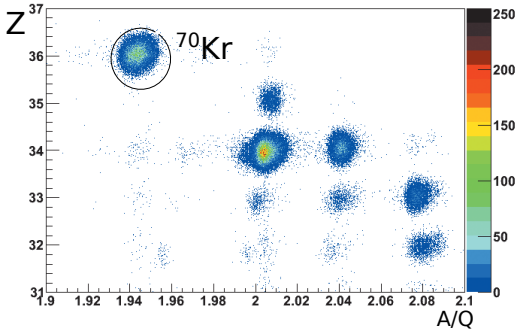

Fig. 1. Identification plot for the isotopes produced in ^{78}Kr fragmentation for the ^{70}Kr setting.

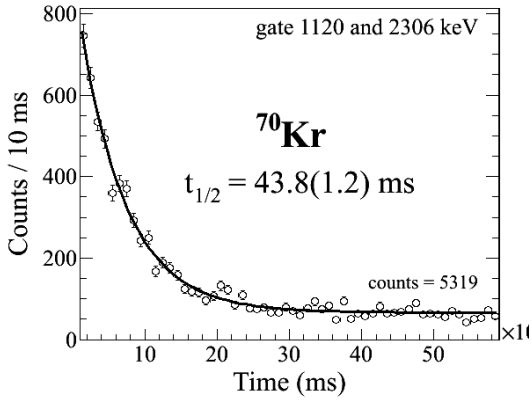

Fig. 2. Preliminary half-live for the beta decay of ^{70}Kr.

*1 IFIC, CSIC-Univ. Valencia
*2 INFN-Legnaro
*3 INFN-Padova
*4 RIKEN Nishina Center
*5 CEN Bordeaux-Gradignan
*6 Surrey University
*7 MTA ATOMKI
*8 Osaka University
*9 CCHEN-Chile
*10 Universität zu Köln
*11 Technische Universität München
*12 IFIN-HH, Bucarest
*13 University of Istanbul
*14 Tokyo Uni. Sci.
*15 CEA-France
*16 GANIL-France
*17 York University

References

1) A.M. Rogers et al., Nuclear Data Sheets 120, 41 (2014).
2) R.K. Wallace and S.E. Woosley, Astro. J. Supp. Ser. 45, 389 (1981).

Discovery of a μs isomer of ^{76}Co†

P.-A. Söderström,[*1] S. Nishimura,[*1] Z. Y. Xu,[*2] K. Sieja,[*3] V. Werner,[*4,*5] P. Doornenbal,[*1] G. Lorusso,[*1] F. Browne,[*1,*6] G. Gey,[*1,*7,*8] H. S. Jung,[*9] T. Sumikama,[*10] J. Taprogge,[*1,*11,*12] Zs. Vajta,[*1,*13] H. Watanabe,[*1,*14] J. Wu,[*1,*15] H. Baba,[*1] Zs. Dombradi,[*13] S. Franchoo,[*16] T. Isobe,[*1] P. R. John,[*17,*18] Y.-K. Kim,[*19] I. Kojouharov,[*20] N. Kurz,[*20] Y. K. Kwon,[*19] Z. Li,[*15] I. Matea,[*16] K. Matsui,[*2] G. Martnez-Pinedo,[*5] D. Mengoni,[*17,*18] P. Morfouace,[*16] D. R. Napoli,[*21] M. Niikura,[*2] H. Nishibata,[*22] A. Odahara,[*22] K. Ogawa,[*1] N. Pietralla,[*5] E. Şahin,[*23] H. Sakurai,[*1,*2] H. Schaffner,[*20] D. Sohler,[*13] I. G. Stefan,[*16] D. Suzuki,[*16] R. Taniuchi,[*2] A. Yagi,[*22] and K. Yoshinaga[*24]

Changes in nuclear shell structure far from stability are largely associated with the monopole component of the proton-neutron interaction. Thus, there is a large ongoing experimental effort aiming to investigate how these shell and sub-shell closures evolve for very exotic nuclei at and below ^{78}Ni. The study of single neutron and proton particle and hole states outside ^{78}Ni is one important way to gain information on this topic. In a recent paper new experimental results on ^{76}Co, one neutron-hole and one proton-hole in ^{78}Ni, were presented. Due to the purity of the excited states, this is a unique case to study the neutron-proton interaction in a region with sparse experimental information.

The ^{76}Co nuclei were produced by in-flight fission of a 345 MeV/u ^{238}U beam on a 3 mm beryllium target and then separated using the BigRIPS fragment separator and the ZeroDegree spectrometer. At F11 the WAS3ABi[1)] silicon detector stack was used for implantation and β-decay correlation measurements and the EURICA spectrometer was used for measuring the energy and time of the γ rays. In total, approximately 1000 ^{76}Co ions were implanted in WAS3ABi during 10 days of measurement.

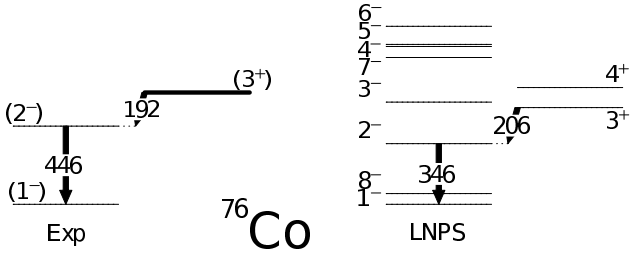

Fig. 1. Proposed experimental level scheme of ^{76}Co compared to shell model calculations using a modified LNPS interaction.

In the experiment, two coincident γ rays of 192 and 446 keV from the decay of a $t_{1/2} = 3$ μs isomeric state of ^{76}Co were observed. The decay of the isomer was assigned to an E1 transition with a reduced transition probability of $B(\mathrm{E1}; 3^+ \rightarrow 2^-) = 1.79 \times 10^{-8}$ W.u. Shell model calculations carried out with an up-to-date LNPS interaction[2,3)] including monopole changes to assure the correct propagation of proton single-particles energies showed the states to be about 70% pure structures of $\pi f_{7/2}^{-1} \otimes \nu g_{9/2}^{-1}$ or $\pi f_{7/2}^{-1} \otimes \nu p_{1/2}^{-1}$ hole configurations for negative and positive parity states, respectively. Thus, the relative $\nu g_{9/2}^{-1}$ and $\nu p_{1/2}^{-1}$ positions could be fine tuned by changing the strength of the $\pi f_{7/2}^{-1} \otimes \nu p_{1/2}^{-1}$ monopole. The results of these calculations are shown in Fig. 1.

Furthermore, a β decaying 8^- state was also observed in the data, consistent with the LNPS shell model calculations. These results will help constrain further developments of theoretical models in the $\pi f_{7/2} \otimes \nu g_{9/2}$ region between ^{60}Ca and ^{78}Ni, where scarce experimental data are available.

References
1) S. Nishimura et al. RIKEN Accel. Prog. Rep. **46**, 182 (2013)
2) K. Sieja and F. Nowacki Phys. Rev. C **85**, 051301 (2012).
3) S. M. Lenzi, F. Nowacki, A. Poves, and K. Sieja Phys. Rev. C **82**, 054301 (2010).

† Condensed from the article in Phys. Rev. C, Vol.92, 051305(R) (2015)

*1 RIKEN Nishina Center
*2 Department of Physics, University of Tokyo
*3 Université de Strasbourg, IPHC
*4 Wright Nuclear Structure Laboratory, Yale University
*5 Institut für Kernphysik, TU Darmstadt
*6 School of Computing, Engineering and Mathematics, University of Brighton
*7 LPSC, Université Grenoble-Alpes, CNRS/IN2P3
*8 ILL
*9 Department of Physics, Chung-Ang University
*10 Department of Physics, Tohoku University
*11 Departamento de Física Teórica, Universidad Autónoma de Madrid
*12 Instituto de Estructura de la Materia, CSIC
*13 Institute for Nuclear Research, Hungarian Academy of Sciences
*14 School of Physics and Nuclear Energy Engineering, Beihang University
*15 School of Physics and State key Laboratory of Nuclear Physics and Technology, Peking University
*16 Institut de Physique Nucléaire, CNRS-IN2P3
*17 INFN Sezione di Padova
*18 Dipartimento di Fisica e Astronomia, Università di Padova
*19 Institute for Basic Science, Rare Isotope Science Project
*20 GSI
*21 INFN, LNL
*22 Department of Physics, Osaka University
*23 Department of Physics, University of Oslo
*24 Department of Physics, Tokyo University of Science

Determination of Q_β for the Gamow-Teller decay of ^{100}Sn and ^{98}Cd

D. Lubos,[*1,*2] J. Park,[*3,*4] N. Warr,[*5] K. Moschner,[*5] M. Lewitowicz,[*6] R. Gernhäuser,[*1] R. Krücken,[*3,*4] S. Nishimura,[*2] H. Sakurai,[*7] G. Lorusso,[*2] J. Wu,[*2] Z. Y. Xu,[*7,*2] H. Baba,[*2] B. Blank,[*8] A. Blazhev,[*5] P. Boutachkov,[*9] F. Browne,[*10,*2] I. Celikovic,[*6] P. Doornenbal,[*2] T. Faestermann,[*1] Y. Fang,[*11,*2] G. de France,[*3] N. Goel,[*9] M. Gorska,[*9] S. Ilieva,[*12] T. Isobe,[*2] A. Jungclaus,[*13] G. D. Kim,[*14] Y.-K. Kim,[*14] I. Kojouharov,[*9] M. Kowalska,[*15] N. Kurz,[*9] Z. Li,[*16] I. Nishizuka,[*17,*2] Z. Patel,[*18,*2] M. M. Rajabali,[*19] S. Rice,[*18,*2] H. Schaffner,[*9] L. Sinclair,[*20,*2] P.-A. Söderström,[*2] K. Steiger,[*1] T. Sumikama,[*17] H. Watanabe,[*21] and Z. Wang[*3]

The heaviest self-conjugate doubly magic nucleus ^{100}Sn is known to have the largest Gamow-Teller decay strength $B(GT)$ of all nuclei.[1)] A precise determination of $B(GT)$ is needed to test the robustness of the $N = Z = 50$ shell closure suggested by shell model calculations. This implies the importance of measuring the β-decay endpoint energy Q_β of ^{100}Sn with better precision. An experiment to study the superallowed Gamow-Teller decay of ^{100}Sn was performed at the RIBF facility of RIKEN Nishina Center in June 2013. ^{100}Sn and a large cocktail of neutron-deficient isotopes down to $N = Z - 2$ were produced by fragmenting a 345 MeV/u ^{124}Xe beam with intensities up to 36 pnA on a 4 mm ^{9}Be target. The nuclei of interest were separated and identified through BigRIPS and the ZeroDegree spectrometer, before being implanted into one of the three double-sided silicon strip detectors (DSSD) of WAS3ABi. The DSSDs were complemented by 10 single-sided silicon strip detectors in a closed-stack geometry for Q_β measurement at maximum efficiency in the downstream direction. WAS3ABi was surrounded by 84 HPGe and 18 $LaBr_3$ detectors of the γ-ray spectrometer EURICA. Thus, gating on the γ-ray transitions of the daughter nuclei results in a high purity of the β^+ energy spectrum. The accurate measurement of the total β^+ energy using WAS3ABi was hindered by processes such as bremsstrahlung, annihilation-in-flight, and particle escape. Hence, neither the measured endpoint nor the experimental distribution of the measured energies could directly be used to determine the Q_β-value. Therefore, Geant4 simulations of the WAS3ABi geometry and physics processes were used to study the detector response and determine the endpoint energy[2)]. For each trial, Q_β was used as the input parameter and positrons were generated in the WAS3ABi geometry to form a simulated energy spectrum. Then, it was compared to the experimental energy spectrum by a χ^2-test. The experimental Q_β resulted in the minimum $\chi^2_{\rm min}$. The uncertainty of χ^2 originating in the simulations is obtained by performing 30 simulations for each trial energy (see Fig. 1). In order to verify this method, the β-decay of ^{98}Cd into the 1691-keV state in ^{98}Ag[3)] was studied (see Fig. 1). The minimum $\chi^2_{\rm min}$ is obtained by $Q_\beta = 2750 \pm 36$ keV, which agrees well with the literature value of 2717(40) keV[4)]. Analysis for Q_β of ^{100}Sn is ongoing, and it will be finalized soon.

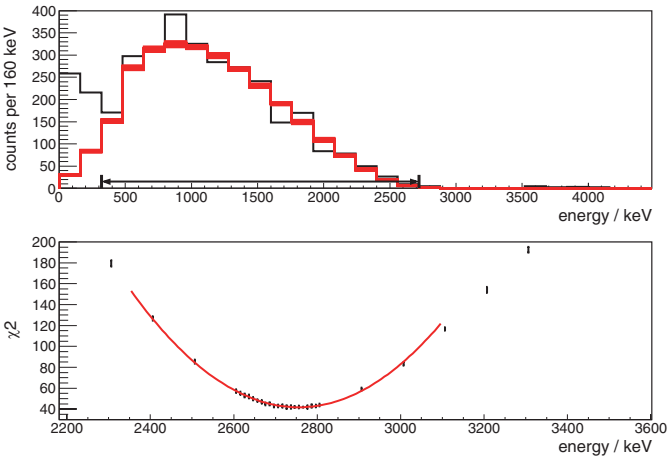

Fig. 1. Complete energy deposit in the experiment (black) of decay products after the implantation of ^{98}Cd nuclei coincident with γ-rays at $E_\gamma = 1176 \pm 2$ keV and 30 simulated spectra (red) of positrons at $Q_\beta = 2737$ keV. The arrow denotes the range of comparison. A parabolic fit yields $\chi^2_{\rm min}$ at $Q_\beta = 2750 \pm 36$ keV.

*1 Physik Department E12, Technische Universität München
*2 RIKEN Nishina Center
*3 TRIUMF
*4 University of British Columbia
*5 Institut für Kernphysik, Universität zu Köln
*6 GANIL
*7 Department of Physics, University of Tokyo
*8 CENBG
*9 GSI Darmstadt
*10 School of Comp., Eng. and Maths., Brighton University
*11 Department of Physics, Osaka University
*12 Institut für Kernphysik, TU Darmstadt
*13 IEM-CSIC
*14 Institute for Basic Science
*15 CERN
*16 School of Physics, Peking University
*17 Department of Physics, Tohoku University
*18 Department of Physics, Surrey University
*19 Department of Physics, Tennessee Tech University
*20 Department of Physics, University of York
*21 Department of Physics, Beihang University

References
1) C. B. Hinke et al., Nature **486**, 341 (2012).
2) N. Warr et al., EPJ Web of Conferences **93**, 07008 (2015).
3) B. Singh, Z. Hu, Nucl. Data Sheets **98**, 335 (2003).
4) N. Wang et al., Chinese Physics C **36**, 1603 (2012).

Investigation of octupole correlations of neutron-rich $Z \sim 56$ isotopes by β-γ spectroscopy

R. Yokoyama,[*1] E. Ideguchi,[*2] G. Simpson,[*3] Mn. Tanaka,[*2] S. Nishimura,[*4] P. Doornenbal,[*4] P.-A. Söderström,[*4] G. Lorusso,[*4] Z. Y. Xu,[*5] J. Wu,[*4,*6] T. Sumikama,[*7] N. Aoi,[*2] H. Baba,[*4] F. Bello,[*8] F. Browne,[*9,*4] R. Daido,[*10] Y. Fang,[*10] N. Fukuda,[*4] G. Gey,[*3,*4,*11] S. Go,[*1,*4] N. Inabe,[*4] T. Isobe,[*4] D. Kameda,[*4] K. Kobayashi,[*12] M. Kobayashi,[*1] T. Komatsubara,[*13] T. Kubo,[*4] I. Kuti,[*14] Z. Li,[*6] M. Matsushita,[*1] S. Michimasa,[*1] C.-B. Moon,[*15] H. Nishibata,[*10] I. Nishizuka,[*7] A. Odahara,[*10] Z. Patel,[*16,*4] S. Rice,[*16,*4] E. Sahin,[*8] L. Sinclair,[*17,*4] H. Suzuki,[*4] H. Takeda, [*4] J. Taprogge,[*18,*19] Zs. Vajta,[*14] H. Watanabe,[*20] and A. Yagi[*10]

It has long been a question whether there exist nuclei with static octupole deformation. The interaction between orbits with $\Delta J = \Delta I = 3$ is responsible for octupole correlations and the nuclei with such orbits close to the Fermi surface are expected to have large octupole correlations. The Possible nucleon numbers where this occurs are Z or $N \sim 34$, 56, 88, and 134. The neutron-rich Ba isotopes ($Z = 56$, $N \sim 88$) are expected to have large octupole correlations and are good candidates for octupole deformation. The even-even Ba isotopes have been studied from $A = 140$ to 148, and low-lying positive- and negative- parity octupole bands connected with enhanced E1 transition rates have been discovered[1]. Although the E1 rates should have a peak at $N = 88$, Ref.[1] revealed that $^{148}Ba_{92}$ has E1 rates as large as those of $^{144}Ba_{88}$, whereas $^{146}Ba_{90}$ has much smaller E1 rates. The theoretical calculations available so far provide different answers for octupole correlations in this region. For example, the microscopic-macroscopic method[2] predicts some β_3 values, whereas Hartree-Fock calculation[3] argues that there is no state with a dipole moment. Therefore, the experimental investigations of more neutron-rich Ba isotopes is required.

We performed β-γ spectroscopy on neutron-rich $Z \sim 56$ isotopes at RIBF. The neutron-rich isotopes were produced using in-flight fission of a 345MeV/nucleon ^{238}U beam bombarding a 3-mm thick Be target. The typical intensity of the primary ^{238}U beam was ~ 6 pnA during the two days of measurement for the Ba region. Fission fragments were identified by measuring the time-of-flight and magnetic rigidity in the second stage of BigRIPS and by measuring the energy loss by using the ion chamber at the final focal plane, F11. The secondary beam was implanted into an active stopper WAS3ABi[4], which consists of five layers of double-sided-silicon-strip detectors for ion-β correlation. The γ rays from the implanted nuclei were detected by using EURICA[5], an array of 12-cluster Ge detectors in which each cluster consists of 7 crystals.

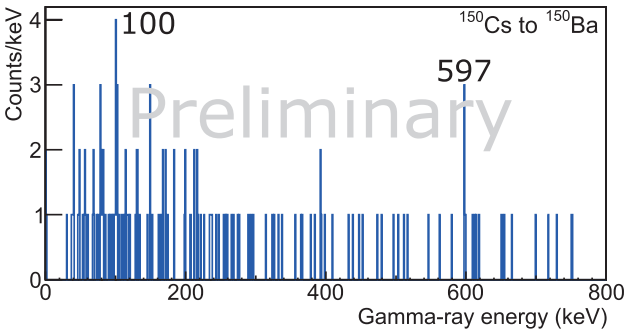

Fig. 1. Preliminary γ-ray energy spectra of the β decay from ^{150}Cs to ^{150}Ba. The time window is 200 ms from the ion implantation.

Figure 1 shows the γ-ray energy spectrum of β-decay events after the implantation of ^{150}Cs. Candidates for peaks are present at energies of 100 and 597 keV. The peaks at 100 keV can be interpreted as the 2^+ to 0^+ γ decays. The energies of the proposed 2^+ level of ^{150}Ba is lower than those in ^{148}Ba, indicating an increase in quadrupole deformation at ^{150}Ba. Test of the significance of the 597-keV peak and examination whether it can be a negative parity state with octupole collectivity are in progress.

*1 Center for Nuclear Study, The University of Tokyo
*2 Research Center for Nuclear Physics, Osaka University
*3 LPSC, Université Grenoble-Alpes, CNRS/IN2P3
*4 RIKEN Nishina Center
*5 Department of Physics, The University of Tokyo
*6 Department of Physics, Peking University
*7 Department of Physics, Tohoku University
*8 Department of Physics, University of Oslo
*9 School of Computing Engineering and Mathematics, University of Brighton
*10 Department of Physics, Osaka University
*11 ILL, Grenoble
*12 Department of Physics, Rikkyo University
*13 Department of Physics, University of Tsukuba
*14 MTA Atomki, Hungarian Academy of Science, Hungary
*15 Department of Display Engineering, Hoseo University
*16 Department of Physics, University of Surrey
*17 Department of Physics, University of York
*18 Instituto de Estructura de la Materia, CSIC
*19 Departamento de Física Teórica, Universidad Autónoma de Madrid
*20 Department of Physiscs, Beihang University

References

1) W. Urban *et. al.*: Nucl. Phys. A **613**, 107 (1997).
2) P. A. Butler *et. al.*: Nucl. Phys. A **533**, 249 (1991).
3) W. Nazarewicz *et. al.*: Nucl. Phys. A **429**, 269 (1984).
4) S. Nishimura *et. al.*: RIKEN APR 46, **182** (2013).
5) S. Nishimura: Nucl. Phys. News **22**, No.3 (2012).

Study of neutron-rich ^{142}Xe using β-decay spectroscopy

A. Yagi,[*1,*2] H. Kanaoka,[*1,*2] A. Odahara,[*1] R. Lozeva,[*3] C.-B. Moon,[*4] H. Nishibata,[*1,*2] T. Shimoda,[*1] P. Lee,[*5] R. Daido,[*1,*2] Y. Fang,[*1,*2] S. Nishimura,[*2] P. Doornenbal,[*2] G. Lorusso,[*2] P.-A. Söderström,[*2] T. Sumikama,[*2] H. Watanabe,[*6] T. Isobe,[*2] H. Baba,[*2] H. Sakurai,[*7,*2] F. Browne,[*8,*2] Z. Patel,[*9,*2] S. Rice,[*9,*2] L. Sinclair,[*10,*2] J. Wu,[*11,*2] Z.Y. Xu,[*12] R. Yokoyama,[*13] T. Kubo,[*2] N. Inabe,[*2] H. Suzuki,[*2] N. Fukuda,[*2] D. Kameda,[*2] H. Takeda,[*2] D.S. Ahn,[*2] D. Murai,[*14] F.L. Bello Garrote,[*15] J.M. Daugas,[*16] F. Didierjean,[*3] E. Ideguchi,[*17] T. Ishigaki,[*1,*2] H.S. Jung,[*18] T. Komatsubara,[*19] Y.K. Kwon,[*19] C.S. Lee,[*5] S. Morimoto,[*1,*2] M. Niikura,[*7] I. Nishizuka,[*20] and K. Tshoo[*19]

Study of neutron-rich $_{54}$Xe isotopes with N>82 is very important for understanding shape evolution from spherical to prolate shapes for nuclei in the mass region beyond the doubly-magic ^{132}Sn nucleus. In particular, the N=88 nucleus of ^{142}Xe is expected to have octupole collectivity in low spin region, because the $^{144}_{56}$Ba nucleus (N=88) is well known for having the large octupole deformation[1]. In this work, to reveal various nuclear structures of ^{142}Xe, the low-spin states in ^{142}Xe were investigated using β-decay spectroscopy of ^{142}I (Z=53).

Neutron-rich ^{142}I was produced by in-flight fission of a ^{238}U beam at the RI Beam Factory (RIBF) in RIKEN. Particle identification for the fission fragments was performed based on the TOF-$B\rho$-ΔE method using the BigRIPS and the ZeroDegree spectrometer[2]. Nuclei were implanted in the 5 double-sided Si-strip detectors (WAS3ABi[3]) at F11. Beta rays and γ rays were measured using the WAS3ABi and the EURICA array consisting of 12 Cluster-type Ge detectors[3], respectively. In order to measure the half-life of the excited states in the time range from a few hundred picoseconds to a few nanoseconds, a fast timing detector system, which consists of 18 $LaBr_3$ detectors for γ rays and 2 plastic scintillators for β rays, was installed[4].

Figure 1 shows the decay curve obtained by the time difference between the implantation of ^{142}I and the detection of β rays in WAS3ABi gated on the known 287-keV γ rays ($2^+ \rightarrow 0^+$) of ^{142}Xe[5]. The half-life of the β decay of ^{142}I was determined to be 229(3) ms, which

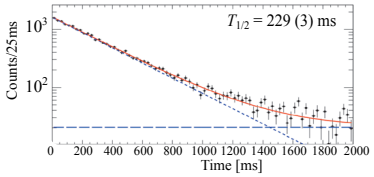

Fig. 1. Decay curve of the β decay gated on the 287-keV γ ray in ^{142}Xe.

was more accurate than the value of 222(12) ms in Ref. 6. Figure 2 shows the energy spectrum of γ-rays emitted after the β decay of ^{142}I. Three known transitions in ^{142}Xe are clearly observed with energies of 287, 403, and 971 keV. The B(E2) value of 0.6(3) e^{2}b^2 determined from the half-life of the 2_1^+ state, which was obtained as 0.22(9) ns by using the fast timing system, is in good agreement with the one obtained by Coulomb-excitation measurement of 0.7(1) e^{2}b^2 in Ref. 7. The deformation parameter β_2 was deduced to be 0.16(3) using the B(E2) value in this work. This indicates that the nucleus ^{142}Xe has a small prolate shape. The decay scheme after the β decay of ^{142}I was newly constructed in this work with 36 levels up to an excitation energy of 3.2 MeV. Two levels in this new decay scheme were assigned as candidates of the (1^-) and (3^-) states which are members of the K=0$^-$ octupole band, populated in high spin region by the spontaneous fission of ^{248}Cm in Ref. 5. A detailed analysis is in progress.

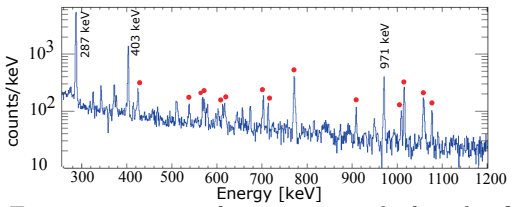

Fig. 2. Energy spectrum of γ-rays emitted after the β decay of ^{142}I. Peaks with closed circles indicate newly observed γ rays in ^{142}Xe.

*1 Department of Physics, Osaka University
*2 RIKEN Nishina Center
*3 IPHC/CNRS and University of Strasbourg
*4 Department of Display Engineering, Hoseo University
*5 Department of Physics, Chung-Ang University
*6 Department of Physics, Beihang University
*7 Department of Physics, University of Tokyo
*8 CEM, University of Brighton
*9 Department of Physics, University of Surry
*10 Department of Physics, University of York
*11 Department of Physics, Peking University
*12 Hong Kong University
*13 CNS, University of Tokyo
*14 Department of Physics, Rikkyo University
*15 Department of Physics, University of Oslo
*16 CEA/DAM
*17 RCNP, Osaka University
*18 Department of Physics, University of Notre Dame
*19 IBS
*20 Department of Physics, Tohoku University

References

1) W. Phillips et al., Phys. Rev. Lett. **57**, 3257 (1986).
2) N. Fukuda et al., Nucl. Instrum. Methods Phys. Res. B **317**, 323 (2013).
3) P.-A. Söderström et al., Nucl. Instrum. Methods Phys. Res. B **317**, 649 (2013).
4) P.-A. Söderström et al., JPS Conf. Proc. **1**, 013046 (2014).
5) W. Urban et al., Eur. Phys. J. A **16**, 303 (2003).
6) R. Kessler et al., GSI 2006-1, 154 (2006).
7) T. Kröll et al., Eur. Phys. J. A **150**, 127 (2007).

New neutron-deficient isotopes from ^{78}Kr fragmentation

B. Blank,[*1] P. Ascher,[*1] M. Gerbaux,[*1] T. Goigoux,[*1] J. Giovinazzo,[*1] S. Grévy,[*1] T. Kurtukian Nieto,[*1] C. Magron,[*1] J. Agramunt,[*2] A. Algora,[*2] V. Guadilla,[*2] A. Montaner-Piza,[*2] A.I. Morales,[*2] S.E.A. Orrigo,[*2] B. Rubio,[*2] D.S. Ahn,[*3] P. Doornebal,[*3] N. Fukuda,[*3] N. Inabe,[*3] G. Kiss,[*3] T. Kubo,[*3] S. Kubono,[*3] S. Nishimura,[*3] H. Sakurai,[*3] Y. Shimizu,[*3] C. Sidong,[*3] P.A. Söderström,[*3] T. Sumikama,[*3] H. Suzuki,[*3] H. Takeda,[*3] P. Vi,[*3] J. Wu,[*3] Y. Fujita,[*4] M. Tanaka,[*4] W. Gelletly,[*5] P. Aguilera,[*6] F. Molina,[*6] F. Diel,[*7] D. Lubos,[*8] G. de Angelis,[*9] D. Napoli,[*9] C. Borcea,[*10] A. Boso,[*11] R.B. Cakirli,[*12] E. Ganioglu,[*12] J. Chiba,[*13] D. Nishimura,[*13] H. Oikawa,[*13] Y. Takei,[*13] S. Yagi,[*13] K. Wimmer,[*13] G. de France,[*14] and S. Go [*15]

The most fundamental property of a nuclear species is its stability or instability with respect to the strong interaction, i.e. whether or not it is particle stable. On the proton-rich side of the valley of stability, if an isotope is sufficiently unbound, it may decay by one- or two-proton emission, the first being the decay mode for odd-Z (proton number) nuclei, whereas the second decay mode occurs for even-Z nuclei. Therefore, reaching the limits of stability allows one not only to test mass models predicting these limits, but also to search for new and exotic decay modes.

Thus two-proton (2p) radioactivity with half-lives of the order of milli-seconds was first observed in the region of iron-nickel-zinc with the known 2p emitters ^{45}Fe, ^{48}Ni, and ^{54}Zn[1]. Just above this region, ^{59}Ge, ^{63}Se, and ^{67}Kr were predicted to be possible new 2p emitters (see e.g.[2]).

In a recent experiment at the BigRIPS separator[3] at the RIKEN Nishina Center, we fragmented a primary ^{78}Kr beam at 345 MeV/A with an intensity of up to 250 pnA on a beryllium target (thickness 4975 μm). The BigRIPS separator was used to separate the isotopes of interest and to detect and identify them by means of the ΔE-ToF-Bρ method. After removal of scattered and incomplete events by means of cuts with beam-line detectors, clean identification spectra could be produced and three new isotopes, ^{63}Se, ^{67}Kr, and ^{68}Kr, were identified for the first time. In addition, ^{59}Ge was also observed, an isotope which was only very recently identified in an experiment at MSU and unreported at the time of the present experiment[4].

Figure 1 shows the identification plot from the present experiment. The three new isotopes and ^{59}Ge are indicated. The observed production rates exceed

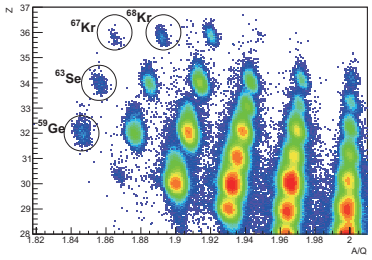

Fig. 1. Identification plot for isotopes produced in a recent BigRIPS experiment using ^{78}Kr fragmentation. New isotopes and possible 2p emitters are indicated in the figure.

rates at other facilities by at least two orders of magnitude. The present experiment thus allowed us to determine the production cross sections for the nuclei transmitted close to the central beam trajectory where the uncertainties due to the momentum distribution of the fragments and the separator transmission are minimal. Figure 2 presents these cross sections and compares them to predictions of EPAX3, an empirical parametrization of fragmentation cross sections[5]. Clearly, EPAX3 overestimates the experimental cross sections a lot.

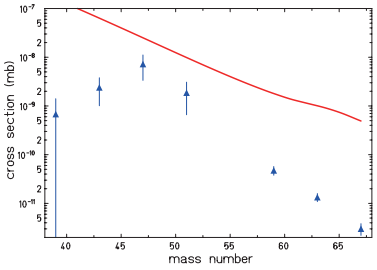

Fig. 2. Comparison of experimentally determined production cross sections for ^{78}Kr fragments with EPAX3 predictions.

The experimental data for the decay of these nuclei are presently under analysis. In particular, the question of whether some of them decay by 2p radioactivity is of prime interest.

*1 CENBG, U. Bordeaux-IN2P3, 33175 Gradignan, France
*2 IFIC, CSIC-U. Valencia, E-46071 Valencia, Spain
*3 RIKEN Nishina Center, Wako, Saitama 351-0198, Japan
*4 Dep. of Physics, Osaka University, Osaka 560-0043, Japan
*5 Dep. of Physics, U. Surrey, Guildford, UK
*6 CCHEN, Casilla 188-D, Santiago, Chile
*7 Inst. Nucl. Phys., U. Cologne, D-50937 Cologne, Germany
*8 Phys. Dep. E12, TU Munich, D-85748 Garching, Germany
*9 INFN, I-35020 Legnaro, Italy
*10 Inst. At. Phys., Bucharest-Margurele, Romania
*11 INFN & Dep. Phys., U. Padova, I-35131 Padova, Italy
*12 Dep. Phys., Istanbul University, Istanbul 34134, Turkey
*13 Dep. Phys., Tokyo University of Science, Chiba, Japan
*14 GANIL, BP 55027, F-14076 Caen, France
*15 Dep. Phys. & Astro., U. Tennessee, Knoxville, USA

References

1) B. Blank *et al.*, Rev. Prog. Phys. **71**, 046301 (2008).
2) B. A. Brown *et al.*, Phys. Rev. C **65**, 045802 (2002).
3) N. Fukuda *et al.*, Nucl. Inst. Meth. B **317**, 323 (2013).
4) A. A. Ciemny *et al.*, Phys. Rev. C **92**, 014622 (2015).
5) K. Sümmerer, Phys. Rev. C **86**, 014601 (2012).

Second campaign of the SEASTAR project

P. Doornenbal,[*1] A. Obertelli,[*1,*2] T. Ando,[*1,*3] T. Arici,[*4] G. Authelet,[*1,*2] H. Baba,[*1] A. Blazhev,[*5] F. Browne,[*6] A.M. Bruce,[*6] D. Calvet,[*1,*2] R.J. Carroll,[*7] F. Château,[*1,*2] S. Chen[*1] L.X. Chung,[*8] A. Corsi,[*1,*2] M.L. Cortés,[*9,*4] A. Delbart,[*1,*2] M. Dewald,[*5] B. Ding,[*10] F. Flavigny,[*11] S. Franchoo,[*11] J.-M. Gheller,[*1,*2] A. Giganon,[*1,*2] A. Gillibert,[*1,*2] M. Górska,[*4] A. Gottardo,[*11] A. Jungclaus,[*12] V. Lapoux,[*1,*2] J. Lee,[*13] M. Lettmann,[*9] B.D. Linh,[*8] J. Liu,[*13] Z. Liu,[*10] C. Lizarazo,[*4,*9] S. Momiyama,[*1,*3] K. Moschner,[*5] T. Motobayashi,[*1] M. Nagamine,[*1,*3] N. Nakatsuka,[*1,*14] M. Niikura,[*1,*3] C. Nita,[*15] C. Nobs,[*6] L. Olivier,[*11] Z. Patel,[*7] N. Paul,[*1,*2] Zs. Podolyak,[*7] J.-Y. Roussé,[*1,*2] M. Rudigier,[*7] T. Saito,[*1,*3] H. Sakurai,[*1,*3] C. Santamaria,[*1,*2] C.M. Shand,[*7] P.-A. Söderström,[*1] I. Stefan,[*11] D. Steppenbeck,[*1] R. Taniuchi,[*1,*3] T. Uesaka,[*1] V. Vaquero,[*12] V. Werner,[*9] K. Wimmer,[*1,*3] Z. Xu,[*13] and the SEASTAR Collaboration

Within the second SEASTAR (Shell Evolution And Search for Two-plus energies At the RIBF) campaign, nuclei "North-East" of the doubly-magic nucleus ^{78}Ni were studied during 9 days of beam time. The experiment was performed in May, 2015 using the DALI2 γ-ray spectrometer[1] and the MINOS liquid hydrogen target system[2]. The set-up was employed at the F8 focus following the BigRIPS[3] fragment separator and reaction products were identified with ZeroDegree[3]. Specifically, in the second campaign 2_1^+ and 4_1^+ energies of ^{82,84}Zn, ^{86,88}Ge, ^{88,90,92,94}Se, ^{96,98,100}Kr, ^{110}Zr, and ^{112}Mo were measured with five different secondary beam settings via knockout reactions.

To produce the secondary beams of interest, a ^{238}U primary beam was accelerated to 345 MeV/nucleon and impinged on a 3-mm thick Be target at the entrance of BigRIPS. The primary beam intensity was about 30 particle-nA. In the five employed settings, BigRIPS was tuned for beam cocktails focusing on ^{85}Ga, ^{89}As, ^{95}Br, ^{101}Rb, and ^{111}Nb ions to enable $(p, 2p)$ and other reactions to populate the 2_1^+ and 4_1^+ states. The particle identification was obtained by the $B\rho$-ΔE-TOF method, employing standard BigRIPS/ZeroDegree detectors. In front of the 100-mm-long MINOS target, beam energies were around 260–270 MeV/nucleon, and total intensities in the order of several kHz. At the end of ZeroDegree, the ions were stopped in the center of the EURICA spectrometer[4] to search for new isomeric decays.

An example for the quality of the Doppler corrected spectra obtained from DALI2 after reconstructing the vertex position with MINOS is given in Fig. 1 for ^{92}Se following $1p1n$-knockout reactions. For this nucleus, an isomeric state was previously observed[5]. However, the $E(2_1^+)$ could not be assigned. Conversely, the 539-keV transition in the in-beam spectrum clearly possesses the highest intensity, and therefore must be the $2_1^+ \rightarrow 0_{gs}^+$ transition. Several other transitions were observed and confirmed in the isomer spectrum of EURICA. In total, data were collected for about 6.5 days, while secondary beam production and user tuning took about 2.5 days for the five applied settings. All 2_1^+ and 4_1^+ energies of interest were observed. Currently, the data and many by-products are under analysis by several groups affiliated to the SEASTAR collaboration.

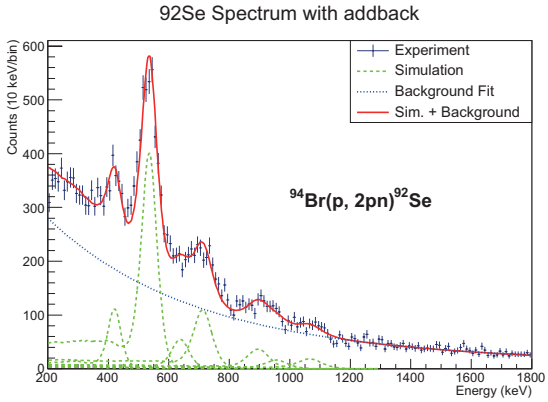

Fig. 1. Doppler-corrected spectrum of ^{92}Se following $1p1n$-knockout reactions from a ^{94}Br secondary beam. The spectrum has been fitted with a double-exponential background (blue dotted) and simulated response functions (green dashed).

*1 RIKEN Nishina Center
*2 CEA Saclay
*3 Department of Physics, The University of Tokyo
*4 GSI Helmholtzzentrum Darmstadt
*5 Institute of Nuclear Physics, University of Cologne
*6 School of Computing Engineering and Mathematics, University of Brighton
*7 Department of Physics, University of Surrey
*8 INST Hanoi
*9 Institut für Kernphysik, TU Darmstadt
*10 Institute of Modern Physics, Chinese Academy of Sciences
*11 IPN Orsay
*12 Instituto de Estructura de la Materia, CSIC
*13 Department of Physics, The University of Hong Kong
*14 Department of Physics, Kyoto University
*15 IFIN-HH

References

1) S. Takeuchi et al.: Nucl. Instr. Meth. A 763, 596 (2014).
2) A. Obertelli et al.: Eur. Phys. J. A 50, 8 (2014).
3) T. Kubo et al.: Prog. Theor. Exp. Phys. 2012, 03C003.
4) P.-A. Söderström et al.: Nucl. Instr. Meth. B 317, 649 (2013).
5) D. Kameda et al.: Phys. Rev. C 86, 054319 (2012).

Intermediate-energy Coulomb excitation of ^{77}Cu

E. Sahin,[*1] V. Modamio,[*1] Z. Y. Xu,[*2] F. Bello,[*1] K. K. Hadyńska-Klęk,[*1] P. Doornenbal,[*3] S. Chen,[*3,*4] A. Jungclaus,[*5] R. Taniuchi,[*6] and the NP1406-RIBF126 collaboration

The present experimental study on ^{77}Cu has been carried out at RI Beam factory (RIBF) of the RIKEN Nishina Center[1]. It will complement our previous study of ^{77}Cu via beta decay of ^{77}Ni at RIKEN within the EURICA campaign. The low-lying states in ^{77}Cu were identified as particle-core excitations through the comparison to the large scale Monte Carlo Shell Model (MCSM) calculations[2,3]. An almost unique way to characterize the states predicted as collective in the calculations is to measure the transition probabilities, i.e. B(E2) strengths. Hence the following Coulomb excitation experiment was performed to study the collective properties of low-lying states in ^{77}Cu. The characterization of such states and in particular the mixing of both collective and single-particle configurations will provide significant information on the shell structure close to ^{78}Ni. A Coulomb excitation measurement of the states due to the proton-core excitations in the case of ^{77}Cu nucleus will also provide an estimation of the collectivity of the 2^+ state in th even-even ^{76}Ni "core".

Exotic secondary beam particles were produced by induced fission of the ^{238}U beam on a 3-mm thick ^{9}Be target. The uranium beam was accelerated to an energy of 345 MeV/nucleon with an average beam intensity of 20 pnA. Fission products were selected and transported by the BigRIPS fragment separator. Coulomb excitation of the fragments was performed on a 900-mg/cm^2 thick ^{197}Au target, mounted in front of the Zero Degree Spectrometer. The DALI2 NaI array was used to detect de-excitation γ ray measured in coincidence with beam-like particles identified in the Zero Degree Spectrometer (ZDS). Two different beam settings of the BigRIPS fragment separator have been employed during the beam time. In the first one the central trajectory was set at ^{73}Cu as a test case to perform the absolute cross-section measurement technique (See Ref.[4] for details). In the second setting, the momentum distribution of the incoming fragments were centered for ^{77}Cu. Figures 1 and 2 show the preliminary particle identification (PID) spectra for ZDS, i.e. after the Coulomb excitation target at F8 position. Note that ^{72}Ni was observed in the first setting which will allow us to obtain the transition strength of the 0_1^+ to 2_1^+ transition and to fill the gap in the seniority parabola of the Ni chain from N=40 to N=46. Data analysis in order to obtain doppler-corrected γ-ray spectra for the extraction of the Coulomb excitation cross sections is still ongoing.

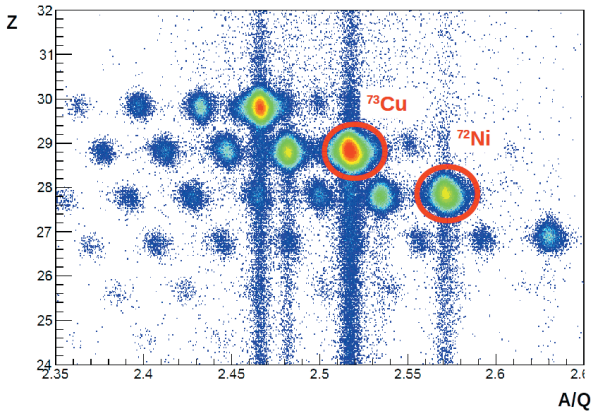

Fig. 1. Setting 1: ^{73}Cu and ^{72}Ni are identified in the Z (atomic number) versus A/Q (mass-to-charge number) plot for ZDS.

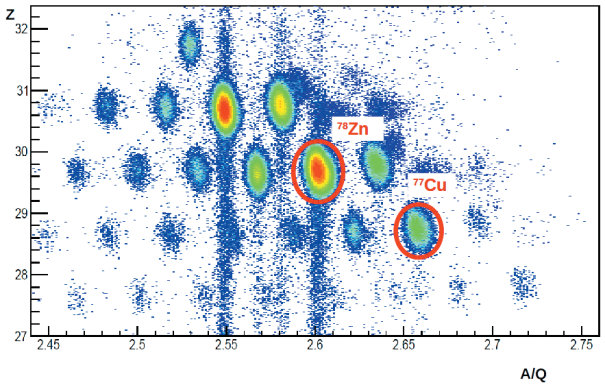

Fig. 2. Setting 2: ^{77}Cu and ^{78}Zn are identified in the Z (atomic number) versus A/Q (mass-to-charge number) plot for ZDS.

*1 University of Oslo, Department of Physics
*2 University of Hong Kong
*3 RIKEN Nishina Center
*4 Peking University
*5 Instituto de Estructura de la Materia, CSIC
*6 University of Tokyo

References

1) T. Onishi *et al.*, J. Phys. Soc. Jpn. **79**, 073201 (2010).
2) Y. Tsunoda, T. Otsuka, N. Shimizu, M. Honma, and Y. Utsuno, Phys. Rev. C **89**, 031301(R) (2014).
3) Y. Tsunoda et al., private communication.
4) P. Doornenbal et al., Phys. Rev. C **90**, 061302(R) (2014).

Coulomb excitation of ^{136}Te studied with the DALI2 spectrometer

V. Vaquero,[*1] A. Jungclaus,[*1] P. Doornenbal,[*2] E. Sahin,[*3] Z.Y. Xu,[*4] S. Chen,[*2,*5] Y. Shiga,[*6] D. Steppenbeck,[*2] R. Taniuchi,[*2,*7] and the NP1306-RIBF98R1 collaboration

In April 2015 an experiment was performed at the RIBF of the RIKEN Nishina Center to study the excitation and decay of a second excited 2^+ state at an excitation energy around 1.5-1.6 MeV in the nucleus ^{136}Te which is predicted by theoretical calculations to be of mixed-symmetry character. The aim was to explore for the first time the potential of the Coulomb excitation technique at relativistic energies for the study of mixed-symmetry states (MSS) in radioactive nuclei. A second aspect of the experiment was to perform a model analysis with exceptional high statistics for the determination of the B(E2; $2_1^+ \rightarrow 0_1^+$) value from measured differential cross sections after Coulomb excitation at relativistic energies. Based on our recent experiences with the analysis of the first Coulex experiments with heavy beams at energies around 130-150 MeV/u performed at RIKEN[1] it became highly desirable to study in detail all systematic uncertainties involved in such an analysis to set the standards for the routinely use of this technique in the future.

The ^{136}Te ions were produced in the projectile fission of a 345-MeV/u ^{238}U beam on a 4-mm ^{9}Be target. The nuclei of interest were separated and identified during their flight through BigRIPS and hit a secondary gold target at the F8 focal plane in which the Coulomb excitation took place. The γ radiation emitted in the decay of the excited states was detected in the DALI2 spectrometer in coincidence with ^{136}Te ions identified in the ZeroDegree (ZD) spectrometer. Over the last months work has been devoted to improve the particle identification (PID) in both the BigRIPS and ZD spectrometer. Preliminary PID plots are shown in Fig.1 while a γ-ray spectrum measured in coincidence with ^{136}Te ions detected in both BigRIPS and ZD is shown in Fig. 2. From the latter figure it is evident that indeed high statistics was accumulated for the Coulomb excitation of the first 2^+ state in ^{136}Te which will allow for a detailed study of the procedure employed to deduce B(E2) values in this type of experiment. Different theoretical calculations[2,3] predict a significant probability for the Coulomb excitation of a second 2^+ state. Therefore, a thorough search for additional lines in the γ-ray spectra obtained in the present experiment will be performed in the near future.

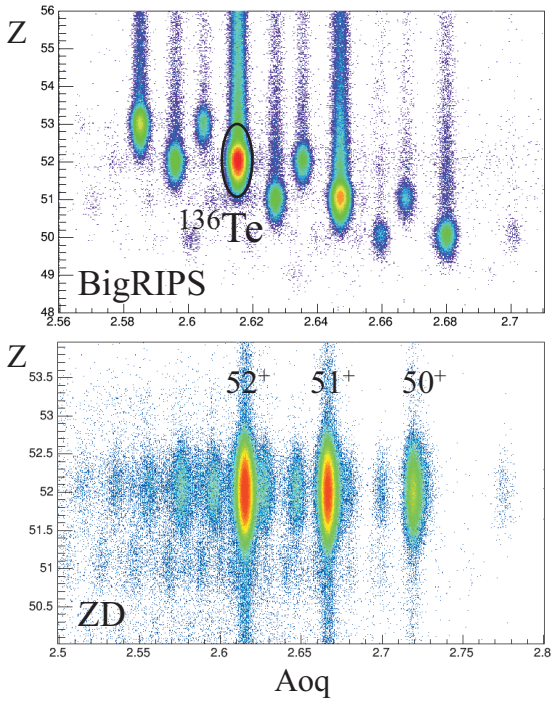

Fig. 1. PID obtained for the BigRIPS and the ZD spectrometer. The ZD plot was obtained requiring the identification of ^{136}Te ions in BigRIPS. Note that the ^{136}Te ions are observed in different charge states in ZD.

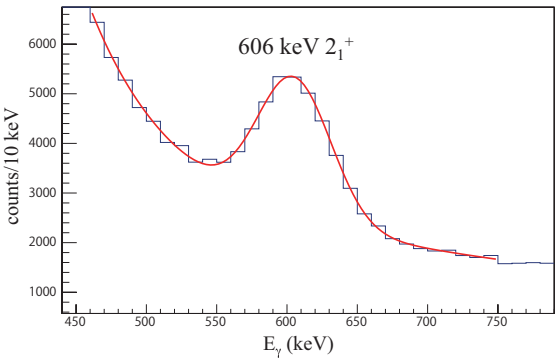

Fig. 2. Gamma-ray spectrum in coincidence with the ^{136}Te ions detected in the ZD spectrometer.

*1 Instituto de Estructura de la Materia, CSIC
*2 RIKEN Nishina Center
*3 Department of Physics, University of Oslo
*4 Department of Physics, University of Hong Kong
*5 State Key Laboratory of Nuclear Physics and Technology, Peking University
*6 Department of Physics, Rikkyo University, Tokyo
*7 Department of Physics, University of Tokyo

References

1) P. Doornenbal et al.: Phys. Rev. C **90**, 061302(R) (2014).
2) N. Shimizu et al.: Phys. Rev. C **70**, 054313 (2004).
3) A.P. Severyukhin et al.: Phys. Rev. C **90**, 011306(R) (2014).

Experimental study of isoscalar and isovector dipole resonances in neutron-rich oxygen isotopes

N. Nakatsuka,[*1,*2] H. Baba,[*2] N. Aoi,[*10] T. Aumann,[*3] R. Avigo,[*5,*14] S. R. Banerjee,[*12] A. Bracco,[*5,*14] C. Caesar,[*3] F. Camera,[*5,*14] S. Ceruti,[*5,*14] S. Chen,[*13,*2] V. Derya,[*4] P. Doornenbal,[*2] A. Giaz,[*5,*14] A. Horvat,[*3] K. Ieki,[*11] N. Imai,[*7] T. Kawabata,[*1] K. Yoneda,[*2] N. Kobayashi,[*8] Y. Kondo,[*9] S. Koyama,[*8] M. Kurata-Nishimura,[*2] S. Masuoka,[*7] M. Matsushita,[*7] S. Michimasa,[*7] B. Millon,[*5] T. Motobayashi,[*2] T. Murakami,[*1] T. Nakamura,[*9] T. Ohnishi,[*2] H. J. Ong,[*10] S. Ota,[*7] H. Otsu,[*2] T. Ozaki,[*9] A. T. Saito,[*9] H. Sakurai,[*2,*8] H. Scheit,[*3] F. Schindler,[*3] P. Schrock,[*3] Y. Shiga,[*11,*2] M. Shikata,[*9] S. Shimoura,[*7] D. Steppenbeck,[*2] T. Sumikama,[*6] I. Syndikus,[*3] H. Takeda,[*2] S. Takeuchi,[*2] A. Tamii,[*10] R. Taniuchi,[*8] Y. Togano,[*9] J. Tscheuschner,[*3] J. Tsubota,[*9] H. Wang,[*2] O. Wieland,[*5] K. Wimmer,[*8] Y. Yamaguchi,[*7] and J. Zenihiro[*2]

Giant resonance is one of the most important phenomena for understanding quantum many-body systems. Neutron-rich nuclei are predicted to have exotic giant resonances owing to their smaller neutron separation energy and excess neutrons. One of the exotic giant resonances in neutron-rich nuclei is a electric dipole resonance found at excitation energies lower than 10 MeV[1]. The identification of the isovector or isoscalar resonances is of great interest to understand the nature of these resonances. In order to study the relationship between the isovector and isoscalar dipole resonances in neutron-rich oxygen isotopes, we performed an experiment at RIBF and measured the dipole resonances of the neutron-rich nuclei ^{20}O, ^{22}O, and ^{24}O. These beams were produced via projectile fragmentation of a 345 MeV/nucleon ^{48}Ca beam on ^{9}Be targets with thicknesses of 2.8 g/cm^2, 2.8 g/cm^2, and 2.2 g/cm^2. The γ rays from the excited beam particles were detected with large volume $LaBr_3$ crystals from INFN Milano[2] in combination with DALI2[3]. Two different targets, 5 g/cm^2 natural gold target for coulomb excitation and 300 mg/cm^2 liquid helium target for inelastic α particle scattering, were used to obtain the isovector and isoscaler dipole strengths, respectively.

A preliminary doppler-corrected γ-ray spectrum of $\alpha(^{20}\mathrm{O},^{20}\mathrm{O}\gamma)\alpha$ reaction is shown in Fig. 1, and the spectrum of $^{\mathrm{nat}}\mathrm{Au}(^{20}\mathrm{O},^{20}\mathrm{O}\gamma)^{\mathrm{nat}}\mathrm{Au}$ reaction is shown in Fig. 2. A clear difference is observed between the spectrum of the different target. This suggests that the comparison of the coulomb excitation and the inelastic α particle scattering is actually effective to distinguish the isovector and isoscaler resonances. Further analysis is in progress to search for the isovector and isoscalar nature of the excited states.

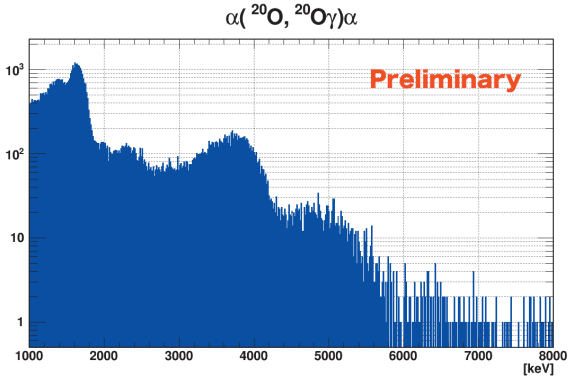

Fig. 1. Preliminary doppler-corrected γ-ray spectrum of $\alpha(^{20}\mathrm{O},^{20}\mathrm{O}\gamma)\alpha$ reaction

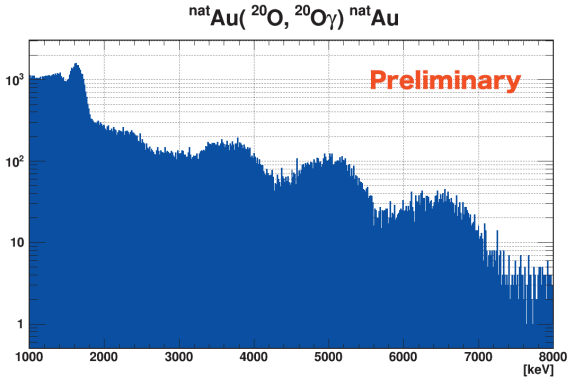

Fig. 2. Preliminary doppler-corrected γ-ray spectrum of $^{\mathrm{nat}}\mathrm{Au}(^{20}\mathrm{O},^{20}\mathrm{O}\gamma)^{\mathrm{nat}}\mathrm{Au}$ reaction

*1 Department of Physics, Kyoto University
*2 RIKEN Nishina Center
*3 Institut für Kernphysik, Technische Universität Darmstadt
*4 Institut für Kernphysik, Universität zu Köln
*5 Istituto Nazionale di Fisica Nucleare Milan
*6 Department of Physics, Tohoku University
*7 Center for Nuclear Study, The University of Tokyo
*8 Department of Physics, The University of Tokyo
*9 Department of Physics, Tokyo Institute of Technology
*10 Research Center for Nuclear Physics, Osaka University
*11 Department of Physics, Rikkyo University
*12 Variable Energy Cyclotron Centre, The Indian Department of Atomic Energy
*13 School of Physics, Peking University
*14 University of Milan

References

1) V. Derya et al., J. Phys. Conf. Ser. **366**, 012012 (2012).
2) A. Giaz et al., Nucl. Instrum. Methods Phys. Res., Sec. A **729**, 910 (2013).
3) S. Takeuchi et al., Nucl. Instrum. Methods Phys. Res., Sec. A **763**, 596 (2014).

Study of the pygmy dipole resonance of ^{132}Sn and ^{128}Sn in inelastic α-scattering

J. Tscheuschner,[*1,*2] T. Aumann,[*1] D. S. Ahn,[*2] R. Avigo,[*3,*4] H. Baba,[*2] K. Boretzky,[*5] A. Bracco,[*3,*4] C. Caesar,[*5] A. Camera,[*3,*4] S. Chen,[*2,*6] V. Derya,[*7] P. Doornenbal,[*2] J. Endres,[*7] N. Fukuda,[*2] U. Garg,[*8] A. Giaz,[*3,*4] M. N. Harakeh,[*9] M. Heil,[*5] A. Horvat,[*1] K. Ieki,[*10] N. Imai,[*11] N. Inabe,[*2] N. Kalantar-Nayestanaki,[*9] N. Kobayashi,[*11] Y. Kondo,[*12] S. Koyama,[*11] T. Kubo,[*2] I. Martel,[*13] M. Matsushita,[*14] B. Million,[*15] T. Motobayashi,[*2] T. Nakamura,[*12] N. Nakatsuka,[*2,*16] M. Nishimura,[*2] S. Nishimura,[*2] S. Ota,[*14] H. Otsu,[*2] T. Ozaki,[*12] M. Petri,[*1] R. Reifarth,[*17] D. Rossi,[*1] A. T. Saito,[*12] H. Sakurai,[*2,*11] D. Savran,[*5] H. Scheit,[*1] F. Schindler,[*1] P. Schrock,[*1] D. Semmler,[*1] Y. Shiga,[*2,*10] M. Shikata,[*12] Y. Shimizu,[*2] H. Simon,[*5] D. Steppenbeck,[*2] H. Suzuki,[*2] T. Sumikama,[*18] D. Symochko,[*1] I. Syndikus,[*1] H. Takeda,[*2] S. Takeuchi,[*2] R. Taniuchi,[*11] Y. Togano,[*12] J. Tsubota,[*12] H. Wang,[*2] O. Wieland,[*3] K. Yoneda,[*2] J. Zenihiro,[*2] and A. Zilges[*7]

In neutron-rich nuclei, the pygmy dipole resonance can be visualized as a vibration of excess neutrons against an isospin symmetric core in the nucleus, which corresponds to a dipole mode. Ongoing to the nature of the resonance, the phenomenon should be a function of the neutron-skin thickness and neutron excess. As the experimental data for this dipole mode are rare, even for stable nuclei[1], interesting open questions remain. One of them is the isospin character of the low-lying dipole strength. In an experiment with stable ^{124}Sn[2], it has been realized that a large fraction of the pygmy strength is of isoscalar character. However, significant differences in the strength distribution with photo-excitation have been observed.

In November 2014, an experiment to investigate the isoscalar character of the pygmy dipole resonance in ^{128}Sn and ^{132}Sn was performed with inelastic α-scattering at RIKEN. The isotopes were produced with a high-intensity primary ^{238}U beam at 345 MeV/u impinging on a beryllium target. The secondary beam of approximately 200 MeV/u was directed towards the liquid helium target, with a thickness of approximately 300 mg/cm^2. At the target position, the emitted γ-rays were measured by 8 large-volume 3.5" $\times$ 8"$LaBr_3$:Ce crystals from the HECTOR-array at INFN Milano[3] and 95 large-volume NaI DALI2[4] crystals.

The particle identification involved a combination of energy loss, magnetic rigidity, and time-of-flight measurements using the BigRIPS and the ZeroDegree spectrometer[5]. The registered hits in the γ-array are selected within a time window to suppress noise stemming from particle hits and the background. As a result, the preliminary energy plot for the γ-rays measured with the crystals from the HECTOR-array, emitted by the excited ^{132}Sn ions, is shown in Fig. 1. The peak at about 4 MeV corresponds to the 2^+ state, which is the lowest excited state in the isotope..

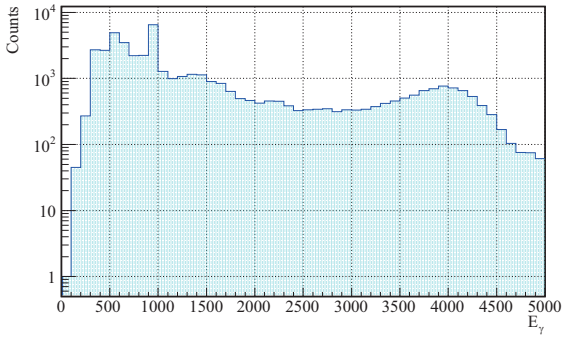

Fig. 1. Doppler-corrected γ-energy spectra measured using crystals from the HECTOR-array, gated on incoming and outgoing ^{132}Sn ions. The 2^+ state at 4 MeV can be identified.

With further investigation of the γ-energy spectra, the strength of the (isoscalar) pygmy dipole resonances can be determined. In addition, the obtained information will allow the isovector and isoscalar parts of the pygmy dipole resonance to be separated in data of experiments already performed at GSI Darmstadt with the R^{3}B setup.

*1 Institut für Kernphysik, TU Darmstadt
*2 RIKEN Nishina Center
*3 INFN sezione di Milano
*4 Dipartimento di Fisica, Universita degli studi di Milano
*5 GSI Helmholtzzentrum Darmstadt
*6 School of Physics, Peking University
*7 Institute für Kernphysik, Universität zu Köln
*8 Department of Physics, University of Notre Dame
*9 KVI-CART Groningen
*10 Department of Physics, Rikkyo University
*11 Department of Physics, University of Tokyo
*12 Department of Physics, Tokyo Institute of Technoloy
*13 Departamento de Fisica Aplicada, Universidad de Huelva
*14 Center for Nuclear Study, University of Tokyo
*15 VECC India
*16 Department of Physics, Kyoto University
*17 Institut für Kernphysik, Goethe Universität Frankfurt
*18 Department of Physics, Tohoku University

References

1) D. Savran et al., Prog. Part. Nucl. Phys. **70**, 210 (2013).
2) J. Endres et al., Phys. Rev. Lett. **105**, 212503 (2010).
3) A. Giaz et al., NIM A**729**, 910 (2013).
4) S. Takeuchi et al., NIM A **763**, 596 (2014).
5) T. Kubo et al., Prog. Theor. Exp. Phys. 03C003 (2012).

E1 strength around threshold in ^{70}Ni†

R. Avigo,[*1,*2] O. Wieland,[*1] A. Bracco,[*1,*2] F. Camera,[*1,*2] H. Baba,[*3] N. Nakatsuka,[*4] P. Doornenbal,[*3] Y. Togano,[*5] J. Tscheuschner,[*6] T. Aumann,[*6] G. Benzoni,[*1] N. Blasi,[*1] K. Boretzky,[*7] S. Brambilla,[*1] S. Ceruti,[*1,*2] S. Chen,[*8] F.C.L. Crespi,[*1,*2] N. Fukuda,[*3] A. Giaz,[*1,*2] K. Ieki,[*9] N. Kobayashi,[*10] Y. Kondo,[*5] S. Koyama,[*10] T. Kubo,[*3] S. Leoni,[*1,*2] M. Matsushita,[*11] B. Million,[*1] A.I. Morales,[*1,*2] T. Motobayashi,[*3] T. Nakamura,[*5] M. Nishimura,[*3] S. Nishimura,[*3] H. Otsu,[*3] T. Ozaki,[*5] L. Pellegri,[*1,*2] A. Saito,[*5] H. Sakurai,[*3] H. Scheit,[*6] P. Schrock,[*6] Y. Shiga,[*3] M. Shikata,[*5] D. Steppenbeck,[*3] T. Sumikama,[*12] S. Takeuchi,[*3] R. Taniuchi,[*10] J. Tsubota,[*5] H. Wang[*3] and K. Yoneda[*3]

The electric dipole response of atomic nuclei is presently attracting increasing attention from the nuclear physics research community. In particular, the E1 strength in neutron-rich nuclei, located at around one particle separation energy (6-12 MeV energy range) is the object of a large effort[1,2] (and references therein). In this energy region structures and accumulations of the E1 strength were measured in a variety of nuclei along along the entire valley of stability, but very scarce data for exotic nuclei are available. These structures are commonly called pygmy dipole resonance (PDR) as they lie at energies below the giant dipole resonance (GDR) and have lesser strength. They are at the center of the scientific debate as the strength is connected to the neutron skin thickness[3], the symmetry energy term of the nuclear equation of state and has important astrophysical implications in explosive nucleosynthesis scenarios.

In order to understand better the characteristics of this PDR strength it is important to study an isotopic chain of a nucleus with increasing neutron number. As the pygmy dipole strength distribution in ^{68}Ni around the threshold has recently been observed,[1,2,3] a high-intensity and high-resolution experiment was performed on ^{70}Ni at RIKEN Radioactive Isotope Beam Factory (RIBF).

A ^{238}U primary beam was accelerated up to an energy of 345 *A*MeV and made to impinge on a thick rotating Be production target. In BigRIPS[4] the Bρ-ΔE- Bρ method was applied to select a secondary beam of ^{70}Ni (30 kcps with 40% purity at a beam energy of 260 *A*MeV). The ^{70}Ni isotope was incident on a 2 g/cm^2 gold secondary target. Reaction products from the secondary target were identified using the ZeroDegree Spectrometer in the large acceptance mode, while the scattering angles were determined using parallel plate avalanche counters.

In order to detect gamma rays from the decay of different nuclear levels, the reaction target was surrounded by a combination of eight large-volume 3.5'' x 8'' LaBr3:Ce detectors (providing high efficiency and resolution[5]) mounted at 30° in the forward direction and of the DALI2 array[6] (consisting of 96 NaI(TI) crystals) at mid and backward angles.

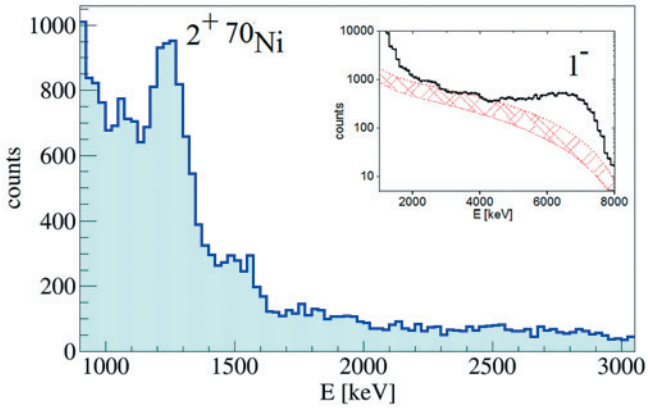

Fig. 1. $2^+ \rightarrow 0^+_{gs}$ E2 transition in ^{70}Ni. In the inset, high-energy γ ray spectra are shown till 8 MeV. The shaded area is the contribution from the thick gold target, deduced from the measured spectra at backward angles and the projectile GDR–tail calculated with a statistical model.

Figure 1 shows the first outcome of the experiment, which is the observation of the first 2+ state of ^{70}Ni. It is planned that the $2^+ \rightarrow 0^+_{gs}$ B(E2) transition strength will be determined. In the inset an important unresolved E1 contribution between 5 and 8 MeV is observed. The E1 character is deduced from angular distribution measurements. This issue will be under investigation in near future. In order to determine the E1 strength distribution in ^{70}Ni an absolute efficiency measurement of the detectors at NewSUBARU is planned in 2016. The analysis of the relation between the strength and the neutron skin in ^{70}Ni together with the data of the measured ^{68}Ni will make an important contribution to the understanding of the features of the pygmy strength.

† Experiment NP1306 -RIBF51R1, November 2014

*1 INFN sezione di Milano
*2 University of Milano
*3 RIKEN Nishina Center
*4 Kyoto University
*5 Department of Physics, Tokyo Institute of Technology
*6 TU Darmstadt
*7 GSI Darmstadt
*8 Peking University
*9 Rikkyo University
*10 University of Tokyo
*11 CNS, University of Tokyo
*12 Tohoku University

References

1) O. Wieland et al. PRL **102,** 092502 (2009).
2) D. Rossi et al. PRL **111**, 242503 (2013).
3) A. Carbone et al. Phys. Rev. C **81,** 041301(R) (2010).
4) T. Kubo et al. Prog. Theor. Exp. Phys. 03C003 (2012).
5) A. Giaz et al. NIM A**729,** 910 (2013).
6) S. Takeuchi et al. NIM A**763**, 596 (2014).

In-beam γ-ray spectroscopy of ^{55}Sc

D. Steppenbeck,[*1] S. Takeuchi,[*2] N. Aoi,[*1,*3] P. Doornenbal,[*1] M. Matsushita,[*4] H. Wang,[*1] H. Baba,[*1] S. Go,[*5] J. Lee,[*1,*6] K. Matsui,[*7] S. Michimasa,[*4] T. Motobayashi,[*1] D. Nishimura,[*1,*8] H. Sakurai,[*1,*7] Y. Shiga,[*1,*9] P.-A. Söderström,[*1] T. Sumikama,[*1] R. Taniuchi,[*1,*7] J. J. Valiente-Dobón,[*10] and K. Yoneda[*1]

The study of the evolution of shell structure has played an important role in the fields of experimental and theoretical nuclear physics over recent decades. On the experimental front, significant advances have been made owing to progress in the production rates of exotic nuclei at radioactive isotope beam facilities worldwide. A few noteworthy examples of shell evolution include the onset of the neutron magic number $N = 16$ in exotic oxygen[1,2], and the weakening of the traditional magic number $N = 28$ approaching the neutron drip line[3]. Moreover, in the pf shell, the onset of a new subshell closure at $N = 32$ has been reported along the Ca[4,5], Ti[6,7], and Cr[8,9] isotopic chains owing to the migration of the $\nu f_{5/2}$ orbital as protons are removed from the $\pi f_{7/2}$ state[10]. More recently, the robustness of the $N = 32$ subshell closure below the $Z = 20$ core, namely, in K[11] and Ar[12] isotopes, has been highlighted. An additional subshell closure was predicted[13] to occur at $N = 34$ in Ti and Ca isotopes; however, the experimental data provided no evidence for this shell gap in ^{56}Ti[7,14]. Later work on the spectroscopy of ^{54}Ca did, however, indicate the presence of a sizable subshell closure at $N = 34$ from the energy of the first 2^+ level[15]. The present work on ^{55}Sc aims at the study of the significance of the $N = 34$ gap along the $Z = 21$ isotopic chain, and the evolution of this neutron magic number as protons are added to the $\pi f_{7/2}$ orbital.

The experiment was performed using ^{70}Zn^{30+} ions with the BigRIPS separator to provide a fast radioactive beam—optimized for the transmission of ^{55}Sc—that was focused on a 10-mm-thick ^{9}Be reaction target at the eighth focal plane of the spectrometer. The beam constituents were identified on an event-by-event basis using particle magnetic rigidities ($B\rho$), times of flight (T), and energy losses in an ionization chamber (ΔE)[16]. The target at F8 was surrounded by the DALI2 γ-ray detector array to measure transitions from nuclear excited states populated by the reactions; ions emerging from the target position were identified by the ZeroDegree spectrometer using the same general ($B\rho$–T–ΔE) techniques as for BigRIPS.

*1 RIKEN Nishina Center
*2 Dept of Physics, Tokyo Institute of Technology
*3 RCNP, Osaka University
*4 Center for Nuclear Study, University of Tokyo
*5 Dept of Science and Engineering, University of Tennessee
*6 Dept of Physics, University of Hong Kong
*7 Dept of Physics, University of Tokyo
*8 Dept of Physics, Tokyo University of Science
*9 Dept of Physics, Rikkyo University
*10 Laboratori Nazionali di Legnaro

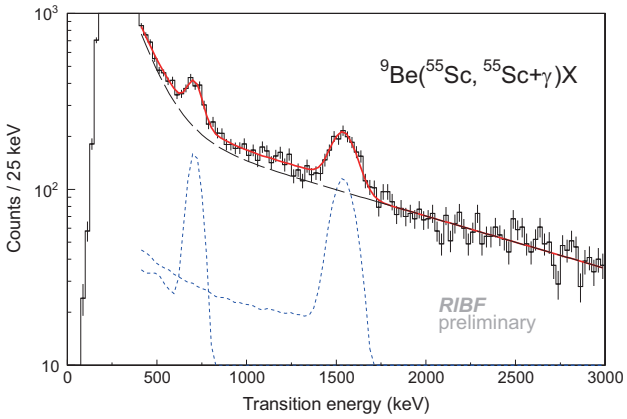

Fig. 1. (colour) Doppler-corrected γ-ray energy spectrum deduced from the inelastic scattering of ^{55}Sc on a ^{9}Be target. The black dashed line is a double exponential fit to the background and the blue dashed lines are the results of GEANT4 simulations; the solid red line is the total (sum) fit. Results are preliminary.

The γ-ray energy spectrum deduced from the ^{9}Be(^{55}Sc, ^{55}Sc+γ)X inelastic scattering reaction is presented in Fig. 1. This work was previously reported, amongst other results, in Ref.[17]. No results on excited states in ^{55}Sc were available prior to the present experiment. From the spectrum in Fig. 1, we report new transitions in ^{55}Sc at energies of 0.71(1) and 1.54(2) MeV. Additional results on the low-lying structure of ^{55}Sc will be reported elsewhere.

References

1) R. Kanungo *et al.,* Phys. Rev. Lett. **102**, 152501 (2009).
2) C. R. Hoffman *et al.,* Phys. Lett. B **672**, 17 (2009).
3) B. Bastin *et al.,* Phys. Rev. Lett. **99**, 022503 (2007).
4) A. Gade *et al.,* Phys. Rev. C **74**, 021302(R) (2006).
5) F. Wienholtz *et al.,* Nature **498**, 346 (2013).
6) R. V. F. Janssens *et al.,* Phys. Lett. B **546**, 55 (2002).
7) D.-C. Dinca *et al.,* Phys. Rev. C **71**, 041302(R) (2005).
8) J. I. Prisciandaro *et al.,* Phys. Lett. B **510**, 17 (2001).
9) A. Bürger *et al.,* Phys. Lett. B **622**, 29 (2005).
10) T. Otsuka *et al.,* Phys. Rev. Lett. **95**, 232502 (2005).
11) M. Rosenbusch *et al.,* Phys. Rev. Lett. **114**, 202501 (2015).
12) D. Steppenbeck *et al.,* Phys. Rev. Lett. **114**, 252501 (2015).
13) T. Otsuka *et al.,* Phys. Rev. Lett. **87**, 082502 (2001).
14) S. N. Liddick *et al.,* Phys. Rev. Lett. **92**, 072502 (2004).
15) D. Steppenbeck *et al.,* Nature **502**, 207 (2013).
16) T. Kubo *et al.,* Nucl. Instrum. Meth. B **204**, 97 (2003).
17) D. Steppenbeck *et al.,* JPS Conf. Proc. **6**, 020019 (2015).

Spectroscopy of unbound oxygen isotopes II

Y. Kondo,[*1,*2] T. Nakamura,[*1,*2] N. L. Achouri,[*3] L. Atar,[*4] T. Aumann,[*4] H. Baba,[*2] K. Boretzky,[*5,*2] C. Caesar,[*5,*2] D. Calvet,[*6,*2] H. Chae,[*7] N. Chiga,[*2] A. Corsi,[*6,*2] H. L. Crawford,[*8] F. Delaunay,[*3] A. Delbart,[*6,*2] Q. Deshayes,[*3] Zs. Dombrádi,[*9,*2] C. Douma,[*10] Z. Elekes,[*9,*2] P. Fallon,[*8] H. Al. Falou,[*11] I. Gašparić,[*12,*2] J. -M. Gheller,[*6,*2] J. Gibelin,[*3] A. Gillibert,[*6,*2] M. N. Harakeh,[*10] A. Hirayama,[*1,*2] C. R. Hoffman,[*13] M. Holl,[*4,*2] A. Horvat,[*4] A. Horváth,[*14] J. W. Hwang,[*7] T. Isobe,[*2] J. Kahlbow,[*4,*2] N. Kalantar-Nayestanaki,[*10] S. Kawase,[*15] S. Kim,[*7] K. Kisamori,[*2] T. Kobayashi,[*16,*2] D. Körper,[*5,*2] S. Koyama,[*17,*2] I. Kuti,[*9,*2] V. Lapoux,[*6,*2] S. Lindberg,[*18,*2] F. M. Marqués,[*3] S. Masuoka,[*19] J. Mayer,[*20,*2] K. Miki,[*21,*2] T. Murakami,[*22,*2] M. A. Najafi,[*10] K. Nakano,[*15,*2] N. Nakatsuka,[*22,*2] T. Nilsson,[*18] A. Obertelli,[*6,*2] F. de Oliveira Santos,[*23] N. A. Orr,[*3] H. Otsu,[*2] T. Ozaki,[*1,*2] V. Panin,[*2] S. Paschalis,[*4] A. Revel,[*23] D. Rossi,[*4] A. T. Saito,[*1,*2] T. Saito,[*17,*2] M. Sasano,[*2] H. Sato,[*2] Y. Satou,[*24] H. Scheit,[*4] F. Schindler,[*4] P. Schrock,[*19] M. Shikata,[*1,*2] Y. Shimizu,[*2] H. Simon,[*5,*2] D. Sohler,[*9,*2] O. Sorlin,[*23] L. Stuhl,[*2] S. Takeuchi,[*1,*2] M. Tanaka,[*25,*2] M. Thoennessen,[*21] H. Törnqvist,[*4,*2] Y. Togano,[*1,*2] T. Tomai,[*1,*2] J. Tscheuschner,[*4] J. Tsubota,[*1,*2] T. Uesaka,[*2] H. Wang,[*2] Z. Yang,[*2] and K. Yoneda[*2]

The NP1312-SAMURAI21 experiment, entitled "Spectroscopy of unbound oxygen isotopes II", was carried out in November-December 2015, aiming at identifying resonance states of the extremely neutron-rich oxygen isotopes ^{27}O and ^{28}O, following the NP1106-SAMURAI02 experiment for ^{25}O and ^{26}O[1] in 2012. The motivation for this series of experiments is exploring the shell evolution towards the possibly doubly magic nucleus ^{28}O (Z=8 and N=20), which is essential to understand the mechanism of the sudden change of the neutron drip line from oxygen to fluorine (Z=9), called "oxygen anomaly."[2] The invariant mass method is applied to reconstruct the decay energies of ^{27}O and ^{28}O, produced by two- and one-proton removal reactions from ^{29}Ne and ^{29}F, respectively.

The experiment was performed using the SAMURAI facility[3] at RIBF. The secondary beams of ^{29}Ne and ^{29}F were produced by the projectile fragmentation of a ^{48}Ca primary beam at 345 MeV/nucleon on a 15-mm thick beryllium target, and they were purified by BigRIPS. In addition to a 15-mm thick aluminum degrader at the first momentum dispersive focal plane (F1) of BigRIPS, a 7-mm thick aluminum degrader was installed at the second dispersive focal plane F5 to reduce the large amounts of light-ion background in the secondary beam. Plastic scintillators with a thickness of 3 mm were installed at the focal planes F3, F5, and F7 for particle identification.

A 15-cm length MINOS[4] target cell filled with liquid hydrogen was installed 4.4 m upstream from the center of the SAMURAI magnet, surrounded by the MINOS TPC and the DALI2 γ-ray detector array.[5] The incident beam was detected by two 1-mm thick plastic scintillators (SBTs) and two drift chambers (BDC1 and BDC2) placed before the MINOS target. The outgoing charged particle and neutrons were separated by the SAMURAI dipole magnet with a 2.9 Tesla field at the center. Standard drift chambers (FDC1 and FDC2) and a plastic scintillator hodoscope (HODF24) were used for the detection of charged fragments. HODF24 was expanded from the existing hodoscope (HODF) by adding eight new paddles, to cover the whole effective area of FDC2. For neutron detection, NeuLAND[6] (new Large Area Neutron Detector for R3B at FAIR) was combined with NEBULA to increase the efficiency for multiple neutron detection.

Data analysis is now in progress.

*1 Tokyo Institute of Technology
*2 RIKEN Nishina Center
*3 LPC-Caen
*4 Technical University Darmstadt
*5 GSI Helmholtzzentrum für Schwerionenforschung, Darmstadt
*6 CEA Saclay
*7 Seoul National University
*8 Lawrence Berkeley National Laboratory
*9 ATOMKI
*10 KVI-CART
*11 Lebanese-French University of Technology and Applied Science
*12 Ruer Bošković Institute, Zagreb
*13 Argonne National Laboratory
*14 Eötvös Loránd University
*15 Kyushu University
*16 Tohoku University
*17 University of Tokyo
*18 Chalmers University of Technology
*19 Center for Nuclear Studies (CNS), University of Tokyo
*20 University of Cologne, Köln
*21 NSCL, Michigan State University
*22 Kyoto University
*23 GANIL
*24 Institure for Basic Science
*25 Osaka University

References
1) Y. Kondo et al., RIKEN Accel. Prog. Rep. **46**, 6 (2013).
2) T. Otsuka et al., Phys. Rev. Lett. **105**, 032501 (2010).
3) T. Kobayashi et al., Nucl. Instrum. and Methods in Phys. Res. Sect. B**317**, 294 (2013).
4) A. Obertelli et al., Eur. Phys. J. A **50**, 8 (2014).
5) S. Takeuchi et al., Nucl. Instrum. and Methods in Phys. Res. Sect. A**763**, 596 (2014).
6) NeuLAND Technical Design Report, http://www.fair-center.de/fileadmin/fair/experiments/NUSTAR/Pdf/TDRs/NeuLAND-TDR-Web.pdf

First commissioning results for SπRIT-TPC

M. Kurata-Nishimura,[*1] G. Jhang,[*3] J. Barney,[*2] J. Estee,[*2] M. Kaneko,[*4] Y. Zhang,[*6*2] J. W. Lee,[*3] P. Lasko,[*5] G. Cerizza,[*2] C. Santamaria,[*2] K. Pelczar,[*5] Y. Kim,[*7] H. Lee,[*7] J. Lukasik,[*5] P. Pawlowski,[*5] D. Suzuki,[*1] T. Isobe,[*1] T. Murakami,[*4] W.G. Lynch,[*2] M.B. Tsang,[*2] and for SπRIT-TPC collaboration

The aim of the SAMURAI Pion-Reconstruction and Ion-Tracker Time-Projection Chamber (SπRIT-TPC) [1] project is to constrain the symmetry energy term in the nuclear-matter equation of state (EOS) at super-saturation density. It is proposed to compare π^+/π^- production ratio among various isospin asymmetry environments combining different unstable Sn beams and stable Sn targets in SAMURAI.

The first commissioning run using ^{79}Se beam was performed outside of the SAMURAI magnet in fall 2015. The performance of SπRIT-TPC and trigger systems were evaluated. Results revealed necessary modifications for upcoming physics campaign.

For the commissioning, the SπRIT-TPC was placed about 7 m away from the center of the SAMURAI magnet and lined up on 60 deg with the ^{79}Se secondary beam. Two targets of 0.5 mm natural Sn foil and 9 mm aluminum plate were mounted on a ladder in front of the TPC field cage window.

The overall readout system[3] was prepared and three types of trigger arrays composed by plastic counters read by MPPCs were installed for opening a gating grid driver. (1) KATANA (KrAkow Trigger Array with amplitude discrimiNAtion) was placed at the exit window to reject the non reacting beam. (2) The Multiplicity Trigger Array[4] was placed on the both sides of TPC to select high multiplicity events. (3) The active collimators was mounted in front of the target to reject beams hitting the target frame. The reaction trigger was provided by a start counter signal, no hit on the active collimator, low energy deposit in KATANA, and multiple hits on Multiplicity Trigger Array. The trigger condition was controlled through a trigger logic board.

The analysis framework, SπRITROOT[5], has been developed for SπRIT-TPC experiment. Using this code, a typical high multiplicity 3D event display is shown in Fig.1. The straight tracks were reconstructed even in dense track regions just after the target.

The total number of reconstructed tracks per event was plotted for two different multiplicity selections with KATANA and Multiplicity Trigger Array in Fig.2. Higher multiplicity requirement resulted in higher multiplicity track events corresponding to central collision events.

The reaction vertex was extrapolated from tracks event by event and the Z-vertex of 84% events was found around the target within 5mm in sigma for high multiplicity events. The event ratio originating from the target depended on the trigger conditions.

The first commissioning of SπRIT-TPC was successfully performed outside of the SAMURAI magnet. The high multiplicity track events were reconstructed and the reaction vertex was found around the target. The gating-grid driver worked with the fast trigger provided by three trigger arrays. Modification of readout electronics and optimization of trigger system is under investigation for coming physics run.

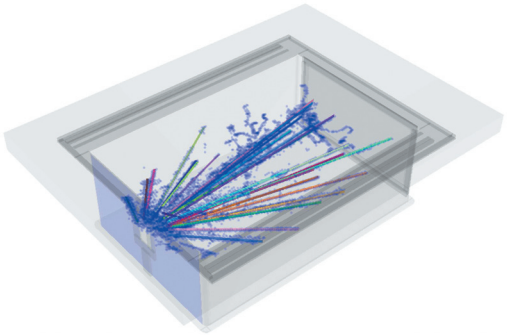

Fig. 1. A typical high multiplicity track event produced with ^{79}Se on Sn (nat.) target. The target was located 8.9 mm upstream from the field cage window.

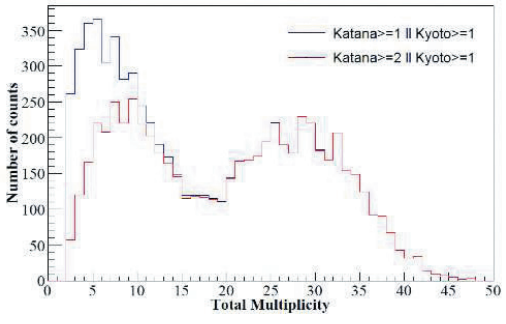

Fig. 2. The total multiplicity in the TPC gated on the multiplicity in the ancillary detectors KATANA and Multiplicity Trigger Array

*1 RIKEN Nishina Center
*3 Department of Physics, Korea Universtiy
*2 National Superconducting Cyclotron Laboratory and Department of Physics and Astronomy, Michigan State University
*4 Department of Physics, Kyoto University
*6 Department of Physics,Tsinghua University
*5 Institute of Nuclear Physics, PAN
*7 Institute for Basic Science, Korea

References

1) R. Shane at al.: Nucl. Instr. Meth. A **784** (2015) 513.
2) M.B. Tsang et al; Phys. Rev. Lett. bf 102 (2009) 122701.
3) T. Isobe et al,; in this report.
4) M. Kaneko et al,; in this report.
5) G. Jhang et al,; in this report.

Study on neutron-neutron correlation in Borromean nuclei via the (p, pn) reaction with the SAMURAI spectrometer

Y. Kubota,[*1,*2] A. Corsi,[*3] G. Authelet,[*3] H. Baba,[*2] C. Caesar,[*4] D. Calvet,[*3] A. Delbart,[*3] M. Dozono,[*1] J. Feng,[*5] F. Flavigny,[*6] J.-M. Gheller,[*3] J. Gibelin,[*7] A. Giganon,[*3] A. Gillibert,[*3] K. Hasegawa,[*8] T. Isobe,[*2] Y. Kanaya,[*9] S. Kawakami,[*9] D. Kim,[*10] Y. Kiyokawa,[*1] M. Kobayashi,[*1] N. Kobayashi,[*11] T. Kobayashi,[*8] Y. Kondo,[*12] Z. Korkulu,[*13] S. Koyama,[*11] V. Lapoux,[*3] Y. Maeda,[*9] F. M. Marqués,[*7] T. Motobayashi,[*2] T. Miyazaki,[*11] T. Nakamura,[*12] N. Nakatsuka,[*14,*2] Y. Nishio,[*15] A. Obertelli,[*3] A. Ohkura,[*15] N. A. Orr,[*7] S. Ota,[*1] H. Otsu,[*2] T. Ozaki,[*12] V. Panin,[*2] S. Paschalis,[*4] E. C. Pollacco,[*3] S. Reichert,[*16] J.-Y. Roussé,[*3] A. T. Saito,[*12] S. Sakaguchi,[*15] M. Sako,[*2] C. Santamaria,[*3] M. Sasano,[*2] H. Sato,[*2] M. Shikata,[*12] Y. Shimizu,[*2] Y. Shindo,[*15] L. Stuhl,[*2] T. Sumikama,[*8] M. Tabata,[*15] Y. Togano,[*12] J. Tsubota,[*12] T. Uesaka,[*2] Z. H. Yang,[*2] J. Yasuda,[*15] K. Yoneda,[*2] and J. Zenihiro[*2]

Dineutron correlation is one of the specific phenomena expected to appear in neutron drip-line nuclei. It has been explored through indirect studies such as the determination of the $E1$ cluster sum rule via the Coulomb breakup reaction.[1] In order to directly determine the momentum distribution of two valence neutrons of the Borromean nuclei ^{11}Li, ^{14}Be, and ^{17,19}B, a kinematically complete measurement was performed at the RIKEN RIBF for the quasi-free (p, pn) reaction on these nuclei.[2] The opening angle between the two neutrons was reconstructed from the measured momentum vectors of all the particles.

The experiment was carried out by using the SAMURAI spectrometer[3] combined with the liquid hydrogen target system MINOS.[4] The beam momentum was determined from the time-of-flight (TOF) between focal planes F7 and F13. The trajectory was measured using the beam drift chambers (BDCs). The momentum vectors of a decay neutron, a knocked-out neutron, and a recoil proton were determined from the TOF and position respectively measured by the NEBULA, the WINDS, and a recoil proton detector (RPD). The position and the angle of a heavy fragment at the entrance and the exit of the SAMURAI spectrometer were measured by the forward drift chambers (FDCs). The rigidity was determined so as to reproduce the set of the tracking information by using the calculated magnetic field.

The resolution of each momentum vector, estimated from the detector responses and angular straggling around the target, is summarized in Table 1. The momentum resolution of the recoil proton was dominated by the angular straggling, while that of the knocked-out neutron was limited by the time resolution of the WINDS. The required resolution of about 20 MeV/c was achieved.

Table 1. Estimated resolution of momentum vectors deduced from the detector responses and angular straggling. The unit is MeV/c.

Particle	Detector	σ_{Px}	σ_{Py}	σ_{Pz}
Beam ^{11}Li	BigRIPS+BDC	0.08	0.08	8
Recoil p	RPD	12	10	12
Knocked-out n	WINDS	15	16	15
Decay n	NEBULA	0.2	0.2	5
Fragment ^{9}Li	FDC	0.1	0.1	12
Total		20	19	25

Figures 1 (a), (b), (c), and (d) show the difference of the sum of the four-vectors of all the particles between the initial and the final states projected onto the x-, y-, and z-direction and the energy, respectively. Owing to the momentum and energy conservation law, in each spectrum the peak should be centered at zero; this is a test of the consistency of both the reconstruction and measurement. The widths of the spectra are consistently explained by the estimated resolution.

Data analysis is currently in progress.

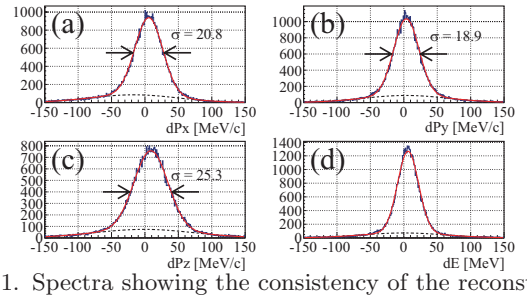

Fig. 1. Spectra showing the consistency of the reconstruction in the (a) x-, (b) y-, and (c) z-direction, and (d) the energy via the verification of the momentum and energy conservation.

*1 Center for Nuclear Study, University of Tokyo
*2 RIKEN Nishina Center
*3 CEA, Saclay
*4 Department of Physics, Technische Universität Darmstadt
*5 Department of Physics, Peking University
*6 IPN Orsay
*7 LPC Caen
*8 Department of Physics, Tohoku University
*9 Department of Applied Physics, University of Miyazaki
*10 Department of Physics, Ehwa Womans University
*11 Department of Physics, University of Tokyo
*12 Department of Physics, Tokyo Institute of Technology
*13 MTA Atomki
*14 Department of Physics, Kyoto University
*15 Department of Physics, Kyushu University
*16 Department of Physics, Technische Universität München

References

1) T. Nakamura *et al.*: Phys. Rev. Lett. **96**, 252502 (2006).
2) Y. Kubota *et al.*: RIKEN Accel. Prog. Rep. **48**, 52 (2015).
3) T. Kobayashi *et al.*: Nucl. Instr. Meth. B**317**, 294 (2013).
4) A. Obertelli *et al.*: Eur. Phys. Jour. A**50**, 8 (2014).

Study of Gamow-Teller transition from ^{132}Sn via the (p, n) reaction in inverse kinematics

J. Yasuda,[*1,*2] M. Sasano,[*1] R.G.T. Zegers,[*3] H. Baba,[*1] D. Bazin,[*3] W. Chao ,[*1] M. Dozono,[*1] N. Fukuda,[*1] N. Inabe,[*1] T. Isobe,[*1] G. Jhang,[*1,*4] D. Kameda,[*1] M. Kaneko, [*5] S. Kawase,[*6] K. Kisamori,[*1,*6] M. Kobayashi,[*6] N. Kobayashi, [*7] T. Kobayashi,[*1,*8] S. Koyama,[*1,*7] Y. Kondo,[*1,*9] A. Krasznahorkay,[*10] T. Kubo,[*1] Y. Kubota,[*1,*6] M. Kurata-Nishimura,[*1] C.S. Lee,[*1,*6] J.W. Lee, [*4] Y. Matsuda, [*11] E. Milman,[*1,*12] S. Michimasa,[*6] T. Motobayashi,[*1] D. Mucher, [*1,*13] T. Murakami, [*5] T. Nakamura,[*1,*9] N. Nakatsuka, [*1,*5] S. Ota,[*6] H. Otsu,[*1] V. Panin, [*1] W. Powell, [*1] S. Reichert, [*1,*13] S. Sakaguchi,[*1,*2] H. Sakai,[*1] M. Sako, [*1] H. Sato,[*1] Y. Shimizu,[*1] M. Shikata,[*1,*9] S. Shimoura,[*6] L. Stuhl,[*1] T. Sumikama,[*1,*8] H. Suzuki,[*1] S. Tangwancharoen, [*1] M. Takaki,[*6] H. Takeda,[*1] T. Tako,[*8] Y. Togano,[*1,*9] H. Tokieda,[*6] J. Tsubota,[*1,*9] T. Uesaka,[*1] T. Wakasa,[*2] K. Yako,[*6] K. Yoneda,[*1] and J. Zenihiro[*1]

We performed measurements on the ^{132}Sn(p, n) reaction at 220 MeV/nucleon in inverse kinematics at RIBF in order to extract Gamow-Teller (GT) transitions from the key doubly magic nucleus ^{132}Sn. This is an essential step toward establishing comprehensive theoretical models for nuclei situated between ^{78}Ni and ^{208}Pb.

The experiment was carried out by using the Wide-angle Inverse-kinematics Neutron Detectors for SHARAQ (WINDS)[1] and the large acceptance SAMURAI spectrometer[2]. A secondary beam of ^{132}Sn was transported onto a 10-mm thick liquid hydrogen target[3], which was surrounded by WINDS to detect recoil neutrons. From the measured neutron time-of-flight and recoil angle, the excitation energy and center-of-mass scattering angle were determined. The SAMURAI spectrometer was used for tagging (p, n) reaction events with particle identification of the outgoing heavy residues. Owing to the large momentum acceptance of SAMURAI, we can measure all the heavy residues with different rigidities in one setting. It allows us to reconstruct the excitation energy spectrum up to high excitation energies including the GT giant resonance (GTGR).

Figure 1 shows scatter plots of neutron energy (E_n) versus laboratory scattering angle ($\theta_{\rm lab}$) for neutrons detected in WINDS, for events associated with the ^{132}Sn beam component. Scatter plots are shown separately for different heavy residues detected in the spectrometer. In Fig. 1(a), one can see a clear kinematical correlation between E_n and $\theta_{\rm lab}$, corresponding to transitions going to the ground state or low-lying excited states in ^{132}Sb. Clear kinematic loci are also visible in Figs. 1(b), 1(c), and 1(d) and shifted to higher excitation energies including the GTGR according to the decay threshold. It means that the γ, $1n$, $2n$, and $3n$ decay channels are successfully measured. The data analysis for obtaining GT distribution is in progress.

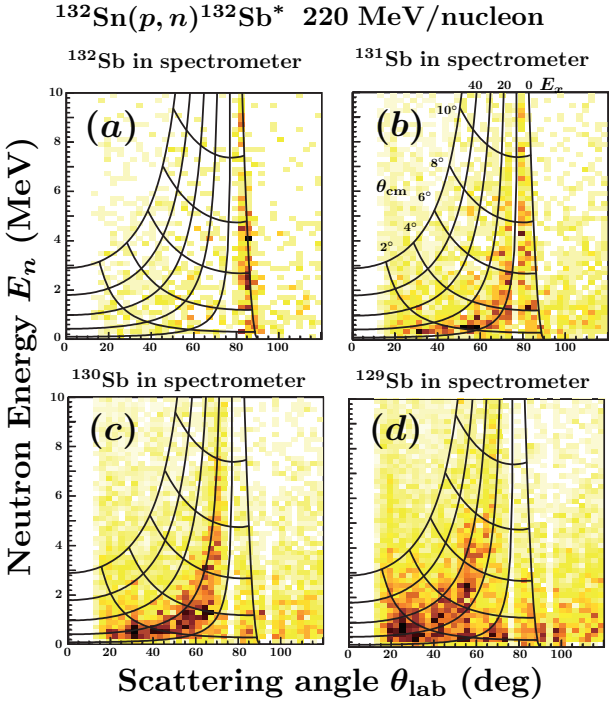

Fig. 1. Neutron spectra as a function of neutron energy (E_n) and scattering angle in the laboratory frame ($\theta_{\rm lab}$) for the ^{132}Sn beam component and for events associated with the heavy residues in the spectrometer: (a) ^{132}Sb, (b) ^{131}Sb, (c) ^{130}Sb, and (d) ^{129}Sb.

*1 RIKEN Nishina Center
*2 Department of Physics, Kyushu University
*3 NSCL Michigan State University
*4 Department of Physics, Korea University
*5 Kyoto University
*6 CNS, University of Tokyo
*7 University of Tokyo
*8 Department of Physics, Tohoku University
*9 Tokyo Institute of Technology
*10 MTA, Atomki
*11 Konan University
*12 Department of Physics, Kyungpook National University
*13 Technical University Munich

References

1) K. Yako *et al.*, RIKEN Accel. Prog. Rep. **45** 137 (2012).
2) T. Kobayashi *et al.*, Nucl. Instr. Meth. B **317**, 294 (2013).
3) M. Kurata-Nishimura *et al.*, RIKEN Accel. Prog. Rep **45**, 122 (2012).

Progress report of Gamow–Teller giant resonance studies at RIBF

M. Sasano,[*1] J. Yasuda,[*2] L. Stuhl,[*1] R.G.T. Zegers,[*3] H. Baba,[*1] W. Chao,[*1] M. Dozono,[*1] N. Fukuda,[*1] N. Inabe,[*1] T. Isobe,[*1] G. Jhang,[*1,13] D. Kamaeda,[*1] T. Kubo,[*1] M. Kurata-Nishimura,[*1] E. Milman,[*1] T. Motobayashi,[*1] H. Otsu,[*1] V. Panin, [*1] W. Powell, [*1] M. Sako, [*1] H. Sato,[*1] Y. Shimizu,[*1] H. Suzuki,[*1] T. Suwat, [*1] H. Takeda,[*1] T. Uesaka,[*1] K. Yoneda,[*1] J. Zenihiro,[*1] T. Kobayashi,[*4] T. Sumikama,[*4] T. Tako,[*4] T. Nakamura,[*5] Y. Kondo,[*5] Y. Togano,[*5] M. Shikata,[*5] J. Tsubota,[*5] K. Yako,[*6] S. Shimoura,[*6] S. Ota,[*6] S. Kawase,[*6] Y. Kubota,[*6] M. Takaki,[*6] S. Michimasa,[*6] K. Kisamori,[*6] C.S. Lee,[*6] H. Tokieda,[*6] M. Kobayashi,[*6] S. Koyama,[*7] N. Kobayashi, [*7] H. Sakai,[*1] T. Wakasa,[*2] S. Sakaguchi,[*2] A. Krasznahorkay,[*8] T. Murakami, [*9] N. Nakatsuka, [*9] M. Kaneko, [*9] Y. Matsuda, [*10] D. Mucher, [*11] S. Reichert, [*11] D. Bazin,[*3] and J.W. Lee[*12]

Among the collective modes[1], the Gamow–Teller (GT) giant resonance is an interesting excitation mode. It is a $0\hbar\omega$ excitation characterized by the quantum-number changes in orbital angular momentum ($\Delta L = 0$), spin ($\Delta S = 1$), and isospin ($\Delta T = 1$), and it is induced by the transition operator $\sigma\tau$. In the stable nuclei in medium or heavier mass regions ($A > 50$), the collectivity in this mode exhibits the GT giant resonance (GTGR), which provides information that is critically important for understanding the isovector part of the effective nucleon-nucleon interaction[2] and the symmetry potential of the equation of the state[3].

We have been rapidly expanding the nuclear chart of GTGR studies at RIBF, since the development of a new method to study GT transitions on unstable nuclei via the charge-exchange (CE) (p, n) reaction with RI beams[4,5]. An experiment at RIBF was performed in Spring 2014 to extract the GT and spin-dipole (SD) transition strengths over a wide excitation energy range covering their giant resonances on the key doubly magic nucleus ^{132}Sn[6]. This is an essential step toward establishing comprehensive theoretical models for nuclei situated between ^{78}Ni and ^{208}Pb. The neutron-drip line in the light mass region is another topic in the GTGR study, for which the first experiment was performed on ^{12}Be by using the SHARAQ spectrometer[7]. In 2015, another experimental program including an exotic nucleus ^{11}Li (spokesperson: L. Stuhl) was newly approved in the NP-PAC meeting.

From an experimental point of view, we employ a low-energy neutron detection system, WINDS, to detect recoil neutrons produced via the (p, n) reaction in inverse kinematics, in combination with a magnetic spectrometer such as SAMURAI[8]. In the progress report last year, we, through a data analysis of the ^{132}Sn(p, n) experiment, showed that the SAMURAI spectrometer provided sufficient particle identification capability and enabled us to separate CE reaction channels from other background reactions. Further background reduction is possible through the upgrade of WINDS. The primary goal of the upgrade plan is to eliminate background due to gamma rays arising from the enviroment through the so-called neutron-gamma discrimination method. Such gamma rays are considered to not be synchronized with the reaction timing, therefore having a flat distribution in time. The contribution of such gamma rays is enhanced in a region of foward scattering angles in the center-of-mass system, because a wide TOF range having background events uniformly distributed in time is compressed to a narrow phase space in that region. The method is being tested using a prototype low-energy neutron detector made from novel plastic scintillator material for the application of the neutron-gamma method. Details of the test are given also in Ref.[9].

*1 RIKEN Nishina Center
*2 Department of Physics,Kyushu University
*3 NSCL Michigan State University
*4 Department of Physics, Tohoku University
*5 Tokyo Institute of Technology
*6 CNS, University of Tokyo
*7 University of Tokyo
*8 MTA, Atomki
*9 Kyoto University
*10 Konan University
*11 Technical University Munich
*12 Department of Physics, Korea University

References

1) M. N. Harakeh and A. M. van der Woude: Giant Resonances (Oxford University Press, Oxford, 2001).
2) S. Fracasso and G. Colo: Phys. Rev. C 72, 064310 (2005).
3) P. Danielewicz: Nucl. Phys. A 727, 233 (2003).
4) M. Sasano et al.: Phys. Rev. Lett. 107, 202501 (2011).
5) M. Sasano et al.: Phys. Rev. C 86, 034324 (2012).
6) J. Yasuda et al.: in this report.
7) K. Yako et al.: RIKEN Accel. Prog. Rep. 45 (2012).
8) T. Kobayashi et al.: Nucl. Inst. Meth. B 317, 294-304 (2013).
9) L. Stuhl et al.: in this report.

Interaction cross section measurement of neutron-rich nuclei ^{17,19}B

A. T. Saito,[*1,*2] T. Nakamura,[*1,*2] Y. Kondo,[*1,*2] Y. Togano,[*1,*2] J. Gibelin,[*3] N. A. Orr,[*3] R. Minakata,[*1,*2] S. Ogoshi,[*1,*2] and SAMURAI DayOne Collaboration

We report the interaction cross section measurements of $2n$-halo nuclei ^{17}B and ^{19}B on a carbon target at 270 and 220 MeV/nucleon, respectively, using the SAMURAI spectrometer at RIBF. The neutron halo is one of the most notable features found in light nuclei located in the vicinity of the neutron drip line. The drip-line nucleus ^{19}B has attracted much attention because of its low two-neutron separation energy (S_{2n}=0.14(39) MeV[1)]) and the high matter radius ($\tilde{r}_m$=3.11(11) fm) determined from the interaction cross section ($\sigma_{\rm I}$=1219(81) mb) at an incident energy of approximately 800 MeV/nucleon[2)]. These results suggest the neutron halo structure in the ground state of ^{19}B, and its microscopic structure is not well understood owing to the large uncertainties of measured S_{2n} and $\sigma_{\rm I}$. Further experimental studies are thus called for to clarify the detailed nuclear structure, such as the valence neutron configuration, core excitation, possible $4n$ halo/skin[2)], and He-Li cluster configuration.[3)] The goal of the present measurement is to obtain the interaction cross section of ^{19}B with an improved accuracy together with that of ^{17}B at approximately 250 MeV/nucleon.

The details of the detector setup of SAMURAI are described in Ref. 4). A cocktail beam of ^{17,19}B was produced via the fragmentation reaction of a ^{48}Ca beam on a 30-mm-thick beryllium target at 345 MeV/nucleon. The ^{17,19}B beams impinged on a carbon secondary reaction target (thickness1.8 g/cm^2) installed at the SAMURAI target area. The particle identification (PID) before the carbon target was performed using BigRIPS with the TOF-ΔE-$B\rho$ method. Figure 1 shows a PID plot of incoming beams reconstructed by TOF measured using plastic scintillators, $B\rho$ obtained from the horizontal position at F5, and ΔE measured using an ionization chamber (ICB) at F13. The beam profile on the target was obtained using two drift chambers (BDC1 and BDC2). The PID plot of the outgoing charged particles from the ^{19}B + C reaction, obtained using SAMURAI, is shown in Fig. 2, where the incident ^{19}B beam is selected. TOF and ΔE were obtained using the plastic scintillator hodoscope (HODF). The $B\rho$ value was reconstructed from the positions and angles measured by two drift chambers (FDC1 and FDC2). The resolution of mass-to-atomic-number ratio (A/Z) and atomic number (Z) for the outgoing ^{19}B are 0.04 and 0.19 (FWHM), respectively. The achieved resolutions are sufficiently high to identify the charged particle unambiguously. The interaction cross sections are then obtained by the transmission method. Further analysis to obtain the final interaction cross sections for ^{17,19}B is in progress.

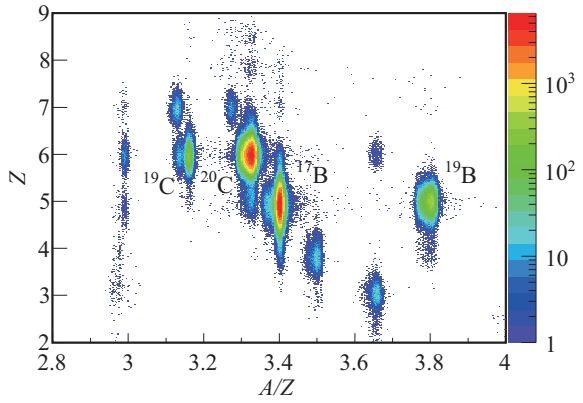

Fig. 1. Particle identification for the beam particles extracted from the data obtained using the standard BigRIPS detectors.

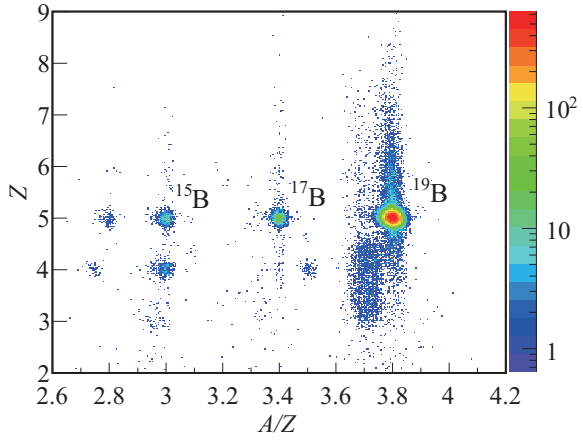

Fig. 2. Particle identification for the outgoing charged particles after the carbon target extracted from the data obtained using the SAMURAI detectors after selecting ^{19}B from Fig. 1.

*1 Department of Physics, Tokyo Institute of Technology
*2 RIKEN Nishina Center
*3 LPC-Caen, ENSICAEN, Université de Caen, CNRS/IN2P3

References

1) L. Gaudefroy *et al.*, Phys. Rev. Lett. **109** 202503 (2012).
2) T. Suzuki *et al.*, Nucl. Phys. A **658** 313 (1999).
3) Y. Kanada-Enyo *et al.*, Phys. Rev. C **52**, 647 (1995).
4) T. Kobayashi *et al.*, Nucl. Instr. Meth. B **317**, 294 (2013).

Time-of-Flight mass measurements of neutron-rich Ca isotopes beyond $N = 34$

M. Kobayashi,[*1] S. Michimasa,[*1] Y. Kiyokawa,[*1] H. Baba,[*2] G.P.A. Berg,[*3] M. Dozono,[*1] N. Fukuda,[*2] T. Furuno,[*4] E. Ideguchi,[*5] N. Inabe,[*2] T. Kawabata,[*4] S. Kawase,[*1] K. Kisamori,[*1,*2] K. Kobayashi,[*6] T. Kubo,[*2] Y. Kubota,[*1,*2] C.S. Lee,[*1,*2] M. Matsushita,[*1] H. Miya,[*1] A. Mizukami,[*7] H. Nagakura,[*6] D. Nishimura,[*7] H. Oikawa,[*7] S. Ota,[*1] H. Sakai,[*2] S. Shimoura,[*1] A. Stolz,[*8] H. Suzuki,[*2] M. Takaki,[*1] H. Takeda,[*2] S. Takeuchi,[*2] H. Tokieda,[*1] T. Uesaka,[*2] K. Yako,[*1] Y. Yamaguchi,[*6] Y. Yanagisawa,[*2] R. Yokoyama,[*1] and K. Yoshida[*2]

The nuclear mass is one of the fundamental quantities used in investigating nuclear structure properties such as shell closures and new magic numbers. The neutron numbers of 32 and 34 have been theoretically suggested to be candidates of new magic numbers in the Ca isotopes[1]. Recently, the prominent shell closure at $N = 32$ was established by measurements of the massses of ^{53}Ca and ^{54}Ca[2]. Moreover, the excitation energy of the 2_1^+ state in ^{54}Ca was reported[3], and the result suggests the existence of an $N = 34$ shell closure in ^{54}Ca. For establishment of the closed-shell nature of ^{54}Ca, mass measurements of the Ca isotopes beyond $N = 34$ are essential. The present work aims at studying the nuclear shell evolution at $N = 32$ and 34 by direct mass measurements of neutron-rich nuclei in the vicinity of ^{54}Ca.

We performed the nuclear mass measurement at the RIKEN RI Beam Factory using the SHARAQ spectrometer. The masses were measured directly by the TOF-$B\rho$ technique. The experimental setup is presented in detail by Kobayashi *et al.*[4].

Here, current status of the data analysis is described. We analyzed the data taken by diamond detectors, which were employed for timing measurement. Time resolution was estimated to be 12 ps (σ), which is a much better value than that in the previous measurement using ^{12}N beams at 320 AMeV[5]. This improvement of the time resolution can be interpreted in terms of the energy deposit in the diamond detector, which was ∼60–100 MeV (∼10 MeV) in the present (previous) experiment.

The mass to charge ratio (A/Q) was reconstructed by the $B\rho$ value from the beam tracking with up to fourth-order aberrations, and calibrated by using the reference nuclei such as $^{53-54}$Ca, $^{49,51-52}$K, $^{46-47}$Ar, $^{43-46}$Cl, $^{41-42}$S, $^{39-42}$P, and ^{38}Si. Figure 1 shows an A/Q spectrum for one of the reference isotopes, ^{54}Ca. The relative mass resolution of ∼1/8000 (σ) has been achieved for $Z \sim 20$ nuclei. The total yield of ^{55}Ca, which is one of the target nuclei, is several thousands. It is expected that the mass of ^{55}Ca can be deduced with the precision of $\sim 3 \times 10^{-6}$.

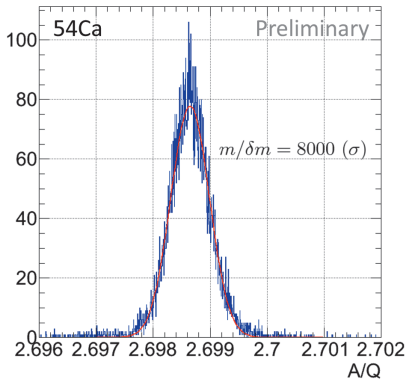

Fig. 1. A/Q spectrum for a reference nucleus, ^{54}Ca.

At present, energy loss in a PPAC, which was used for the $B\rho$ measurement, has not been considered in the mass calibration. It will be included in the fitting to reduce the residuals of the calibration. Further analysis is in progress.

References

1) T. Otsuka *et al.*: Phys. Rev. Lett. **87**, 082502 (2001).
2) F. Wienholtz *et al.*: Nature **498**, 349 (2013).
3) D. Steppenbeck *et al.*: Nature **502**, 207 (2013).
4) M. Kobayashi *et al.*: RIKEN Accel. Prog. Rep. **48**, 59 (2015).
5) S. Michimasa *et al.*: Nucl. Instr. Meth. B **317**, 305 (2013).

*1 Center for Nuclear Study, University of Tokyo
*2 RIKEN Nishina Center
*3 JINA and the Department of Physics, University of Notre Dame
*4 Department of Physics, Kyoto University
*5 RCNP, Osaka University
*6 Department of Physics, Rikkyo University
*7 Department of Physics, Tokyo University of Science
*8 NSCL, Michigan State University

Isomer spectroscopy of neutron-rich nuclei near $N = 40$

Y. Kiyokawa,[*1] S. Michimasa,[*1] M. Kobayashi,[*1] R. Yokoyama,[*1] D. Nishimura,[*2] S. Ota,[*1] A. Mizukami,[*2] H. Oikawa,[*2] K. Kobayashi,[*3] H. Baba,[*4] G.P.A. Berg,[*5] M. Dozono,[*1] N. Fukuda,[*4] T. Furuno,[*6] E. Ideguchi,[*7] N. Inabe,[*4] T. Kawabata,[*6] S. Kawase,[*1] K. Kisamori,[*1,*4] T. Kubo,[*4] Y. Kubota,[*1,*4] C.S. Lee,[*1] M. Matsushita,[*1] H. Miya,[*1] H. Nagakura,[*3] H. Sakai,[*4] S. Shimoura,[*1] A. Stolz,[*8] H. Suzuki,[*4] M. Takaki,[*1] H. Takeda,[*4] S. Takeuchi,[*4] H. Tokieda,[*1] T. Uesaka,[*4] K. Yako,[*1] Y. Yamaguchi,[*3] Y. Yanagisawa,[*4] and K. Yoshida[*4]

A study on isomeric γ decays in the vicinity of the neutron-rich nuclei of $N = 40$ has been performed at the RIKEN Nishina Center RI Beam Factory. Neutron-rich nuclei were produced by fragmentation of a ^{70}Zn primary beam at 345 MeV/nucleon in a ^{9}Be target. The fragments were separated and identified on an event-by-event basis via the TOF-Bρ-Δ E method using the BigRIPS, the High Resolution Beam Line, and the SHARAQ spectrometer, and were implanted in a plastic active stopper. Delayed γ-rays were detected using two clover-type high-purity germanium detectors and sixteen NaI(Tl) detectors located outside the vacuum chamber at the downstream side of the final focal plane of the SHARAQ beam line by a DAQ system with an independent trigger from the beamline DAQ system. The data of the delayed γ-rays were correlated with the data of particles identified using a common timestamp. Data of all the delayed γ-rays were recorded without any hardware time window. Delayed γ-rays within < 5 ms from beam implantation were regarded as valid events. This is much shorter than the beam rate and there was almost no chance of incorrect identification of particles owing to multiple beam implantation during the time range. The experimental setup is presented in detail in Ref.[1]).

We identified 8 isomers with half-lives in the microsecond range, including the discovery of 2 new isomers in very neutron-rich nuclei, ^{58}Sc^{m} and ^{61}Ti^{m}, and obtained a wealth of spectroscopic information such as γ-ray energy, half-lives, and γ-ray relative intensities for a wide range of neutron-rich exotic nuclei. The isomers that We observed in the present experiment are summarized in Tables 1 and 2 along with the γ-ray energies (E_γ) and the half-lives ($T_{1/2}$). Figure 1 shows the γ-ray energy spectra of the new isomers.

The known isomers observed in the present experiment are consistent with the previous work. Further analysis is in progress.

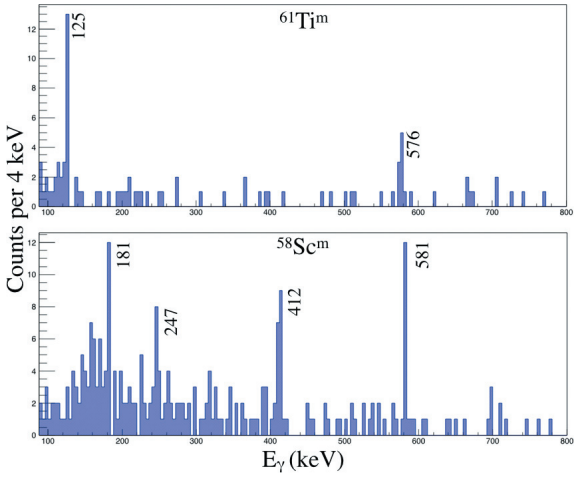

Fig. 1. Delayed γ-rays energy spectra of new isomers identified in the present work. Peaks are labeled with energies in keV.

Table 1. γ-ray energies and half-lives of previously known isomers observed in the present work.

Isomers	E_γ[keV]	$T_{1/2}$[μs]
^{60}V^{m} [Ref.[2,3])]	99.6(1)$_{stat}$; 103.7(2)$_{stat}$	0.221(13)
^{59}Ti^{m} [Ref.[3])]	108.9	0.572(19)
^{56}Sc^{m} [Ref.[3,4])]	140.6(2)$_{stat}$; 187.8(3)$_{stat}$; 587.5(1)$_{stat}$;728.0(4)$_{stat}$	0.228(24)
^{54}Sc^{m} [Ref.[3–5])]	110.6	2.82(9)
^{50}K^{m} [Ref.[2,3])]	128.3(1)$_{stat}$;172.5(1)$_{stat}$	0.132(9)
^{43}S^{m} [Ref.[3,6])]	320.6	0.414(14)

Table 2. New isomers observed in the present work along with the γ-ray energies (E_γ), half-lives ($T_{1/2}$), and γ-ray relative intensities (I_γ).

Isomers	E_γ[keV]	$T_{1/2}$[μs]	I_γ(%)
^{61}Ti^{m}	576.1(3)$_{stat}$	0.23(9)	100
	125.2(4)$_{stat}$	0.32(13)	50(27)
^{58}Sc^{m}	580.9(2)$_{stat}$	0.49(15)	100
	412.3(5)$_{stat}$	0.86(50)	85(36)
	247(2)$_{stat}$	1.25(83)	26(19)
	180.5(4)$_{stat}$	0.58(20)	27(14)

*1 Center for Nuclear Study, the University of Tokyo
*2 Tokyo University of Science
*3 Rikkyo University
*4 RIKEN Nishina Center
*5 JINA and the Department of Physics, University of Notre Dame
*6 Department of Physics, Kyoto University
*7 RCNP, Osaka University
*8 NSCL, Michigan State University

References

1) Y. Kiyokawa *et al.*, RIKEN. Accel. Prog. Rep. **48**, 60 (2015).
2) J.M. Daugas *et al.*, Phys. Rev. C **81**, 034304 (2010).
3) D. Kameda *et al.*, Phys. Rev. C **86**, 054319 (2012).
4) H.L. Crawford *et al.*, Phys. Rev. C **82**, 014311 (2010).
5) R. Grzywacz *et al.*, Phys. Rev. Lett. **81**, 766 (1998).
6) F. Sarazin *et al.*, Phys. Rev. Lett. **84**, 5062 (2000).

The $(^{16}O, ^{16}F(0^-))$ reaction to study spin-dipole 0^- states

M. Dozono,[*1] T. Uesaka,[*2] K. Fujita,[*3] N. Fukuda,[*2] M. Ichimura,[*2] N. Inabe,[*2] S. Kawase,[*1] K. Kisamori,[*1] Y. Kiyokawa,[*1] K. Kobayashi,[*4] M. Kobayashi,[*1] T. Kubo,[*2] Y. Kubota,[*1] C. S. Lee,[*1] M. Matsushita,[*1] S. Michimasa,[*1] H. Miya,[*1] A. Ohkura,[*3] S. Ota,[*1] H. Sagawa,[*2,*5] S. Sakaguchi,[*3] H. Sakai,[*2] M. Sasano,[*2] S. Shimoura,[*1] Y. Shindo,[*3] L. Stuhl,[*2] H. Suzuki,[*2] H. Tabata,[*3] M. Takaki,[*1] H. Takeda,[*2] H. Tokieda,[*1] T. Wakasa,[*3] K. Yako,[*1] Y. Yanagisawa,[*2] J. Yasuda,[*3] R. Yokoyama,[*1] K. Yoshida,[*2] and J. Zenihiro[*2]

We proposed the parity-transfer $(^{16}O, ^{16}F(0^-))$ reaction as a powerful tool to study spin-dipole (SD) 0^- states in nuclei[1]. The parity-transfer reaction has a unique selectivity to unnatural-parity states, which is an advantage over the other reactions used thus far. As the first $(^{16}O, ^{16}F(0^-))$ measurement, the experiment for a ^{12}C target was performed with the SHARAQ spectrometer. The known 0^- state at $E_x = 9.3$ MeV in ^{12}B[2] serves as a benchmark to verify the effectiveness of this reaction. The experimental setup and method can be found in Ref.[3].

The preliminary result of the excitation-energy spectrum for the $^{12}C(^{16}O, ^{16}F(0^-))^{12}B$ reaction at $\theta_{lab} = 0^\circ - 0.25^\circ$ is shown in Fig. 1. The energy resolution is 2.6 MeV in FWHM. We note that the events at $E_x \sim -10$ MeV are due to the $(^{16}O, ^{16}F(0^-))$ reaction on hydrogens in the plastic scintillator used as a reaction target. The obtained distribution is largely different from those previously obtained by other reaction probes such as (n, p) and $(d, ^2He)$ (e.g., see Fig. 1 in Ref.[4]). A distinct difference is that the 1^+ ground-state Gamow-Teller (GT) transition is strongly hindered. Furthermore, an enhancement at $E_x \sim 9$ MeV can be seen, which is due to the 0^- state at $E_x = 9.3$ MeV. Therefore, the obtained distribution shows high selectivity of the present reaction to 0^- states.

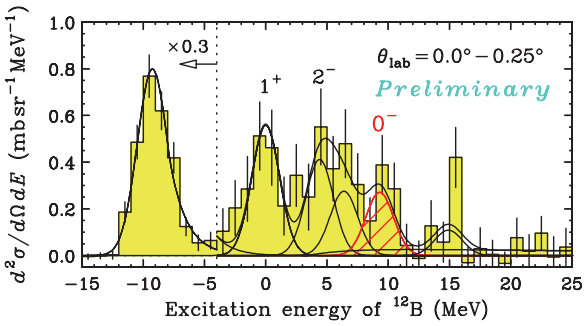

Fig. 1. Preliminary result of the excitation-energy spectrum for the $^{12}C(^{16}O, ^{16}F(0^-))^{12}B$ reaction at $\theta_{lab} = 0^\circ - 0.25^\circ$.

In order to extract the yield of the 0^- state, we performed peak fitting, and the results are shown as the solid lines in Fig. 1. Figure 2 shows the angular distribution for the 0^- state at $E_x = 9.3$ MeV together with the results for the 1^+ g.s. and the 2^- state at $E_x = 4.4$ MeV. The solid curves denote the results calculated by the distorted-wave Born approximation (DWBA). The DWBA calculations predict the oscillatory patterns of the cross sections that are different depending on the spin-parity. The 0^- has the strong forward peaking, while the other states, 1^+ and 2^-, have the first maximum at finite angles. These patterns reproduce the experimental data very well. Thus, the oscillatory pattern of the angular distribution allows a clear spin-parity determination for the unnatural-parity state. Further analysis is underway to finalize experimental results.

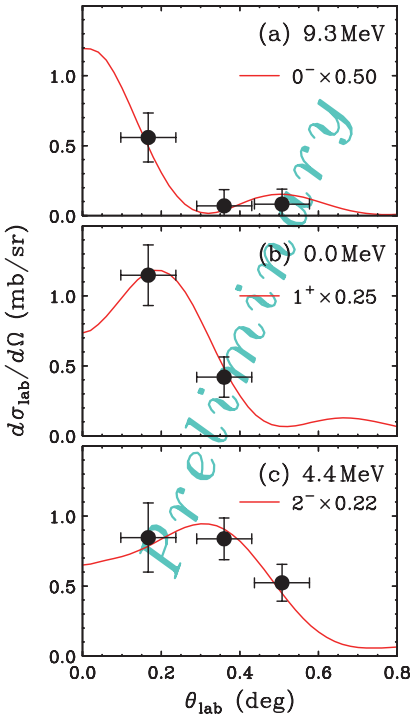

Fig. 2. Measured and calculated differential cross sections for $E_x = 9.3$ MeV, 0.0 MeV, and 4.4 MeV states.

*1 Center for Nuclear Study, University of Tokyo
*2 RIKEN Nishina Center
*3 Department of Physics, Kyushu University
*4 Rikkyo University
*5 Center for Mathematics and Physics, University of Aizu

References
1) M. Dozono et al.: RIKEN Accel. Prog. Rep. **45**, 10 (2012).
2) H. Okamura et al.: Phys. Rev. C **66**, 054602 (2002).
3) M. Dozono et al.: RIKEN Accel. Prog. Rep. **48**, 58 (2015).
4) H. Okamura et al.: Phys. Lett. B **345**, 1 (1995).

Spectroscopy of single-particle states in oxygen isotopes via the ^{A}O$(p, 2p)$ reaction

S. Kawase,[*1,*2] T. L. Tang,[*1] T. Uesaka,[*3] D. Beaumel,[*3,*4] M. Dozono,[*3] T. Fujii,[*1,*3] T. Fukunaga,[*3,*5] N. Fukuda,[*3] A. Galindo-Uribarri,[*6] S. H. Hwang,[*7] N. Inabe,[*3] T. Kawahara,[*3,*8] W. Kim,[*7] K. Kisamori,[*1,*3] M. Kobayashi,[*1] T. Kubo,[*3] Y. Kubota,[*1,*3] K. Kusaka,[*3] C. S. Lee,[*1,*3] Y. Maeda,[*9] H. Matsubara,[*3] S. Michimasa,[*1] H. Miya,[*1,*3] T. Noro,[*3,*5] A. Obertelli,[*10] S. Ota,[*1] E. Padilla-Rodal,[*11] S. Sakaguchi,[*3,*5] H. Sakai,[*3] M. Sasano,[*3] S. Shimoura,[*1] S. S. Stepanyan,[*7] H. Suzuki,[*3] M. Takaki,[*1,*3] H. Takeda,[*3] H. Tokieda,[*1] T. Wakasa,[*3,*5] T. Wakui,[*3,*12] K. Yako,[*1] Y. Yanagisawa,[*3] J. Yasuda,[*3,*5] R. Yokoyama,[*1,*3] K. Yoshida,[*3] and J. Zenihiro[*3]

^{14,22,24}O$(\vec{p}, 2p)$ reaction measurements (SHARAQ04 experiment) were carried out with a polarized proton target at the RIBF to measure single-particle spectra and determine spin-orbit splitting of proton single-particle orbits in ^{14,22,24}O as a function of their neutron number. Beams that included oxygen unstable isotopes bombarded the solid polarized proton target[1)] and two scattered protons were detected with the drift chambers and plastic scintillators, which were located on both left and right sides of the beamline. The residual nuclei were momentum-analyzed by using the first doublet quadrupole magnets (SDQ) and the first dipole magnet (D1) of the SHARAQ spectrometer. For further details about the experimental setup and conditions see Ref. 2.

The $(p, 2p)$ events were tagged by identifying two scattered protons and reaction residues. The particle identification of the reaction residues was performed by using the position information both before and after the D1 magnet, TOF from the target to the S1 focal plane, which is located at the downstream of the D1 magnet, and the energy loss in plastic scintillators at the downstream of the target. Figure 1 shows the correlation between the proton number Z and the mass-to-charge ratio A/Q at the focal plane S1 for the ^{22}O secondary beam. The reaction residues were successfully identified.

After the identification of the reaction, spectroscopic factors for the ground states of ^{13}N, ^{21}N, and ^{23}N were deduced by comparing the experimental cross sections and DWIA calculations with computer code THREEDEE.[3)] In the calculation, global Dirac optical model potentials[4)] were used. For the NN interaction, the

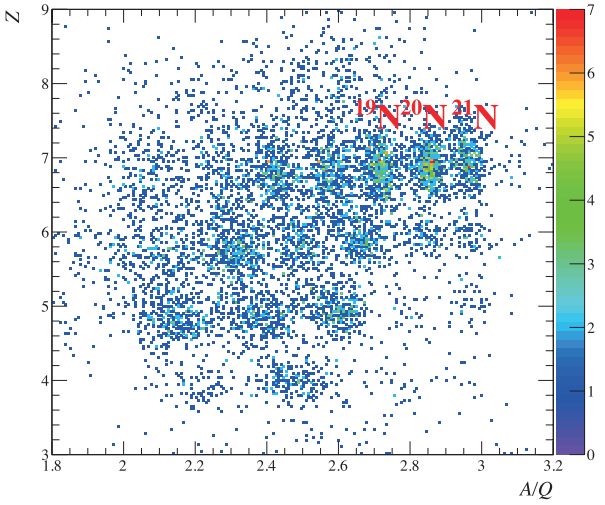

Fig. 1. Correlation between Z and A/Q at the focal plane S1.

observables calculated from the phase-shift analysis of the NN elastic scattering by Arndt[5)] were used.

Both experimental and calculated cross sections of ^{22,24}O$(p, 2p)$ were dropped by a factor of 3 compared to that of ^{14}O$(p, 2p)$. This can be understood partially by the effect of stronger binding energy of protons. The preliminary values of the spectroscopic factors are 1.06±0.05 (^{14}O$(p, 2p)^{13}$Ng.s.), 1.01±0.08 (^{22}O$(p, 2p)^{21}$Ng.s.), and 1.0±0.3 (^{24}O$(p, 2p)^{23}$Ng.s.). Here, only the statistical errors are indicated. No significant difference in the spectroscopic factors was observed among these ground-state transitions.

In the near future, the spectroscopic factors will be compared to the shell model calculations and their reductions will be discussed. The deduction of the vector analyzing power of the reaction will also be done.

*1 Center for Nuclear Study (CNS), University of Tokyo
*2 Present address: Faculty of Engineering Sciences, Kyushu University
*3 RIKEN Nishina Center
*4 Institut de Physique Nucléaire d'Orsay
*5 Department of Physics, Kyushu University
*6 Oak Ridge National Laboratory
*7 Department of Physics, Kyungpook National University
*8 Department of Physics, Toho University
*9 Department of Applied Physics, University of Miyazaki
*10 CEA Saclay
*11 Instituto de Ciencias Nucleares, Universidad Nacional Autónoma de México
*12 CYRIC, Tohoku University

References

1) T. Wakui *et al.*, Nucl. Instrum. Meth. A **550**, 521 (2005).
2) S. Kawase *et al.*, RIKEN Accel. Prog. Rep., **46**, 30 (2013).
3) N. S. Chant and P. G. Roos, Phys. Rev. C **15**, 57 (1977).
4) E. D. Cooper *et al.*, Phys. Rev. C **47**, 297 (1993).
5) R. A. Arndt *et al.*, Phys. Rev. D **35**, 128 (1987).

Spectroscopic factors of the proton bound states in ^{23,25}F

T. L. Tang,[*1] S. Kawase,[*1] T. Uesaka,[*2] D. Beaumel,[*2,*3] M. Dozono,[*2] T. Fujii,[*1,*2] N. Fukuda,[*2] T. Fukunaga,[*2,*4] A. Galindo-Uribarri,[*5] S. H. Hwang,[*6] N. Inabe,[*2] D Kameda,[*2] T. Kawahara,[*2,*7] W. Y. Kim,[*6] K. Kisamori,[*1,*2] M. Kobayashi,[*1] T. Kubo,[*2] Y. Kubota,[*1,*2] K. Kusaka,[*2] C. S. Lee,[*1] Y. Maeda,[*8] H. Matsubara,[*2] S. Michimasa,[*1] H. Miya,[*1,*2] T. Noro,[*2,*4] A. Obertelli,[*9] S. Ota,[*1] E. Padilla-Rodal,[*10] S. Sakaguchi,[*2,*4] H. Sakai,[*2] M. Sasano,[*2] S. Shimoura,[*1] S. S. Stepanyan,[*6] H. Suzuki,[*2] M. Takaki,[*1,*2] H. Takeda,[*2] H. Tokieda,[*1] T. Wakasa,[*2,*4] T. Wakui,[*2,*11] K. Yako,[*1] Y. Yanagisawa,[*2] J. Yasuda,[*2,*4] R. Yokoyama,[*1,*2], K. Yoshida,[*2] and J. Zenihiro,[*2] for SHARAQ04 collaboration

The proton quasi-free knockout reaction on ^{23}F (^{25}F) was studied in SHARAQ04 experiment at RIBF, RIKEN[1]. The spectrum of excitation energy of the residue ^{22}O (^{24}O) was deduced and partitioned by the neutron thresholds[2]. The orbital angular momentum of each partition was identified by comparison with the DWIA calculation, and then the sum of the spectroscopic factors (SFs) was extracted [3]. Figure 1 shows the spectra of excitation energy.

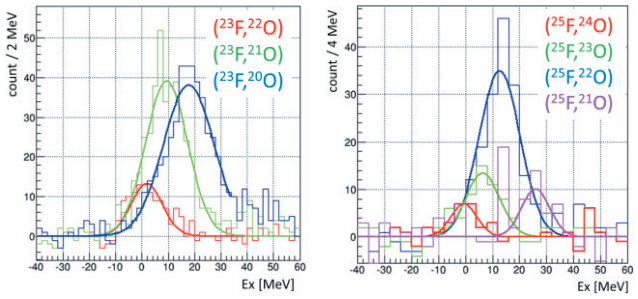

Fig. 1. Spectra of excitation energy of ^{23}F(p,2p) (left) and ^{25}F(p,2p) (right).

In ^{23}F(p,2p), the partition (^{23}F,^{22}O) originates from the $1d_{5/2}$ shell and the SF is 0.4 ± 0.1. The partitions (^{23}F,^{21,20}O) originate from the p-shell with the sum of the SFs of 4.8 ± 0.7. In ^{25}F(p,2p), the partitions (^{25}F,^{24,23}O) originate from the $1d_{5/2}$ shell and the sum of the SFs is 0.9 ± 0.7. The partitions (^{25}F,^{22,21}O) originate from the p-shell with the sum of the SFs of 4.4 ± 0.9.

The sum of the SFs of the $1d_{5/2}$ proton of ^{25}F can be understood as a result of the double magic of ^{24}O [4]. The sum of the SFs of the p-shell for both ^{23}F and ^{25}F are approximately 75% of the shell limit. This result is similar to most stable isotopes. The extraordinary small SF of the $1d_{5/2}$ of ^{23}F needs explanations.

The independent particle model should be valid in ^{23}F because the experimental proton shell gap between the $1d_{5/2}$ and $1p_{1/2}$ is 10 MeV, and the proton-neutron interaction energy is only 0.7 MeV. There could be missing strength at higher excitation energies. The wave function of ^{23}F $|^{23}F\rangle$ can be expressed as a linear combination of proton single particle wave functions $|p\rangle$ coupled to ^{22}O wave functions $|^{22}O\rangle$, such that

$$|^{23}F\rangle = \sum_{i,j} \beta_{ij} \left[|p\rangle_i |^{22}O\rangle_j \right],$$

where β_{ij} is the square root of the SF, and the square bracket [ ] represents the angular and isospin coupling and anti-symmetry operator. The known parities of the excited states of ^{22}O are all negative above 6.9 MeV (1-neutron threshold is 6.8 MeV). Because the residual interaction cannot mix different parity states, the sum of the SFs of the $1d_{5/2}$ shell is almost limited up to 1-neutron threshold. However, the knowledge of the excited states is not complete that there could be undiscovered positive parity states above the neutron threshold.

A mean field calculation suggests that ^{23}F is slightly deformed ($\beta_2 = -0.2$) [5,6]. The deformed oxygen core has to be expanded into many excited states of free oxygen; therefore, the deformation could reduce the knockout cross section. In the reaction aspect, the (p,2p) cross section of a slightly deformed nucleus will be different from that of a spherical nucleus due to the focusing effect [7].

In conclusion, the SFs of the proton bound states of ^{23}F and ^{25}F were deduced. The $1d_{5/2}$ proton of ^{25}F is a strong candidate of a single particle orbit. The nature of the $1d_{5/2}$ proton of ^{23}F requires further study. The results will be compared with the shell model calculation in the near future.

*1 Center of Nuclear Study (CNS), University of Tokyo
*2 RIKEN Nishina Center
*3 Institut de Physique Nucléaire d'Orsay
*4 Department of Physics, Kyushu University
*5 Oak Ridge National Laboratory
*6 Department of Physics, Kyungpook National University
*7 Department of Physics, Toho University
*8 Department of Applied Physics, University of Miyazaki
*9 CEA Saclay
*10 Instituto de Ciencias Nucleares, Universidad Nacional Autónoma de México
*11 CYRIC, Tohoku University

References

1) S. Kawase *et al.*: CNS annual report 2012, (2013) 13.
2) T. L. Tang *et al.*: RIKEN Accel. Prog. Rep. **48** (2015) 57.
3) T. L. Tang *et al.*: CNS annual report 2014 (to be published).
4) R. V. F. Janssens: Nature **459** (2009) 1069.
5) G. A. Lalazissis *et al.*: The. Euro. Phys. Jour. A **22** (2004) 37.
6) M. K. Sharma *et al.*: Chin. Phys. C **39** (2015) 064102
7) P. A. Deutchman *et al.*: Nucl. Phys. A **283** (1977) 289.

Spin-dipole response of ^{4}He by exothermic charge exchange (^{8}He,^{8}Li*(1$^+$))

H. Miya,[*1] S. Shimoura,[*1] K. Kisamori,[*1,*2] M. Assié,[*3] H. Baba,[*2] T. Baba,[*4] D. Beaumel,[*3] M. Dozono,[*1] T. Fujii,[*2] N. Fukuda,[*2] S. Go,[*1] F. Hammache,[*3] E. Ideguchi,[*5] N. Inabe,[*2] M. Itoh,[*6] D. Kameda,[*2] S. Kawase,[*1] T. Kawabata,[*4] M. Kobayashi,[*1] Y. Kondo,[*7] T. Kubo,[*2] Y. Kubota,[*1,*2] C. S. Lee,[*1,*2] Y. Maeda,[*8] H. Matsubara,[*9] S. Michimasa,[*1] K. Miki,[*5] T. Nishi,[*10] M. Kurata-Nishimura,[*2] S. Ota,[*1] H. Sakai,[*2] S. Sakaguchi,[*11] M. Sasano,[*2] H. Sato,[*2] Y. Shimizu,[*2] H. Suzuki,[*2] A. Stolz,[*12] M. Takaki,[*1] H. Takeda,[*2] S. Takeuchi,[*2] A. Tamii,[*5] H. Tokieda,[*1] M. Tsumura,[*4] T. Uesaka,[*2] K. Yako,[*1] Y. Yanagisawa,[*2] and R. Yokoyama[*1]

The spin dipole (SD) ($\Delta S = \Delta L = 1$) is one of the spin-isospin responses. On a double-closed nucleus, the SD excitation contribution is large because of the nucleon configuration. ^{4}He is leghtest of the double-closed nucleus, and has a simple configuration. It is easy to understand the SD response. This is important for the study of supernova nucleosynthesis with the neutrino-nucleus reaction[1].

We conducted the exothermic charge-exchange (CE) reaction ^{4}He(^{8}He, ^{8}Li*(1$^+$))^{4}H. CE reactions are used as a powerful probe to study the spin-isospin responses. The exothermic reaction enables targets to excite at low momentum transfer due to the high reaction Q-value. The kinematics of this reaction are closed of the neutrino-nucleus reaction, in contrast to the case in previous experiments. In this article, the angular distribution of the reaction is reported.

The reaction was measured with the BigRIPS[3], the high-Resolution beamline[4], and the SHARAQ spectrometer[5] at RIKEN RIBF. The liquid-^{4}He[6] was installed at the target position of the SHARAQ. The secondary ^{8}He beam irradiated the target at an intensity of about 2 MHz. In order to determine the missing mass energy and scattering angle, the trajectory and momenta of ^{8}He and ^{8}Li were measured by using LP-MWDCs[7] and CRDCs[8] in the beamline and SHARAQ. The detail experimental setup is discribed in another report[9].

Figure 1 shows the cross section angular distribution obtained from the (^{8}He,^{8}Li*(1$^+$)). The vertical and horizontal axes are the differential cross section and scattering angle in the center-of-mass frame, respectively. The closed circles were reduced from the experimental data. The cross sections were summed over the excitation energy in the range from 0 MeV to 30 MeV for the continuum state of ^{4}H. The experimental data were compared with the DWBA calculation with FOLD[10]. The lines show the calculated cross sections on the angular momentum transfer of $\Delta L = 0, 1, 2, 3$. The experimental data qualitatively indicated SD transition.

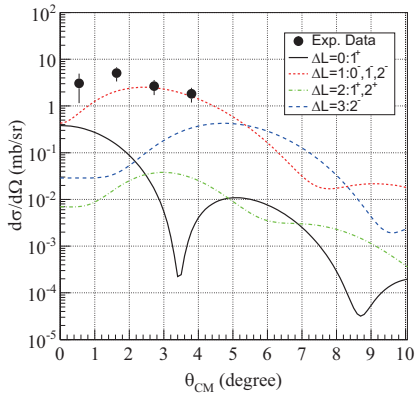

Fig. 1. Cross section angular distribution obtained from the (^{8}He,^{8}Li*(1$^+$)) reaction. Closed circles donate the experimental data. The lines show the DWBA calculation on the angular momentum transfer of $\Delta L = 0, 1, 2, 3$.

Comparison between the experimental data and the theoretical calculation of the isovector type SD response of ^{4}He is now in progress.

*1 Center for Nuclear Study, The University of Tokyo
*2 RIKEN Nishina Center
*3 Institut de Physique Nucléaire, Orsay
*4 Department of Physics, Kyoto University
*5 Research Center Nuclear Physics, Osaka University
*6 Cyclotron and Radioisotope Center, Tohoku University
*7 Department of physics, Tokyo Institute of Technology
*8 Department of Applied Physics, University of Miyazaki
*9 National Institute of Radiological Sciences
*10 Department of physics, The University of Tokyo
*11 Department of Physics, Kyushu University
*12 National Superconducting Cyclotron Laboratory, Michigan State University

References

1) T. Suzuki *et al.*, Phys. Rev. C **74**, 034307 (2006).
2) W. G. Love, M. A. Franey, Phys. Rev. C **24**, 1073 (1981).
3) T. Kubo *et al.*, Nucl. Instr. Meth. B **204**, 97-113 (2003).
4) T. Kawabata *et al.*, Nucl. Instr. Meth. B **266**, 4201-4204 (2008).
5) S. Michimasa *et al.*, Nucl. Instr. Meth. B **317**, 305-310 (2013).
6) H. Ryuto *et al*, Nucl. Instr. Meth. A555, 1-5 (2005).
7) H. Miya *et al.*, Nucl. Instr. Meth. B **317**, 701-704 (2013).
8) K. Kisamori *et al.*, CNS Ann. Rep. 2011 (2013).
9) H. Miya *et al.*, RIKEN Prog. Rep. **46** 25 (2013).
10) J. Cook *et al.*, 'Computer code FOLD/DWHI', Frorida State University (1988).

Magnetic moment measurement of isomeric state in ^{99}Zr and characterization of the abrasion-fission mechanism

F. Boulay,[*1,*2,*3] J. M. Daugas,[*2,*3] G. S. Simpson,[*4] Y. Ichikawa,[*3] A. Takamine,[*3] D. S. Ahn,[*3] K. Asahi,[*5] H. Baba,[*3] L. Balabanski,[*3,*6] T. Egami,[*7] T. Fujita,[*3,*8] N. Fukuda,[*3] C. Funayama,[*5] T. Furukawa,[*9] G. Georgiev,[*10] A. Gladkov,[*3,*11] M. Hass,[*12] K. Imamura,[*3,*13] N. Inabe,[*3] Y. Ishibashi,[*3,*14] T. Kawaguchi,[*7] T. Kawamura,[*8] W. Kim,[*11] Y. Kobayashi,[*15] S. Kojima,[*5] A. Kusoglu,[*10,*16] S. Momiyama,[*17] I. Mukul,[*12] G. Neyens,[*18] M. Niikura,[*17] H. Nishibata,[*8] T. Nishizaka,[*7] A. Odahara,[*8] Y. Ohtomo,[*3,*5] D. Ralet,[*10] T. Sato,[*5] Y. Shimizu,[*3] T. Shimoda,[*8] T. Sumikama,[*3] H. Suzuki,[*3] H. Takeda,[*3] L. C. Tao,[*3,*19] Y. Togano,[*5] D. Tominaga,[*7] H. Ueno,[*3] H. Yamazaki,[*3] and X. F. Yang,[*18]

The region of neutron-rich isotones N=59 is on the border of a sudden change of the ground state shape of nuclei[1,2]. A direct consequence is the existence of many nuclei with isomeric states in this region. These nuclei are well produced by fission. Measuring the magnetic moment of these states often allows a clear determination of their single-particle structure and allows us to determine the spin parity of the isomeric state.

The production of spin-aligned nuclei is primordial for these types of studies; however, the explanations of the production mechanisms of such nuclei are not well known. An alignment of 18(8)% was previously measured for isomers produced in the abrasion-fission reaction[4,5]. The purpose of the experiment described here is to probe different momentum regions and determine the one with the highest alignment rate. Owing to the high beam intensity delivered by RIBF, three different momentum selections of ^{99}Zr were probed with sufficient statistics accumulated.

Thus, the NP1306-RIBF99 experiment performed at RIKEN with the BigRIPS spectrometer has two aims. The first is to measure the magnetic moment of the ^{99}Zr isomeric state. The second is to measure the alignment ratio of the ^{99}Zr produced by the abrasion-fission reaction of a ^{238}U beam sent at 345 MeV/A on a 100-μm-thick target of ^{9}Be.

The time-dependent perturbed angular distribution (TDPAD)[3] method was used to perform such measurements. The ^{99}Zr nuclei were selected and identified through BigRIPS and were implanted in a non-disturbing copper crystal at F8. An external magnetic field of 0.250 T was applied to induce a Larmor precession of the nuclei. This perturbation modified the number of photons emitted at a given angle depending on the time. To detect this variation, 4 germanium detectors were placed around the crystal at 90° relative to each other.

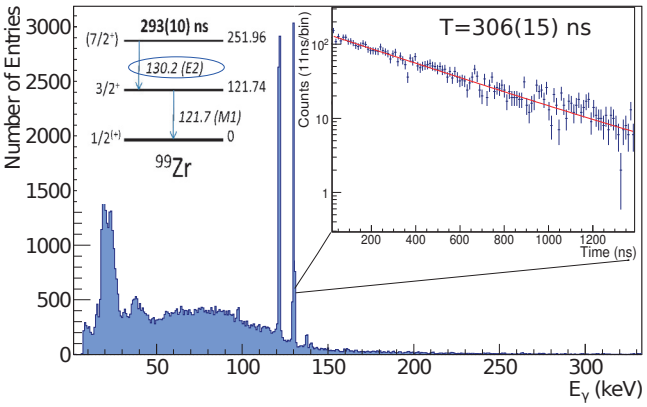

Fig. 1. Preliminary gamma energy spectra measured for ^{99}Zr with the decay curve associated to the 130.2 keV line.

The online analysis did not allow us to extract a preliminary magnetic moment measurement. The analysis is in progress. However, some basic observables could be preliminarily extracted to confirm the expected properties. In Fig. 1, the gamma energy spectra associated with ^{99}Zr is shown. We can see the two characteristic lines from the decay of the isomeric state at 251.96 keV. The fit on the decay curve for the line at 130.2 keV gives a lifetime of 306(15) ns, which is compatible with the adopted value of 293(10) ns.

*1 GANIL CEA/DSM CNRS/IN2P3
*2 CEA DAM
*3 RIKEN Nishina Center
*4 LPSC
*5 Department of Physics, Tokyo Institute of Technology
*6 IFIN/HH/ELI-NP
*7 Department of Physics, Hosei University
*8 Department of Physics, Osaka University
*9 Department of Physics, Tokyo Metropolitan University
*10 CSNSM
*11 Department of Physics, Kyungpook National University
*12 Weizmann Institute
*13 Department of Physics, Meiji University
*14 Department of Physics, University of Tsukuba
*15 Department of Informatics and Engineering, University of Electro Communications
*16 Physics Department, Istanbul University
*17 Department of Physics, University of Tokyo
*18 K. U. Leuven
*19 School of Physics, Peking University

References

1) S. Hilaire, M. Girod Eur. Phys. J. A 33, 237 (2007).
2) A.G. Smith et al., Phys. Lett. B 591, 55 (2004).
3) G. Neyens, Rep. Prog. Phys. 66, 633 (2003).
4) G. Ilie et al., Phys. Lett. B 687, 305 (2010).
5) G. Neyens et al., Acta Phys. Pol. B 38, 1237 (2007).

First dedicated in-beam X-ray measurement at GARIS

C. Berner,[*1,*3] H. Baba,[*3] R. Gernhäuser,[*1] S. Hellgartner,[*1] W. Henning,[*2,*3] D. Kaji,[*3] R. Lutter,[*4] L. Maier,[*1] K. Morimoto,[*3] K. Morita,[*3] D. Mücher,[*1] and Y. Wakabayashi[*3]

We report on an experiment aiming at in-beam X-ray spectroscopy of heavy and superheavy elements (SHE). The goal is to establish K-X-ray spectroscopy as a sensitive tool to identify SHE produced in fusion reactions. SHE are usually identified via the alpha-decay products, which have to be connected to well-known elements. However, various theories predict spontaneous fission as the dominant decay mode for the daughter nuclides. Additionally, half-lives of these elements are expected to increase to values[1,2] impeding the identification of SHE solely by their decay. The in-beam identification of the characteristic X-rays would independently allow to identify the charge number of the produced SHE.

We performed dedicated experiments for in-beam X-ray recoil-decay-tagging spectroscopy at GARIS in order to study the dependence of the mean K-X-ray multiplicity $\langle M_K \rangle$ on the mass-number of the produced evaporation residue. $\langle M_K \rangle$ is predicted[3] to increase to values well above one when approaching the SHE-region (see Fig. 1).

The fact that a single compound nucleus can emit more than one X-ray after formation is a consequence of the filling times of an empty inner atomic orbit (typically $10^{-13} \ldots 10^{-14}$ s[4]) being significantly shorter than the typical lifetime of nuclear levels decaying by electron conversion (typically the pico-second range).Therefore many subsequent conversions are possible in the decay cascade of a compound nucleus.

Experiments were performed at the RIKEN Nishina Centre for Accelerator based Science by using the gas-filled magnet separator GARIS for superheavy element detection. A high-purity, low-energy planar germanium LEGe-detector[a] was adapted to the GARIS system at the target place for the first time in order to measure the element-characteristic, prompt X-ray emission.

In September and October 2014, first tests concerning the rate-acceptance and resolution-deterioration of the LEGe-detector as well as background studies due to different targets in heavy-ion fusion reactions have been carried out. By measuring the γ-ray background during the reaction ^{248}Cm(^{48}Ca, xn)$^{296-x}$Lv* with I = 650 pnA average beam-intensity at a distance of 76 cm to the target the detector performance was excellent: Superior energy-resolution of ΔE_{FWHM} = 800 eV ($@E_x$ = 74 keV) at a trigger rate of 133 kcps. Additionally, neutron damage was measured to be negligible due to the thin and planar structure of the detector: Analysis of the neutron edges in the spectra showed a minimum detector lifetime of more than 40 days at full beam intensity before any visible neutron damage would influence the measurement.

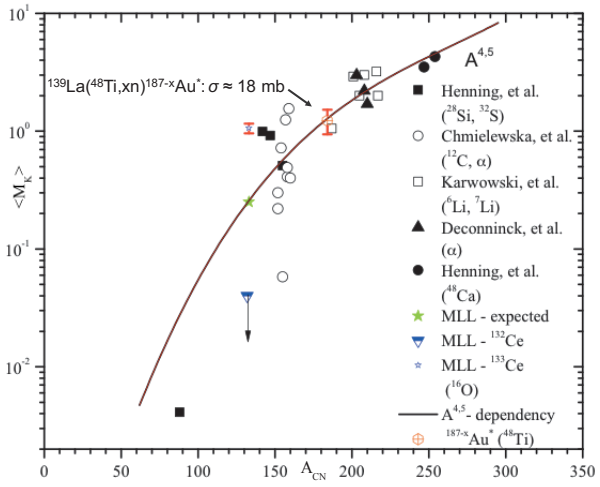

Fig. 1. Experimental values for the mean K-X-ray multiplicity $\langle M_K \rangle$ as a function of the mass number A_{CN}.

Dedicated X-ray spectroscopy was performed in June, 2015: The reaction ^{139}La(^{48}Ti, xn)$^{187-x}$Au was chosen to show the general feasibility of this new detection method. Due to space limitations, a fixed target of ^{139}La with 300 µm/cm^2 on 3 µm Ti-backing had to be used. Therefore, intensity of the ^{48}Ti beam (E = 242 MeV) was limited to 45 pnA. The production cross-section of the compound nucleus $^{187-x}$Au was measured to be σ = 18.5 ± 4.6 mb. As can be seen in Fig. 1, the measured value for the multiplicity-value reveals an excellent agreement with the semi-empirical prediction of $\langle M_K \rangle$ = 1.23 ± 0.29. Encountering the absolute detection efficiencies as well as the total dead-time of the electronics a detection-limit in cross-section can be estimated for in-beam X-ray spectroscopy using a whole array of LEGe-detectors to be 220 pb. This value - being nearly two orders of magnitude lower than the current limit for in-beam γ-ray spectroscopy - encourages for further studies.

*1 Department of Physics, Technische Universität München
*2 ANL, Argonne National Laboratory
*3 RIKEN Nishina Center
*4 Faculty of Physics, Ludwig Maximilians Universität
a) Canberra Type LEGe1010

References

1) A. Staszczak et al., Phys. Rev. C **87**, 024320 (2013).
2) Y.Oganessian, Rep. Prog. Phys. **78**, (2015).
3) W. Henning, Nucl. Phys. A **400**, (1983).
4) H.J. Karwowski et al., Phys. Rev. C **25**, (1982).

Isotope identification in nuclear emulsion plate for double-hypernuclear study

S. Kinbara,[*1] H. Ekawa,[*2] T. Fujita,[*3] S. Hayakawa,[*4] S. H. Hwang,[*5] Y. Ichikawa,[*3] K. Imamura,[*3] H. Itoh,[*1] H. Kobayashi,[*1] R. Murai,[*1] K. Nakazawa,[*1] M. K. Soe,[*1] A. Takamine,[*3] A. M. M. Theint,[*1] H. Ueno,[*3] and J. Yoshida[*1]

Double-Λ hypernuclei and twin single-Λ hypernuclei are quite important objects, since they give us the Λ-Λ and Ξ-*N* interaction. In the KEK-E373 experiment, only the NAGARA event was uniquely identified as a $_{\Lambda\Lambda}{}^{6}$He among seven events in nuclear emulsion, and the Λ-Λ interaction is found to be weakly attractive in the *s*-shell double-Λ hypernucleus.[1), 2)] To understand the Λ-Λ and Ξ-*N* interaction in a unified way up to the *p*-shell nuclei, it is necessary to uniquely identify as many nuclides as possible. For such detection, we find that the recognition of daughter particles from the decay of the double-Λ hypernucleus is key issues. It can be very useful for ionization-loss measurement, which will be reflected in particle-track thickness or width in the emulsion. Although the relation between energy losses, *dE/dx*, and their ranges has been calibrated by specific a rays with monochromatic energies of natural radioisotopes in the emulsion, we have no experience in recognizing the relation between particle track widths and their charges.

To develop a particle-identification (PID) method, fully stripped particles of ^{1}H, ^{2}H, ^{3}H, ^{3}He, ^{4}He, ^{7}Li, ^{9}Be and ^{11}B were exposed to the emulsion. Those particles were produced as fragments of the ^{12}C beam with an energy of 70 AMeV and intensity of 10 pnA at the ^{9}Be target (t = 0.5 mm). Wedge-shaped degraders made of Al with a thickness of 962 mg/cm^2 and 426 mg/cm^2 were used to degrade the particle energies. Additionally, Al and Fe degraders, which were combined with several thickness plates, were installed to get suitable particle energies for stopping in the emulsion in front of the emulsion stack.

An emulsion stack had a size of 3×7 cm^2 and a thickness of 6 mm, and was exposed to one particle with a density of nearly 10^4 particles/cm^2. To obtain the parameter for calibrating a track haloes depending on the incident angle θ, all emulsion stacks were exposed with angles of θ = 0°, 25°, 50°, 75°. We exposed ^{1}H horizontally (θ = 90°) to all emulsion plates as a baseline of track width, which depends on the optical and photographic development conditions on plate by plate of the emulsion.

The raw image taken with a CCD camera attached to an optical microscope is shown in Fig.1 a). Based on this image a), the blurred image of b) by Gaussian kernel was obtained. By subtracting the blurred image b) from the raw image a), an image of c) with a uniform background was obtained. In this image c), the track width was defined as the distance between two inflection points, which were obtained from the brightness distribution by using the fitting function, $F=A$*tanh(Gauss(x,μ,σ)). We assumed a track to be made of many cylinders with a thickness of 1 μm, and obtained the track volume as collection of cylinders.

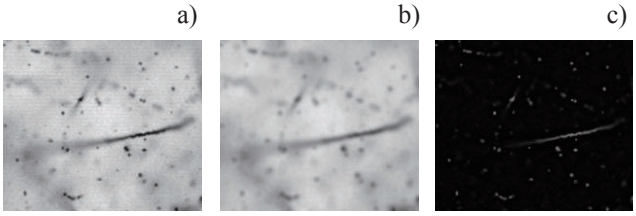

Fig. 1. Process to obtain track width with uniform background from a) to c).

The volumes of five nuclides (θ = 75°) were obtained along the track between 10 μm and 100 μm from the stopping point. Since the track width becomes narrow near the stopping point, we omitted the track volume around there. Two large volumes, which would suddenly appear, were removed among the ten cylinders, and the average volume in an interval of 10 μm was obtained from the eight cylinders. The preliminary result on the volume ratios for the five nuclides of ^{1}H, ^{4}He, ^{7}Li, ^{9}Be and ^{11}B corresponding to horizontally exposed ^{1}H (θ = 90°) is shown in Fig. 2. Although the recognition for the different charged particles seems good around 100 μm in three standard deviations, it is quite necessary to develop the analysis in the region near the stopping point. Data fluctuation around there causes worse convergence in a more short range region.

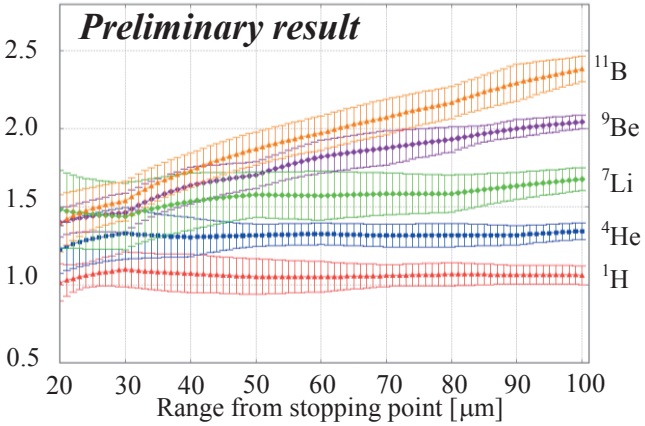

Fig. 2. Volume ratio for each nuclides (θ = 75°) to ^{1}H (θ = 90°) .

* This work shall be published in HYP2015 JPS. Conf. Proc.

References

1) H. Takahashi *et al.*, Phys. Rev. Lett. **87**, 212502 (2001).
2) J. K. Ahn *et al.*, Phys. Rev. C **88** 014003 (2013).

[*1] Physics Department, Gifu University
[*2] Department of Physics, Kyoto University
[*3] RIKEN Nishina Center
[*4] Department of Physics, Osaka University
[*5] Japan Atomic Energy Research Institute

Measurement of nuclear magnetic moment of neutron-rich ^{39}S

Y. Ishibashi,[*1,*2] Y. Ichikawa,[*1] A. Takamine,[*1] A. Gladkov,[*1,*3] K. Imamura,[*1,*4] T. Fujita,[*1.*5] T. Sato,[*6] K. Asahi,[*6] T. Egami,[*7] C. Funayama,[*6] T. Kawaguchi,[*7] S. Kojima,[*6] L. C. Tao,[*1,*8] D. Nagae,[*1] T. Nishizaka,[*7] Y. Ohtomo,[*6] A. Ozawa,[*2] D. Tominaga,[*7] H. Yamazaki,[*1] A. Yoshimi,[*9] and H. Ueno[*1]

Ground-state nuclear electromagnetic moments of unstable nuclei have been measured with the β-ray detected nuclear magnetic resonance (β-NMR) method [1] using fragmentation-induced spin-polarized radioactive isotope (RI) beams[2]. In this method, a resonance can be observed when all three conditions are met at the same time: 1) a polarized RI beam is produced; 2) the frequency range of the oscillating magnetic field in β-NMR measurements covers a resonance frequency; and 3) polarization is maintained in the stopper material during count time. These conditions complicate β-NMR measurements. In order to investigate the production of spin polarization separately from the resonance scan, a new adiabatic field rotation (AFR) system has been developed.[3,4]

The experiment was carried out at the RIKEN Projectile Fragment Separator (RIPS) at the RI Beam Factory operated by RIKEN Nishina Center in September 2015. Nuclear spin-polarized ^{39}S nuclei were produced by bombarding ^{48}Ca ions on a 0.52-mm-thick ^{9}Be target for the first time. The $^{48}Ca^{17+}$ ions were accelerated up to 63 MeV/nucleon and the intensity of the primary beam was typically ∼200 pnA on the target. The fragments emitted into the angle from 1.5° to 5.9° relative to the primary beam with the momentum $p = p_0 \times (1.02 \pm 0.02)$, where p_0 is the peak in the distribution, were selected by the RIPS. A wedge-shaped degrader (148.8 mg/cm^2) was used for energy loss separation, and then, the ^{39}S ions were transported to the AFR and β-NMR apparatus. Next, they were implanted into a CaS crystal together with inseparable fragments as contaminants that became low energy β-ray emitters. Under these conditions, the beam purity of ^{39}S was about 70%.

First, AFR measurements were conducted with ^{39}S nuclei. The experimental setup of the AFR measurement is described in Ref. 5). The maximum asymmetry change (AP) is normalized to be a product of the asymmetry parameter A and polarization P. The AP values for AFR measurements of ^{39}S in CaS are shown in Fig. 1, where the plot points 1-5 correspond to the conditions shown in Table 1. Table 1 shows the time sequence of beam on/off period, selected momentum, selected angle, and obtained yield of β-ray from ^{39}S (Y_β). As per the results of AFR measurements, we were successfully in achieving nuclear spin-polarization.

Second, β-NMR measurements by means of the adiabatic fast passage (AFP) method were carried out with ^{39}S nuclei. The experimental setup of the AFP-NMR measurement is the same as described in Ref. 6). Because the range of theoretically predicted g-factor is very wide, a fast switching system was used.[7] In this measurement, the g-factor search was performed in the region $0.14 < g < 1.49$. The results of the AFP-NMR measurements are under analysis.

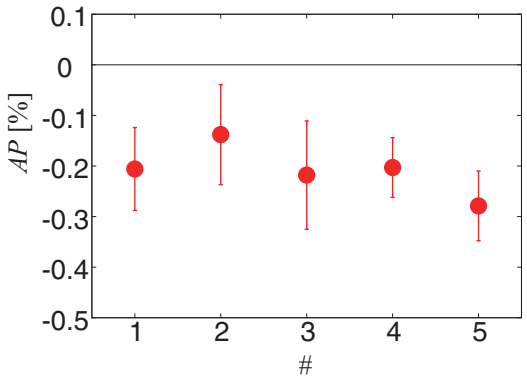

Fig. 1. Obtained AP value of ^{39}S at room temperature.

Table 1. Measurement conditions and obtained Y_β

#	Time sequence	Momentum [%]	Angle	Y_β [cps]
1	2 s - 30 s	$1 \le \Delta p/p_0 \le 4$	$\theta \ge 1.5°$	140
2	2 s - 30 s	$1 \le \Delta p/p_0 \le 4$	$\theta \ge 1.0°$	150
3	8 s - 24 s	$1 \le \Delta p/p_0 \le 4$	$\theta \ge 1.5°$	240
4	16 s - 16 s	$1 \le \Delta p/p_0 \le 4$	$\theta \ge 1.5°$	310
5	16 s - 16 s	$0 \le \Delta p/p_0 \le 4$	$\theta \ge 1.5°$	420

*1 RIKEN Nishina Center
*2 Institute of Physics, University of Tsukuba
*3 Department of Physics, Kyungpook National University
*4 Department of Physics, Meiji University
*5 Department of Physics, Osaka University
*6 Department of Physics, Tokyo Institute of Technology
*7 Department of Physics, Hosei University
*8 School of Physics and State Key Laboratory of Nuclear Physics and Technology, Pekin University
*9 Research Core for Extreme Quantum World, Okayama University

References

1) K. Sugimoto et al., Phys. Lett. **18**, 38 (1965).
2) K. Asahi et al., Phys. Lett. B **251**, 488 (1990).
3) H. Ogawa et al., Phys. Lett. B **451**, 11 (1999).
4) Y. Ishibashi et al., Nucl. Instrum. Meth. B **317**, 714 (2013).
5) A. Gladkov et al., in this report.
6) Y. Ichikawa et al., RIKEN Accel. Prog. Rep. **48**, 64 (2014).
7) N. Yoshida et al., Nucl. Instrum. Meth. B **317**, 705 (2013).

Polarization measurements of ^{39}S for β-NMR studies

A. Gladkov,[*1,*2] Y. Ichikawa,[*1] Y. Ishibashi,[*1,*3] A. Takamine,[*1] T. Fujita,[*1,*4] K. Imamura,[*1,*5] T. Nishizaka,[*6] H. Ueno,[*1] W. Y. Kim,[*2] L. C. Tao,[*1,*7] T. Egami,[*6] H. Yamazaki,[*1] D. Tominaga,[*6] K. Asahi,[*8] T. Kawaguchi,[*6] Y. Ohtomo,[*1,*8] C. Funayama,[*8] S. Kojima,[*8] and T. Sato[*8]

In this experimental campaign, we focus on the search for the ground state electromagnetic moments of S isotopes close to the magic number $N = 28$, for which erosion of the shell gap has been suggested[1,2]. As the AP value obtained for ^{41}S is quite small[3], the AP value achieved for ^{39}S whose decay scheme has been partly established[4] is tested before the ^{41}S and ^{43}S measurements. Here A and P denote the asymmetry parameter for the β-ray emission and the degree of polarization, respectively.

For these purposes, we employ the method of β-nuclear magnetic resonance (β-NMR) in combination with adiabatic fast passage technique (AFP) and the particles of interest are provided by the well-established method to produce spin-polarized RI beams[5]. However, in order to conduct the β-NMR measurement in an efficient way, it is highly desirable to determine the optimal beam settings resulting in the largest value of the figure-of-merit $Y \times P^2$ beforehand, where Y and P denote the yield and polarization of the secondary beam, respectively. Therefore, we employ the adiabatic field rotation (AFR) system[6,7] that enables us to determine the polarization through a change in the β-ray asymmetry caused by the adiabatic rotation of the holding field, without the use of the NMR technique and prior to the actual β-NMR measurement.

A strong holding field B_0 provides better preservation of polarization and higher probability of spin reversal. To increase the magnetic field within the space and motor power limitations, the magnet part of the AFR device was modified by employing the Halbach array magnet configuration[8] instead of a common dipole design. The type of Halbach array that we use consists of eight Nd magnet segments placed in such a way that the entire construction forms a circular shape. Each segment has a different direction of the magnetic field so that the magnetic field lines are within the magnet material. Thus, the key feature of the array is that the magnetic field is mostly enclosed within the array and is negligibly weak outside of it, providing the most efficient use of the magnet material. With such a configuration, a 0.495 T magnetic field was obtained, which is almost twice as large as that for the previous dipole design.

In addition, the rectangular planar plastic scintillators were replaced with cylindrical scintillators covering a solid angle of nearly 2π sr. This allowed us to enlarge the stopper so that it is the same size as that in the β-NMR setup.

The AFR experiment was conducted at the RIPS facility at the RIBF prior to the β-NMR measurements. A secondary beam of ^{39}S was produced from the projectile fragmentation reaction of ^{48}Ca on a 0.5 mm-thick beryllium target at an energy of 63 MeV/nucleon and beam current of 200 pnA at the target. In order to ensure polarization of ^{39}S, an emission angle selection $\theta_F > 2^\circ$ was applied with a momentum window of $p_F = p_0 \times (1.02 \pm 0.02)$. Here p_0 represents the central momentum of the fragment. In these conditions, a beam purity of 77% was achieved by the two-stage $B\rho$ selection. After separation, the particles of interest were implanted in a 0.5 mm-thick CaS stopper within the AFR setup. The emitted β-rays were detected by two pairs of plastic scintillators placed above and below the stopper.

The measurements were carried out according to the following sequence. The stopper was irradiated for 16 s of the beam-on period. The AFR magnet array was then rotated by 180° for 150 ms. As the rotation causes small vibrations, an additional margin of 70 ms was added to ensure stabilization. After that the β-particles were counted for 16 s. The AP value was calculated from the four-fold ratio considering four configurations of up/down direction of the rotating field and normal/reversed spin of the implanted particles.

In this measurement, an AP value of $-0.37 \pm 0.12\%$ was obtained with 3.1σ significance on the CaS stopper. The determined beam settings were applied in the β-NMR measurements following the AFR experiment to determine the g-factor of the ^{39}S ground sate. Further analysis of data obtained from both experiments is in progress.

*1 RIKEN Nishina Center
*2 Department of Physics, Kyungpook National University
*3 Department of Physics, University of Tsukuba
*4 Department of Physics, Osaka University
*5 Department of Physics, Meiji University
*6 Department of Physics, Hosei University
*7 The School of Physics and State Key Laboratory of Nuclear Physics and Technology, Pekin University
*8 Department of Physics, Tokyo Institute of Technology

References

1) R. W. Ibbotson et al.: Phys. Rev. C **59**, 642 (1999).
2) S. Grévy et al.: Eur. Phys. J. A **25**, 11 (2005).
3) H. Shirai et al.: RIKEN Accel. Prog. Rep. **47**, 39 (2014).
4) J. C. Hill et al.: Phys. Rev. C **21**, 384 (1980).
5) K. Asahi et al.: Phys. Lett. B **251**, 488 (1990).
6) H. Ogawa et al.: Phys. Lett. B **451**, 11 (1999).
7) Y. Ishibashi et al.: Nucl. Instrum. Meth. B **317**, 714 (2013).
8) K. Halbach: Nucl. Instrum. Meth. **169**, 1 (1980).

β-NMR measurement in coincidence with β-delayed γ rays of ^{39}S

L. C. Tao,[*1,*2] Y. Ichikawa,[*1] H. Ueno,[*1] Y. Ishibashi,[*1,*3] A. Takamine,[*1] A. Gladkov,[*1,*4] T. Fujita,[*1,*6] K. Asahi,[*7] T. Egami,[*8] C. Funayama,[*7] K. Imamura,[*1,*5] T. Kawaguchi,[*8] S. Kojima,[*7] T. Nishizaka,[*8] T. Sato,[*7] D. Tominaga,[*8] and H. Yamazaki[*1]

We aim to measure the ground-state magnetic moment of neutron-rich S isotopes. The β-NMR measurement of ^{39}S was carried out before ^{41}S and ^{43}S, in order to check the AP value that was produced through fragmentation reaction and was kept in a CaS stopper[1]. The β-decay of ^{39}S was reported but spin parities of the produced ^{39}Cl excited states have not been fixed other than the two excited states whose energies respectively are 396 keV and 1697 keV[2]. β-γ spectroscopy with polarized beams was carried out to establish a complete decay scheme including fixed spin parities, which is required for an accurate evaluation of AP value.

This experiment was carried out at the RIPS of RIBF in December 2015. A beam of ^{39}S was obtained from the fragmentation of ^{48}Ca projectiles at $E = 63$ MeV/nucleon on a ^{9}Be target with a thickness of 0.5 mm. The intensity of ^{48}Ca beam on the Be target was typically 200 pnA. The isotope separation of ^{39}S was performed with RIPS where an emission angle of $\theta_{\mathrm{F}} > 2.0°$ and a momentum window of $p_{\mathrm{F}} = p_0 \times (1.02 \pm 0.02)$ were selected in order to produce spin polarization in ^{39}S. Here, p_0 represents the central momentum of fragment ^{39}S.

The ^{39}S beam was then transported to the final focal plane and implanted into a 0.5-mm-thick CaS stopper in the β-NMR apparatus. The β-NMR apparatus consists of a collimator, a CaS crystal stopper, a dipole magnet, a radio frequency Helmholtz coil and scintillator telescopes located above and below the stopper. The CaS stopper was mounted between the poles of the dipole magnet. The experimental setup for NMR measurement was same as described in Ref[1]. The β-delayed gamma rays of ^{39}S that stopped in the CaS crystal were detected using two high purity Ge detectors that were diagonally placed at a distance of 30 cm from the stopper. Fig. 1 shows the photograph of the experimental setup around the stopper. The data acquisition system was triggered by a gamma-hit event defined by a logical OR of signals from the Ge detectors.

In this experiment, we also observed six gamma-ray peaks with energies of 396 keV, 485 keV, 874 keV, 904 keV, 1300 keV and 1697 keV, which had been observed in the previous experiment[2]. As an example, the energy spectrum of 396 keV is shown in Fig. 2. The further analysis to obtain the polarization effect in coincidence with the β rays is in progress.

Fig. 1. Photograph of experimental setup. The top part of one Ge detector is seen on the right side of the figure, and the other detector is located behind the dipole magnet. Two sets of plastic scintillators are inserted between the poles of the magnet.

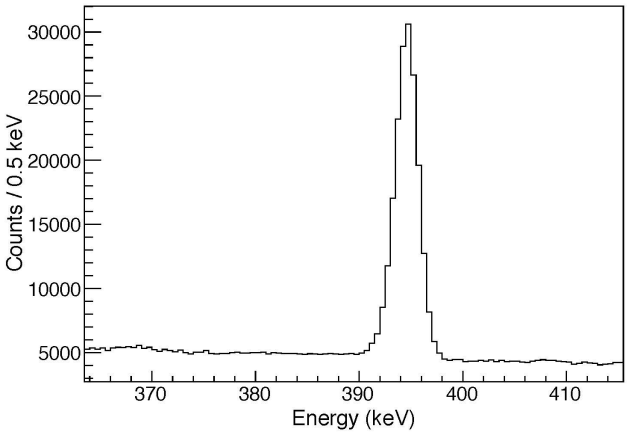

Fig. 2. γ ray spectrum with the energy of 396 keV.

*1 RIKEN Nishina Center
*2 School of Physics and State Key Laboratory of Nuclear Physics and Technology, Peking University
*3 Department of Physics, University of Tsukuba
*4 Department of Physics, Kyungpook National University
*5 Department of Physics, Meiji University
*6 Department of Physics, Osaka University
*7 Department of Physics, Tokyo Institute of Technology
*8 Department of Physics, Hosei University

References

1) Y. Ishibashi et al., RIKEN Accel. Prog. Rep. **49** (in this report).
2) J. C. Hill, R. F. Petry, K. H. Wang: Phys. Rev. C **21**, 384 (1980).

First application of the Trojan Horse Method with a radioactive ion beam: study of the ^{18}F$(p,\alpha)^{15}$O reaction at astrophysical energies†

S. Cherubini,[*1,*2,*3] M. Gulino,[*1,*3,*4] C. Spitaleri,[*1,*2] G.G. Rapisarda,[*1,*2] M. La Cognata,[*1] L. Lamia,[*2] R.G. Pizzone,[*1] S. Romano,[*1,*2] S. Kubono,[*3,*5] H. Yamaguchi,[*5] S. Hayakawa,[*1,*5] Y. Wakabayashi,[*5] N. Iwasa,[*6] S. Kato,[*7] T. Komatsubara,[*8] T. Teranishi,[*9] A. Coc,[*10] N. de Séréville,[*11] F. Hammache,[*11] G. Kiss,[*12] S. Bishop,[*3,*13] and D.N. Binh[*5,*14]

The results of a pioneering experiment where the Trojan Horse Method[1,2] was applied for the first time for measuring the cross section of an astrophysically important reaction, namely ^{18}F$(p,\alpha)^{15}$O at Nova energies[3,4], using a radioactive beam were published in Phys. Rev. C **92**, 015805 (2015).

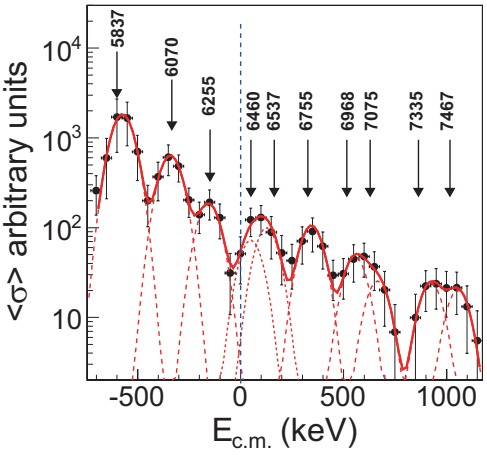

Fig. 1. The nuclear cross section spectrum as a function of the p-^{18}F cm energy. The blue vertical line shows the position of the threshold for the ^{18}F+p reaction (E_{th} = 6.41 MeV). The red dashed lines represent Gaussians used for fitting the data. The numbers above the arrows represents the peak positions in ^{19}Ne excitation energy obtained from the fitting procedure.

The experiment was performed at the RIKEN Nishina Center using the CRIB apparatus from the University of Tokyo. The primary beam of ^{18}O delivered by the AVF cyclotron was used to produce a ^{18}F radioactive beam with intensity in the range of 10^5-10^6 pps.

The nuclear cross section and the astrophysical factor S(E) were extracted from the data for the reaction ^{18}F$(p,\alpha)^{15}$O. These are shown in Figs. 1 and 2 respectively. In order to improve the results obtained in this work, a new measurement of the same reaction was performed again in Fall 2015. The new experiment is also reported in this Accelerator Progress Report[5].

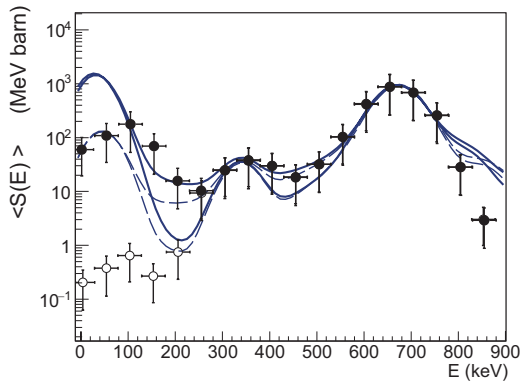

Fig. 2. The ^{18}F(p, α)^{15}O astrophysical S-factor from this work. The full dots are THM experimental data with the assumption of $J^\pi = 3/2^+$ for the resonance at E = 6460 keV, the open ones corresponds to the assumption of $J^\pi = 5/2^-$ (the difference from this last assumption to the other possible value $1/2^-$ and $3/2^-$ being negligeable within the errors). The solid and dashed lines shown in the figure are calculations presented and discussed in Ref.[6] smeared to the present experimental resolution.

† Condensed from the article in Phys. Rev. C **92**, 015805 (2015)

*1 INFN-LNS, Catania, Italy
*2 Dipartimento di Fisica ed Astronomia, Università di Catania
*3 Riken, Nishina Center
*4 Università di Enna KORE
*4 RIKEN, Nishina Center
*5 Center for Nuclear Study, The University of Tokyo
*6 Department of Physics, Tohoku University
*7 Department of Physics, Yamagata University
*8 Rare Isotope Science Project, Institute for Basic Science
*9 Department of Physics, Kyushu University
*10 Centre de Spectrométrie Nucléaire et de Spectrométrie de Masse, IN2P3
*11 Institut de Physique Nucléaire, IN2P3
*12 Institute for Nuclear Research (MTA-ATOMKI)
*13 TUM
*14 30 MeV Cyclotron Center, Tran Hung Dao Hospital

References

1) R. E. Tribble et al., Rep. Prog. Phys. **77**, 106901 (2014).
2) S. Cherubini et al., ApJ **457**, 855, (1996).
3) A. S. Adekola et al., Phys. Rev., **C83** 052801 (R) (2011).
4) A. M. Laird et al., Phys. Rev. Lett., **110**, 032502 (2013).
5) S. Cherubini et al.: In this report.
6) C. E. Beer et al., Phys. Rev., **C 83**, 042801 (2011)

Different mechanism of two-proton emission from excited states of proton-rich nuclei ^{23}Al and ^{22}Mg†

Y. G. Ma,[*1] D. Q. Fang,[*1] X. Sun,[*1] P. Zhou,[*1] Y. Togano,[*2] N. Aoi,[*2] H. Baba,[*2] X. Z. Cai,[*1] X. G. Cao,[*1] J. G. Chen,[*1] Y. Fu,[*1] W. Guo,[*1] Y. Hara,[*3] T. Honda,[*3] Z. Hu,[*4] K. Ieki,[*3] Y. Ishibashi,[*5] Y. Ito,[*5] N. Iwasa,[*6] S. Kanno,[*2] T. Kawabata,[*7] H. Kimura,[*8] Y. Kondo,[*2] K. Kurita,[*3] M. Kurokawa,[*2] T. Moriguchi,[*5] H. Murakami,[*2] H. Ooishi,[*5] K. Okada,[*3] S. Ota,[*7] A. Ozawa,[*5] H. Sakurai,[*2] S. Shimoura,[*7] R. Shioda,[*3] E. Takeshita,[*2] S. Takeuchi,[*2] W. Tian,[*1] H. Wang,[*1] J. Wang,[*4] M. Wang,[*4] K. Yamada,[*2] Y. Yamada,[*3] Y. Yasuda,[*5] K. Yoneda,[*2] G. Q. Zhang,[*1] and T. Motobayashi[*2]

For proton-rich nuclei, the proton decay mechanism is complicated, especially for two-proton (2p) radioactivity[1]. The proton-rich nucleus ^{23}Al has attracted a lot of attention in recent years since it may play a crucial role in understanding the depletion of the NeNa cycle in ONe novae[2]. The measurement of its reaction cross section and fragment momentum distribution has shown that the valence proton in ^{23}Al is dominated by the d wave but with an enlarged core[3]. The spin and parity of the ^{23}Al ground state was found to be $J^{\pi}=5/2^{+}$[4]. Also of great interest is ^{22}Mg because of its importance in determining the astrophysical reaction rates for ^{21}Na(p,γ)^{22}Mg and ^{18}Ne(α,p)^{21}Na reactions in the explosive stellar scenarios.

An experiment was performed to study the two-proton decay channels of ^{23}Al and ^{22}Mg using the RIPS beamline at the RI Beam Factory (RIBF) operated by RIKEN Nishina Center and Center for Nuclear Study, University of Tokyo.

In this study, we examined the relative momentum spectrum (q_{pp}) and opening angle (θ_{pp}) of the two protons in the three-body decay system for ^{23}Al and ^{22}Mg. Without any cut in the excitation energy, a broad q_{pp} spectrum and structure-less θ_{pp} distribution are observed. These results indicate that the main mechanism of two proton emission from ^{23}Al and ^{22}Mg are sequential or three-body emission with very weak correlation between the two protons. However, since the decay mode for different excited states or excitation energies is different, it is interesting to check q_{pp} and θ_{pp} spectrum at different excitation energies. For the diproton or ^{2}He emission, a clear peak should appear at small relative momentum as well as opening angle. Fig. 1 show the experimental results of the above two distributions for ^{23}Al in the excitation energy window $10.5 < E^{*} < 15$ MeV. Evident peaks at $q_{pp} \sim 20$ MeV/c (a) and small opening angle (b) are absent. Instead, the q_{pp} spectrum is broad and the θ_{pp} distribution is structure-less. Similar analysis has been done in different E* windows other than $10.5 < E^{*} < 15$ MeV and similar behaviors for q_{pp} and θ_{pp} are observed.

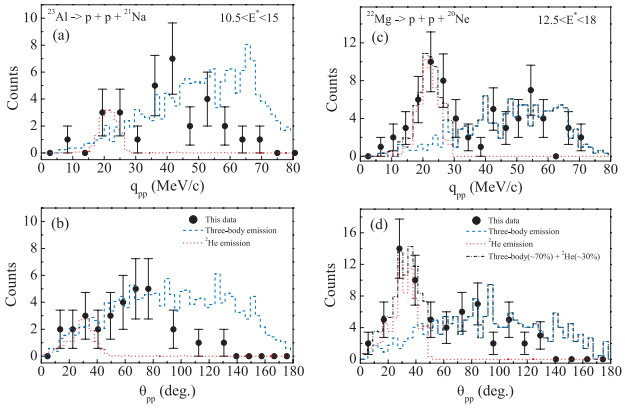

Fig. 1. Relative momentum (a) and opening angle (b) distributions between two protons by the decay of ^{23}Al into two protons plus ^{21}Na for $10.5 < E^{*} < 15$ MeV; (c) and (d) are the results by the decay of ^{22}Mg into two protons plus ^{20}Ne for $12.5 < E^{*} < 18$ MeV.

For ^{22}Mg, Fig. 1 shows the q_{pp} (c) and θ_{pp} (d) data in the excitation energy window $12.5 < E^{*} < 18$ MeV. The peaks of the q_{pp} distribution at 20 MeV/c and of the corresponding small θ_{pp} are clearly observed. These features are consistent with the diproton emission mechanism. However, no significant enhancements for $q_{pp} \sim 20$ MeV/c and small θ_{pp} are observed for other E^{*} windows.

In order to quantitatively understand the q_{pp} and θ_{pp} spectra, a Monte Carlo simulation has been performed. A mixture of diproton and simultaneous three-body decay or sequential decay was used to fit the q_{pp} and θ_{pp} data. As shown in the figure, the sequential decay is overwhelmingly dominant for ^{23}Al. For ^{22}Mg, on the other hand, the diproton or ^{2}He emission peaks are well reproduced by the simulation. The fraction of the diproton emission is determined to be around 30%.

† Condensed from the article in Phys. Lett. B **743**, 306 (2015)

*1 Shanghai Institute of Applied Physics, CAS
*2 RIKEN Nishina Center
*3 Department of Physics, Rikkyo University
*4 Institute of Modern Physics, CAS
*5 Institute of Physics, University of Tsukuba
*6 Department of Physics, Tohoku University
*7 Center for Nuclear Study (CNS), University of Tokyo
*8 Department of Physics, University of Tokyo

References

1) V. I. Goldansky, *Nucl. Phys.* **19** (1960) 482.
2) V. E. Iacob et al., *Phys. Rev. C* **74** (2006) 045810.
3) D. Q. Fang et al., *Phys. Rev. C* **76** (2007) 031601(R).
4) A. Ozawa et al., *Phys. Rev. C* **74** (2006) 021301(R).

Observation of resonances in ^{14}C with ^{10}Be+α resonant elastic scattering at CRIB

H. Yamaguchi,[*1] D. Kahl,[*1] S. Hayakawa,[*1] Y. Sakaguchi,[*1] and K. Abe,[*1] for CRIB collaboration

A measurement of ^{10}Be+α resonant elastic scattering was conducted at CRIB on the interests of cluster structure in the ^{14}C nucleus[1–3]. In 2015, the main measurement was performed using the thick-target method in inverse kinematics. The ^{10}Be radioactive isotope (RI) beam was produced via the ^{11}B(d, ^{3}He)^{10}Be reaction in inverse kinematics using a 1.2-mg/cm^2-thick deuterium gas target and a ^{11}B beam at 5.0 MeV/u and 700 pnA accelerated with an AVF cyclotron. The ^{10}Be beam was separated and purified by magnetic analysis and velocity selection with a Wien filter. The experimental setup at the final focal plane was similar to the previous one in the ^{7}Be+α experiment[4], but we placed an extra silicon detector telescope instead of the NaI detectors, and we used two parallel-plate avalanche counters (PPACs) as the beam counter. The new setup enabled us to perform a reliable analysis on the angular distribution with a better position sensing of the beam and recoiled particles. The parallel-plate avalanche counters (PPACs) measured timing and position of the incoming ^{10}Be beam with a position resolution of 1 mm or better. The beam finally traveled into the gas target, a chamber filled with helium gas at 700 Torr and covered with a 20-μm-thick Mylar film as the beam entrance window. The ^{10}Be beam energy at the entrance of the helium gas target was 25 MeV, and the purity was better than 95%, with a typical intensity of 10^4 pps. α particles recoiling to the forward angles were detected by the ΔE-E detector telescopes. We used two sets of detector telescopes in the gas-filled chamber, where each telescope consisted of two layers of silicon detectors, which had thicknesses of 20 μm and 480 μm. The central telescope was located at 555 mm from the beam entrance window, and the other telescope was at an angle of 9°, looking from the entrance window position. Each detector in the telescope had an active area of 50 × 50 mm, and 16 strips for one side, making pixels of 3 × 3 mm^2.

The dominant particle measured at the telescopes was α particle, which was distinguished from other particles with the ΔE-E information. We selected events in which the beam particle was entering into the target and an α particle was detected at the telescope in coincidence with the ^{10}Be beam particle at the PPAC. A precise energy loss function of the ^{10}Be beam in the helium gas target was obtained by a direct energy measurement at seven different target pressures interpolated with a calculation using the SRIM code. The scattering position, or equivalently the center-of-mass energy $E_{\rm cm}$, was determined by a kinematic reconstruction on event-by-event basis, which uses the energy loss function, the beam trajectory measured with the PPACs, and the energy and position of the recoiled α particle at the telescope. The number of events for each small energy division was converted to the differential cross section $d\sigma/d\Omega$, using the solid angle of the detector, the number of beam particles, and the effective target thickness. The number of beam particles was precisely known by the single counting of the beam particle with the PPAC, simultaneously recorded in the measurement. The background contribution evaluated by the argon-target run data was subtracted from the helium-target spectrum. Finally we obtained the excitation function of the ^{10}Be+α resonant scattering for 14–19 MeV as shown in Fig. 1a, where events with the laboratory angle of the recoiled α particle $\theta_{\rm lab}$=0–8° (corresponding to the center-of-mass angle $\theta_{\rm cm}$=164–180°) were selected. The excitation function obtained here has a similar peak structure with a previous measurement[5]. The resonant information including J^π will be obtained with an analysis with R-matrix calculation.

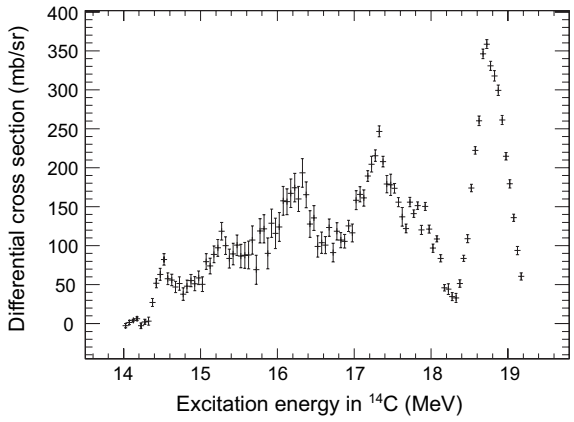

Fig. 1. Excitation function of the ^{10}Be+α resonant scattering for $\theta_{\rm lab}$=0–8°.

[*1] Center for Nuclear Study, University of Tokyo

References

1) T. Suhara and Y. Kanada-En'yo: Phys. Rev. C **82**, 044301 (2010).
2) T. Suhara and Y. Kanada-En'yo: Phys. Rev. C **84**, 024328 (2011).
3) H. Yamaguchi et al.: RIKEN Accelerator Progress Report **48**, 67 (2015).
4) H. Yamaguchi et al.: Phys. Rev. C **87**, 034303 (2013).
5) M. Freer et al.: Phys. Rev. C **90**, 054324 (2014).

New Trojan Horse study of the $^{18}F(p,\alpha)^{15}O$ reaction at astrophysical energies

S. Cherubini,[*1,*2,*3] G. D'Agata,[*1,*2] M. Gulino,[*1,*3,*4] M. La Cognata,[*1] S. Palmerini,[*1] R.G. Pizzone,[*1] S. Romano,[*1,*2] R. Spartà,[*1] C. Spitaleri,[*1,*2] H. Yamaguchi,[*5] K. Abe,[*5] O. Beliuskina,[*5] S. Hayakawa,[*5] D.M. Kahl,[*5] Y. Sakaguchi,[*5] S. Kubono,[*3] D. Suzuki,[*3] N. Iwasa,[*6] K.Y. Chae,[*7] M. Kwag,[*7] H.S. Jung,[*8] D.N. Binh,[*9] V. Guimarães,[*10] and S. Bishop[*11]

The first experiment on the application of the Trojan Horse Method[1,2] was to measure the cross section of an astrophysically important reaction, namely $^{18}F(p,\alpha)^{15}O$ at nova energies[3,4] via the $^{18}F(p,\alpha^{15}O)n$ reaction with three bodies in the final state, using a radioactive beam. This experiment has been recently published in Ref. 5 and it is also presented in this report.[6] Indeed, the whole idea of the Trojan Horse Method is to study a suitably chosen reaction proceeding via a quasi-free mechanism with three body in the final state, in the present case $^{18}F(d,\alpha^{15}O)n$, in order to infer pieces of information on the process of astrophysical interest, $^{18}F(p,\alpha)^{15}O$ in this case.

In order to improve the statistics as well as the quality of data, a new measurement was performed at the RIKEN Nishina Center using the CRIB apparatus from the University of Tokyo during October-November 2015. As in the previous work, the primary beam of ^{18}O delivered by the AVF cyclotron was used to produce a ^{18}F radioactive beam with intensity in the range of 10^5-10^6 pps. After the standard CRIB apparatus, the radioactive beam of ^{18}F was tracked by two PPACs and finally used to bombard thin (100-200 $\mu g/cm^2$) CD_2 targets. The distance between the PPACs was optimized on the basis of the experience acquired in the previous experiment. In addition, the detection system based on the ASTRHO (A Silicon Array for Trojan HOrse) setup[7] was upgraded. In particular eight double position sensitive silicon detectors (45×45 mm^2 active area, 500 μm thick) mounted on a square geometry were used to detect outgoing particles with an exit angle of roughly 10 to 40 deg. Another set of two double sided multi strip silicon detectors (50 $\times$ 50 mm^2, 500 μm thick) was used to detect particles with exit angles ranging from approximately 4 to 10 deg.

One of the main problems encountered in the data analysis of the previous work came from the existence of various reaction channels with different sets of three particles in the final state. Though it was shown that it is possible to disentangle the events coming from the reaction channel of interest from the others by applying various kinds of cuts in the phase space[5], the possibility of having a direct identification in Z of the outgoing particles, at least for the heavier ones, was one of the major improvements in this measurement. To this end, a 20 μm thick silicon strip detector was used as ΔE stage in front of each of the aforementioned double sided multi strip detectors, such that the ΔE-E telescopes cover angles from roughly 4 to 10 deg. This will also result in a higher detection efficiency because we expect that we will be able to recover regions of the phase space that had to be discarded in the previous data analysis.

As already mentioned, the experiment was successfully performed in fall 2015 over a period of 18 days divided into two runs. Given the much longer period of actual data acquisition (15 days vs 2) and the higher detection efficiency, we also expect that we will be able to significantly increase the accumulated statistics with respect to the previous experiment. The data analysis of the new set of data has started and we expect to obtain preliminary results within fall 2016.

*1 INFN-LNS, Catania, Italy
*2 Dipartimento di Fisica e Astronomia, Università di Catania, Catania, Italy
*3 Riken, Nishina Center, Wako, Saitama, Japan
*4 Università di Enna KORE, Enna, Italy
*5 Center for Nuclear Study, The University of Tokyo, Japan
*6 Department of Physics, Tohoku University, Sendai, Japan
*7 Department of Physics, Sungkyunkwan University, Suwon, Republic of Korea
*8 Department of Physics, Chung-Ang University, Seoul, Republic of Korea
*9 30 MeV Cyclotron Center, Tran Hung Dao Hospital, Hoan Kiem District, Hanoi, Vietnam
*10 Universidade de São Paulo, Instituto de Física, Departamento de Física Nuclear, São Paulo, Brasil
*11 TUM, Garching, Germany

References

1) R. E. Tribble et al., Rep. Prog. Phys. **77**, 106901 (2014).
2) S. Cherubini et al., ApJ, **457**, 855, (1996).
3) A. S. Adekola et al., Phys. Rev., **C83** 052801 (R) (2011).
4) A. M. Laird et al., Phys. Rev. Lett., **110**, 032502 (2013).
5) S. Cherubini et al., Phys. Rev. C **92**, 015805 (2015)
6) S. Cherubini et al., in this report.
7) S. Cherubini et al., *ASTRHO: an Array of Silicons for TRojan HOrse studies with RIBs*, in preparation.

^{17}F elastic scattering and total reaction cross section on ^{58}Ni target around Coulomb barrier

C. J. Lin,[*1] L. Yang,[*1] N. R. Ma,[*1] H. M. Jia,[*1] H. Yamaguchi,[*2] M. Mazzocco,[*3*4] L. J. Sun,[*1] D. X. Wang,[*1] S. Hayakawa,[*2] D. Kahl,[*2] S. M. Cha,[*5] G. X. Zhang,[*6] F. Yang,[*1] Y. Y. Yang,[*7] C. Signorini,[*3*4] Y. Sakaguchi,[*2] K. Abe,[*2] A. Kim,[*5] K. Y. Chae,[*5] M. S. Kwag,[*5] D. Pierroutsakou,[*4] C. Parascandolo,[*4] M. La Commara,[*4*8] E. Strano[*4*9]

The reaction mechanisms of weakly bound nuclear systems have attracted much attention lately[1]. Because of the small binding energy, the weakly bound projectiles can easily break up into smaller fragments when they interact with the target[2]. Moreover, the consequence of the breakup channel on the fusion process is still controversial[3]. Therefore, a detailed knowledge on the breakup process is important for a deep understanding of the reaction mechanism of weakly bound systems.

In view of this fact, ^{17}F[4] was chosen to study the breakup mechanism of the ^{17}F+^{58}Ni system. For this purpose, a new detector array has been designed, to perform a complete-kinematics measurement. The array consists of ten detector units, each of which contains one ion chamber (IC), followed by one double-side silicon detector (DSSD), and two thick quartered silicon detectors (QSDs). Based on this array, the energy and angle correlations between the breakup fragments can be measured to reconstruct the intermediate state of the breakup process. The elastic scattering and other reaction channels can also be measured to investigate the total reaction cross-section. The resolution of single detector unit is around 4%. Thus, the inelastic channel may not be distinguished. However, the influence can be estimated because there is only one excited state below the breakup threshold of ^{17}F.

The experiment was performed at the CRIB (CNS Radio Isotope Beam) separator from Dec.10 to 19, 2015. The radioactive ^{17}F was produced by the ^{2}H(^{16}O,^{17}F) reaction using a 6.6 MeV/u ^{16}O primary beam impinging on a H_2 gas target. Four different ^{17}F secondary beam energies were obtained. The former, 59.7 MeV, was achieved with a gas pressure of 254 torr and a Al degrader with a thickness of 5 μm. By increasing the gas pressure and Al degrader up to 262 torr and 12 μm, as well as 316 torr and 17 μm, the beam energies of 49.7 MeV and 46 MeV were obtained, respectively. The latter, 65 MeV, was achieved with a gas pressure of 250 torr and without a degrader. After selection by the WF and tracked by two PPACs, the secondary beam, with an intensity of 6-10×10^5 pps, was then impinged on the secondary target, ^{58}Ni, with a thickness of 1 mg/cm^2. The identification of particles obtained using the first detector unit ($\theta_{\rm lab}$ from 15.2° to 30.5°) is shown in Fig. 1. It can be seen that ^{17}F, ^{16}O, and p can be distinguished clearly.

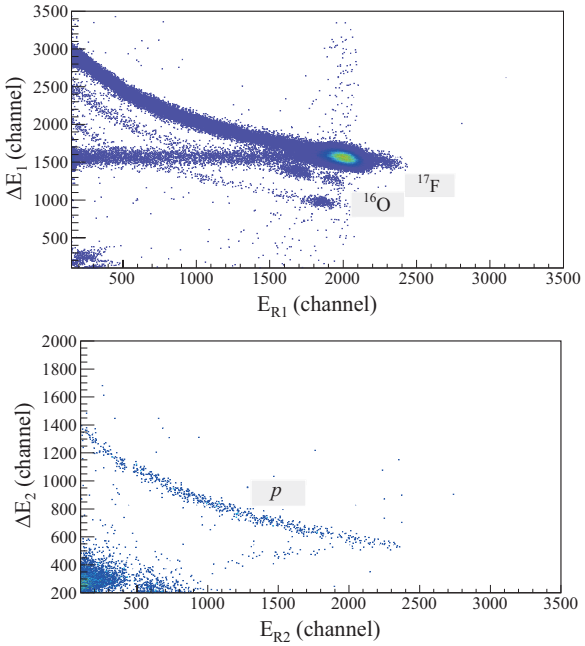

Fig. 1. Identification of particles yielding from ^{17}F+^{58}Ni at $E_{\rm lab}$(^{17}F)=59.7 MeV. Symbols ΔE$_1$ and E$_{R1}$ represent the IC and DSSD, respectively, and ΔE$_2$ and E$_{R2}$ are the two QSDs. The horizontal tail of ^{17}F arises from the radiation damage and/or channeling effect of the solid detector.

The data analysis is in progress now.

*1 Department of Nuclear Physics, China Institute of Atomic Energy
*2 Center for Nuclear Study, University of Tokyo
*3 University of Padova
*4 INFN
*5 Department of Physics, Sungkyunkwan University
*6 Department of Physics, Beihang University
*7 Institute of Modern Physics, Chinese Academy of Sciences
*8 University of Naples
*9 University of Catania

References

1) N. Keeley, R. Raabe, N. Alamanos, and J. L. Sida: Prog. Part. Nucl. Phys. **59**, 579 (2007).
2) N. Keeley, N. Alamanos, K. W. Kemper and K. Rusek: Prog. Part. Nucl. Phys. **63**, 396 (2009).
3) J. F. Liang and C. Signorini: Int. J. Mod. Phys. E **14**, 1121 (2005).
4) M. Mazzocco, C. Signorini, D. Pierroutsakou et al.: Phys. Rev. C **82**, 054604 (2010).

Measurement of alpha elastic scattering on ^{15}O

A. Kim,[*1,*2] D. H. Kim,[*1] G. W. Kim,[*1] S. Y. Park,[*1] E. K. Lee,[*1] K. I. Hahn,[*1] K. Y. Chae,[*2] S. W. Hong,[*2] S. M. Cha,[*2] M. S. Gwak,[*2] E. J. Lee,[*2] J. H. Lee,[*2] J. Y. Moon,[*3] S. H. Choi,[*4] S. H. Bae,[*4] H. Yamaguchi,[*5] S. Hayakawa,[*5] Y. Sakaguchi,[*5] K. Abe,[*5] N. Imai,[*5] N. Kitamura,[*5] O. Beliuskina,[*5] Y. Wakabayashi,[*6] S. Kubono,[*6] V. Panin,[*6] N. Iwasa,[*7] K. Daid,[*8] and A. A. Chen[*9]

The γ rays emitted from novae are dominated by e^+-e^- annihilation, of which main source is believed to be the β^+ decay of ^{18}F. The amount of ^{18}F produced in nova depends significantly on the reaction rates of ^{18}F$(p,\alpha)^{15}$O and ^{18}F$(p,\gamma)^{19}$Ne and the former one is known as the most important destructive reaction.[1] This reaction rate is thought to be dominated by two resonances, $3/2^-$ and $3/2^+$, which are located at E_x = 6.74 MeV and 7.07 MeV in ^{19}Ne, respectively. In particular, the interference term between the strong $3/2^+$ state at 7.07 MeV and the other $3/2^+$ states around the proton threshold (6.41 MeV) is known to affect the reaction rate significantly in the astrophysically important energy region.[2] However, the $3/2^+$ states at E_x = 6.42 and 6.45 MeV are still controversial while the $3/2^-$ state at 665 keV above the proton threshold was observed clearly.[2–6] Therefore, to confirm the energies and J^π assignments of these resonances, the study of ^{19}Ne using ^{15}O + α would be very useful because alpha threshold energy(3.53 MeV) is much lower than the proton threshold energy(6.41 MeV).

A measurement of alpha elastic scattering on ^{15}O was performed using the thick target method, which can provide a continuous excitation function in inverse kinematics because energy loss occurs steadily through thick gas cell filled with ^{4}He. The primary beam, ^{15}N (7.0 MeV/u, 0.6 pμA), was transported from the AVF cyclotron of the RIKEN Accelerator Research Facility to the low-energy RI beam separator, called CRIB at the Center for Nuclear Study, University of Tokyo[7] and impinged on a hydrogen gas target with a thickness of 1.09 mg/cm^2. The primary target was cooled to 90 K by liquid nitrogen in order to prevent the target window from breaking due to heat.[8]

The secondary beam, ^{15}O, was obtained by the $p(^{15}$N,$n)^{15}$O reaction. The ^{15}O beam was selectively purified by a Wien filter system so that the beam purity was 99.9% at the focal plane (F3) of CRIB as shown in Fig. 1.

The final intensity of ^{15}O beam was 6×10^5 counts/s

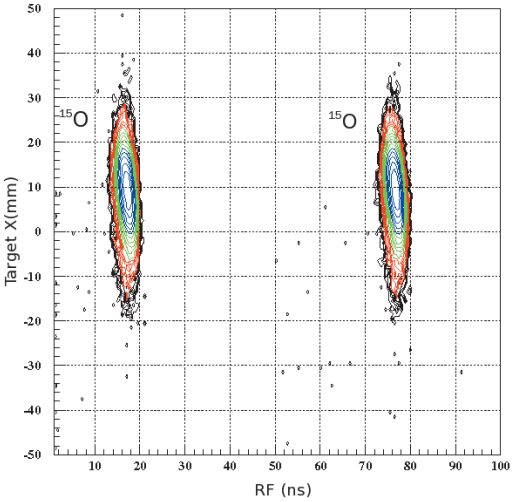

Fig. 1. Secondary beam distribution in F3 after Wien filter.

at the target. The F3 chamber was filled with the helium gas of 600 Torr, which was maintained at room temperature. For detecting the recoiling alpha particles, two sets of the ΔE-E telescope at 0° and 15° were installed in the F3 chamber, which was located at a distance of 200 mm from the entrance window of the chamber. The effective target thickness was 2.63 mg/cm^2. The thicknesses of two detectors are 20 μm and 480 μm, respectively. The energy of the ^{15}O beam was well-defined with 36.0$\pm$0.5 MeV after the entrance window (Mylar 20 μm-thick) of the F3 chamber, which means the measured energy was E_x=3.53-11.13 MeV in ^{19}Ne. For subtraction of the background, we performed the measurement of ^{15}O + Ar using Ar gas target. The data are being currently analyzed.

*1 Department of Physics, Ewha Womans University
*2 Department of Physics, SungKyunKwan University
*3 RISP, Institute of Basic Science
*4 Department of Physics and Astronomy, Seoul National University
*5 Center for Nuclear Study, University of Tokyo
*6 RIKEN Nishina Center
*7 Department of Physics, University of Tohoku
*8 School of Physics and Astronomy, University of Edinburgh
*9 Department of Physics and Astronomy, McMaster University

References

1) M. Hernanz et al., Astrophys. J. **526**, L97 (1999).
2) C. E. Beer et al., Phys. Rev. C **83**, 042801(R) (2011).
3) D. W. Bardayan et al., Phys. Rev. Lett. **89**, 262501 (2002).
4) A. St. J. Murphy et al., Phys. Rev. C **79**, 058801 (2009).
5) K. Y. Chae et al., Phys. Rev. C **74**, 012801(R) (2006).
6) A. M. Laird et al., Phys. Rev. Lett. **110**, 032502 (2013).
7) Y. Yanagisawa et al., RIKEN Accel. Prog. Rep. **30**, 183 (2001).
8) H. Yamaguchi et al., Nucl. Instrum. Methods Phys. Res. Sect. A **589**, 150 (2008).

RI beam production at BigRIPS in 2015

Y. Shimizu,[*1] N. Fukuda,[*1] H. Takeda,[*1] H. Suzuki,[*1] D.S. Ahn,[*1] T. Sumikama,[*1] D. Murai,[*1,*2] N. Inabe,[*1] T. Komatsubara,[*1] K. Kusaka,[*1] M. Ohtake,[*1] Y. Yanagisawa,[*1] K. Yoshida,[*1] and T. Kubo[*1]

The radioactive isotope (RI) beam production at the BigRIPS fragment separator[1] in 2015 is presented. Table 1 summarizes the experimental programs that involved the use of the BigRIPS separator in this period and the RI beams produced for each experiment.

The first uranium beam time started in March with the ImPACT program at the ZeroDegree spectrometer. To study the nuclear-transmutation reaction for the long-lived fission products, ^{135}Cs, ^{108,107}Pd, ^{94,93}Zr, and ^{90}Sr were produced by the in-flight fission of the ^{238}U beam. The SEASTAR campaign were performed to measure $E(2_1^+)$ energies of ^{110}Zr, ^{100}Kr, ^{94}Se, ^{88}Ge, and ^{84}Zn. The polarized ^{2}H beam experiment was performed to investigate the three nucleon force. The ^{78}Kr primary beam was provided for the first time. We have measured the production yields and the production cross sections for a variety of RI beams produced by projectile fragmentation of the ^{78}Kr beam[2]. Highly proton-rich isotopes, such as ^{67}Kr, ^{63}Se, and ^{59}Ge, from the ^{78}Kr beam were delivered to the EURICA experiments. Search for new proton-rich isotopes was performed. The spring beam time ended with the Rare RI Ring commissioning using the ^{78}Kr primary beam.

Table 1. List of experimental programs together with RI beams produced at the BigRIPS separator in 2015.

Primary beam (Period)	Proposal No.	Course	RI beams
^{238}U 345 MeV/nucleon (Mar. 26 – May 8)	IMPACT14-01	ZeroDegree	^{135}Cs, ^{108,107}Pd, ^{94,93}Zr, ^{90}Sr
	NP1406-RIBF126	ZeroDegree	^{77,73}Cu
	NP1306-RIBF98R1	ZeroDegree	^{136}Te
	MS-EXP15-03	BigRIPS	^{132}Sn
	MS-EXP15-02	BigRIPS	^{132}Sn
	NP1312-RIBF18R1 (SEASTAR)	ZeroDegree	^{111}Nb, ^{101}Rb, ^{95}Br, ^{89}As, ^{85}Ga
	PE15-01	ZeroDegree	
^{2}H 190 MeV/nucleon (May 12 – May 16)	NP1112-RIBF65-02	BigRIPS	^{2}H (primary beam)
^{78}Kr 345 MeV/nucleon (May 24 – Jun. 22)	NP1112-RIBF94-02	ZeroDegree	^{72,70}Kr
	NP0702-RIBF4R1	EURICA	^{67}Kr, ^{63}Se, ^{59}Ge, ^{51}Ni
	NP1112-RIBF82	EURICA	^{66,64}Se, ^{60}Ge
	NP1112-RIBF93	EURICA	^{71,70}Kr
	DA14-02-04	BigRIPS	^{59}Ge
	MS-EXP15-04	Rare RI Ring	^{78}Kr (primary beam)
^{238}U 345 MeV/nucleon (Oct. 20 – Nov. 14)	MS-EXP15-01	ZeroDegree	^{212}Ra, ^{136}Sn
	IMPACT15-01	SAMURAI	
	MS-EXP15-06	SAMURAI	^{94,93}Zr, ^{80,79}Se
	MS-EXP15-07	SAMURAI	
	MS-EXP15-08	BigRIPS	^{132}Sn
	MS-EXP15-09	BigRIPS	^{132}Sn
	NP1412-RIBF124R1	F8	^{76}Zn
	NP1306-RIBF99	F8	^{99}Zr
^{48}Ca 345 MeV/nucleon (Nov. 19 – Dec. 4)	MS-EXP15-10	BigRIPS	^{48}Ca (primary beam)
	MS-EXP15-11	SAMURAI	^{1}H
	NP1312-SAMURAI21	SAMURAI	^{29}Ne, ^{29}F, ^{24}O, ^{20}F
	MS-EXP15-12	Rare RI Ring	^{38}K

[*1] RIKEN Nishina Center
[*2] Department of Physics, Rikkyo University

The second uranium beam time started in October with the ImPACT program at the SAMURAI spectrometer. A machine study was conducted to investigate particle identification and isotope separation in the region around atomic number $Z = 88$[3]. ^{29}Ne and ^{29}F were produced by projectile fragmentation of a ^{48}Ca beam to study resonance states of the neutron-rich oxygen isotopes ^{27,28}O using the SAMURAI spectrometer. The autumn beam time ended with the Rare RI Ring experiment using the ^{38}K RI beam.

The number of the experiments using the RI beams at the BigRIPS separator is tallied in Table 2, for various primary beams in each year. A total of 115 experiments have been performed so far. Figure 1 shows the RI beams produced at the BigRIPS separator from March 2007 to December 2015 on the table of the nuclides. The number of RI beams produced at the BigRIPS separator amounted to about 400. The number of new isotopes reached about 140. Production yields for more than 1400 RI beams have been measured.

References
1) T. Kubo: Nucl. Instr. Meth. B **204**, 97 (2003).
2) H. Suzuki et al.: In this report.
3) T. Sumikama et al.: In this report

Table 2. Number of experiments performed using RI beams in each year.

Year	^{238}U	^{124}Xe	^{86}Kr	^{78}Kr	^{70}Zn	^{48}Ca	^{18}O	^{16}O	^{14}N	^{4}He	^{2}H	Yearly total
2007	4		1									5
2008	2					4						6
2009	3					3			3	1		10
2010						10	1		2		1	14
2011	4	2					2					8
2012	6	3			1	4	6					20
2013	4	2					3					9
2014	11				1	3		1			1	17
2015	15			6		4					1	26
Total	49	7	1	6	2	28	12	1	5	1	3	115

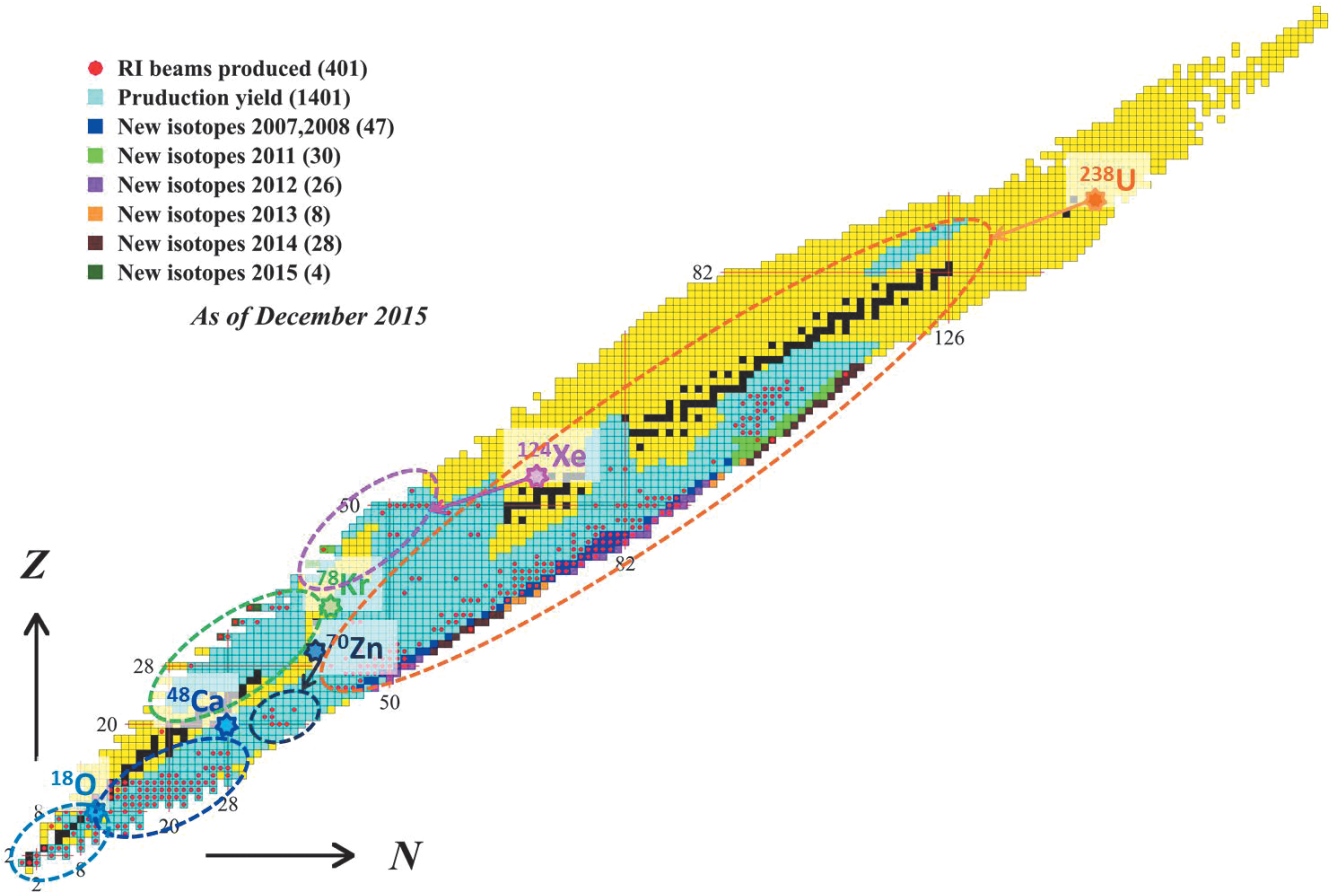

Fig. 1. RI beams produced at the BigRIPS separator from March 2007 to December 2015.

Production cross section measurement for radioactive isotopes produced from ^{78}Kr beam at 345 MeV/nucleon by BigRIPS separator

H. Suzuki,[*1] T. Sumikama,[*1] N. Fukuda,[*1] H. Takeda,[*1] Y. Shimizu,[*1] D.S. Ahn,[*1] D. Murai,[*1,*2] N. Inabe,[*1] K. Yoshida,[*1] K. Kusaka,[*1] Y. Yanagisawa,[*1] M. Ohtake,[*1] Z. Korkulu,[*1] T. Komatsubara,[*1] H. Sato,[*1] and T. Kubo[*1]

We have measured the production rates and the production cross sections for a variety of radioactive isotopes (RIs), which were produced from a ^{78}Kr beam at an energy of 345 MeV/nucleon using the BigRIPS separator[1], for the first time. Proton-rich isotopes with atomic numbers $Z = 22-37$ were produced by the projectile fragmentation of the primary beam on a 5-mm-thick Be production target. The particle identification of RIs was based on the TOF-$B\rho$-ΔE method in the second stage of the BigRIPS[2].

The production cross sections were deduced from the measured production rates and the transmission efficiency in the BigRIPS separator, which was simulated with the calculation code LISE^{++}[3]. In the LISE^{++} simulation, the parametrization for momentum distribution of the RIs was adjusted, because the exponential tails in the low-momentum regions observed in the experiment fell off faster than those calculated by the LISE^{++} with the original parametrization. In preliminary, we used the parameters of the momentum distribution, which were obtained in the production cross-section measurement of proton-rich nuclei produced from the 345-MeV/nucleon ^{124}Xe beam. The parameters of the angular distribution were not changed from the original values in the code.

Figure 1 shows the production cross sections of RIs obtained in the ^{78}Kr-beam campaign. The solid and dashed lines in Fig. 1 show the cross sections predicted from the empirical formulae EPAX3.1a[4] and EPAX2.15[5], respectively. EPAX3.1a predicts the cross sections better than EPAX2.15, which overestimates most of them. The measured cross sections of RIs with a wide range of Z are fairly well reproduced by EPAX3.1a; however, some isotopes show systematic discrepancies around the very neutron-deficient region. In the case of ^{67}Kr, which is the most neutron-deficient Kr isotope in our measurement, the experimental cross section is $(3.2 \pm 1.4) \times 10^{-12}$ mb (preliminary), while the value calculated using the EPAX3.1a formula is 4.25×10^{-10} mb. Further, we also observe that the discrepancy becomes significant with increasing Z number. These discrepancies were also observed in proton-rich RIs produced from the 345-MeV/nucleon ^{124}Xe beam[6].

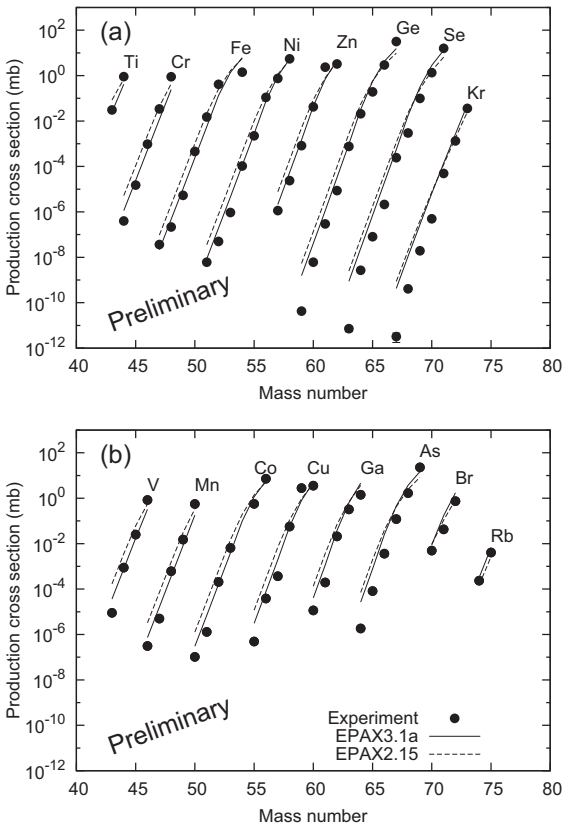

Fig. 1. Production cross sections of RIs produced in the ^{78}Kr + Be reaction at 345 MeV/nucleon with the predictions of EPAX parametrizations (Preliminary). (a) Results for even-Z isotopes. (b) Results for odd-Z isotopes. Solid and dashed lines show the values predicted using the EPAX3.1a and EPAX2.15 formulae, respectively.

*1 RIKEN Nishina Center
*2 Department of Physics, Rikkyo University

References

1) T. Kubo: Nucl. Instrum. Meth. Phys. Res. **B 204**, 97 (2003).
2) N. Fukuda et al.: Nucl. Instrum. Meth. Phys. Res. **B 317**, 323 (2013).
3) O.B.Tarasov, D.Bazin: Nucl. Instr. and Meth. **B 266**, 4657 (2008) (references therein; LISE^{++} site, http://lise.nscl.edu, Michigan State University)
4) K. Sümmer: Phys. Rev. C **86**, 014601 (2012).
5) K. Sümmer and B. Blank: Phys. Rev. C **61**, 034607 (2000).
6) H. Suzuki et al.: Nucl. Instrum. Meth. Phys. Res. **B 317**, 756 (2013).

Production cross-section measurements for the systematics of Na and Mg isotopes with ^{48}Ca beam

D. S. Ahn,[*1] N. Fukuda,[*1] H. Suzuki,[*1] T. Sumikama,[*1] Y. Shimizu,[*1] T. Takeda,[*1] D. Murai,[*1, *2] N. Inabe,[*1] K. Yoshida,[*1] K. Kusaka,[*1] Y. Yanagisawa,[*1] M. Ohtake,[*1] T. Komatsubara,[*1] H. Sato,[*1] and T. Kubo[*1]

Na and Mg isotopes were produced by projectile fragmentation of a ^{48}Ca beam at an energy of 345 MeV/nucleon using the BigRIPS separator[1]. We measured the systematics of the production cross-section for Na and Mg isotopes in an unstable isotope region toward a very neutron-rich region. The systematics are useful to predict the production rates of rare isotopes. In addition, we performed a drip-line search of Na isotopes. The drip-line is important to understand the nuclear structure and the benchmark for nuclear models in a very neutron-rich region.

The $B\rho$ was tuned for each isotope in each setting and the ^{39}Na isotope was obtained using the $B\rho$ tuned for the center orbit of ^{36}Ne and ^{39}Na isotopes ("^{36}Ne + ^{39}Na setting"). The same target (Be: 20 mm) and the same thick degraders were used for the F1 (Al: 15 mm) and F5 (Al: 7 mm) degraders. The F5 degrader was used to reject the light particles. Particle identification was performed using the TOF-$B\rho$-ΔE method and the background events were eliminated using various correlations of the difference observable from each beam line detector[2),3)]. The production cross-sections of $^{27\text{-}39}$Na and $^{29\text{-}40}$Mg isotopes were measured and the results for the ^{40}Mg isotope were higher than those obtained with the NSCL[4] measurement. The heaviest known isotopes are ^{37}Na and ^{40}Mg. One event of the ^{39}Na isotope was detected in the "^{36}Ne + ^{39}Na setting" with an irradiation time of 9.4 h. The error of the event is large, hence it is difficult to determine whether ^{39}Na is bound. The nuclear binding of ^{39}Na is still an open question, and more experimental data for the ^{39}Na isotope are needed to unambiguously establish the nuclear binding of ^{39}Na. We obtained the production cross-section for one event for ^{39}Na as a preliminary result. The detailed analysis is in progress. Figure 1 and 2 show the production cross-sections of Na and Mg isotopes, respectively, toward the very neutron-rich region. The red and blue circles represent the experimental results obtained from the 2015 and 2014 experiments in Figure 1 and 2015 and 2010/2014 experiments in Figure2, respectively. These are the preliminary results. The black line represents the empirical formula of the EPAX 2.15[5] parameterizations in the LISE^{++} calculation[6]. Overall, our experimental results of the production cross-sections are in good agreement with the EPAX 2.15 parameterization in the region of $^{27\text{-}37}$Na and $^{29\text{-}38}$Mg. However, the measured production cross-sections of the ^{39}Na and ^{40}Mg isotopes are smaller than the EPAX 2.15 parameterizations and a large discrepancy exists in the production cross-section.

*1 RIKEN Nishina Center
*2 Department of Physics, Rikkyo University

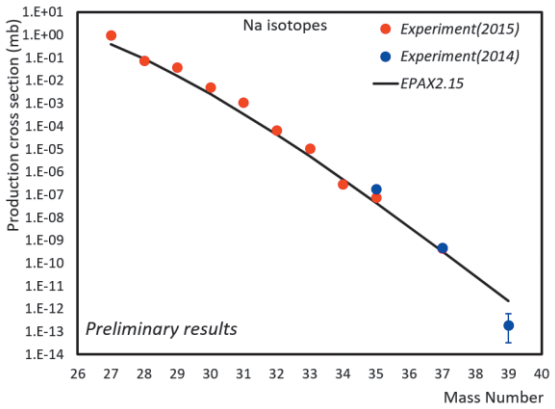

Fig. 1. Preliminary results of production cross-sections of Na isotopes toward the very neutron-rich region. The red and blue circles represent the experimental results obtained from the 2015 and 2014 experiments, respectively. The black line represents the EPAX 2.15 parameterizations.

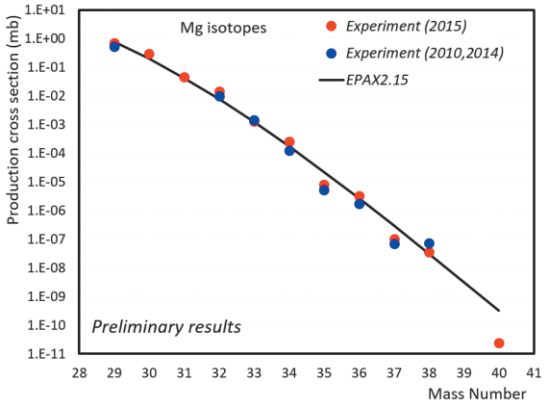

Fig. 2. Preliminary results of production cross-sections of Mg isotopes toward the very neutron-rich region. The red and blue circles represent the experimental results obtained from the 2015 and 2010/2014 experiments, respectively. The black line represents the EPAX 2.15 parameterizations.

References

1) T. Kubo et al., Nucl. Instrum. Meth. Phys. Res. **B204**, 97 (2003).
2) N. Fukuda et al., Nucl. Instrum. Meth. Phys. Res. **B317**, 323 (2013).
3) D. S. Ahn et al., to be submitted.
4) T. Baumann et al., Nature **449**, 1022-1024 (2007).
5) K. Sümmer and B. Blank, Phys. Rev. **C 61**, 034607 (2000)
6) O. B. Tarasov and D. Bazin, Nucl. Instrum. Meth. Phys. Res. **B266**, 4657 (2008).

RI-beam production using BigRIPS separator in regions heavier than those belonging to lead isotope

T. Sumikama,[*1] N. Inabe,[*1] N. Fukuda,[*1] H. Takeda,[*1] Y. Shimizu,[*1] H. Suzuki,[*1] D. S. Ahn,[*1] D. Murai,[*2] H. Sato,[*1] K. Kusaka,[*1] Y. Yanagisawa,[*1] M. Ohtake,[*1] K. Yoshida,[*1] and T. Kubo[*1]

The regions of the nuclear chart that are heavier in terms of atomic weight, i.e. with an atomic number $Z \sim 80$ and more, are the key to understand the nucleosynthesis of elements up to uranium. In our previous study,[1)] an RI beam with $Z > 80$ was produced using the projectile-fragmentation reaction of a ^{238}U beam at RIBF. A 0.3-mm thick degrader was used in the BigRIPS separator[2)] for the RI beam separation, but a large amount of fission fragments unexpectedly decreased a purity. In the present study, an RI beam heavier than the lead isotope was produced using a thicker degrader, with a thickness of 2 mm, to eliminate the fission fragments.

The RI beam around $^{208}_{86}$Rn was produced via the projectile-fragmentation reaction of a 345-MeV/u ^{238}U beam. The production target was a 3-mm thick Be. To separate the primary ^{238}U beam, the He-like ions (charge-state $Q = Z - 2$) were selected at the first dipole D1. The 2-mm-thick wedge degrader was placed at the first momentum dispersive focal plane F1, and the fully-stripped ions were selected at the second dipole D2 after F1. Under these conditions, the charge-state combination for the fission fragments with $Z < 60$ was restricted to Li-like and fully stripped ions at D1 and D2, respectively, or $Z - Q \geq 4$ at D1. Due to a low probability of these combinations, the fission fragments were separated very well. The second wedge degrader with a thickness of 1 mm was used in the middle of the second stage of BigRIPS for further purification. The He-like ions were selected at all the dipole magnets used in the second stage. The particle-identification (PID) plot measured at the second stage of BigRIPS is shown in Fig. 1 (a). The contaminants in the form of the fission fragments were negligibly eliminated. The PID was confirmed by the γ rays emitted from a known isomeric state in ^{208}Rn, as shown in Fig. 1 (b). The high purity of ^{208}Rn allowed us to complete the γ-ray measurement within 30 minutes. Figure 2 shows the mass to charge ratio for the Rn isotopes. Each Rn isotope was well separated from the others. A small component with a different charge state may be included within the width of the distribution because the A/Q of the nucleus with $A = 208$ and $Q = 84$, for example, is very close to that with $A = 203$ and $Q = 82$ or $A = 213$ and $Q = 86$. To distinguish the charge states, the total kinetic energy was measured by using six stacked Si detectors, each with a thickness of 1 mm. This analysis is still in progress.

*1 RIKEN Nishina Center
*2 Department of Physics, Rikkyo University

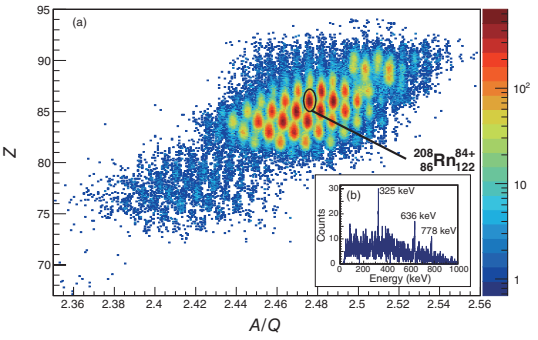

Fig. 1. (a) Particle identification plot for the RI beam measured at the second stage of BigRIPS. The atomic number Z versus the mass to charge ratio is shown. (b) The γ-ray energy spectrum of the known isomeric state in ^{208}Rn, indicated by the circle in (a). Three γ-ray peaks can be clearly observed.

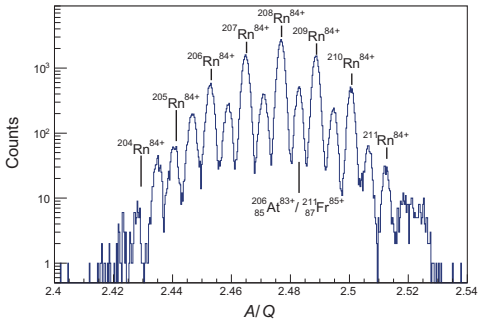

Fig. 2. Mass to charge ratio of the radon isotope ($Z = 86$) obtained from Fig. 1 (a) with the gate of $85.8 < Z < 86.2$. The radon isotopes with $Q = 84$ were observed between the masses 204 and 211, as can be seen for the isotopes labeled using lines. $^{206}_{85}$At^{83+}/$^{211}_{87}$Fr^{85+} shows a typical example of the contaminants for isotopes with $Z = 85$ and 87.

References

1) N. Inabe et al.: RIKEN Accel. Prog. Rep., Vol. 48 (2015), p. 73.
2) T. Kubo et al.: Prog. Theor. Exp. Phys., 03C003 (2012).

Development of a slowed-down beam of ^{82}Ge at RIBF

T. Sumikama,[*1] D. S. Ahn,[*1] N. Fukuda,[*1] N. Inabe,[*1] T. Kubo,[*1] Y. Shimizu,[*1] H. Suzuki,[*1] H. Takeda,[*1] N. Aoi,[*2] D. Beaumel,[*3] K. Hasegawa,[*4] E. Ideguchi,[*2] N. Imai,[*5] T. Kobayashi,[*4] M. Matsushita,[*5] S. Michimasa,[*5] H. Otsu,[*1] S. Shimoura,[*5] and T. Teranishi[*6]

RI beams with around 15 MeV/u are necessary for the study of the nuclear shell structure using the nucleon transfer reaction. The RI-beam energy at RIBF is typically 250 MeV/u after the first stage of the BigRIPS[1]. The RI beam is slowed down using energy degraders. However, the control of the energy spread and the beam size becomes difficult due to the increase in the beam emittance after the use of energy degraders. Two methods were proposed to efficiently produce a slowed-down beam at RIBF. One is the slowed-down method with the momentum-compression scheme[2], and the second method is the use of an RF deflector, called OEDO (Optimized Energy Degrading Optics for RI beams).[3] This paper reports on the first test experiment to produce a slowed-down beam of ^{82}Ge with the energy of 13 MeV/u using the momentum-compression scheme.

The RI beam of ^{82}Ge was produced by the projectile fragmentation of the ^{238}U beam with the energy of 345 MeV/u. The primary target of beryllium with a thickness of 7 mm was used. A wedge degrader was placed at the momentum-dispersive focus F1 to purify the RI beam, as shown in Fig. 1. The thickness for the central trajectory was 5 mm. A second wedge-shaped degrader with a thickness of 2.0 mm was placed at the momentum-dispersive focus F5. The wedge angle was designed to compress the momentum spread. The ion-optics mode obtained after using this degrader was changed to achieve the momentum achromat. The momentum spread of 6% was compressed to 3%, as shown in Fig. 2. Three energy degraders were also placed at the achromatic foci, F2, F3, and F7. The energy after beam-line detectors at F8 was measured by using the time of flight between F8 and F9, as shown in Fig. 3. The ^{82}Ge beam with the energy of 13 MeV/u at the central trajectory was successfully produced. The transmission efficiency from F2 to F8 was 2%. There was a reduction of 1/10 mainly due to out of focus at F7.

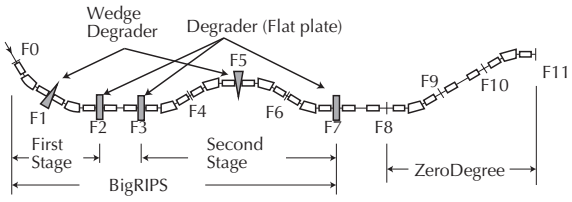

Fig. 1. Schematic view of the combination of degraders in the BigRIPS and ZeroDegree separators. The wedge-shaped degrader was placed at the momentum dispersive foci, F1 and F5, of BigRIPS.

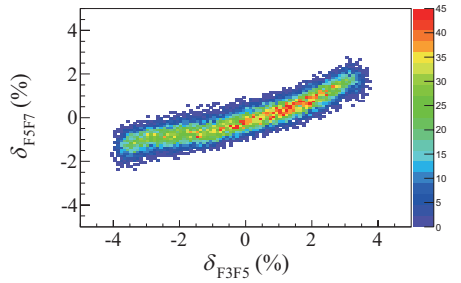

Fig. 2. Results of the momentum compression at the second stage of BigRIPS. δ_{F3F5} and δ_{F5F7} are $(p-p_0)/p_0$ before and after using the momentum-compressive degrader, where p is the momentum and p_0 is the momentum at the central trajectory.

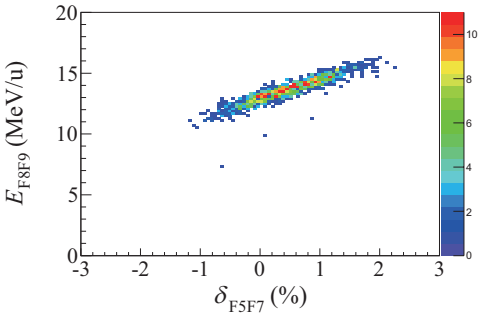

Fig. 3. Energy after all beam-line detectors at F8 as a function of δ_{57}. The particle with $-0.6 < \delta_{57} < 1.5\%$ was transported to the ZeroDegree spectrometer.

*1 RIKEN Nishina Center
*2 RCNP, Osaka University
*3 INPO, CNRS/IN2PS
*4 Department of Physics, Tohoku University
*5 CNS, University of Tokyo
*6 Department of Physics, Kyushu University

References

1) T. Kubo et al.: Prog. Theor. Exp. Phys. (2012) 03C003.
2) T. Sumikama et al.: Energy focusing and RI-beam purification using two energy degraders at fragment separator BigRIPS, RNB8 conference, Grand Rapids, Michigan, May 26 − 30, 2009.
3) M. Matsushita et al.: New energy-degrading scheme for low-energy reaction measurements of rare isotope beams, EMIS conference, Grand Rapids, Michigan, May 11 − 15, 2015.

Target study for magnetic moment measurement of ^{40}Sc

Y. Ishibashi,[*1,*2] D. Nagae,[*1] Y. Abe,[*1] Y.E. Ichikawa,[*2] T. Moriguchi,[*2] S. Suzuki,[*2] Y. Tajiri,[*2] A. Ozawa,[*2] and H. Ueno[*1]

We report a target study on the measurement of the μ moment of ^{40}Sc using the β-ray detected nuclear magnetic resonance (β-NMR) method[1] at the Research Center for Nuclear Physics, Osaka University. In order to apply the β-NMR method, a spin-polarized nucleus is needed. A spin-polarized ^{40}Sc nucleus was produced in the ^{40}Ca($\vec{p}$,n)^{40}Sc reaction. In the reaction, the polarization of the beam particles was transferred to each nucleus. The $\vec{p}$ was produced using a polarized ion source[2], and it was accelerated at E/A = 72 MeV using an AVF cyclotron. The polarized proton beam was implanted on a CaS, a CaO, and a CaF_2 target to produce polarized ^{40}Sc. The targets were placed at the center of the β-NMR apparatus at room temperature.

The higher the purity of ^{40}Sc, the more efficiently it can be measured; therefore, we performed purity measurement and comparison of the three targets. The β-ray emitted from ^{40}Sc were detected with plastic scintillator telescopes located above and below the targets. In order to deduce the purity of the ^{40}Sc, half-lives were measured using three targets. Figure 1(a), 1(b), and 1(c) are β-decay time spectra obtained using CaS, CaO, and CaF_2 targets, respectively. The time spectra obtained from the accumulated β rays in the ^{40}Sc experiment were fitted with two or three exponential functions in addition with a constant background arising from the long-lived impurities. The least squares method was applied to the analysis. The results of the fitting analysis are shown in Fig. 1(a), 1(b), and 1(c). The obtained half-lives were slightly longer than the reported half-life of 182.3(7) ms. The estimated impurities of ^{32}Cl($T_{1/2}$ = 298 ms), ^{29}P($T_{1/2}$ = 4.142 s), ^{13}N($T_{1/2}$ = 9.965 m), and ^{37}K($T_{1/2}$ = 1.225 s) have much longer half-lives than that of ^{40}Sc. Thus, the ^{40}Sc isotopes were correctly produced in the ^{40}Ca($\vec{p}$,n)^{40}Sc reaction. The purities of the ^{40}Sc are obtained to be 23^{+36}_{-23}%, 23^{+33}_{-23}%, and 37±4% using CaS, CaO, and CaF_2 targets, respectively.

From the half-life measurements, the purity of the ^{40}Sc using CaF_2 was determined to be the highest. Thus, we applied a CaF_2 target for the measurement of the μ moment of ^{40}Sc by the β-NMR method. In order to maintain the spin polarization, a static magnetic field B = 543 mT was applied. The up/down ratio R of the β-ray counts is written as $R_0 \sim a(1 + A_\beta P)/(1 - A_\beta P)$, where a, A_β, and P denote a constant factor representing asymmetries in counter solid angle and efficiencies, the β-ray asymmetry parameter, and the degree of spin-polarization, respectively. An oscillating magnetic field perpendicular to the static field was applied to the CaF_2 target using an rf coil. If the frequency of the rf field corresponds to the resonance field for the spin-polarized ^{40}Sc, the direction of the spin polarization is changed by the NMR. Then, the ratio changes to $R \sim a(1 - A_\beta P)/(1 + A_\beta P)$. The β-ray asymmetry $A_\beta P$ is written as $A_\beta P = \sqrt{(R_0/R) - 1}/\sqrt{(R_0/R) + 1}$. The μ moment is derived from the frequency of the observed peak or dip in the $A_\beta P$ spectrum. The analysis is in progress.

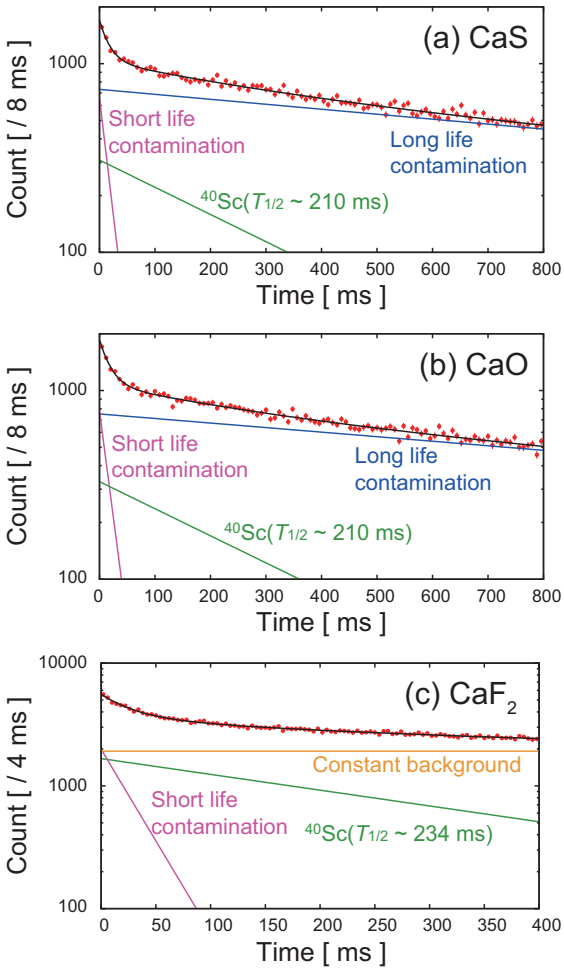

Fig. 1. β decay spectra for ^{40}Sc.

References

1) K. Sugimoto et al., J. Phys. Soc. Jpn. **21**, 213 (1966).
2) K. Hatanaka et al., Nucl. Instr. and Meth. **217**, 397 (1983).

*1 RIKEN Nishina Center
*2 Institute of Physics, University of Tsukuba

Giant dipole resonance built on hot rotating nuclei produced during evaporation of light particles from the ^{88}Mo compound nucleus†

M. Ciemała,[*1,2] M. Kmiecik,[*1] A. Maj,[*1] K. Mazurek,[*1] A. Bracco,[*3,4] V.L. Kravchuk,[*5,6] G. Casini,[*7] S. Barlini,[*7,8] G. Baiocco,[*9] L. Bardelli,[*7,8] P. Bednarczyk,[*1] G. Benzoni,[*4] M. Bini,[*7,8] N. Blasi,[*4] S. Brambilla,[*4] M. Bruno,[*9] F. Camera,[*3,4] S. Carboni,[*7,8] M. Cinausero,[*5] A. Chbihi,[*2] M. Chiari,[*7,8] A. Corsi,[*3,4] F.C.L. Crespi,[*3,4] M. D'Agostino,[*9] M. Degerlier,[*5] B. Fornal,[*1] A. Giaz,[*3,4] F. Gramegna,[*5] M. Krzysiek,[*1] S. Leoni,[*3,4] T. Marchi,[*5] M. Matejska-Minda,[*1,10] I. Mazumdar,[*11] W. Meczyński,[*1] B. Million,[*4] D. Montanari,[*3,4] L. Morelli,[*9] S. Myalski,[*1] A. Nannini,[*7,8] R. Nicolini,[*3,4] G. Pasquali,[*7,8] S. Piantelli,[*7] G. Prete,[*5] O.J. Roberts,[*12] Ch. Schmitt,[*2] J. Styczeń,[*1] B. Szpak,[*1] S. Valdré,[*7,8] B. Wasilewska,[*1] O. Wieland,[*4] J.P. Wieleczko,[*2] M. Ziebliński,[*1] J. Dudek,[*13] and N. Dinh Dang[*14]

Studying the Giant Dipole Resonance (GDR) properties at high temperature and increasing angular momentum is one of the most important tools to investigate the nuclear structure under extreme conditions. The evolution of the GDR width with angular momentum and temperature reflects the role played by quantal and thermal fluctuations in the mechanism of damping of the giant resonance. To test predictions of damping mechanisms in a more comprehensive way, the GDR studies should be based on exclusive and rather complete measurements, which include, in addition to γ-rays, the detection of the recoiling residual nuclei and emitted particles. The present article reports on an exclusive experiment performed to measure the GDR width of the ^{88}Mo nucleus, produced in the reaction ^{48}Ti + ^{40}Ca at 300 and 600 MeV bombarding energies, which correspond to the average temperatures T = 2.1 and 3 MeV, respectively. The data were analyzed using the statistical model Monte Carlo code *GEMINI++*. It allowed extracting the GDR parameters by fitting the high energy γ-ray spectra. The GDR strength functions and extracted GDR widths were compared with theoretical predictions based on the Lublin-Strasbourg-Drop (LSD) macroscopic model, supplemented with thermal shape fluctuations analysis (LSD+TFM)[1)], and the Phonon Damping Model (PDM)[2)]. These predictions were convoluted with the population matrices of evaporated nuclei from the statistical model. As it can be seen from the comparison (Fig. 1), the theoretical predictions by both models are in a rather good agreement with the experimental data, especially at the highest energy. A possible onset of a saturation of the GDR width was observed around T = 3 MeV.

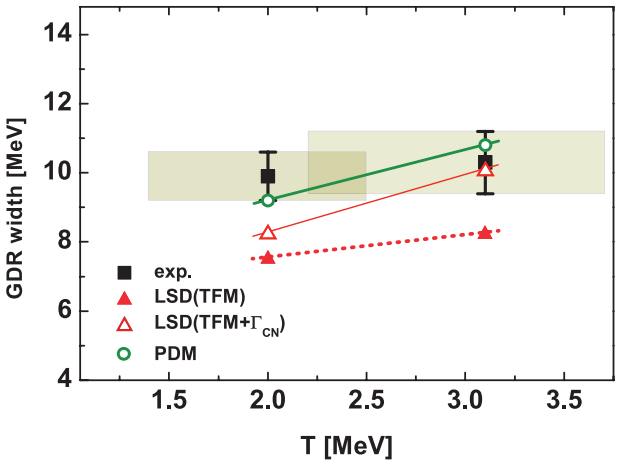

Fig. 1. Temperature dependence of the GDR width. The experimental values (full squares) are compared with the predictions of the LSD+TFM (triangles) and PDM (circles). The results of calculations based on the LSD+TFM used either GDR width at T = 0 equal to Γ_0=5 MeV (full triangles) or $\Gamma(T) = \Gamma_0 + \Gamma_{CN}$ (open triangles) with the T-dependent evaporation width Γ_{CN}. The experimentally extracted GDR widths are bounded in the shaded areas determined by the width of the experimental temperature distributions and the vertical error bars. The straight lines connecting the theoretical predictions are drawn to guide the eyes.

† Condensed from the article in Phys. Rev. C **91**, 054313 (2015)

*1 Department of the Structure of Atomic Nucleus, Institute of Nuclear Physics PAN
*2 GANIL
*3 Dipartimento di Fisica, Universitá di Milano
*4 INFN sezione di Milano, Milano
*5 INFN, Laboratori Nazionali di Legnaro
*6 Kurchatov institute, National Research Centre "Kurchatov Institute"
*7 INFN sezione di Firenze
*8 Dipartimento di Fisica, Universitá di Firenze
*9 Dipartimento di Fisica e Astronomia, Universitá di Bologna and INFN sezione di Bologna
*10 Heavy Ion Laboratory, University of Warsaw
*11 Department of Nuclear and Atomic Physics,Tata Institute of Fundamental Research
*12 Department of Physics, University of York
*13 Physics Department, Institut Pluridisciplinaire Hubert Curien and Université de Strasbourg
*14 RIKEN Nishina Center

References

1) K. Pomorski, J. Dudek, Phys. Rev. C **67** (2003) 044316. J. Dudek, K. Pomorski, N.Schunck and N. Dubray, *Eur. Phys. J. A* **20** (2004) 15.
2) N. Dinh Dang and A. Arima, Phys. Rev. Lett. **80** (1998) 4145; N. Dinh Dang, *Phys. Rev. C* **85** (2012) 064323.

Experimental investigation on the temperature dependence of the nuclear level density parameter†

B. Dey,[*1] D. Pandit,[*1] S. Bhattacharya,[*2] K. Banerjee,[*1] N. Quang Hung,[*3] N. Dinh Dang,[*4] D. Mondal,[*1] S. Mukhopadhyay,[*1] S. Pal,[*1] A. De,[*5] and S.R. Banerjee[*1]

Recently there have been ample experimental efforts to comprehend the spin dependence of the level density parameter $a = k^{-1}$. In a few measurements of angular momentum J gated neutron evaporation spectra in $A \sim 119$, 97, and 62, it was seen that the value of the inverse level density parameter k decreased with increasing J, which indicated that the level density increases with J. On the other hand, the values k extracted from the α evaporation spectra in the mass regions of $A \sim 180$ and 120 are either constant or increase with J. However, theoretical calculations for similar masses show that k should increase with J for all the systems. Thus, extremely exciting but conflicting experimental results on the spin dependence of the level density parameter motivate one to carry out further investigations.

This work reports on the angular momentum gated neutron evaporation spectra at different excitation energies (30 – 50 MeV) for the reaction ^{4}He + ^{93}Nb. The specific advantage of using a light-ion reaction is that the major residues are of similar nature and in our case they are $^{93-95}$Tc, depending on the excitation energy of the compound nucleus. However, for excitation energies above 42 MeV, another channel contributes ($\sim$ 20%) due to (α, α2n) populating ^{91}Nb. Nevertheless, the deformations of all the nuclei populated in the decay chain are similar and of the order of $\beta \sim 0.05$. The shell effects are also very small and similar. Therefore, the neutron evaporation spectra will have the contribution from similar kind of nuclei only.

The experiment was performed at the Variable Energy Cyclotron Centre (Kolkata) using the α beam from the K-130 cyclotron. A self-supporting 1 mg/cm^2 thick target of 99.9% pure ^{93}Nb target was used. Four different beam (^{4}He) energies of 28, 35, 42, and 50 MeV were used to populate the compound nucleus ^{97}Tc at the excitation energies of 29.3, 36.0, 43.0, and 50.4 MeV, respectively. The maximum populated angular momenta for fusion were 16, 18, 19, and 20$\hbar$, respectively. The evaporated neutrons from the compound nucleus were detected by a liquid organic scintillator (BC501A) based neutron detector that was placed at a distance of 1.5 m from the target position and at an angle of 125 degrees to the beam axis. The experimental data are compared with the predictions by several theoretical models including those by the finite temperature (FT) BCS and FTBCS1 theories. The latter[1)] includes the effect due to quasiparticle-number fluctuations beyond the FTBCS theory.

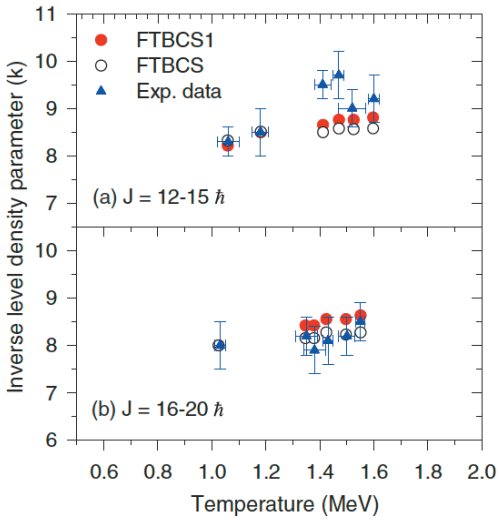

Fig. 1. Temperature dependence of k compared with the calculations of FTBCS and FTBCS1 theories.

As can be seen from Fig. 1, the increase of k with temperature T observed in the data is reproduced by the results of theoretical calculations within the FTBCS and FTBCS1 theories. The agreement is better for the higher J window, whereas for the lower J window the theory underestimates the two data points at $T = 1.41$ MeV ($J = 15\hbar$) and 1.47 MeV ($J = 13\hbar$). The FTBCS and FTBCS1 predict similar results, indicating that pairing reentrance effect, predicted by the FTBCS1 theory at finite T band J, might have a minor effect on k in this case. However, to have a thorough understanding of the effect of collectivity and pairing reentrance on the decrease of k with increasing J, much more theoretical and experimental studies are needed. Moreover, it may be noted that the effect of angular momentum on k is not observed for higher masses but is only apparent in low- and medium-mass $A \leq 120$ nuclei. Hence, more experimental data at both high- and low-mass regions are required to understand this behavior.

Reference
1) N. Quang Hung and N. Dinh Dang, Phys. Rev. C **84** (2001) 054324

† Condensed from the article in Phys. Rev. C **91**, 044326 (2015)

*1 Experimenatl Nuclear Physics Section, VECC
*2 Faculty of Physics, Barasat Govt. College
*3 School of Engineering, TanTao University
*4 RIKEN Nishina center
*5 Department of Physics, Raniganj Girls College

2. Nuclear Physics (Theory)

Impurity effects of the Λ particle on the 2α cluster states of ^{9}Be and ^{10}Be†

M. Isaka*1 and M. Kimura*2

A unique and interesting aspect of hypernuclei is the structure change caused by the addition of a Λ particle as an impurity, which is the so-called "*impurity effect*." From this point of view, the structure of Be hyper-isotopes is of particular interest, because Be isotopes have a 2α cluster core surrounded by valence neutrons[1–3]. For example, in ^{9}Be, the first excited state $1/2^+$ is considered to have a $^{8}\mathrm{Be}(0^+) + n(s_{1/2})$ configuration, which can be regarded as a Hoyle analogue state with the replacement of an α particle by a neutron, while the ground state has a relatively compact $2\alpha + n$ structure. In the neutron-rich side, exotic structures associated with 2α clustering appear. In ^{10}Be, the coexistence of different structures has been discussed based on the concept of the molecular orbits of valence neutrons around the 2α clustering[4]. Since the two valence neutrons are considered to occupy different molecular orbits in the 0_1^+, 0_2^+, and 1^- states, the degree-of-clustering varies depending on the neutron occupation. In particular, the 0_2^+ state is considered to be largely deformed with a well-developed 2α cluster structure, whereas the ground state is rather compact. Therefore, we can expect the modification of the excitation spectra by the addition of a Λ particle. Furthermore, it is interesting to investigate the dynamical changes of these structures.

To investigate such phenomena, we applied an extended version of the antisymmetrized molecular dynamics for hypernuclei, which we call HyperAMD[5], to $^{10}_{\Lambda}$Be and $^{11}_{\Lambda}$Be in the same manner as our previous work for $^{12}_{\Lambda}$Be[6].

Figures 1(a) and (b) compare the excitation spectra of $^{10}_{\Lambda}$Be and $^{11}_{\Lambda}$Be with those of the core nuclei. It is clearly seen that the excited states of these hypernuclei are shifted up in the excitation spectra, namely the positive-parity states in $^{10}_{\Lambda}$Be and the $K^\pi = 0_2^+ \otimes \Lambda$ band built on the $1/2_2^+$ state in $^{11}_{\Lambda}$Be. In other words, the excitation energies of the well-pronounced 2α cluster states are increased significantly. This is because the energy gain of the Λ particle is considerably different between the ground and these excited states. To see the difference of the energy gain clearly, we calculate the binding energy of the Λ particle B_Λ defined as,

$$B_\Lambda = E(J^\pi; {}^{A}\mathrm{Be}) - E(J^\pi \otimes \Lambda; {}^{A}_{\Lambda}\mathrm{Be}), \qquad (1)$$

for each state. In Figs. 1(c) and (d), it is found that the B_Λ of the well-pronounced cluster states are much smaller than those of the ground states. The difference of B_Λ is mainly due to the difference in the deformation of each state, essentially coming from the degrees of the 2α clustering.

In this article, we also discuss the changes caused to the 2α clustering by the addition of a Λ particle. It is found that the Λ particle largely reduces the rms radii of the excited states with large nuclear quadrupole deformation β, which mainly comes from the reduction of the inter-cluster distance between 2α.

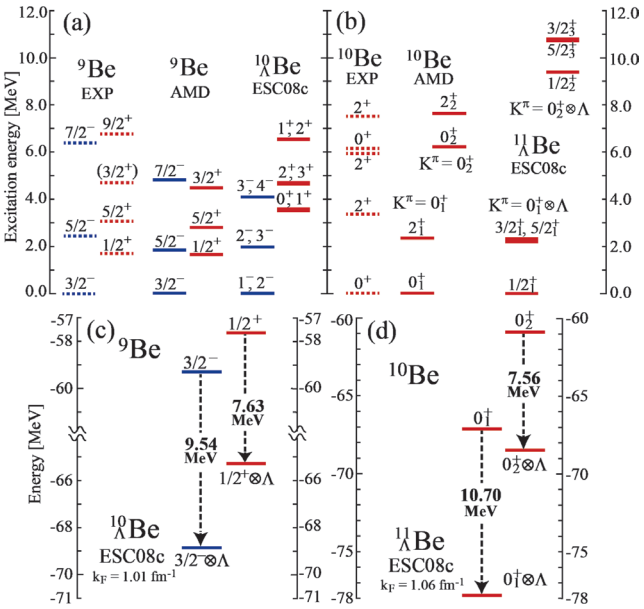

Fig. 1. (a) Calculated excitation spectra of ^{9}Be and $^{10}_{\Lambda}$Be. (b) Same as (a) but for ^{10}Be and $^{11}_{\Lambda}$Be. (c) Calculated values of B_Λ by using YNG-ESC08c as the ΛN interaction in $^{10}_{\Lambda}$Be (d) Same as (c) but for $^{11}_{\Lambda}$Be.

References
1) S. Okabe, Y. Abe, and H. Tanaka, Prog. Theory. Phys. **57**, 866 (1977).
2) N. Itagaki and S. Okabe, Phys. Rev. C**61**, 044306 (2000).
3) Y. Kanada-En'yo, M. Kimura, and A. Ono, Prog. Theor. Exp. Phys. **2012**, 01A202 (2012).
4) Y. Kanada-En'yo, H. Horiuchi, and A. Doté, Phys. Rev. C**60**, 064304 (1999).
5) M. Isaka, M. Kimura, A. Doté, and A. Ohnishi, Phys. Rev. C**83**, 044323 (2011).
6) H. Homma, M. Isaka, and M. Kimura, Phys. Rev. C**91**, 014314 (2015).

† Condensed from the article in Phys. Rev. C **92**, 044326 (2015)

*1 RIKEN Nishina Center
*2 Department of Physics, Hokkaido University

Excited states above the Hoyle state

Y. Funaki*1

In ^{12}C, there exists besides the Hoyle state (the second 0^+ state of ^{12}C) a number of other α gas states above the Hoyle state that one can qualify as excited states of the Hoyle state. For a description of those states, it is useful to adopt a generalized THSR wave function[1], as the so-called THSR wave function[2,3] is known to be the best to describe the Hoyle state[4]. The part of the 3α THSR wave function that contains the c.o.m. motion of the α particles contains two Jacobi coordinates $\boldsymbol{\xi}_1$ and $\boldsymbol{\xi}_2$. As a natural extension of the original THSR wave function, it is possible to associate two different width parameters B_1, B_2 with the two Jacobi coordinates. In this case the translationally invariant THSR wave function has the following form:

$$\Psi^{\rm thsr}_{3\alpha} = \mathcal{A}\left[\exp\left(-\frac{4}{3B_1^2}\boldsymbol{\xi}_1^2 - \frac{1}{B_2^2}\boldsymbol{\xi}_2^2\right)\phi_1\phi_2\phi_3\right]. \quad (1)$$

With this type of generalized THSR wave function, one can get a much richer spectrum of ^{12}C. Axial symmetry has been assumed and the four B parameters are taken as Hill-Wheeler coordinates. In Fig. 1, the calculated energy spectrum is shown. One can see that besides the ground state band, there are many J^π states obtained above the Hoyle state. All these states turn out to have large rms radii ($3.7 \sim 4.7$ fm), and therefore can be considered as excitations of the Hoyle state. The Hoyle state can thus be considered as the "ground state" of a new class of excited states in ^{12}C. In particular, the nature of the series of states $(0_2^+, 2_2^+, 4_2^+)$ and the 0_3^+ and 0_4^+ states have recently been widely discussed from the experimental side[5–9].

In Fig. 1, the $E2$ transition strengths between J and $J\pm2$ states and monopole transitions between 0^+ states are shown with corresponding arrows. We note the very strong $E2$ transitions inside the Hoyle band, $B(E2; 4_2^+ \to 2_2^+) = 591$ e^{2}fm^4 and $B(E2; 2_2^+ \to 0_2^+) = 295$ e^{2}fm^4. The transition between the 2_2^+ and 0_3^+ states is also very large, $B(E2; 2_2^+ \to 0_3^+) = 104$ e^{2}fm^4. There have been attempts to interpret the Hoyle band as a rotational band of a spinning triangle as this was successfully done for the ground state band[10]. However, the situation may not be as straightforward as it seems[11]. Since the two transitions $2_2^+ \to 0_2^+$ and $2_2^+ \to 0_3^+$ are of similar magnitude, no clear band head can be identified. Whether they can be qualified as members of a rotational band or of a vibrational band or a mixture of both is an open question. One should also realize that the 0_3^+ state is strongly excited from the Hoyle state by monopole transition whose strength is obtained from the extended THSR calculation to be $M(E0; 0_3^+ \to 0_2^+) = 35$ fm^2. Therefore, the 0_3^+ state seems to be a state where one α particle has been lifted out of the condensate to the next higher S level with a node. This is confirmed by the S^2 factor, which is calculted to be close to unity for the ^{12}C$(0_1^+)+\alpha(S)$ channel. We can also conclude that the 2_3^+ and 4_3^+ states, together with the 0_3^+ state, form the higher nodal rotational band, from the Reduced Width Amplitude analysis. On the other hand, the 0_4^+, 2_4^+ and 4_4^+ states all have the largest contribution from the ^{8}Be$(2^+)+\alpha(D)$ channel, indicating that these states are built out of an α particle orbiting in a D-wave around a (correlated) two α pair, also in a relative $0D$ state.

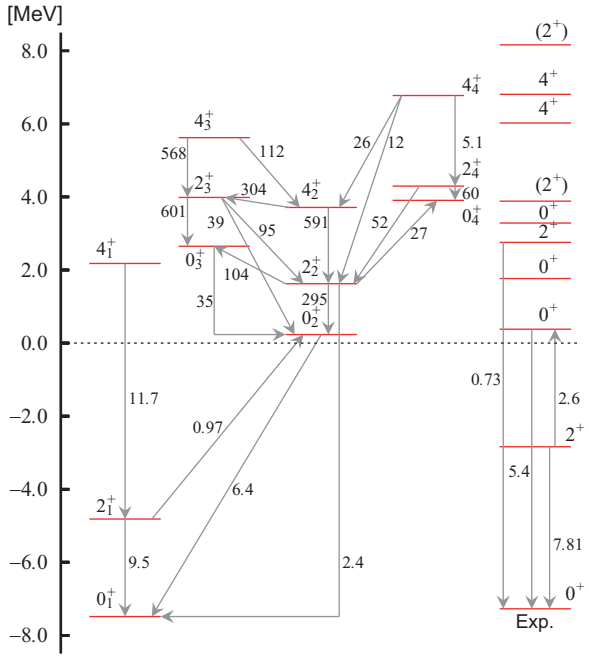

Fig. 1. Spectrum of ^{12}C obtained from the extended THSR approach in comparison with experiment.

*1 RIKEN Nishina Center

References
1) Y. Funaki *et al.*, Prog. Part. Nucl. Phys. **82**, 78 (2015).
2) A. Tohsaki *et al.*, Phys. Rev. Lett. **87**, 192501 (2001).
3) Y. Funaki *et al.*, Prog. Theor. Phys. **108**, 297 (2002).
4) Y. Funaki *et al.*, Phys. Rev. C **67**, 051306(R) (2003).
5) M. Itoh *et al.*, Nucl. Phys. A **738**, 268 (2004).
6) M. Itoh *et al.*, Phys. Rev. C **84**, 054308 (2011).
7) M. Freer *et al.*, Phys. Rev. C **80**, 041303(R) (2009).
8) W. R. Zimmerman *et al.*, Phys. Rev. Lett. **110**, 152502 (2013).
9) M. Freer *et al.*, Phys. Rev. C **83**, 034314 (2011).
10) D. J. Mańin-Lámbarri *et al.*, Phys. Rev. Lett. **113**, 012502 (2014).
11) Y. Funaki, Phys. Rev. C **92**, 021302 (2015).

Shell-model fits for $N = 82$ isotones

M. Honma,[*1] T. Otsuka,[*2,*3,*4] T. Mizusaki,[*5] Y. Utsuno,[*6,*3] N. Shimizu,[*3] and M. Hjorth-Jensen[*4,*7,*8]

Owing to the well-established shell gap at $Z = 50$ and 82, the shell model has been successfully applied for describing the structure of the $N = 82$ isotones with $50 < Z < 82$ by taking the valence single-particle orbits $0g_{7/2}$, $1d_{5/2}$, $0h_{11/2}$, $2s_{1/2}$ and $1d_{3/2}$ on top of an inert ^{132}Sn core. The $N = 82$ isotones show various interesting features. For example, the excitation energy of the first 2^+ state increases as a function of Z and shows a prominent maximum at $Z = 64$, suggesting the development of a subshell gap. The lighter isotones with $Z < 64$ are dominated by mixed configurations of the lower two orbits ($g_{7/2}$ and $d_{5/2}$) with excitations to the upper orbits, while for the heavier ones the unique-parity high-j orbit $h_{11/2}$ plays a crucial role. The systematics of yrast spectra and the property of some isomers are successfully explained by the seniority scheme. In addition, the development of the octupole collectivity has been observed in the low-lying states connected by strong $E3$ transitions.

It is interesting to investigate to what extent such variety of nuclear structures can be described within the shell-model framework. The effective interaction is a key ingredient to address this problem, which can be either determined purely empirically[1] or derived microscopically from the realistic nucleon-nucleon potential. The latter attempt has been extensively developed,[2,3] and the importance of the three-body force has been suggested to account for the deviation of the shell-model results from the experimental observations. Another possible approach for a better description of the experimental data is to modify such a microscopically determined effective interaction[4] by fitting the calculated energies to the experimental data. In this report, we present such fitting calculations for the $N = 82$ isotones. The similar analysis for Sn isotopes was reported previously.[5]

The single-particle energies of the $d_{5/2}$, $d_{3/2}$, and $h_{11/2}$ orbits relative to the $g_{7/2}$ are taken from the experimental energy spectra of ^{133}Sb,[7] and only that of the $s_{1/2}$ orbit is determined by the fit. Starting from the microscopically derived effective interaction based on the N3LO potential,[6] we have carried out iterative fitting calculations. In the latest fit, 26 linear combinations of the fit parameters (*i.e.* 160 two-body matrix elements with $A^{-0.3}$ mass dependence and the single-particle energy of the $s_{1/2}$ orbit) have been modified, and we have attained a rms error of 142 keV for 338 energy data of 22 isotones.

Figure 1 illustrates the quality of the fit. It can be seen that the overall agreement between the shell-model results and the experimental data is quite good including the "magic"-like feature at Z=64. The fit is successful also for odd-Z cases. The semi-empirical approach presented here would be useful not only for the analysis of experimental data but also as a reference for clarifying various effects such as the three-body forces that are not included in the present microscopic approach. It is also interesting to extend the scope of this interaction beyond the semi-magic nuclei by combining it with a suitable proton-neutron interaction.

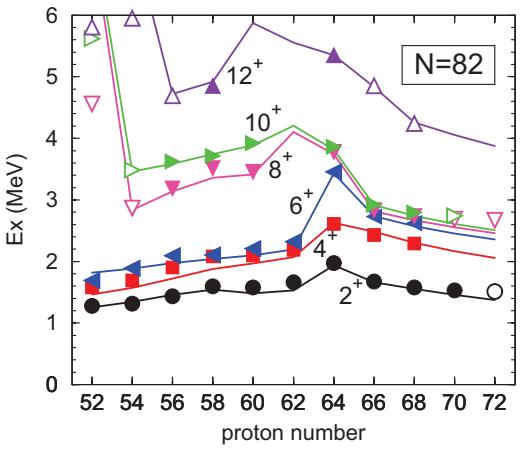

Fig. 1. Comparison of excitation energies of even-spin yrast states between the experimental data (symbols) and the shell-model results (lines). Experimental data are taken from Ref.[8] Open symbols indicate that the spin or parity assignment is uncertain. The shell-model results are obtained by using the efficient shell-model code MSHELL64[9].

*1 Center for Mathematical Sciences, University of Aizu
*2 Department of Physics, University of Tokyo
*3 Center for Nuclear Study, University of Tokyo
*4 National Superconducting Cyclotron Laboratory, Michigan State University
*5 Institute of Natural Sciences, Senshu University
*6 Advanced Science Research Center, Japan Atomic Energy Agency
*7 Department of Physics and Astronomy, Michigan State University
*8 Department of Physics, University of Oslo

References

1) B. H. Wildenthal: Phys. Rev. Lett. **22**, 1118 (1969).
2) A. Holt *et al.*: Nucl. Phys. A **618**, 107 (1997).
3) L. Coraggio *et al.*: Pnys. Rev. C **80**, 044320 (2009).
4) M. Hjorth-Jensen *et al.*: Phys. Rep. **261**, 125 (1995).
5) M. Honma *et al.*: RIKEN Accel. Prog. Rep. **45**, 35 (2012).
6) D. R. Entem *et al.*: Phys. Rev. C **68**, 041001(R) (2003).
7) M. Sanczhez-Vega *et al.*: Phys. Lett. **80**, 5504 (1998).
8) Data extracted using the NNDC WorldWideWeb site from the ENSDF database.
9) T. Mizusaki *et al.*: MSHELL64 code (unpublished).

Soft negative-parity excitations of rotating super- and hyperdeformed states around ^{40}Ca studied by Skyrme-RPA calculations

M. Yamagami [*1] and K. Matsuyanagi[*2]

Soft mode connected to the violation of symmetries is one of the central issues in nuclear physics. It emerges when the correlations increase by the addition of nucleons for a closed major shell or a change in the shell structure caused by weakly bound orbits, isovector properties of the nuclear force, and so on. Here, we discuss soft modes emerging from the superdeformed (SD) state toward a non-axial reflection-asymmetric shape due to the change in the shell structure by collective rotation.

We have already investigated the rotational bands of the SDf^4 and SDf^8 states in ^{36}Ar and the SDf^8 and hyperdeformed (HD) states in ^{40}Ca and ^{44}Ti by performing mean-field calculations with the Skyrme energy density functional (Skyrme-EDF)[1]. Here, the SDf^4 (SDf^8) state has four (eight) nucleons in single-particle (sp) levels originating from the $f_{7/2}$ shell, and the sp levels from $f_{7/2}$ and $g_{9/2}$ shells are occupied in the HD state.

In the present study, we predict the emergence of soft modes in these rotating SD and HD states by means of random phase approximation (RPA) calculation with the Skyrme-EDF.[2]

As an illustrative example, the vibrational energy E_{vib} of the SDf^8 state in ^{40}Ca is shown as a function of ω_{rot} in Fig. 1. Here, the size of the symbol is proportional to the isoscalar octupole transition strength $B(IS3)$.

At $\omega_{rot} = 0$, excitation with large transition strength $B(IS3) = 195.2$ W.u. appears at $E_{vib} = 5.46$ MeV. In this state, $S_{K=0}$ is dominant (98.2 %). Here, S_K is the K-component of $B(IS3)$. The main configuration is a particle-hole (ph) excitation $[330]1/2 \rightarrow [440]1/2$. Other ph excitations from hole states originating from the $f_{7/2}$ shell to particle states from the $g_{9/2}$ shell also contribute largely.

The vibrational energy of the $K = 0$ state is strongly lowered by the rotational alignment of the $[440]1/2$ levels that have rapid down-sloping as a function of ω_{rot}. We obtain the vibrational state up to the critical rotational frequency $\hbar\omega_{rot}^{(c)} = 1.60$ MeV, where a sudden change of the internal structure occurs when the $[440]1/2$ levels are occupied in our framework. The properties at $\omega_{rot}^{(c)}$ are listed in Table 1. Due to the Coriolis K-mixing effect, $S_{K=1}$ becomes dominant.

We can expect the continuity of this trend such that the vibrational energy will decrease further and cross the yrast line. Specifically, we predict the emergence of the soft mode of the SD state that leads to the transition to a non-axial reflection-asymmetric shape (banana shape).

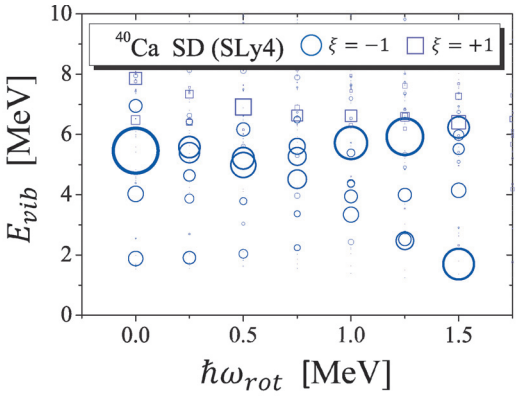

Fig. 1. E_{vib} of the SDf^8 state in ^{40}Ca as a function of $\hbar\omega_{rot}$. The size of the symbol is proportional to the $B(IS3)$ value. Circles and boxes represent the negative-parity excitations with x-signature $\xi = -1$ and $+1$, respectively. Here, Skyrme SLy4 is used.

	$\hbar\omega_{rot}^{(c)}$ [MeV]	E_{vib} [MeV]	$B(IS3)$ [W.u.]	$S_{K=0}$ [W.u.]	$S_{K=1}$ [W.u.]
^{36}Ar (SDf^4)	2.25	1.21	47.7	8.5	39.2
^{36}Ar (SDf^8)	1.25	1.81	289.4	162.8	125.1
^{40}Ca (SDf^8)	1.60	1.37	170.3	26.7	132.6
^{44}Ti (SDf^8)	1.50	1.47	154.1	44.5	101.4
^{40}Ca (HD)	1.75	2.33	544.9	371.6	171.9
^{44}Ti (HD)	1.75	1.82	315.3	33.7	258.9

Table 1. Properties of negative-parity excitations at $\omega_{rot}^{(c)}$ in the SDf^4, SDf^8, and HD states around ^{40}Ca. Here, Skyrme SLy4 is used.

We also predict the emergence of soft modes in the SD and HD states around ^{40}Ca systematically. The properties at $\omega_{rot}^{(c)}$ are summarized in Table 1. In the HD states, the rotational alignment of the $[550]1/2$ orbits originating from the $h_{11/2}$ shell plays a key role, and the ph configurations between the $h_{11/2}$ shell and the $g_{9/2}$ shell produce extremely large transition strength.

In conclusion, we emphasize the role of rotational alignment of special high-j orbits, the $[440]1/2$ orbits in the SDf^4 and SDf^8 states and the $[550]1/2$ orbits in the HD states, for the emergence of the soft modes toward banana shape around ^{40}Ca.

*1 Department of Computer Science and Engineering, University of Aizu
*2 RIKEN Nishina Center

References

1) T. Inakura et al., Nucl. Phys. **A710**, 261 (2002).
2) M. Yamagami et al., JPS Conf. Proc. **6**, 030051 (2015).

Pairing Reentrance in warm rotating ^{104}Pd nucleus†

N. Quang Hung,[*1,*2] N. Dinh Dang,[*2] B.K. Agrawal,[*3] V.M. Datar,[*4] A. Mitra,[*4] and D.R. Chakrabarty[*4]

The recent series of experiments conducted at the Bhabha Atomic Research Center (BARC) for the reaction $^{12}C + {}^{93}Nb \rightarrow {}^{105}Ag^* \rightarrow {}^{104}Pd^* + p$ at the incident energy of 40 - 45 MeV has observed an anomalous enhancement of the nuclear level density (NLD) of ^{104}Pd nucleus at low excitation energy E^* and high angular momentum J[1]. This enhancement is similar to that previously predicted by the shell-model Monte Carlo (SMMC)[2] and FTBCS1 calculations[3] for a warm rotating ^{72}Ge nucleus. Both the SMMC and FTBCS1 have pointed out that the local enhancement of NLD at low T and high J is associated with the pairing reentrance effect. The latter occurs when the angular momentum of the system is sufficiently high so that the pairing correlation, which is zero at low $T < T_1$, reappears at $T > T_1$. The goal of this work is to apply the FTBCS1 theory including finite angular momentum to study if the enhanced NLD observed in ^{104}Pd can be interpreted as the first evidence of pairing reentrance in a warm rotating finite nucleus.

The FTBCS1 theory at finite temperature and angular momentum is obtained based on the conventional finite-temperature Bardeen-Cooper-Schrieffer (FTBCS) theory that takes into account the effect of quasiparticle-number fluctuations (QNF) on the pairing field[3]. The numerical calculations are carried out for ^{104}Pd nucleus, whose single-particle spectra are taken from the axially deformed Woods-Saxon potential including the spin-orbit and Coulomb interactions. The quadrupole deformation parameter β_2 potential is adjusted so that the NLD obtained at different values of J fit best the experimental data, especially in the region where the enhancement of NLD is observed. The variation of β_2 with J is plotted in Fig. 1 (a). This figure clearly shows that ^{104}Pd nucleus undergoes a shape transition from the prolate shape ($\beta_2 > 0$) to the oblate one ($\beta_2 < 0$) at around $J = 20\ \hbar$, which is reasonable in this mass region because of an alignment of protons in $g_{9/2}$ and neutrons in $h_{11/2}$ orbits. Figs. 1 (d) - (e) depict the NLD as a function of excitation energy E^* obtained within the FTBCS1 and the conventional FTBCS theories.

It is found that due to the QNF, the FTBCS1 gaps at different J values decrease monotonically with increasing E^* and do not collapse at the critical value $E^* = E^*_c$ as in the case of the FTBCS. As a result, the pairing reentrance takes place only in the pairing gaps obtained within the FTBCS1 (*e.g.*, for protons at $J = 20\hbar$ and neutrons and at $J = 30\hbar$), whereas this effect does not appear in the FTBCS gaps. This leads to the local enhancements of the NLD obtained within the FTBCS1 at low E^* ($2 < E^* < 5$ MeV) and high J, in agreement with the experimental data. This agreement indicates that the observed enhancement of the NLD might be the first experimental detection of the pairing reentrance in a finite nucleus.

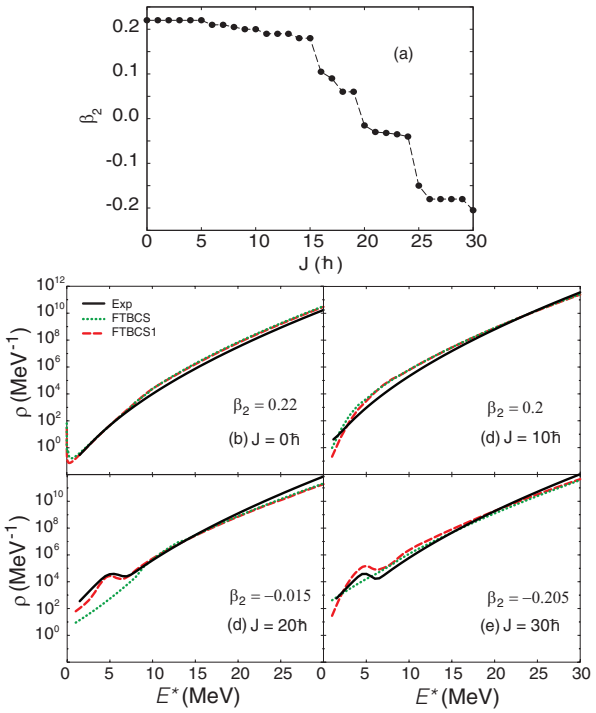

Fig. 1. (Color online) (a) - Quadrupole deformation parameter β_2 as functions of the total angular momentum J obtained within the FTBCS1 theory. [(b) - (e)] - Total NLD as function of excitation energy E^* obtained within the FTBCS (dotted lines) and FTBCS1 (dashed lines) at different values of J and β_2. The solid lines are the experimental data.

References

1) A. Mitra *et al.*, J. Phys. G **36**, 095103 (2009); A. Mitra *et al.*, EPJ Web of Conf. **2**, 04004 (2010); V.M. Datar, A. Mitra, D.R. Chakrabarty, Proceedings of the DAE Sym. on Nucl. Phys., University of Delhi, Dec 37, 2012, Vol. 57, p. 184 (2012).
2) D.J. Dean, K. Langanke, H.A. Nam, W. Nazarewicz, Phys. Rev. Lett. **105**, 212504 (2010).
3) N.Q. Hung and N.D. Dang, Phys. Rev. C **78**, 064315 (2008), Phys. Rev. C **84**, 054324 (2011).

† Condensed from the article in Act. Phys. Pol. B **8**, 551 (2015)

*1 Institute of Research and Development, Duy Tan University
*2 RIKEN Nishina Center
*3 Theory Division, Saha Institute of Nuclear Physics
*4 Nuclear Physics Division, Bhabha Atomic Research Center

Effects of thermal shape fluctuations and pairing fluctuations on the giant dipole resonance in warm nuclei†

A.K. Rhine Kumar,*1 P. Arumugam,*1 and N. Dinh Dang*2

The study of giant dipole resonance (GDR) at high temperature (T) and angular momentum (J) has been an interesting area of research, which has revealed several structural properties of nuclei at extreme conditions. Being a fundamental mode of photo excitation, GDR can probe nuclei at extreme conditions and even those with exotic structures. Since the nucleus is a tiny system, the thermal fluctuations inherent in finite systems are expected to be large. The shape degrees of freedom being crucial for nuclear structure, the deformation parameters are closely associated with the order parameters for the related transitions. Hence the thermal shape fluctuations (TSF) are the most dominant ones, and at low T the fluctuations in the pairing field can also contribute significantly. Many models have been used to study the effect of both these fluctuations separately, but the combined effect of these two was not investigated until our recent efforts.

In our recent work[1)], we have outlined some of our results from a theoretical approach for such warm nuclei where all these effects are incorporated along within the thermal shape fluctuation model (TSFM) extended to include the fluctuations in the pairing field. In this article, we present the complete formalism based on the microscopic-macroscopic approach for determining the deformation energies and a macroscopic approach which links the deformation to GDR observables. The TSFM built on Nilsson-Strutinsky calculations with a macroscopic approach to GDR was employed. The nuclear shapes are related to the GDR observables using the Hamiltonian written in terms of the dipole operator $\mathcal{D}$ and pairing operator P as $H = H_{osc}+\eta\, D^{\dagger}D +\chi\, P^{\dagger}P$, where H_{osc} stands for the anisotropic harmonic oscillator hamiltonian, the parameter η characterizes the isovector component of the neutron and proton average field and χ is the strength of the pairing interaction. The pairing interaction changes the oscillator frequencies $[\omega_{\nu}^{osc}(\nu = x, y, z)]$ to $\omega_{\nu} = \omega_{\nu}^{osc} - \chi\omega^{P}$, where $\omega^{P} = [(Z\Delta_P + N\Delta_N)/(Z + N)]^2$ with χ having the units of MeV^{-1}. Pairing renormalizes the dipole-dipole interaction strength to $\eta = \eta_0 - \chi_0\sqrt{T}\omega^{P}$, with χ_0 having the units of MeV$^{-5/2}$. The T-independent parameters η_0 and χ_0 are chosen to reproduce the GDR width at $T = 0$ and to obtain the overall agreement with the experimental widths at $T \neq 0$. The effective GDR cross-sections is calculated by averaging all the cross-sections $\sigma(E_{\gamma}, \beta, \gamma.\Delta_P, \Delta_N)$ obtained from thermal fluctuations of quadrupole shapes by using the formula for the expectation value of an observable $\mathcal{O}$ as $\langle\mathcal{O}\rangle_{\beta,\gamma,\Delta_P,\Delta_N} = \int \mathcal{O}W(T, \beta, \gamma, \Delta_P, \Delta_N)\mathcal{D}[\alpha]/\int W(T, \beta, \gamma, \Delta_P, \Delta_N)\mathcal{D}[\alpha]$ with $W(T, \beta, \gamma, \Delta_P, \Delta_N) = \exp[-F(T; \beta, \gamma, \Delta_P, \Delta_N)/T]$, $\mathcal{D}[\alpha] = \beta^4|\sin 3\gamma|\, d\beta\, d\gamma\; d\Delta_P\; d\Delta_N$. The total free energy (F_{TOT}) at a fixed deformation is calculated using the expression $F_{TOT} = E_{LDM} + \sum_{p,n}\delta F$. Each cross section $\sigma(E_{\gamma}, \beta, \gamma.\Delta_P, \Delta_N)$ is a sum of the Lorentzians, whose widths are given as $\Gamma_i = \Gamma_0(E_i/E_0)^{\delta}$ with Γ_0 and E_0 being the width and energy in the case of a spherical nucleus, respectively. The energy predicted by the liquid drop model (LDM) is calculated by summing up the Coulomb and surface energies corresponding to a triaxially deformed shape defined by the deformation parameters β and γ.

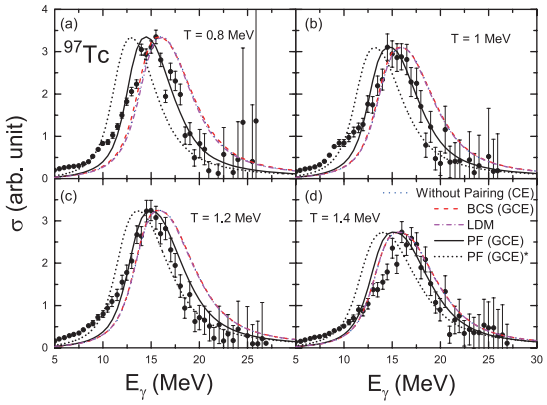

Fig. 1. The GDR strength functions for ^{97}Tc at different T are compared with the results obtained by using the pairing fluctuations (PF) within a grand canonical ensemble approach (GCE). Experimental data are shown by solid circles. The legend PF (GCE)* denotes that the calculations are with the parameter $\delta = 1.9$; in all other calculations δ =1.8.

We discussed our results for the nuclei ^{97}Tc, ^{120}Sn, ^{179}Au, and ^{208}Pb, and corroborated with the experimental data available. The TSFM could explain the data successfully at low temperature only with a proper treatment of pairing and its fluctuations (Fig. 1). More measurements with better precision could yield rich information about several phase transitions that can happen in warm nuclei.

Reference

1) A.K. Rhine Kumar, P. Arumugam, and N. Dinh Dang, Phys. Rev. C **90** (2014) 044308.

† Condensed from the article in Phys. Rev. C **91**, 044305 (2015)

*1 Department of Physics, Indian Institute of Technology Roorkee
*2 RIKEN Nishina center

Stability of the wobbling motion in an odd-A nucleus†

K. Tanabe[*1,*2] and K. Sugawara-Tanabe[*1,*3]

Recently, the transverse wobbling mode was proposed in the yrast band near the ground state before the first backbending in ^{135}Pr[1]. The transverse wobbling mode is the wobbling motion around the middle moment of inertia (MoI)[2], which does not exist in the pure rotor as discussed in the context of classical mechanics[3] and by Bohr-Mottelson[4] quantum mechanically. Regarding the particle-rotor model, as long as the rigid MoI is adopted, there is no chance to find transverse wobbling, because the single-particle oscillator strength ω_k and the rigid MoI are derived from a common radius, and their magnitudes increase or decrease in the same direction as functions of γ periodically with a span of $2\pi/3$. On the other hand, the hydrodynamical (hyd) MoI changes its role in every span of $\pi/3$ in an opposite direction to ω_k. Thus, there remains a possibility to find the transverse wobbling mode for the particle-rotor model with hyd MoI.

We extend the Holstein-Primakoff (HP) boson expansion method to the odd-A case[5–8] by introducing two kinds of bosons for the total angular momentum $\vec{I}$ and the single-particle angular momentum $\vec{j}$. We can identify the nature of each band by referring to two kinds of quantum numbers (n_α, n_β) which indicate the wobbling of $\vec{I}$ and the precession of $\vec{j}$, respectively. In this paper we extend this method to the particle-rotor model with hyd MoI. We choose a representation in which I_y and j_x are diagonal because the hyd MoI is maximum around the y-axis with the relation $\mathcal{J}_y^{\rm hyd} \geq \mathcal{J}_x^{\rm hyd} \geq \mathcal{J}_z^{\rm hyd}$ in the range of $0 \leq \gamma \leq \pi/6$, while ω_k favors $\vec{j}$ to align along the x-axis in the same range of γ. We notice that, if we choose the diagonal representation for $\vec{I}$ and $\vec{j}$ in the same direction, we cannot find any stable physical solution for common values of γ and V (the strength of the single-particle potential[5–8]) in the range of $11/2 \leq I \leq 33/2$. We solve the energy-eigenvalue equation to obtain two real solutions, i.e., ω_+, which is the higher energy, and ω_-, which is the smaller one. In the symmetric limit of $\gamma = 30°$ and $V = 0$, ω_+ corresponds to the wobbling motion around the y-axis with the maximum MoI, while ω_- corresponds to the precession of j around the x-axis.

We adopt j =11/2, $\mathcal{J}_0$ =25 MeV^{-1} ($\mathcal{J}_k^{\rm hyd} = \frac{4}{3}\mathcal{J}_0 \sin^2\left(\gamma + \frac{2}{3}\pi k\right)$), β =0.18 and γ =26° (proposed by Ref.[1]), and V = 1.6 MeV (related to the single-particle strength with these β, γ and j by Wigner-Eckart theorem)[8]. In Fig. 1 we compare the energies labeled by (n_α, n_β)= (0,1) and (0,0) with the exact ones obtained by diagonalizing the same Hamiltonian. The exact levels are reproduced by the approximate ones labeled (0,1), the precession mode of j, irrespective of $I - j$. Both ω_+ and ω_- monotonically increase with I, and never decrease.

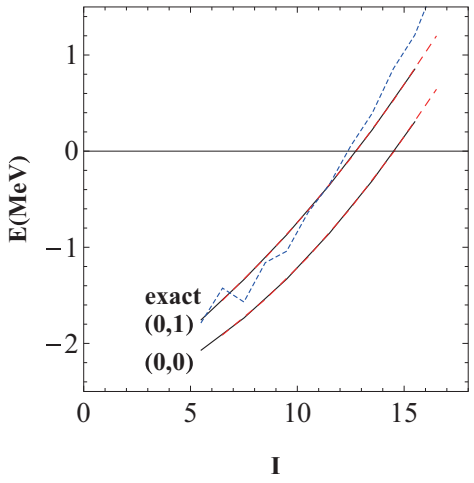

Fig. 1. Comparison of the excitation energy in the leading order approximation[5] with the exact results as functions of I. The solid lines correspond to $I - j$ =even, the red dashed lines to $I - j$ =odd, and the dotted blue lines to the exact results. The attached numerals (0,1) and (0,0) correspond to quantum numbers of (n_α, n_β).

In conclusion, there is no transverse wobbling mode within the framework of the particle-rotor model even with the hyd MoI.

† Condensed from the article at the autumn meeting of Japan Physical Society, Osaka City University, Sept. 27th (2015)

*1 RIKEN Nishina Center
*2 Department of Physics, Saitama University
*3 Otsuma Women's University

References

1) J. T. Matta *et al.*, Phys. Rev. Lett. **114**, 082501 (2015).
2) S. Frauendorf, F. Dönau, Phys. Rev. C **89**, 014322 (2014).
3) L. D. Landau, E. M. Lifshitz: *Mechanics* (Physics-Mathematics Institute, Moskow, 1958), Sect. 37.
4) A. Bohr, B. R. Mottelson: *Nuclear Structure* (Benjamin, Reading, MA, 1975), Vol. II.
5) K. Tanabe, K. Sugawara-Tanabe, Phys. Rev. C **73**, 034305 (2006).
6) K. Tanabe, K. Sugawara-Tanabe, Phys. Rev. C **77**, 064318 (2008).
7) K. Sugawara-Tanabe, K. Tanabe, Phys. Rev. C **82**, 051303(R) (2010).
8) K. Sugawara-Tanabe, K. Tanabe, N. Yoshinaga, Prog. Theor. Exp. Phys. **2014**, 063D01 (2014).

Constraints on the neutron skin and the symmetry energy from the anti-analog giant dipole resonance in ^{208}Pb†

Li-Gang Cao,[*1,*2] X. Roca-Maza,[*3,*4] G. Colò,[*3,*4] and H. Sagawa[*5,*6]

Different experimental methods, either direct or indirect, have been proposed to extract the value of neutron-skin thickness in finite nuclei, that is, the difference between neutron and proton root-mean-square radii,

$$\Delta R_{np} \equiv \langle r^2 \rangle_n^{1/2} - \langle r^2 \rangle_p^{1/2}. \quad (1)$$

The neutron skin thickness has received much attention from both experimental and theoretical viewpoints because it is one of the most promising observables in nuclear structure for constraining the density dependence of symmetry energy around the nuclear saturation density. The symmetry energy plays an important role in understanding the mechanisms of different phenomena in nuclear physics and nuclear astrophysics. It directly affects the properties of exotic nuclei, dynamics of heavy-ion collisions, structure of neutron stars, and simulations of core-collapse supernova.

We investigate the impact of neutron skin thickness, ΔR_{np}, on the energy difference between the anti-analog giant dipole resonance (AGDR), $E_{\rm AGDR}$, and isobaric analog state (IAS), $E_{\rm IAS}$, in a heavy nucleus ^{208}Pb. The AGDR has $J^\pi = 1^-$, and $T = T_0 - 1$ with respect to the isospin of parent nucleus T_0. We employ a family of systematically varied Skyrme energy density functionals. The calculations are performed within the fully self-consistent Hartree-Fock (HF) plus charge-exchange random phase approximation (RPA) framework. We confirm a linear correlation with our microscopic approach and compare our results with available experimental data on ^{208}Pb in order to extract a preferred value for ΔR_{np} and, in turn, for the symmetry energy parameters. In Ref.[1] (denoted as Exp1), the AGDR was separated from other excitations by means of the multipole decomposition analysis of the ^{208}Pb$(\vec{p},\vec{n})$ reaction at a bombarding energy $T_p = 296$ MeV; the polarization transfer observables were quite instrumental in the separation of the non-spin flip AGDR from the spin-flip spin dipole resonance (SDR) in the multipole decomposition analysis. The energy difference between the AGDR and IAS was determined to be $E_{\rm AGDR} - E_{\rm IAS} = 8.69 \pm 0.36$ MeV. Another experimental measurement has been reported in Ref.[2] (Exp2); the ^{208}Pb$(p, n\gamma p)$ ^{207}Pb reaction with a beam energy of 30 MeV was used to excite the AGDR and to measure its γ-decay to the isobaric analog state, coinciding with proton decay of the IAS. The energy difference between the AGDR and IAS was determined to be $E_{\rm AGDR} - E_{\rm IAS} = 8.90 \pm 0.09$ MeV. Averaging the results from two available experimental data, our analysis gives $\Delta R_{pn} = 0.236 \pm 0.018$ fm, $J = 33.2 \pm 1.0$ MeV and a slope parameter of the symmetry energy at saturation $L = 97.3 \pm 11.2$ MeV. Good agreement is obtained in comparing our new results of neutron-skin thickness and symmetry energy J with the values extracted using several different experimental methods within the error bars as shown in Fig. 1. In contrast, the extracted L value is somewhat larger than previously obtained values. Possible hints on whether model dependence can explain this difference are provided.

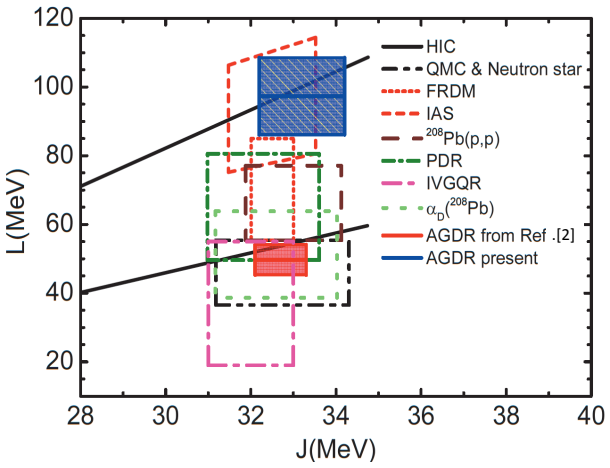

Fig. 1. (Color online) Values of the slope parameter L and symmetry energy J at the saturation density extracted in the current work compared with the values from other experimental data extracted using several different methods.

References
1) J. Yasuda et al., Prog. Theor. Exp. Phys. **063**D02 (2013).
2) A. Krasznahorkay et al., arXiv:1311.1456, (2013).

† Condensed from the article in Phys. Rev. C **92**, 034308 (2015)

*1 School of Mathematics and Physics, North China Electric Power University
*2 State Key Laboratory of Theoretical Physics, Institute of Theoretical Physics, Chinese Academy of Sciences
*3 Dipartimento di Fisica, Università degli Studi di Milano
*4 Istituto Nazionale di Fisica Nucleare (INFN), Sez. di Milano
*5 RIKEN Nishina Center
*6 Center for Mathematics and Physics, University of Aizu

Variational study of the equation of state for neutron star matter with hyperons†

H. Togashi,[*1,*2] E. Hiyama,[*1] Y. Yamamoto,[*1] and M. Takano[*2]

The equation of state (EOS) for dense nuclear matter plays a crucial role in the study of neutron star (NS) structure. As there are relatively large uncertainties in hyperon-nucleon (YN) and hyperon-hyperon (YY) interactions, the fraction of hyperons in NS matter is still far from being understood. In particular, recently observed masses of PSRs J1614-2230 ($M = 1.97 \pm 0.04 M_\odot$)[1)] and J0348+0432 ($M = 2.01 \pm 0.04 M_\odot$)[2)] impose severe constraints on the EOS of nuclear matter including hyperons. In this report, we investigate how uncertainty in the odd-state part of bare $\Lambda\Lambda$ interactions affects the structure of NSs by using EOSs constructed with the cluster variational method for hyperonic nuclear matter containing Λ and Σ^- hyperons.

Following the cluster variational method for pure nucleon matter[3)], we use the Hamiltonian composed of bare baryon interactions. For the nucleon sector, the Argonne v18 two-nucleon potential and the Urbana IX three-nucleon potential are adopted. For the hyperon sector, central two-body potentials are employed as the ΛN, $\Sigma^- N$, and $\Lambda\Lambda$ interactions[4,5)], which are constructed to reproduce the experimental data of hypernuclei. Here, it is noted that there are no experimental data on double-Λ hypernuclei to determine the odd-state part of the $\Lambda\Lambda$ interaction. Therefore, we prepare four different odd-state $\Lambda\Lambda$ interactions (Type 1–4), whose parameters are chosen so that the odd-state $\Lambda\Lambda$ interaction becomes monotonically more repulsive from Type 1 to Type 4. Using these baryon interactions, we calculate the energies of hyperonic nuclear matter for each odd-state $\Lambda\Lambda$ interaction model and apply the obtained EOSs to calculations of the NS structure.

The numerical results are shown in Table 1. It is seen that the onset density of Λ in NS matter is insensitive to the odd-state $\Lambda\Lambda$ interaction, whereas that of Σ^- decreases as the odd-state $\Lambda\Lambda$ interaction becomes more repulsive. Furthermore, the obtained maximum mass of NSs increases with the repulsion of the odd-state $\Lambda\Lambda$ interaction, but it is still smaller than the recently observed masses of heavy NSs[1,2)].

Table 1. Onset densities of Λ and Σ^- hyperons and maximum masses of NSs for four different odd-state $\Lambda\Lambda$ interactions. The values of the onset densities are given in fm^{-3} and the maximum masses are in $M_\odot$.

$\Lambda\Lambda$ interaction	Type 1	Type 2	Type 3	Type 4
Λ onset density	0.42	0.42	0.42	0.42
Σ^- onset density	0.76	0.72	0.70	0.68
Maximum mass	1.48	1.53	1.57	1.62

† Condensed from the article in Phys. Rev. C **93**, 035808 (2016).

*1 RIKEN Nishina Center
*2 Research Institute for Science and Engineering, Waseda University

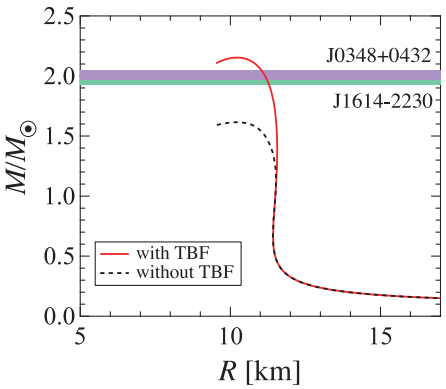

Fig. 1. Mass-radius relations of NSs obtained from EOSs based on the most repulsive odd-state $\Lambda\Lambda$ interaction (Type 4) with and without a phenomenological three-baryon force (TBF). The horizontal bands show the masses of PSRs J1614-2230[1)] and J 0348+0432[2)].

Therefore, we finally consider a phenomenological three-baryon force (TBF) for YNN, YYN, and YYY systems[6)] in order to explain the masses of heavy NSs. Figure 1 shows the mass-radius relations of NSs obtained from the EOS with the most repulsive odd-state $\Lambda\Lambda$ interaction (Type 4) including the hyperon TBF. Also shown is the result without the hyperon TBF. The maximum mass with the TBF becomes larger than that without the TBF due to the strong repulsion among three baryons. In Fig. 1, the horizontal green and purple bands show the masses of PSRs J1614-2230[1)] and J0348+0432[2)], respectively. It is found that the obtained result with TBF is consistent with these observations. The influence of the TBF on the NS structure is discussed in more detail in Ref.[7)].

References

1) P. B. Demorest et al., Nature **467**, 1081 (2010).
2) J. Antoniadis et al., Science **340**, 6131 (2013).
3) H. Togashi and M. Takano, Nucl. Phys. A **902**, 53 (2013).
4) E. Hiyama et al., Phys. Rev. C **66**, 024007 (2002).
5) E. Hiyama et al., Phys. Rev. C **74**, 054312 (2006).
6) Y. Yamamoto et al., Phys. Rev. C **90**, 045805 (2014).
7) H. Togashi et al., Phys. Rev. C **93**, 035808 (2016).

Joint project for large-scale nuclear structure calculations in 2015

N. Shimizu,[*1] T. Abe,[*2] T. Otsuka,[*2,*1] N. Tsunoda,[*1] and Y. Utsuno[*3,*1]

A joint project for large-scale nuclear structure calculations has been promoted since the year 2002 based on a collaboration agreement between the RIKEN Accelerator Research Facility (currently RIKEN Nishina Center) and the Center for Nuclear Study, the University of Tokyo. Currently, we maintain 16 PC servers with Intel CPUs for large-scale nuclear shell-model calculations. In 2015, we reinforced the system by introducing two computer nodes equipped with Intel Xeon CPUs with 32 cores and 20 cores, respectively. Based on this project, we performed shell-model calculations of the various nuclides that have been measured or are proposed to be measured at the RIKEN RI Beam Factory, such as ^{37,38}Si[1], ^{50}Ar[2], ^{27,29}F, ^{29}Ne, ^{54,56,58,60}Ti, and ^{8,9}C, under various collaborations with many experimentalists. Theoretical studies have also been performed in parallel. Among them, hereafter, we briefly show four achievements of this project.

We have investigated shell evolution in neutron-rich nuclei around $N = 28$ by comparing recent experimental data taken in RIBF with shell-model calculations using the SDPF-MU interaction[3]. Low-lying unnatural-parity levels in ^{37}Si[1] are well reproduced. This indicates that the $N = 20$ shell gap is almost unchanged on increasing the neutron number due to the cross-shell $T = 1$ monopole matrix elements whose strengths are nearly zero. The SDPF-MU interaction also successfully accounts for the 2^+_1 level in ^{50}Ar[2]. The calculation suggests that the $N = 32$ shell gap is preserved in Ar isotopes. In addition, we predict that the $N = 34$ shell gap is enlarged on decreasing the proton number from $Z = 20$. This prediction provides a strong motivation for measuring the 2^+_1 level in ^{52}Ar in the SEASTAR project.

Among the *ab initio* subjects directly related to the experiments at the RIBF, the study of the nuclear structure of proton-rich carbon isotopes (^{8}C and ^{9}C) via neutron-transfer reactions using a ^{10}C secondary beam is ongoing in collaboration with the experimentalists. For ^{8}C, the energies of the 0^+ ground and 2^+ excited states have been calculated using KSHELL in smaller basis spaces (from two to four major shells). No-core MCSM calculations in larger basis spaces (from five to seven major shells) on the K computer are awaited, so as to obtain the converged ground-state and excitation energies. The evaluation of the spectroscopic factor is also planned to investigate the cross section of neutron-transfer reactions in the near future. In association with this study, we also focus on the anomalously large magnetic dipole moment of the ^{9}C nucleus. For this purpose, we are now carrying out the no-core MCSM calculations for that in a relatively large basis space (up to seven major shells) on the K computer.

We proposed a new method of estimating the level density stochastically based on nuclear shell-model calculations[4]. In order to count the number of eigenvalues of the shell-model Hamiltonian matrix, we performed contour integration of a complex function, $f(z) = \langle\phi|\frac{1}{z-H}\phi\rangle$, with H being the Hamiltonian matrix. $|\phi\rangle$ is taken as a random vector to estimate the trace stochastically. The shifted Krylov subspace method enables its efficient computation. By using this method, we successfully reproduced the experimentally observed parity equilibration of the level densities of ^{58}Ni.

As an attempt to connect medium-mass neutron-rich nuclei to the nuclear force, we derived the effective interaction for the shell model starting from the nuclear force. Standard many-body perturbation theory can only be applied to a single major shell because of the divergence appearing in perturbative expansion. However, in this area of the nuclear chart, the larger model spaces of at least more than one major shell have to be considered. Then, we developed a novel revision of the many-body perturbation theory, named the Extended Kuo-Krenciglowa (EKK) method.[5] We applied the EKK method to derive the effective interaction for the valence space of the sd+pf-shell, starting from the χEFT N^{3}LO interaction. Three-nucleon force (3NF) is also added as an effective two-body force by integrating out one of the three nucleons as the hole line of the ^{16}O core. Then, we performed the shell-model calculations of even-even isotopes of Ne, Mg, and Si and succeeded in reproducing the basic properties of those nuclei, *i.e.* the binding energies, excitation energies of the first 2^+ states, E2 transition probabilities, and so on. In particular, it is well known, as the "island of inversion", that the shell gap of $N = 20$ is broken for Ne and Mg, but not for Si. We reproduced the physics of "island inversion" well and our work is the first calculation of this subject starting from the nuclear force and microscopic theories.

*1 Center for Nuclear Study, the University of Tokyo
*2 Department of Physics, the University of Tokyo
*3 Japan Atomic Energy Agency

References

1) K. Steiger *et al.*, Eur. Phys. J. A **51**, 117 (2015).
2) D. Steppenbeck *et al.*, Phys. Rev. Lett. **114**, 252501 (2015).
3) Y. Utsuno *et al.*, Phys. Rev. C **86**, 051301(R) (2012).
4) N. Shimizu *et al.*, Phys. Lett. B **753**, 13 (2016).
5) N. Tsunoda *et al.*, Phys. Rev. C **89**, 024313 (2014).

3. Nuclear Data

Measurements of secondary neutrons produced from thin Be and C by 50 MeV/u ^{238}U beam

H.S. Lee,[*1,*4] J.H. Oh,[*1,*4] N.S. Jung,[*1,*4] A. Lee,[*1,*4] L. Mokhtari Oranj,[*2] N. Nakao,[*3,*4] and Y. Uwamino[*4]

Neutron production is one of the important subjects for shielding calculation of particle accelerator facilities, such as RIBF/RIKEN. However, the number of high-energy heavy ion accelerators in the world is small. The accuracy of shielding calculations of such facilities has been studied until now. In particular, the information of neutron production is very rare if the accelerated particles are heavy ions such as uranium. The neutron production yields were measured using a 50 MeV/u ^{238}U beam of RIBF for the shielding design of the Rare Isotope Science Project (RISP) ion accelerator in Korea.

In this study, the interesting energy of the ^{238}U beam is lower than 100 MeV/u because another group had already performed a similar study using an energy of 345 MeV/u at RIBF[1]. The charge-stripper chamber was chosen as the experimental station as shown in Fig. 1. The produced neutrons were measured when the 50 MeV/u ^{238}U beam hit the thin Be stripper or C stripper target in the chamber. For this measurement, the activation analysis was applied using Bi, Co, and Al samples, which were attached on the outer surface of the stripper chamber. We chose four different emission angles of neutron productions as shown in Fig. 1. The gamma rays from activated samples were measured using an HPGe detector and analyzed using HYPEGAM[2] software. The beam intensity of ^{238}U was monitored by a phase probe (PPM04) and calibrated by the current of a Faraday cup (FCM04).

The radionuclide yields were calculated using the gamma-ray spectra and well-known reaction cross-sections of Bi, Co, and Al with high-energy neutrons. The energy distributions of the produced neutrons were calculated using the unfolding method. The SAND-II code[3] was applied.

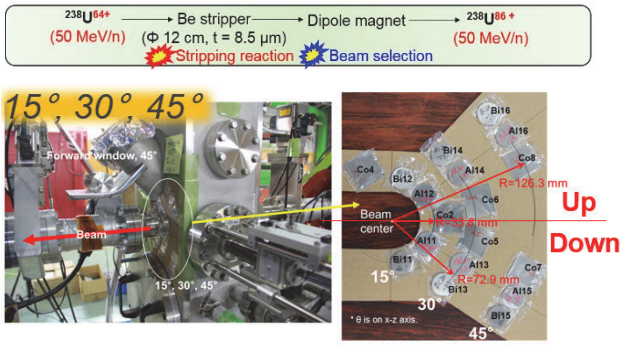

Fig. 1. Experimental setup at the charge-stripper chamber and the arrangement of activation samples in the forward direction. (Charge stripping process is described above)

*1 Pohang Accelerator Laboratory, POSTECH
*2 Division of Advanced Nuclear Engineering, POSTECH
*3 Shimizu Corporation
*4 RIKEN Nishina Center

In this study, the entire experimental process was simulated using two Monte Carlo codes, PHITS[4] and FLUKA[5]. The spatial distribution of neutron fluence, one of the important results, was calculated using PHITS as shown in Fig. 2. The radionuclide production rates[6] of Bi samples were measured for different angles, 15°, 30°, 45°, and 90° as shown in Fig. 2. The angular distribution of the production rate was regenerated in good agreement with the theoretical trend. The comparison between the measured and calculated data by the two codes showed reasonable agreements, but the PHITS results were a greater underestimation relative to the FLUKA results.

Each neutron-induced reaction of Bi, Co, and Al samples has its own threshold energy. The neutron spectra above 10 MeV were obtained from the production yields of each reaction through the unfolding process[6]. The spectra calculated using FLUKA were in a good agreement with the unfolded one for every emission angle. However, the PHITS results showed a large discrepancy. The reason for the discrepancy has been reviewed carefully. The different physics models of two codes used in this energy range has been supposed as the first candidate reason.

These experimental results are very important to compensate for the fact that no proven data exist below approximately 300 MeV/u for benchmarking ^{238}U induced neutron production. The enhanced analysis is ongoing to confirm the discrepancy between the PHITS and FLUKA results or between the calculated results and experimental data.

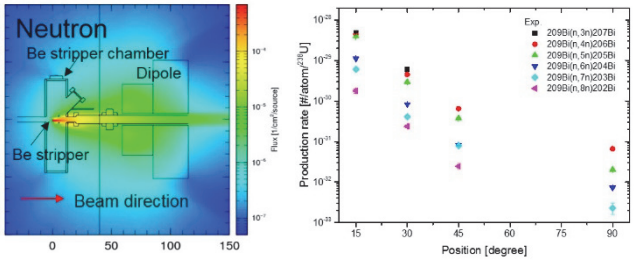

Fig. 2. Distribution of neutron fluence in the reaction area (left) and angular distribution of radionuclide yields in Bi samples (right).

References

1) N. Nakao et al.: Proc. IPAC2014, (2015) p.1811.
2) H.D. Choi et al., Nucl. Eng. Tech. **44**, 781 (2012).
3) P.J. Griffin et al.: SAND93-3957, Sandia Nat. Lab. (1994).
4) K. Nitta et al., Phys. Rev. C **52**, 2620 (1995).
5) A. Ferrari et al.: CERN-2005-10, CERN (2005).
6) J.H. Oh et al.: presented at ISORD-8, Jeju (2015).

Coulomb breakup reactions of long-lived fission products, ^{79}Se, ^{93}Zr, and ^{107}Pd

S. Takeuchi,[*1,*2] T. Nakamura,[*1,*2] M. Shikata,[*1,*2] Y. Togano,[*1,*2] Y. Kondo,[*1,*2] J. Tsubota,[*1,*2] T. Ozaki,[*1,*2] A. T. Saito,[*1,*2] A. Hirayama,[*1,*2] T. Tomai,[*1,*2] H. Otsu,[*1] H. Wang,[*1] Y. Watanabe,[*3] S. Kawase,[*3] for ImPACT Collaboration

Nuclear transmutation of long-lived fission products (LLFPs) mixed in nuclear radioactive wastes is one of the candidate techniques for the reduction and/or reuse of LLFPs, and has been investigated since several decades. High-level radioactive wastes including LLFPs have to be kept in the deep and hard rock stratum to separate them from human environments with current disposal methods owing to their large radiations and high heats. Among the LLFPs, transmutations of ^{79}Se, ^{93}Zr, ^{107}Pd, and ^{135}Cs are important owing to their long half-lives of 0.3M, 1.6M, 6.5M, and 2.3M years, respectively. These LLFPs can be transmuted to be stable or short-lived nuclei; however the reaction rates relevant to these isotopes are not sufficient for transmutation techniques.

In order to accumulate nuclear reaction data for further developments, we performed nuclear reaction experiments using LLFPs as secondary beams[1]. In particular, we focused on (γ,n) and (n,γ) reactions for LLFPs and neighboring nuclei. The neutron capture (n,γ) for LLFPs is an important reaction for transmutation; however there are several difficulties to conduct these experiments. An alternative way may be by measuring photo-absorption (γ,n) cross sections (σ_{abs}) connected to (n,γ) cross sections via the principle of detailed balance. The σ_{abs} for LLFPs can be measured indirectly by Coulomb breakup reactions with fast RI beams of LLFPs in inverse kinematics. We focused on the measurements of Coulomb breakup reactions of ^{79,80}Se, ^{93,94}Zr, and ^{107,108}Pd to obtain σ_{abs}.

The secondary beams of ^{79,80}Se, ^{93,94}Zr, and ^{107,108}Pd with an energy of 200 MeV/nucleon were produced by in-flight fission reactions of a ^{238}U primary beam with 345 MeV/nucleon on a ^{9}Be production target and identified by BigRIPS[2]. In the experiment using the ZeroDegree (ZD) spectrometer[2], we performed inclusive measurements for Coulomb breakup reactions of ^{93,94}Zr and ^{107,108}Pd. Secondary targets of Pb and C with thicknesses of 0.52 g/cm^2 and 0.32 g/cm^2, respectively, were placed at the F8 focus and surrounded by DALI2[3] to detect de-excitation γ rays. The reaction products were analyzed and identified by the ZD spectrometer with the two Bρ settings. In the first setting, the Bρ value was adjusted to set non-reacted secondary beams to be centered (0% setting), which accepted momentum distributions up to -3% corresponding to three neutron removal channels for ^{107}Pd, for example. In another setting, the Bρ value was adjusted to be -3% relative to the 0% setting with the acceptance of six neutron removal channels for ^{107}Pd. Combining these two settings, Coulomb breakup cross sections will be obtained after subtracting nuclear components estimated by breakup reactions on the C target. Figure 1 shows the mass-to-charge distribution of reaction products in the ^{107}Pd + Pb reaction obtained by the ZD spectrometer with the -3% setting. By counting the yields for each isotope, Coulomb breakup cross sections will be deduced and converted to σ_{abs}.

Exclusive measurements were also made using the SAMURAI spectrometer[4] to obtain Coulomb breakup cross sections to be converted to the relevant excitation function. The secondary beams of ^{79,80}Se and ^{93,94}Zr were bombarded on Pb and C targets with thicknesses of 0.54 g/cm^2 and 0.26 g/cm^2, respectively. Charged particles produced in breakup reactions were analyzed by the SAMURAI spectrometer and neutrons were detected by NEBULA[4] and NeuLAND[5]. DALI2 was placed at the target area to detect de-excitation γ rays to identify reaction channels.

The analyses for both experiments are currently in progress. This work was funded by ImPACT Program of Council for Science, Technology and Innovation (Cabinet Office, Government of Japan).

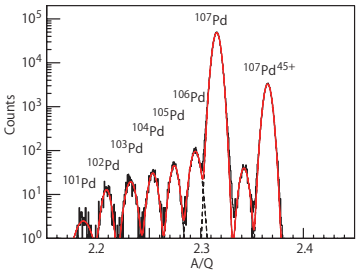

Fig. 1. Mass-to-charge ratio (A/Q) for Pd isotopes in the ^{107}Pd + Pb reaction.

References

1) H. Wang et al., S. Kawase et al.: In this report.
2) T. Kubo et al., Prog. Theor. Exp. Phys. **2012**, 3C003 (2012).
3) S.Takeuchi et al., Nucl. Instrum. Methods Phys. Res. A **763**, 596 (2014).
4) T. Kobayashi et al., Nucl. Instrum. Methods Phys. Res. B **317**, 294 (2013).
5) https://www.gsi.de/work/fairgsi/rare_isotope_beams/r3b/neuland.htm

*1 RIKEN Nishina Center
*2 Department of Physics, Tokyo Institute of Technology
*3 Faculty of Engineering and Sciences, Kyushu University

Cross section measurement of residues in proton- and deuteron-induced spallation reactions of ^{93}Zr and ^{93}Nb

S. Kawase,[*1] Y. Watanabe,[*1] K. Nakano,[*1] T. Kin,[*1] S. Araki,[*1] H. Wang,[*2] H. Otsu,[*2] H. Sakurai,[*2] S. Takeuchi,[*3] Y. Togano,[*3] T. Nakamura,[*3] Y. Maeda[*4] for ImPACT-RIBF collaboration

The long-lived fission products (LLFPs), which are produced in nuclear reactors have been an important issue because of the difficulty of their disposal owing to their remarkably long lifetimes. Therefore, a treatment method to transform the LLFPs into short-lived and/or low-toxic materials is strongly desired, and nuclear transmutation technology is one of the promising candidates for this. However, the reaction data of LLFPs required for the design of optimum pathways of the transmutation process are currently quite scarce.

We performed an experiment to measure isotopic production cross section of ^{93}Zr, which is an LLFP nuclide with a half-life of 1.61×10^6 years, using proton- and deuteron-induced spallation reactions at the RIKEN RI Beam Factory (RIBF). For the experimental setup, see Ref.[1)]

Figure 1 shows one of the plots, which was used for particle identification using the ZeroDegree spectrometer (ZDS). Each reaction residue was successfully identified with a 10σ separation of mass number A. The isotopic production cross section was obtained from the production yield for each nuclide and the number of beam particles. The transmission ratio in the ZDS was estimated from the position distribution at a dispersive focal plane F9. Then the cross sections were compared with the calculations using PHITS[2)] with the Intra-Nuclear Cascade model of Liège (INCL)[3)] and the Generalized Evaporation Model (GEM)[4)]. Figure 2 shows the preliminary results for Nb, Zr, Sr, and Kr isotopes corresponding to proton- and deuteron-injection. The calculations reproduced the experimental cross section to some extent, but they underestimate the number of evaporated neutrons and hence the resulting cross sections are distributed in an A region slightly larger than the experimental ones. Further examination of the calculation models is needed.

The analysis for the spallation reaction on ^{93}Nb, which was included in the ^{93}Zr beam setting, is underway. The cross sections of ^{93}Nb will be compared with the experimental data obtained using the activation method[5)] in order to verify the effectiveness of the method used in this experimental series.

This work was funded by the ImPACT Program of the Council for Science, Technology and Innovation (Cabinet Office, Government of Japan).

*1 Faculty of Engineering Sciences, Kyushu University
*2 RIKEN Nishina Center
*3 Graduate School of Science and Engineering, Tokyo Institute of Technology
*4 Department of Applied Physics, University of Miyazaki

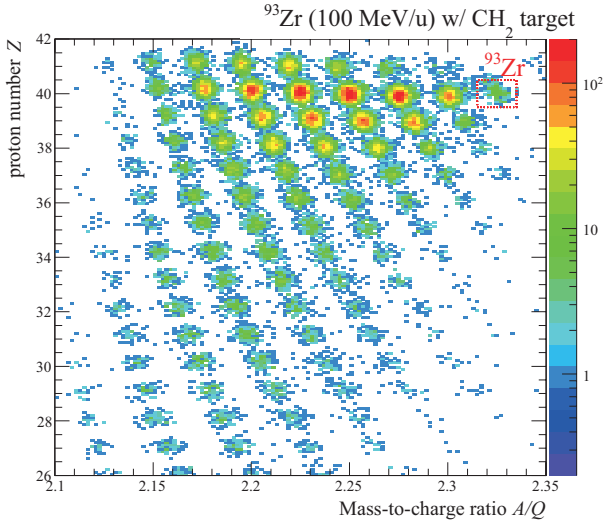

Fig. 1. Correlation of proton number Z and mass-to-charge ratio A/Q of reaction residues produced from ^{93}Zr beam at 100 MeV/u and CH_2 target.

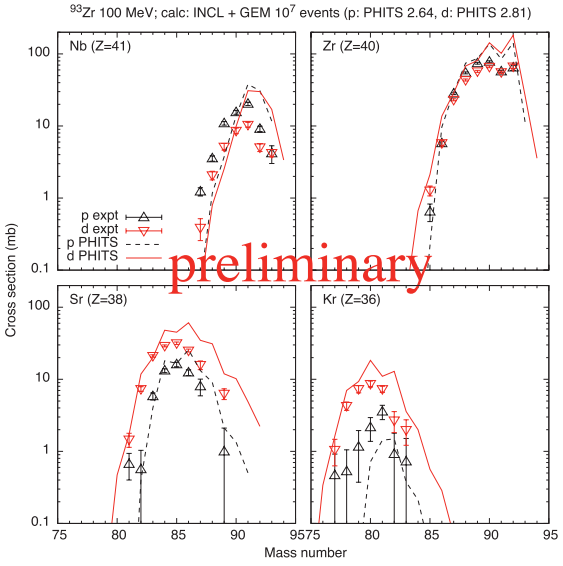

Fig. 2. Experimental and calculated cross sections for spallation reactions of ^{93}Zr at 100 MeV/u with protons and deuterons.

References

1) H. Wang *et al.*, In this report.
2) T. Sato *et al.*, J. Nucl. Sci. Technol., **50**, 913 (2013).
3) A. Boudard *et al.*, Phys. Rev. C **87**, 014606 (2013).
4) S. Furihata, Nucl. Instr. and Meth. B **171**, 251 (2000).
5) Yu. E. Titarenko, Phys. Atom. Nucl. **74**, 537 (2011).

Simulation of thick-target transmission method for interaction cross sections of ^{93}Zr on ^{12}C

M. Aikawa,[*1,*2] S. Ebata,[*1] and S. Imai[*3]

The interaction cross section provides valuable knowledge pertaining nuclear physics[1] and engineering since it is an essential quantity related to nuclear radii and the transmutation of nuclear wastes. In addition, its excitation function is also important; however, the data of radioactive isotopes are very few and insufficient because it requires huge experimental effort at each energy. Therefore, we propose the thick-target transmission (T3) method to obtain the excitation functions of the interaction cross sections[2].

The T3 method can derive the excitation function through iterative measurements of beam attenuations with different target thicknesses. Similar to the ordinary transmission method, the interaction cross section σ_I can be derived from the following equation:

$$\sigma_I = \frac{-1}{n_T \Delta L} \ln \frac{N_i(L+\Delta L)}{N_i(L)}, \quad (1)$$

where n_T, L, ΔL and $N_i(L)$ are the number density of the target, thickness of moderator, thickness of reaction target and the number of transmitted incident particles at L, respectively. In other words, $N_i(L)$ passed through the moderator part with L is used as a beam on the reaction part of the thickness ΔL. We performed a simulation with the PHITS code[3] for the interaction cross sections of ^{93}Zr on ^{12}C, which are typical examples of long-lived fission fragments and stable nuclei. The cross sections are equivalent to inclusive cross sections of ^{12}C-induced transmutation reaction on ^{93}Zr.

The parameters adopted in the simulation are set to cover the expected peak area. The energy is set to 100 MeV/nucleon, which is similar to the recent experiment[4]. The target density and thicknesses are 2.260 g/cm^3 and 0.02 cm ($0 \leq L \leq 0.2$ cm) and 0.004 cm ($0.2 \leq L \leq 0.24$ cm), respectively. The trial number is 10^5 which are consistent with an intensity of 1,000 pps and individual irradiation period of 100 s. Calculations with different target thicknesses were iteratively performed in the simulation. The beam attenuation and energy at the downstream of the target can be obtained in each calculation and are shown as a function of the target thickness in Fig. 1. The interaction cross sections thus obtained with the moderator part from Eq. (1) are shown in Fig. 2 with expected values of PHITS derived from the traditional transmission method with thin-targets and energy adjustments. The behaviors of the cross sections are in good agreement, and therefore the T3 method may be applicable in real experiments. The derived cross sections, however, have large uncertainties in the low energy region because the uncertainties are accumulated in the moderator part of the target. We continue to investigate the method in more detail to propose a new experiment and also perform additional simulations of other radioactive isotopes.

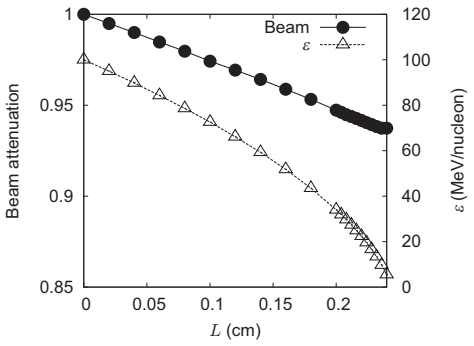

Fig. 1. The attenuation (solid circles with solid line) and energy (open triangles with dotted-line) of the incident beam are shown as a function of the target thickness.

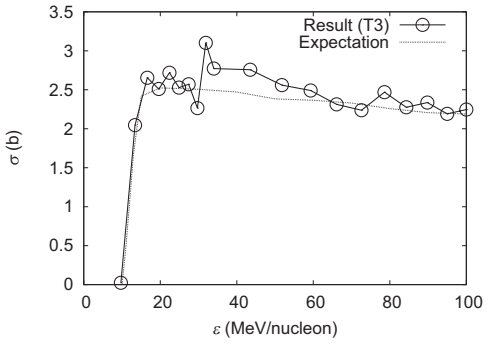

Fig. 2. Interaction cross sections of ^{93}Zr on ^{12}C. The results of the simulation (open circles with solid line) are shown with the expected values in PHITS (dotted-line).

This work was funded by ImPACT Program of Council for Science, Technology and Innovation (Cabinet Office, Government of Japan).

References

1) I. Tanihata et al., Phys. Rev. Lett. **55**, 2676 (1985).
2) M. Aikawa et al., under submission.
3) T. Sato et al., J. Nucl. Sci. Technol. **50**, 913 (2013).
4) H. Wang et al., In this report.

*1 Faculty of Science, Hokkaido University
*2 RIKEN Nishina Center
*3 Institute for the Advancement of Higher Education, Hokkaido University

Nuclear data study for the development of transmutation technology

S. Ebata,[*1] M. Aikawa,[*1] and S. Imai[*2]

Nuclear transmutation is a promising technology for the disposal of nuclear waste with high-level radioactivity. High-level radioactive waste includes the minor actinides (MA), with $Z > 89$, and long-lived fission products (LLFP). For the reduction of MA, the accelerator-driven system (ADS) has been studied globally, e.g. J-PARC[1] plans to establish an ADS test facility. However, an effective procedure to reduce LLFP has not been found yet. A major hurdle to development is the lack of reaction data for LLFP, especially for reactions induced by a charged particle. The demands for this data is high, although experiments with a LLFP target have difficulties related to the high radioactivity and chemical instability.

Recent progress at the radioisotope beam facility allows us to utilize LLFP nuclei as the beam. Experiments for the LLFP reaction data with inverse kinematics are performed.[2] Activities of our data centre for the transmutation study are to accumulate related data, to distribute them to the public, and to estimate the physical quantities, through the followings:

- Developing a new data format
- Thick-target yield (TTY) for the transmutation
- Excitation function of the interaction cross section

The new data format is represented in XML which is both human- and machine-readable.[3] We are confirming its availabilities to store and to search data, including previous one. The labelling of data is key for an effective data format. Figure 1 shows the format under development. The outline of the format is almost

Fig. 1. The parts of data labelled in the Bibliography.

completed, although there are practical problems, e.g. the expression of the reaction formula for inverse kinematics. The detailed rules will be determined in the near future.

*1 Faculty of Science, Hokkaido University
*2 Institute for the Advancement of Higher Education, Hokkaido University

The TTY strongly depends on the matter properties, but might be useful data for nuclear engineering, although the cross section is the most fundamental information. To avoid an experiment with the radioactive target directly, we have suggested a conversion method between the TTYs of the original reaction system and the inverse kinematics system.[4] The method is based on the common cross section between these systems and the energy dissipations of the projectile which can be described by the stopping power due to the target matter properties. The conversion coefficient depends on the incident energy of the projectile, but we found that it can be replaced by a constant value in a high energy region. The method is applied to more specific systems considering the kinds of projectile and energy, using the PHITS[5] simulation.

The excitation function of the cross section has significance for nuclear structure (e.g. radius) and for the quantity reflected with matter properties (e.g. TTY). To measure the excitation function, we propose a simple method, which is the thick-target transmission (T3) method.[6] The basic concept of the method is the extension of the ordinary transmission method to that with a thick target. In the T3 method, the target has also the role of beam moderator and its thickness corresponds to the energy of the incident particle. While adding a thin target Δx to the target, we count the number $I(x)$ of projectile passed through the target at each thickness x, and can calculate the interaction cross section, $\sigma_{\mathrm{Int.}}(x)$, from the beam attenuation;

$$\sigma_{\mathrm{Int.}}(x) \propto -\frac{1}{\Delta x}\ln\frac{I(x+\Delta x)}{I(x)}. \quad (1)$$

If the LLFP beams can be chosen in the T3 method, the $\sigma_{\mathrm{Int.}}(x)$ corresponds to the cross section of transmutation. The availability of the T3 method might be decided from the competition between efforts to change the thickness and beam energy.

We report the activities for the nuclear data study of transmutation, and will carry out them with the cooperation among nuclear data, theorists and experimentalists.

This work was funded by ImPACT Program of Council for Science, Technology and Innovation (Cabinet Office, Government of Japan).

References

1) http://j-parc.jp/Transmutation/en/index.html
2) H. Wang et al., Phys. Lett. B**754**, 104 (2016).
3) M. Aikawa et al., RIKEN Accel. Prog. Rep. **47**, 70 (2014).
4) S. Imai et al., RIKEN Accel. Prog. Rep. **48**, 98 (2015).
5) T. Sato et al., J. Nucl. Sci. Technol **50**, 913 (2013).
6) M. Aikawa et al., In this report.

Compilation of nuclear reaction data from the RIBF in 2015

D. Ichinkhorloo,[*1] M. Aikawa,[*1,*2] S. Ebata,[*1] S. Imai,[*3] N. Otuka,[*2,*4] A. Sarsembayeva,[*1] and B. Zhou[*1]

Nuclear data such as the data of cross sections, radiations emitted from radioactive isotopes, level properties of isotopes are used widely in many fields. Nuclear data play a key role in understanding the nature of nuclear structures and nuclear reactions. On the other hand, as the fundamental input to various codes for nuclear applications, they are also very important in medical radiotherapy, shielding and radiation protection, and some related engineering works. Therefore, it is of great significance to build a nuclear database for providing nuclear data service in various fields.

EXFOR[1)] is the name of the data library containing experimental nuclear reaction data. The EXFOR library contains numerical data, bibliographic information, and experimental information including sources of uncertainties. On the contrary, such data and information can be retrieved from the database by nuclear data users. Additional information, such as experimental setups, is also available.

Experimental data are found in the EXFOR database, which is maintained by the International Atomic Energy Agency (IAEA)[2)] and the International Network of Nuclear Reaction Data Centres (NRDC). The NRDC collaborates for database compilation and related software development. One of the NRDC members is the Hokkaido University Nuclear Reaction Data Centre (JCPRG)[3)]. JCPRG has contributed to about 10 percent of the data on charged-particle nuclear reactions in the EXFOR library. In the JCPRG, compiled nuclear reaction data in the NRDF (Nulear Reaction Data File) and EXFOR formats are available through the online search system of the NRDF and EXFOR libraries[1)], respectively.

Under collaboration with the NRDC network, experimental data published in scientific journals are continuously surveyed. Among the data obtained, the charged-particle and photon induced data obtained from the facilities in Japan should be compiled by JCPRG. The compiled files of nuclear data produced at the RIBF are translated into the EXFOR format for the benefit of nuclear data users. In this article, we report on our activities in 2015, especially the compilation of experimental nuclear reaction data from the RIBF.

In 2015, we compiled 29 new papers reporting on experiments performed in Japan. Among them, 11 papers were from the RIBF data and satisfied the compilation scope of the EXFOR library. All data are accessible by the entry numbers listed in Table 1. For higher quality of contents, the corresponding authors were requested to provide numerical data of the compiled papers. Most of the compiled RIBF data in 2015 are provided by the authors. Such additional information is also available with a list of compiled RIBF data on the JCPRG website.

Table 1. Entry numbers with references compiled from the RIBF data in 2015

Entries	E2461[4)]	E2462[5)]	E2463[6)]
	E2465[7)]	E2466[8)]	E2467[9)]
	E2468[10)]	E2471[11)]	E2473[12)]
	E2474[13)]	E2482[14)]	
Total		11	

We established an effective procedure to compile all of the new publications during the last five-year collaboration with the RIKEN Nishina Center. Therefore, most of recent experimental nuclear reaction data from the RIBF have successfully been compiled in the EXFOR library. It is recommended that such collaboration should be further developed for experiments at the RIBF. By using these compilations, experiment data from the RIBF can also be served in a more convenient and fast manner for nuclear research and studies in other fields.

References

1) http://www.jcprg.org/exfor/
2) http://www-nds.iaea.org/
3) http://www.jcprg.org/
4) J. Hu et al., Phys. Rev. C **90**, 025803 (2014).
5) M. U. Khandaker, et al., Nucl. Data Sheets **119**, 252 (2014).
6) H. S. Jung et al., Phys. Rev. C **90**, 035805 (2014).
7) N. Sato et al., Radiochim. Acta **102**, 211 (2014).
8) M. Murakami et al., Appl. Radiat. Isot. **90**, 149 (2014).
9) M. U. Khandaker et al., J. Radioanal. Nucl. Chem. **302**, 759 (2014).
10) K. Tshoo et al., Phys. Lett. B **739**, 19 (2014).
11) M. Takechi, et al., Phys. Rev. C **90**, 061305(R) (2014).
12) M. U. Khandaker et al., Nucl. Instrum. Methods Phys. Res., Sect. B **346**, 8 (2015).
13) T. Moriguchi et al., Nucl. Phys. A **929**, 83 (2014).
14) Zs. Vajta et al., Phys. Rev. C **91**, 064315 (2015).

*1 Faculty of Science, Hokkaido University
*2 RIKEN Nishina Center
*3 Institute for the Advancement of Higher Education, Hokkaido University
*4 NDS, IAEA

New EXFOR editor: a review of recent developments

A. Sarsembayeva,[*1] S. Imai,[*2] S. Ebata,[*1] M. Chiba,[*3] N. Otuka,[*4,*5] and M. Aikawa[*1,*5]

EXFOR[1] is an experimental nuclear reaction data library maintained by the IAEA on behalf of the International Network of Nuclear Reaction Data Centres (NRDC)[2]. It is accessible publically and is widely used in fields of scientific research such as nuclear physics, design and operation of nuclear power plants, medical isotopes, and radiotherapy. Currently, 14 data centers of the NRDC are present worldwide, and they collaborate mainly for collection, dissemination, compilation, and exchange of experimental data using the EXFOR format. The Hokkaido University Nuclear Reaction Data Centre (JCPRG, formerly Japan Charged-Particle Nuclear Reaction Data Group) became a member of the NRDC Network in the early 1980s[3]. JCPRG compiles and accumulates charged particle nuclear reaction data produced in accelerator-based facilities in Japan. A web-based Hyper Editor for Nuclear Data Exchange Libraries (HENDEL) was adopted to compile experimental nuclear reaction data in Nuclear Reaction Data File (NRDF) and EXFOR formats[4]. In an EXFOR compilation workshop (6-10 Oct. 2014, Vienna), EXFOR compilers emphasized that it is important to develop an OS independent EXFOR editor system[5]. In order to establish an OS independent EXFOR editor system, Java was selected as a programming language. A stand-alone type application for compiling experimental nuclear reaction data For EXFOR (ForEX) is being developed.

When we started the development of the program, our goal was to develop a fast, light, and user-friendly editor to compile nuclear reaction data with maximum flexibility. To achieve user-friendliness, we implemented the following functions: 1) collapsible/expandable items, 2) add/remove buttons, 3)a filterable suggestion field, 4) text filtering for a table, and 5) a dynamic suggestion field. In addition to the new functions, some external tools such as DANLO and CHEX can be executed in ForEX. DANLO is a tool to extract a dictionary of codes in EXFOR and is utilized for ForEX. CHEX is a checking program for the EXFOR format.

(1) Collapsible/expandable item
Many types of information and data are required as input for each keyword. For instance, the reaction information consists of information about the projectile, target, emitted particles, and so on. However, while inputting other data, it is unnecessary to view the reaction information. Therefore, the collapsible/expandable function is implemented for each item.

(2) Add/remove buttons
Similar to the concept of collapsible/expandable items, the number of input areas must be minimum at first. These areas can be added/removed interactively by buttons.

(3) Filterable suggestion field
Since there are several codes for some keywords, compilers often find it very difficult to select the correct code. Therefore, filterable suggestion fields were implemented to allow compilers to save time and avoid mistakes.

(4) Text filtering for a table
Similar to the concept of filterable suggestion fields, codes can be suggested by a keyword input. In particular, there are several codes related to reactions that are similar; therefore, with text filtering, an appropriate list of reaction codes can be obtained easily.

(5) Dynamic suggestion field
The purpose of a dynamic suggestion fields is to make data input easier and more reliable. For example, the compiler chooses an input from one list, which restricts the related contents of another list. The dynamic suggestion field presents two suggestion fields working in conjunction with one another, prompting end users with only relevant data.

A new EXFOR editor system, ForEX, is being developed in Java as a stand-alone application. ForEX can provide an environment for compiling numerical data with its bibliographic and experimental information in the EXFOR format. The input part of the program has been developed and tested on Linux and Windows platforms; however the output and import functions of the program are still under development. Testing on the Mac OS is in progress.

*1 Faculty of Science, Hokkaido University
*2 Institute for the Advancement of Higher Education, Hokkaido University
*3 Sapporo-Gakuin University
*4 Nuclear Data Section, International Atomic Energy Agency
*5 RIKEN Nishina Center

References

1) EXchange FORmat, `https://www-nds.iaea.org/exfor/exfor.htm`, 2016/03/03.
2) N. Otuka (ed.), Report INDC(NDS)-0401 Rev.6, IAEA (2014).
3) Nuclear Reaction Data Centre, `http://www.jcprg.org/`, 2016/03/03.
4) Web-based Editor for Nuclear Data, `http://www.jcprg.org/hendel/`, 2016/03/03.
5) V. Semkova, B. Pritychenko (eds.), Report INDC(NDS)-0672, IAEA (2015).

4. Hadron Physics

Determination of the detector acceptance correction for the PHENIX $W \to \mu$ analysis

S. Park*1 for the PHENIX collaboration

The cross section and single spin asymmetry of parity violating W production in longitudinally polarized proton collisions have been studied at the Relativistic Heavy Ion Collider as an important probe for sea quark polarization in the proton. At PHENIX, W bosons can be measured via their decays into electrons at midrapidities ($|\eta| < 0.35$) and muons at forward/backward rapidities ($1.2 < |\eta| < 2.4$). Since the preliminary result of the $W \to \mu$ channel was obtained with the high statistics data sample of 2013[1], analysis progress has been made towards the publication. One important component is to get the final acceptance correction of the forward muon spectrometer that is applied on the measured W candidates to calculate the total cross section. The total cross section of $W \to l\nu$ in proton-proton collisions can be written as:

$$\sigma(pp \to W^{+(-)}X) \times BR(W^{+(-)} \to l^{+(-)}\nu) = \frac{1}{\mathcal{L}} \frac{(N_{obs} - N_{bg})(1 - f_Z)}{< A \cdot \epsilon >} \quad (1)$$

where $\mathcal{L}$ is total integrated luminosity, $N_{obs(bg)}$ is the number of observed signal (background) events, $A \cdot \epsilon$ is the acceptance and total efficiency correction, and f_Z is the fraction of leptonic decays of Z bosons in the signal.

In order to determine the detector acceptance, Monte-Carlo (MC) simulation samples were produced using the PYTHIA event generator and the PHENIX detector simulation packages based on GEANT3. The MC samples were passed through the same analysis software as the real data. Realistic detector responses such as data driven detector hit efficiency, gain and pedestal calibrations, dead HV modules and readout channels under different beam and detector condition are considered. Figure 1a shows an example of azimuthal distributions of single muon candidates in the north side of the detector for a representative data sample and MC sample.

In this study, we also found that the detector performance varied throughout the data taking periods. This is mainly caused by instability of the readout channels and the number of enabled HV modules of the PHENIX Muon Tracking Chambers[2]. The number of inactive readout channels and disabled HV modules were scanned for different data taking period in 2013, and we found variations especially in readout channels. The possible causes of the variation in readout channels are problems in gain and pedestal calibrations or detector malfuctions while the HV module status changes typically when the background rate is high. When an output current of a module exceeds a set current, the HV channel in the module becomes disabled to protect the detector. Therefore, we introduced azimuthal angle dependent correction factors between data and MC to include this fluctuation in the simulation. Figure 1b shows the averaged data distribution along with the MC plot for the representative data sample. The averaged data distribution is obtained by summing the entire 2013 data set with a weight of luminosity for different data taking periods. Then, the ratio between the averaged data and MC is taken as the correction factor for each bin. Using the correction factors, $A \cdot \epsilon$ is being estimated including the trigger, reconstruction and analysis cut efficiencies. Currently, the estimation of systematic uncertainty for $A \cdot \epsilon$ is also ongoing and will be finalized in the immediate future.

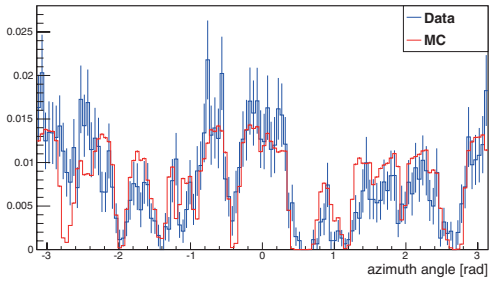

(a)

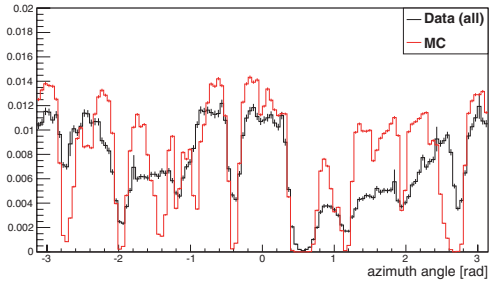

(b)

Fig. 1. (a) Azimuthal distributions of a representative data sample (blue) and MC (red). Each bin covers about 0.05 rad. (b) Azimuthal distributions of averaged data (black) and the same MC plot (red) as in (a).

*1 RIKEN Nishina Center

References
1) R. Seidl: RIKEN Accel. Prog. Rep. **48**, 104 (2014).
2) H. Akikawa et al.: Nucl. Instr. and Meth. A 499, 537 (2003).

Overall trigger efficiency estimation for W analysis at PHENIX

C. Kim,[*1,*2] I. Nakagawa,[*2] S. Park,[2] and R. Seidl [*2] for the PHENIX collaboration

The large uncertainty of flavor-separated spin contributions of anti-quarks to the spin 1/2 can be constrained using W analysis at PHENIX. The observable is a single longitudinal spin asymmetry (A_L), originating from parity-violating W production calculated by collecting single muons from W bosons. The muons were collected via multiple muon sensitive Global Level 1 (GL1) triggers from 2011 to 2013 during data recording periods. Owing to the heavy Monte-Carlo simulation dependence and necessity of precise W cross-section measurement, precise estimation of the trigger efficiency is essential.

However, there are a few difficulties to overcome in actual trigger efficiency estimation.

First, owing to the use of multiple triggers (e.g., 13 for 2013 data), more than 1 trigger can be fired in a given muon event. Though the probabilty of multiple triggers fired for an event drops following a Poisson distribution, it is important to know the number of fired triggers as well as their combination. Therefore, we investigated all possible trigger combinations and yields in the data, and then obtained a list of highly contributing combinations. By measuring these combinations' relative fraction in the data and their efficiency, the overall efficiency of all muon triggers in the data can be estimated. The top plot in Fig. 1 shows a fraction of 77 trigger combinations in the final data. Note that each trigger combination's fraction was measured in a certain pseudorapidity (η) window to take into account its η dependence.

Second, there exists a linear correlation between the trigger efficiency and the W signal likelihood ($Wness$). The $Wness$ is a key parameter of the analysis; it is a probability that indicates how close an event is to the W signal. The higher the $Wness$ ($\rightarrow 1$), more likely the event is the W signal. In this analysis, only a very small fraction of the data with a high $Wness$ (≥ 0.92) is used as the final candidates for the evaluation and we need to know the average trigger efficiency of the fraction. It is appropriate to measure the trigger efficiency with these candidates however, owing to the scarcity of high-$Wness$ candidates, statistical uncertainty dominates if we directly measure the efficiency with these candidates only. Therefore, we separate the data into a few $Wness$ windows (e.g., $0.1 < Wness < 0.2$), estimate each efficiency separately, and then extrapolate the efficiency from low $Wness$ to high $Wness$ for the average efficiency in the high-$Wness$ region. The bottom plot of Fig. 1 shows each trigger combination's extrapolated efficiency in the high-$Wness$ region.

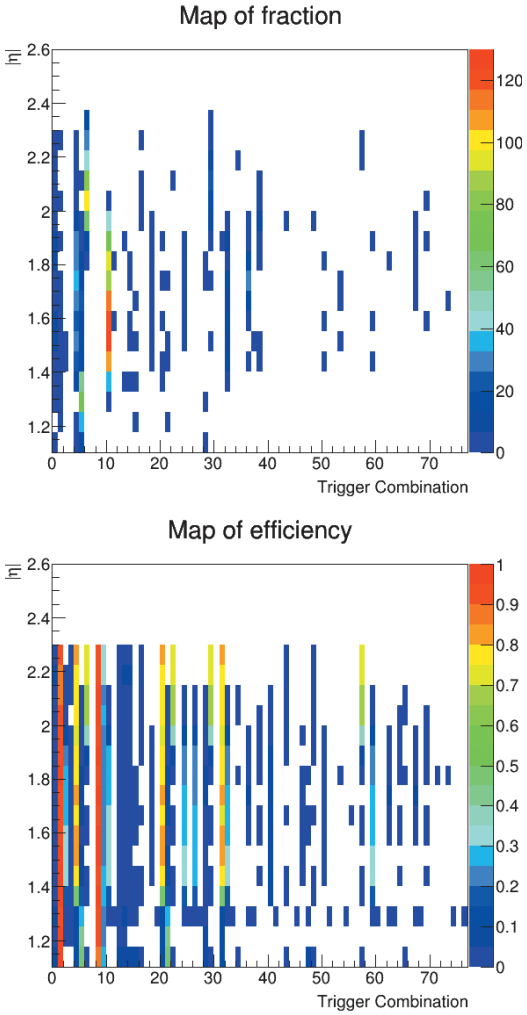

Fig. 1. Map of specific trigger combination fractions in the data (top) and their efficiency (bottom).

The combination of triggers, their relative fractions, and extrapolated efficiencies are currently being cross-checked using multiple analyzers to obtain the final asymmetry result.

[*1] Department of Physics, Korea University
[*2] RIKEN Nishina Center

Status of longitudinal double helicity asymmetries (A_{LL}) in $\pi^{\pm}$ productions in $\sqrt{s} = 510$ GeV polarized $p + p$ collisions in RHIC-PHENIX experiment

T. Moon[*1,*2] for the PHENIX collaboration

The spin of the proton is 1/2 which is explained by the angular momentum sum rule in terms of quark and gluon components. Results of EMC experiments and others suggested that the quarks and anti-quarks contribute to only about 30% of the proton spin. Gluons and the orbital angular momentum of quarks and gluons probably account for the rest of the proton spin. Spin analysis using $\pi^{\pm}$ production is particularly interesting in investigating the contribution of the gluons to the proton spin.

The Relativistic Heavy Ion Collider (RHIC) is a unique facility providing longitudinally polarized $p+p$ collisions. It enables us to expore the role of gluons in the intrinsic properties of the proton.

In perturbative Quantum Chromodynamics, pion production is sensitive to the gluon helicity distributions (Δg) in the proton because their production is dominated by gluon-related interactions (q-g and g-g scatterings) in the p_T region probed in PHENIX, 4.8 GeV/c $< p_T <$ 16.5 GeV/c. The gluon helicity distribution (Δg) can be constrained by measuring the double helicity asymmetries (A_{LL}) in π^0 and $\pi^{\pm}$ production in longitudinally polarized $p+p$ collisions. The asymmetry is defined as

$$A_{LL}(p_T) = \frac{\sigma_{++} - \sigma_{+-}}{\sigma_{++} + \sigma_{+-}} \quad (1)$$

where, $\sigma_{++(+-)}$ denotes the $\pi^{\pm}$ cross section from a collision with the same (opposite) helicity.

Yet, unlike the π^0 which can be triggered via photons in an Electro-Magnetic Calorimeter (EMCal) and Ring Imaging Cerenkov Detector (RICH), no dedicated charged hadron trigger exists and thus the $\pi^{\pm}$ statistics are less than for π^0.

However, $\pi^{\pm}$ analysis at mid-rapidity has the advantage of confirming the sign of gluon polarization (ΔG) in the proton simply by ordering the longitudinal double helicity asymmetries (A_{LL}) of the pion charges.

The result of $\pi^{\pm}$ analysis with data taken at $\sqrt{s} =$ 200 GeV has already been published in 2009[1]. In 2013, PHENIX recorded a total integrated luminosity of 145 pb^{-1} at $\sqrt{s} = 510$ GeV within a 30 cm vertex region which is 10 times higher than the previous one. The figure of merit ($\int L P_B^2 P_Y^2 dt$) considering beam polarization (P_B and P_Y) was also higher. Therefore, the result of the ongoing analysis is expected to help determine the sign of the gluon polarization (ΔG) with a higher precision.

*1 RIKEN Nishina Center
*2 Department of Physics, Yonsei University

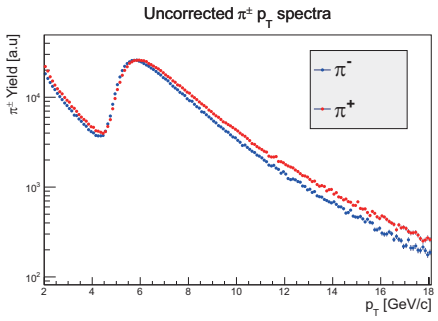

Fig. 1. p_T spectra of $\pi^{\pm}$

Charged particles including $\pi^{\pm}$ are reconstructed using the drift chamber (DC), pad chambers (PC) covering the pseudo-rapidity range $|\eta| < 0.35$, and azimuthal angle $\Delta\phi = \pi$. When a charged particle passes through a di-electric medium, CO_2 gas in the RICH, at a speed faster than the phase velocity of light in the medium, it emits the Cerenkov light which then fires the array of photomultiplier tubes (PMT). In the momentum region of interest, only $e^{\pm}$ and $\pi^{\pm}$ emit light and can thus be preselected by RICH activity. $e^{\pm}$ deposits most of its energy in the EM showers. On the other hand $\pi^{\pm}$ on average deposits only a third of their energy in the EMCal. Therefore, $\pi^{\pm}$ is separated from other particles using the RICH and the EMCal. In addition to the cuts mentioned above, the acceptance cut and the track matching with hit on the EMCal and PCs were required. Fig.1 shows $\pi^{\pm}$ p_T spectra after applying the cuts. A turn on curve is cleary observed at a p_T of 4.8 GeV/c because $\pi^{\pm}$ survives from the cut requirement. However, some background may remain, as mentioned.

(1) conversion electron reconstructed with wrong p_T
(2) $\pi^{\pm}$ originating from hadronic decay

In the PHENIX tracking algorithm, the tracks are not propagated to the decay vertex but to the event vertex. So the tracks for types (1) and (2) may not be reconstructed correctly and cuts are carefully being applied to the tracks at present. After the cut optimization, both the cross section and A_{LL} will be measured.

In summary, $\pi^{\pm}$ analysis was started at $\sqrt{s} = 510$ GeV. With more statistical data, a more precise measurement of A_{LL} in $\pi^{\pm}$ production is expected.

Reference

1) A. Adare et al. (PHENIX Collaboration), Phys. Rev. D 91, 032001 (2015).

Quality assurance of PHENIX spin database for Run 15 at RHIC

S. Karthas,[*1] I. Nakagawa,[*2] and A. Deshpande[*1]

The PHENIX collaboration at Brookhaven National Laboratory takes advantage of the spin-polarized proton beam at RHIC in order to perform spin dependent analyses. All spin relevant information are stored in a spin database accessible to the collaboration. All the information were obtained over the 10.9 weeks of proton-proton collisions, 5.1 weeks of proton-Gold collisions, and 1.9 weeks of proton-Aluminum collisions at RHIC in 2015.

Due to some glitch of the accelerator control system, there are some occasions when incorrect or null information are recorded in the database. The following is a review and status of the quality assurance (QA) analysis of the database of all physics runs taken in Run 15. This QA was necessary to ensure sufficient accuracy of the data available to the collaboration in this database for data analyses.

The first step of the QA was to check if any of the physics runs were missing from the database. In the first pass over the database there were a total of 24 missing runs. The reasons for missing runs included the following: PHENIX magnet trips midway while collecting data, unsuccessful crossing shift calibrations, and issues with the data acquisition system. Of these 24 missing runs, two have been recovered and likely 13 will be recoverable since these runs were not included as a result of an unsuccessful calibration. Those remaining, for which there was a magnet trip, will not be used for physics analyses.

Next, it was necessary to check that each run was assigned to the proper RHIC fill number so the spin patterns and polarizations for each run could be cross-checked with the polarimetry group. The initial fill time is provided by the Collider Accelerator Department (CAD) as the time of beam injection and the PHENIX data acquisition system recorded the begin and end run times. In order to verify that a run was assigned the proper RHIC fill number, it was checked that the begin run time was after its associated begin fill time and before the begin fill time for the next fill. This method proved that all physics runs were originally assigned to the proper RHIC fill number.

The spin patterns and crossing shifts in the spin database were checked for consistency across all runs in each fill. The spin pattern is a record of the spin direction for each bunch of protons in the collider for a given fill. The crossing shift is a PHENIX specific quantity that defines the shift in the bunch number from the zeroth bunch along the bunch train. This was necessary because within a fill the crossing shift or spin pattern should not change, but in the spin database this occurred occasionally. The spin patterns were also checked for consistency with the CAD database. For inconsistencies in the crossing shift throughout a fill, the Global Level 1 scalars were assessed to indicate the reason for the anomaly. These scalars are scaled down numbers of triggered events, which indicate the presence of unfilled bunches for this QA. If no reason was found and the bunch crossings were normal, the anomalous run(s)'s crossing shift was changed to the crossing shift of all other runs in that fill. In addition, there were some fills that indicated an abnormal crossing shift and were addressed on a fill-by-fill basis. There were 7 fills for which one or more crossing shifts were inconsistent and 5 of those have been resolved. The remaining fills are still under investigation. Two fills had inconsistent spin patterns with CAD. These were corrected on a run-by-run basis.

The polarization of the beam is the percentage of each proton bunch that is spin polarized in the designated spin direction. It is known that the polarization gradually decays while the polarized beam is stored in the ring for 6 to 7 h. While several physics runs are taken during this period, assigning a simple average polarization of the fill to each run is not necessarily representative of the actual polarization of the run. We introduce 'dynamic polarization' to reflect the polarization decay for later runs in the fill by solving the following formula:

$$P_{dyn} = P_{init} + P_{slope} * (brt - bft) \quad (1)$$

where P_{dyn} is the dynamic polarization, P_{init} is the initial fill polarization, P_{slope} is the slope of the fill polarization provided by the polarimetry group, bft is the begin fill time, and brt is the begin run time. The uncertainty for the dynamic polarization was calculated by simple error propagation.

$$\Delta P_{dyn} = \sqrt{(\Delta P_{init})^2 + (\Delta P_{slope} * (brt - bft))^2} \quad (2)$$

The dynamic polarizations will be re-calculated once the final polarization values are released after thorough offline analysis is carried out by the polarimeter group.

*1 Department of Physics and Astronomy, State University of New York at Stony Brook
*2 RIKEN Nishina Center

Gain calibration of the PHENIX Shower Max Detector (SMD)

J. Yoo,[*1,*2] I. Nakagama,[*1] M. Kim[*1,*3]

In order to measure the energies and positions of very forward neutrons after proton-proton and heavy ion collision, Zero Degree Calorimeters (ZDCs) and Shower Max Detector (SMD) are located ±1800 cm away from the collision point.[1)] The SMD is composed of 7 vertical and 8 horizontal plastic scintillator stripes. The SMD measures the shower profile of high energy neutrons come from interaction point. The incident neutron position is reconstructed using following equation[1)]:

$$\text{Position} = \frac{\sum_{i=1}^{\#\text{hit SMD}} (\text{smd energy})_i \times (\text{smd position})_i}{\sum_i (\text{smd energy})_i}$$

where sum runs for number of hit SMD strips that have signals above the threshold and 'smd energy' is the observed energy in a given SMD strip, and 'smd position' is the center position of the corresponding strip. As the reconstructed position of an incident neutron is weighted by the energy deposit in the SMD strips, the gain of each strip should be matched in order to reconstruct the neutron position correctly.

The gain matching result for horizontal SMD strips is discussed in this report. Gain matching was carried out using a ^{60}Co source. ^{60}Co emits gamma-rays with decay energies of 1.173 or 1.332 MeV. The source rate was of a similar order of to that of the cosmic ray rates; thus, the cosmic backgrounds are subtracted from the ADC spectra in order to extract the ADC distribution from the source.

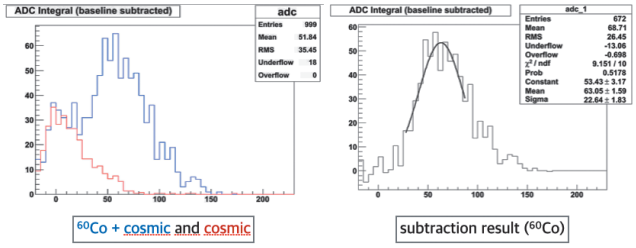

Fig. 1. Distributions of ADC data from ^{60}Co with cosmic rays (left) and ^{60}Co (right).

Figure 1 (left panel) shows the raw ADC spectra with/without a source. The right panel shows the extracted spectrum after the cosmic background subtraction. In order to quantify the gain, we attempted Gaussian fitting of the ADC peak. The model dependence of the fitting function was evaluated using different functions (Landau, and Landau + Gaussian).

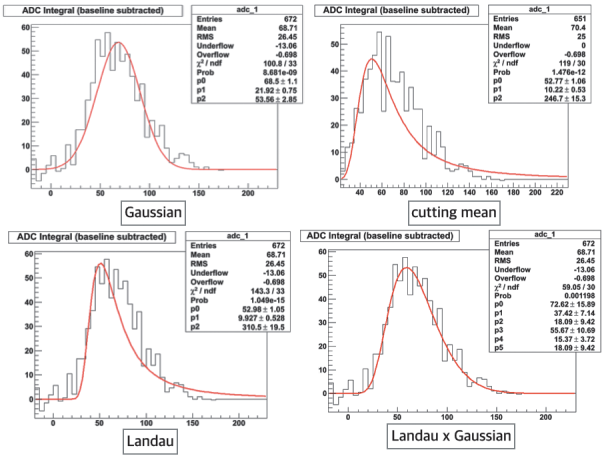

Fig. 2. Fitting results according to methods of mean calculation at detector 1.

Figure 2 shows four kinds of fitting for the same data. The 'cutting mean' excludes the low ADC region to minimize the effect of low statistics. The mean value estimated from the Gaussian fit gives the central value of the gain and the variation of different fits gives the systematic error.

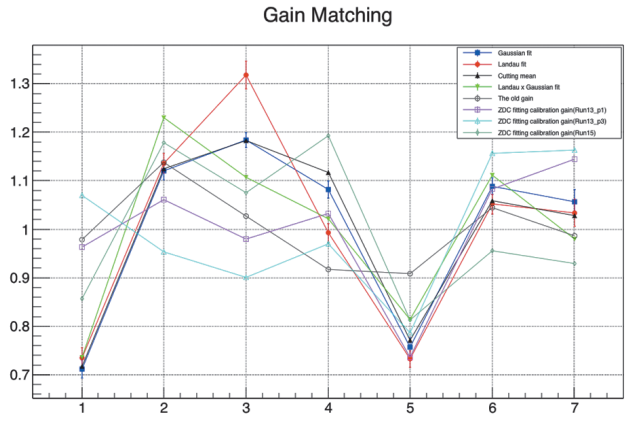

Fig. 3. Relative SMD gain according to calibration method.

The gain values obtained from different fits as well as the ones used for past analyses are plotted in Fig. 3. The resulting gain will then be determined by reconstructing the position distribution using real data.

*1 RIKEN Nishina Center
*2 Department of Physics, Korea University
*3 Department of Physics and Astronomy, Seoul National University

Reference

1) M. Kim, PHENIX analysis note 1246.

Measurement of transverse single spin asymmetry for J/ψ production in polarized p+p and p+Au collisions at PHENIX

C. Xu,[*1] H. Yu,[*1] and X. Wang[*1,*2]

Large transverse single-spin asymmetries (TSSAs) were first observed in 1976 at large x_F in pion production from transversely polarized proton-proton collisions at $\sqrt{s} = 4.9$ GeV, and they were subsequently observed in hadronic collisions over a range of energies extending up to $\sqrt{s} = 200$ GeV at RHIC energy. In order to describe large TSSAs, two approaches have been developed since the 1990s. One approach requires higher-twist contributions in the collinear factorization scheme and the other approach utilizes parton distribution functions and/or fragmentation functions that are unintegrated in the partonic transverse momentum, k_T. These functions are generally known as transverse-momentum-dependent distributions (TMDs). These two approaches have different but overlapping kinematic regimes of applicability, and they have been shown to correspond exactly in their region of overlap[1].

Heavy-flavor production mainly come results from gluon-gluon interaction at RHIC energy. J/ψ production has been extensively studied over the last decades, but the details of the production mechanism remain an open question. The measurement of heavy-flavor TSSA can serve to isolate gluon dynamics within the nucleon. It was proposed in 2008 by Yuan[2] that within the framework of non-relativistic QCD (NRQCD), the TSSA of J/ψ production can be sensitive to the J/ψ production mechanism. It should be noted that the relationship between the TSSA and the production mechanism is not quite as simple in the collinear higher-twist approach.

The J/ψ production have been measured by the PHENIX muon spectrometers at forward and backward rapidities ($1.2 < |\eta| < 2.4$), where two muons enter the same arm. TSSA for the $J/\psi \to \mu^+\mu^-$ decay channel were determined by subtracting a background asymmetry from the inclusive signal as

$$A_N^{J/\psi} = \frac{A_N^{Incl} - r \cdot A_N^{BG}}{1 - r}, \quad r = \frac{N_{Incl} - N_{J/\psi}}{N_{Incl}} \qquad (1)$$

The first measurement of TSSAs in J/ψ production was published in 2010. The data were taken by the PHENIX during the 2006 and 2008 polarized proton runs at $\sqrt{s} = 200$ GeV; the integrated luminositis are 1.8 pb^{-1} and 4.5 pb^{-1}, and the averaged polarizations are 53% and 45% respectively. The p_T and x_F dependencies are studied, for rapidity regions of $-2.2 < y < -1.2$, $|y| < 0.35$. and $1.2 < y < 2.2$, and for p_T up to 6 GeV/c[3]. The results are statistically limited and they are consistent with zero. During 2015 RHIC run, PHENIX recorded 50 pb^{-1} polarized p+p collisions with a much higher average polarization of 60%. We expect that the statistical errors of the measurement will be improved significantly. The expected statistical uncertainty of inclusive J/ψ A_N from 2015 p+p collision is shown in the Fig 1.

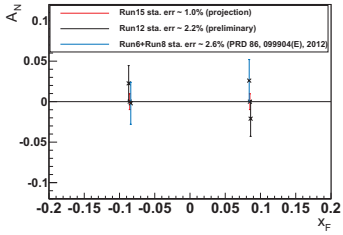

Fig. 1. Projected statistical uncertainty of inclusive J/ψ A_N from the 2015 polarized p + p collisions at 200 GeV.

In additional to the polarized p+p collision, RHIC also successfully ran polarized proton beam collisions with large nuclear Au targets. A recent theoretical study proposed that scattering a polarized proton on the saturated nuclear may provide a unique way of probing the gluon and quark TMDs. Measuring the ratio of A_N in polarized p+Au and p+p at 200 GeV might shade a light on the test for saturation physics[4]. The measurement of $J/\psi A_N$ in these two polarized collision systems are in progress. The invariant mass distributions of dimuons in p + p and p + Au are shown in Fig 2. Invariant mass distributions are fitted using a third-order polynomial and two Gaussian functions.

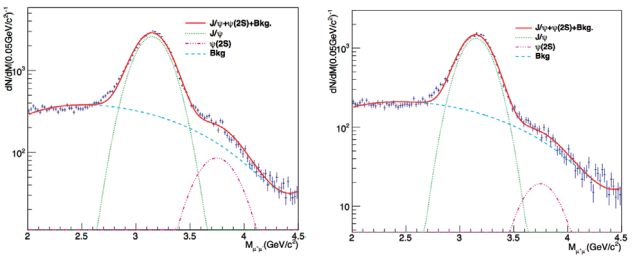

Fig. 2. Invariant mass distribution for p+p and p+Au collisions in 2015 run.

*1 Department of Physics, New Mexico State University
*2 RIKEN Nishina Center

References
1) X.-D. Ji, J.-W. Qiu, W. Vogelsang, Phys. Rev. Lett **97**, 082002 (2006).
2) F. Yuan, Phys. Rev. D**78**, 014024 (2008).
3) PHENIX collaboration: Phys. Rev. D **82**, 112008 (2010), D **86**, 099904 (2012).
4) Y. Kovchegov, M. Sievert, ArXiv: 1201.5890 [hep-ph] (2012).

Studies on transverse spin properties of nucleons at PHENIX

Y. Goto*1 for the PHENIX Collaboration

For understanding the polarized structure of the nucleon, we have performed measurements with polarized proton collisions at RHIC using the PHENIX detector. A 3-D picture including the transverse structure of the nucleon provides a conclusive understanding of the nucleon structure beyond the simple parton picture. It shows many-body correlation of partons and presents the orbital motion inside the nucleon. It is described by extending or generalizing the picture of the 1-D parton distribution, and measured with transversely polarized proton collisions. Experimentally, it is measured as single transverse-spin asymmetry $A_N = (d\sigma \uparrow - d\sigma \downarrow)/(d\sigma \uparrow + d\sigma \downarrow)$, where $d\sigma \uparrow$ ($d\sigma \downarrow$) is the production cross section when the protons are polarized up (down).

A_N has shown unexpected large asymmetry in the forward-rapidity region and required development of many models based on perturbative QCD. There are two theory frameworks. One is the so-called Sivers effect in the initial state. It is described by Sivers distribution function, which represents transverse-momentum dependence of partons inside the transversely-polarized nucleon, or higher-twist distribution function, which shows quark-gluon and multi-gluon correlations. The other is the so-called Collins effect with transversity distribution in the initial state combined with final-state effect. The transversity distribution represents a correlation between the transversely polarized nucleon and the transversely polarized partons inside. The final-state effect is described by Collins fragmentation function or higher-twist fragmentation function.

In 2006, an electromagnetic calorimeter system called Muon Piston Calorimeter (MPC) was installed in a small cylindrical hole in the muon magnet piston. It consists of lead tungstate crystals and covers the forward and backward rapidity region, $3.1 < |\eta| < 3.9$. Measurements of A_N in forward electromagnetic clusters [1] and π^0 and η mesons[2] with the MPC showed large forward asymmetry increasing with Feynman x (x_F) as shown in the previous measurements. In front of the MPC, preshower detectors[3] were installed in 2014. We will measure prompt photon asymmetry, which is sensitive to the Sivers effect, and π^0 correlations with jet-like clusters, which are sensitive to the Collins effect.

We also measured asymmetry of open heavy-flavor production, or charmed meson production. Since heavy-flavor production is dominated by the gluon-fusion process and has no final-state effect, it is sensitive to the gluon inside the nucleon. We have already had a good knowledge on the quark sector where twist-3 quark-gluon correlation functions contribute to the A_N, however the gluon sector where twist-3 tri-gluon correlation functions contribute is largely unknown . Figure 1 shows our preliminary results for A_N measurement of the single-muon from charmed-meson decay in 2012. Much improved results are expected to be obtained in 2015 through the use of the forward silicon vertex detector (FVTX) installed in 2012. The FVTX can identify secondary decay vertex of the charmed meson by measuring the distance of the closest approach of the muon track from the initial collision vertex. A_N of μ^+ and μ^- will be measured at an error level of 1%. In theoretical calculations, they are expected to be different so that charm and anti-charm contributions can be distinguished. Asymmetry of heavy-flavor production has also been measured in J/ψ channel[4].

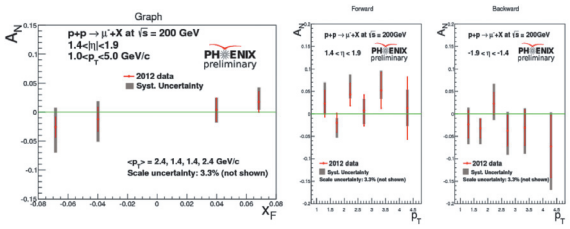

Fig. 1. A_N of the single-muon from charmed-meson decay; (left) x_F dependence, (center) p_T dependence of the forward muon, $x_F > 0$, (right) p_T dependence of the backward muon, $x_F < 0$.

After the 2016 RHIC run, the PHENIX detector will be upgraded by replacing the present central magnet with a solenoid, which will make the forward direction available. We have proposed a forward spectrometer to cover rapidity region $1 < \eta < 4$, with a capability of measuring hadrons, photons, electrons, muons and jets[5]. The forward upgrades will extend our ability to investigate the Sivers and Collins effects by performing full jet reconstruction; the Sivers effect through the observation of the A_N of the final-state jet itself, and the Collins effect through an azimuthal anisotropy in the distribution of hadrons in the jet.

*1 RIKEN Nishina Center

References

1) A. Adare *et al.* [PHENIX Collaboration], Phys. Rev. D **90**, no. 1, 012006 (2014).
2) A. Adare *et al.* [PHENIX Collaboration], Phys. Rev. D **90**, no. 7, 072008 (2014).
3) S. Campbell *et al.* [PHENIX Collaboration], arXiv:1301.1096 [nucl-ex].
4) X. Wang for the PHENIX Collaboration: in this report.
5) Y. Goto for the PHENIX Collaboration: RIKEN Accel. Prog. Rep., Vol.47 (2014), p.93.

Investigation of prompt photon asymmetries using the MPC-EX detector at Brookhaven National Laboratory

D. Kapukchyan*1 for the PHENIX collaboration

Measurements of transverse single spin asymmetries (TSSA) and theoretical predications for them did not match during the 1980s and 1990s. These experiments showed that, at energies on the order of 10 GeV, TSSAs were not as small as predicted by collinear QCD. The results of these experiments persisted even at energies as high as 500 GeV and it seemed that they would not go away.

Such observations have shown that a further development of QCD and pQCD is required in order to understand the possible sources of these TSSAs. Developments in pQCD have shown that both initial state and final state effects can give rise to transverse spin asymmetries. The initial state effects include the Sivers Transverse Momentum Dependent (TMD) PDF picture and collinear higher twist effects. The Sivers TMD picture arises from the correlation between the proton spin and the transverse momentum of the quark.

The focus of our project is to measure the Sivers Effect and other effects to the TSSAs will be neglected here. In order to measure the Sivers effect the prompt (direct) photon asymmetries (A_N) will have to be measured. The prompt photons are the result of the $p+p$ collision itself and not the result of any photons that may arise as a result of a decay from the various other products of such a collision. This asymmetry will say something about the direction the quarks were moving with respect to the proton's spin (i.e. Sivers effect) since the direct photon products will be sensitive to this motion.

In Run 15 at Brookhaven National Labs (BNL) such a measurement was taken using an upgrade to the existing Muon Piston Calorimeter (MPC) at the PHENIX detector. This upgrade is an extension of the MPC detector and aptly named MPC extension (MPC-EX). During Run 15 the MPC-EX ran and collected data for $p+p$ collisions at $\sqrt{s} = 200$ GeV energy as well as $p + Au$ collisions at the same energy. BNL is able to produce transversely polarized proton beams which is ideal for measuring A_N since the Sivers effect requires transversely polarized protons.

The main issue in measuring direct photons is eliminating the photon signal that occurs as a result of photons that have decayed from other products of the collision. The main decay mode that is troubling is $\pi^0 \rightarrow \gamma + \gamma$. Since the energy of the collisions is so high that the two photons produced as a result of this decay will have a very small angle between them. The MPC is able to distinguish π^0s with energies up to 20 GeV. The MPC-EX has the advantage over the MPC in that in can distinguish π^0s up to 80 GeV thus eliminating a greater portion of this decay mode and will allow much better isolation of the direct photon signal.

Our analysis has and will consist of trying to eliminate the π^0 decays first. The simulated data is currently being used to find the best method to do this and will be compared to the real data in the coming year. In order to reconstruct the π^0, the energies and hits in the MPC-EX need to be calibrated and aligned with the MPC data. This data will then be used to obtain the photon energies and momenta which can then be used to find out if they came from a π^0 or not. Once the π^0 signal has been eliminated then the prompt photons can be studied and the asymmetry calculated.

My analysis thus far has consisted at looking at minimum ionization peaks (MIP) in the MPC-EX and using that to make cuts on where to search for the hits. Once the hits were identified this led to trying to find tracks in the detector in Hough space. Hough space is easier to work with since it normalizes the z-coordinate (direction of motion) to one, which allows for an easier way to work with the tracks since we have reduced our space coordinates by one and only need to worry about the other directions. Once the track is identified the other directions (x and y) will say something about the showers that developed and make it easier to track their size and energy.

My focus currently is to reconstruct single track π^0s using the showers and hits from the detector. This task is made difficult by the fact that as the showers grow they will eventually overlap with the track and showers created from another photon. The challenge will be in trying to distinguish these kind of events. Even after distinguishing most of these events there will still remain some events that are the result of a π^0 but did not get rejected either because the signal was at the edge of the detector or because of the resolution of the detector. Once the location of the photon signals for a π^0 decay have been determined the opening angle between the photons can be used to reconstruct the origin of the π^0 and its energy. Thus leading a way for the calculation of A_N.

Reference

1) S. Campbell *et al.* [PHENIX Collaboration], arXiv:1301.1096 [nucl-ex].

*1 Department of Physics and Astronomy, University of California Riverside

Analysis of displaced electron tracks with the silicon vertex tracker in Au+Au collisions $\sqrt{s_{NN}}$ = 200 GeV at RHIC-PHENIX†

H. Asano,[*1,*2] A. Adare,[*3] Y. Akiba,[*2] S. Bathe,[*4,*2] J. Bryslawskyj,[*4] T. Hachiya,[*2] T. Koblesky,[*3] M. Kurosawa,[*2] D. McGlinchey,[*3] T. Moon,[*5,*2] K. Nagamishima, [*6,*2] H. Nakagomi,[*7,*2] R. Nouicer,[*8] T. Rinn[*9] Z. Rowan,[*4] T. Sumita,[*2] A. Taketani,[*2] and the PHENIX VTX group

The PHENIX Collaboration at the Relativistic Heavy Ion Collider (RHIC) has measured open heavy flavor production in minimum bias Au+Au collisions at $\sqrt{s_{NN}}$ = 200 GeV via the yields of electrons from semileptonic decays of charm and bottom hadrons. Previous heavy flavor electron measurements indicated substantial modification in the momentum distribution of the parent heavy quarks due to the quark-gluon plasma created in these collisions[1]. However, at that time, PHENIX was not able to distinguish electrons from charm and bottom hadrons independently.

For the specific purpose of separating the contributions of electrons from charm and bottom hadrons at midrapidity, the PHENIX Collaboration has added micro-vertexing capabilities in the form of a silicon vertex tracker (VTX) in 2011. The different lifetimes and kinematics for charm and bottom hadrons decaying to electrons enables separation of their contributions with measurements of displaced tracks (i.e. the decay electron not pointing back to the collision vertex).

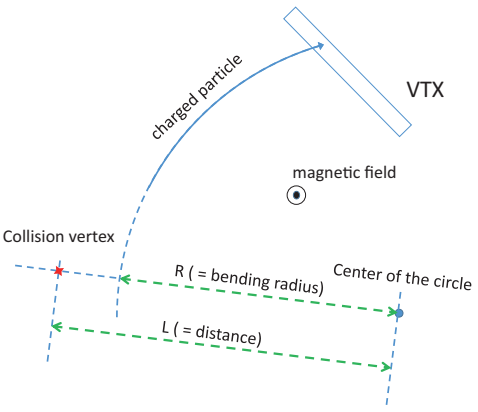

Fig. 1. Illustration of the definition of $\mathrm{DCA}_T \equiv L$ - R in the transverse plane.

We measured the distance of closest approach of electron tracks in the transverse plane (DCA_T) as illustrated in Fig.1 and subtracted various backgrounds: misidentified hadrons, mis-reconstructed electron, conversion electrons, electrons from Dalitz decay, kaon decay electrons, heavy-quarkonia decay.

After subtracting those backgrounds, we performed an unfolding procedure to fit the DCA_T distribution as shown in Fig.2. The sum of the background components, electrons from charm and bottom decays is shown as the red curve for direct comparison with the data. The gray band indicates the region in DCA_T considered in the unfolding procedure.

In conclusion, we have succeeded in separation of electrons from charm and bottom hadrons decay by using the VTX detector.

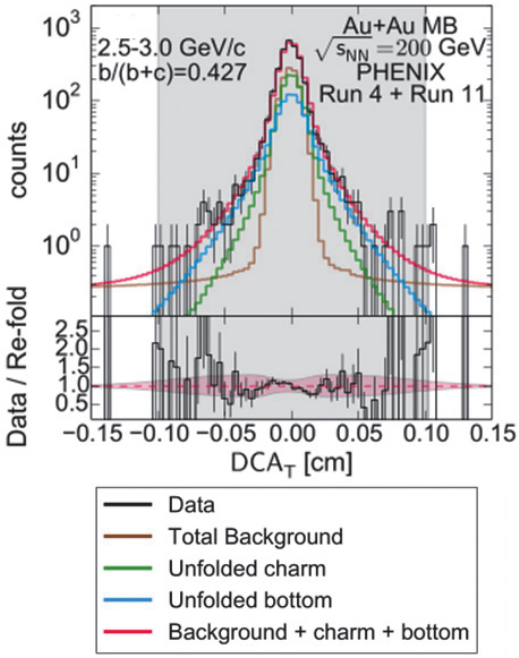

Fig. 2. The DCA_T distribution for measured electrons compared to the decomposed DCA_T distributions for background components, electrons from charm decays, and electrons from bottom decays.

† Condensed from the article in Phys. Rev. C 93, 034904 (2016)

*1 Department of Physics, Kyoto University
*2 RIKEN Nishina Center
*3 Department of Physics, University of Colorado Boulder
*4 Department of Natural Science, City University of New York
*5 Department of Physics, Yonsei University
*6 Department of Physics, Hiroshima University
*7 Graduate School of Pure and Applied Sciences, University of Tsukuba
*8 Brookhaven National Laboratory
*9 Department of Physics and Astronomy, Iowa State University

References

1) A. Adare et al., Phys.Rev.Lett. **98** 17230 (2007)
2) M Baker et al., Proposal for a Silicon Vertex Tracker (VTX) for PHENIX Experiment, 2004 BNL72204-2004, Physics Dept. BNL

Current status of open heavy flavor measurements in RHIC-PHENIX RUN14

K. Nagashima,[*1,*2] A. Adare,[*2] Y. Akiba,[*1] H. Asano,[*1,*4] S. Bathe,[*1,*5] J. Bryslawskeyj,[*5] T. Hachiya,[*1] T. Koblesky,[*3] M. Kurosawa,[*1] D. Mcglinchey,[*3] T. Moon,[*1,*6] H. Nakagomi,[*7] R. Nouicer,[*8] T. Rinn,[*9] Z. Rowan,[*5] T. Sumita,[*1] and A. Taketani[*1]

The Quark Gluon Plasma (QGP) existed in the early universe. We are studying the physical property of the QGP at RHIC-PHENIX. It can be characterized by the quark energy loss mechanism. Especially heavy quarks (charm and bottom) are important probes of the QGP. They are predominantly produced during hard scattering in the initial stage of a heavy-ion collision produces them dominantly, since the charm and bottom masses are larger than the temperature of the QGP. Additionally the energy loss of heavy quarks would be expected to be smaller than that of light quarks due to lower collisional energy loss and the Dead-Cone-Effect that leads to a strong suppression of small angle gluon radiation. The silicon vertex tracker (VTX) was installed and used to measure the first data in 2011. It can separate the charm and bottom hadron decay electrons with the distance of closest approach (DCA). The DCA of a track is calculated separately in the transverse plane (DCA_T) and the beam direction (DCA_L) as shown in Fig.1.

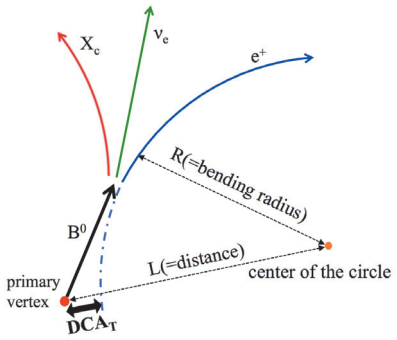

Fig. 1. DCA_T is defined as DCA_T = L - R in the transverse (bending) plane

We focus on DCA_T for the analysis because DCA_T has a better resolution than DCA_L in the design performance. In order to estimate the charm and bottom hadron invariant yields separately, we use a DCA cocktail method subtracting all background components estimated by simulations and data, and a Bayesian inference technique based on a Markov Chain Monte Carlo (MCMC).

PHENIX reported the nuclear modification factor $R_{\rm AA}$ of electrons from charm and bottom hadron decays separately based on Au+Au collisions at $\sqrt{s_{NN}}$ = 200 GeV recorded in 2004 and 2011.[1,2] We found that suppression of electrons from bottom hadron decays is lesser than that from charm for the region 3 < $p_{\rm T}$ < 4 GeV/c.[3,4] Accordingly, we plan to measure the centrality dependence of $R_{\rm AA}$ over a broader $p_{\rm T}$ range with high statistics data recorded in 2014. It is expected to have 10 times more statistics than the data recorded in 2011. VTX performances was the same in 2014 and 2011, as a result of comparing DCA_T resolutions as shown in Fig.2. We finished the calibration

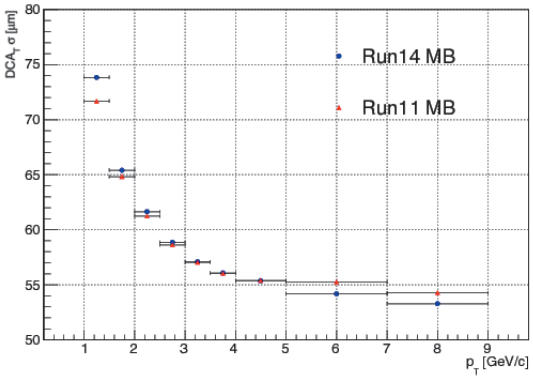

Fig. 2. DCA_T resolution as a function of $p_{\rm T}$ in Run14 AuAu (blue) and Run11 AuAu (read). The comparison shows that detector performances are much the same.

and quality assurance of the 2014 data and obtained the electron DCA_T distribution in each centrality bin. The next step is to estimate the normalization and shape of all background components in order to decomvolute the electron DCA_T distribution. Eventually we will obtain the invariant cross section of both charm and bottom hadrons, and compare it with the p+p collision data recorded in 2015 to estimate $R_{\rm AA}$.

*1 RIKEN Nishina Center
*2 Department of Physics, Hiroshima University
*3 Department of Physics, University of Colorado, Boulder
*4 Department of Physics, Kyoto University
*5 Department of Natural Science, Baruch College, CUNY
*6 Department of Physics, Yonsei University
*7 Department of Physics, University of Tsukuba
*8 Brookhaven National Laboratry
*9 Department of Physics, Iowa State University

References

1) A. Adare et al; Phys. Rev. C **84**, 044905 (2011).
2) A. Adare et al; arXiv:1509.04662.
3) T. Hachiya et al: In this report.
4) H. Asano et al: In this report.

Single electron yields from semileptonic charm and bottom hadron decays in Au+Au collisions at $\sqrt{s_{NN}} = 200$ GeV†

T. Hachiya,[*1] A. Adare,[*2] Y. Akiba,[*1] H. Asano,[*1,*3] S. Bathe,[*1,*4] J. Bryslawskeyj,[*4] T. Koblesky,[*2] M. Kurosawa,[*1] D. Mcglinchey,[*1] T. Moon,[*1,*5] K. Nagashima,[*1,*6] H. Nakagomi,[*1,*7] R. Nouicer,[*8] T. Rinn,[*9] Z. Rowan,[*4] T. Sumita,[*1] and A. Taketani[*1]

The PHENIX experiment measured open heavy flavor production in minimum bias Au+Au collisions at $\sqrt{s_{NN}} = 200$ GeV using single electrons from semileptonic decays of charm and bottom hadrons. Previous measurement of electrons from inclusive heavy flavor decays showed strong suppression at high transverse momentum, $p_T > 5$ GeV/c, when compared with that in $p+p$ collisions[1)]. In order to understand the suppression, we installed the silicon vertex tracker (VTX). VTX allows separating the charm and bottom contributions by measuring the distance of the closest approach of electrons to the primary vertex (DCA).

Data analysis was performed in three steps. First, we measured the DCA of inclusive electrons using Au+Au events recorded in 2011. The electrons contain a large amount of backgrounds (BG) that are Dalitz decays of π^0 and η, photon conversions, K_{e3} decays, and $J/\psi \to e^+e^-$ decays. Most of them are rejected based on the requirement of the pair-wise hit in VTX because the pair of hits are created by e^+e^- pairs of BG's, such as $\gamma \to e^+e^-$.

Second, we determined the BG DCA distribution for 1)misidentified hadrons, 2)random matching of electrons with VTX hits, 3) π^0, η, K_{e3}, and J/ψ decays and photon conversions. 1) is evaluated by the event swap method and 2) is evaluated by embedding single simulated electrons into the real events. 3) is estimated using GEANT-based detector simulation with the input of measured spectra. All BG DCA distributions are normalized based on the BG yield obtained in the single electron measurement in 2004[1–3)].

Third, to extract the charm and bottom components, we developed the unfolding method that employs the Bayesian inference technique with the Markov chain Monte Carlo sampler. The method performed simultaneous fitting with the DCA distributions and inclusive heavy flavor electrons yield[1,2)] as a function of p_T.

From the unfolding result, the fraction of bottom electrons to inclusive heavy flavors was shown in Fig. 1. The red line and the pink band represent the center value and the systematic errors, respectively. The gray line is the FONLL prediction in $p+p$ collisions. We found the steeper rise in $2 < p_T < 4$ GeV/c with a possible peak compared with the central FONLL calculations.

The nuclear modification factors R_{AA} of charm and bottom electrons can be calculated separately using this result with additional constraints in $p+p$[4)] and previous Au+Au measurement[1,2)]. Figure 2 indicates that both charm and bottom electrons are strongly suppressed at high p_T, and bottom electrons are less suppressed than charm electrons in $3 < p_T < 4$ GeV/c.

For further improvement, we are analyzing large amounts of the Au+Au and $p+p$ data recorded in 2014 and 2015[5)].

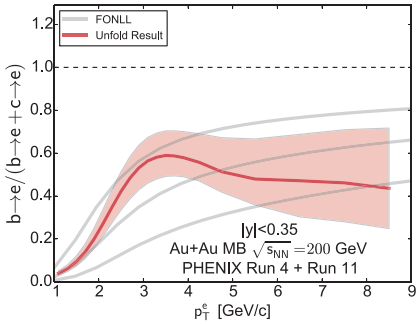

Fig. 1. Bottom electron fraction in minimum bias Au+Au collisions. The FONLL calculations are also shown (gray lines)

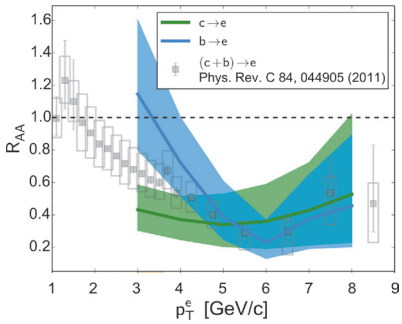

Fig. 2. R_{AA} for charm and bottom electrons as a function of p_T.

References
1) A. Adare et al., Phys. Rev. Lett. **98** 172301 (2007).
2) A. Adare et al., Phys. Rev. C **84** 044905 (2011).
3) H. Asano at al., In this report.
4) M. M. Aggarwal et al., Phys. Rev. Lett. **105** 202301 (2010).
5) K. Nagashima at al., In this report.

† Condensed from the article in arXiv:1509.04662

*1 RIKEN Nishina Center
*2 Department of Physics, University of Colorado, Boulder
*3 Department of Physics, Kyoto University
*4 Department of Natural Science, Baruch College, CUNY
*5 Department of Physics, Yonsei University
*6 Department of Physics, Hiroshima University
*7 Department of Physics, University of Tsukuba
*8 Brookhaven National Laboratory
*9 Department of Physics, Iowa State University

Measurements of directed, elliptic, and triangular flow in Cu+Au collisions at $\sqrt{s_{NN}} = 200$GeV†

H.Nakagomi*1*2 for the PHENIX collaboration

In relativistic high-energy heavy-ion collisions, a hot and dense nuclear matter called quark-gluon plasma (QGP) is considered to exist. Until now several measurements and theoretical calculations have suggested the successful formation of QGP and the produced QGP is a nearly perfect fluid.

The measurements of the azimuthal anisotropies of particle emission is a strong tool to investigate the property of QGP. In relativistic heavy-ion collisions, the initial spatial anisotropy of the overlap region of the off-center nuclear-nuclear collisions is converted to an anisotropy in momentum space through the pressure gradient. Namely, azimuthal anisotropic flow originates from the initial spatial geometry and is considered to result from the hydrodynamic expansion of QGP. Thus, azimuthal anisotropy provides us with the initial spatial condition and the bulk property of QGP. The azimuthal anisotropic flow is expressed as the coefficients of the Fourier expansion series as follows,

$$\frac{dN}{d\phi} \propto 1 + \sum_{n=1} 2v_n \cos(n(\phi - \Psi_n)) \quad (1)$$

where $v_n = \langle\cos(n(\phi - \Psi_n))\rangle$(n=1,2,3,4...) is the magnitude of azimuthal anisotropy. ϕ is the azimuthal angle of each particle and Ψ_n called the n_{th} order Event Plane that is the azimuthal direction in which more particles are emitted. The first order coefficient is the magnitude of directed particle emission called Directed flow. In symmetric collision systems, the signal of Directed flow around the collision point is very small due to the symmetric interaction region. The second order coefficient is the magnitude of elliptical particle emission called Elliptic flow. So far the measurements of v_2 have been hardly studied in symmetric collision systems and concluded the viscosity η/s of QGP is small. The third harmonic coefficient is the magnitude of triangular particle emission called Triangular flow. v_3 originates from the initial nucleon fluctuation. The combined even and odd harmonic coefficients provide more stringent constraint on the initial condition and the viscosity of QGP than v_2 measurement alone.

In 2012, Cu and Au collisions were operated at RHIC. This was the first asymmetric heavy-ion collision for controling initial spatial geometry. In Cu+Au collisions systems, asymmetric initial conditions lead to an asymmetric pressure gradient and particle production for the Cu and Au side. The measurements of v_n in the Cu+Au collisions further constrain viscosity and initial conditions.

Figure 1 shows the sizable v_1 measured as the function of transverse momentum p_T for four multiplicity classes. The v_1 is measured with respect to the Cu spectator neutrons that do not participate in the collisions. In all multiplicity classes, high p_T particles that come from the Au nuclei are indicated by negative v_1.

Figures 2,3 illustrate v_2 and v_3 measured as functions of p_T compared to the hydrodynamical calculation. The event-by-event hydrodynamical calculation with two different viscosities reproduce v_2 and v_3 simultaneously.

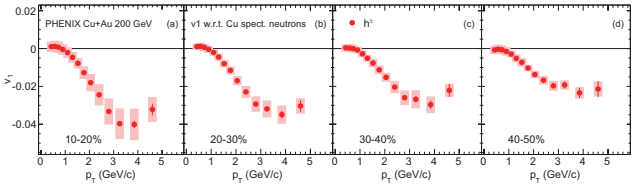

Fig. 1. $v_1(p_T)$ for four different multiplicity classes

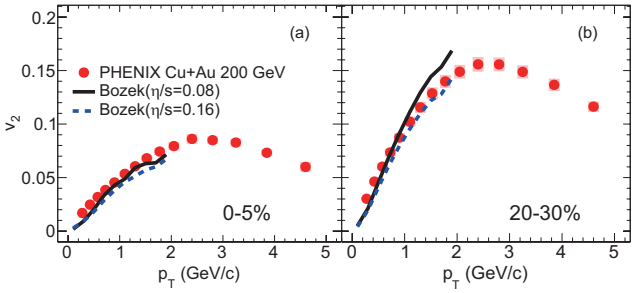

Fig. 2. $v_2(p_T)$ for two different multiplicity classes compared to hydrodynamical calculation

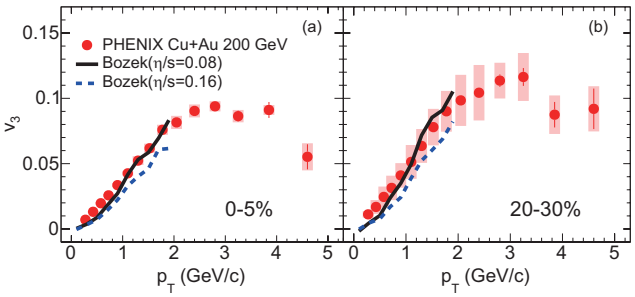

Fig. 3. $v_3(p_T)$ for 2 different multiplicity classes compared to hydrodynamical calculation

References

1) A. Adare et al., (PHENIX Collaboration), Phys. Rev. Lett. **107**, 252301 (2011).
2) M. R. Haque, M. Nasim, B. Mohanty, Phys. Rev. C **84**, 067901 (2011).
3) P. Bozek, Phys. Lett. B 717, 287 (2012).
4) A. Adare et al., (PHENIX Collaboration), Phys. Rev. C **92**, 034913 (2015).

† Condensed from the article in arXiv:1509.07784 (2015)

*1 RIKEN Nishina Center
*2 Graduate School of Pure and Applied Sciences University of Tsukuba

Searching for mini-QGP in p+p collisions using a high multiplicity trigger with the FVTX

S. Han*1*2 and the PHENIX collaboration

There have been many reports via RHIC and LHC experiments about the collective behavior of matter formed in high-energy heavy-ion collisions such as Au+Au and Pb+Pb. This non-zero elliptic flow has been considered to indicate strong evidence of the formation of the quark gluon plasma (QGP). On the other hand, it has been believed no QGP formation exist in small systems such as $p+p$ or p+A collisions because the system is too small to attain a thermal equilibrium. However, recent LHC results have shown collective behaviors from high-multiplicity events (when the total number of tracks is larger than 110) in $p+p$ collisions both at $\sqrt{s}$ =7 and 13 TeV[1)], and in p+Pb collisions at $\sqrt{s_{NN}}$ =5.02 TeV[2)]. A ridge structure on the near-side of two-particle correlations was observed where the near side corresponds to the region of small azimuthal angular difference between the particles. Inspired by these results, PHENIX also studied collective behaviors in small systems such as p+Au, d+Au, and ^{3}He+Au[3)] collisions.

In order to explore the possible collective behavior in the smallest system, i.e., $p+p$ collisions at RHIC energies, we implemented a high-multiplicity trigger to the existing readout system of the forward vertex detector (FVTX) before RHIC Run-15 to tag events of multiple tracks at forward rapidity. The FVTX is a new silicon strip detector that was installed before starting RHIC Run-12 to measure the precise event vertex position and trajectory of charged particles at the rapidity range of $1.2 < |\eta| < 2.2$. The FVTX has four stations per arm, which consist of 48 number of mini-strip silicon sensors. A previous study showed that there is a very weak correlation between tracks measured at central arms (CNT, $|\eta| < 0.35$) and the beam beam counter (BBC, $3.4 < |\eta| < 3.8$) in $p+p$ collisions. We decided to use the FVTX to trigger high-multiplicity events in $p+p$ collisions. That is because the FVTX detector is closer to mid-rapidity than the BBC, so we could expect a stronger correlation between CNT-FVTX than that between CNT-BBC.

The logic of the FVTX trigger system relies on the basic unit of the FVTX reconstruction, the wedge. The wedge consists of two silicon strip sensors, readout chips, and high-density interconnect. Each station contains 24 wedges. In the FVTX trigger system, the number of online tracks simply indicates the number of the fired wedges according to the logic of the threshold, so the number of online tracks cannot be larger than 24. More over, the number of offline tracks indicates reconstructed roads from the PHENIX raw data files according to the road reconstruction logic. Fig. 1 shows correlations between the number of offline tracks and online tracks. The number of offline tracks is supposed to show a linear correlation with the number of online tracks. In our trigger, we can clearly observe a correlation between the number of online tracks and the number of offline tracks. However, when comparing Fig. 2 with Fig. 1, there seems to be a larger off-diagonal component with more online tracks than offline tracks.

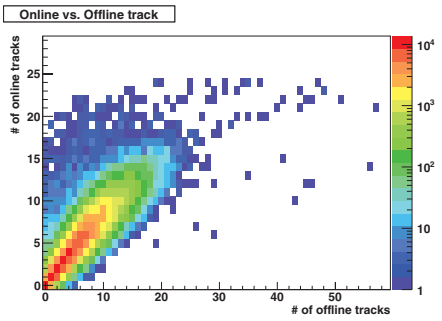

Fig. 1. Correlation of number of tracks between online and offline reconstructions at p-going side in p+Au collisions.

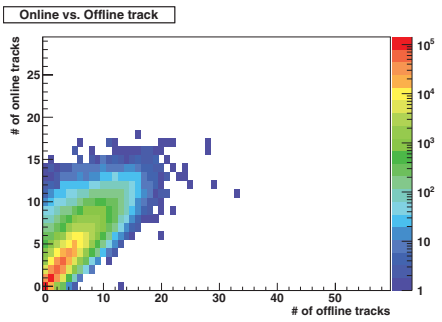

Fig. 2. Correlation of number of tracks between online and offline reconstructions in p+p collisions.

We still need to find a way how to remove the off-diagonal part in the correlation between online and offline track numbers, particularly on the $p+p$ collisions. A data analysis of two-particle correlations in $p+p$ collisions at $\sqrt{s}$ =200 GeV is ongoing.

*1 RIKEN Nishina Center
*2 Department of Physics, Ewha womans university

References

1) CMS Collaboration:J. High Energy Phys. **09** (2010) 091.
2) CMS Collaboration:Phys. Lett. B **718**, 795 (2013).
3) PHENIX Collaboration:Phys. Rev. Lett. **115**, 142301.

Silicon tracker for sPHENIX

I. Nakagawa,[*1] Y. Akiba,[*1] and G. Mitsuka[*1]

sPHENIX is a proposal[1] to be built in the experimental hall after the PHENIX experiment is decommissioned in 2016 at the Relativistic Heavy Ion Collider (RHIC). The experiment is scheduled during 2022 - 2024 in oder to address on fundamental unanswered questions about the nature of the strongly coupled Quark-Gluon Plasma (QGP), discovered experimentally at RHIC to be a perfect fluid. These questions include how and why the QGP behaves as a perfect fluid in the vicinity of strongest coupling, near the temperature at which the phase transition takes place, whether there are quasiparticles that play an important role in the dynamics of the QGP, and how the strongly coupled QGP evolves to become a weakly coupled system at asymptotically high temperature. These questions can only be fully addressed with a detector which can measure jet production and jet properties at RHIC energies, at temperatures near the phase transition where the coupling is strongest and by comparing these measurements to higher temperature QGP measurements at the Large Hadron Collider. Taken together, these data will provide valuable insight into the thermodynamics of Quantum Chromodynamics (QCD), the theory which governs the interactions of the quarks, the building blocks of nuclei.

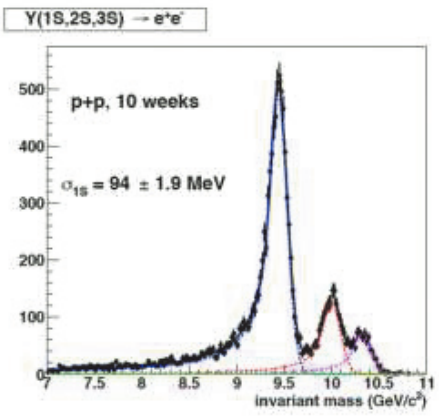

Fig. 1. Simulated invariant mass of three Υ states assuming the designed momentum resolution of the silicon tracker.

sPHENIX design is thus optimized to measure jets, jet correlations and upsilons to determine the temperature dependence of transport coefficients and the color screening length in the QGP. It will do this with high rate, large acceptance, hadronic and electromagnetic calorimetry and precision tracking. It will have mass resolution sufficient to distinguish separately the three states of the Υ family.

The measurement of the Υ family places the most stringent requirement on momentum resolution at lower momentum. The large mass of the Upsilon means that one can primarily focus on electrons with momenta of $\sim 4-10$ GeV/c. The $\Upsilon(3S)$ has about 3% higher mass than the $\Upsilon(2S)$ state and to distinguish them clearly one needs invariant mass resolution of ∼100 MeV, or $\sim 1\%$ as demonstrated in Fig. 1. This translates into a momentum resolution for the daughter $e^{\pm}$ of $\sim 1.2\%$ in the range $4-10$ GeV/c.

In order to meet the requirement to distinguish the three Υ states, the silicon strip tracker is under development. The silicon strip tracker covers the acceptance $|\eta| < 1$ and has full azimuthal coverage, $\Delta\phi = 2\pi$. It consists of 3 stations (from inner to outer, called S0, S1 and S2) as illustrated in Figure 2. In each of the S0 and S1 stations, sensor modules are mounted on the front and back of a single support and cooling structure to form two closely spaced tracking layers. To achieve hermeticity, alternate support and cooling structures are staggered in radius and offset in azimuthal angle so that the alternating sensor modules overlap in azimuth. The S2 station contains a single tracking layer, again with alternate support and cooling structures staggered in radius and offset in azimuth to achieve hermeticity of the active area. The R&D status is discussed in elsehwere[2),3)].

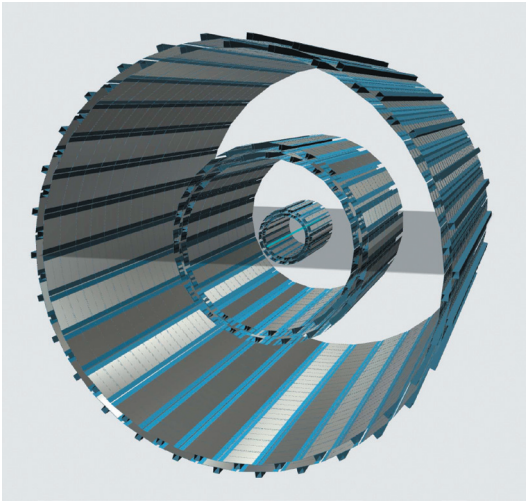

Fig. 2. The silicon tracker for sPHENIX.

*1 RIKEN Nishina Center

References

1) sPHENIX pre-Conceptual Dsign Report (2015) .
2) Y. Akiba (et. al) in this report.
3) G. Mitsuka (et. al) in this report.

Forward Jet asymmetry measurements in fsPHENIX

R.Seidl*1 and A.Vossen*2

The current PHENIX detector's small acceptance has substantially limited the possibilities to study the spin structure of the nucleon in more detail. With the inception of a new, large acceptance jet and charmonium detector for heavy ion physics, sPHENIX[1], some incremental improvements are possible in the sPHENIX acceptance (-1< η < 1) but almost all interesting observables for spin and cold nuclear matter physics require forward coverage. The main reasons are that at forward rapidities both higher and lower Bjorken x can be probed than previously accessible. The lower x region is interesting for the study of the gluon spin where even a moderate polarization can substantially impact the total contribution to the proton spin. The higher x region is important as it relates to the valence region and above for transverse spin effects.

The so-called fsPHENIX project (for forward sPHENIX)[2] proposed to augment the sPHENIX acceptance at the least by a forward hadronic calorimeter and GEM tracking planes in the rapidity region of 1.3 to 4. This minimal solution is relatively cost-effective and would allow the measurement of jets as well as charged hadrons within jets in these forward rapidities. With other detector additions or refurbishing, fsPHENIX can also become a zero-day detector for an electron-ion collider if realized at Brookhaven.

One of the main transvsere spin measurements is the access to the tensor charge, which is an important test quantity in lattice calculations. This chiral-odd object has so far been mostly accessed via the Collins fragmentation function[5] which has been extracted in e^+e^- annihilation[6]. Transversity is only known at moderately low x (0.05 to 0.3) accessible in semi-inclusive deep inelastic scattering (SIDIS). Recently STAR has managed to access a similar x region in transvsersely polarized proton-proton collisions at central rapidity via hadron in jet azimuthal asymmetries. Performing these measurements in forward rapidities, one can extend the measurement to x regions so far not accessed and at a high scale.

We have performed MC studies using either the currently extracted parameterizations[3] or use the Soffer bound[4]. Since no data exsits at the higher x we are interested in at forward rapidities these two expected asymmetry curves realistically reflect the amound of uncertainty at present. In addition, we have performed a realistic study of the experimentally achievable uncertainties taking into account jet axis smearing, beam remnant backgrounds as well as underlying event contributions assuming a rather moderate integrated luminosity of 268 fb $^{-1}$ at a collision energy of 500 GeV. In Fig. 1 the statistical uncertainties on the expected negative hadron measurements are not visible and with expected asymmetries as large as 10% the d quark transversity can be constrained. With increasing rapidity as well as jet transvsere momentum one can reach the high x values needed to eventually perform the integral and obtain the tensor charges. The lower x regions in turn can be used to experimentally confirm that factorization holds if compared to SIDIS. Last, when the backward going beam is transversly polarized instead of the forward going beam with a similar measurement the potential linear polarization of gluons in the nucleon can be probed for the first time. More details on these as well as other key measurements at RHIC can be obtained from the recently completed new RHIC spinplan[7].

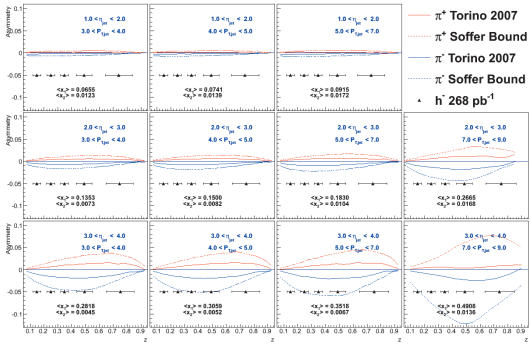

Fig. 1. Expected h$^-$ Collins asymmetry uncertainties (black points) compared to positive (red) and negative (blue) pion asymmetires based on the Torino extraction[3] (full lines) or the Soffer bound[4] (dashed lines) as a function of fractional hadron energy z for various bins in jet rapidity and momentum. The average kinematics are also shown.

References
1) A. Adare *et al.*, arXiv:1501.06197 [nucl-ex].
2) https://indico.bnl.gov/materialDisplay.py?materialId=5&confId=764
3) M. Anselmino, M. Boglione, U. D'Alesio, A. Kotzinian, F. Murgia, A. Prokudin and C. Turk, Phys. Rev. D **75**, 054032 (2007).
4) J. Soffer, Phys. Rev. Lett. **74**, 1292 (1995).
5) A. Airapetian *et al.* [HERMES Collaboration], Phys. Rev. Lett. **94**, 012002 (2005).
6) R. Seidl *et al.* [Belle Collaboration], Phys. Rev. Lett. **96**, 232002 (2006).
7) E. Aschenauer *et al.*, arXiv:1602.03922.

*1 RIKEN Nishina Center
*2 Indiana University

Towards measurment of direct photons via external conversions in high multiplicity pp collisions at 13 TeV

H.Murakami[*1,*2]

A Large Ion Collider Experiment (ALICE) at the CERN, LHC is dedicated to the study of Quark Gluon Plasma (QGP), a strongly interacting QCD medium. The study of the QGP was mainly performed by using relativistic heavy ion collisions. The collective behavior of hadronic particles has been observed in high multiplicity pp and p-Pb collisions at the LHC.[1] These observations could be indicating the formation of thermalized systems such as the QGP, even in small systems.[2] A direct photon is an ideal probe to study such thermalized systems due to its penetrating nature. In this study, we aim to measure direct photons produced in high multiplicity pp collisions at $\sqrt{s}$ =13 TeV.

In the ALICE experiment, we measure direct photons in two ways, via a calorimeter or via the measurement of photon conversions (external conversions). The latter allows us to measure very low transverse momentum p_{T} photons. The main tracking system[3] of the ALICE detector consists of the Inner Tracking System (ITS), the Time Projection Chamber (TPC), and the Time of Flight (TOF). Direct photons will convert into dielectrons in the material of the ITS and TPC, and leave two tracks. For multiplicity estimation, V0 detectors, which are made of two arrays of scintillation counters are used and they are set on both sides of the ALICE interaction point.

Photons are produced in several stages during the time-space evolution of the QGP and there are mainly two groups: direct photons and decay photons. The former originates from quark-anti-quark annihilation and the QCD Compton scattering, and the latter comes from particle decay such as $\pi^0 \rightarrow \gamma\gamma$. It is difficult to measure direct photons separately, since there is huge background from decay photons. Therefore, we measure all the emitted photons(inclusive photons) and decay photons. The invariant yield of direct photons $\gamma_{\mathrm{dir}}(p_{\mathrm{T}})$ can be expressed in terms of the inclusive photons $\gamma_{\mathrm{inc}}(p_{\mathrm{T}})$ and that of decay photons $\gamma_{\mathrm{dec}}(p_{\mathrm{T}})$:

$$\gamma_{\mathrm{dir}}(p_{\mathrm{T}}) = \gamma_{\mathrm{inc}}(p_{\mathrm{T}}) - \gamma_{\mathrm{dec}}(p_{\mathrm{T}}) \quad (1)$$

$$= (1 - \frac{\gamma_{\mathrm{dec}}(p_{\mathrm{T}})}{\gamma_{\mathrm{inc}}(p_{\mathrm{T}})}) \cdot \gamma_{\mathrm{inc}}(p_{\mathrm{T}}) \quad (2)$$

$$= (1 - R_{\gamma}^{-1}(p_{\mathrm{T}})) \cdot \gamma_{\mathrm{inc}}(p_{\mathrm{T}}), \quad (3)$$

where the fraction of inclusive photons above decay photons $R_{\gamma}(p_{\mathrm{T}})$ is called the direct photon fraction. If $R_{\gamma}(p_{\mathrm{T}})$ is larger than unity, direct photons are produced in the collision. The fraction can be calculated from the decay photon spectrum. The major source of decay photons are π^0 and η , and other sources are calculated by using m_{T} scaling based on these neutral meson's p_{T} spectra. Therefore, the determination of the p_{T} spectra of neutral meson is very important.

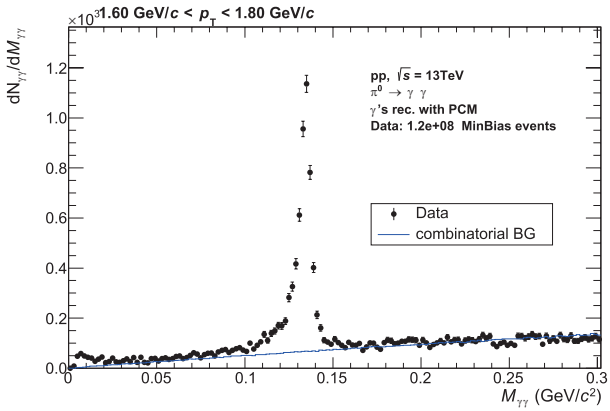

Fig. 1. Invariant mass distribution of reconstructed photon pairs $M_{\gamma\gamma}$

In this paper, we report the status of neutral meson analysis. In 2015, ALICE successfully collected over 400M events which correspond to 0.007 pb^{-1} in $\sqrt{s}$ =13 TeV pp collisions with minimum bias (MB) trigger and we used this data sample. The first step of the analysis is to find photons with the V^0 reconstruction method. The V^0 is the secondary vertex from unknown particle decays such as $\Lambda^0, \overline{\Lambda^0}, K_s^0, \gamma$. In order to select pure photon samples from V^0 particles, several cuts such as particle identification cuts, a 2D cut for dielectrons and a cut using the Armenteros-Podolanski plot[4] were applied. Figure 1 shows the invariant mass spectrum of reconstructed photon candidates which are from external conversion pairs. The blue line is the combinatorial background(BG), which is calculated using the event mixing technique, in which photons are taken from different events and combined to form pairs. On top of the BG, a clear peak can be seen for π^0 mass 0.135 GeV/c^2. Subtraction of BG and evaluation of the invariant raw yield of π^0 are work in progress. Not only the raw yield of π^0, but also that of η will be calculated and eventually, we will evaluate the invariant cross section. Moreover, we will carry out an analysis focused on high multiplicity events.

*1 Department of Physics, University of Tokyo
*2 RIKEN Nishina Center

References

1) The CMS collaboration, J. High Energy Phys. 09 (2010) 091.
2) C.Shen et al, arXiv:nucl-th/1504.07989v1(2015).
3) The ALICE Collaboration, JINST 3, S08002 (2008).
4) J. Podolansky and R. Armenteros. Phil. Mag. 45(13), 1954.

Neutral pion production in pp collisions at LHC energies

S. Yano*1,*2

ALICE, one of the experiments at the Large Hadron Collider (LHC) at CERN, is aimed at studying heavy-ion collisions and the properties of a deconfined state of matter, the quark-gluon plasma (QGP)[1]. High-p_{T} particle production is a powerful tool for characterizing the QGP because the interaction between fast partons depends on the QGP transport properties. The hadron yields in heavy-ion collisions can be quantified by the nuclear modification factor (R_{AA}), which is the ratio of the particle yield in heavy-ion collisions normalized by the number of inelastic nucleon–nucleon collisions to the yield in pp collisions. Previous experiments have shown that R_{AA} at high p_{T} is significantly smaller than 1, which can be explained by the energy loss of fast partons traversing in QGP.

The ALICE experiment includes a high-resolution and high-granularity electromagnetic calorimeter called PHOS[1]. One of the main physics goals achievable by PHOS is the study of energy loss through the measurement of high-p_{T} neutral mesons (π^0 and η). Three PHOS modules are installed in the ALICE experiment, which covers azimuthal angles in the range $260° < \phi < 320°$ and pseudorapidity $|\eta| < 0.125$. PHOS provides a photon trigger (PHOS trigger) owing to its requirement of the measured energy to be above a threshold. The threshold was set to be 2 and 4 GeV in pp collisions at $\sqrt{s} = 8$ TeV. By using the PHOS trigger, high-p_{T} neutral mesons can be efficiently measured in the ALICE experiment. This paper describes the analysis status of neutral-pion production measured with the PHOS trigger and minimum-bias (MB) trigger data in pp collisions. Further, neutral-pion production in pp collisions at $\sqrt{s} = 8$ TeV are compared with the results for other LHC energies (0.9, 2.76, and 7 TeV)[2,3]. In this analysis, MB-trigger ($0.3nb^{-1}$) and PHOS-trigger ($70nb^{-1}$) data are used in pp collisions at $\sqrt{s} = 8$TeV.

The invariant cross section is predicted by the pQCD theory considering the particle production mechanism as follows[4].

$$E\frac{d\sigma}{d^3p}(pp \to \pi^0 X) = \frac{F(x_{\mathrm{T}})}{p_{\mathrm{T}}^n} \quad (1)$$

The exponent n in the LO QCD should be 4; however, in reality, it is approximately 6 owing to scaling violation. Eq.(1) can be converted by using $x_{\mathrm{T}} = 2\sqrt{s}/p_{\mathrm{T}}$ as below.

$$\sqrt{s}^n E\frac{d\sigma}{d^3p}(pp \to \pi^0 X) = \left(\frac{2}{x_{\mathrm{T}}}\right)^n F(x_{\mathrm{T}}) = G(x_{\mathrm{T}}) \quad (2)$$

The $G(x_{\mathrm{T}})$ is expected not to depend on the collision energy, but only on x_{T}[4]. Therefore, the following equation is expected between different collision energies. This is called x_{T} scaling

$$\sqrt{s_1}^n E\frac{d\sigma_1}{d^3p}(x_{\mathrm{T}}) = \sqrt{s_2}^n E\frac{d\sigma_2}{d^3p}(x_{\mathrm{T}}) \quad (3)$$

The exponent n depends on the energy, and at RHIC energies, a good scaling behavior is observed for $n = 6.24$. The results of LHC energies are shown in Fig. 1. The exponent n is extrapolated using the global fit of these 3 energies and n is 5.08. As is evident, the high p_{T} region of each energy shows very good agreement with each other; however, all low p_{T} regions violated the scaling because of the soft QCD.

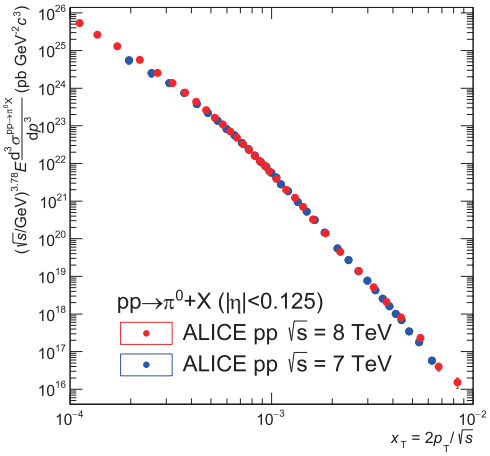

Fig. 1. The x_{T} scaling result of LHC and RHIC.

x_{T} scaling at high p_{T} is observed at LHC energies. The exponent n is smaller than RHIC. At high x_{T} regions, good scaling is observed. The results imply that the particle production mechanism at LHC energies is the same as the previous experiment.

*1 Department of Physics Science, Hiroshima University
*2 RIKEN Nishina Center

References
1) The ALICE Collaboration, JINST 3, S08002 (2008).
2) The ALICE colaboration, Phys. Lett. B **717**, pp. 162 - 172 (2012).
3) The ALICE colaboration, Eur. Phys. J. C 74-3108 (2014).
4) F Arleo, S J Brodsky, D S Hwang and A M Sickle, Phys. Rev. Lett **105** 062002 (2010).

Long-range correlation of V^0 particles in p-Pb collisions at $\sqrt{s_{NN}}$ = 5.02 TeV with the ALICE detector

Y. Sekiguchi,[*1,*2] H. Hamagaki,[*2] and T. Gunji[*2]

Measuring correlations in particle production as a function of the azimuthal angular space and rapidity space is very useful for investigating particle production in high-energy nucleus-nucleus collisions. The long-range correlations in the rapidity space in near-side angular pairs of dihadron correlations were first observed in Au-Au collisions at $\sqrt{s_{NN}}$= 200 GeV at RHIC[1,2]. This long-range correlations are derived from the collective expansion of the initial geometry fluctuations. Unexpectedly, a similar structure has also been observed in high-multiplicity pp collisions at $\sqrt{s_{NN}}$ = 7 TeV by the CMS experiment[3]. It is very interesting to study the correlation in p-Pb collisions because the initial gluon density and magnitude of the collective expansion are very different from those in other collision systems. The azimuthal anisotropy parameter v_2 of K, π, and p shows mass ordering at low transverse momentum ($p_{\rm T}$) and the trend is similar to Pb-Pb collisions[4]. The mass ordering is a characteristic feature of collective expansion. This analysis aims to further explore the partonic collectivity by extracting v_2 of K^0_s and Λ in p-Pb collisions at $\sqrt{s_{\rm NN}}$ = 5.02 TeV with the ALICE detector. The correlations between the unidentified charged hadrons as trigger particle and K^0_s and $\Lambda(\bar{\Lambda})$ as associated particles at $|\eta|$ <0.8 are measured as a function of the azimuthal angle difference $\Delta\phi$ and pseudo-rapidity difference $\Delta\eta$. K^0_s and Λ decay into $\pi^+ + \pi^-$ and $p^+ + \pi^-$ with a characteristic decay pattern, called V^0. Topological cuts are required to reduce the combinatorial background. The correlation function as a function of $\Delta\eta$ and $\Delta\phi$ between two charged particles is defined as $\frac{1}{N_{\rm trig}}\frac{{\rm d}^2N_{\rm asso}}{{\rm d}\Delta\eta{\rm d}\Delta\phi} = \frac{S(\Delta\eta,\Delta\phi)}{B(\Delta\eta,\Delta\phi)}$, where $N_{\rm trig}$ is the total number of triggered particles in the event class and $p_{\rm T}$ interval, the signal distribution $S(\Delta\eta,\Delta\phi) = \frac{1}{N_{\rm trig}}\frac{{\rm d}^2N_{\rm same}}{{\rm d}\Delta\eta{\rm d}\Delta\phi}$ is the associated yield per trigger particle from the same event, and the background distribution $B(\Delta\eta,\Delta\phi) = \alpha\frac{{\rm d}^2N_{\rm mixed}}{{\rm d}\Delta\eta{\rm d}\Delta\phi}$ accounts for pair acceptance and pair efficiency. B is constructed by taking the correlations between the trigger particles in one event and the associated particles in other events in the same event class. The α factor is chosen so that it is unity at $\Delta\eta \sim 0$ because the acceptance is flat along $\Delta\phi$. This correlation function is studied for different $p_{\rm T}$ intervals and different event classes. The correlation function in peripheral collisions is subtracted from that in central collisions to remove the auto-correlations from jets. Figure 1 shows the projection of the subtracted correlation functions onto $\Delta\phi$. To quantify azimuthal anisotropy (v_2), the Fourier coefficients are extracted by fitting with the function $a_0 + 2a_1\cos(\Delta\phi) + 2a_2\cos(2\Delta\phi)$. The $v_{\rm n}$ coefficient can be obtained as $v_{\rm n}^{{\rm K^0_s},\Lambda} = V_{\rm n}^{{\rm K^0_s},\Lambda}/\sqrt{V_{\rm n}^{\rm h-h}}$, where $V_n^i = a_{\rm n}^{\rm i}/(a_0^{\rm i} + b^{\rm i})$, in which i is the index of h-h or h-V0 pairs (h denotes undefined hadrons) and b is the baseline determined by averaging over 1.2< $|\Delta\eta|$ <1.6 on the near side of the 60-100% event class. Figure 2 shows the extracted v_2 coefficient for K^0_s and $\Lambda(\bar{\Lambda})$ compared to p and K as a function of $p_{\rm T}$. Mass ordering between the v_2 of K^0_s and $\Lambda(\bar{\Lambda})$ as well as the kaon and proton is observed.

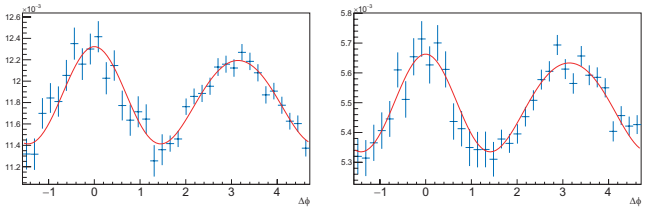

Fig. 1. Projection of the subtracted correlation functions of the associated K^0_s (top) and Λ (bottom) yield per trigger particle with 1.5<$p_{\rm T,trig}$, $p_{\rm T,asso}$ <2.5 GeV.

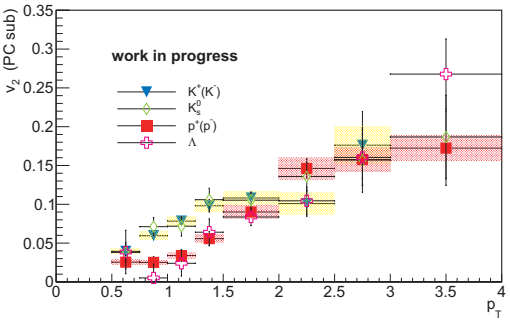

Fig. 2. v_2 of K^0_s, $\Lambda(\bar{\Lambda})$ compared with one of kaon and proton. Error bars and shaded bands show statistical uncertainties and systematic, respectively.

*1 RIKEN Nishina Center
*2 Center for Nuclear Study, the University of Tokyo

References

1) STAR Collaboration, Phys. Rev. C**80** 064912 (2009)
2) PHOBOS Collaboration, Phys. Rev. Lett. **104** 062301(2010)
3) CMS Collaboration, JHEP **09** 091(2010)
4) ALICE Collaboration, Phys. Lett. B, **726** 164-177(2013)

Search for exotic dibaryons at LHC-ALICE

K. Terasaki,[*1,*2] H. Hamagaki,[*2] and T. Gunji[*2]

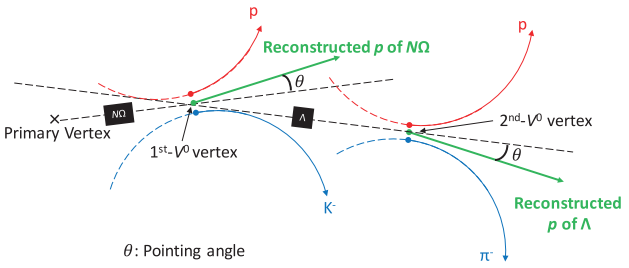

Fig. 1. Decay topology of the $N\Omega$ dibaryon.

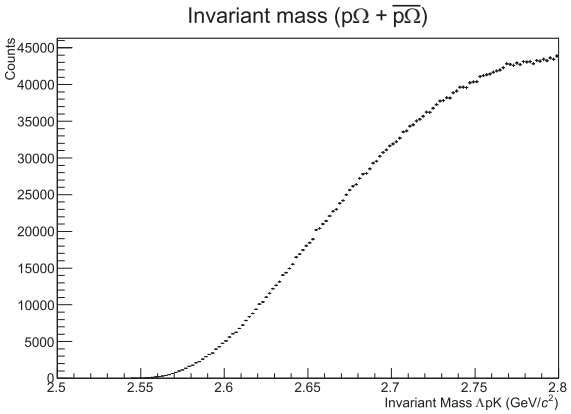

Fig. 2. Invariant mass distribution for ΛpK in Pb-Pb collisions.

H dibaryon (uuddss)[1] is one of the most investigated dibaryon candidates and its experimental searches were recently carried out in heavy-ion collisions, where various hadrons are produced abundantly [2,3]. Besides exploring a bound state of dibaryons, the measurements of baryon-baryon correlations provide us with the information on baryon-baryon interactions and equation of the state for dense matter.

ALICE is the dedicated experiment to study Quark Gluon Plasma (QGP), a hot and dense Quantum chromodynamics (QCD) medium, via heavy-ion collisions at LHC. The two main tracking detectors in the central barrel are the Inner Tracking System (ITS) and the Time Projection Chamber (TPC). The ITS consists of six cylindrical layers of silicon detectors for particle tracking and reconstructing the secondary vertex. The TPC surrounds the ITS and comprises a 90 m^3 cylinder filled with $Ne/CO_2/N_2$ (90/10/5). It is also used for particle identification via the energy deposit (dE/dx) measurement.

As a dibaryon candidate other than H dibaryon, it is predicted by lattice QCD calculations that the $N\Omega$ system has enough attraction to form a bound state[4]. The analysis strategy for searching $N\Omega$ is based on topological particle identification. The decay pattern is shown in Fig. 1.

Our assumed decay topology of the $N\Omega$ dibaryon is as follows.

(1) $N\Omega$ dibaryon decays into p, K^-, and Λ at the 1st-V^0 vertex.
(2) Λ decays into p and π^- at the 2nd-V^0 vertex.

The reconstruction of a $N\Omega$ candidate via this decay topology starts with the reconstruction of Λ (i.e., the search of the 2nd-V^0 vertex in Fig. 1). The V^0 decays are determined by two tracks that are emitted from a secondary vertex and might come close to each other. The minimum distance between the two tracks is called the Distance-of-Closest-Approach (DCA). The V^0 decay point is determined using DCA. The protons and pions are selected from all 2nd-V^0 candidates and the invariant mass of Λ is calculated. In a similar way, the 1st-V^0 vertex is determined by selecting protons and kaons from all V^0 candidates. A criterion for selecting the appropriate 1st- and 2nd-V^0 candidate is the cut on the pointing angle. It is the angle between the reconstructed flight-path and the reconstructed momentum of the V^0 particle.

Figure 2 shows the invariant mass distribution in the decay channel $N\Omega \to \Lambda pK$ for Pb-Pb data at $\sqrt{s_{NN}} = 2.76$ TeV. A 3σ dE/dx cut in the TPC is used for the PID of p, K, and π. The invariant mass of Λ at 2nd-V^0 is restricted between 1.111 GeV/c^2 $< m_\Lambda <$ 1.120 GeV/c^2 and is combined with the four-vectors of proton and kaon at the 1st-V^0 vertex. The cuts on the DCA and the cosine of the pointing angle for both V^0 vertex are < 1.0 cm and > 0.9, respectively. There is no significant signal in the invariant mass distribution so far, however the cut optimization is ongoing. Other dibaryon candidates such as $\Omega\Omega$, $\Lambda^*\Lambda^*$ will also be evaluated.

*1 RIKEN Nishina Center
*2 Center for Nuclear Study, Graduate School of Science, University of Tokyo

References
1) R. L. Jaffe, Phys. Rev. Lett. **38**, 195 (1977).
2) N. Shah for the STAR Collaboration, Nucl. Phys. A **914**, 410 (2013).
3) ALICE Collaboration arXiv:1506.07499 [nucl-ex] CERN-PH-EP-2015-069.
4) F. Etminan et al. (HAL QCD Collaboration), Nucl. Phys. A **928**, 89 (2014).

RHICf experiment to measure cross section and asymmetry in very forward neutral particle production at RHIC

T. Sako*1 for the RHICf Collaboration

The origin of cosmic rays is a long-standing mystery in astrophysics. To determine the energy and particle type of the primary cosmic ray from the observed air shower particle distributions, we rely on the Monte Carlo simulation of air showers. However, the lack of knowledge in hadronic interaction modeling results in uncertainty in this interpretation. To understand this process, the Large Hadron Collider forward (LHCf) experiment[1] measured forward particle production at the LHC up to the particle energy in a fixed target setting of 9×10^{16} eV ($\sqrt{s}$=13 TeV). LHCf reported a scaling of π^0 production spectra at $\sqrt{s}$=2.76, and 7 TeV proton-proton collisions[2]; in addition, it continues analyzing 13 TeV data. To confirm the scaling or its violation in a wider energy range and to extrapolate the knowledge beyond the LHC energy range, the RHICf collaboration was launched.

Another mystery in forward particle production, single transverse-spin asymmetry (SSA), was found in the RHIC experiments[3]. It is believed that the SSA in neutron production originates from the interference between the amplitudes of spin-flip pion exchange and non spin-flip meson exchange. SSA can shed light on the fundamental process of forward particle production and improve our understanding of air shower development. The excellent position resolution of the RHICf detector improves the measurement accuracy of SSA and enables us to test the proposed mechanism[4].

For RHICf, an LHCf detector is installed in front of the zero degree calorimeter of the STAR experiment,

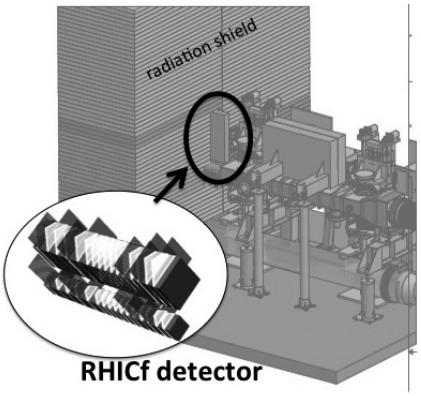

Fig. 1. CAD drawing of the RHICf installation. The RHICf detector can fit in the narrow slot of the radiation shield near the STAR interaction point.

*1 Institute for Space-Earth Environmental Research / Kobayashi-Maskawa Institute for the Origin of Particles and the Universe, Nagoya University

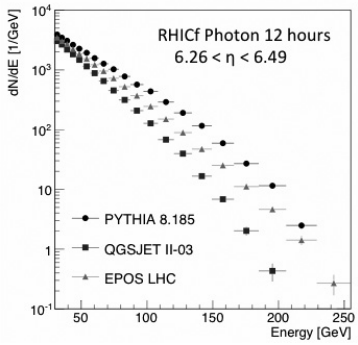

Fig. 2. Expected photon spectra observed in 12h operation for three different hadronic interaction models.

as shown in Fig.1[5]. The proton-proton collisions with $\sqrt{s}$ =510 GeV at the RHIC enable RHICf to study particle production at the cosmic-ray equivalent energy of 1.4×10^{14} eV. Figure 2 shows the expected photon spectra observed in RHICf operation for 12h. It is found that the statistical errors are negligibly small with respect to the difference between predictions by three major hadronic interaction models. RHICf will also measure spectra, or differential cross sections, of π^0's and neutrons. In neutron measurement, RHICf has a position determination resolution better than 1 mm[6], while the former SSA measurements were performed with 10 mm resolution.

Although the original plan for RHICf was to operate it in the PHENIX site[7], according to the long-term plan of RHIC, RHICf was finally approved by PAC in 2015 to be operated in 2017 with STAR. The detailed plan of installation, commissioning, and data collection were intensively discussed with the STAR team in 2015. The STAR and RHICf teams have exchanged an MOU in early 2016.

References

1) LHCf Technical Design Report, CERN-LHCC-2006-004.
2) O. Adriani et al.: PRD received, arXiv:1507.08764 [hep-ex].
3) Y. Fukao, M. Togawa, et al.: Phys. Lett. B **650**, 325 (2007).; PHENIX Collaboration, Phys. Rev. D **88**, 032006 (2013).
4) B. Z. Kopeliovich, I. K. Potashnikova, I. Schmidt, and J. Soffer: Phys. Rev. D **84**, 114012 (2011).
5) RHICf Collaboration, LOI, arXiv:1401.1004; proposal, arXiv:1409.4860.
6) K. Kawade et al.: JINST, **9** P03016 (2014).
7) Y. Goto for the RHICf Collaboration: RIKEN Accel. Prog. Rep. **48**, 107 (2015).

Fragmentation function measurements in Belle†

R. Seidl,[*1] F. Giordano,[*2] M. Leitgab,[*2] A. Vossen,[*3] H. Li,[*3] W. W. Jacobs,[*3] N. Kobayashi,[*4] M. Grosse-Perdekamp,[*2] A. Ogawa,[*5] C. Hulse[*6] and G. Schnell[*6,*7]

Fragmentation functions (FFs) describe the transition of highly-energetic, asymptotically free partons into final state hadrons. They are a quantity which cannot be obtained from first principles QCD but need to be extracted from experiments. In turn FFs can be used as a tool to extract information about the nucleon structure for different parton flavors. In particular, FFs are commonly used in polarized semi-inclusive deep-inelastic scattering and proton-proton collisions to access the spin structure of the nucleon. The cleanest way to access FFs is in electron-positron annihilation due to the lack of hadrons in the initial state. However, only charge square weighted sums over all kinematically availabe quarks and antiquarks are accessible at leading order of the strong coupling α_S in e^+e^- annihilation. To overcome this partially, instead of detecting a single hadron in the final state, two hadrons, preferrably in opposite hemispheres as defined by the thrust axis, have been measured. The combination of charges and hadron types then gives additional information about the FFs if one assumes the hadrons to be fragmenting off different partons. For example, same-sign pions and opposite sign-pions contain different combinations of favored (e.g., $u \to \pi^+$) and disfavored ($d \to \pi^+$) FFs when considering up and down type (anti)quarks only.

The di-hadron cross sections have been extracted from a dataset of 655 fb^{-1} taken by the Belle experiment at the asymmetric-energy e^+e^- collider KEKB. The data was corrected for particle-misidentification, momentum smearing, contributions of QED processes not related to fragmentation (such as τ pair production), acceptence and efficiencies as well as initial state photon radiation[1]. The final cross sections were then extracted for 6 pion and kaon and charge combinations with different physics content. The cross sections, differential in the fractional energies of the two hadrons $z_{1,2} = 2E_{h,1,2}/\sqrt{s}$ relative to the initial, leading order parton energies $\sqrt{s}/2$, can be seen in Fig. 1. For the same hadron types the same sign combinations are generally suppressed in comparison to opposite sign combinations. Additional strangness, especially if likely being created in the fragmentation process such as for same sign kaons seems further suppressed. The assumption whether di-hadrons originated from the same parton or different partons has been tested by selecting hadron pairs in the same or opposite hemispheres when applying an additional thrust criterion. As can be seen in Fig. 2, same-hemisphere dihadrons decrease rapidly as soon as the sum of their fractional energies exceeds unity in agreement that opposite-hemisphere di-hadrons are generally produced off different partons.

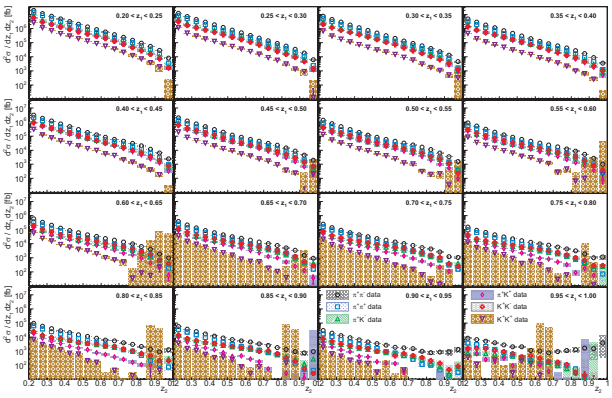

Fig. 1. Di-hadron cross sections as a function of fractional energy z_2 in bins of the fractional energy z_1 without a topology requirement on the two hadrons. Individual hadron combinations are $\pi^+\pi^-$ (black), $\pi^+\pi^+$ (blue), π^+K^- (green), π^+K^+ (pink), K^+K^- (red) and K^+K^+ (purple) including systematic uncertainties as shaded areas.

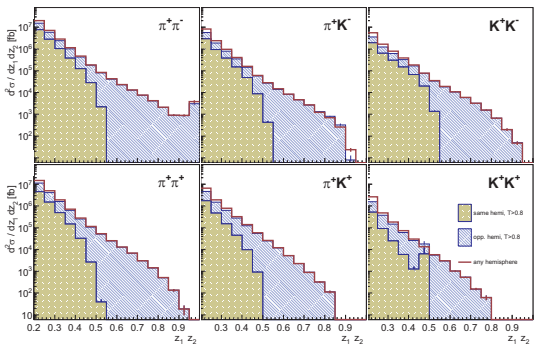

Fig. 2. Stacked di-hadron cross sections as a function of the diagonal fractional energy ($z_1 = z_2$) bins for same (grey area) and opposite (blue area) hemispheres and in comparison to no hemisphere and thrust selection (red).

† Condensed from the article in Phys. Rev. **D92**, 092007 (2015)

*1 RIKEN Nishina Center
*2 Physics department, University of Illinois
*3 Physics department, Indiana University
*4 Department of Physics, Tokyo Institute of Technology
*5 Brookhaven National Laboratory
*6 Department of Physics, University of the Basque Country
*7 Ikerbasque

References

1) M. Leitgab *et al.* [Belle Collaboration], Phys. Rev. Lett. **111**, 062002 (2013).

Progress of Drell–Yan experiment by SeaQuest at Fermilab

K. Nagai,[*1,*2] Y. Goto,[*2] Y. Kunisada[*1] Y. Miyachi,[*3] S. Miyasaka,[*1] K. Nakano,[*1] S. Nara,[*3] S. Sawada,[*2,*4] T.-A. Shibata,[*1,*2] S. Tamamushi[*1] for the E906/SeaQuest Collaboration

The E906/SeaQuest experiment is a Drell–Yan experiment at Fermi National Accelerator Laboratory (Fermilab). SeaQuest aims to accurately measure the flavor asymmetry of antiquarks ($\bar{d}/\bar{u}$) in the proton at large Bjorken x ($0.1 \lesssim x \lesssim 0.45$). E866 measured the flavor asymmetry around Bjorken $x \sim 0.3$. E866 indicated that the flavor asymmetry decreases in that region, although the uncertainty was large.[1)] The behavior has not been reproduced by any theory. The measurement by SeaQuest will improve the understanding of the internal structure of the proton.

The flavor asymmetry is derived from the ratio of proton-proton and proton-deuteron Drell–Yan cross sections. SeaQuest uses a 120-GeV proton beam extracted from Fermilab Main Injector and liquid target of hydrogen and deuterium. A pair of μ^- and μ^+ is created in the Drell–Yan process. It passes through a focusing magnet, which is located right behind the targets. The muon pair is detected by four tracking stations (Stations 1, 2, 3, and 4). Stations 1, 2, and 3 consist of drift chambers and hodoscopes. Station 4 consists of proportional tubes and hodoscopes. Station 4 is located behind a hadron absorber and is used for the identification of the muons. Another magnet is placed between Station 1 and Station 2 in order to determine muon momenta. We reconstruct the muon momenta using hit positions measured at the four stations.

SeaQuest acquired 0.8×10^{18} beam protons on target for 20 months from 2013 to 2015. It started acquiring another set of data in October 2015. In total, we will accumulate 3.4×10^{18} beam protons on target.

Two months' data acquired in 2014 are used to perform the data analysis. We successfully reconstructed the invariant-mass (M) distribution of muon pairs.[2)] The Drell–Yan events were selected with $M > 4.2$ GeV. Figure 1 shows the z-vertex distribution of muon pairs. The hydrogen and deuteron targets are located at $z = -150$ cm through -100 cm, and a beam dump, which is the iron core of the focusing magnet, is located at $z = 0$ cm through 500 cm. The closed circles in Fig. 1 are all the muon pairs in the real data. The open circles at $z < -50$ cm are the muon pairs that originate from the target, and the open circles at $z > -50$ cm are the muon pairs that originate from the beam dump. The muon pairs around $z = -50$ cm are discarded because the z-vertices are highly inaccurate and it cannot be determined where the muon pairs originated from. The open circles are consistent with the distributions estimated by the simulation (the solid lines) well except for the upstream region ($z \sim -200$ cm).

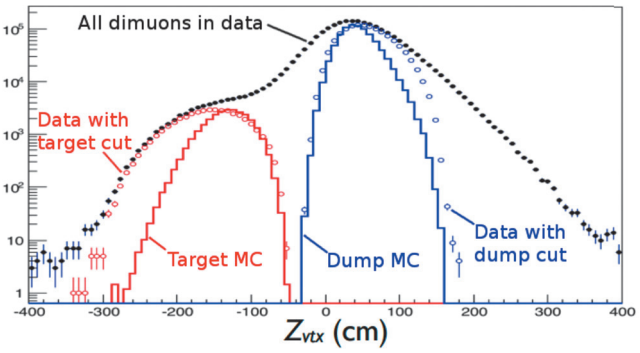

Fig. 1. The z-vertex distribution of muon pairs whose invariant masses are larger than 4.2 GeV/c^2. The circles show z-vertex distribution of the muon pairs in real data. The solid lines are estimated z-vertex distributions of muon pairs from target (red line) and that of muon pairs from dump (blue line) in the simulation.

The z-vertex of muon pairs from the target in the real data distributes around $z = -160$ cm, which is slightly more upstream than the actual target position ($-150 < z < -100$ cm). This is because the calibration of the magnetic field is not accurate by 2%. It has been tuned.

A very preliminary result of the flavor asymmetry was derived using the two months of data. The systematic uncertainty is large at present, mostly arising from the beam-intensity dependence of measurement efficiencies. We are improving the analysis method to minimize the systematic uncertainty.

References

1) E.A. Hawker et al.: Phys. Rev. Lett. **80**, 3715 (1998).
2) K. Nagai et al.: RIKEN Accel. Prog. Rep., **48**, 123 (2015).

*1 Graduate School of Science and Engineering, Tokyo Institute of Technology
*2 RIKEN Nishina Center
*3 Faculty of Science, Yamagata University
*4 Institute of Particle and Nuclear Studies, KEK

5. Hadron Physics (Theory)

P-odd spectral density of quark-gluon plasma at weak coupling

H. -U. Yee[*1,*2]

Topological fluctuations of QCD is one of the fundamental aspects of QCD dynamics in the plasma of quarks and gluons. They lead to thermal fluctuations of axial charge density that has distinct P- and CP-odd parities, which induces several unique phenomena such as chiral magnetic effect[1]. At weak coupling regime in high enough temperature, the rate of topological fluctuations is $\Gamma_s \sim \alpha_s^5 \log(1/\alpha_s) T^4$, and this dependence on the coupling constant also governs how fast the axial charge, once created, decays in time. If the time scale one is interested in is faster than this, the axial charge is approximately conserved. The boundary of validity regime of hydrodynamics is $\alpha_s^2 T$, the scale of hard electromagnetic probes such as photon emission rates is $d\Gamma/d^3k \sim \alpha_{EM}\alpha_s T$, the scale of heavy quark momentum diffusion is $\kappa \sim \alpha_s^2 T^3$, and the jet quenching parameter is $\hat{q} \sim \alpha_s^2 T^3$. Therefore, for many interesting dynamics in the quark-gluon plasma at weak coupling regime, the axial charge can be considered as a conserved charge.

Due to its unique P- and CP-odd parities, the axial charge leads to an interesting P-odd structure in the current-current thermal correlation functions of the plasma. The retarded current-current correlation function $G_R^{ij}(k) \equiv (-i)G_{ra}^{ij}(k) = (-i)\langle J_r^i(k) J_a^j(-k)\rangle$ written in the ra-basis of Schwinger-Keldysh formalism, encodes "chiral magnetic conductivity"[2] $\sigma_\chi(k)$ by $G_R^{ij}(k) \sim i\sigma_\chi(k)\epsilon^{ijl}k^l$, that is responsible for the chiral magnetic effect with arbitrary momentum of the magnetic field: $\vec{J} = \sigma_\chi(k)\vec{B}(k)$. It has been well-established that the zero momentum limit of $\sigma_\chi(k)$ is topologically protected by chiral anomaly coefficient: $\lim_{k\to 0}\sigma_\chi(k) = N_c N_F \mu_A/(2\pi^2)$ where μ_A is axial chemical potential.

To get a better picture of full real-time P-odd correlation functions, one starts with the fluctuation-dissipation relation

$$G_{rr}^{ij}(k) = \big(1/2 + n_B(k^0)\big)\,\rho^{ij}(k)\,, \tag{1}$$

where $\rho^{ij}(k) \equiv \big(G_{ra}^{ij}(k) - G_{ar}^{ij}(k)\big)$ is the spectral density that governs the strength of thermal fluctuations represented by the left-hand side. From the hermiticity of current operator, one can show that $\rho^{ij}(k)$ is a hermitian matrix in terms of spatial indices i, j: with rotational invariance, it allows to have a P-odd structure $\rho^{ij}(k) \sim i\rho^{\rm odd}(k)\epsilon^{ijl}k^l$ with a real function $\rho^{\rm odd}(k)$. We call $\rho^{\rm odd}(k)$ "P-odd spectral density"[3]. It is easy to show that it is the imaginary part of the chiral magnetic conductivity: $\rho^{\rm odd}(k) = -2\,{\rm Im}(\sigma_\chi(k))$.

Contrary to the real part of $\sigma_\chi(k)$ in $k \to 0$ limit, the P-odd spectral density is sensitive to real-time thermal dynamics of quark-gluon plasma as it governs the P-odd part of thermal current-current fluctuations, and it shares many common features with the P-even spectral density that is responsible for dissipative transport coefficients in hydrodynamic regime. Like P-even spectral densities, $\rho_{\rm odd}(k)$ is an odd function of $k^0 \equiv \omega$ with a small ω expansion $\rho^{\rm odd}(k) \sim 2\xi_5\omega + \cdots$, where ξ_5 is one of the second order transport coefficients in chiral anomalous hydrodynamics[4]: $\vec{J} = \sigma_0\vec{B} + \xi_5 d\vec{B}/dt$. Like the ordinary electric conductivity, the ξ_5 turns out to be non-analytic in coupling constant, and the leading log computation requires a re-summation of all ladder diagrams with HTL re-summation of exchanged gluons, that eventually leads to solving second order differential equations in momentum space. For 2-flavor QCD, we have obtained[3]

$$\xi_5 = -\frac{2.003}{g_s^4\log(1/g_s)}\frac{\mu_A}{T}\,. \tag{2}$$

For other kinematics of momentum k, the P-odd spectral density generally gives P- and CP-odd emission rates of spin-polarized (that is, circular polarized) virtual photons with momentum k. To see this, the unique P- and CP-odd observable in photon emissions is given by the spin polarization[5]: $\Gamma^{\rm odd} = \Gamma(\epsilon^+) - \Gamma(\epsilon^-)$ where $\epsilon^\pm$ are circular polarization vectors of photons. Using the results in Ref.[5] that relates $\Gamma^{\rm odd}$ with the P-odd part of current-current correlation functions, one can show that

$$\frac{d\Gamma^{\rm odd}}{d^3k} = -\frac{e^2}{(2\pi)^3}n_B(\omega)\rho^{\rm odd}(k)\Big|_{\omega=|\vec{k}|}\,. \tag{3}$$

We have computed $d\Gamma^{\rm odd}/d^3k$ in complete leading order at weak coupling[6], by computing 1) hard Compton/pair annihilation rates, 2) soft t- or u-channel exchange contributions with HTL re-summation, and 3) Landau-Pomeranchuk-Migdal re-summation of soft collinear Bremstrahlung and inelastic pair annihilation processes.

*1 Department of Physics, University of Illinois
*2 RIKEN Nishina Center

References
1) K. Fukushima, D. E. Kharzeev and H. J. Warringa, Phys. Rev. D **78**, 074033 (2008).
2) D. E. Kharzeev and H. J. Warringa, Phys. Rev. D **80**, 034028 (2009).
3) A. Jimenez-Alba and H. U. Yee, Phys. Rev. D **92**, no. 1, 014023 (2015).
4) D. E. Kharzeev and H. U. Yee, Phys. Rev. D **84**, 045025 (2011).
5) K. A. Mamo and H. U. Yee, Phys. Rev. D **88**, no. 11, 114029 (2013).
6) K. A. Mamo and H. U. Yee, arXiv:1512.01316 [hep-ph].

Legendre expansion of longitudinal two-particle correlations

A. Monnai*1 and B. Schenke,*2

One of the most remarkable findings regarding high-energy heavy ion colliders is the fluidity of the quark-gluon plasma (QGP), which is supported by the fact that the anisotropy of azimuthal momentum distribution, characterized by the Fourier coefficients v_n, is large compared with that of the geometrical shape of the produced medium. Thus far, numerous efforts have been made to understand the transverse dynamics of the QGP by introducing event-by-event fluctuations as well as off-equilibrium corrections.

However, the longitudinal dynamics has not been throughly investigated. The isotropization mechanism in a heavy-ion system is not fully understood, and no direct experimental evidence for the fluidity of the QCD medium in the longitudinal direction has been found yet.

In this study, we extend the (3+1)-dimensional viscous hydrodynamic model MUSIC[1] to finite baryon density and introduce more realistic setups to study the forward rapidity dynamics. For longitudinally and transversely fluctuating initial conditions, the Monte-Carlo Glauber model is extended to three dimensions by introducing a variation of the Lexus model,[2] where the modification of the rapidity distribution of the valence quarks after each sub-collision is taken into account to calculate the net baryon distribution. The modification is controlled by the kernel

$$Q(y-y_P, y_P-y_T, y-y_P) = \lambda \frac{\cosh(y-y_P)}{\sinh(y_P-y_T)} + (1-\lambda)\delta(y-y_P), \quad (1)$$

where y is the rapidity and the subscripts T and P denote target and projectile, respectively. λ is a parameter to be determined experimentally. The entropy distribution is obtained by depositing entropy between the last sub-collision pairs. The finite-density equation of state is constructed by interpolating those of hadron resonance gas and lattice QCD, where the latter is obtained in the Taylor expansion method, at a connecting temperature near the crossover. Relaxation-type equations derived from the kinetic theory are employed as the viscous hydrodynamic equations.

We probe the longitudinal properties of the QGP in hydrodynamics by decomposing the two-particle rapidity correlation into Legendre polynomials, which have recently been measured at the ATLAS Collaboration at the CERN Large Hadron Collider,[3]

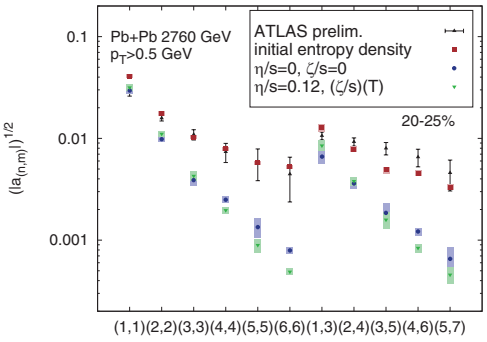

Fig. 1. (Color online) Calculations of $\sqrt{|a_{n,m}|}$ compared with experimental data.

$$a_{n,m} = \int C_N(\eta_1,\eta_2) \times \frac{T_n(\eta_1)T_m(\eta_2)+T_n(\eta_2)T_m(\eta_1)}{2}\frac{d\eta_1}{Y}\frac{d\eta_2}{Y}, \quad (2)$$

where $T_n(\eta_p) = \sqrt{n+1/2}P_n(\eta_p/Y)$ is the scaled Legendre polynomial and C_N is the two-particle correlation defined as

$$C_N(\eta_1,\eta_2) = \frac{C(\eta_1,\eta_2)}{C_p(\eta_1)C_p(\eta_2)}, \quad (3)$$

$$C_p(\eta_1/2) = \frac{1}{2Y}\int_{-Y}^{Y} C(\eta_1,\eta_2)d\eta_{2/1}, \quad (4)$$

to remove the effects of residual centrality dependence. Note that a good analogy can be made between this quantity and the transverse flow harmonics v_n.

Figure 1 shows $\sqrt{|a_{n,m}|}$ before and after the hydrodynamic evolution of Pb-Pb collisions at 2.76 TeV for 20-25% centrality. As shown, the hydrodynamic result is close to the LHC data at $n = 1$ but has stronger n dependence. The hydrodynamic evolution tends to smear out short range correlations more efficiently. Viscous effects are small. The Legendre coefficients of the initial entropy distribution appear to agree with the data, but the estimations at different centralities indicate that this is a coincidence. This disagreement may be due to the lack of post-hydrodynamic treatments. Our recent calculations suggest that they agree with experimental data when short range correlations from resonance decays are considered.[4]

† Condensed from the articles in Phys. Lett. B **752**, 317 (2016)
*1 RIKEN Nishina Center
*2 Physics Department, Brookhaven National Laboratory, Upton, NY 11973, USA

References
1) B. Schenke, S. Jeon, C. Gale, Phys. Rev. Lett. **106**, 042301 (2011).
2) S. Jeon, J. I. Kapusta, Phys. Rev. C **56**, 468 (1997).
3) Tech. Rep. ATLAS-CONF-2015-020, CERN, Geneva, 2015.
4) G. Denicol *et al.*, in preparation.

Constraining shear viscosity of QCD matter at forward rapidity†

G. Denicol,*1 A. Monnai*2 and B. Schenke*1

The quark-gluon plasma (QGP) is a high-temperature phase of QCD. Its materialization at BNL Relativistic Heavy Ion Collider and LHC Large Hadron Collider has opened up a possibility to observe the QCD medium quantitatively. One of the goals of heavy-ion phenomenology is to constrain the microscopic properties of the QGP, namely, the equation of state (EoS) and the transport coefficients. With the advent of lattice QCD techniques, we have a good understanding of the EoS near the vanishing chemical potential; however speculations still surround the transport coefficients. One such conjecture is the *lower boundary* of shear viscosity, $\eta/s = 1/4\pi$, derived from the framework of the Anti-de Sitter/conformal field theory (AdS/CFT) correspondence[1].

We use a full three-dimensional viscous hydrodynamic model MUSIC[2] to explore *forward rapidity* regions. In particular, we show in our description of the experimental data that the AdS/CFT-conjectured minimum boundary would not hold in QCD.

The input to the hydrodynamic model are chosen as follows[3]. The fluctuating initial conditions for the entropy and the net baryon distribution are calculated using the Monte-Carlo Glauber model with rapidity dependence implemented by the modified Lexus model. The EoS is that of (2+1)-flavor lattice QCD with the Taylor expansion method, connected to that of hadron resonance gas in low-temperature regions at a connecting temperature T_c. Since the hadron gas at low T and the perturbative QCD gas at high T are known to have large viscosity, we can parametrize the shear viscosity as

$$\begin{aligned}(\eta T/(\epsilon+P))(T) &= (\eta T/(\epsilon+P))_{\rm min} \\ &+ a\times(T_c-T)\theta(T_c-T) \\ &+ b\times(T-T_c)\theta(T-T_c), \end{aligned} \quad (1)$$

where $(\epsilon+P)/T$ replaces s in the finite density system considered in this study. The four scenarios are plotted in Fig. 1. Hydrodynamic and initial condition parameters are independently chosen for each scenario so that rapidity distribution is reproduced.

Figure 2 shows the numerical results on the rapidity dependence of elliptic flow v_2 in Au-Au collisions at $\sqrt{s_{NN}} = 200$ GeV for four different sets of a and b. We see that $(\eta T/(\epsilon+P))_{\rm min} = 0.04$ with large hadronic viscosity is favored by the PHOBOS Collaboration data[4]. Similarly, our calculation of triangular flow v_3 indicates that the $b = 2$ scenario is better than the $b = 0$ one. It is worth noting that (i) the temperature-independent

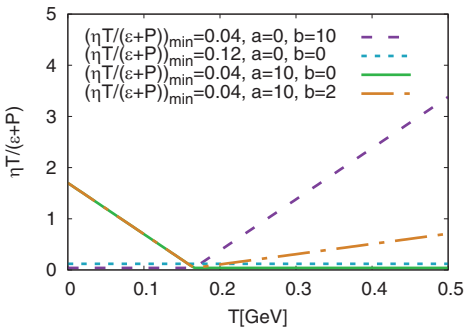

Fig. 1. (Color online) Four models of temperature-dependent shear viscosity.

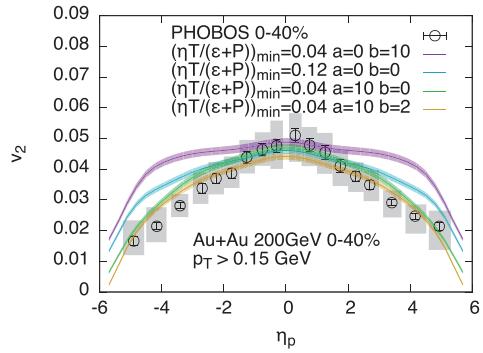

Fig. 2. (Color online) Rapidity dependence of v_2 for different $\eta T/(\epsilon+P)$ parameterizations.

$\eta T/(\epsilon+P) = 0.12$, which has been known to work well at mid-rapidity, is not preferred at forward rapidity, and (ii) this is an experimental indication that the AdS/CFT minimum boundary $\eta/s = 1/4\pi \simeq 0.08$ can be crossed near the quark-hadron crossover. It can be interpreted that one needs a much smaller minimum than what was conventionally used for the whole temperature range when temperature dependence is introduced because of the effects of large shear viscosity at lower and higher temperatures.

References
1) P. Kovtun, D. T. Son, A. O. Starinets, Phys. Rev. Lett. **94**, 111601 (2005).
2) B. Schenke, S. Jeon, C. Gale, Phys. Rev. Lett. **106**, 042301 (2011).
3) A. Monnai, B. Schenke, Phys. Lett. B **752**, 317 (2016).
4) B. B. Back *et al.* [PHOBOS Collaboration], Phys. Rev. C **72**, 051901 (2005).

† Condensed from the articles in arXiv:1512.01538 [nucl-th]

*1 Physics Department, Brookhaven National Laboratory
*2 RIKEN Nishina Center

Axial current generation by P-odd domain in QCD matter†

I. Iatrakis,[*1] S. Lin,[*2] and Y. Yin[*3]

It is believed that parity-odd domains are produced in heavy ion collisions. The effect of parity odd domains can be modeled by an external θ field, which couples to topological charge density $q = \frac{g^2}{32\pi^2}\epsilon^{\mu\nu\rho\sigma} tr G_{\mu\nu} G_{\rho\sigma}$, where g is the strong coupling constant and G is the gluon field strength. An external θ field can induce nonvanishing q. According to the axial anomaly equation

$$\partial_\mu J^\mu_A = -2q, \tag{1}$$

a nonvanishing q can generate chiral imbalance, which can be characterized by axial chemical potential μ_A. The μ_A is a key component of the chiral magnetic effect (CME). The CME predicts the generation of electric current along an external magnetic field in deconfined quark-gluon plasma with chiral imbalance[1)]

$$\mathbf{j}_V = \frac{N_c e^2}{2\pi^2}\mu_A \mathbf{B}. \tag{2}$$

The CME is currently being intensvely researched through heavy ion collision experiments at relativistic heavy ion collider (RHIC) and large hadron collider (LHC). The goal of this paper is to explore the response of the axial current to the θ field and the backreaction of the axial charge to the θ field.

We can write the response of q to θ as $q(\omega, k) = -G^R(\omega, k)\theta(\omega, k)$, with the response function in the hydrodynamic limit given by

$$G^R(\omega, k) = -\chi - \frac{i\Gamma_{CS}\omega}{2T} - \frac{\kappa_{CS}}{2}k^2 + \cdots. \tag{3}$$

Here, the first term represents the topological susceptibility, which is highly suppressed in deconfined quark-gluon plasma. The second term is the Chern-Simon (CS) diffusion, where Γ_{CS} is the diffusion rate. This term is known to be responsible for axial charge generation. The third term is present when the external θ field is spatially inhomogeneous. We note that the corresponding transport coefficient κ_{CS} is measurable on the lattice in the static limit $\omega \to 0$. It measures the response of q to spatial inhomogeneity of the θ field. More interestingly, we found in a model-independent way that it leads to the generation of axial current along the gradient of θ

$$\mathbf{j}_A = \kappa_{CS}\nabla\theta. \tag{4}$$

We also confirmed the current through a holographic model calculation.[2)] It is worth noting that the holographic calculation also considers the contribution of the conventional diffusive current. We argued that this current could be phenomenologically important in the context of heavy ion collisions as compared to the chiral separation effect and the chiral electric separation effect. A schematic view of axial current generation is shown in Fig.1.

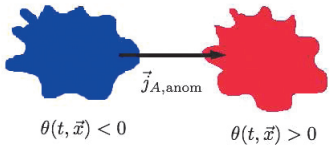

Fig. 1. A schematic view of axial current generation along the gradient of the θ field.

We also considered the backreaction of the axial charge to the effective θ field. In the homogeneous limit $k = 0$, the θ field generates an axial charge density

$$n_A = \frac{\Gamma_{CS}}{T}\theta \tag{5}$$

through the diffusion of the topological charge and axial anomaly. Using axial charge susceptibility χ_A (not to be confused with topological susceptibility), it gives rise to an axial chemical potential

$$\mu_A = \left(\frac{\Gamma_{CS}}{\chi_A T}\right)\theta. \tag{6}$$

Following Ref.[3)], we identify μ_A with $\partial_t\theta$. By comparing this with Eq. 6, we obtain an exponential decay for the effective θ field with the decay time scale set as $\tau_{sph} = \frac{\chi_A T}{2\Gamma_{CS}}$. The physical reason for the backreaction is that the presence of axial charge modifies the gluon potential such that the topological charge density is changed to partially balance out the axial charge. This results in a damping of the topological nontrivial configurations like sphaleron. Thus, we refer to τ_{sph} as the sphaleron damping rate. In terms of the θ field, it is realized as the exponential decay of the field. We also confirmed the backreaction in a holographic model calculation.[2)]

References

1) D. Kharzeev, L. McLerran and H. Warringa, Nucl. Phys. A **803**, 227 (2008).
2) I. Iatrakis, S. Lin and Y. Yin, J. of High Energy Phys. **030**, 09 (2015).
3) D. Kharzeev, Annals. Phys. **325**, 205 (2010).

† Condensed from the article in Phys. Rev. Lett. **114**, 25 (2015)

*1 Department of Physics and Astronomy, Stony Brook University
*2 RIKEN Nishina Center
*3 Department of Physics, Brookhaven National Laboratory

Anomalous chiral effects in heavy ion collisions†

J. Liao*1,*2

Anomalous chiral effects, notably the Chiral Magnetic Effect (CME), are remarkable phenomena that stem from highly nontrivial interplay of QCD chiral symmetry, axial anomaly, and gluonic topology. It is of fundamental importance to search for these effects in experiments. The heavy ion collisions provide a unique environment where a hot chiral-symmetric quark-gluon plasma is created, gluonic topological fluctuations generate chirality imbalance, and very strong magnetic fields $|\vec{\mathbf{B}}| \sim m_\pi^2$ are present during the early stage of such collisions. For recent reviews, see[1–3].

The CME predicts the generation of charge current $\vec{\mathbf{J}}$ along magnetic field $\vec{\mathbf{B}}$ for a chiral medium in the presence of axial charge imbalance: $\vec{\mathbf{J}} = C_A \mu_A \vec{\mathbf{B}}$ where μ_A characterizes chirality imbalance. In non-central heavy ion collisions, the CME may lead to an out-of-plane charge separation effect, contributing to the reaction-plane dependent azimuthal correlation observable: $\gamma_{H_\alpha H_\beta} =< \cos(\phi_i + \phi_j - 2\Psi_{\rm RP}) >_{\alpha\beta}$ with H_α, H_β labeling the hadron species and $\phi_{i,j}$ the azimuthal angles of the two final state charged hadrons. The $\Psi_{\rm RP}$ denotes reaction plane angle. However, the measured correlation suffers from elliptic flow driven background contributions and can not be entirely attributed to CME. The separation of flow-driven background and possible CME signal is the most pressing issue in current CME search.

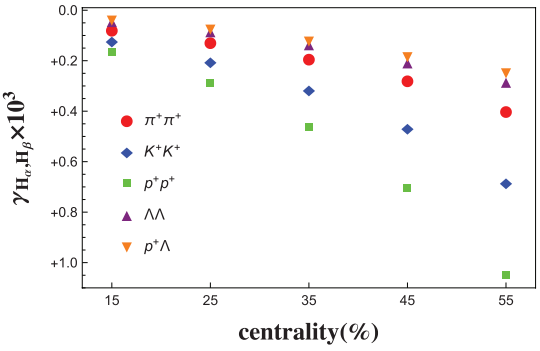

Fig. 1. Correlations $\gamma_{H_\alpha,H_\beta}$ vs centrality for 3-flavor case.

To draw a definitive conclusion, it is vital to develop anomalous hydrodynamic simulations that quantify the CME signals with realistic initial conditions as well as account for background contributions. Recently a first attempt has been made in[4] to consistently quantify contributions to observed charge correlations from both the CME signal and background contributions in one and same framework that integrates anomalous hydro with data-validated bulk viscous hydro simulations. The anomalous hydrodynamic equations for pertinent currents are solved in a linearized way on top of the bulk evolution. The results from this computation have demonstrated that the same-charge correlation data by STAR can be described quantitatively with CME and TMC together, computed with modest magnetic field lifetime ($\sim$ 1fm/c) and realistic initial axial charge density. To further test this interpretation, predictions have been made for the azimuthal correlations of various identified hadron paris (see Fig. 1), to be compared with future data.

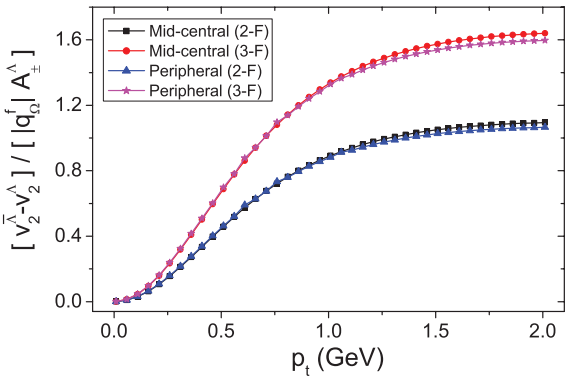

Fig. 2. Normalized $\bar\Lambda$ and Λ elliptic flow splitting, $[v_2^{\bar\Lambda} - v_2^{\Lambda}]/[|q_\Omega^f| A_\pm^\Lambda]$, for symmetric 2-flavor(2-F) and 3-flavor(3-F) cases (for $15-30\%$ and $60-92\%$ centrality).

Studying CME-related anomalous transport phenomena provides an independent avenue for the search of CME. Global fluid rotation (quantified by nonzero vorticity $\vec{\omega}$) bears close similarity to a magnetic field $\vec{\mathbf{B}}$ and can induce Chiral Vortical Effects (CVE). In the presence of fluid rotation, a new gapless collective mode called Chiral Vortical Wave (CVW) has recently been found in[5]. The CVW arises from interplay between vector and axial charge fluctuations induced by CVE. For the rotating quark-gluon plasma in non-central collisions, the CVW-induced charge transport leads to the formation of flavor-wise quadrupole in the fireball. Such phenomenon could be manifested through the elliptic flow splitting of Λ and $\bar\Lambda$ baryons (with predictions shown in Fig. 2) that may be experimentally measured.

† Condensed from the articles in Phys. Rev. D. **92**, 071501(R) (2015) and in Phys. Lett. B **756**, 42 (2016).

*1 RIKEN Nishina Center
*2 Department of Physics, Indiana University

References

1) D. E. Kharzeev, J. Liao, S. A. Voloshin and G. Wang, Prog. Part. Nucl. Phys. **88**, 1 (2016).
2) J. Liao, Pramana **84**, no. 5, 901 (2015).
3) J. Liao, arXiv:1601.00381 [nucl-th].
4) Y. Yin and J. Liao, Phys. Lett. B **756**, 42 (2016).
5) Y. Jiang, X. G. Huang and J. Liao, Phys. Rev. D **92**, no. 7, 071501 (2015).

Transverse momentum dependent jet model for quark fragmentation functions†

W. Bentz *1*2 and K. Yazaki *1

Fragmentation functions (FFs) describe the semi-inclusive production of hadrons in deep inelastic scattering (DIS) of leptons on nuclear targets[1]. The leading order process for the case of pion production is represented by Fig. 1, which shows a high energy virtual quark with momentum k and polarization s after the interaction with the lepton, fragmenting into the observed pion with momentum p and a spectator state, which includes a quark and, in general, also unobserved hadrons. The FF describing this process has the form

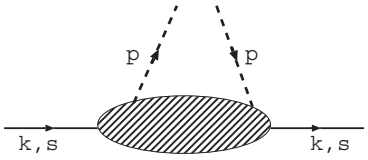

Fig. 1. Cut diagram representing the process where a quark with momentum k and polarization s fragments into a pion with momentum p. The shaded oval represents the spectator states, and the cut goes through the shaded oval.

$$F^{(q\to\pi)}(z,\mathbf{p}_\perp;\mathbf{s}) = D^{(q\to\pi)}(z,\mathbf{p}_\perp^2) + \frac{1}{m_\pi z}\left(\mathbf{p}_\perp\times\mathbf{s}\right)^3 H^{\perp(q\to\pi)}(z,\mathbf{p}_\perp^2)\,, \quad (1)$$

where the direction of the 3-momentum of the fragmenting quark is assumed along the z axis. The produced pion has a fraction z of the initial quark's longitudinal momentum and transverse momentum $\mathbf{p}_\perp$. The two functions in (1) are the unpolarized FF $D^{(q\to\pi)}$ and the so-called Collins function $H^{\perp(q\to\pi)}$. The observed single-spin asymmetries in semi-inclusive pion production in DIS of polarized electrons on unpolarized protons[2] have shown that the Collins function is non-zero, while more precise information has not yet been obtained.

The two FFs of (1) are subject to important sum rules. If we consider only the case of inclusive pion production and quark flavor $SU(2)$ for simplicity, the sum rules for the longitudinal and transverse momentum, and the ispospin sum rule are expressed as follows:

$$\sum_{\tau_\pi}\int_0^1 \mathrm{d}z\, z\int \mathrm{d}^2p_\perp D^{(q\to\pi)}(z,\mathbf{p}_\perp^2) = 1\,, \quad (2)$$

$$\sum_{\tau_\pi}\int_0^1 \frac{\mathrm{d}z}{2zm_\pi}\int \mathrm{d}^2p_\perp \mathbf{p}_\perp^2 H^{\perp(q\to\pi)}(z,\mathbf{p}_\perp^2) = 0\,, \quad (3)$$

$$\sum_{\tau_\pi}\tau_\pi\int_0^1 \mathrm{d}z\int \mathrm{d}^2p_\perp D^{(q\to\pi)}(z,\mathbf{p}_\perp^2) = \frac{\tau_q}{2}\,. \quad (4)$$

Here the isospin labels for the pions and quarks are $\tau_\pi = (1,0,-1)$ for (π^+,π^0,π^-), and $\tau_q = (1,-1)$ for (u,d).

In this work we extend our previous quark-jet model description[3] of the unpolarized FF to the polarized case. In order to account for multi-fragmentation processes, we make a product ansatz for $F^{(q\to\pi)}$ in terms of the functions describing the elementary fragmentation processes. The proper treatment of the spin of the quark in the intermediate states requires several more elementary FFs, in addition to the elementary counterparts of the two functions in (1). We have worked out the coupled integral equations for the two FFs in Eq.(1), which can readily be used for numerical calculations. An important result of our investigation is that the sum rules (2) - (4) are satisfied automatically in this transverse momentum dependent jet-model.

Important tasks for future investigations are to obtain numerical solutions of the integral equations derived in this work, as well as the extension to include additional hadron production channels.

This work was supported by the Japanese Ministry of Education, Culture, Sports, Science and Technology (Kakenhi Grant No. 25400270).

References

1) V. Barone, A. Drago, and P.G. Ratcliffe, Phys. Rept. **359**, 1 (2002).
2) M. Aghasyan et al. (CLAS Collab.), Phys. Lett. **B 704**, 397 (2011).
3) T. Ito, W. Bentz, I.C. Cloët, A.W. Thomas, K. Yazaki, Phys. Rev. **D 80**, 074008 (2009).

† Condensed from an article by W. Bentz et al, to be published in Phys. Rev. **D** (2016).

*1 RIKEN Nishina Center
*2 Department of Physics, Tokai University

Perturbative matching for quasi-PDFs between continuum and lattice

T. Ishikawa*1

Parton distribution functions (PDFs) play an important role in understanding the structure of nucleons. In the search for the nucleon structure through experiment, the PDF is important; however it is currently estimated using the model assumption. Its direct lattice QCD calculation is impossible because it basically involves light-cone dynamics. In principle, the calculation can be made by operator product expansion; this method, however, is quite difficult because in the higher moments, the signal-to-noise ratios worsen. Recently, a strategy has been proposed, in which a computable quantity on the lattice (quasi-PDF) can be related to the (normal) PDF by perturbative matching.[1] The relation between the normal-PDF $q(x,\mu)$ and the quasi-PDF $\widetilde{q}(x,P_3,\Lambda)$ can be written as

$$\widetilde{q}(x,\Lambda,P_3)=\int_{-1}^{1}\frac{dy}{|y|}Z\left(\frac{x}{y},\frac{\mu}{P_3},\frac{\Lambda}{P_3}\right)q(y,\mu)+\cdots, \quad (1)$$

where x is the momentum fraction of the parent hadron being carried by a quark, μ is the renormalization scale, and Λ is the UV cutoff scale. The quasi-PDF is presented by

$$\widetilde{q}(\tilde{x},\Lambda,P_3)=\int\frac{d\delta z}{2\pi}e^{-i\tilde{x}P_3\delta z}\langle\mathcal{N}(P_3)|O_{\delta z}|\mathcal{N}(P_3)\rangle, \quad (2)$$

where the matrix element (ME) is defined as the transition amplitude between the in- and out-nucleon states with momentum P_3 in the z-direction; the non-local operator elongated in the z-direction is described as

$$O_{\delta z}=\int_x\overline{\psi}(x+\hat{\mathbf{3}}\delta z)\gamma_3 U_3(x+\hat{\mathbf{3}}\delta z;x)\psi(x), \quad (3)$$

with a Wilson line operator $U_3(x+\hat{\mathbf{3}}\delta z;x)$. The essential part in Eq. (2) is the nonperturbative ME, which we call quasi-PDF ME and write $\mathcal{M}_{\delta z}(P_3)$. This ME can be calculated using the lattice QCD simulation because it is not time-dependent. We need a matching to convert the ME obtained from the lattice calculation to the continuum counterpart, which has been omitted in the current lattice calculations and is a main purpose of this report.

To achieve matching between lattice and continuum, we have two choices: matching "in momentum space" or "in coordinate space". The first one is similar to the continuum matching in Eq. (1). In this approach, δz is first integrated out; thus, the z-component of the incoming and outgoing momentum at the vertex is fixed to be $\tilde{x}P_3$. However, we take the second approach, which is simple and more easily controllable in the actual lattice QCD simulation. The matching is achieved by a δz dependent matching factor:

*1 RIKEN Nishina Center

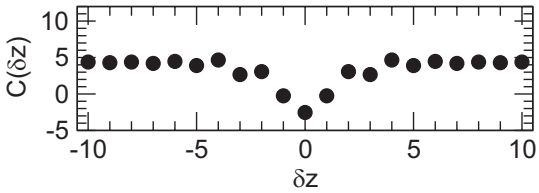

Fig. 1. One-loop coefficient of the matching factor.

$$[\mathcal{M}_{\delta z}(P_3)]^{\rm cont}=Z(\delta z)\,[\mathcal{M}_{\delta z}(P_3)]^{\rm latt}. \quad (4)$$

As the matching factor for operators does not depend on the external states, we can set $P_3=0$ for the calculation of the amplitude.

The transition amplitude involves power divergences, which arises from the Wilson line operator in both continuum and lattice. The power divergence must be subtracted nonperturbatively so that the theory is well-defined. There are several ways to perform the subtraction and we choose to use a static $Q\bar{Q}$ potential that shares the same power divergence. The Wilson line operator with a contour $\mathcal{C}$, $W_{\mathcal{C}}$, can be renormalized as

$$W_{\mathcal{C}}=e^{\delta m\ell(\mathcal{C})}W_{\mathcal{C}}^{\rm ren}, \quad (5)$$

where the superscript "ren" indicates that the operator is renormalized, $\ell(\mathcal{C})$ denotes the length along the contour $\mathcal{C}$, and δm denotes the mass renormalization of a test particle moving along the contour $\mathcal{C}$.[2] By choosing the renormalization condition for the static $Q\bar{Q}$ potential at a distance R_0 so that $V^{\rm ren}(R_0)=V_0$, the mass renormalization can be obtained as[3] $\delta m=(V_0-V(R_0))/2$. Using the renormalization condition above, we can define power divergence free ME as

$$\mathcal{M}_{\delta z}^{\rm S}(P_3)=e^{\frac{V(R_0)-V_0}{2}|\delta z|}\mathcal{M}_{\delta z}(P_3). \quad (6)$$

We only show the matching factor between continuum and lattice here using a naive fermion for simplicity, while it is not realistic for the actual simulation. We calculate it at one-loop order with HYP2 link smearing of the Wilson line and with mean-field improvement. Figure 1 shows the one-loop coefficient of the matching factor

$$Z(\delta z)=1+\frac{g^2}{(4\pi)^2}\frac{4}{3}C(\delta z)+O(g^4). \quad (7)$$

Using this, we can obtain the ME in continuum and the quasi-PDF can be calculated. We are currently planning to perform the actual simulation with this matching strategy.

References

1) X. Ji, Phys. Rev. Lett. **110**, 262002 (2013).
2) H. Dorn, Fortsch. Phys. **34**, 11 (1986).
3) B. U. Musch et al., Phys. Rev. D **83**, 094507 (2011).

Chiral contamination in nucleon correlation functions†

B. C. Tiburzi *1

The study of excited-state contamination in nucleon correlation functions is motivated by lattice QCD computations. In particular, the Euclidean time dependence of two- and three-point functions is used to extract the nucleon mass and current matrix elements using standard lattice techniques. The long-time limit is used as a filter for the ground-state nucleon, such as exhibited in the effective mass of the two-point function, which has the behavior

$$M_{eff}(\tau) = \log \frac{G(\tau)}{G(\tau + a)} \to M_N + |Z'|^2 e^{-\Delta E \tau}, \quad (1)$$

where the exponential term arises from coupling to an excited state. A flat effective mass indicates saturation from the ground state, however, stochastically determined nucleon correlation functions exhibit a well-known signal-to-noise problem at long times. Without an increase in statistics, one can attempt to minimize $|Z'|^2$ through construction of better nucleon interpolating operators. Such operators have reduced coupling to excited states; and, to this end, we investigate the nature of pion-nucleon excited states using chiral perturbation theory. One should note that the signal-to-noise problem is considerably more detrimental to the case of three-point functions due to the necessity of two Euclidean time separations, and the lack of a positivity condition.

We have determined the pion-nucleon (also the pion-delta) contributions to nucleon two- and three-point correlators as a function of Euclidean time. Originally the computation was performed for a continuum of excited states[2], and then revisited for a discrete set of states relevant for a torus[1]. Strictly speaking, the nucleon operator of chiral perturbation theory is local, and the results are only applicable to extended lattice nucleon operators provided their characteristic size R is much smaller than the length scale introduced by the chiral symmetry breaking scale, $R \ll \Lambda_\chi^{-1}$. A discussion of this is contained in[3], where the effective field theory mapping of lattice interpolating operators is also detailed.

To perform these computations of unamputated correlation functions using chiral perturbation theory, the crucial observation is that the results can be cast in the form

$$G_\chi(\tau) = |Z_O|^2 e^{-M_N \tau} \Big[1 + |Z_{\pi N}|^2 e^{-\Delta E_{\pi N} \tau} \Big], \quad (2)$$

where, for simplicity, we illustrate the case of the two-point function. The overlap $|Z_O|^2$ is determined by the short-distance dynamics of the nucleon interpolating operator. The relative overlap, $|Z_{\pi N}|^2$, however, is a long-distance correction that can be determined universally using chiral perturbation theory. The two-point function exhibits no surprises. Specializing to the case of the iso-vector, axial-vector current matrix element in the nucleon, we compute the ratio of three-point to two-point functions using chiral perturbation theory, namely

$$G_A(\tau, t) = \langle 0 | O_N(\tau) J^+_{\mu 5}(t) O^\dagger_N(0) | 0 \rangle \Big/ G_\chi(\tau), \quad (3)$$

and the result is shown in Figure 1. We find that the dominant excited-state contamination arises, not surprisingly, from nucleon to pion-nucleon intermediate states. For insufficient time separation, such excited-state contamination drives the axial-current correlation function upwards. On the basis of perturbative pion-nucleon interactions, we conclude that the consistent lattice underestimation of the nucleon axial charge, g_A, is not likely due to contamination from pion-nucleon states. Lattice QCD studies with well-localized interpolating operators would allow for confrontation with this prediction.

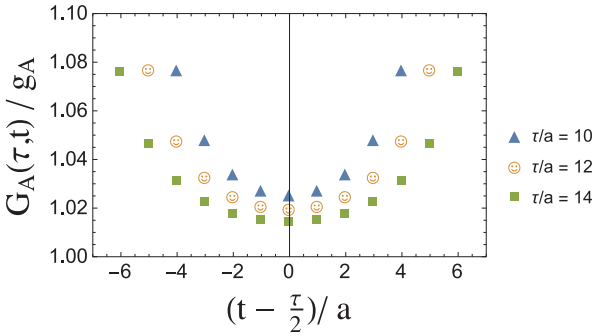

Fig. 1. Excited-state contamination in the axial-vector three-point function of the nucleon. The contamination is plotted as a function of the current-insertion time t (relative to the source-sink midpoint) for three values of the source-sink separation τ. The lattice spacing a is taken to be 0.1 fm. Excited states with pions tend to drive the axial correlator upwards, potentially leading to overestimation of the axial charge of a few percent.

† Condensed from Reference[1]

*1 Department of Physics, The City College of New York (CUNY); and RIKEN Nishina Center

References

1) B. C. Tiburzi, Phys. Rev. D **91**: 094510 (2015), arXiv:1503.06329 [hep-lat].
2) B. C. Tiburzi, Phys. Rev. D **80**: 014002 (2009), arXiv:0901.0657 [hep-lat].
3) O. Bär, Phys. Rev. D **92**: 074504 (2015), arXiv:1503.03649 [hep-lat].

High-precision calculation of the strange nucleon electromagnetic form factors†

J. Green,[*1] S. Meinel,[*2,*3] M. Engelhardt,[*4] S. Krieg,[*5,*6] J. Laeuchli,[*7] J. Negele,[*8] K. Orginos,[*9,*10] A. Pochinsky,[*8] and S. Syritsyn[*2]

The nucleon electromagnetic form factors describe how electric charge and current are distributed inside protons and neutrons. Protons and neutrons primarily contain up and down quarks, but virtual strange-anti-strange quark pairs also give minute contributions to the form factors. Isolating these contributions has been a long-standing challenge for experiment and theory. The strange electromagnetic form factors, G_E^s and G_M^s, can be accessed in elastic electron-proton scattering by analyzing the small parity-violating effects arising from Z-boson exchange. The available experimental results, which focus on momentum transfers Q^2 in the vicinity of $0.2\,\mathrm{GeV}^2$, are consistent with zero but constrain the relative contribution of the strange quarks to be within a few percent[1)].

Ab-initio calculations of G_E^s and G_M^s are possible using lattice QCD. This is a formidable task because it requires the computation of quark-disconnected diagrams, which are very noisy. The noise originates both from the gauge-field fluctuations of the QCD path integral, and from the stochastic methods needed to evaluate the disconnected quark loops. In this work, we performed a lattice QCD calculation of the strange nucleon electromagnetic form factors using a novel variance reduction method called *hierarchical probing*[2)]. Our lattice results for G_E^s and G_M^s, along with model-independent fits using the z expansion, are shown in Fig. 1. This is the first time that both G_E^s and G_M^s are resolved from zero with high significance. In addition, our calculation was performed in a larger lattice volume and at a closer-to-physical light-quark mass (corresponding to $m_\pi = 317$ MeV) than previous work.

From the z-expansion fits of the Q^2-dependence, we determined the strange electric and magnetic charge radii $(r^2_{E,M})^s \equiv -6\,\mathrm{d}G^s_{E,M}/\mathrm{d}Q^2|_{Q^2=0}$, and the strange magnetic moment $\mu^s \equiv G_M^s(0)\,\mu_N$ (where μ_N is the nuclear magneton). We also performed simple extrapolations of these quantities to the physical pion mass, obtaining

$$\begin{aligned}(r_E^2)^s &= -0.0067(10)(17)(15)\ \mathrm{fm}^2,\\ (r_M^2)^s &= -0.018(6)(5)(5)\ \mathrm{fm}^2,\\ \mu^s &= -0.022(4)(4)(6)\ \mu_N.\end{aligned}$$

The first two uncertainties given here originate from the statistical and systematic uncertainties in the lattice QCD calculation itself, and the last uncertainty results from the extrapolation to the physical point. For comparison, a global analysis of parity-violating asymmetry data for elastic electron-proton scattering gives $\mu^s = -0.26(26)\ \mu_N$[1)], which is consistent with our result but has a much larger uncertainty.

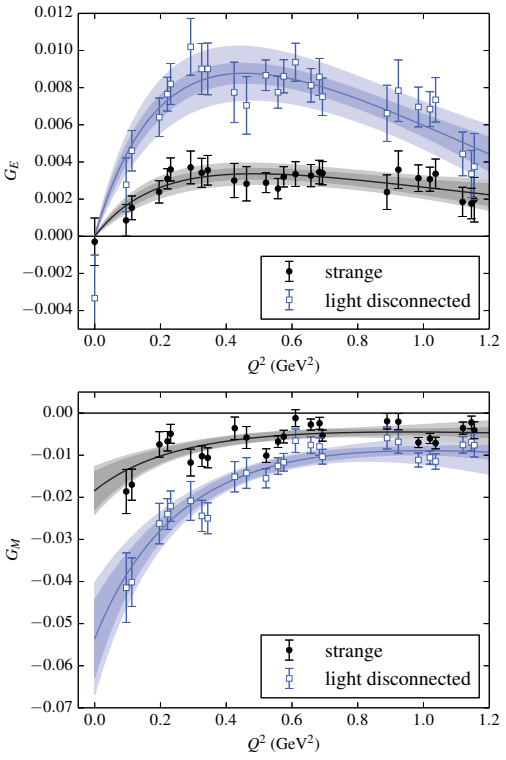

Fig. 1. Strange-quark and disconnected light-quark electric and magnetic form factors of the nucleon, for a light-quark mass corresponding to $m_\pi = 317$ MeV.

† Condensed from the article in Phys. Rev. D **92**, 031501 (2015)

*1 Institut für Kernphysik, Johannes Gutenberg-Universität Mainz
*2 RIKEN Nishina Center
*3 Department of Physics, University of Arizona
*4 Department of Physics, New Mexico State University
*5 Bergische Universität Wuppertal
*6 IAS, Jülich Supercomputing Centre, Forschungszentrum Jülich
*7 Department of Computer Science, College of William and Mary
*8 Center for Theoretical Physics, Massachusetts Institute of Technology
*9 Physics Department, College of William and Mary
*10 Thomas Jefferson National Accelerator Facility

References

1) R. González-Jiménez, J. A. Caballero, and T. W. Donnelly, Phys. Rev. D **90**, 033002 (2014).
2) A. Stathopoulos, J. Laeuchli, and K. Orginos, SIAM J. Sci. Comput. **35(5)**, S299–S322 (2013).

6. Particle Physics

Lattice determination of $|V_{us}|$ with inclusive hadronic τ decay experiment†

T. Izubuchi,[*1, *2] and H. Ohki[*2]

The Kobayashi-Maskawa matrix element $|V_{us}|$ is an important parameter for flavor physics, which is relevant for searching new physics beyond the standard model in particle physics. Thus far, $|V_{us}|$ has been most precisely determined by kaon decay experiments. As an alternative, $|V_{us}|$ can also be determined independently from τ decay. A conventional method is to use the so-called finite energy sum rule with polynomial weight function $\omega(s)$ and spectral function $\rho^{(J)}_{V/A}$ with spin $J = 0, 1$ as

$$\int_0^{s_0} \omega(s)\rho(s)ds = -\frac{1}{2\pi i}\oint_{|s|=s_0} \omega(s)\Pi(s)ds, \qquad (1)$$

where $\Pi(s)$ is a hadronic vacuum polarization (HVP) function. Here, $\rho(s)$ on the left hand side is related to the differential τ decay rate by hadronic V and A currents with u, s flavors as

$$\frac{dR_{us;V/A}}{ds} = \frac{12\pi^2|V_{us}|^2 S_{EW}}{m_\tau^2}(1-y_\tau)^2 \times \left[(1+2y_\tau\rho^{(0+1)}_{us;V/A} - 2y_\tau\rho^0_{us;V/A})\right], \qquad (2)$$

where $y_\tau = s/m_\tau^2$, and S_{EW} is a known short-distance electroweak correction. The HVP function $\Pi(s)$ on the right hand side in Eq.(1) is analytically calculated using OPE based on perturbative QCD (pQCD). Thus, the value of momentum s_0 should be sufficiently large to use a perturbative OPE result. By combining both the inclusive τ decay experiments and pQCD, one can obtain $|V_{us}|$. Recent analyses suggest that there is 3 σ discrepancy between the two results obtained from the method that uses the inclusive τ decay and the CKM unitarity constraint. While there might be a possibility that such a discrepancy could be explained by the effect of new physics, we should note that OPE yields a potential problematic uncertainty in the determination of $|V_{us}|$ from the inclusive hadronic τ decay by using the finite energy sum rule [a)]. Thus, it is important to reduce the uncertainty of the QCD part, so that the so-called $|V_{us}|$ puzzle can be resolved.

In this report, for the purpose of resolving this problem, we would like to propose an alternative method of determining $|V_{us}|$, in which we use non-perturbative lattice QCD results for $\Pi(s)$ in addition to pQCD. Combining the two inputs, we expect that more reliable results could be obtained. In order to use lattice QCD inputs, we adopt a different weight function $\omega(s)$ that has poles in the Euclidean momentum region. As an illustrative example, we assume a weight function as $\omega(s) = \frac{1}{(s+Q_1^2)(s+Q_2^2)\cdots(s+Q_N^2)}$, where $-Q_k^2 < 0$ (for $k = 1, ..., N$), and $N \geq 3$. Taking $s_0 \to \infty$ in Eq.(1), we obtain

$$\int_0^\infty \rho(s)\omega(s)ds = \sum_k^N \mathrm{Res}\left(\Pi(-Q_k^2)\omega(-Q_k^2)\right). \qquad (3)$$

The lattice result is used for residues on the right hand side. The left hand side can be evaluated up to $s = m_\tau^2$ from experimental data, and we use a pQCD result for $s > m_\tau^2$. There is an advantage of using this method. As the above weight function $\omega(s)$ is highly suppressed in the high momentum region, the uncertainty introduced by pQCD can be reduced. In fact, Fig. 1 shows the dependence of weight function on the ratio of the OPE contribution of the spectrum integral in Eq.(3) to the contribution of the dominant kaon pole. As shown in Fig. 1, the OPE contribution can be suppressed by adding poles in the weight function.

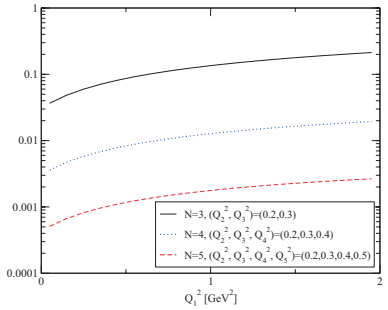

Fig. 1. Dependence of Q_1^2 on the ratio of the pQCD and kaon pole contribution. For pQCD result, $D = 0$ OPE ($N_f = 3$) and a conventional value of $|V_{us}|$ are used.

As a preliminary study, we calculate $|V_{us}|$ determined from $\rho^{(0)}_A$. As for the lattice calculation of $\rho^{(0)}_A$, we use the lattice result of $L = 48$ near the physical quark mass[b)]. Using a weight function with three poles of $(Q_1^2, Q_2^2, Q_3^2) = (0.1, 0.2, 0.3)$, we obtain a statistical relative error of 0.3%, which is competitive with previous results. As a future work, we will estimate systematic uncertainties such as lattice discretization, unphysical mass, and contributions from other channels, in particular pQCD effects.

References

1) P. A. Boyle et al., Int. J. Mod. Phys. Conf. Ser. **35**, 1460441 (2014) doi:10.1142/S2010194514604414 [arXiv:1312.1716 [hep-ph]].

† All the results shown here are preliminary.

*1 Physics Department, Brookhaven National Laboratory
*2 RIKEN Nishina Center

a) For a recent study of the inclusive τ decay by using the finite energy sum rule, see[1)].

b) We thank RBC-UKQCD collaboration and Kim Maltman for providing lattice HVP and experimental data.

Standard-model prediction for direct CP violation in $K \to \pi\pi$ decays

C. Kelly*1 for the RBC and UKQCD collaborations

A first-principles calculation of the amount of direct CP-violation in the Standard Model has long been a goal of the particle physics community. Utilizing recent computational and theoretical advances, the RBC & UKQCD collaborations have performed the first realistic determination of this quantity.

Direct CP-violation occurs in the decays of neutral kaons into two pions and is parameterized by a quantity ϵ', which is very small ($\mathcal{O}(10^{-6})$) in the Standard Model and therefore offers a sensitive probe for the new physics expected to account for the preponderance of matter over antimatter in the observable universe.

In $K \to \pi\pi$ decays, the final $\pi\pi$ state can have isospin quantum numbers of either $I = 2$ or 0, and ϵ' manifests as a difference in the complex phases of the corresponding amplitudes, A_2 and A_0. These amplitudes receive significant contributions from hadronic-scale QCD effects, necessitating the use of lattice QCD. Such calculations require powerful computers, in our case the IBM Blue Gene/Q supercomputers at RBRC, ANL and Edinburgh University, and would otherwise take several thousand years on a typical laptop.

Our most recent determination of A_2[1] was performed with large physical volumes, physical pion masses and energy-conserving kinematics. We measured A_2 with two different lattice spacings, thereby enabling a continuum limit to be performed. We obtained a very precise result: $\mathrm{Re}(A_2) = 1.50(4)(14) \times 10^{-8}$ and $\mathrm{Im}(A_2) = -6.99(20)(84) \times 10^{-13}$, where the errors are statistical and systematic, respectively. The latter arise mainly from the use of perturbation theory in the renormalization of the underlying lattice matrix elements, and can be reduced by improved perturbative calculations or by renormalizing at higher energies.

Calculating A_0 is significantly more challenging, requiring novel techniques for statistical error reduction and for measuring with energy-conserving kinematics. Our ground-breaking calculation, reported in Physical Review Letters[2], is the first *ab initio* determination of A_0 with controllable errors. The calculation was performed on a single lattice with a somewhat coarse lattice spacing but a large physical volume, resulting in controlled finite-volume errors (∼7%) but relatively large discretization errors (∼12%). Nevertheless the largest systematic errors are again associated with the perturbative truncation in the renormalization factors (∼15%) and Wilson coefficients (12%). We are presently working to raise the renormalization scale in order to reduce these errors.

As part of the calculation we also measure the $I = 0$ $\pi\pi$-scattering phase-shift at the physical kaon mass,

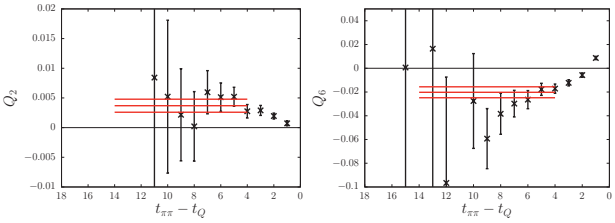

Fig. 1.: The Q_2 and Q_6 three-point functions, plotted in lattice units as functions of $t_{\pi\pi} - t_Q$, with the time dependence removed. The horizontal lines show the central value and errors.

for which we obtain $\delta_0 = 23.8(4.9)(1.2)^\circ$, which is roughly 2.7σ smaller than phenomenological expectations[3,4]. This is possibly due to the existence of excited-state contamination hidden by the rapidly diminishing signal-to-noise ratio; more statistics are needed to confirm this hypothesis.

For the $I = 0$ $K \to \pi\pi$ amplitude, we obtained

$$\mathrm{Re}(A_0) = 4.66(1.00)(1.26) \times 10^{-7}\ \mathrm{GeV} \quad (1)$$

$$\mathrm{Im}(A_0) = -1.90(1.23)(1.08) \times 10^{-11}\ \mathrm{GeV} \quad (2)$$

where the errors are statistical and systematic, respectively. Our value for $\mathrm{Re}(A_0)$ agrees with the experimental value of $3.3201(18) \times 10^{-7}$ GeV and serves as a test of our method. $\mathrm{Im}(A_0)$ was heretofore unknown.

In Fig. 1 we plot the matrix elements Q_2 and Q_6 which comprise the dominant contributions to the real and imaginary parts of A_0, respectively.

Combining our lattice values for $\mathrm{Im}(A_2)$ and $\mathrm{Im}(A_2)$ with the more precise experimental determinations of the real parts, we obtain the following result.

$$\mathrm{Re}\left(\frac{\varepsilon'}{\varepsilon}\right) = \mathrm{Re}\left\{\frac{i\omega e^{i(\delta_2-\delta_0)}}{\sqrt{2}\varepsilon}\left[\frac{\mathrm{Im}A_2}{\mathrm{Re}A_2} - \frac{\mathrm{Im}A_0}{\mathrm{Re}A_0}\right]\right\} \quad (3)$$

$$= 1.38(5.15)(4.59) \times 10^{-4}\,, \quad (4)$$

which is 2.1σ below the experimental value $16.6(2.3) \times 10^{-4}$. While currently in broad agreement, the possibility of resolving a discrepancy is clear motivation for continued study. With continued effort we expect that a 10% error relative to the measured value of $\mathrm{Re}(\varepsilon'/\varepsilon)$ can be achieved within 5 years.

*1 RIKEN Nishina Center, Brookhaven National Laboratory

References

1) T. Blum *et al.* [RBC and UKQCD Collaborations], Phys. Rev. D **91**, 7, 074502 (2015) [arXiv:1502.00263 [hep-lat]].
2) Z. Bai *et al.* [RBC and UKQCD Collaborations], Phys. Rev. Lett. **115**, no. 21, 212001 (2015) [arXiv:1505.07863 [hep-lat]].
3) G. Colangelo, J. Gasser and H. Leutwyler, Nucl. Phys. B **603**, 125 (2001) [hep-ph/0103088].
4) G. Colangelo, E. Passemar and P. Stoffer, Eur. Phys. J. C **75**, 172 (2015) [arXiv:1501.05627 [hep-ph]].

Dipolar quantization and the infinite circumference limit of 2d CFT†

T. Tada*1

We elaborate on our previous work[1], where a new term *dipolar quantization* was introduced, and further argue that adopting $L_0 - (L_1 + L_{-1})/2$ as the Hamiltonian yields an infinite circumference limit in two-dimensional conformal field theory. One of the physical significances of this new Hamiltonian is that the time translational vector field coincides with the electric field of an electric dipole located at $z = 1$, as opposed to in the ordinary radial quantization case. The new theory then exhibits a continuous and strongly degenerated spectrum as well as the Virasoro algebra with a continuous index.

First, let us define the following "charges":

$$\mathcal{L}_\kappa \equiv \frac{1}{2\pi i}\oint^t dz g(z) f_\kappa(z) T(z), \tag{1}$$

where $T(z) = T_{zz}(z)$ is the holomorphic part of the energy-momentum tensor of the original CFT. Further, the integration is performed along the path where the Euclidean time t assumes a constant value. The relationship between the Euclidean time t and the z coordinate is best summarized by introducing a new coordinate w as

$$w = t + is, \tag{2}$$

where s represents the Euclidean space part. Then, the following relations are imposed:

$$\frac{\partial w}{\partial z} = \frac{1}{g(z)}, \tag{3}$$

$$f_\kappa(z) = e^{\kappa w}. \tag{4}$$

Now we can define $\mathcal{L}_\kappa$ by choosing an appropriate value of $g(z)$. In particular, for $\kappa = 0$, we have the expression for the Hamiltonian for $g(z)$ below corresponding to the case for the ordinary radial quantization and for the dipolar quantization:

$$\mathcal{L}_0 = \frac{1}{2\pi i}\oint^t dz g(z) T(z) = \begin{cases} L_0 & \text{for } g(z) = z \\ L_0 - \frac{L_1 + L_{-1}}{2} & \text{for } g(z) = -\frac{(z-1)^2}{2} \end{cases}. \tag{5}$$

One can then calculate the commutation relations between $\mathcal{L}_\kappa$'s as follows:

$$[\mathcal{L}_\kappa, \mathcal{L}_{\kappa'}] = (\kappa - \kappa')\mathcal{L}_{\kappa+\kappa'} + \begin{cases} \frac{c}{12}(\kappa^3 - \kappa)\delta_{\kappa+\kappa',0} & \text{for } g(z) = z \\ \frac{c}{12}\kappa^3 \delta(\kappa + \kappa') & \text{for } g(z) = -\frac{(z-1)^2}{2} \end{cases}. \tag{6}$$

Here, for $g(z) = -\frac{(z-1)^2}{2}$, κ assumes all the real values, while κ is an integer for $g(z) = z$. By using this commutation relation with the Hamiltonian

$$H = \mathcal{L}_0 + \bar{\mathcal{L}}_0, \tag{7}$$

where $\bar{\mathcal{L}}_0$ stands for a member of another set of similar "charges", one can construct a state with an arbitrary value of energy in the following manner. First, consider an eigenstate of $\mathcal{L}_0$ with an eigenvalue α and with an additional index σ labeling a possible degeneracy:

$$|\alpha, \sigma\rangle, \tag{8}$$

so that

$$\mathcal{L}_0|\alpha, \sigma\rangle = \alpha|\alpha, \sigma\rangle. \tag{9}$$

In this case, operating on $|\alpha, \sigma\rangle$ with $\mathcal{L}_\kappa$ yields

$$\mathcal{L}_\kappa|\alpha, \sigma\rangle = |\alpha - \kappa, \sigma\rangle. \tag{10}$$

Thus, starting from the vacuum or any other energy eigenstate, we can construct an eigenstate for $\mathcal{L}_0$ with an arbitrary eigenvalue because κ can assume any real value.

Further, one can show that

$$\mathcal{L}_\kappa^\dagger = \mathcal{L}_{-\kappa}, \tag{11}$$

where † stands for the Hermitian conjugation. One of the idiosyncrasies we find in this formulation is a different inner product of the Hilbert space. For the choice of $g(z) = -\frac{(z-1)^2}{2}$, the following holds:

$$(L_{-1})^\dagger = L_{-1}, \quad (L_0)^\dagger = 2L_{-1} - L_0, \quad (L_1)^\dagger = L_1 - 4L_0 + 4L_{-1}. \tag{12}$$

Equation (13) shows that the operations of the Hermitian conjugation operations in dipolar quantization on L_{-1}, L_0 and L_1 are closed among themselves. In addition, they definitely assume a different form from those in radial quantization. Nonetheless, if we compute the Hermitian conjugate for the combination $L_0 - (L_1 + L_{-1})/2$, which is the Hamiltonian for dipolar quantization, it proves to be Hermitian (in the sense of dipolar quantization):

$$\begin{aligned} &\left(L_0 - \frac{L_1 + L_{-1}}{2}\right)^\dagger \\ &= 2L_{-1} - L_0 - \frac{L_1 - 4L_0 + 4L_{-1} + L_{-1}}{2} \\ &= L_0 - \frac{L_1 + L_{-1}}{2}. \end{aligned} \tag{13}$$

Thus, we presented a new conformal symmetric quantum system with novel Hamiltonian and Hilbert space.

References

1) N. Ishibashi and T. Tada, J. Phys. A **48**, no. 31, 315402 (2015) [arXiv:1504.00138 [hep-th]].

† Condensed from arXiv:1602.01190 [hep-th].

*1 RIKEN Nishina Center

Revision of the brick wall method for calculating the black hole thermodynamic quantities†

F. Lenz,[*1,*3] K. Ohta,[*2] and K.Yazaki[*3]

The brick wall method was proposed by t'Hooft[1)] for calculating the contributions of a scalar field to the thermodynamic quantities of black holes, and it has become a common tool for studying thermodynamic properties in the spaces with horizons. We examine the method in Rindler space, which has been often used as a near horizon approximation for black holes, by developing an accurate numerical method for the calculation. We find that the previous works[1–3)] overestimated the partition function and the entropy by almost 2 orders of magnitude. The origin of the discrepancy between our results and theirs is clarified by repeating the calculations of the latter in our framework. We also carry out the analogous studies for the scalar field in de Sitter space and confirm that our method is applicable to the important case of spherically symmetric spaces.

Rindler space is defined by the following coordinate transformation from the Minkowski space.

$$t, x, \mathbf{x}_\perp \to \tau, \xi, \mathbf{x}_\perp :$$
$$t(\tau,\xi) = \frac{1}{a} e^{a\xi} \sinh a\tau, \quad x(\tau,\xi) = \frac{1}{a} e^{a\xi} \cosh a\tau, \quad (1)$$

where a is the acceleration of a particle at $\xi = \tau = 0$ ($x = \frac{1}{a}, t = 0$) in Minkowski space. In the following calculation, we use $a = 1$, measuring all quantities in units of powers of a. A noninteracting scalar field with mass m satisfies the equation of motion,

$$(\partial_\tau^2 - \partial_\xi^2 - (\nabla_\perp^2 - m^2)e^{2\xi})\phi(\tau,\xi,\mathbf{x}_\perp) = 0. \quad (2)$$

The solution vanishing asymptotically at $\xi \to \infty$ is

$$\phi(\tau,\xi,\mathbf{x}_\perp) = e^{-i\omega\tau} e^{i\mathbf{k}_\perp \mathbf{x}_\perp} K_{i\omega}(\sqrt{m^2 + k_\perp^2}\, e^{\xi}), \quad (3)$$

where K is the MacDonald function.

In order to calculate the thermodynamic quantities, we restrict the system in the transverse directions to a square with area $\mathcal{A}$ using the periodic boundary condition in the usual way. The brick wall method uses the Dirichlet boundary condition at ξ_0 with the distance from the horizon $l = e^{\xi_0}$ on the order of the Planck length, l_P. The eigenvalue equation for ω is

$$K_{i\omega}(\sqrt{k_\perp^2 + m^2} e^{\xi_0}) = 0, \quad (4)$$

which results in discrete spectra $\omega_n(k_\perp), n = 1, 2, \ldots$ for each $k_\perp$. The partition function is then given by

$$\ln Z(\beta) = -\frac{\mathcal{A}}{2\pi} \sum_{n=1}^{\infty} \int_0^\infty k_\perp dk_\perp \ln(1 - e^{-\beta\omega_n(k_\perp)}), \quad (5)$$

where $\beta = 2\pi$ at the Unruh temperature.

In the previous works, the eigenvalues of ω are obtained by the WKB approximation and the sum over n for the partition function (5) is replaced by the integral from 0 to ∞ under the assumption that many n's contribute to the sum, leading to the well known closed expressions for the thermodynamic quantities[1–3)] in the case of a massless scalar field. We have solved the equation for $m = 0$ numerically with high accuracy and found that only a small number of n's contribute to the sum with $n = 1$ term dominating at the Unruh temperature. The origin of the overestimation in the previous works is the contribution of the region $0 \le n < 1$, where the spectrum is absent.

The results of our calculation for the partition function $\ln Z$ and the entropy $S = (1 - \beta\partial_\beta) \ln Z$ at the Unruh temperature based on the numerical solutions of eq.(4) are shown in TABLE I together with the closed expressions of the previous works (WKB). They are given in units of $\mathcal{A}/4l^2$ which equals the Beckenstein-Hawking entropy for $l = l_P$. Our result for $\ln Z$ with only the $n = 1$ term in (5) is also shown, demonstrating the dominance of this term. The previous works are seen to overestimate $\ln Z$ by 68 and S by 37.

TABLE I $\ln Z$ and S in units of $\mathcal{A}/4l^2$

	$\ln Z$ ($n = 1$)	$\ln Z$ (total)	S
eq.(4)	1.27×10^{-5}	1.30×10^{-5}	9.68×10^{-5}
WKB		$1/360\pi$	$1/90\pi$

Another important difference between our calculation and the previous ones is that ours is sensitive to the boundary condition at the brick wall because of the sensitivity of eigenvalues for small n's while the previous ones are insensitive owing to the assumption that many n's contribute to the sum in equation (5)

The dominance of the $n = 1$ mode implies that the longitudinal degrees of freedom are practically frozen at the Unruh temperature and the thermodynamic properties are determined by the transverse degrees of freedom.

† Condensed from the article in Phys. Rev. D, Vol.**92**, 064018 (2015)

*1 Institue for Theoretical Physics, University of Erlangen-Nuernberg
*2 Institute of Physics, University of Tokyo
*3 RIKEN Nishina Center

References

1) G.'t Hooft, Nucl. Phys. **B 256**, 727 (1985).
2) L. Susskind and J. Uglum, Phys. Rev. D **50**, 2700 (1994).
3) S. Mukohyama and W. Israel, Phys. Rev. D **58**, 104005 (1998).

Direct detection of composite dark matter via electromagnetic polarizability†

E. T. Neil*1,*2 for the LSD Collaboration

Direct-detection experiments are becoming increasingly sensitive, quickly approaching the expected irreducible background from coherent scattering of cosmic neutrinos[1]. Most dark matter candidates which couple to the visible sector through Standard Model force carriers have been ruled out by several orders of magnitude. However, models of *composite dark matter* provide an intriguing exception.

A dark sector consisting of electroweak-charged fermions and a new strongly-coupled gauge force can give rise to neutral composite bound states, which will nevertheless interact with the Standard Model through photon and Z-boson exchange. These exchanges are described by momentum-dependent electromagnetic form factors, which are highly suppressed for small momentum transfers (typical in direct-detection experiments.)

Making predictions within composite dark matter models can be challenging, due to the strongly-coupled nature of the underlying interactions. Lattice simulations provide an important tool to give quantitative information about such theories. Here we consider a specific model known as "Stealth Dark Matter"[2], based on a dark confining SU(4) gauge theory. Due to symmetry considerations, stealth dark matter has the novel feature that its leading interaction with photons is through the dimension-7 electric polarizability operator,

$$\mathcal{O}_F = C_F B^* B \, F^{\mu\alpha} F^{\nu}_{\alpha} v_\mu v_\nu \ , \qquad (1)$$

where $F_{\mu\nu}$ is the electromagnetic field-strength tensor, B is the "baryon" composite dark matter field, and v_μ is the four-velocity of B. Because this is a two-photon vertex, scattering of "stealth baryons" off of ordinary nuclei thus involves a virtual photon loop, leading to an order-of-magnitude nuclear uncertainty partly due to the poorly constrained effects of nuclear excited states.

The unknown coefficient C_F must be determined by a non-perturbative lattice calculation. We generate a series of SU(4) gauge configurations with lattice volume $V = 32^3 \times 64$, and apply the standard background field method[3] to study the polarizability and determine C_F. The "baryon" ground-state energy is determined from a two-point correlation function in the presence of an applied background electric field, $\mathcal{E}$. The polarizability operator induces a quadratic Stark shift in the mass of the "baryon" proportional to C_F,

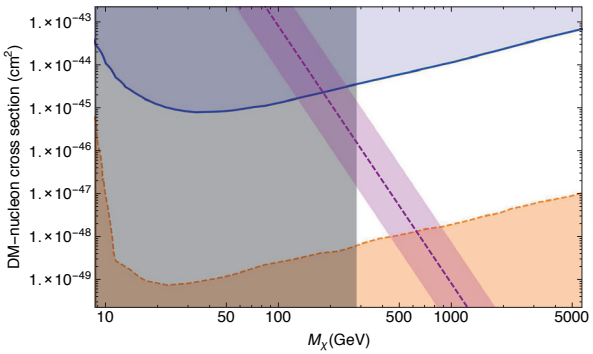

Fig. 1. Predicted spin-independent xenon scattering cross section per nucleon for stealth dark matter due to the electric polarizability (purple band). The width of the purple band indicates the uncertainty in the nuclear two-photon matrix element. The top region (blue) is excluded by the LUX experiment[4], while the left shaded region (grey) is excluded by the LEP II bound on charged mesons[2]. The bottom region (orange) shows the expected coherent neutrino background[1].

$$E_B = m_B + 2C_F|\mathcal{E}|^2 + \mathcal{O}\left(\mathcal{E}^4\right) \ . \qquad (2)$$

Repeating the calculation of E_B for several values of $\mathcal{E}$ and fitting to this formula allows us to determine C_F.

In units of the "baryon" mass M_B, we find that the value of C_F is similar for SU(4) and SU(3) gauge theories, obtaining $C_F M_B^3 \approx 1.3$ at relatively heavy fermion masses. This translates into the direct-detection scattering cross section shown in Fig. 1. Although the signal is strongly suppressed for heavy dark matter, scaling as $1/M_B^6$, there remains an intriguing window up to $M_B \sim 1$ TeV where this candidate may still be detectable above the coherent neutrino background. Because interaction through the polarizability scales as Z^4/A^2, where Z and A are the atomic and mass numbers of the target, stealth dark matter would provide a distinctive signature if a signal were found in experiments using different nuclear targets.

† Condensed from the article in Phys. Rev. Lett. **115**, 171803 (2015)
*1 RIKEN Nishina Center
*2 Department of Physics, University of Colorado, Boulder

References

1) J. Billiard, L. Strigari, and E. Figueroa-Feliciano, Phys. Rev. **D89** (2014), 023524.
2) T. Appelquist et al. (LSD Collaboration): Phys. Rev. **D92** (2015), 075030.
3) W. Detmold, B. C. Tiburzi, and A. Walker-Loud, Phys. Rev. **D81** (2010), 054502.
4) D. S. Akerib et al. (LUX Collaboration): Phys. Rev. Lett. **112** (2014) 9, 091303.

7. Astrophysics and Astro-Glaciology

Diagnose oscillation properties observed in an annual ice-core oxygen isotope record obtained from Dronning Maud Land, Antarctica

Y. Hasebe,[*1,*2] Y. Motizuki,[*1,*2] Y. Nakai,[*1] and K. Takahashi[*1]

Ice cores are time capsules that consist of snow accumulated in layers over a range of years; the deeper an ice core is, the older the age of it is. Analysing water isotopes in ice cores is one of the ways to understand climate change in the past. In particular, the oxygen isotope ratio δ^{18}O in water, H_2O, has been established as the temperature proxy in glaciology[1]. Here, δ^{18}O is defined as

$$\delta^{18}\mathrm{O} = \left\{ \frac{(^{18}\mathrm{O}/^{16}\mathrm{O})_{\text{Ice core}}}{(^{18}\mathrm{O}/^{16}\mathrm{O})_{\text{SMOW}}} - 1 \right\} \times 1000\ [‰], \quad (1)$$

where SMOW (Standard Mean Ocean Water) indicates an international standard of the water isotope ratio. The objective of this work is to investigate the relationship between the temperature and solar activity by analyzing the oscillation properties of the δ^{18}O data.

Figure 1 shows the δ^{18}O time-series record from AD 1025 to 1997. These data were obtained from ice cores drilled in Dronning Maud Land (DML), East Antarctica[2]. The temporal resolution of the record is annual. In Fig. 1, the DML δ^{18}O data are translated into the temperature deviation from the mean using the commonly-accepted proportional relationship[1].

Figures 2 and 3 show the results of our time series analysis using Fourier analysis (FT) and auto-regressive model (AR)[3]. Here, the AR method has higher resolution than FT. As the first step, we analysed the data from AD 1825 to 1997. This is because the dating of this portion of the ice core is considered to be relatively precise. As shown in Fig. 2, we obtained a clear signal of a 21-year periodicity using the AR. This peak almost corresponds to the peak of FT within the range of the FT's step size. Next, we analysed the overall data from AD 1025 to 1997. As shown in Fig. 3, we obtained signals of periodicity around

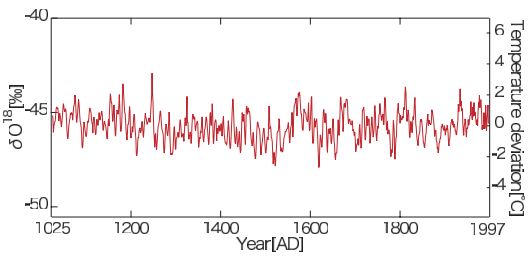

Fig. 1. Oxygen isotope ratio (δ^{18}O) time series record (left vertical axis) in DML[2] and corresponding temperature deviation (right vertical axis) are shown.

*1 RIKEN Nishina Center
*2 Department of Physics, Saitama University

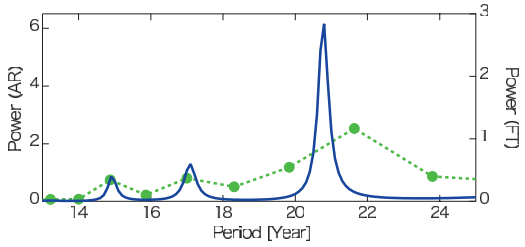

Fig. 2. Power spectra obtained from analysing the δ^{18}O record from AD 1825 to 1997. The solid blue line and green circles represent the results obtained using the auto-regressive model (AR) and by Fourier analysis (FT), respectively.

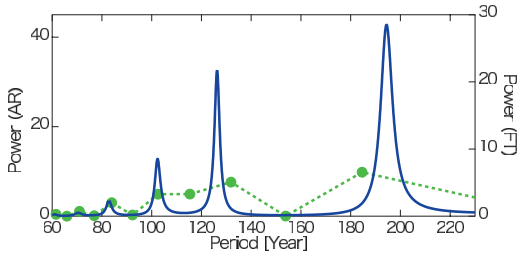

Fig. 3. Power spectra for the data from AD 1025 to 1997.

102, 126, and 194 years using the AR.

Furthermore, we also analyzed the measured surface temperature record in the southern hemisphere from AD 1850 to 2015 (HadCRUT4)[4]. We then confirmed that these observed surface temperatures have a 21-year oscillation periodicity. This result is the same as that of DML (Fig.2). It is thus confirmed that the DML δ^{18}O data actually reflected temperature history.

From the observed sunspot numbers and ^{14}C content in tree rings, ∼11, ∼22, ∼90, and ∼200 years are known to be solar activity cycles. In our analysis, nearly 22 and 200 year cycles were obtained. Therefore, the temperature modulation in the DML ice core record is suggested to be related with the solar activity cycles. The significance analysis for the obtained signals is in progress.

References

1) V. Masson-Delmotte et al.: Journal of climate **21**, 3359-3387 (2008).
2) W. Graf et al.: Annals of Glaciology **35**, 195-201 (2002).
3) D. B. Percival and A. T. Walden: *Spectral analysis for physical applications* (Canbridge University Press, England, reprinted 1998).
4) C. P. Morice et al.: Geophys. Res. **117**, D08101 (2012).

Box-model simulation for variation of atmospheric chemical composition caused by solar energetic particles

Y. Nakai,[*1] Y. Motizuki,[*1] M. Maruyama,[*1] H. Akiyoshi,[*1,*2] and T. Imamura[*2]

The atmospheric effect of energetic particles from the giant solar flares (solar energetic particles: SEPs) has been attracting attention in recent years. High-energy protons in SEPs can intrude down to the stratosphere and cause dissociation of nitrogen molecules in the middle atmosphere. This induced an increase in reactive odd nitrogen species (NOy) and decrease in ozone through subsequent chemical reactions over a period lasting longer than the SEP events, which typically continue for 3-7 days. The concentration variations of several chemical species with SEP events have been observed, and related simulations have been attempted.[1-3)]

We have investigated the variation of chemical composition induced by SEP protons using the box-model simulation, which includes multitudinous reactions for various ionic and neutral chemical species in the middle atmosphere, but no transport processes.[4,5)] The box-model simulations in the altitude range of 20-65 km were applied to the SEP event in October-November 2003. In this simulation, we adopted 77 chemical species including both positive and negative ions and 482 chemical reactions including various types of ionic reactions for the gas phase chemistry in the middle atmosphere.[5)] The simulation was performed using commercial software (FACSIMILE, MCPA Software Ltd).

The prompt products generated through radiolysis processes by the SEP protons induce subsequent ionic and neutral reactions (SEP-induced reactions). Thus, the production rates of the prompt products are estimated using the G-values (amount of products per absorbed energy of 100 eV)[6,7)] under the assumption that the yield of the prompt products is determined only with the energy deposit in the air. The day-by-day energy deposits with two peaks during the SEP event were estimated through the calculation of daily ion-pair creation rate by the SEP protons[2)]. We also assume that the prompt products are charged and neutral products generated from nitrogen and oxygen molecules.[4,5)]

Figure 1 shows the preliminary results of the energy deposit rate in a unit volume of the air, the variation of the ozone concentration (ΔO_3), and that of the NOy concentration (ΔNOy) at a 50km altitude in the northern polar region for the SEP event in October-November 2003. The variation of each chemical species induced by SEP protons was estimated as the difference between the result considering both SEP-induced and photochemical reactions and that considering only photochemical reactions using the same initial condition. The ΔO_3 responds to the increase in energy deposit very quickly. After the SEP event, the ΔO_3 increases again but does not completely recover to the pre-event value. On the other hand, ΔNOy increases during the SEP event and recovers very slowly after the event, maintaining its value for a few weeks or more. The depletion of ozone after the SEP event presumably remains because of the ozone consumption in the catalytic reaction cycle involving NOy.

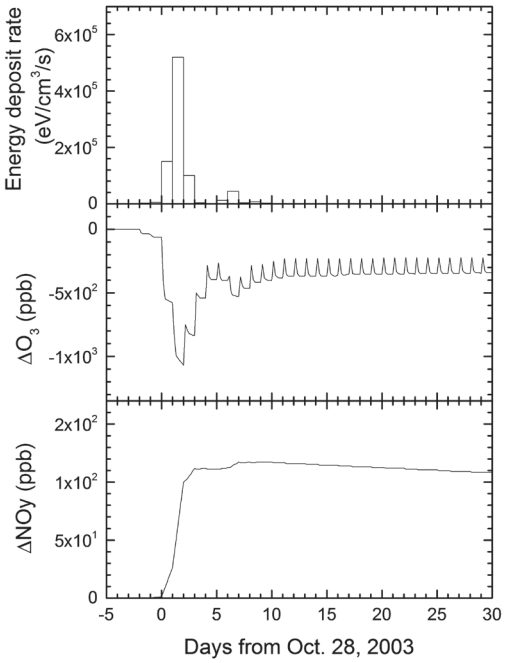

Figure 1. Preliminary results for the energy deposit rate in a unit volume of the air, the variation of the ozone concentration and that of NOy at a 50km altitude, caused by SEP protons. The SEP event started on October 28, 2003.

In near future, the variations estimated by the box-model for a short term will be input into a three-dimensional chemical climate model[8)] as instantaneous perturbation for investigation of the global and long-term influence.

References

1) B. Funke *et al*., Atmos. Chem. Phys. **11**, 9089 (2011);
2) C.H. Jackman *et al.*, Atmos. Chem. Phys. **8**, 765 (2008).
3) P.T. Verronen *et al.*, Geophys. Res. Lett. **35**, L20809 (2008).
4) K. Sekiguchi *et al*., RIKEN Accel. Prog. Rep. **46**, 124 (2013).
5) Y. Nakai *et al*., RIKEN Accel. Prog. Rep. **48**, 168 (2015).
6) C. Willis and A. W. Boyd, Int. J. Radiat. Phys. Chem. **8**, 71 (1976).
7) H. Mätzing, Adv. Chem. Phys. LXXX, 315 (1991).
8) H. Akiyoshi *et al*., J. Geophys. Res., in press.

*1 RIKEN Nishina Center
*2 National Institute for Environmental Studies

Overview of the chemical composition and characteristics of Na^+ and Cl^- distributions in samples from Antarctic ice core DF01 (Dome Fuji) drilled in 2001

Y. Motizuki,[*1] K. Takahashi,[*1] Y. Nakai,[*1] Y. Iizuka,[*2] K. Suzuki,[*3] and H. Motoyama[*4]

Ice core samples contain information about the geological history of Earth, including past climate changes. Dome Fuji, situated at the highest point of land in central Antarctica, is considered one of the best drilling locations for procuring samples for reconstructing past climates and environments.

We present here fundamental data on the concentrations of dissolved ions in shallow samples, between depths of 7.7 m and 65.0 m, from the Dome Fuji ice core drilled in 2001. A total of 1435 samples were obtained for analysis. The measured anions were $HCOO^-$, CH_3COO^-, $CH_3SO_3^-$, F^-, Cl^-, NO_2^-, NO_3^-, SO_4^{2-}, $C_2O_4^{2-}$, and PO_4^{3-}, and the cations were Na^+, K^+, Mg^{2+}, Ca^{2+}, and NH_4^+. The measurements were carried out using ion chromatography. The temporal resolution of the depth profiles of the ion concentrations was less than one year. No significant correlations were observed among these ions except between Na^+ and Cl^-.

Figure 1 shows the ion balance in the core, based on the averaged ion concentrations of the samples. As shown in this figure, the ion balance in the ice core was far different from that of sea salt, a result consistent with a finding of previous studies[1),2)]. The previous studies and our data imply the probability that precipitation around Dome Fuji might reflect conditions in the stratosphere.

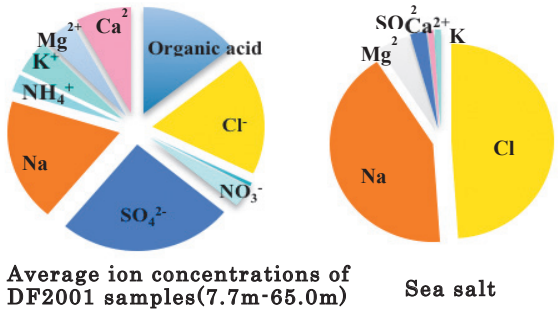

Fig. 1. Relative ion composition of the ice core (left) and sea salt (right).

In several samples, however, synchronous concentration peaks of Cl^- and Na^+ were identified, and the Cl^-/Na^+ ratios of the corresponding samples were close to the sea salt ratio. Figure 2 shows a plot of Cl^- vs. Na^+ concentrations and several samples exhibit Cl^-/Na^+ ratios close to that of the sea salt (dashed line). This observation indicates the possibility that climate conditions were such that precipitation containing sea salt occurred in the Dome Fuji area. The effect of sea salt can hardly be recognized around Dome Fuji thus far. This is a new finding by the analysis of high-resolution depth profiles of Na^+ and Cl^- concentrations. On the other hand, the Cl^-/Na^+ ratio of samples that did not exhibit Na^+ and Cl^- peaks in the depth profile differed from that previously reported for the covering snow[3), 4)]. This result implies that Cl^-, but not Na^+, was redistributed after the snow had fallen. According to Fujita et al., (in press)[5)], it is probable that high concentrations of sulphate made the Cl^- ion mobile in ice cores and the concentration of Cl^- was smoothed out. This might account for the alteration of Cl^-/Na^+ ratios and the distribution, exhibiting the dotted line in Fig. 2, has been achieved. To interpret these observations and elucidate the climatic conditions that might account for them, further studies to examine the transportation of water into Antarctica and the metamorphism of ice, such as isotopic analyses of δD and $\delta^{18}O$, will be required.

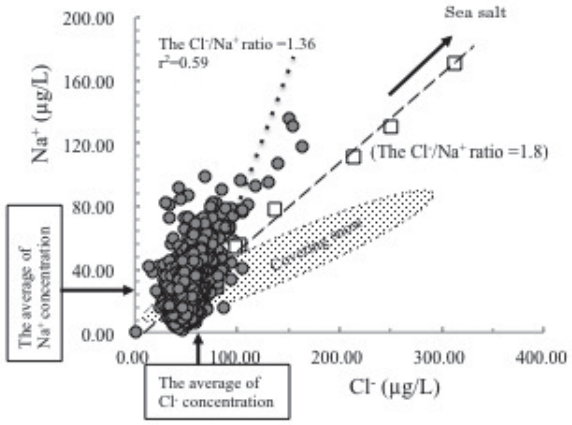

Fig. 2. Scatter plot of Na^+ vs. Cl^- concentrations in shallow samples, between 7.7 m and 65.0 m depth, from the Dome Fuji ice core drilled in 2001.

*1 RIKEN Nishina Center
*2 Hokkaido University, Institute of Low Temperature
*3 Shinshu University, Faculty of Science
*4 National Institute of Polar Research, Ice Core Cetnter

References

1) K. Kamiyama et al.. J. Geophys. Res. **94**, 18,519 (1998).
2) E. Fourré et al.. Earth Planet. Sci. Lett. **245**, 56 (2006).
3) K. Hara et al. J. Geophys. Res. **109**, D20208 (2004).
4) Y. Iizuka. et al.. J. Geophys. Res. **113**, D07303 (2008).
5) S. Fujita et al.. J. Glaciology, in press.

8. Accelerator

Energy upgrade for biological applications

N. Fukunishi,[*1] M. Fujimaki,[*1] M. Komiyama,[*1] K. Kumagai,[*1] T. Maie,[*1] T. Hirano,[*1,*2] Y. Watanabe,[*1] and T. Abe[*1]

Energetic heavy ions have been used as an effective tool for inducing mutations of flowers, crops and microbes at RIKEN Nishina Center. Typical beams used in these applications are 135-MeV/nucleon C, N and Ne beams, a 95-MeV/nucleon Ar beam, and a 90-MeV/nucleon Fe beam. All of them are accelerated by RRC.[1)] However, the beam energies of Ar and Fe ions are insufficient to obtain nearly flat distributions of Linear Energy Transfer (LET) within thick (or in-water) irradiated samples. It sometimes causes a difficulty such that the dependence of the effectiveness of mutagenesis on LET becomes unclear. Hence an upgrade for beam energies available at the existing in-air irradiation port for biological samples (E5H) is urgently required.

Our solution to this problem is the usage of IRC.[2)] IRC is originally designed to accelerate ions up to 127 MeV/nucleon using RILAC, RRC, and IRC in series or up to 114 MeV/nucleon using RILAC2, RRC, fRC, and IRC in series. However, the maximum beam energy obtained by IRC can be increased up to 160 MeV/nucleon by employing a new acceleration scheme as follows. The injector is AVF cyclotron. It accelerates Ar ions up to 3.7 MeV/nucleon. The ions extracted from AVF are charge-stripped there, injected into RRC, and accelerated up to 66 MeV/nucleon. After RRC, additional charge stripping and energy degradation to 62 MeV/nucleon should be performed by using a thick carbon disk, which is inevitable to compensate for an energy mismatch inherent to this non-orthodox acceleration scheme.

160-MeV/nucleon Ar ions extracted from IRC are transported to the existing E5H irradiation port by extending the RIBF beam transport system as shown in Fig. 1. A beam extracted from IRC is deflected by DAKR dipole magnet in order to separate the beam from the existing SRC-injection line. The section from IRC extraction to DMR2 makes a dispersive IRC-extracted beam doubly achromatic. The beam is bended up by DMR3 and bended down by DMR4 to shift the beam vertically by 3 m to compensate for the existing floor level difference. Here, the doubly achromatic condition is also fulfilled in the vertical direction. The section from DMR5 to DMR6 forms an achromatic bending system of 90 deg. The section from DMR7 and DMR8 is also doubly achromatic. After that, the beam line is joined to the existing beam delivery fishbone at DMA1. The section immediately after DMR2 to DMR6 is not newly constructed but utilizes the existing IRC-bypassing[3)] beam line in the reverse direction. Note that the IRC-bypassing beam line was constructed to inject a beam accelerated by RRC directly to SRC in order to perform light-ion experiments. The maximum magnetic rigidity of the new branch beam line is 4.4 Tm, which covers not only 160-MeV/nucleon $^{40}Ar^{18+}$ ions but also heavier ions such as $^{56}Fe^{26+}$ ions.

Beam commissioning was made in January 2015. We extracted a 160-MeV/nucleon Ar beam in the proposed non-orthodox acceleration scheme. We found no sizable beam loss along the whole new beam transport system and confirmed that our optical design of the new branch beam line worked well. In addition, we successfully produced a uniform irradiation field of 10 cm in diameter and obtained a depth-dose curve of Ar ions as expected from numerical simulations. Details of the beam commissioning are given in Ref. 4.

One problem observed in the beam commissioning was sizable (~ 40%) beam loss during acceleration at IRC. The cause of this abnormal behavior was fixed in the additional beam test performed in October 2015. The observed beam loss was induced by a half integer resonance in the vertical betatron motion. The vertical tune at beam extraction is 0.6, which is not so close to 0.5 but strong harmonic magnetic fields induced at the beam extraction region of IRC created problems. These strong harmonic fields are effective for outer most ions accelerated in the standard acceleration schemes to secure a sufficient clearance from a baffle slit attached to the IRC chamber wall. In October, we reduced harmonic magnetic fields by rebalancing excitation currents of outer trim coils and obtained a transmission efficiency of up to nearly 100%.

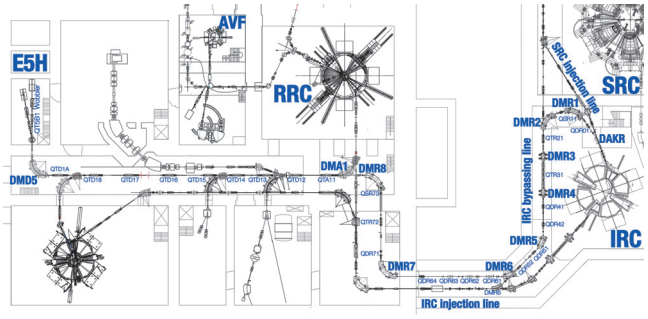

Fig. 1. Layout of RIBF beam transport system.

References

1)Y. Yano : Proc. 12th Int. Conf. Cyclotrons and their Applications, Berlin, Germany (1989) p. 13.
2) J. Ohnishi et al. : Proc. 17th Int. Conf. on Cyclotrons and Their Applications, Tokyo, Japan (2004) p. 197.
3) Y. Watanabe et al. : Accel. Prog. Rep. **42**, 111-112 (2009).
4) N. Fukunishi et al. : Proc. HIAT2015, MOPA04 (2015).

*1 RIKEN Nishina Center
*2 Faculty of Agriculture, University of Miyazaki

Installation of changeover switches for dipole and quadrupole magnet on a new beam transport line

K. Kumagai [*1] and N. Fukunishi [*1]

A new beam transport line dedicated to provide high-energy beams for biological experiments was constructed in the last year[1), 2)]. Beam commissioning of the beam line was carried out from January 24th to 25th in 2015. A 160MeV/u ^{40}Ar beam was transported from a beam exiting point of IRC to the confluent point connected to the existing beam line within 30 min. After the beam commissioning succeeded, an Ar beam was transported to the E5 experimental vault and beam irradiation to seaweed samples was carried out promptly.

One-third of dipole magnets and two-thirds of quadruple magnets on the new beam transport line were operated with existing power supplies by switching or changing the polarity of the magnet. At the time of commissioning, the switching of the magnets and/or their polarity was performed manually. The switching of all magnets took several hours. Because it was assumed that the frequency in use of the beam line becomes larger by having succeeded in the beam commissioning, we decided to install power source changeover switches to switch magnets and/or their polarity automatically using buttons.

Table 1 summarizes the scheme of the switching for the dipole magnets and Table 2 shows that for the quadrupole magnets. The automatic transfer switch type SSK-C produced by KYORITSU KEIKI CO., LTD. was used to switch dipole magnets, and type SSK-E was used to switch quadrupole magnets. Both switches have the functions of instantaneous excitation and mechanical holding. In the case of quadrupole magnets, two families of circuits can be switched using one switch. In the case of resistive load, these switches were designed such that switching was possible in the state in which an electric direct current spread in, but the inductance of the magnet might damage the contacts of switches. We designed the switches such that they are not able to switch when an electric current flows. In addition, they were not able to switch when the current sensing device broke down. An electric current passing through the circuit was detected by the current sensing device using a shunt resistor. It is designed such that a switch becomes effective when the electric current is less than approximately 1.6 mA for a dipole magnet and 3 mA for a quadrupole magnet.

The interlock signals of overheat and the coolant stop of both magnets are equipped in the power supply, but the signals originating from a magnet that is not connected are unnecessary. Therefore, the interlock was designed to be masked using the auxiliary contacts of the switching device.

Table 1. Scheme of switching for dipole magnets.

Channel	Power supply	Specification	New beam line		IRC bypass beam line
1	BT_D10_4	330A-60V	DMR3	⇔	DMK9 [a)]
2	BT_D10_3	330A-85V	DMR4	⇔	DMH8 [a)]
3	BT_D8_2	330A-155V	DMR5	⇔	DMH7 [a)]

[a)] Polarity Change

Table 2. Scheme of switching for quadrupole magnets.

Channel	Power supply	New beam line		Injection beam line to SRC		IRC bypass beam line
1	BT_QB4_1 BT_QB4_2	QDR63a QDR63b	⇔	QDG21a QDG21b		
2	BT_QB4_4 BT_QB4_5	QDR64a QDR64b	⇔	QSG23 QSG24		
3	BT_QA5_1 BT_QA5_2	QTR72b QTR72c	⇔	QDG26a QDG26b		
4	BT_QA5_3 BT_QA5_4	QDR71a QDR71b	⇔	QDG41a QDG41b		
5	BT_QA5_5 BT_QA5_6	QSR73 QSR74	⇔	QDG51a QDG51b		
6	BT_QB4_6	QTR72a	⇔	QSG25		
7	BT_QB1_1 [c)] BT_QB1_2 [c)]	QDR31c QDR31b	⇔			QTH81a [a)] QTH81b [a)]
8	BT_QB1_3 [c)]	QDR31a	⇔			QTH81c [a)]
9	BT_QB5_1			QSH17 [b)]	⇔	QSH61
10	BT_QC2_2 BT_QC2_3	QDR61a QDR61b	⇔	QDG11a QDG11b	⇔	QTG92a QTG92c
11	BT_QC2_4 BT_QC2_5	QDR62a QDR62b	⇔	QDG12a QDG12b	⇔	QDG93a QDG93b
12	BT_QC1_2 BT_QC2_1	QDR01a QDR01b	⇔	QDK02a QDK02b		
13	BT_QA6_5 [c)]	QSR11	⇔			QTG92b

[a)] Polarity Change
[b)] On the injection beamline to IRC
[c)] Specification of these power supplies is 150A-40V and that of the rest of the power supplies is 150A-30V.

The switches were manufactured from June to August. In September, installation, wiring and a check of wiring and magnet polarity were carried out. The first irradiation after installing the switches was carried out from 5th to 7th October and was finished satisfactorily. The next irradiation is scheduled for 27th to 29th January, 2016.

[*1] RIKEN Nishina Center

References

1) K. Kumagai et al., RIKEN Accel. Prog. Rep. 48, 189 (2015).
2) Y. Watanabe et al., RIKEN Accel. Prog. Rep. 48, 19 (2015).

Progress in high-temperature-oven development for 28 GHz ECR ion source†

J. Ohnishi,*1 Y. Higurashi,*1 and T. Nakagawa*1

We have been developing a high-temperature oven using UO_2 at the 28 GHz superconducting ECR ion source since 2013. Our high-temperature oven uses a tungsten crucible joule-heated with a DC current of 450–510 A. The crucible must be heated to a temperature higher than 2000°C to achieve a UO_2 vapor pressure of 0.1–1 Pa.[1] Some improvements have been made so far, and U^{35+} beams with a beam current of 100 μA could be continuously extracted from the 28 GHz ECR ion source for longer than two weeks. However, the high-temperature oven has not been used yet for providing U beams to the accelerators. This is because the use of the oven involves a higher trouble risk than the existing sputtering method, and it is not significantly superior to the sputtering method in the case of operation of a beam current of about 100 μA. However, the high-temperature oven cannot be expected to be more effective than the sputtering method in the stable operation of extracting U beams with a beam current higher than 200 μA.

Figure 1 shows shapes of the tested crucibles and Table 1 summarizes the test results. In the first test using the R34-type crucibles, the blockage of the vapor ejection hole by the UO_2 film often occurred. This was because the temperature of the cap and upper part of the crucible body is lower than that of the bottom part of the crucible according to the analysis by ANSYS.[2] In the next R41-type crucible, we decreased the thicknesses of the cap and the fitted section between the body and cap. In runs 5–7, the frequency at which the vapor ejection hole became blocked decreased. However, the oven voltage became unstable at high- temperature operations. This was presumed to be due to the local temperature rise in the upper and lower rods of the crucibles according to ANSYS. In the next R43-type crucible, the oven voltage was stabilized by increasing the diameter of the upper and lower rods from 2 mm to 2.2 mm. In run 10, we could increase the U^{35+} beam current by 20% by shifting the crucible position. Further, in the R435-type, we increased the diameter of the vapor ejection hole from 3 mm to 4 mm, and then we successfully operated the oven continuously for approximately 17 days without blockage of the vapor ejection hole.

In the next test, we are planning to approximately double the crucible size to increase the continuous operation period. Moreover, we are also planning to improve a thermal shield that was easy to break, and to connect the upper and lower support structures of the crucible to reduce the magnetic force acting on the crucible.

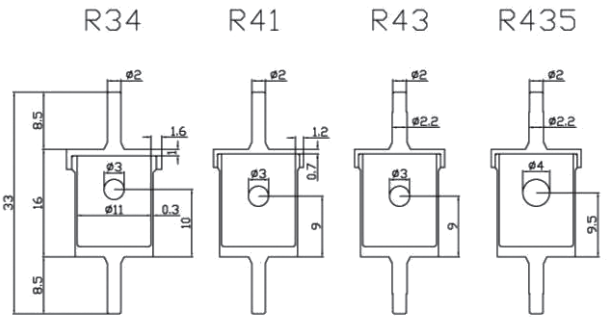

Fig. 1. Schematic of the tungsten crucibles used.

Table 1. Summary of the high-temperature oven operation results.

Run No.	Operation period	Crucible type	Oven power (W)	U^{35+} current (μA)	Operation time (h)	UO_2 Consumption rate (mg/h)	Comment
1	4/10-12/2013	R34	400-600	40-80	22	-	First test
2	7/8-16/2013, 7/22-27, 10/7-11	R34	550-650	60 (typ.)	291	2.5	Blockage of the ejection hole was observed directly by opening the ion source (7/10, 19)
3	11/5-15/2013, 11/19-22	R34	550-600	70-90	294	2.4	Blockage
4	12/10-13/2013	R34	550-600	60-80	77	0.6 (?)	
5	1/14-22/2014	R41	560-580	55-65	188	2.6	New type. No blockage
6	1/23-29/2014, 2/13-15, 2/25-28, 3/4-6	R41	480-510	55-70	283	1.7	Blockage removed by high-power (640 W) operation
7	3/11-26/2014	R41	530-660	40-70	311	1	Blockage. Unstable on high-power operation
8	6/24-7/6/2014	R43	570-660	70-100	257	4.7	Thick upper and lower rods. Oven current increased.
9	9/8-9/18/2014	R43	540-560	70-80	195	2.1	No blockage
10	2/5-3/11/2015	R43	560-630	80-100	326	2.6	Crucible moved forward by 25 mm. U^{35+} current increased by 20%. Blockage observed.
11	6/30-8/5/2015	R435	450-500	80-100	411	2.4	Ejection hole ϕ3 -> ϕ4. Thermal shield added. Oven power decreased. No blockage.

References
1) J. Ohnishi, et al.: Rev. Sci. Instr. 85, 02A941 (2014).
2) http://www.ansys.com/

† Condensed from the article in Rev. Sci. Instr. 87, 02A709 (2016).

*1 RIKEN Nishina Center

Search for suitable scintillation materials for the pepper-pot type emittance meter for diagnostics of low-energy heavy ion beams from an ECR ion source†

T. Nagatomo,[*1] V. Tzoganis,[*1,*2,*3] M. Kase,[*1] T. Nakagawa[*1] and O. Kamigaito[*1]

For diagnostics of the low-energy and high-intensity heavy ion beams extracted from an ECR ion source (ECRIS), we are developing an emittance meter (EM) based on the pepper-pot method[1]. Inside the ECRIS, to generate a multiply charged ion beam, ions and high-temperature electrons are confined together as plasma in a strong mirror magnetic field. The mirror field is the superposition of a radial hexapolor and axial solenoidal fields. Therefore, a heavy ion beam extracted from the ECRIS has no longer a round nor a gaussian shape, and has a triangular spacial distribution. Hence, it is important to measure the transverse phase space distribution (x, p_x, y, p_y) simultaneously to improve transport efficiency through the accelerator complex. The pepper-pot EM is perfectly suited to obtain the 4D distribution. Furthermore, because of the high processing power of PC, analyzing time by the pepper-pot EM is estimated as a few seconds. It is remarkably faster than the estimation time of ~ 10 min by a slit-scanning EM that is currently employed at RIKEN.

The simplest way to obtain a beam-spot image is to utilize a scintillation plate; for example, a plate with its surface covered with a scintillator, KBr, is commonly used as a beam viewer. However, there is no utilizable quantitative scintillation data, such as degradation of light emission for high- intensity and low-energy ion beam from the ECRIS. If a scintillator has comparably rapid light degradation that depends on the ion beam intensity, the obtained transverse 4D distribution in turn results in distortion. Therefore, as the first step, we have evaluated the applicability of several scintillators whether they are applicable to the imaging screen for this purpose.

Scintillation crystal plates made of quartz, Eu-doped CaF_2, Th-doped CsI, and KBr were tested. The 18-GHz superconducting-ECRIS was used to produce the proton-, $^{12}C^{4+}$-, $^{16}O^{4+}$- and $^{40}Ar^{11+}$-beams. The extraction voltages were 6.5 kV and 10.0 kV for the proton beam and the others, respectively. Each sample was placed behind the pepper-pot mask which has a 49 × 49 array of pinholes with diameters of 0.1 mm and a pitch of 2 mm. Figure 1 shows typical images of the beam spots with the proton beam, for which the current was typically 50 μA. In the case of the proton beam, the fluorescence intensities of all the scintillation materials tested, except for quartz, degraded exponentially with increasing irradiation time as shown in Fig. 2. The time constant was a few minutes with continuous proton-beam irradiation. A quartz surface impinged by the proton beam exhibited no degradation of fluorescence intensity as seen in other samples, however, with heavy-ion beams, even the quartz showed similar degradation of the fluorescent intensity as the others. Heavier ions are considered to prefer knocking out atoms on the material lattice to ionization, which induces the light emission. As a result, it is difficult to use common scintillation materials for the imaging plate, which is directly exposed to continuous heavy ion-beam impacts. Thus, the heavy ion beams must be converted into light particles, for example, a micro channel plate can convert ions into electrons.

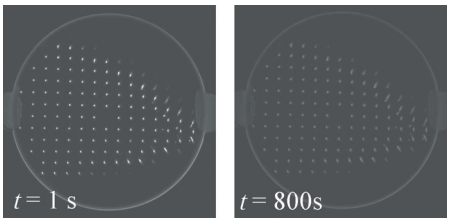

Fig. 1. Obtained images of the proton-beam spots with a CaF_2(Eu) crystal. The photos on the left and right were taken at the irradiation time of 1 s and 800 s, respectively.

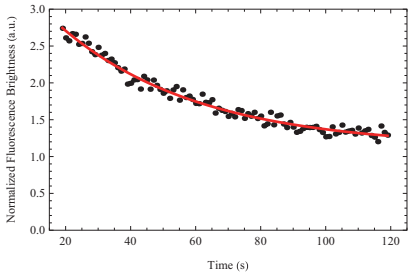

Fig. 2. Obtained degradation of fluorescence intensity induced by proton beam impinging on a KBr crystal.

† Condensed from the article in Rev. Sci. Instrum., **87**, 02B920 (2016).

*1 RIKEN Nishina Center
*2 Cockcroft Institute, Daresbury, Warrington WA4 4AD, United Kingdom
*3 Department of Physics, University of Liverpool, Liverpool, Merseyside L69 3BX, United Kingdom

Reference

1) H.R. Kremers et al., Rev. Sci. Instrum. **84**, 025117 (2013).

Design of input coupler for RIKEN superconducting quarter-wavelength resonator

K. Ozeki,[*1] E. Kako,[*2] O. Kamigaito,[*1] H. Nakai,[*2] K. Okihira,[*3] H. Okuno,[*1] N. Sakamoto,[*1] K. Sennyu,[*3] K. Suda,[*1] K. Umemori,[*2] Y. Watanabe,[*1] K. Yamada,[*1] and T. Yanagisawa[*3]

At the RIKEN Nishina Center, the construction of an accelerator system based on the superconducting quarter-wavelength resonator (QWR) is underway as a prototype with the goal of developing basic technologies for the superconducting linear accelerator for ions.[1] For the heat flows that stem from the input coupler, the residual resistivity ratio (RRR) of the copper plating on the input coupler has an opposite influence on the dynamic loss and thermal conduction (for higher/lower RRR, lower/higher dynamic loss and higher/lower thermal conduction, respectively). The discussion on the minimization of heat flows into the cavity and thermal shield had suggested that a relatively low RRR (5-20) is preferable, and the cold window should be as close to the cavity as possible.[2]

In the above study, the thickness of the copper plating was fixed at 20 μm. However, as shown in Fig. 1, it was found that the RRR of the copper plating changed depending on the thickness of the copper plating. Therefore, we determined the optimal thickness of the copper plating. Figure 2 shows the heat flows into the cavity estimated for various sets of thickness and RRR of the copper plating, which were derived by the linear fitting of measured RRR data.

Because a realizable cold-window position was decided by the actual configuration of the coupler (13.5 mm), the heat flows into cavity with the realizable cold-window position were compared. Figure 3 suggests the optimum thickness of the copper plating to be 25-30 μm. However, the RRR for 25 μm adopted in this estimation seems to have less certainty. An actual RRR for 25 μm may be lower than that obtained by linear fitting (See Fig. 1). In that case, the heat flow into the cavity becomes larger than the estimated value. Therefore, we decided to set the thickness of the copper plating to 30 μm.

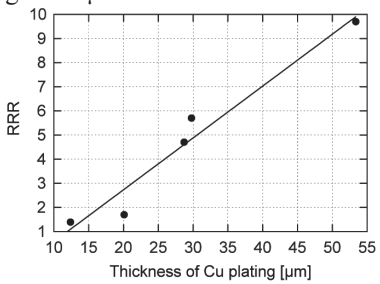

Fig. 1. Measured RRRs of copper plating for various thicknesses of copper plating. The solid line shows the result of linear fitting.

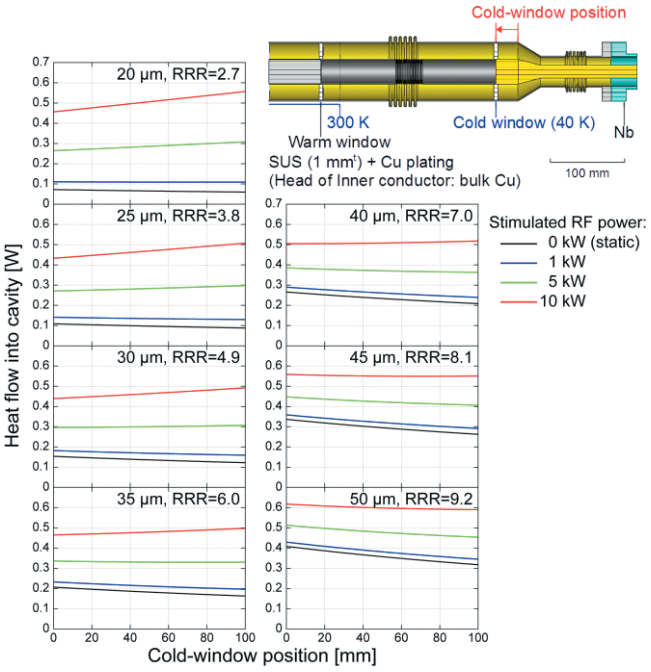

Fig. 2. Heat flows into the cavity as a function of cold-window position for various sets of thickness and RRR of copper plating. The configuration of the input coupler and the definition of cold-window position are also shown.

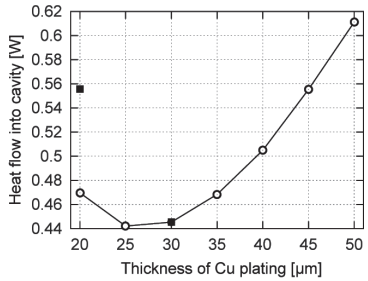

Fig. 3. Heat flows into the cavity for various thicknesses of copper plating (open circle) with realizable cold-window position. Stimulated RF power is 10 kW. As a reference, heat flows based on measured RRRs are also shown (filled square).

This work was funded by ImPACT Program of Council for Science, Technology and Innovation (Cabinet Office, Government of Japan).

References

1) N. Sakamoto et al.: Proc. of SRF2015, WEBA06 (2015).
2) K. Ozeki et al.: Proc. of SRF2015, THPB084 (2015).

*1 RIKEN Nishina Center
*2 High Energy Accelerator Research Organization
*3 Mitsubishi Heavy Industries Mechatronics Systems, Ltd.

Study of plasma window for larger aperture

N. Ikoma,[*1,*2] T. Kikuchi,[*2] H. Kuboki,[*3] H. Hasebe,[*1] H. Imao,[*1] T. Nagatomo,[*1] H. Okuno,[*1] and O. Kamigaito[*1]

Many applications in accelerator-based science are expected of the plasma window (PW) that can work as the interface between the vacuum and the high pressure region. It can be used for the efficient confinement of helium or hydrogen gas in beam line for electron stripping[1] or used as beam windows in high-power target system. The Small aperture, however, is one of the key issues for the PW that needs to be overcome. The first PW invented by Ady Hershcovitch in 1995[2] had an aperture of 2.3 mm. We started its development with the help of Ady Hershcovitch.[3] Now, its aperture has been enlarged up to 6 mm in diameter. For further enlargement, we studied the dependence of PW performance in the condition of different lengths of the PW.

PW consists of three cathodes with thoriated tungsten tip, cathode housing, five insulated cooling plates, and an anode plate (Fig. 1). They are made of 99.9999 % oxygen-free copper (OFC) because of its high thermal conductivity. Each part has internal channels for water cooling.

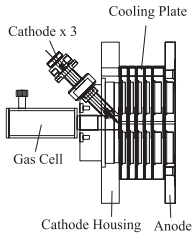

Fig. 1. Schematic of Plasma Window.

First, we measured the pressure reduction factor i.e., the ratio of vacuum chamber pressure to gas cell pressure, and applied voltage with different numbers of the cooling plates from one to seven (Fig. 2). In this experiment, we used He gas. The current and flow rate were 36 A/cathode and 17.1 slm, respectively. 12 cooling plates and 140 V are required to obtain the factor 100 by extrapolation. We will evaluate the contribution of the plasma length to the pressure reduction factor from the difference between the measured pressure reduction factors with and without plasma.

Second, we measured the pressure reduction factor in the condition of 12 A × three cathodes and 36 A × one cathode (Table 1). This experiment was carried out using Ar gas because we could not ignite PW by He under a small current such as 12 A. Its flow rate was 9.9 slm. We obtained the higher pressure reduction factor than He gas. In addition, The condition of 12 A × three cathodes has a higher pressure reduction factor because plasma fills in the cooling plates uniformly. In addition, we can reduce the load per one cathode to increase the number of cathodes.

Plasma spectroscopy on the plasma in PW under various conditions is on-going (Fig. 3). We will obtain their physical quantities such as temperature and density of free electron in the plasma to discuss the optimum condition for an aperture larger than 1cm.

This project is supported by the ImPACT Fujita program.

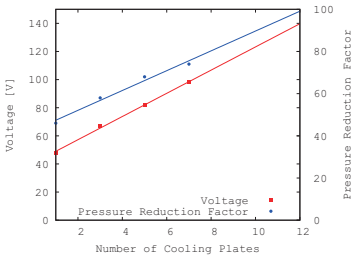

Fig. 2. Dependence of voltage and pressure reduction factor on the number of cooling plates.

Table 1. Number of cathodes and pressure reduction factor.

Current × Cathode	Pressure Reduction Factor
12 A × 3	133
36 A × 1	122

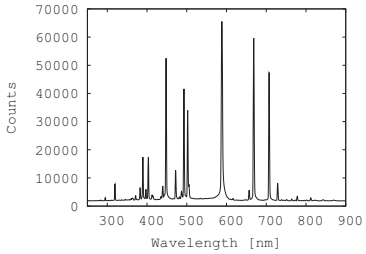

Fig. 3. Spectrum of He plasma.

*1 RIKEN Nishina Center
*2 Department of Nuclear System Safety Engineering, Nagaoka University of Technology
*3 High Energy Accelerator Research Orgainzation

References

1) H. Okuno et al., Phys. Rev. ST Accel. Beams **14** 033503 (2011).
2) A. Hershcovitch, J. Appl. Phys. **78**, 5283 (1995).
3) H. Kuboki et al., J. Radioanal. Nucl. Chem. **299**, 1029 (2014) .

Plasma spectroscopy for ECR ion source tuning at RIKEN

H. Muto,[*1] M. Kase,[*1] K. Kobayashi,[*1] M. Nishimura,[*1] S. Kubono,[*1]
Y. Ohshiro,[*2] Y. Kotaka,[*2] H. Yamaguchi,[*2] T. Hattori,[*3] and S. Shimoura[*2]

A grating monochromator with a photomultiplier was installed at the Hyper-ECR ion source, and the light intensities of gaseous and metal ion beams were observed during beam tuning.[1~3] During beam tuning, the charge distribution of ions extracted from the ECR plasma has been measured using a magnetic beam analyzer and a Faraday cup. After beam extraction, the ion beam intensity was maximized in order to reach the highest possible efficiency. During this process, a coincidental appearance of the same Q/M species occurs in the ECR plasma and their separation by a magnetic beam analyzer is extremely difficult. Especially, in the case of $^{6}Li^{3+}$ beam tuning, Helium is used as supporting gas to keep the plasma condition stable and it is almost impossible to separate $^{6}Li^{3+}$, H_2^+, and He^{2+} (Q/M = 1/2) using a magnetic analyzer. Therefore, observing the light intensity of desired ion species from a photomultiplier combined with a monochromator was decided to tune the beam.[4] The conceptual diagram of this work is presented in Fig.1.

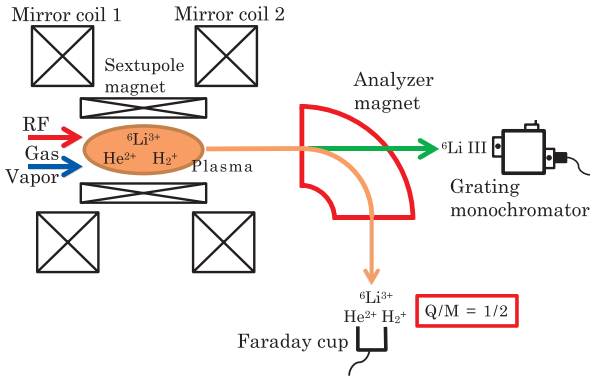

Fig. 1. Conceptual image of beam separation by an optical monochromator.

Figure 2 shows the light intensity of the ^{6}Li III line spectrum (λ = 516.7 nm) as a function of the analyzed $^{6}Li^{3+}$ beam intensity measured by the Faraday cup at the extraction section behind the beam deflector of the AVF cyclotron.[4] The AVF cyclotron has a sufficient high resolution for this process (ΔM/M = 1/1200). The $^{6}Li^{3+}$ beam intensity was tuned by controlling the RF power, the flow rate of the supporting gas, and the position of the micro oven in the ECR chamber. This result clearly shows a linear correlation of a light intensity and a beam intensity. Figure 3 shows the time charts of $^{7}Li^{3+}$ beam current and ^{7}Li III light intensity (λ = 449.8 nm) during beam tuning recorded by a pen recorder.[4] As the $^{7}Li^{3+}$ beam current increased, the light intensity of the ^{7}Li III spectrum also increased. These results clearly show a linear correlation of these two values.

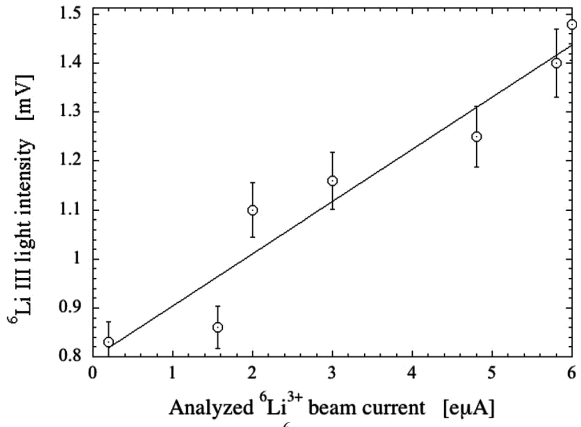

Fig. 2. Light intensity of ^{6}Li III line spectrum as a function of analyzed $^{6}Li^{3+}$ beam intensity measured by a Faraday cup positioned at the extraction section after beam deflector of the cyclotron.[4]

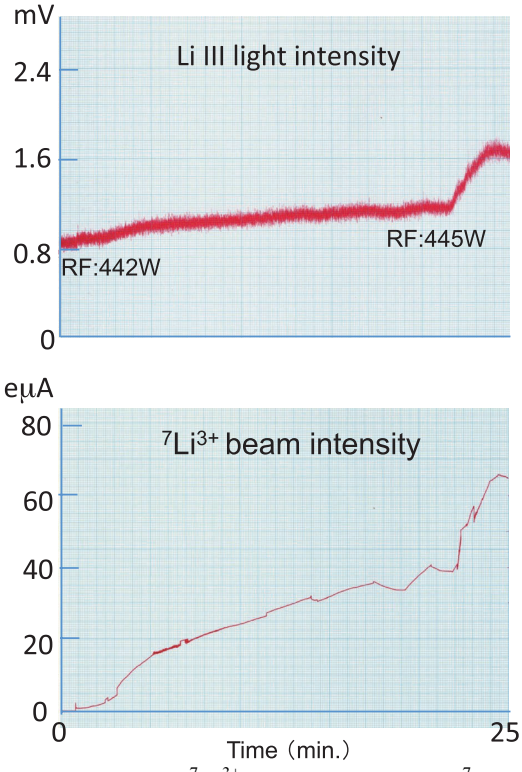

Fig. 3. Time charts of $^{7}Li^{3+}$ beam intensity and ^{7}Li III light intensity during beam tuning.

References

1) H.Muto et al., Rev. Sci. Instrum. **84**, 073304 (2013).
2) H.Muto et al., Rev. Sci. Instrum. **85**, 02A905 (2014).
3) H.Muto et al., Physics Procedia **66**, 140 (2015).
4) H.Muto et al., Rev. Sci. Instrum. **85**, 126107 (2014).

*1 RIKEN Nishina Center
*2 CNS, University of Tokyo
*3 HIMAC, NIRS

Status of cryopumps in accelerator facilities

Y. Watanabe,[*1] E. Ikezawa,[*1] M. Kase,[*1] S. Watanabe,[*1] K. Yamada,[*1]
M. Nishida,[*2] K.Oyamada,[*2] J. Shibata,[*2] K. Yadomi,[*2] and A. Yusa [*2]

The vacuum pumping system of accelerator facilities [1] consists of cryopumps for main evacuation, turbomolecular pump systems for high-vacuum evacuation prior to main evacuation, and rough pumping systems. In addition, two kinds of differential pumping systems are used for the evacuation of an additional chamber pumping system in the RRC and the IRC and for that of a sub-vacuum of resonator (sub-pumping system) in the IRC and the SRC. The status of cryopumps in accelerator facilities is listed in Table 1. Multiple cryopumps are used for the main evacuation of accelerator facilities, and several cryopumps are also used in some ion sources, beam transport lines, and other facilities. Cryopumps with a capacity of 10 m^3/s are used for resonators and valleys; 5 m^3/s, for a part of the resonators in RILAC and RRC; 4 and 2.3 m^3/s, for DTL and RFQ in RILAC2 and FT resonators in IRC and SRC, respectively. These cryopumps and its compressors are maintained regularly for every 10,000-12,000 h and 24,000-30,000 h, respectively. These current vacuum pressures are almost better than the design vacuum pressure of accelerator facilities. However, those of RILAC/CSM and RRC are worse than the design vacuum pressure at present because some vacuum leaks have been observed in each facility. These details of the vacuum leaks in 2015 are summarized in Ref. 2).

Many malfunctions caused by age-related deterioration have been recently occurring because almost all cryopumps have been in operation for over 10 years. Some cryopump's compressors of RILAC, RRC, fRC, IRC and SRC were recently replaced with new ones. Furthermore, some malfunctions of the cryopump's compressors, which were guessed to be an influence of an environmental radiation caused by an increase of beam intensity, have been frequently occurring; the number of malfunctioned compressors in RILAC2, IRC and SRC were respectively two, six, and one in the last three years. It is thought that because a dose in RILAC2, IRC and SRC were very high during a beam irradiation from a measurement of residual radioactivity [3]. For example, the maximum dose rate was found to be 34 mSv/h at the neighbor of the G01 Faraday cup (SRC deflection beam line), and two cryopump's compressors of the IRC-NE valley have malfunctioned a few times in the last three years. These malfunctions were caused because some inverters and electrical components of the compressor deteriorated by environmental radiation. Therefore, all six cryopump's compressors of the IRC-NE valley and the NW resonator cavities and two cryopump's compressors of the SRC-resonator No.1 and No.2 cavities were relocated from the north side of the N-sector magnet to right under the W-sector magnet and from the south side of sector magnet No.1 to the west side of resonator No.2 in the summer of 2015, respectively. No malfunctioned compressors have been thus far.

Malfunctions caused by age-related deterioration and environmental radiation will increase in the future, and we have to take the following measures. First, standardize a maker and a model number of cryopumps and compressors. When a cryopump malfunctions accidentally, we can easily exchange a malfunctioned component with another facility's component as a substitute component. Second, shield and relocate cryopump's compressors to a place far from a higher environmental radiation for further high-energy beam intensity. Third, do not to use a compressor equipped with an inverter in the future. Several malfunctions of compressor occured because inverters of compressors deteriorated by environmental radiation. Forth, decrease the temperature of the rf shield for a cryopump with a water cooling system. Because the rf voltage of the resonator increases, the temperature of the rf shield and inside the cryopump increases.

Table 1. Status of cryopumps in accelerator facilities.

	RILAC/CSM *	RILAC2 *	AVF *	RRC	fRC	IRC	SRC
Total volume(m^3) of facility	(72)	(6)	0.9	30	16	35	90
Number of cryopump	13	9	2	14	6	14	22
Total pumping speed (m^3/s)	(56.3)	(16.2)	14	120	60	128	164.6
Design vacuum pressure (Pa)	$1x10^{-5}$	$7x10^{-6}$	$5x10^{-5}$	$3\sim4x10^{-6}$	$4x10^{-5}$	$1x10^{-5}$	$5x10^{-6}$
Current vacuum pressure (Pa)	$1\sim7\ x10^{-5}$ **	$4\sim7x10^{-6}$	$2x10^{-5}$	$0.4\sim2x10^{-5}$ **	$0.3\sim1x10^{-5}$	$2\sim4x10^{-6}$	$2\sim4x10^{-6}$
Number of malfunctions ***	4	2	0	9	2	7	8
(Influence of environmental radiation)	(0)	(2)	(0)	(0)	(0)	(6)	(1)
Number of replaced new compressors ***	1	0	0	5	1	1	3

* Excluding ion sources and beam transport lines. ** Vacuum leaks have been observed. *** Three years from 2013 to 2015.

*1 RIKEN Nishina Center
*2 SHI Accelerator Service Ltd.

References

1) S. Yokouchi et al., Accel. Prog. Rep. **41**, 101-103 (2008).
2) S. Watanabe et al.: in this report.
3) K. Tanaka et al.: in this report.

Nishina RIBF water-cooling system

T. Maie,[*1] K. Kusaka,[*1] M. Ohtake,[*1] Y. Watanabe,[*1] E. Ikezawa,[*1] M. Kase.[*1]
M. Oshima,[*2] H. Hirai,[*2] K. Kobayashi, [*3] and J. Shibata [*3]

1. Operation condition

In fiscal year 2015, the Nishina and RIBF water-cooling systems were operated for six and five months, respectively. These operation periods correspond to the scheduled beam service time of RIBF, i.e., five months. In addition, Nishina's water-cooling system was used not only for full RIBF operation but also for the AVF standalone and AVF+RRC operations. During FY2015, there was no significant problem that resulted in beam service interruption for both Nishina and RIBF water-cooling systems. However, they were affected by small problems.

2. Trouble report

The most number of problems were related water leaks from a coupling and a joint and they also include the problem of the coolant pump being shut down for maintenance every year. Other problems include, the movement of the control valve of owing to the increase in radiation caused by the problems in the inverter of the water-cooling pumps and the accelerator driving.

3. Periodic maintenance

Routine maintenance works listed below are performed during the scheduled summer and winter maintenance periods of the RIBF accelerators.

1) Cleaning of the cooling towers
2) Checking and overhauling the cooling-water pumps
3) Checking the control system of the RIBF water-cooling system
4) Checking the inverter of the RIBF water-cooling pumps
5) Cleaning of the plate heat exchangers
6) Checking and overhauling the air compressor
7) Replacing some superannuated hoses, joints and valves used in the system
8) Cleaning of the strainers and filters used in the deionized water production system
9) Extending the sensing-wires of the water leakage alarm to floors of new areas

In addition, 2-3 times go the work that pro-backup, changes electricity and a cooling installation in a year during an accelerator outage to be affected by cooling facilities than a stop of steam and the cold water by rolling blackouts of RIKEN inside and a periodic inspection of the co-generation in the Nishina center.

4. Establishment, and improvememt

New cooling facilities were not used, instead the old ones were improved by remodeling the coolant plumbing system and the SQUID monitors of the valve of the Big RIPS back up plumbing for 2015. We are planning to update the absorption-style refrigerator in the RIBF facilities in 2016.

Photograph of the Cleaning the cooling towers

References

1) T. Maie et al.: RIKEN Accel. Prog. Rep. 47(2013)
2) T. Maie et al.: RIKEN Accel. Prog. Rep. 48(2014)

*1 RIKEN Nshina Center
*2 Nippon Kucho Service Co., Ltd
*3 SHI Accelerator Service Co., Ltd

Development of pepper-pot emittance monitor for AVF cyclotron

Y. Kotaka,[*1] Y. Ohshiro,[*1] H. Yamaguchi,[*1] N. Imai,[*1] H. Muto,[*4]
T. Nagatomo,[*2] M. Kase,[*2] K. Hatanaka,[*3] and S. Shimoura[*1]

In order to improve the injection efficiency from the Hyper ECR ion source (Hyper ECRIS) to the Riken AVF cyclotron, a pepper-pot emittance monitor[1] has been developed. The horizontal (x) and vertical (y) beam elements are coupled in this injection beam line because three solenoid coils and two Glaser coils exist. Consequently, a four-dimensional distribution (x, x', y, y') of the beam is necessary for measurement. In this report, we present the performance of the pepper-pot emittance monitor, which can measure four-dimensional distributions.

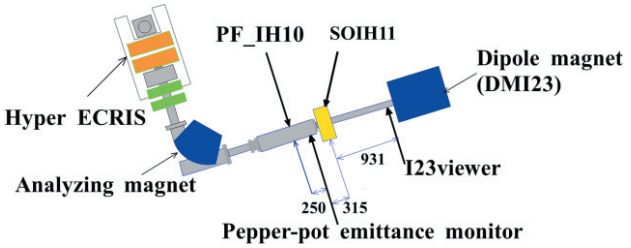

Fig. 1. Top view of Hyper ECRIS and the beam line

Figure 1 shows the test set to determine the performance of the pepper-pot emittance monitor. The figure shows a top view of the beam line from the Hyper ECRIS to DMI23. DMI23 is a dipole magnet that bends the beam in the vertical direction. On the straight line from the analyzing magnet to DMI23, a beam profile monitor (PF_IH10), a pepper-pot emittance monitor, a solenoid coil (SOIH11) and a viewer plate (I23viewer) exist in this order. PF_IH10 is used for the alignment of the pepper-pot emittance monitor.

We irradiated the pepper-pot emittance monitor with a $^{4}He^{2+}$ 20 keV ion beam (51eμA). The beam image of the pepper-pot emittance monitor is shown in the left part of Fig. 2. Using this, the four-dimensional distribution is calculated and indicated as the vector in the right part of Fig. 2.

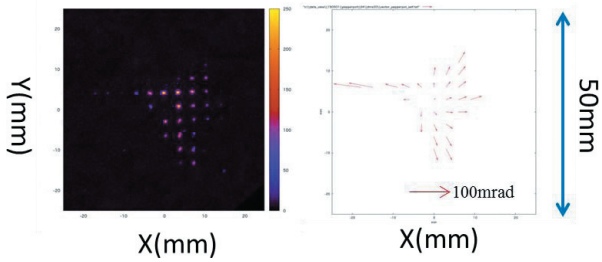

Fig. 2. Distribution of beam vector measured by the pepper-pot emittance monitor

Then, we transfer the four-dimensional distribution to the position of the I23veiwer. The transfer matrix of SOIH11 is constructed using the real solenoid model[2]. The result is shown as the image on the x-y plane in the left part of Fig. 3. The right part of Fig. 3 shows the beam image of the I23viewer. Comparing the left and right images of Fig. 3, we find that both shapes and positions are similar.

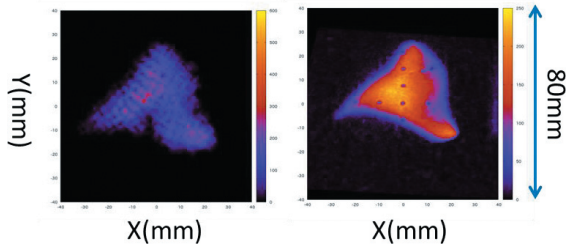

Fig. 3. The left image is the image obtained from the four-dimensional distribution transferred to the position of the I23viewer and the right image is a beam image on the I23viewer.

In order to obtain further confirmation, we also transfer the four-dimensional distribution to the exit of DMI23 and the result is shown as the image on the x-y plane in the left part of Fig. 4. For comparison, we place another pepper-pot emittance monitor at the exit of DMI23 and measure another four-dimensional distribution. This beam image is shown in the right part of Fig. 4. Both shapes and positions are similar.

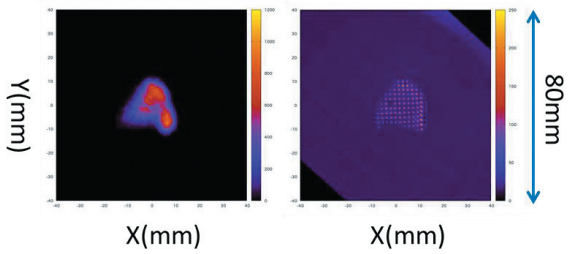

Fig. 4. The left image is the image obtained from the four-dimensional distribution transferred to the exit of DMI23 and the right image is the image obtained from another pepper-pot emittance monitor.

These results show that our pepper-pot emittance monitor has the necessary performance to be useful for the analysis of the injection beam line. After this, we are going to design the transport system of the injection beam line using the four-dimensional distribution.

*1 Center for Nuclear Study, University of Tokyo
*2 RIKEN Nishina Center
*3 RCNP, Osaka University
*4 Center of General Education, Tokyo University of Science, Suwa

References

1) T.Hoffmann et al.: Proc. 9th BIW, Cambridge, USA, (2000), p.432-439.
2) H. Wiedemann: Particle Accelerator Physics, 3rd ed. (Berlin, Springer, 2007)

HTc-SQUID beam current monitor at the RIBF†

T. Watanabe,*1 N. Fukunishi,*1 M. Kase,*1 S. Inamori,*2 and K. Kon*2

For measuring the DC current of heavy-ion beams non-destructively at high resolution, we developed a high critical temperature (HTc) superconducting quantum interference device (SQUID) beam current monitor for use in the radioactive isotope beam factory (RIBF) at RIKEN[1]. Because of its low vibration, a pulse tube refrigerator cools the HTc fabrications that include the SQUID such that the size and operational costs of the system are reduced. Two years ago, we significantly reinforced the magnetic shielding system. The new strong magnetic shielding system can attenuate the external AC magnetic noise by 10^{-10}. With the aim of practical use in acceleration operation, we disassembled the prototype high-Tc SQUID current monitor (SQUID monitor), installed improved parts, and re-assembled it. Last year, we installed the SQUID monitor in the beam transport line in the RIBF. We are presently using the SQUID monitor for measuring of the current of beams of heavy-ions such as uranium.

To increase the beam current resolution of the SQUID monitor, we investigated the improvement of the coupling efficiency between the magnetic field that is generated at the bridge circuit and the input coil of the HTc SQUID. We developed a new HTc SQUID[2] with a high-permeability core that was installed in the two input coils of the HTc SQUID. Furthermore, to increase the magnetic field produced by the bridge circuit, we successfully fabricated an HTc current sensor with two coils using a newly developed spraying machine[3]. In general, the performance of monitors such as the SQUID monitor is determined by the signal to noise ratio. To improve the measurement resolution,

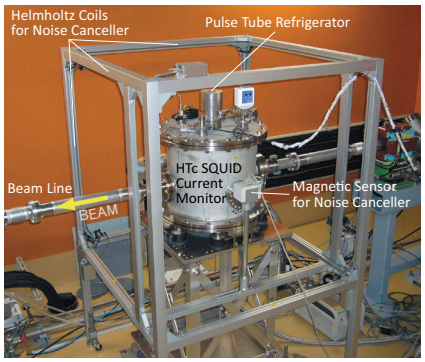

Fig. 1. SQUID monitor equipped with the noise canceller system, which was installed in the transport line between the fRC and the IRC .

† Condensed from the the proceedings in 2015 International Beam Instrumentation Conference (IBIC 2015)
*1 RIKEN Nishina Center
*2 TEP Corporation

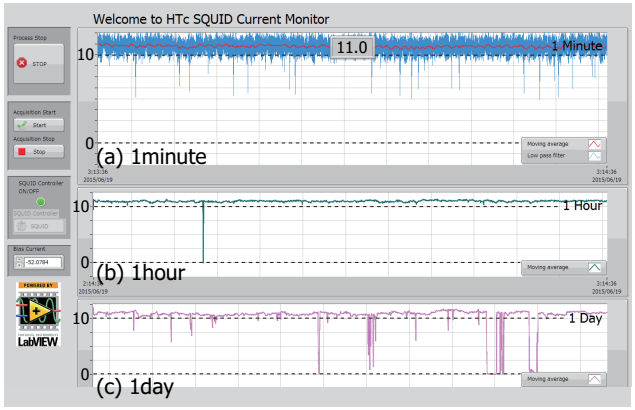

Fig. 2. The 11 μA $^{78}Kr^{36+}$ intensity of the beam (50 MeV/u) was successfully measured with a 500 nA resolution.

it is important to attenuate external magnetic noise. Therefore, we developed a hybrid magnetic shielding method based on the properties of perfect diamagnetic materials (superconductors) and ferromagnetic materials[4].

Figure 1 shows the SQUID monitor equipped with the noise cancellation system, which was installed in the transport line between the fRC and the IRC. We successfully measured the intensity of an 11 μA beam of $^{78}Kr^{36+}$ (50 MeV/u) with a 500 nA resolution (Fig. 2). We calibrated the SQUID output voltage with a simulated beam current beforehand. Prolonged 1 min, 1 h, and 1 day recordings of the Kr beam current extracted from the fRC were achieved. In these recordings, several dips in beam intensity due to the ECR ion source discharge can be observed. The amplitude of the ripples in the modulated beam current increased with the beam current. Although we can measure the intensity of a sub-μA beam, a two orders of magnitude lower current resolution is required at the RIBF. Therefore, we are now investigating the possibility of coating a thin layer (70 μm) of Bi_2-Sr_2-Ca_1-Cu_2-O_x (Bi-2212) on a silver (Ag) substrate capable of corresponding to the complex shape.

This work was supported by JSPS KAKENHI Grant Number 15K04749.

References

1) T. Watanabe et al., Proc. 2010 Beam Instrumentation Workshop (BIW10), 523-532 (2010).
2) M. I. Faley, Applications of High-Tc Superconductivity, 148-176 (2011).
3) T. Watanabe et al., J. Supercond. Nov. Magn., **26** (4), 1297-1300 (2013).
4) T. Watanabe et al., IOP Publishing Journal of Physics: Conference Series, **507**, 042047 (2014).

Radiation monitoring in the RIBF using ionization chamber

M. Nakamura,*1 K. Yamada,*1 A. Uchiyama,*1 H. Okuno,*1 and M. Kase*1

In recent years, we have attempted to monitor radiation due to beam loss in the RIBF by using self-made ionization chambers (ICs)[1)-3)] In the course of RIBF operations, the septum electrode of the electrostatic deflection channel (EDC) of the RRC was damaged by a $^{238}U^{86+}$ beam. To avoid such serious damages, the part of the septum where the ion beams can easily irradiate was cut off and molded into a "V-shaped" edge. By observing the following RIBF operations, we could recognize that such septum is effective for reducing the beam loss at the EDC and avoiding the damage to the septum. Last year, we conducted tests by inputting the alarm signal from the IC signal near the EDC of the RRC. We recognized that this method was safer and easier than the former calibration method[1, 2)]. Hence, in this report, for confirming the validity of this calibration method for the ICs set at other parts in the RIBF, we investigated the introduction of the alarm signal from the IC near the EDC of the SRC using the same method.

Usually, we input the alarm signal from the IC near the EDC of the SRC to the BIS after the calibration experiments[1, 2)]. In these experiments, the ion beams were attenuated to less than 1/10 and irradiated to the EDC for a fairly short time and the IC voltages were measured. From these results, we can estimate the alarm levels of the IC to the BIS. However, it can be very dangerous to irradiate heavy-ion beams to the EDC of the SRC because of a sudden increase in the temperature of the septum. Therefore, we consider the alarm levels of the IC from the signals of the TCs set at the septum. When the temperature of the TC set at the first EDC septum of the SRC becomes 42℃, the alarm signal is input to the BIS. Hence, we compared the value of the first septum temperature with the signal of the IC set near the EDC of the SRC in the machine time of the $^{48}Ca^{20+}$ beam. The result is shown in Fig. 1. The data showed little dispersion and the calibration curve in Fig. 1 can be drawn. From this curve, we can see that the voltage of the IC becomes approximately 1.5 V when the temperature of the first septum reaches 42℃, which is shown as a red dotted line in Fig. 1. Then we can decide the alarm level for the BIS.

We input the alarm signal to the BIS from November 25to December 5, 2015 when the $^{48}Ca^{20+}$ ion was accelerated at 345 MeV/nucleon. On November 26, the BIS by the alarm signal from the IC acted and stopped the operations of the RIBF. Fig. 2 shows the IC signal for November 26 from 12:00 to 24:00. At 17:35, the signal suddenly rose to 2.4 V and the alarm signal was sent to the BIS. After this signal, the alarm reached the BIS in the machine time of the $^{48}Ca^{20+}$ beam in 2015. The cause of the unusual signal shown in Fig. 2 is unknown.

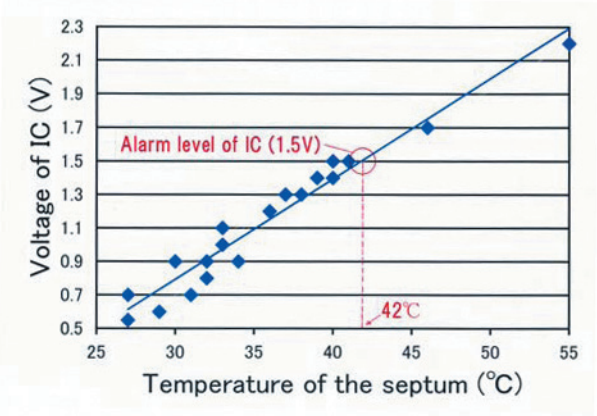

Fig. 1 Correlation of IC voltage and temperature of first septum of EDC

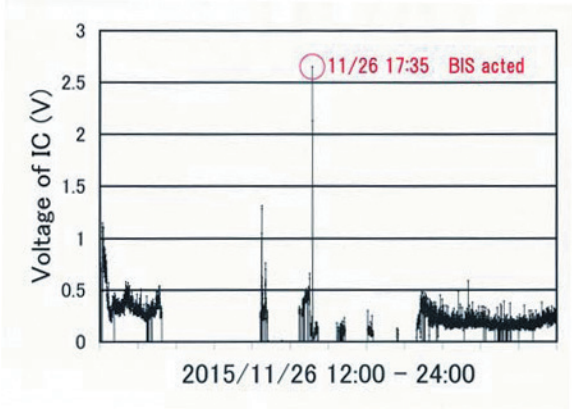

Fig. 2 Signal from the IC near the EDC of the SRC

In previous reports[1, 3)], we showed that some problems with the $^{48}Ca^{20+}$ ion beam in the EDC of the SRC frequently occur when the IC output signal rises to about 4 V. On the other hand, the beam loss at the EDC reduced in this machine time compared with the previous times. For this reason, we presumed that the alarm level reduced to 1.5 V. This cause is still not clear. However, if the beam loss at the EDC changes each time, we can easily reset the IC alarm level in every machine time by considering the correlations of the IC signal and TCs temperature.

In any case, as described above, we could confirm that faster alarm signal to the BIS can be input from the IC near the EDC of the SRC. Thus, we investigated to input the alarm signal from IC in SRC to the BIS when every ion is accelerated in the RIBF.

*1 RIKEN Nishina Center

References
1) M. Nakamura et al.: RIKEN Accel. Prog. Rep. **44**, 293 (2011).
2) M. Nakamura et al.: RIKEN Accel. Prog. Rep. **45**, 228 (2012).
3) M. Nakamura et al.: RIKEN Accel. Prog. Rep. **47**, 310 (2014).
4) M. Nakamura et al.: RIKEN Accel. Prog. Rep. **48**, 237 (2015).

Improvement of the RIBF control system

M. Komiyama,[*1] A. Uchiyama,[*1] M. Fujimaki,[*1] K. Kumagai,[*1] N. Fukunishi,[*1]
M. Hamanaka,[*2] T. Nakamura,[*2] and S. Fukuzawa[*2]

We report on two aspect of the RIBF control system; one is the maintenance of the aging components in the system to maintain stable operation of the accelerators and the other is safe operation of the accelerators based on the improvement of their performance.

The Network-I/O (NIO) system is one of the control systems for magnet power supplies in the RIBF accelerator complex,[1] which is a commercially available system manufactured by Hitachi Zosen Corporation. The NIO system consists of three types of controllers: the NIO-S board, the NIO-C board, and the branch board. The NIO-S board is a slave board attached directly to the magnet power supply and controls it based on the signals received from an upper-level control system through the NIO-C board. The NIO-C board works as a master board for the NIO-S boards and is designed to operate in the VME computing machines. The NIO-C and NIO-S boards are connected using an optical fiber cable through a branch board. Since one NIO-S board can control only one magnet power supply, there are about 500 NIO-S boards, and this corresponds to 60% of the total magnet power supply used in the RIBF accelerator complex. The existing NIO system has been working stably; however, the production of the present NIO-S and NIO-C boards was terminated because some parts used for communication were not available. Therefore, we decided to develop fully compatible successors to the existing NIO-S and NIO-C boards, and first, a successor of the NIO-S board was developed in 2013.[2] However, a problem was found during the performance tests; some types of magnet power supplies could not be controlled by the successor because the widths of some output pulses produced were slightly different from those produced by the existing board. After the pulse width of the successor was adjusted to match with that of the existing NIO-S board, we confirmed a normal operation of the successor in 2015. The development of a successor for the NIO-C board has also been started since 2014. The specifications required for the successor of this board are essentially the same as that for the existing one; however we decided to design the new board to run in a control system constructed by PLC modules instead of the VME computing environment currently used, in order to achieve cost reduction and functional scalability. The successor of the NIO-C board is based on FA-M3, manufactured by Yokogawa Electric Corporation, [3] according to recent trends in the control systems of RIBF accelerators based on EPICS. One of the advantages of adopting FA-M3 is that a simple control system can be set up because a Linux-based PLC-CPU (F3RP61) is available in the FA-M3 system and F3RP61 can work not as only a device controller but also as an EPICS Input/Output Controller (IOC).[4] This means that additional hardware to serve as an EPICS IOC is not required for F3RP61. Following the development of the hardware for the successor in 2014, its software was developed in 2015. The successor of the NIO-C board is not only equivalent to the existing one in terms of functionality some new functions have also been added to control any NIO-S board from an NIO-C board by using its serial port. In the existing NIO system, there are only two ways to control an NIO-S board: one is by entering a command from the VME computer and the other is by entering a command directly from a serial port of an NIO-S board. Therefore, the new function is expected to help identify the cause of the problem at the time of its occurrence.

The second aspect is the contribution towards a safe operation of the accelerators. Following an annual increase in the beam intensities supplied from the RIBF accelerators, various functions have been added to the control system and the beam interlock system (BIS) [5] to operate the accelerators safely. As a part of the improvements, we connected the interlock signals indicating failure of old magnet power supplies for the AVF cyclotron and RRC and their beam transport lines to the BIS in 2015 by modifying a part of the magnet power supplies to take out the interlock signals. As a result, signals from almost all magnet power supplies in RIBF are connected to the BIS except for the magnets installed in the junction building and the vault of ion sources for AVF cyclotron. Furthermore, current signals detected by the beam spill monitors installed in the fRC were also connected to the BIS in 2015. With this improvement, the amount of beam loss in all cyclotrons except the AVF cyclotron can be monitored by the BIS, and it has become possible to prevent damages to the hardware of the RIBF accelerator complex from significant beam losses for high-power heavy-ion beams. For a further increase on the beam intensities supplied from the RIBF accelerators in the near future, we will expand the number and type of signals managed by the BIS appropriately.

*1 RIKEN Nishina Center
*2 SHI Accelerator Service Ltd.

References

1) O. Kamigaito et al.: Proc. IPAC2014, (2014), p.800.
2) M. Komiyama et al.: RIKEN Accel. Prog. Rep. Vol. 48 (2015). p. 194.
3) http://www.yokogawa.co.jp/itc/itc-index-ja.htm
4) M. Komiyama, et al.: Proc. ICALEPCS2009, (2009), P. 275.
5) M. Kobayashi-Komiyama et al.: RIKEN Accel. Prog. Rep. Vol. 39 (2006), p. 239.

Control system renewal for efficient operation of RIKEN 18 GHz electron cyclotron resonance ion source†

A. Uchiyama,[*1] K. Ozeki,[*1] Y. Higurashi,[*1] M. Kidera,[*1] M. Komiyama,[*1] and T. Nakagawa[*1]

The RIKEN 18 GHz electron cyclotron resonance ion source (18 GHz ECRIS)[1] is used as an external ion source at the RIBF accelerator complex to produce an intense beam of medium-mass heavy ions. In the RIBF control system, Experimental Physics and Industrial Control System (EPICS) is adapted in order to integrate controllers for operation of power supplies of the magnet, vacuum systems, beam diagnostic system, etc.[2] However, a non-EPICS-based system has hardwired controllers, and it is used in the 18 GHz ECRIS control system as an independent system. For this reason, an unintegrated control system between the ECRIS and the RIBF accelerator complex causes inefficient cross-operation. For efficient operation of the 18 GHz ECRIS, the control system should be upgraded by a remote control system with EPICS.

Rapid development of the renewal method is necessary because the 18 GHz ECRIS is used for both RIBF injection and standalone experiments at the RILAC. Therefore, we use the 28 GHz SC-ECRIS control system technology[3] for constructing the 18 GHz ECRIS control system. The control system features are used to adapt the programmable logic controllers (PLCs) to embedded EPICS technology and construct superior client systems. The 18 GHz ECRIS control system includes several types of distributed systems for remote control and Ethernet services. For control of the main devices (e.g., gas valves, 18 GHz ECRIS rod position), a Yokogawa F3RP61-2L module, which acts as an EPICS input/output controller (IOC), is combined with FA-M3 PLCs.[4] A beam diagnostic system (e.g., Faraday cup, beam profile monitor) is constructed with the EPICS using Linux-based IOCs connected with N-DIMs, which are the original Ethernet-based control devices at the RIKEN Nishina Center.[5] The negatively biased disk and the oven system are placed in the high-voltage terminal. For components installed at the locations, it is necessary to provide insulation between the controller and components. Consequently, an FA LINK (proprietary specification, Yokogawa Electric Corporation) and optical fibers are adopted for connection with the high-voltage stage (See Fig. 1).

For the software, basic components, such as a data archiver, and a GUI-based operator interface, are implemented as well as RIBF control system. The operational log system[6] is also adopted for the 18 GHz ECRIS control system. By completely logging 18 GHz ECRIS operations, for example gas valve and rod position operations, the operational logs can support the generation of ion beams, because the logged data can be used to develop an ion beam.

The 18 GHz ECRIS system can be operated without serious problems. Especially, we successfully achieved stable ^{48}Ca beams[7][8] in 2015 using this renewal control system, because a more sensitive operation, for example fine tuning of the MIVOC[9] temperature and micro-oven[10] voltage, is possible, which was not the case with the old hardwired control system.

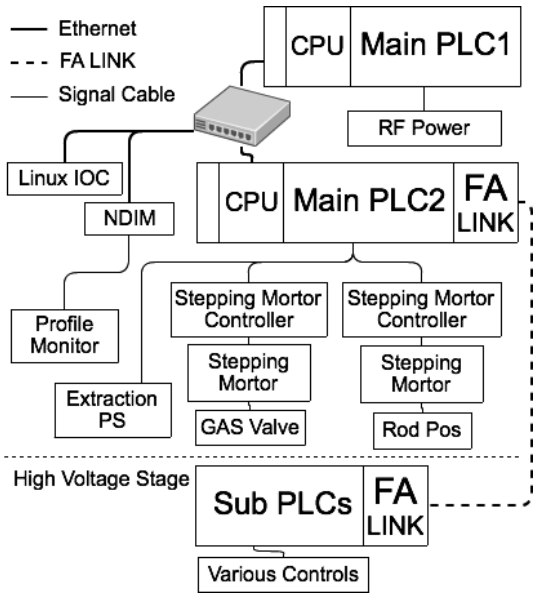

Fig. 1. Outline of the hardware for this renewal system.

References
1) T. Nakagawa et al., Nucl. Instrum. Meth. B **226**, 392 (2004).
2) M. Komiyama et al.: Proc. ICALEPCS14, SanFrancisco, CA, USA (2014), p.348.
3) M. Komiyama et al.: Proc. ICALEPCS09, Kobe, Japan, (2009), p.275.
4) A. Uchiyama et al.: Proc. PCaPAC08, (2008), p.145.
5) M. Fujimaki et al., RIKEN Accel. Prog. Rep. **37**, 279 (2004).
6) A. Uchiyama et al., RIKEN Accel. Prog. Rep. **48**, 195 (2015).
7) M. Nishida et al.,in this report.
8) E. Ikezawa et al., in this report.
9) M. Kidera et al., Rev. Sci. Instrum. **75**, 1473 (2004).
10) K. Ozeki et al., Rev. Sci. Instrum. **85**, 02A924 (2014).

† Condensed from the article in Rev. Sci. Instrum. **87**, 02A722 (2016)

*1 RIKEN Nishina Center

EPICS PV management and method for RIBF control system†

A. Uchiyama,*1 M. Komiyama,*1 and N. Fukunishi*1

For the RIBF, we constructed a control system based on the Experimental Physics and Industrial Control System (EPICS) for magnet power supplies, beam diagnostic instruments, vacuum control systems, and so on.[1] Different types of devices are connected via the EPICS Input/Output Controllers (IOCs) as front-end controllers for accelerator operation. For example, VME-based IOCs are adapted for magnet power supplies, and beam diagnostic and vacuum systems (e.g., Faraday cup and beam profile monitor) are constructed using Linux-based IOCs connected with N-DIM.[2] Additionally, CAMAC, GPIB, Programmable Logic Controller, and others are also utilized as control devices with EPICS for various applications in the RIBF control system. In October 2015, the EPICS-based RIBF control system consisted of 51 IOCs that contain approximately 110,000 EPICS records in total. Note that the EPICS record consists of some fields, and the behavior of the record is defined by cording the fields.

On the other hand, since the RIBF control system has been constructed by extending the control system of the RIKEN Accelerator Research Facility (RARF), the relationship among the IOCs, the Process Variables (PVs), and controllers are complicated. The PV is a named piece of data with a set of attributes in the EPICS-based system. Therefore, we have constructed a system to manage the EPICS PV to solve the complication of the relationship and PV name.

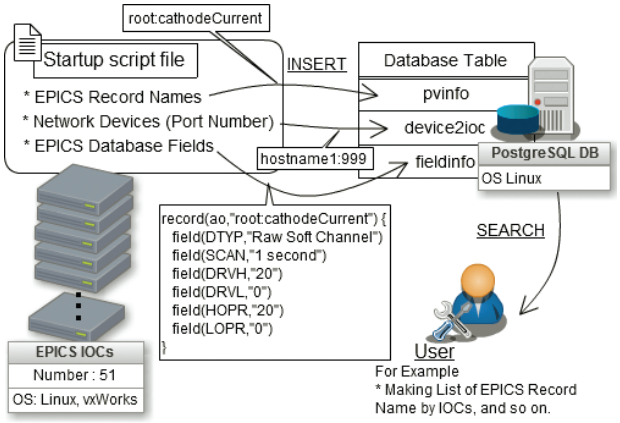

Fig. 1. System chart of the developed program and inserted data.

In the RIBF control system, common EPICS programs (EPICS-base, application programs, runtime database, and additional extensions programs) are stored in the network attached storage (NAS), and they are shared by all EPICS IOCs using the network file system or file transfer protocol. The NAS, manufactured by NetApp, provides a centralized system with a high availability. On the other hand, the IOCs mount common EPICS programs and the management server is also mounted with the shared storage to read common EPICS programs. Therefore, by reading the startup script files and accessing the EPICS runtime database files, the developed program can parse the runtime database files, which is coded in startup script file. In this developed system, the EPICS PV information is separately stored in the PostgreSQL-based database by parsing the startup script files and EPICS runtime database files (See Fig. 1). Additionally, the information of the network-based devices, which are managed by the IOC, is inserted in the database. This developed program is coded in PHP and is regularly invoked from Crontab services, which run on Linux; thus, the data are always in the latest state.

Because the EPICS PVs and fields information are stored in the PostgreSQL-based database, the information is available for use for various purposes by using the network communication. Therefore, we developed command-line-based tools to obtain the information, and it was implemented in the operational log system.[3] The operational log system is one of the electric log systems for recording and viewing the accelerator operating time and contents of an operated device.

By using this system, the names of the required PVs are never missed from the list because creating the lists with a program is easy. By developing Web applications, searching the IOC hostname from the EPICS record name becomes possible. Furthermore, because this developed system has an autocomplete feature, searching by EPICS record name is possible without requiring the completed EPICS record name.

Using the inserted information, alive monitoring will be implemented in the near future for the RIBF control system. By using alive monitoring system, it will become possible to enhance the reliability of the control system.

References
1) M. Komiyama et al.: Proc. ICALEPCS14, SanFrancisco, CA, USA (2014), p.348.
2) M. Fujimaki et al.: RIKEN Accel. Prog. Rep. **37** (2004), p.279.
3) A. Uchiyama et al.: RIKEN Accel. Prog. Rep. **48** (2015), p.195.

† Condensed from the article in proceedings of the 15 th International Conference on Accelerator and Large Experimental Control Systems. Melbourne, Australia, (2015)

*1 RIKEN Nishina Center

New operation interface for rf voltage and phase of RIBF cyclotrons using rotary encoder

K. Yamada,[*1] S. Ishikawa,[*2] R. Koyama,[*2] K. Yadomi,[*2] and N. Sakamoto[*1]

The RIBF accelerator complex can accelerate all kinds of ions up to $\beta = v/c = 0.7$ via a four-stage cascade of ring cyclotrons, i.e., the RIKEN Ring Cyclotron (RRC), fixed-frequency Ring Cyclotron (fRC), Intermediate-energy Ring Cyclotron (IRC), and Superconducting Ring Cyclotron (SRC). The rf systems for these cyclotrons are controlled by using an individual programmable logic controller (PLC) for every rf resonator. The remote control interface for the fRC, IRC, and SRC accomplished in 2006 has been actualized by an Ethernet connection to PLCs using a PC base driver and SCADA software of Wonderware InTouch 9.5. The remote control interface had some problems such as slow response and disconnection of network owing to the use of an older-generation PLC. Thus, we have constructed a new operation interface to remotely control the rf voltage and phase using rotary encoders such as that for the RRC instead of using mouse clicks in order to realize smooth and comfortable operation of the cyclotrons.

Figure 1 shows a schematic of the new remote control system. The remote control interface is directly connected to an additional PLC (OMRON CS1H) installed in the control room. The signals of rotary encoders are counted by fast counter modules of the PLC and converted to set point data for the rf voltage and phase, which are stored in the PLC memory. The data are distributed to relay PLCs installed in the vicinity of the existing RF control PLCs for the fRC, IRC, and SRC through a private data link network using Controller Link. Each relay PLC is connected to the existing RF control PLCs via an open field network, DeviceNet, because the existing PLCs were already discontinuous product but they had been incorporated in the DeviceNet master module.

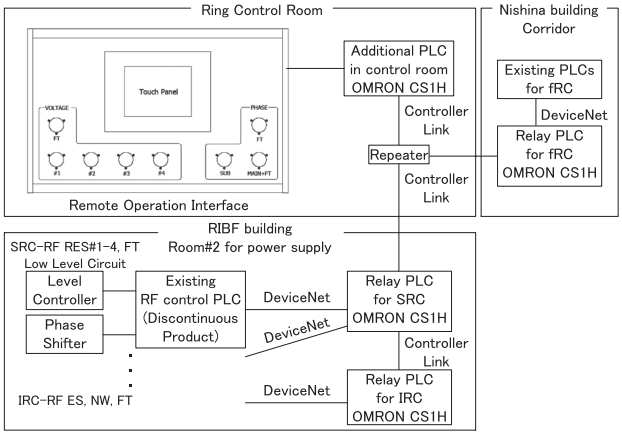

Fig. 1. Schematic of the new remote control system for RIBF cyclotrons.

As shown in Fig. 2, two hardware buttons, eight rotary encoders, and a touch panel are mounted on the interface. One of the hardware buttons is a LOCK button and the other is a SET button similar to the RRC interface. The control inhibition has to be released by the LOCK button to start the operation using encoders, and the control is automatically inhibited after 3 min. A control target cyclotron, fRC, IRC, or SRC has to be selected using the touch panel. When the lock is released, the all present set points of the rf voltage and phase on the existing RF control PLCs are imported to the memory on the PLC installed in the control room, and the operation using the conventional PC base control is invalidated, which ensures compatibility. The group of rotary encoders on the left is for rf voltage control, whereas the group on the right is for rf phase control. The voltage setting of all the rf resonators can be adjusted individually. The phase setting of the main acceleration resonators is adjusted using a rotary encoder simultaneously, and the phase setting of the flat-top resonator is adjusted independently. All the present values of voltage and phase, set points, and control step sizes are indicated on the touch panel. The control step size can be selected using the touch panel. The present set points can be saved to memory by pushing the SET button up to ten times.

The new system was successfully commissioned in March 2015 and was operated during the RIBF experiments without problems. Owing to the introduction of the new interface, smooth operation with a response ten times faster than that of previous systems and no network connection issues will lead to optimum tuning of the rf voltage and phase for the RIBF cyclotrons.

Fig. 2. Remote control interface for the new system.

*1 RIKEN Nishina Center
*2 SHI Accelerator Service Ltd.

Development of a buffer gas-free Buncher for SCRIT experiments

K. Yamada,[*1] T. Oonishi,[*2] K. Kurita,[*1] M. Togasaki,[*1] R. Toba,[*3] and M. Wakasugi[*2]

We developed low-energy–ion beam buncher[1] for ion beam injection into the SCRIT device at the Self-Confinig Radioactive isotope Ion Target (SCRIT)[2] facility. This apparatus makes it possible to convert a continuous beam from Electron-beam-driven RI separator for SCRIT (ERIS)[3] to a pulsed beam with 500 μs duration. This buncher is based on a linear radio-frequency quadrupole (RFQ) buncher widely used in the world. However no buffer gas is used and this buncher works in ultra-high vacuum condition. The new-type buncher we have developed stacks continuously injected ions using RF fringing fields created at both ends of the RFQ electrodes, and extracts them as a pulsed beam. In off-line test experiments, we found the DC to pulse conversion efficiency. We also found that the efficiency is greatly improved by combining with pre-bunching at the ion source using grid action.

Figure 1 shows the schematics of the off-line experimental setup of the system together with the longitudinal potential diagrams. This consists of an ion source with a grid, RFQ electrode with barrier electrodes as both ends, and the analyzing magnet. Three Faraday cups were used as beam diagnostic device as shown in the figure. The RFQ has a total length of 914 mm and a bore radius of r_0 = 8.0 mm. RF field with less than 500-V amplitude is supplied in the frequency range from 0.3 MHz to 3 MHz from an LC resonance circuit. The ion source is a surface ionization type, and it provides alkali metal ions ($^{133}Cs^+$, $^{85\text{-}87}Rb^+$, $^{39\text{-}41}K^+$, and $^{23}Na^+$) beam. Accelerating voltage V_{Acc} = 6.0 kV. The voltage V_{Bar} applied to barriers 1 and 2 was slightly lower than V_{Acc}, V_{Acc} - V_{Bar} = 1.5 V, and higher than the DC voltage V_{DC} applied to the RFQ electrodes, $V_{Bar} - V_{DC}$ = 5~10 V. With this condition, continuously injected ions are decelerated by the RF fringing field in between the barrier and the RFQ. Stacked ions are extracted from the buncher when the potential of the barrier electrode 2 is switched to V_{DC} – 120 V. This operation was repeated with appropriate frequency.

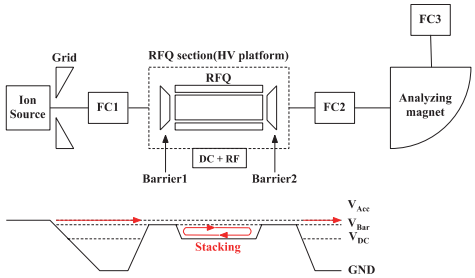

Fig.1. Experimental setup of the buncher system together with the longitudinal potential diagram (DC injection).

From the observed waveforms at FC1-3, we estimated the number of ions at each position. The stacking efficiency is defined as the ratio between the number of ions injected in the operation period (N_{inj}) and the extracted yields of pulsed beam (N_{ext}), $\varepsilon = N_{ext}/N_{inj}$. Figure 2 shows example of waveforms of pulsed Cs ion beams observed at FC3 at the operation frequency of 2 Hz. Red and green lines indicates cases of continuous beam injection and pre-bunched beam injection respectively. Pre-bunching enhances the yield of the pulsed beam by approximately three times. Estimated DC-pulse conversion efficiency is shown Fig. 3 as a function of the operation frequency. The efficiency increases with the operation frequency, and the typical value for continuous beam injection, for instance, is approximately 5% at the 2 Hz operations. The efficiency for the case of the pulsed beam is always enhanced and roughly 30% at the operation frequency of less than 10 Hz. This is due to the enhancement of the peak intensity of the pre-bunched beam and by significantly reducing the stacking time in the RFQ.

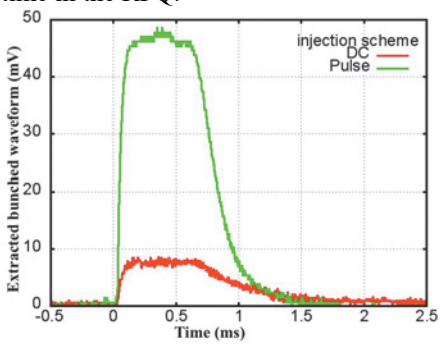

Fig. 2. Waveforms observed by FC3 for each injection schemes at the frequency of 2 Hz.

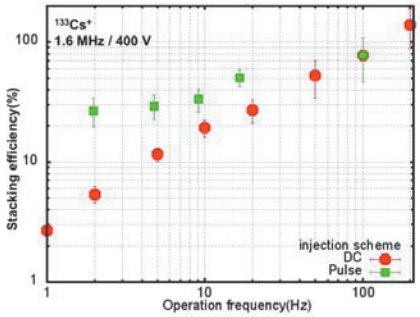

Fig. 3. Operation frequency dependence of stacking efficiency for each injection scheme.

*1 Department of Physics, Rikkyo University
*2 Riken Nishina Center
*3 Department of Nuclear Engineering, Nagaoka University of Technology

References

1) M. Togasaki et al.: to be published in HIAT proceedings.
2) M. Wakasugi et al., Nucl. Instr. and Meth. A 532, 216 (2004).
3) M. Wakasugi et al., Nucl. Instr. Meth. B317, 668 (2013).

Lithium ion production for laser ion source†

M. Okamura,[*1,*2] K. Palm,[*3] C. Stifler,[*4] D. Steski,[*1] S. Ikeda,[*5,*2] M. Kumaki,[*6,*2] and T. Kanesue[*1]

The use of laser ion source (LIS) is an effective and simple method for creating a wide variety of ions. However, this method has not yet been extensively tested on alkali metal targets owing to their high reactivity. In this report, we investigated the Li plasma properties in laser ablation for the future application of alkali metal beam acceleration because Li ion beams can be used for neutron beam creation[1].

Li oxidizes rapidly when exposed to the atmosphere. To limit the exposure of the targets, special precautions were taken when producing the targets. The metals were polished, rolled to an appropriate thickness using a rolling mill, and immediately stored in a portable vacuum chamber. When the targets were installed, argon gas flow was employed to reduce the exposure to oxygen. Then, the target chamber was immediately pumped down to vacuum. The attempted target thickness was 1.0 mm, although it was not easy to achieve good accuracy. The targets were irradiated with a neodymium-doped yttrium aluminum garnet (Nd:YAG) laser operating at 1.4 J, with a wavelength of 1064 nm and a pulse length of 6 ns. The laser was focused on the target with a plano-convex focusing lens with a focal length of 100 mm. The distance of the lens from the target was adjustable from outside of the target vacuum chamber, thus allowing the beam to be focused and defocused. The incident angle between the laser path and the beam line was 20°. The target chamber and subsequent beam line were held below 1.8×10^{-4} Pa for the duration of the experiment. A Faraday cup (FC) with a φ = 10 mm aperture was placed 2.4 m away from the targets to measure the beam current. The suppressor voltage of the FC was set to −3.5 kV. The positively charged particles in the plasma were analyzed using an electrostatic ion analyzer (EIA). The selected ions were detected by a secondary electron multiplier (SEM). The total distance between the detector and target was 3.7 m. The ion species and charge states were determined by the time of flight information in the SEM signal and the applied voltage to the EIA.

In the experiment, we detected H, Li, and O ions. Unfortunately, the apparatus cannot distinguish ions of different species but which have the same mass to charge ratio. Therefore, some detected signals may be contributed by different species. The entire view of the experimental setup was explained in our previous publication[2].

A focused laser beam with power density of the order of 10^{12} W/cm^2 was used to create high-charge-state Li beams. A fresh laser spot was always supplied in the motorized stage for every laser shot. The analysis showed oxygen charge states ranging from O^{1+} to O^{8+} as well as $^7Li^{3+}$, $^7Li^{2+}$, $^7Li^{1+}$, and $^6Li^{3+}$. The beam composition data can be seen in Fig. 1.

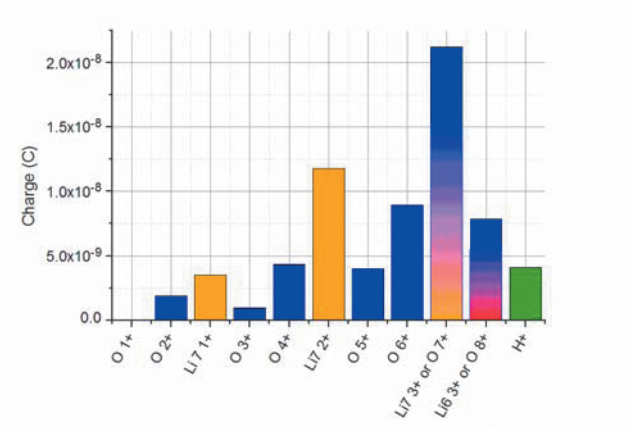

Fig. 1. Species and charge state distribution in the plasma from the Li target. The charges were counted at 1.0 m from the target with a 1.0 cm^2 sensing area.

The LIS could create high-charge-state ions from the Li target. There was an apparent oxygen contamination in the beams. We also found that the Li target was clearly oxidized in the vacuum chamber held below 1.8 x 10^{-4} Pa. To adopt a laser ion source with a Li target for industrial applications, oxidization and the time-consuming target preparation need to be overcome.

References

1) E. Norbeck, Jr. and C. S. Littlejohn, Phys. Rev. **108**, 3 (1957).
2) S. Ikeda et al., Rev. Sci. Instrum. **85**, 02B913 (2014).

† Condensed from the article in Rev. Sci. Instrum. 87, 02A901 (2016)

*1 Collider-Accelerator Department, BNL
*2 RIKEN Nishina Center
*3 Department of Physics, Cornell University
*4 Engineering Physics Systems Department, Providence College
*5 Interdisciplinary Graduate School of Science and Engineering, Tokyo Institute of Technology
*6 Research Institute for Science and Engineering, Waseda University

Response of an axial magnetic field to injection of laser ablation plasma

S. Ikeda,[*1,*2] M. Okamura,[*3] and K. Horioka[*2]

An ion source using laser ablation plasma can provide various types of heavy ion pulsed beam with relatively simple configuration, such as the source operated in the Brookhaven National Laboratory.[1)] In addition to this advantage, the plasma is expected to become a high current ion source because of the high density and high drift velocity. To achieve this, guiding of the expanding plasma with axial magnetic field is necessary and the mechanism needs to be made clear. During the above interaction, the magnetic field is distorted by the plasma while the distortion generates magnetic pressure affecting the plasma dynamics. The distortion is determined by a competing process between the convection by the plasma and the diffusion into the plasma. In the case of laser ablation plasma, both effects play some roles and vary within the plasma plume due to the distribution of the conductivity and the plasma velocity. Therefore, the magnetic field should evolve within the plume while giving rise to a structure within the plume. Hence, we investigated the response of an axial magnetic field against the plume injection with a magnetic probe, and then compared the result with plasma behavior.

Figure 1 shows the experimental setup. We produced the plasma plume using a 4×10^8 W/cm^2 Nd:YAG laser from an iron target in a chamber evacuated to 4×10^{-4} Pa. A coil 50 mm in diameter and 5 mm in length was placed at a distance of 260 mm from the target to generate the magnetic field that was 65 G at the center. A disk with a 14-mm-diameter aperture was placed between the target and the coil to define the plasma plume diameter. A magnetic probe was placed in the coil. A 20-turns pickup coil 6.4 mm in diameter and 2.0 mm in length was attached to the probe edge. By integrating the voltage signal from the probe, we measured the variation in the longitudinal component of the magnetic field. We also measured the plasma ion current density at a distance of 740 mm with a biased ion probe.

From the current density measurement, we found that the head of the plasma plume is preferentially guided and directed. In addition, the plume was estimated to pass through the coil from 5 to 30 μs.

Figure 2 shows the field response ΔB_z as a function of the distance from the coil center z at various time (8, 10, 14 μs) from the laser pulse. At any given point

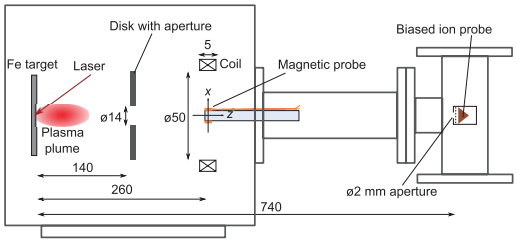

Fig. 1. Schematic of the experimental setup for magnetic field measurement.

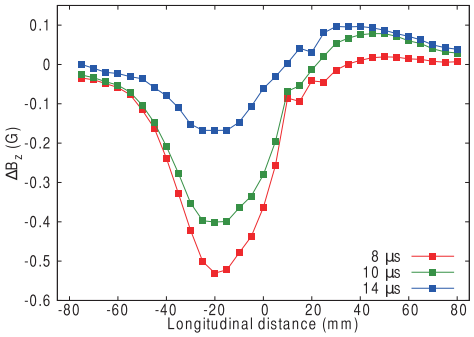

Fig. 2. Variation of magnetic field ΔB_z as a function of the distance from the coil center z at various time (8, 10, 14 μs) from the laser pulse.

of time, ΔB_z was negative in $z < 0$ and positive in $z > 0$. The absolute value of ΔB_z in $z < 0$ was larger than in $z > 0$, and additionally, ΔB_z changed from negative to positive in $z > 0$. These results mean that the magnetic field was distorted asymmetrically with respect to the midplane of the coil. On the other hand, ΔB_z in $z < 0$ in earlier time was smaller than that in later time. This means that the head of the plume distorts the field to a greater extent. Because the head is faster than the tail, this indicates that the different convective effect depending on the velocity leads to the different distortion within the plume.

The larger distortion by the head and the preferential guiding of the head as mentioned above show that the difference of the distortion results in the difference of the guiding effect.

From the investigation, we found that the magnetic field evolves within the plume asymmetrically, which leads to structure in the plume.

*1 RIKEN Nishina Center
*2 Interdisciplinary Graduate School of Science and Engineering, Tokyo Institute of Technology
*3 Collider Accelerator Department, Brookhaven National Laboratory

Reference

1) T. Kanesue *et al.*: *Proceedings of IPAC2014, Dresden, Germany*, p 1890 (2014).

Peformance of a fast kicker magnet for Rare-RI Ring†

H. Miura,[*1] Y. Abe,[*2] Z. Ge,[*2] K. Hiraishi,[*3] Y. Ichikawa,[*3] I. Kato,[*1] T. Moriguchi,[*3] D. Nagae,[*2] S. Naimi,[*2] T. Nishimura,[*1] S. Omika,[*1] A. Ozawa,[*3] F. Suzaki,[*1,*2] S. Suzuki,[*3] T. Suzuki,[*1] N. Tadano,[*1] Y. Tajiri,[*3] Y. Takeuchi,[*1] T. Uesaka,[*2] M. Wakasugi,[*2] T. Yamaguchi,[*1] Y. Yamaguchi,[*2] and Rare-RI ring collaborators

A fast kicker magnet is indispensable for injecting beams into the rare-RI ring individually[1)]. Therefore, we developed a distributed-constant type fast kicker magnet. The kicker magnet is equivalent to an electronic circuit that is a π-type LC circuit.

Based on the detailed simulations of the equivalent electronic circuit of the prototype kicker magnet, we optimized the inductance, capacitance, and mutual inductance. We used these simulation results to develop a new kicker magnet. The new kicker magnet parameters are designed to be $L = 100$ nH and $C = 350$ pF to improve impedance matching, and an additional capacitance of 2600 pF was attached to the entrance of the kicker magnet to prevent reflection.

We applied the search coil method to measure the magnetic field. The result of the magnetic field of the new kicker magnet at 20 kV is shown in Fig.1. The propagation time from a trigger signal input, which corresponds to 0 ns in Fig.1, until the peak of the kicker magnet field, is approximately 545 ns.

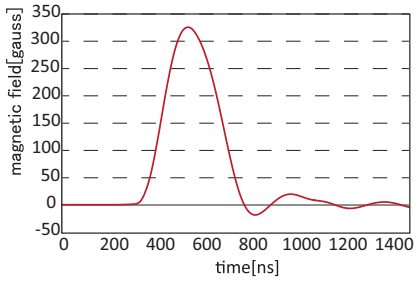

Fig. 1. Typical magnetic field of a new kicker magnet.

In June 2015, we carried out the first commissioning of the rare-RI ring using a $^{78}Kr^{36+}$ beam with an energy of 168 MeV/nucleon. The kick angle of 11.4 mrad is required for injection into the rare-RI ring. For the present beam condition, a magnetic field of 434 G is required. Thus, the kicker power supply should be charged up to 26.6 kV.

We tested an individual injection method using the new kicker magnet. To confirm the injection of the beam, a plastic scintillation counter was placed in the central orbit at the detector chamber after the next straight section of the rare-RI ring. When the beam is kicked correctly, it is counted by the plastic scintillation counter. We measured the number of counts by changing the charging voltage, as shown in Fig. 2. This figure shows the relative injection efficiency because the width of the plastic scintillation counter is smaller than that of the acceptance of the ring.

We tested the ejection of the stored beam using the same kicker magnet after 700 μs storage. A plastic scintillation counter was placed at the exit of the ring. We measured the number of events counted by the plastic scintillator by changing the ejection timing; the charging voltage of the kicker magnet was 26.6 kV. The result is shown in Fig. 3. This plastic scintillation has sufficient width to cover the extractable acceptance of the ring. From this result, the kicker magnet has a flat top of approximately 100 ns because the duration until the extraction efficiency up to 90 % of the peak is approximately $\pm$ 50 ns.

The present result shows that the individual injection method and ejection was successfully performed.

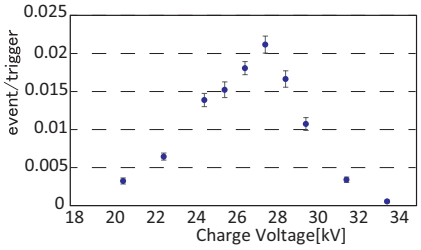

Fig. 2. Number of injected events by the plastic scintillation detector as a function of the charging voltage of the kicker magnet.

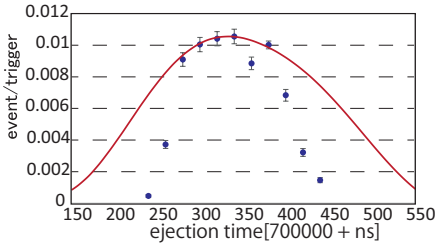

Fig. 3. Number of events counted by the plastic scintillation detector at the exit of the storage ring as a function of ejection delay timing.

Reference

1) Y. Yamaguchi et al., Phys. Scr. T166, 014056 (2015).

† Condensed from the article in Proceedings of HIAT2015, Yokohama,Japan

*1 Department of Physics, Saitama University
*2 RIKEN Nishina Center
*3 Institute of Physics, University of Tsukuba

9. Instrumentation

Ion-optical study of additive and subtractive modes of BigRIPS

H. Takeda,[*1] T. Kubo,[*1] N. Fukuda,[*1] H. Suzuki,[*1] D. S. Ahn,[*1] Y. Shimuzu,[*1] T. Sumikama,[*1] D. Murai,[*1] N. Inabe,[*1] K. Yoshida,[*1] K. Kusaka,[*1] Y. Yanagisawa,[*1] M. Ohtake,[*1] H. Sato,[*1] T. Komatsubara,[*1] and H. Geissel[*2]

One of the important features of the in-flight fragment separator BigRIPS[1)] is a two-stage separation scheme. Rare-isotope (RI) beam is produced and separated in the first stage (F0-F2) with an energy-loss degrader at the momentum dispersive focus F1. Particle identification and momentum analysis are performed event-by-event in the second stage (F3-F7) with the momentum dispersive foci F4, F5, and F6.[1,2)] Another energy-loss degrader placed at F5 is often used to separate unwanted isotopes produced in the first degrader at F1 as a result of the charge state change or the secondary reaction.

The two stages act independently and their isotopic separation power can be added or subtracted, depending on the experimental condition. When the separation powers of the two stages are added, the horizontal spatial distance at the final focus F7 would increase. Because widths also increase, improvement of the final resolving power will depend on the experimental condition.

The additive and subtractive modes can be switched by changing the sign of the magnification of a matching section F2-F3 in between the two stages. In a previous report,[3)] we have introduced a new ion-optical system for the additive mode. The F2-F3 magnification is reversed compared to the standard (subtractive) mode by adding one focus in the horizontal direction at the mid-point between F2 and F3. We performed machine studies to examine the two modes in this year.

In April 2015, we compared the additive and subtractive modes under the same conditions for the first and second stages. Only the matching section F2-F3 was changed. Isotopes around ^{132}Sn produced in a ^{238}U^{86+} + Be 5 mm reaction at 345 MeV/nucleon were used to measure the optical properties. 5-mm- and 3-mm-thick wedge-shaped aluminum degraders were placed at F1 and F5, respectively. Magnetic rigidity of the first dipole (D1) was 7.1 Tm and the other dipoles (D2-D6) were tuned so that the ^{132}Sn isotope came at the center at each focus.

Table 1 shows the measured mass dispersions at F2, F3, and F7 together with the LISE^{++} simulation. We can see that the mass dispersion became large at F7 in the additive mode as expected. However, there are some discrepancies in the additive mode between the measured and calculated values compared to those of the subtractive mode. These discrepancies may come from the discrepancies in the F2-F3 transfer matrix elements. For example, the measured and calculated magnifications were 0.78 and 1.01, respectively, while they agreed in a few % in the subtractive mode. The reason for the difference is under consideration. We also found that the telescopic condition was not fulfilled due to the very large $(a|x)$ value in the additive mode. The measured and calculated values were 1.89 and 2.14 mrad/mm, respectively. According to this $(a|x)$ term, isotopes that come off-center at F2 have large angles at F3 and the track reconstruction in the second stage would become worse. The transmission is also affected. The ^{132}Sn yield in the additive mode was about 30% less than that in the subtractive mode. Events with a large angle caused by the large $(a|x)$ term may be lost after F2. Reduction of the $(a|x)$ term is under consideration.

Table 1. Mass dispersion in mm/ΔA at F2, F3, and F7. See text for the RI beam setting in this measurement.

	subtractive		additive	
	measured	LISE^{++}	measured	LISE^{++}
F2	5.82	6.05	5.54	6.05
F3	-6.33	-6.41	4.72	6.11
F7	0.23	-0.71	12.1	18.5

Purities of the ^{132}Sn isotope are almost the same in both additive and subtractive modes, being 8% and 6% for the F1 slit at ±2 mm and ±64.2 mm, respectively, when the F2 and F7 slits are optimized for ^{132}Sn. The purities are dominated by the contamination from the same isotones, which occupy almost the same position at F2 in our case. The additive mode gives the same separation for such isotones as the subtractive mode. Therefore, the purities were not improved in the additive mode as we had expected. Altering the combination of energy and degrader thickness is required for isotone separation.

In November 2015, we performed another machine study for the two-stage separation. We applied the same conditions for the first stage as in April. Thickness of the aluminum degrader at F5 was changed (0 mm, 2 mm, 3 mm, and 5 mm) to investigate systematically the isotope separation in the subtractive mode. The measured mass dispersions at F7 varied from −7 to 11 mm/ΔA as a function of the F5 degrader thickness and were well reproduced with LISE^{++} simulations. Detailed analysis, including transmission, purity, and so on, is in progress.

*1 RIKEN Nishina Center
*2 GSI Helmholtzzentrum für Schwerionenforschung GmbH

References
1) T. Kubo: Nucl. Instr. Meth. **B204**, 97 (2003).
2) N. Fukuda et al.: Nucl. Instr. Meth. **B317**, 323 (2013).
3) H. Takeda et al.: RIKEN Accel. Prog. Rep. **48**, 208 (2015).

PPAC high-rate study with $Z \sim 50$ beams (MS-EXP15-09)

H. Sato,[*1] K. Kumagai,[*1] D.S. Ahn,[*1] N. Fukuda,[*1] N. Inabe,[*1] T. Komatsubara,[*1] T. Kubo,[*1] K. Kusaka,[*1] D. Murai,[*1] M. Ohtake,[*1] Y. Shimizu,[*1] T. Sumikama,[*1] H. Suzuki,[*1] H. Takeda,[*1] Y. Yanagisawa,[*1] and K. Yoshida[*1]

Position-sensitive Parallel Plate Avalanche Counter (PPAC) is one of the important focal plane detectors for the $B\rho$ measurement at RIBF[1]. Owing to the fast response of the PPAC with the delay line readout, the PPAC operated under the counting-rate of several MHz with the 2.5 MeV/u ^{4}He beam[2]. However, sometimes a discharge of the PPAC due to high-rate heavy-ion beams results in damage to the electrodes and causes the high voltage (HV) modules to trip[1]. Therefore, it is important to investigate the tolerance of the PPAC against intense heavy-ion beams.

An endurance test of the PPAC against high-rate heavy-ion beams was carried out in November 2015. Two double-PPACs[1] were placed in the F3 chamber of the BigRIPS separator. The upstream and downstream PPAC are named as F3-1 and F3-2, respectively. The size of F3-1 (F3-2) is 150 mm(X) × 150 mm(Y) (240 mm(X) × 150 mm(Y)). Each double-PPAC has two delay-line PPACs in its case, termed A- and B-side. Each PPAC is equipped with an anti-discharge unit, which is currently under development [3]. A mixed beam of around ^{132}Sn was used, whose energy at F3 was around 220 MeV/u. The beam size in σ at F3-1 was 2.1 mm (X) and 3.1 mm (Y), and at F3-2 the beam size was 7.5 mm (X) and 9.0 mm (Y).

Before irradiating the PPACs with intense beams, the HV dependence of individual detection efficiencies for each cathode was measured with a 1 kHz beam (Fig. 1). Subsequently, the HV was adjusted for all cathodes so as to realize the individual efficiency of around 95%. At that time, the total efficiency for X and Y plane, η_X and η_Y, was 99.86% and 99.92%, respectively. Here, η_X is defined as

$$\eta_X = \{1-(1-\eta_{F3\text{-}1AX})(1-\eta_{F3\text{-}1BX})\} \times \{1-(1-\eta_{F3\text{-}2AX})(1-\eta_{F3\text{-}2BX})\},$$

where $\eta_{F3\text{-}1AX}$ is the individual efficiency of the X cathode of the A-side PPAC at F3-1; η_Y is similarly defined.

Under this HV condition, PPACs were irradiated with high-rate beams in the range from 1 kHz to 1000 kHz, and the occurrence of the discharge and the change of the total efficiency were monitored. Firstly, there was neither discharge nor trip of the voltage modules even in the case of irradiation with the 600 kHz and 1000 kHz beams for 70 and 60 minutes, respectively. Secondly, the total efficiency decreased as beam rate increased as shown in Table 1. If the electrodes in the PPACs sustain damage, this decrease of the total efficiency will happen and will be irreversible. However, η_X and η_Y obtained with the 1 kHz beam in runs 612 and 621, which were performed just after irradiation with the 600 kHz and 1000 kHz beam respectively, reproduce the values obtained with the first 1 kHz beam in run 602. Thus, we can conclude that the electrodes in the PPACs were not damaged by the high-rate beams up to 1000 kHz. The reason for the decrease of η_X and η_Y can be explained by the property of the delay line: the total delay time of the signal (118 ns for 150 mm delay line length and 192 ns for 240 mm) results in the dead time of the PPAC. As a result, the efficiency decreases for high-rate beams.

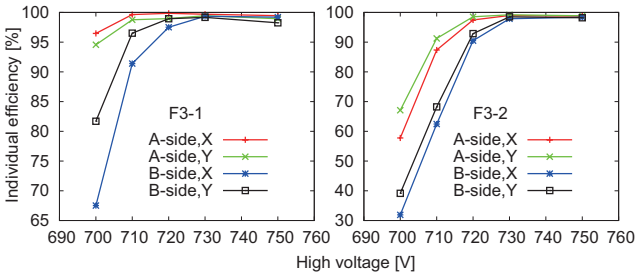

Fig. 1. Individual efficiency of each cathode. The adjusted voltage for each PPAC is as follows: F3-1A, 700 V; F3-1B, 720 V; F3-2A, 720 V; F3-2B, 730 V.

Table 1. Total efficiencies of η_X and η_Y.

run number	beam rate @F3 [kHz]	irradiation time [min]	η_X [%]	η_Y [%]
602	1	5	99.86	99.92
605	50	10	99.70	99.83
606	100	10	99.74	99.80
608	200	10	99.57	99.72
609	400	10	98.89	99.30
610	600	10	97.71	98.52
612	1	5	99.95	99.96
613	600	30	97.65	98.49
615	600	30	97.75	98.52
616	1000	30	90.83	93.30
617	1000	30	92.94	94.57
621	1	5	99.94	99.96

*1 RIKEN Nishina Center

References
1) H. Kumagai et al.: Nucl. Instrum. Meth. B **317**, 717 (2013).
2) H. Kumagai et al.: Nucl. Instrum. Meth. A **470**, 562 (2001).
3) Y. Sato et al.: JPS Conf. Proc. **6**, 030124 (2015).

ANSYS code calculations for measuring beam spot temperature

Z. Korkulu,[*1] K. Yoshida,[*1] Y. Yanagisawa[*1], and T. Kubo[*1]

RIBF cyclotrons can accelerate very heavy ions such as uranium up to 345 MeV/nucleon. The goal beam intensity is expected to be 1 particle μA (6.2×10^{12} pps), which corresponds to a beam power of 82 kW in the case of ^{238}U[1]. An important aspect in increasing beam intensity is limiting the maximal temperature due to beam energy loss in the material. Controlling this absorbed power is a key challenge. Therefore, a high-power production target system[2,3] was designed and constructed in 2007 for the BigRIPS separator[4,5]. The water-cooled rotational disk targets and ladder-shaped fixed targets are currently in operation.

As the fixed ladder-shaped target, a Be taper of 3-mm thickness was irratiated by a ^{238}U beam of 345 MeV/nucleon, up to 38 pnA with a beam spot size of 1.5-mm diameter. This target was tightly mounted on a water-cooled target holder using a 5-mm thick aluminum fixing plate. Although the present primary beam intensity is much lower than the goal value, the beam spot temperature at various conditions was measured and compared with thermal simulations to examine the beam power tolerance and to evaluate the cooling capacity of the high-power production target. The finite element thermal analysis code, ANSYS[6], was used to model thermal distributions in the targets.

Figure 1 shows the quarter model of the ladder-shaped target and the result of the temperature distribution calculated by the steady-state thermal analysis. The mesh of the target body is generated using three-dimensional hexahedral elements 0.2 mm in size. The input power was given as the heat generation, which is approximately 87 W/mm^3. In addition, the total absorbed power in the whole Be target, not the quarter model, is approximately 460 W for 35 pnA intensity. Owing to the high energy deposition in the target, the target system is cooled using a forced convection mode. For forced convection, the heat transfer coefficient of the cooling channel was calculated (using JAERI formula[7]) and used in the simulation. For this simulation, the cooling water (25°C) flowed at 3.5 l/min through the cooling channel. To ensure efficient heat transfer, the temperature-dependent thermal conductivity of Be and Al were used at temperatures between 25 and 750°C. As shown in Fig. 1, the maximum temperature of the target center was approximately 650°C under the above mentioned conditions. Figure 2 shows the calculated and measured beam spot temperature on a Be target as a function of the primary beam intensity of ^{48}Ca, ^{78}Kr, and ^{238}U. For all primary beams, the temperature is always below the melting temperature (1278°C) of the Be target for beam intensities

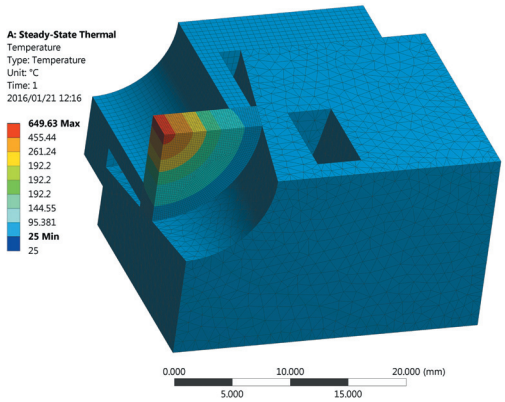

Fig. 1. Quarter finite element analysis model and the calculated temperature distrubiton in the Be target.

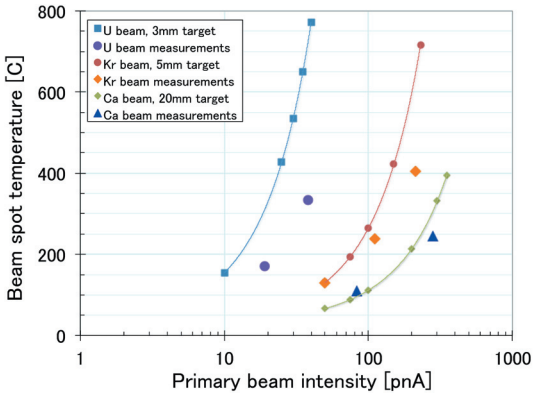

Fig. 2. Calculated and measured beam spot temperature on a Be target as the function of a different primary beam intensity.

used in the simulation. In order to reach the goal intensity, it is recommended to use a water-cooled rotating disk target with a suitable velocity so that different parts of the target are irradiated by bunches.

Presently, the beam spot temperature calculated using the ANSYS code is higher than the measured beam spot temperature[8]. Discrepancy between the measured temperature and the simulation can be caused by the suboptimal spatial resolution of the thermal camera system. Since the spatial resolution of the thermal camera is approximately 2 mm, some improvements to achieve a more accurate measurement will be necessary.

*1 RIKEN Nishina Center

References

1) Y. Yano, Nucl. Instr. Meth. B **261**, 1009 (2007).
2) A. Yoshida et. al., Nucl. Instr. Meth. A **521**, 65 (2004).
3) A. Yoshida et. al., Nucl. Instr. Meth. A **590**, 204 (2008).
4) T. Kubo, Nucl. Instr. Meth. B **204**, 97 (2003).
5) T. Kubo et al., IEEE Trans. Appl. Sup. **17**, 1069 (2007).
6) ANSYS, Inc. Product Release 16.0, USA.
7) J. Boscary et al., Fusion Eng. Des. **43**, 147 (1998).
8) Y. Yanagisawa et al.: In this report.

Measurement of beam-spot temperature on production target at BigRIPS

Y. Yanagisawa,*1 K. Yoshida,*1 Z. Korkulu,*1 and T. Kubo*1

The primary beam intensity until U beams at the RIBF is increasing yearly towards the final goal of 1 puA with 350 MeV/nucleon. The target needs to withstand the beam intensity. We report on the measurement of the beam-spot temperature on the production target for the BigRIPS for the primary ^{48}Ca, ^{78}Kr, and ^{238}U beams.

For the BigRIPS, two types of targets are used. One is a ladder-shaped target with water cooling, which is a fixed target for a low-beam-power experiment (a few kilowatts of energy loss) and the other is a water-cooled rotating disk target for a high-beam-power experiment. Details of the target system are described in ref. 1). We have measured the temperature of the surface of the target using an infrared thermos-viewer at a distance of 14 m from the target.

Figure 1 shows the beam-spot temperature on the fixed- and rotating-Be target as a function of the primary beam intensity at the exit of the SRC of ^{48}Ca, ^{78}Kr and ^{238}U beams with a beam-spot size approximately 1.5 mm in diameter. The maximum intensities of the ^{48}Ca, ^{78}Kr, and ^{238}U beams in these measurements are 480 pnA, 270 pnA, and 38 pnA, respectively. The calculated beam-spot temperature for the fixed targets is described in ref. 2). We can observe the image of the temperature distribution for the rotating Be target for the first time. Figure 2 shows the temperature image of the 15-mm-thick Be target at 100 rpm bombarded by 48Ca with 420 pnA as an example. A significant change of the beam-spot temperature due to the difference in rotational speeds, 100 rpm and 300 rpm, was not observed.

By Comparing the observed temperatures for the fixed- and rotating-Be target of the same thickness for ^{48}Ca and ^{78}Kr, it can be seen that the latter has a 5-8 times gain in the primary beam intensities. The results indicate that we have a sufficient margin for the lighter primary beams below Kr with an intensity of 1 puA.

We also measured the beam-spot temperature only on a fixed target for ^{238}U with 38 pnA, as shown in Fig. 1. In the case of the 3-mm-thick Be target, its maximum temperature is 333 degrees, which is sufficiently lower than the melting point of Be. However, the center of the target had a melted mark and small cracks with spike shapes on the downstream side after the experiment, as shown in Fig. 3. Although the reason for this is currently under investigation, we have assumed that the fixed target reaches the critical limit in this intensity. We are planning to introduce the rotating target in ^{238}U next time. Even if the rotating target has an eightfold gain as compared to the fixed one, as is the case for Kr beams, it is difficult for the target to withstand the goal intensity, i.e., 1 puA for ^{238}U beams. We will have to improve the target system based on various measurement data including the beam-spot temperature and its model calculations.

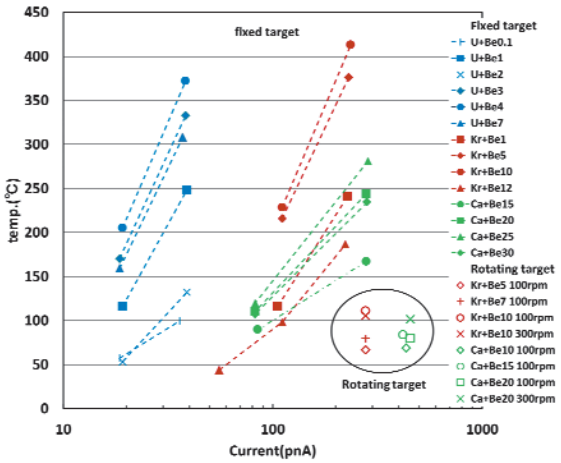

Fig.1 Beam-spot temperature on a Be target as a function of the primary beam intensity of ^{48}Ca, ^{78}Kr, and ^{238}U beams.

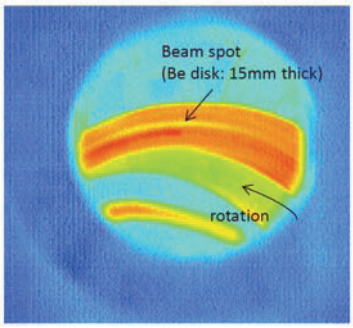

Fig.2 Observed temperature image in the 15-mm-thick rotating Be target with 100 rpm bombarded by ^{48}Ca with 420 pnA.

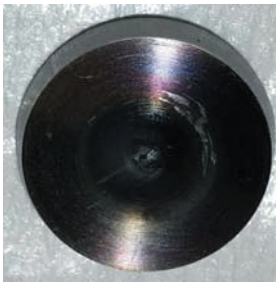

Fig.3 The downstream side of the 3-mm-thick Be target bombarded by a ^{238}U beam with 38 pnA after the experiment.

References

1) A. Yoshida et al.: Nucl. Instrum. Meth. Phys. Res. A 655, 10 (2011) and their references.
2) Z. Korkulu et al.: In this report.

*1 RIKEN Nishina Center

Temperature measurements of the high power beam dump of the BigRIPS separator

K. Yoshida,[*1] Y. Yanagisawa,[*1] Z. Korkulu,[*1] H. Takeda,[*1] K. Kusaka,[*1] M. Ohtake,[*1] N. Fukuda,[*1] H. Suzuki,[*1] D. S. Ahn,[*1] Y. Shimizu,[*1] T. Sumikama,[*1] N. Inabe,[*1] and T. Kubo[*1]

The high-power beam dump[1,2] that stops intense primary beams from the super-conducting cyclotron SRC is one of the crucial devices of the BigRIPS fragment separator. The beam dump consists of the side dump and the exit dump. The two exit beam dumps, for an intense ^{238}U beam and for the other beams, were designed to handle various ion beams with intensities up to 1 pμA.[2] Two exit dumps had the same structure except for the distance from the dump surface and the cooling channel; 1 mm for ^{238}U and 3 mm for the other. The latter exit beam dump and the side dump were constructed in 2007. Since then, it has been successfully operated with various beams including a ^{238}U beam although the available beam intensity was low. The design of the beam dumps was based on the sophisticated thermal model simulation[1,2] and its validity has not been verified because the available beam intensity was not so high. Recently the intense ^{48}Ca beam became available. As the first step of the evaluation of the cooling capacity of the beam dump, the temperature measurements of the exit beam dump were performed with the intense ^{48}Ca beam.

The inner-side exit beam dump[1,2] that was made by the Cu-Cr-Zr alloy and the M8 screw threads were formed as the cooling channels was irradiated by the ^{48}Ca beam with an energy of 345 MeV/n and intensity of 460 pnA. Cooled water with a temperature of 13 ℃, pressure of 1.0 MPa, and flow speed of 10 m/s were supplied to the dump as the coolant. Temperatures are measured by using a thermocouple (T. C.) mounted on the dump at 3 mm behind the dump surface. By changing the position of the dump, horizontal distribution of the temperature was measured against the beam spot. Various beam heat densities were obtained by tuning the first superconducting quadrupole triplet STQ1 located upstream of the dump. The spot sizes of the beam at the dump were estimated from the primary beam profile (size and angle) measured separately at the second focus F2 located at the downstream of the dump. The first order matrix of the ion optics of the BigRIPS separator was used for the estimation.

In Fig.1, the observed temperatures are shown for three different beam spot sizes, resulting in the different heat densities. The results of finite element calculations using the ANSYS code[3] are also shown in the figure. In the calculations, thermal conductivity was assumed to be a constant at 375 W/mK. The heat transfer coefficient of the cooling channel was also assumed to be 90 - 130 kW/m^{2}K for wall temperatures of 15 - 180℃, which corresponded to three times larger values of that of smooth tube with same diameter (ϕ 8).[4] The heat transfer coefficient of the smooth tube was calculated with the JAERI formula.[5] As seen in the lower panels of Fig. 1, a good agreement was obtained between the results of the thermal model simulation and the observed temperatures. It suggests that the estimation of the cooling capacity of the beam dump is reasonable since similar model calculations were made in the estimation.

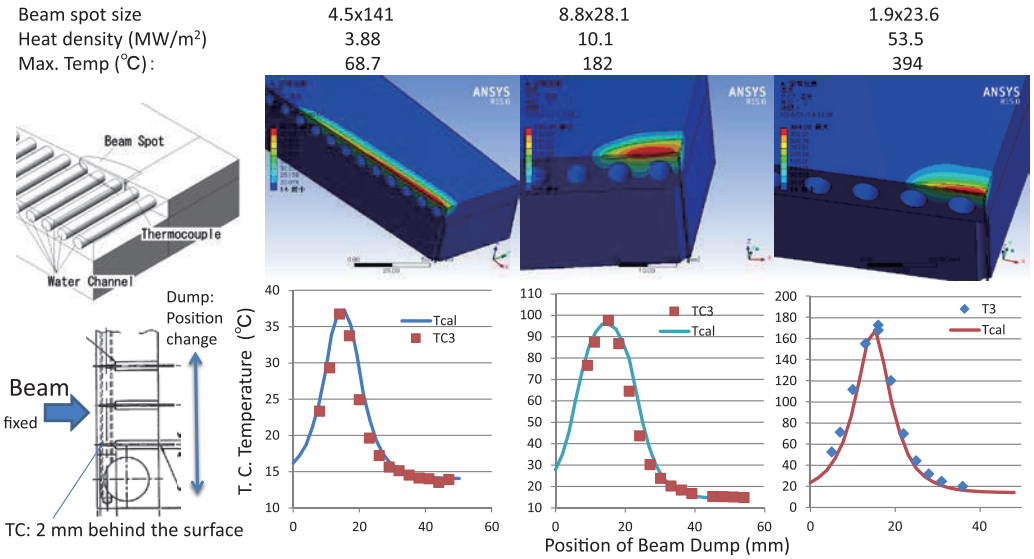

Fig.1 Beam dump temperatures for various beam sizes. Dots are measured values and lines and 2D figures are the results of the ANSYS calculations.

*1 RIKEN Nishina Center

References

1) N. Fukuda et al., RIKEN Accel. Prog. Rep. **41**, 119 (2008).
2) K. Yoshida et al., Nucl. Instr. Methods **B 317**, 373 (2013).
3) ANSYS Inc. Product Release 15.0, USA.
4) K. Masaki et al., Fusion Eng. Des. **61-62**, 171 (2002).
5) J. Boscary et al., Fusion Eng. Des. **43**, 147 (1998).

Production of low-energy 4.17 MeV/nucleon ^{9}C beam with polyethylene degrader at RIPS

E. Milman,[*1,*3] T. Teranishi,[*2] S. Sakaguchi,[*1,*2] K. Abe,[*4] Y. Akiyama,[*1,*2] D. Beaumel,[*1,*5] S. Chebotaryov,[*1,*3] T. Fukuta,[*1,*2] A. Galindo-Uribarri,[*6] S. Hayakawa,[*4] S. Hwang,[*7] Y. Ichikawa,[*1] N. Imai,[*4] D. Kahl,[*4] R. Kaku,[*1,*2] T. Kaneko,[*1,*8] D. Kim,[*1,*9] W. Kim,[*3] N. Kitamura,[*4] Y. Norimatsu,[*1,*2] E. Romero-Romero,[*6] D. Sakae,[*1,*2] Y. Sakaguchi,[*4] M. Sasano,[*1] K. Tateishi,[*1] T. Uesaka,[*1] K. Yamada,[*1,*8] and H. Yamaguchi[*4]

Theoretically, four low-lying ^{10}N levels are expected as broad and overlapping resonances[1,2]. The level structure of ^{10}N is very important to understand resonances in ^{10}Li because ^{10}N and ^{10}Li are the mirror nuclei expected to have a similar structure. The information of ^{10}Li levels can be used to constrain the ^{9}Li+n potential, which is required for constructing the three-body model of the borromean nucleus ^{11}Li.

We proposed to measure the excitation function of the (differential) cross section and vector analyzing power (A_y) for the ^{9}C+p reaction to determine these broad resonances[3]. The thick-target method in inverse kinematics[4] will be used for the measurement. In this method, the excitation functions for the cross section and A_y will be scanned with a single beam energy utilizing the energy loss of the beam particle in the target. The range of center-of-mass energy is set to 1−5 MeV to cover the theoretically expected ground state of ^{10}N and several excited states.

In September 2015, a test ^{9}C+p resonant scattering experiment was conducted at RIPS, where the production of a low-energy ^{9}C beam was tested and the excitation function was measured with an unpolarized polyethylene ($(CH_2)_n$) target. A ^{9}C beam was produced using a 70-MeV/nucleon ^{12}C primary beam with an intensity of 400 particle-nA and a 4-mm Be primary target at RIPS. The configuration of RIPS is described in Ref. [5]. A wedge-type degrader with d/R at 0.8, where d is the central thickness of the degrader and R is the range of ^{9}C with a central momentum, was used at F1 to degrade the ^{9}C beam energy. In order to realize a high transmission efficiency of ^{9}C from F1 to F2, a conventional aluminum F1 degrader was replaced with a new $(CH_2)_n$ degrader, because the multiple scattering effect, which is serious at d/R ∼0.8, can be highly reduced with a low-Z material.

The central thickness of the $(CH_2)_n$ degrader was set to 316 mg/cm^2 so that the energy loss of the ^{9}C beam was equal to the energy loss in the standard Al degrader with 444 mg/cm^2 thickness. The wedge angle of the degrader was set to 5 mrad based on the LISE++ code[6] calculation.The intensity of the ^{9}C beam was measured at F2 for the two cases using the standard Al degrader and the $(CH_2)_n$ degrader at F1. The latter was 1.8 times higher than the former, which shows improvement of transmission using the low-Z material for the F1 degrader.

The ^{9}C beam energy was determined using the time-of- flight (ToF) measured between a 0.5-mm-thick plastic scintillator installed at F2 and one of two position-sensitive Parallel Plate Avalanche Counters (PPAC) at the F3 focal plane. The energy of the ^{9}C beam was precisely controlled by a rotatable thin polyethylene degrader installed at the F2 focal plane. The correction for the energy loss in the PPACs was calculated based on the SRIM code[7]. The beam energy determined in this analysis was 4.17 MeV/nucleon with an energy spread of $\sigma = 0.73$ MeV/nucleon.

The identification of the secondary beam particles was conducted based on the RF and ToF information. Thus the measured purity and intensity of the ^{9}C beam were 15% and 2.4×10^4 pps at F3, respectively. These purity and intensity values are sufficiently high for the planned resonant scattering experiment.

In conclusion, a 4.17-MeV/nucleon ^{9}C beam was successfully produced with a thick F1 degrader at RIPS. In the experiment, the transmission of the degraded beam was improved by suppressing multiple scattering effects in the thick F1 degrader using a low-Z material.

*1 RIKEN Nishina Center
*2 Department of Physics, Kyushu University
*3 Department of Physics, Kyungpook National University
*4 CNS, The University of Tokyo
*5 IPN Orsay
*6 Oak Ridge National Laboratory
*7 JAEA
*8 Department of Physics, Toho University
*9 Department of Physics, Ewha Womans University

References

1) S. Aoyama, K. Kato, K. Ikeda, Phys. Lett. B **414**, 13 (1997).
2) E. Caurier et al., Phys. Rev. C **66**, 024314 (2002).
3) T. Teranishi, S. Sakaguchi, T. Uesaka et al., AIP Conf. Proc. **1525**, 552 (2013).
4) K.P. Artemov et al., Sov. J. Nucl. Phys. **52**, 408 (1990).
5) T. Kubo et al., Nucl. Instr. Meth. B **70**, 309 (1992).
6) O. B. Tarasov, D. Bazin, Nucl. Instr. Meth. B **266**, 4657 (2008).
7) J.F. Ziegler, M.D. Ziegler, J.P. Biersak, Nucl. Instr. Meth. B **268**, 1818 (2010).

SpiRITROOT: an analysis framework for the SπRIT experiment

G. Jhang,[*1,*2] J. W. Lee,[*1,*2] G. Cerizza,[*2] T. Isobe,[*3] and M. B. Tsang[*2] for the SπRIT collaboration

The main detector in the SπRIT(SAMURAI pion Reconstruction and Ion Tracker) experiment is the SπRIT-TPC (time projection chamber)[1]. The GET electronics[2] as front-end readout electronics reads the charge and time with 12,096 pad electrodes of the TPC and stores structured binary-encoded data. To decode and analyze this data in a consistent and systematic manner, we provide a software framework to the collaborators that accounts for both simulation and data analysis.

SpiRITROOT is the analysis framework for the SπRIT experiment developed on the structure of FairRoot[4]. FairRoot provides a highly modulized programming environment that allows developers to maintain the code in an organized manner and to simplify the analysis process for users. SpiRITROOT has two parts: the simulation and the experimental data flow. A Schematic of these parts is shown in Fig. 1. Each rectangle indicates a stage inside the software framework. Each stage has entries (blue text) corresponding to tasks.

In the *simulation data flow*, collision events generated by external programs such as PHITS[5] and pBUU[6] are fed to SpiRITROOT to simulate the detector response through the GEANT4 package. After simulating the events, the digitization stage takes over with its three tasks: drift task, pad response task, and electronics task. The drift task calculates the number of ionized electrons, their drift time, and their dispersion from the ionized point. The pad response task calculates the amplification and dispersion by the anode wires. Finally, the electronics task simulates the response pulse from the electronics using a reference pulse measured from the cosmic data.

In the *experimental data flow*, the data are read by the unpacker stage. The GETDecoder task unpacks the binary data, while the STConverter task maps the signals of each channel to each pad. In addition, the ANAROOT task has been added to unpack and decode data from RIBFDAQ, which contains information from the KATANA and multiplicity trigger arrays[7].

The reconstruction stage is common to both data flows. The pulse shape analysis task analyzes the shaped pulse from the electronics to find the hit position and energy loss. The hit clustering task collects groups of hits satisfying certain criteria, such as proximity between hits, into clusters to determine the closest position to the ionized point. The linear tracking task, developed mainly to identify tracks and analyze the commissioning experiment data, is used to fit the straight tracks and determine the reaction vertices. The Riemann tracking task identifies and separates the tracks in the event and provides approximate track parameters, such as the curvature and dip angle, using a simple helix fit. Finally, the GENFIT[9] task analyzes the tracks using a Kalman filtering algorithm and provides information on physical observables such as momentum, mass, and charge to perform particle identification taking into account the energy loss.

SpiRITROOT is working successfully in analyzing the experimental data. One of the useful tools provided to the users for online analysis is the event display, which allows to visualize the reconstructed events in 3D. The brief report on commisssioning experiment and one example of 3D-reconstructed collision event are presented in Ref.[8]

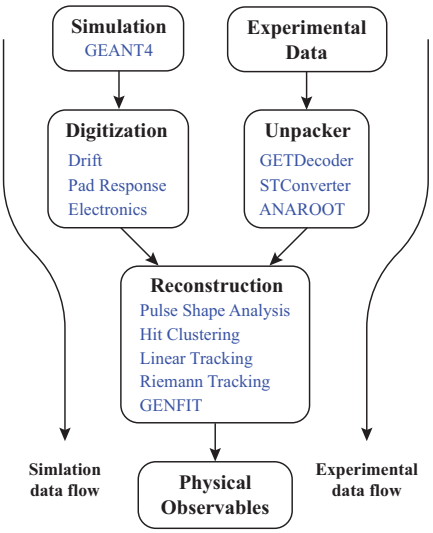

Fig. 1. Simple description of the data flow in SpiRITROOT. Both the simulation and experimental data are analyzed in the single framework.

*1 Department of Physics, Korea University
*2 NSCL, Michigan State University
*3 RIKEN Nishina Center

References
1) R. Shane *et al.*, Nucl. Instr. Meth. A **784**, 513 (2015).
2) E. Pollacco *et al.*, Phys. Procedia **37**, 1799 (2013).
3) T. Isobe *et al.*, in this report.
4) M. Al-Turany *et al.*, J. Phys. Conf. Ser. **396**, 022001 (2012).
5) T. Sato *et al.*, J. Nucl. Sci. Technol. **50:9**, 913-923 (2013)
6) J. Hong and P. Danielewicz, Phys. Rev. C **90**, 024605 (2014).
7) M. Kaneko *et al.*, in this report.
8) M. Kurata-Nishimura *et al.*, in this report.
9) C. Höppner *et al.*, Nucl. Instr. Meth. A **620**, 518 (2010).

Construction of readout system for SPiRIT-TPC

T. Isobe,[*1] M. Kurata-Nishimura,[*1] H. Baba,[*1] M. Kaneko,[*2] T. Murakami,[*2] W.G. Lynch,[*3] J. Barney,[*3] J. Estee,[*3] S. Tangwancharoen,[*3] G. Jhang,[*4] and J.W. Lee[*4] for the SPiRIT Collaboration

SPiRIT Time Projection Chamber (TPC) is being constructed for the study of density dependent symmetry energy using heavy RI collision at RIKEN-RIBF[1]. A novel readout system, General Electronics for TPC (GET)[2], for the signal coming from the TPC has been employed for the SPiRIT-TPC[3].

At the end of summer 2015, 48 AsAd boards for the amplification and digitization of signal were mounted on the TPC as shown in the Picture 1. During the installation of AsAd boards, the performance of the system was carefully checked. After we mounted half of the electronic components, we found that there were large gain deviations between different pads. This was a serious problem for the TPC, as TPC needs a uniform gain so that it can achieve good tracking and proper triggering. The reason for this was the instability in the power that was provided to the AGET ASIC chips on the readout board, which can be improved by changing the components on the AsAd board. After this modification, we mounted all the boards on the TPC again and checked the uniformity of gain by pulsing the ground wire, which generates a potential around the amplification region. As shown in Fig. 2, the uniformity of the gain is good enough for the reconstruction of charged particle trajectories.

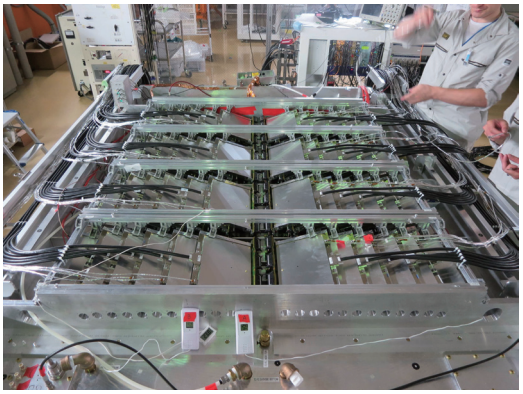

Fig. 1. GET electronics mounted on SPiRIT TPC. Each AsAd board is shielded with Al cover.

The GET system employs NARVAL[4] as DAQ system, GANIL run control (RC), and GANIL user interface (UI). We employ the GANIL RC and graphical UI for controlling SPiRIT system. In order to control RIBF-DAQ along with GET in the same framework, a software of the SOAP server that communicates with GANIL RC was developed. As demonstrated in the graphical UI shown in Fig. 3, a user can control the CoBo boards, which are back-end electronics of GET, as well as RIBF-DAQ system named Babirl/GTO. Fig. 3 also demonstrates the DAQ data throughput on the disk of ∼100 MB/s/CoBo, which corresponds to 1.2 GB/s in total.

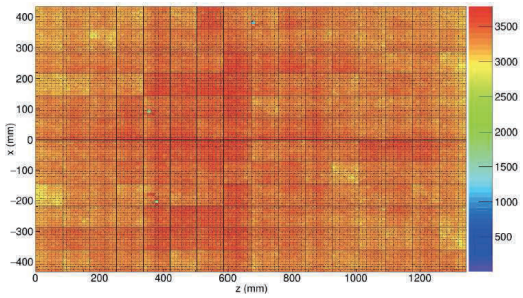

Fig. 2. Gain uniformity of TPC pads. 5.3V signal is pulsed through the ground wire of TPC. Out of 108×112=12096 pads, 3 pads show lower gain while other pads show good gain uniformity.

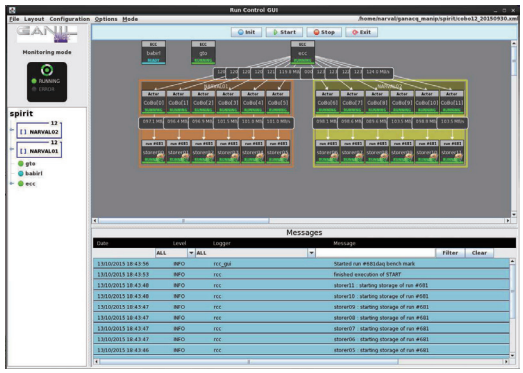

Fig. 3. Graphical UI of SPiRIT DAQ. Babirl, which is RIBF common DAQ system, and GTO can be controlled through this UI.

The commissioning of the readout system including SPiRIT-TPC was carried out during 2015 fall as reported in this annual report.

*1 RIKEN Nishina Center
*2 Department of Physics, Kyoto University
*3 National Superconducting Cyclotron Laboratory, Michigan State University
*4 Department of Physics, Korea University

References

1) S. Rebecca et al., Nucl. Inst. and Met. A **784**, 513 (2015).
2) E. Pollacco et al., Physics Procedia **37**, 1799 (2012).
3) T. Isobe et al., RIKEN Accel. Prog. Rep. **48**, 204 (2015).
4) X. Grave., Proc. 14th IEEE NPSS RT Conf, 65(2005).

Multiplicity trigger array for the SπRIT experiment

M. Kaneko,[*1] [*2] T. Murakami,[*1] T. Isobe,[*2] M. Kurata-Nishimura[*2] for the SπRIT collaboration

In the SπRIT (SAMURAI pion Reconstruction and Ion Tracker) experiment, it is important to identify the charged pions that are generated from heavy ion collisions of high centrality and reconstruct their momenta to determine the π^+/π^- ratio, which contains information on the nuclear symmetry energy. To accumulate data that focuses on symmetry energy, it is also important for the trigger system to have sensitivity to the event centrality. As it is well known that the impact parameter correlates with multiplicity of the collision, higher-centrality collisions are extractable preferentially by triggering events with high multiplicity. While detail analysis on charged particle multiplicity will be necessary through SπRIT-TPC,[1)] the impact parameter within at least 5 fm as a central collision must be survived at the stage of triggering.

We have developed an trigger detector sensitive to multiplicity for the SπRIT-TPC data acquisition, which is called the "multiplicity trigger array". This detector consists of 30 extruded scintillator bars that are in close contact with both sides of the TPC, which is shown in Fig.1 as enclosed with an orange dotted line, using 60 bars in total. The walls of the TPC are 1mm thick aluminum windows allowing light fragment particles from the reaction to pass through and be detected by the external triggering system. The dimensions of each scintillator bar are 450 mm*50 mm*10 mm, which are coated with oxidized titanium to improve light reflection. Each bar has a hole of about 1.5 mmϕ centered along its length for a wave length shifting fiber. The collected light will be detected by 1.3 mm^2 MPPC attached to the ends of the fiber.

For readout electronics, the VME-EASIROC[2)] is used. This module was developed by Tohoku and KEK group in 2014, for the readout of multi-MPPC detector systems. EASIROC (Extended Analogue Silicon PhotoMultiplier ReadOut Chip) is used for 32 photodiodes readout developed by Omega in France.[3)] Each chip has a parallel circuit of preamplifiers, shapers, and discriminators. VME-EASIROC has two EASIROC chips on the board and is capable of reading out 64 MPPCs. The parameters of the EASIROC are variably controlled by the onboard FPGA communicating via an SiTCP connection to another computer. We can also obtain the information of the MPPC signal by the ADC onboard chip and the MHTDC logic implemented in the FPGA. The calculation logic for multiplicity is located on the FPGA, which is done by counting the number of discriminator signals that surpass the threshold value. After the calculation, the result will be compared with the user set threshold of multiplicity and generate a trigger signal within about 52 ns for the whole VME-EASIROC module.

In the fall of 2015, the SπRIT-TPC was commissioned by performing an experiment using a ^{79}Se beam impinging on Al and Sn targets. The SπRIT-TPC was setup outside the SAMURAI magnet and surrounded by the multiplicity trigger array. The histogram in Fig.2 shows charged particle multiplicity with the condition of coincidence between at least one hit in the multiplicity trigger array and the beam start counter located just upstream of the TPC. It is clear that most of the events had low multiplicity originating due to non-central collisions. In perspective of the real experiment, analyzing commissioning data is crucial to find the optimal trigger conditions for rejecting peripheral-type collisions.[4)]

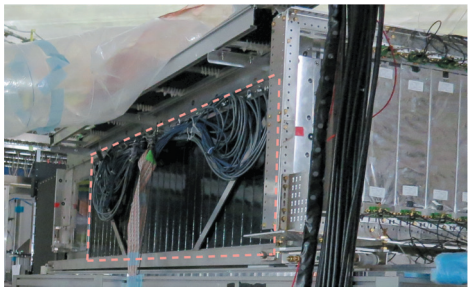

Fig. 1. One-sided view of multiplicity trigger array.

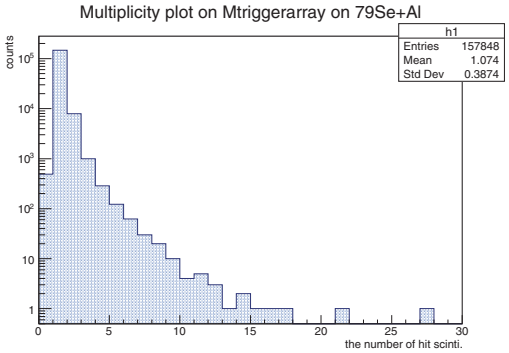

Fig. 2. Multiplicity plot of charged particle detected by multiplicity trigger array in the ^{79}Se commissioning run.

*1 Department of Physics, University of Kyoto
*2 RIKEN Nishina Center

References
1) R. Shane et al.: Nucl. Instr. Meth. A **784**, 513 (2015).
2) T. Shiozaki: Master's thesis, Department of Physics, Tohoku university (2014).
3) Omega group. EASIROC DATA SHEET. (2011).
4) M. Kurata-Nishimura et al.: in this report.

Performance test of the silicon tracker for the heavy-ion-proton experiments at SAMURAI

V. Panin,[*1] M. Kurokawa,[*1] K. Yoneda,[*1] H. Baba,[*1] J. C. Blackmon,[*2] Z. Elekes,[*3] Z. Halász,[*3] D. H. Kim,[*4] T. Motobayashi,[*1] H. Otsu,[*1] B. C. Rasco[*2] A. Saastamoinen,[*5] L. G. Sobotka,[*6] L. Trache,[*7] and T. Uesaka[*1]

An essential component of the future setup of the heavy-ion-proton (HI-p) experiments[1] at SAMURAI will be an array of GLAST-type[2] single-sided silicon strip detectors (SSDs) situated downstream of the target. These detectors will be used for precise tracking and identification of outgoing protons and heavy residues. Each detector is 325 μm thick and has dimensions of 87.6×87.6 mm^2 with a readout-pitch size of 864 μm. A key feature of the SSDs is their wide dynamic range, which allows for simultaneous detection of protons and heavy ions, which deposit to a single SSD energy ranging from ∼100 keV up to several hundreds MeV, respectively. This feature is achieved via custom-designed ASIC dual-gain preamplifiers providing low-gain (LG) and high-gain (HG) readouts coupled to the high-density processing circuit HINP[3].

A performance test with the SSDs and their new electronics was conducted at the HIMAC facility in Japan, using beams of protons with energies between 150 and 230 MeV as well as heavy-ion beams ^{12}C, ^{84}Kr, and ^{132}Xe (primary and secondary) at a few hundreds MeV/u. Only 32 central strips out of the 128 strips of a single sensor were fully instrumented by the newly designed ASIC preamplifiers, and only those channels were read-out during the experiment.

The results of the performance test are summarized in Fig. 1. Using the secondary beam, obtained by fragmentation of the primary ^{132}Xe at an energy of 200 MeV/u (see PID plot in Fig. 1(A,B)), the response of the LG readout was investigated for a wide range of nuclear charge Z. A good linearity of the LG readout was observed (Fig. 1(D)) along with a deposited-energy dE resolution of $\sigma(dE/E) \approx 1.4\%$, which is close to the designed value. The cross-talk ratio between a fired and a neighbouring strip is found to be ∼1% after the add-back analysis combining HG and LG data. Saturation of the LG readout was observed at $dE \gtrsim 650$ MeV, although the reconstruction of even larger dE was possible owing to a certain amount of interstrip hits in which dE is divided between the adjacent strips.

The performance of the HG readout was tested with ^{12}C and proton beams. Good linearity of the HG dynamic range was confirmed. The required detection threshold of $dE \gtrsim 100$ keV for protons can be achieved with the present configuration. The total detection efficiency of protons was found to be above 97%. Thus, it is confirmed that the combined dynamic range of the detector spans from ∼100 keV to ∼650 MeV, which in perspective would allow the simultaneous detection of protons and Z ≈ 50 heavy ions at RIBF energies.

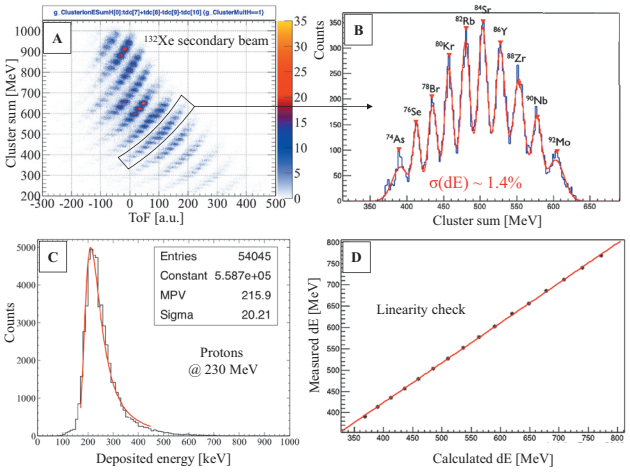

Fig. 1. Performance results of the silicon tracker in the HIMAC test experiment. Figure A: particle identification (PID) of the secondary beam from ^{132}Xe at 200 MeV/u, where dE measured by the SSD (cluster sum after the add-back) is plotted against the time of flight (ToF). Figure B: dE response of the SSD with the indicated resolution $\sigma(dE)$ for the selected species in Figure A and the multiple-gauss fit (red line). Figure C: dE response of the HG readout with respect to 230 MeV protons and Landau fit (red line). Figure D: comparison of the measured and calculated dE response in the SSD (symbols) with a linear fit (red line).

The design and production of the missing preamplifier circuits is currently in progress and is expected to be completed in 2016. Hence, a sufficient amount of dual-gain readouts will be provided for all four silicon trackers (*i.e.*, $4 \times 128 = 512$ strips) intended for the actual HI-p experiments.

*1 RIKEN Nishina Center
*2 Louisiana State University
*3 Institute for Nuclear Research, MTA Atomki
*4 Ewha Womans University
*5 Cyclotron Institute, Texas A&M University
*6 Washington University
*7 IFIN-HH

References

1) V. Panin *et al.*: RIKEN Accel. Prog. Rep., Vol 48 (2015), 53.
2) R. Bellazzini *et al.*: Nucl. Instr. Meth. Phys. Res. A, Vol. 512 (2003), 136-142.
3) G. L. Engel *et al.*: Nucl. Instr. Meth. Phys. Res. A, Vol, 573 (2007), 418-426.

Development for proton detector NINJA at SAMURAI magnet gap with VME-EASIROC readout

N. Chiga,[*1] T. Saito,[*1,*2] T.Isobe,[*1] and H. Otsu[*1]

SAMURAI has various properties for nuclear spectroscopic studies. Up to now, experimental programs measuring heavy residual and neutrons in coincidence have been performed. On the other hand, projectile velocity protons have not been considered for coincidence measurement since they cannot go to the downstream of the magnet due to the strong focusing by the SAMURAI magnet. Therefore, a new proton detector array NINJA(Nimble detector array for Nucleons with JAck-knife like trajectory) have been constructed. The NINJA located inside the SAMURAI gap and can be operated under the strong magnetic field of SAMURAI. NINJA enables us to provide exotic decay channels such as *d*-bar (singlet s state on $p + n$ system) decay from excited states of nuclei. It is also expected to detect one of the protons from the (p,2p) reaction at forward angle combined with the SAMURAI-MINOS configuration.

Properties of NINJA are shown in Tab. 1. Geometry of NINJA was designed to be used on various experiment without interfering with other particle trajectories than that of protons.

Table 1. Specifications of NINJA

Structure of detector	1 X-layer, 1 Y-layer
Scintillator	EJ-200
Formation of Scintillator	X-layer (18 slats) 60×720 mm^2×10 mm^t Y-layer (12 slats) 60×1100 mm^2×10 mm^t
Readout structure	WLS,MPPC(double side)
Readout circuit	VME-EASIROC
Slide limit	800 mm
Cable length	Vacuum side：4.5 m Atmosphere side：0.5 m

The NINJA consists of plastic scintillator with optical readout by MPPC mounted at top and bottom side through wave length shift fiber (WLS) KURARAY YB-5. The WLS is mounted on backside ditch of the plastic scintillator. At both ends of the WLS, dedicated connectors[1], are attached so as to be connect MPPCs optically. The signals from MPPCs are read-out by the EASIROC circuit[2] implemented on VME bus. In parallel this readout, we separately prepared a hand-made single channel readout circuit to obtain the response of MPPC and their HV dependence of readout efficiency.

A supporting structure of the NINJA was designed to compose the array within 25 mm in depth. The size of the supporting structure is minimized to enlarge the active area of NINJA.

Readout cable layout were determined by estimating it on a CAD software. Low consumption cable at high frequency (S-02162-B) was chosen for vacuum side. The signals are transmitted through a vacuum feed through attached at the bottom side of the extension duct of the SAMURAI gap chamber. From the feed through to the read-out circuit, the LEMO-16 pair exchange cables with 50 cm length and 17 pair to 34 pair cables with 20 cm is used to minimize the length of the cables. The high voltages for each MPPCs are supplied via hand-made AC coupled circuit connected to the exchange cable.

The support structure of NINJA can be slid along a rail which is mounted inside the SAMURAI vacuum chamber as shown in Fig. 1. The position of the detector can be determined depending on trajectories of protons, which are given by the magnetic field and proton momenta in interest.

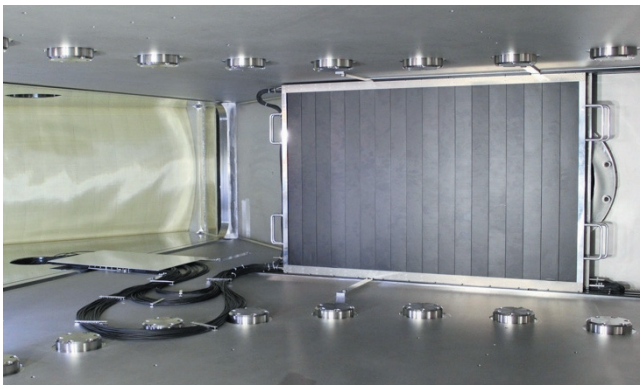

Fig. 1: NINJA inside the SAMURAI Gap.

In the last experiment[3),4)], the position is optimized for the 200 MeV protons with a 2.4T of SAMURAI magnetic field.

From this experiment, we found that noise reduction is necessary so as to use NINJA as a trigger source, while it works well as a parasitic detector. The NINJA will be used to every SAMURAI experiment with *n*-HI coincidence configuration.

References

1) H. Kawamuko et al., Proceedings of science PoS (PD07)043 (2007).
2) T. Shiozaki, “Development of a MPPC multi-channel readout system for the Σp scattering experiment”, Master's thesis, Tohoku university (2014).
3) S. Takeuchi et al., in this report.
4) Y. Kondo, et al., in this report.

*1 RIKEN Nishina Center
*2 Department of Physics, University of Tokyo

Frame design for the γ-ray detector array CATANA

N. Chiga,[*1] H. Otsu,[*1] M. Shikata,[*1,*2] T. Ozaki,[*1,*2] A. T. Saito,[*1,*2] T. Nakamura,[*1,*2] Y. Kondo,[*1,*2] and Y. Togano[*1,*2]

The γ-ray detector array CATANA[1] is being constructed to measure the E1 response of the neutron-rich nuclei. 200 CsI(Na) detectors compose CATANA, and are configured the packed layout (barrel shape) to realize the high detection efficiency and position resolution. This report describes the design of the CATANA frame and its concepts.

Since CATANA will be used in many experiments with SAMURAI, The frame should have the high maintainability and flexibility. The CsI(Na) crystals will be configured to have a barrel like structure (CsI unit) to achieve the high efficiency as shown in the left side of Fig. 1. To achieve the high maintainability, the 10 detectors will be supported by a frame shown in the right side of Fig. 1 , and the barrel like configuration will be realized by using 20 CsI units. The CsI(Na) crystal and PMT are connected by using an inlaid support on the top of the crystal. An O-ring is put for light shielding between the inlaid support and the crystal. The detector is connected to the CsI unit by a jig. Individual detector can be easily removed from the CsI unit, for the high maintainability. Fine adjustment of the detector positions can be done on the CsI unit. The total weight of the CsI unit is about 25 kg so as to handle it without a crane operation. A side plate of CsI unit has numerous small holes for the easy and clean cabling.

Figure 2 shows the main frame of the CATANA (left) and half of the top part (right). The CsI unit is mounted on the main frame by a guide attached to the main frame. The guide is made of a synthetic resin to isolate the CsI unit electrically. The frame width along the beam line and the frame height are 59 cm and 276 cm, respectively. The width is almost half of the present DALI frame[2], so as to put a reaction target closer to the SAMURAI magnet. The whole frame can be craned by using eyebolts on the main frame. The top part of the main frame can be opened to the direction perpendicular to the beam line for easier work around the reaction target put at the center of CATANA. The shaft for the opening is a trapezoidal screw to fix the position of the frame without any locking mechanism. Ladders for cables are put on a plate to support the CsI unit (shown in purple in Fig. 2). The bottom part of the main frame has space at both sides to put a high-voltage power supply for PMTs and/or circuits for signal processing. The space follows the EIA standard for 19-inch racks. The parts for seismic reinforcement are put under the main frame. The offsets of heights can also be attached under the main frame, to cope with the different beam-line height depending on the focal planes such as F8 of BigRIPS.

The CATANA frame construction is now in progress.

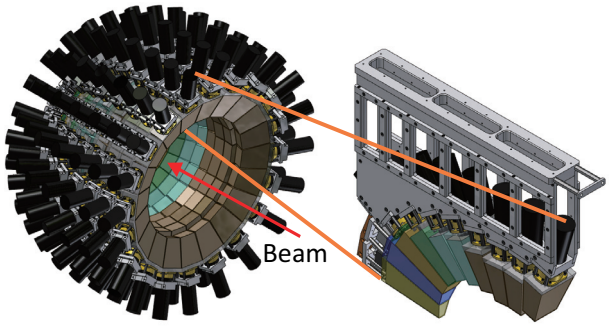

Fig. 1. Configuration of CsI(Na) detectors in CATANA (left) and the support frame for 10 detectors (right).

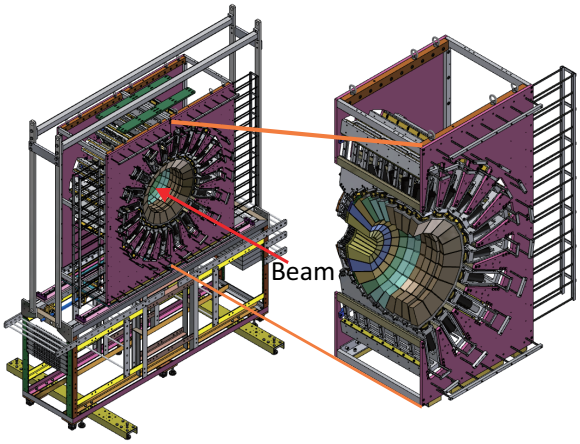

Fig. 2. The frame of CATANA with 200 CsI(Na) crystals.

References

1) Y. Togano et al.: RIKEN. Accel. Prog. Rep. **47**, 179 (2013).
2) S. Takeuchi et al.: Nucl. Instr. and Meth. A **763**, 596 (2014).

*1 RIKEN Nishina Center
*2 Department of Physics, Tokyo Institute of Technology

Status of the $(p, 2p)$ silicon tracker for upcoming fission experiments with the SAMURAI spectrometer

S. Reichert,[*1,*2] M. Sako,[*2] M. Sasano,[*2] D. Mücher,[*3] H. Baba,[*2] C. Berner,[*1] M. Böhmer,[*1] N. Chiga,[*2] R. Gernhäuser,[*1] W. F. Henning,[*4] T. Kobayashi,[*5] Y. Kubota,[*2,*6] R. Lang,[*1] L. Maier,[*1] V. Panin,[*2] L. Stuhl,[*2] E. Takada,[*7] T. Uesaka,[*2] L. Werner, [*1] and J. Yasuda[*2,*8]

For studying the fission induced by the $(p, 2p)$ reaction with RI beams of heavy unstable nuclei[1], a $(p, 2p)$ setup with high missing mass resolution will be installed[2,3]. Therefore a collaboration between RIKEN and TUM is developing two major new detector components: A time-of-flight (TOF) detector assembly to determine the energy of light charged particles, and a silicon tracker array presented here. Typical energies of the detected protons range 80 to 200 MeV, resulting in a low energy loss of 60 to 150 keV.

The silicon tracker is a two-arm setup with three layers of 100 μm thick, single-sided strip detectors with a pitch of 100 μm[3]. The strips of the first two layers are oriented vertically to determine the first-order polar angles, while the third layer strips are oriented horizontally. With an additional beam tracking by drift chambers in front of the target, we derive high-resolution reconstruction for both polar and azimuthal angles. Results of Geant4 simulations with 3-mm-thick CH_2 show an expected angular resolution of $\sigma \sim 3$ mrad.

The silicon wafers were designed by M. Sako and purchased by RIKEN. They were sent to TUM in November 2015. The PCB design and the electronics for readout are from TUM. Preliminary tests of the individual detector PCBs were conducted in Munich before the PCBs were subsequently shipped to Japan where integration into the BABIRL DAQ system was performed.

For one detector, maximum trigger rates of 15 kHz in raw data mode and 50 kHz in zero suppressed, pedestal corrected mode (normal mode) were achieved. These rates are currently limited by the data transfer to the BABIRL-DAQ computer and have to be scaled down by the number of detectors for the full setup to 1 kHz. Using a coincidence trigger signal from beam tracking detectors and the abovementioned TOF detectors, we expect only rates below 100 Hz in a typical experimental scenario at HIMAC and RIBF.

The small energy loss in the silicon renders the detector noise level a critical issue. The noise level can be evaluated in raw data mode with random triggers (pedestal run).

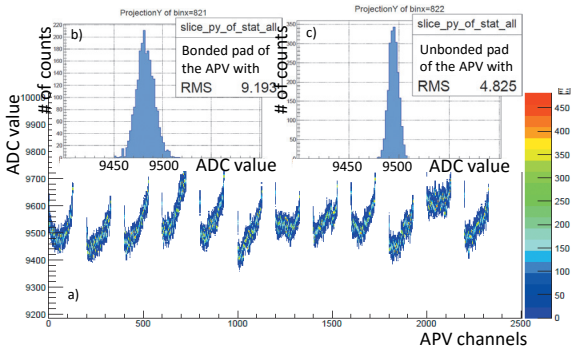

Fig. 1. Pedestal run of the first layer with 768 strips. Here they are divided into 12 groups representing the 12 APV25s with 128 channels each (64 bonded).

Figure 1(a) shows the ADC values for all the APV channels used for the detector in the first layer where every second channel is bonded. Typical noise levels for bonded channels are in the range of $\sigma = 10$ ADC units, see Fig. 1(b), while the unbonded, reference channels in Fig. 1(c) show a more narrow distribution of $\sigma = 5$ ADC units. With a calibration of 0.5 to 0.6 keV per ADC unit, we expect a signal to noise ratio of 10:1 in the experiment. Recently performed runs of cosmic ray measurements (energy loss of 35 keV) validate this expectation, and the protons were clear above the set 5 σ thresholds.

This new setup was tested at the end of February 2016 at HIMAC with the reactions of ^{16}O$(p, 2p)^{15}$N and ^{132}Xe$(p, 2p)$ fission each with $E = 290$ MeV/nucleon and 10^5 pps in inverse kinematic. In particular, for the first reaction we will be able to demonstrate the missing mass spectroscopy based on our setup by reconstructing kinetic curves for the first excited state at 6.3 MeV with an uncertainty better than $\sigma = 1$ MeV.

*1 Department of Physics, Technical University Munich
*2 RIKEN Nishina Center
*3 Department of Physics, University of Guelph
*4 ANL
*5 Department of Physics, Tohoku University
*6 Center for Nuclear Studies, University of Tokyo
*7 NIRS
*8 Kyushu University

References

1) D. Mücher, M. Sasano et al.: Proposal RIBF NP-PAC-12 *Fission Barrier Studies of Neutron-Rich Nuclei via the (p,2p) Reaction* (2013).
2) D. Mücher, S. Reichert et al.: RIKEN Accel. Prog. Rep. 48 (2015).
3) S. Reichert, M. Sako et al.: RIKEN Accel. Prog. Rep. 48 (2015).

Development of the He-filling system for the SAMURAI spectrometer

V. Panin,[*1] S. Chebotaryov,[*1,*2] S. Sakaguchi,[*3] Z. Elekes,[*4] N. Chiga,[*1] and H. Otsu[*1]

In the upcoming Light-Ion experiments SAMURAI 12/13 and in the HI-Proton experiments SAMURAI 24/25/28/29, the SAMURAI gap will be filled by He at 1 atm pressure, as required by the use of large-sized windows at the entrance and exit ends of the spectrometer to maximize its angular acceptance.

A test window was constructed with the total area of 1200 × 3340 mm^2, which can replace the existing window for outgoing charged particles. The chosen material for the He-window was the 100-μm PET film KEL86W.

To validate the design of the He-window and the air-replacement method, a He filling test was performed using a test chamber with volume V≈1.4 m^3. The PET film was superposed onto a 2-mm rubber frame and both were attached to the chamber's flange by a segmented metal frame to provide sufficient gas tightness. He was injected into the chamber and the air-He mixture was ejected to the atmosphere through the outlet port on the opposite side of the chamber. Time-dependence of the absolute O_2 concentration, $C^{O_2}(t)$, in the chamber was monitored by the O_2 sensors with a precision of 0.1%. The sensors were placed at three different heights: 2 cm (bottom), 27.5 cm (middle), and 55 cm (top) in the center of the chamber to control the homogeneity of the He-air mixture. The O_2 sensors were controlled via an external PC and their data were read out every 5 seconds.

The air concentration, $C^{air}(t)$, at every moment of time t was determined as follows:

$$C^{air}(t) = \frac{C^{O_2}(t)}{20.9\%} \times 100\%, \qquad (1)$$

where 20.9% is the C^{O_2} in the air at normal conditions. Hence, the He concentration is determined as:

$$C^{He}(t) = 100\% - C^{air}(t). \qquad (2)$$

The results of the gas-replacement test are summarized in Fig. 1. The total time of gas ventilation required to reach C^{He}≈95% (or C^{O_2}≈1%) was around 3 h and 35 min with an average input He-flow F_{in}≈20 L/min.

The air replacement as a function of time t is described by the basic room-purge equation:

$$C^{air}(t) = C^{air}(t_0)\exp(-\frac{F_{in}}{V}(t - t_0)), \qquad (3)$$

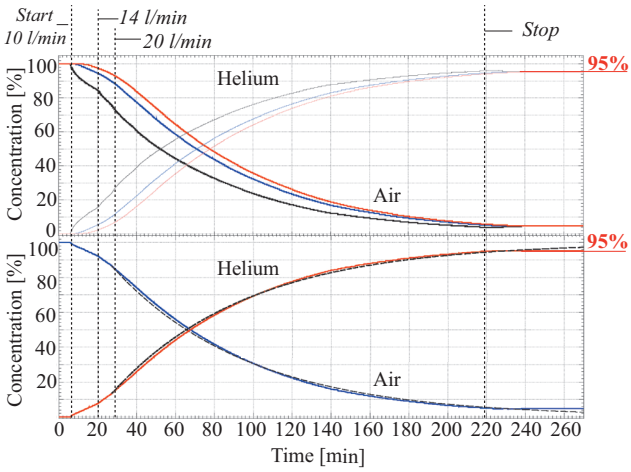

Fig. 1. Top figure: time-dependence of the air (bold lines) and He (faint lines) concentrations, derived from the data of the bottom (red line), middle (blue line) and top (black line) O_2 sensors. Bottom figure: same as the top figure, but the concentrations (He - red line, air - blue line) are averaged between the three sensors. The dashed curves in the bottom figure are calculated using equation 3. The vertical dashed lines indicate the start and the end of He injection as well as the time points when the injected He-flow changed to the indicated values.

where V is the volume of the chamber and t_0 is the start time of the ventilation. This function is plotted in the bottom graph of Fig.1 (dashed curves) and is in good agreement with the data. Based on this, one can estimate for the SAMURAI gap with V≈10 m^3 and input He-flow F_{in}≈20 L/min, the necessary time to reach C^{He}=95% is about 25 h with a consumption of about 30 m^3 of He-gas (at 1 atm).

No He leak was found after stopping the ventilation and sealing the chamber. C^{He} and C^{O_2} remained constant for at least 4 consecutive days. Moreover, no significant change in pressure (< 1mbar) was observed during and after the ventilation.

In conclusion, good performance of the He-window design and the feasibility of the applied gas-filling method, which is in agreement with theoretical expectations, have been confirmed. In future, a large exit window (5340×1000 mm^2) will be constructed and tested with the SAMURAI gap under experimental conditions.

*1 RIKEN Nishina Center
*2 Department of Physics, Kyungpook National Universityty
*3 Department of Physics, Kyushu University
*4 Institute for Nuclear Research, MTA Atomki

Beta-delayed neutron measurement with new detector NiGIRI

V.H. Phong,[*1,*2] S. Nishimura,[*1] J. Liu,[*3] T. Lokotko,[*3] Z. Li,[*4] and J. Lee[*3]

A new scintillation detector system NiGIRI[1] (Neutron, ion and gamma ray identification for Radioactive Isotope beam) is under development to measure the energies of neutrons for decay and reaction studies using the time-of-flight technique[2]. The design of the NiGIRI detector is based on a novel plastic scintillation material EJ-299-33, which has a superior pulse shape discrimination (PSD) capability[3]. Each scintillator bar (30x55x127 mm^3) is coupled by two PMTs (Hamamatsu H11265-200 and R8520-20-12) allowing to locate the interaction position along the scintillator bar from the time difference between two PMT signals.

A feasibility study of the NiGIRI has been conducted in conjunction with the newly developed plastic scintillator strip detector (MaCi) coupled with the multianode PMT (Hamamatsu H8500B) as a start detector. An array of 26 NiGIRI detectors were arranged in a half-barrel configuration surrounding the start detector and attached into the EURICA support frame with a flight path of approximately 50 cm. The waveform output from each detector was recorded by four flash ADC modules (CAEN V1730B) with a sampling rate of 2 ns synchronized with the RIBF DAQ and EURICA DAQ by sharing the clock with LUPO modules. A customized DAQ for the flash ADC with the capability of processing high data throughput has been developed.

Offline digital pulse processing was performed to extract useful information such as timing and pulse height to reconstruct the implantation and decay position in the start detector as well as time-of-flight between the start detector and NiGIRI detectors in the sub-nano second resolution. By applying a charge integration method with the optimized parameters, a clear separation between neutrons and gamma rays was obtained as shown in Fig. 1 while the time-of-fight was obtained by using the pulse fitting method.

The test experiment has been carried out in the parasitic mode with the SEASTAR campaign. Figure 1 shows the experimental setup. The RI beam after reaction target at F8 focal plane and the Zero Degree Spectrometer (ZDS) tuned for selecting isotopes around ^{95}Kr was implanted into the MaCi detector at the F11 focal plane while beta delayed neutrons and gamma rays were measured by the NiGIRI and the EURICA array.

Figure 2 shows the time-of-flight spectrum combining all NiGIRI detectors with the decay curve reconstructed in the MaCi detector for the beta-correlated gamma and neutron events identified with NiGIRI detectors. The delayed neutron events were selected by gating on a 200 ms window after the RI implantation in MaCi. Possible high energy neutrons have been detected from this spectrum.

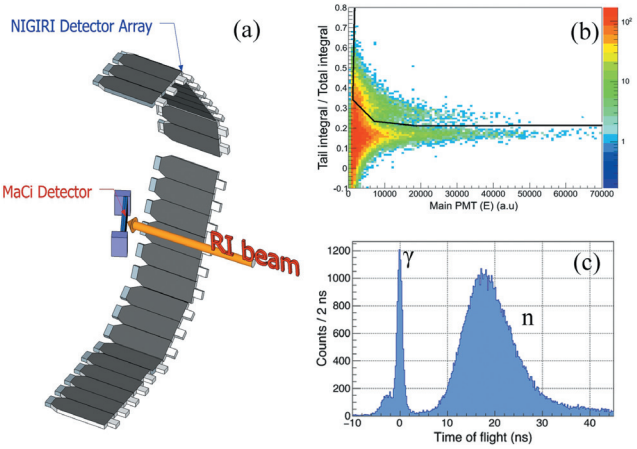

Fig.1. A schematic view of the experimental setup employing the NiGIRI and MaCi detectors (a). ^{252}Cf source test: PSD versus total integral. PSD cut (black lines) has been applied to select neutron events (b). The time-of-flight spectrum from all NiGIRI detectors after applying PSD cut (c) (small tail prior to gamma ray peak appeared due to backscattering).

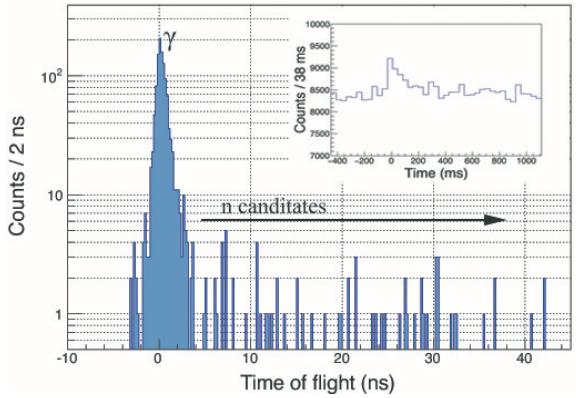

Fig.2. Combined neutron time-of-flight spectrum associated with the implantation of the RI beam in the MaCi detector. The inserted figure shows the time correlation between decay events and implantation events from the MaCi detector.

Further analysis with the available spectroscopic information of delayed gamma rays from EURICA is undergoing. The result from this test experiment is expected to provide useful information for the upcoming BRIKEN project to measure the beta-delayed neutron emission probability.

References

1) H. Masuzwa et al., RIKEN Accel. Prog. Rep. **48** (2016).
2) Matei et al.; *Proceedings of Science, PoS (NIC IX)*, **138** (2008).
3) S. Nyibule et al.; Nucl. Instr. Meth. A **728**, 36-39 (2013).

[*1] RIKEN Nishina Center
[*2] Faculty of Physics, VNU University of Science, Hanoi.
[*3] Department of Physics, The University of Hong Kong
[*4] School of Physics, Peking University

Low-pressure MWDC system for ESPRI experiment (Ⅱ)

Y. Matsuda,[*1,*2] J. Zenihiro,[*2] S. Terashima,[*2,*3] and H. Sakaguchi[*2,*4]

Elastic scattering of protons with RI beams (ESPRI) has been used to study the ground-state properties of unstable nuclei[1]. In ESPRI experiments, the trajectories of the RI beams, the energy and intensity of which are respectively 200-300 MeV/nucleon and 10^{5-6} particles per second, should be measured. Recently, in order to improve the detection efficiency and tracking resolution, a low-pressure multi wire drift chamber (MWDC) system was constructed[2]. This report describes the characteristics evaluated with various beams (^{132}Xe and its secondary beams) and detector gases (CH_4, C_2H_6, and i-C_4H_{10}).

The experiment was performed at NIRS-HIMAC. Figure 1 shows the detection efficiency for the 300 MeV/nucleon Xe beam when the pressure of each gas was controlled at 50 Torr. The beam intensity was 5×10^3 particles per pulse (pulse width of 1 s). The threshold voltage of the ASDs was −20 mV. The definition of symbols in Fig. 1 is the same as in Sec. 2.3 of Ref. 3. For all the gases, the efficiency reaches 100%. While the voltage increased with an increase in the pressure, the voltage at $\leq$ 50 Torr was almost unchanged. Figure 2 shows the position resolution for an X plane. For all gases at 50–200 Torr, the resolution reaches about 50 μm (rms).

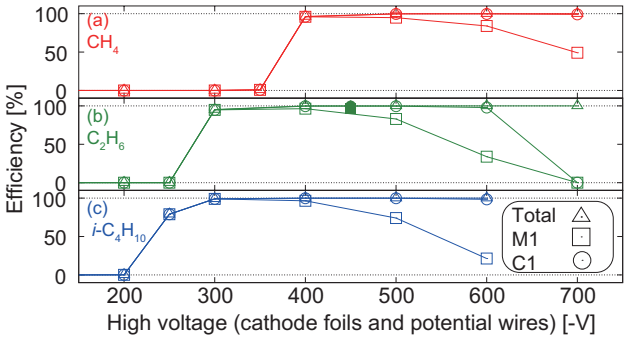

Fig. 1. Detection efficiency at 50 Torr for Xe beam. (a) CH_4, (b) C_2H_6, and (c) i-C_4H_{10}.

Next, the dependence of these quantities on the beam intensity and energy was investigated. The data corresponding to 300 $\times10^3$ particles per pulse are plotted with closed markers in Fig. 1 and 2. The data indicate negligibe intensity dependence. This is because of a small cell size of 5 mm. The results for the 200 MeV/nucleon Xe beam were the same as above.

Finally, the detection efficiency for a cocktail beam was investigated. Figure 3 shows the total detection efficiency for the Z =25, 35, and 40 particles when the pressure of each gas is 50 Torr. Except for the absolute voltage, a specific difference of the tendency does not exist among the gases.

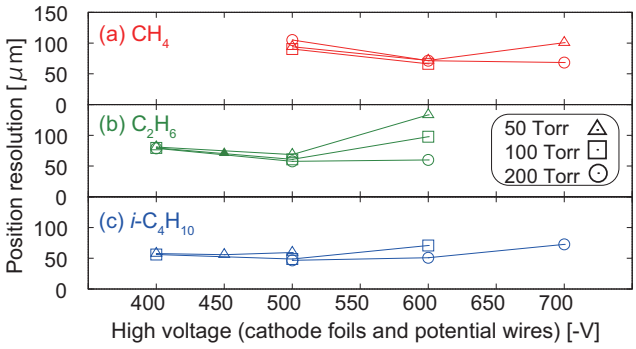

Fig. 2. Position resolution at 50-200 Torr for Xe beam. (a) CH_4, (b) C_2H_6, and (c) i-C_4H_{10}.

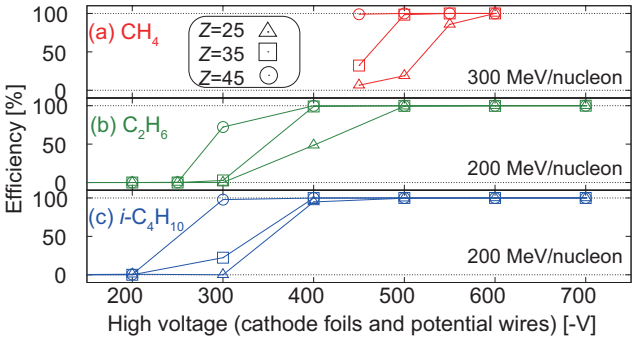

Fig. 3. Total detection efficiency at 50 Torr for secondary beams. (a) CH_4, (b) C_2H_6, and (c) i-C_4H_{10}.

In summary, we evaluated the characteristics of a low-pressure MWDC system with heavy-ion beams. The detection efficiency and position resolution reach 100% and about 50 μm, respectively, with all the tested gases (CH_4, C_2H_6, and i-C_4H_{10}). These results demonstrate that the constructed system is suitable as a beam tracker for ESPRI experiments, and the system shows potential for experiments using various heavy-ion beams.

*1 Department of Physics, Konan University
*2 RIKEN Nishina Center
*3 School of Physics and Nuclear Energy Technology, Beihang University
*4 RCNP, Osaka University

References

1) Y. Matsuda et al.,: Phys. Rev. C 87, 034614 (2013); S. Terashima et al.,: RIKEN Accel. Prog. Rep. 47, xviii (2014).
2) Y. Matsuda et al.,: RIKEN Accel. Prog. Rep. 48, 211 (2015).
3) Y. Matsuda et al.,: Nucl. Instr. Meth. A 670, 25 (2012).

Development of a new low-energy neutron detector with pulse shape discrimination properties for (p,n) experiments

L. Stuhl,[*1] M. Sasano,[*1] K. Yako,[*2] J. Yasuda,[*3] and T. Uesaka[*1]

We are planning to investigate the spin-isospin responses of light nuclei near the neutron drip line[1] using a new experimental technique[2] to measure the (p,n) reaction in inverse kinematics. This method has already been successfully applied to ^{132}Sn isotope[3] at RIKEN. In these inverse kinematical reactions, the detection of recoil neutrons is crucial for missing mass reconstruction, but it is affected by the high gamma-ray background (∼1 kHz). Therefore, reducing the background event rate is of high priority. To achieve a higher signal-to-noise ratio in neutron detection, the possibility of online separation of neutrons and gammas is a key challenge.[4] One must ensure that only useful (p,n) events are tagged during the experiment. This helps in conducting experiments with higher intensity and efficiency at the same time.

We are designing a neutron detector system (as an upgrade for WINDS[5] (Wide-angle Inverse-kinematics Neutron Detector for SHARAQ)) using new advantages of the plastic scintillator composition.[6] From the very beginning of neutron detection, pulse shape discrimination (PSD) between neutrons and gamma rays in plastic scintillators has been an unsolved problem. The new EJ-299-34 type plastic scintillator[7,8] by Eljen Technology can perform neutron and gamma-ray discrimination neutron pulses contain more light in their tail region than gamma-ray pulses. The first prototype of large volume ($30\times5\times2.5$ cm^3) plastic scintillator detector bars has already been designed and constructed. It is wrapped with mylar foil and coupled to two Hamamatsu H7195 photomultiplier tubes (PMTs) at each end.

PSD measurements were performed by irradiating the scintillator with an unshielded ^{252}Cf source, which was placed on the surface of the scintillator. The charge integration method[9] with analog electronics was applied to perform PSD. The parameters of discrimination were empirically optimised. To quantify the efficiency of the neutron and gamma peak separation of our scintillator bar, the Figure of Merit (FoM) was obtained while projecting the bidimensional discrimination spectrum at a given energy. The FoM values were calculated in a manner similar to that described in Blanc et al.[9]

The obtained PSD spectrum for the prototype detector is presented in Fig 1. FoM values of 0.77 at 300 keVee and 0.81 at 500 keVee energies were obtained for our large volume detector. A similar type of detector with significantly smaller size (2”× 2” (in diam.)) and shape (circular cylinder) was investigated in Cester et al.[7], where FoM values of 0.92 at 300 keVee and 1.05 at 500 keVee were deduced. In this study a digital read out module (CAEN V1720) was used, which could also increase the efficiency of PSD. We believe that the lower FoM values obtained in our measurements are essentially due to the larger scintillator volume of our detector that probably blurs light collection.

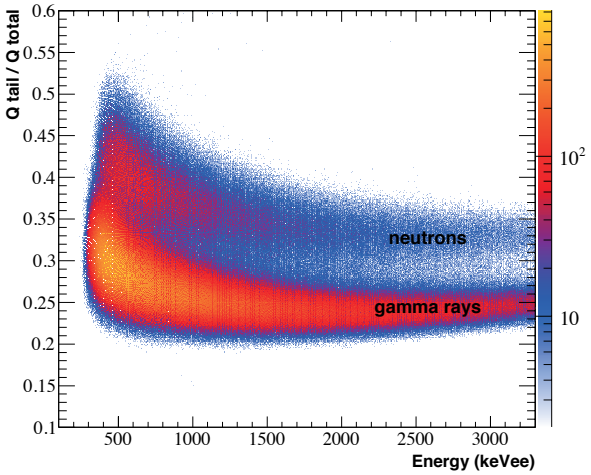

Fig. 1. Neutron/gamma discrimination spectra from prototype detector when exposed to a ^{252}Cf neutron source.

The position sensitivity of the PSD along the scintillator bar was also tested. We conclude that the PSD capability decreases by only less than 15% when the distance between the source and the PMT along the detector bar changes from 5 cm to 25 cm.

Henceforth, the CAENs V1730D module will be used in the construction of digital readout systems. We are planning to complete the development and further optimize the PSD, while increasing the FoM and decreasing the separation threshold. Construction of all detector bars and study of the properties of the upgraded spectrometer in experimental conditions are also scheduled.

*1 RIKEN Nishina Center
*2 CNS, University of Tokyo
*3 Department of Physics, Kyushu University

References
1) L. Stuhl et al.: RIKEN Accel. Pr. Rep. **48**, 54 (2015).
2) M. Sasano et al., Phys. Rev. Lett. **107**, 202501 (2011).
3) M. Sasano et al.: RIKEN Accel. Pr. Rep. **48**, 51 (2015).
4) M. Sasano et al.: In this report.
5) J. Yasuda et al.: RIKEN Accel. Pr. Rep. **48**, 203 (2015).
6) N. Zaitseva et al., Nucl. Instr. Meth. A **668**, 88 (2012).
7) D. Cester et al., Nucl. Instr. Meth. A **735**, 202 (2014).
8) S.A. Pozzi et al., Nucl. Instr. Meth. A **723**, 19 (2013).
9) P. Blanc et al., Nucl. Instr. Meth. A **750**, 1 (2014).

Hyperpolarization of flowing water by dynamic nuclear polarization

K. Yamada, [*1, *2] K. Tateishi,[*1] and T. Uesaka[*1]

Magnetic resonance angiography (MRA) is a technique for imaging blood vessels based on magnetic resonance imaging (MRI) for the evaluation of aneurysms, stenosis, occlusions, and so on. To obtain clear images, imaging time need to be done for a long for signal averaging, and this makes the resolution, in particular of heart, worse due to the beating. To overcome this problem, the injection of polarized water into a blood vessel was demonstrated[1]. Both the imaging time and the resolution were improved through the use of this method. In this experiment, the polarized ^{1}H spins in water were generated by dynamic nuclear polarization (DNP) method. The method can be used to polarize > 30% of ^{1}H spins using cryogenics and sub-terahertz devices, however, about 90% of the polarization was relaxed before injection, due to the short spin-lattice relaxation time of ^{1}H spins.[2] In this work, we adopted the flow-DNP method to polarize ^{1}H spins in flowing water for simplicity.

The DNP method is used to transfer electron spin polarization to nuclei with microwave irradiation. We applied it to flowing water (flow-DNP).[3] This is a very compact, cheap, and versatile method for polarizing liquid-state samples. We would like to apply this method not only to MRA but also for various studies such as on proteins using high-resolution NMR system.[4]

Experimental setup of flow-DNP is shown in Fig. 1. A microwave cavity with a frequency of 9 GHz is placed in the electromagnet. The external magnetic field is set at 0.3 T. Water is flowed into the cavity by a pump. The tube in the cavity is filled with gels functionalized with radicals to slow down the flow rate only inside the cavity. The microwave irradiates the radicals with an incident power of 3 W. Although the polarized water is looped back to the pump in current setup, it will be sent to the MRI system in the future. The coil in the NMR is placed in the downstream direction of the cavity to check the polarization. The enhancement factor ϵ of the polarization is given as

$$\epsilon = 1 - \rho f s \frac{|\gamma_e|}{\gamma_n},$$

where ρ is the coupling factor, f is the leakage factor, s is the saturation factor, and γ_e and γ_n are the gyromagnetic ratios of the electron and ^{1}H, respectively. With the above setup, ρ, f, and s are estimated to be 0.07, 0.90, and 1, respectively,[3] and the expected polarization is 0.0041 %.

[*1] RIKEN Nishina Center
[*2] Department of Physics, Toho University

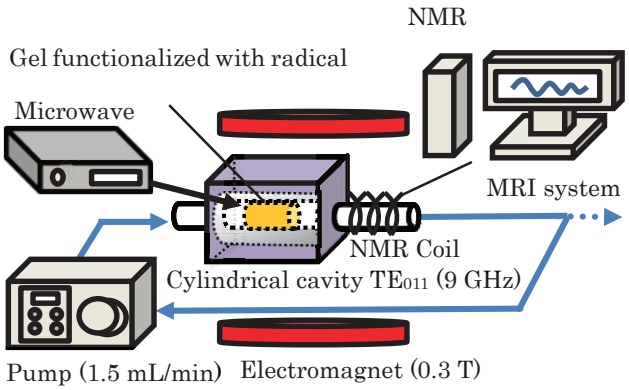

Fig. 1. Experimental set up for flow-DNP.

We constructed the system except for the gel this time, and detected the NMR signal of ^{1}H spins in the flowing water with a flow rate of 1.5 mL/min for demonstration. The result is shown in Fig. 2. Although the line width is a little broad compared to the one obtained from a conventional solution NMR, it is narrow enough for flow-DNP. Next year, we will synthesize the gel and carry out the flow-DNP experiment.

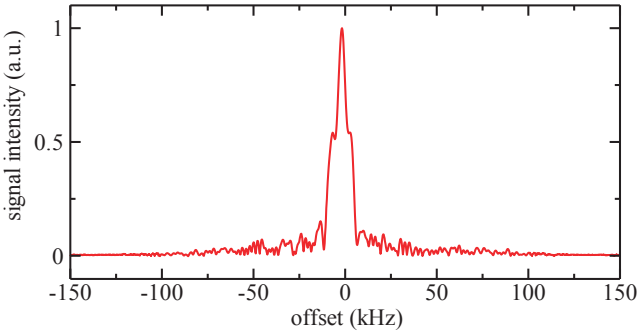

Fig. 2. NMR signals of the ^{1}H spins in flowing water in thermal equilibrium. Offset means the difference between the resonance frequency of ^{1}H and the frequency of electromagnetic waves.

References

1) J. Ardenkjaer-Larsen et al., Magn. Reson. Med. **71**, 50 (2014).
2) Q. Chappuis et al., J. Phys. Chem. Lett. **6**, 1674 (2015).
3) M. D. Lingwood et al., J. Magn. Reson. **205**, 247 (2010).
4) M. Reese et al., J. Am. Chem. Soc. **131**, 15086 (2009).

Design study of triplet-resonance circuit to polarize ^{13}C spins utilizing dynamic nuclear polarization and cross polarization

T.Kaneko,[*1,*2] K.Tateishi,[*1] and T.Uesaka[*1]

Techniques to polarize nuclear spins can be applied not only in the field of nuclear/particle physics for polarized targets but also in the field of chemistry and medicine. [1] In this decade, dynamic nuclear polarization (DNP) has attracted a lot of attention for analytical science. DNP is the method of transferring the electron spin polarization to nuclei using microwave irradiation. For example, polarized pyruvate is used for metabolic imaging.[1] The transition from pyruvate to alanine or lactate in the body can be imaged using magnetic resonance imaging (MRI) systems.

For the above-mentioned application, ^{13}C spins are useful. All organic molecules contain carbon. In addition, chemical shift difference (distinguishability of molecules in the spectrum) is larger than the ^{1}H spins and the spin-lattice relaxation time (T_1: shooting time) is also longer than ^{1}H. However, ^{1}H spins are ideal for DNP because of faster spin diffusion. The gyromagnetic ratio of a ^{1}H spin is 4 times larger than that of ^{13}C spin.

Our strategy involves the following. First, ^{1}H is polarized using DNP. Subsequently, the polarization is transferred from the ^{1}H spins to ^{13}C spins using a cross polarization (CP) technique. The CP is the polarization transfer sequence between heteronuclear spins using radio-frequency irradiation. In this report, we designed a resonator with a cylindrical cavity for DNP and a double-resonance LC-circuit for CP.

The cylindrical cavity was designed using on electromagnetic simulator (CST Microwave Studio). The frequency was 18 GHz, which resonated with electron spins at 0.65 T. Details of the double-resonance circuit are described in Ref. 2. The circuit is tuned for ^{1}H and ^{13}C spins with a frequency of 28 and 7 MHz, respectively. Both circuits are still under development.

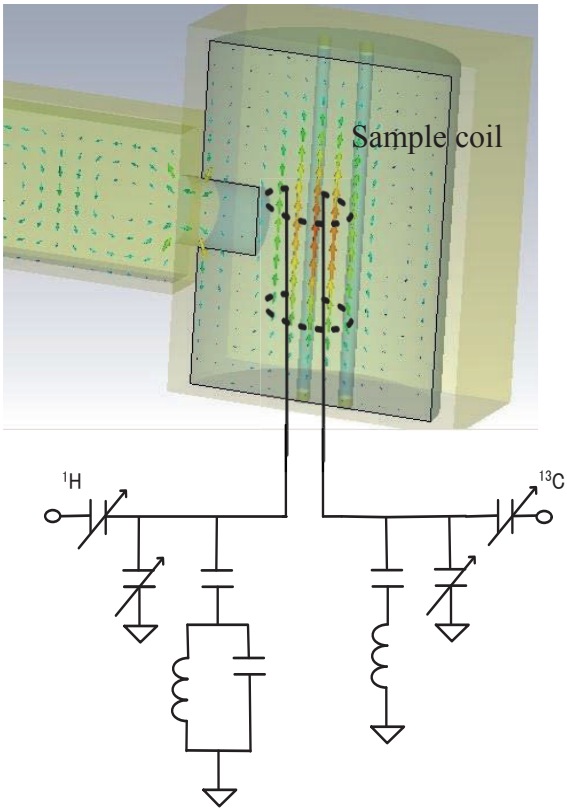

Fig. 1. Design of triplet-resonance resonator (e/^{1}H/^{13}C) to combine with DNP and CP. The coil for double-resonance LC-circuit is inserted in the cylindrical cavity. The resonance frequency is 18000/28/7 MHz, respectively.

Many polarized nuclei, such as ^{1}H, ^{2}H, ^{13}C, ^{15}N, ^{19}F and so on, are used for chemical and medical applications. To this end, our polarization transfer scheme is quite useful. Nuclear spins can be polarized by changing the double-resonance LC-circuit for CP.

References

1) K.Golman et al, *Cancer Res* 66.22, 10855-10860 (2006).
2) S.Kan, M. Fan, and J. Courtieu, Rev. Sci. Inst.51, 887 (1980).

*1 RIKEN Nishina Center
*2 Department of Physics, Toho University

Dependence of spin-polarized proton target performance on microwave resonator thickness parameter and operation temperature

S. Chebotaryov, *1,*3 S. Sakaguchi, *1,*2 W. Kim, *3 E. Milman, *1,*3 K. Tateishi, *1 and T. Uesaka *1

A spin-polarized proton target provides opportunities to experimentally study spin-dependent interactions with unstable nuclei. Such a target is required because unstable nuclei are short-lived species and have to be provided as an RI-beam. Such an experimental study has not been possible until recently owing to the lack of a polarized target that is applicable to RI-beam experiments. Conventional polarized targets use a high magnetic field of a few tesla and sub-kelvin temperatures to attain high polarization. However, in experiments the energy of recoil protons can be as low as few tens of megaelectronvolts. Thus the maximum magnitude of the magnetic field used has to be constrained to several tens of millitesla to prevent significant distortion of proton trajectories. The Center for Nuclear Study, University of Tokyo, and the RIKEN group has developed a spin-polarized proton target system suitable for use in RI-beam experiments,[1] which made it possible to conduct an experimental study of spin-dependent interactions in unstable nuclei.

The method of generating spin polarization employed in the target system is based on the cross-polarization technique[2], where the polarization of an electron system is transferred to the protons in the presence of an oscillating magnetic field. The field is generated as a standing electromagnetic wave using a microwave resonator. The type of resonator employed in our system is the so-called loop-gap resonator (LGR); its schematics is presented in Fig. 1. This resonator is made of a sheet of CuFlon material, which consists of a copper metal clad on both sides of a thin Teflon sheet.[3].

In this report, we study the polarization performance of the target system at different temperatures, specifically how performance depends on temperature-dependent parameters of an LGR used for creating the oscillating magnetic field. The goal is to choose the optimal parameters of the LGR to obtain maximum polarization at a target normal operating temperature of −173 °C. As for LGR, the use of a thicker copper layer tends to give better results in terms of resonator performance, while for target operation, a thinner copper layer is preferable as it disturbs the trajectories of recoil protons less significantly. For 10 MeV protons, the angular resolution will vary from ±0.5° to ±1.6° (sigma), for an LGR with copper layer thicknesses of 4.4 µm and 36 µm, respectively.

We measured a series of dependences of the polarization signal intensity P as a function of the square root of microwave power $\sqrt{P_{MW}}$ supplied to the LGR from an RF amplifier. The magnetic field generated inside the LGR is proportional to $\sqrt{P_{MW}}$: $H_1 \propto \sqrt{P_{MW}}$. Measurements were performed at −40 °C, −80 °C, and −173 °C using two types of LGRs with copper layer thicknesses of 4.4 µm and 36 µm with all other conditions being equal. In Fig. 2 the results of the measurements are presented.

Fig. 1. Schematics of the loop-gap resonator.

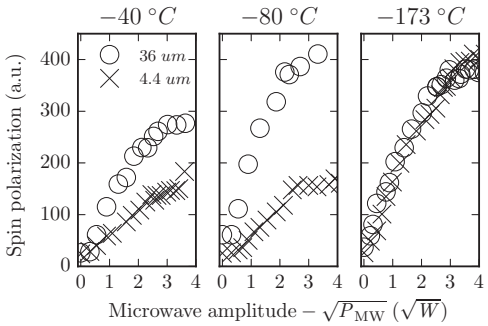

Fig. 2. Dependence of polarization on microwave amplitude at different temperatures (measurement error is comparable to symbol size).

At a temperature of −173 °C, the thickness of the LGR copper layer does not play an important role, while at higher temperatures measurable difference starts to appear. In the case of the 4.4 µm LGR, a decrease in polarization performance vs. temperature is more pronounced in comparison to the 36 µm one. If the temperature is above −173 °C, to maximize polarization performance, the use of the LGRs with a thicker copper layer is preferable. To better understand the performance of the polarized target at different temperatures and to be able to build a quantitative model, a more detailed study of magnetic field dependence from temperature in the LGR itself is required.

*1 RIKEN Nishina Center
*2 Department of Physics, Kyushu University
*3 Department of Physics, Kyungpook National University

References

1) T. Wakui et al., Nucl. Instr. Meth. Phys. Res. A **550**, 521 (2005).
2) A. Henstra et al., Chem. Phys. Lett. **165**, 6 (1990).
3) B. Ghim, et al., J. Magn. Reson., Ser A **120**, 72 (1996).

Pressure dependence of effective gas gain of THGEM in deuterium gas

C.S. Lee,[*1,*2] S. Ota,[*2] H. Tokieda,[*2] Y.N. Watanabe,[*3] R. Saiseau,[*4] and T. Uesaka[*1]

A low-pressure gaseous active target called CNS active target (CAT) has been developed for a deuteron inelastic scattering off unstable nuclei[1]. The CAT consists of a combination of gas electron multipliers (GEMs) and time projection chamber (TPC) as a vertex tracker, and Si detectors as a total kinetic energy detector for high momentum recoil particles. Three 400 μm-thick thick gas electron multipliers (THGEMs) are employed for the amplification inside the TPC in order to achieve an effective gas gain of 10^4 at 0.4 atm deuterium gas. This gas gain of 10^4 fulfils the detection of the minimum energy deposition of our interest, 5 keV/cm, which is the energy loss per centimeter of a recoiling deuteron to 9° in the centre-of-mass frame from ^{132}Sn(d, d') reaction at 100 MeV/nucleon. The properties of a double THGEM configuration in 0.2-, 0.3- and 0.4-atm deuterium were investigated for the first time by corresponding authors[2]. In addition to the previous work, the pressure dependence and the long-term stability of the effective gas gain were investigated by using a triple THGEM configuration.

A schematic view of the experimental setup is shown in Fig. 1. The collected electrons on the readout pad were integrated with a charge-sensitive preamplifier, which has a conversion gain of 200 mV/pC and a time-constant of 80 ns. The output signal from the preamplifier was treated by a shaping amplifier (ORTEC 571), and the pulse height of the shaped signal was recorded by a multi-channel analyser (MCA) (Kromek 102). The effective gas gain G_{eff} is derived from the equation:

$$G_{eff} = \frac{Q_{pads}}{q_e \cdot \Delta E / W_i} \quad (1)$$

where G_{eff} is the effective gas gain of GEM, ΔE is the energy loss of particle, W_i is mean energy for ion-electron pair creation of certain gas (36.4 eV for D_2), q_e, the elementary charge, and Q_{pads} is the collected charges on the readout pad. Figure 2 shows the obtained gain curves including the achievable gain from a triple THGEM configuration for 0.18-0.5 atm D_2 as a function of the voltage between the upper and the lower electrodes of THGEM, ΔV_{THGEM}. A triple THGEM configuration provides the effective gas gain of more than 10^4 for every pressure, and even more than 10^5 for under 0.35-atm.

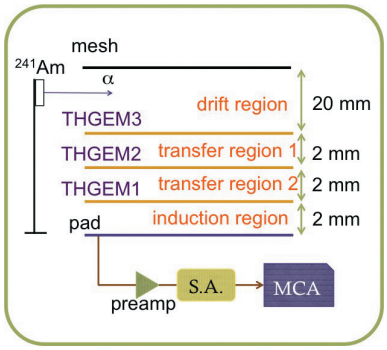

Fig. 1. Experimental setup of this work. Voltages to the THGEMs are supplied from a single channel of a HV module, by using a register chain, where each ΔV_{THGEM} is equally provided.

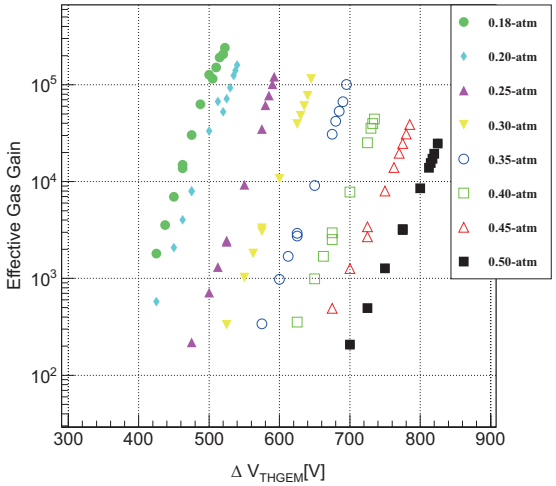

Fig. 2. Gain curves of a triple THGEM configuration at 0.18-0.5 atm D_2 as a function of ΔV_{THGEM}.

Every set of measurements for each pressure was suspended when a normal spectrum can hardly be taken due to the discharge problem. In this measurement, the ratio of the voltages on each electrode of the THGEMs was retained in constant by using a resistance chain. The strength of the transfer field was 2.25 to 4.16 kV/cm/atm where the transfer efficiency is almost maximum and reached a plateau. The strength of the induction field was 3.0 to 5.56 kV/cm/atm.

*1 RIKEN Nishina Center
*2 Center for Nuclear Study, Graduate School of Science, The University of Tokyo
*3 Department of Physics, The University of Tokyo
*4 University Paris-Sud

References

1) S. Ota *et al.*, CNS Annual Report **2011** CNS-REP-90(2013) 70-71.
2) C.S. Lee *et al.*, JINST **9** (2014) C05014.
3) M. Tokuda *et al.*, JINST **7** (2012) C04006.

Development of ^{178m2}Hf isomer target

N. Kitamura,[*1] Y. Yamaguchi,[*1] S. Michimasa,[*1] N. Imai,[*1] and H. Haba[*2]

Since the discovery of superdeformation in the nucleus, many superdeformed states have been observed [1]. As the further deformed state, hyperdeformation, in which the ratio of the long axis to the short axis is 3 : 1, has been predicted as extreme quadrupole deformation[2]. However, no such state had been discovered yet. Furthermore, recent theoretical calculation predicts that even a deformed torus shape appears at a high-spin state[3]. Such deformed states will provide us with a stringent test of our understanding of nuclear physics. The key to produce such states is transferring high angular momentum to the nucleus. If the high-spin target or beam is available, it would be more probable to populate such an exotic state. Thus, we are developing a target of ^{178m2}Hf, [a] which has a high spin of 16$\hbar$ and a long half-life of 31 y. Among several reactions, the ^{176}Yb$(\alpha, 2n)$ reaction is known to have a relatively high cross section to produce ^{178m2}Hf[4]. The pioneering work to produce 3×10^{14} atoms of ^{178m2}Hf was performed in Dubna[5]. The isomeric state was produced by the fusion reaction of $(\alpha, 2n)$ with an enriched ^{176}Yb target. At an incident energy of 35.5 MeV, the cross section was 9 mb and the isomer ratio was 0.5 %. The AVF cyclotron at RIBF can provide 40-MeV α beams of 10 eμA, which are enough to make a nanogram sample of ^{178m2}Hf with a beam time of a few days. Before stepping into mass production, we performed the feasibility study for production. There are three issues to be checked. The first issue is the measurement of the excitation function of the production cross section of ^{178m2}Hf to optimize the incident beam energy. The second issue is the production cross sections of ^{175,172}Hf, which will be the main contaminants after the irradiation. Since they have relatively short half-lives, 70 d and 1.87 y, respectively, the radioactivities of these contaminants will be much larger than that of ^{178m2}Hf if we use a natural Yb target. The production cross sections of these nuclei determine the degree of enrichment required for ^{176}Yb. The third issue is the heat damage to the Yb target. It is not obvious that the target can withstand the high-intensity α beam since the melting point of Yb is about 824 °C.

The experiment was performed at the C03 beam line of the AVF cyclotron. An α beam of 40 MeV irradiated a target stack for 8 hours. The target stack was made of ten ^{nat}Yb foils with a thickness of 20 μm each. The Yb foils were sandwiched by two 2-μm Ti foils to check the energy of the beam using the monitor reaction ^{nat}Ti$(\alpha, xn)^{51}$Cr. The target was placed on the water-cooled Ta Faraday cup to measure the total dose of the beam. In addition, He gas was flown on the surface of the target to take the heat away. The irradiation time was determined by the regulation for production of ^{175}Hf in this facility.

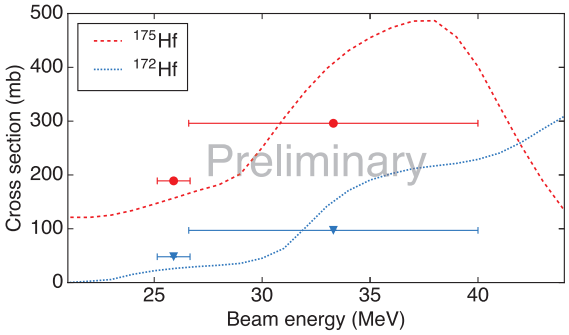

Fig. 1. Experimental cross sections for ^{nat}Yb$(\alpha, xn)^{175}$Hf (circles) and ^{172}Hf (triangles) are compared with the calculations by PACE4 (dashed and dotted, respectively). The horizontal errorbars stand for the loss of energy in the foils.

When we opened the chamber and checked the target after cooling for 3 days, it turned out that the first ten foils, one Ti and nine Yb, were adhered. On the other hand, the last two foils, Yb and Ti, could be separated. This means that as long as the foils are attached tightly to the water-cooled Faraday cup, they can withstand the 10-eμA α beams. γ rays were measured by a HPGe detector to evaluate the radioactivities produced. The deduced cross section of ^{51}Cr was found to be consistent with the value with an incident energy of 40 MeV. The cross sections of ^{nat}Yb$(\alpha, xn)^{175,172}$Hf are presented in Fig. 1. The PACE4 code[7] reproduced these experimental values. For detecting the decay from ^{178m2}Hf, we have to measure γ rays in triple coincidence to distinguish them from other activities. We are now preparing Ge detectors array GRAPE[8] for the measurement.

*1 Center for Nuclear Study, University of Tokyo
*2 RIKEN Nishina Center

a) There are two isomeric states in ^{178}Hf. One is ^{178m1}Hf with a half-life of 8.0 s, the other is ^{178m2}Hf.

References

1) X. L. Han and C. L. Wu, At. Data Nucl. Data Tables **63**, 117 (1996).
2) J. Dudek et al., Phys. Lett. B **211**, 252 (1988).
3) T. Ichikawa et al., Phys. Rev. Lett. **109**, 232503 (2012).
4) S. A. Karamian, Yad. Fiz. **68**, 1827 (2005).
5) Yu. Ts. Oganessian et al., J. Phys. G: Nucl. Part. Phys. **18**, 393 (1992).
6) IAEA-TECDOC-924, Vienna (1997)
7) http://lise.nscl.msu.edu/pace4.html
8) S. Shimoura, Nucl. Instrum. Methods A **525**, 188 (2004).

Construction of OEDO beamline

S. Michimasa,[*1] S. Shimoura,[*1] M. Matsushita,[*1] N. Imai,[*1] K. Yako,[*1] H. Yamaguchi,[*1] S. Ota,[*1] E. Ideguchi,[*2] H. Sakurai,[*3] K. Yoshida,[*3] and K. Yamada[*3]

The OEDO system is a new beamline proposed for high-quality slow-down RI beams[1]. The OEDO is an abbreviation of **O**ptimized **E**nergy **D**egrading **O**ptics for RI beam. The idea behind it is to manipulate the timing degree-of-freedom in the phase space of RI beam. To obtain a high-quality beam with a small spot size and a small energy spread, the OEDO system shifts the spreads of positions and angles to the timing spread of the beam, which corresponds to the rotation of the phase space ellipse on the position- (angle-)timing plane to obtain a small position (angle) spread. Radiofrequency (RF) electric ion-optical elements can rotate a phase space ellipse of spatial and timing components, as beams from a cyclotron have an RF bunch structure.

The main components of the OEDO system are: An RF deflector[2] synchronized with the cyclotron's RF and 2 sets of triplet quadrupole (TQ) magnets to achieve point-to-parallel/parallel-to-point ion optics. The OEDO system is to be installed downstream of a momentum-dispersive focus with a reasonable dispersion. The first TQ associates the beam energy with beam angle at the RF deflector, and the second TQ makes a small achromatic focus. This dispersion condition is fulfilled in the first half of the High-Resolution (HR) beamline[3]. Therefore, the OEDO system will be implemented in the HR beamline by installing new electric/magnetic elements and rearranging the existing magnets. In FY2014, the main part of the construction budget was funded and the OEDO project was launched. We are continuously improving the design of the beamline with respects to the magnet configuration and an ion-optics.

Figure 1 shows the magnet arrangement for the OEDO beamline downstream of the F6 focal plane of the BigRIPS. The specifications of the RF deflector for the OEDO system are shown in the inset table of Fig. 1. The magnet configuration was confirmed to function as a phase-space rotator for slow-down beams by ion optics calculation. The slow-down scheme of the OEDO beamline is shown in Fig. 2. In Fig.2(a),an RI beam at 250 MeV/u is transported to FE8, where the momentum dispersion is tuned to be 1 m. A monoenergetic degrader is installed at FE8 to slow RIs down to 50 MeV/u, which corresponds to a rotation of the phase space ellipse on the plane of the beam energy (δ) and flight time (t). In Fig.2(b), the first half of the OEDO system, set to be point-to-parallel optics,

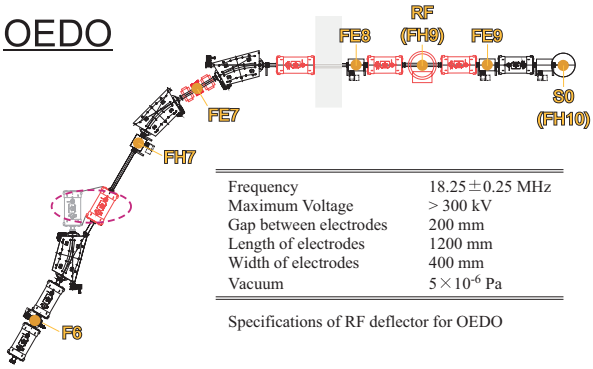

Fig. 1. Magnet configuration of the OEDO beamline

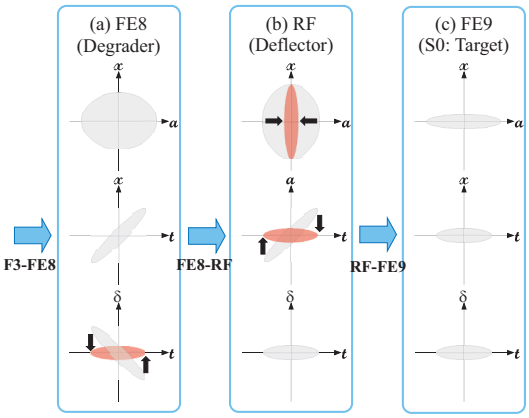

Fig. 2. Phase space rotation in OEDO beamline

rotates the phase space ellipse on the x-a plane. Then, the RF deflector reduces the timing (t) dependence of angle (a). In Fig.2(c), the second half of the OEDO system, also set to be parallel-to-point optics, rotates the phase space ellipse on the x-a plane in the reverse direction. Finally, a small beam spot and a small energy spread are achieved at the FE9 and S0 foci.

Based on the result, we estimated the higher order aberrations of the OEDO beamline using a Monte-Carlo simulation[5].

This work was funded by ImPACT Program of Council for Science, Technology and Innovation (Cabinet Office, Government of Japan).

References

1) S. Shimoura *et al.*, CNS Annual Report 2013, CNS-REP-93, 56 (2015) 56.
2) K. Yamada *et al.*, Nucl. Phys. A **746**, 156c (2004).
3) S. Michimasa *et al.*, Nucl. Instrum. Meth. in Phys. Res. **B317**, 305 (2013).
4) T. Kubo *et al.*, Nucl. Instrum. Meth. in Phys. Res. **B204**, 97 (2003).
5) M. Matsushita *et al.*, In this report.

*1 Center for Nuclear Study, University of Tokyo
*2 RCNP, Osaka University
*3 RIKEN Nishina Center

Simulation study of a new energy-degrading beamline, OEDO

M. Matsushita,[*1] S. Shimoura,[*1] S. Michimasa,[*1] N. Imai,[*1] K. Yako,[*1] H. Yamaguchi,[*1] S. Ota,[*1] E. Ideguchi,[*2] H. Sakurai,[*3] K. Yoshida,[*3] and K. Yamada[*3]

The OEDO (**O**ptimized **E**nergy **D**egrading **O**ptics for RI beam) beamline is one of the solutions to degrade intense RI beams provided in RIBF, which will make possible further research on exotic nuclei/states by using the transfer reaction in the energy region around a few tens MeV, fusion reaction in around a few MeV and others [1]. The application of a material energy degrader is a general method to degrade a fast beam, while it induces momentum- and angular aberrations that lead to broadenings of beam spot[2]. The OEDO beamline employed an RF electric beam deflector (RF deflector) to cancel the aberrations based on the time structure of the secondary beams[3]. Simulation of this beamline has been performed for optimization and feasibility studies.

In the simulation, beam transportations by magnetic devices were reconstructed by beam transfer matrix obtained in COSY infinity[4], while interactions with materials and electric fields were simulated by the code based on GEANT4[5]. Conditions of the simulation are schematically shown in Figure 1, where a neutron-rich nucleus ^{132}Sn and neutron-deficient nucleus ^{56}Ni were used as typical examples. Initial momentum and angular distributions were generated by using the LISE++ code[6] to estimate the production via a projectile-fission reaction of the ^{238}U primary beam and a projectile-fragmentation reaction of the ^{124}Xe primary beam for ^{132}Sn and ^{56}Ni, respectively. Secondary beams separated by BigRIPS[7] were transported to OEDO beamline with energies of 250 MeV/u and 210 MeV/u (ΔP/P= $\pm$3%) for ^{132}Sn and ^{56}Ni, respectively. Secondary beams were degraded to 50 MeV/u by a mono-energetic degrader located at FE8 focus, and transported to the RF deflector with point-to-parallel optics to convert from position to angular dispersion. In order to make beams focused at FE9, the RF deflector compensates the angular aberrations by its dynamic electric field oscillating with a cyclotron resonance frequency. If an additional deceleration is required, another energy degrader is employed at FE9.

The OEDO beamline consisting of the RF deflector works as a separator using a velocity filter. Timing differences from the focusing phase of the RF deflector are transformed to position differences at FE9. As shown in Figure 2, a clear separation obtained for Ni isotopes indicates large enough differences in time-of-flight (TOF) caused by the velocity differences. In the case of ^{132}Sn, on the other hand, it cannot be obtained due to insufficient TOF differences and bending power of the RF deflector against a particle with large A/Q ratio. Development of an alternative transport is on going, which consciously enhances the capability of beam purification for neutron-rich nuclei in medium/heavy mass region, such as ^{132}Sn.

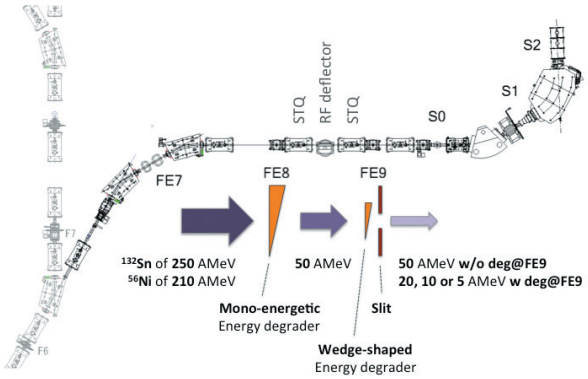

Fig. 1. Simulation condition and a scheme of two-staged energy deceleration in OEDO.

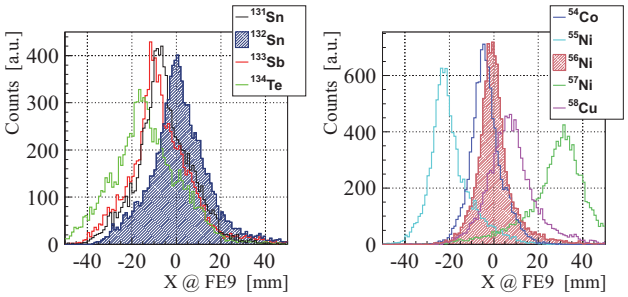

Fig. 2. Position distribution at FE9 obtained for ^{132}Sn (^{56}Ni) and contaminants are shown in left (right) panel.

This work was funded by ImPACT Program of Council for Science, Technology and Innovation (Cabinet Office, Government of Japan).

References

1) S. Shimoura et al., CNS Anual Rep. **2013**, 55 (2013).
2) E. Ideguchi, Prog. Theor. Exp. Phys. **2012**, 03C005 (2012).
3) S. Michimasa et al. : in this report.
4) `http://www.bt.pa.msu.edu/index_cosy.html`.
5) `http://geant4.cern.ch/`.
6) `http://lise.nscl.msu.edu/lise.html`.
7) T. Kubo et al., Nucl. Instrum. Meth. in Phys. Res. **B204**, 97 (2003).

*1 Center for Nuclear Study, University of Tokyo
*2 Research Center for Nuclear Physics, Osaka University
*3 RIKEN Nishina Center

Performance of a resonant Schottky pick-up in the commissioning of Rare RI Ring†

F. Suzaki,[*1,*2] Y. Abe,[*1] Z. Ge,[*1] K. Hiraishi,[*3] Y. Ichikawa,[*3] I. Kato,[*2] H. Miura,[*2] T. Moriguchi,[*3] D. Nagae,[*1] S. Naimi,[*1] T. Nishimura,[*2] S. Omika,[*2] A. Ozawa,[*3] S. Suzuki,[*3] T. Suzuki,[*2] N. Tadano,[*2] Y. Tajiri,[*3] Y. Takeuchi,[*2] T. Uesaka,[*1] M. Wakasugi,[*1] T. Watanabe,[*1] K. Yamada,[*1] T. Yamaguchi,[*2] Y. Yamaguchi,[*1] J. Zenihiro,[*1] and Y. Yano[*1]

The Rare RI Ring is a storage ring dedicated to the measurement of the masses of unstable nuclei to study their nuclear structure and nucleosynthesis[1]. We employ the isochronous mass spectrometry method aiming at a relative mass precision of 10^{-6}. For such high-precision measurement, reaching the isochronous condition in the ring up to a precision of 10^{-6} is essential. As a monitor for the tuning of the isochronous field, we adopt a resonant Schottky pick-up. Figure 1 a) shows the resonant Schottky pick-up installed in the ring. When the beam passes through the resonant Schottky pick-up, an electromagnetic field is induced in the resonant cavity. Figure 1 b) shows the magnetic field induced at the resonance frequency $f_{\rm res}$. The change of magnetic flux is detected by a pick-up loop inside the cavity. Similar resonant Schottky pick-ups have been used at GSI[2] in Germany and IMP[3] in China. From the results of an offline test, we obtained $f_{\rm res} = 171.43$ MHz, shunt impedance $R_{\rm sh} = 161$ kΩ, and unloaded quality factor $Q_0 = 1880$[4].

In June 2015, we commissioned the Rare RI Ring using a Kr beam with an energy of 168 MeV/u. In the commissioning, we successfully observed the signals of a single Kr ion in the Schottky spectrum, as shown in Fig. 2. The upper part of Fig. 2 is a spectrogram of Kr. In this plot, the horizontal and vertical axes are the resonance frequency and time, respectively. The frequency shift is considered to be caused by the momentum change due to the interactions with the residual gas in the ring. The vacuum was still of the order of 10^{-5} Pa without the baking procedure. The lower part of Fig. 2 is a zoomed FFT spectrum in a frame of 32 ms. The frequency width is 224 Hz at FWHM; therefore, the frequency resolution is 1.29×10^{-6}. The measured signal power is $P = -68.9$ dBm, where P is obtained by integrating the peak in the Schottky spectrum after subtracting thermal noise background. For comparison, we calculated the expected signal power $P_{\rm cal}$ by using the following equation which represents the signal power of a single ion with charge q[2]: $P_{\rm cal} = 1/8(qef)^2 R_{\rm load}$, where e = elementary charge, f = revolution frequency, and $R_{\rm load}$ is calculated from the equation $R_{\rm load} = R_{\rm sh}/Q_0 \times Q_{\rm load}$. Taking into account the gains of two amplifiers and transmission losses, $P_{\rm cal}$ = -66.1 dBm. The observed Schottky signal power P is in good agreement with the expected $P_{\rm cal}$. In conclusion the performance of the resonant Schottky pick-up is sufficient in terms of sensitivity and resolution.

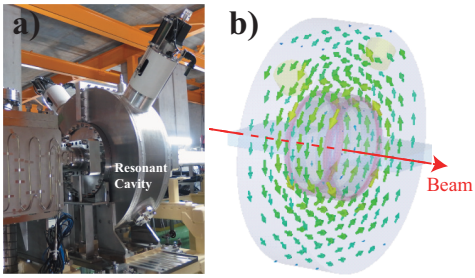

Fig. 1. a) A photograph of the resonant Schottky pick-up. b) Magnetic field in the resonant cavity induced by the beam.

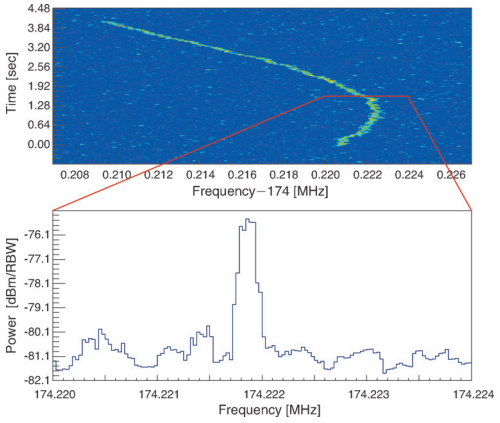

Fig. 2. Upper: A spectrogram of a single ^{78}Kr ion. Lower: A zoomed FFT spectrum in a frame of 32 ms.

References
1) Y. Yamaguchi et al., Nucl. Instrum. Methods Phys. Res. B 317, 629 (2013).
2) F. Nolden et al., Nucl. Instrum. Methods Phys. Res. A 659, 69 (2011).
3) J. X. Wu et al., Nucl. Instrum. Methods Phys. Res. B 317, 623 (2013).
4) F. Suzaki et al., JPS Conf. Proc. 6, 030119 (2015).

† Condensed from the article in Proceedings of HIAT2015, Yokohama, Japan

*1 RIKEN Nishina Center
*2 Department of Physics, Saitama University
*3 Institute of Physics, University of Tsukuba

Online results for the injection ion optics of the Rare RI Ring

Z. Ge,[*1,*2] Y. Abe,[*1] F. Suzaki,[*1,*2] D. Nagae,[*1] S. Naimi,[*1] T. Uesaka,[*1] Y. Yamaguchi,[*1] T. Yamaguchi,[*2] A. Ozawa,[*3] H. Miura,[*2] S. Omika,[*2] Y. Takeuchi,[*2] S. Suzuki,[*3] Y. Yano[*1] for the Rare RI Ring collaboration

The Rare RI Ring (R3) is a cyclotron-like storage ring designed for mass measurements of exotic nuclei far from stability at Radioactive Ion Beam Factory in RIKEN[1]. In order to successfully transport the nuclei of interest individually[1] to the central orbit of the Rare RI Ring, we calculated the injection ion optics for the Rare RI Ring beam line, which connects the Rare RI Ring spectrometer to the BigRIPS separator. For the upstream optics from F3 to S_0, the target position of the SHARAQ spectrometer, the standard high-resolution achromatic mode is used[2]. The total optical matrix is calculated from S_0 to the kicker magnet position[3], and two important foci, ILC1 and ILC2, are shown in Fig. 1, where 2 PPACs are placed to evaluate the matrix elements for beam tuning quantitatively.

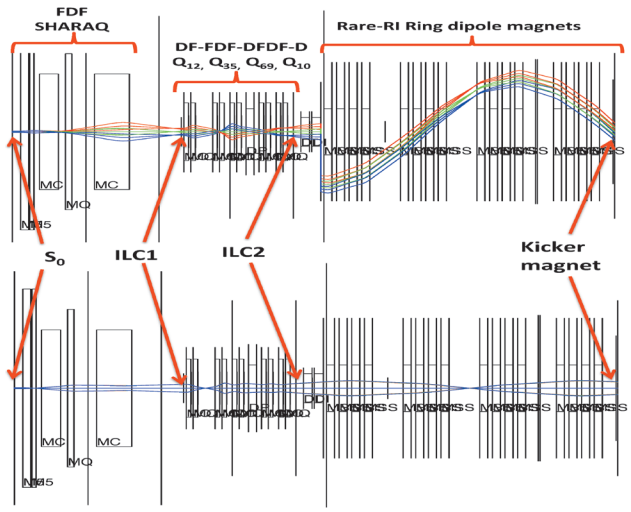

Fig. 1. Envelopes of the beam transport from SHARAQ S_0 to kicker magnet in the horizontal and vertical plane by third order calculation using *COSY INFINITY*.

During online beam tuning, we chose the configuration of the three SHARAQ quadrupoles (SQ1-3)[2] and the ten quadrupoles (Q1-10) between ILC1 and ILC2 to be FDF-DF-FDF-DFDF-D (D indicts indicates "Defocus" and F indicates "Focus") configuration in the lateral direction, which is suited for the small vertical acceptance as shown in Fig. 1 (bottom) for fast tuning of the beam. To complete the fast tuning method developed for SHARAQ spectrometer[2], we first design the optics of the injection line with many focus planes. Then we calculate the response functions of each quadruple magnet by *COSY INFINITY*. During beam tuning, we cancelled the momentum-dispersion effects by combining information at the dispersive focal plane. Once the matrix elements of the experimental values are evaluated, it is used for correcting the magnet setting precisely.

*1 RIKEN Nishina Center
*2 Department of Physics, Saitama University
*3 Institute of Physics, University of Tsukuba

Table 1. Currents (C_{SQ1-3} and C_{Q1-10}) of the quadrupole magnets (SQ1-3 and Q1-10) of the injection line

Condition	Configuration	EXP. (A)	Cal. (A)
F	C_{SQ1}	33.28	33.1
D	-C_{SQ2}	61.20	61.0
F	C_{SQ3}	61.59	61.3
DF	-C_{Q1}=C_{Q2}	226.8	480.8
FDF	C_{Q3}=-C_{Q4}=C_{Q5}	715.4	723.8
DFDF	-C_{Q6}=C_{Q7} =-C_{Q8} =C_{Q9}	200.9	295.7
D	-C_{Q10}	25.8	27.4

Table 2. Matrix elements of ILC1 and ILC2 evaluated from the experiment and calculated by *COSY INFINITY*

Matrix Element	EXP. (ILC1)	Cal. (ILC1)	EXP. (ILC2)	Cal. (ILC2)
(x| a)	0.02±0.007	0	0.19 ± 0.010	0.04
(y| b)	5.40±0.007	0	−6.66±0.010	-0.07

We performed the tuning method using the designed ion-optical mode for the first commissioning run of Rare RI Ring in June 2015, for which we use the $^{78}Kr^{36+}$ beam with the energy of 168 MeV/nucleon. With this ion-optical mode we successfully carried out the individual injection of the Rare RI Ring, and we succeeded in storing the $^{78}Kr^{36+}$ ions for a few seconds.

Table 1 indicates the measured magnet current values and their corresponding calculated values via *COSY INFINITY* (the magnetic fields corresponding to the currents of the magnets here). The transfer matrix element of the two important focal planes ILC1 and ILC2 are listed in Table 2. The measured values of the matrix elements after beam tuning are consistent with the calculated values for the horizontal direction, while they differ in the vertical direction due to a misalignment in the beamline.

References

1) A. Ozawa et al., Prog. Theor. Exp. Phys. 03C009, 2012.
2) T. Uesaka et al., Prog. Theor. Exp. Phys. 03C007, 2012.
3) Y. Yamaguchi et al., Nucl. Instrum. Methods Phys. Res. B 317, 629 (2013).

Circulation detector for Rare RI Ring

D. Nagae,[*1] Y. Abe,[*1] Y. Yamaguchi,[*1] F. Suzaki,[*1,*2] S. Naimi,[*1] Z. Ge,[*1,*2] H. Miura,[*2] S. Ohmika,[*2] Y. Takeuchi,[*2] T. Nishimura,[*2] N. Tadano,[*2] I. Kato,[*2] T. Yamaguchi,[*2] T. Suzuki,[*2] Y. Ichikawa,[*3] Y. Tajiri,[*3] K. Hiraishi,[*3] T. Matsumoto,[*3] T. Moriguchi,[*3] S. Suzuki,[*3] A. Ozawa,[*3] Y. Yanagisawa,[*1] H. Suzuki,[*1] H. Baba,[*1] S. Michimasa,[*4] S. Ota,[*4] H. Miya,[*4] T. Watanabe,[*1] M. Wakasugi,[*1] T. Uesaka,[*1] and Y. Yano[*1]

A circulation detector consisting of a carbon foil and a multichannel plate (MCP) has been developed for confirming that particles can be stored and for evaluating the revolution time in the Rare RI Ring[1]. Although the basic concept of the circulation detector is the same as those developed at GARIS and Tsukuba[2], and GSI[3], an enlargement of the sensitive area is required to cover a large beam profile in the Rare-RI Ring. A schematic view of the detector is shown in Fig. 1. A large and thin carbon foil (100×50 mm^2 and 60 μg/cm^2) was developed at RIKEN[4]. A stored particle generates secondary electrons when passing through the carbon foil. Secondary electrons are accelerated by an acceleration electric field $E_{\rm acc}$ applied between the carbon foil and an acceleration grid, and they are then deflected at 90 degree towards the MCP by an electrostatic mirror field $E_{\rm mir}$ applied between two parallel grids. These grids are made of gold-plated tungsten wires with a diameter of 40 μm. The acceleration field ($E_{\rm acc}$) and the mirror field ($E_{\rm mir}$) are chosen to satisfy the relation $2E_{\rm acc} = E_{\rm mir}$.

The circulation detector was used in the first commissioning experiment where the ^{78}K primary beam was used. The detector was used in the same manner in the second commissioning experiment using the secondary beam of ^{36}Ar and ^{35}Cl produced by the fragmentation reaction of a primary beam of ^{48}Ca at an energy of 345 MeV/nucleon on a ^{9}Be target with a thickness of 25 mm. A circulation time spectrum of ^{78}Kr is shown in Fig. 2. Particles were successfully stored approximately 60 turns. A revolution frequency was estimated to be 2.639 MHz from the circulation time spectrum. Figures 3(a) and 3(b) are circulation time spectra for ^{36}Ar and ^{35}Cl, respectively. ^{36}Ar ions and ^{35}Cl ions were circulated for approximately 40 turns and 10 turns, respectively. The preliminary revolution times of 378.32(6) ns and 386.3(1) ns were obtained for ^{36}Ar and ^{35}Cl, respectively.

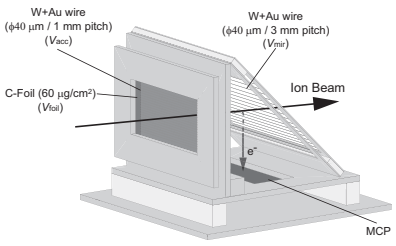

Fig. 1. Schematic view of the circulation detector.

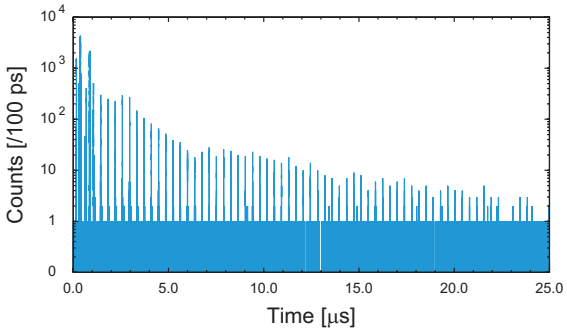

Fig. 2. Circulation time spectrum of ^{78}Kr. Noise generated by the kicker magnet is observed at approximately 0.05 μs.

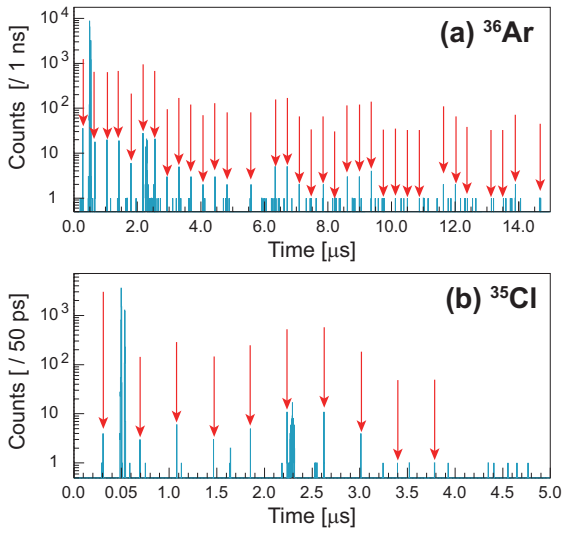

Fig. 3. Circulation time spectra of (a) ^{36}Ar and (b) ^{35}Cl. Arrows indicate signals corresponding to particles.

*1 RIKEN Nishina Center
*2 Department of Physics, Saitama University
*3 Institute of Physics, University of Tsukuba
*4 Center for Nuclear Study, University of Tokyo

References

1) A. Ozawa et al., Prog. Theor. Exp. Phys. 03C009 (2012).
2) T. Mizota et al., Nucl. Instr. and Meth. A **305**, 125 (1991).
3) F. Busch et al., Nucl. Instr. and Meth. **171**, 71 (1980).
4) H. Hasebe et al., RIKEN Accel. Prog. Rep. **42**, 133 (2009).

Study on background suppression of charged particles using GARIS-II filled with He-H_2 mixture

D. Kaji,[*1] K. Morimoto,[*1] S. Yamaki,[*1,*2] H. Haba,[*1] Y. Komori,[*1] S. Yano,[*1] R. Aono,[*1,*3] Y. Namba,[*1,*3] and S. Goto[*1,*3]

The performance of a gas-filled recoil ion separator (GARIS-II) has been evaluated using various asymmetric fusion reactions[1–3]. The feasibility of a high transmission under a low-background condition is a key issue for superheavy elements (SHEs) produced with a low cross section of pb-order. In previous work[1], it was found that GARIS-II filled with a He-H_2 mixture as a filled gas is promising to suppress background particles. To aid future study of SHEs, the usefulness of a He-H_2 mixture was investigated further in this work. As a typical example, the results for ^{218,217}Pa, which were produced via the reaction of ^{197}Au(^{24}Mg,xn) [x=3,4], are given here.

The products of ^{218,217}Pa were separated in-flight from projectiles and other by-products using the GARIS-II, and then they were guided into a double sided silicon detector after passing through a time-of-flight detector. The separator was filled with a He-H_2 mixture with various H_2 mixing ratios (0, 10, 20, and 30%). The gas pressure was maintained at 53 Pa. Recently, a new gas-mixing system, shown in Fig. 1, was developed as the previous system used a commercial gas with fixed mixing ratio. This system enables the mixing ratio to be tuned under constant pressure. The system was well calibrated by a gas analyzer.

The reaction products of ^{218,217}Pa, which were assigned to α-transitions of 9.616 and 8.337 MeV with half-lives of 113 μs and 3.8 ms respectively as shown in Fig. 2, were measured by varying the fraction of H_2 composition from 0 to 30%. The reaction products of ^{217,218}Pa including long-lived isotopes of ^{215,214}Ac are clearly identifiable with an increasing mixing ratio. The values of the equilibrium charge state $\overline{q}$, which are deduced from the optimum magnetic rigidity $B\rho$ values, are plotted against the H_2 composition in Fig. 3. The $\overline{q}$ in pure H_2 is estimated to be 3.80 using empirical systematics, obtained using a Dubna gas-filled recoil separator DGFRS[4]. Interpolated values of $\overline{q}$ between 4.47 and 3.80 in the case of pure He and H_2 are indicated as a broken line in Fig. 3. It seems that the measured $\overline{q}$ values agree well with the linear interpolation of the DGFRS.

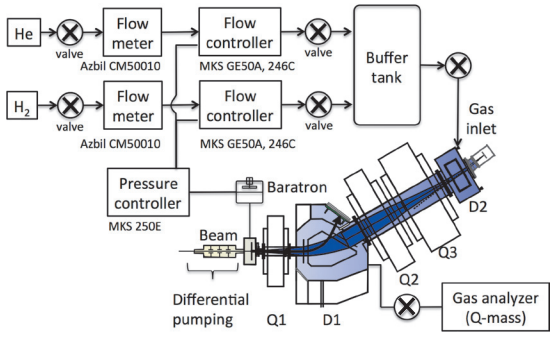

Fig. 1. New gas control system for GARIS-II filled with He-H_2 mixture.

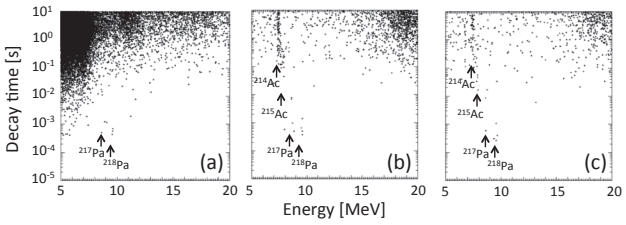

Fig. 2. Two-dimensional scatter plots, obtained by a time-position correlation analysis, of decay time against decay energy. Fractions of H_2 composition are (a) 0%, (b) 10%, and (c) 30%.

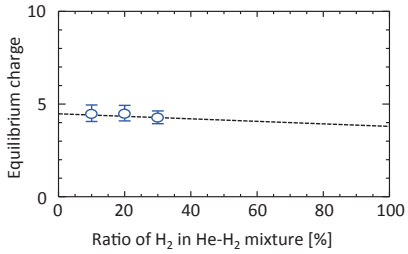

Fig. 3. Equilibrium charge state of ^{217}Pa ions moving in a He-H_2 mixture. The broken line is the linear interpolation between the experimentally obtained $\overline{q}$ of 4.47 and the estimated $\overline{q}$ of 3.80 from the DGFRS's work[4].

*1 RIKEN Nishina Center
*2 Department of Physics, Saitama University
*3 Graduate school of Science and Technology, Niigata University

References

1) D. Kaji et al., RIKEN Accel. Prog. Rep 48, 214 (2015).
2) D. Kaji et al., RIKEN Accel. Prog. Rep 47, 213 (2014).
3) D. Kaji et al., RIKEN Accel. Prog. Rep 46, 189 (2013).
4) Y.T. Ogganessian et al., Phys. Rev. C64, 064309 (2001).

Current status of a gas-cell system for precision experiments with GARIS-II

Y. Ito,[*1] P. Schury,[*1,*2] M. Wada,[*1,*2] F. Arai,[*1,*3] I. Katayama,[*1] I. Murray,[*1] K. Okada,[*4] M. Reponen,[*1] T. Sonoda,[*1] A. Takamine,[*1] H. Wollnik,[*1,*5] H. Haba,[*1] D. Kaji,[*1] K. Morimoto,[*1] K. Morita,[*1,*6] S. Kimura,[*2,*3] and H. Koura[*7]

We constructed a gas cell for precision experiments on fusion-evaporation residues coupled with GARIS-II. In the last report[1)], we presented the commissioning results. In this report, we present the current status of the whole system, from the gas cell to the multi-reflection time-of-flight mass spectrograph (MRTOF) (Fig. 1).

For precision mass measurement with MRTOF[2)], we installed an upstairs radio-frequency ion trap system after extraction from the gas cell. The ion trap system comprises a flat trap[3)] (FT) and a pair of resistive ion traps (RT). The RT stores and pre-cools ions before transferring them to the FT. For this function, we adopted four silicon electrodes with electrical contacts at both edges and 30 mm from the FT side. The electrodes have 6 mm width and 145 mm length which corresponds to the resistance of 330(10) Ω and an inter-strip gap of 8.4 mm. Ions extracted from the gas cell were first stored in the RT for several milliseconds, and then, they were transfered to the FT and bunched in the FT (3 ms). The ion bunch was ejected to the experimental room located downstairs through a 3-m beam transport line (BTL). To accelerate the ion bunch, we used pulsed drift tubes (PDT) that hace a 15 mm inner diameter and 150 mm length. The PDT was switched from -1.5 kV to a GND potential of the BTL with 200 ns rise time when the ions are traveling in the tube. As a result, the ions gain 1.5 keV and are transported in the grounded BTL. In the middle of the BTL, we installed a Bradbury-Nielsen (BN) gate that has a 50 μm gold-coated tungsten wire with a 0.5 mm pitch and is capable of eliminating unwanted ions by fast voltage switching. After the BN gate, we placed another PDT that is switched oppositely to the one upstairs. The ions are decelerated to be ∼50 eV from the PDT by focusing lenses toward a downstairs trap system identical to the one upstairs. The decelerated ions were re-bunched in the same manner as those upstairs and ejected toward the MRTOF at the TDC start time to measure time-of-flight.

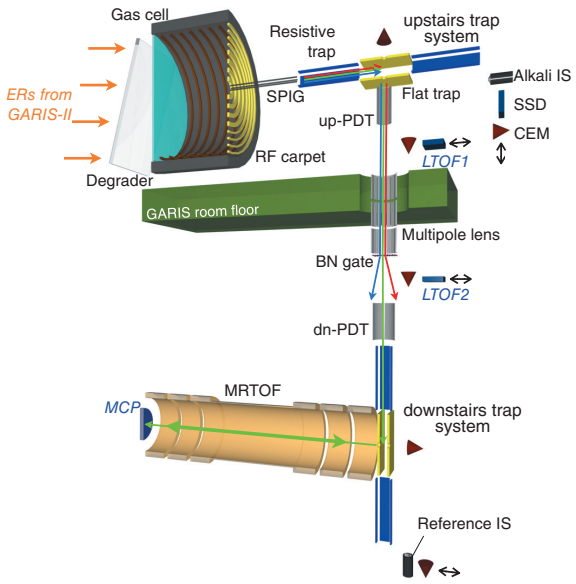

Fig. 1. Schematic view of the gas cell setup with MRTOF.

Using several diagnostics, SSD and channeltron (CEM) detectors, we evaluated efficiencies. First, we counted the ^{205}Fr rate by SSD in front of the gas cell; then we counted the ^{205}Fr^{+} rate by SSD at LTOF2 located after the BN gate. The efficiency to LTOF2 compared to the incoming ^{205}Fr was given as 19%. Second, we measured the BTL transmission efficiency using SSDs at LTOF1 and LTOF2, and obtained the efficiency of 70%. By using the pre-measured gas-cell efficiency of 29%[1)], we could obtain the efficiency of 94% for the upstairs trap system. Finally, the re-trapping efficiency for the downstairs trap system was measured to be 1.6% using the ^{205}Fr^{+} rate at MCP after the MRTOF and ^{205}Fr^{+} rate at LTOF2. In total, the overall efficiency of 0.3% was obtained.

The bottleneck was after re-trapping efficiency that was expected to be more than 20%. We recently found mis-wiring to apply DC voltages for the downstairs trap system. The potential created with this wiring resulted in an unreasonable potential configuration for transferring ions to the FT. We fixed the problem and will check the efficiencies in next beam time.

*1 RIKEN Nishina Center
*2 Institute of Particle and Nuclear Studies (IPNS), High Energy Accelerator Research Organization (KEK)
*3 Department of Physics, University of Tsukuba
*4 Department of Physics, Sophia University
*5 Department of Chemistry and Biochemistry, New Mexico State University
*6 Department of Physics, Kyushu University
*7 Advanced Science Research Center, Japan Atomic Energy Research Institute (JAEA)

References

1) P. Schury et al.: RIKEN Accel. Prog. Rep. 48, 22 (2015).
2) P. Schury et al.: arXiv:1512.00141.
3) Y. Ito et al.: Nucl. Instrum. Meth. B 317, 544 (2013).

Extraction of multi-nucleon transfer reaction products in the ^{136}Xe and ^{198}Pt system

Y. Hirayama,[*1] Y.X. Watanabe,[*1] H. Miyatake,[*1] M. Wada,[*1,*2] H.S. Jung,[*1] M. Oyaizu,[*1] Y. Kakiguchi,[*1] M. Mukai,[*2,*3] S. Kimura,[*2] H. Ishiyama,[*4] S.C. Jeong,[*4] N. Imai,[*5] and T. Sonoda[*3]

We have developed the KEK Isotope Separation System (KISS)[1] to study the β-decay properties of the neutron-rich isotopes with neutron numbers around $N = 126$ for astrophysics research.[2–4] We extracted elastic events of ^{198}Pt and unstable nuclei of ^{199}Pt and ^{196,197,198}Ir produced in the ^{136}Xe beam and ^{198}Pt target system. We successfully dissociated the molecular ions by using a new multi-pole ion-guide (MPIG) system and measured the lifetime of the unstable nuclei of ^{199}Pt[3] and ^{196}Ir.

We performed on-line tests using the ^{136}Xe beam with an energy of 10.75 MeV/nucleon and a maximum intensity of 20 pnA. The ^{136}Xe beam was directed onto the ^{198}Pt target placed in the gas cell, and was stopped at a tungsten beam dump after passing through the gas cell. The thermalized and neutralized reaction products were re-ionized in the gas cell, and the ions were extracted and detected after mass separation using a Channeltron detector for ion counting. The lifetimes were measured by using newly developed β-ray telescopes[5] whose background rate was reduced to 0.09 cps.

In our previous experiment, the extracted $^{198}Pt^+$ ions formed molecular ions such as $^{198}PtH_2^+$, $^{198}PtH_2O^+$, and $^{198}PtAr_2^+$ with the intensity ratio of 1, 1, and 6, respectively, relative to the intensity of $^{198}Pt^+$ ions. The extraction efficiency of the most intense $^{198}PtAr_2^+$ ion was 0.2 %. In order to reduce the amount of the molecular ions and increase the extraction yields, we developed three MPIGs which were installed at the exit of the gas cell to dissociate the molecular ions by applying a DC voltage of 15 V between the first and the second MPIGs as well as to transport the ions from the high pressure region to the low pressure region and, then, accelerate them by applying a high voltage of 20 kV. Figure 1 shows the measured mass distribution of $^{198}Pt^+$ ions extracted from KISS through the MPIGs. In the present measurement, we can successfully dissociate the molecular ions. Considering the molecular ion formation probability in the previous experiment, the extraction efficiency of $^{198}Pt^+$ ion with the most intensity was recovered to be 0.3%, which was a factor of about 1.5 higher than of 0.2% for $^{198}PtAr_2^+$ ion. This indicates that almost all molecular ions dissociated to $^{198}Pt^+$ ion.

We extracted the laser-ionized iridium isotopes ^{196,197,198}Ir atoms. Figure 2 shows the measured lifetime of the ^{196}Ir ($t_{1/2} = 52(1)$ s) isotope. The measured lifetime $t_{1/2} = 67(13)$ s was in good agreement with the reported value.

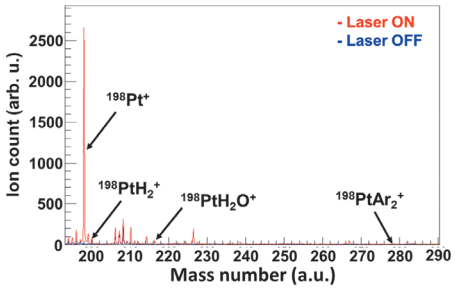

Fig. 1. Measured mass distribution of the platinum ions. Red and blue lines indicate the spectra measured with and without the irradiation of ionization lasers, respectively.

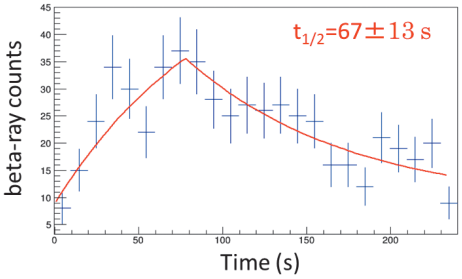

Fig. 2. Lifetime measurement of ^{196}Ir.

To extend this study to more neutron-rich nuclei, we have been developing a doughnut-shaped gas cell to increase the available primary beam intensity and a low-background beta-ray telescope.

References

1) Y. Hirayama et al., Nucl. Instr. and Meth. **B353**, 4 (2015).
2) S.C. Jeong et al.: KEK Report 2010-2.
3) Y. Hirayama et al.: RIKEN Accel. Prog. Rep. **48**, 233 (2015).
4) H. Ishiyama et al.: RIKEN Accel. Prog. Rep. **45**, 151 (2012).
5) S. Kimura et al.: RIKEN Accel. Prog. Rep. **48**, 234 (2015).

*1 Wako Nuclear Science Center (WNSC), Institute of Particle and Nuclear Studies (IPNS), High Energy Accelerator Research Organization (KEK)
*2 Department of Physics, University of Tsukuba
*3 RIKEN Nishina Center
*4 Institute for Basic Science, Rare Isotope Science Project
*5 Center for Nuclear Study, University of Tokyo

Measuring luminosity of electron scattering from Xe isotopes at the SCRIT experiment

A. Enokizono,[*1,*2] K. Adachi,[*1,*2] T. Fujita,[*1,*2] M. Hori,[*1] K. Kurita,[*1,*2] T. Ohnishi,[*2] T. Suda,[*2,*3] T. Tamae,[*2,*3] K. Tsukada,[*2,*3] M. Wakasugi,[*2] M. Watanabe,[*2] and K. Yamada[*1,*2]

The SCRIT (Self-Confining RI ion Target)[1] device has been developed to make the experiment of electron scattering off short-lived nuclei possible at high luminosity (10^{27}cm^{-2}s^{-1}). The charged density distribution of the target nucleus is derived from the angular distribution of elastic scattering cross-section of electrons. At the SCRIT experiment, the angle and momentum distributions of scattered electrons are measured by the electron spectrometer (WiSES), and the luminosity of the electron-nucleus scatterings is measured by the luminosity monitor (LMon). Here the luminosity is obtained by measuring photons from the bremsstrahlung process which is calculatable with less ambiguity even for previously unmeasured nuclei.

The LMon, which is located ∼7 m downstream along the beam line from the electron-target interaction region, consists of 7 CsI calorimeters to measure the photon energy, and plastic fiber scintillators to measure the 2D hit distribution of photons[2]. In August 2015, a commissioning test using stable ^{132}Xe target was performed at the beam energy $E_e = 150$ MeV. In order to estimate the background from residual gases, the LMon measures photons for both periods with and without trapped ^{132}Xe.

Figure 1 shows the total energy distributions that are calculated by summing up energy deposits in the 7 CsIs. Each CsI energy was calibrated by using the cosmic data and GEANT4 simulation. The left panel of Figure 2 shows the photon hit rates measured run-by-run. Each run is typically ∼20-30 min long. It is shown that the background photons from the residual gases (ION OFF) occupy the majority of the total event rate (ION ON), and the net photon event rate from Xe target (ION ON-OFF) is ∼10-15 kHz. The run-by-run luminosities, as shown in the right panel of Fig. 2, are estimated as $L = N_{br}/t\sigma_{br}\epsilon$ where σ_{br} is the cross-section of the bremsstrahlung process for a given energy range[3] and ϵ is the detection efficiency evaluated by GEANT4. The net photon event rate (N_{br}/t) and the integral of σ_{br} are limited only above 50 MeV to avoid a huge background of low energy photons. The average luminosity during this commissioning experiment is estimated to be $(2.02\pm0.12)\times10^{26}$cm^{-2}s^{-1} including systematic uncertainties. The systematic error that originates in the CsI energy resolution is the largest contribution (2.8%). The energy pile-up contribution, which appears as entries above 150 MeV in Fig. 1 if more than two photons from independent bremsstrahlung processes hit CsIs within a trigger window, is found to be negligible.

In summary, we have performed a commissioning experiment for SCRIT using ^{132}Xe at $E_e = 150$ MeV, and demonstrated that the luminosity measured by LMon reached $\sim 2\times10^{26}$cm^{-2}s^{-1}. Since the background rate is found to be more than 3-4 times higher than the signal event rate, the next important step is to carefully investigate the background contributions by GEANT4 simulation. It should also be noted that more recent studies of the electron beam improved the luminosity by a couple of factors, and the result will be reported in near future.

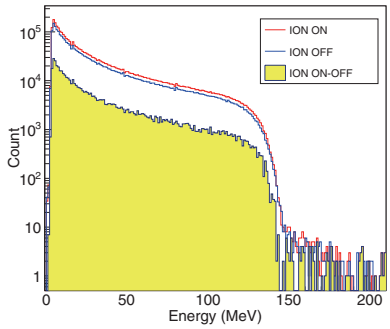

Fig. 1. Total energy distributions of CsI with Xe trap (ION ON), without Xe trap (ION OFF) and the difference between the two (ION ON-OFF).

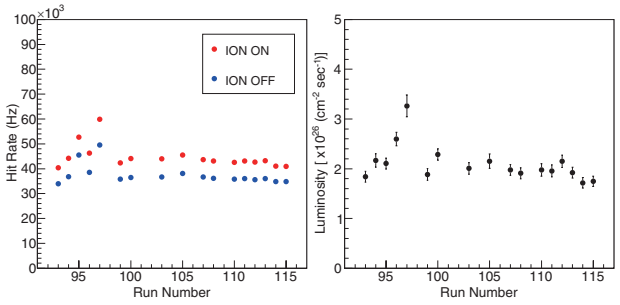

Fig. 2. Run dependence of photon hits rates at CsI (left), and the measured luminosity (right).

*1 Department of Physics, Rikkyo University
*2 RIKEN Nishina Center
*3 Research Center for Electron-Photon Science, Tohoku University

References
1) M. Wakasugi *et al.*: NIM **B317**, 668 (2013).
2) S. Yoneyama *et al.*: Accel. Prog. Rep. **48**, 227 (2015).
3) Y. S. Tsai, Rev. Mod. Phys. **46**, 815 (1974).

Current status of RI beam production at electron-beam-driven RI separator for SCRIT (ERIS)

T. Ohnishi,[*1] S. Ichikawa,[*1] M. Togasaki,[*1,*2] K. Kurita,[*1,*2] and M. Wakasugi[*1]

The ERIS[1] (electron-beam-driven RI separator for SCRIT) at the SCRIT electron scattering facility[2] is an online isotope separator system used to produce low-energy RI beams for electron-scattering experiments of unstable nuclei. Recent developments of the ERIS were reported in Ref. 3. In this year, we performed an operation for a long period of time using stable ions to evaluate the stability of the ERIS. In addition, improvements were made to increase rate of unstable nuclei. In this paper, we report the results and the present status of the ERIS.

The operation of the ERIS started on May 8, 2015. Beams of stable xenon ions were used for the optimization of the ion transport line and the commissioning of the new electron spectrometer, WiSES[4]. In this operation, the ionization chamber and the transfer tube equipped with the cathode head were the same as in the case of the production of unstable nuclei. These parts were heated using self-resistance heating with a large current, about 325 A, and the temperature was maintained at about 2273 K. The maximum current of ^{132}Xe was about 400 nA. After seven months of operation, the cathode head was broken on December 2, 2015.

Figure 1 shows the long-term trend of the cathode voltage and the vacuum degree of the acceleration chamber, which is one order higher than that of the ion source. For constant current operation, the cathode voltage affects the condition of the electrodes. When the cathode voltage decreased and became constant, the connection between the cathode head and the transfer tube improved. Finally, the cathode voltage increased rapidly, because the cathode head became thinner and it broke.

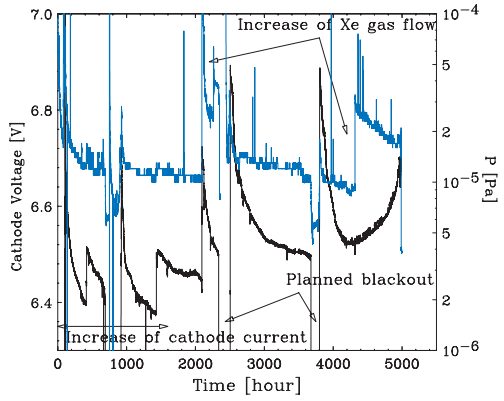

Fig. 1. Long-term trends of cathode voltage (black) and pressure of the acceleration chamber (blue). The period is from May 8 to December 2, 2015. During the operation, there were two planned blackouts.

This operation period was much longer than in 2013, about 2 months. One of the key points was a high vacuum degree because of the minor damage to electrodes caused by a small amount of residual gas. The other key point was considered as small thermal stress. The cathode current was continuously applied during the operation period except for during the planned blackout. Therefore, damage from the thermal stress caused by the variation of the temperature was estimated to be very small.

In order to increase the extraction rate of unstable nuclei, a new ionization chamber of the ERIS is considered. Figure 2 shows a schematic of the new ionization chamber. By applying a voltage higher than the anode voltage to the entrance and exit grid electrodes, stacking of ions is expected to occur inside the ionization chamber. For positive ion extraction, voltage lower than the anode voltage is applied only to the exit grid. The optimization of the exit grid voltage improves the extraction using the extractor. This new chamber is still being manufactured.

In summary, we performed a stability test of the ERIS with the long-term operation. This gives us very useful information about the stable operation with high temperature conditions. Plans to improve the efficiency of the ERIS, mainly the extraction efficiency, are underway.

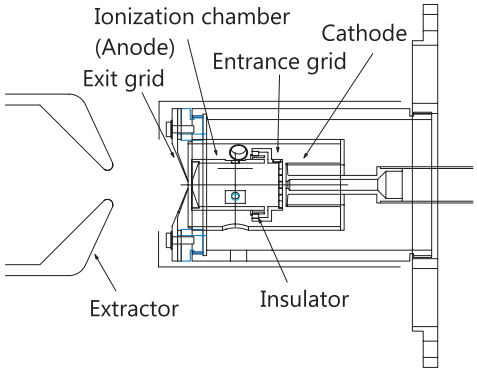

Fig. 2. Schematic of new ionization chamber of ERIS. The entrance and exit grid electrodes are connected to the ionization chamber through an insulator.

*1 RIKEN Nishina Center
*2 Department of Physics, Rikkyo University

References

1) T. Ohnishi et al., Nucl. Instr. Meth. B**317**, 357 (2013).
2) M. Wakasugi et al., Nucl. Instr. Meth. B**317**, 668 (2013).
3) T. Ohnishi et al., Accel. Prog. Rep. **48**, 229 (2015).
4) K. Tsukada et al., Accel. Prog. Rep. **48**, 23 (2015).

Commissioning of SCRIT electron scattering facility with stable nuclear targets

K. Tsukada,[*1,*2] K. Adachi,[*1,*3] A. Enokizono,[*1,*3] T. Fujita,[*1,*3] M. Hori,[*1,*3] K. Kurita,[*1,*3] T. Ohnishi,[*1] T. Suda,[*1,*2] T. Tamae,[*1,*2] K. Yamada,[*1,*3] M. Wakasugi,[*1] and M. Watanabe[*1]

The SCRIT electron scattering facility has been developed at RIBF for realizing electron scattering off unstable nuclei. Construction of a magnetic spectrometer, WiSES (Window-frame Spectrometer for Electron Scattering), and a luminosity monitor almost finished in November 2014, and the detector commissioning started[1,2]. ERIS (electron-beam-driven RI separator for SCRIT) and an ion transportation system have been continuously developed up until now to increase the target ion trapped in the SCRIT.

This year, commissioning experiments with several kinds of stable nuclear targets have been performed in order to evaluate the performance of SCRIT facility.

Metal wires of diameter 50 μm made of tungsten and titanium were horizontally mounted at the center of the SCRIT device as stable nuclear targets. By changing the position of these wires remotely, the luminosity can be controlled. Figure 1 shows the angular distribution of elastic scattering events corrected by the acceptance for the tungsten target. These data were taken in July 2015. Although a DWBA calculation[3] is consistent with our results in the forward region, there are small discrepancies of around 50°.

The xenon ion beams have been stably provided by ERIS[4]. For the commissioning, ^{132}Xe was used as a stable target because the natural abundance of ^{132}Xe is 26.9%, which is the largest in the series of xenon isotopes. Figure 2 shows the vertex point distribution along the beam line. These data were taken in December 2015. As shown in the inner figure of Fig. 2, the conditions of ^{132}Xe and the empty target interchanged every 50 ms with an interval of 10 ms.

The difference between Ion IN and Ion OUT is clearly seen. Figure 3 shows the angular distribution of elastic events corrected by the acceptance after background subtraction. In the present analysis, it is assumed that the xenon ions are distributed uniformly in the SCRIT. In the forward region, the calculation and our results are almost consistent. The statistics, however, is not enough in the backward region to discuss the consistencies. Even now, the data taking are being continuously taken by using the ^{132}Xe target with an electron energy of 150 MeV.

In summary, the angular distributions of a stable nuclear target have been measured and compared with a DWBA calculation. Before proceeding to experiments with unstable nuclei, we need more studies with stable targets to understand the acceptance.

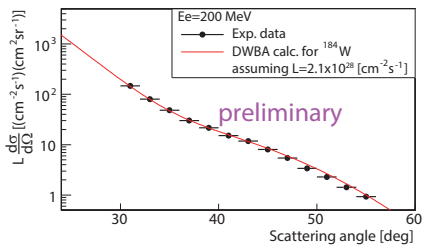

Fig. 1. Obtained differential cross section for tungsten target at the electron beam energy of 200 MeV. The solid line is a calculation by DWBA code assuming averaged luminosity of 2.1×10^{28} [cm^{-2}s^{-1}].

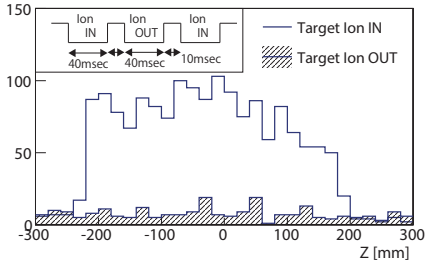

Fig. 2. Vertex point distribution along the beam line. Inner figure shows the time structure of the target conditions.

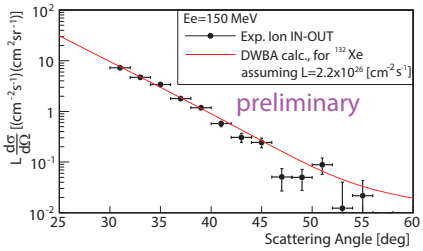

Fig. 3. Obtained differential cross section for ^{132}Xe target at the electron beam energy of 150 MeV. The solid line is a calculation by DWBA code assuming averaged luminosity of 2.2×10^{26} [cm^{-2}s^{-1}].

*1 RIKEN Nishina Center
*2 ELPH, Tohoku University
*3 Department of Physics, Rikkyo University

References
1) K. Tsukada *et al.*, Accel. Prog. Rep. **48**, 23 (2015).
2) S. Yoneyama *et al.*, Accel. Prog. Rep. **48**, 227 (2015).
3) B. Drepher *et al.*, a phase-shift calculation code for elastic electron scattering, communicated by J. Friedrich.
4) T. Ohnishi *et al.*, in this progress report.

New design of timing-controller circuit board for accelerators in the SCRIT facility

M. Watanabe,[*1] A. Enokizono,[*1,2] M. Hara,[*1] T. Hori,[*1] S. Ichikawa,[*1] K. Kurita,[*2] T. Ohnishi,[*1] T. Suda,[*1,3] T. Tamae,[*1,3] M. Togasaki,[*1] K. Tsukada,[*1,3] M. Wakasugi,[*1] and K. Yamada[*2]

A timing-controller circuit board installed in the electron injection system at the SCRIT facility[1] has been designed for electron beam injection from a racetrack microtron (RTM) into the storage ring (SR2). However, it is used to inject the electrons into the electron-beam driven RI separator[2] (ERIS) at the SCRIT facility. For electron injection into the SR2, the frequency of the beam pulse frequency is 2.0 Hz. On the other hand, a higher frequency is desired to have a high intensity beam of RIs of ERIS.

The SR2 was developed as the electron storage ring in order to provide synchrotron radiation for basic research and/or application for industries as the lithography light source. Consequently, the timing controller system for the electron injection does not have the function to inject the beam into another facility such as ERIS. In order to satisfy both injection conditions into SR2 and ERIS, the timing-controller should have a function to switch the beam between the storage ring SR2 and ERIS and to change the injection conditions. In this report, we detail the new design for the timing-controller circuit board. The circuit board has functions for processing internal pulse triggers and external triggers to utilize various injection parameters for ERIS. Therefore, we added a switching function onto the new board.

We used the 74HC logic IC family to construct the circuit as the original circuit is designed using the 74HC logic IC family and it is relatively easy to buy this from the vendors. In addition, almost all of the 74HC family is provided in DIP packages. The speed of 74HC is high enough for more than 1 kHz frequency. The final goal of the frequency is 100 Hz for this new board.

Figure 1 shows a simplified circuit diagram for one channel. Each channel has two trigger inputs (Ext. TRG and TRG), interlock signal inputs (Ext. I/L and I/L), and one trigger selector input. One board has five channels inside.

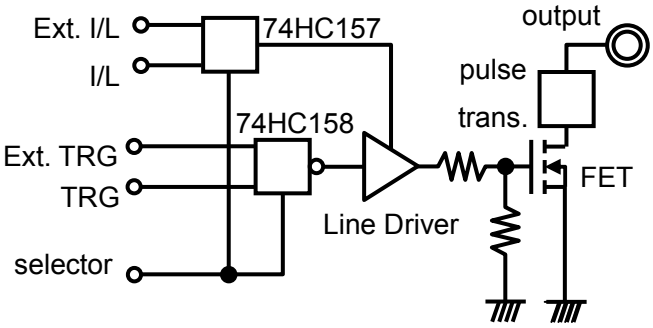

Fig. 1. Simplified schematic of the circuit.

*1 RIKEN Nishina Center
*2 Department of Physics, Rikkyo University
*3 ELPH, Tohoku University

Figure 2 is the photo of the developed circuit board. The white connector at the right side is for the connection to the mother board of the timing-controller system. In the connector, there are 5 coaxial connectors for internal trigger input, 5 interlock signal pins (24 V), and DC 15 V power line. The 15 V is converted into 5 V by a regulator IC to provide electric power for the logic ICs. On the left side, there are 5 coaxial connectors for external trigger inputs, 5 external interlock pins, and int./ext. selector pins. The selector pins can be used by either short/open or 5 V / 0 V states. To use the 5 V / 0 V states as selectors, IC 62003 has to be installed into the IC socket next to the input pins.

Other than the input connectors, there are a few DIP switches on the board. One of them is a selector switch that select the terminator for the external trigger input. It is possible to choose either 50 ohm or 1M ohm. Other switches are “interlock ON” switch and “interlock flip” switches.

Output trigger lines are insulated from the logic system of this circuit board by pulse transformers. Input signals into the pulse transformers are supplied by the series of driver ICs and FETs to provide sufficient voltage and power for 50 ohm impedance lines. The pulse peak heights from the FETs are close to the 15 V power line. The outputs from the pulse transformers should be similar to the input signals, since the ratio of the transformer is 1:1. In order to modify the pulse shape of the output, zener diodes are used to control the output pulse heights. All output pulse except for the output for the RF driver is set at 5 V heights. The widths of the pulses depends on the input trigger widths.

The newly designed circuit boards have been already installed, and they are confirmed to work at the frequency of 100 Hz.

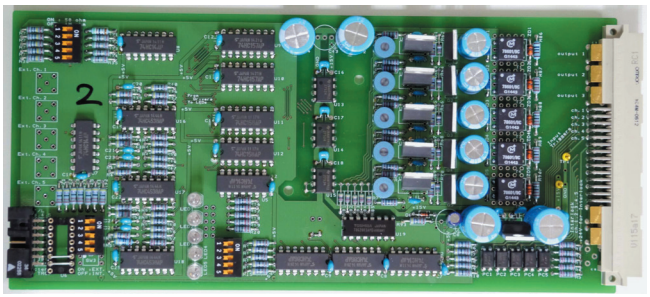

Fig. 2. Photo of the timing-controller circuit board. The left side is for the external trigger input area, and the right internal. The black connector at the left bottom is selector pins for the int./ext. input switches.

References

1) M. Wakasugi et al.: Nucl. Instr. And Meth. B**317**, 668 (2013)
2) T. Ohnishi et al.: Phys. Scr. T**166**, 014071 (2015)

All-solid-state continuous-wave laser source at 313 nm for laser cooling of Be^+ ions

A. Takamine,[*1] H. Ohmae,[*2] M. Wada,[*1,*3] and H. Katori[*2]

An all-solid-state laser system operated at a wavelength of 313 nm is developed for laser cooling of Be^+ ions aimed at hyperfine anomaly measurements of Be isotope ions, including the neutron halo nucleus ^{11}Be[1], and sympathetic cooling of highly charged ions with Be^+ ions.

Laser beams at 313 nm were traditionally produced by second-harmonic generation (SHG) of a 626 nm radiation obtained from a dye laser[2]. However, compared with such a liquid laser, a solid-state laser is more suitable for long-term operation because of its reliability and stability. In recent years, solid-state laser systems to provide light in a single-mode at 313 nm have been demonstrated: sum-frequency generation (SFG) of a 532 nm frequency doubled Nd:YAG laser and a 760 nm Ti:sapphire laser[3], frequency quintupling of a 1565 nm amplified fiber laser system[4], SHG of a 626 nm laser light by SFG of amplified fiber laser systems at 1550 nm and 1051 nm[5], and frequency doubling of a 626 nm light from a cooled down diode laser[6]. Although some of these can produce 313 nm light with a high power of more than 100 mW, they are expensive. The procedure in Ref.[6] is the cheapest but it requires a very high finesse SHG cavity, which might cause a noisy output because the fluctuation of the cavity length needs to be suppressed to the level much smaller than the ratio of the laser wavelength to the finesse and the fluctuation of the laser frequency is required to be much smaller than the ratio of the free spectral range to the finesse.

We develop a cost-efficient laser system with a reasonably high output power as shown in Fig. 1. Laser light at 939 nm from a Littrow configuration external-cavity diode laser (ECDL) is amplified up to ∼2 W through a tapered amplifier (TA) chip (m2k-TA-095-2000). The high power 939 nm light is delivered through an optical fiber and divided into two beams. One is injected into a SHG cavity with a type-I phase-matching BiB_3O_6 crystal to produce 470 nm laser light. The other 939 nm beam and the 470 nm SHG output beam are injected into a SFG cavity with a type-I phase-matching BBO crystal to produce 313 nm laser light with an expected power of ∼5 mW, which is high enough for laser cooling of Be^+ ions. The cavity lengths are controlled by using Pound-Drever-Hall locking[7] with the reflected pump beams from the input couplers, which are monitored by photodetectors (PDs). The sidebands required for the locking scheme are generated by an electro optical modulator (EOM).

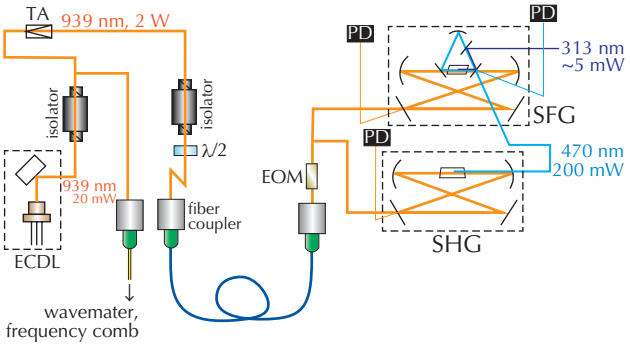

Fig. 1. Schematic diagram of the laser setup.

Figure 2 (a) shows the measurement results of the injection current dependence of the output power from the TA chip at 22.01 °C with a seed light of 10 mW. The output power of the single-mode laser light from the fiber output coupler was 900 mW with a fiber input of 1.72 W, including the amplified spontaneous emission background. The highest 620 mW power of the 470 nm laser was obtained from SHG at a pump power of 900 mW, as shown in Fig. 2 (b), which means we achieved a high second harmonic conversion efficiency of ∼70 %. Although tuning of SFG cavity is now under way, we have a high degree of expectation for this novel scheme to produce laser light at 313 nm intense enough for laser cooling experiments.

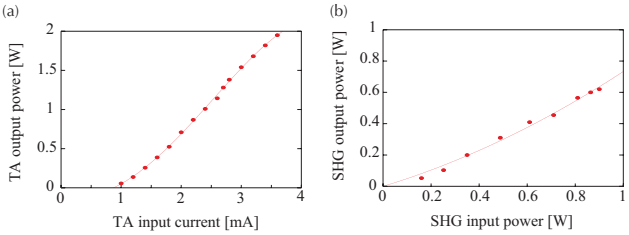

Fig. 2. (a) TA output power as a function of injection currents with a seed light of 10 mW at 939 nm. (b) Output power of SHG as a function of the input power of 939 nm laser light.

*1 RIKEN Nishina Center
*2 Quantum Metrology Laboratory, RIKEN
*3 Wako Nuclear Science Research Center, KEK

References

1) A. Takamine et al.: Nucl. Instrum. Meth. B in press doi:10.1016/j.nimb.2015.12.027
2) C. Monroe et al.: Phys. Rev. Lett. **75**, 4011 (1995).
3) H. Schnitzler et al.: Appl. Opt. **41**, 7000 (2002).
4) S. Vasilyev et al.: Appl. Phys. B **103**, 27 (2011).
5) A. C. Wilson et al.: Appl. Phys. B **105**, 741 (2011).
6) F. M. J. Cozijin et al: Opt. Lett. **38**, 2370 (2013).
7) R. W. P. Drever et al.: Appl. Phys. B **31**, 97 (1983).

An injection-locked Titanium:Sapphire laser for high-resolution in-jet resonance ionization spectroscopy at PALIS

M. Reponen,[*1] T. Sonoda,[*1] M. Wada,[*2] D. Matsui,[*3] V. Sonnenschein,[*3] T. Takamatsu,[*3] and H. Tomita[*3]

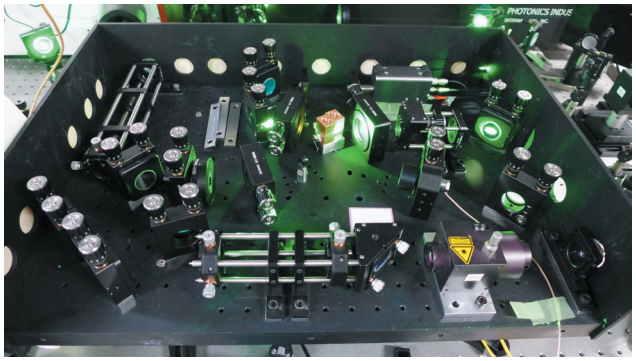

Fig. 1. Injection-locked laser in operation

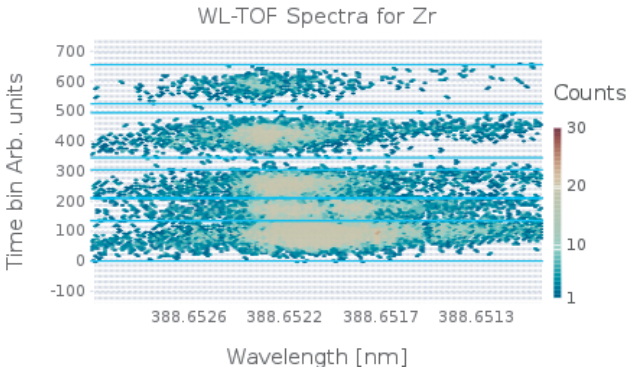

Fig. 2. Wavelength vs. time-of-flight spectra for stable Zr.

The PArasitic Laser Ion-Source (PALIS)[1)] of the SLOWRI -facility[2)] at RIKEN Nishina Center is a gas-cell -based device intended for producing pure, low-energy beams of exotic nuclei. The device primarily operates by first stopping and neutralizing the discarded fraction of the isotopes produced in projectile fragmentation and in-flight fission reactions, followed by selective re-ionization by lasers and subsequent mass separation.

The present PALIS laser system consists of broadband, high-power dye lasers and of a Titanium:Sapphire laser operating at a 10 kHz repetition rate. The combination of dye and solid-state lasers coupled with harmonic generation capability provides high-pulse power and a broad wavelength coverage from the near-infrared to deep UV regions thus enabling access to a wide selection of ionization schemes. The wide $\geq$1.5 GHz bandwidth of these lasers is optimal for efficient in-gas-cell resonance ionization where the atomic transitions are broadened owing to the high buffer gas pressure (up to 1000 mbar).

The broad overall linewidth in the case of the in-gas-cell resonance laser ionization masks the small perturbations the nucleus exerts on the atomic energy levels. The inability to resolve features such as hyperfine structure and isotope shift limits the applicability of in-gas-cell resonance ionization spectroscopy (RIS).

However, upon exiting the gas cell, the buffer gas expands to a supersonic jet where the temperature and pressure, and thus the primary line broadening mechanisms, are greatly suppressed[3)]. In order to take advantage of this environment and to provide a high-resolution RIS capability for the PALIS -facility, a program to develop a narrowband Titanium:Sapphire laser has been initiated. The ring cavity based slave resonator is an evolution of the design from the University of Mainz[4)] and from the University of Jyväskylä[5)]. The laser produces a narrowband output by utilizing the so-called injection-locking that enables bandwidth down to ~20 MHz, while preserving the high pulse power required to efficiently drive atomic transitions. The laser, presented in Fig. 1, has been designed and constructed in collaboration with the University of Nagoya, where it has also been commissioned via resonance ionization of zirconium using a transition at 388.65 nm combined with an non-resonant ionization step (see Fig. 2). Initial results indicate a total resolution of $\leq$500 MHz, sufficient to partially resolve the hyperfine structure in ^{91}Zr and isotope shift $\delta\nu^{90,A}$.

The near future plan is to study the laser properties in detail in order to determine the fundamental bandwidth and stability, and to expand the laser wavelength range to 732 nm and 980 nm regions in order to gain access to elements such as copper and silver. Following this, the initial off-line in-jet RIS of stable copper isotopes will be performed at PALIS in order to verify the lasers feasibility for nuclear laser spectroscopy.

*1 RIKEN Nishina Center
*2 Institute for Particle and Nuclear Studies (IPNS), High Energy Accelerator Res Org. (KEK)
*3 Department of Quantum Engineering, University of Nagoya

References

1) T. Sonoda et.al AIP Conf. Proc. 1104, 132 (2009).
2) M. Wada et al. , Hyp. Int. **199**, 269 (2011).
3) R. Ferrer et al. Nucl. Instrum. Methods. Phys. Res. B **291**, 29 (2011).
4) T. Kessler et al., Las. Phys. **18**, 842 (2008).
5) V. Sonnenschein: PhD Thesis, JYFL Res. Report No. **1**/2015.

Development of magnetic field coils for laser spectroscopy of atoms in He II

T. Fujita,[*1,*2] K. Imamura,[*1,*3] D. Tominaga,[*4,*1] T. Kawaguchi,[*4,*1] T. Egami,[*4,*1] T. Nishizaka,[*4,*1] T. Kobayashi,[*5] A. Takamine,[*1] T. Furukawa,[*6,*1] H. Ueno,[*1] T. Shimoda,[*2] and Y. Matsuo[*4,*1]

Nuclear spins and electromagnetic moments are important properties for investigating nuclear structures. To determine these properties of low yield exotic nuclei, we have been developing OROCHI (Optical RI-atom Observation in Condensed Helium as Ion-catcher) method, which is a laser spectroscopic method using superfluid helium (He II) as a stopping material for energetic ion beams. In this method, we measure the atomic Zeeman and hyperfine structure (HFS) splitting energies of neutralized atoms in He II using laser-radio frequency (RF)/microwave (MW) double resonance method[1]. Then, the nuclear spins and moments are deduced. The effectiveness of the OROCHI method was confirmed by the experiments using energetic $^{84-87}$Rb beams at the RIPS beam line, RIKEN[2]. In addition, the Zeeman and HFS splittings of stable Rb, Cs, and Au atoms in He II have been observed in offline experiments. Improvement of measurement accuracy and precision leads us to discuss higher order effects such as hyperfine anomaly. Recently, the measurement accuracy is successfully improved by one order of magnitude by scanning the MW frequency using phase-locking[3]. In order to increase the precision, we installed a new set of magnetic field coils to suppress the inhomogeneity of an applied magnetic field. We here report the current status of HFS measurement of stable Au atoms.

Figure 1 shows our offline experimental apparatus. An open-topped cubic quartz cell was fully filled with He II. The Au sample was placed 1 cm above the He II surface. The Au atoms were prepared in He II by laser sputtering of the sample with two pulsed lasers[4]. The atoms were optically pumped by irradiation with the frequency-quadrupled laser radiation of an LD-pumped pulsed 1054 nm Nd:YLF laser at a 3 kHz repetition rate. We set RF coils and an MW loop antenna for the double resonance method. The emitted laser-induced-fluorescence (LIF) photons were focused onto a photomultiplier tube (PMT) through a monochromator for wavelength selection.

In the previous experiments, a pair of circular coils was located near the quartz cell. The obtained resonance peaks, which are expected to be Lorentzian shapes, were distorted because it was difficult to apply a uniform magnetic field in the observation region due to limitations of space inside the cryostat[5]. In our new setup, we constructed a set of large square coils, which can be placed outside the cryostat. The coils are represented in orange in Fig. 1. Figure 2 shows the resonance spectrum obtained using the new coils. The measurement precision was improved by one order of magnitude as compared with the previous work[5] owing to the reduced inhomogeneities in the applied magnetic field as well as the increment of the LIF counts. The achieved precision is satisfactory for the discussion of hyperfine anomaly. However, the obtained spectrum was slightly distorted by the inhomogeneities of the magnetic fields, presumably due to environmental magnetic fields.

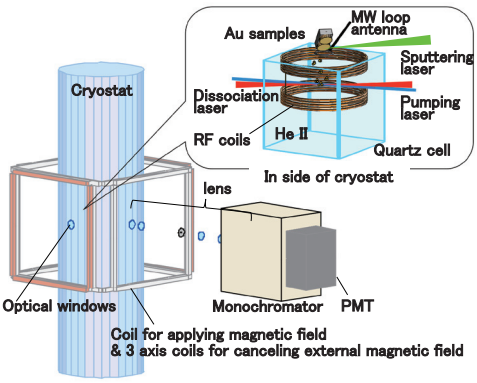

Fig. 1. Experimental apparatus.

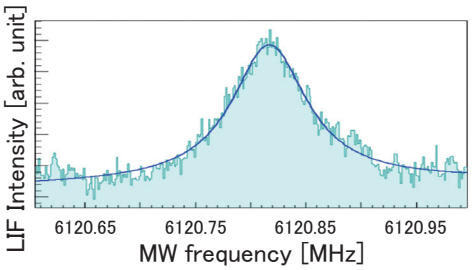

Fig. 2. MW resonance spectrum of ^{197}Au.

Next, we plan to measure HFS splittings using three-axis coils for canceling environmental magnetic fields, shown as gray coils in Fig. 1. After the test experiment, we will start the measurement for stable Ag atoms, which belong to the same group of atom as Au and have two stable isotopes.

*1 RIKEN Nishina Center
*2 Department of Physics, Osaka University
*3 Department of Physics, Meiji University
*4 Department of Physics, Hosei University
*5 RIKEN Center for Advanced Photonics
*6 Department of Physics, Tokyo Metropolitan University

References

1) S. Lang et al.: Europhys. Lett. **30**(4), 233 (1995).
2) X.F. Yang et al.: Phys. Rev. A **90**, 052516 (2014).
3) K. Imamura et al.: Hype. Interact. **230**, 73 (2015).
4) T. Furukawa et al.: Phys. Rev. Lett. **96**, 095301 (2006).
5) T. Fujita et al.: RIKEN Accel. Prog. Rep. **47**, 212 (2014).

Intensity evaluation of laser-RF double resonance signal of Rb atoms in superfluid helium cryostat

K. Imamura,[*1,*2] T. Furukawa,[*3,*1] T. Wakui,[*4,*1] T. Fujita,[*1,*5] M. Hayasaka,[*6,*1] M. Matsumoto,[*6,*1] T. Egami,[*7,*1] D. Tominaga,[*7,*1] H. Odashima,[*2] H. Ueno,[*1] and Y. Matsuo[*7,*1]

A laser spectroscopy technique named OROCHI (Optical Radioisotope atom Observation in Condensed Helium as Ion-catcher) has been developed in RIKEN. Owing to the intriguing properties of superfluid helium as a host matrix of atoms, high energetic ions provided from accelerator facilities can be efficiently utilized to measure nuclear properties such as nuclear spins and moments[1]. In the OROCHI experiment, energetic ions are injected into superfluid helium and neutralized during their stopping process. By applying a circularly polarized laser, neutralized atoms exhibit spin polarization. We observe the variation intensity of emitted photons from atoms using laser-RF (radio frequency)/MW(microwave) double resonance spectroscopy to measure Zeeman/hyperfine splitting of atoms. The measurement enables us to deduce the nuclear spin/moment values. Thus far, we have conducted a series of experiments using $^{84-87}$Rb ion beams at the RIPS separator[2]. The successful measurement of Zeeman splitting of Rb atoms and the deduction of the nuclear spin value of $^{84-87}$Rb show the applicability of the OROCHI method to rare isotopes.

However, there are several technical difficulties when applying OROCHI to low-yield spices also emerged. One of the main difficulties is the low intensity of the double resonance signal induced by RF or MW fields. The resonance signal observed in the on-line experiment was approximately three times lower than that observed in the off-line test experiments. To identify the cause of this discrepancy, we conducted experiments to evaluate the appropriate signal intensity of the double resonance using a pyrex gas cell that contains Rb and He gases using two types of setups. One was basically the same scheme as the off-line test experiment described in Ref 1). The difference was that the gas cell was placed in a quartz cubic cell instead of a superfluid helium liquid. In the other setup, the gas cell was placed at the center of the cryostat used for the on-line experiment. In the experiments, we used an external cavity laser diode (ECLD) as a pumping laser with on intensity was of approximately 1.0 mW (with a diameter of 3 mm, and a wavelength of 795 nm). Both the static magnetic field and fixed-frequency oscillating RF field were applied to atoms using Helmholtz coils and RF coils, respectively. Magnetic resonance peaks caused by the RF field were obtained by sweeping the strength of the statistic magnetic field.

Figures 1(a) and (b) show the intensity dependence of the resonance peak against the RF field intensity using the off-line and on-line setups, respectively. As seen in Fig.1, we find that the resonance signal of the off-line setup reaches the saturation region with an RF intensity of two orders of magnitude smaller than the case of the on-line setup. This large discrepancy in RF intensity dependence is attributed to the followings. In the setup used for the on-line experiment, the transmission line to provide RF power is approximately 10 times longer than that used in the off-line test experiment. This long transmission line may be the reason for the significant loss in the RF field. The second possible reason is the difference in the shapes of the RF coils. The RF coils used in the on-line experiment is slightly smaller than the coils used in the off-line experiment because of the geometric limitation of the cryostat for the beam experiment. This might have lowered the intensity of the applied RF field. The third reason is the large width of resonance spectra due to the inhomogeneity of the static magnetic field. Broadened resonance spectra require a larger RF field power to saturate the resonance peaks. The improvement in the experimental setup to solve the problems mentioned above is now in progress.

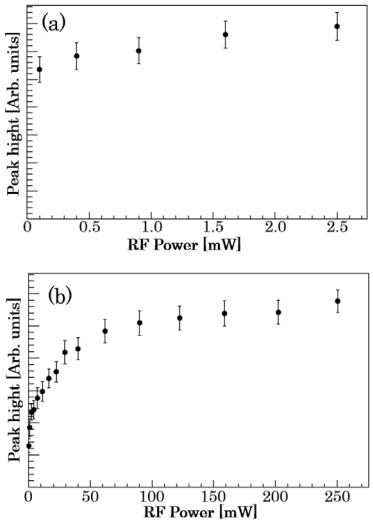

Fig. 1. RF power dependence of resonance peak heights

*1 RIKEN Nishina Center
*2 Department of Physics, Meiji University
*3 Department of Physics, Tokyo Metropolitan University
*4 Tohoku University, CYRIC
*5 Department of Physics, Osaka University
*6 Department of Physics, Tokyo Gakugei University
*7 Department of Physics, Hosei University

References
1) T. Furukawa et al.: Hyperfine Interact. **196**, 191(2010).
2) X. F. Yang et al.: Phys. Rev. A **90**, 052516(2014).

Formation of uniform heavy-ion beam for industrial utilization

T. Kambara*1 and A. Yoshida*1

RIKEN provides 70 MeV/A Kr and 95 MeV/A Ar beams from RIKEN Ring Cyclotron (RRC) to private companies under fee-based utilization. The customers irradiate their samples in atmosphere with a beam of uniform flux distribution and specified LET. In order to address their requirements, we installed a dedicated irradiation setup at the E5A beam line with a pair of wobbler magnets, scatterer foil, and variable energy degrader.[1] The principle is the same as that for biological irradiation at RRC.[2] Here, we report the formation and characterization of the uniform beam-intensity distribution.

The ion beam experiences multiple scattering at the scatterer foil and its angular distribution has a Gaussian form. Accordingly, the lateral beam-intensity distribution at downstream has a Gaussian form $\exp(-d^2/\sigma^2)$, where d is the distance from the spot center, and the spot width σ is proportional to the distance from the foil. In addition, the wobbler magnets deflect the beam so that the beam center traces a circle, whose radius is denoted as R. Combining these effects, we can obtain a uniform dose distribution for the irradiation. According to the customers' requests, we aim at a uniform beam flux within 50-mm diameter at the irradiation position, approximately 4 m downstream from the scatterer. The dose at a distance r from the center of the circle is proportional to:

$$F(r) = \exp\left[-(r^2+R^2)/\sigma^2\right] \sum_{n=0}^{\infty} \frac{1}{(n!)^2} \left(\frac{Rr}{\sigma^2}\right)^{2n}. \quad (1)$$

The shape of $F(r)$ is determined by a parameter R/σ, and the intensity distribution is nearly uniform within radius R when $R/\sigma \gtrsim 1$.

We evaluated the effects of the scatterer and the wobbler magnets by measuring the lateral beam-flux distribution at the irradiation position. As the scatterer, we used a gold foil with a thickness of 73 μm for the Ar beam and 46 μm for the Kr beam. The beam-flux distribution was measured with a Si detector that moved across the beam in 5-mm steps on a motor-driven linear slider. The count rate of the Si detector at each position was normalized by the total flux counted by a plastic scintillator upstream. With the wobbler OFF, we obtained the width σ of the beam-spot distribution and with the wobbler ON, we evaluated the beam uniformity and compared it with Eq. 1.

Figure 1 shows the results for the Ar beam and Fig. 2 for the Kr beam. The dots denote the normalized count rate of the Si detector. The open dots are not included in the following analyses because they are out of the aperture at the beam extraction window that

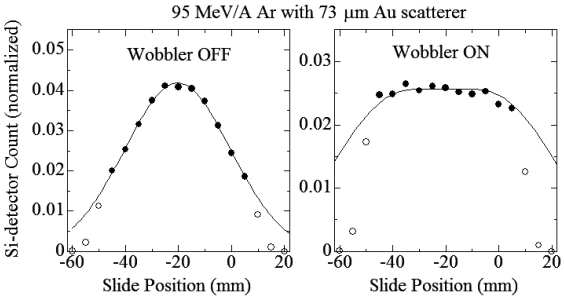

Fig. 1. Flux distribution of Ar beam without (left) and with (right) wobbler. The line in the graph on the left is the best-fit Gaussian function for the data of black dots, the line on the right is calculated using Eq. 1.

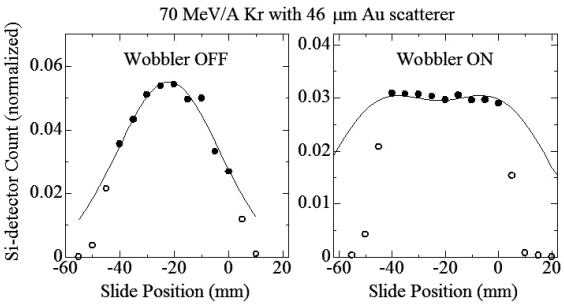

Fig. 2. Same as Fig. 1 for Kr beam.

was 60 mm ϕ for Ar and 50 mmϕ for Kr. The best-fit Gaussian functions to the measurements with the wobbler OFF, shown by lines in the left-hand side figures, give the beam-spot widths σ of 28.25 mm for the Ar beam and 26.5 mm for the Kr beam. With the wobbler ON, the beam-spot center drew a circle with a radius $R = 28.8$ mm for Ar ($R/\sigma = 1.02$) and 29 mm for Kr ($R/\sigma = 1.09$). The beam uniformity is within ± 10 % for Ar and ± 5 % for Kr within the aperture. The lines in the figures on the right-hand side show the calculation results using Eq. 1, which well reproduces the measurements.

The Bethe-Molière formula[3] of multiple scattering well reproduced the angular width of multiple scattering deduced from the measured σ, and it can be a useful guideline for heavier ions.

*1 RIKEN Nishina Center

References

1) T. Kambara and A. Yoshida, RIKEN Accel. Prog. Rep. **48**, 239 (2015).
2) T. Kanai et al., NIRS-M-91 (HIMAC-004), (1993).
3) H. A. Bethe, Phys. Rev. **89**, 1256 (1953).

Gamma-ray inspection of rotating object

T. Kambara,[*1] H. Haba,[*1] and A. Yoshida[*1]

We are developing a new method to determine the spatial distribution of positron-emitting RIs on a rotating object, based on the same working principle as medical PET systems, but simpler and less expensive. In the method called gamma-ray inspection of rotating object (GIRO), an object with positron-emitting sources continuously rotates and a couple of gamma-ray detectors move in parallel back and forth on either side of the object. The rate of simultaneous detection of two positron-annihilation gamma rays as a function of the detector position and orientation of the object yields a sinogram, from which the source distribution on the object is reconstructed by a maximum-likelihood expectation maximization (ML-EM) algorithm. The principle and some results of test measurements with a prototype instrument have been reported.[1,2] The instrument has since been modified so that the detectors move back and forth instead of the rotating object.

We used ^{22}Na sources for the test measurements: two point-like sources (1.55 and 64 kBq) and one with a two-dimensional RI distribution (149 kBq). Since we required more intense sources with more variety of activity-distribution patterns, we attempted to use new two-dimensional sources with ^{89}Zr nuclide ($T_{1/2}$=78 hours), which was produced by a ^{89}Y(d,2n)^{89}Zr reaction at the AVF cyclotron with a 24-MeV deuteron beam. We prepared a filter paper cut out to letters ("RIKEN RIBF" with a character height of 26 mm) and figures of a circle (60 mm ϕ), a square (40 mm × 40 mm), and a rectangle (30.5 mm × 83 mm), and dripped a hydrochloric acid solution of ^{89}Zr on them. The paper pieces were then dried and sealed between plastic sheets and used as sources for GIRO. GIRO was equipped with two NaI scintillation detectors with 6-mm wide and 3-cm thick vertical collimators. The object rotated at 150 rpm, and the linear motion of the detectors was 2-mm/step and 1 step/10s over a ±74-mm range. The source distributions were reconstructed from the sinograms by ML-EM,[3] and compared with those obtained by imaging plates.

Figure 1 shows an image of a composite of the square, rectangle, and circle. The average activity was approximately 1.17 MBq during the measurement time of 19.4 hours. The GIRO image (right) reproduces not only the shape of the source but also the gross pattern of the activity distribution on the source taken by an imaging plate (left). Figure 2 shows an image of the source cut out as letters. The average activity was approximately 1.15 MBq during the measurement of 16.8 hours. The letters are only roughly reproduced.

The present experiments show that GIRO can well reproduce the gross structure of the two-dimensional source distribution, but the reproduction of structures finer than the collimator width is difficult.

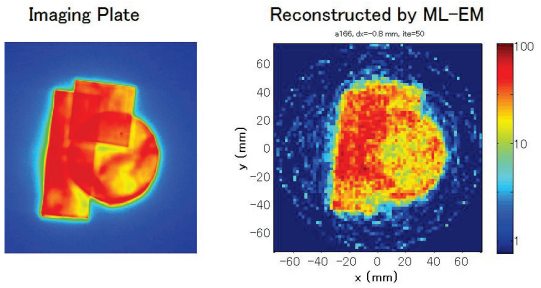

Fig. 1. Imaging plate (left) and image reconstructed from sinogram by GIRO (right) of a composite of figures.

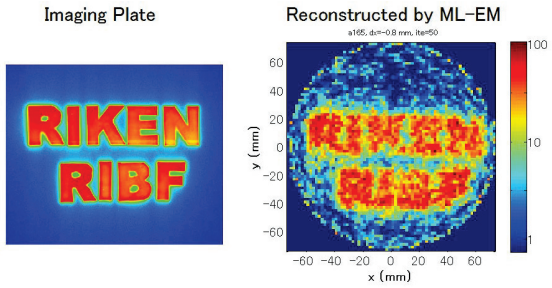

Fig. 2. Imaging plate (left) and image reconstructed from sinogram by GIRO (right) of letters.

References

1) T. Kambara, H. Takeichi, and A. Yoshida: RIKEN Accel. Prog. Rep. **47**, 216 (2014).
2) T. Kambara, A. Yoshida and H. Takeichi: Nucl. Instr. Meth. A **797**, 1 (2015).
3) H. Takeichi, T. Kambara, and A. Yoshida: RIKEN Accel. Prog. Rep. **47**, 217 (2014).

*1 RIKEN Nishina Center

Development of a new cluster reconstruction method for GEM Tracker for the J-PARC E16 experiment

W. Nakai,[*1,*2] for the J-PARC E16 Collaboration

The aim of the J-PARC E16 experiment[1)3)] is to measure the mass spectra of vector mesons in nuclear matter at J-PARC to study the origin of hadron mass.

We developed the Gas Electron Multiplier[2)] Tracker (GEM Tracker) for a tracking detector. In this paper, we present a new universal analysis method to handle the signals of the GEM Tracker for a wide incident angle.

The detector requires a position resolution of 100 μm up to an incident angle of 30 degrees under a high counting rate environment of up to 5 kHz/mm^2. The GEM Tracker consists of a drift cathode, triple-GEM stack, and readout strip board. We chose a strip pitch of 350 μm to achieve the required position resolution and a very thin drift gap of 3 mm in order to reduce the signal pile-up in a high counting rate. We will record waveforms of strip signals using a flash ADC and the sampling rate of the ADC is 40 MS/s. The dynamic range of the preamplifier is 0.1 pC, and the shaping time is 50 ns.

We already achieved the required position resolution at an incident angle of up to 30 degrees with two types of analysis methods. One of the following two types of analysis methods has to be chosen according to the incident angle; the center of gravity (COG) method for 0 degrees, and the timing method, which uses arrival times of signals on each strip, for 15 and 30 degrees[4)].

We developed a new universal method independent of the incident angle, which reconstructs charge clusters generated in the drift gap by fitting several waveforms of successive strips simultaneously (two-dimensional fitting). The fitting function is

$$F(x,t) = \sum_{i=1}^{N} q_i \times I(t - z_i/v_d) \times G(x - x_i; \sigma = 300\ \mu\mathrm{m}),$$

where q_i, x_i, and z_i are fit parameters, v_d is drift velocity, N is the number of charge clusters, I is an impulse response function of preamp, and G is a Gaussian. An example of the fitting is shown in Fig 1. Because of gaussian fitting for the x-direction, the horizontal positions of clusters can be derived with the same accuracy as the COG method. Because of fitting by the impulse response of the preamp for the t-direction, the arrival timing of clusters can be obtained with the same accuracy as the timing method. Therefore, it is expected that better or equal resolution can be achieved for all incident angles.

The test experiment using a 1.0 GeV/c pion beam was performed at the J-PARC K1.1BR beam line. The result is shown in Fig 2. Using the new method, the obtained position resolution improved for all incident angles and was 74 μm for the 30 degrees track.

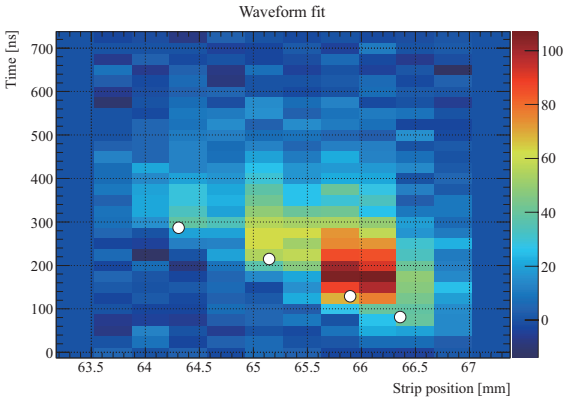

Fig. 1. Example of waveform fitting. Fitting results are indicated by white circles. Each white circle shows a cluster arrival timing and position.

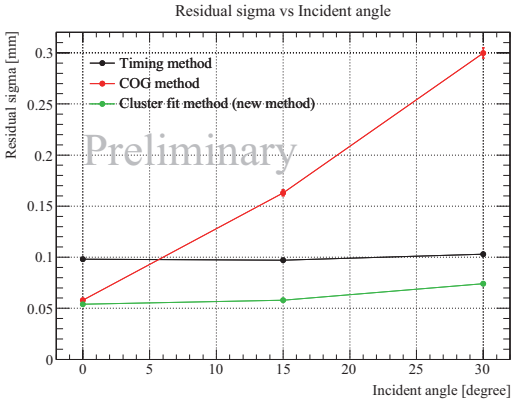

Fig. 2. Standard deviation of residual distribution as a function of incident angle. The black and red points have been reported in Ref. 4 and the green points are present study.

References

1) S. Yokkaichi et al.: in this report.
2) F. Sauli, Nucl. Instr. Meth. Phys. Res. A **386**, 531 (1997).
3) Y. Morino et al., JPS Conf. Proc. **8**, 022009 (2015).
4) Y. Komatsu et al., Nucl. Instr. Meth. Phys. Res. A **732**, 241-244 (2013).

*1 Department of Physics, The University of Tokyo
*2 RIKEN Nishina Center

Study of the effect of radiation damage on the quantum efficiency of a CsI photocathode

K. Kanno[*1,*2] for the J-PARC E16 Collaboration

We measured the effect of radiation damage on the quantum efficiency of a CsI photocathode. This study is of great importance for the performance of the J-PARC E16[1] hadron blind detector (HBD), which uses a CsI photocathode to detect Cherenkov photons produced by an incident electron in the CF_4 radiator. In the E16 experiment, the HBD is required to identify electrons with high efficiency in the high-rate neutron environment (<10 MeV, 3 kHz/cm^2). The radiation damage of a CsI photocathode caused by these neutrons will degrade the sensitivity of the photocathode to Cherenkov photons. This degradation of a photocathode decreases the electron detection efficiency of the HBD.

We performed a test experiment at the RIKEN AVF cyclotron to estimate the effect of the radiation damage on a CsI photocathode caused by a high-rate neutron environment. The radiation damage was evaluated by comparing the quantum efficiency before and after the experiment. In the experimental area, low-energy neutrons were produced by stopping an α-particle beam at 12.5 MeV/u from the cyclotron at a beam dump. A CsI photocathode contained in a prototype HBD was irradiated with these low-energy neutrons. It should be noted that the CsI photocathode was not directly irradiated with the α-particle beam. The photocathode was not exposed to air at all, because the water contaminant caused the CsI photocathode to change its composition and degraded the quantum efficiency.[2] The prototype was operated under CF_4 gas flow, and the water contaminant was monitored and maintained below 15 ppm, which ensured that the photocathode did not deteriorate at all owing to the water contaminant. The CsI photocathode was evaporated by Hamamatsu Photonics K.K. and the thickness was 300 nm. The neutron rate evaluated with a ^{3}He gas-filled neutron monitor in the area and a GEANT4 simulation was approximately 17 kHz/cm^2 (<10 MeV) at the position the prototype was located, which was higher than that of the E16 experiment by a factor of approximately six. The photocathode was irradiated for 35 h in total, and this duration corresponded to approximately nine days in the E16 experiment in terms of the total amount of neutrons.

The result is shown in Fig. 1. The top panel represents the quantum efficiency of the CsI photocathode before and after the irradiation. The bottom panel represents the systematic errors in the relative value of quantum efficiency. This systematic error arises from the calibration error of our quantum efficiency measurement system. Thus, the enhancement of the quantum efficiency after the irradiation over the wavelength of 120–200 nm is significant. Although we detected no changes in the CsI photocathode by visual inspection, this enhancement might be caused by the change in the surface structure of the photocathode by high-rate neutrons. The surface structure of a photocathode affects the photoelectron escape probability from the photocathode.[3] Even though further studies are required to understand this enhancement, this result ensures that the quantum efficiency does not decrease for at least nine days in the E16 experiment.

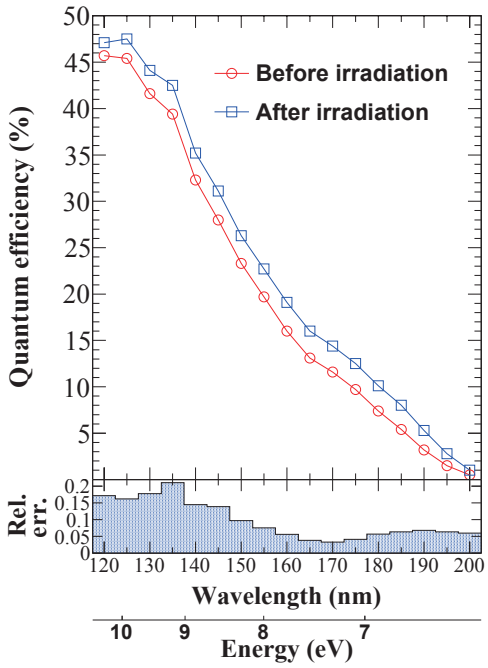

Fig. 1. Quantum efficiency of the photocathode (top panel) and its systematic error (bottom panel) as a function of wavelength and energy.

References

1) S. Yokkaichi *et al.*: in this report.
2) A. Breskin: Nucl. Instr. and Meth. A **371**, 116 (1996).
3) C. Lu, K. T. McDonald: Nucl. Instr. and Meth. A **343**, 135 (1994).

*1 RIKEN Nishina Center
*2 Department of Physics, Graduate School of Science, The University of Tokyo

Performance of the FVTX high-multiplicity trigger system for the RHIC-PHENIX experiment Run15

T. Nagashima[*1,*2] for the PHENIX collaboration

Protons and neutrons, which are components of familiar substances, are composed of quarks and gluons that bind quarks together. Immediately following the big bang, under extremely high-density and high-temperature conditions, quarks and gluons are considered to escape from the boundary of nucleons. This liquid-like state is called quark-gluon plasma (QGP).

Relativistic Heavy Ion Collider(RHIC) is the first accelerator aimed at investigating QGP. In particle angular correlations of generated particles in a Au+Au colliding system that was performed at RHIC until 2005, elliptic azimuthal anisotropy considered to be due to QGP was observed. Conventionally, QGP was considered to be observed only in nucleus+nucleus collisions because the energy density is not high enough in small colliding systems. However, several experiment groups at the LHC have recently reported that similar azimuthal anisotropy was observed in small colliding systems, such as p+p[1]. At RHIC, similar results have been observed in d+Au and 3He+Au collisions, but detailed investigation of p+p collisions has not been done so far.

The PHENIX experiment group introduced a new high-multiplicity trigger system using the Forward Silicon Vertex Detector (FVTX) for observation of the elliptic azimuthal anisotropy in the p+p colliding system in RHIC. The trigger signal is generated based on the number of tracks detected in the FVTX detector. The FVTX trigger was operated using the AND/OR operations of south and north trigger signals in Run15 p+p collision. The trigger was commissioned at the beginning of Run15 and started recording physics data by March 2015. Figure 1 shows the integrated triggered events in the p+p collision plotted as a function of the run number. The trigger accumulated 500M events in p+p collisions.

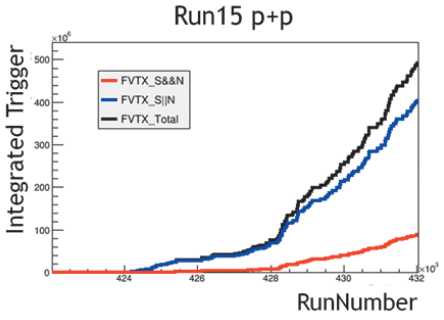

Fig. 1. FVTX trigger statistics. Red : South AND North. Blue : South OR North. Black : Sum of AND and OR.

Figure 2 shows the distribution of the number of tracks detected in the FVTX with a normalized scale on a vertical axis. Compared to the minimum bias trigger, the FVTX trigger shows a higher average number of tracks. Especially in the high-multiplicity region, the FVTX trigger have more statistics by a factor of 100.

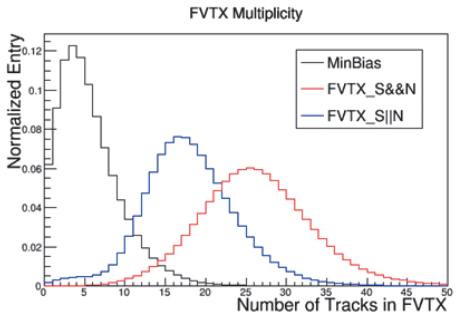

Fig. 2. Distribution of number of FVTX tracks for each trigger.

The stability of the trigger is evaluated in Figure 3 by correlating the average number of tracks in FVTX as a function of the run number. The trigger was operated in different multiplicity trigger thresholds, which caused variations in the average in earlier runs in the plots. There are significantly lower average runs, which appeared discretely. They cannot be explained by the change of the above mentioned trigger condition and the reason of this behavior is under investigation.

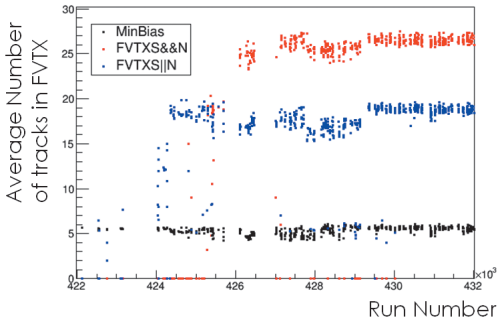

Fig. 3. Average number of tracks as a function of run number.

The FVTX triggered samples will be used for two-particle correlation analysis, one of the methods used to study the anisotropy of the generated matter from collision. The analysis of multiplicity dependence in Run15 p+p collision is underway.

Reference

1) V. Khachatryan et al.: CMS Collaboration, JHEP 1009 091 (2010)

*1 RIKEN Nishina Center
*2 Department of Physics, Rikkyo University

R&D of silicon strip detector for the sPHENIX tracker

G. Mitsuka,[*1] Y. Akiba,[*1] and I. Nakagawa[*1]

The sPHENIX detector is a major upgrade to the PHENIX detector at the Relativistic Heavy Ion Collider (RHIC) at Brookhaven National Laboratory (BNL) and is designed for exploring a vast range of physics areas including heavy quarkonia suppression via the three ϒ states and tagging of charm and beauty jets[1]. A precision tracking detector inside the 1.5 T BaBar superconducting solenoid, as well as a silicon vertex detector currently operated in PHENIX, play a crucial role in reducing fake track contributions and improving the momentum resolution, leading to the separation of the three ϒ states and to the separation of charm and bottom quarks[2]. In this report, we will discuss the design, technology choices, and R&D status of the prototype sPHENIX silicon tracker with a special emphasis on the high-density integrated (HDI) circuit and modularized silicon sensors.

The HDI circuit connects the readout chips to the downstream frontend boards, and custom 128-channel front-end ASIC 'FPHX'[3] chips are planned. The design of the HDI has taken into account (1) the effects of both common-mode and differential-mode noise, (2) the desire to minimize the geometrical size, and (3) the desire to limit the material budget. For the first point, the HDI design for the silicon tracker follows the PHENIX-FVTX design that is coupled to the FPHX chips and copes with the effects of both common-mode and differential-mode noise by surrounding the signal layers by the grounding layers[4]. The second point is very important for the silicon tracker S0 and S1 stations (see the other Reports[2] for details), as they must be made compact for installation in a tiny space relative to the S2 station. The third point is especially important for the S1 station, where the effects of multiple scattering are most significant and thus may cause poor momentum resolution.

Considering the requirements listed above, we started the HDI R&D by placing a higher priority on the S0 and S1 stations compared with the S2 station. The current design of the HDI for the S1 station has seven layers of flexible printed circuits and has dimensions of 28 mm (W) × 500 m (H). The length of the HDI in the beam direction varies from 10 cm to 40 cm. The size of the HDI is well below the geometrical requirements. The prototype HDI has a thickness of approximately 0.5 % of a radiation length on average. The seven layers of flexible printed circuits have been designed with a special emphasis on the reduction of any unwanted microstrip antenna and on good impedance matching even at a distance of ∼ 40 cm from the FPHX chip. The prototype HDIs for the S1 station will be produced by Yamashita Materials Corporation and will be ready for further assembly in early 2016. Figure 1 shows the layout of the HDIs for the S1 station.

One silicon sensor, two HDIs with ten FPHX chips for each, and one CFRP support frame are assembled into a silicon sensor module as shown in Fig. 2. Because of the readout structure of the silicon sensors, the HDIs are glued onto both ends of the silicon sensors. In order to reduce the amount of material used, the two HDIs are completely separated and not connected.

In the assembly, the bonding of the FPHX chips to the silicon sensor and their attachment to the two HDIs are being performed as well. Hayashi watch-works Co., Ltd, which has experience producing the PHENIX VTX pixel detectors, will be employed for the assembly of the prototype module.

The first prototype module for the S1 station will be tested at RIKEN and BNL. The sPHENIX silicon outer tracker uses essentially the same electronics as the PHENIX FVTX detector, namely the FPHX chip and frontend circuits. The test bench at RIKEN that was originally set up for the high-multiplicity trigger development for the FVTX detectors can be applied again to test prototype sensor modules, with minor modifications in the readout configuration. The test is planned for 2016 spring and summer.

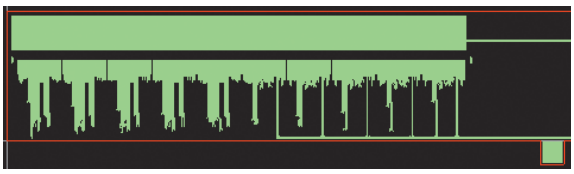

Fig. 1. Layout of the HDIs for the S1 station. The green area indicates the analog and digital circuits.

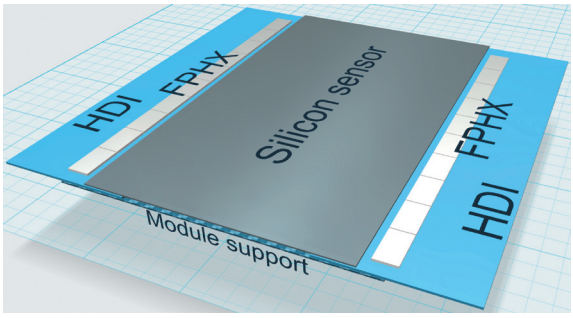

Fig. 2. CAD drawing for the silicon sensor module for the S1 station.

*1 RIKEN Nishina Center

References
1) A. Adare et al., arXiv:1501.06197.
2) Y. Akiba, G. Mitsuka, and I. Nakagawa, In this report; I. Nakagawa, Y. Akiba, and G. Mitsuka, In this report.
3) J. R. Hoff, T. N. Zimmerman, R. J. Yarema, J. S. Kapustinsky and M. L. Brookes, Nuclear Science Symposium Conference Record (NSS/MIC), 2009 IEEE, 75–79 (2009).
4) C. Aidala et al., Nucl. Instrum Methods A 755, 44–61 (2014).

Development of sensor prototype for sPHENIX Silicon Tracker

Y. Akiba,[*1] I. Nakagawa,[*1] and G. Mitsuka[*1]

sPHENIX is a new detector at RHIC[1], which will be used for measuring jets, direct photons and Upsilon. The detector has electronmagnetic and hadronic calorimeters to measure jets and a high precision tracker. The tracker is contained inside a 1.5 T superconducting solenoid which was previously used for Babar experiment at SLAC.

We aim to construct a large silicon tracker for sPHENIX[2] and are working on the research and development of the silicon detector. The tracker consists of three tracking stations (from inner to the outer, called S0, S1 and S2) covering $-1 < \eta < 1$ and $\Delta\phi = 2\pi$.

The basic building block of the silicon tracker is a sensor module, which consists of a sensor, two High Density Interconnects (HDIs) for read-out, and mechanical support. We are currently developing a prototype of the silicon module used for the S1 layer. In this paper we report the status of a prototype silicon strip sensor for the S1 silicon module. The status of HDI is reported by another paper[3].

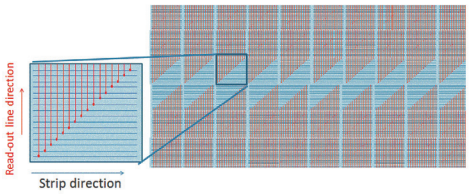

Fig. 1. Conceptual design of the S1 strip sensor.

Figure 1 illustrates the conceptual design of the S1 sensor. The sensor is a single sided, AC coupled sensor. The active area of the sensor, 96 mm (z) × 45.5 mm (ϕ), is divided into 10 × 6 blocks. Each block has 128 short strips that are 58 μm in pitch and 9.6 mm long, and run parallel to the z (beam) direction. In Fig. 1, the strip runs horizontally. The read-out lines of the strips, indicated by red lines in the figure, run perpendicular to the strips and bring the signals to the read-out chips placed at the upper and the lower edge of the sensor. The upper and the lower 3 blocks are connected upwards and downwards, respectively. This arrangement reduces the channel count to save the cost of the detector. Although signals in the 3 strips are combined and cannot be distinguished in the read-out chip, the offline track reconstruction program should distinguish the correct hit strip by requiring a good χ^2 for tracks fitted to all layers simultaneously. The probability of misidentifying the hit strip is low owing to the expected low channel occupancy. The occupancy is $\simeq 0.2\%$ even in central Au+Au collisions.

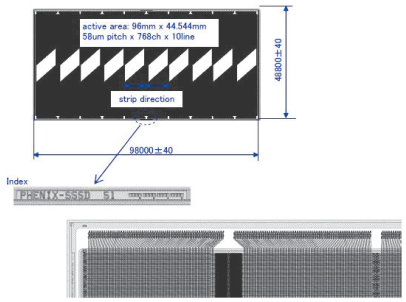

Fig. 2. A drawing of the S1 prototype sensor.

FPHX chip, which is used for FVTX silicon detector of PHENIX, is utilized to read-out the sensor. The read-out pad pitch of the sensor is thus matched to that of FPHX chip (75 μm). FPHX chip has low power consumption, about 64 mW per chip, which reduces the need for cooling for the sensor module. A FPHX chip has 128 ch and is used to read-out 3 blocks that are combined together. A total of 20 FPHX chips, 10 at the upper edge and 10 at the lower edge, are used to read-out one sensor.

The sensor will be manufactured by Hamamatsu Photonics Co. (HPK). Figure 2 is a part of a design drawing of the sensor made by HPK. Two sensors will be fabricated on one 6-inch wafer. The size of the sensor is maximized to fabricate two sensors on a 6-inch wafer.

We will produce two types of sensors in the same design. One is 320-μm thick, which is the standard thickness of wafers that HPK uses. The other one is 240-μm thick, which is made by thinining the 320 μm sensor. The thinner sensor results in lower scattering of charged particle and thus improve the momentum resolution of tracks. However, the signal generated by a hit will be reduced. We will evaluate the S/N ratio for MIP particles for both types of sensors to determine which one we will use for the production.

The design of the sensor at HPK has been complete and they are manufacturing the sensors. We expect the delivery of the sensors by early 2016.

References

1) sPHENIX preliminary Conceptual Design Report (2015).
2) I. Nakagawa, in this report.
3) G. Mitsuka, in this report.

*1 RIKEN Nishina Center

Implementation of the TDC function in the GTO

T. Yoshida,[*1] H. Baba[*2] and K. Ieki[*1]

The field-programmable gate array (FPGA) has become a popular device and has been widely adopted for physics measurements[1] in recent years. An FPGA-based NIM logic module has been developed[2] called a Generic Trigger Operator (GTO). Advanced logic circuits have successfully been introduced in the GTO[3,4]. The present article describes the implementation of the time-to-digital converter (TDC) function in the GTO.

There are several attempts to develop the TDC function in FPGAs[5,6]. The conversion time of a conventional TDC is typically 10–100 μs, while that of an FPGA-based TDC is only tens of nanoseconds. The block diagram of the TDC function in an FPGA is shown in Fig. 1. The shaded triangles are delay units. FF denotes to the flip-flop component. The coarse timing value is obtained using the global clock. When a 50-MHz clock is applied, the coarse timing value will be a 20-ns step. To obtain the fine timing value beyond the clock frequency, the tapped delay line (the cascade chain of the delay units in Fig. 1) and FF array are used. An input signal is delivered to the FF components whenever the signal passes through the delay units. The value of the FF array is latched by the global clock which achieves mostly equal-length wiring. The encoder seeks transitions of "0→1" and "1→0" in the FF array. The former transition corresponds to the leading edge of the input signal, and the latter one is the trailing edge. Thus, this TDC is capable of measuring both the edges of the signal at the same time. In this work, the look-up-table (LUT) and the carry-logic (CL) components are adopted as a delay unit. These are called as LUT-DL TDC and CL-DL TDC, respectively. The LUT-DL TDC uses 45 LUT components and a 50-MHz global clock. The CL-DL TDC consists of 113 CL components and a 162.5-MHz global clock. The conversion times are 40 ns (2 global clocks) for the LUT-DL TDC and 18.5 ns (3 global clocks) for the CL-DL TDC.

The differential non-linearity (DNL) has been measured to investigate the performance of the developed TDC function. The linearity of the coarse timing is quite good as the global clock is generated from the quartz resonator that has a frequency stability of 10^{-6}. However, the linearity of the fine timing depends on the variation of the propagation delay of the LUT/CL components and the wiring length in the FPGA. Figure 2 shows the result of the DNL measurement for the fine timing. The measurement method is the same as that in Ref. 6. The least significant bit (LSB) of the LUT-DL TDC and CL-DL TDC is 446 ps and 54.6 ps, respectively. The bin number corresponds to the n-th LUT/CL components. The LUT-DL TDC has a good performance because the DNL is much less than 1 LSB in any bin. However, some bins of the CL-DL TDC reach ±1 LSB, which implies there are missing values in the converted result. This DNL for the CL-DL TDC may be improved by fine tuning the wiring length in the FPGA.

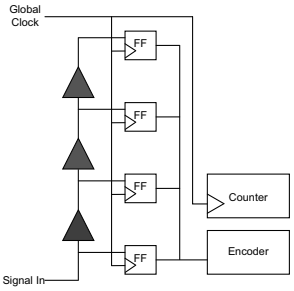

Fig. 1. Block diagram of TDC in the GTO.

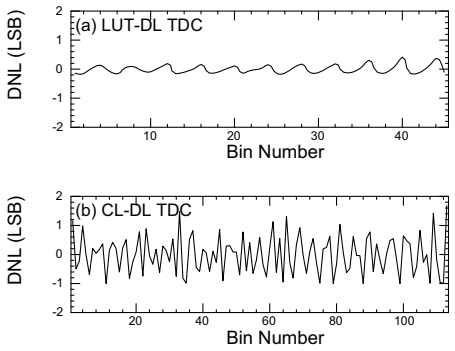

Fig. 2. The differential non-linearity of the developed TDC.

Two types of TDC functions have successfully been introduced in the GTO. Its conversion time is very fast and the linearity is reasonable. Based on this result, the particle-identified trigger for future BigRIPS experiments will be established by analyzing the time-of-flight, position and delta-E information in the GTO.

*1 Department of Physics, Rikkyo University
*2 RIKEN Nishina Center

References

1) H. Sadrozinski and J. Wu : Applications of Field-Programmable Gate Arrays in Scientific Research (CRC Press, 2011).
2) H. Baba et al.: RIKEN Acc. Prog. Rep. **46**, 213 (2013).
3) H. Baba et al.: RIKEN Acc. Prog. Rep. **47**, 235 (2014).
4) H. Baba et al.: In this report.
5) J. Wu and Z. Shi : 2008 IEEE Nuclear Science Symposium Conference Record, (2008) p. 19.
6) X. Qin et al.: IEEE Trans. Nucl. Sci. **60**, 3550 (2013).

New functions in Generic Trigger Operator

H. Baba,[*1] T. Ichihara,[*1] T. Isobe,[*1] T. Ohnishi,[*1] K. Yoshida,[*1] Y. Watanabe,[*1] S. Ota,[*2] S. Shimoura,[*2] S. Takeuchi,[*3] and Y. Togano[*3]

The Generic Trigger Operator (GTO) module[1] is a field-programmable gate array (FPGA)-based NIM logic module. Common trigger firmware[2] manages trigger generation to ensure event synchronization between multiple CAMAC and VME front-end systems. GTO modules implementing this firmware are permanently installed at experiments of BigRIPS, SHARAQ, EURICA, SUNFLOWER, SAMURAI, and R3. Recently, advanced functions of scaler, gate-and-delay generator (GG) and selector have been developed for GTO. Here, we report these new functions.

Scaler

The scaler function has been introduced in the GTO module. Scaler values can be readout via the Ethernet. The functionality of the scaler firmware is as follows.

- 20-channel scaler inputs : Each scaler has a 32-bit counter depth.
- Gate input : When the gate input function is enabled, scaler circuits count up only when the gate signal is issued.
- Veto input : Inhibit counting.
- Read latch input : The readout value is held by the read latch signal. Scaler circuits are still operational even if the read latch is issued.
- Clear input : Clear the scaler values to zero.

As additional functions, 1-Hz/1-kHz/10-kHz clock signals and level/pulse signals can be output.

Gate-and-Delay Generator

The firmware of the 4-channel GG has been developed. Two different GG functions are introduced: clock-asynchronous and clock-synchronous GG. The clock-asynchronous GG is based on the D-Flip Flop delay chain (details are described in Ref. 1). The gate and delay circuits are driven according to the leading edge of the input signal. The clock-synchronous GG is implemented by simply counting up the clock signal. In this case, input signals are synchronized by the internal clock. The specification of each GG function is described bellow.

- clock-asynchronous GG
  - Gate-width range : T_{wid} = 51 ns to 2.6 ms.
  - Delay range : T_{dl} = 51 ns to 2.6 ms.
  - Minimum step of T_{wid} and T_{dl} : 1.2 ns.
  - Timing jitter : $\sigma \simeq T_{dl} \times 10^{-4}$.

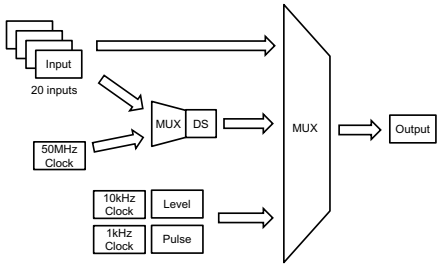

Fig. 1. Functional diagram of the selector firmware

- clock-synchronous GG
  - Clock interval : T_{int} = 20 ns to 10 μs.
  - Gate-width range : T_{wid} = 20 ns to 171 s.
  - Delay range : T_{dl} = 20 ns to 171 s.
  - Timing jitter : $\sigma = T_{int}/2\sqrt{3}$.

In the case of the clock-synchronous GG, the clock signal is variable. The minimum clock interval (T_{int}) is 20 ns, which originates from a 50-MHz crystal resonator. This clock can be divided into 1/1 to 1/256 frequency in FPGA. Thus, the clock interval is varied between 20 ns and 10 μs. The timing jitter of the output signal in clock-synchronous GG depends on T_{int} because deterministic jitter is generated when the input signal is synchronized by the clock. On the other hand, the timing jitter in clock-asynchronous GG is a random jitter.

Selector

A selector firmware has been developed to remotely switch signal sources. The functional diagram is shown in Fig. 1. There are 8 output channels. Each output channel can be chosen from signal sources by the multiplexer (MUX) circuit. The signal sources of the 20 inputs, down scaler (DS), 1k/10k-Hz clock, pulse, and level signals are available. Input signals and 50-MHz clock signals can be decimated using the DS circuit: this function is the so-called rate divider or down scaler.

These new functions implemented as firmware are utilized in RIBF experiments. In addition, the development of the time-to-digital converter (TDC) in the GTO is examined. The details of the TDC firmware are described in Ref 3.

*1 RIKEN Nishina Center
*2 Center for Nuclear Study, University of Tokyo
*3 Department of Physics, Tokyo Institute of Technology

References
1) H. Baba et al.: RIKEN Acc. Prog. Rep. **46**, 213 (2013).
2) H. Baba et al.: RIKEN Acc. Prog. Rep. **47**, 235 (2014).
3) T. Yoshida et al.: In this report.

Upgrade of trigger circuits and DAQ modules for SAMURAI

Y. Togano,[*1,*2] T. Isobe,[*2] H. Baba,[*2] J. Tsubota,[*1,*2] S. Araki,[*3] S. Kawase,[*3] Y. Kondo,[*1,*2] S. Takeuchi,[*1,*2] and H. Otsu[*2]

Many kinds and a large number of detectors are employed in experiments with SAMURAI. Users often need many complex triggers by using many kinds of detectors to select a certain reaction channel. In addition, the trigger rate is often as high as 2 kHz. To cope with such increased number of triggers and higher trigger rate, the circuits and modules for the data acquisition system (DAQ)[1] were upgraded, which consisted of two parts, introduction of a trigger selection module and installation of new modules to shorten the dead time of the DAQ system. This paper reports on these two upgrades.

For experiments at SAMURAI, the four trigger inputs of the normal GTO module[2] is often not enough. Therefore the trigger selector GTO[3] was newly introduced. Figure 1 shows the diagram of the new trigger circuits for SAMURAI. The trigger selector GTO named as sdgto02 can input 16 triggers and can output downscaled individual triggers and "or" of them. The output from sdgto02 coincides with the "Beam" trigger generated from F13 plastics, and then vetoed by the busy signal and SSM (bit signal to synchronize circuits with DAQ start/stop) from the normal GTO module named as sdgto01. The accepted trigger is distributed to all DAQ branches of the SAMURAI DAQ system. This circuit configuration was used for the SAMURAI21 experiment[4].

The SAMURAI DAQ system consists of many DAQ branches such as B3F, BDC, FDC1, FDC2-1, FDC2-2, NEBULA, and HODF. The details of the SAMURAI DAQ system can be found in Ref. 1. The B3F branch accumulates information from beam-line plastics and triggers. The BDC branch is used to accumulate data from BDC1, BDC2, and ICB. The FDC1, FDC2-1, and FDC2-2 branches are for drift chambers. The data from FDC2 are processed by using two DAQ branches, FDC2-1 and FDC2-2, to cope with the large number of channel of FDC2. The NEBULA branch is for the neutron detector NEBULA. The HODF branch is used to accumulate data from HODF (+ICF and TED, depending on experiments).

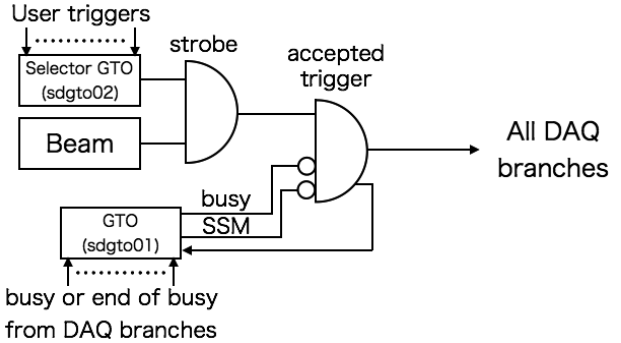

Fig. 1. Diagram of new trigger circuits of SAMURAI.

Table 1. Summary of typical dead time of the DAQ branches in SAMURAI21 and DAY-ONE experiments.

	SAMURAI21 [μs]	DAY-ONE [μs]
B3F	145	360
FDC1	180	170
FDC2-1	210	270
FDC2-2	180	220

To shorten the dead time of the DAQ system[1], we upgraded the system for the B3F branch and changed the VME controller for the FDC1, FDC2-1, and FDC2-2 branches. The B3F branch is replaced by a VME-based system from a CAMAC-based system. The new VME-based system contains TDC (MTDC32 from Mesytec GmbH), QDC (MQDC32 from Mesytec GmbH), two scalers (SIS3820 from SIS GmbH), and a interrupt register (RPV-130 from Repic Co.). The VME controllers for the FDC1, FDC2-1, and FDC2-2 branches are replaced from SBS-620 (SBS Technologies) to V7768 (Abaco systems).

Table 1 summarizes the typical dead time of DAQ branches in SAMURAI21 experiment and SAMURAI DAY-ONE experiment. For the B3F branch, the dead time was 145 μs, much shorter than that of the previous system (360 μs) in the SAMURAI DAY-ONE experiment[5]. For FDC2-1 and FDC2-2, the dead time in SAMURAI21 was $\sim$20% shorter than those in the DAY-ONE experiment. The time resolution of the F13 plastics with the new VME system was obtained to be about 46 ps for the SAMURAI21 experiment, showing that the performance of the VME crate is enough for SAMURAI.

With these upgraded DAQ branches, the live time in the SAMURAI21 experiment was 75% for 1.1 kHz triggers. The bottleneck of the dead time is BDC, which had 240 μs dead time in the SAMURAI21 experiment, which can be improved by replacing the VME controller to V7768.

*1 Department of Physics, Tokyo Institute of Technology
*2 RIKEN Nishina Center
*3 Faculty of Engineering Sciences, Kyusyu University

References

1) H. Otsu et al.: RIKEN Accel. Prog. Rep. **46**, 146 (2013).
2) H. Baba et al.: RIKEN Accel. Prog. Rep. **47**, 235 (2014).
3) H. Baba et al.: In this report.
4) Y. Kondo et al.: In this report.
5) T. Kobayashi et al.: Nucl. Instrum. Meth. B **317**, 294 (2013).

Tests of the Advanced Implantation Detector Array (AIDA) at RIBF

C.J. Griffin,[*1] T. Davinson,[*1] A. Estrade,[*1] D. Braga,[*2] I. Burrows,[*3] P. Coleman-Smith,[*3] T. Grahn,[*4] A. Grant,[*3] L.J. Harkness-Brennan,[*4] G. Kiss,[*5] M. Kogimtzis,[*3] I. Lazarus,[*3] S. Letts,[*3] Z. Liu,[*1] G. Lorusso,[*5] K. Matsui,[*5,*6] S, Nishimura,[*5] R.D. Page,[*4] V. Phong,[*5] M. Prydderch,[*2] V. Pucknell,[*3] S. Rinta-Antila,[*4] O. Roberts,[*7] D. Seddon,[*4] J. Simpson,[*3] J. Strachan,[*3] S.L. Thomas[*2] and P.J. Woods[*1]

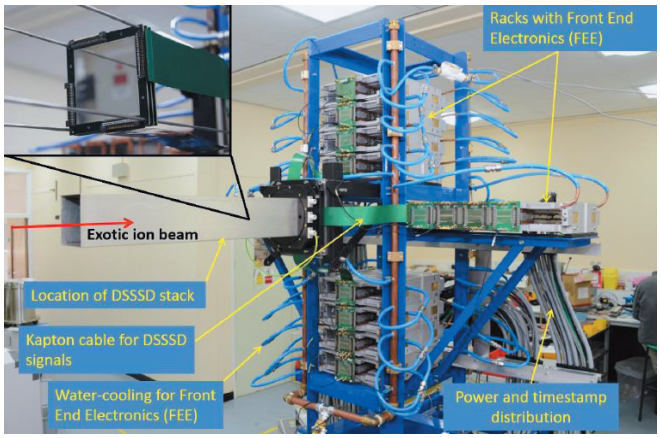

Fig. 1: A photograph of the fully constructed AIDA assembly.

The Advanced Implantation Detector Array (AIDA)[1] represents the latest generation of silicon implantation detectors for use in decay spectroscopy measurements of exotic nuclei at fragmentation beam facilities.

Designed to improve upon current generation, AIDA features high detector pixilation and fast overload recovery (~1 μs), required at modern RI facilities with increasingly high secondary beam intensity and access to isotopes with very short half-lives.

Application specific integrated circuits (ASICs)[2] were specifically designed to meet the above requirements. One ASIC can process 16 data channels, each with two dedicated preamplifiers: one, with selectable gain to cover the low and medium energy ranges of up to 1 GeV, and the other, a low-gain amplifier covering the full dynamic range of 20 GeV. Detector signals are carried via flexible Kapton PCBs to the front end electronics (FEE) cards, which support 64 channels of instrumentation. The FEE cards contain: multiple analogue-to-digital converters (ADCs) for use in signal processing; a field-programmable gate array (FPGA) for control, signal processing and data management; and additional supporting electronics.

As each FEE card runs a separate data acquisition system (DAQ), reading data from just 64 channels, dead-time is vastly reduced compared to current generation detectors dealing with high pixelation. Fig. 1 shows the full AIDA assembly.

To study the response of AIDA to implantation of heavy ions, in-beam tests have been conducted at the Radioactive Ion Beam Factory (RIBF) at RIKEN. The tests were conducted parasitically to experiments part of the SEASTAR campaign, placing AIDA at the F11 focal plane. In the most recent test configuration, AIDA comprised three MSL BB18-1000 type DSSSDs, each with a thickness of 1 mm and featuring 128 strips with a 0.625 mm pitch in both the x and y directions.

These tests have demonstrated both the capability of AIDA to detect position and energy of fast fragment beams and their decay products, as well as our ability to integrate multiple DAQs – AIDA, and the BigRIPS in-beam detectors for particle identification – into one data stream. DAQ integration is achieved through the timestamping of all data items in each data stream, which are then time-ordered in the analysis software. This forms one continuous stream of data containing information on the implant positions, decay positions and energies, and particle identification data from BigRIPS. A method has also been developed by which the BRIKEN/AIDA DAQs can be synchronised, which will be tested with the full-scale BRIKEN array once it has been assembled. In addition to this, an online monitor has been developed to check the status of the DAQ synchronisation and to provide some basic analysis in real-time.

Preliminary analysis of the data collected during these tests is underway, from which we hope to see some early results in the near future. Further steps must still be taken to better understand the efficiency of the analysis software in correlating implants and decays, and in characterising the background to reduce the likelihood of random correlations. With promising progress being made on all fronts, AIDA is planned for use at RIBF throughout 2016-2017 with two main focuses: β-decay half-life and decay spectroscopy measurements with the EURICA γ-ray detector, and measurements of β-delayed neutron emission probabilities as part of the BRIKEN collaboration.

[*1] School of Physics and Astronomy, University of Edinburgh
[*2] STFC Rutherford Appleton Laboratory
[*3] STFC Daresbury Laboratory
[*4] School of Physical Sciences, University of Liverpool
[*5] RIKEN Nishina Centre
[*6] Department of Physics, University of Tokyo
[*7] School of Engineering and Mathematics, University of Brighton

References

1) C.J. Griffin, T. Davinson, A Estrade et al., POS(NIC XIII) 097 2014
2) D. Braga, P. J. Coleman-Smith, T. Davinson, I. H. Lazarus, R. Page, and S. Thomas in ANIMMA 2nd International Conference, IEEE, 2011.

CCJ operations in 2015

S. Yokkaichi,[*1] H. En'yo,[*1] T. Ichihara,[*1] and Y. Watanabe[*1]

1 Overview

The RIKEN Computing Center in Japan (CCJ)[1] commenced operations in June 2000 as the largest offsite computing center for the PHENIX[2] experiment being conducted at the RHIC.Since then, the CCJ has been providing numerous services as a regional computing center in Asia. We have transferred several hundred TBs of raw data files and nDST [a] files from the RHIC Computing Facility (RCF)[3] to the CCJ. A joint operation of the CCJ with the RIKEN Integrated Cluster of Clusters (RICC)x has been continuing since July 2009. In April 2015, a new system "HOKUSAI Greatwave" was launched by RIKEN ACCC[4] and the joint operation is successful. New hierarchical archive system and dedicated PC nodes are provided to CCJ by them. The number of dedicated PC nodes is reduced from 20 to 10 in this April.

Many analysis and simulation projects are being carried out at the CCJ, and these projects are listed on the web page `http://ccjsun.riken.go.jp/ccj/proposals/`. As of December 2015, CCJ has contributed 31 published papers and 41 doctoral theses.

2 Computing hardware and software

In 2015, computing hardware (nodes and RAIDs) and software (OS, batch queuing systems, database engine, and so on) were changed slightly from those described in the previous APR.[1] In summary, we have 28 computing nodes, two login servers, one main server (users home directory, NIS, DNS, NTP), two disk servers, and 10 computing nodes in the ACCC computing room. In total, 422 (= 384 + 72) jobs can be processed simultaneously by these computing nodes.

Table 1 lists the numbers of malfunctioning SATA or SAS disks in the HP servers, namely, computing nodes and NFS/AFS servers.

Table 1. Number of malfunctioning HDDs in 2011-2015

Type	Size	Total	2015	14	13	12	11
SATA	1 TB	192	14	11	16	20	9
	2 TB	120	10	0	2	5	4
SAS	146 GB	38	3	2	0	1	1
	300 GB	24	1	1	0	0	1

One database (postgreSQL[5]) server and one AFS[6] server are operated in order to share the PHENIX computing environment. Now only the SL5[7] environment is shared by the computing nodes, which have approximately 0.9 TB of library files. We have two data-transfer servers on which the grid environment[9] is installed for the data transfer to/from RCF. Two other servers were retired in Jan. 2015 and reserved.

New NFS server HP DL380eGen8 and Infortrend 16TB SAS RAID, which serve user home areas were purchased in Mar. and Apr. 2015, respectively, and deployed in Oct. 2015, in place of SUN M4000. The xfs[8] is used as the home and work area served by the server.

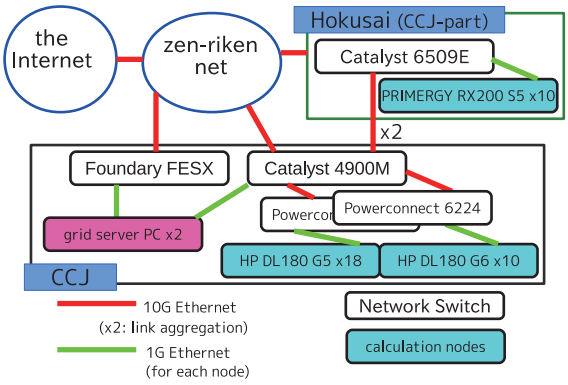

Fig. 1. Schematic view of the network configuration as of December 2015.

The High Performance Storage System (HPSS)[10] that had been in use for 15 years, was retired in Aug. 2015 and 863 TB (785 TiB) of data accounting for 1.66 million files were migrated to the new archive system in HOKUSAI. At the same time, network connection was changed. Between CCJ main switch and HOKUSAI, two 10G Ethernet are used. Toward outside RIKEN, one 10G is used between the main switch and the zen-riken net. Another 10G line of our grid server for the data transfer between RCF has also been retained.

Batteries of three 10KVA UPS were replaced in Mar. 2016. The main network switch will also be replaced in Jun. 2016.

[*1] RIKEN Nishina Center

[a] term for a type of summary data files in PHENIX

References

1) S. Yokkaichi et al.: RIKEN Accel. Prog. Rep. **48**, 248 (2015).
2) `http://www.phenix.bnl.gov/`
3) `https://www.racf.bnl.gov/`
4) `http://accc.riken.jp/`
5) `http://www.postgresql.org/`
6) `http://www.openafs.org/`
7) `http://www.scientificlinux.org/`
8) `http://xfs.org/`
9) `http://www.globus.org/toolkit/docs/latest-stable/gridftp/`
10) `http://www.hpss-collaboration.org/`

Computing and network environment at the RIKEN Nishina Center

T. Ichihara,[*1] Y. Watanabe,[*1] and H. Baba[*1]

We are operating Linux/Unix NIS/NFS cluster systems[1,2] at the RIKEN Nishina Center (RNC).

Figure 1 shows the current configuration of the Linux/Unix servers at the RNC. We have adopted Scientific Linux (SL), which is a clone of Red Hat Enterprise Linux (RHEL), as the operation system.

The host *RIBF.RIKEN.JP* is used as the mail server, NFS server of the user home directory /rarf/u/, and the NIS master server. This is the core server for the RIBF Linux/Unix cluster with approximately 600 registered user accounts. The hosts *RIBF00/RIBF01* are used as SSH login servers to provide access to external users, and as general-purpose computational servers and gateways to the RIBF intranet.

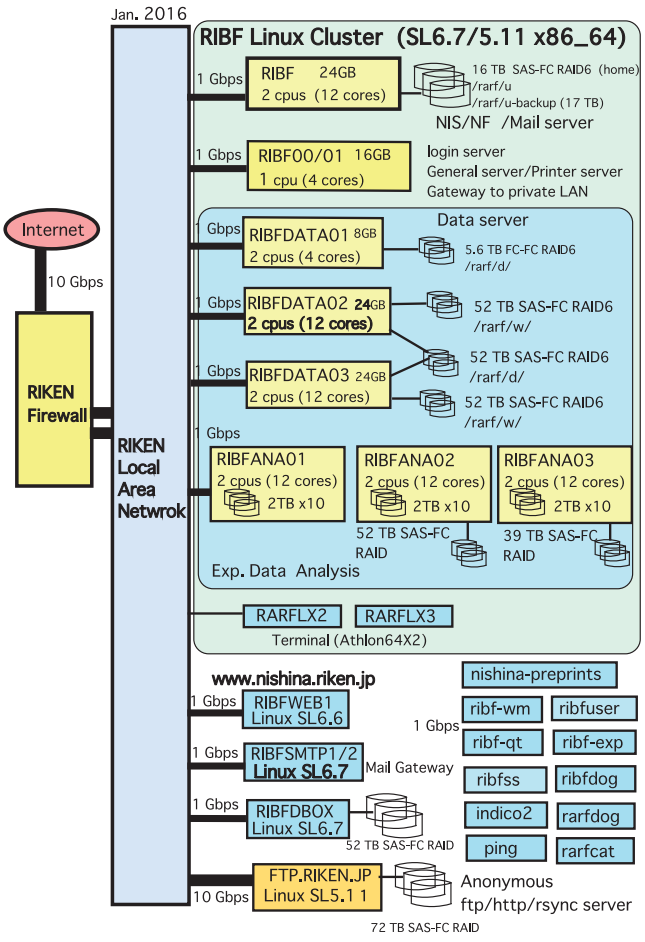

Fig. 1. Configuration of the RIBF Linux cluster.

A research record server *RIBFDBOX* was installed, and is started operation in April 2015. This server consists of an HP DL-320e server, a 52 TB SAS RAID6 system, and Proself 4 software. All of the experiment data, except for the large volume of raw data of RIBF experiments, were recorded to this research record server. The 52 TB storage system was divided into two partitions of 26 TB each. One is used for the data storage area of the experiment record and the other is used for the backup of the data.

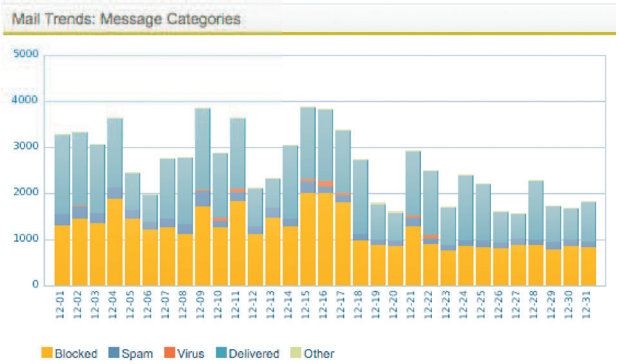

Fig. 2. Mail Trends:Message categories in Dec. 2016

A new streaming server *RIBFSS* was installed to replace the previous streaming server. Wowza Streaming Engine V4.3 software, which is capable of streaming RTMP protocol, is used for the streaming software. Any web browser plugged in with Adobe flash player is capable of playing the streaming contents.

The hosts *RIBFSMTP1/2* are the mail front-end servers, which are used for tagging spam mails and isolating virus-infected mails. The Sophos Email Protection-Advanced software (PMX) has been updated to the latest version PMX 6.3.0. Figure 2 shows the Mail Trends of the PMX in Dec. 2015. As shown in the figure, 50% of the incoming mails were blocked by the IP blocker. The red bar indicates the virus-infected mails blocked by the PMX. Approximately 0.7 % of the incoming mails were infected by viruses in this month, which is six times the yearly average. We noticed that half of the viruses blocked by the PMX in Dec. 2015 were harmful ransamware[3].

An anonymous ftp server, *FTP.RIKEN.JP*, is managed and operated at the RNC. Major Linux distributions, including Scientific Linux, Ubuntu and CentOS, are mirrored daily for the convenience of their users and for facilitating high-speed access. The average network traffic of this server is 40 MB/s.

*1 RIKEN Nishina Center

References

1) http://ribf.riken.jp/comp/
2) T. Ichihara et al.: RIKEN Accel. Prog. Rep. 48, 249 (2015).
3) https://en.wikipedia.org/wiki/Ransomware

III. RESEARCH ACTIVITIES II
(Material Science and Biology)

1. Atomic and Solid State Physics (Ion)

Site change of hydrogen owing to lattice distortion in Nb alloys†

C. Sugi,[*1, *2] E. Yagi,[*1, *2] Y. Okada,[*2] S. Koike,[*3] T. Sugawara,[*4] T. Shishido,[*4] and K. Ogiwara[*1]

An interaction of hydrogen with solute atoms is one of the fundamental problems on hydrogen in metals, because various hydrogen-related properties are strongly affected by alloying. In order to understand the interaction, the knowledge of the atomistic state of hydrogen in alloys is highly required. However, such information has been extremely limited, because of experimental difficulties. Therefore, the channelling method utilizing a nuclear reaction of $^{1}H(^{11}B,\alpha)\alpha\alpha$ with a $^{11}B^{+}$ beam of about 2 MeV had been newly developed.[1)] Hydrogen can be detected by measuring emitted α particles. This method has been demonstrated to be very useful to locate hydrogen dissolved in metals.[1,2)] The lattice location of hydrogen has hitherto been investigated systematically in detail in Nb alloyed with undersized Mo atoms up to 60 at. % by the channelling method at room temperature with a tandem accelerator. Their atomic radii are 1.43 Å for Nb and 1.36 Å for Mo atoms. This alloy system forms a solid solution over the entire Mo concentration (C_{Mo}) range, maintaining a bcc crystal structure, although the lattice parameter changes.

It has been demonstrated that the lattice location changes very sensitively with C_{Mo} and, with the help of measurement of width of X-ray reflection lines (Fig. 1), that such change can be interpreted in terms of lattice distortion induced by alloying.[3)] Broadening of reflection lines serves as a measure of lattice distortion averaged over the whole specimen. At low C_{Mo}, lattice is strongly distorted around Mo atoms. Hydrogen is trapped by a Mo atom to be located at a T_{tr} site, which is displaced from an original tetrahedral (T) site by about 0.6 Å towards the Mo atom, so as to reduce the distortion around Mo atom. There exists a strong attractive interaction between hydrogen and Mo atoms.[4)] With increasing C_{Mo}, the lattice distortion is reduced owing to interference between strain fields around individual Mo atoms, and most of the H atoms occupy T sites as in Nb. For C_{Mo} higher than 39 at. %, the lattice distortion gradually increases again with increasing C_{Mo} because of the increase in the number of undersized Mo atoms in a unit cell, but not so strongly as that at low C_{Mo}, i.e., up to an intermediate level (the range II in Fig. 1). In this case, H atoms are distributed over T and d-T sites, which are displaced from T sites to their nearest neighbour octahedral (O) sites by about 0.25 Å. The T-site occupancy is energetically more favourable than the d-T-site occupancy. Hydrogen preferentially occupies T sites in undistorted or very weakly distorted region, but, as the concentration of available T sites is limited, excess H atoms occupy d-T sites in the region distorted at the intermediate level.[3)] Therefore, it is expected that H atoms are located at T sites in the alloys whose lattice is very weakly distorted.

Then, in the present study, the site occupancy of hydrogen in Nb alloyed with 50 at. % of oversized Ta atoms with a very closer atomic radius to Nb atoms, 1.44 Å, $Nb_{0.50}Ta_{0.50}H_{0.021}$ and $Nb_{0.50}Ta_{0.50}H_{0.053}$, was investigated by the channelling method at room temperature. It was observed that H atoms are located at T sites, irrespective of hydrogen concentration (C_H), in contrast with the results on Nb alloyed with similar concentration of undersized Mo atoms, $Nb_{0.52}Mo_{0.48}$ (C_H=0.0097–0.05). In approximately the same C_H range as that in the $Nb_{0.50}Ta_{0.50}$ alloys, in the $Nb_{0.52}Mo_{0.48}$ alloys, at low C_H, most of the H atoms are located at T sites and excess H atoms are at d-T sites, while at high C_H, most of them are at d-T sites.[3)]

Widths of X-ray diffraction lines in the $Nb_{0.50}Ta_{0.50}$ alloys are much smaller than those in the $Nb_{0.52}Mo_{0.48}$ alloys and are very close to those in pure Nb (Fig. 1), indicating much smaller lattice distortion in the $Nb_{0.50}Ta_{0.50}$ alloys than in the $Nb_{0.52}Mo_{0.48}$ alloys, owing to the smaller size difference between Nb and Ta atoms. The present result on site occupancy of hydrogen in the $Nb_{0.50}Ta_{0.50}$ alloys is in good agreement with the expectation. Therefore, considering also the hitherto obtained results for Nb alloyed with 2–5 at. % Ta atoms, it is concluded that the site occupancy of hydrogen in Nb-Mo and Nb-Ta alloys can be well explained on the basis of the lattice distortion induced by alloying.

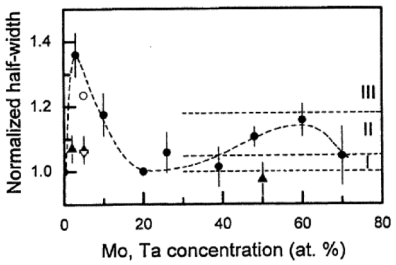

Fig. 1. The half-widths of the {321} X-ray reflection lines of the non-H-doped Nb-Mo (●) and Nb-Ta (▲) alloys. Open symbols, Nb-Mo (○) and Nb-Ta (▽), represent those by Matsumoto et al.[5)]

† Condensed from the article in J. Phys. Soc. Jpn. **82** 074601 (2013).

*1 RIKEN Nishina Center
*2 School of Science and Engineering, Waseda University.
*3 Department of Physics II, Tokyo University of Science.
*4 Institute for Materials Research, Tohoku University.

References

1) E. Yagi. T. Kobayashi, S. Nakamura, Y. Fukai, and K. Watanabe: J. Phys. Soc. Jpn. **52**, 84 (1983).
2) E. Yagi, T. Kobayashi, S. Nakamura, Y. Fukai, and K. Watanabe: Phys. Rev. B **31**, 1640 (1985).
3) E. Yagi et al.: J. Phys. Soc. Jpn. **79**, 044602 (2010).
4) E. Yagi, S. Nakamura, F. Kano, T. Kobayashi, K. Watanabe, Y. Fukai, and T. Matsumoto: Phys. Rev. B **39**, 57 (1989).
5) T. Matsumoto et al.: J. Phys. Chem. Solids **36**, 215 (1975).

Superconducting proximity effects in Nb/rare-earth bilayers

H. Yamazaki*1

A systematic study of the superconducting proximity effects in Nb/rare-earth (RE) bilayers is reported, where RE indicates Gd, Tb, Dy, and Ho (the first four heavy RE elements in the periodic table). Gd, Tb, and Dy are in the ferromagnetic state below 293 K, 222 K, and 85 K, respectively, while Ho exhibits conical ferromagnetism (inhomogeneous magnetism) below ~20 K.

Using the epitaxial growth of $Al_2O_3(11\bar{2}0)$/Nb(110)/RE(0002), a single-crystal layer of RE was fabricated. The thickness of the RE layer, t_{RE}, was varied from 10 nm to 20 nm with an interval of Δt_{RE}=0.4 nm. The superconducting transition temperature T_c of the samples was measured. We carried out a periodicity analysis on the $T_c(t_{RE})$ data using a quantitative fast Fourier transform (FFT) method. The results of the analysis are summarized in Fig. 1. With the exception of the longest period (~3.5 nm) for Gd, two types of variations are confirmed in the element dependence of the oscillation period. Here, we refer to the longer periods (more than 1 nm) as λ_L and the shorter periods (about 1 nm) as λ_S. The spin modulation period intrinsic to Ho, λ_{spin}^{Ho}(=3.4 nm; open circle), is located within a broad distribution of λ_L for Ho. We identify a linear change in λ_L (shown as a broken line) from Gd to Dy. The line is extrapolated to Ho, giving an extrapolated value of 2.45 nm at Ho.

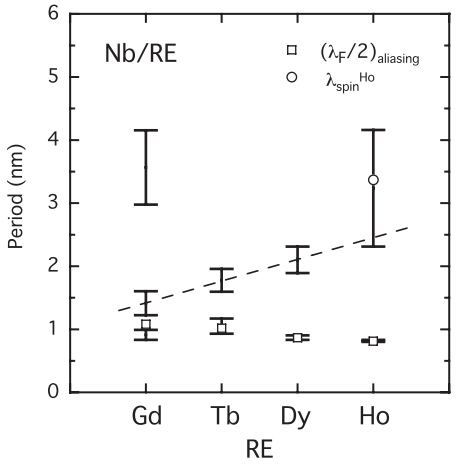

Fig. 1. Summary of the FFT analysis: periods of the oscillation components in $T_c(t_{RE})$ for Gd, Tb, Dy, and Ho (in order of atomic number). The broken line represents a linear extrapolation of the λ_L values for Gd, Tb, and Dy, to Ho. We observe a good agreement between $(\lambda_F/2)_{aliasing}$ (open squares) and the short-wavelength period λ_S. The helical spin-modulation period in bulk Ho at low temperatures (~2K) corresponds to λ_{spin}^{Ho}=3.4 nm (open circle).

*1 RIKEN Nishina Center

According to the picture of the RKKY interaction between valence electrons and 4*f* moments, the exchange energy E_{ex} at 0 K scales linearly with the 4*f* spin moment *S*, where *S*=7, 6, 5, and 4 μ_B for Gd, Tb, Dy, and Ho, respectively. The spatial period of the FFLO-like oscillation, λ_{FFLO}, in the REs therefore increases from Gd to Ho at low temperatures, as long as $\lambda_{FFLO} \propto v_F/E_{ex}$ holds (a clean ferromagnet) and the Fermi velocity v_F is almost unchanged for the REs. The broken line actually suggests that λ_L increases as $S(\propto E_{ex})$ decreases. Further, the values of λ_L for Gd and Ho are in good agreement with the literature data for λ_{FFLO}.[1, 2] Hence, we infer that the broken line indicates the element dependence of λ_{FFLO}.

The Fermi wavelength λ_F of each RE was calculated from λ_{FFLO} (the broken line) and the experimental values of E_{ex} for the Δ_2 valence states.[3] To date, there is little experimental data of v_F and λ_F for REs. The open squares show the calculated results of $(\lambda_F/2)_{aliasing}$, i.e., the aliased $\lambda_F/2$ by discrete-thickness sampling. We recognize that the values of $(\lambda_F/2)_{aliasing}$ reproduce λ_Ss well. This suggests that λ_Ss reflect the formation of quantum well states (QWSs) in the RE layer, as observed in the superconducting Pb film.[4] QWSs require the full penetration of Cooper pairs into the RE layer through the entire thickness. Accordingly, the presence of λ_Ss indirectly proves the presence of triplet pairs in the REs. It is possible that some local probes supplied by RI beams detect the triplet pairs converted from the singlet pairs of Nb owing to the exchange field in REs.

References

1) J. S. Jiang, D. Davidovic, D. H, Reich, and C. L. Chien, Phys. Rev. Lett **74**, 314 (1995).
2) F. Chiodi, J. D. S. Witt, R. G. J. Smits, L. Qu, Gábor B. Halász, C. -T. Wu, O. T. Valls, K. Halterman, J. W. A. Robinson, and M. G. Blamire, EPL, **101**, 37002 (2013).
3) C. Schüßler-Langeheine, E. Weschke, Chandan Mazumdar, R. Meier, A. Yu. Grigoriev, G. Kaindl, C. Sutter, D. Abernathy, G. Grübel, and Manuel Richter, Phys. Rev. Lett. **84**, 5624 (2000).
4) Y. Guo, Y.-F. Zhang, X.-Y. Bao, T.-Z. Han, Z. Tang, L.-X. Zhang, W.-G. Zhu, E. G. Wang, Q. Niu, Z. Q. Qiu, J.-F. Jia, Z.-X. Zhao, and Q.-K. Xue, Science **306**, 1915 (2004).

Evaluation of single event transient error rate related to operation frequency on 64bit SOI micro processor

A. Maru,[*1] K. Sakamoto,[*1] H. Shindou,[*1] S. Kuboyama,[*1] and K. Suzuki[*1]

Silicon on Insulator (SOI) devices are the focus for recent electronic applications due to their excellent characteristics which are low power consumption and possibility of miniaturization. They also have excellent characteristics with regard to the angle of radiation tolerance. Single event latch up (SEL) has never occurred in SOI devices due to their cross-sectional structure. Since the SOI transistor has been electrically isolated from others by buried oxide (BOX), electrical circuits with excellent single event upset (SEU) and single event transient (SET) tolerance can be composed by using SOI transistors. In addition, the Japan Aerospace Exploration Agency (JAXA) focused on SOI devices for space applications and has been continuously involved in research and development since 2005. JAXA has developed the Micro Processer Unit (MPU) and Application Specific Integrated Circuit (ASIC) for space applications by combining SOI devices and radiation hardness by design (RHBD) techniques.[1)] They are used in numerous spacecraft. Recently, it was reported in certain project that many SEUs were observed in the SOI product used in satellites. Reported error rates of SEUs on the orbit was higher than the calculated error rates from radiation tests on the ground. Therefore, it was suggested that some defects exist in this device.

From our analysis, it was identified that one defect in this device was due to a parasitic diode on the drain area of the SOI transistor, as shown in Fig.1. We identified the parasitic diode was created in one fabrication process of the SOI transistor, so we tried to fix this defect by changing the process condition of the SOI transistor. The evaluation results of the SOI device, which was fabricated using a fixed process condition indicated that it had high radiation tolerance. Under static test conditions, no error was observed on this device. However, a few errors were observed under dynamic test conditions (continuous memory data read/write condition). It is presumed that the cause of this error is temporal read miss due to SET.

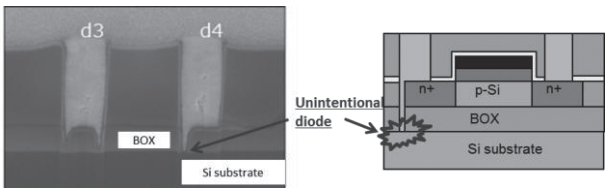

Fig. 1. Cross-sectional structure image of SOI transistor with unintentionally formed parasitic diode.

[*1] Japan Aerospace Exploration Agency

In the case of error due to SET, the error rate depends on the operation frequency of the device. Therefore we evaluated the error rate operation frequency dependence of this SOI device for calculating the error rate on the orbit.

The test sample was irradiated with a Kr-ion beam of 713 MeV using the RIKEN RILAC+RRC. Total fluence was set to 5×10^{7} ~ 1×10^{8} ions/cm^{2} at the chip surface. The operation frequency of the device was set to 0.5, 5, 50 MHz. The irradiation test was performed under dynamic test conditions.

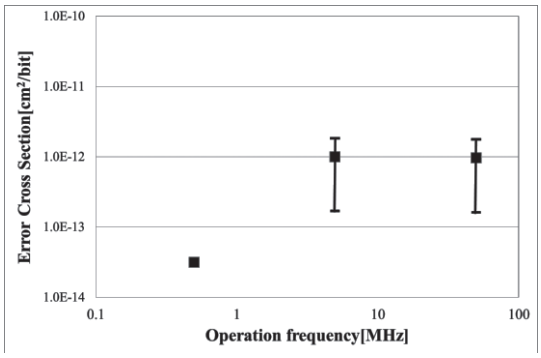

Fig. 2. SOI device irradiation test result under a dynamic test condition.

Figure 2 shows the data of error cross section which depends on operation frequency. The operation frequency dependence was not observed within the uncertainty of the data. Note that the value of error cross section is extremely low, so this error seldom occurs. Based on the evaluation results of error cross section, the calculated error rate on the orbit can be almost ignored.

The SOI device which was fabricated using the fixed process condition, indicated excellent radiation tolerance. We confirmed that the error rate on the orbit of this device can be almost ignored because the SET error cross section value is extremely low. Operation frequency dependence of SET error cross section could not be observed clearly, so we will evaluate this device with a wider frequency range in future work.

Reference

1) A. Makihara et al., RADECS, Vol.1 (2011), 164-168.

2. Atomic and Solid State Physics (Muon)

μSR study of the Cu-spin correlation in heavily electron-doped high-T_c T'-cuprates

T. Adachi,[*1,*2] M. A. Baqiya,[*3] I. Watanabe,[*1] and Y. Koike[*1,*3]

In the history of research on high-T_c superconductivity, numerous efforts have been made to the establishment of the phase diagram of both hole-doped and electron-doped cuprates. However, Matsumoto et al. reported that superconductivity appears even in the parent compound of $x = 0$ and in a wide range of x in $Nd_{2-x}Ce_xCuO_4$ with the so-called T' structure through the appropriate reduction of excess oxygen from the as-grown films, resulting in a completely different phase diagram from that formerly suggested.[1] The superconductivity in the parent compounds of T'-cuprates has also been confirmed for polycrystalline powdered samples of $La_{1.8}Eu_{0.2}CuO_4$.[2] These suggest that the superconductivity in electron-doped T'-cuprates cannot be understood in terms of the doping of carriers into Mott insulators as in the case of hole-doped cuprates.

Recently, through improved reduction annealing, we have succeeded in obtaining high-quality superconducting (SC) single crystals of underdoped T'-$Pr_{1.3-x}La_{0.7}Ce_xCuO_{4+\delta}$ with $x = 0.05 - 0.10$ whose ground states were believed to be antiferromagnetic (AF).[3] Transport measurements have revealed that the strongly localized state of carriers accompanied by the pseudogap due to AF fluctuations in the as-grown crystal changes to a Kondo state without the pseudogap in the SC crystal through reduction annealing. Moreover, our recent μSR measurements of SC crystals of $x = 0.10$ have revealed fast depolarization of muon spins and recovery of asymmetry in a long time region at low temperatures, suggesting the coexistence of superconductivity accompanied by a short-range magnetic order.[4] These results as well as the superconductivity in the parent compounds can be understood in terms of our proposed band picture based on the strong electron correlation.[3,4]

One of the next issues is investigating how superconductivity disappears through Ce doping. Our previous μSR measurements of the SC polycrystal of T'-$Pr_{1-x}LaCe_xCuO_{4+\delta}$ (PLCCO) with $x = 0.14$ revealed slowing down of the Cu-spin fluctuations at low temperatures, but no short-range magnetic order was observed.[5] Therefore, we performed μSR measurements using PLCCO single crystals in the heavily overdoped regime of $x = 0.17$ and 0.20 to obtain detailed information on the Cu-spin correlation. ZF and longitudinal-field μSR measurements were carried out using a MiniCryo and a fly-past-type ^{3}He cryostat at temperatures down to 0.3 K at RIKEN-RAL.

Figure 1 shows ZF μSR spectra of heavily overdoped PLCCO with $x = 0.20$ where superconductivity disappears. At high temperatures around 200 K, the depolarization of muon spins is slow, indicating that the development of the Cu-spin correlation is weak. It is found that, with decreasing temperature, the depolarization of muon spins becomes fast due to the growing effect of Pr^{3+} moments. At low temperatures, it is found that the recovery of the asymmetry in a long time region corresponding to the development of the Cu-spin correlation[5] is negligibly small. This suggests that the Cu-spin correlation is barely developed in the non-SC heavily overdoped regime of PLCCO. Combined with the results in the underdoped[4] and optimally doped[5] regimes, it is concluded that the Cu-spin correlation is crucial for the appearance of superconductivity in T'-cuprates.

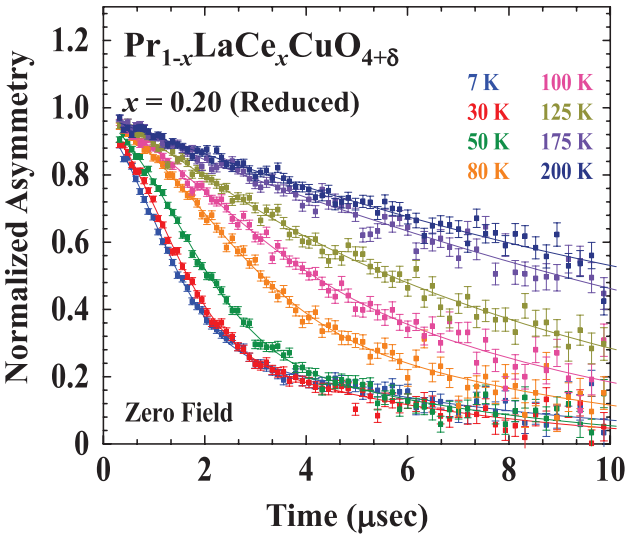

Fig. 1. Zero-field μSR time spectra of the non-superconducting heavily overdoped single crystal of T'-$Pr_{1-x}LaCe_xCuO_{4+\delta}$ with $x = 0.20$.

References

1) O. Matsumoto et al., Physica C **469**, 924 (2009).
2) T. Takamatsu et al., Appl. Phys. Express **5**, 073101 (2012).
3) T. Adachi et al., J. Phys. Soc. Jpn. **82**, 063713 (2013).
4) T. Adachi et al., arXiv: 1512.08095.
5) Risdiana et al., Phys. Rev. B **82**, 014506 (2010).

*1 RIKEN Nishina Center
*2 Department of Engineering and Applied Sciences, Sophia University
*3 Department of Applied Physics, Tohoku University

Magnetic ordering in $YBa_2Cu_3O_6$

S.S. Mohd-Tajudin,[*1,*2] T. Nishizaki,[*3] A. Kikkawa,[*4] N. Adam,[*1,*2] E. Suprayoga,[*2,*5] S. Sulaiman,[*1]
M.I. Mohamed-Ibrahim,[*1] and I.Watanabe[*2]

The high-T_c cuprate oxide superconductor $YBa_2Cu_3O_{6+x}$ (YBCO) is a Mott insulator and its electromagnetic properties can be controlled by the oxygen content x. In the range $0 \leq x \leq 0.4$, YBCO is in the antiferromagnetic (AFM) ordered state below room temperature. The magnetic transition temperature T_N decreases with increasing x. As x increases further, the AFM ordered state disappears and the superconducting state appears at $x \geq 0.4$. Cu ions have localized d electrons in a $3d^9$ configuration.[1)] Thus, Cu ions control the magnetism of the YBCO system.

We characterized the magnetic susceptibility of single crystal YBCO with $x = 0$ that had been annealed at 580℃ in

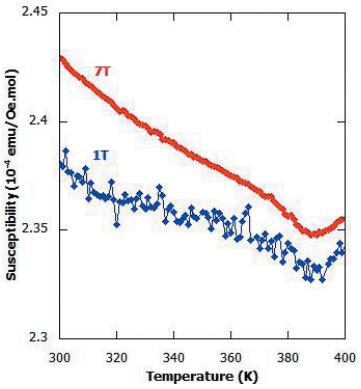

Fig. 1: Magnetic susceptibility of YBCO single crystals with x=0 measured under magnetic field of 1 and 7 T using SQUID.

Ar atmosphere using SQUID. $T_N = 365$ K is observed, but the magnetic transition is smeared out. This could be due to the inhomogeneous distribution of oxygen deficiency in the samples. In order to understand and clarify the magnetic ordering at the ground state of YBCO we used a muon spin rotation and relaxation (μSR) technique. The μSR experiment can detect the magnetic ordered state by the appearance of muon precession in a zero external field (ZF). Accordingly, the μSR experiment was performed in RAL (R486). A clear muon-spin precession was observed up to 279 K as shown in Fig. 2 (a). The observation of the muon-spin precession indicates clearly the appearance of a long-range magnetic ordered state in YBCO.[2,3)] Figure 2 (b) shows the slow damping of the non-oscillating signal above room temperature. This may be due to the fluctuating field or the nuclear dipole field that originates from the copper nuclei. Thus, we can say that the sample is in a paramagnetic state. A fast relaxing component was observed between 330 and 365 K

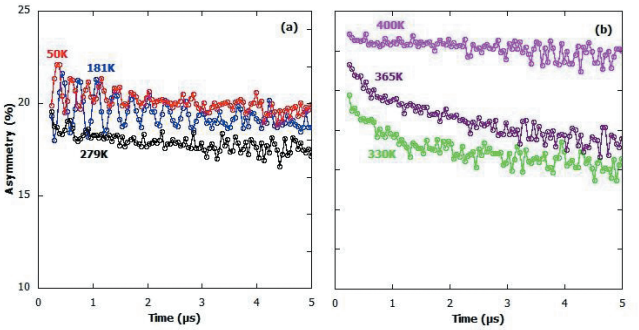

Fig. 2: ZF-μSR time spectra of YBCO single crystals with x=0 observed (a) below room temperature and (b) above room temperature.

and it increased with decreasing temperature. Therefore, T_N was se to 330 K from the current μSR experiment. The magnetic transition of μSR yields different results compared with the magnetic susceptibility measurement. We need more data points from the μSR point of view to elucidate macroscopic magnetic transition at high temperature.

References

1) J.M. Tranquada et al.: Phys. Rev. Lett. **60** 156 (1988).
2) N. Nishida et al.: Jpn. J. Appl. Phys. **26** L1856 (1987).
3) M. Pinkpank et al.: Physica C **317-318** 299 (1999).

[1] School of Distance Education, Universiti Sains Malaysia
[2] RIKEN Nishina Center
[3] Kyushu Sangyo University
[4] RIKEN Center for Emergent Matter Science (CEMS)
[5] Physics Department, Institut Teknologi Bandung

μSR study of an insulator near high-T_c honeycomb lattice superconductors

S. Shamoto*1 and I. Watanabe*2

A high-T_c layered superconductor, $Li_{0.48}(THF)_yHfNCl$ (T_c=25.5 K), was discovered by Yamanaka group in 1998[1]. The crystal structure has double honeycomb lattice of $[HfN]_2$[2]. The crystal structures of a series of double honeycomb lattice superconductors have been studied by our neutron diffraction experiments. The band structure is calculated by using LAPW+LDA[3]. Electrons are doped by alkali metal intercalation at K point in the bottom of conduction bands. The density of states $N(0)$ in 2-dimensional system is inversely propotional to the estimated transfer integral t_{dd} or band width W. If the $N(0)$ is the only variable parameter in the material like alkali doped fullerene superconductors, T_c varies as a function of the transfer integral t_{dd} estimated from the obtained crystal parameters based on Harrison values[4]. We found that the same honeycomb lattice material $Li_{0.16}YOCl$ was an insulator with small t_{dd}. In additon, this material shows spin glass like magnetism at H=100 Oe, although this sample includes non-magnetic impurity phases of LiCl and Y_2O_3. This magnetic behavior is not expected for a material with non-magnetic elements, although spin fluctuation senarios are theoretically discussed[5,6]. In addition, alkali fullerenes such as bcc Cs_3C_{60} exhibit antiferromagnetism as the Mott-Hubbard inslating state[7].

According to our zero-field μSR study under magnetic field, no explicit magnetic order has been observed for the $Li_{0.16}YOCl$ down to T= 2.5 K as shown in Fig. 1. The time dependent relaxation is also measured under magnetic fields. The μ^+ asymmetry is recovered by increasing an applied field. From the analysis of the decoupling curve of the asymmetry versus field, we found the relaxation rate can be represented by an $H^{0.3}$ dependence in the range from 70 G to 3950 G as shown in Fig. 2. This behaviour is similar to that observed in the solitons of polyacetylene[8]. The exponent may suggest a correlation to the spin diffusion dimension in the $[YO]_2$ honeycomb lattice.

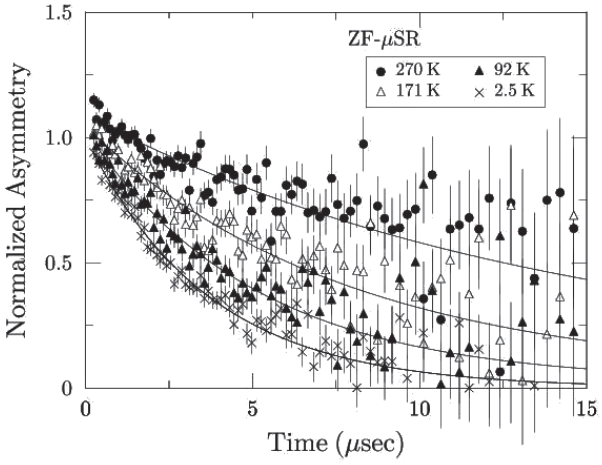

Fig. 1. The time spectra of decay positron asymmetry at various temperatures for $Li_{0.16}YOCl$.

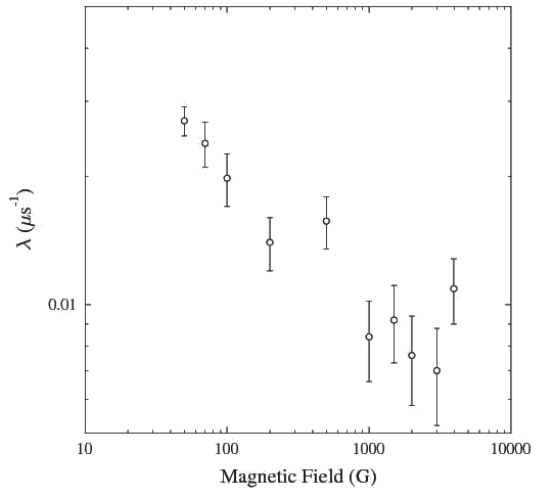

Fig. 2. Observed relaxation rates as a function of magnetic field for $Li_{0.16}YOCl$ at T=2.5 K.

References

1) S. Yamanaka *et al*., Nature **392**, 580-582 (1998).
2) S. Shamoto, T. Kato *et al*., Physica C, **306**, 7-14 (1998).
3) R. Weht *et al*., Europhys. Lett. **48**, 320 (1999).
4) W. A. Harrison, "Electronic Structure and the Properties of Solids", Dover.
5) K. Kuroki, Sci. Technol. Adv. Mater. **9**, 044202 (2008).
6) T. Watanabe and S. Ishihara, J. Phys. Soc. Jpn. **82**, 034704 (2013).
7) P. Jeglic *et al.*, Phys. Rev. B **80**, 195424 (2009).
8) K. Nagamine *et al*., Phys. Rev. Lett. B **53**, 1763 (1984).

*1 Advanced Science Research Center, Japan Atomic Energy Agency
*2 RIKEN Nishina Center

Investigation of magnetic ground states in mixed kagome systems $(Rb_{1-x}Cs_x)_2Cu_3SnF_{12}$ II

T. Suzuki,[*1,*3] K. Katayama,[*2] I. Watanabe,[*3] and H. Tanaka[*2]

The Heisenberg kagome antiferromagnet (HKAF) has attracted much attention in magnetism because lots of frustration and quantum effects have been indicated by theories. For example, in the classical spin model case for HKAF, the $q = 0$ or $\sqrt{3} \times \sqrt{3}$ magnetic structure is stabilized when the next-nearest-neighbor interaction is considered. In the case of $S = 1/2$ kagome lattice, exotic magnetic ground states have been theoretically predicted. For example, numerical calculations revealed that the ground state is a magnetically disordered spin liquid. In the ground state, triplet excitations are gapped, and there exists the continuum of low-lying singlet states below the triplet gap. Valence-bond crystals having a periodic arrangement of singlet dimers have also been proposed as the magnetic ground state of $S = 1/2$ HKAF. Experimentally, many types of HKAFs have been investigated as the candidate for the ideal kagome spin lattice material. For example, "jarosite" materials $AM_3(OH)_6(SO_4)_2$ (A = NH_4, Na, or K, M = Fe, Cr), m−MPYNN·BF_4, $Cu_3V_2O_7(OH)_2{\cdot}2H_2O$, $[Cu_3(titmb)_2(OCOCH_3)_6{\cdot}H_2O$, β−$Cu_3V_2O_8$, etc.

A new candidate for the ideal kagome lattice which has an exotic magnetic ground state was reported[1]. The cupric compound $A_2Cu_3SnF_{12}$ (A = Cs, Rb), which is the subject in this study, is a newly synthesized family of $S = 1/2$ HKAF. For $Cs_2Cu_3SnF_{12}$, the $q = 0$ magnetic structure is observed below $T_N = 20$ K. On the other hand, for $Rb_2Cu_3SnF_{12}$, the first realization of the "pinwheel" valence bond solid ground state in the $S = 1/2$ HKAF is confirmed by inelastic neutron measurements.

Recently, the ground state of mixed kagome $(Rb_{1-x}Cs_x)_2Cu_3SnF_{12}$ was investing by Katayama *et al*[2]. By magnetic susceptibility and specific heat measurements on single crystals, they reported a ground-state phase diagram, which shows the existence of a quantum phase transition from the valence-bond-glass (VBG) phase to the AF phase at $x_c = 0.53$. In this critical concentration, the spin gap and the ordered state disappear at least down to 1.8 K from the magnetic susceptibility measurement results. The characteristic properties at the quantum phase transition point is of great interest, and the information about it will contribute to a further understanding of the properties of the ground states in the kagome lattice compound. In the previous beam time, we carried out the longitudinal-field muon-spin-relaxation (LF-μSR) measurements in the sample of $x_c = 0.53$ down to 0.3 K, and we reported that internal magnetic fields fluctuate at 0.3 K, and that no tendency towards a magnetic phase transition is observed. The purpose of this study is to microscopically investigate the spin dynamics including fluctuating frequencies and values of internal magnetic fields down to lower temperatures.

In zero field (ZF), a low frequency rotational behavior due to dipole-dipole interactions between F^- and μ^+[3] is observed, and to extract the Cu spins dynamics from the entire spectra includung rotational signals, longitudinal fields above 100 gauss are applied. Figure 1 (a) shows the LF-μSR time spectra at 26 mK in the case of $x_c = 0.53$ above 100 gauss. The time spectra are analyzed using the two components function as follows:

$$A(t) = A_1 \exp(-\lambda_1 t) + A_2 \exp(-\lambda_2 t) \quad (1)$$

Here, λ_1 and λ_2 are the muon spin relaxation rates. A ratio of A_1/A_2 is fixed to be 0.97. Fig. 1 (b) shows the obtained LF dependence of muon spin relaxations λ_1 and λ_2. No step-like change in the LF-dependence appears, and λ_1 and λ_2 monotonously decrease with increasing the LF. These results suggest that internal magnetic fields at the muon sites fluctuate with widely spread frequencies down to 26 mK.

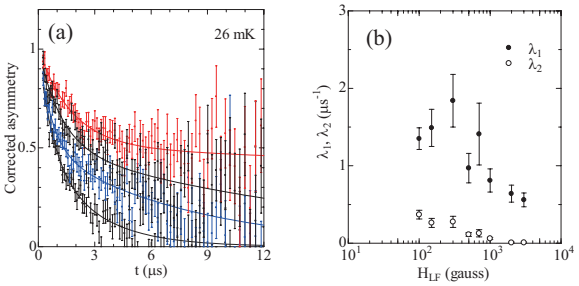

Fig. 1. (a) LF-μSR time spectra at 26 mK in 100, 700, 1000, and 3000 gauss shown from bottom to top. The solid lines represent the fitted results. (b) LF-dependence of the muon spin relaxation rates at 26 mK.

References

1) T. Ono *et al.*, Phys. Rev. B **79**, 174407 (2009).
2) K. Katayama *et al.*, Phys. Rev. B **91**, 214429 (2015).
3) J. H. Brewer *et al.*, Phys. Rev. B **33**, 7813 (1986).

*1 Shibauta Institute of Technology
*2 Department of Physics, Tokyo Institute of Technology
*3 RIKEN Nishina Center

μSR Result on Magnetic ground state of $Ce_{1-x}La_xT_2Al_{10}$ (T = Ru, Os)

N. Adam,[*1,*2] H. Tanida,[*3] D. T. Adroja,[*4] M. Sera,[*3] T. Takabatake,[*3] and I. Watanabe[*1]

Ce-based caged-type compounds, CeT_2Al_{10} (T= Ru, Os) have generated great interest due to their Kondo semiconducting state and an anomalously high magnetic ordering temperature $T_0 \sim 30$ K with spin gap formation at low temperatures [1-2]. Neutron diffraction studies of CeT_2Al_{10} for T= Ru and Os revealed small ordered moments, 0.34 μB and 0.29 μB, along the *c*-axis respectively although these two compounds exhibit a large anisotropy of magnetic susceptibility $\chi_a > \chi_c > \chi_b$ [3,4]. This indicates that the moment direction is governed by the anisotropic magnetic exchange and not by the CEF anisotropy [5,6].

In order to investigate the relation between the moment direction and the spin gap energy, magnetic Ce ($4f^1$) is substituted with nonmagnetic La ($4f^0$), as in $Ce_{1-x}La_xT_2Al_{10}$, assuming that it would change the magnetic moment due to different lattice parameters. However, an unusually ordered state is realized. In the case of $Ce_{0.9}La_{0.1}Os_2Al_{10}$, neutron diffraction studies have shown that the ordered moment remains along the *c*-axis and the Ce moment reduces with an increasing La concentration without any changes in the spin direction [6]. Compared to $Ce_{1-x}La_xRu_2Al_{10}$, the direction of the ordered moment changes from *c*-axis to *b*-axis and the moment is reduced to 0.18 μB after 7% La doping [7].

In order to gain further information on the microscopic change in magnetism, we performed muon spin relaxation (*μSR*) on a $Ce_{1-x}La_xRu_2Al_{10}$ (x = 0.05, 0.07, 0.10) and $Ce_{1-x}La_xOs_2Al_{10}$ (x = 0.10, 0.24, 0.50) alloy. The *μSR* experiments were carried out using the JANIS in CHRONUS (Port-4) spectrometer in longitudinal geometry at RIKEN-RAL, UK. Fig. 1 (a-d) shows the zero-field (ZF) *μSR* spectra of $Ce_{1-x}La_xRu_2Al_{10}$ (x = 0.07 and 0.10) and Fig. 2 (a-d) shows the ZF- *μSR* spectra for $Ce_{1-x}La_xOs_2Al_{10}$ (x = 0.24 and 0.50). The panels on the left side of the figures show the spectra at low temperatures, while those on the right side show the spectra at high temperatures.

As shown in the Figs. 1(a), 1(c), and 2(a), the spectra exhibit clear signs of oscillation with strong damping confirming the long range magnetic ordering of the Ce moment below T_0. Meanwhile in Figs. 1(b), 1(d) and 2(b), we can observe the magnetic transition at 24 K, 21 K, and 8 K, respectively. On the other hand, the *μSR* spectra of $Ce_{1-x}La_xOs_2Al_{10}$ (x = 0.5) at 2 K in Fig. 2(c) reveal a non-magnetic ground state below T_0. The same behavior can be observed in Figs. 1(b), 1(d), 2(b), and 2(d) above the magnetic transition temperature which is a typical muon response to static distribution of the nuclear dipole moment.

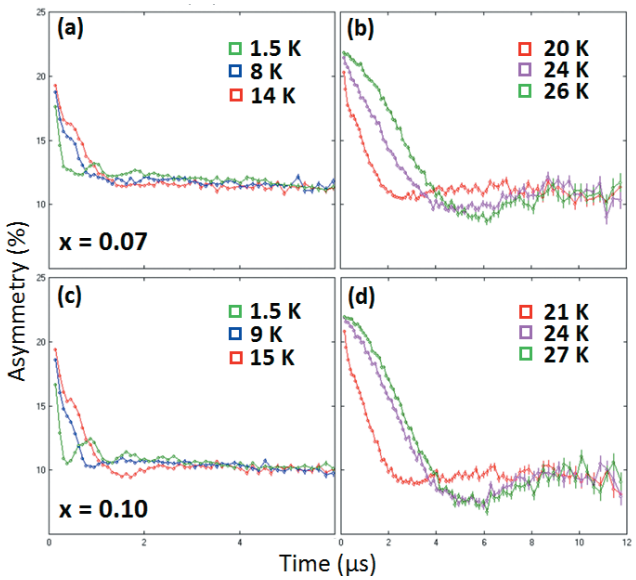

Fig. 1 ZF-*μSR* of $Ce_{1-x}La_xRu_2Al_{10}$

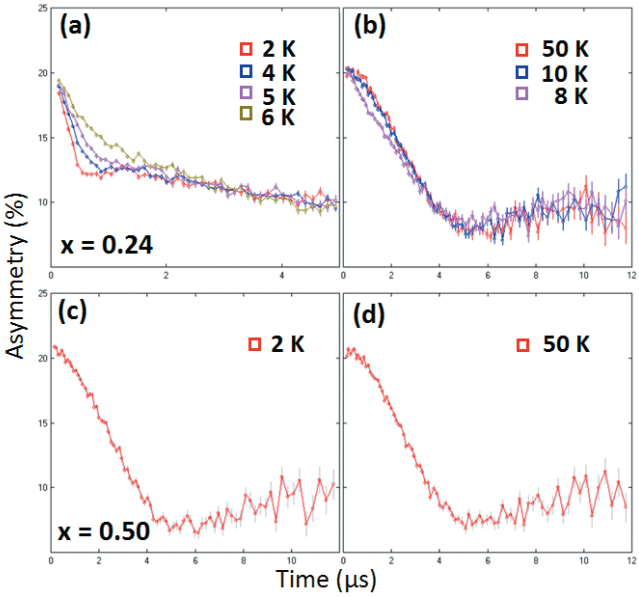

Fig. 2 ZF-*μSR* of $Ce_{1-x}La_xOs_2Al_{10}$

*1 RIKEN Nishina Center
*2 Computational Chemistry and Physics Laboratory, Universiti Sains Malaysia
*3 ADSM, Hiroshima University
*4 ISIS Facility, Rutherford Appleton Laboratory

References

1) A. M. Strydom, Physica B, **404**, 2981 (2009).
2) T. Nishioka *et al.*, JPSJ, **78**, 123705 (2009).
3) D. D. Khalyavin *et al.*, Phys. Rev. B **82**, 100405(R) (2010).
4) H. Kao *et al.*, J. Phys. Soc. Jpn. **80**, 073701 (2011).
5) J.-M. Mignot *et al.*, Phys. Rev. B **89**, 161103 (2014).
6) D.T. Adroja *et al.*, Phys. Rev. B **92**, 094425 (2015).
7) H. Tanida *et al.*, JPS Conf. Proc. **3**, 011073 (2014).

μSR study on the Kondo semiconductor $(Ce_xLa_{1-x})Ru_2Al_{10}$

N. Adam,[*1,*2] H. Tanida,[*1,*3] M. Sera,[*3] T. Nishioka,[*4] and I. Watanabe[*1,*2]

The Kondo semiconductors CeT_2Al_{10} (T = Fe, Ru, and Os) have been attracting much attention because of their unusual antiferromagnetic (AFM) ordering at $T_0 \sim 30$ K for T = Ru and Os .[1,2] Below T_0, the AFM moment (m_{AF}) is parallel to the orthorhombic c axis[3,4] although the easy magnetization axis is the a axis with a large magnetic anisotropy, $\chi_a \gg \chi_c \gg \chi_b$. By substituting magnetic Ce ($4f^1$) with nonmagnetic La ($4f^0$), a further unusual ordered state is realized; the direction of m_{AF} is switched from the c to b axis, although the b axis is the magnetic hardest axis.[5] Nonetheless, T_0 is not significantly reduced, and the Kondo semiconducting behavior is maintained by the substitution. On further reducing the Ce concentration, T_0 decreases smoothly and disappears at a critical Ce concentration of $x \sim 0.45$. This indicates that the interaction of the transition is long-ranged, like the RKKY interaction. However, the transition temperature, $T_0 \sim 30$ K, is too high for an usual magnetic transition because (1) the T_N of isomorphous GdT_2Al_{10}, which is expected to show the highest ordering temperature in a series of RT_2Al_{10} systems, is only 16−18 K, and (2) the distance between the nearest Ce sites is greater than 5 Å. These imply that magnetic interactions are not key parameters for the transition, but there could be an unknown parameter related to the $c-f$ hybridization effect.

Previously, we examined the microscopic magnetism of $CeRu_2Al_{10}$ and the related Rh−doped one by means of μSR in RAL,[6] together with numerical calculations by using the density functional theory.[7] By substituting Ru with Rh which possesses an extra $4d$ electron compared to Ru, electronic properties are drastically changed, and $m_{AF} \parallel a$ is realized instead of $m_{AF} \parallel c$.[8] From our results, we have concluded that (1) the critical Rh concentration is less than 3%; (2) there are two muon stopping sites, which is supported by the DFT calculation; (3) internal fields, H_{int} (H_{Large} and H_{Small}), are very sensitive to spin structure; and (4) transferred hyperfine field could be essential for their non-mean field like behavior.

In order to examine the microscopic magnetism in $(Ce_xLa_{1-x})Ru_2Al_{10}$, we performed zero-field μSR using randomly mounted small single crystals. Figure 1 shows the preliminary results of the temperature dependence of H_{int} in $(Ce_{0.9}La_{0.1})Ru_2Al_{10}$. The data for $x = 1$ are also shown for comparison.[6] For $x = 1$, H_{Large} exhibits the usual mean-field behavior, whereas H_{Small} shows non-mean-field behavior. For $x = 0.9$, a similar behavior is obtained in H_{Large}. On the other hand, H_{Small} exhibits a behavior significantly different from that of H_{Small} for $x = 1$. Thus, H_{Large} is robust, while H_{Small} is strongly affected by the substitution. Considering the mean-field behavior of H_{Large}, the development of m_{AF} should be regarded a mean-field type. Thus, the non-mean field behavior of H_{Small} for $x = 0.9$ could also be related to the hyperfine anomaly. It should be noted that the temperature dependence of H_{Small} for $x = 0.9$ is very similar to that of H_{Large} in the Rh-doped $CeRu_2Al_{10}$, aside from a large difference in magnitude.[6] This could be a key to identify the muon sites and the origin of the hyperfine anomaly.

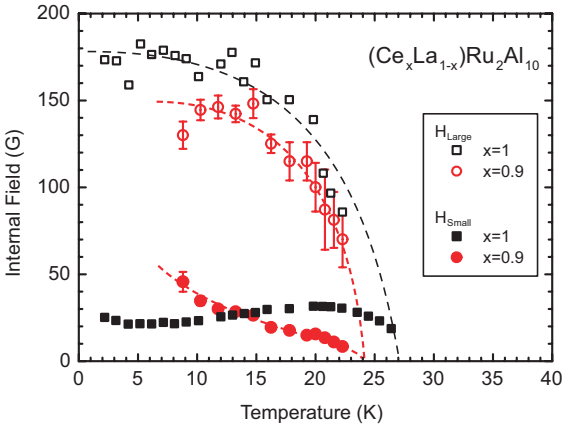

Fig. 1. Preliminary results of the temperature dependence of the internal magnetic fields in $(Ce_{0.9}La_{0.1})Ru_2Al_{10}$. The data for $x = 1$ are also shown for comparison.[6] Dotted curves are guides to the eyes.

*1 RIKEN Nishina Center
*2 Computational Chemistry and Physics Laboratory. Universiti Sains Malaysia
*3 ADSM, Hiroshima University
*4 Neutron Science Laboratory, ISSP, University of Tokyo
*5 Graduate School of Integrated Arts and Science, Kochi University

References
1) A. M. Strydom, Physica B **404**, 2981 (2009).
2) T. Nishioka et al., J. Phys. Soc. Jpn. **78**, 123705 (2009).
3) D. D. Khalyavin et al., Phys. Rev. B **82**, 100405(R) (2010).
4) H. Tanida et al., Phys. Rev. B **84**, 233202 (2011).
5) H. Tanida et al., Phys. Rev. B **88**, 045135 (2013).
6) H. Guo et al., Phys. Rev. B **88**, 115206 (2013).
7) N. Adam et al., J. Phys. Conf. Series. **551**, 012053 (2014).
8) R. Kobayashi et al., J. Phys. Soc. Jpn. **82**, 093702 (2013).

Disappearing of the Ir-ordered state in the Pyrochlore iridates $(Nd,Ca)_2Ir_2O_7$ studied by μSR

R. Asih,[*1,*2] S. S. Mohd-Tajudin,[*1,*3] N. Adam,[*1,*3] K. Matsuhira,[*4] T. Nakano,[*2] Y. Nozue,[*2] and I. Watanabe[*1,*2,*3]

Pyrochore iridates, $R_2Ir_2O_7$ (R-227, R = Y and rare-earth element), are an ideal platform to study the interplay between electron correlation (U) and spin-orbit coupling (SOC) in which the electron correlation (U) can be systematically tuned by changing the ionic radius of R-ion (r).[1] Among pyrochlore systems, these compounds have the widest structure stability[2] and experimentally have revealed systematic metal-insulator transition (MIT) and systematic variation of properties with R.[3] The MIT temperature, T_{MI}, decreases monotonically as the ionic radius of R^{3+} increases, and its boundary lies between R = Nd and Pr.[3] Accordingly the study on a change in the magnetically ordered state in $Nd_2Ir_2O_7$ and its doped-systems is important to discuss an intrinsic critical behavior of the electronic state in $R_2Ir_2O_7$.

In this study, we report the effect of Ca substitution on the magnetic ordered state of Ir^{4+} spins in $Nd_2Ir_2O_7$ investigated by muon-spin relaxation. $Nd_2Ir_2O_7$ shows metallic behavior at high temperature and undergoes MIT at temperatures around 33 K,[3] and the magnetic order in this material also seem to occur simultaneously at T_{MI} without any lattice distortion.[4] In our previous μSR results on $Nd_2Ir_2O_7$,[5] we observed the coherent magnetically ordered state of Ir^{4+} spins just below T_{MI} and confirmed that Nd^{3+} moments mainly grew below 15 K as observed in the neutron diffraction.[6]

As observed in the electrical resistivity and the DC magnetization measurements, in which the T_{MI} and magnetic transition (T_M) decrease by increasing Ca doping, we expected the Ca substitution to dramatically suppress the magnetic order of Ir^{4+} spins in $(Nd_{1-x}Ca_x)_2Ir_2O_7$. Figure 1 shows the zero-field (ZF) time spectrum of $(Nd_{1-x}Ca_x)_2Ir_2O_7$ at a temperature of 1.5 K. The spontaneous muon spin precession is still observed in the sample with 3 % of Ca-doped, and it becomes less well-defined at a higher Ca substitution. A heavily damped muon-spin precession with fast damping rate is the characteristic in the time spectrum at a high Ca concentration. A phenomenological function of

$$A_{(t)} = A_1 e^{-\lambda_1 t} + A_2 e^{-\lambda_2 t} + A_3 cos(\gamma_\mu H_{int} + \varphi) e^{-\lambda_3 t} \quad (1)$$

is used to fit the time spectra. λ_1 and λ_2 are the slow and fast relaxation rates, respectively, while λ_3 is the damping rate of muon-spin precession. H_{int} and φ are the internal field at the muon site and the initial phase of muon precession, respectively.

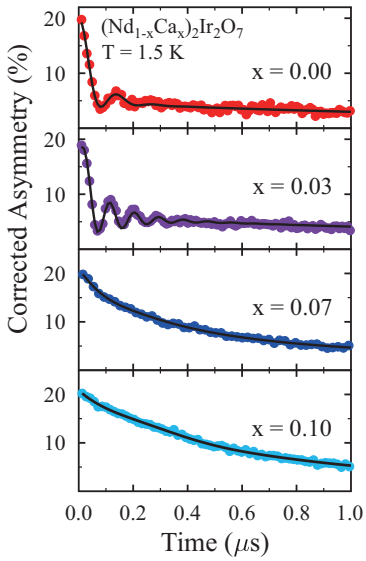

Fig. 1. Zero-field time spectrum of $(Nd_{1-x}Ca_x)_2Ir_2O_7$ in the early time region at a temperature of 1.5 K. The solid lines are fits to Eq. 1.

A spontaneous muon spin precession was observed in the sample with 3 % of Ca concentration at a temperature below 12.5 K, which is lower than the T_{MI} of this sample. At higher Ca concentrations, x = 0.07 and 0.10, no static ordering was observed at temperature below 1.5 K. Although the T_{MI} of these samples is estimated to be approximately 10 K and 5 K, respectively. This indicates that the carrier doping would strongly suppress the magnetic ordering rather than the changes in the electrical transport properties.

*1 RIKEN Nishina Center
*2 Department of Physics, Osaka University
*3 School of Distance Education, Universiti Sains Malaysia
*4 Graduate School of Engineering, Kyushu Institute of Technology

References

1) X. Wan et al., Phys. Rev. B **83**, 205101 (2011).
2) J. S. Gardner, M. J. P. Gingras, and J. E. Greedan, Rev. Mod. Phys. **82**, 53 (2010)
3) K. Matsuhira et al., J. Phys. Soc. Jpn. **80**, 094701 (2011).
4) J. Yamaura et al., Phys. Rev. Letter **108**, 247205 (2012).
5) H. Guo et al., Phys. Rev. B **88**, 060411(R) (2013).
6) K. Tomiyasu et al., J. Phys. Soc. Jpn. **81**, 034709 (2012).

μSR investigation of novel magnetism in the 4d Heisenberg-Kitaev honeycomb compound α-$RuCl_3$

S. Yoon,[*1,*2] S.-H. Do,[*3] Y. S. Kwon,[*4] K.-Y. Choi,[*3] I. Watanabe,[*1,*2] and B. J. Suh[*2]

The Kitaev honeycomb spin model has been considered as an approach to study the spin liquid state.[1)-3)] This model is based on the two-dimensional honeycomb network of magnetic ions with strong spin orbit coupling. This environment can suppress the Heisenberg AF exchange,[4),5)] and it can result in anisotropic exchange depending on the bond direction.[5)] This exchange leads to a highly frustrated spin state with spatial and spin degrees of freedom.[1)-3)] This fractional spin excitation that reflects the frustrated spin state can be translated by an emergence of Majorana fermions with their own antiparticles.[1)-3),5)]

Honeycomb ruthenate, α-$RuCl_3$, was suggested as a candidate to realize the Kitaev spin model.[6)] It provides proper environments for the Kitaev spin model, a cubic environment composed of Cl^- ions for revealing strong spin orbit coupling, and honeycomb layers connected by weak van der Waals forces for realizing the ideal two-dimensional environment for Kitaev exchanges.[6)] It exhibits two distinct magnetic anomalies, at 6 K, and 14 K in the DC susceptibility. Also, significant exchange anisotropy is found by observing the different Weiss temperatures with opposite signs in the different external field orientations.[7)-9)]

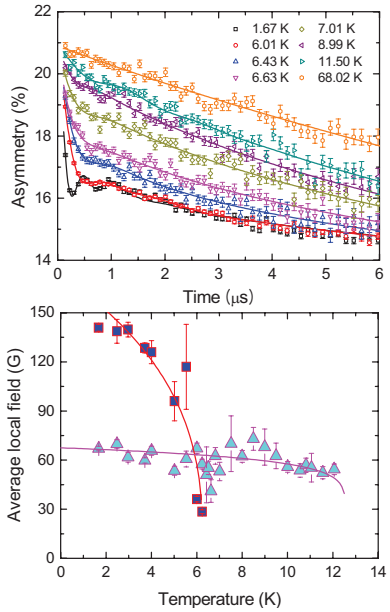

Fig. 1. (upper panel) Time differential spectra of the muon polarization at several temperatures in the zero field condition, and (lower panel) temperature dependence of the internal field extracted by fitting muon time spectra at the zero field with an assumption of the magnetic ordered state

*1 RIKEN Nishina Center
*2 Department of Physics, The Catholic University of Korea
*3 Department of Physics, Chung-Ang University
*4 Department of Emerging Materials Science, DGIST

Our synthesized honeycomb ruthenate single crystal shows three distinct anomalies at 6 K, 9.5 K, and 12.5 K in the result of the heat capacity measurement, and the magnetic susceptibility exhibits the result similar to those in the previous reports.[7)-9)] Besides, this material is found to be similar to the ideal two-dimensional environment as a rhombohedral lattice was revealed in the crystal structure analysis. In this environment, the effects induced by stacking faults in the honeycomb layers are expected to decrease. For instance, different magnetic transitions emerge from different stacking orders in the neutron diffraction results.[10)] Additionally, a single anomaly at 14 K is revealed in honeycomb ruthenate with a monoclinic lattice.[11)]

Fig. 1 shows the muon time spectra at several temperatures in the zero field condition (upper panel), and the temperature dependence of internal fields extracted by fitting muon time spectra with an assumption of the magnetic ordered state (lower panel). The muon time spectra obtained at the zero field exhibit the clear oscillation below 6 K, and changes of the initial asymmetry, which indicate the magnetic ordered state. In addition, single exponential relaxation is exhibited over 13 K. With these phenomena, we analyzed the muon time spectra based on the magnetic ordered state below 13 K as shown in Fig. 1 (lower panel). Furthermore, we observed similar relaxations between 4 μs and 6 μs at 1.7 K, and 6 K. These relaxations can provide evidence of the frustrated spin state.

In summary, we performed a microscopic investigation of honeycomb ruthenate with a rhombohedral lattice using spin polarized muons. We analyzed the muon polarizations below 13 K in the zero field condition with an assumption of the magnetic ordered state revealed by the clear oscillation below 6 K, and single exponential relaxation over 13 K.

References

1) W. Witczak-Krempa *et al.*, Annu. Rev. Condens. Matter Phys. **5**, 57 (2014).
2) J. G. Rau *et al.*, arXiv:1507.06323.
3) R. Schaffer *et al.*, arXiv:1512.02224.
4) A. Kitaev, Ann. Phys. **321**, 2 (2006).
5) G. Jackeli, and G. Khaliullin, Phys. Rev. Lett. **102**, 017205 (2009).
6) K. W. Plumb *et al.*, Phys. Rev. B **90**, 041112 (2014).
7) Y. Kubota *et al.*, Phys. Rev. B **91**, 094422 (2015).
8) J. A. Sears *et al.*, Phys. Rev. B **91**, 144420 (2015).
9) M. Majumder *et al.*, Phys. Rev. B **91**, 180401 (2015).
10) A. Banerjee *et al.*, arXiv:1504.08037.
11) R. D. Johnson *et al.*, Phys. Rev. B **92**, 235119 (2015).

Investigation of the magnetic ground state of frustrated spin system $Rb_2Cu_2Mo_3O_{12}$

S. Ohira-Kawamura,[*1,*2] K. Tomiyasu,[*3] and I. Watanabe[*2]

$Rb_2Cu_2Mo_3O_{12}$ is a quantum spin system having a spin-1/2 one-dimensional (1D) zig-zag chain, where spin frustration is expected to result from competition between the first and second neighbor exchange interactions, J_1 and J_2.[1)] Based on the ratio J_1/J_2, it has been suggested that the magnetic ground state of this system is novel incommensurate spin-singlet.[2)] However, evidence for the spin-singlet ground state has not been bared experimentally. Magnetic susceptibility drops at low temperature but exhibits a nonzero value,[1)] and a powder inelastic neutron scattering measurement did not reveal an energy gap, whereas dispersive spin excitations arising from an incommensurate propagation vector were observed.[3)] In order to clarify the magnetic ground state of $Rb_2Cu_2Mo_3O_{12}$, we performed a muon spin relaxation (μSR) experiment on this material at the RIKEN-RAL Muon Facility.

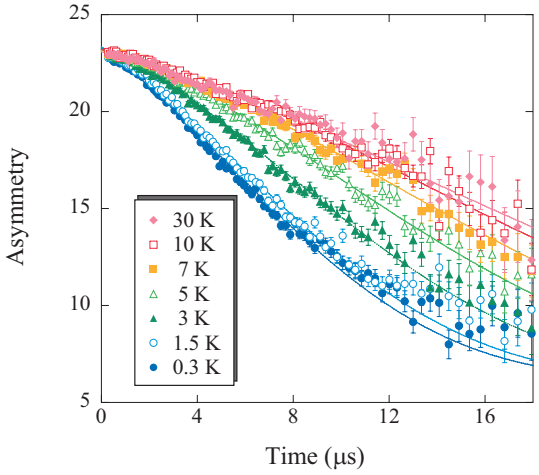

Fig. 1. ZF-μSR time spectra observed at various temperatures.

Figure 1 shows the time spectra observed at various temperatures under zero-field (ZF). The relaxation is gradually enhanced below 10 K, while it shows little change below ∼1.5 K. The enhancement of the relaxation is moderate, and a Gaussian-like relaxation is sustained even at the lowest temperature. This behavior indicates the existence of a nonmangetic ground state without any magnetic order.

The ZF-μSR time spectra are fitted with a relaxation function $A(t) = AG_{\mathrm{KT}}(\Delta, t)\mathrm{e}^{-\lambda t}$, where $G_{\mathrm{KT}}(\Delta, t)$ is a Gaussian Kubo-Toyabe function that describes a random and static field, Δ the distribution width of the random field, and λ the relaxation rate of the muon spin. The temperature dependences of Δ and λ are shown in Figs. 2(a) and 2(b), respectively. They show similar trends. They are almost independent of temperature above ∼10 K, where the system is paramagnetic. As temperature decreases, both parameters increase simultaneously and saturate at ∼1 K. We note that the spectra cannot be fitted with a constant Δ value in the whole measured temperature range. Such a temperature dependence of the relaxation rate has been reported in a several spin-singlet systems,[4)] and in most cases, the relaxation rate starts to increase concomitantly with the formation of spin-singlet pairs. In the present system, the magnetic susceptibility shows a broad maximum at ∼14 K, and then decreases with decreasing temperature.[1)] Therefore, the ZF-μSR result indicates the appearance of the spin-singlet state in $Rb_2Cu_2Mo_3O_{12}$.

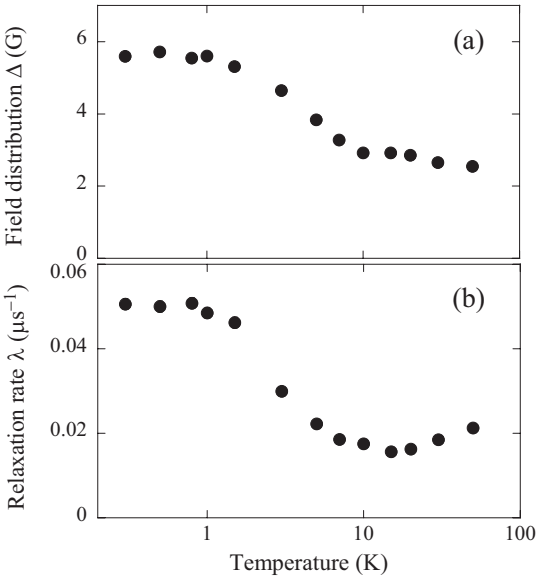

Fig. 2. Temperature dependence of (a) the field distribution width Δ and (b) the relaxation rate λ.

*1 J-PARC Center, Japan Atomic Energy Agency
*2 RIKEN Nishina Center
*3 Department of Physics, Tohoku University

References
1) M. Hase et al., Phys. Rev. B **70**, 104426 (2004).
2) T. Tonegawa and I. Harada, J. Phys. Soc. Jpn. **58**, 2902 (1989).
3) K. Tomiyasu et al., Appl. Phys. Lett. **94**, 092502 (2009).
4) For example, B. W. Lovett et al., Phys. Rev. B **61**, 12241 (2000); S. Ohira-Kawamura et al., J. Phys.: Conf. Ser. **225**, (2010) 012041.

Spin dynamics for p electrons in CsO_2 and NaO_2

D. P. Sari,[*1,*2] R. Asih,[*1,*2] I. Watanabe,[*2] A. Kumar,[*3] and G. Blake[*3]

Alkali metal superoxides (AO_2) such as NaO_2, KO_2, RbO_2, and CsO_2 forming ionic crystals that adopt crystal structures related to rocksalt structures are ideal model system for the study of the p-electron magnetism. The magnetic properties of KO_2 and RbO_2 systems have already been well investigated, unlike those of NaO_2 and CsO_2, because of the ease of fabricating the sample. In a superoxide anion $(O_2)^-$, there is one unpaired spin (S = ½) because three electrons occupy a pair of degenerate antibonding π^* molecular orbitals. AO_2 compounds undergo structural distortion splitting the π^* energy levels and lifting the orbital degeneracy similar to the Jahn-Teller effect for degenerate orbitals. Orbital ordering similar to that found in transition metal systems may be expected, but has scarcely been studied experimentally.

The neutron diffraction, EPR, and AFMR measurements revealed the crystal structure of KO_2, RbO_2, and CsO_2 to be FM in the crystallographic *ab* plane and AFM along the crystallographic *c* axis.

From the NMR study on CsO_2 by Klanjsek et al., a huge, nonmonotonic temperature dependence of the exchange coupling originating from thermal liberations of O_2^- molecules above ~70 K was observed. Tomonaga-Lutingger liquid behavior (~15K – 40K) was observed, in which antiferromagnetic (AFM) spin chains are formed as a result of p-orbital ordering, and then magnetic phase transition occurs again jumping to the ordered Neel state at around ~10 K [1]. The latter supports the prediction of susceptibility measurement in which an anomaly in the magnetic susceptibility was observed around 10 K, indicating a possible crossover from 1D chain character which was fit with the original Boner-Fisher formulation (15 K – 70 K) to 3D AFM ordering [2].

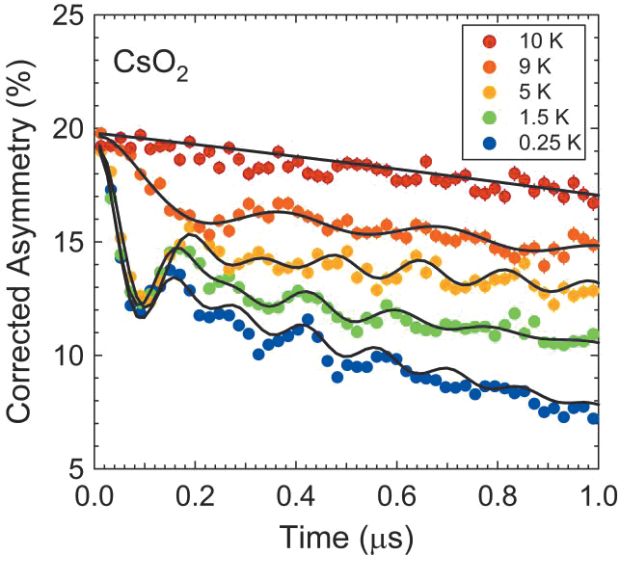

Fig. 1. ZF-μSR time spectrum for CsO_2 for the first microsecond from 10 K down to base temperature.

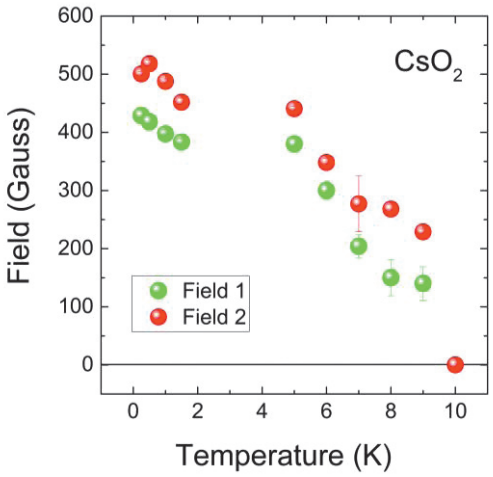

Fig. 2. Internal Field from at least 2 muon sites in CsO_2.

We performed μSR measurement at the Continuous Muon Facility PSI, Switzerland. We obtained time spectra show a non-ordered state still until 10 K and then the internal field appeared at around 8 K from at least 2 muon sites in CsO_2 and tends to increase with decreasing temperature [Figs. 1 and 2]. There is no clear enhancement in the depolarization rate due to the spin dynamics observed around the transition temperature. We confirm that this sample is of good quality based on our susceptibility measurement with a small contribution of the paramagnetic state in the low temperature regime.

The sample quality of NaO_2 revealed by our susceptibility measurement was not very good. We only observed a paramagnetic state from the M-H curve. Unfortunately, we could not obtain μSR data from the PSI for NaO_2 owing to a cryostat problem. We only have ZF-μSR data obtained using the Pulsed Muon at the RIKEN-RAL Muon Facility in the UK. The initial asymmetry from room temperature to 6 K shows a gradually decreasing trend, indicating fast depolarization behavior with a small volume fraction. Furthermore, in the next measurement at the RIKEN-RAL, we plan to determine whether NaO_2 is magnetically ordered in the ground state, like CsO_2.

*1 RIKEN Nishina Center
*2 Department of Physics, Osaka University
*3 Zernike Institute for Advanced Materials, University of Groningen

References

1) M. Klanjsek et al., Phys. Rev. Lett. **115**, 057205 (2015).
2) S. Riyadi et al., Phys. Rev. Lett. **108**, 217206 (2012).

μSR study of spin dynamics in Cu-based organic-inorganic hybrid systems

E. Suprayoga,[*1,*2] A. A. Nugroho,[*2] D. Onggo,[*2] and I. Watanabe[*1]

The muon-site is a very important parameter to study the hyperfine interaction between muon and electrons and to discuss ordered states of electronic spins in magnetic materials. In the previous report,[1] we have estimated muon-sites in organic-inorganic hybrid materials of $(C_6H_5CH_2CH_2NH_3)_2CuCl_4$ (PEA) and $(C_2H_5NH_3)_2CuCl_4$ (EA) by taking into account the minimum electrostatic potential energy based on the density functional theory (DFT). Accordingly, we estimated six muon-site candidates in EA and eight candidates in PEA; nevertheless, only one site was experimentally achieved on both materials with an internal field of around 200 G at 4 K.[2] A new achievement for PEA has been obtained at the RIKEN-RAL muon facilities. The internal field of PEA increases by decreasing the temperature with 240 G at 1.5 K. This result can be used to discuss the magnetic interaction mechanism between magnetic layers in PEA system.

In order to understand the magnetic interaction in EA and PEA systems and to explain the experimental results, we performed DFT and dipole field calculations by using the HOKUSAI, RIKEN supercomputer. To begin with, we put a muon at the minimum potential position in a bulk structure of $2 \times 2 \times 1$ supercell to study the localization of the muon. To obtain the final stable muon position, we made a self-consistency test by using the generalized gradient approximation (GGA) and augmented plane wave (APW) pseudopotential methods as implemented in the VASP package.[3] During the self-consistency, the muon moved to the side of $CuCl_4$ octahedral, pushed the nearest Cu^{2+} ion and deformed the local crystal structure due to change in the local potential around the muon, as shown in Fig. 1 and 2.

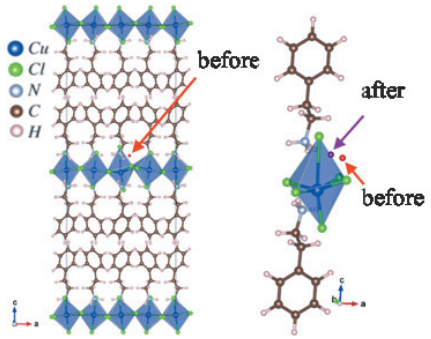

Fig. 1. Local structure deformation of $(C_6H_5CH_2CH_2NH_3)_2CuCl_4$ (PEA) by the injected muon.

*1 RIKEN Nishina Center
*2 FMIPA, Institut Teknologi Bandung

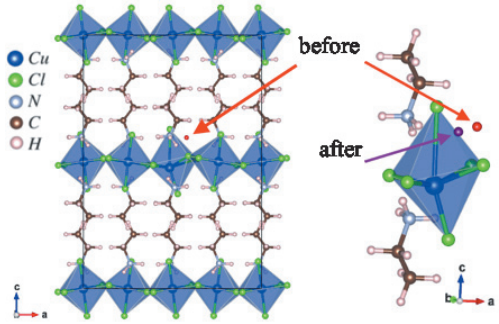

Fig. 2. Local structure deformation of $(C_2H_5NH_3)_2CuCl_4$ (EA) by the injected muon.

In order to confirm our muon-site candidates, we calculated electronic dipole fields at the muon position coming to the magnetic moment of Cu^{2+} spins. We assumed the ferromagnetic spin alignment as previously suggested from the susceptibility measurement[4] and calculated electronic dipolar fields in three different orientations along the a-, b-, and c- axes to find the ground-state condition. We also considered other quantum effects such as the zero-point vibration motion of the muon, the spatial distribution of the magnetic moments, and the deformation of the surrounding electronic orbital by the injected muon.

Our DFT calculation results on both Cu-hybrid systems show the appearance of magnetic moment distribution of Cl^- as well as that of Cu^{2+} ions. We estimated the size of magnetic moment around 0.5 μ_B and 0.1 μ_B for Cu^{2+} and Cl^- ions, respectively, to calculate dipole fields at the muon site. In order to obtain the accurate muon position, we suggested the supercell calculation to see local deformation of the ionic position due to injected muon. Finally, by including those effects, we can compare the experimental results of internal fields at the muon-site in order to determine the spin structure of Cu-hybrid EA and PEA. Detailed calculations and further discussion of the magnetic interaction mechanism between magnetic layers on those hybrids are under way and we expect to obtain the final results and conclusions very soon.

References

1) E. Suprayoga et al.: RIKEN Accell. Prog. Rep. **48**, 267 (2015).
2) A. A. Nugroho et al.: RIKEN Accell. Prog. Rep. **45**, 193 (2012).
3) G. Kresse and J. Furthmuller: Phys. Rev. **54**, 11169 (1996).
4) L. J. De Jongh et al.: Physica **58**, 277 (1972).

Study of frustrated antiferromagnetic states by μSR

M. Abdel-Jawad,[*1] Y. Ishii,[*2] Y. Oshima,[*1] R. Kato,[*1] and I. Watanabe[*3]

A series of organic salts, $(Cation)[Pd(dmit)_2]_2$ (dmit=1,3-dithiole-2-thione-4,5-dithiolate) has a triangular exchange network of S = 1/2 units of molecular dimers[1]. The strength of the spin frustration can be controlled by the choice of the cation. In such triangular magnets, geometrical frustration is thought to play an important role in determining the magnetic state, as the antiferromagnetic (AF) transition temperature is found to increase proportionally to the deviation from the almost regular triangular exchange networks. It is thought that $EtMe_3Sb[Pd(dmit)_2]_2$[2] does not show any AF order owing to strong spin frustrations. The exchange interaction J in these materials is on the order of 200 to 300 K.

Recent longitudinal field (LF) μSR measurements were performed on $EtMe_3Sb[Pd(dmit)_2]_2$, a quantum spin liquid (QSL) candidate. Preliminary analysis suggests that the field dependence of the muon relaxation rate, λ, is proportional to $1/\sqrt{B}$ in a field range of $1 \leq B_{ext} \leq 1000$ G at low-temperatures. Such behaviour is expected from one-dimensional (1D) spin diffusion, a surprising result considering the quasi two dimensional nature of the electronic structure of $Pd(dmit)_2$-based compounds.

To study how geometrical frustration affects the nature of the spin fluctuations, we have performed μSR measurements on $Et_2Me_2P[Pd(dmit)_2]_2$, a Mott insulator with an AF transition of 14 K. Analysis in the paramagnetic temperature region of the μSR spectra was performed using the following formula:

$$A(t) = A_0 \exp(-\lambda t) \times G_{KT}(\Delta, H_{LF}, t)$$

where $G_{KT}(\Delta, H_{LF}, t)$ is the Kubo-Toyabe function, which is due to nuclear dipoles, and λ is the muon depolarization rate, which describes the degree of electron spin fluctuation. Δ values were determined with the zero field (ZF) data and were assumed to be LF independent.

Figure 1 shows that the LF dependence of λ at 100 K in $Et_2Me_2P[Pd(dmit)_2]_2$ is a combination of two different spin fluctuation motions. At low fields, λ follows a power law LF dependence with an exponent of -0.86, a value close to the -1/2 value expected from a spinon 1D spin diffusion motion, whereas at higher magnetic fields a logarithmic dependence of λ emerges, indicative of a purely 2D spin diffusion or 1D ballistic spin motion[3,4]. The inset of Fig. 1 shows that the temperature dependence of λ at ZF, which is dominated by the 1D spin diffusion motion, increases with decreasing temperature in contrast to the temperature dependence of λ at 100 G, which peaks at 100 K and is dominated by 2D spin diffusion or 1D ballistic spin motion. This 100 K maximum of λ at 100 G is interesting as it correlates with the thermoelectric power maximum and the onset of the anomalous dielectric constant[5] of the same compound.

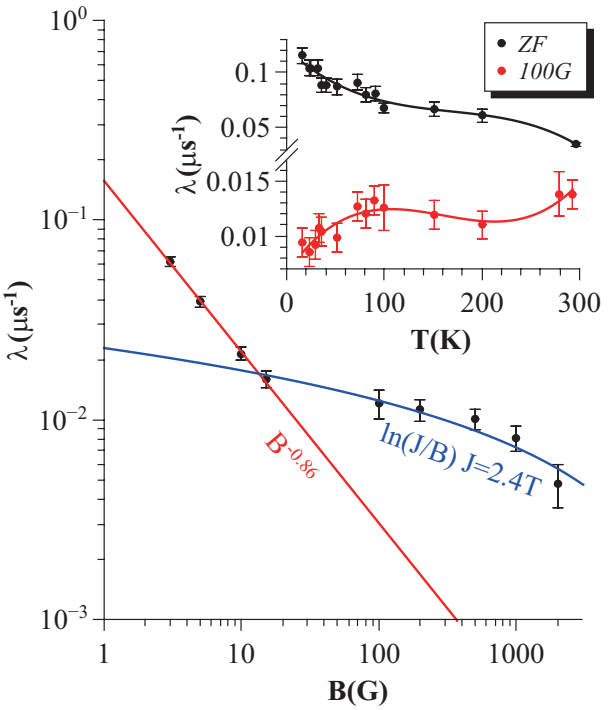

Fig. 1. Dependence of the longitudinal relaxation rate λ on the applied longitudinal field at 100 K in $Et_2Me_2P[Pd(dmit)_2]_2$. (Inset) Temperature dependence of the relaxation rate λ of $Et_2Me_2P[Pd(dmit)_2]_2$ at a zero field and a 100 G longitudinal field.

LF μSR measurements in $Et_2Me_2P[Pd(dmit)_2]_2$ have shown that decreasing geometrical frustration on the spin-liquid level not only increases the AF transition temperature but changes the nature of the spin fluctuations from the purely 1D diffusion motion of a spinon. Further, LF μSR measurements are required to properly quantify the ratio between the two different spin motions, their relation to charge transport, and the degree of geometrical frustration.

*1 Condensed Molecular Materials Laboratory, RIKEN
*2 Shibaura Institute of Technology
*3 RIKEN Nishina Center

References

1) K. Kanoda and R. Kato, Annu. Rev. Condens. Matter Phys. **2**, 167 (2011).
2) M. Yamashita et al., Science, **328**, 1246 (2010).
3) F. L. Pratt et al., Phys. Rev. Lett. **96**, 247203 (2006).
4) F. L. Pratt et al., Physica B **404**, 585589 (2009).
5) M. Abdel-Jawad et al., Phys. Rev. B **88**, 075139 (2013).

Antiferromagnetic ordering in organic $\pi - d$ hybrids [Pd(tmdt)$_2$]

R. Takagi,[*1] I. Watanabe,[*2] S. S. Mohd-Tajudin,[*2,*3] R. Asih,[*2,*4]
K. Kanoda,[*5] S. Ogura,[*6] B. Zhou,[*6] and A. Kobayashi[*6]

Emergent phenomena in the systems of interacting electrons are expected to be more diverse when electrons are accommodated by multi-orbitals with distinctive characters. [M(tmdt)$_2$], a family of organic $\pi - d$ hybrids, are multi-orbital correlated electron systems, where a transition metal ion, M, is coordinated with organic ligands, tmdt, from both sides.[1–3] The orbitals near the Fermi level are a d-orbital in M and π-orbitals in tmdt.[4,5] The energy-level difference between the d and π orbitals depends on M, and leads to the diverse ground states; paramagnetic metals with appreciable electron correlations for M = Ni and Pt, an antiferromagnetic (AF) metal (T_N = 110 K) for M = Au, and a one-dimensional AF Mott insulator (T_N = 13 K) for M = Cu.[6–11]

For the M = Ni, Pt, and Pd compounds, the π and d orbitals are well separated in terms of energy; their conduction bands are composed of only π orbitals. Although the Ni and Pt systems are paramagnetic metals as expected, we recently found that the Pd system was exceptional. It showed a decrease in ESR signal intensity and broadening of the NMR spectra below 100 K.[12,13] A broad peak appeared around 50 K in the temperature dependence of the NMR relaxation rate.[13] These results suggest that an AF ordering inhomogeneously appears in the sample. The inhomogeneously-ordered state might be a long-range-ordered state, which cannot be explained by the band calculation and implies the importance of the electron correlation of the π-orbitals and/or spin-orbit coupling in this system.

In order to achieve full confirmation of the appearance of magnetic ordering and to investigate the magnetic ground state, we carried out zero-field (ZF) μSR measurements on [Pd(tmdt)$_2$] polycrystalline sample in the DOLLY area at Paul Scherrer Institut. Figure 1(a) shows the ZF-μSR time spectra of [Pd(tmdt)$_2$] at various temperatures. It can clearly be seen that the relaxation becomes faster at lower temperatures and that the shape of the relaxation function changes with temperature. At 50 K and 10 K, muon-spin precession signals were observed. This provides clear evidence for the appearance of a long-range-ordered magnetic state in [Pd(tmdt)$_2$] at least below 50 K. The slow relaxation of the non-oscillating signal can originate from tempo-

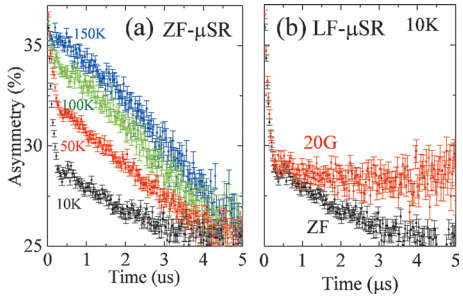

Fig. 1. (a)ZF-μSR time spectra of [Pd(tmdt)$_2$] observed at 10, 50, 100, and 150 K. (b) LF-μSR time spectra observed at 10 K.

rally fluctuating fields and/or small static local fields. To determine whether the spin state in the ground state is static or not and to find the residual spin dynamics, we performed μSR measurements under a longitudinal field (LF). As shown in Fig. 1(b), the slowly relaxing signal was suppressed and became nearly flat on applying a field of 20 G. This indicates the existence of a small static field, thus ruling out the temporally fluctuating fields that are slower than the μSR time scale (10^{-6}–10^{-11} sec). The small static field might originate from the nuclear dipolar fields in a possible paramagnetic volume within the sample. This suggests that the magnetically-ordered state of [Pd(tmdt)$_2$] is a inhomogeneously-ordered state, which is consistent with the preceding NMR and ESR results.

*1 RIKEN Center for Emergent Matter Science (CEMS)
*2 RIKEN Nishina Center
*3 School of Distance Education, Universiti Sains Malaysia
*4 Department of Physics, Osaka University
*5 Department of Applied Physics, University of Tokyo
*6 Department of Chemistry, College of Humanities and Sciences, Nihon University

References

1) A. Kobayashi *et al.*, J. Phys. Soc. Jpn. **75**, 051002 (2006).
2) H. Seo *et al.*, J. Phys. Soc. Jpn. **77**, 023714 (2008).
3) H. Seo *et al.*, J. Phys. Soc. Jpn. **82**, 054711 (2013).
4) S. Ishibashi *et al.*, J. Phys. Soc. Jpn. **77**, 024702 (2008).
5) S. Ishibashi *et al.*, Crystals **2**, 1210 (2012).
6) H. Tanaka *et al.*, Science **291**, 285 (2001).
7) Y. Hara *et al.*, J. Phys. Soc. Jpn. **77**, 053706 (2008).
8) B. Zhou *et al.*, Adv. Mater. **21**, 3596 (2009).
9) B. Zhou *et al.*, Inorg. Chem. **49**, 6740 (2010).
10) R. Takagi *et al.*, Phys. Rev. B **85**, 184424 (2012).
11) R. Takagi *et al.*, Phys. Rev. B **93**, 024403 (2016).
12) S. Ogura *et al.*, unpublished.
13) R. Takagi *et al.*, unpublished.

Solute-vacancy clustering in Al-Mg-Si and Al-Si alloys

K. Nishimura,[*1,*3] K. Matsuda, [*1,*3] T. Namiki,[*1] S. Lee,[*1] N. Nunomura,[*2]
I. Watanabe,[*3] M. A. Jaward,[*3] S. Yoon,[*3] T. Matsuzaki,[*3] and F. L. Pratt[*4]

The Al-Mg-Si (6xxx series) aluminum alloys are in high demand as materials for vehicles because of their low weight, excellent formability and age hardenability.[1,2] The usual process for heat treatment is solution heat treatment at approximately 820 K followed by quick quenching with water, resulting in a supersaturated solid solution (SSSS). After storage at room temperature (called natural aging, NA), the alloy undergoes artificial aging (AA) at around 420 K, leading to a precipitation sequence:[3]
SSSS $\rightarrow$Mg/Si/vacancy cluster $\rightarrow$Guinier Preston (GP) zone $\rightarrow\beta''\rightarrow\beta'\rightarrow\beta(Mg_2Si)$.

It is well known that the early stage of solute clustering of Mg and Si proceeds quite quickly and is completed in less than an hour, even at room temperature.[4-6] A long-standing problem for industries is that NA treatment often results in a negative effect on the mechanical strength in the following AA.[3,7] The microstructures of the precipitations have been studied intensively using transmission electron microscopy (TEM)[8] and atom probe tomography (APT)[9] to reveal the age hardening mechanism. These techniques, however, require time consuming sample preparation; thus, it is difficult to directly observe the early stage of clustering. Differential scanning calorimetry (DSC)[10] has been widely used to investigate precipitation processes and cluster formation, but in principle, this method cannot be used for isothermal measurements because the peak positions in a heat flow spectrum depend on the heating rate. From various studies on Al-Mg-Si alloys, it has been found that vacancy behavior is considered to play an important role in the aging process, enhancing the diffusion of solute Mg and Si atoms and nucleation of clusters. Positron annihilation spectroscopy (PAS)[5,6] and muon spin relaxation spectroscopy (μSR)[11,12] have been successfully used to investigate the vacancy and clustering behavior in Al-Mg-Si alloys.

New observations of time dependent muon spin relaxation of an Al-1.6%Mg_2Si alloy at the isothermal condition at 280 K, 290 K, and 300K are presented in this report. All the samples underwent heat treatment at 848 K for 1 h and subsequent quenching in ice water (STQ). Approximately 10 min after STQ, the sample was inserted in an ARGUS muon spectrometer, and then, zero-field μSR measurement was performed at a constant temperature. The observed spin relaxation spectra were fit using a Gaussian function with standard deviation $1/\sigma$ using the WIMDA program,[13] where σ is a measure of the depolarization rate of the muon spins. The deduced values of the muon spin depolarization rates at 280 K showed little change in the time range between 20 and 100 min, then gradually decreased with time, and finally decreased linearly in a logarithmic time scale about 400 min after STQ. The depolarization rates at 290 K decreased slowly with time in the early stage till about 30 min, and then decreased linearly in a logarithmic time scale. Those at 300 K decreased in a logarithmic time scale from the early stage, but there are three different time regions. These time variations of the depolarization rates are quite similar to those of the positron annihilation lifetime in Al-Mg-Si alloys,[5] thus, they can be interpreted in terms of the clustering kinetics of a Mg/Si/vacancy. From an Arrhenius plot of the relaxation rates against the reciprocal measured temperature, the activation energy for clustering of Mg or Si atoms in an Al-1.6%Mg_2Si sample is deduced.

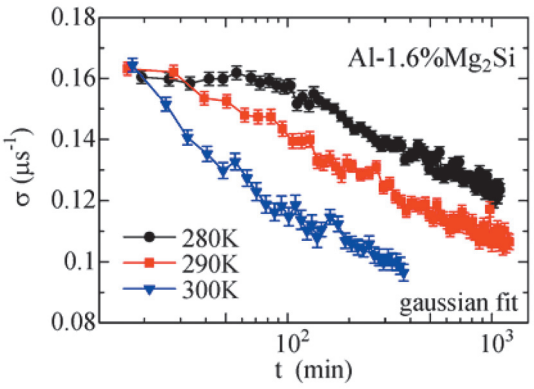

Fig. 1. Aging time dependences of zero-field spin relaxation rate for Al-1.6%Mg_2Si sample at constant temperatures of 280, 290, and 300 K.

*1 Department of Materials Science and Engineering, U. Toyama
*2 Information Technology Center, U. Toyama
*3 RIKEN Nishina Center
*4 ISIS Facility, RAL

References

1) K. Matsuda et al., Mater. Trans. **43**, 2789 (2002).
2) T. Moons et al., Scripta Mater. **35**, 939 (1996).
3) S. Pogatscher et al., Acta Mater. **59**, 3352 (2011).
4) H. Seyedrezai et al., Mater. Sci. Eng. **A525**, 186 (2009).
5) J. Banhart et al., Phys. Rev. B **83**, 014101 (2011).
6) A. Somoza et al., Phys. Rev. B **61**, 14454 (2000).
7) S. Pogatscher et al., Phy. Rev. Lett. **112**, 225701 (2014).
8) C. D. Marioara et al., J. Mater. Sci. **41**, 471 (2006).
9) M.W. Zandbergen et al., Acta Mater. **101**, 136 (2015).
10) S. Kim et al., Mater. Trans. **54**, 297 (2013).
11) S. Wenner et al., Phys. Rev. B **86**, 104201 (2012).
12) S. Wenner et al., Acta Mater. **61**, 6082 (2013).
13) F. L. Pratt, Physica B**289,** 710 (2000).

Li-ion diffusion in Li-ion battery material $LiFe_{1-x}Mn_xPO_4$

I. Umegaki,[*1] H. Nozaki,[*1] G. Kobayashi,[*2] R. Kanno,[*3] M. Månsson,[*4] A. Berlie,[*5] I. Watanabe,[*5] and J. Sugiyama[*1]

For the development of on-board batteries, the Li-ion battery is required to operate at high voltages. For realizing a practical Li-ion battery, a solid solution of the olivine-type lithium iron/manganese phosphate ($LiFePO_4$ and $LiMnPO_4$) is used as the positive electrode material. Olivine lithium phosphate is superior in terms of stability and is a low cost material. The tetrahedron PO_4 is so stable that oxygen desorption hardly occurs. Compared to other positive electrode materials such as $LiCoO_2$, olivine lithium phosphate is produced at a low cost because it contains no transition metals. High charge/discharge voltage can be steadily obtained for the $Li(Fe,Mn)PO_4$ solid solution. It is noted that the $LiFe_{1-x}Mn_xPO_4$ (x∼0.7) solid solution is used for the realization of a practical Li-ion battery.

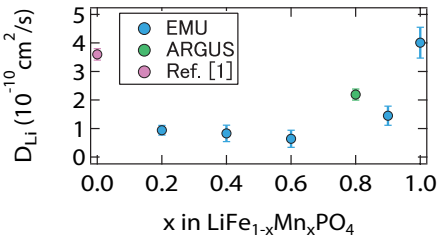

Fig. 1. x dependence of the D_{Li} at 300 K. The data for $x = 0$ is reported in Ref. 1 and the data for $x = 0.2, 0.4, 0.6, 0.9$ and 1 have been obtained with EMU spectrometer in ISIS.

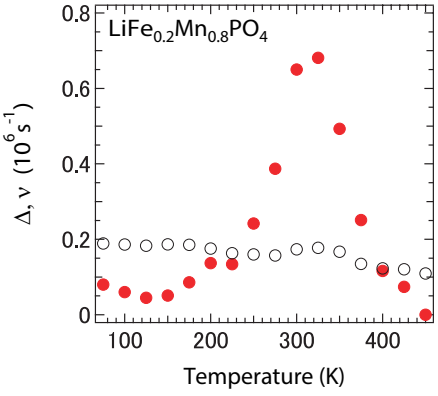

Fig. 2. Temperature dependences of (a) Δ(open circle) and (b) ν (closed circle) obtained for $LiFe_{0.2}Mn_{0.8}PO_4$.

We investigated Li diffusion in $LiFePO_4$ and $LiMnPO_4$ by μ^+SR[1]. However, we could not obtain information about Li diffusion for $LiMnPO_4$, because μ^+SR spectra were strongly affected by magnetic moment of Mn^{2+}. Although the diffusive nature of Lithium is represented in the dynamic Kubo-Toyabe (KT) type relaxed signal in zero field (ZF) μ^+SR measurements, the small changes in KT signal are hidden by fast relaxed signal caused by the magnetic moment of Mn^{2+}. In order to avoid the magnetic effect due to Mn^{2+}, we meausred μ^+SR spectra on $LiFe_{1-x}Mn_xPO_4$ with smaller x to presume the Li diffusive nature in $LiFe_{1-x}Mn_xPO_4$ with larger x (Fig. 1).

In order to investigate Li-ion diffusion in the solid solution similar to the one used in the practical battery, we measured μ^+SR spectra on $LiFe_{0.2}Mn_{0.8}PO_4$. In x=0.8 samples, the ZF-μ^+SR spectrum is fitted by the sum of the exponentially relaxed static KT function and fast relaxation, asumming the volume fraction determined for smaller x as the initial value. Then, the ZF-μ^+SR spectrum exhibits dynamic KT function at temperatures above 150 K. By fitting the ZF- and LF-spectra with a dynamic KT function, the field fluctuation rate (ν), relaxation rate (λ) and the field distribution width (Δ) were obtained. For x=0.8, ν rapidly starts to increase and Δ starts to decrease at 150 K (Fig. 2). This indicates that Li-ion diffusion occurs above 150 K. The diffusion coefficient is estimated as $D_{Li} = 2.1\times10^{-10}(cm^2/s)$ at 300 K.

By utilizing ARGUS spectrometer to obtain a large asymmetry for the KT signal, we obtained additional data to the systematic results taken with EMU spectrometer for the solid solution, $LiFe_{1-x}Mn_xPO_4$ with x =0.2 - 1. There appers to be a peak in D_{Li} between x=0.6 and x=1 (Fig. 1). However, we cannot conclude that D_{Li} has a small peak around x=0.8 since we have measured only for x=0.6 and 0.9. We would like to study in detail the region between x=0.6 - 0.9, since the composition is very close to that used in a practical Li-ion battery.

We also measured μ^+SR spectrum on x=0 sample, however, the obtained data was unsatisfactory. It is reported in Ref. 1 that D_{Li}=$3.6\times10^{-10}(cm^2/s)$ at 300 K. Since D_{Li} changes drastically between x=0 and 0.2, we need to try to confirm such large changes.

The activation energy E_a was estimated from the relation E_a=$k_BT\ln(\nu)$ to be 53.0 meV for x=0.8. There may be a peak in E_a between x=0.6 and 1 (not shown).

*1 Toyota Central Research and Development Labs., Inc.
*2 Institute for Molecular Science
*3 Tokyo Institute of Technology
*4 KTH Royal Institute of Technology
*5 RIKEN Nishina Center

Reference
1) J. Sugiyama et al., Phys. Rev. B **85**, 054111 (2012).

Development of RF cavity for MuSEUM experiment in a zero magnetic field

K. S. Tanaka[*1,*2] on behalf of J-PARC MuSEUM Collaboration

The MuSEUM (Muonium Spectroscopy Experiment Using Microwave) group is planning to measure the energy of the ground state hyperfine structure (HFS) of muonium at J-PARC/MLF[1]. Muonium is a hydrogen-like bound state that consists only of leptons, and its HFS is a good probe for testing the QED theory. The latest experiment at LAMPF obtained the following value:[2]

$$\Delta_{\mathrm{Mu}}^{\mathrm{ex}} = 4.463302765(53)\ \mathrm{GHz}\ (12\ \mathrm{ppb})\ . \qquad (1)$$

The total precision was limited by the statistical uncertainty. We will achieve a precision more than 10 times better than that of the latest experiment by using the high intensity muon beam provided at J-PARC/MLF. We plan to measure muonium HFS in a zero magnetic field at D Line[3] and in a high magnetic field at H Line.

The measurement procedure of the experiment is as follows:

- Muons with their spins polarized to the upstream direction are provided from J-PARC/MLF muon beam line.
- RF cavity located in the center of the magnet containing pure Krypton gas. Muons stop by collisions in the gas and polarized muonium are formed by electron capture process with Krypton.
- High momentum decay positrons are emitted preferentially in the direction of the muon spin. By driving the transitions with an applied microwave magnetic field, the muon spin can be flipped and the angular distribution of high momentum positrons is changed from predominantly upstream to downstream with respect to the beam direction.

In this paper, the development of the RF cavity for the zero field experiment is described.

Figure 1 shows the cavity for zero field experiment. The inner diameter of the cylindrical cavity for the zero field experiment is tuned so that the resonance frequency of the TM110 mode matches the transition frequency of muonium HFS of 4.463 GHz. Frequency sweep is enabled in the range of 20 MHz by the insertion system of a tuning bar made of conductive material.

A microwave is delivered by a coaxial cable and coupled into the cavity by the input loop. The microwave power in the cavity is picked up by a loop coil and measured by the thermal power sensor (R&S NRP-Z51). The measured power is feedback to the signal generator to stabilize the input microwave power at a level of 0.02 % which brings no systematic uncertainty.

Figure 2 shows the dependence of resonance frequency on the displacement of the tuning bar. The red line shows the transition frequency of the hyperfine splitting and the red band shows the sweep range of the measurement. As shown in this figure, tunability of the cavity is enough for the measurement.

Thus, the RF system for the zero field experiment is ready. We will start the first measurement of muonium HFS in a zero field in 2016.

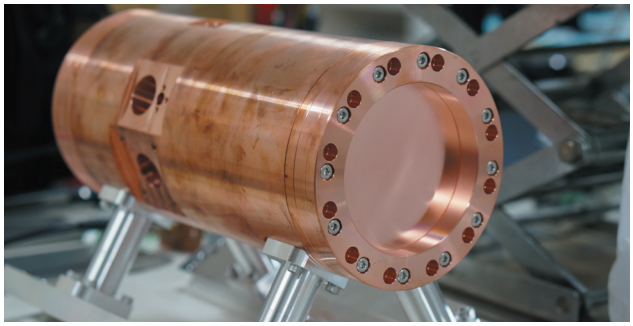

Fig. 1. Photo of the cavity for zero field experiment. The inner radius is 41 mm and the axial length is 230 mm.

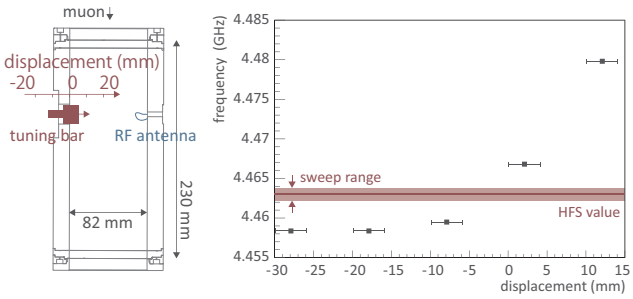

Fig. 2. The left figure shows the cross-sectional view of the cavity. The tuning bar is inserted from the side surface to tune the resonance frequency of the cavity. Right figure shows the relation between the resonance frequency and the displacement of the tuning bar. The red line shows a transition frequency of HFS and the red band is a sweep range to observe the resonance line shape.

*1 RIKEN Nishina Center
*2 Graduate School of Arts and Sciences, University of Tokyo

References

1) K. S. Tanaka on behalf of MuSEUM Collaboration.: RIKEN Accel. Proog. Rep. **47**, 277 (2014).
2) W. Liu *et al.*, Phys. Rev. Lett. **82**, 711 (1999).
3) S. Kanda on behalf of MuSEUM Collaboration.: in this report.

Development of magnetic shield for the MuSEUM experiment

S. Kanda[*1,*2] for the MuSEUM Collaboration

Muonium is a hydrogen-like atom consisting of a positive muon and an electron. Precision spectroscopy of its ground state hyperfine splitting (HFS) is the most stringent test of bound-state QED theory and the most precise determination of the muon mass. At J-PARC, the MuSEUM (Muonium Spectroscopy Experiment Using Microwave) collaboration is planning a new measurement of muonium HFS proceed in two stages; indirect measurement under a 1.7 T high magnetic field and direct measurement under a precise controlled zero magnetic field. The zero-field experiment is a preliminary measurement with existing facility toward the definitive high-field experiment, which requires a new muon beam line under construction. Our goal is to improve the precision of muonium HFS by about one order of magnitude in both experiments.

Spectroscopy of muonium HFS is performed by the measurement of positron angular asymmetry from muonium decay, which depends on the muonium energy state. The hyperfine transition is induced by microwave and muon spin flips when the transition occurs. Result of the most recent zero-field experiment[1] is 4.463022 (1.4) GHz (300 ppb) where the error is the statistical uncertainty. In the zero-field measurement of muonium HFS, one of the major sources of systematic uncertainty is the non-uniformity of a magnetic field in the muonium formation volume. According to the numerical simulation, requirement for the field non-uniformity is less than 100 nT peak-to-peak.

To perform the zero-field experiment, we developed muon and positron detectors[2], three-dimensional muon stopping distribution imager[3], RF cavity[4], magnetic field monitor, and magnetic shield of permalloy (high-permeable alloy of nickel and iron). Figure 1 shows the developed magnetic shield and field probe with a moving system. The shield was designed based on the results of a stray field analysis by the finite-element method. It consists of a three-layered box made of permalloy where the layer thickness is 1.5 mm and interlayer distance is 50 mm. The magnetic field strength is measured by a high-precision fluxgate probe (MTI FM3500) with a resolution of 0.5 nT. Without shielding, the typical magnetic field strength in the target volume was 100 μT and field non-uniformity was about 20 μT peak-to-peak.

Figure 2 shows the measurement result of the stray field inside the magnetic shield. The magnetic probe was moved on the beam-axis. The target volume corresponds to the probe position ranging from -150 mm to 80 mm. Typical field strength was suppressed to about 150 nT. A shielding factor, i.e., the ratio of the field strength with magnetic shield $B_{\rm w}$ and without shield $B_{\rm wo}$ was estimated at $B_{\rm wo}/B_{\rm w} = 700$. The field non-uniformity was about 30 nT peak-to-peak and the performance specification of the magnetic shield satisfied the requirement.

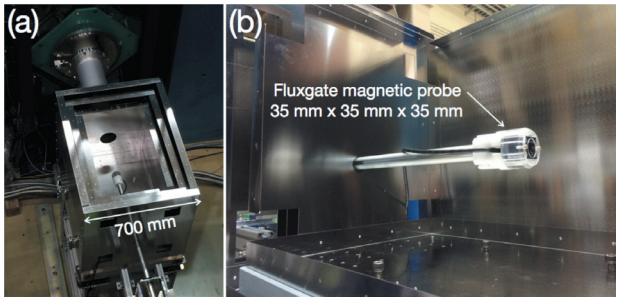

Fig. 1. Magnetic shield and fluxgate probe

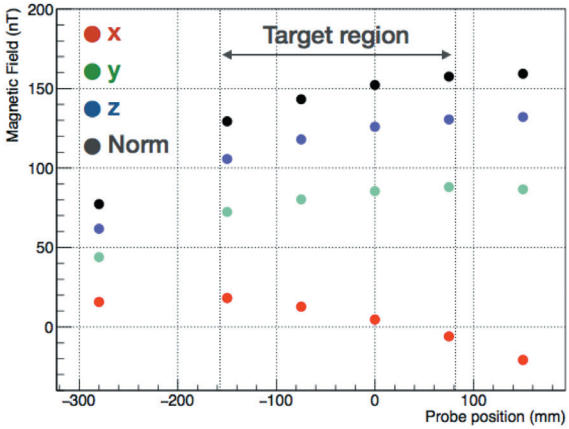

Fig. 2. Magnetic field distribution

The measured field non-uniformity was acceptable for the experiment. However, a factor of two higher shielding factor is expected from the simulation and laboratory measurement results. The field investigation implied that the shield is magnetized by the environmental magnetic field during assembly. Magnetization of inner layers of the shield should be suppressed by the attenuation current supplied by the degaussing coils. The degaussing device and method are under study. The development of every other experimental component has been completed and the first trial of zero-field measurement is scheduled in Feb. 2016 at J-PARC MLF MUSE.

*1 Department of Physics, University of Tokyo
*2 RIKEN Nishina Center

References

1) D.E. Casperson *et al.*, Phys. Lett. B, **59**, 397 (1975).
2) S. Kanda *et al.*, JPS Conf. Proc. **8**, 025006 (2015).
3) S. Kanda *et al.*, KEK-MSL Prog. Rep. 2014, 46 (2015).
4) K.S. Tanaka., In this report.

Ultra-slow muon production at the RIKEN-RAL muon facility based on muonium emission from silica aerogel

S. Okada,[*1] S. Aikawa,[*1] G. Beer,[*2] J. Brewer,[*3] K. Ishida,[*1] M. Iwasaki,[*1] S. Kanda,[*4] H. Kawai,[*5] R. Kitamura,[*4] Y. Ma,[*1] G. Marshall,[*3] T. Mibe,[*6] Y. Oishi,[*1] A. Olin,[*3] M. Otani,[*6] N. Saito,[*6] M. Sato,[*1] M. Tabata,[*5] and T. Tsukihana[*7]

Positive muons having an energy of a few eV, the so-called ultra-slow muons, are generated by laser ionization of thermal muonium atoms (Mu) in vacuum. By accelerating them through an electrostatic field, a variable-energy muon beam with an extraordinarily small energy spread can be realized[1,2]. This technique has therefore attracted attention for advanced μSR studies and for measurement of the muon anomalous magnetic moment, g-2, and electric dipole moment at J-PARC[3].

One of the key issues with ultra-slow muon production is how to generate more Mu in vacuum. Recently, we successfully observed Mu emission into vacuum from a silica aerogel with a uniform surface[4], and subsequently realized that a silica aerogel having a non-uniform structure with hole-like regions created by laser ablation leads to an emission that is higher than that for uniform one by one order of magnitude[5]. Compared to the conventional tungsten heated to 2300 K[1,2], this room-temperature silica-aerogel has significant advantages: it is easy to handle because of no significant heat radiation; its lower Mu energy distribution leads to a smaller emittance of the ionized source; its smaller spatial spread and smaller Doppler broadening results in more efficient use of the available laser power.

As the next step, we will perform a demonstration and R&D study of the actual ultra-slow muon production using a silica-aerogel target at the RIKEN-RAL muon facility (Port 3). The new experimental setup is shown in Fig. 1. Ultra-slow muons will be extracted at an angle of 45-degrees to avoid a straight beam background with a rotationally-symmetric electrostatic field (SOA lens); these muons will be detected by a Micro-Channel Plate (MCP) detector with a slit system to evaluate the beam characteristics. The Mu spin is controlled using three-axis Helmholtz coils. A μSR counter set is used for measurement of the Mu production rate, control of Mu spin and optimization of stopping.

Commissioning runs without the laser system were peformed in September and December 2015. After installing the laser system in early 2016, we plan to produce the first ultra-slow muon beam with an aerogel target. Then, we hope to start optimization towards a higher yield with the shape of the structured aerogel target and by efficiently increasing the Lyman-α irradiation using reflection mirrors installed near the target.

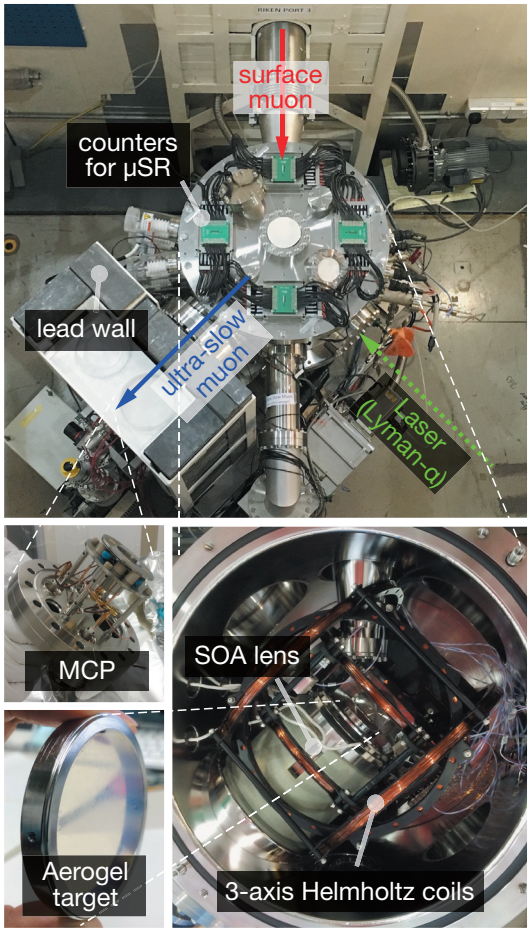

Fig. 1. New experimental setup at the Port 3 beam line of the RIKEN-RAL muon facility for ultra-slow muon study based on muonium emission from a silica aerogel target.

*1 RIKEN Nishina Center
*2 Department of Physics and Astronomy, UVic
*3 Science Division, TRIUMF
*4 Department of Physics, The University of Tokyo
*5 Department of Physics, Chiba University
*6 IPNS, KEK
*7 RIKEN Center for Advanced Photonics

References

1) K. Nagamine et al., Phys. Rev. Lett. **74**, 4811 (1995).
2) P. Bakule et al., NIM B **266**, 355 (2008).
3) M. Aoki et al., Conceptual Design Report for The Measurement of the Muon Anomalous Magnetic Moment g−2 and Electric Dipole Moment at J-PARC, (2011).
4) P. Bakule et al., Prog. Theor. Exp. Phys. 103C01 (2013).
5) G. A. Beer et al., Prog. Theor. Exp. Phys. 091C01 (2014).

Development of a slow muon detection system for a muon acceleration

R. Kitamura[*1,*2] for the J-PARC muon g-2/EDM Collaboration

The measured value of the muon anomalous magnetic moment (g-2) differs from the theoretical value by about three standard deviations[1]. Given that muon anomalous magnetic moment may provide important evidence for the physics beyond the Standard Model, more precise measurements are awaited. A new experiment for the precise measurement of the g-2 and the search for the muon EDM using novel techniques has been planned at J-PARC. One of the most important techniques is the world's first muon RF acceleration to 212 MeV.

For efficient beam capture in the RF accelerator, the input muon beam should have low emittance and low energy (5.6 keV in our case). The conventional surface muon beam typically has 4 MeV energy and large emittance; therefore we plan to develop the low-emittance input beam by using the following method. The muon beam is irradiated onto a thin metal foil. Some of the muons are decelerated to the sub-keV[2] band after passing the foil. Subsequent acceleration to 5.6 keV by an electro-static "SOA lens" will give us a low-emittance beam.

An experiment to establish the muon deceleration and electro-static acceleration was planned in Feb. 2016. Figure 1 shows the experimental setup. After deceleration and acceleration, the muons are transported to the detection system by a series of electro-static quadrupoles and an electro-static bending. The detection system consists of a microchannel plate (MCP) surrounded by scintillation counters with MPPCs. In this paper, we report on the development of the slow muon detection system.

The MCP counts the number of muons with energy in the order of a few keV. The gains of MCP for several kinds of particles including low-energy electrons were measured in order to confirm the muon detection capability[3]. The measured gain for the electron with 500 eV was 2.1×10^7 and is sufficiently large for the detection. The gain depends on the number of secondary electrons generated by the bombardment of the incident particle on the surface of the MCP. The estimated number of secondary electrons for the low-energy muon is expected to be more than that for the electron based on our measurements and the calculation of the energy deposit. We conclude that the expected gain for the muon is sufficiently high to count the low-energy muons.

The scintillation counters are utilized for muon identification by detecting the decay positron from the muon stopped in the MCP. A large acceptance and a large light yield are required to detect as many decay positrons as possible with high efficiencies. The positron counters consist of plastic scintillators, wavelength shifting fibers, and MPPCs to satisfy those requirements. In the cosmic-ray test, we observed the mean light yields of more than 120 photo emissions and obtained counting efficiencies of more than 99.8 % with 90 % confidence level[4].

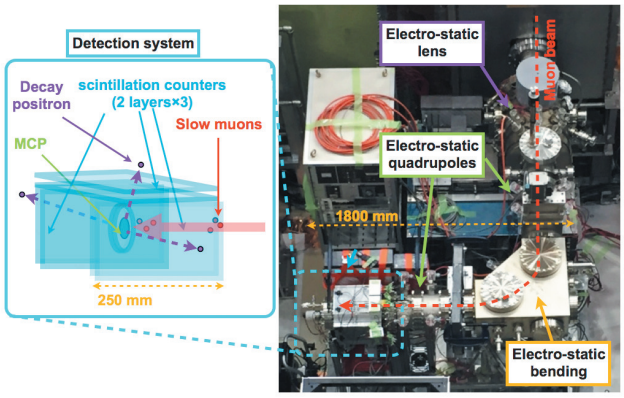

Fig. 1. Detection system for the slow muons comprising detectors (MCP and decay positron counters), the electro-static lens, and the electro-static bending.

Finally, the expected signal and background rates were evaluated using the GEANT4 simulation. The simulation showed that the dominant backgrounds at the MCP were decay positrons from incident beam muons; many muons were stopped at the thin metal foil used for the deceleration or the electro-static bending, and subsequently the decay positrons directly impacted the MCP. A lead shield configuration was optimized with the simulation in order to reject these positron backgrounds. The noise to signal ratio after the optimization was evaluated to be 4.9×10^{-3}. We concluded that it is sufficiently low for the experiment.

In summary, we developed two kinds of detectors, MCP and positron counters, to measure the intensity of the slow muons. We confirmed their good performances and we are ready for demonstration with the muon beam.

*1 RIKEN Nishina Center
*2 Department of Physics, University of Tokyo

References
1) G.W.Bennett *et al.*, Phys. Rev. D **73**, 072003 (2006).
2) Y. Kuang *et al.*, Phys. Rev. A **35**, 3172 (1987).
3) R. Kitamura *et al.*: The JPS 2015 Annual Meeting, 2015, 21aDF8 (2015)
4) R. Kitamura *et al.*: The JPS 2015 Autumn Meeting, 2015, 25aSG7 (2015)

FAMU experiment: studies on the muon transfer process in a mixture of hydrogen and higher Z gas

A. Vacchi,[*1,*2] E. Mocchiutti,[*1] D. Guffanti,[*1,*3] on behalf of the FAMU collaboration

The final objective of the FAMU experiment is to measure the proton Zemach radius by measuring the hyperfine splitting of the μp ground state[1), 2)]. The experimental method requires a detection system suited for time resolved X-ray spectroscopy. The results of the first measurements performed at the RIKEN-RAL muon facility are presented in this paper.

The characteristic X-rays from muonic atoms formed in different targets have been detected using a HPGe detector and five scintillating counters based on LaBr3(Ce) crystals, whose output was recorded for 5 μs using a 500 MHz digitizer to measure both energy and time spectrum of the detected events. With a detailed pulse analysis, considering also the pile-up events, the expected characteristic X-rays and lifetimes of various elements were measured.

The measurement of the Zemach radius of the proton Rp was measured in ordinary hydrogen; therefore, a comparison with the value extracted from muonic hydrogen may reinforce or delimit the proton radius puzzle. In the proposed laser spectroscopy experiment[3), 4)], muonic hydrogen atoms are formed in a hydrogen gas target. In subsequent collisions with H2 molecules, the μp de-excite to the thermalized μp in the (1S) F =0 state. A laser tuned on the HFS resonance induces singlet-to-triplet transitions; therefore, the μp atoms in the (1S) F =1 state are de-excited back to the singlet state and the transition energy is converted into additional kinetic energy of the μp system. Thus the μp atom gains about two-thirds of the hyperfine transition energy (≈ 120 meV).

The energy dependence of the muon transfer from muonic hydrogen to another higher-Z gas is exploited to detect the occurred transition in μp. Although in theory, the muon-transfer rate at low energies λpZ is energy independent, this is not the case for few gases. Oxygen[5), 6)] exhibits a peak in the muon transfer rate λ_{pZ}^{epith} at the epithermal energy. Thus, by adding small quantities of oxygen to hydrogen, one can observe the number of HPF transitions, which take place from the muon-transfer events, by measuring the time distribution of the characteristic X-rays of the added gas.

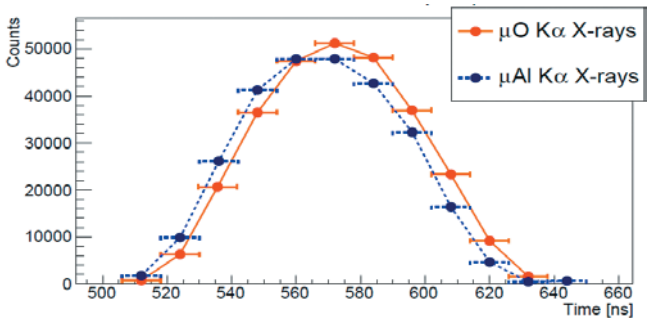

Fig. 1. Time difference between prompt signal (Aluminium X-rays) and delayed signal (Oxygen X-rays).

In the first FAMU experimental test, four different targets were exposed to the muon beam: a pure graphite block and three gas mixtures (pure H2, H2+2%Ar, H2+4%CO2) contained in an aluminum vessel. The aim was to study detector response in the environment of the muon beam at RIKEN-RAL through the measurement of the muon transfer rate at room temperature.

The characteristic X-rays of muonic atoms were detected using scintillating counters based on LaBr3(Ce) crystals (energy resolution 2.6% at 662 keV and decay time τ = 16 ns) readout by Hamamatsu R11265-200 PMTs and two HPGe detectors were used to obtain a benchmark spectrum. Hence, the waveforms were processed off-line to reconstruct the time and energy of each detected X-ray. By studying the differences between the time distribution (see Fig. 1) of prompt events, represented by X-rays originating from μAl atoms formed in the vessel and the delayed X-rays emitted by μO(Ar), atoms it was possible to measure the muon transfer rate from hydrogen to oxygen (argon). The results will be submitted for publication in an international journal.

At present, the collaboration is focussed on the measurement of the temperature dependence of the muon transfer rate by the mean of the cryogenic target in order to determine the best high-Z gas type, concentration and temperature. The experiment is on-going at RIKEN RAL. Figure 2 shows the top view of the apparatus. Beam pipe is on the left and the target is surrounded by the hodoscope, 9 LaBr3(Ce), four HPGe, and three lutetium aluminate detectors. Measurement of the Zemach radius with laser setup will be carried out in 2017.

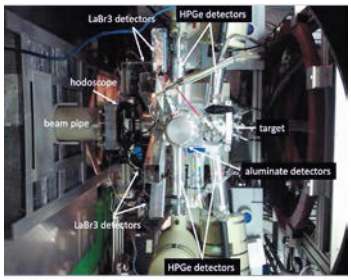

Fig. 2. FAMU, 2016 layout.

References

1) D. Bakalov, C. Rizzo et al., Phys. Lett. A172 (1993).
2) D. Bakalov, A. Adamczak et al., NIM B281 (2012).
3) D. Bakalov, A. Adamczak et al., Hyperfine Interact. 136-137 (2001).
4) D. Bakalov, A. Adamczak et al., Phys. Lett. A379 (2105).
5) F. Mulhauser, H. Schneuwly, Hyperfine Interact. 82 (1993).
6) A. Werthmüller, A. Adamczak et al., Hyperfine Interact. 116 (1998).

*1 INFN Trieste and RIKEN Nishina Center
*2 Department Math, Info, Physics, University of Udine
*3 INFN GSSI

Development of mid-infrared laser for the measurement of muonic hydrogen atom hyperfine splitting energy

S. Aikawa,[*1,*2] K. Ishida,[*2] M. Iwasaki,[*1,*2] S. Kanda,[*4] Y. Ma,[*2] Y. Matsuda,[*5] T. Matsuzaki,[*2] K. Midorikawa,[*3] Y. Oishi,[*2,*6] S. Okada,[*2] M. Sato,[*2] N. Saito,[*3] A. Takamine,[*2] K. Tanaka,[*2,*5] H. Ueno,[*2] S. Wada,[*3] and M. Yumoto[*3]

Recently, the proton charge radius was measured using laser spectroscopy of the 2*s*-2*p* Lamb shift in muonic hydrogen (μp). Laser spectroscopy of μp resulted in 10 times higher precision of the proton charge radius determination than that of the ordinary measurements such as e-p scattering and hydrogen spectroscopy.[1)] As verification of the charge radius measurement, e-p scattering experiments were conducted at Mainz[2)] and the Jefferson Lab[3)], but the discrepancy in the results was not resolved. This raised a question as to whether the magnetic radius of the proton measured with muons will be consistent with that measured by electrons. Thus, we plan an independent measurement of the proton structure, i.e., the Zemach radius, to answer this question by using the hyperfine transition from singlet to triplet in the 1*s* state of muonic hydrogen atoms using the laser-spin-pumping method.[4)]

Two important requirements of the laser in this experiment are a high energy and narrow spectrum width. We need to generate pulse energy exceeding 40 mJ at 6.7 μm. In addition, a narrow spectrum width of 50 MHz is required. A mid-infrared laser system that produces pulse energy of 10 mJ at 6.1 μm has already been developed at RIKEN.[5)]

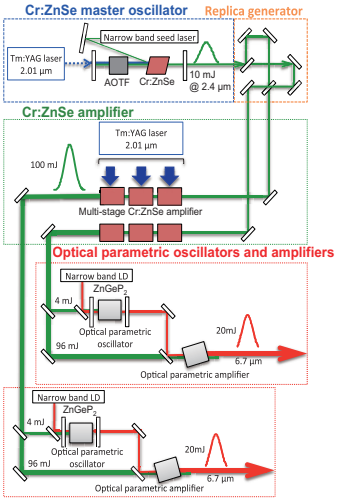

Fig. 1. Schematic of the laser

Based on this, we plan to construct a new laser system. The schematic of the laser is shown in Fig. 1. The laser system consists of a Cr:ZnSe master oscillator, Cr:ZnSe power amplifiers, and optical parameteric oscillators (OPOs) / amplifieers (OPAs). The Cr:ZnSe master oscillator and the power amplifier generate 100 mJ pulse energy per line at 2.4 μm. The pulse is introduced to the $ZnGeP_2$ nonlinear crystal (ZGP) OPO to achieve radiation at 6.7 μm. Two independent optical parametric oscillators and amplifiers will be prepared to achieve 40 mJ laser power in total and avoid damages to the ZGP crystal, which is difficult to synthesize with a large diameter. To realize a narrow band spectrum width of 50 MHz, we will introduce a single mode laser diode (LD) of 100 kHz as a seed laser. In this paper, we report the output characteristics of a Cr:ZnSe master oscillator (laser) and a single pass Cr:ZnSe power amplifier.

Figure 2 shows the output energy of the Cr:ZnSe laser. A maximum pulse energy of 5.8 mJ was obtained at 2.4 μm with a pump energy of 18 mJ. The conversion efficiency reached 32% at maximum. This value is excellent compared with those of other lasers for example, the Ti:Al_2O_3 laser and Nd:YAG laser.

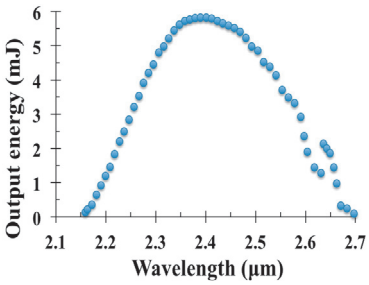

Fig. 2. Output energy of the for Cr:ZnSe laser

The output enegy extracted from the Cr:ZnSe power amplifier is shown in Fig. 3. The incident energy from the Cr:ZnSe laser was 5.5 mJ at 2.4 μm, and it was amplified to 26.3 mJ with increasing pump energy. A maximum conversion efficiency of 41.5 % was obtained with a pump energy of 50.2 mJ. This is, to the best of our knowledge, the highest conversion efficiency ever attained for a single-pass Cr:ZnSe power amplifier.

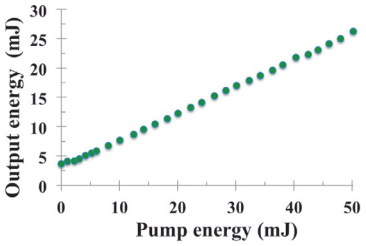

Fig. 3. Output energy extracted from the Cr:ZnSe power amplifier.

Based on the above results, to obtain an energy of 100 mJ at 2.4 μm, we need a pump energy of 240 mJ. However, if we introduce such an energy to the Cr:ZnSe, it will be damaged because the damage threshold on the surface of Cr:ZnSe is about 90 mJ. Therefore, we will construct three-stage Cr:ZnSe power amplifiers to solve this problem.

In the next stage, we will optimize the conversion efficiency of the Cr:ZnSe laser and the power amplifiers by controlling the crystal length and Cr^{2+} concentration. In addition, we will construct a three-stage Cr:ZnSe power amplifier and an OPO to generate radiation at 6.7 μm.

*1 Department of Physics, TokyoTech
*2 RIKEN Nishina Center
*3 RIKEN Center for Advanced Photonics
*4 Department of Physics, The University of Tokyo
*5 Graduate School of Arts and Science, The University of Tokyo
*6 IMSS, KEK

References

1) R. Pohl et al., Nature 466, 213 (2010).
2) J. C. Bernauer et al., Phys. Rev. Lett.105 242001 (2010).
3) X. Zhan et al., Phys. Lett. B705 59 (2011).
4) M. Sato et al., JPS Conf. Proc., 025005 (2015)
5) M. Yumoto et al., OSA/Nonlinear optics, NW4A.19 (2013)

3. Radiochemistry and Nuclear Chemistry

Production of neutron deficient Rf isotopes in ^{208}Pb + ^{48,50}Ti reactions

S. Goto,[*1] R. Aono,[*2,*1] D. Kaji,[*2] K. Morimoto,[*2] H. Haba,[*2] K. Ooe,[*1] and H. Kudo[*3]

Asymmetric nuclear fission in which mass of fissioning nucleus splits asymmetrically is obtained in low-energy induced fission and spontaneous fission (SF) of actinides. This type of fission is considered to be strongly influenced by shell effect of fission fragments, but it has not been explained quantitatively. Rutherfordium has many isotopes decaying by SF. Systematic research of fission properties, i.e., mass and total kinetic energy (TKE) distributions of fission fragments, can provide various information to clarify the asymmetric fission mechanism. In this work, as a preparatory experiment to measure fission properties of neutron deficient Rf isotopes (especially ^{253,254}Rf) conditions of production of these nuclides were optimized.

Experiments were performed at RIKEN Linear Accelerator facility (RILAC) using the gas-filled recoil ion separator (GARIS). Beam energies of ^{50}Ti in laboratory system were 242 and 249 MeV as acceleration energy, and that of ^{48}Ti was 242 MeV. Typical beam intensity of ^{50}Ti was about 140 pnA, and ^{48}Ti was about 190 pnA. Sixteen targets were prepared with vacuum evaporation of 98.4 %-enriched ^{208}Pb onto 60 μg cm^{-2} C-backing. Target thicknesses were 170–370 μg cm^{-2}. The targets were mounted on a rotating wheel with 30 cm in diameter. For cooling the targets, the wheel was rotated at 2000 rpm. Alminum degraders of 0, 0.8, 2.0, and 3.0 μm thicknesses were placed for every four targets. In order to measure an excitation function without changing accelaration energy, a target ID system was used.[2] This system allows to associate an event detected at a focal plane with a target where a reaction occured. Evaporation residues (ERs) recoilling out the target were separated from the beam and by-products using GARIS. Optimum mangetic regirity of GARIS was 2.048 T m. ERs passed through time-of-flight detectors, and were implanted into a position sensitive detector (PSD) at the focal plane of GARIS.

At first, ^{208}Pb was bomberded with ^{50}Ti to produce ^{256}Rf mainly. The number of SF events of ^{256}Rf were 132. By normalizing the obtained production cross section with the previous value,[3] transmission efficiency of GARIS was about 50 %. Since TKE distribution of ^{256}Rf was reported,[1] these data can be used to calibrate energies of fission fragments.

Next, ^{253,254}Rf were produced through ^{208}Pb + ^{48}Ti reaction. Figure 1 shows the decay time of SF events tagged by different thick targets, which are labeled by the occupied angle in the target wheel. The events with long decay time in region (c) and (d) may be ^{253}Rf and ^{255}Rf, respectively. Thirteen events with short decay time were identified as ^{254}Rf. The excitation function constructed from observed events in Fig. 1 is shown in Fig. 2. This is in good agreement with reported excitation function of ^{208}Pb(^{48}Ti, 2n)^{254}Rf.[3] Furthermore, the obtained half life was $20.9^{+8.0}_{-4.5}$ μs, which was consistent with $29.6^{+0.7}_{-0.6}$ μs of reference value.[3] Now, detailed analysis of TKE distribution of ^{254}Rf is carried out.

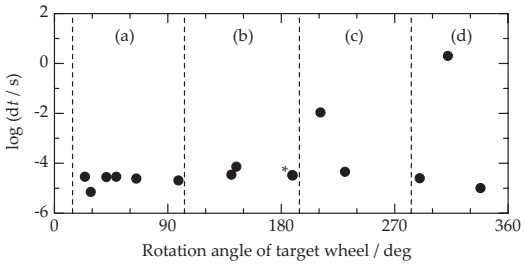

Fig. 1. Decay time of SF events in ^{208}Pb + ^{48}Ti reaction at $E_{\rm lab}$ = 242 MeV. The abscissa shows a rotation angle from a specific position. Regions of (a) to (d) correspond to the excitation energies, (a) E^* = 22.2 MeV, (b) 26.3 MeV, (c) 29.5 MeV, and (d) 17.8 MeV. *Two symbols almost overlapped.

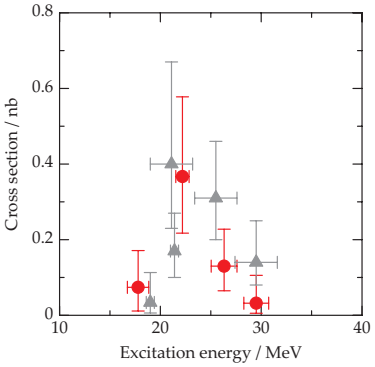

Fig. 2. Excitation functions of ^{254}Rf production in ^{208}Pb + ^{48}Ti reaction. Circles and triangles show results of this work and reference,[3] respectively.

*1 Graduate School of Science and Technology, Niigata Univ.
*2 RIKEN Nishina Center
*3 Faculty of Science, Niigata Univ.

References
1) J. F. Wild et al., J. Alloys and Comp. **213/214**, 86 (1994).
2) D. Kaji et al., Nucl. Instr. and Meth. **A792**, 11 (2015).
3) I. Dragojević et al., Phys. Rev. C **78**, 024605 (2008).

Off-line experiments of isothermal gas chromatography for Zr and Hf tetrachlorides

K. Shirai, *1 Y. Oshimi, *1 S. Goto, *1 K. Ooe, *1 H. Haba, *2 and H. Kudo*3

The periodic table today contains 118 elements, and elements with $Z \geq 104$ are called superheavy elements. Gas-phase chemical separation is one of the most utilized techniques to study chemical properties of the superheavy elements. Gas-phase chromatography is a method for determining the adsorption enthalpy (ΔH_{ads}) of an element of interest in a volatile compound based on its adsorption-desorption processes on a column surface. To clarify chemical properties of element 104, Rf, gas chromatographic behaviors of chlorides of Rf and its homologs, Zr and Hf, have been studied. The reported sequence of volatility was Zr ≳ Rf > Hf,[1,2] but the relation between Zr and Hf chlorides differs from the sequence of sublimation expected from their vapor pressure curves in macro-scale.[3] In this study, we investigated gas chromatographic behaviors of Zr and Hf chlorides at off-line to clarify this contradiction.

Radiotracers of ^{88}Zr ($T_{1/2}$=83.4 d) and ^{175}Hf ($T_{1/2}$=70 d) were produced via ^{89}Y(d, $3n$) and ^{175}Lu(d, X) reactions, respectively, using a 24-MeV deuteron beam supplied by the RIKEN K70 AVF cyclotron. These tracers were chemically separated from the target materials by means of anion exchange chromatography and stored in 1 M HCl solution. The solution of radiotracers of ^{88}Zr and ^{175}Hf in tracer-scale, or $MOCl_2 \cdot 8H_2O$ (M=Zr, Hf) water solution mixed the tracer solution in the macro-scale, was infiltrated into a carbon filter plugged into the chlorination part (see Fig. 1). Oxychlorides of Zr and Hf were converted tooxide flushing air at 650℃, and then the oxides were converted to tetrachlorides with carbon tetrachloride at 500－600℃ in He gas. The formed tetrachlorides of Zr and Hf were collected on a carbon filter at the MCl_4 part. Then, $ZrCl_4$ and $HfCl_4$ evaporated at 400℃ and passed through an isothermal column (φ4.0 mm i.d. and 30 cm long) at various temperatures (macro-scale: 80, 100, 125, and 140℃, tracer-scale: 140, 150, 160, and 170℃). Cumulative yields of the volatile species passing through the column and collecting at the cooling part were obtained through γ-ray measurement.

Figure 2 shows the dependence of the yields of Zr and Hf on the temperature of the isothermal column for 4.5 min of collection time in the macro- and tracer-scale. In the macro-scale (ca.10^{18} molecules) the adsorption enthalpies of $ZrCl_4$ and $HfCl_4$ were considerd to be –82.8 and –78.4 kJ mol^{-1}, respectively. The relationship between these adsorption enthalpies is in agreement with the relationship expected from the vapor pressure curves.

On the other hand, the adsorption enthalpies of Zr and Hf tracer-scale (ca.10^{10} molecules) were –93.0 and –93.1 kJ mol^{-1}, respectively, which differ from those at the macro-scale. In the macro-scale, $ZrCl_4$ and $HfCl_4$ cover the column surface, and interact with the same chemical species. In contrast, in the tracer-scale, the volatile compounds adsorbed on the quartz surface, and the strengths of interaction were almost the same for Zr and Hf. Because the retention time of chlorides of Zr and Hf chloride in the tracer-scale are smaller than those in the macro-scale, tetrachloride is subjected to strong interactions by the quartz surface.

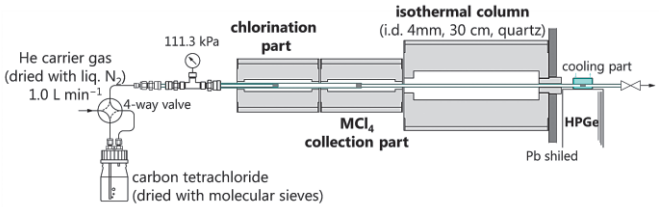

Fig. 1. Schematic view of the experimental set-up for off-line isothermal gas-chromatography of $ZrCl_4$ and $HfCl_4$.

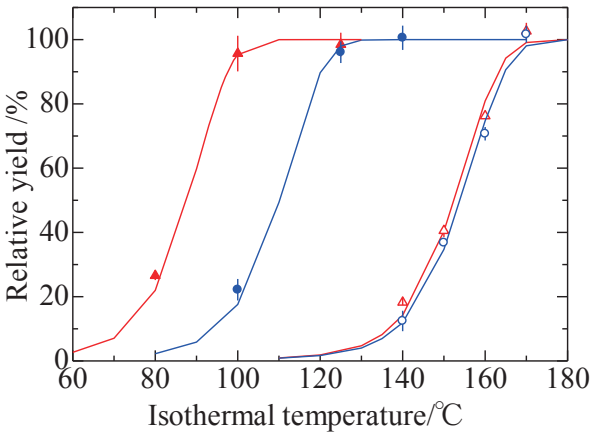

Fig. 2. Yields of Zr and Hf as a function of isothermal temperature. Circles and triangles show Zr and Hf, respectively. Close and open symbols show macro- and tracer-scale, respectively. Curves indicate results of Monte Carlo simulation.[4]

*1 Graduate School of Science and Technology, Niigata University
*2 RIKEN Nishina Center
*3 Faculty of Science, Niigata University

References

1) B. Kadkhodayan et al., Radiochim. Acta **72**, 169 (1996).
2) A. Türler et al., J. Alloys Compd. **271**, 287 (1998).
3) R. P. Tangri, D. K. Bose., Thermochimica Acta **244**, 249 (1994).
4) I. Zvára., Radiochim. Acta **38**, 95 (1985).

Adsorption behavior of No with a TTA chelate extractant from HF/HNO_3 acidic solutions

Y. Fukuda,[*1] H. Haba,[*2] A. Toyoshima,[*3] H. Kikunaga,[*4] Y. Komori,[*2] S. Yano,[*2] K. Hayashi,[*1] S. Ooe,[*5] and A. Yokoyama[*2,*5]

In a study on the fluoride complexation of a super-heavy element, rutherfordium (Rf), we focus on the extraction with an acidic chelate extractant, 2-thenoyltrifluoroacetone (TTA), which is sensitive to the valence of the metal complex. Recently, we developed a reversed-phase chromatography technique with TTA and performed Rf experiments with this technique in various HF/0.01 M HNO_3 concentrations.[1)]

The isotope ^{261}Rf used in the experiments decays into its daughter ^{257}No. The α-particle energies of ^{257}No (E_α = 8.22, 8.32 MeV) are close to that of ^{261}Rf (E_α = 8.28 MeV). Therefore, these energies are difficult to distinguish from each other. In the Rf experiments, two types of ^{257}No α-events are expected to be observed. One is from ^{257}No produced from the α-decay of ^{261}Rf after its chemical separation. It reflects the chemical behavior of Rf. The other is of ^{257}No deposited during the collection of ^{261}Rf, which reflects the chemical behavior of No. In order to correct the contribution of ^{257}No, we observe the adsorption behavior of No in the same systems of the Rf experiments.

Similar to the Rf experiments, the isotope ^{255}No ($T_{1/2}$ = 3.10 min) was produced in the ^{248}Cm(^{12}C, 5n) reaction with an 84 MeV ^{12}C beam at the RIKEN K70 AVF cyclotron. The reaction products were rapidly transported with a KCl/He gas-jet system to a chemistry laboratory and were deposited on the collection site of the on-line Automated Rapid Chemistry Apparatus (ARCA) for 180 s. After deposition, the products were dissolved in 85 μL of various HF/0.01 M HNO_3 solutions and fed into a 1.6 mm i.d. × 7.0 mm TTA resin column at a flow rate of 0.1 mL/min. The effluent from the column was collected on a Ta disk as fraction 1. The remaining products in the column were then stripped with 250 μL of 0.1 M HF/0.1 M HNO_3 solution at a flow rate of 1.0 mL/min and then collected on another Ta disk as fraction 2. Both samples were evaporated to dryness using hot He gas and a halogen heating lamp. The samples were assayed with a rapid α/SF detection system for the aqueous chemistry of super-heavy elements at RIKEN. In order to determine the chemical yield, ^{162}Yb was simultaneously produced from the Gd content in the Cm target and was measured by a Ge detector after the measurement of ^{255}No. The average chemical yield of ^{162}Yb in all the experiments was approximately 17%.

From 195 cycles of the No experiments, a total of 1042 α-events indicating the production of ^{255}No were registered in the energy range of 7.60–8.20 MeV. The adsorption probability, %ads, of No with a fixed volume of the effluent was evaluated using the following equation:

$$\%ads = Fr2 / (Fr1 + Fr2) \times 100, \quad (1)$$

where Fr1 and Fr2 are the radioactivities observed in fraction 1 and 2, respectively. The decay of No was taken into account in the correction for the %ads values. The results for %ads of ^{255}No as a function of $[F^-]_{eq}$ in the range of 1.93×10^{-5} to 1.66×10^{-3} M are shown in Fig. 1. In the Rf experiments, [1)] the %ads values of ^{261}Rf were constant at approximately 60% in the $[F^-]_{eq}$ range up to 5×10^{-4} M and then steeply decreased at $[F^-]_{eq} = 9 \times 10^{-4}$ M. On the other hand, in the No experiments, it was found that the %ads values of ^{255}No were less than 10% in the entire range of $[F^-]_{eq}$.

In order to evaluate the %ads values of ^{261}Rf, we assumed in the previous report[1)] that the adsorption of No was negligible. Based on the present work, it was confirmed that No was adsorbed to TTA to a small extent and the %ads values of ^{261}Rf can be determined with greater precision.

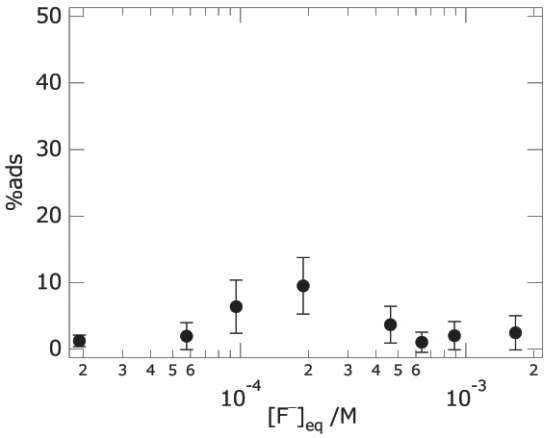

Fig. 1 Adsorption probability, %ads, of ^{255}No plotted as a function of $[F^-]_{eq}$ in TTA column chromatography.

*1 Graduate School of Natural Science and Technology, Kanazawa University
*2 RIKEN Nishina Center
*3 Advanced Science Research Center, Japan Atomic Energy Agency
*4 Research Center for Electron Photon Science, Tohoku University
*5 Institute and College of Science and Engineering, Kanazawa University

Reference

1) Y. Kitayama, Y. Fukuda, H. Haba, K. Tsukada, A. Toyoshima, H. Kikunaga, M. Murakami, Y. Komori, M. H. Huang, T. Taniguchi, S. Ueno, K. Hayashi, Y. Yatsu, I. Chiyonishio, K. Murakami, A. Yokoyama: RIKEN Accel. Prog. Rep. **48**, 281 (2015).

Extraction behavior of Mo and W from sulfuric acid into Aliquat336 as model experiments for seaborgium (Sg)

A. Mitsukai,[*1,*2] A. Toyoshima,[*2] Y. Kaneya,[*1,*2] Y. Komori,[*3] H. Haba,[*3] M. Asai,[*2] K. Tsukada,[*2] T.K Sato,[*2] K. Ooe[*4] D. Sato, [*4] M. Murakami, [*4] and Y. Nagame[*1,*2]

It is known that for inorganic metal complexes such as a sulfato, the ionic radius of the metal center plays an important role in its complex formation. Unlike its lighter homologs, Mo and W the sulfato complex of seaborgium is hard to form, because the theoretically predicted ionic radius of Sg is larger than those of the homologs. Experimental assessment of the sulfato complex formation of Sg, therefore, provides information on its ionic radius, which would be influenced by strong relativistic effects.[1] A rapid solvent extraction apparatus is, however, required to be developed to explore the complex formation of Sg because the half-lives ($T_{1/2}$) of the ^{265a,b}Sg isotopes are so short (around 10 s) and their production cross sections in the ^{248}Cm(^{22}Ne, 5n)^{265a,b}Sg reaction are extremely small.[2] In the present study, we examined the extraction behavior of carrier-free ^{181}W ($T_{1/2}$ = 121.8 d) using a newly developed Flow Solvent Extractor (FSE) to find suitable experimental conditions for future Sg experiments. On-line experiments with the short-lived ^{93m}Mo ($T_{1/2}$ = 6.85 h) and ^{179}W ($T_{1/2}$ = 37 min) nuclides were also carried out using the FSE connected to a Membrane Degasser (MDG), which was developed for the dissolution of gas-jet transported products.[3]

At the RIKEN AVF cyclotron, ^{93m}Mo and ^{179}W were produced in the ^{nat}Nb(d, 2n)^{93m}Mo and ^{nat}Ta(d, xn)^{179}W reactions, respectively. The reaction products were transported to the chemistry laboratory by a gas-jet method and were dissolved with 6 M sulfuric acid using the MDG. This aqueous solution was then immediately mixed with an organic solvent of 0.2 M Aliquat336 dissolved in toluene using a spiral PTFE tube with 1-mm inner diameter. The mixture with a volume of 1.5 mL throughout the PTFE tube was collected in a sample vial. After centrifuging, the aqueous and organic solutions were separately taken in measurement tubes for γ-ray spectrometry with a Ge detector. The distribution ratio (D) is defined as the ratio of ratio activity per volume between each phase as $D = (A_{org} / V_{org}) / (A_{aq} / V_{aq})$, where A_{org} and A_{aq} are radioactivities in the organic and aqueous phases, respectively, and V_{org} and V_{aq} are the volume of the organic and aqueous phases, respectively. Off-line experiments with the relatively long-lived ^{181}W produced in the ^{nat}Ta(d, n)^{181}W reaction were also carried out to compare with the on-line experiments.

*1 Graduate School of Science and Technology, Ibaraki University
*2 Advanced Science Research Center, Japan Atomic Energy Agency
*3 RIKEN Nishina Center
*4 Graduate School of Science and Technology, Niigata University

In Fig. 1, the variation of the distribution ratios of Mo and W are shown as a function of extraction time, which is the time required to pass through the spiral PTFE tube. In the previous batch-wise extraction experiments, the D values of Mo and W at the equilibrium are approximately 15 and 2.[4] It is found that, in the off-line experiment, the extraction of ^{181}W reaches the equilibrium in less than 50 s because its D value increases up to the equilibrated value of 2 within 50 s. This equilibration time is much shorter than the time of about 120 s for W observed in our previous experiments.[4] This result indicates that the extraction kinetics of W was enhanced with the FSE. However, in the on-line experiment, the equilibration time of Mo of approximately 50 s was much longer than that of less than 5 s, [4] and the extraction of W did not reach equilibrium within 50 s. This is probably due to slow chemical reactions other than extraction in the MDG and FSE. In future, the kinetics of these elements will be improved by using heating or supersonic systems.

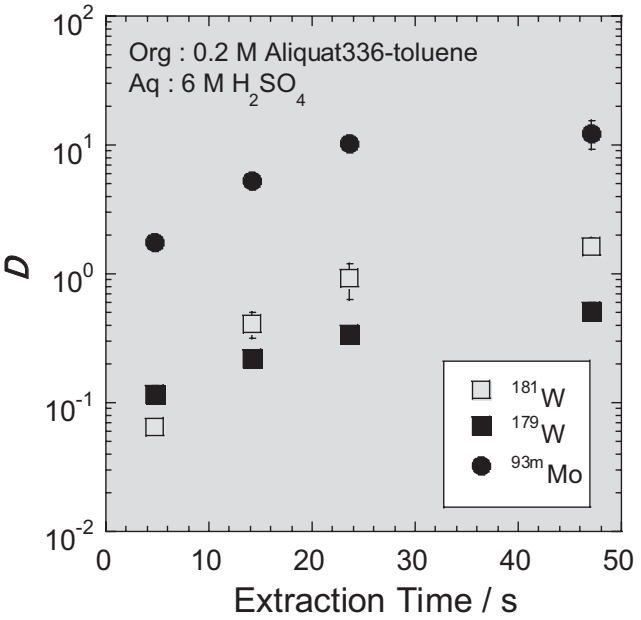

Fig. 1. Dependence of the distribution ratio (D) of Mo and W on extraction time in the spiral PTFE tube of the FSE system.

References

1) V. Pershina: in *The Chemistry of Superheavy Elements. 2nd edition*, edited by M. Schädel and D.Shaughnessy (Springer-Verlag, Berlin, 2014), p. 158
2) H. Haba et al., Phys. Rev. C **85**, 024611 (2012).
3) Y. Komori et al.: in this report.
4) A. Toyoshima et al,; RIKEN Accel. Prog. Rep. **48**, 283 (2014).

Solid-liquid extraction of Nb and Ta with Aliquat 336 resin from HF solutions for chemical experiment of element 105, Db

D. Sato,[*1,*2] M. Murakami,[*1] K. Ooe,[*1] R. Motoyama,[*1] H. Haba,[*2] Y. Komori,[*2]
A. Toyoshima,[*3] A. Mitsukai,[*3] H. Kikunaga,[*4] S. Goto,[*1] and H. Kudo[*5]

The elements with atomic number ≥ 104 are called super-heavy elements. Aqueous chemistry experiments with these elements have been performed often by a column chromatographic method. In particular, an anion-exchange experiment of element 105, Db was successfully performed in 13.9 M hydrofluoric acid solution using Automated Rapid Chemical Apparatus, ARCA.[1] Chemical species of Db in HF solution were, however, still not identified. We have, therefore, studied liquid-liquid extraction behavior of Nb and Ta, which are lighter homologues of Db, with Aliquat 336 for investigating the charge of extracted complexes of these elements from HF solution. From these results, it was found that, although the extraction behavior of Nb was different from that of Ta, univalent anionic fluoride complexes were extracted for both Nb and Ta by Aliquat 336.[2] Based on these results, it is expected that information on the chemical species of Db in HF solution would be obtained by applying this extraction system to the solid-liquid extraction experiment with ARCA. The solid-liquid extraction experiments of Nb and Ta with an Aliquat 336 resin from HF solutions were conducted by a batch method for the column experiment with ARCA in this work.

Long-lived radiotracers, ^{95g}Nb ($T_{1/2}$ = 34.97 d) and ^{179}Ta ($T_{1/2}$ = 665 d), were produced by deuteron irradiation on Zr and Hf metallic foil targets with natural isotopic abundance, respectively, using the RIKEN K70 AVF Cyclotron. These radiotracers in the targets were chemically isolated by an ion-exchange. A 32 wt% Aliquat 336 resin was prepared by mixing MCI GEL CHP20/P30 with Aliquat 336 dissolved in methanol for about 1 day, which was followed by drying in an oven at 80 ˚C.[3] The ^{95g}Nb and ^{179}Ta tracers were dissolved in 400 μL of 1-27 M HF, and then mixed with 10-15 mg of the 32 wt% Aliquat 336 resin in a syringeless filter tube. After shaking for 5 min, the solution was separated from the resin by filtration, and 250 μL of the solution in each sample was pipetted into another sample tube. For measurement of initial radioactivity, A_{ini}, in the aqueous solutions, control experiments without the Aliquat 336 resin were also conducted. The radioactivities of these samples were measured with a Ge detector. The distribution coefficients, K_d of ^{95g}Nb and ^{179}Ta were obtained by the following equation:

$$K_d = \frac{(A_{ini} - A_s)/m_r}{A_s/V_s}. \quad (1)$$

Here, A_s is the radioactivity of solution, m_r is the weight of the resin used and V_s is the volume of a liquid phase.

The dependences of K_d values of ^{95g}Nb and ^{179}Ta on the initial HF concentration, $[HF]_{ini}$ were investigated with the 32 wt% Aliquat 336 resin from 1-27 M HF solutions. The obtained results were shown in Fig.1. It is revealed that the K_d values of ^{179}Ta are decreased with increasing $[HF]_{ini}$, while those of ^{95g}Nb show a minimum at 10 M HF. The decreases of the K_d values of both the elements are due to an increase of HF_2^- ion.[1] Comparing with our earlier results on liquid-liquid extraction of these elements,[2] this solid-liquid extraction behavior of ^{179}Ta is found to be very similar to that in liquid-liquid extraction. Thus, the same complex, TaF_6^- ion as that in liquid-liquid extraction is probably extracted by the Aliquat 336 resin. However, the solid-liquid extraction behavior of ^{95g}Nb was partly different from that in Ref. [2]. While distribution ratios of ^{95g}Nb in Ref. [2] decreased gradually with increasing $[HF]_{ini}$, a gradual increase of K_d values is observed above 10 M HF in the present solid-liquid extraction. This suggests that the extracted complexes of ^{95g}Nb in solid-liquid extraction might be different from those in liquid-liquid extraction. Further investigation of the extracted species of ^{95g}Nb in solid-liquid extraction is needed for identification of the Nb species.

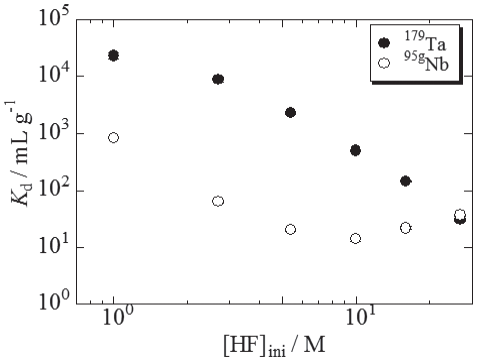

Fig.1 The adsorption behavior ^{95g}Nb and ^{179}Ta on Aliquat 336 resin as a function of $[HF]_{ini}$

[*1] Graduate School of Science and Technology, Niigata University
[*2] RIKEN Nishina Center
[*3] Japan Atomic Energy Agency
[*4] Research Center for Electron Photon Science, Tohoku University
[*5] Department of Chemistry, Faculty of Science, Niigata University

References

1) K. Tsukada *et al.*: Radiochim. Acta. **97**, 83 (2009).
2) D. Sato *et al.*: Accel. Prog. Rep. **47**, 247 (2014).
3) H. Haba *et al.*: Radiochim. Acta. **95**, 1 (2007).

Extraction behaviors of chloride complexes of Nb and Ta with triisooctyl amine for chemical experiment of dubnium (Db)

R. Motoyama,[*1,*2] K. Ooe,[*1] M. Murakami,[*1] H. Haba,[*2] S. Goto,[*1] and H. Kudo[*3]

It has been reported that the anion-exchange behavior of the 105th element, Db, in HF/HNO_3 solution is similar to that of Nb rather than Ta.[1] In our laboratory, the extraction behaviors of fluoride complexes of Nb and Ta with tributyl phosphate (TBP)[2] and Aliquat 336[3] have been investigated. The extraction yield of Ta is greater than that of Nb in these systems. For the extraction of Db with TBP from 1.0 M HF, the behavior of Db was significantly different from that of Ta.[4] To clarify the similarity of the extraction behavior between Db and Nb, systems where the extraction yield of Nb is greater than that of Ta should be studied. We investigated the extraction behaviors of Nb and Ta from HCl with triisooctyl amine (TiOA) on a tracer scale. It has been reported that the extraction yield of Nb is greater than that of Ta on a macro scale.[5]

Radiotracers, ^{95g}Nb ($T_{1/2}$ = 34.991 d) and ^{179}Ta ($T_{1/2}$ = 1.82 y), were produced from ^{nat}Zr(d,xn) and ^{nat}Hf(d,xn) reactions, respectively, using the RIKEN AVF cyclotron. These radiotracers were chemically isolated from the target materials through an anion-exchange method and preserved in 1 M HF. An appropriate amount of this solution was evaporated to dryness and preserved in concentrated HCl (stock solution). An aliquot of the stock solution was evaporated to dryness and dissolved in an appropriate concentration of HCl. In a 1.5 mL polypropylene tube, 600 µL of 8–10 M HCl containing the tracers was mixed with an equal volume of 0.12 M TiOA in xylene, and the mixture was shaken for a fixed time. After centrifugation, 420 µL aliquots of each phase were separated into sample tubes. The radioactivity of each phase was measured with a Ge detector. We calculated the distribution ratios (D) of ^{95g}Nb and ^{179}Ta using the following equation:

$$D = (A_{org} / V_{org}) / (A_{aq} / V_{aq}),$$

where A_{org} and A_{aq} are the radioactivities in organic and aqueous phases, respectively, and V_{org} and V_{aq} are the volumes of the organic and aqueous phases, respectively.

The extraction kinetics from 10 M HCl into 0.12 M TiOA in xylene were investigated by changing the shaking time from 1 min to 60 min. It was found that the D values of ^{95g}Nb and ^{179}Ta were almost constant in the examined range of shaking time. This result shows that the extraction equilibrium is achieved quickly.

The dependence of the D values of ^{95g}Nb and ^{179}Ta extracted into 0.12 M TiOA in xylene is shown in Fig.1 as a function of the HCl concentration (8–10 M). The D values of ^{95g}Nb are approximately 10^2 times greater than those of ^{179}Ta. The D values of ^{179}Ta are greater than the values in the literature, although those of ^{95g}Nb are in agreement with those in the literature. In the course of the investigation, the D values of ^{179}Ta decreased with time lapsed from the preparation of the stock solution, while those of ^{95g}Nb stayed constant (Fig. 2). The decreasing trend of the D values of ^{179}Ta may be caused by hydrolysis of the Ta species or an effect of residual fluoride ions in the stock solution. The preparation methods of the Ta tracer may be considered for the study of the extraction behavior of a chloride complex of Ta. A detailed investigation is necessary to solve the problem.

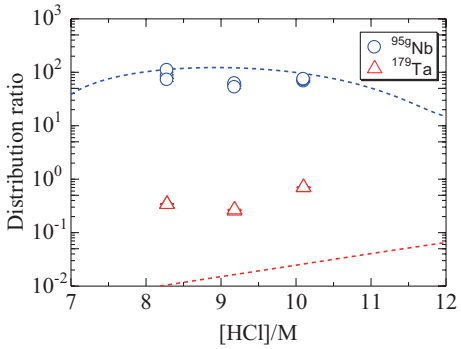

Fig. 1. The distribution ratios of ^{95g}Nb and ^{179}Ta extracted into 0.12 M TiOA in xylene as a function of the HCl concentration. Dashed lines indicate the literature values of Nb and Ta. [5]

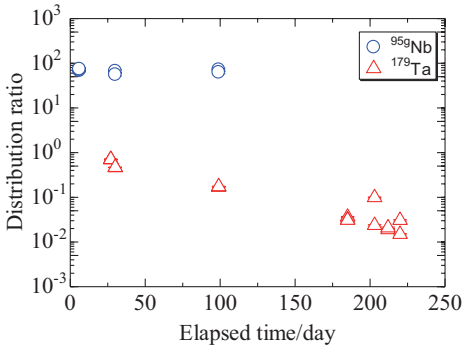

Fig. 2. Variation of the distribution ratios of ^{95g}Nb and ^{179}Ta from 10 M HCl extracted into 0.12 M TiOA in xylene as a function of time lapsed from the preparation of the stock solution.

References

1) Y. Kasamatsu et al., Chem. Lett. **38**, 1084 (2009).
2) S. Tsuto et al., RIKEN Accel. Prog Rep. **47**, 270 (2014).
3) D. Sato et al., RIKEN Accel. Prog Rep. **47**, 271 (2014).
4) M. Murakami et al., RIKEN Accel. Prog Rep. **48**, 279 (2015).
5) T. Ishimori et al., Nihon Genshiryoku Gakkaishi **3**, 698 (1961).

*1 Graduate School of Science and Technology, Niigata University
*2 RIKEN Nishina Center
*3 Faculty of Science, Niigata University

Development of an automated batch-type solid-liquid extraction apparatus and extraction of Zr, Hf, and Th by triisooctylamine from HCl solutions for chemistry of element 104, Rf†

Y. Kasamatsu,[*1] A. Kino,[*1] T. Yokokita,[*1] K. Nakamura,[*1] Y. Komori,[*1,2] K. Toyomura,[*1] T. Yoshimura,[*3] H. Haba,[*2] J. Kanaya,[*2] M. Huang,[*2], Y. Kudou,[*2] N. Takahashi,[*1] and A. Shinohara[*1]

Online rapid chemical experiments on a "one-atom-at-a-time" basis using an accelerator are needed for the superheavy element chemistry. An apparatus for rapid and repetitive chemistry in online use is essential. So far, the pioneering works opened up the chemistry of new elements and revealed their properties as *d*-block metal elements in the periodic table.[1)] On the other hand, equilibration of the chemical reactions has not been confirmed for the short-lived superheavy elements, although this confirmation is important to investigate the detailed chemical properties of these elements such as complex formation. Only in the fluoride complexation studies, the equilibrated data were obtained for the lighter homologues in online experiments.[1)] The K_d values of Rf obtained in the ion-exchange chromatography under such conditions were clearly different from those of Zr and Hf. Investigation of the complex formation of Rf with other ligands is very important for an understanding of its chemical properties. However, it might be difficult to obtain well equilibrated data or to observe the time dependence of the distribution behaviors for superheavy elements.

In this work, we developed an automated batch-type solid-liquid extraction apparatus to study time dependence of extraction behavior, and performed the online extraction experiments of Zr and Hf in TIOA/HCl system. By comparing the results with those in "offline" extraction, applicability of the apparatus for Rf was investigated.

In the offline experiment, the 18–57 wt% TIOA resin and 6.2–10.9 M HCl containing the ^{88}Zr and ^{175}Hf tracer solution were mixed in a PP tube and the mixture was shaken for 2–120 min at 25 ± 1 °C. Then, we measured the sample γ-ray spectroscopically using a Ge semiconductor detector. In all solid-liquid extraction experiments, control experiments without the resin were performed to determine the radioactivity of the control solution. The *R* values were determined from the following equation:

$$R = A_r V_s / A_s w_r = (A_c - A_s) V_s / A_s w_r, \quad (1)$$

where A_r and A_s are the radioactivities on the resin and in the solution, respectively, V_s is the volume (mL) of the solution, and w_r is the mass of the dry resin (g). A_c denotes the radioactivity of the control solution. In this study, the *R* value in equilibrium is described as the K_d value in solid-liquid extraction.

An AutoMated Batch-type solid-liquid Extraction apparatus for Repetitive experiments of transactinides (AMBER) was developed. All the operations were controlled by PC with fixed time intervals in online extraction experiments.

In the online experiment, the ^{89g,m}Zr and ^{175}Hf nuclides were produced in the ^{89}Y(*p*, *n*)^{89g,m}Zr and ^{175}Lu(*p*, *n*)^{175}Hf reactions, respectively, using the K70 AVF cyclotron at RIKEN. The product nuclides were transported by the gas-jet system to the chemistry laboratory and deposited on a collection site of AMBER for 60 s. Then, the deposited sample was dissolved in 160–230 μL of 6–11 M HCl. The solution passed through the valves, and then entered the chemical reaction container containing the 31 wt% TIOA resin. After shaking the container with a vortex mixer for 10–120 s, only the liquid phase was pushed out of the container by the compressed air at 0.5 MPa, and was assayed by γ-ray spectroscopy. The residual Zr and Hf species adsorbed on the resin were stripped by washing the resin three times with about 220 μL of a mixture solution of 5.1 M HNO_3 and 0.01 M HF. We measured the first two fractions of the stripping solution γ-ray spectroscopically. A control extraction experiment without the resin was also performed.

In the offline experiment, the chemical reactions of Zr and Hf were found to be fast in the TIOA/HCl extraction when the TIOA concentrations were above 30 wt%. Based on these results, we determined the suitable experimental conditions for online experiment. By using the developed apparatus, we successfully performed an online solid-liquid extraction experiment with the AVF cyclotron at RIKEN. The *R* values of Zr and Hf obtained with shaking times of 10–120 s were approximately constant and the average value at each HCl concentration was consistent with the K_d values obtained in the offline experiment in 7–11 M HCl. This result suggests that the chemical reactions in the present extraction reach equilibrium within 10 s and the K_d values of Zr and Hf were obtained in the online experiment. In the extraction using AMBER with shaking for 10 s, the solution sample for measurement was prepared about 35 s from the start of the dissolution of the products transported by the gas-jet system. The present extraction experiment would be applicable to the 68-s ^{261}Rf experiment.

† Condensed from the article in Radiochim. Acta **103**, 513 (2015).

*1 Graduate School of Science, Osaka University
*2 RIKEN Nishina Center
*3 Radioisotope Research Center, Osaka University

Reference

1) M. Schädel and D. Shaughnessy: *The Chemistry of Superheavy Elements*, 2nd ed. (Springer, Heidelberg, 2014).

Solvent extraction of Zr and Hf using the online flow-type extraction apparatus for superheavy elements

Y. Kasamatsu,[*1] K. Nakamura,[*1] T. Yokokita,[*1] Y. Shigekawa,[*1] Y. Yasuda,[*1] N. Takahashi,[*1] Y. Kuboki,[*2] H. Haba,[*2] M. Murakami,[*2] Y. Komori,[*2] T. Yoshimura,[*3] and A. Shinohara[*1]

Thus far, ion-exchange and solid-liquid extraction experiments have often been performed in solution chemistry on superheavy elements.[1] Solvent extraction experiments were also conducted using rapid solvent extraction apparatuses. However, sufficient distribution data for discussion on complex formation were hardly obtained in the extraction of short-lived superheavy elements because it is difficult to achieve rapid equilibration and phase separation. Stable repetitive extractions and *a*-particle detections are also difficult in online extraction experiments. We developed an online flow-type solvent extraction apparatus to accomplish rapid solvent extraction and phase separation with the short-lived ^{261}Rf (68 s).[2] In this experiment, by using the developed apparatus, we performed the online solvent extraction of Zr and Hf (homologues of Rf) produced with the AVF cyclotron at RIKEN to check the performance of the apparatus and to search for suitable conditions of Rf experiments.

The developed extraction apparatus involves a reactor tube (extraction unit, EU) filled with PTFE chips to mix aqueous and organic solutions well (shortening of the diffusion length between these solutions is expected). Rapid phase separation between aqueous and organic solutions was achieved with a flow-type phase separator (PS) using a PTFE membrane filter. We found that separation with the purity of each phase greater than 95% was accomplished with a 1-step separator. The entire setup of the online extraction experiment at RIKEN is shown in Fig. 1. ^{89g,m}Zr and ^{173}Hf were produced in the ^{nat}Sr(α, x*n*) and ^{nat}Yb(α, x*n*) reactions, respectively. The nuclear reaction products were rapidly transported to the dissolution apparatus in the chemistry room by the He/KCl gas-jet system. The solvent extraction of Zr and Hf was performed in a 7.8, 9.2, and 10.4 M HCl/0.01 M Aliquat 336 carbon tetrachloride solution system. 30-cm EU was used and the flow rate was 500 μL/min for both phases. The length of EU required to reach equilibrium was tested beforehand through an offline extraction experiment using the apparatus. The eluted aqueous and organic solutions were separately collected and subjected to γ-ray measurement, and the distribution ratios, *D* (the ratio of metal concentration in organic solution to that in aqueous solution), were determined.

The obtained *D* values are shown in Fig. 2. In this figure, the equilibrium *D* values obtained beforehand in the offline batch extraction experiment are also shown for comparison.

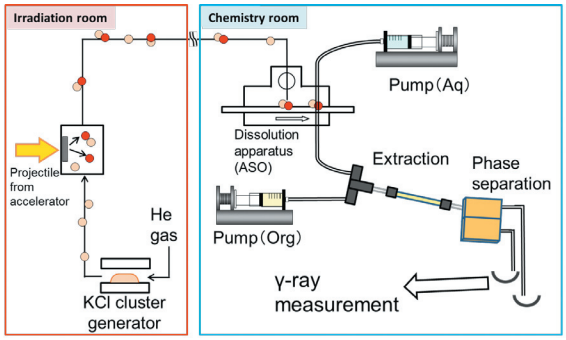

Fig. 1. The entire setup of the online extraction experiment at RIKEN

The *D* values obtained in the present online experiment basically match the tendency of the *D* values in equilibrium. This result indicates that extraction equilibrium of the chemical reactions involved in the present solvent extraction was achieved in the online experiment using the apparatus. At 9.2 M HCl, the *D* values of both Zr and Hf were slightly lower than the equilibrium data. Repetitive extraction was not performed in the present experiment. Thus, these low *D* values might be due to uncertainty of the data; if not, the length of the EU was insufficient (not equilibrated). We need to investigate the reproducibility of the data in the online experiment. The time taken to accomplish one extraction procedure was approximately 1 min, which is suitable for Rf experiments. In conclusion, we were able to check the movement of the developed apparatus and obtained the *D* values of Zr and Hf in an online experiment.

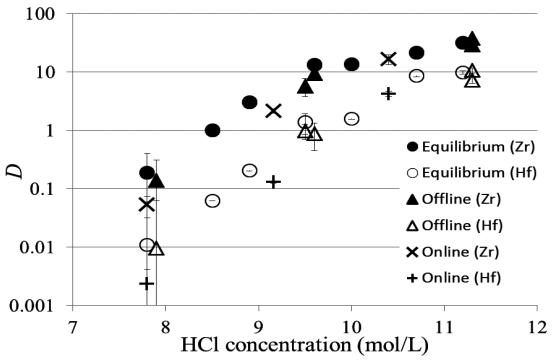

Fig. 2. The *D* values of Zr and Hf

[*1] Graduate School of Science, Osaka University
[*2] RIKEN Nishina Center
[*3] Radioisotope Research Center, Osaka University

References

1) M. Schädel, D. Shaughnessy: *The Chemistry of Superheavy Elements*, 2nd ed. (Springer, Heidelberg, 2014).
2) Y. Kudou et al.: RIKEN Accel. Prog. Rep. **44**, 262 (2011).

Solvent extraction behavior of Zr and Hf with di(2-ethylhexyl)phosphoric acid for aqueous chemistry of Rf

R. Yamada,[*1] K. Ooe,[*1] M. Murakami,[*1] H. Haba,[*2] Y. Komori,[*2] S. Goto,[*1] and H. Kudo[*3]

Studies on the complex formation of element 104, rutherfordium (Rf), in aqueous solutions have been mainly performed using inorganic ligands such as halide ions.[1, 2] Few experiments with organic ligands have been reported and little is known about the complex formation between Rf and organic ligands. In a previous study,[3] we reported the solvent extraction behavior of zirconium (Zr) and hafnium (Hf), which are lighter homologs of Rf, with a chelating agent, 2-thenoyltrifluoroacetone (TTA), to find suitable experimental conditions for complexation studies of Rf. As another candidate for the chelate extraction of Rf, di(2-ethylhexyl)phosphoric acid (HDEHP) was used in this study; HDEHP is widely used in analytical chemistry in addition to TTA, and many experimental data with HDEHP was reported in the analysis and discussion of our results.

Radiotracers of ^{88}Zr ($T_{1/2}$ = 83.4 d) and ^{175}Hf ($T_{1/2}$ = 70 d) were produced in the ^{89}Y(d, 3n) and ^{nat}Lu(d, xn) reactions, respectively, using the RIKEN K70 AVF cyclotron. Metal foils of Y and Lu (of 100 and 125 μm thickness, respectively) were used as targets. The incident energy of the deuteron beam was 24 MeV. The produced radiotracers were chemically separated from the target materials through an anion exchange and a solvent extraction method. A perchloric acid solution of 600 μL containing ^{88}Zr and ^{175}Hf radiotracers was mixed with an equal volume of HDEHP in toluene in a perfluoroalkoxy (PFA) sample tube. The mixture was shaken for 2 hours at 25 ºC. After centrifugation for 1 min, a 420 μL aliquot from each phase was separately pipetted into a polypropylene tube. The radioactivity of each phase was measured with a Ge detector, and the distribution ratio (D) was evaluated using the following equation:

$$D = (A_o/V_o)/(A_a/V_a), \qquad (1)$$

where A denotes the radioactivity of either ^{88}Zr or ^{175}Hf, V is the volume of the aqueous or organic phase, and the subscripts a and o refer to the aqueous and organic phases, respectively.

The D values of ^{88}Zr and ^{175}Hf in 3 M $HClO_4$ are shown in Fig. 1 as a function of the HDEHP concentration in toluene. In the previous TTA extraction experiment, [3] the D values of Zr was 10 times that of Hf, while the order of the D values was reversed in the extraction with HDEHP as shown in Fig. 1. The reason for this difference between TTA and HDEHP extraction is a very interesting topic for the chemical studies of Rf as well as Zr and Hf chemistry.

*1 Institute of Science and Technology, Niigata University
*2 RIKEN Nishina Center
*3 Faculty of Science, Niigata University

However, at present, we need further investigation for the interpretation of this result. HDEHP is known to form a dimer species,[4] and the dimer of HDEHP coordinates to metal ions as chelating agent. Therefore, in the extraction of tetravalent metal ions (M^{4+}) with HDEHP, the extraction reaction would be described by the following equation:

$$M^{4+} + 4(HDEHP)_{2(o)} \rightleftharpoons M(HDEHP \cdot DEHP)_{4(o)} + 4H^{+}. \qquad (2)$$

From eq. (2), the log D vs. log [$(HDEHP)_2$] plot is expected to show a linear relation with a slope of 4. This slope value indicates the number of HDEHP dimer molecules involved in the extraction reaction, and the extraction mechanism can be deduced from a slope analysis of the plot. A least-squares fit to the data in Fig. 1 showed a good linear relation with a slope of 3.9 ± 0.1 for both of ^{88}Zr and ^{175}Hf. Therefore, this result suggests that the main extracted species of Zr and Hf would be Zr(HDEHP·DEHP)$_4$ and Hf(HDEHP·DEHP)$_4$, respectively, in 3 M $HClO_4$. In 1 M $HClO_4$, the slope value of the log D vs. log [$(HDEHP)_2$] plot was 3.0 ± 0.1 for both Zr and Hf. Because these two elements have a great tendency to hydrolyze, the formation of hydrolyzed species such as $ZrOH^{3+}$ and $HfOH^{3+}$ might affect the extraction process. This change of extraction mechanism with acid concentration was also observed in the previous results with TTA.

For the Rf experiment, a rapid solvent extraction experiment of Zr and Hf using the flow injection analysis (FIA) technique will be performed with the HDEHP and TTA extraction system.

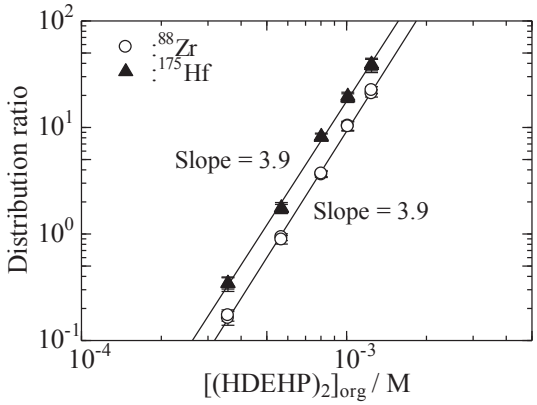

Fig. 1. Dependences of the distribution ratios of ^{88}Zr and ^{175}Hf in 3 M $HClO_4$ against the dimeric HDEHP concentration in toluene.

References

1) H. Haba et al., J. Nucl. Radiochem. Sci. **3**, 143 (2002).
2) H. Haba et al., J. Am. Chem. Soc. **126**, 5219 (2004).
3) A. Tanaka et al., RIKEN Accel. Prog. Rep. **48**, 288 (2015).
4) N. Miralles et al., Anal. Sci. **8**, 773 (1992).

^{99}Ru Mössbauer spectroscopy of Na-ion batteries of Na_2RuO_3 (II)

K. Takahashi,[*1] Y. Kobayashi,[*1,*2] H. Haba,[*2] and M. Okubo[*3]

Sodium-ion batteries are candidates for next-generation rechargeable batteries that use Na^+ ions as charge carriers. High-power and low-cost batteries incorporating Na^+ ions are strongly expected to be energy storage devices, because sodium is much more abundant and easier to isolate compared to lithium. There have been many investigations targeting the development and production of novel Na^+-containing electrodes as suitable cathodes. It is particularly important to develop novel cathode materials with high capacity as well as high operating potential. Yamada et al. recently reported the electrochemical properties of a new Na–Ru–O system, incorporating $Na[Na_{1/3}Ru_{2/3}]O_2$, as the cathode material. Na_2RuO_3 has a layered structure in which the first layer is composed of Na while the second layer contains Na and Ru in the ratios 1:3 and 2:3, respectively, and provides the redox reaction associated with Na^+ ion extraction and insertion, leading to the possibility of high energy density of 140 mAh/g[1].

The crystal structure of $Na[Na_{1/3}Ru_{2/3}]O_2$ has two possible phases, *ordered* and *disordered*, depending on the synthetic conditions[1,2]. The two phases exhibit significant differences in their electrochemical properties. In this study, the *ordered* Na_2RuO_3 as the starting composition and Na-deficient $Na_{2-x}RuO_3$ were characterized by means of XRD and ^{99}Ru Mössbauer spectroscopy in order to clarify the change of oxidation state and coordination environment of the Ru atoms caused by the deficiency of Na^+ ions.

$Na_{2-x}RuO_3$ (x=0, 0.5, 1.0, 1.5) samples in the *ordered* phase were prepared by a solid-state reaction. A mixture of RuO_2 and $NaHCO_3$ were pressed and sintered at 850ºC for 48 h in an Ar atmosphere. Powdered samples were used for XRD and ^{99}Ru Mössbauer spectroscopy.

The source nuclide, ^{99}Rh ($T_{1/2}$=15.0 d) of ^{99}Ru Mössbauer spectroscopy was produced by the ^{99}Ru(p,n)^{99}Rh reaction at the AVF Cyclotron (K70-MeV). For the (p,n) reactions, the p-beam was used to bombard the 96 %-enriched ^{99}Ru metallic powder target. The energy and intensity of the p-beam were 12 MeV and 10 μA, respectively. After p-irradiation for about 24 h, the Mössbauer source was estimated to have an activity of 500 MBq[3]. ^{99}Ru Mössbauer spectra were obtained using a Mössbauer spectrometer (Wissel, MVT-1000) and a multichannel analyzer (FAST, MCS3). Due to the relatively high energy of the Mössbauer γ-ray (89.8 keV), both the source and the absorbers were maintained at low temperature in a liquid-helium cryostat during the measurements. The Mössbauer γ-rays were detected by a 2-mm- thick NaI(T1) scintillator. Velocity was calibrated by measuring the Mössbauer absorption lines of ^{57}Fe in an iron foil sample against a ^{57}Co/Rh source.

The XRD pattern of *ordered* Na_2RuO_3 indicated that this compound crystallized in a monoclinic unit cell with a = 0.541 nm, b = 0.937 nm, c = 1.085 nm, β = 99.64º [3]. The ^{99}Ru Mössbauer spectrum of Na_2RuO_3 obtained is shown in Fig. 1(a). The spectrum shows a doublet with isomer shift (δ) of –0.30(5) mm/s, quadrupole splitting (ΔE_Q) of 0.29(5) mm/s, and linewidth (Γ) of 0.33 mm/s. The δ value is typical of Ru^{IV}. The linewidth observed in *ordered* Na_2RuO_3 is much smaller than that of $Na[Na_{1/3}Ru_{2/3}]O_2$[4], due to the calcination temperature and period for sample preparation. The Mössbauer spectrum of Na-deficient $Na_{0.5}RuO_3$ (Fig. 1 (b)) shows a doublet with δ = −0.41(1) mm/s and ΔE_Q = 0.46(1) mm/s, also indicating Ru^{IV}. It means that the Ru ions are located in an equivalent coordination environment, despite the considerable sodium-ion deficiency. The XRD pattern of $Na_{0.5}RuO_3$ indicated a modification of the crystal structure from monoclinic in the starting material to tetragonal in the product due to the reduction of Na between RuO_6 layers. Detailed discussion about the oxidation states and coordination environment of the Ru atoms as a function of the deficiency of Na in $Na_{2-x}RuO_3$ is under consideration.

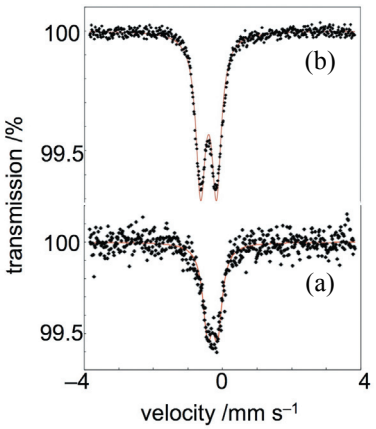

Fig. 1. ^{99}Ru Mössbauer spectra of (a) *ordered* Na_2RuO_3 and (b) Na-deficient $Na_{0.5}RuO_3$at 4.2 K.

References

1) M. Tamaru et al., *Electrochem. Commun.*, **33**, 23 (2013).
2) K. M. Mogare et al., *Z. Anorg. Allg. Chem.*, **630**, 547 (2004).
3) Y. Kobayashi et al., *J. Phys.*, **217**, 012023 (2010).
4) M. Okubo et al., *RIKEN Accel. Prog. Rep.*, **48** (2015) .

*1 Dep. of Eng. Sci., University of Electro-Commun.
*2 RIKEN Nishina Center
*3 Dep. of Eng., University of Tokyo

Quantitative study on metallofullerene separation by chemical reduction

K. Akiyama,[*1,*2] K. Chiba,[*1] H. Haba,[*2] and S. Kubuki[*1]

Endohedral metallofullerene (EMF) is expected to be applied in electronics and medicine because of its excellent donor-acceptor properties and unique structure. Among these useful applications, the application in nuclear medicine using radioactive metallofullerenes is promising. However, the production yield of EMFs is generally low: for example, the yield of EMFs in whole fullerene species is less than 1% with the commonly employed arc discharge method. Therefore, the separation and purification of EMFs from a large amount of empty fullerene species are needed. In general, high-performance liquid chromatography (HPLC) is employed for the separation/purification of EMFs from empty fullerenes. Because this method is not always efficient from the viewpoint of cost and time consumption, a more efficient method is required to be developed.

Recently, low-cost separation methods for EMFs using the chemical redox reaction were reported.[1,2] Considering the separation of carrier-free radioactive EMFs, separations through the reduction of EMFs using an electron donor are expected to be suitable because these methods do not include a process using a large amount of carriers such as the formation of the precipitate. However, these separation methods have some problems because the separation efficiency is not very high and the number of steps is large. Currently, we are attempting to develop a separation method with higher efficiency and smaller number of steps than the other methods through the chemical reduction of EMFs. In this study, we employed the radio-tracer method to acquire quantitative data for the separation by chemical reduction for determining the best separation condition.

To obtain the radio tracer of ^{139}Ce, a dried La_2O_3 pellet (600 mg/cm^2) was irradiated with 3 μA of 24 MeV deuteron for 2 h at the RIKEN AVF cyclotron. After the irradiation, ^{139}Ce and the target material La were converted into their nitrate forms, dissolved in ethanol, and then injected into porous carbon rods for fullerene generation. Radioactive ^{139}Ce EMFs were produced by the arc discharge method and extracted together with empty fullerenes from the soot by CS_2. Mixed solutions of polar solvents (acetonitrile: MeCN, acetone, and methanol: MeOH) and small amounts of electron donors (triethylamine: TEA, tripropylamine: TPA, tetrahydrofurane: THF, *N*,*N*,-dimethylformanide: DMF, pyridine, and aniline) for the reduction of EMFs were added into these CS_2 solutiosn and then stirred. To separate the produced EMF anion from the residual empty fullerene precipitate, these solutions were passed through a membrane filter. A few drops of an aqueous solution of dichloroacetatic acid were added into the filtrate samples for neutralizing the EMF anion, and the neutralized EMFs were re-dissolved in chlorobenzene (F). The residual empty fullerenes on membrane filters were dissolved in CS_2 for recovery from a filter (P). The γ ray emitted from these solutions and filter were detected using a Ge detector.

Figure 1 shows the rate% of radioactivity observed in F, P, and filter for each sample. In principle, radioactivity observed in F is derived from radioactive EMFs separated from empty fullerenes and that in P is derived from radioactive EMFs that remained in the empty fullerene precipitate. Accordingly the rate% of F indicates the separation efficiency of EMFs. Considering the donor number (DN) which is known as an index indicating the strength of the electron donor properties, the electron donors used in this study can be arranged according to their performance as TEA >TPA >aniline >pyridine >DMF >THF.[3] In the case of MeCN as the polar solvent, a rate% greater than 80% in F was found with alkylamines such as TPA and TEA. These results indicate that good electron donors such as TPA and TEA easily reduce EMFs. From the viewpoint of the polarity of the solvent, the rate% of F for the solvents with large polarity such as MeCN is found to be larger than that for the solvents with small polarity such as acetone. On the other hand, the rate% of F for MeCN which is a non-protic solvent is superior to that for MeOH which is a protic solvent in spite of both polarities being comparable.

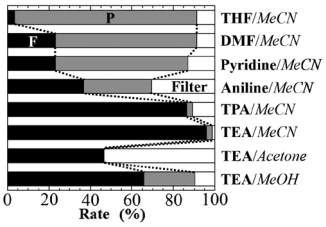

Fig. 1. Observed radioactivity in solution F (black), solution P (gray), and filter (white) for each sample.

*1 Department of Chemistry, Tokyo Metropolitan University
*2 RIKEN Nishina Center

References

1) K. Akiyama et al., J. Am. Chem. Soc. **134**, 9762 (2012).
2) T. Kodama et al., Chem. Lett. **34**, 464 (2005).
3) V. Gutmann: The Donor-Acceptor Approach to Molecular Interactions (Plenum, New York, 1978).

Production cross sections of (*d*,*x*) reactions on natural platinum†

M. U. Khandaker*1,*2 and H. Haba*2

An accurate knowledge of nuclear reaction phenomena of light charged particles with platinum shows significance due to its various applications in science and technology. The microscopic experimental cross-sections of platinum are very useful for the production of medical radioisotopes, the verification of nuclear reaction theory, the thin layer activation analysis, etc. Recently, we investigated deuteron-induced reaction cross sections from various target elements because measured data of the (*d*,*x*) processes are limited compared to those of (*p*,*x*) processes. A survey of literature shows that several investigations have been conducted for the ^{nat}Pt(*d*,*x*) reactions leading to various applications. As an example, the production of the ^{198g}Au via the ^{nat}Pt(*d*,*x*) reaction finds applications in targeted radiotheraphy and imaging procedures [1,2]. Its half-life is suitable for an uptake and residence time of antibodies especially in the treatment of solid tumors without a significant loss of activity. Due to the monoisotopic characteristic of ^{197}Au target, the ^{197}Au(*n*,γ)^{198}Au reaction with a nuclear reactor of quite moderate power is currently being utilized as a commercial production route for ^{198}Au in many countries for clinical use [2]. But the successive and simultaneous formation of ^{199}Au via the secondary ^{198}Au(*n*,γ)^{199}Au reaction is significant because of its very high cross-section, and therefore causes a small portion of ^{199}Au isotopic impurity and reduce the specific activity of ^{198}Au. Thus, measurements of new experimental cross-sections via the deuteron irradiation on natural platinum are expected to provide new production pathways for the no-carrier-added ^{198}Au.

The objective of the present study was to report the latest cross sections of the ^{nat}Pt(*d*,*x*) ^{192,193,194,195,196m2,196,198m,198,199}Au, ^{195m,197}Pt and $^{190(g+m1+0.086m2),192(g+m1),194m}$Ir reactions that were measured with a high precision over the energy range of 2–24 MeV using the AVF cyclotron facility of the RIKEN RI Beam Factory, Wako, Japan. Details on the irradiation technique, radioactivity determination, and data evaluation procedures are available in Ref. [3]. Owing to the space limitation of this report, we present only the ^{nat}Pt(*d*,*x*)^{198g}Au cross sections and the deduced yield in Figs. 1 and 2, respectively. Measured cross sections with an overall uncertainty are listed in Ref. [3]. The cross-sections were normalized by using the ^{nat}Ti(*d*,*x*)^{48}V monitor cross sections recommended by IAEA. Measured data were critically compared with the available literature data and theoretical data, and only partial agreements were obtained with the earlier experimental and theoretical data extracted from the TENDL-2013.

The deduced thick-target yields indicate that a low amount of no-carrier-added ^{198g}Au could be obtained on an enriched ^{198}Pt (100%) target with the yield of 22 MBq/μA-h at 15 MeV deuteron energy from a cyclotron.

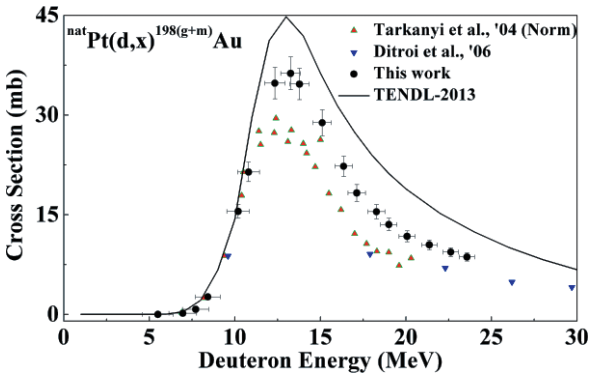

Fig. 1. Excitation function of the ^{nat}Pt(*d*,*x*)^{198g}Au reaction.

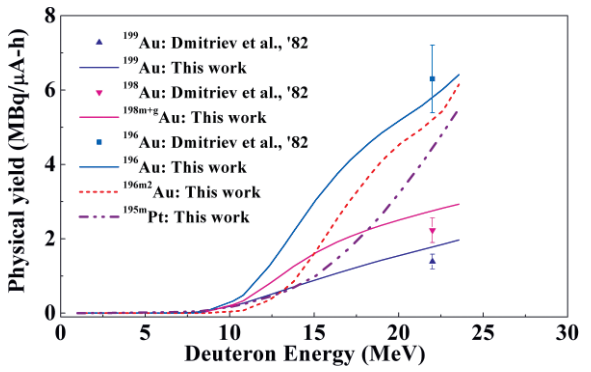

Fig. 2. Physical thick target yields for the $^{199,198g+m,196,196m2}$Au and ^{195m}Pt radionuclides.

References

1) J. Horiuchi, M. Takeda, H. Shibuya, S. Matsumoto, M. Hoshina, S. Suzuki: Radiotherapy and Oncology **21**, 29 (1991).
2) D. E. Berning, K. V. Katti et al.: Nucl. Med. & Bio. **25,** 577 (1998).
3) M. U. Khandaker, H. Haba et al.: Nucl. Instrum. Meth. Phys. Res. B **362**, 151 (2015).

† Condensed from the article in Nucl. Inst. Meths. B. **362**, 151 (2015).

*1 Department of Physics, University of Malaya
*2 RIKEN Nishina Center

Measurement of production cross sections of Re isotopes in the $^{nat}W(d,x)$ reactions

Y. Komori,[*1] M. Murakami,[*1,*2] and H. Haba[*1]

Chemical characterization of superheavy elements is one of the most important and challenging subjects in the field of nuclear chemistry. We plan to conduct model experiments for chemical studies of element 107, Bh, using radiotracers of its homologs, Tc and Re. Long-lived ^{95m}Tc ($T_{1/2}$ = 61 d), ^{183}Re ($T_{1/2}$ = 70 d), and ^{184m,g}Re (m: $T_{1/2}$ = 169 d; g: $T_{1/2}$ = 35.4 d) are useful for the model experiments. These isotopes are producible in the deuteron-induced reactions on ^{nat}Mo and ^{nat}W (nat: natural isotopic abundance) using the RIKEN AVF cyclotron. Previously, we measured production cross sections of Tc isotopes in the ^{nat}Mo(d,x) reactions for quantitative production of ^{95m}Tc.[1] In this work, we have measured the cross sections of Re isotopes in the ^{nat}W(d,x) reactions up to 24 MeV.

The cross sections were measured using a stacked-foil technique. The target stack consisted of twenty sets of ^{nat}W foils (99.95% purity, 40.7 mg/cm^2 thickness) and ^{nat}Ti foils (>99.6% purity, 4.7 mg/cm^2 thickness). The Ti foils were used to calibrate the beam current and the incident energy via the monitor reaction ^{nat}Ti(d,x)^{48}V.[2] The size of all foils was 15 × 15 mm^2. The target stack was irradiated for 1 h with a 24-MeV deuteron beam supplied from the RIKEN AVF cyclotron. The average beam current was 0.18 μA. After the irradiation, each foil was subjected to γ-ray spectrometry with a Ge detector.

The excitation functions were measured for the ^{nat}W(d,x)^{181,182a,182b,183,184m,184g,186g}Re, ^{187}W, ^{182g,184}Ta reactions. Figure 1 shows the excitation function of the ^{nat}W(d,x)^{183}Re reaction. Our results are in good agreement with those of Tárkányi et al.[3] and Duchemin et al.[4] and slightly smaller than others.[5–7] Figure 2 shows the excitation function of the ^{nat}W(d,x)^{184m}Re reaction. There are only two reports[4,5] on the cross sections of ^{184m}Re and our data confirmed the results reported by Duchemin et al.[4] It can be seen that the theoretical model code TALYS (TENDL-2014)[8] reproduces well the experimental cross sections of ^{183}Re. However, the code significantly overestimates the excitation function of ^{184m}Re though it can reproduce the shape of the function. As for ^{184g}Re, our results are slightly smaller than those in the literature.[3–5] The TALYS code slightly underestimates our excitation function of ^{184g}Re, though it reproduces the shape of the function. Thick-target yields of ^{183,184m,184g}Re were deduced from the measured cross sections. The deduced yields of ^{183,184m,184g}Re at 24 MeV are 1.7, 0.043, and 1.2 MBq/μA·h, respectively. Based on the present results, we produced ^{183,184m,184g}Re by typical irradiations of a 200 mg/cm^2-thick ^{nat}W target foil with the 24-MeV deuteron beam with 5-μA for 3 h. These Re isotopes were chemically separated as no-carrier-added forms from the target material and by-products by using anion-exchange and alumina columns. We are using these radiotracers to develop a rapid solvent extraction apparatus and to determine suitable experimental conditions to study the aqueous chemistry of Bh.[9]

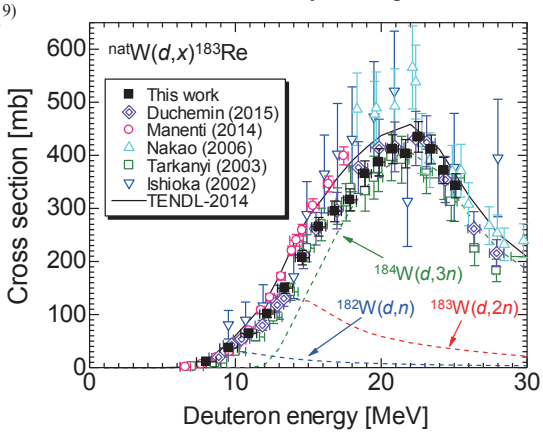

Fig. 1. The excitation function of the ^{nat}W(d,x)^{183}Re reaction. The errors of the cross sections were evaluated by propagating those of counting statistics in the radioactivity measurement, detector efficiency, and γ-ray intensity. The error in the deuteron energy corresponds to the energy degradation in each foil.

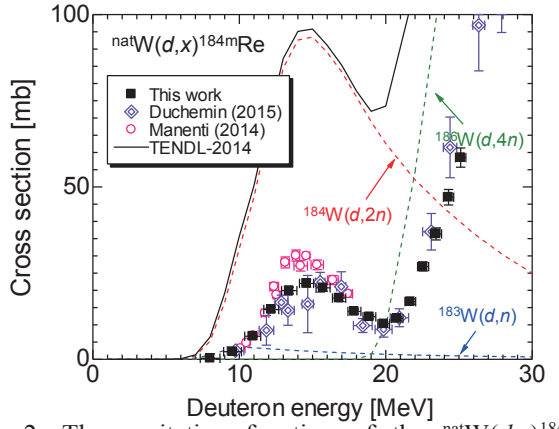

Fig. 2. The excitation function of the ^{nat}W(d,x)^{184m}Re reaction.

*1 RIKEN Nishina Center
*2 Graduate school of Sci. and Technol., Niigata Univ.

References

1) Y. Komori et al.: RIKEN Accel. Prog. Rep. **48**, 296 (2015).
2) IAEA: IAEA report IAEA-TECDOC-1211, 2001.
3) F. Tárkányi et al.: Nucl. Instrum. Meth. B **211**, 319 (2003).
4) C. Duchemin et al.: Appl. Radiat. Isot. **97**, 52 (2015).
5) S. Manenti et al.: Radiochim. Acta. **102**, 669 (2014).
6) M. Nakao et al.: Nucl. Instrum. Meth. A **562**, 785 (2006).
7) N. S. Ishioka et al.: J. Nucl. Sci. Technol. Suppl. **2**, 1334 (2002).
8) A. J. Koning et al.: TENDL-2014: TALYS-based Evaluated Nuclear Data Library, 2014.
9) Y. Komori et al.: Pacifichem 2015, Honolulu, Hawaii, U.S.A., Dec. INOR 1758, 2015.

Alpha particle induced cross section measurements on natural and enriched Cd at 50 MeV

F. Ditrói, [*1] S. Takács, [*1] H. Haba, [*2] Y. Komori, [*2] M. Aikawa, [*3,*2] Z. Szűcs, [*1] and M. Saito [*4,*2]

In year 2015 two series of measurements have been performed in January and December at the AVF cyclotron of RIKEN Nishina Center in the frame of a bilateral agreement between the Hungarian Academy of Sciences and the Japan Society for the Promotion of Science. One of those series was the investigation of alpha particle induced cross sections on ^{nat}Cd and enriched ^{116}Cd targets. The energy of the alpha beam was calibrated by using Time of Flight (TOF) methods before the December experiments. The results of this was also used to correct the results of the January experiments, because it turned out that the nominal 50 MeV alpha energy provided by the accelerator actually corresponds to 51.2 MeV energy. The enriched cadmium was deposited on Cu backing while the natural cadmium foils were pure metal foils from Goodfellow. In both irradiations we used thin Ti foils for monitoring the beam parameters, while in the enriched cadmium experiments also the Cu backing served as monitor.

The radioisotope ^{117m}Sn with 13.6 d half-life, which has already been used as a bone cancer pain relief agent, turned to be more important in medical applications. ^{117m}Sn has several advantages in modern cancer therapy. It has conversion electron radiation with an average energy of 140 keV allowing about 300 μm effective treatment range, the half-life is convenient for production, labelling and delivery within several hundreds of kilometers, its 159 keV gamma line is also convenient for using the commercial imaging techniques e.g. gamma camera. Taking into account all these properties ^{117m}Sn is a unique candidate between all potential medical isotopes[1].

The first stack was assembled from enriched ^{116}Cd deposited on 12 μm Cu backing. The average thickness of the Cd layer was measured as 21.9 μm. For further monitoring several Ti foils with nominal thickness of 12 μm were also inserted between the Cd targets.

The alpha induced cross sections on both natural and enriched ^{116}Cd and ^{nat}Cd targets have already measured by several authors[2,3,4], the purpose of the present study was to resolve the big discrepancies of the different results and to extend the energy range of the measurements (see Figs. 1 and 2). The preliminary results are shown in Fig.1 for the enriched targets and in Fig. 2 for natural cadmium, both for the medically important ^{117m}Sn radioisotope. On Fig. 1 our results are much higher than the others under 30 MeV, that is why we have measured the spectra in the December experiment much longer, in order to separate the contribution from other isotopes. At list one of the previous results on natural cadmium is obviously wrong (Fig. 2), so our contribution may give the correct results, as the it is confirmed by the shape and amplitude of the TENDL prediction.

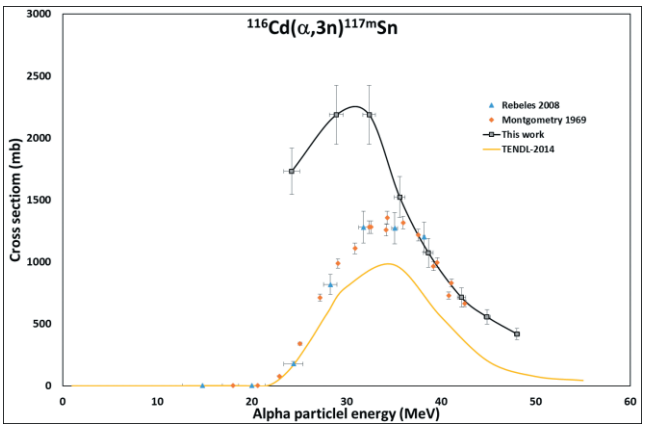

Figure 1. Preliminary result of cross sections for the ^{116}Cd(α,3n)^{117m}Sn reaction

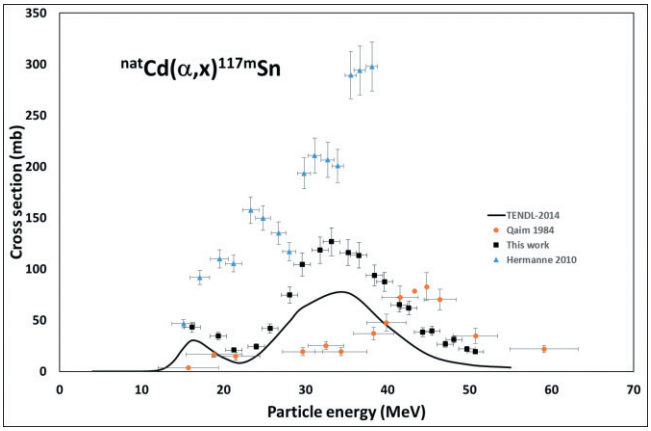

Figure 2. Preliminary result of cross sections for the ^{nat}Cd(α,3n)^{117m}Sn reaction

References

1) R. Nigel et al.: J. Radioanal. Nucl. Chem. **305**, 99 (2015).
2) S.M. Qaim, H. Doehler: Appl. Radiat. Isot. **35**, 645 (1984).
3) R.A. Rebeles et al.: Nucl. Instrum. Methods Phys. Res. B **266**, 4731 (2008).
4) D.M. Montgometry, N.T. Porile: Nucl. Phys. A **130**, 65 (1969).
5) T. Watanabe et al., Proceedings of the 5th International Particle Accelerator Conference (IPAC2014), 3566 (2014).
6) T. Watanabe et al., Proceedings of the 12th Annual Meeting of Particle Accelerator Society of Japan, p. 1198 (2015).

[*1] Institute for Nuclear Research, Hungarian Academy of Sciences
[*2] RIKEN Nishina Center
[*3] Faculty of Science, Hokkaido University
[*4] Graduate School of Science, Hokkaido University

Excitation function of α-induced reaction on ^{nat}Pd for ^{103}Ag production

M. Aikawa,[*1,*2] M. Saito,[*3,*2] H. Haba,[*2] Y. Komori,[*2] S. Takács,[*4] F. Ditrói,[*4] and Z. Szücs[*4]

Radioactive isotopes (RIs) are available in many application fields, such as engineering and medicine. Production of such RIs is possible through various reactions involving combinations of projectiles and targets. The best process to obtain RIs can be discussed based on the information of all the reactions. The production cross sections induced by neutrons and light charged-particles thus constitute fundamental information for the applications.

One such RI for medical applications is ^{103}Pd ($T_{1/2}$ = 16.991 d) for brachytherapy[1,2] and targeted radionuclide therapy as part of the ^{103}Pd/^{103m}Rh *in vivo* generator[3]. In addition to direct ^{103}Pd production, the production of its generator, ^{103}Ag, is worthly of investigation. ^{103}Ag has the isomeric state ^{103m}Ag at 134.4 keV ($T_{1/2}$ = 5.7 s, IT: 100%), which cumulatively contributes to ^{103g}Ag ($T_{1/2}$ = 65.7 min, $\epsilon + \beta^+$: 100%) production through IT decay. In the case of α-induced reactions on ^{nat}Pd, only experimental data are available only below 37 MeV[4]. Therefore, we performed an experiment to obtain the excitation function of ^{nat}Pd(α,x)^{103}Ag up to about 50 MeV. This experiment is promising as it would provide fundamental information for establishing the best process for ^{103}Ag/^{103}Pd production.

The experiment was performed at the RIKEN AVF cyclotron by using the stacked foil technique and the activation method. ^{nat}Pd foils (purity: 99.95%, Nilaco, Japan) were used with ^{nat}Ti monitor foils (purity: 99.9%, Goodfellow, UK). The thicknesses of the Pd and Ti foils were 9.80 mg/cm^2 and 4.95 mg/cm^2, respectively. The stacked target consisted of 12 sets of the Pd-Pd-Ti-Ti foils to reduce the possible recoil effect in every second foil. The target was irradiated for 2 h by the 51.2 MeV α beam with the average intensity of 55.7 pnA. This beam energy was measured by the time-of-flight method using a plastic scintillator monitor[5]. γ rays from the irradiated foils were measured by HPGe detectors.

According to the NuDat 2.6 database[6], there are many specific γ lines from ^{103g}Ag decays. We adopted the intense γ line at 118.74 keV (31.2%) to derive the production cross sections of ^{103g}Ag since the γ line at 148.20 keV (28.3%) overlaps with that of ^{111m}Cd ($T_{1/2}$ = 48.54 min, IT: 29.1%) at 150.824 keV. Our preliminary result is shown in Fig. 1 with the previous experimental data[4] and theoretical calculation of

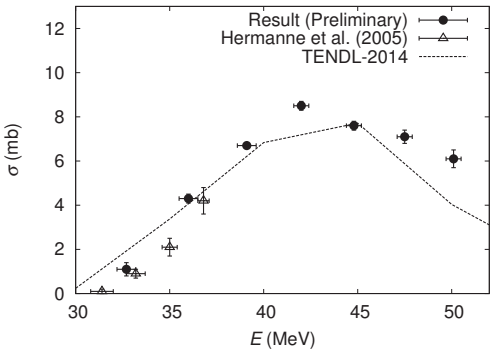

Fig. 1. Excitation function of the ^{nat}Pd(α,x)$^{103g+m}$Ag reaction. Our preliminary result (solid circles) with statistical errors is compared with the previous experimental data (open triangles)[4] and the theoretical calculation[7] of ^{102}Pd(α,x)^{103}Ag with normalization of the ^{102}Pd abundance.

^{102}Pd(α,x)^{103}Ag in TENDL-2014[7] with normalization of the ^{102}Pd abundance (1.02%). Our result shows slightly larger values than the previous data[4] below 37 MeV. The peak could be found at around 42 MeV in our result but at around 45 MeV in TENDL-2014[7]. Further analysis will be performed on the data and the Ti monitor reaction to finalize the result.

In summary, we performed an experiment on ^{nat}Pd(α,x)$^{103g+m}$Ag by using the stacked foil technique and the activation method. The preliminary result of the excitation function of the reaction shows slightly different values from the previous experiment and theoretical calculation. The final result based on further analysis will be reported in a separate paper. We will also analyze the spectral data to derive production cross sections of other RIs.

This work is supported by the Japan - Hungary Research Cooperative Program, JSPS and HAS.

References

1) S. Nag et al., Int. J. Radiat. Oncol. Biol. Phys. **44**, 789 (1999).
2) A. Hermanne et al., Radiochim. Acta **92**, 215 (2004).
3) Z. Szücs et al., Appl. Rad. Isot. **67**, 1401 (2009).
4) A. Hermanne et al., Nucl. Instr. Meth. B **229**, 321 (2005).
5) T. Watanabe et al.: Proc. 5th Int. Part. Accel. Conf. (IPAC2014) (2014), p.3566.
6) National Nuclear Data Center: the NuDat 2 database, http://www.nndc.bnl.gov/nudat2/.
7) A.J. Koning et al.: TENDL-2014: TALYS-based evaluated nuclear data library.

*1 Faculty of Science, Hokkaido University
*2 RIKEN Nishina Center
*3 Graduate School of Science, Hokkaido University
*4 MTA ATOMKI, Hungarian Academy of Sciences

Excitation functions of deuteron-induced reactions on natural nickel †

A. R. Usman,[*1,*2] M. U. Khandaker,[*1,*2] H. Haba,[*1] M. Murakami,[*1] and N. Otuka[*3]

Nickel (Ni) has been given priority over several other materials in a recent IAEA Coordinated Research Project on Nuclear Data Libraries for Advance Systems - Fusion Devices. Ni also can be used as a target material for the production of radionuclides by accelerators leading to medical and industrial applications. Co radionuclides such as ^{55,56,57}Co found potential applications in medicine and other basic research fields due to their suitable decay characteristics [1]. ^{55}Co found important applications in labelling bleomycin and in the studies of cerebral and cardiac problems via PET. ^{57}Co plays a significant role as a calibration standard in γ-ray spectrometry and single photon emission computed tomography (SPECT) [2]. A detailed literature survey of experimental data via deuteron bombardment of nickel show large discrepancies among the previous data. More so, experimental data via the deuteron bombardment process are relatively scarce, leading to further need of enriching the database. In this article, new experimental cross-sections of several radionuclides were reported via deuteron irradiation of some stacked foils made from natural Ni. A well-established stacked foil activation technique combined with γ-ray spectrometry was employed to determine the cross-sections of the ^{nat}Ni(d,x)$^{55\text{-}58,60}$Co, ^{57}Ni, ^{52g,54}Mn, and ^{61}Cu reactions for the deuteron energy range of 24 MeV down to the respective thresholds [3].

Using a water-cooled target holder that served as a Faraday cup, two stacks were irradiated for 2.00 h and 2.07 h, respectively, with a 24-MeV deuteron beam energy and about 200 nA beam current from the AVF cyclotron of RIKEN RI Beam Factory, Japan [3]. The beam intensity was determined from the activity of the Ti foil placed at the front of the stacks, and considered as a constant to deduce cross-sections for each foil in the stack. The ^{nat}Ti(d,x)^{48}V monitor reaction (σ = 217.54 mb at E_d = 23.88 MeV) recommended by the IAEA [3] was adopted to evaluate the beam intensity.

The production cross-sections of $^{55\text{-}58,60}$Co, ^{57}Ni, ^{52g,54}Mn, and ^{61}Cu radionuclides were reported in the tables and figures in Ref. [3], together with extensive reviews of EXFOR data base and also TENDL-2014. Owing to space, only excitation functions of $^{60m+g}$Co and ^{52g}Mn are given here. Only two earlier studies reported the cross-sections of ^{60}Co, and they are inconsistent with each other as shown in Fig. 1. The prediction by the Talys code extracted from TENDL-2014 database could not also give a good approximate of the excitation function of ^{60}Co. A separate experiment based on the optimized experimental condition for ^{60}Co may be helpful to obtain a more reliable excitation function of this radionuclide. Unlike proton production route, the production cross-sections of ^{52g}Mn via deuteron irradiation was scarcely reported. The TENDL-2014 could not accurately predict the excitation function of this radionuclide.

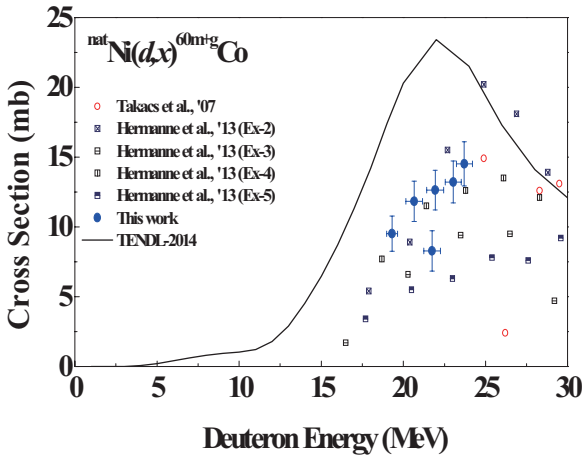

Fig. 1. Excitation function of the ^{nat}Ni(d,x)$^{60m+g}$Co reaction.

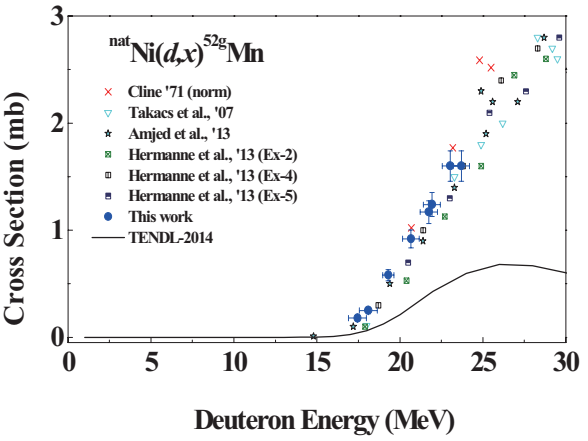

Fig. 2. Excitation function of the ^{nat}Ni(d,x)^{52g}Mn reaction.

References

1) M.C. Lagunas-Solar, J.A. Jungerman: Int. J. Appl. Radiat. Isot. **30**, 25 (1979).
2) F.S. Al-Saleh et al.: Appl. Radiat. Isot. **65,** 104 (2007).
3) A. R. Usman et al.: Nucl. Instrum. Meth. Phys. Res. B **368**, 112 (2016).

† Condensed from the article in Nucl. Inst. Meths. B. **368**, 112 (2016).

*1 RIKEN Nishina Center
*2 Department of Physics, University of Malaya
*3 Nuclear Data Section, International Atomic Energy Agency

Cross checking of monitor reactions at RIKEN AVF cyclotron using 50 MeV alpha particle beams

S. Takács,[*1] F. Ditrói,[*1] Z. Szűcs,[*1] H. Haba,[*2] Y. Komori,[*2] M. Aikawa,[*3,*2] and M. Saito[*4,*2]

In the frame of a bilateral agreement between the Hungarian Academy of Sciences (HAS) and the Japan Society for the Promotion of Science (JSPS), experiments were performed to determine activation cross sections for a variety of radionuclides, which were produced in alpha particle induced nuclear reactions on ^{27}Al, ^{nat}Ti, ^{nat}Cu, ^{nat}Pd, ^{nat}Cd, ^{116}Cd, and ^{nat}Ge target materials, using the conventional stacked-foil-target technique and activation method. Experiments were performed during two separate beam time allocations in January 2015 and in December 2015. In both series of experiments alpha particle beams with E_α = 51.2 MeV energy were used, measured by the time of flight method. Irradiations took place in a special vacuum chamber for irradiation times of one or two hours with a beam current of 50 nA. The activity of the irradiated target foils was assessed by high purity Ge gamma-spectrometers. Decay of the produced radionuclides was followed for several half-lives in order to identify the sources of the possible interfering gamma radiations accurately. Reactions on the ^{27}Al, ^{nat}Ti, and ^{nat}Cu target materials are most frequently used for monitoring the beam parameters, such as actual beam energy, beam intensity, or energy loss of the bombarding particles in the irradiated target material. Recommended cross section values are provided for those monitor reactions by the International Atomic Energy Agency (IAEA)[1] and are freely available on the Internet. Since the recommended data available by IAEA were evaluated one by one, independently, a cross-check of the reaction cross section is advised. The aim of our measurements regarding the ^{27}Al, ^{nat}Ti, and ^{nat}Cu targets was to contribute the cross-checked data sets to the database maintained by the Nuclear Data Section (NDS), IAEA and extend the energy range of the recommended data up to 50 MeV, where necessary. A stack containing thin Al, Ti, and Cu metallic foils was irradiated to cross-check the ^{27}Al(α,x)^{22}Na, ^{27}Al(α,x)^{24}Na, ^{nat}Ti(α,x)^{51}Cr, ^{nat}Cu(α,x)^{66}Ga, ^{nat}Cu(α,x)^{67}Ga, and ^{nat}Cu(α,x)^{65}Zn monitor reactions. As indicated by the first preliminary results shown in Figs. 1 and 2, there is only a small inconsistency among the recommended values of the investigated monitor reactions. Experimental data measured on ^{27}Al, ^{nat}Ti, and ^{nat}Cu in the same stack show that the recommended values provided in the IAEA database are relatively in good agreement. However, the shapes of the recommended curves and the new experimental data show some deviations, which require further analysis and verification. Preliminary data show that the amplitude of the recommended excitation functions and the experimental values have maximum difference of 7%, which should be confirmed later, since some of the data collection is still running and data evaluation is in progress.

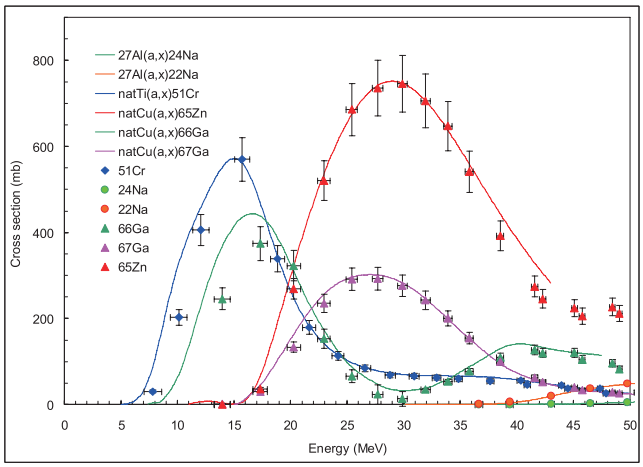

Figure 1. Preliminary results are shown on cross section data for the ^{27}Al(α,x)^{22,24}Na, ^{nat}Ti(α,x)^{51}Cr, ^{nat}Cu(α,x)^{66,67}Ga, and ^{nat}Cu(α,x)^{65}Zn reactions. Solid curves denote the IAEA recommended values, which are in acceptable agreement with our measurements; however, the shape of the excitation functions should be confirmed.

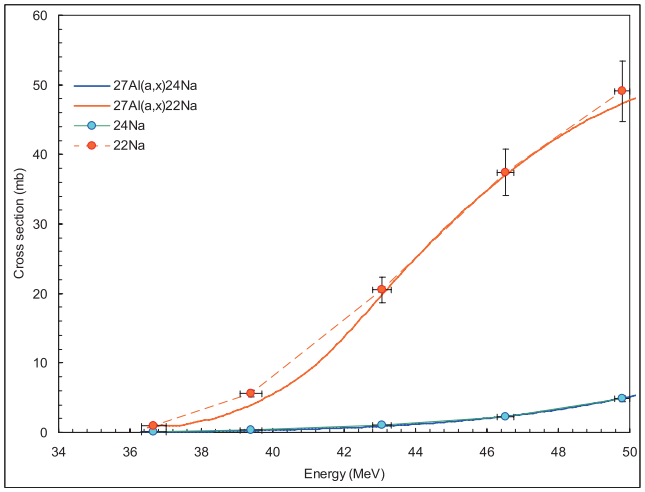

Figure 2. Preliminary results are shown on cross section data for the ^{27}Al(α,x)^{22,24}Na reactions. Solid curves denote the IAEA recommended values. The shape of the excitation functions should be confirmed.

Reference

1) https://www-nds.iaea.org/medical/monitor_reactions.html

*1 Institute for Nuclear Research, Hungarian Academy of Sciences
*2 RIKEN Nishina Center
*3 Faculty of Science, Hokkaido University
*4 Graduate School of Science, Hokkaido University

4. Radiation Chemistry and Biology

The defect of non-homologous end joining substantially enhanced the focus formation of Rad51 after X-ray irradiation, but not after heavy-ion irradiation

M. Izumi[*1] and T. Abe[*1]

DNA double-strand breaks (DSBs) are caused by exposure of DNA to ionizing radiation, and these are repaired primarily by non-homologous end joining (NHEJ), homologous recombination (HR), or microhomology mediated end joining (MMEJ) in mammalian cells [1]. Accelerated heavy-ion particles with a high linear energy transfer (LET) induce complex clustered DNA damage, which is considered an obstacle to efficient repair and induces different biological effects compared to low-LET radiation. To analyze the repair mechanism for DSBs caused by heavy-ions, we investigated cell sensitivity to heavy-ions by using a wild-type CHO cell and two CHO mutant lines deficient in HR[2] or NHEJ[3] in the previous study[3] and observed that HR is mainly involved in the repair pathway induced by high-LET ionizing radiation[4]. However, several studies suggest that NHEJ is also involved in DSB repair caused by heavy ion[5,6], and the repair mechanism is still controversial.

In this report, we investigated the formation of Rad51 foci, which is involved in strand transfer and is essential for HR[7], using CHO cells and mutant cell line (V3) deficient in NHEJ. The number of Rad51 foci per cell in V3 cells was twice that in CHO cells 1 h after X-ray irradiation, suggesting that NHEJ and HR work competitively to some extent (Fig. 1). In contrast, the number of Rad51 foci in V3 cells was similar to that in CHO cells 1 h after C-ion irradiation (LET = 80 keV/μm), suggesting that HR works mainly in DSB repair.

The number of Rad51 foci was maximum immediately after X-ray irradiation and decreased gradually, whereas the number of Rad51 foci increased from 1 h to 8 h and then slightly decreased from 8 h to 16 h after C-ion irradiation, indicating that DSBs induced by C-ion are repaired slowly compared to those induced by X-ray. In addition, the number of Rad51 foci significantly increased in V3 cells than in CHO cells 16 h after C-ion irradiation. This result suggests that NHEJ is also involved in repair pathway. The processing of damaged DNA strands by various enzymes may enable NHEJ to repair DSBs caused by heavy-ion irradiation at a later period. As the apoptosis in CHO cells starts 18-24 h after irradiation, the results of survival may not necessarily reflect the repair process directly.

Now we are investigating the localization of 53BP1 and Rif1 after heavy-ion irradiation, which are involved in the selection of repair pathways for repairing DSB[8,9]. Our preliminary experiments showed that Rad51 foci were only observed in S-G2 cells after heavy-ion irradiation (data not shown). Therefore, we are also planning to examine how cell cycle affects repair kinetics.

*1 RIKEN Nishina Center

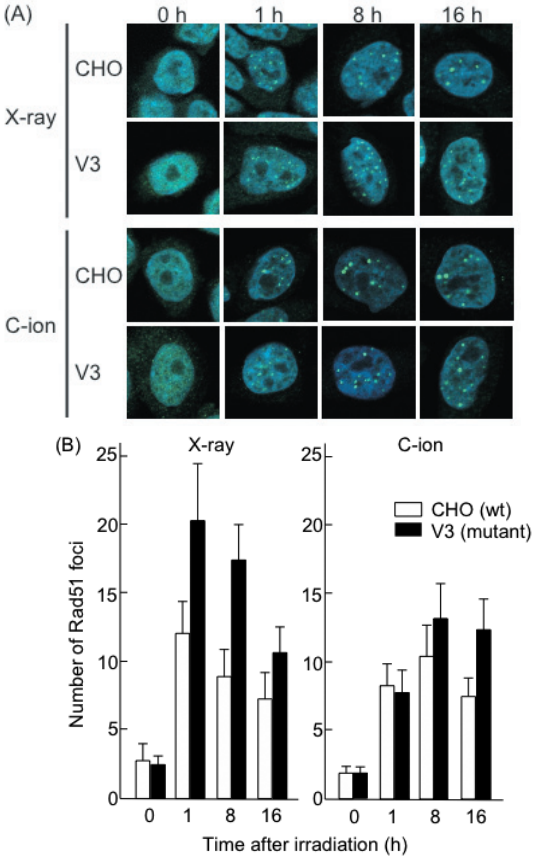

Fig. 1 (A) Representative images of CHO or V3 nuclei (blue) with Rad51 foci (green). Cells were irradiated with 5 Gy of X-ray or carbon ions and fixed with 4% paraformaldehyde at indicated time points from irradiation. Foci formation of Rad51 was detected using immunofluorescence staining. (B) Kinetics of Rad51 foci formation in CHO (open box) or V3 (closed box) cells. Rad51 foci were scored in 2D by using a Zeiss microscope with ApoTome from 1-16 h post irradiation. The average number of foci per Rad51-positive cells is shown. Error bars represent the standard deviations.

References

1) L.S. Symington and J. Gautier: Annu. Rev. Genet. **45,** 247-271 (2011).
2) R.S. Tebbs et al.: Proc. Natl. Acad. Sci. USA **92,** 6354 (1995).
3) S.R. Peterson et al.: Proc. Natl. Acad. Sci. USA **92,** 3171 (1995).
4) M. Izumi and T. Abe: RIKEN Accel. Prog. Rep. **47,** 253, (2014).
5) A. Takahashi et al.: Radiat. Res. **182,** 338-344 (2014).
6) A. Bajinskis et al.: Mut. Res. 731, 125-132 (2012).
7) A. Shinohara et al: **69,** 457 (1992).
8) C. Escribano-Diaz et al.: Mol. Cell **49**, 872 (2013).
9) J. R. Chapman et al.: Mol. Cell **49,** 858 (2013).

Low-dose high-LET heavy ion-induced bystander signaling (II)

M. Tomita,[*1,*2] T. Tsukada,[*2] and M. Izumi[*2]

Radiation-induced bystander response (RIBR) is a cellular response induced in nonirradiated cells that receive bystander signals from directly irradiated cells within an irradiated cell population.[1)] RIBR induced by low doses of high-LET radiations is an important issue concerning the health of astronauts and in heavy-ion radiation cancer therapy. Here, we investigated the underlying molecular mechanisms and biological implications of RIBR induced by such low doses of high-LET radiations.

The clonogenic cell survival of normal human fibroblast WI-38 cells irradiated with Ar ions (310 keV/μm) is shown in Fig. 1. At a higher dose region (0.5 Gy and above), the surviving fractions of cells harvested 16–24 h after irradiation was similar to those of cells harvested immediately (0 h) after irradiation [Fig. 1A]. On the other hand, a strong cell-killing effect at doses below 0.08 Gy was observed in the cells harvested 16–24 h after irradiation [Fig. 1B]. Such an effect was not observed in the cells harvested immediately after irradiation. Previously, we reported that cells irradiated with high-LET Fe ions (1000 keV/μm) showed similar results.[2)] These results suggest that an adequate incubation period is necessary for bystander signal induction and transfer.

Previously, we reported that gap-junction intercellular communication (GJIC), cyclooxygenase-2 (COX-2) protein, and nitric oxide (NO) were involved in high-LET Fe-ion-induced bystander signal transfer.[2)] Figure 2 shows the progress of results reflecting new data. Lindane and NS-398 (an inhibitor of GJIC and COX-2, respectively) were dissolved in DMSO (a scavenger of reactive oxygen species). c-PTIO is a scavenger of NO. DMSO (0.1%), lindane (Lin, 50 μM), c-PTIO (20 μM), or NS-398 (50 μM) was added to the medium 2 h before irradiation[3)] with 0.1 Gy of Fe ions (1000 keV/μm) [Fig. 2A] or 0.05 Gy of Ar ions (310 keV/μm) [Fig. 2B]. The obtained results for the cells irradiated with Fe and Ar ions were almost similar. DMSO did not significantly suppress the bystander cell killing. In contrast, lindane, NS-398, and c-PTIO significantly ($P < 0.05$) suppressed cell death to similar levels. Cells pretreated with both c-PTIO and lindane did not exhibit a significantly higher surviving fraction than those pretreated with lindane or c-PITO alone. These results suggest that bystander signaling through GJIC and the cell culture medium induces the bystander cell killing effect in a coordinated manner.

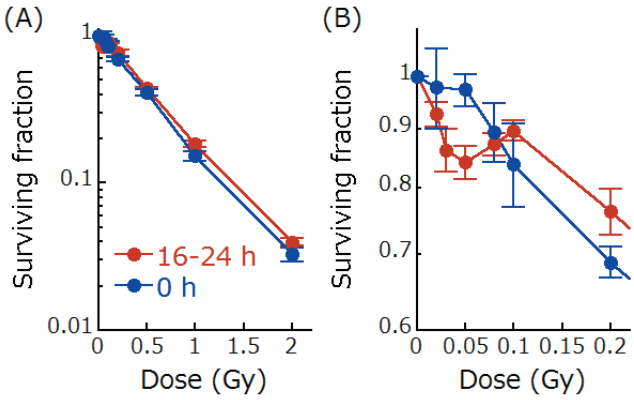

Fig. 1. Survival curves of WI-38 cells. Confluent monolayers of WI-38 cells were irradiated with 95 MeV/u Ar ions and the cells were harvested immediately (0 h) or 16–24 h after irradiation. The surviving fraction was determined by using a colony forming assay. Panel A shows all data obtained in this study. Panel B shows the surviving fractions at doses of 0.2 Gy and below. The error bars represent the standard errors of the mean (SEM) (n = 3–6).

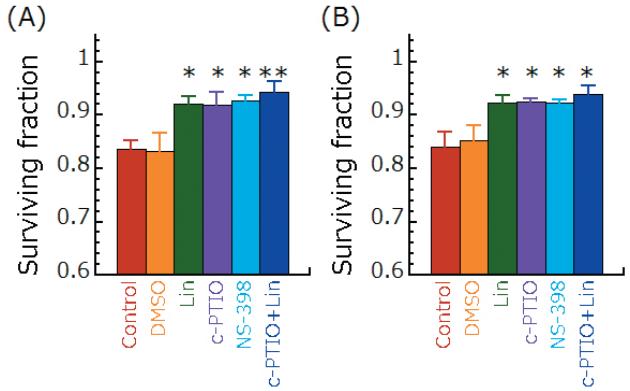

Fig. 2. Effect of inhibitors or scavengers. Panels A and B show the surviving fractions in the cells irradiated with 0.1 Gy of Fe ions and 0.05 Gy of Ar ions, respectively. $*P < 0.05$ and $**P < 0.01$, for comparison with control and drug-treated cultures.

References

1) M. Tomita and M. Maeda: J. Radiat. Res. **56**, 205 (2015).
2) M. Tomita et al.: RIKEN Accel. Prog. Rep. **48**, 302 (2015).
3) M. Tomita et al.: Radiat. Res. **179**, 200 (2013).

*1 Radiation Safety Research Center, Central Research Institute of Electric Power Industry
*2 RIKEN Nishina Center

Effects of several LET conditions on the mutation isolation system in fruit flies

K. Tsuneizumi[*1] and T. Abe[*1]

Heavy-ion beam mutagenesis is generally recognized as an effective method for mutation breeding[1, 2]. Although this method was greatly successful with plants, its application is limited for animals. Therefore, we plan to acquire more basic data to set up optimal conditions for the irradiation system by heavy-ion beam, using *Drosophila melanogaster* (fruit fly) as the model.

In a previous study, we developed and improved a stable mutant isolation system using fruit flies using carbon-ion beam irradiation. Then, we estimated the suitable state of the F1 progeny that includes a possibility of chromosome damage. It is important to know when the flies with high probabilities of DNA damage are born. Since DNA damage to important genes for survival can be judged by the homozygotes born in the F3 progeny, we measured a frequency of the lethal rate of the F3 progeny[3]. The progeny born 4 days after irradiation at 10 Gy dose levels recorded the maximum frequency of lethal rate[3].

In this report, we measured the survival and the lethal rates at 4-days samples with various linear energy transfer (LET) values of [22.5, 30, 50, 80, 100, 200, and 300 keV/μm] at different dose levels (1, 3, 10, 20, 30, 40, 60, and 80 Gy) using carbon-ion beam or argon-ion beam to estimate the influence of LET of heavy-ion beam on the biological effects.

Irradiated male flies were crossed with virgin female flies in the manner shown in reference 4. We focused on 4-days samples because they showed maximum frequency of lethal rate of the F3 progeny[3]. We compared the survival rate with those at different LET conditions. The survival rate decreases with increasing dose of LET irradiation (Fig. 1). When the strength of LET was beyond 100 keV/μm, the survival rate decreased remarkably, and the population of the F1 generation to establish mutant flies decreased sharply (Fig. 1). Furthermore, even when the exposure doses exceeded 20 Gy, survival rates decreased remarkably, and the population in the F1 generation decreased sharply.

Then, we compared the lethal rates at different LET condition. When the exposure doses exceeded 20 Gy, the lethal rates had high numerical values (Fig. 2). But these data could not establish the lethal mutants because there were only a few numbers of the F1 generation. In other words, it is impossible to search the mutant lines for large-scale screening, and it is impossible to estimate the good irradiation conditions.

The good exposure doses for the purpose of large-scale screening of mutant lines are 1-3 Gy. The good LET values for irradiation are 22.5-80 keV/μm (Fig. 1). In the case of 22.5, 30, and 50 keV/μm, the lethal rate for 3-Gy irradiation is higher than that for 1-Gy irradiation (Fig. 2). Thus, these data suggest that 3-Gy irradiation is better than any other condition. In the case of 80 keV/μm, the lethal rate for 1-Gy irradiation is higher than that for 3-Gy irradiation (Fig. 2). Therefore, these data suggest that 1-Gy irradiation is better than any other conditions.

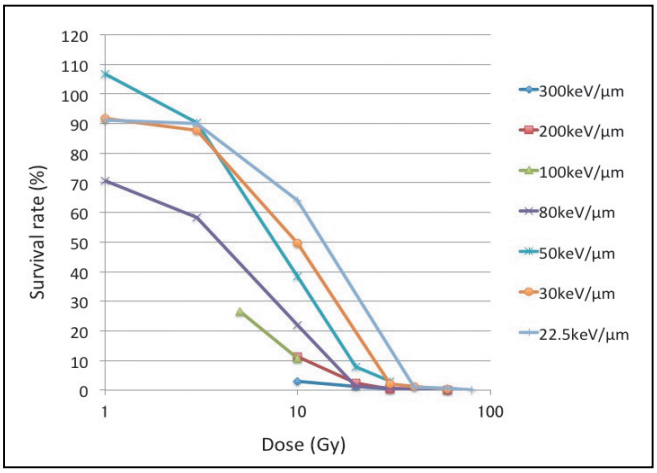

Fig. 1. Correlation between survival rate and exposure dose. Parental male flies were irradiated with carbon-ion beams (LET = 22.5, 30, 50, 80, 100 keV/μm) or argon-ion beams (LET = 200, 300 keV/μm). The frequency of survival rate of the F1 progeny is measured using 4-days samples.

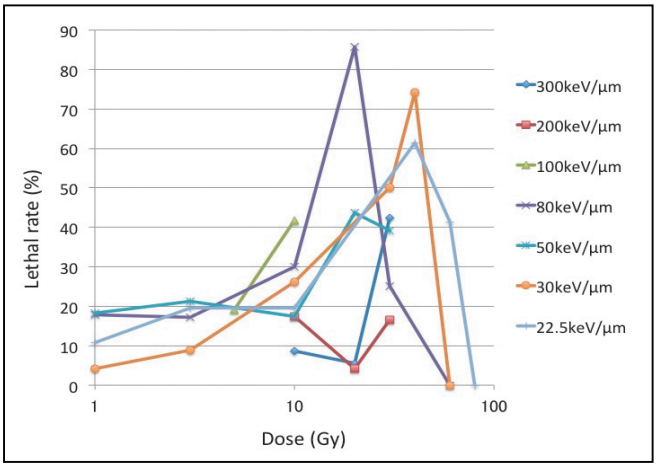

Fig. 2. Correlation between lethal rate and exposure dose. The frequency of lethal rate of the F3 progeny is measured using 4-days samples.

*1 RIKEN Nishina Center

References

1) T. Abe et al.: in Plant Mutation Breeding and Biotechnology, edited by Q. Y. Shu et al. (CABI, Oxfordshire, 2012), p.99.
2) A. Tanaka et al.: J. Radiat. Res. **51**, 223 (2010).
3) K. Tsuneizumi et al.: RIKEN Accel. Prog. Rep. **48**, 303 (2015).
4) K. Tsuneizumi et al.: RIKEN Accel. Prog. Rep. **47**, 285 (2014).

Development of a high-performance bioinformatics pipeline for rice exome sequencing

H. Ichida,[*1] Y. Shirakawa,[*1] R. Morita,[*1] Y. Hayashi,[*1] and T. Abe[*1]

Heavy-ion beams cause DNA double strand breaks in a cell along with the beam direction and induce mutations, including insertions, deletions, inversions, and base substitutions in genome. Recent advances in massively parallel (aka "next generation") DNA sequencing technology enabled us to perform a comprehensive analysis of genomic mutations in base-pair resolution. We have been establishing heavy ion beam-irradiated rice progenies as a bioresource that are subjected to screening experiments to meet scientific and agricultural needs. Although among crops, rice has a relatively small genome size (approximately 400 million bases per haploid), most parts are filled with repetitive and junk elements and only 10% is predicted to encode proteins. We have developed a system to enrich rice exons, which are genomic regions transcribed and translated into proteins, and to determine their nucleotide sequences. By this strategy, called exome sequencing, it is possible to reduce sequencing costs significantly by eliminating meaningless sequences and focusing on the regions encoding proteins.

In the present study, we have developed a high-performance bioinformatics pipeline for analyzing rice exome sequencing results, and we identify the most significant mutations without the need for prior knowledge. The pipeline was implemented on Hokusai GreatWave, which is a parallel computing platform operated by Advanced Center for Computing and Communication, RIKEN. In the pipeline, raw sequencing reads (100–150 bp in length) are mapped to reference Nipponbare sequences using Burrows-Wheeler Aligner (BWA) software[1)], sorted, and realigned, and the data is stored in the standard BAM format. Programs with 3 distinct algorithms (GATK[2)], Pindel[3)], and Bedtools[4)]) are used to identify the mutations. We implemented a filter to remove duplicated and unreliable mutation candidates. The list of mutations were stored in tab-delimited text file and accessible from generic spreadsheet software. In parallel, the quality of raw reads were checked by FastQC[5)] program and the results were stored as an HTML-formatted report for review. The entire process was executed automatically and in parallel through a batch job controlling system. The deployment of an in-house bioinformatics pipeline enabled reliable comparison of results from different experiments (batches), since the pipeline is controlled by a versioning system; therefore, it is possible to reproduce exactly the same program and database versions any time.

To test the validity of variant calling and the following filtration, we analyzed the exome sequencing results from 8 individual rice mutants obtained via carbon- and neon-ion irradiations. As the result, there were 62,024 mutation candidates in GATK and Pindel outputs, but most of those mutations are common among the mutants and are likely to be intra-cultivar polymorphisms between our parental Nipponbare line and the reference sequence. Our newly implemented filtering program effectively removed such variations and identified 117 line-specific mutations, which are likely to be caused by heavy-ion beam irradiations. PCR and sequencing analysis showed that among the randomly-chosen 87 loci, 85 had the defined mutations. These results indicates that the process for narrowing down the candidates, which was implemented in the pipeline is reasonable and greatly improves the efficiency, as confirmed in subsequent experiments. This pipeline is a fundamental resource for rapid, comprehensive, and cost-effective genome-wide mutation screening and analysis of rice.

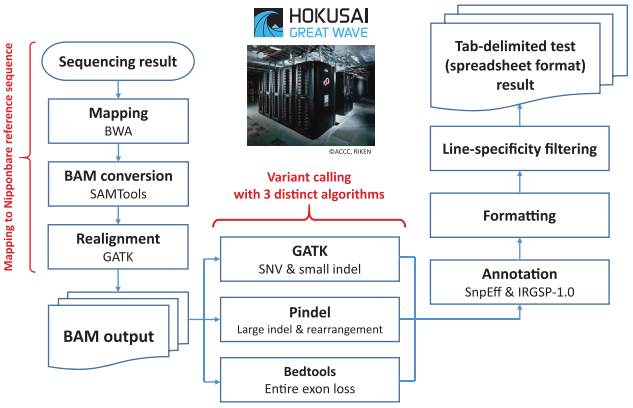

Fig. 1. A flow chart of the developed bioinformatics pipeline for exome sequencing datasets

*1 RIKEN Nishina Center

References
1) H. Li and R. Durbin: Bioinformatics **25**, 1754–60 (2009).
2) A. McKenna et al.: Genome Res. **20**, 1297–1303 (2010).
3) K. Ye et al.: Bioinformatics **25**, 2865-28-71 (2009).
4) A. R. Quinlan and I. M. Hall: Bioinformatics **26**, 841-842 (2010).
5) S. Andrews: available from *http://www.bioinformatics.babraham.ac.uk/projects/fastqc.*

Molecular characterization of mutations induced in *PLASTOCHRON2* by a heavy-ion beam in dry rice seeds

R. Morita,[*1] Y. Shirakawa,[*1] K. Ichinose,[*1] Y. Hayashi,[*1] S. Usuda,[*1] H. Tokairin,[*1] T. Sato,[*1,*2] and T. Abe[*1]

Rice is one of the most important crop plants and is also an important model plant, because its entire genome sequence is available. In this work, we studied heavy-ion beam induced mutations in rice plants. Heavy-ion beams have been recognized as a useful mutagen for mutation breeding, because they can induce mutations at high rates with relatively low irradiation doses in plants. For inducing mutations in rice, we used imbibed seeds or dry seeds. When imbibed rice seeds were irradiated with ion beams, mutations could be induced with a relatively low dose of radiation. As a result, the time for ion-beam irradiation was shorter. The disadvantage of using imbibed seeds, however, is that these seeds cannot be used for long as seed germination will occur. Therefore, we cannot irradiate imbibed rice seeds during a period that is not suitable for cultivation of rice plants. However, when dry rice seeds were used for ion-beam irradiation, we could store the irradiated seeds for long time periods (at least several months). Therefore, the dry rice seeds could be irradiated even if the machine time fell during a period unsuitable for cultivation. Previously, we have reported several mutations induced by heavy-ion beam irradiation to imbibed rice seeds [1-3]. However, there is no information in the literature regarding the types of mutations inuduced by heavy-ion beam irradiation on dry rice seeds. To reveal the types of mutations induced by heavy-ion beams on dry rice seeds, we irradiated dry rice seeds (*Oryza sativa* L. cv. Nipponbare) with carbon ions ($^{12}C^{6+}$ ions, 25 Gy, LET: 30 keVμm^{-1}) in the RIKEN RI-beam factory. We obtained one plastochron mutant, named 6-279, from the M_2 population. The mutant line 6-279 showed a phenotype with a short plastochron. For example, when a wild-type (WT) plant prouduced its 4th leaf, 6-279 produced its 7th leaf (Fig. 1). It has been reported that the mutants of *PLASTOCHRON1* (*PLA1*) or *PLASTOCHRON2* (*PLA2*) genes show similar short plastochron phenotypes [4, 5]. A sequence analysis of both *PLA1* and *PLA2* genes revealed that 6-279 showed a 2 bp deletion accompanied by a 1-bp filler DNA in the first exon of *PLA2* gene (Fig. 2). These mutaions caused a frameshft in *PLA2* gene, resulting a premature stop codon. There was no mutation in the *PLA1* gene of this mutant. These results suggest that 6-279 is a mutant of *PLA2* gene.

In the present study, we identified one mutation induced by heavy-ion beam irradiation to rice dry seeds. To characterize the types of mutations induced by heavy-ion beams on dry rice seeds, it is important to analyze a number of rice mutants, which is currently in progress.

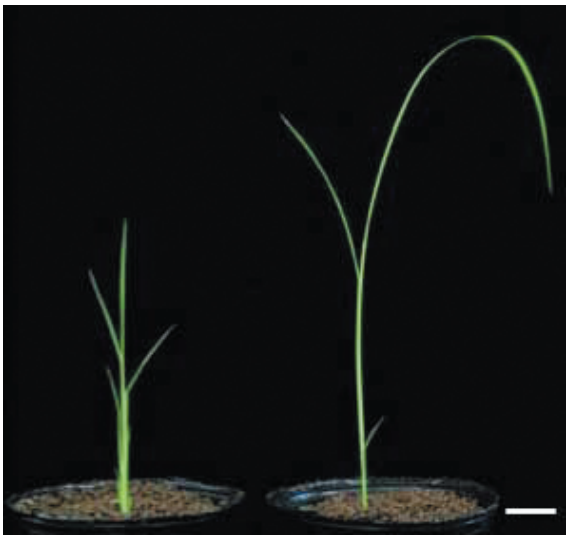

Fig. 1 Phenotipic characterization of 6-279 mutant. 6-279 (left) produced its 7th leaf whereas WT plant (right) produced its 4th leaf. Scale bar = 1 cm.

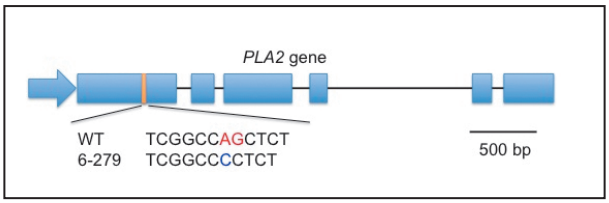

Fig. 2 Schematic representation of *PLA2* gene. *PLA2* gene consists of 6 exons. A 2 bp deletion with a filler DNA was detected in the first exon of the *PLA2* gene. The deleted 2 bp in 6-279 is shown in red, and the filler DNA is indicated in blue. The boxes and lines indicate exons and introns of *PLA2* gene, respectively. The Arrow indicates the direction of the *PLA2* gene.

References

1) R. Morita et al.: RIKEN Accel. Prog. Rep. **45**, 212 (2012).
2) S. Kogure et al.: RIKEN Accel. Prog. Rep. **45**, 213 (2012).
3) S. Kogure et al.: RIKEN Accel. Prog. Rep. **46**, 260 (2013).
4) J. Itoh et al.: Plant Cell **10**, 1511 (1998).
5) T. Kawakatsu et al.: Plant Cell **18**, 612 (2006).

[*1] RIKEN Nishina Center
[*2] Graduate School of Life Science, University of Tohoku

Effect of Ar-ion beam irradiation on imbibed seed of rice

Y. Hayashi, *1 R. Morita, *1 K. Ichinose, *1 S. Usuda, *1 H. Tokairin, *1 T. Sato, *2 and T. Abe*1

Linear energy transfer (LET) is an important factor for mutation induction by heavy-ion beam irradiation. The following ions are applicable for irradiation of biological samples at the RIBF: C, N, Ne, Ar, and Fe. The LET values of these ions calculated at the surface of the sample are 22.5, 30.0, 61.5, 280.0, and 624.0 keV/μm, respectively. It is possible to control the LET value by selecting a particular ion or using a range shifter of automatic irradiation system[1]. It has been reported that high-LET irradiation causes large deletion or chromosome aberration in Arabidopsis[2-4]. Furthermore, our previous study revealed that Ar-ion irradiation causes larger deletion than C- or Ne-ion irradiation in rice[5]. In this study, we estimated the effect of high-LET irradiation on the mutation efficiency in rice using an Ar-ion beam.

Imbibed seeds of rice (*Oryza sativa* L. cv. Nipponbare) were exposed to Ar-ions accelerated to 95 MeV/u at the RIBF. The dose range of the Ar-ion beam (LET 290 keV/μm) was 5 to 20 Gy. The irradiated seeds were sown in soil in pots and grown in a greenhouse. The survival rates were investigated for two-week old seedlings. We estimated the optimum dose for mutation induction from the results of the survival rate. The seed fertilities and mutation frequency were observed in two experiments after irradiation with pre-determined doses. The first experiment was a comparison between doses of 2,5 Gy and 5 Gy. The second one was a comparison between doses of 5 Gy and 7.5 Gy. The number of irradiated seeds for each dose was 750. The seed fertility was evaluated using the percentage of fertile seeds per panicle in the first experiment, and using the number of fertile seeds in one panicle in the second experiment. The mutation frequency was calculated using the percentage of M_1 lines, which showed chlorophyll deficient mutants (CDM) in M_2 progenies.

The survival rate of M_1 seedlings significantly decreased for doses over 10 Gy (Fig. 1). The growth inhibition was more severe as the dose increased (Fig. 2). These results indicate a higher inhibition effect of Ar-ions on growth and survival compared to C-ions[6]. The effect of dose on fertility in M_1 plants is shown in Fig. 3. The ratio of M_1 plants with low fertility increased as the dose increased. Nearly 40% of the M_1 plants had less than fifty seeds per panicle at a dose of 7.5 Gy.

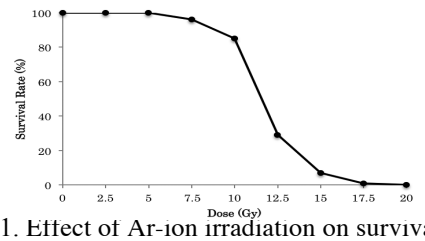

Fig. 1. Effect of Ar-ion irradiation on survival rate.

The mutation rates obtained with Ar-ion irradiation were 6.1%-8.7% (Table 1). These results are almost the same as those of C-ion irradiation (LET:50 keV/μm) with a dose of 15 Gy[6]. Mutation frequency is the most important factor for determining the effective condition in mutagenesis. However, seed fertility is also an important factor because sterility is an undesirable trait for breeding. Furthermore, a low fertility increases the risk of outcross in the field. Considering the results of both factors, irradiations with doses of 2.5 Gy and 5.0 Gy is adequate for mutation breeding using Ar-ions in rice.

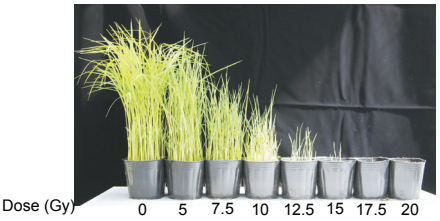

Fig. 2 Growth condition of M_1 seedlings after 2 week.

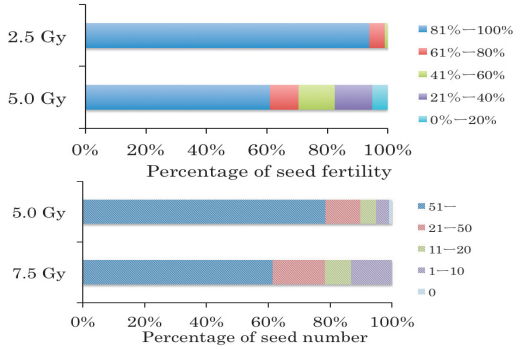

Fig. 3 Effect of dose on seed fertility in M_1 plants. The average seed fertility and fertile seed number in control Nipponbare were 92% and 108.6, respectively.

Table 1 Effect of Ar-ion irradiation on survival rate and mutation frequency

Dose (Gy)	Fertile M_1 line	Survival Rate (%)	Total CDM	Frequency of CDM
2.5	686	91.5	42	6.1
5	684	91.2	42	6.1
5	690	92	49	7.1
7.5	623	83.1	54	8.7

*1 RIKEN Nishina Center
*2 Graduate School of Agriculture, Tohoku University

References

1) 1) H. Ryuto et al., Plant Biotechnol. **25**, 119 (2008).
2) T. Hirano et al., Mutat. Res. **735**, 19 (2012).
3) Y. Kazama et al., Genes Genet. Syst. **88**, 189 (2013).
4) T. Hirano et al., Plant J. **82**, 93 (2015).
5) S. Kogure et al., RIKEN Accel. Prog. Rep. **47**, 289 (2014).
6) Y. Hayashi et al., RIKEN Accel. Prog. Rep. **42**, 285 (2009).

Relationship between early-flowering mutation and LET-Gy combination of ion beam irradiation in einkorn wheat

K. Murai,[*1] Y. Kazama,[*2] and T. Abe[*2]

Bread wheat (*Triticum aestivum*) is a hexaploid species with the genome constitution AABBDD that were derived from three wild diploid ancestral species: the A genome from *T. urartu*, the B genome from *Aegilops speltoides* or another species classified in the Sitopsis section, and the D genome from *Ae. tauschii*. Therefore, the hexaploid wheat genome contains triplicated homoeologous genes, and unfortunately, this characteristic increases the difficulty of screening for mutants in bread wheat. To avoid this problem, we have chosen to use cultivated diploid einkorn wheat (*T. monococcum*) with A^m genome, similar to the A genome in bread wheat, for developing a large-scale mutant panel[1]. To avoid the rainy season for harvesting, early maturing is one of the more important properties of bread wheat in East Asia, including Japan. Therefore, we focused on identifying early-flowering mutations in the screening of the mutant panel.

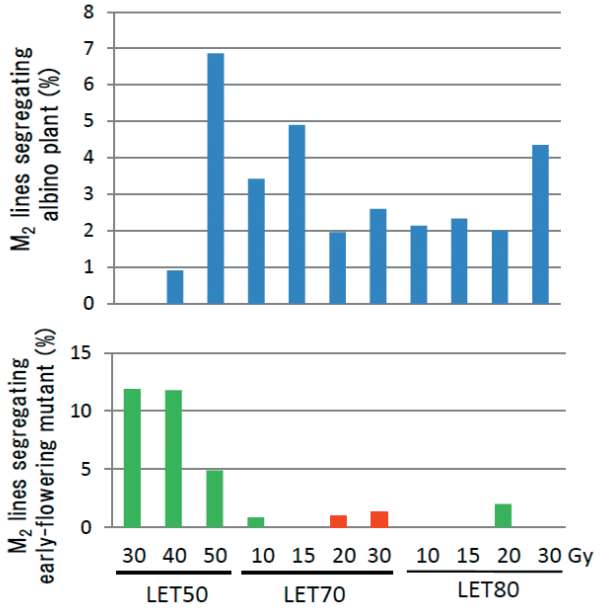

Fig. 1. Appearance of albino plants and early-flowering mutant plants in M_2 generation. Percentages (%) of M_2 lines segregating mutant plants are shown in each LET-Gy combination of ion beam irradiation. Green and red bars indicate early-flowering mutants and extra early-flowering mutants, respectively.

[*1] Department of Bioscience, Fukui Prefectural University
[*2] RIKEN Nishina Center

This work was supported by Council for Science, Technology and Innovation (CSTI), Cross-ministerial Strategic Innovation Promotion Program (SIP), "Technologies for creating next-generation agriculture, forestry and fisheries".

In a previous study, we identified four extra early-flowering mutants, named *extra early-flowering1* (*exe1*), *exe2*, *exe3*, and *exe4*, which were headed 30–45 days earlier than the wild-type strain KU104-1[2]. Here we report our recent study on the relationship between the early-flowering mutation and the LET-Dose (Gy) combination of ion beam irradiation.

Dry seeds of the diploid einkorn wheat (*T. monococcum*) strain KU104-1 were irradiated with 10, 15, 20, 30, 40, or 50 Gy of $^{12}C^{6+}$ ions with 50, 70, or 80 keV μm^{-1} LET to determine the optimal conditions for mutant generations, using the E5 beam line of Ring Cyclotron (RRC) in the RIKEN RI-beam factory. The germination rate was examined using the irradiated seeds (called M_1 seeds) that were sown in wet-paper-containing petri-dishes. 150 seeds (50 seeds with three replications) were tested for each LET-Gy combination. The germination rate was not affected by ion beam irradiation. The M_1 seedlings were planted in the field in October 2013, and the survival ratio was observed in May 2014 at the heading stage. The survival ratio was reduced to less than 80 % when LET of ion beam was 70 or 80 keV μm^{-1}. The harvested seeds from each individual M_1 plant were used to produce the next generation (M_2) lines. 23 - 134 M_2 lines (997 lines in total) for each LET-Gy combination were sown in October 2014 in the fields; ten seeds of each M_2 line were sown. The frequency of lines with albino plant(s) among the ten plants was determined to assess the comparative mutation ratio of the different irradiation conditions. The frequency of albino plants in the M_2 generation was different for different LET-Gy combinations (Fig. 1). The highest ratio was observed for the LET50-50Gy treatment condition. The data of survival ratio suggests that LET50-50Gy treatment was the optimal condition for einkorn wheat.

In the mutant screening in 2015, we observed early-flowering mutation within one week and extra early-flowering mutation before one week, compared with the wild-type. Fig. 1 shows the percentages of the M_2 lines segregating (extra) early-flowering and mutant plant(s). The early-flowering mutants were obtained under relatively moderate treatment conditions with LET50, while extra early-flowering mutants were obtained under harsher treatment conditions with LET70. The genes for early-flowering phenotypes would be good candidates in genome editing for fine-tuning of heading time in wheat.

References

1) K. Murai et al.: Nuclear Instruments and Methods in Physics Research B 314. **2013**, 59.
2) A. Nishiura et al.: Breeding Science 64. **2014**, 213.

Improvement of DelMapper: software for deletion mapping of non-recombining region

K. Ishii,[*1] Y. Kazama,[*1] T. Ikeda,[*1] and T. Abe[*1]

Genetic mapping is usually constructed by calculating recombination rate as a measure of distance between genetic markers. However, this method cannot be applied to the non-recombining region such as sex chromosomes. To map the DNA markers or genes on the Y chromosome in *Silene latifolia*, we have developed new deletion mapping software, Del Mapper.[1)] Deletion mapping is an approach for mapping DNA markers or genes in the non-recombining region by collecting mutants having deletion on the mapping region and ordering the markers to have the least total number of chromosomal breakpoints in all mutants. DelMapper conducts deletion mapping with a new approach that boils down seeking the best marker order to solving traveling salesman problem.

DelMapper calculates the numbers of breakpoints in all possible permutations of the markers by applying the branch and bound algorithm. To promote greater efficiency of calculation, markers are clustered and each cluster is treated as a single virtual marker. When calculating the numbers of breakpoints in each permutation, DelMapper adds two virtual markers to the both ends of the mapping region. One virtual marker represents the essential chromosomal region that cannot be deleted and is presumed to be present in all mutants. There are two alternatives for the other virtual marker. Under the "Del" option, the mapping region is assumed to be located on the terminal of the chromosome and the virtual marker is regarded to be deleted. Under the "Any" option, the region is assumed to be located on the intermediate of the chromosome and the presence/absence of the marker is dependent on that of the neighboring marker. When run with the "Del" option, a previous version of DelMapper tends to output an increased number of marker orders with the least number of breakpoints. This problem is potentially caused by concentrated deletions on the specific marker (e.g., marker B3 in Fig. 1). Such situation can be produced by the collection of mutants showing the same phenotype. In such cases, the concentrated deletions are located next to the terminal virtual marker. At the same time, "solitary deletions" that do not extend beyond the border of clusters appears due to disjunction of deletions that are to be continuous (Fig. 1; deletions in clusters B and C in Mutants 3, 5, and 6).

To cope with this problem, we added a routine to calculate the number of "solitary deletions." In addition to the number of breakpoints, DelMapper counts the number of "solitary deletions" in all given permutations of markers. Users can adopt the permutation(s) of the markers with the least number of "solitary deletions" in those with the least number of breakpoints as the mapping result. As a verification of the effects of the routine, we made 30 virtual maps that consisted of 71 markers, 41 mutants, and 500 instances of deleted markers and had a tendency of biased deletion on the specific markers by a Perl script DelMapMaker.[1)] We tested DelMapper whether it could reconstruct these maps. DelMapper run with the "Any" option output an average of 1.3 marker orders with the least number of "solitary deletions" in those with the least number of breakpoints regardless of the implementation of the routine. On the other hand, DelMapper run with the "Del" option output an average of 2.5 marker orders before the implementation, while after the implementation, it did an average of 1.3 marker orders, which was the same value as that with the "Any" option.

In this study, we successfully decreased the number of the false-positive best marker orders from the output of DelMapper with the "Del" option, which enables users to conduct more clear deletion mapping.

A

Cluster			A			B			C					
Marker	L	A1	A2	A3	B1	B2	B3	C1	C2	C3	R	P	S
Mutant1	1	1	0	0	0	0	0	1	1	1	0	3	0
Mutant2	1	0	0	0	0	0	0	0	1	1	0	3	0
Mutant3	1	1	1	1	1	0	0	0	0	0	0	1	0
Mutant4	1	1	1	0	0	0	0	1	1	1	0	3	0
Mutant5	1	1	1	1	1	1	0	0	0	0	0	1	0
Mutant6	1	1	1	1	0	0	0	0	0	0	0	1	0
Total												12	0

B

Cluster			C			A			B					
Marker	L	C2	C3	C1	A1	A2	A3	B1	B2	B3	R	P	S
Mutant1	1	1	1	1	1	0	0	0	0	0	0	1	0
Mutant2	1	1	1	0	0	0	0	0	0	0	0	1	0
Mutant3	1	0	0	0	1	1	1	1	0	0	0	3	2
Mutant4	1	1	1	1	1	1	0	0	0	0	0	1	0
Mutant5	1	0	0	0	1	1	1	1	1	0	0	3	2
Mutant6	1	0	0	0	1	1	1	0	0	0	0	3	2
Total												12	6

Fig.1 Two examples of the result of DelMapper with the "Del" option. L and R indicate virtual markers representing the ends of the mapping region. "0" and "1" indicate that the markers are absent and present in the corresponding mutant, respectively. P and S indicate the numbers of breakpoints and "solitary deletion," respectively. The routine calculating "solitary deletions" helps users to determine that the marker order of (A) is more plausible than (B) because of the smaller number of "solitary deletions" although the numbers of breakpoints are same.

[*1] RIKEN Nishina Center

Reference

1) Y. Kazama and K. Ishii et al.: Sci. Rep. **6**, 18917 (2016).

A new physical mapping of the *Silene latifolia* Y chromosome†

Y. Kazama,[*1] K. Ishii,[*1] W. Aonuma,[*2] T. Ikeda,[*1] H. Kawamoto,[*2] A. Koizumi,[*2] D.A. Filatov,[*3] M.V. Chibalina,[*3] R. Bergero,[*4] D. Charlesworth,[*4] T. Abe,[*1] and S. Kawano[*2]

The majority of angiosperms are hermaphrodites and only 6% are dioecious (with separate males and females); some of these plants have sex chromosomes. Plant sex chromosomes are excellent for studying the early stages of sex chromosome evolution because they have evolved independently in different species, more recently than in animals.

Dioecious plants have sex-determining systems that are thought to involve two different genes, a stamen promoting gene and a pistil-suppressing gene. The dioecious plant, *Silene latifolia*, has such two sex determining genes on the Y chromosome (gynoecium-suppressing function; GSF, and stamen-promoting function; SPF). These sex-determining genes have not yet been identified, and their evolution has not yet been studied. Maps of the genes on the X and Y chromosomes are needed to identify Y-linked sex-determining genes, compare gene orders in the X and Y, and determine whether the Y has lost regions present on the X chromosome. However, most of the Y chromosome is non-recombining, making genetic mapping impossible. Mapping Y-chromosome deletion mutants is therefore the only way to map the Y chromosome. Previous Y chromosome maps [1), 2)] used small numbers of markers. We developed a new *S. latifolia* Y map with more markers to achieve high reliability and developed a new deletion mapping software tool, DelMapper.

We collected 41 mutants with Y-chromosome deletions from progeny plants derived from seeds or pollen irradiated by carbon-ion beams or γ-rays as described previously.[3)] The mutants include 15 hermaphrodites, one female-like mutant, 10 asexuals, 14 mutants with non-maturing anthers, and one male plant. These mutants were genotyped for the presence/absence of deletions at 71 Y-linked markers by PCR amplification (STS-markers). Hermaphroditic mutants must have deletions of the GSF, while asexual mutants have lost the SPF. Our use of numerous genic markers improves our ability to locate the GSF and SPF regions in comparison with the use of non-genic markers.

To find the marker order, DelMapper obtains the best fit to the data by solving a "Travelling Salesman problem", minimizing the number of chromosome breaks required. Minimization of the chromosome breaks is a standard approach for deletion mapping, and the novelty of our method is that it can deal with many markers. We verified this approach by testing DelMapper using simulated datasets with known gene orders. The accuracy of DelMapper depends strongly on the number of individuals with mutant phenotypes, and on the total number of deletions in the dataset, but the number of markers used is less important. Our simulations allow us to determine the accuracy of maps made using DelMapper.

The analyzed data included 442 instances of deleted markers among the 41 mutants. Based on our simulations, the accuracy of a map based on such a dataset is expected to be 90%. Our new Y-chromosome map infers that markers MK17 and ScQ14 are the closest to the GSF and SPF genes, respectively,[1),2)] and it locates both of them on the putative p arm (the chromosome arm that does not include the pseudo autosomal region (PAR): see Fig. 1). We locate GSF between MK17 and genic contig20685Y, in an interior region of the p arm. SPF is located between ScQ14 and the genic contig 03376Y. This new map with these added genic markers provides improved ability to locate the GSF and SPF regions, in comparison with the previous maps.

Our new map will greatly facilitate the isolation of sex-determining factors and will be instrumental in other research focusing on sex chromosomes.

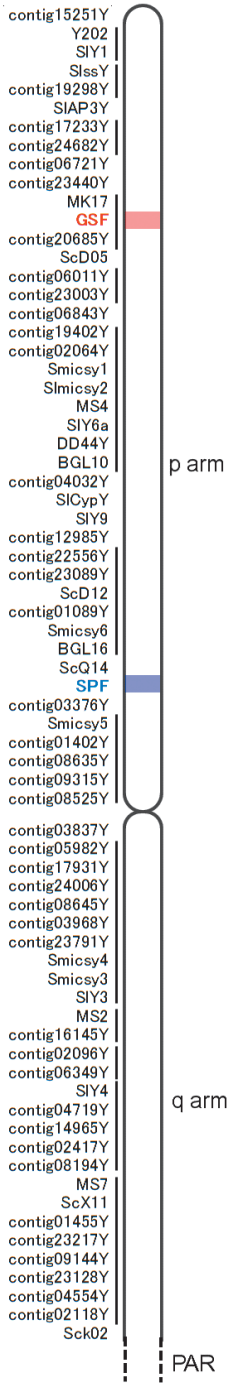

Fig.1 The new *S. latifolia* Y map. Markers indicated by bars are closely linked and their orders were not determined.

†Condensed from the article in Scientific Rep. **5**, 18917 (2016)

[*1] RIKEN Nishina Center
[*2] Department of Integrated Sciences, Graduate School of Frontier Sciences, The University of Tokyo
[*3] Department of Plant Sciences, University of Oxford
[*4] Institute of Evolutionary Biology, University of Edinburgh

References

1) S. Lebel-Hardenack et al., Genetics **160**, 717 (2002).
2) J. Zluvova et al., Genetics **170**, 1431 (2005).
3) N. Fujita et al., G3 (Bethesda) **2**, 271 (2012).

Sexual reproduction observed in the loss-of-apomixis mutants of guineagrass induced by heavy-ion beam irradiation

M. Takahara,[*1] R. Morita,[*2] Y. Kazama,[*2] T. Abe,[*2] T. Takamizo,[*1] and H. Nakagawa[*1, *3]

Apomixis, an asexual mode of reproduction, provides a method for reproducing clonal plants through the seed. By using apomixis in the breeding program, we can develop a new efficient method for fixing desirable genotypes of F_1 hybrids and simplifying commercial seed production. Therefore, we aimed to isolate the gene(s) controlling apomixis from a tropical forage grass, guineagrass (*Panicum maximum* Jacq.). In a previous study, we found two mutant lines (SM-1 and SM-2) that were suggested to have lost the apomictic pathway of reproduction and to propagate using the sexual mode of reproduction.[1), 2)] In the present study, we analyzed the mode of reproduction of these loss-of-apomixis mutants with two methods: the progeny test using amplified fragment length polymorphism (AFLP) patterns and embryo sac analysis. The results showed that they lost the apomictic mode of reproduction.

The M_1 plants of SM-1 and SM-2 were generated from the dry seeds of an apomictic cultivar "Natsukaze" irradiated with $^{20}Ne^{10+}$ (63 keV/μm) ions at 200 Gy and with $^{56}Fe^{24+}$ (624 keV/μm) ions at 20 Gy, respectively.[1)] Forty M_2 plants of each line were grown in a field. DNA from the leaves of each M_2 plant was extracted and analyzed using the AFLP method. For the embryo sac analysis, inflorescences at anthesis were fixed in Farmer's fixative (100% ethanol:acetic acid = 3:1), and then dehydrated and cleared as described previously.[3)] The cleared pistils were observed with a differential interference contrast microscope (Nomarski).

The AFLP patterns of 40 M_2 plants are shown in Fig.1. In case of the apomictic cultivar "Natsukaze", the AFLP results show the same pattern among progenies. In contrast, all the AFLP patterns of M_2 plants of both SM-1 and SM-2 were different from each other. This result suggested that SM-1 and SM-2 propagated with the sexual mode of reproduction.

To confirm the sexual mode of reproduction of SM-1 and SM-2, embryo sac analysis was performed. In the case of guineagrass, an apomictic embryo sac has four nuclei (an egg, two synergids, and a polar nucleus; Fig. 2A), while a sexual embryo sac has eight nuclei (an egg, two synergids, two polar, and three antipodal cells' nuclei; Fig. 2B). The most clear differences between the sexual and apomictic embryo sacs are whether antipodal cells are formed or not, and whether the number of polar nuclei is two or one. [3)] In the embryo sac analysis of SM-1 and SM-2, we observed a few sexual embryo sacs (Fig. 2B), many aborted embryo sacs (Fig. 2C), and no apomictic embryo sac in each line. These results suggested that they lost the apomictic pathway of reproduction.

Our previous results suggested that the deleted region in the loss-of-apomixis mutants were relatively small.[2)] We are currently searching for the genes located within these deletion regions.

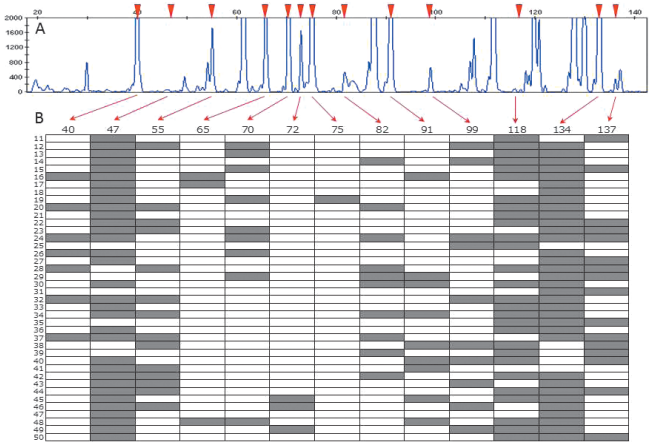

Fig. 1. AFLP patterns of M_2 plants in the sexual mutant line SM-2. (A) The AFLP pattern of "Natsukaze" detected by the ABI 3130xl capillary sequencer (as a reference). Red arrowheads indicate the loci that are polymorphic among M_2 plants. (B) Schematic presentation of AFLP patterns of M_2 plants in SM-2. White box shows the presence of the peak, and gray box shows the absence of the peak. Similar results have been obtained for SM-1 (not shown).

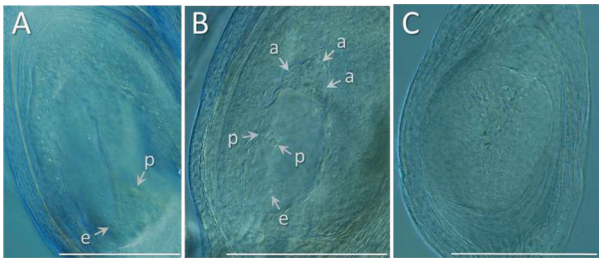

Fig. 2. Typical embryo sacs in guineagrass. (A) Apomictic embryo sac observed in "Natsukaze" (apomictic cultivar). (B and C) Sexual embryo sac (B) and aborted ovule (C) observed in the loss-of-apomixis mutants. a, antipodal cell; e, egg cell; p, polar nuclei. Synergid cells are small and difficult to observe in both types.[3)] Bar = 200 μm.

*1 National Agriculture and Food Research Organization (NARO) Institute of Livestock and Grassland Science
*2 RIKEN Nishina Center
*3 Hamamatsu Photonics K. K.

References

1) M. Takahara et al.: RIKEN Accel. Prog. Rep. **46,** 263 (2013).
2) M. Takahara et al.: RIKEN Accel. Prog. Rep. **47,** 294 (2014).
3) H. Nakagawa: JARQ **24,** 163-168 (1990).

Induction of flower color mutants by heavy-ion irradiation to leaf blades of spray-mum 'Southern Chelsea'

Y. Tanokashira,[*1] M. Tamari,[*1] S. Nagayoshi,[*1] Y. Hayashi,[*2] T. Hirano,[*2*3] and T. Abe[*2]

Heavy-ion beam irradiation effectively induces mutations and has been used in plant breeding[1]. Ar-ion beam irradiation is expected to provide a different spectrum of mutant phenotypes from the C-ion irradiation due to their different LET values. Therefore, we irradiated Chrysanthemum tissue with an Ar-ion beam in order to obtain flower color mutants. We previously reported the induction of flower color mutants by Ar-ion irradiation to cuttings of spray-mum 'Southern Chelsea', which was developed by Kagoshima Prefecture[2]. In addition, we reported the effects of Ar-ion beam irradiation on the regeneration of leaf blades[3]. Here, we report the induction of flower color mutants by leaf blades irradiation.

Leaf blades of the spray-mum cultivar 'Southern Chelsea', having pink flowers, were irradiated with an Ar-ion beam (LET: 310 keV/μm) at doses of 0.1, 0.3, 0.5, 1, 2, and 3 Gy, and a C-ion beam (LET: 23 keV/μm) at doses of 1, 2, and 3 Gy. After irradiation, these tissues were cultured in vitro. Adventitiously regenerated buds were cut and grown to plantlets in vitro and they were transferred to a greenhouse to investigate the occurrence of flower color mutations.

Twenty plants among 1,716 irradiated regenerants showed flower color mutation [Table 1] The regenerants were white, light pink, deep pink, light reddish yellow, and orange, suggesting that increase, decrease, disappearance of anthocyanin and the increase of carotenoid were induced in these mutants, respectively [Table 1].

Table 1. Flower color mutation induced by heavy-ion beam irradiation.

Variation source		Regeneration rate[1] (%)	Number of plants[2]	Number of Flower-color mutants							Number of mutants	Mutation rate (%)
Line class	Dose (Gy)			White	Light pink	Deep pink	Deep reddish yellow	Light reddish yellow	Orange	Other		
Ar	0.1	95.6	420		2	3					5	1.2
	0.3	90.9	438			2					2	0.5
	0.5	65.9	264		2			1	1		4	1.5
	1	37.8	192	1					4		5	2.6
	2	8.7	6								0	0
	3	3.0	12								0	0
	Total		1,332	1	4	5	0	1	5	0	16	
C	1	83.8	138			1				1	2	1.4
	2	64.3	114							1	1	0.9
	3	46.2	132	1							1	0.8
	Total		384	1	0	1	0	0	0	2	4	
	0	100	84								0	0

1) The relative regeneration rate means the rate of regenerated shoots after the ion beam irradiation to radiationless regenerated shoots which were developed from directly adventitious shoots.

2) Regenerated and flowered plants after irradiation.

*1 Kagoshima Prefectural Institute for Agricultural Development
*2 RIKEN Nishina Center
*3 University of Miyazaki

These results were the same as those obtained by irradiation to cuttings with a C-ion beam. The mutation rates in flower color changes with Ar-ion beam irradiation were 0.5-2.6% at 0.1-1 Gy, and those with C-ion were 0.8-1.4% at 1-3 Gy [Table 1]. Irradiation to cuttings could cause simultaneous mutation in both anthocyanin and carotenoid content and yellow flower mutants were obtained[2]. However, irradiation to leaf blades could not cause the simultaneous mutation in the anthocyanin and carotenoid content in this examination. Some mutants also showed flower-shape variation by Ar-ion beam irradiation [Figure 1]. Relative regeneration rate decreased to less than 10% under Ar-ion irradiation at doses of 2 Gy, and no flower color mutants were obtained at these doses. All of the regenerated plants irradiated with Ar-ion beam showed less growth than non irradiated control plants.

Ar-ion beam irradiation to leaf blades is not thought to be suitable for practical breeding in 'Southern Chelsea' because its regeneration rate and mutation rates are lower than that of cuttings in flower color. Currently, we are investigating the stability of flower color of the mutants derived from Ar-ion irradiation.

This work was supported by the Council for Science, Technology and Innovation (CSTI), Cross-ministerial Strategic Innovation Promotion Program (SIP), "Technologies for creating next-generation agriculture, forestry and fisheries" (funding agency: Bio-oriented Technology Research Advancement Institution , NARO).

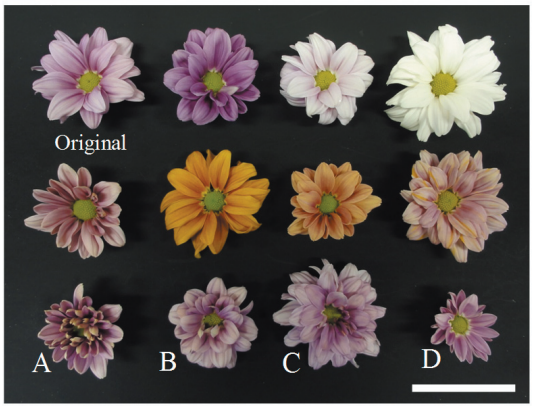

Fig.1 Spectrum of mutant phenotypes. (A,B,C,D) Mutants showing different flower shapes. Bars = 5cm.

References

1) T. Abe et al., Breed. Res.**16**, 67 (2014).
2) Y. Tanokashira et al., RIKEN Accel. Prog. Rep.**47**, 297 (2014).
3) Y. Tanokashira et al., RIKEN Accel. Prog. Rep.**48**, 306 (2015).

Production of mutant line with early flowering at a low temperature in spray-type chrysanthemum cultivar induced by C-ion beam irradiation

K. Sakamoto,[*1] Y. Takatori,[*1] R. Chiwata,[*2] T. Matsumura,[*1] K. Tsukiashi,[*1] Y. Hayashi,[*3] and T. Abe[*3]

Chrysanthemum (*Dendranthema grandiflorum*) is one of the major cut flowers. Saga Prefecture has developed 5 original cultivars of spray-type chrysanthemum by crossbreeding in 2011. However, the white-flower cultivar 'Saga SK3' showed delayed flowering under a low temperature. Recently, heavy-ion beam irradiation was reported as an effective method for breeding chrysanthemum with early flowering at a low temperature[1]. Therefore, in this study, we aimed to develop early-flowering mutants of 'Saga SK3' by heavy-ion beam irradiation and selected an earlier-flowering mutant line.

In 2012, 6-cm-long cuttings without leaves of 'Saga SK3' were irradiated with C-ion beams (LET 22.6 keV/μm) at doses of 3 and 6 Gy. After irradiation, these cuttings were cultured in cell trays for rooting in a greenhouse. The survival rates of irradiated plants were all 100% (Table 1). The terminal buds of the cuttings were pinched off, and new shoots were allowed to grow from the axillary buds. This procedure was repeated twice or thrice for isolating chimeric structures. Then, shoots elongated after pinching were planted in a greenhouse, and these plants were grown in the January flowering cropping system in 2013 under low temperature controlled at a minimum of 13℃. 'Saga SK3' flowered 63 days after lighting stop. Individual selections from these plants flowered until 56 days after lighting stop by the standard method in Saga Prefecture. We found that 9 individuals flowered until 56 days after lighting stop from the 464 plants obtained after 6-Gy irradiation (Table 1), and we selected 5 individuals from them. On the other hand, no plant flowered until 56 days after lighting stop at a dose of 3 Gy. These results suggest that the minimum effective dose of C-ion beam irradiation using cuttings in chrysanthemum for inducing early-flowering mutation is more than 3 Gy.

In 2014 and 2015, we planted each line in a greenhouse for line selection. In 2014, we planted the 5 lines in the February flowering cropping system under low temperature controlled at a minimum of 12℃. Although 'Saga SK3' flowered 92 days after lighting stop, we selected two lines that had flowering dates earlier by 32 and 37 days compared to that of 'Saga SK3'. In 2015, we selected one line, 24-SK3-i6-4, from the two lines in the March flowering cropping system under low temperature controlled at a minimum of 13℃. The flowering date of this line was 7 days earlier than that of 'Saga SK3' (Table 2, Fig. 1). Furthermore, this line was almost not different from 'Saga SK3' in terms of the flower size, petal color, and plant height (Table 2, Fig. 2).

As a result, we selected one suitable early-flowering mutant line, 24-SK3-i6-4, which seems to retain the original flower characteristics of 'Saga SK3' after 6-Gy irradiation with C-ion beams. We are planning to investigate the characteristics of the mutant line further for commercial production in our prefecture.

Table 1. Effects of C-ion beam irradiation on induction of early-flowering mutation[z].

Beam dose (Gy)	No. of cuttings irradiated	Survival rate (%)	No. of plants investigated	No. of flowering plants[y]	No. of early-flowering mutants[x]	No. of selected plants
0	20	100	30	24	0	-
3	60	100	489	271	0	-
6	60	100	464	271	9	5

[z] Planting date: 2012/10/24. Lighting stop date: 2012/12/5. Minimum temperature controlled at 13℃.
[y] No. of plants flowered until 70 days after lighting stop.
[x] No. of plants flowered until 56 days after lighting stop.

Table 2. Characteristics of selected line in March flowering croping system in 2015[z].

Line or cultivar	Flowering date	Days to flowering in short days	Plant height (cm)	Weight of 85 cm cut flower (g)	Number of flowers
24-SK3-i6-4	Mar. 23	56	119.7 ± 1.0[y]	92.7 ± 12.1	18.3 ± 2.8
Saga SK3	Mar. 30	63	106.4 ± 1.6	83.6 ± 7.1	15.6 ± 1.7

[z] Planting date: 2014/11/21. Lighting stop date: 2015/1/26. Minimum temperature controlled at 13℃.
[y] Mean ± SE

Saga SK3 24-SK3-i6-4

Fig. 1. Photographs of original cultivar 'Saga SK3' and selected line, 24-SK3-i6-4, on 23 Mar. in 2015.

Saga SK3 24-SK3-i6-4

Fig. 2. Flower of 'Saga SK3' and selected line, 24-SK3-i6-4.

[*1] Saga Prefectural Agriculture Research Center
[*2] Saga Prefectural Higashimatsuura Agriculture Extention Center
[*3] RIKEN Nishina Center

Reference

1) Ueno et al., Hort. Res. (Japan) 12, 245 (2013).

Agronomic characteristics of new edible chrysanthemum cultivar 'Yamaen K4' induced by heavy-ion beam irradiation

S. Endo,[*1] Y. Saito, [*1] A. Abe,[*1] and T. Abe[*2]

Boiled petals of chrysanthemum are a traditional food in Tohoku district and Niigata prefecture. The edible flower cultivars (Shokuyou-giku) were converted from ornamental cultivars with sweetness and a little bitterness. In recent times, edible chrysanthemum has been widely used as a color decoration in Japanese food. The edible petals of chrysanthemum are classified into purple petals and yellow petals. The former type is shipped in autumn as a seasonal product, while the latter is shipped nearly throughout the year. The amount of production of edible chrysanthemum in Yamagata prefecture is the largest in Japan. In Yamagata, edible chrysanthemum is successively shipped in combination with some other cultivars. However, the main yellow flower cultivar 'Kotobuki' shows a trend of reduction in shipment quantity and deterioration in quality due to the smaller flower size from late September. Thus, an increase in shipment quantity is required in the off-season month of October. Therefore, we developed new yellow edible chrysanthemum, 'Yamaen K4', harvested from the middle of October to the middle of November by mutation breeding using heavy-ion beam irradiation.

In 2006, petals of yellow flower cultivar 'Etenraku' (bred using somaclonal variation of 'Kotobuki' in Yamagata prefecture [1]) were picked and sterilized. Subsequently, petals were cut into approximately 1-cm squares and cultured on MS medium containing 5 mg/l BA and 5 mg/l NAA. Then, they were irradiated with a $^{12}C^{6+}$ ion beam (135 MeV/nucleon, LET 22.6 keV/μm) at 10 Gy at the RIKEN RI-beam factory. Irradiated samples had been incubated at 25°C in 68.9 μmol m^{-2} s^{-1} (PPFD) with 16 h day length for some time, and redifferentiated shoots were transplanted on an MS medium for plant elongation and rooting. Rooted plants were transferred to pots and acclimated to the outside air environment. In 2007, cutting seedlings made from 859 individual lines were planted into a greenhouse in November. These plants were evaluated during 2008-2011, and they had showed some mutation of the flowering period (Table 1), flower configuration, and other agronomic characteristics. Finally, one mutant line was selected in 2011. After it passed the field test, it was applied for seed and seedling registration in February 2015 and published for application in July as 'Yamaen K4'.

The flowering period of 'Yamaen K4' was from October to November and was different from that of the original cultivar, 'Etenraku', the flowering period of which is from July to September. The harvesting period was approximately 2-3 weeks from the middle ofOctober to the middle of November regardless of planting date and year (Table 2). Flower head diameters were approximately 80-90 mm in the early profit stage, and these values are slightly less than those of 'Etenraku'. However, the average flower head weight during the harvesting period is the same as that of 'Etenraku', and it depends on the small reduction in the flower head diameter of 'Yamaen K4'. The main color of the inner side of the ray floret is 7B or 7C (reference number of RHS Color Chart), that of the outer side is 7D or 8A, and all values are higher than the corresponding values for 'Etenraku' (Fig. 1, Table 3). The ray floret type is spatulate and incurved, and the ratio of the former type is greater than that for 'Etenraku'. The total number of ray florets in the flower head is the same as for 'Etenraku'. In 2010, the yield per stock was 2,429 g at the 7 May planting and 1,765 g at the 6 June planting, which indicate that the early planting yield tendency is as high as the late planting yield. However, planting before the beginning of June makes it difficult to harvest and control because the plant height increases beyond 110 cm. In 2011, it was easier to handle because the plant height was 86 cm in the case of planting at 27 June, and the yield per stock at that time was 1,569 g (Table 2). The tasting evaluation of 'Yamaen K4' was good and almost the same as for 'Etenraku' .

Table 1. Mutation of flowering date using heavy-ion beam irradiation

Amount of individuals (%)				
Early[z]	Equivalent[z]	Late[z]	Not yet flowering[y]	Total
5 (0.6)	218 (25.4)	477 (55.5)	159 (18.5)	859

z ; Early ; flowering 2 weeks before from original, Late ; flowering 2 weeks after from original, Equivalent ; other, y ; Containing decreased growth and dead individuals

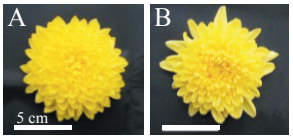

Fig. 1. Flower head of 'Yamaen K4' (A) and original cultivar 'Etenraku' (B)

Table 2. Characteristics of 'Yamaen K4' and standard cultivar (2011)

Planting date	Cultivar	Harvest date		Plant height (cm)[z]	Marketable yield per		Weight per Marketable flower head (g)
		Earliest	Latest		Number of flower head	Weight (g)	
6 Jun.	Yamaen K4	14 Oct.	14 Nov.	110	598	1,794	3.0
	Etenraku	12 Aug.	14 Nov.	56	413	1,188	2.9
	Kotobuki	29 Aug.	21 Nov.	88	640	1,593	2.5
16 Jun.	Yamaen K4	14 Oct.	14 Nov.	95	376	1,442	3.8
	Etenraku	12 Aug.	21 Nov.	50	367	1,132	3.1
	Kotobuki	12 Sep.	7 Nov.	89	573	1,589	2.8
27 Jun.	Yamaen K4	17 Oct.	14 Nov.	86	396	1,569	4.0
	Etenraku	1 Sep.	14 Nov.	47	188	597	3.2
	Kotobuki	26 Sep.	25 Oct.	77	361	1,116	3.1

z : Mean (n=5) , y : Mean in early stage of harvest period (n=30)

Table 3. Flower head morphology of 'Yamaen K4' and original cultivar (2013)

Cultivar	Flower head diameter (mm)[z]	Ray floret[z]		Number of disc floret[z]	Main color of ray floret[x]	
		Number	Type[y]		Inner	Outer
Yamaen K4	87	215	3,2	30	7C	7D
Etenraku	91	220	2,3	17	7D	5D

z : Mean in the early stage of harvest period (n=20), y : 1;ligulate, 2;incurved, 3;spatulate, 4;guilled, 5;funnel shaped, x : Reference number of RHS Color Chart (Japan garden plants standard color chart)

Reference

1) Hirono et al., Breed. Res. 1 (suppl. 2). **323**, (1999). (in Japanese)

[*1] Horticultural Experiment Station of Yamagata Integrated Agricultural Research Center
[*2] RIKEN Nishina Center

Isolation of dwarf mutants induced with C-ion beam irradiation in pea cultivar "Kishu-usui"

Y. Kotani,[*1] S. Ueyama, [*1] T. Hirano, [*2,*3] and T. Abe[*3]

Wakayama Prefecture is one of the major pea (*Pisum sativum* L.) production regions in Japan. We developed Kishu-usui, which is a major cultivar of peas in Wakayama. However, the cultural practices and harvesting operations for Kishu-usui are difficult, because the plant is tall. Therefore, we tried to obtain dwarf mutants, which had a short internode, by heavy-ion beam irradiation for Kishu-usui.

On 13 June 2011, we irradiated dry seeds of Kishu-usui with C-ion beams (LET 33 keV/μm) at doses of 30, 50, and 70 Gy. The germination rate of M_1 seeds at all doses was 100% four days after imbibition. The survival rates of M_1 plants a month after sowing in a greenhouse were 83%, 87%, and 53% at 30, 50, and 70 Gy, respectively.

We collected self-pollinated M_2 seeds of every M_1 plant. The M_2 seeds were sown on 5 September 2012. The dwarf mutants were obtained at all doses, and the frequencies of the dwarf mutants tended to increase with increasing irradiation doses (Table 1). Finally, 16 dwarf mutants were selected for M_2. Especially, the two best mutants were obtained at 30 Gy, and their internode length was 50 to 70% of the internode length at 0 Gy.

The self-pollinations were repeated for selected mutants. On 18 September 2014, the M_4 seeds and Kishu-usui were sown and dwarf mutants were obtained (Fig. 1). Then, the elite line '30Gy①-12-5-55' was selected.

The number of nodes of 30Gy①-12-5-55 was almost equal to that of Kishu-usui (Table 2). However, the plant height and internode length of 30Gy①-12-5-55 were about half those of Kishu-usui. In addition, the first date of flowering, first date of harvesting, node order of flowering, and node order of harvesting of 30Gy①-12-5-55 were almost the same as those of Kishu-usui. The shape of the pod, shape of the unripe seed, weight of the pod, and weight of the unripe seed of 30Gy①-12-5-55 were about the same as those of Kishu-usui. However, it was observed that some of the main stems of 30Gy①-12-5-55 were broken (Fig. 2).

These results suggest that C-ion beam irradiation at doses of over 30 Gy may be effective for creating dwarf mutants and that the dwarf mutants, whose height and internode length are about half those of Kishu-usui, can be isolated.

Table 1. Effect of C-ion beam irradiation on frequency of dwarf mutants[z] of Kishu-usui in M_2 generation.

Dose (Gy)	Number of plants	Number of dwarf mutants	Frequency of dwarf mutants (%)
0	350	0	0.0
30	802	4	0.5
50	759	6	0.8
70	129	6	4.7

[z]Internode length of selected plants by visual judgement was 90% or less than the internode length at 0 Gy. Internode length at 0 Gy:n=9

Table 2. Conparison of no. of nodes, plant height, and internode length for 30Gy①-12-5-55(M_4 plant) and Kishu-usui.

Cultivar or Line	No. of node	Plant height (cm)	Internode length[z] (cm)
30Gy①-12-5-55	53.9	247.1	4.6
Kishu-usui	54.6	485.9	8.9

Data were recorded from Mar. 30 to Apr. 2 , 2015.

[z]Plant height/No. of node (cm)

30Gy①-12-5-55:n=8 Kishu-usui:n=5

Fig. 1. Kishu-usui (left) and M_4 mutant line (right).

Fig. 2. Broken main stem of 30Gy①-12-5-55(M_4 plant). Arrowheads indicate the broken point.

*1 Horticultural Experiment Center, Wakayama Agricultural Experiment Station
*2 University of Miyazaki, Department of Biochemistry and Applied Bioscience
*3 RIKEN Nishina Center

Robust strains isolated by heavy-ion beam irradiation and endurance screening in the green algae, *Haematococcus pluvialis*

T. Takeshita,[*1] K. Takita,[*1] S. Ota,[*1,*2] T. Yamazaki,[*1,*2] Y. Kazama,[*3] T. Abe,[*3] and S. Kawano[*1,*2]

Haematococcus pluvialis is an egg-shaped or spherical unicellular green microalga ranging from 20-50 μm in diameter, belonging to the green algal genus Volvocales (Chlorophyceae). After endospore formation, the alga releases zoospores with two flagellars that grow and become the nonmotile palmela cell. The green cell becomes a cyst following exposure to an environmental stress factor such as strong light or low nutrients, and accumulates astaxanthin, which exerts a strong antioxidative effect, in the cell[1]. If it is possible to obtain a strain with high tolerance to environmental stress (i.e., a robust strain), it seems that the percentage of cell death is decreased, and it is therefore possible to improve productivity. In this study, we attempted to isolate robust strains of *H. pluvialis* using heavy-ion beam irradiation and endurance screening.

Heavy-ion beams of carbon (C), argon (Ar) or iron (Fe) were irradiated on *H. pluvialis* at various doses (C: 0-200 Gy; Ar: 0-100 Gy; Fe: 0-75 Gy), and the number of colony forming units was counted (Fig. 1). The LETs were 22.5 keV/μm, 309 keV/μm, and 790 keV/μm, for C, Ar, and Fe, respectively; thus, the number of colonies formed changed in the order of LETs in *H. pluvialis,* and the overkill reported with *Arabidopsis* did not occur [2].

The cell culture irradiated with the heavy-ion beam of each ion species and dose was inoculated on an agar plate (Fig. 1). To isolate robust strains, the plates were subjected to endurance screening, which included incubation for 3-12 months until the nutrient medium dried up. Most of the cells were died to emit white fluorescence under UV irradiation.

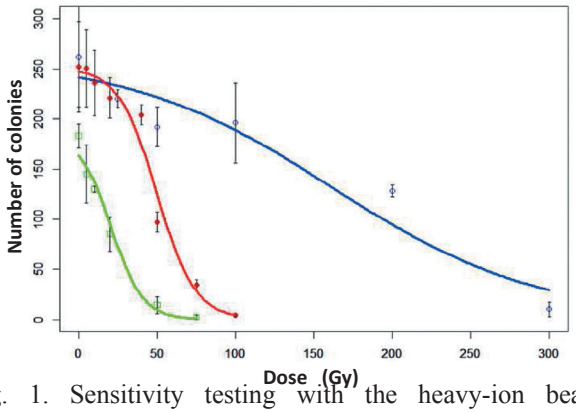

Fig. 1. Sensitivity testing with the heavy-ion beam. Following heavy-ion beam irradiation of *H. pluvials* with each dose of the C ion (○), Ar ion (●) and Fe ion (□), 3,000 cells from each culture were inoculated on an agar plate (n=4 or 5).

*1 Department of Integrated Biosciences, Graduate School of Frontier Sciences, University of Tokyo
*2 JST, CREST.
*3 RIKEN Nishina Center

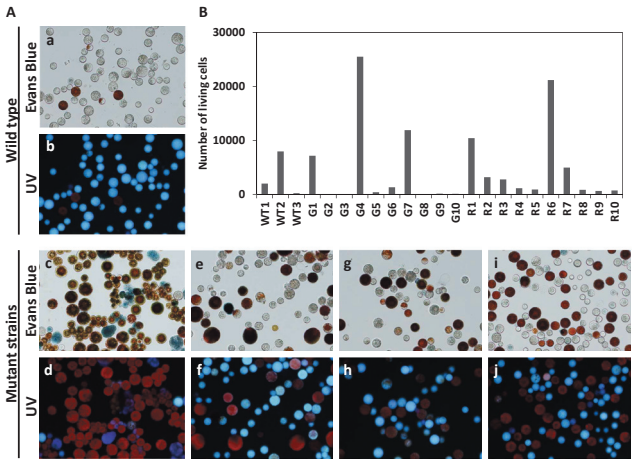

Fig. 2. Microscopic observation (A) and number of living cells (B) in robust strains. WT (a, b), G4 (c, d), G7 (e, f), R1 (g, h), R6 (i, j) in A. Number of living cells (total cell no. × survival rate) in B. Dead cells are stained with Evans blue and emit the white fluorescence under UV irradiation.

After selecting robust strains that were still alive as the red or green cells from dead cells emitting white fluorescence through the use of microscopic observation, they were cultivated with continuous light, and each set of 10 strains maintained a red or a green character. The red strain is a candidate for high astaxanthin accumulation and the green strain is a candidate for high proliferation with chlorophylls. The culture scale was increased to the BBM liquid medium in 100-mL flasks under continuous light (125 μmol photons·m^{-2}·s^{-1}), and sodium acetate solution (final concentration: 45 mM) was added to induce astaxanthin accumulation. The survival rate of the wild type strain (WT1-3) at 7 days post-inoculation was 0-6.2% under these conditions (Fig. 2Aa,b and B). The number of living cells, as determined by cell count, and survival rate were high in G4 (91.8%), G7 (74.9%), R1 (47.2%), and R6 (61.7%) (Fig. 2Ac-h and B). Isolates G4, G7, R1, and R6 indicated high chlorophyll and carotenoid production rates, and G7 and R1 showed conspicuously high carotenoid production (data not shown).

The heavy-ion beams irradiated into the four robust strains were the Ar ion beam at 25 Gy, and C ion beam at 100 Gy. Under these irradiation conditions, approximately 200 colonies formed on an agar plate (Fig. . It is thought that the irradiation conditions are suitable for the variant construction of *H. pluvialis*.

This study was supported by JST, CREST (to SK).

References

1) Wayama et al., Plos One **8**(1), e53618 (2013).
2) Kazama et al., Plant Biotechnol. **25**(1), 113-117 (2008).

Particle beam radiation of the ectomycorrhizal basidiomycete *Tricholoma matsutake* that produces the prized, but uncultivable, mushroom "matsutake"

H. Murata,[*1] T. Abe,[*2] H. Ichida,[*2] Y. Hayashi,[*2] T. Shimokawa,[*1] H. Neda,[*1] T. Yamanaka,[*1] M. Sunagawa,[*1] and A. Ohta[*3]

Tricholoma matsutake is an ectomycorrhizal basidiomycete that produces the economically important edible mushroom "matsutake" in association with Pinaceae plants. The annual, worldwide yield of matsutake is estimated to be 2,000 t, which represents a total retail value of over US$500 million. In Japan, the annual yield of matsutake in the past decade ranged from 50 to 150 t per year, which is much lower than previous annual yields, which reached 12,000 t in 1941. Such a concerning downward trend in the matsutake yield has also occurred elsewhere, including in South Korea, the northeastern provinces of China, and Bhutan.

Mushrooms are fruiting bodies (i.e., the sexual reproductive stage) that contain a tremendous amount of basidiospores. In general, homokaryotic basidiospores are produced after meiosis in dikaryotic hyphae, which result from mating between two monokaryotic hyphae, or between monokaryotic and dikaryotic ones[1,2]. While some ectomycorrhizal mushrooms that are regarded as early colonizers frequently propagate and expand their colonies through spore dispersal, thereby heavily relying on sexual reproduction, and spread elsewhere, those regarded as late colonizers, such as *T. matsutake*, expand their colonies through vegetative hyphal growth, thereby persisting in a preexisting area. However, it has been proven recently that late colonizers also require spore dispersal, thus making them genetically mosaic[3].

Currently, no method is available to cultivate *T. matsutake* to produce fruiting bodies, although methods for artificial mycorrhization and shiro formation have been established in vitro. In fact, in axenic in vitro culture systems, *T. matsutake* associates with a broad range of tree species, including those that naturally harbor arbuscular mycorrhizal fungi, albeit via a root endophytic association, as well as with *Betula platyphylla*, a deciduous broad-leaved tree that shares the same habitat as *Pinus densiflora* and *Tsuga sieboldii*[4]. The most important issue in matsutake cultivation may be the lack of any suitable cultivars. There is a precedent for developing cultivars of fungi that are difficult to cultivate, as the ectomycorrhizal mushroom *Lyophyllum shimeji* is now commercially cultivated to produce the prizedstrains from nature that grow well in a barley-based spawn. Such *L. shimeji* strains were further bred to generate cultivars that were suitable for large-scale mushroom production[5]. Therefore, the creation of strains that are suitable for fruiting, or even spawning like *L. shimeji*, is a key factor for the artificial cultivation of matsutake.

In the present study, we determined whether heavy particle beams could be used to isolate *T. matsutake* mutants. Because we previously obtained some mutants whose traits may be desirable for spawn cultivation and which exhibited a survival rate of ca. 30% following gamma-ray irradiation (500 Gy), we used Ar- and Fe-ions at radiation doses ranging from 0 to 500 Gy. Of these heavy ion beams, Ar irradiation (400–500 Gy) resulted in a survival rate of 12%, while Fe irradiation (large particles, 100–300 Gy) resulted in a survival rate of ca. 65%; following irradiation, some mutants exhibited abnormal mycelial morphologies on an agar plate at the first screening (Fig. 1). However, such mutant phenotypes reverted to the wild-type during the second screening. This phenomenon may be attributed to the fact that we picked a piece of mycelia, rather than a single hypha, wherein the survivor with the wild-type phenotype was mixed with, and eventually overtook, the mutant mycelia. Another issue is that the *T. matsutake* hypha is composed of multinucleated cells, and even a monokaryon isolated from a single spore becomes multinucleated during vegetative growth[6]. Therefore, we conclude that irradiation with heavy particle beams is useful for developing cultivars for matsutake fruiting, although some issues regarding how to obtain stable mutants need to be addressed.

Fig. 1. A putative mutant generated by Fe-ion radiation (300 Gy: left) that generates a large amount of aerial hypae unlike the wild-type (right)

*1 Forestry and Forest Products Research Institute
*2 RIKEN Nishina Center
*3 Shiga Forest Research Center

References
1) K. Babasaki et al., Biosci. Biotechnol. Biochem. **76**, 100 (2003).
2) J. Heitman et al., Sex in fungi, ASM Press (2007).
3) H. Murata et al., Mycorrhiza **15**, 505 (2005).
4) H. Murata et al., Mycorrhiza **25**, 237 (2015).
5) A. Ohta, Mycoscience **35**, 147 (1994).
6) H. Murata et al., Mycoscience **56**, 287 (2015).

Microbeam divergence from glass capillaries compared with simulation for biological use

T. Ikeda,[*1] R. J. Bereczky,[*1] T. Kobayashi,[*1] Y. Sakai,[*2] and T. Abe[*1]

Heavy-ion beam irradiation at relatively low doses induces mutations at a high rate without severely inhibiting growth. As DNA, which is relevant to mutation, is localized in a cell, micrometer-sized beams should be used to irradiate the DNA effectively. When a megaelectronvolt-energy ion beam is transmitted through a tapered glass capillary with a micrometer-sized outlet, the extracted beam can be utilized as an ion microbeam for cell irradiation [1]. The capillary is closed by a thin end-window at the outlet to maintain the inner vacuum so that the outlet can be close to the target cells in water solution. In the case of thinner capillaries (order of 1 μm), the divergence of the transmitted beam has been investigated. However, larger outlets (10 μm or more) with end-windows need further study because the probability of mishitting the neighboring cells due to larger lateral momentum components of ions should be determined before experiments.

In our experiment, He^{2+} ions with an energy of 4.5 MeV from the Pelletron accelerator at RIKEN were used and transmitted through capillaries with different outlet diameters of the order of 10 μm, where the inlet diameter and the length were 800 μm and ~5 cm, respectively. The beam profile was obtained with pieces of a plastic tracking detector, CR-39, in air 6 mm downstream of the capillary and then compared with simulated data using SRIM (TRIM) code. The distance between the capillary outlet and the target was determined so that the ion hit points are sufficiently separated from each other to be observed by a microscope with good statistics. The beam divergence inside the capillary is parameterized in the simulation, where ions start at the upstream side surface of the end-window with a homogeneous distribution for initial positions and with a distribution of lateral momentum components expressed by a single parameter, σ_θ, the standard deviation of a Gaussian distribution. Most of the experimental hit point distributions on the CR-39 pieces are well reproduced even when single σ_θ was selected properly. In this case, a difference in σ_θ of 0.1° reflects a large change in chi-square for the comparison [2]. However, some of the capillaries showed more out-going events. This fact implies the divergence inside the capillary may have multi-parameter σ_θ's. This idea has been reported by Hasegawa et al. [3], who introduced a 'core' component as well as a 'halo' component. Figure 1 shows the hit point distributions of the experimental and simulated results as a function of the distance between a hit point and the beam axis (or the weighted center for experiments), r in micrometers. As a trial, σ_θ of 1.35° for Fig.1(a) and σ_θ of 3.00° for (b) were selected after a rough scan in σ_θ. Both plots do not show an agreement between the experimental and simulated data. Figure 1(c) shows that simulated data of linear combination (a) ×1 + (b) ×0.32 reproduce the experimental spectrum, where the coefficient of the combination was obtained by chi-square fitting. It shows that more than one component of the beam spread during the transmission is needed. In order to reduce the halo component, how and what amount of such events is generated and what shape of the capillary is best should be investigated. We have started a realistic GEANT4 simulation that allows us to install the complicated capillary shape [4]. Figure 1(d) shows a typical event display with a capillary outlet size of 20 μmϕ and end-window of 3 μm[T]. After the installation of the measured capillary, a simulation with not only parallel incoming beams but also spread/focused beams adjusted by a Q-magnet upstream of the capillary is scheduled.

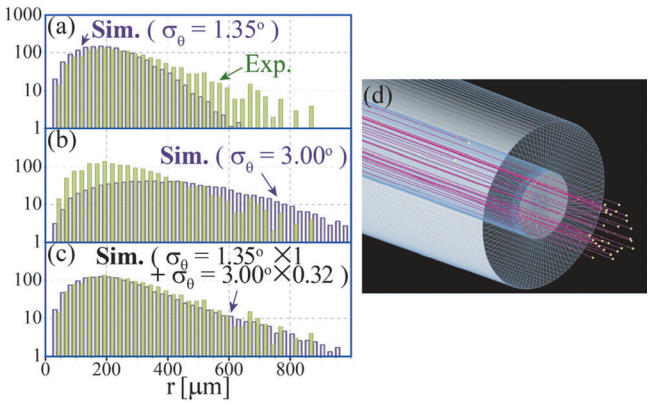

Fig. 1. Comparison between experimental (green) and simulated (purple) spectra. The experimental spectra are the same through (a)-(c). The heights of the spectra for the simulated results in (a) and (c) are normalized so that the peak heights are similar to those of the experimental results. The normalization factor for (b) is the same as that for (a). (d) A typical event display of GEANT4 for the trajectories of He^{2+} with 4.5 MeV stopping (at yellow points) in water solution.

*1 RIKEN Nishina Center
*2 Department of Physics, Toho University

References

1) R. J. Bereczky et al.: Abstract of 12th Int. Workshop on Microbeam Probes of Cellular Radiation Response, Fukui, Japan, (2015), p. 74.
2) R. J. Bereczky et al., RIKEN Accel. Prog. Rep. **48**, 316 (2015).
3) J. Hasegawa et al., J. Appl. Phys. **110**, 044913 (2011).
4) T. Ikeda et al., Surf. Coat. Technol. **206**, 859 (2011).

IV. OPERATION RECORDS

Program Advisory Committee meetings for nuclear physics and for materials and life experiments

K. Yoneda, *1 K. Ishida, *1 H. Yamazaki, *1 N. Imai, *2 Y. Watanabe, *3 K. Yako, *2
H. Miyatake, *3 H. Ueno, *1 and H. Sakai*1

The Program Advisory Committees (PAC) is in charge of reviewing scientific proposals submitted for use of the accelerator facility of RIKEN Nishina Center (RNC). In Fiscal Year 2015, two PAC meetings were held; one for proposals of nuclear physics (NP-PAC), and one for proposals of materials and life experiments (ML-PAC). The NP-PAC reviewed experimental proposals at RIBF, whereas the ML-PAC reviewed proposals at Rutherford Appleton Laboratory (RAL) and RIBF.

NP-PAC

The 16th NP-PAC meetings were held on December 3 – 5, 2015[1]. From this NP-PAC meeting, Institute of Particle and Nuclear Studies (IPNS), KEK, participated in the cooperative operation of the NP-PAC meeting together with RNC and Center for Nuclear Study (CNS), the University of Tokyo. The experimental proposals which utilize KISS were called for the first time.

In the 16th NP-PAC meeting, 34 proposals were reviewed, and 26 proposals were approved as grade S or A. The outcome of these NP-PAC meetings is summarized in Table 1.

Before this NP-PAC meeting, eight PAC members were renewed. The 16th NP-PAC members are as follows:
B.M. Sherrill (NSCL, MSU, the chair), A. Andreyev (The University of York), A. Bracco (INFN), H. Iwasaki (MSU), I. Hamamoto (Univ. of Lund/RIKEN Nishina Center), W. Loveland (Oregon State University), S. Nakamura (Tohoku University), T. Nilsson (Chalmers University of Technology), K. Ogata (RCNP, Osaka University), T. Rauscher (University of Hertfordshire), H. Simon (GSI), O. Sorlin (GANIL), A. Tamii (RCNP, Osaka University), Y. Utsuno (JAEA), P. Van Duppen (K.U. Leuven), Y.-H. Zhang (IMP).

ML-PAC

The 12th ML-PAC meeting was held on February 16 – 17, 2016[2]. In this meeting, 47 RAL proposals and 3 RIBF proposals were reviewed. The summary of the outcome of the meeting is given in Table 2.

Table 1. Summary of the outcome of the 16th NP-PAC meeting. The proposals ranked with S and A are treated as the "approved" proposals.

16th NP-PAC (December 3 – 5, 2015)	requested proposals (days)	approved proposals (days)
GARIS (RILAC)	4 (89.5)	4 (57.5)
CRIB (AVF)	5 (55.5)	3 (32)
RIPS (RRC)	3 (29)	3 (20)
BigRIPS/ZDS	11 (101)	8 (45.5)
SHARAQ	1 (15)	1 (8)
SAMURAI	9 (81)	6 (23.5)
Proposal for Scientific Program	1 (11)	1 (8)
Construction	0 (-)	0 (-)
Total	34 (382)	26 (195.5)

Table 2. Summary of the outcome of the 12th ML-PAC meeting.

12th ML-PAC (February 16 – 17, 2016)	requested proposals (days)	approved proposals (days)
RAL	47 (234.5)	43 (125)
RIBF	3 (28.5)	3 (28.5)
Total	50 (263)	46 (153.5)

The 12th ML-PAC members (including two new members) are as follows:
A. Hiller (ISIS, RAL, the chair), T. Azuma (RIKEN), R. Kadono (KEK), A. Kawamoto (Hokkaido Univ.), N. Kojima (Univ. of Tokyo), K. Kubo (ICU), P. Mendels (Univ. Paris, Orsay), S. Sulaiman (Universiti Sains Malaysia), H. Yamase (NIMS), S. Yoshida (Thera Projects Associates), and X.G. Zheng (Saga Univ.).

References

1) http://www.nishina.riken.jp/RIBF/NP-PAC/index.html
2) http://www.nishina.riken.jp/RIBF/ML-PAC/index.html

*1 RIKEN Nishina Center
*2 Center for Nuclear Study, the University of Tokyo
*3 Wako Nulcear Science Center, Institute of Particle and Nuclear Studies, KEK

Beam-time statistics of RIBF experiments

K. Yoneda, *1 H. Ueno, *1 and H. Sakai*1

This report describes the statistics of the beam times (BTs) at the RIBF facility in Fiscal Year (FY) 2015. In the following, the BTs are categorized into two groups: high-energy-mode and low-energy-mode BTs. In the former mode, the beams were delivered in the acceleration scheme of AVF, RILAC, or RILAC2 → RRC → (fRC → IRC →) SRC, where the accelerators in parentheses can be skipped in the cascade acceleration, depending on the beam species used. In the latter mode, the acceleration scheme is AVF or RILAC (→ RRC).

BTs in the high-energy mode were scheduled from April to June, and from October to December 2015, considering the restriction of utility-power use, budgetary constraints, maintenance schedule of the accelerator system and co-generation system, as well as other constraints. In the series of experiments in spring, the primary beams of ^{238}U, ^{2}H, and ^{78}Kr were provided to users, and in the autumn series, the primary beams of ^{238}U and ^{48}Ca were provided. 11 experiments approved by the RIBF Program Advisory Committees[1] with the approved beam time of 62 days were conducted in total. 10.7 days were used for the facility development programs, defined as machine study (MS) experiments. Other than these, a new isotope search experiment and two nuclear transmutation experiments were conducted as the Nishina Center mission programs.

The summary of the high-energy-mode BTs in FY2015 is given in Fig. 1 as a bar chart. Compared to the beam time in FY2014, the user time decreased, reflecting the shorter total running time in FY2015. The increase of the machine study is mainly due to the commissioning experiments of the Rare RI Ring, which were conducted twice, 3 days in spring and 2 days in autumn.

The summary for the low-energy mode is shown in Fig. 2. Here the BTs are classified by the accelerator operation modes, AVF standalone, RILAC standalone, and RRC. In FY2015, the use of the low-energy mode increased compared to FY2014. This is because most of the low-energy-mode experiments after December 2014 had to be postponed due to lack of the operation budget, and BTs were assigned to those experiments with a higher priority in FY2015. The shorter operation in the high-energy mode also allowed the relatively long BT assignments to the low-energy-mode experiments.

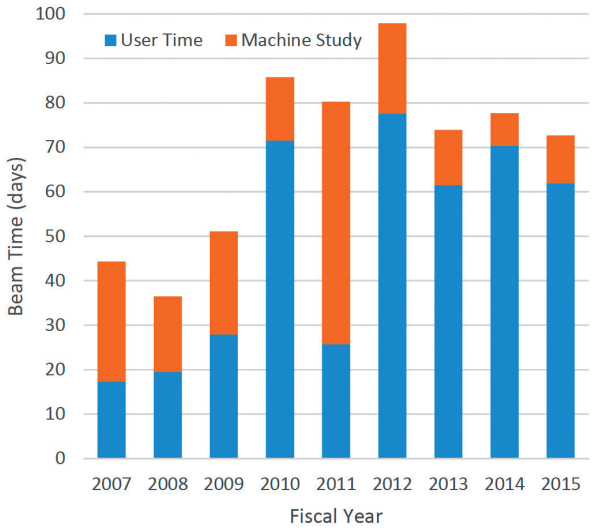

Fig. 1. Bar chart showing the BT statistics for high-energy-mode experiments from FY2007 to FY2015. The accelerator tuning time and Nishina Center mission time are not included.

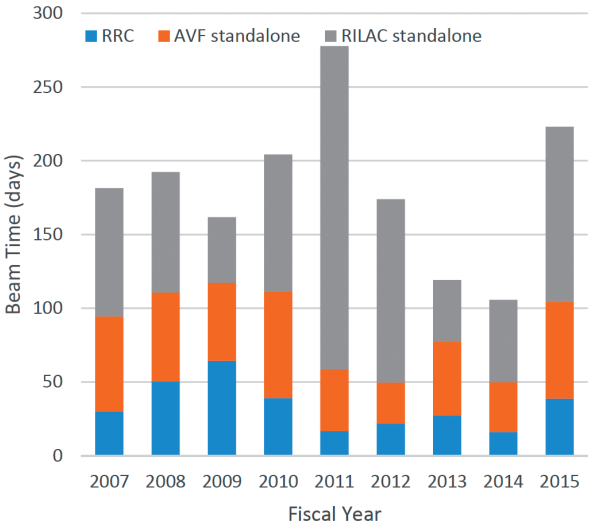

Fig. 2. Bar chart showing the BT statistics for low-energy-mode experiments from FY2007 to FY2015.

Reference

1) K. Yoneda, K. Ishida, H. Yamazaki, N. Imai, Y. Watanabe, K. Yako, H. Miyatake, H. Ueno, and H. Sakai: In this report.

*1 RIKEN Nishina Center

Electric power condition of Wako campus in 2015

E. Ikezawa, *[1] M. Kato, *[1] H. Yamasawa, *[1] and M. Kase*[1]

The monthly electrical power consumption data for the RIKEN Wako campus (Wako) and RIKEN Nishina Center (RNC) and the energy supply by the cogeneration systems (CGSs) are shown in Fig. 1. The hourly average electrical power consumption on a day for RNC in 2015 is shown in Fig. 2. The annual data of the electrical power consumption and energy supply in 2015 are listed in Table 1. The total electrical power consumption of Wako in 2015 was 157,905 MWh, which was the same as that in 2014. However, the total electrical power consumption of RNC in 2015 was 75,154 MWh, which was 3% higher than that in 2014. When the RI Beam Factory (RIBF) experiments using the uranium (^{238}U) beam were conducted, the maximum electrical power supply to Wako from the Tokyo electric power corporation (TEPCO) reached 21.9 MW with a CGS output of 3.9 MW on April 29, 2015, and the maximum electrical power consumption of RNC reached 17.6 MW on October 20, 2015.

A complete overhaul of the gas turbine of CGS #1 after 4,000 h of operation was carried out in September 2015.

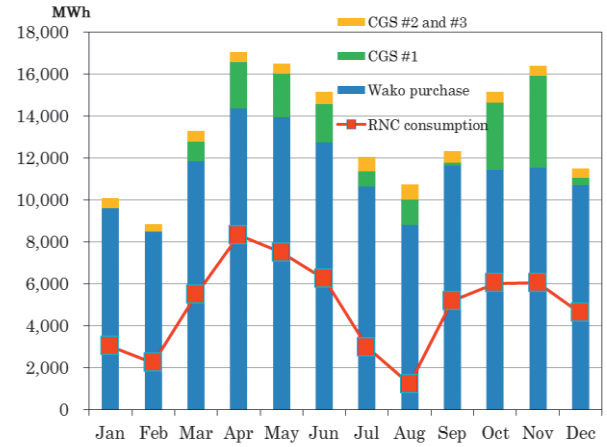

Fig.1. Monthly electrical power consumption and energy supply by CGSs in 2015.

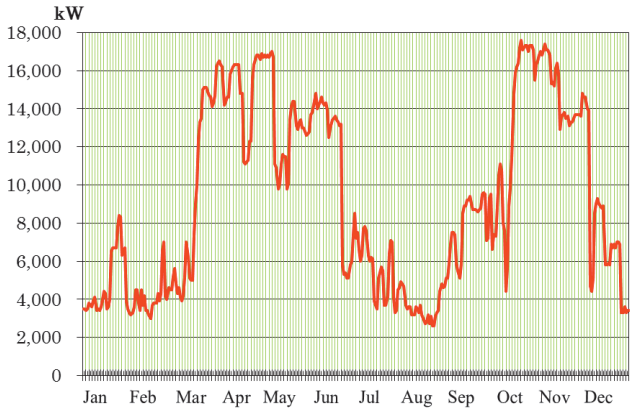

Fig.2. Hourly average electrical power consumption on a day for RNC in 2015.

Table 1. Annual data of electrical power consumption and energy supply in 2015.

	Total (MWh)	Note	% of 2014
Wako purchase	135,577	Total electrical power supply to Wako from TEPCO	97%
Wako consumption	157,905	Wako electrical power consumption (CGSs + TEPCO)	100%
RNC purchase	57,996	Total electrical power supply to RNC from TEPCO	98%
CGS #1	17,158	CGS #1 total electrical power output	128%
CGS #2 and #3	6,345	CGS #2 and #3 total electrical power output	139%
RNC consumption	75,154	RNC total electrical power consumption	103%

*[1] RIKEN Nishina Center

Radiation safety management at RIBF

K. Tanaka,*1 Y. Uwamino,*1 H. Sakamoto,*1 R. Hirunuma-Higurashi,*1 H. Mukai,*2 A. Akashio,*1 T. Okayasu,*1 R. Suzuki,*3 M. Takekoshi,*3 Y. Yamauchi,*3 S. Fujita,*1 H. Aiso,*1 K. Igarashi,*1 S. Iizuka,*1 and N. Usudate*1

The results of radiation monitoring at RIBF, carried out at the border of the facility and the radiation-controlled area are reported. The residual doses along the accelerator setups are also presented. In 2015, on an average, a 345 MeV/u ^{238}U beam was provided at an intensity of 30 particle nA intensity in April, May, October, and November. A ^{78}Kr beam of 300 particle nA was used in May and June, and a ^{48}Ca beam of 400 particle nA in November and December.

The dose rates at the site boundary, where the legal limit is 1 mSv/y, were monitored. Neutron and γ-ray monitors were used, and the annual dose in 2015 was found to be smaller than the detection limit after the background correction. The detection limit of the neutron monitor is 2 μSv/y and that of the γ-ray monitor is 8 μSv/y. Therefore, it was inferred that the annual dose at the boundary was less than 10 μSv/y, which is considerably lower than the legal limit.

The dose rates at the boundary of the radiation-controlled area were also monitored. The neutron and γ-ray monitors were used at three locations: roofs of the RRC, IRC, and BigRIPS. Figure 1 shows the annual neutron dose at the RRC and IRC roofs since 1999. The dose in 2015 at the BigRIPS roof is newly plotted because it had been lower than the detection limit of 3 μSv/y before. Even the highest annual dose of 325 μSv/y at the IRC roof is lower than the legal limit of 5.2 mSv/y.

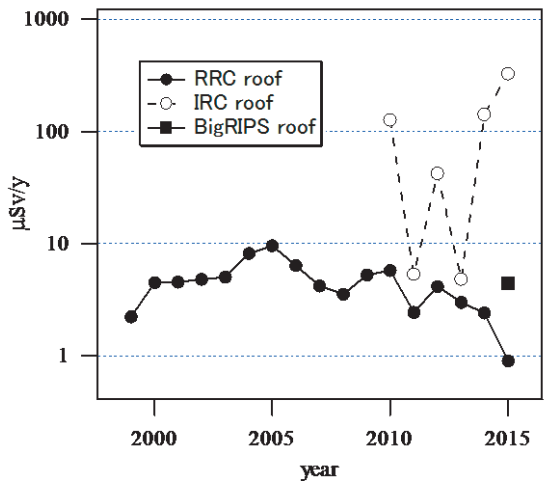

Fig.1 Radiation dose at the boundary of the radiation-controlled area.

*1 RIKEN Nishina Center
*2 Japan Environment Research Corporation
*3 Daiwa Atomic Engineering Corporation

The radioactivity in the closed cooling system at BigRIPS was measured. The water for the F0 target, the exit beam dump, and the sidewall dump were sampled after the 2015 operation of RIBF. The results are shown in Table 1. A liquid scintillation counter was used for the low energy β ray of 18 keV from H-3 nuclide. A Ge detector was also used for γ rays emitted from other radionuclides. The water in the closed cooling systems was replaced in December 2014, therefore it can be said that the detected radioisotopes were generated during 2015. The radionuclides, except for H-3, were already filtered by an ion exchange resin in the closed cooling systems. Although the overall value of contamination was less than the legal limit for drain water, as shown in Table 1, the water from the closed cooling system will be dumped into the drain tank before the next operation to prevent contamination in the room in case of a water leakage.

Table 1. Concentrations of radionuclide in the cooling water at BigRIPS, the allowable legal limits for drain water, and the ratios of concentration to the allowable limit.

Cooling water	Nuclide	Concentration[a] (Bq/cm^3)	Limit[b] (Bq/cm^3)	Ratio to limit [a/b]
BigRIPS F0 target	H-3	7.2	60	0.12
	Be-7	1.1e-2	30	3.3e-3[1)]
			summation	0.12
BigRIPS exit beam dump	H-3	14	60	0.23
	Be-7	1.8e-2	30	6.0e-4
	Co-56	5.7e-4	0.3	1.9e-3
	Co-57	9.6e-4	4	2.4e-4
	Co-58	2.1e-3	1	2.1e-3
	Mn-54	5.2e-3	1	5.2e-3
			summation	0.24
BigRIPS side-wall beam dump	H-3	7.3	60	0.12
	Be-7	1.6e-2	30	5.4e-4
	Mn-54	2.8e-3	1	2.8e-3
			summation	0.12

1) read as 3.3×10^{-3}

The residual radioactivity at the deflectors of the cyclotrons was measured just before the maintenance work. The residual dose depends on factors such as the beam intensity, accelerator operation time, and cooling time. The dose rates from 1986 are shown in Fig. 2. The dose rates for FRC, IRC, and SRC are shown after the year 2006, when the RIBF operation started. For AVF, the dose rate increased in 2006 because the radioisotope production was started and the beam intensity increased.

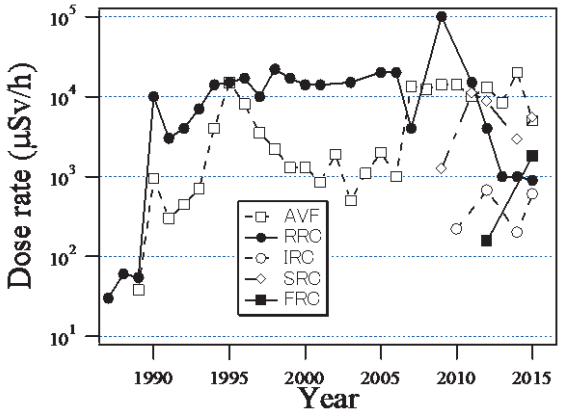

Fig. 2. Dose rates of residual radioactivity at the deflectors of 5 cyclotrons.

Table 2. Dose rates measured at beam lines in 2015. Points 1−26 indicate the locations where measurements were taken as shown in Fig. 3. At point 24-27, the secondary radioactive-isotope beams (RI) were provided whose intensities are limited to 10^7 particle per second.

Point	Dose rate (μSv/h)	Date (M/D)	Particle	Energy (MeV/u)	Intensity (pnA)	Cooling time (h)
1	120	11/18	α	7.25	2750	7
2	85	6/29	Kr-78	10.75	860	158
3	200	7/27	C-12	70	10	165
4	60	6/29	Kr-78	50	530	158
5	1200	12/9	Ca-48	45	715	113
6	1200	12/9	Ca-48	45	715	113
7	80	12/9	Ca-48	45	715	113
8	120	6/29	Kr-78	45	341	159
9	200	12/9	Ca-48	114	650	114
10	130	12/9	Ca-48	114	650	114
11	12000	12/9	Ca-48	345	650	114
12	34000	12/9	Ca-48	345	650	114
13	1100	6/29	Kr-78	345	341	159
14	1600	6/29	Kr-78	345	341	159
15	7000	6/29	Kr-78	345	341	159
16	500	6/29	Kr-78	345	341	159
17	120	6/29	Kr-78	345	341	159
18	180	12/9	Ca-48	345	650	114
19	80	12/9	Ca-48	345	650	114
20	400	12/9	Ca-48	345	650	114
21	32000	12/9	Ca-48	345	650	114
22	5000	12/9	Ca-48	345	650	114
23	23000	12/9	Ca-48	345	650	114
24	400	12/9	RI	<345		114
25	110	12/9	RI	<345		114
26	150	12/9	RI	<345		114
27	500	12/9	RI	<345		114

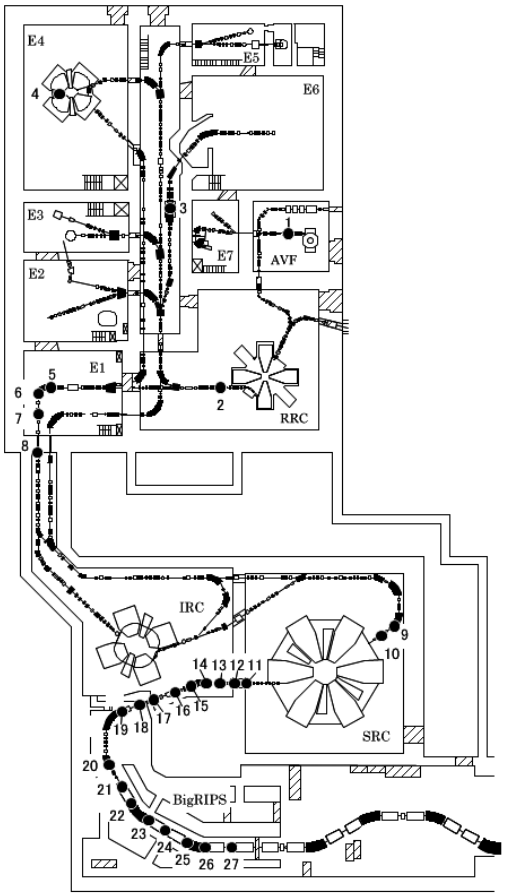

Fig.3. Layout of the beam lines at RIBF. The measurement locations listed in Table 2 are indicated.

The residual radioactivity along the beam lines was measured after almost every experiment. Figure 3 shows locations of measurement points where high residual doses were observed. Table 2 lists the dose rates, beam conditions, and cooling time at the measurement points. The maximum dose was 34 mSv/h at point 12, which is in the vicinity of the G01 faraday cup.

The E-learning module, which can be accessed anytime and from anywhere, even from the outside RIKEN, was newly designed and used for the re-training to the radiation workers at RIBF. About 700 radiation workers have completed the training in 2015.

RILAC operation

E. Ikezawa,*1 T. Ohki,*2 M. Kase,*1 T. Nakagawa,*1 N. Sakamoto,*1 H. Okuno,*1 N. Fukunishi,*1 M. Komiyama,*1 A. Uchiyama,*1 T. Maie,*1 M. Nagase,*1 M. Fujimaki,*1 T. Watanabe,*1 H. Hasebe,*1 H. Imao,*1 H. Kuboki,*1 K. Ozeki,*1 K. Suda,*1 Y. Higurashi,*1 K. Yamada,*1 Y. Watanabe,*1 S. Watanabe,*1 T. Nagatomo,*1 H. Yamauchi,*2 K. Oyamada,*2 M. Tamura,*2 A. Yusa,*2 K. Kaneko,*2 and O. Kamigaito*1

The RIKEN heavy-ion linac (RILAC) has operated steadily throughout the reporting period and has supplied various ion beams for different experiments. Some statistics regarding the RILAC operation from January 1 to December 31, 2015 are given in Table 1. The total beam service time of the RILAC accounted for 85.8% of its operation time. The two operation modes of the RILAC, the standalone mode and the injection mode, in which the beam is injected into the RIKEN Ring Cyclotron (RRC), accounted for 73.8% and 26.2% of the total beam service time of the RILAC, respectively. For beam experiments and machine study of the RI Beam Factory (RIBF), a 2.675-MeV/nucleon ^{48}Ca-ion beam accelerated by the RILAC was injected into the RRC from November 14 to December 4. Table 2 lists the beam service times in the standalone mode of the RILAC allotted to the e2 and e3 beam courses in target room no. 1 in 2015. The e2 beam course was used in experiments with the GARIS2. The e3 beam course was used in experiments with the GARIS. Table 3 lists the operation time of the 18-GHz ECR ion source in 2015.

We carried out the following improvements and overhauls during the reporting period.

1) In the RF systems, the DC high-voltage power supplies were subjected to annual inspection. The major components of mechanical parts were subjected to simple inspection.
2) Three water pumps were overhauled. The other water pumps were subjected to simple inspection. All cooling towers were subjected to monthly inspection and annual cleaning. In addition, bearings for the fans and the fan motors of the cooling towers for rf systems and the cavities of the RILAC and the CSM were replaced with new ones.
3) All the turbomolecular pumps were subjected to annual inspection. Cryogenic pumps used for the RILAC no. 6 cavity and the CSM A4 cavity were overhauled.

We faced the following mechanical problems during the reporting period.

1) The contact fingers of the direct current blocker for the final vacuum tube of the RILAC no. 6 rf system had melted because of the excessive rf current. We replaced it with a new one.
2) The final vacuum tube of the FC-RFQ rf system had a problem. We replaced it with a new one.
3) Water was found to have splashed in the stem of the FC-RFQ cavity and the stub of the x-rebuncher because of leakage from each cooling pipe joint. We replaced it with a new one.
4) Water was found to have splashed in the 5 kW dummy load resistance of the RILAC no. 4 rf system and the end drift tube of the CSM A6 cavity because of leakage from each cooling pipe. We repaired the pipes with a repair material as a stopgap measure.

Table 1. Statistics of RILAC operation from January 1 to December 31, 2015.

Operation time of RILAC	3255.9	h
Mechanical problems	22.0	h
Standalone RILAC	2063.6	h
Injection into RRC	731.5	h
Total beam service time of RILAC	2795.1	h

Table 2. Beam service time of the standalone RILAC allotted to each beam course in target room no. 1 in 2015.

Beam course	Total time (h)	%
e2	583.7	28.3
e3	1479.9	71.7
Total	2063.6	100.0

Table 3. Operation time of the 18-GHz ECR ion source in 2015.

Ion	Mass	Charge state	Total time (h)
He	4	2	72.0
N	14	3	83.9
Na	23	7	466.6
Mg	24	7	264.0
Ar	40	11	477.6
Ca	48	10,11	1665.5
Ti	48	11	92.6
Ti	50	11	157.4
Kr	82	18	576.0
Kr	86	11	72.0
Total			3927.6

*1 RIKEN Nishina Center
*2 SHI Accelerator Service Ltd.

AVF operations in 2015

T. Nakamura,[*2] K. Suda,[*1] M. Fujimaki,[*1] N. Fukunishi,[*1] S. Fukuzawa,[*2] M. Hamanaka,[*2] H. Hasebe,[*1] Y. Higurashi,[*1] E. Ikezawa,[*1] H. Imao,[*1] S. Ishikawa,[*2] T. Kageyama,[*1] O. Kamigaito,[*1] M. Kase,[*1] M. Kidera,[*1] K. Kobayashi,[*2] M. Komiyama,[*1] Y. Kotaka,[*3] R. Koyama,[*2] K. Kumagai,[*1] T. Maie,[*1] M. Nagase,[*1] T. Nagatomo,[*1] T. Nakagawa,[*1] M. Nakamura,[*1] M. Nishida,[*2] N. Tsukiori,[*2] M. Nishimura,[*2] J. Ohnishi,[*1] Y. Ohshiro,[*3] H. Okuno,[*1] K. Ozeki,[*1] N. Sakamoto,[*1] J. Shibata,[*2] A. Uchiyama,[*1] T. Watanabe,[*1] Y. Watanabe,[*1] K. Yadomi,[*2] K. Yamada,[*1] and S. Yamaka[*3]

In 2015, the total annual operation time of the K70 AVF cyclotron (denoted as AVF hereafter) was 3282 hours as shown in Table 1. The total beam supply time was 2051 hours, which was increased by 349 hours compared with that in 2014. The beam supply time was classified into four categories: “Injection to RRC”, “Injection to RRC-SRC”, “Injection to RRC-IRC-E5”, and “AVF standalone”. One of the categories “Injection to RRC-IRC-E5” was a new beam course. The beam was supplied for the first time in January 2015. The supply time for the AVF standalone was 1587 hours, which was 548 hours longer than that in 2014. It was increased mainly by CRIB experiments, and the supply time to the CRIB was three times longer than that in 2014. The beam tuning times for the AVF and the others are shown in Table 1. The tuning time for the AVF is defined as the sum of periods from the start of the cycling of AVF magnets to the end of the spot tuning (in the case of AVF standalone) or to the start of beam transport to the RRC.

All of the beams accelerated by the AVF in 2015 are listed in Table 2. The following beams were accelerated for the first time in 2015: α (7.25, 10.0 MeV/u) and ^{16}O (6.6 MeV/u). The supplied courses were as follows (in order of the decreasing supplied time): E7A (CRIB), C03 (RI production), RRC-E5, RRC-SRC, RRC-E6, E7B (student experiment), and RRC-IRC-E5.

Table 1. AVF operation statistics in 2015.

	2014	2015
Total operation time (h)	2942	3282
Beam tuning (AVF)	773	785
Beam tuning (others)	467	446
Injection to RRC (E5 or E6)	208	324
Injection to RRC-SRC	455	124
Injection to RRC-IRC-E5	-	15
AVF standalone	1039	1587
Beam course (AVF standalone) (h)		
E7A (CRIB)	335	1097
E7B (student experiment)	58	28
C03 (RI production)	646	462

The total fault time was 47 hours (included in the supply time). The main faults are listed in Table 3 in descending order of the time spent on restoration, and the details are indicated below.

*1 RIKEN Nishina Center
*2 SHI Accelerator Service Ltd.
*3 Center for Nuclear Study, the university of Tokyo

Table 2. AVF beam list in 2015.

Particle	E (MeV/u)	Course	Supplied time (h)
p	12	C03	69
d	12	C03	172
d	3.97	RRC-SRC	124
α	6.5	Student exp.	28
α	7.25	C03	23
α	10	C03	8
α	12.5	C03	101
^{7}Li	5.6	E7A	81
^{11}B	5	E7A	181
^{12}C	3.97	RRC-E6	114
^{12}C	7	C03 / RRC-E5	32.4 / 46.4
^{15}N	7	E7A	186
^{16}O	6.6	E7A	217
^{18}O	5.5	E7A	432
^{18}O	6.07	C03	56
^{40}Ar	3.8	RRC-IRC-E5	15
^{40}Ar	5.2	RRC-E5	70
^{56}Fe	5	RRC-E5	22
^{84}Kr	3.97	RRC-E5	72

(1) During d beam tuning, a loss of vacuum occurred at the RF cavity No.2. An O-ring between the insulator ceramics and a coupling terminal plate was damaged. We replaced it with a new one. In addition, the high-voltage plate power supply of the RF system was interrupted due to a failure of two cooling fans. These fans were replaced.

(2) During ^{40}Ar beam supply, the RF system No.1 failed, and could not be operated. There was no output from the power unit of a wide band amplifier. We replaced the unit with a spare.

(3) During ^{15}N beam tuning, a mirror coil, an extraction high-voltage, and a vacuum pump of the HYPER-ECR ion source failed. The beam was supplied by the SC-ECR ion source instead of the HYPER-ECR because time was needed to investigate the cause of the failure.

Table 3. Main faults in 2015. See text for details.

	Date	Time for restoration (h)
(1)	September 2nd	9
(2)	July 5th	8
(3)	September 20th	4

Present status of the liquid-helium supply and recovery system

T. Dantsuka,[*1,*2] H. Okuno,[*1] M. Nakamura,[*1] M. Kase,[*1] S. Tsuruma,[*1]
M. Ohshima,[*2] H. Miura,[*2] H. Shiraki,[*2] H. Hirai,[*2] H. Hazama,[*2] and H. Shiba[*2]

The liquid-helium supply and recovery system,[1)] which can produce liquid helium at a liquefaction rate of 200 L/h from pure helium gas, has been under stable operation since the beginning of April 2001. The volumes of liquid helium supplied each year from 2001 to 2014 are shown in Fig. 1. The volume gradually increased from 2001 to 2013 with two declines in 2009 and 2011. In 2014, the supplied volume decreased due to a malfunction of the system.

The purity of helium gas recovered from the laboratories gradually improved after the construction of the system was completed. Currently, the impurity concentration in the recovered gas rarely exceeds 200 ppm. The volume of helium gas recovered from each building in the Wako campus and the volume transported to the liquid helium supply and recovery system were measured. The recovery efficiency, which is defined as the ratio of the amount of recovered helium gas to the amount of supplied liquid helium, was calculated. The recovery efficiency for the buildings on the south side of the Wako campus, such as the Cooperation Center building of the Advanced Device Laboratory, the Chemistry and Material Physics building, and the Nanoscience Joint Laboratory building, increased to more than 90%.

At the end of September 2014, the system experienced a malfunction. The motor of the helium compressor failed and we could not supply liquid helium for a period of two and a half months. One cause for the motor failure was deterioration due to age. We updated the inverter of the helium compressor in March 2014.

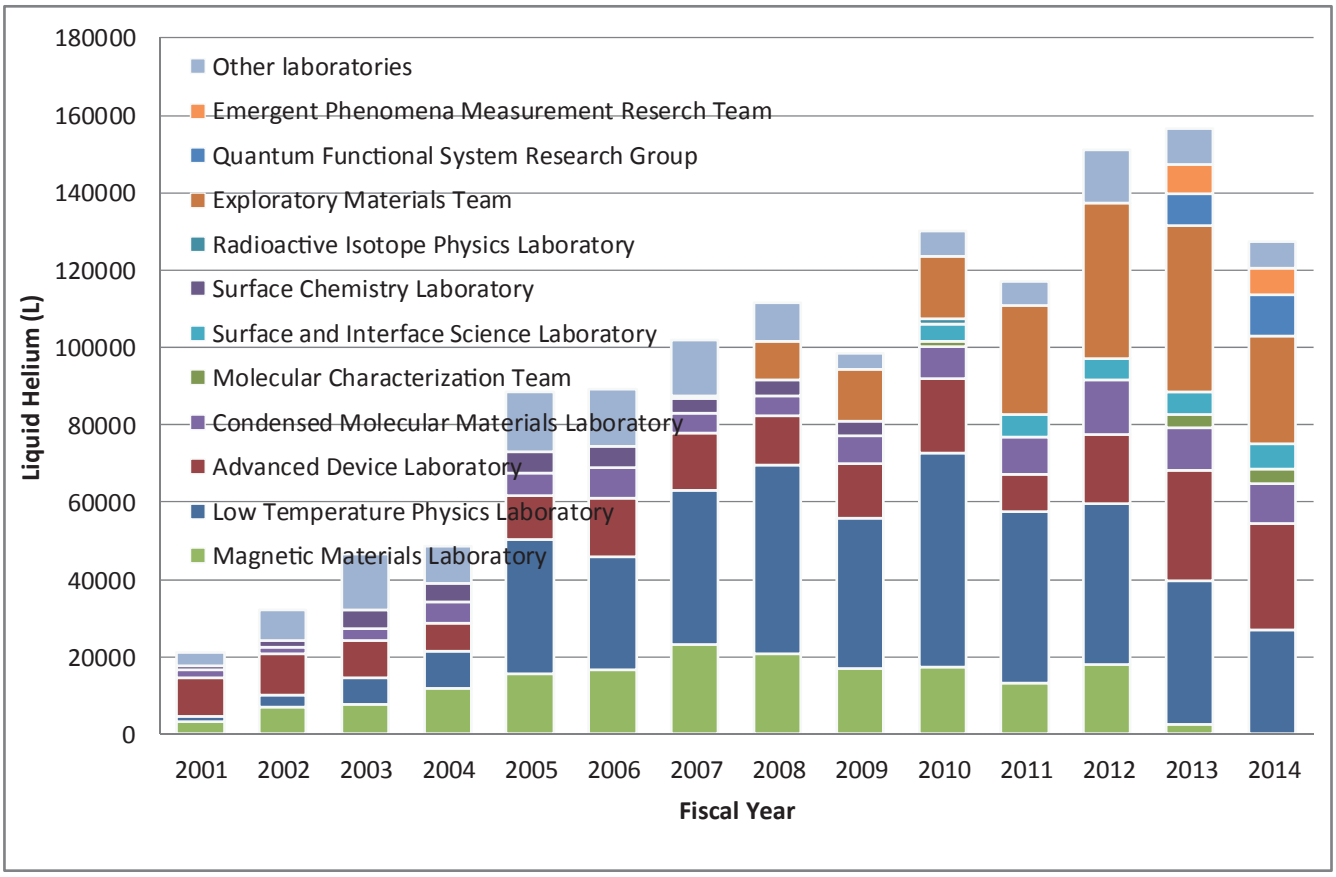

Fig.1. Volumes of liquid helium supplied to the various laboratories for each fiscal year from 2001 to 2014.

*1 RIKEN Nishina Center
*2 Nippon Air Conditioning Service K.K

Reference

1) K. Ikegami et al.: RIKEN Accel. Prog. Rep. 34, 349 (2001).

Present status of the BigRIPS cryogenic plant

K. Kusaka,[*1] M. Ohtake,[*1] T. Kubo,[*1] K. Yoshida,[*1] M. Ohshima,[*2] A. Mikami,[*2] H. Shiba,[*2] H. Hazama,[*2] H. Miura,[*2] H. Shiraki,[*2] H. Hirai,[*2] M. Haneda,[*2] M. Kubota,[*2] M. Noguchi,[*3] and N. Suzuki[*3]

Periodic maintenance of the helium compressor unit is crucial to ensure long-term continuous operations of BigRIPS[1]. Since the total operation time of the helium compressor unit has reached to 52,060 h in July 2015, the main compressor and the motor unit were shipped to the manufacturer's factory for maintenance. The compressor unit was disassembled and its interior was cleaned. All the components were checked carefully and no significant mechanical damage was found. They were reassembled with new mechanical seals and bearings.

The main motor unit was also disassembled. The rotor and the stator coils were cleaned and varnished. The abrasion of the size of +30–50 μm was found at the anti-coupling side bearing bracket. The bracket was repaired by the bushing method, so that its surface became highly smooth (+7–10 μm) and a new motor bearing could be installed. In addition to mechanical checks electrical properties of the motor unit were successfully tested. The rebuilt compressor and main motor unit were installed on site in September.

In September 2014 we have started the continuous operation of the BigRIPS cryogenic plant and stopped the main compressor in July 2015. After the summer maintenance, we started the cryogenic plant in mid−September and stopped the compressor in December 2015. During these continuous operations, we faced some troubles on the compressor unit. One is an unusual noise that was produced by the main motor unit in May 2015. We greased the motor unit and maintained the continuous operation. In other incidents, the compressor unit suddenly stopped that happened twice in May 2015. The failure of the temperature transducer for the discharge helium gas caused false interlock stops. We replaced the temperature transducer and continued the operation. After these incidents, we have started measuring the vibrations of the main compressor unit for sound operations.

Figure 1 shows the vibration velocities in the axial and vertical directions as a function of the total operation time. We measured vibrations both at the high-pressure (HP) and low-pressure (LP) sides of the main compressor unit using the handy vibration tester OH-580A[4]. It is clearly seen that the vibration velocity changed drastically before and after the maintenance.

In addition to maintaining the mechanical components of the compressor unit, we replaced the activated charcoal and molecular sieves in the adsorbent vessel in August 2015. We observed the oil contamination level of the oil-removal module using an oil check kit.

Figure 2 shows an estimate of the oil contamination level at the entrance of the third coalescer vessel as a function of the coalescer filter operation time. As stated by Kusaka et al.[2], the amount of oil drain from the vessel is directly related to the oil contamination level. The navy blue, green, and, yellow diamonds represent the estimates for the 2008-2009, 2010-2011, and 2012-2013 operations, respectively. The coalescer filters used in those periods were discontinued[3]. The estimate for the 2014-2015 operation with successive new coalescer filters is shown as pink diamonds. The oil contamination measurement values using the oil check kit are also shown. The open triangles, squares, circles, and diamonds represent the results for the 2008-2009, 2010-2011, 2012-2013, and 2014-2015 operations, respectively. The performance efficiency of the new filter elements seems to be similar to or better than that of the discontinued ones.

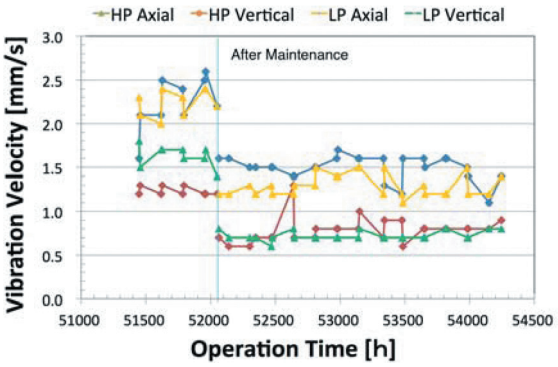

Fig. 1. Vibration velocity of the compressor unit.

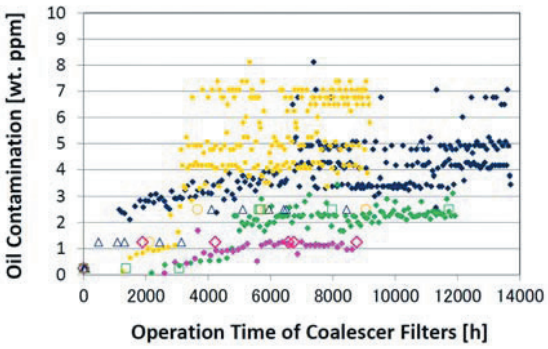

Fig. 2. Oil contamination at the entrance of the third coalescer vessel.

References

1) K. Kusaka et al.: RIKEN Accel. Prog. Rep. **41**, 244 (2008).
2) K. Kusaka et al.: RIKEN Accel. Prog. Rep. **43**, 309 (2010).
3) K. Kusaka et al.: RIKEN Accel. Prog. Rep. **48**, 330 (2015).
4) http://www.testo.jp.

*1 RIKEN Nishina Center
*2 Nippon Kucho Service Co., Ltd.
*3 Mayekawa Mfg. Co., Ltd.

Maintenance of vacuum for accelerators

S. Watanabe,[*1] Y. Watanabe,[*1] E. Ikezawa,[*1] N. Sakamoto,[*1] N. Yamada,[*1] M. Kase,[*1]
K. Oyamada,[*2] M. Nishida,[*2] K. Yadomi,[*2] J. Shibata,[*2] and A. Yusa[*2]

The maintenance of vacuum for accelerators in 2015 is described as follows.

At the RILAC on January 2015, pressure rises were found in cavities No.5 and No.6. The pressures were on the order of 10^{-4}Pa. A helium leak detector was used to find the leak points of the vacuum. The cavities had inner cylinders which were in nested structure and several parts around the chamber. When helium gas was blown on the chamber, the helium leak detector reacted. However the exact location of the leak could not be pinpointed because the helium gas was spread on the chamber. Scratches and cracks on the chamber would have high possibilities of having a leak point. To find the scratches and cracks, dye penetrant inspection was adopted. The scratches and cracks on the surface can be seen using this method. One scratch on the port of the cavity No.5 and 3 scratches on the port of the cavity No.6 were found. A sealing agent was applied to the scratches. The pressure in cavity No.6 was improved to an order of 10^{-6}Pa. However the leak I cavity No.5 could not be fixed. In July, a vacuum leak was found in a chamber called 014. The point of the leak was in a gate valve. Hence, this gate valve was replaced with another one. The vacuum leak was fixed. A controller of a pressure gauge (TPG300) broke down in March. The causes were that a condenser and DC/DC converter were broken. Both the condenser and converter were replaced with new ones. The controller of the pressure gauge was repaired.

The operations in the cyclotrons are described as follows. After summer maintenance in August, the air in the chamber of the AVF could not be evacuated. The chamber was deformed so that the vacuum in the chamber could not be sealed. However, the air could be evacuated when a magnet of AVF was excited. This phenomenon is explained as follows. The temperature of the seals would increase owing to the excited magnet. The gap between two sealing faces became narrow and the leak rate of the vacuum decreased. This phenomenon occurs often. Then, polls were put in the chamber to support the deformed chamber. However some slacken bolts used with the polls were found. The cause of the deformation of the chamber was these slacken bolts. To fix the bolts, the bolts replaced with those with double nuts. In September, vacuum leaks occurred in RF No.2. The leaks were in an insulator and coupling terminal. The O-rings used in the two pats were replaced with new.

The RRC usually runs on a pressure on the order of 10^{-6} Pa. However there was a buildup of pressure in cavity No.1. The pressure was on the order of 10^{-5} Pa. Therefore, the cavity was checked for a leak of vacuum. Leaks were found in cooling pipes No.48 and 52. However the location of the leaks could not be pinpointed. To investigate the leak points, the cavity should be taken apart. To fix the leak, the cavity should be repaired. The other leak of vacuum occurred in cavity No.1 in September. The leak point was in a broken insulator. To fix the leak, the insulator was replaced with a new one. In January, the pressure in cavity No.2 increased to the order of 10^{-4} Pa. Residual gases in the cavity were measured using a quadrupole mass spectrometer. A large spectrum of H_2O was found. The cause of pressure increase was that water leaked from some cooling pipes. The water was leaked from some pipes at cavity No.2. Two pipes having leakage were found using compressed air in March. In June, the cavity was exposed to the atmosphere and the cooling pipes were checked. Several water joints were slacked. The joints were tightened and water leak was fixed. A bellows connected with cavity No.2 had a leak point. The leak point was fixed using sealing agent.

At the fRC, the pressure of the vacuum in the cavity decreased when the magnet was excited. This phenomenon could be due to the fact that excitation of the magnet heated part of the ceiling and the gap between the ceiling faces became narrow owing to the heat. Despite a leak point in the cavity, there will be no problem in running the fRC.

At IRC, the pressure in the IRC was kept high on the order of 10^{-4} Pa. In October, a broken glass of a viewing port was found in the South Pole-box. The viewing port was replaced with a blank flange. The pressure of the vacuum was enhanced to the order of 10^{-6} Pa.

*1 RIKEN Nishina Center
*2 HIS Accelerator Service Ltd.

Operation of fee-based activities by the industrial cooperation team

A. Yoshida,[*1] T. Kambara,[*1] H. Haba,[*1] S. Shibata,[*1] K. Takahashi,[*1] and S. Yanou[*1]

The operation of fee-based activities by the industrial cooperation team in 2015, utilization of heavy-ion beams to industry and distribution of radioisotopes, are summarized below.

RIKEN Nishina Center opens the AVF cyclotron, RILAC, and RIKEN Ring Cyclotron (RRC) to private companies in Japan for a fee.[1] At RRC, three fee-based beamtimes were successfully performed at E5A beamline; two beamtimes with a 70-MeV/A ^{84}Kr beam were performed in July and December, and one beamtime with a 95-MeV/A ^{40}Ar beam was performed in December. Another article in this report describes the technical details of beam preparation and characterization.[2] At the AVF cyclotron, a beamtime was performed in March with an RI beam of ^{7}Be ($T_{1/2}$ = 53 days) from the CNS RI beam separator (CRIB) at E7A beamline, but it was cancelled owing to a technical problem.

Since 2007, RIKEN has been distributing radioisotopes (RIs) produced at the AVF cyclotron to users in Japan for a fee in collaboration with the Japan Radioisotope Association[3] (JRIA). The RIs are produced by the RI Applications Team. According to a material transfer agreement (MTA) drawn between JRIA and RIKEN, JRIA mediates the transaction of RIs and distributes them to users. In April 2015, the MTA was amended to add a new nuclide ^{85}Sr ($T_{1/2}$ = 65 days) to the list of distributed nuclides that included ^{65}Zn ($T_{1/2}$ = 244 days), ^{109}Cd ($T_{1/2}$ = 463 days), and ^{88}Y ($T_{1/2}$ = 107 days). The ^{85}Sr nuclide is produced by the $^{\mathrm{nat}}\mathrm{Rb}(d,x)^{85}\mathrm{Sr}$ reaction[4] and supplied as solution in hydrochloric acid with a concentration of 0.1 M. The maximum radioactivity of one package is 10 MBq. Because ^{85}Sr and ^{88}Y have short half-lives, they are not stocked like ^{65}Zn and ^{109}Cd but are produced in a scheduled beamtime after an order is accepted. Therefore, the RIs are delivered after two or more months. Details can be found on the on-line ordering system J-RAM[5] of JRIA.

In 2015, we delivered three shipments of ^{109}Cd with a total activity of 4 MBq, two shipments of ^{65}Zn with a total activity of 10 MBq, and one shipment of ^{88}Y with an activity of 1 MBq. The final recipients of the RIs were five universities and one hospital. Figure 1 shows the yearly trends in terms of the number of orders and the amounts of the distributed RIs. Compared to 2014, the amount of distributed ^{109}Cd decreased by a factor of 5.5 and that of ^{65}Zn by 4.4, whereas the amount of ^{88}Y was the same.

Information on the RIs can be obtained from JRIA through JRAM or FAX (03-5395-8055).

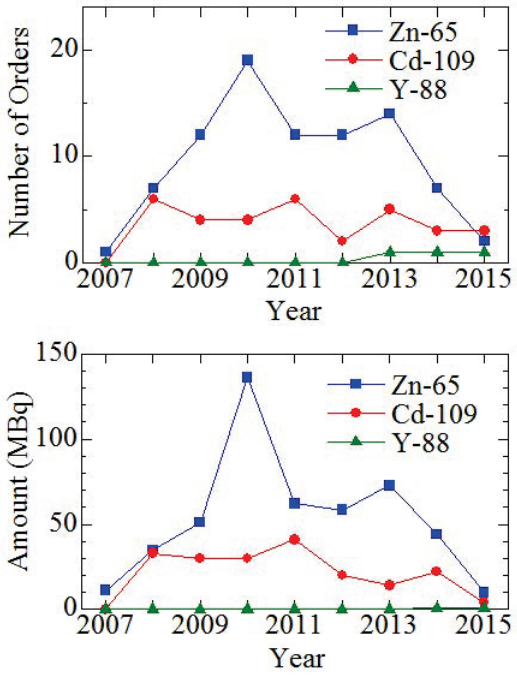

Fig. 1. Number of orders (upper) and amount (lower) of RIs distributed yearly from 2007 to 2015. The distribution of ^{88}Y started in 2010.

References

1) http://ribf.riken.jp/sisetu-kyoyo/ (Japanese).
2) T. Kambara et al.: in this report.
3) http://www.jrias.or.jp/ (Japanese), http://www.jrias.or.jp/e/ (English).
4) S. Yano et al., RIKEN Accel. Prog. Rep., **48**, 299 (2015).
5) https://www.j-ram.net/jram/DispatchTopPage.do (Japanese).

*1 RIKEN Nishina Center

Operation of the tandem accelerator

T. Kobayashi*1 and M. Hamagaki*2

The tandem accelerator (Pelletron 5SDH-2, 1.7 MV max.) (Fig.1) was operated for a total of 84 days for experiments during the annual reporting period from Jan 1 to Dec 31, 2015.

Fig.1 The Pelletron tandem accelerator and beamlines

A total of 20 days were spent on machine inspection, dose measuring, troubleshooting, beam test, and recovery from electric power failure.

The ion species accelerated in this year are H^+, He^+ , Au^{3+} and Au^{7+} with energies ranging from 1.0 to 7.0 MeV, as summarized in Table 1. So far, the ion species of H, He, Li, B, C, N, O, Si, Ti, Ni, Cu and Au have been accelerated with our accelerator.

Experimental studies on the following subjects were performed, and some of them are still in progress.

(1) Characterization of chemical vapor deposition (CVD) single crystal diamond semiconductor detector by using heavy ions (5 days)
(2) Metallic nanoparticle formation by ion irradiation in liquid (24 days)
(3) Microbeam irradiation of living cells using a glass capillary with a thin lid (32 days)
(4) Study of $^{10}B(\alpha, p)$ reaction (15 days)
(5) Study of helium microbeam using tapered glass capillaries (5 days)
(6) Analyses using elastic scattering (3 days)
 (a) Rutherford backscattering spectrometry (RBS)
 (b)Elastic recoil detection analysis (ERDA) of diamond-like carbon (DLC) thin films and polymers for determining hydrogen distribution.

Starting this fiscal year of 2016, the managing laboratory of the tandem accelerator has been switched from Atomic Physics Research Unit to RNC Research Instruments Group.

Table 1 The beam conditions and the experiments conducted in the tandem accelerator

Ion	Energy [MeV]	Beam current [nA]	Experiment	Operation time [days]
$^{1}H^{+}$	1.0 – 3.0	0.01 – 50	Irradiation	63
$^{4}He^{+}$	1.5 – 2.3	1 – 10	RBS, ERDA	20
$^{197}Au^{3+}$	4.0	0.01 – 1	Irradiation	2
$^{197}Au^{6+}$	7.0	0.01 – 1	Irradiation	2

*1 RIKEN Center for Advanced Photonics
*2 Atomic Physics Research Unit, RIKEN

Operation report on the ring-cyclotrons in the RIBF accelerator complex

M. Nishida,[*3] K. Ozeki,[*1] T. Dantsuka,[*1] M. Fujimaki,[*1] T. Fujinawa,[*1] N. Fukunishi,[*1] S. Fukuzawa,[*3] M. Hamanaka,[*3] H. Hasebe,[*1] Y. Higurashi,[*1] E. Ikezawa,[*1] H. Imao,[*1] S. Ishikawa,[*3] T. Kageyama,[*1] O. Kamigaito,[*1] M. Kase,[*1] M. Kidera,[*1] K. Kobayashi,[*3] M. Komiyama,[*1] Y. Kotaka,[*2] R. Koyama,[*3] K. Kumagai,[*1] T. Maie,[*1] M. Nagase,[*1] T. Nagatomo,[*1] T. Nakagawa,[*1] M. Nakamura,[*1] T. Nakamura,[*3] M. Nishimura,[*3] J. Ohnishi,[*1] H. Okuno,[*1] N. Sakamoto,[*1] J. Shibata,[*3] K. Suda,[*1] N. Tsukiori,[*3] A. Uchiyama,[*1] S. Watanabe,[*1] T. Watanabe,[*1] Y. Watanabe,[*1] K. Yadomi,[*3] K. Yamada,[*1] and H. Yamasawa[*1]

In this report, the operation of the ring-cyclotrons in the RIBF accelerator complex from January to December 2015 is presented. Table 1 summarizes the accelerated beams in these cyclotrons. The availability is defined by the ratio of the actual beam time to the scheduled beam time, which is an index of the reliability of beam supply. The delivered beam time in 2015 was 3173.1 h. The ratio of experiments that used the beam extracted from the SRC and the other accelerators was 75% (2388.6 h) and 25%.

The ^{238}U beam was supplied for three periods as follows:

1) Mar. 25th to Apr. 17th for five experiments
2) Apr. 27th to May 8th for two experiments
3) Oct. 19th to Nov. 14th for eight experiments.

A maximum beam intensity of 48.8 particle nA was achieved owing to several factors, such as the increase of the beam current in the ion source, conversion of the injection buncher from the mesh type to cavity type, adoption of a new carbon material for the rotating charge stripper,[1)] improvement of the transmission efficiency in the cyclotrons, and improvement of the vacuum in the RRC.

The polarized deuteron beam was supplied from May 11th to 16th. Although the energy (190 MeV/u) was lower than the certified energy according to the design of SRC (250 MeV/u for M/q = 2 ions), a single-turn extraction was achieved at the acceleration test before the experiment.

The ^{78}Kr beam was supplied in six experiments with a maximum intensity of 310 particle nA, in the RILAC2-RRC-fRC-IRC-SRC mode for the first time (May 23rd to Jun. 22nd). The high-intensity beam production test was performed using an exit beam dump in the BigRIPS, and a beam power of 13.1 kW (486 particle nA) was obtained, which was the power record in the RIBF.

The ^{48}Ca beam was supplied in four experiments (Nov. 17th to Dec. 4th). The maximum intensity reached 689 particle nA owing to the improvement in the ion source and transmission efficiency by the refinement of the rotating charge stripper.

For the machine study, a test to transport the beam extracted from the IRC to E5B was performed. The ^{40}Ar beam was successfully accelerated up to 160 MeV/u in the AVF-RRC-IRC mode and transported to the E5B. In addition, ^{4}He was accelerated in the RILAC2-RRC mode for the first time to be extracted from the RRC. The beam current shown in the table is the converted value to a duty of 100% (the measured current was 0.86 particle μA with a duty of 0.9%).

For the experiments that used a beam extracted from the RRC, ^{48}Ca and ^{12}C (RIPS), ^{84}Kr for industrial use (E5A), ^{86}Kr for the JAXA group (E3A), and ^{136}Xe for the KEK/KISS group (E2A) were supplied. In addition, biological experiments (E5B) were conducted as usual.

Table 1. Summary of the accelerated beams in 2015

Beam particle	Energy (MeV/u)	Acceleration mode	Beam course	Beam current (particle nA)		Beam time (h)		Down time (h)	Availability (%)
				Requested	Actual	Scheduled	Actual		
^{12}C	70	AVF-RRC	E6 (RIPS)	400.0	583.3	108.0	115.8	0.4	106.9
^{12}C	135		E5B (Biology)	1.0	583.3	38.0	38.0	0.0	100.0
^{40}Ar	95		E5B (Biology)/E5A (MS)	1.0	76.5	70.0	70.0	0.0	100.0
^{56}Fe	90		E5B (Biology)	1.0	6.3	22.0	22.0	0.0	100.0
^{84}Kr	70		E5A (Industry)	0.1	5.6	72.0	72.0	0.0	100.0
^{86}Kr	36	RILAC-RRC	E3A (JAXA)	1.0	8.8	12.0	12.0	0.0	100.0
^{48}Ca	63		E6 (RIPS)	300.0	417.6	216.0	212.8	3.3	97.0
^{4}He	7.3	RILAC2-RRC	A02 (MS)	N/A	95000.0	24.0	24.0	0.0	100.0
^{136}Xe	10.75		E2B (KEK/KISS)	50.0	750.0	96.0	95.9	0.3	99.6
^{238}U	10.75		A01 (MS)/A11 (MS)/E5A (Material)	2.0	2500.0	72.0	72.0	0.0	100.0
^{40}Ar	160	AVF-RRC-IRC	E5B (MS/Biology)	N/A	30.0	54.0	54.0	0.0	100.0
pol. *d*	190	AVF-RRC-SRC	BigD-pol	10.0	290.0	96.0	123.9	22.5	105.6
^{48}Ca	345	RILAC-RRC-IRC-SRC	BigRIPS/SAMURAI/ZDS	400.0	689.0	396.0	396.0	19.5	95.1
^{78}Kr	345	RILAC2-RRC-fRC-IRC-SRC	BigRIPS/ZDS/EURICA/Rare-RI Ring	30.0	486.1	732.0	732.0	72.2	90.1
^{238}U (1st)	345		BigRIPS/ZDS	15.0	31.4	552.0	553.0	47.9	91.5
^{238}U (2nd)	345		BigRIPS/ZDS	20.0	39.5	228.0	252.0	25.3	99.5
^{238}U (3rd)	345		BigRIPS/SAMURAI/ZDS	15.0	48.8	588.0	605.7	86.6	88.3

*1 RIKEN Nishina Center
*2 Center for Nuclear Study, the University of Tokyo
*3 SHI Accelerator Service Ltd.

Reference

1) H. Hasebe et al.: in this report.

V. EVENTS

CHEP2015 - 21st International Conference on Computing in High Energy and Nuclear Physics

Y. Watanabe

The 21st international conference on Computing in High Energy and Nuclear Physics (CHEP2015) was held from 13th to 17th April, 2015 at the Okinawa Institute of Science and Technology (OIST) in Okinawa, Japan. It was jointly organized by High Energy Accelerator Research Organization (KEK), International Center for Elementary Particle Physics (ICEPP), The University of Tokyo, Okinawa Institute of Science and Technology Graduate University (OIST), Research Center for Nuclear Physics (RCNP), Osaka University, and RIKEN Nishina Center for Accelerator-Based Science, and supported by Ministry of Education, Culture, Sports, Science and Technology (MEXT), Okinawa Convention & Visitors Bureau (OCVB), and Okinawa Prefecture.

CHEP is a major series of international conferences for physicists and computing professionals from the High Energy and Nuclear Physics community, Computer Science, and Information Technology which provides an international forum to exchange the experiences and needs of the community, and to review recent, ongoing, and future activities. Since the first CHEP conference was held in 1985 Amsterdam, Netherlands, it is held in every one and half a year. It was the second time to be held in Japan since held in Tsukuba in 1991.

The scope of CHEP 2015 is represented by keywords which are categorized in two areas: Application and Technologies.

APPLICATION(13 keywords): DAQ, Trigger, Simulation, Reconstruction, Data analysis, Date Stores, Experiment frameworks for WAN distributed computing, Middleware and services for production-quality infrastructures, Outreach, Multi-discipline/multi-experiment topic, Computing models, Data preservation, and Monitoring.

TECHNOLOGIES(18 keywords): Controls systems, Event processing frameworks, Data structures and algorithms, Data handling/access, Databases, Storage systems, Computing facilities and infrastructures, Software design, Software development process, Performance and validation tools, Continuous integration systems, Parallel programming, Networking, Collaborative tools, Cloud computing, Virtualization, High performance computing, and CPU architectures GPU FPGA.

In numbers, CHEP 2015 attracted a very high number of oral and poster contribution, 535 in total, and hosted 450 participants from 28 countries. There were 34 plenary talks and 254 oral presentations in 6 parallel sessions. Among 247 posters, eight posters presented by young scientists were selected as "Poster award", and lighting talks by each winner took place just before the closing session.

The conference proceedings have been published electronically in the Journal of Physics: Conference Series (JPCS), Volume 664 (2015) (doi:10.1088/1742-6596/664/00/001001).

The next 22nd CHEP conference will be held on October 12th-14th 2016, in San Francisco, hosted by SLAC and LBNL.

Fig. 1. Opening talk of the conference by Dr. Ken Peach

Fig. 2. Applause at the time of the conference end

TAN15 - 5th International Conference on the Chemistry and Physics of the Transactinide Elements

H. Haba* on behalf of the TAN15 Local Organizing Committee

The 5th International Conference on the Chemistry and Physics of the Transactinide Elements (TANs) was held on May 25–29, 2015, at the Urabandai Royal Hotel, located in the Urabandai area, in the northwest region of Fukushima prefecture, Japan. This conference was co-organized by the Nishina Center for Accelerator-Based Science, RIKEN (co-chair: Kosuke Morita) and the Advanced Science Research Center, Japan Atomic Energy Agency (co-chair: Yuichiro Nagame). TAN15 was the fifth in a series of conferences dedicated to the recent achievements in chemistry and physics of transactinide elements. The previous TAN conferences were held in Seeheim, Germany (1999), Napa, United States (2003), Davos, Switzerland (2007), and Sochi, Russia (2011). The scientific program covers both theories and experiments of 1) heaviest-element synthesis, 2) nuclear reactions, 3) nuclear structure, 4) chemistry, 5) atomic properties, and 6) other related topics.

The number of registrants was 86 from 13 countries. There were 2-special, 5-plenary, 12-invited, and 30-oral talks, and 20 poster presentations. In this report, the highlights from the RIKEN RI Beam Factory are briefly introduced.

Kosuke Morita (RIKEN/Kyushu University) claimed the discovery of element 113 by the cold fusion reaction of ^{209}Bi(^{70}Zn,n)^{278}113 based on the convincing three α-decay chains of ^{278}113 which connected to the known nuclides of ^{266}Bh, ^{262}Db, and ^{258}Lr. Yasuo Wakabayashi (RIKEN) reported productions of new isotopes of ^{215}U and ^{216}U in the ^{136}Ba, ^{137}Ba, ^{138}Ba + ^{82}Kr reactions. Hiromitsu Haba (RIKEN) presented production and decay properties of ^{261}Rf, ^{262}Db, ^{265}Sg, and ^{266}Bh available for chemical studies using a gas-jet transport system installed to GARIS. Using unique pre-separated ^{265}Sg atoms, Alexander Yakushev (GSI Helmholtzzentrum für Schwerionenforschung GmbH) investigated the chemical synthesis and the gas-chromatographic separation of the first organometallic compounds of TANs, $Sg(CO)_6$. Yukiko Komori (RIKEN) presented a rapid solvent extraction apparatus coupled to the GARIS gas-jet system for future aqueous chemistry studies of the heaviest TANs such as Sg and Bh. Yoshitaka Kasamatsu (Osaka University) investigated co-precipitation behavior of Rf with $Sm(OH)_3$ as well as solvent extraction behavior of Rf in HCl solutions into Aliquat336. Toward the aqueous chemistry of Db at the RIKEN AVF cyclotron, Shin-ichi Goto (Niigata University) measured an excitation function for the ^{248}Cm(^{19}F,5n)^{262}Db reaction. Daiya Kaji (RIKEN) demonstrated a performance of a new recoil separator, GARIS II. Michiharu Wada (RIKEN) introduced the Multi-reflection Time-Of-Flight (MR-TOF) mass spectrograph under development at GARIS II for precision mass measurements of TAN nuclei. Yuta Ito (RIKEN) received the Best Poster Award for his presentation "Development of a Gas Cell System for SHE-Mass Project at RIKEN".

The next TAN conference will be organized by the German colleagues in 2019.

Fig. 1. Conference photo taken at a garden of the Urabandai Royal Hotel.

* RIKEN Nishina Center

The 9th Nishina School

H. Ueno*1 and T. Kishida*1

The Nishina School was initiated by the RIKEN Nishina Center (RNC) to promote international cooperation in the field of nuclear physics in the Asian Regions through human-resource development. Under this program, select undergraduate students from Peking University and Seoul National University have been participating in a two-week summer program since 2008 and 2012, respectively. They have been attending the Nishina School jointly since 2013.

The 9th Nishina School was held from July 27 to August 7, 2015. The curriculum of the School was designed to introduce the essence of nuclear physics to five undergraduate students from Peking University and five from Seoul National University. The program for the first week consisted of lectures and basic experimental training. During the second week, they gained hands-on experience in conducting experiments. On the last day of the School, the students gave presentations. The program timetable is shown in Fig. 1.

The management policy of the Nishina School has been decided by the Nishina School Steering Committee since its establishment in 2014. This year, the Committee meetings were held five times, on February 24, May 8, July 2, September 18, and December 16, 2015. Kishida, Principal of the Nishina School, also attended all of the meetings as an observer. The Committee decided to incorporate three different experimental trainings: i) mass spectroscopy of natural abundant Xe isotopes utilizing a part of the SCRIT system, ii) ion trapping of charged particles of aluminum powder with a simple trap electrode built by the students, and iii) X-ray and gamma-ray detection with advanced gas and semi-conductor detectors. Technical instructions for these experimental training were provided by the SCRIT Team, the SLOWRI Team, and the High Energy Astrophysics Laboratory.

All the students seemed to appreciate the invaluable experience and enjoy the School and life at RNC. Figure 2 shows a photograph taken at the opening ceremony on July 27.

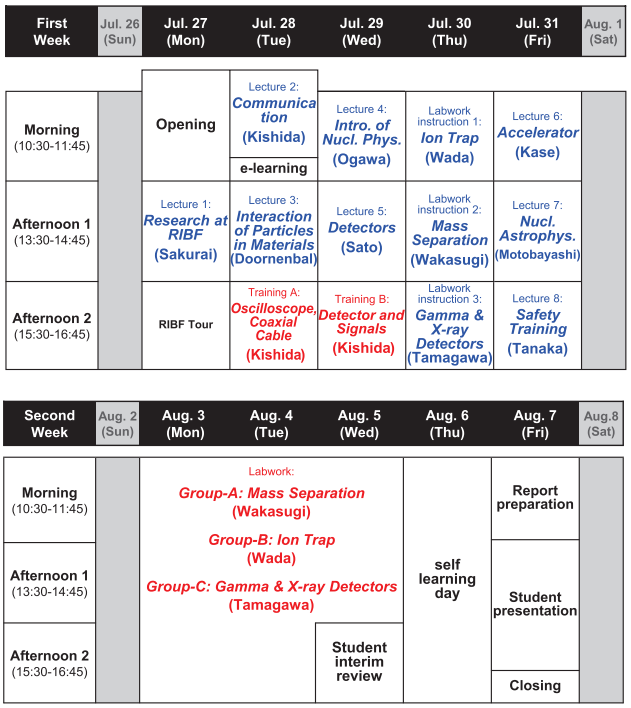

Fig. 1. The curriculum and timetable of the Nishina School. The lectures and experimental training are indicated in blue and red, respectively.

Fig. 2. Photograph of the Nishina School 2015 participants.

*1 RIKEN Nishina Center

HIAT2015-13th International Conference on Heavy ion Accelerator Technology†

N. Sakamoto*1 and O. Kamigaito*2

The 13th International Conference on Heavy ion Accelerator Technology (HIAT2015) was held at WORKPIA YOKOHAMA in the downtown of the city of Yokohama city from September 7 to 11, 2015. It was jointly hosted by the RIKEN Nishina Center, RCNP (Osaka Univ.), NIRS, University of Tsukuba and JAEA-Takasaki.

HIAT2015 was the 13th in a series of conferences, dating back to 1973 first held in Daresbury and followed by Strasbourg (1977), Oak Ridge (1981), Buenos Aires (1985), Strasbourg-Heidelberg (1989), Legnaro (1992), Canberra (1995), Argonne (1998), Delhi (2002), Brookhaven (2005), Venice (2009), and Chicago (2012). HIAT is an international conference dedicated to the design, construction, development and operation of heavy-ion accelerators and their components. It focuses on the operational experience of existing facilities, achievements in heavy-ion accelerator physics and technology, progress on the implementation of new projects and infrastructure upgrades, and trends in the proposal and design of heavy ion accelerators as well as their main systems and components. The conference is mainly devoted to the accelerator teams of any institution, laboratory or university which are running or developing heavy ion facilities or their components for studies in the fields of nuclear physics and astrophysics as well as the applications of heavy ion beams in medicine, accelerator mass spectrometry, material analysis and processing, nuclear waste management, dynamics of nuclear fusion and fission, radiation science and dosimetry, development and production of radionuclides, environmental metrology, etc.

The topics of HIAT2015 were the subjects featured at the first conference that have been modified as follows: 1)Electrostatic Accelerators, 2)Room Temperature and Supaeconducting Linacs, 3)Room Temperature and Supperconducting Cyclotrons, 4)Synchrotrons and Storage Rings, 5)Radioactive Ion Beam Facilities, 6)Ion Sources and Traps, 7)Main Accelerator Systems and Components (e.g. Radiofrequency, Cavities, Magnets, Vacuum, Control, Beam Diagnostics, Cryogenics, Radioprotection, Mass Spectrometry, Microbeam Facilities).

Prior to the conference, a welcome reception was held on Sunday and posters were presented by students who successfully received financial support from the organizing committe. The conference started on Monday with the welcome address by the director of the Nishina Center, Hideto En'yo. In the sessions that followed, the current status on commissioning of new facilities, progresses on accelerator devices, new design of heavy-ion accelerators and their components etc. were widely discussed. There were 18 invited talks and 32 contributed oral presentations. One of the common issues was how to realize very intense heavy-ion beams with highly efficient accelerators. On Monday and Wednesday, poster sessions were held. 47 posters were presented and technical issues were discussed actively. On Friday Richard C. Pardo presented a summary of the conference.

The number of registrants was 120 (not including the number of exhibitors and accompanying persons), from 14 countries. Fig. 1 shows a conference photo taken on Thursday. The HIAT2015 conference turned out to be a great success and it is worth noting that the research activities in this field have become much more vibrant since the last HIAT conference.

The conference proceedings has been published in JACoW(http://www.jacow.org/). The next HIAT conference hosted by IMP will be held in 2018.

*1 Executive Board Chair of HIAT2015, RIKEN Nishina Center
*2 Conference Chair of HIAT2015, RIKEN Nishina Center

Fig. 1. Conference photo taken in the plenary hall

RIBF Users Meeting 2015

N. Imai,[*1] T. Sumikama,[*1] S. Ota,[*1] M. Asai,[*1] P. Fallon,[*1] T. Isobe,[*1] N. Itagaki,[*1] Y. Kanada-En'yo,[*1] M. Kimura,[*1] Y. Kondo,[*1] J. Lee,[*1] H. Miyatake,[*2] T. Nakamura,[*1] A. Obertelli,[*1] K. Ogata,[*1] H. Sakurai,[*3,4] S. Shimoura,[*5] T. Uesaka,[*3] H. Ueno,[*3] K. Yako,[*1] K. Yoneda,[*3] and K. Yoshida[*1]

The RIBF Users Meeting 2015[1] was successfully held on September 10 and 11 in 2015. This meeting aims at mutual understanding among RIBF users through discussion on latest results obtained every year at RIBF. The number of participants was 140, which was more than the number registered. We discussed actively the topics of relevant fields. At the RIBF Users Meeting 2013 held in June 2013, it was decided that the next meeting will be scheduled for March 2015 for the convenience of the users outside Japan. However, the cancellation of NP-PAC scheduled to be held in the June 2015, the Users Meeting was also postponed to September. The Users meeting is usually held during the RIBF collaboration days where the users discuss the ideas of experimental proposals in advance of the NP-PAC meeting.

Since the range of each experimental field varies widely depending on the nuclei interest and the energies of the beams, we allocated 10 minutes for discussion time following 15 minutes talk for each contribution to gain understanding of each other's field. The program mainly consists of reports from large collaborations, i.e., Rare-RI Ring, SUNFLOWER, SAMURAI, EURICA, GARIS, KISS, CRIB, SHARAQ and OEDO. Newly introduced was a new activity of the ImPACT program which attempts to establish a nuclear transmutation method to dispose long lived fission products produced by nuclear power plants. As the last session of the first day, the poster session was hosted by the director of the Nishina Center. We enjoyed discussion during poster presentation in a relaxed atmosphere served with refreshments

Two winners of the RIBF Thesis Awards 2015 were also celebrated at the event. Originally started as the RIBF Users Group Thesis Awards in 2012, this was the fourth time for the Awards to be presented. The Awards honor the achievements of young scholars who earned their doctoral degrees based on experiments and theoretical works related to the physics research conducted at RIBF. Starting from 2015, the Awards were co-hosted by the director of the Nishina Center and RIBF UEC, and name changed to the RIBF Thesis Awards. The winners were Dr. Z.Y. Xu (Univ. of Hong Kong), and Dr. Y. Ito (RIKEN Nishina Center) for the thesis titled "Beta-decay spectroscopy on neutron-rich nuclei in a range of Z = 26 ~ 32" and "A multi-reflection time-of-flight mass spectrograph for high-precision mass measurements of short-lived nuclei", respectively. After the ceremony, Dr. Xu presented a talk on the thesis. Dr. Ito will give a talk at the next Users Meeting.

We also allocated time for two special sessions. One featured the introduction of the activities of GRETINA in USA by Dr. P. Fallon. The highlights of their achievements up to now as well as the prospect of future development were presented. Though the current main γ-ray spectrometer at RIBF, DALI-2, is composed of approximately 200 NaI(Tl) crystals, we should change to spectrometers which has finer energy resolution like germanium detectors. The reason is that the level density will increase in the high-Z region and the level scheme will be complex in the odd nuclei. We agreed to continue with discussion on this issue.

Topics of the other was the upgrade plan of RIBF. Since overseas facilities such as FRIB and FAIR will be commissioned from around 2020, the time has come to discuss the future direction of RIBF. Prof. H. Sakurai from the Nishina Center presented a plan to increase the beam intensity by one order of magnitudes. The plan calls for the construction of a superconducting injector linac and a new fRC in order to bypass the old RRC (RIKEN Ring Cyclotron). Users, on the other hand, requested to install the experimental devices to make full use of the high primary beam intensity. After the meeting, mostly domestic users continued to discuss with the Nishina Center on this issue and finally agreed to the updated plan which includes several experimental devices. The plan was submitted to Science Council Japan in March 2016 to be reviewed.

The next RIBF Users Meeting will be held at the beginning of September in 2016. Though we allocated 10 minutes discussion for each contribution, it turned out that the time was still not sufficient. At the next Users Meeting, we will reduce the number of collaboration reports and instead secure more time for discussion.

Reference

1) http://indico2.riken.jp/indico/conferenceOtherViews.py?view=standard&confId=1961

*1 RIBF Users group UEC
*2 WNSC, KEK
*3 RIKEN Nishina Center
*4 Univ. of Tokyo
*5 CNS, Univ. of Tokyo

Quark Matter 2015

Y. Akiba,[*1] H. Hamagaki[*2] and T. Hatsuda[*1]

The Quark Matter 2015 (QM2015) is the XXV international conference on ultrarelativistic heavy-ion collisions. The aim of this conference series held every year and a half is to unravel the mystery of strongly interacting matter at extreme environments created in the ultrarelativistic heavy-ion collisions in the early universe and the central core of super dense stars. From September 27 to October 3, 699 physicists from 33 countries gathered in Fashion Mart, Kobe, Japan.

QM2015 was hosted by the Science Council of Japan and the Physical Society of Japan, and co-hosted by the RIKEN Nishina Center and the Center for Nuclear Study, the University of Tokyo. 19 domestic and foreign institutions, 9 domestic and foreign companies, and 2 foundations from Kobe city had made substantial contributions and financial supports to organize QM2015. The conference was chaired and co-chaired by the present authors.

Major scientific topics of QM2015 included (1) QCD at High Temperature, (2) Baryon Rich QCD Matter, (3) QGP in Small Systems, (4) Initial State Physics and Approach to Equilibrium, (5) Jets and High p_T Hadrons, (6) Open Heavy Flavors and Strangeness, (7) Quarkonia, Electromagnetic Probes, (8) Collective Dynamics, (9) Correlations and Fluctuations, (10) Quark Matter in Astrophysics, (11) Relations to Other Strongly Coupled Systems, (12) New Theoretical Developments, and (13) Future Experimental Facilities, Upgrades, and Instrumentation.

The QM2015 program started on September 27 with the public lectures by Ryugo Hayano (Univ. Tokyo) and Hiroshi Ooguri (Caltech/IPMU) concurrently with the student day lectures. More than 240 students and postdocs attended the student day lectures. After the opening talk by Gordon Baym (Univ. Illinois) on September 28, the first three days (Sep.28-Sep.30) were devoted to parallel sessions and poster sessions. Plenary sessions followed for the last three days (Oct.1-Oct.3). There were 168 parallel talks, 410 poster entry and 32 plenary talks. In addition, 8 flash talks selected from the posters were presented on the last day. The Young Scientist Prize for Nuclear Physics was awarded to the select individuals who gave parallel talks, namely, Natasha Sharma (Univ. of Tennessee), Darren McGlinchey (Univ. of Colorado), Zhenyu Chen (Rice Univ.), and Alexander Rothkopf (Heidelberg Univ.). Moreover, the Zimanyi Medal granted to a young theoretical physicist under 40 who has made extraordinary contributions to the field of high energy nuclear physics, was awarded to Chihiro Sasaki (Wroclaw Univ.). Details of the scientific contents and presentation slides can be viewed online: http://qm2015.riken.jp/

*1 RIKEN Nishina Center
*2 Center for Nuclear Study, The University of Tokyo

Fig. 1 and Fig.2 show some statistics regarding the QM2015 participants. The blue and the red correspond to male and female participants, respectively.

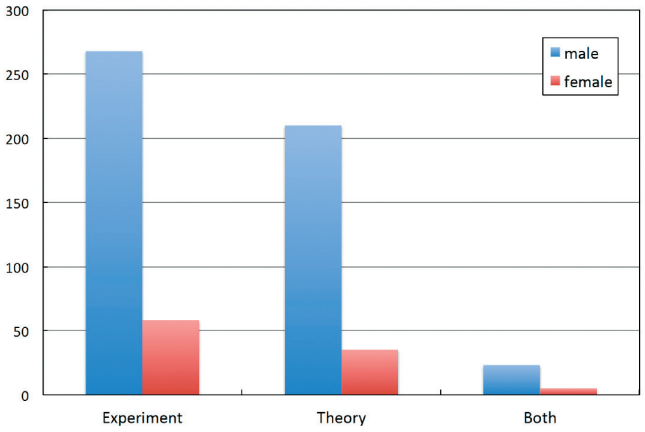

Fig. 1. Number of experimentalists and theorists participating in QM2015.

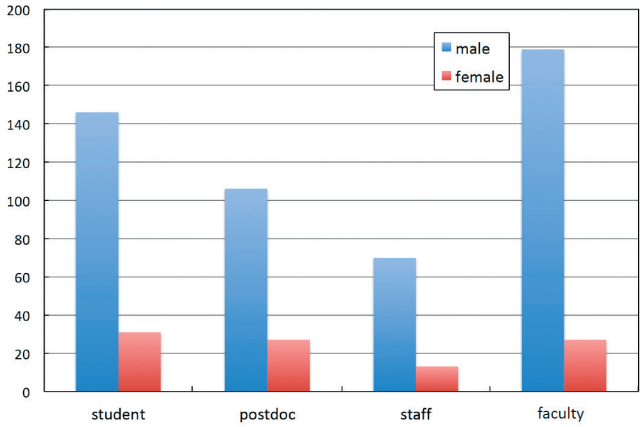

Fig.2. Number of students, postdocs and staffs/faculties participating in QM2015.

Physics with Fragment Separators - 25th Anniversary of RIKEN Projectile Fragment Separator (RIPS25)

Reported by T. Kubo

A symposium entitled "Physics with Fragment Separators - 25th Anniversary of RIKEN Projectile Fragment Separator (RIPS25)" was held on December 6-7, 2015 at Shonan Village Center in Hayama, Kanagawa, Japan to celebrate the 25th anniversary of the RIKEN Projectile-Fragment Separator, RIPS, at RIKEN Nishina center.

With the RIPS separator producing its first RI beams in November 1989, the physics programs using RI beams at intermediate energies started in January 1990. Since then, the RIPS facility has been pioneering in a variety of key experiments in RI-beam physics, such as those of reaction studies of exotic nuclei with RI beams as well as with spin-polarized RI beams. The RIPS25 symposium celebrated the great achievements that the RIPS separator had contributed in making in the last 25 years, reviewing how RI-beam physics has been established as one of the key fields of nuclear physics. Furthermore the future directions of the fields were discussed as well.

The RIPS25 symposium was jointly organized by RIKEN Nishina Center and the Center for Nuclear Study (CNS), Univ. of Tokyo, chaired by Toshiyuki Kubo, RIKEN and co-chaired by Susumu Shimoura, CNS. A total of 65 participants joined the symposium, which included 16 from foreign institutes, 23 from domestic institutes, and 26 from RIKEN. Figure 1 shows a group photograph of the participants. The numbers of oral and poster presentations were 25 and 13, respectively.

The invited speakers and invited participants (labeled by *) are listed as follows:

N. Aoi (RCNP, Osaka U.)
T. Aumann (TU Darmstadt / GSI)
D. Beaumel (IPN Orsay)
A. Chakrabarti (VECC, India)
M. Fukuda (Osaka U.)
A. Gade (NSCL, MSU)
H. Geissel (GSI)
K. I. Hahn (Ewha Womans U., S. Korea)
I. Hamamoto (RIKEN / U. of Lund)
M. Ishihara (RIKEN)
Y. Kondo (Tokyo Tech.)
D. J. Morrissey (NSCL, MSU)
A. C. Mueller (CNRS)
E. Yu. Nikolski (Kurchatov Institute)
S. Nishimura (RIKEN)
K. Ogata (RCNP, Osaka U.)
N. A. Orr (LPC CAEN)
T. Otsuka (U. of Tokyo)
S. Sakaguchi (Kyushu U.)
H. Ueno (RIKEN)
M. Wada (RIKEN)
Y. Ye (Peking U.)
*W. Henning (RIKEN/Argonne)
*J. A. Nolen (Argonne)
*A. Ozawa (U. of Tsukuba)
*H. Sakai (RIKEN)
*Y. Yano (RIKEN)

The speakers from the organizer side were as follows:

T. Kubo (RIKEN)
H. Sakurai (RIKEN)

Fig. 1. Group photograph of the symposium

VI. ORGANIZATION AND ACTIVITIES OF RIKEN NISHINA CENTER

(Activities, Members, Publications & Presentations)

1. Organization

1.1 Organization Chart as of March 31, 2016

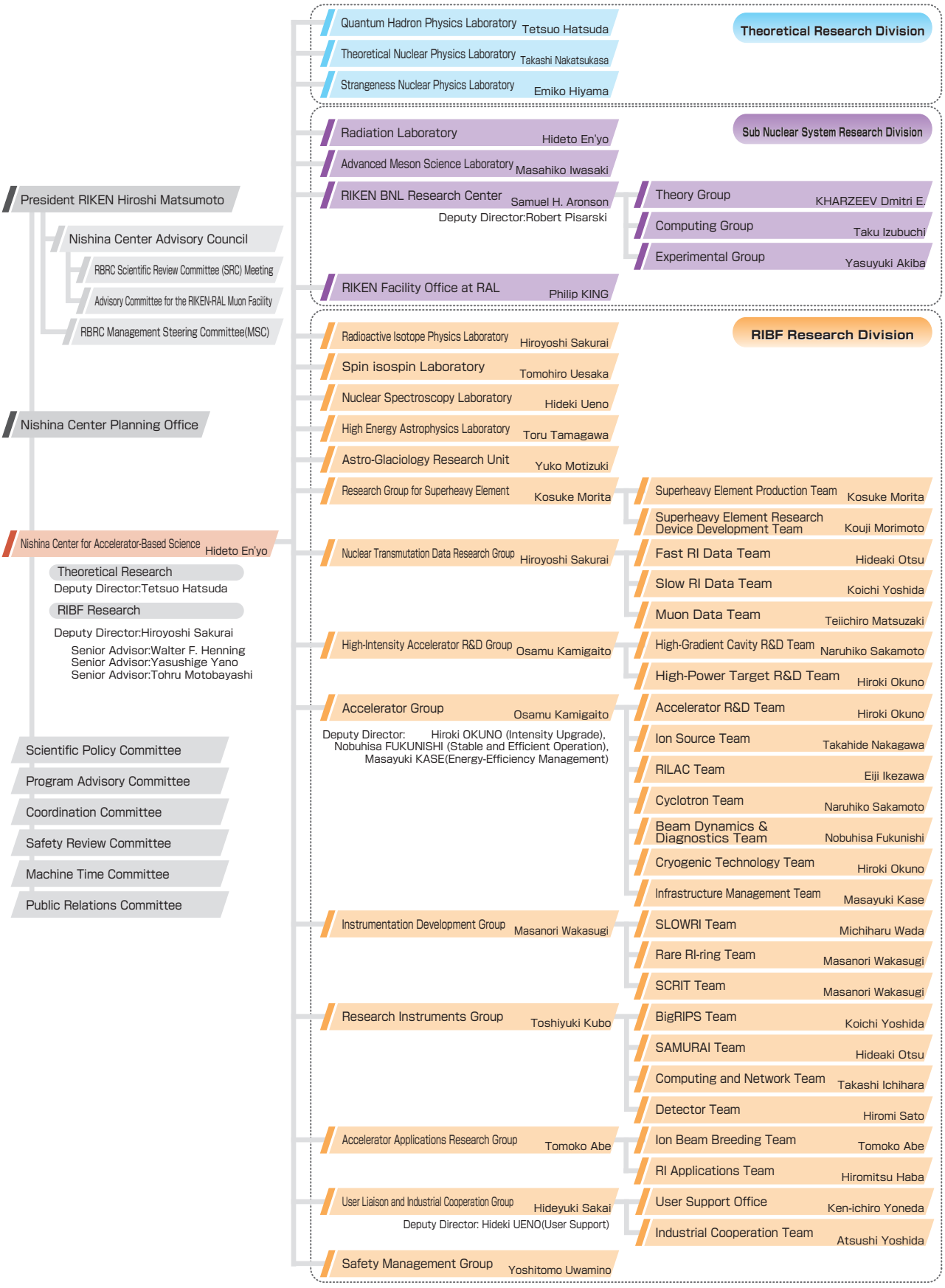

1.2 Topics in FY2015

In fiscal year 2015, 4.8 months operation was achieved along with the acquisition of fundamental nuclear transmutation data for the ImPACT (Impulsing Paradigm Change through Disruptive Technologies Program) project.

Accelerator system of RIBF has greatly improved with the upgrade of the beam intensity of the heavy ion in the RI beam generating system by threefold. This upgrading was accomplished two year ahead of schedule. RIBF has been highly available to the users even by the standard of research environment worldwide.

IUPAC recognized element 113 discovered as a new element by the research group led by Group Director Kosuke Morita (now Research Group for Superheavy Element), and gave the group the honor of naming and determining the two-letter symbol for the element. Element 113 will then become the first element to be named through the discovery made by an Asian research institution.

As a result of biological irradiation of the heavy ion in cooperation with public companies, the Ion Beam Breeding Team succeeded in the selective breeding of tear-free onion. Named ‘smile ball’, the new breed of onion is being marketed. Paid use of RI beams in the radiation resistance test of the semiconductor for use in space has been promoted for industrial application.

Year	Date	Topics in Management
2015	Sep. 1	Team Leader Michiharu WADA moves to the part-time position (Prof., Institute of Particle and Nuclear Studies, KEK)
	Nov. 1	New Appointment Group Leader of Theory Group: Dmitri E. KHARZEEV
2016	Jan. 12	Interim Review of the Chief Scientist, Osamu KAMIGAITO
	Mar. 8	Interim Review of Associate Chief Scientist, Toru TAMAGAWA
	Mar. 31	End of Theoretical Nuclear Physics Laboratory

2. Finances

As mentioned in “1.2 Administrative Topic in FY2015”, RNC executed approximately 4.8 months of RIBF operation. Breakdown expenses of the RNC FY2015 budget and a transition for the past five years are shown in following graphs.

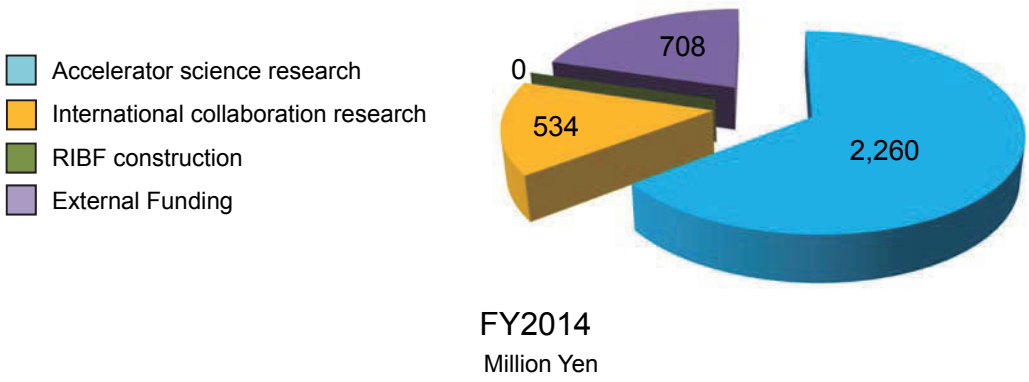

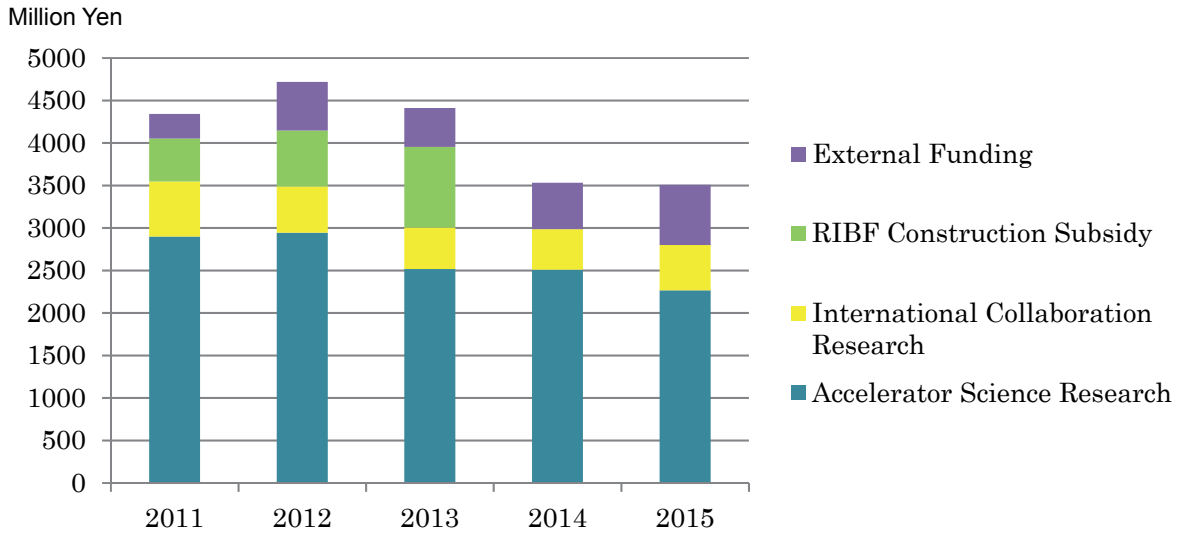

3. Staffing

At the start of FY 2015, April 1 2015, there were 230 personnel affiliated with RNC and 408 researchers visiting RNC for research purpose. The following graphs show a breakdown of personnel into seven categories as of April 2015, and a transition of the number of each category.

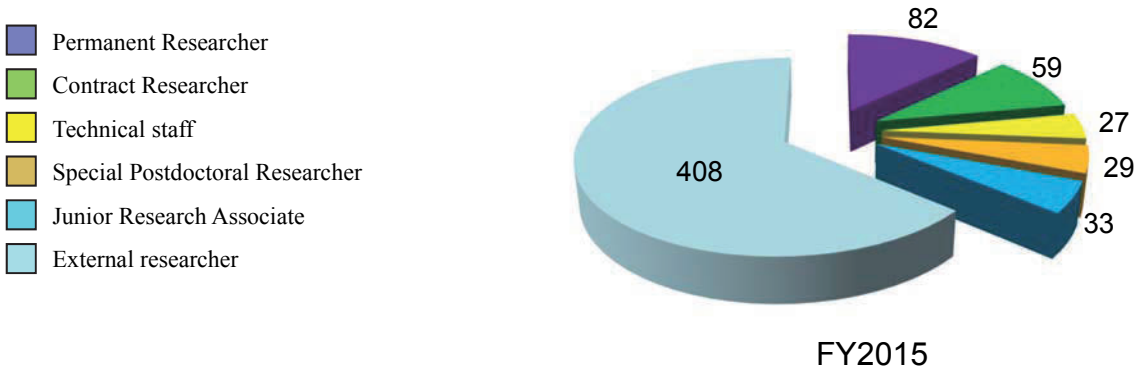

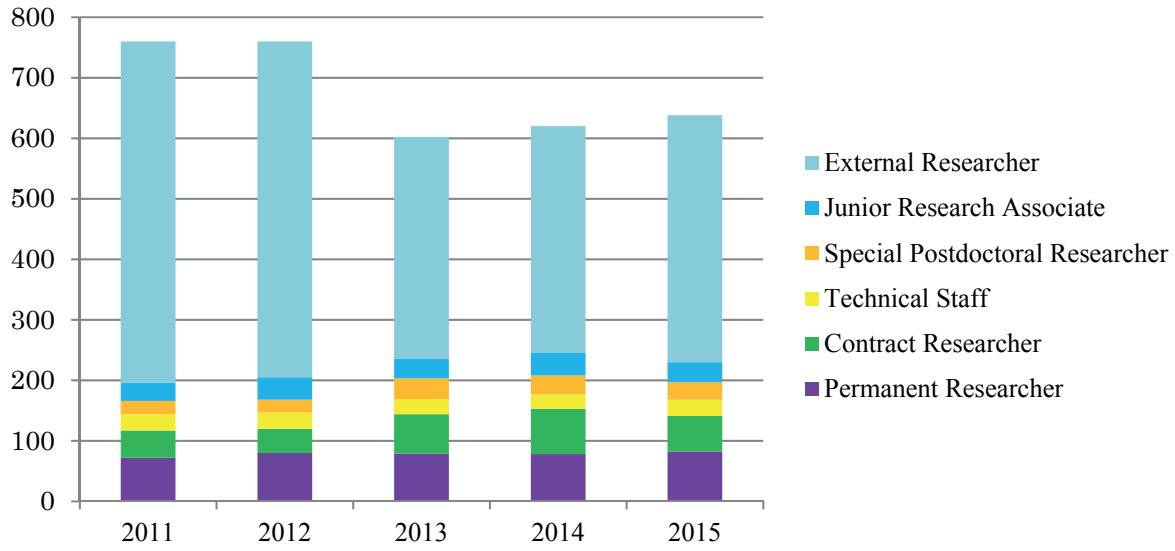

4. Research publication

Publication in the past 10 years

The number of papers published annually from RNC is shown graphically using the data of Thomson Reuiters' Web of Science Documents. The type of documents is "Article" and "Review". Articles from 2013and before, however, include the proceedings of meetings.

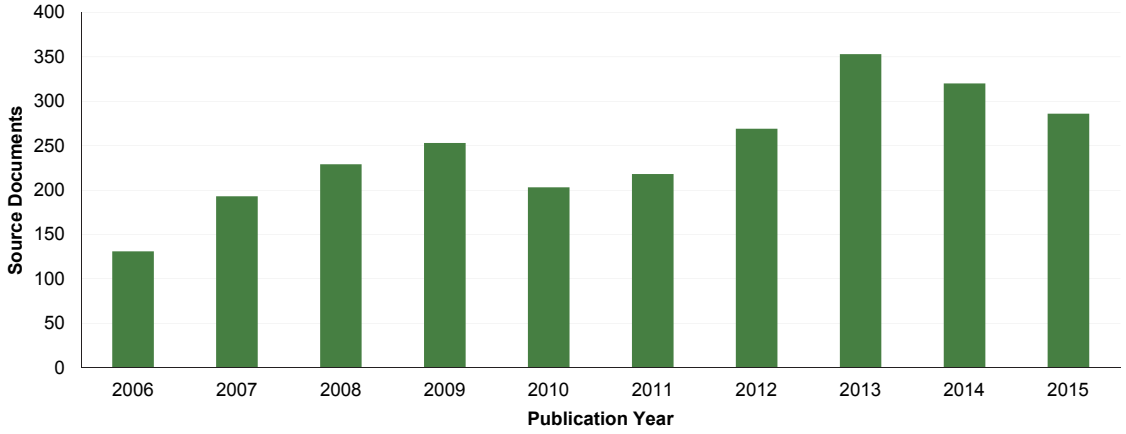

Citation Analysis for past 3 years (2015 data is insufficient due to incomplete citation)

As of June 20, 2016

Indicators \ Year	2013	2014	2015
Total number of papers	353	320	286
Total number of citations	3039	1891	647
Number of papers in top 10%	47	47	37
Percentage of papers in top 10%	13.31	14.69	12.94
Number of papers in top 1%	8	3	2
Percentage of papers in top 1%	2.27	0.94	0.70

5. Management

Headed by the RNC Director Hideto En'yo, the RIKEN Nishina Center for Accelerator-Based Science (RNC) consists of:

9 Laboratories
1 Research unit
9 Groups with 25 Teams
2 overseas research center with 3 Groups

as of the latter half of FY2015. There are also three 'Partner Institutes' which conduct research in the laboratories set up in RNC.

RNC is managed by its Director who takes into consideration the majority decision of the RNC Coordination Committee. The Nishina Center Planning Office under the auspices of President of RIKEN is responsible for administrative matters of RNC.

The management of RNC is supported by the following committees:

Scientific Policy Committee
Program Advisory Committee
Safety Review Committee
RIBF Machine Time Committee
Public Relations Committee

There are also committees to support the President of RIKEN and/or the Director of RNC such as:

Nishina Center Advisory Council with two subcommittees
RBRC Scientific Review Committee (SRC) and
Advisory Committee for the RIKEN-RAL Muon Facility
RBRC Management Steering Committee (MSC)

Nishina Center for Accelerator-based Science

Executive Members (as of March 31, 2016)

Hideto EN'YO	Director RNC; Chief Scientist, Director of Radiation Laboratory
Tetsuo HATSUDA	Deputy Director (Theoretical Research), RNC; Chief Scientist, Director of Quantum Hadron Physics Laboratory
Hiroyoshi SAKURAI	Deputy Director (RIBF Research), RNC; Chief Scientist, Director of Radioactive Isotope Physics Laboratory; Group Director, Nuclear Transmutation Data Research Group
Walter F. HENNING	Senior Advisor
Yasushige YANO	Senior Advisor
Tohru MOTOBAYASHI	Senior Advisor
Minami IMANISHI	Assistant

RNC Coordination Committee

The following subjects relevant to the RNC management are deliberated under the chairmanship of the RNC Director:
Establishment of the new organization or reorganization in RNC
Personnel management of RNC researchers
Research themes and research budget
Approval of the Partner Institutes
Evaluation of the management of RNC and the response to the recommendations by external evaluation
The RNC Coordination Committee is held monthly.

Members (as of March 31, 2016)

Hideto EN'YO	Director, RNC; Chief Scientist, Director of Radiation Laboratory
Hiroyoshi SAKURAI	Deputy Director, RNC; Chief Scientist, Director of Radioactive Isotope Physics Laboratory; Group Director, Nuclear Transmutation Data Research Group
Tetsuo HATSUDA	Deputy Director, RNC; Chief Scientist, Director of Quantum Hadron Physics Laboratory
Walter F. HENNING	Senior Advisor
Yasushige YANO	Senior Advisor
Tohru MOTOBAYASHI	Senior Advisor
Masahiko IWASAKI	Chief Scientist, Director of Advanced Meson Science Laboratory
Tomohiro UESAKA	Chief Scientist, Director of Spin isospin Laboratory
Hideki UENO	Chief Scientist, Director of Nuclear Spectroscopy Laboratory; Deputy Group Director, User Liaison and Industrial Cooperation Group
Toru TAMAGAWA	Associate Chief Scientist, Director of High Energy Astrophysics Laboratory
Takashi NAKATSUKASA	Associate Chief Scientist, Director of Theoretical Nuclear Physics Laboratory
Emiko HIYAMA	Associate Chief Scientist, Director of Strangeness Nuclear Physics Laboratory
Kosuke MORITA	Group Director, Research Group for Superheavy Element; Team Leader, Superheavy Element Production Team
Osamu KAMIGAITO	Group Director, Accelerator Group; Group Director, High-Intensity Accelerator R&D Group
Hideyuki SAKAI	Group Director, User Liaison and Industrial Cooperation Group
Hiroki OKUNO	Deputy Group Director, Accelerator Group; Team Leader, Accelerator R&D Team; Team Leader, Cryogenic Technology Team; Team Leader, High-Power Target R&D Team
Nobuhisa FUKUNISHI	Deputy Group Director, Accelerator Group; Team Leader, Beam Dynamics & Diagnostics Team
Masayuki KASE	Deputy Group Director, Accelerator Group; Team Leader, Infrastructure Management Team
Tomoko ABE	Group Director, Accelerator Applications Research Group; Team Leader, Radiation Biology Team
Yoshitomo UWAMINO	Group Director, Safety Management Group
Toshiyuki KUBO	Group Director, Research Instruments Group; Team Leader, Detector Team
Masanori WAKASUGI	Group Director, Instrumentation Development Group; Team Leader, Rare RI-ring Team; Team Leader, SCRIT Team
Eiji IKEZAWA	Team Leader, RILAC Team
Takashi ICHIHARA	Team Leader, Computing and Network Team
Naruhiko SAKAMOTO	Team Leader, Cyclotron Team; Team Leader, High-Gradient Cavity R&D Team
Hiromi SATO	Team Leader, Detector Team
Takahide NAKAGAWA	Team Leader, Ion Source Team
Hiromitsu HABA	Team Leader, RI Applications Team
Koji MORIMOTO	Team Leader, Superheavy Element Device Development Team
Atsushi YOSHIDA	Team Leader, Industrial Cooperation Team
Koichi YOSHIDA	Team Leader, BigRIPS Team; Team Leader, Slow RI Data Team
Ken-ichiro YONEDA	Team Leader, User Support Office
Michiharu WADA	Team Leader, SLOWRI Team
Hideaki OTSU	Team Leader, SAMURAI Team; Team Leader, Fast RI Data Team

Teiichiro MATSUZAKI	Team Leader, Muon Data Team
Yasuyuki AKIBA	Vice Chief Scientist; Group Leader, Experimental Group, RIKEN BNL Research Center
Katsuhiko ISHIDA	Vice Chief Scientist, Advanced Meson Science Laboratory
Tsukasa TADA	Vice Chief Scientist, Quantum Hadron Physics Laboratory
Yuko MOTIZUKI	Research Unit Leader, Astro-Glaciology Research Unit
Kanenobu TANAKA	Deputy Group Director, Safety Management Group
Noriko SHIOMITSU	Director, Nishina Center Planning Office
Mitsuru KISHIMOTO	Deputy Director, Nishina Center Planning Office

Nishina Center Planning Office

The Nishina Center Planning Office is responsible for the following issues:
- Planning and coordination of RNC's research program and system
- Planning and management of RNC's use ofbudget
- Public relations activities

Members (as of March 31, 2016)

Noriko SHIOMITSU	Director, Head of Nishina Center Planning Office
Mitsuru KISHIMOTO	Deputy Director, Nishina Center Planning Office; Administration Manager, RBRC; Administration Manager, RIKEN Facility Office at RAL
Kazunori MABUCHI	Deputy Manager, Nishina Center Planning Office
Yasutaka AKAI	Administrative Officer of Nishina Center Planning Office; Deputy Administration Manager, RBRC
Yukari ONISHI	Chief, Nishina Center Planning Office
Kumiko SUGITA	Special Administrative Employee
Yuko OKADA	Task-Specific Employee
Yukiko SATO	Task-Specific Employee
Kyoji YAMADA	Special Temporary Employee
Yoshio OKUIZUMI	Temporary Employee
Masatoshi MORIYAMA	Consultant for Advisory Committee, Research Review, etc.
Rie KUWANA	Temporary Staff

Scientific Policy Committee

The Scientific Policy Committee deliberates on the following issues:
- Research measures and policies of RNC
- Administration of research facilities under RNC's management

The Committee members are selected among professionals within and outside RNC. The members were not chosen nor the Committee held in FY2015.

Program Advisory Committee

The Program Advisory Committee reviews experimental proposals submitted by researchers and reports the approval/disapproval of the proposals to the RNC Director. The Committee also reports to the RNC Director the available days of operation at RIBF or the Muon Facility at RAL allocated to researchers.

The Committee is divided into three categories according to the research field.

(1) Nuclear Physics Experiments at RIBF (NP-PAC): academic research in nuclear physics
(2) Materials and Life Science Researches at RNC (ML-PAC): academic research in materials science and life science
(3) Industrial Program Advisory Committee (In-PAC): non-academic research

Program Advisory Committee for Nuclear Physics Experiments at RI Beam Factory (NP-PAC)

The 16th NP-PAC was held on December 3-5, 2015 at RIBF.

Members (as of March 31, 2016)

Bradley. M.SHERRILL (Chair)	Prof., Director, National Superconducting Cyclotron Laboratory, Michigan State University
Andrei ANDREYEV	Prof., The University of York.
Angela BRACCO	Prof., Dipartiment di Fisica, The Istituto Nazionale di Fisica Nucleare
Piet Van Duppen	Prof., Instituut voor Kern- en Stralingsfysica, Departement Natuurkunde en Sterrenkunde, University of Leuven (K.U.Leuven)
Hironori Iwasaki	Associate Prof., National Superconducting Cyclotron Laboratory, Michigan State University
Walter D. LOVELAND	Prof., Department of Chemistry, Oregon State University, USA
Thomas NILSSON	Prof., Department of Fundamental Physics, Chalmers Univ. of Technology
Thomas Rauscher	Department of Physics, University of Basel
Haik Simon	GSI
Olivier Sorlin	GANIL(Grand Accélérateur National d'Ions Lourds)
Yuhu Zhang	Institute of Modern Physics, Chinese Academy of Sciences

Yutaka UTSUNO	Senior Scientist, Advanced Science Research Center, JAEA
Kazuyuki Ogata	Associate Prof., Theoretical Nuclear Physics, Research Center for Nuclear Physics, Osaka University
Atsushi TAMII	Associate Prof., Experimental Nuclear Physics Division, Research Center for Nuclear Physics, Osaka University, Japan
Satoshi N. Nakamura	Prof., Nuclear Experiment Group, Faculty of Science, Tohoku University
Ikuko Hamamoto	Prof. Emeritus, The Lund Univ., Senior Visiting Scientist, RNC

Program Advisory Committee for Materials and Life Science Researches at RIKEN Nishina Center (ML-PAC)

Members (as of March 31, 2016)

Adrian HILLIER (Chair)	ISIS, RAL
Philippe MENDELS	Prof., Laboratorie de Physique des Solides, Universite Paris-SUD
Shukri SULAIMAN	Prof. Universiti Sains Malaysia
Toshiyuki AZUMA	Chief Scientist, Atomic Molecular & Optical Physics Laboratory, RIKEN
Ryosuke KADONO	Prof., Division Head, Muon Science Laboratory, Institute of Materials Structure Science, KEK
Atsushi KAWAMOTO	Prof., Graduate School of Science, Hokkaido University
Kenya KUBO	Prof., Department of Material Science, International Christian University,
Norimichi KOJIMA	Full Time Research Fellow, Toyota Physical and Chemical Research Institute
Atsushi SHINOHARA	Prof., Graduate School of Science, Osaka University
Xu-Guang ZHENG	Prof., Department of Physics Faculty of Science and Engineering, Saga University
Hiroyuki YAMASE	Senior Researcher, National Institute for Materials Science
Shigeo YOSHIDA	Research Consultant, RIKEN Center for Sustainable Resource Science, RIKEN

Industrial Program Advisory Committee (In-PAC)

The 5th In-PAC was held on January 13, 2016 at RNC.

Members (as of March 31, 2016)

Akihiro IWASE (Chair)	Prof., Graduate School of Engineering, Osaka Prefecture University
Toshiyuki AZUMA	Chief Scientist, Atomic, Molecular & Optical Physics Laboratory, RIKEN
Kenya KUBO	Prof., The College of Liberal Arts, International Christian University
Hitoshi NAKAGAWA	Central Research Laboratory, Hamamatsu Photonics K.K.
Nobuhiko NISHIDA	Full Time Research fellow, Toyota Physical and Chemical Research Institute
Toshinori MITSUMOTO	Chief Engineer, Quantum Equipment Division, Sumitomo Heavy Industries, Ltd

Safety Review Committee

The Safety Review Committee is composed of two sub committees, the Safety Review Committee for Accelerator Experiments and the Hot-Lab Safety Review Committee. These Committees review the safety regarding the usage of radiation generating equipment based on the proposal submitted to RNC Director from the spokesperson of the approved experiment.

Safety Review Committee for Accelerator Experiments

Members (as of March 31, 2016)

Takashi KISHIDA (Chair)	Senior Research Scientist, Radioactive Isotope Physics Laboratory
Kouji MORIMOTO	Team Leader, Superheavy Element Device Development Team
Eiji IKEZAWA	Team Leader, RILAC Team
Hiromitsu HABA	Team Leader, RI Applications Team
Shinichiro MICHIMASA	Assistant Prof., Center for Nuclear Study, University of Tokyo
Hidetoshi YAMAGUCHI	Lecturer, Center for Nuclear Study, University of Tokyo
Hiroshi WATANABE	Lecturer, Radioactive Nuclear Beam Group, IPNS, KEK
Hiromi SATO	Team Leader, Detector Team
Atsushi YOSHIDA	Team Leader, Industrial Cooperation Team
Koichi YOSHIDA	Team Leader, BigRIPS Team
Naoki FUKUDA	Nishina Center Research Scientist, BigRIPS Team
Naruhiko SAKAMOTO	Team Leader, Cyclotron Team

Ex officio members

Yoshitomo UWAMINO	Group Director, Safety Management Group
Kanenobu TANAKA	Deputy Group Director, Management Group
Hisao SAKAMOTO	Nishina Center Technical Scientist, Safety Management Group

Hot-Lab Safety Review Committee

Members (as of March 31, 2016)

Masako IZUMI (Chair)	Senior Research Scientist, Radiation Biology Team
Yoshitomo UWAMINO	Group Director, Safety Management Group
Hisao SAKAMOTO	Nishina Center Technical Scientist, Safety Management Group
Hiroki MUKAI	Assigned Employee, Safety Management Group
Kanenobu TANAKA	Deputy Group Director, Safety Management Group
Hiromitsu HABA	Team Leader, RI Applications Team

RIBF Machine Time Committee

Upon request of the RNC Director, the RIBF Machine Time Committee deliberates on the machine time schedule of RIBF, and reports the results to him.

Members (as of March 31, 2016)

Hideyuki SAKAI (Chair)	Group Director, User Liaison and Industrial Cooperation Group
Tomoko ABE	Group Director, Accelerator Applications Research Group
Nobuhisa FUKUNISHI	Deputy Group Director, Accelerator Group
Osamu KAMIGAITO	Group Director, Accelerator Group
Masayuki KASE	Deputy Group Director, Accelerator Group
Toshiyuki KUBO	Group Director, Research Instruments Group
Kouji MORIMOTO	Team Leader, Superheavy Element Research Device Development Team
Hiroki OKUNO	Deputy Group Director, Accelerator Group
Hiroyoshi SAKURAI	Chief Scientist, Radioactive Isotope Physics Laboratory
Hideki UENO	Chief Scientist, Nuclear Spectroscopy Laboratory
Tomohiro UESAKA	Chief Scientist, Spin isospin Laboratory
Yoshitomo UWAMINO	Group Director, Safety Management Group
Masanori WAKASUGI	Group Director, Instrumentation Development Group
Ken-ichiro YONEDA	Team Leader, User Support Office
External members	
Susumu SHIMOURA	Professor, Center for Nuclear Study, University of Tokyo
Hidetoshi YAMAGUCHI	Lecturer, Center for Nuclear Study, University of Tokyo
Hiroari MIYATAKE	Professor, Radioactive Nuclear Beam Group, IPNS, KEK
Observers	
Hideto EN'YO	Director, RNC
Nobuaki IMAI	Chair, RIBF-UEC, Associate Prof. Center for Nuclear Study, University of Tokyo
Hiromitsu HABA	Team Leader, RI Applications Team
Kosuke MORITA	Group Director, Research Group for Superheavy Element
Tohru MOTOBAYASHI	RIBF Synergetic-Use Coordinator
Koichi YOSHIDA	Team Leader, BigRIPS Team; Team Leader, Slow RI Data Team
Kanenobu TANAKA	Deputy Group Director, Safety Management Group
Mitsuru KISHIMOTO	Deputy Director, Nishina Center Planning Office
Hideaki OTSU	Team Leader, Fast RI Data Team

Public Relations Committee

Upon request of the RNC Director, the Public Relations Committee deliberates and coordinates the following matters:
(1) Creating public relations system for theRNC
(2) Prioritization of the public relations activities for the RNC
(3) Other general and important matters concerning the public relations of RNC

Members (as of March 31, 2016)

Hiroshi TSUBOI	Executive Director; Director, Head of Nishina Center Planning Office
Hiroyoshi SAKURAI	Deputy Director, RNC; Chief Scientist, Radioactive Isotope Physics Laboratory
Tetsuo HATSUDA	Deputy Director, RNC; Chief Scientist, Quantum Hadron Physics Laboratory
Tohru MOTOBAYASHI	RIBF synergetic-use coordinator
Walter F. HENNING	Senior Advisor
Yasushige YANO	Senior Advisor
Masahiko IWASAKI	Chief Scientist, Advanced Meson Science Laboratory
Tomohiro UESAKA	Chief Scientist, Spin isospin Laboratory
Hideki UENO	Chief Scientist, Nuclear Spectroscopy Laboratory
Toru TAMAGAWA	Associate Chief Scientist, High Energy Astrophysics Laboratory
Takashi NAKATSUKASA	Associate Chief Scientist, Theoretical Nuclear Physics Laboratory
Emiko HIYAMA	Associate Chief Scientist, Strangeness Nuclear Physics Laboratory
Koji HASHIMOTO	Associate Chief Scientist, Mathematical Physics Laboratory
Kosuke MORITA	Group Director, Research Group for Superheavy Element
Osamu KAMIGAITO	Group Director, Accelerator Group
Hideyuki SAKAI	Group Director, User Liaison and Industrial Cooperation Group

RBRC Management Steering Committee (MSC)

RBRC MSC is set up according to the Memorandum of Understanding between RIKEN and BNL concerning the collaboration on the Spin Physics Program at the Relativistic Heavy Ion Collider (RHIC). The 21st MSC was held on July 17, 2015 at RIBF.

Members (as of March 31, 2016)

Yoichiro MATSUMOTO	Executive Director, RIKEN
Shoji NAGAMIYA	Science Advisor, RIKEN
Hideto EN'YO	Director, RNC
David LISSAUER	Deputy Chair, Physics Department, BNL
Berndt MUELLER	Associate Laboratory Director for Nuclear and Particle Physics, BNL
Satoshi OZAKI	Senior Advisor, BNL

Nishina Center Advisory Council

NCAC 2016 is the forth AC meeting since the establishment of the Nishina Center which promotes all of RIKEN's accelerator based science including the RIKEN BNL Research Center and the RIKEN-RAL Muon Facility. NCAC has two sub-councils for the RBRC and the RAL Muon Facility respectively. The 1st NCAC was held in January, 2009. The 2nd NCAC was held in May, 2011. Thr 3rd NCAC was held in July, 2014.

The mission of NCAC is set by the Terms of Reference presented by President Matsumoto based on the Initiative for Scientific Excellence and the fundamental issues about research activities and research administration. NCAC submits its report to the President of RIKEN, and to the Director of Nishina Center if necessary.

The members of NCAC are recommended by the Director of Nishina Center to the President of RIKEN from among highly knowledgeable individuals and experts worldwide.

Members (as of March 31, 2016)

Sydney GALES (Chair)	Professor Dr., Director of Research IPN Orsay CNRS, Scientific Director, ELI-N
Robert V.F. JANSSENS	Division Director, Physics Division, Argonne National Laboratory (ANL)
Jochen WAMBACH	Professor, ECT* Director
Witold NAZAREWICZ	Professor, Michigan State University
Kinichi IMAI	Professor Emeritus, Kyoto University
Richard G. MILNER	Professor, Department of Physics, MIT
Angella BRACCO	Professor, Università degli Studi di Milano e INFN
Reiner KRÜCKEN	Dr. Deputy Director of TRIUMF
Hirokazu TAMURA	Professor, Department of Physics, Graduate School of Science, Tohoku University
Tokushi SHIBATA	Dr. Adviser, Chiyoda technol corporation Oarai Research Laboratory
Elvezio MORENYONI	Prof.Dr. Paul Scherrer Institut
Yoshitaka ITOW	Professor, Institute for Space-Earth Environmental Research, Nagoya University
Lia MERMINGA	Professor, Associate Lab Director, SLAC National Accelerator Laboratory
Akira YAMAMOTO	Head, Special Professor, HIGH ENERGY ACCELERATOR RESEARCH ORGANIZATION, KEK
Hidenori TAKAGI	Prof. Dr. Max-Planck Institute for Solid State Research

RBRC Scientific Review Committee (SRC)

Members (as of March 31, 2016)

Richard MILNER (Chair)	Prof., Director, Laboratory for Nuclear Science, MIT
Shinya AOKI	Prof., Yukawa Institute for Theoretical Physics, Kyoto University
Alfred MUELLER	Prof., Department of Physics, Columbia University
Albert De ROECK	Prof., LPC Fellow, LHC Physics Center, Fermilab
Xiandong JI	Prof., Department of Physics, University of Maryland
Julia VELKOVSKA	Prof., Department of Physics and Astronomy, Vanderbilt University

Advisory Committee for the RIKEN-RAL Muon Facility

Members (as of March 31, 2016)

Andrew D TAYLOR (Chair)	Executive Director, STFC National Laboratories, UK
Jean-Michel POUTISSOU	Senior research scientist Emeritus, TRIUMF, Canada
Klaus P. JUNGMANN	Prof., University of Groningen, Netherlands
Roberto De RENZI	Prof., Department of Physics and Earth Sciences, University of Parma, Italy
Yasuyuki MATSUDA	Assoc. Prof., Graduate School of Arts and Sciences, the University of Tokyo, Japan
Jun SUGIYAMA	Principal Research Scientist, Toyota Central R&D Labs., INC, Japan

6. International Collaboration

Country	Partner Institute	Objects	RNC contact person
Austria	Stefan Meyer Institute for Subatomic Physics	Experimental and theoretical hadron physics, especially in exotic hadronic atoms and meson and baryon nuclear bound states	Masahiko IWASAKI, Chief Scientist, Director of Advanced Meson Science Laboratory
Belgium	Katholieke Universiteit te Leuven	Framework	Michiharu WADA, Team Leader, SLOWRI Team
Canada	TRIUMF	Accelerator-based Science	Hiroyoshi SAKURAI, Deputy Director, Chief Scientist, Radioactive Isotope Physics Laboratory
China	China Nuclear Physics Society	Creation of the council for China -Japan research collaboration on nuclear physics	Hiroyoshi SAKURAI, Deputy Director, Chief Scientist, Radioactive Isotope Physics Laboratory
	Peking University	Nuclear Science	Hiroyoshi SAKURAI, Deputy Director, Chief Scientist, Radioactive Isotope Physics Laboratory
		Strategic cooperation (Nishina School)	Hiroyoshi SAKURAI, Deputy Director, Chief Scientist, Radioactive Isotope Physics Laboratory
	Shanghai Jiao Tong University	International Joint Graduate School Program	Takashi NAKATSUKASA, Associate chief scientist, Theoretical Nuclear Physics Laboratory
	ZHEJIANG University	International Joint Graduate School Program	Isao WATANABE, Advanced Meson Science Laboratoy
	Institute of Modern Physics, Chinese Academy of Science	Physics of heavy ions	Hiroyoshi SAKURAI, Deputy Director, Chief Scientist, Radioactive Isotope Physics Laboratory
	School of Nuclear Science and Technology, Lanzhou University	Framework	Yue MA, Advanced Meson Science Laboratory
	School of Physics, Nanjing University	Framework	Emiko HIYAMA, Associate chief scientist, Strangeness Nuclear Physics Laboratory
	Department of Physics, Faculty of Science, The Univ. of Hong Kong	Experimental and educational research collaboration in the area of experimental nuclear physics	Hiroyoshi Sakurai, Deputy Director, Chief Scientist, Radioactive Isotope Physics Laboratory
EU	European Gamma-Ray Spectroscopy Pool Owners Committee	The use of Euroball ditector at RIKEN	Shunji NISHIMURA, Radioactive Isotope Physics Laboratory
	European Center for Theoretical Studies in Nuclear Physics and Related Areas (ECT*)	Theoretical physics	Tetsuo HATSUDA, Deputy Director, Chief Scientist, Quantum Hadron Physics Laboratory
	CERN	RD-51:R&D programme for micro-pattern gas detectors (MPGD)	Satoshi YOKKAICHI, Senior Research Scientist, Radiation Laboratory
		Collaboration in the ALICE Experiment as an Associate Member	Satoshi YOKKAICHI, Senior Research Scientist, Radiation Laboratory
		Collaboration in the ALICE Experiment	Satoshi YOKKAICHI, Senior Research Scientist, Radiation Laboratory
Finland	University of Jyvaskyla	Basic nuclear physics and related instrumentation	Michiharu WADA, Team Leader, SLOWRI Team
France	National Institute of Nuclear Physics and Particle Physics (IN2P3)	Physics of heavy ions	Tohru MOTOBAYASHI, RIBF synergetic-use coordinator
	CNRS, CEA,GANIL, Université Paris Sud, etc.	Creation of an International Associated Laboratory (LIA) French-Japanese International Associated Laboratory for Nuclear Structure Problems	Tohru MOTOBAYASHI, RIBF synergetic-use coordinator
	CEA-DSM	The use of MINOS device at RIKEN	Tomohiro UESAKA, Chief Scientist, Spin Isospin Laboratory
	SIMEM Graduate School, Department of Physics, Caen University	Framework	Tomohiro UESAKA, Chief Scientist, Spin Isospin Laboratory
Germany	Technische Universität München	Nuclear physics, hadron physics, nuclear astrophysics	Emiko HIYAMA, Associate chief scientist, Strangeness Nuclear Physics Laboratory
	Max-Planck Gesellschaft	Comprehensive agreement	Hiroyoshi SAKURAI, Deputy Director, Chief Scientist, Radioactive Isotope Physics Laboratory
	GSI	Physics of heavey ions and accelerator	Hiroyoshi SAKURAI, Deputy Director, Chief Scientist, Radioactive Isotope Physics Laboratory
	GSI and Reactions with Relativistic Radioactive Beam Collaboration (R3B)	The use of NeuLAND device at RIBF	Tomohiro Uesaka, Chief Scientist, Spin Isospin Laboratory
	Department of Physics, Technische Universität Darmstadt	Framework	Emiko Hiyama, Associate chief scientist, Strangeness Nuclear Physics Laboratory
Hungary	The Institute of Nuclear Research of the Hungarian Academy of Sciences (ATOMKI)	Nuclear physics, Atomic Physics	Tomohiro UESAKA, Chief Scientist, Spin Isospin Laboratory
Indonesia	ITB, UNPAD, ITS, UGM, UI	Material science using muons at the RIKEN-RAL muon facility	Isao WATANABE, Advanced Meson Science Laboratoy
	Universitas Hasanuddin	Agricultural science and related fields involving heavy-ion beam mutagenesis using Indonesian crops	Tomoko ABE, Group Director, Accelerator Applications Research Group

Country	Partner Institute	Objects	RNC contact person
Italy	National Institute of Nuclear Physics (INFN)	Physics of heavy ions	Tohru MOTOBAYASHI, RIBF synergetic-use coordinator
	Applied Physics Division, National Institute for New Technologies, Energy and Environment (ENEA)	Framework	Tohru MOTOBAYASHI, RIBF synergetic-use coordinator
Korea	Seoul National University	Nishina School	Hiroyoshi SAKURAI, Deputy Director, Chief Scientist, Radioactive Isotope Physics Laboratory
		International Joint Graduate School Program	Itaru NAKAGAWA, Radiation Laboratory
	Institute of Basic Science, Rare Isotope Science Project	Rare ion accelerator and related fields	Hiroyoshi SAKURAI, Shunji NISHIMURA
	Department of Physics, Kyungpook National University	Framework	Tomohiro UESAKA, Chief Scientist, Spin Isospin Laboratory
	College of Natural Sciences of Kyungpook National University	International Joint Graduate School Program	Tomohiro UESAKA, Chief Scientist, Spin Isospin Laboratory
	College of Science, Yonsei University	Framework	Tomohiro UESAKA, Chief Scientist, Spin Isospin Laboratory
	Department of Physics, Yonsei University	International Joint Graduate School Program	Yasuyuki AKIBA, Radiation Laboratory
	Department of Physics, Korea University	Framework	Yuji GOTO, Radiation Laboratory
	College of Natural Science, Ewha Women's University	Framework	Tomohiro UESAKA, Chief Scientist, Spin Isospin Laboratory
	College of Natural Sciences, INHA Univ.	Framework	Emiko Hiyama, Associate chief scientist, Strangeness Nuclear Physics Laboratory
Malaysia	Universiti Sains Malaysia	Muon Science	Isao WATANABE, Advanced Meson Science Laboratoy
Poland	the Henryk Niewodniczanski Institute of Nuclear Physics, Polish Academy of Sciences(IFJ PAN)	Framework	Hiroyoshi SAKURAI, Deputy Director, Chief Scientist, Radioactive Isotope Physics Laboratory
Romania	"Horia Hulubei" National Institute of Physics and Nuclear Engineering Bucharest-Magurele, Romania	Framework	Tomohiro UESAKA, Chief Scientist, Spin Isospin Laboratory
Russia	Joint Institute for Nuclear Research (JINR)	Framework	Tomohiro UESAKA, Chief Scientist, Spin Isospin Laboratory
	Russian Research Center "Kurchatov Institute"	Framework	Hiroyoshi SAKURAI, Tomohiro UESAKA, Osamu KAMIGAITO, Masanori WAKASUGI
Switzerland	Paul Scherrer Institute	Improve the performance and reliability of accelerator systems	Osamu KAMIGAITO, Director, Chief Scientist, Accelerator Group
UK	The Science and Technology Facilities Council	Muon science using the ISIS Facility at the Rutherford Appleton Laboratory	Philip KING, Director of RIKEN-RAL muon facility
	University of Liverpool	International Joint Graduate School Program	Hiroyoshi SAKURAI, Deputy Director, Chief Scientist, Radioactive Isotope Physics Laboratory
USA	BNL	The Spin Physics Program at the Relativistic Heavy Ion Collider(RHIC)	Hideto EN'YO, Director of RNC
	Columbia University	The development of QCDCQ	Taku IZUBUCHI, Group Leader, Computing Group, RBRC
	Michigan State University	Comprehensive The use of TPC(Time Projection Chamber)	Tomohiro Uesaka, Chief Scientist, Spin Isospin Laboratory Hiroyoshi Sakurai, Deputy Director, Chief Scientist, Radioactive Isotope Physics Laboratory & Tadaaki Isobe, Radioactive Isotope Physics Laboratory
Vietnam	Vietnam Atomic Energy Commission	Framework	Tohru MOTOBAYASHI, RIBF synergetic-use coordinator
	Institute for Nuclear Sciences and Technique	Nuclear Physics	Hiroyoshi Sakurai, Deputy Director, Chief Scientist, Radioactive Isotope Physics Laboratory
	Hanoi University of Science	International Joint Graduate School Program	Hiroyoshi SAKURAI, Deputy Director, Chief Scientist, Radioactive Isotope Physics Laboratory
	Institute of Physics, Vietnam Academy of Science and Technology	Framework	Hiroyoshi SAKURAI, Deputy Director, Chief Scientist, Radioactive Isotope Physics Laboratory

7. Awards

Awardee, Laboratory / Team	Award	Organization	Date
Larry McLerran, Theory Group, RBRC	Herman Feshbach Prize in Theoretical Nuclear Physics	American Physical Society	April
Takuya Maeyama, Special Postdoctoral Researcher, Beam Dynamics & Diagnostics Team	JSRC (Japanese Society of Radiation Chemistry) Young Scientist Award	Japanese Society of Radiation Chemistry	May 27
Takuya Maeyama, Special Postdoctoral Researcher, Beam Dynamics & Diagnostics Team	JSRC Young Investigators Travel Award (From ICRR 2015)	Japanese Society of Radiation Chemistry	May 29
Takuya Maeyama (Special Postdoctoral Researcher), Nobuhisa Fukunisi (Team Leader), Kenichi Ishikawa (visiting Scientsit) Beam Dynamics & Diagnostics Team	JRR(Journal of Radiation Research) Award at ICRR 20 15	Japanese Society of Radiation Chemistry	May 29
Tadashi Fujinawa (Research Consultant), Accelerator Group	Hoshino Prize	The Institute of Electrical Installation Engineers of Japan	Jun 5
Stefan Meinel, Computing Group, RBRC	Kenneth G. Wilson Award at the Lattice 2015 conference	RIKEN, Univ. of Tsukuba, Nagoya Univ. etc.	July
Takahide Nakagawa, Team Leader, Ion Source Team	The 11th PASJ Award for Technical Contributions	Particle Accelerator Society of Japan	Aug. 4
Masako Yamada, formerly affiliated with Radiation Laboratory	The 11th PASJ Award for Young Scientists	Particle Accelerator Society of Japan	Aug. 4
T. Motobayashi, Senior Advisor and H. Sakurai, Chief Scientist and Deputy Director of the Nishina Center	The Nishina Memorial Prize 2015	Nishina Memorial Foundation	Dec. 7
T. Motobayashi, Senior Advisor of the Nishina Cente	The Outstanding Referee	The Outstanding Referees Program instituted by APS	Jan. 8
Katsuhiko Ishida, Associate Chief Scientist of the Advanced Meson Science Laboratory and Tutomu Mibe, Visiting Scientist of the Advanced Meson Science Laboratory and the Radiation Laboratory	Nishikawa Prize	The Foundation For High Energy Accelerator Science	Feb. 15
Research Group for Superheavy Element	The certificate of appreciation	Wako-shi	Mar. 4
Yuma Kikuchi, Special Postdoctoral Researcher of the Spin isospin Laboratory	The 10th Young Scientist Award	Physical Society of Japan	Mar. 20
Kosuke Morita, Group Director, Research Group for Superheavey Element	The Japan Academy Prize	The Japan Academy	Apr. 20

8. Brief overview of the RI Beam Factory

Intensity of Primary Beams

Achieved beam intensities (as of March 2016)

^{238}U	49 pnA	(345 MeV/u, Oct. 2015)
^{124}Xe	38 pnA	(345 MeV/u, Jun. 2013)
^{86}Kr	30 pnA	(345 MeV/u, Nov. 2007)
^{78}Kr	486 pnA	(345 MeV/u, May. 2015)
^{70}Zn	123 pnA	(345 MeV/u, Jun. 2014)
^{48}Ca	530 pnA	(345 MeV/u, Nov. 2014)
^{18}O	1,000 pnA	(345 MeV/u, Jun. 2010)
^{14}N	400 pnA	(250 MeV/u, Oct. 2010)
^{4}He	1,000 pnA	(250 MeV/u, Oct. 2009)
d	1,000 pnA	(250 MeV/u, Oct. 2010)
pol. d	120 pnA, P~80%	(250 MeV/u, May. 2015)

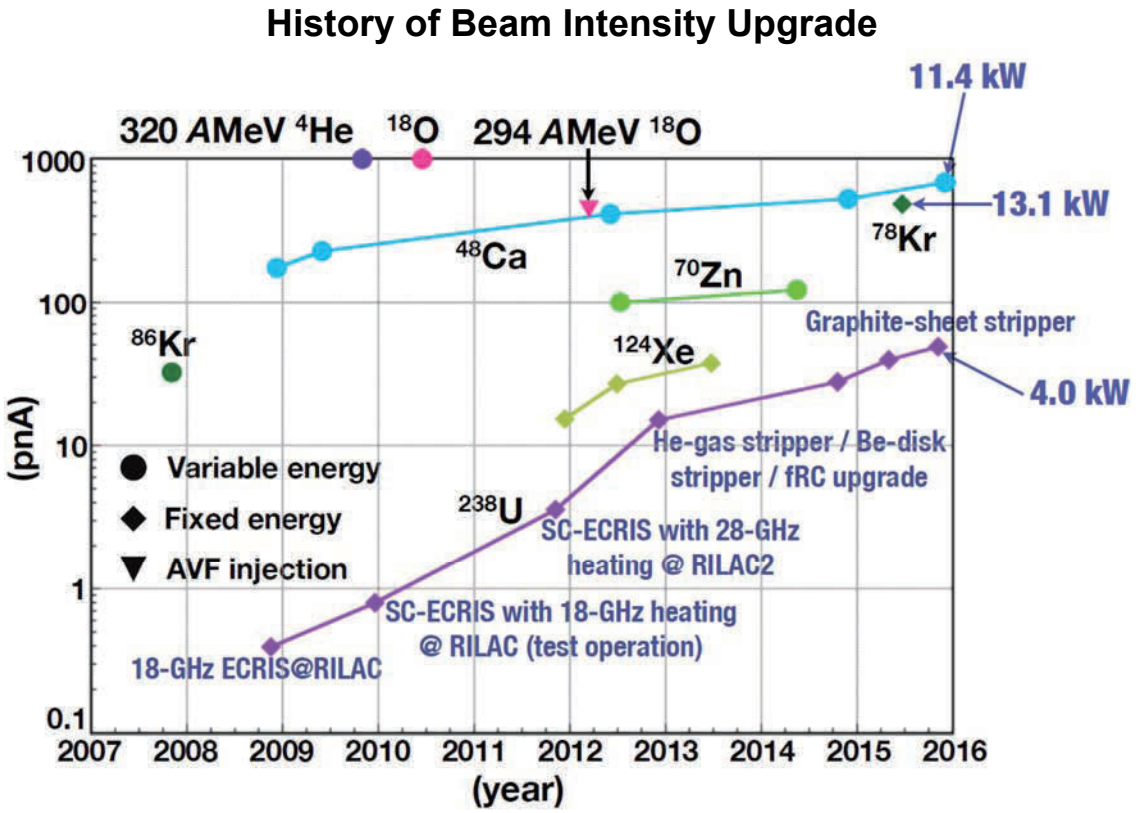

Total beam time for experiments

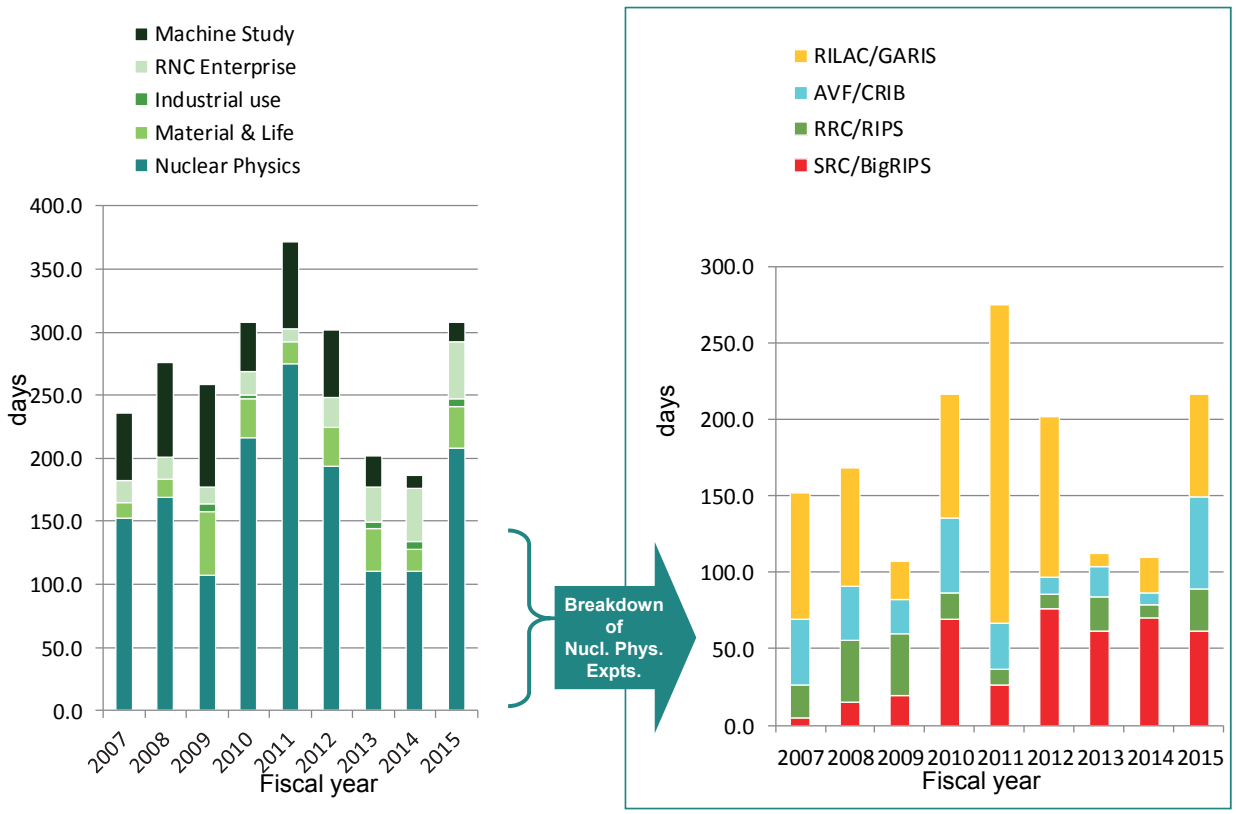

Total beam time allocated to BigRIPS experiments

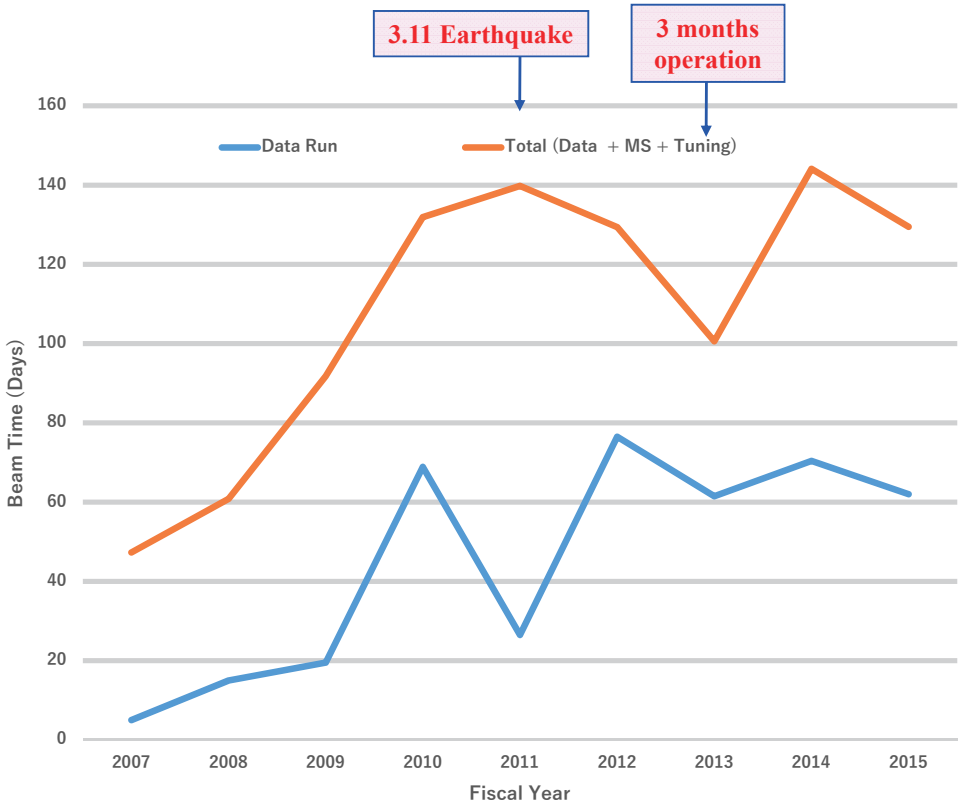

Theoretical Research Division
Quantum Hadron Physics Laboratory

1. Abstract

Atomic nuclei are made of protons and neutrons bound by the exchange of pion and other mesons. Also, protons and neutrons are made of quarks bound by the exchange of gluons. These strong interactions are governed by the non-Abelian gauge theory called the quantum chromodynamics (QCD). On the basis of theoretical and numerical analyses of QCD, we study the interactions between the nucleons, properties of the dense quark matter realized at the center of neutron stars, and properties of the hot quark-gluon plasma realized in the early Universe. Strong correlations common in QCD and cold atoms are also studied theoretically to unravel the universal features of the strongly interacting many-body systems. Developing perturbative and non-perturbative techniques in quantum field theory and string theory are of great importance not only to solve gauge theories such as QED and QCD, but also to find the theories beyond the standard model of elementary particles. Various theoretical approaches along this line have been attempted.

2. Major Research Subjects

(1) Perturbative and non-perturbative methods in quantum field theories
(2) Theory of spontaneous symmetry breaking
(3) Lattice gauge theory
(4) QCD under extreme conditions
(5) Nuclear and atomic many-body problems

3. Summary of Research Activity

(1) Perturbative and non-perturbative methods in quantum field theories

(1-1) 10^{th} order QED calculation and the lepton anomalous magnetic moments

First preliminary value of the tenth-order QED contribution to the electron anomalous magnetic moment $a_e=(g-2)/2$ was reported by us in 2012. Since then, we have been improving and establishing its accuracy: We reevaluated the most difficult and large set of the Feynman diagrams by using advanced techniques of numerical calculation especially suitable to RIKEN's supercomputer. As a result, we have obtained precise values for the eighth- and tenth-order terms. Assuming the validity of the standard model, it leads to the world-best value of the fine-structure constant $\alpha^{-1}(a_e)=137.035\ 999\ 1570(29)(27)(18)(331)$, where uncertainties are from the eighth-order term, tenth-order term, hadronic and electroweak terms, and the experimental measurement of a_e. This is the most precise value of α available at present in the world and provides a stringent constraint on possible theories beyond the standard model.

(1-2) Picard–Lefschetz theory and the sign problem

Understanding strongly-correlated quantum field theories and many-body systems has been one of the ultimate goals in contemporary physics. Exact diagonalization of a Hamiltonian provides us with complete information on the system; however, it usually es the huge computational cost and is limited to small systems. For large systems, numerical simulation on discretized space-time with quantum Monte Carlo method is a powerful ab initio tool based on the importance sampling. In many quantum systems of nterest, however, it suffers from the so-called sign problem; large cancellation occurs between positive and negative quantities to physical signals, so that the computational time grows exponentially with the system size. So far, many attempts have been ed overcome the sign problem, which include the two promising candidates, the complex Langevin method and the etz-thimble method. In particular, the Lefschetz-thimble approach is a generalization of the steepest descent method for multiple ory integrals. In the past few years, we have studied extensively the mathematical basis of the Lefschetz-thimble method as well practical applications to quantum systems such as the real-time path integral for quantum tunneling, zero-dimensional bosonic rmionic models, the one-site Hubbard model, and Polyakov-loop effective models for QCD. We have shown that the interference multiple Lefschetz thimbles is important to reproduce the general non-analytic behavior of the observables as a function of the al parameter. Such an interference is a key to understand the sign problem of finite-density QCD.

unctional renormalization group

BEC-BCS crossover in cold fermionic atoms

We have developed a fermionic functional renormalization group (FRG) and applied this method to describe the superfluid phase transition of the two-component fermionic system with an attractive contact interaction. The connection between the fermionic FRG approach and the conventional Bardeen-Cooper-Schrieffer (BCS) theory with Gorkov and Melik-Barkhudarov (GMB) correction was clarified in the weak coupling region by using the renormalization group flow of the fermionic four-point vertex with particle-particle and particle-hole scatterings. To go beyond the BCS+GMB theory, coupled FRG flow equations of the fermion self-energy and the four-point vertex are studied under an Ansatz concerning their frequency/momentum dependence. We found that the fermion self-energy turns out to be substantial even in the weak coupling regime, and the frequency dependence of the four-point vertex is essential to obtain the correct asymptotic-ultraviolet behavior of the flow for the self-energy. The superfluid transition temperature and the associated chemical potential were evaluated in the region of negative scattering lengths.

Tricritical point of the superconducting transition

The order of the phase transition in the Abelian Higgs model with complex scalar fields became of interest because of the analyses of the spontaneous symmetry breaking due to radiative corrections in 3+1 dimensions, and of a superconductor near the critical point with the dimensionally reduced Ginzburg-Landau theory. Indeed, the fluctuations of the gauge field were of great importance and may even turn the second-order transition to first-order at least for strongly type-I superconductors. We analyzed

the order of the superconducting phase transition via the functional renormalization group approach: We derived for the first time fully analytic expressions for the ß functions of the charge and the self-coupling in the Abelian Higgs model with N-component scalar field in d = 3 dimensions. The result supports the existence of two charged fixed-points: an infrared (IR) stable fixed point describing a second-order phase transition and a tricritical fixed point controlling the region of the parameter space that is attracted by the former one. It was found that the region separating first and second-order transitions can be uniquely characterized by the critical Ginzburg-Landau parameter, $\kappa_c \approx 0.62/\sqrt{2}$ for N=1.

- **Chiral dynamics under strong magnetic field**

  The magnetic field is not only interesting as a theoretical probe to the dynamics of QCD, but also important in cosmology and astrophysics: A class of neutron stars called magnetars has a strong surface magnetic field of order 10^{10} T while the primordial magnetic field in early Universe is estimated to be even as large as ~ 10^{19} T. In non-central heavy-ion collisions at RHIC and LHC, a magnetic field of the strength ~ 10^{15} T perpendicular to the reaction plane could be produced and can have impact on the thermodynamics and transport properties of the quark-gluon plasma. We investigated the quark-meson model in a magnetic field using the functional renormalization group equation beyond the local-potential approximation. We considered anisotropic wave function renormalization for mesons in the effective action, which allows us to investigate how the magnetic field distorts the propagation of neutral mesons. We found that the transverse velocity of mesons decreases with the magnetic field at all temperatures. Also, the constituent quark mass is found to increase with magnetic field, resulting in the crossover temperature that increases monotonically with the magnetic field.

(1-4) Emergent space-time

In quantum field theories, symmetry plays an essential and exceptional role. Focusing on some proper symmetry and delving into its meaning have been proven to be one of the most fruitful strategies. A recent example is the SO(2, 4) symmetry in AdS/CFT correspondence which leads to unexpected connection between gravity and gauge theory defined in different dimensions. We offer another example of quantum field theory where symmetry plays a central role and reveals interesting phenomena: Our focal point is the global conformal symmetry in two dimensional conformal field theory (2d CFT), which is homomorphic to SL(2, R). We have shown that 2d CFT admits a novel quantization which we call dipolar quantization. Usually the study of the quantum field theory starts by defining the space-time where the field is situated. On the other hand, in our case, we first obtain quantum system and then the nature of space-time emerges. This is in accordance with the general ideas of emergent space-time such as those discussed in matrix models.

(2) Theory of spontaneous symmetry breaking

(2-1) Dispersion relations of Nambu-Goldstone modes at finite temperature and density

We clarified the dispersion relations of Nambu-Goldstone (NG) modes associated with spontaneous breaking of internal symmetries at finite temperature and/or density. We showed that the dispersion relations of type-A and type-B NG modes are linear and quadratic in momentum, whose imaginary parts are quadratic and quartic, respectively. In both cases, the real parts of the dispersion relations are larger than the imaginary parts when the momentum is small, so that the NG modes can propagate for long distances. We derived the gap formula for NG modes in the presence of explicit symmetry breaking. We also discussed the gapped partners of type-B NG modes, when type-A and type-B NG modes coexist.

(2-2) Effective field theory for space-time symmetry breaking

We studied the effective field theory for space-time symmetry breaking from the local symmetry point of view. By gauging space-time symmetries, the identification of Nambu-Goldstone (NG) fields and the construction of the effective action were performed based on the breaking pattern of diffeomorphism, local Lorentz, and isotropic Weyl symmetries as well as the internal symmetries including possible central extensions in nonrelativistic systems. Such a local picture provides a correct identification of the physical NG fields, while the standard coset construction based on global symmetry breaking does not. We also revisited the coset construction for space-time symmetry breaking: Based on the relation between the Maurer-Cartan one-form and connections for space-time symmetries, we classified the physical meanings of the inverse Higgs constraints by the coordinate dimension of broken symmetries. Inverse Higgs constraints for space-time symmetries with a higher dimension remove the redundant NG fields, whereas those for dimensionless symmetries can be further classified by the local symmetry breaking pattern.

(2-3) Nambu-Goldstone modes in dissipative systems

Spontaneous symmetry breaking (SSB) in Hamiltonian systems is a universal and widely observed phenomena in nature, e.g., the electroweak and chiral symmetry breakings, superconductors, ferromagnets, solid crystals, and so on. It is also known that the SSB occurs even in dissipative systems such as reaction diffusion system and active matters. The translational symmetry in the reaction diffusion system is spontaneously broken by a spatial pattern formation such as the Turing pattern in biology. The rotational symmetry is spontaneously broken in the active hydrodynamics which describes collective motion of biological organisms. We found that there exist two types of NG modes in dissipative systems corresponding to type-A and type-B NG modes in Hamiltonian systems. By taking the O(N) scalar model obeying a Fokker-Planck equation as an example, we have shown that the type-A NG modes in the dissipative system are diffusive modes, while they are propagating modes in Hamiltonian systems. We pointed out that this difference is caused by the existence of two types of Noether charges, Q^a_R and Q^a_A : Q^a_R are symmetry generators of Hamiltonian systems, which are not generally conserved in dissipative systems. Q^a_A are symmetry generators of dissipative systems described by the Fokker-Planck equation and are conserved. We found that the NG modes are propagating modes if Q^a_R are conserved, while those are diffusive modes if they are not conserved.

(3) Lattice gauge theory

(3-1) Hadron interactions from lattice QCD

One of the most important goals in nuclear physics is to determine baryon-baryon interactions directly from QCD. To achieve this goal, the HAL QCD Collaboration has been developing a novel lattice QCD formulation (HAL QCD method) and performing first-principles numerical simulations. We have calculated the spin-orbit forces for the first time from QCD by the HAL QCD method, and

have observed the attraction in the $^3P_2$ channel related to the P-wave neutron superfluidity in neutron star cores. Our calculation of the N-Ω interaction shows that this system is bound in the $^5S_2$ channel. We have shown that the Ω–Ω interaction in the spin-singlet channel is in the unitary region where the scattering length becomes large. Three-nucleon forces have been calculated for several heavy quark masses. Our lattice calculations was extended to the heavy quark systems, e.g. the exotic tetraquark, T_{cc} and T_{cs}. Properties of the light and medium-heavy nuclei (^{4}He, ^{16}O, ^{40}Ca) have been calculated by combining the nuclear many-body techniques and the nuclear forces obtained from lattice QCD. Also, we have theoretically and numerically shown that the Luscher's method traditionally used in studying the hadron-hadron interactions does not lead to physical results for baryon-baryon interactions unless the lattice volume is unrealistically large, so that the HAL QCD method is the only reliable approach to link QCD to nuclear physics.

As a part of the High Performance Computing Infrastructure (HPCI) Project 5, we have completed the generation of (2+1)-flavor full QCD configurations with a large box, V=(8 fm)^3, and with nearly physical pion mass, 145MeV, on the 10Pflops super computer "K". We are currently in the process of calculations of baryon-baryon interactions using these configurations.

(3-2) Momenta and Angular Momenta of Quarks and Gluons inside the Nucleon

Determining the quark and gluon contributions to the spin of the nucleon is one of the most challenging problems in QCD both experimentally and theoretically. Since the quark spin is found to be small (~ 25% of the total proton spin) from the global analysis of deep inelastic scattering data, it is expected that the rest should come from the gluon spin and the orbital angular momenta of quarks and gluons. We made state-of-the-art calculations (with both connected and disconnected insertions) of the momenta and the angular momenta of quarks and gluons inside the proton. The u and d quark momentum/angular momentum fraction extrapolated to the physical point is found to be 0.64(5)/0.70(5), while the strange quark momentum/angular momentum fraction is 0.024(6)/0.023(7), and that of the gluon is 0.33(6)/0.28(8). This implies that the quark spin carries a fraction of 0.25(12) of the proton spin. Also, we found that the quark orbital angular momentum, which turned out to be dominated by the disconnected insertions, constitutes 0.47(13) of the proton spin.

(4) QCD under extreme conditions

(4-1) Production and Elliptic Flow of Dileptons and Photons in the semi-Quark Gluon Plasma

A notable property of peripheral heavy-ion collisions at RHIC and LHC is the elliptic flow which is a measure of the transfer of initial spatial anisotropy to momentum anisotropy. Both the PHENIX experiment at RHIC and the ALICE experiment at LHC have announced a puzzling observation; a large elliptic flow for photons, comparable to that of hadrons. We considered the thermal production of dileptons and photons at temperatures above the QCD critical temperature (T_c) on the basis of semi-QGP, a theoretical model for describing the quark-gluon plasma (QGP) near T_c. With realistic hydrodynamic simulations, we have shown that the strong suppression of photons in semi-QGP due to the inhibition of colored excitations tends to bias the elliptical flow of photons to that generated in the hadronic phase. This increases the total elliptic flow for thermal photons significantly towards the experimental data.

(4-2) Deriving relativistic hydrodynamics from quantum field theory

Hydrodynamics describes the space-time evolution of conserved quantities, such the energy, the momentum, and the particle number. It does not depend on microscopic details of the system, so that it can be applied to many branches of physics from condensed matter to high-energy physics. One of the illuminating examples is the recent success of relativistic hydrodynamics in describing the evolution of QGP created in heavy-ion collisions. Inspired by the phenomenological success of relativistic hydrodynamics in describing QGP, theoretical derivations of the relativistic hydrodynamics have been attempted on the basis of the kinetic theory, the fluid/gravity correspondence, the non-equilibrium thermodynamics, and the projection operator method. In our study, a most microscopic and non-perturbative derivation of the relativistic hydrodynamics from quantum field theory was given on basis of the density operator with local Gibbs distribution at initial time. Performing the path-integral formulation of the local Gibbs distribution, we derived the generating functional for the non-dissipative hydrodynamics microscopically. Moreover, we formulated a procedure to evaluate dissipative corrections.

(4-3) Hadron-quark crossover in cold and hot neutron stars

We studied bulk properties of cold and hot neutron stars (NS) on the basis of the hadron-quark crossover picture where a smooth transition from the hadronic phase to the quark phase takes place at finite baryon density. By using a phenomenological equation of state (EOS) "CRover" which interpolates the two phases at around 3 times the nuclear matter density (ρ_0), it is found that the cold NSs with the gravitational mass larger than two solar mass can be sustained. This is in sharp contrast to the case of the first-order hadron-quark transition. The radii of the cold NSs with the CRover EOS are in the narrow range (12.5±0.5) km which is insensitive to the NS masses. Due to the stiffening of the EOS induced by the hadron-quark crossover, the central density of the NSs is at most 4 ρ_0 and the hyperon-mixing barely occurs inside the NS core. This constitutes a solution of the long-standing hyperon puzzle first pointed out by Takatsuka et al. The effect of color superconductivity (CSC) on the NS structures was also examined with the hadron-quark crossover picture. For the typical strength of the diquark attraction, a slight softening of the EOS due to two-flavor CSC takes place and the maximum mass is reduced by about 0.2 solar mass. The CRover EOS is generalized to the supernova matter at finite temperature to describe the hot NSs at birth. The hadron-quark crossover was found to decrease the central temperature of the hot NSs under isentropic condition. The gravitational energy release and the spin-up rate during the contraction from the hot NS to the cold NS were also estimated.

(5) Nuclear and atomic many-body problems

(5-1) Giant dipole resonance in hot nuclei

Over the last several decades, extensive experimental and theoretical works have been done on the giant dipole resonance (GDR) in excited nuclei covering a wide range of temperature (T), angular momentum (J) and nuclear mass. A reasonable stability of the GDR centroid energy and an increase of the GDR width with T (in the range ~1–3 MeV) and J are the two well-established results. Some experiments have indicated the saturation of the GDR width at high T: The gradual disappearance of the GDR vibration at much higher T has been observed. Experiments on the Jacobi transition and the GDR built on superdeformed shapes at high rotational frequencies

have been reported in a few cases. We have demonstrated that thermal pairing included in the phonon damping model (PDM) is responsible for the nearly constant width of GDR at low temperature T < 1 MeV. We have also shown that the enhancement observed in the recent experimentally extracted nuclear level densities in ^{104}Pd at low excitation energy and various angular momenta is the first experimental evidence of the pairing reentrance in finite (hot rotating) nuclei. The results of calculations within the PDM were found in excellent agreement with the latest experimental data of GDR in the compound nucleus ^{88}Mo.

(5-2) Hidden pseudospin symmetries and their origins in atomic nuclei

The quasi-degeneracy between single-particle orbitals, (n,l,j=l+1/2) and (n−1,l+2,j=l+3/2), indicates a hidden symmetry in atomic nuclei, the so-called pseudospin symmetry (PSS). Since the introduction of the concept of PSS in atomic nuclei, there have been comprehensive efforts to understand its origin. Both splittings of spin doublets and pseudospin doublets play critical roles in the evolution of magic numbers in exotic nuclei discovered by modern spectroscopic studies with radioactive ion beam facilities. Since the PSS was recognized as a relativistic symmetry in 1990s, many special features, including the spin symmetry (SS) for anti-nucleon, and other new concepts have been introduced. We have published a comprehensive review article (Liang et al., Phys. Rept. 2015) on the PSS and SS in various systems, including extensions of the PSS study from stable to exotic nuclei, from non-confining to confining potentials, from local to non-local potentials, from central to tensor potentials, from bound to resonant states, from nucleon to anti-nucleon spectra, from nucleon to hyperon spectra, and from spherical to deformed nuclei. We also summarized open issues in this field, including the perturbative nature, the supersymmetric representation with similarity renormalization group, and the puzzle of intruder states.

(5-3) Efimov Physics in cold atoms

For ultra-cold atoms and atomic nuclei, the pairwise interaction can be resonant. Then, universal few-body phenomena such as the Efimov effect may take place. We carried out an exploratory study suggesting that the Efimov effect can induce stable many-body ground states whose building blocks are universal clusters. We identified a range of parameters in a mass and density imbalanced two-species fermionic mixture for which the ground state is a gas of Efimov-related universal trimers. An explicit calculation of the trimer-trimer interaction reveals that the trimer phase is an SU(3) Fermi liquid stable against recombination losses. We proposed to experimentally observe this phase in a fermionic mixture of ^{6}Li-^{53}Cr atoms. We have also written a comprehensive review article on theoretical and experimental advances in Efimov physics.

(5-4) Supersymmetric Bose-Fermi mixtures

Some special Bose-Fermi mixtures of cold atoms and molecules in optical lattices could be prepared in such a way as they exhibit approximate supersymmetry under the interchange of bosons and fermions. Since supersymmetry is broken at finite temperature and/or density, an analog of the Nambu-Goldstone excitation, dubbed the “Goldstino”, should appear. We evaluated the spectral properties of the Goldstino in a Bose-Fermi mixture of cold atoms and molecules. We derived model independent results from sum rules obeyed by the spectral function. Also, by carrying out specific calculations with random phase approximation, analytic formula for the dispersion relation of Goldstino at small momentum was obtained.

Members

Chief Scientist (Lab. Head)

Tetsuo HATSUDA (Deputy Director, RNC)

Vice Chief Scientist

Tsukasa TADA

Research & Technical Scientists

Takumi DOI (Senior Research Scientist)
Yoshimasa HIDAKA (Senior Research Scientist)
Pascal Raphaël Gabriel NAIDON (Senior Research Scientist)
Haozhao LIANG (Research Scientist)

Nishina Center Research Scientist

Makiko NIO

Special Postdoctoral Researchers

Kanabu NAWA (– Mar. 31, 2015)
Takashi SANO (– Mar. 31, 2015)
Kazuhiko KAMIKADO (– Mar. 31, 2016)
Noriaki OGAWA (Apr. 1, 2014 –)
Shingo TORII (Apr. 1, 2015 – Mar. 31, 2016)
Hiroshi OKI (Apr. 1, 2015 –)
Toshifumi NOUMI (– Oct. 1, 2015)

Foreign Postdoctoral Researchers

Gergely Peter FEJOES (– Jul.15, 2015)
Vojtech KREJCIRIK (– May 31, 2015)
Di-Lun YANG (Sep. 1, 2015 –)

Postdoctoral Researchers

Yoichi IKEDA (– Mar. 31, 2016)
Shinsuke YOSHIDA (– Mar. 31, 2015)
Koich HATTORI (– Mar. 31, 2016)

Research Consultant

Takeo INAMI (– Sep. 19, 2015)

Junior Research Associate
Masaru HONGO (Univ. of Tokyo, - Mar. 31, 2016)

International Program Associate
Zhaoxi LI (Oct. 1, 2015 – Mar. 31, 2016)
Shihang SHEN (Dec. 1, 2015 –)

Visiting Researcher
Taro KIMURA (JSPS Fellow, Apr. 1, 2015 – May 31, 2015)
Kanako YAMAZAKI (JSPS Fellow, Apr. 1, 2015 – Mar. 31, 2016)
Kei SUZUKI (JSPS Fellow, Apr. 1, 2015 – Mar. 31, 2016)

Senior Visiting Scientist
Koichi YAZAKI (Univ. of Tokyo)

Visiting Scientists
Noriyoshi ISHII (Osaka Univ.)
Yoshitaka HATTA (Kyoto Univ.)
Motoi TACHIBANA (Saga Univ.)
Masashi HAYAKAWA (Nagoya Univ.)
Toichiro KINOSHITA (Cornell Univ.)
Kenji SASAKI (Univ. of Tsukuba)
Shinya AOKI (Kyoto Univ.)
Hiroshi SUZUKI (Kyushu Univ.)
Keiko MURANO (Osaka Univ.)
Daisuke KADOH (KEK)
Yuji HIRONO (Univ. of Tokyo)
Tatsuyuki TAKATSUKA (Iwate Univ.)
Hong MAO (Hangzhou Normal Univ.)
Arata YAMAMOTO (Univ. of Tokyo)
Sho OZAKI (KEK)
Takashi OKA (Univ. of Tokyo)
Keitaro NAGATA (KEK)
Takashi INOUE (Nihon Univ.)
Kazuyuki KANAYA (Univ. of Tsukuba)
Sachiko TAKEUCHI (Japan College of Social Work)
Takayuki MATSUKI (Tokyo Kasei Univ.)
Takumi IRITANI (Kyoto Univ.)
Hiroshi TOKI (Osaka Univ.)
Tetsuo MATSUI (Univ. of Tokyo)
Makoto TAKIZAWA (Showa Pharm. Univ.)
Teiji KUNIHIRO (Kyoto Univ.)
Shoichi SASAKI (Tohoku Univ.)
Tatsumi AOYAMA (Nagoya Univ.)
Atsushi NAKAMURA (Hiroshima Univ.)
Takeo INAMI (Chuo Univ., National Taiwan University)
Koji HASHIMOTO (Osaka Univ.)
Minoru ETO (Yamagata Univ.)
Kanabu NAWA (Univ. of Tokyo)
Gergely FEJOS (Osaka Univ.)
Takashi SANO (AIST)
Shinsuke YOSHIDA (Niigata Univ., Central China Normal University)
Toshifumi NOUMI (The Hong Kong University of Science and Technology)
Shinya GONGYO (Kyoto Univ., CNRS)
Yoichi KAZAMA (Univ. of Tokyo)
Kazuo FUJIKAWA (Nihon Univ.)

Student Trainees
Yasuki TACHIBANA (Univ. of Tokyo)
Tomoya HAYATA (Univ. of Tokyo)
Koichi MURASE (Univ. of Tokyo)
Yuya TANIZAKI (Univ. of Tokyo)
Ryuichi KURITA (Univ. of Tokyo)
Kota MASUDA (Univ. of Tokyo)
Masanori YAMADA (Univ. of Tsukuba)
Terukazu ICHIHARA (Kyoto Univ.)
Yuta KIKUCHI (Kyoto Univ.)
Shoichiro TSUTSUI (Kyoto Univ.)
Takaya MIYAMOTO (Kyoto Univ.)
Shihang SHEN (Peking Univ.)

Part-time Workers
Yuki MINAMI (Oct. 1, 2014 – Mar. 31, 2015)
Yasuki TACHIBANA (– Sep. 18, 2015)
Tomoya HAYATA (– Apr. 30, 2015)
Koichi MURASE (– Oct. 3, 2015)
Kayo YAMAJI

List of Publications & Presentations

Publications
[Journal]
(Original Papers) *Subject to Peer Review

Yoichi Kazama, Shota Komatsu, and Takuya Nishimura, “On the singlet projector and the monodromy relation for psu(2, 2|4) spin chains and reduction to subsectors,” Journal of High Eenergy Physics 1509, 183 (2015).*

Yuya Tanizaki, Yoshimasa Hidaka, Tomoya Hayata, “Lefschetz-thimble analysis of the sign problem in one-site fermion model,” New Journal of Physics 18, 033002 (2016).*

Jean-Paul Blaizot, Yoshimasa Hidaka, Daisuke Satow, “Spectral properties of the Goldstino in supersymmetric Bose-Fermi mixtures,” Physical Review A92, 063629 (2015).*

Yuji Hirono, Yoshimasa Hidaka, “Jarzynski-type equalities in gambling: role of information in capital growth,” Journal of Statistical Physics, 161, 721 (2015).*

Yoshimasa Hidaka, Kazuhiko Kamikado, Takuya Kanazawa, Toshifumi Noumi, “Phonons, Pions and Quasi-Long-Range Order in Spatially Modulated Chiral Condensates,” Physical Review, D92, 034003 (2015).*

Yoshimasa Hidaka, Shu Lin, Robert D. Pisarski, Daisuke Satow, “Dilepton and photon production in the presence of a nontrivial Polyakov loop,” Journal of high energy physics, 10, 005 (2015).*

Tomoya Hayata, Yoshimasa Hidaka, Masaru Hongo, Toshifumi Noumi, “Relativistic hydrodynamics from quantum field theory on the basis of the generalized Gibbs ensemble method,” Physical Review D92, 065008 (2015).*
Yoshimasa Hidaka, Toshifumi Noumi, Gary Shiu, “Effective field theory for spacetime symmetry breaking,” Physical Review D92, 045020 (2015).
C. Gale, Y. Hidaka, S. Jeon, S. Lin, J. -F. Paquet, R.D. Pisarski, D. Satow, V.V. Skokov, G. Vujanovic, “Production and Elliptic Flow of Dileptons and Photons in the semi-Quark Gluon Plasma,” Physical Review Letters 114, 072301 (2015).*
Tomoya Hayata, and Yoshimasa Hidaka, “Dispersion relations of Nambu-Goldstone modes at finite temperature and density” Physical Review D 91, 056006 (2015).*
Ryoji Anzaki, Kenji Fukushima, Yoshimasa Hidaka, and Takashi Oka, “Restricted phase-space approximation in real-time stochastic quantization,” Annals of Physics. 353, 107 (2015).*
T. Kimura, “Linking loops in ABJM and refined theory,” Journal of High Energy Physics 07, 030 (2015).*
T. Kimura and M. Murata, “Transport Process in Multi-Junctions of Quantum Systems,” Journal of High Energy Physics 07, 072 (2015).*
Yuki Iimori and Shingo Torii, “Relation between the Reducibility Structures and between the Master Actions in the Witten Formulation and the Berkovits Formulation of Open Superstring Field Theory,” Journal of High Energy Physics 10 (2015) 127.*
Pascal Naidon, Shimpei Endo, and Antonio M García-García, “Scattering of universal fermionic clusters in the resonating group method,” Journal of Physics B: Atomic, Molecular, and Optical Physics, 49, 034002 (2015).*
Shimpei Endo, Antonio M. García-García, and Pascal Naidon, “Universal clusters as building blocks of stable quantum matter,” Physical Review A 93, 053611 (2015).*
K. Fujikawa, C.H. Oh, K. Umetsu, and Sixia Yu, “Separability criteria with angular and Hilbert-space averages,” Annals of Physics 368 (2016) 248.*
K. Fujikawa, “Yang-Mills theory and fermionic path integrals,” Modern Physics Letters A31 (2016) 1630004.*
K. Fujikawa, “ The gradient flow in λφ^{4} theory ,” Journal of High Energy Physics 03 (2016) 021.*
K. Fujikawa and A. Tureanu, “Neutrino-antineutrino Mass Splitting in the Standard Model: Neutrino Oscillation and Baryogenesis,” Modern Physics Letters A 30, 1530016 (2015).*
K. Fujikawa, Mo-Lin Ge, Yu-Long Liu and Qing Zhao, “Uncertainty principle, Shannon-Nyquist sampling and beyond,” Journal of Physical Society of Japan 84, (2015) 064801.*
K. Suzuki, P. Gubler and M. Oka, “D meson mass increase by restoration of chiral symmetry in in nuclear matter,” Physical Review C 93, 045209 (2016).*
P. Gubler, K. Hattori, S.-H. Lee, M. Oka, S. Ozaki and K. Suzuki, “D mesons in a magnetic field,” Physical Review D 93, 054026 (2016).*
K. Suzuki and T. Yoshida, “Cigar-shaped quarkonia under strong magnetic field,” Physical Review D 93, 051502(R) (2016).*
K. Masuda, T. Hatsuda and T. Takatsuka, “Hadron–quark crossover and hot neutron stars at birth,” Progress of Theoretical and Experimental Physics 2016, no. 2, 021D01 (2016).*
P. Gubler, N. Yamamoto, T. Hatsuda and Y. Nishida, “Single-particle spectral density of the unitary Fermi gas: Novel approach based on the operator product expansion, sum rules and the maximum entropy method,” Annals of Physics 356, 467 (2015).
G. Baym and T. Hatsuda, “Polarization of Direct Photons from Gluon Anisotropy in Ultrarelativistic Heavy Ion Collisions,” Progress of Theoretical and Experimental Physics 2015, no. 3, 031D01 (2015).*
F. Lenz, K. Ohta and K. Yazaki, “Revision of the brick wall method for calculating the blacl hole thermodynamic quantities,” Physical Review D 92, 064018 (2015)*.
G. Fejos, “Functional dependence of axial anomaly via mesonic fluctuations in the three flavor linear sigma model,” Physical Review D 92, 036011(2015).*
K. Fukushima, Y. Tanizaki, “Hamilton dynamics of the Lefschetz thimble integration akin to the complex Langevin method,” Progress of Theoretical and Experimental Physics (2015) 111A01.*
D. Mesterhazy, J. H. Stockemer, Y. Tanizaki, “From quantum to classical dynamics: The relativistic O(N) model in the framework of real-time functional renormalization group,” Physical Review D 92 (2015) 076001.*
Y. Tanizaki, H. Nishimura, K. Kashiwa, “Evading the sign problem in the mean-field approximation through Lefschetz-thimble path integral,” Physical Review D 91 (2015) 101701.*
Y. Tachibana and T. Hirano, “Interplay between Mach cone and radial expansion and its signal in gamma-jet events,” Physical Review C 93, 054907 (2016) .*
N. Ishibashi, T. Tada, “Infinite circumference limit of conformal field theory,” Journal of Physics A: Mathematical and Theoretical 48 (2015) 315402.*
K. Fukushima, K. Hattori, H.-U. Yee, and Y. Yin, “Heavy Quark Diffusion in Strong Magnetic Fields at Weak Coupling and Implication to Elliptic Flow,” Physical Review D 93 (2016) 074028. *
K. Hattori, T. Kojo, and N. Su, “Mesons in strong magnetic fields: (I) General analyses,” Nuclear Physics A951 (2016) 1-30. *
K. Hattori, K. Itakura, S. Ozaki, and S. Yasui, “QCD Kondo effect: quark matter with heavy-flavor impurities,” Physical Review D 92 (2015) 065003. *
S. Ozaki, T. Arai, K. Hattori, and K. Itakura, “Euler-Heisenberg-Weiss action for QCD+QED,” Physical. Review D 92 (2015) 1, 016002. *
S. Cho, K. Hattori, S. H. Lee, K. Morita, and S. Ozaki, “Charmonium Spectroscopy in Strong Magnetic Fields by QCD Sum Rules: S-Wave Ground States,” Physical Review D 91 (2015) 045025. *
Yoshitaka Hatta, Bo-Wen Xiao, and Di-Lun Yang, “Non-boost-invariant solution of relativistic hydrodynamics in 1+3 dimensions,” Physical Review D 93, 016012, (2016).*
Shi Pu and Di-Lun Yang, “Transverse flow induced by inhomogeneous magnetic fields in the Bjorken expansion,” Physical Review D 93, 054042, (2016).*
S. Ohnishi, Y. Ikeda, T. Hyodo and W. Weise, “Structure of the $\Lambda(1405)$ and the $K^- d \to \pi \Sigma n$ reaction,” Physical Review C 93, no. 2, 025207 (2016).*
K. Sasaki, S. Aoki, T. Doi, T. Hatsuda, Y. Ikeda, T. Inoue, N. Ishii and K. Murano (HAL QCD Collaboration), “Coupled channel approach to strangeness S = -2 baryon-baryon interactions in Lattice QCD,” Progress of Theoretical and Experimental Physics 2015, 113B01 (2015).*
M. Yamada, K. Sasaki, S. Aoki, T. Doi, T. Hatsuda, Y. Ikeda, T. Inoue, N. Ishii, K. Murano and H. Nemura (HAL QCD Collaboration),
“Omega-Omega interaction from 2+1 flavor lattice QCD,” Progress of Theoretical and Experimental Physics 2015, 071B01 (2015).*

T. Inoue, S. Aoki, B. Charron, T. Doi, T. Hatsuda, Y. Ikeda, N. Ishii, K. Murano, H. Nemura and K. Sasaki (HAL QCD Collaboration), "Medium-Heavy Nuclei from Nucleon-Nucleon Interactions in Lattice QCD," Physical Review C 91, 011001(R) (2015).*

M. Deka, T. Doi, Y.-B. Yang, B. Chakraborty, S.-J. Dong, T. Draper, M. Glatzmaier, M. Gong, H.-W. Lin, K.-F. Liu, D. Mankame, N. Mathur and T. Streuer (chiQCD Collaboration), "Lattice Study of Quark and Glue Momenta and Angular Momenta in the Nucleon," Physical Review D 91,014505(2015).*

Yuki Nakaguchi, Noriaki Ogawa, Tomonori Ugajin,"Holographic Entanglement and Causal Shadow in Time-Dependent Janus Black Hole," Journal of High Energy Physics, 1507 (2015) 080.*

Koji Hashimoto, Noriaki Ogawa, Yasuhiro Nakaguchi, "Holographic Heavy Quark Symmetry," Journal of High Energy Physics, 1506 (2015) 040.*

Y. Tanimura, K. Hagino, and H.Z. Liang, "Three-dimensional mesh calculations for covariant density functional theory", Progress of Theoretical and Experimental Physics 2015, 073D01 (2015).*

D.-Y. Cheng, X. Liu, and T. Matsuki, "Prediction of charmoniumlike structures in the hidden-charm di-eta decays of higher charmonia," Journal of Physics G: Nuclear Particle Physics 42, 015002 (2015).*

D.-Y. Cheng, X. Liu, and T. Matsuki, "Hidden charm decays of *X*(3915) and *Z*(3930) as the P-wave charmonia, " Progress of Theoretical and Experimental Physiscs 2015 043B05 (2015).*

Qing-Tao Song, Dian-Yong Chen, Xiang Liu, and T. Matsuki, "*D*_{s1}^*(2860) and *D*_{s3}^*(2860): Candidates for *1D* charmed-strange mesons, " European Physical Journal *C* 75, 30 (2015).*

Bo Wang, Cheng-Qun Pang, Xiang Liu, and T. Matsuki, "Pseudotensor meson family," Physical Review D91,014025 (2015).*

D.-Y. Cheng, X. Liu, and T. Matsuki, "Observation of e^+e^- → χ_{c0}ω and missing higher charmonium ψ(4S), " Physical Review D91, 094023 (2015).*

Qin-Tao Song, Dian-Yong Chen, Xiang Liu, and T. Matsuki, "Charmed-strange mesons revisited: mass spectra and strong decays," Physical Review D 91, 054031 (2015).*

Kan Chen, Cheng-Qun Pang, Xiang Liu, and T. Matsuki, "Light axial vector mesons," Physical Review D 91, 074025 (2015).*

Qin-Tao Song, Dian-Yong Chen, Xiang Liu, and T. Matsuki, "Higher radial and orbital excitations in the charmed meson family," Physical Review D 92, 074011-1-16 (2015).*

Cheng-Qun Pang, Bo Wang, Xiang Liu, and T. Matsuki, "High-spin mesons below 3 GeV," Physical Review D 92, 014012-1-16 (2015).*

(Review)

Haozhao Liang, Jie Meng, Shan-Gui Zhou, "Hidden pseudospin and spin symmetries and their origins in atomic nuclei", Phys. Rept. 570 (2015)*

K. Masuda, T. Hatsuda and T. Takatsuka, "Hyperon Puzzle, Hadron-Quark Crossover and Massive Neutron Stars," European Physical Journal A52 (2016) 65 *

D. R. Chakrabarty , N. Dinh Dang, V. M. Datar, "Giant dipole resonance in hot rotating nuclei," The European Physical Journal A52 (2016) 143*

[Proceedings]

(Original Papers) *Subject to Peer Review

K. Suzuki, P. Gubler and M. Oka, "D meson properties in nuclear medium from QCD sum rules," to appear in Proceedings of 12th international conference on Hypernuclear and Strange Particle Physics(HYP2015), Tohoku University, Sendai, September 7-12, 2015.

Y. Tanizaki, H. Nishimura, K. Kashiwa, "Lefschetz-thimble path integral for solving the mean-field sign problem," Proceedings of Science (LATTICE 2015) 282 (2015), 33rd International Symposium on Lattice Field Theory (LATTICE 2015), July 14-18, 2015, Kobe International Conference Center, Kobe.

K. Hattori, L. McLerran, B. Schenke, "Geometrical scaling of jet fragmentation photons,," to appear in Nuclear Physics A, proceedings of 25th International conference on ultrarelativistic nucleus-nucleus collisions, Quark Matter 2015 (QM2015), Kobe Fashion Mart, Kobe, Japan, September 27-October 3, 2015.*

K. Hattori, K. Itakura, "Photon and dilepton spectra from nonlinear QED effects in supercritical magnetic fields induced by heavy-ion collisions," to appear in Nuclear Physics B Proceedings Supplement, proceedings of 7th International conference on Hard and Electromagnetic Probes of High-energy Nuclear Collisions (Hard Probes 2015), McGill University, Montreal, Canada, June 29-July3, 2015.*

M. Kitazawa, M. Asakawa, T. Hatsuda, T. Iritani, E. Itou and H. Suzuki, "Thermodynamics and reference scale of SU(3) gauge theory from gradient flow on fine lattices," 33rd International Symposium on Lattice Field Theory (Lattice 2015), Kobe, Japan, July 14-18, 2015.

T. Amagasa, S. Aoki, Y. Aoki, T. Aoyama, T. Doi, K. Fukumura, N. Ishii, K.-I. Ishikawa, H. Jitsumoto, H. Kamano, Y. Konno, H. Matsufuru, Y. Mikami, K. Miura, M. Sato, S. Takeda, O. Tatebe, H. Togawa, A. Ukawa, N. Ukita, Y. Watanabe, T. Yamazaki and T. Yoshie, "Sharing lattice QCD data over a widely distributed file system," 21st International Conference on Computing in High Energy and Nuclear Physics (CHEP2015) April 13–17, 2015, Okinawa, Japan, Journal of Physics: Conference Series, 664, 042058 (2015).*

Y. Tanimura, K. Hagino, and H.Z. Liang, "Three-dimensional mesh calculations for covariant density functional theory", in NUCLEAR STRUCTURE AND DYNAMICS '15 (Proceedings of NSD15, Portoroz, Slovenia, 14-19 June 2015), AIP Conference Proceedings 1681, 030008 (2015).*

T. Matsuki, Dian-Yong Chen, and Xiang Liu, "Charged charmonium-like structures and the initial single chiral particle emission mechanism, " AIP Conference Proceedings 1701, 050010 (2016), XIth Quark Confinement and the Hadron Spectrum held at St. Petersburg, Russia, September 8-12, 2014, arXiv:1502.03906.

T. Matsuki, D.-Y. Cheng, and X. Liu, "The Initial Single Chiral Particle Emission Mechanism and the Predictions of Charged Charmonium-like Structures," Acta Physica Polonica Supplement 8, 153-158 (2015).

[Book]

(Original Papers) *Subject to Peer Review

J.Y. Guo, H.Z. Liang, J. Meng, and S.G. Zhou, "Chapter 6: Relativistic symmetries in nuclear single-particle spectra", in Relativistic Density Functional for Nuclear Structure, edited by J. Meng (International Review of Nuclear Physics: Volume 10), World Scientific, 2016, pages 219-262.*

[Others]

風間洋一(訳), ヤン　チェン・ニン（著）「マックスウェル方程式とゲージ理論の概念的起源」,パリティ　2015 年 9 月号，30(9),13-21.

風間洋一，書評「超ひも理論をパパに習ってみた」,数理科学　2015 年 9 月号，53(9),60.
風間洋一，「弦理論は原理論か」,パリティ　2015 年 11 月号，30(11),6-13.
日高義将,「南部-ゴールドストンの定理の半世紀ぶりの一般化」，パリティ　2016 年 4 月号，31(4),19-25.
仁尾真紀子，「電磁気学と場の理論」，数理科学　2016 年 3 月号, 54(3), 14-19.

Oral Presentations

[International Conference etc.]

Yoichi Kazama, “Cognate structure at weak and strong coupling for three-point functions,” Invited lecture,エトヴェシ大学，ブダペスト，October 21, 2016.

Yoichi Kazama, “AdS/CFT and Integraibility: Cognate structure at weak and strong coupling for three-point functions,” Invited talk, NCTS(National Center for Theoretical Sciences) Annual theory meeting, National Tsing Hua University, Hsinchu, Taiwan, December 11, 2015.

K. Fujikawa, ”Quadratic divergences and naturalness,” invited talk, Conference on new physics at the Large Hadron Collider, March 4, 2016, Singapore.

K. Fujikawa, ”Lorentz invariant CPT breaking,” invited talk, Memorial meeting for Abdus Salam's 90th birthday, January 25, 2016, Singapore.

K. Fujikawa, ”Yang-Mills theory and path integrals,” invited talk, 60 years of Yang-Mills gauge field theories, May 27, 2015, Singapore.

Gergely Fejos, “Chiral symmetry restoration with functional renormalization group methods,” Theory Seminar, Wigner Research Centre, Budapest, Hungary, January 9, 2015.

Gergely Fejos, “Functional renormalization group method in quantum field theory and its applications in strongly coupled systems,” Theory Seminar, RCNP, Osaka University, Toyonaka, February 2, 2015.

Yoshimasa Hidaka, “Symmetry breaking and gapless excitations,” Topological Science Kick-off Symposium 2016, Keio University, 14-15 Mar. 2016.

Yoshimasa Hidaka, “Phonons, pions and quasi-long-range order in spatially modulated chiral condensates,” Molecule-type workshop on “Selected topics in the physics of the Quark-Gluon Plasma and Ultrarelativistic Heavy Ion Collisions,” YITP, September 14-26, 2015.

Yoshimasa Hidaka, “Magnetic Catalysis vs. Magnetic Inhibition,” QCD Chirality Workshop 2015, University of California, Los Angeles, USA, January 21-23, 2015.

K. Suzuki, P. Gubler and M. Oka, “*D* meson properties in nuclear medium from QCD sum rules,” 12th International Conference on Hypernuclear and Strange Particle Physics (HYP2015), Tohoku University, Sendai, September 7-12, 2015.

Pascal Naidon, “What determines the Efimov three-body parameter?” Invited talk, the International Workshop on Critical Stability in Few-Body Systems, RIKEN, Wako, January 26, 2015.

Pascal Naidon, “Scattering of universal fermionic clusters,” Selected Presentation at the 21st International Conference on Few-Body Problems in Physics, , Chicago, Illinois, USA, May 18, 2015.

Pascal Naidon, “Scattering of universal fermionic clusters,” Invited Presentation at the International Workshop on Critical Stability in Few-Body Systems, February 4, 2016, RIKEN, Wako, Japan.

Pascal Naidon, “Scattering of universal fermionic clusters,” Invited Presentation at the International Workshop on Critical Stability in Few-Body Systems, February 4, 2016, RIKEN, Wako, Japan.

Y. Tanizaki, Y. Hidaka, T. Hayata, “Lefschetz-thimble and complex Langevin approaches to Silver Blaze of one-site Hubbard model,” KEK Theory Workshop December 1-5, 2015, KEK, Tsukuba, Japan.

Y. Tanizaki, H. Nishimura, K. Kashiwa, “Lefschetz-thimble path integral for solving the mean-field sign problem,” 33rd International Symposium on Lattice Field Theory (LATTICE 2015), July 14-18, 2015, Kobe International Conference Center, Kobe, Japan.

Y. Tachibana, “Jet medium interactions,” invited talk, 6th Asian Triangle Heavy Ion Conference(ATHIC 2016), New Delhi, India, Feburary 19, 2016.*

Y. Tachibana and T. Hirano, “Interplay between Mach cone and radial expansion in jet events,” 25th International conference on ultrarelativistic nucleus-nucleus collisions, Quark Matter 2015 (QM 2015), Kobe Fashion Mart, Kobe, Japan, September 27-October 3, 2015.*

Y. Tachibana and T. Hirano, “Hydrodynamic excitation by jets in the expanding QGP,” Hard Probes 2015, McGill University, Montréal, June 30, 2015.*

Tsukasa Tada, “Dipolar quantization and the Hilbert space structure,” KEK Theory workshop 2015 December 1-5, 2015, KEK, Tsukuba, Japan.

T. Hatsuda, “Lattice QCD approach to nuclear physics,” invited lecture at ECT* doctoral training program on Computational Nuclear Physics - Hadrons, Nuclei and Dense Matter, Trento, Italy, April 13 - May 22 (2015).

T. Hatsuda, “QCD Spectral Functions,” invited talk, ECT* workshop on New perspectives on Photons and Dileptons in Ultrarelativistic Heavy-Ion Collisions at RHIC and LHC, Trento, Italy, Nov. 30 - Dec. 11 (2015).

Tatsumi Aoyama, “Numerical evaluation of QED contribution to lepton g-2,” plenary talk, 33rd International Symposium on Lattice Field Theory (LATTICE 2015), July 14-18, 2015, Kobe International Conference Center, Kobe, Japan.

K. Hattori, L. McLerran, B. Schenke, “Jet fragmentation photons in ultrarelativistic heavy-ion collisions,” 25th International conference on ultrarelativistic nucleus-nucleus collisions, Quark Matter 2015(QM2015), Kobe Fashion Mart, Kobe, Japan, September 27-October 3, 2015.*

K. Hattori, K. Itakura, “Photon and dilepton spectra from nonlinear QED effects in supercritical magnetic fields induced by heavy-ion collisions,” 7th International conference on Hard and Electromagnetic Probes of High-energy Nuclear Collisions (Hard Probes 2015), Montreal, Canada.*

K. Hattori, “Nonlinear QED effects on photon and dilepton spectra in supercritical magnetic fields,” New perspectives on Photons and Dileptons in Ultrarelativistic Heavy-Ion Collisions at RHIC and LHC, ECT*, Dec. 9, 2015.

K. Hattori, “Charmonium spectroscopy in strong magnetic fields by QCD sum rules,” Hadrons and Hadron Interactions in QCD -- Effective theories and Lattice --} (HHIQCD2015), YITP, Kyoto Univ., Mar. 10, 2015.

K. Hattori, “Photon propagation in strong magnetic fields,” QCD Chirality Workshop 2015, UCLA, Jan. 21-23, 2015.

Di-Lun Yang, “Two novel analytic solutions in relativistic hydrodynamics and magneto-hydrodynamics”, ITP seminar, Vienna University of technology, March 10, 2016, Vienna, Austria.

Di-Lun Yang, “Collective flow of photons in strongly coupled gauge theories”, Nuclear physics colloquium, ITP Goethe University Frankfurt am Main, March 3rd, 2016, Frankfurt, Germany.

K. Kamikado ,“Phase diagram of the U(2) x U(2) scalar model in three dimension” , 33rd International Symposium on Lattice Field Theory (LATTICE 2015), July 14-18, 2015, Kobe International Conference Center, Kobe, Japan.

T. Noumi, “Effective Field Theory for Spacetime Symmetry Breaking,” Gordon Research Conference “String Theory and Cosmology,” Hong Kong University of Science and Technology, Hong Kong, May 31- June 5 2015.

Y. Ikeda, “Status of Lattice QCD Simulations for Normal and Exotic Hadrons," Plenary invited talk, 12th International Conference on Low Energy Antiproton Physics(LEAP2016), March 6-11, 2016, Kanazawa-Kagekiza, Kanazawa, Japan.

Y. Ikeda, “Search for Tetraquarks from lattice QCD simulation," Invited talk, International Workshop on ``Critical Stability in Few-Body Systems,"

Feb. 1-5, 2016, RIKEN, Wako, Saitama, Japan.

Y. Ikeda, “Lattice QCD study of $Z_c(3900)$," Plenary invited talk, the 31st Reimei WorkShop on Hadron Physics in Extreme Conditions at J-PARC,

Jan. 18-20, 2016, JAEA, Tokai, Ibaraki, Japan.

Y. Ikeda, “Structure of $Z_c(3900)$ from coupled-channel scattering on the lattice,” Symposium on “Quarks to Universe in Computational Science (QUCS 2015),” November 4-8, 2015, Nara Kasugano International Forum, Nara, Japan.

Y. Ikeda, “Structure of $Z_c(3900)$ from lattice QCD," Plenary invited talk, Frontiers in hadron and nuclear physics with strangeness and charm, October 19 - 23, 2015, ECT*, Trento, Italy.

Y. Ikeda, “$Z_c(3900)$$ from coupled-channel HAL QCD approach on the lattice,” Invited talk, 33rd International Symposium on Lattice Field Theory (Lattice2015), July 14-18, 2015, Kobe International Conference Center, Kobe, Japan.

Y. Ikeda, “On the structure of $Z_c(3900)$ from lattice QCD,” Invited talk, 10th International Workshop on the Physics of Excited Nucleons (NSTAR2015), May 25-28, 2015, Osaka University, Suita, Japan.

M. Nio, “Status of QED contributions to lepton g-2,” g-2/EDM 10th collaboration meeting, J-PARC, Toukai, June 25, 2015.

T. Doi, for HAL QCD Collaboration, “Baryon Interactions from Lattice QCD with physical masses,” Invited talk, “The 31st Reimei Workshop on Hadron Physics in Extreme Conditions at J-PARC,” J-PARC, Tokai, Japan, Feb. 17-21, 2015.

T. Doi, for HAL QCD Collaboration, “Nuclear Physics from Lattice QCD,” Invited Talk, “Symposium on Quarks to Universe in Computational Science (QUCS 2015),” Nara Kasugano International Forum IRAKA, Nara, Japan, 4-8 Nov. 2015.

T. Doi, for chiQCD Collaboration, “A Lattice Study of Quark and Glue Momenta and Angular Momenta in the Nucleon,” Invited Talk, “The 10th Circum-Pan-Pacific Spin Symposium on High Energy Spin Physics (Pacific Spin 2015),”

Academia Sinica, Taipei, Taiwan, 5-8 October 2015.

T. Doi, for HAL QCD Collaboration, “Towards lattice QCD baryon forces at the physical point: First results,” “The 12th International Conference on Hypernuclear and Strange Particle Physics (HYP2015),” Tohoku University, Sendai, September 7-12, 2015.

T. Doi, for HAL QCD Collaboration, “First results of baryon interactions from lattice QCD with physical masses (1) -- General overview and two-nucleon forces --,” “The 33rd International Symposium on Lattice Field Theory (Lattice 2015),” Kobe, Japan, July 14-18, 2015.

T. Doi, for HAL QCD Collaboration, “Three-Nucleon Forces from Lattice QCD,” “Hadrons and Hadron Interactions in QCD – Effective theories and Lattice – (HHIQCD2015),” Yukawa Institute for Theoretical Physics (YITP), Kyoto, Japan, Feburary15-March 21 2015.

T. Doi, for HAL QCD Collaboration, “HAL QCD method for hadron interactions on the lattice,” Invited Talk, “Multi-Hadron and Nonlocal Matrix Elements in Lattice QCD (MNME 2015),” BNL, Upton, USA, February 5-6, 2015.

M. Hongo and Y. Hidaka, “Chiral-magnetohydorynamics from quantum field theory,” 13th international eXtreme QCD conference (eXtreme QCD 2015), Central China Normal University, Wuhan, September 21-23, 2015.

Noriaki Ogawa, “Physical Approach to Fish Retinal Cone Mosaic,” RIKEN-NCBS Joint Meeting for Theoretical Biology, RIKEN, Wako, April 7-10, 2015.

Noriaki Ogawa, “Physical Modeling for Development of Fish Retinal Patterns,” YITP Long-Term Workshop on Non-equilibrium Physics, Yukawa Institute for Theoretical Physics(YITP), Kyoto, July 24, 2015.

Noriaki Ogawa, Tetsuo Hatsuda, Atsushi Mochizuki, Masashi Tachikawa, “Theoretical Analysis of Fish Retinal Cone Mosaic Formation,” 5th China-Japan-Korea Colloquium on Mathematical Biology & 25th Annual Meeting of Japan Society of Mathematical Biology, Doshisha University, Kyoto, August 26-29, 2015.

Noriaki Ogawa, “Nambu and Living World: Symmetry Breaking and Pattern Selection in Cellular Mosaic Formation,” Osaka CTSR - Kavli IPMU - RKEN iTHES International Workshop “Nambu and Science Frontier,” Osaka University, Toyonaka, November 17, 2015.

Di-Lun Yang,“Collective flow of photons in strongly coupled gauge theories”, YITP Nuclear Theory seminar, Kyoto University, November 19, 2015, Kyoto, Japan.

Di-Lun Yang, “Two novel analytic solutions in relativistic hydrodynamics and magneto-hydrodynamics”, H-ken colloquium, Nagoya University, March 28, 2016, Nagoya, Japan.

H.Z. Liang, Lecture: “Relativistic symmetries in atomic nuclei”, Lectures on Covariant Density Functional Theory in Nuclear Physics, Jan 21-25, 2016, Changchun, China.

H.Z. Liang, Invited talk: “Towards the self-consistent and relativistic study of spin-isospin excitations in deformed nuclei”, SKLTP-BLTP Joint Workshop on Physics of Strong Interaction, Oct 29-Nov 3, 2015, Guilin, China.

H.Z. Liang, “Localized form of Fock terms in nuclear covariant density functional theory”, YITP long-term workshop: Computational Advances in Nuclear and Hadron Physics, Sep 21-Oct 30, 2015, Kyoto, Japan.

H.Z. Liang, Invited talk: “Towards the self-consistent and relativistic study of spin-isospin excitations in deformed nuclei”, The 5th Conference: Collective Motion in Nuclei under Extreme Conditions, Sep 14-18, 2015, Krakow, Poland.

H.Z. Liang, Invited lecture: “Covariant density functional theory and nuclear spin-isospin excitations”, The 14th CNS International Summer School, Aug 26-Sep 1, 2015, Wako, Japan.

H.Z. Liang, Invited talk: “Hidden pseudospin and spin symmetries in nuclei”, NORDITA Workshop “Chiral Bands in Nuclei”, Apr 20-22, 2015, Stockholm, Sweden.

[Domestic Conference]

日高義将,「自発的対称性と南部ゴールドストーンモード」, 理研研究会『これからの弦理論橋本研 closing 研究会～』, 大河内ホール, 理研, 和光, 2015 年 2 月 21-22 日.

服部恒一，板倉数記，「高強度磁場がひきおこす光子の分裂」，日本物理学会第 70 回年次大会，早稲田大学，東京, 2015 年 3 月 21-24 日.
日高義将，早田智也，本郷優，南佑樹，野海俊文,「相対論的流体の有効ラグランジアンと自発的対称性の破れ」,日本物理学会第 70 回年次大会，早稲田大学，東京, 2015 年 3 月 21-24 日.
日高義将，「QGP の基礎的性質概観（粘性など）」 チュートリアル研究会「重イオン衝突の物理 : 基礎から最先端まで」，理研，和光, 2015 年 3 月 25-27 日.
日高義将，「自発的対称性の破れと南部ゴールドストーンモード」，第 43 回北陸信越地区素粒子論グループ合宿研究会，国立妙高青少年自然の家，2015 年 5 月 15-17 日.
日高義将，集中講義「有限温度・有限密度の場の量子論 : 基礎から最近の話題まで」 千葉大学, 2016 年 3 月 8-9 日.
日高義将，集中講義「平衡系，非平衡系における場の量子論」，中央大学, 2016 年 1 月 6-8 日.
日高義将，「有限温度・有限密度の場の量子論: 基礎から応用まで」，三者若手夏の学校，ホテルたつき，蒲郡，2015 年 8 月 17 日-22 日.
日高義将，「南部ゴールドストンの定理とその発展」，シンポジウム講演，日本物理学会 第 71 回年次大会，東北学院大学，仙台，2016 年 3 月 19-22 日.
板倉数記，服部恒一，「強磁場中の光子が示す複屈折に対する媒質効果」，日本物理学会第 70 回年次大会，早稲田大学，東京，2015 年 3 月 21-24 日.
安井繁宏，服部恒一，板倉数記，尾崎翔，「低温高密度クォーク物質における近藤効果」，日本物理学会第 70 回年次大会，早稲田大学，東京, 2015 年 3 月 21-24 日.
上門和彦，“First and second order phase transitions in the U(2)xU(2) chiral model,”三者若手夏の学校，ホテルたつき，蒲郡，2015 年 8 月 17 日-22 日.
上門和彦, “Phonons, Pions and Quasi-Long-Range Order in Spatially Modulated Chiral Condensates,”研究会「熱場の量子論とその応用」，京都大学基礎物理学研究所，京都市，2015 年 8 月 31 日−9 月 2 日.

Theoretical Research Division
Theoretical Nuclear Physics Laboratory

1. Abstract

Nuclei are finite many-particle systems composed of protons and neutrons. They are self-bound in femto-scale (10^{-15}m) by the strong interaction (nuclear force) whose study was pioneered by Hideki Yukawa. Uncommon properties of the nuclear force (repulsive core, spin-isospin dependence, tensor force, etc.) prevent complete microscopic studies of nuclear structure. There exist number of unsolved problems even at present. In addition, radioactive beam facilities reveal novel aspects of unstable nuclei. We are tackling these old problems and new issues in theoretical nuclear physics, developing new models and pursuing large-scale calculations of quantum many-body systems. We are also strongly involved in research on other quantum many-body systems, to resolve mysteries in the quantum physics.

2. Major Research Subjects

(1) Nuclear structure and quantum reaction theories
(2) First-principle calculations with the density functional theory for many Fermion systems
(3) Computational nuclear physics

3. Summary of Research Activity

(1) Microscopic determination of nuclear reaction path and inertial mass

Nuclear reaction at low energy is described by the quantum scattering theory. However, when many nucleons are involved in the reaction processes, the full treatment becomes impractical. In this case, it is very useful to find the optimal collective coordinate to describe the reaction. Based on the time-dependent density-functional theory, we can achieve this by solving a set of equations, the moving mean-field equation and the moving RPA equation, which we derived previously using a theory of large amplitude collective motion. This requires complicated coding and large computational resources. We have developed a computer program based on the three-dimensional real-space representation and applied this to reaction of light nuclei, such as ^{8}Be and ^{16}O. We have succeeded to derive the fission path of ^{8}Be into two alpha particles. At the same time, the inertial mass parameter for this reaction is microscopically determined. It turns out that the collective inertial mass is equal to the reduced mass in a asymptotic region and increases near the touching region of two alpha's.

(2) Energy density functional approaches to superheavy nuclei

We have performed a systematic calculation for superheavy nuclei using the energy density functional methods. A purpose of this study is to quantify the theoretical uncertainty of the energy density functional methods. Comparing the results with known experimental data, we have found nice agreement. However, in unknown territories of the superheavy nuclei, we do not know the predictive power of the method. To quantify the uncertainty, we use many different kinds of modern energy density functionals and compare the results to each other. Surprisingly, the results agree with each other in open-shell region where the nuclei are well deformed. On the other hand, in the semi-magic and the transitional regions, the predicted values are scattered. Most probably, this is associated with missing correlations, such as shape fluctuation effects, and indicates necessity of further extension of the model.

(3) Energy and mass number dependence of total reaction cross sections of nuclei

We have systematically analyzed nuclear reaction data that are sensitive to nuclear size, namely, proton-nucleus total reaction cross sections and differential elastic cross sections, using a phenomenological black-sphere approximation of nuclei that we are developing. In this framework, the radius of the black sphere is found to be a useful length scale that simultaneously accounts for the observed proton-nucleus total reaction cross section and first diffraction peak in the proton elastic differential cross section. This framework is expected to be applicable to any kind of projectile that is strongly attenuated in the nucleus. On the basis of a cross-section formula constructed within this framework, we find that a less familiar $A^{1/6}$ dependence plays a crucial role in describing the energy dependence of proton-nucleus total reaction cross sections

(4) Deformed nuclei in the black-sphere approximation of nuclei

In order to access the information of nuclear equation of state, such as the value of L, we have studied total reaction cross sections by focusing on the empirical data of the interaction cross section measured at ~900 MeV per nucleon, as a first step. Since the data of Ne and Mg isotopes have already been obtained with the energy of ~240 MeV per nucleon at the RI Beam Factory of RIKEN, systematic analyses are indispensable. For the analyses, we adopt the black-sphere approximation of nuclei. Since we have to face the nuclear deformation in this region of nuclei, we change the black sphere into a spheroid of the same volume in order to take into account nuclear deformation. So far, we have obtained the results showing rather small effect from nuclear deformation. This study is now in progress.

(5) Giant Dipole Resonance built on hot rotating nuclei produced during evaporation of light particles from Mo-88 compound nucleus

We succeeded to show that the phonon damping model (PDM by Dang & Arima 1998), which was extended to finite angular momentum in 2012, describes very well the most recent data of the giant dipole resonance (GDR) built on hot rotating nuclei produced during evaporation of light particles from ^{88}Mo compound nucleus by the experimentalists in Krakow and Milano.

(6) Reentrance phenomenon of superfluid pairing in hot rotating nuclei

We applied the FTBCS1 theory (proposed and developed by Dang and Hung in 2008) at finite temperature and angular momentum to study the pairing phenomenon and level density in ^{104}Pd, of which an enhancement of level density at low excitation energy and high angular momentum has been experimentally observed by the experimentalists at BARC (Mumbai). The quantitative agreement between experiment and theory suggests that this enhancement is indeed the first experimental evidence of the reentrance of superfluid pairing in a finite nucleus.

(7) Effects of thermal shape fluctuations and pairing fluctuations on the giant dipole resonance in warm nuclei

We presented the complete formalism based on the microscopic - macroscopic approach for determining the deformation energies and a macroscopic approach which links the deformation to GDR observables. We discussed our results for the nuclei ^{97}Tc, ^{120}Sn, ^{179}Au, and ^{208}Pb, and corroborate with the experimental data available. We showed that the thermal-shape fluctuation model could explain the data successfully at low temperature only with a proper treatment of pairing and its fluctuations.

(8) Experimental investigation on the temperature dependence of the nuclear level density parameter

In collaboration with the experimentalists at the VECC (Kolkata), who studied the effect of temperature T and angular momentum J on the inverse level density parameter k by populating the compound nucleus ^{97}Tc in the reaction ^{4}He + ^{93}Nb at four incident beam energies of 28, 35, 42, and 50 MeV, we compared the T dependence of k for two angular momentum windows with different theoretical predictions as well as with the results of calculations within the FTBCS1. We found that the experimental data are in good agreement with the theoretical calculations at higher J but deviate from all the calculations at lower J.

(9) Review of three-decay study of giant dipole vibration in hot rotating nuclei

In collaboration with D. Chakrabarty and V. Datar, we have written and submitted to The European Physical Journal A – Hadrons and Nuclei an invited review article, entitled “Giant dipole vibration in hot rotating nuclei". The review has been accepted for publication and is now in production.

(10) Gauge symmetry in the large-amplitude collective motion of superfluid nuclei

The adiabatic self-consistent collective coordinate (ASCC) method is a practical method for describing the large-amplitude collective motion in atomic nuclei with superfluidity and an advanced version of the adiabatic time-dependent Hartree-Fock-Bogoliubov theory. We investigate the gauge symmetry in the ASCC method on the basis of the Dirac-Bergmann theory of constrained systems. We have shown that the gauge symmetry in the ASCC method originates from the constraint on the particle number in the collective Hamiltonian, and that it is partially broken by the adiabatic expansion. The validity of the adiabatic expansion under the general gauge transformation is also confirmed.

Members

Associate Chief Scientist (Lab. Head)

Takashi NAKATSUKASA

Research & Technical Scientist

Akihisa KOHAMA (Senior Research Scientist)
Haozhao LIANG (concurrent: Quantum Hadron Physics Laboratory, Jul.1, 2015 –)

Nishina Center Research Scientist

Dang Dinh NGUYEN

Special Postdoctoral Researchers

Kohei WASHIYAMA (– Mar. 31, 2015)
Koichi SATO

Foreign Postdoctoral Researcher

Haozhao LIANG (– Mar. 31, 2015)

Research Consultants

Akitsu IKEDA
Kenichi MATSUYANAGI

Visiting Scientists

Kazuhiro OYAMATSU (Aichi Shukutoku Univ.)
Kei IIDA (Kochi Univ.)
Yasuyuki SUZUKI (Niigata Univ.)
Hung Quang NGUYEN (Tan Tao Univ.)
Kazuyuki OGATA (Osaka Univ.)
Takashi ABE (Univ. of Tokyo)
Naoyuki ITAGAKI (Kyoto Univ.)
Kazuko TANABE (Otsuma Women's Univ.)
Kaori KAKI (Shizuoka Univ.)

Student Trainees

Rhine Kumar Arayakkandi Keechiprath
(Indian Inst. of Tech. Roorkee)

Part-time Workers

Kiyomi ARAI
Noriko OKAYASU
Tsuneyo SUZUKI
Miki KANOU
Mie DOI (Oct. 1, 2014 –)
Naomi MURAKAMI (Jan. 1, 2015 – Mar. 31, 2015)
Shiduka ASANO (Oct. 5, 2015 –)

List of Publications & Presentations

Publications

[Journal]

(Original Papers) *Subject to Peer Review

S. Yoon, F. Dalfovo, T. Nakatsukasa, and G. Watanabe, "Multiple period states of the superfluid Fermi gas in an optical lattice", New J. Phys.18 (2016) 023011 (10 pages).

K. Wen, K. Washiyama, F. Ni, and T. Nakatsukasa, "Time-dependent density functional studies of nuclear quantum dynamics in large amplitudes", Acta Physica Polonica B Proceedings Supplement 8 (2015) 637-644.

S. E. Agbemava, A. V. Afanasjev, T. Nakatsukasa, and P. Ring, "Covariant density functional theory: Reexamining the structure of superheavy nuclei", Phys. Rev. C 92 (2015) 054310 (21 pages).

K. Matsuyanagi, M. Matsuo, T. Nakatsukasa, K. Yoshida, N. Hinohara, K. Sato, "Microscopic derivation of the quadrupole collective Hamiltonian for shape coexistence/mixing dynamics", J. Phys. G 43 (2016) 24006 (20 pages).

N. Quang Hung, N. Dinh Dang, B.K. Agrawal, V.M. Datar, A. Mitra, and D. R. Chakrabarty, *Pairing reentrance in warm rotating 104-Pd nucleus*, Acta Physica Polonica B - Proceedings Supplement 8 (2015) 551.

N. Quang Hung, N. Dinh Dang, B.K. Agrawal, V.M. Datar, A. Mitra, and D. R. Chakrabarty, *Reentrance phenomenon of superfluid pairing in hot rotating nuclei*, J. Phys.: Conference Series 627 (2015) 012006.

M. Ciemala, M. Kmiecik, A. Maj, V.L. Kravchuk, S. Barlini, G. Casini, F. Gramegna, F. Camera, A. Corsi, L. Bardelli, M. Bini, P. Bednarczyk, B. Fornal, M. Krzysiek, M. Matejska-Minda, K. Mazurek, W. Meczynski, S. Myalski, J. Styczen, B. Szpak, B. Wasilewska, M. Zieblinski, M. Cinausero, T. Marchi, V. Rizzi, G. Prete, M. Degerlier, G. Benzoni, N. Blasi, A. Bracco, S. Brambilla, F. Crespi, S. Leoni, B. Million, O. Wieland, D. Montanari, R. Nicolini, A. Giaz, G. Baiocco, M. Bruno, M. D'Agostino, L. Morelli, M. Chiari, A. Nannini, G. Pasquali, S. Piantelli, S. Valdre, A. Chbihi, J.P. Wieleczko, I. Mazumdar, O. J. Roberts, J. Dudek, N. Dinh Dang, *Giant Dipole Resonance built on hot rotating nuclei produced during evaporation of light particles from Mo-88 compound nucleus*, Phys. Rev. C 91 (2015) 0454313.

B. Dey, D. Pandit, S. Bhattacharya, K. Banerjee, N. Quang Hung, N. Dinh Dang, D. Mondal, S. Mukhopadhyay, S. Pal, A. De, S. R. Banerjee, *Experimental investigation on the temperature dependence of the nuclear level density parameter*, Phys. Rev. C 91 (2015) 044326.

A.K. Rhine Kumar, P. Arumugam, and N. Dinh Dang, *Effects of thermal shape fluctuations and pairing fluctuations on the giant dipole resonance in warm nuclei*, Phys. Rev. C 91 (2015) 044305.

N. Dinh Dang, Thermal pairing and giant dipole resonance in highly excited nuclei, J. Phys.: Conf. Series 580 (2015) 012050.

K. Sato, “Gauge symmetry in the large-amplitude collective motion of superfluid nuclei”, Progress of Theoretical and Experimental Physics (2015) 123D01.

(Review)

K. Matsuyanagi, M. Matsuo, T. Nakatsukasa, K. Yoshida, N. Hinohara, and K. Sato, "Microscopic derivation of the quadrupole collective Hamiltonian for shape coexistence/mixing dynamics", Journal of Physics G: Nuclear and Particle Physics 43, 024006 (2016).

[Proceedings]

(Original Papers) *Subject to Peer Review

S. Ebata and T. Nakatsukasa, "Repulsive aspects of pairing correlation in nuclear fusion reaction", JPS Conf. Proc. 6 (2015) 020056 (6 pages).

W. Horiuchi, T. Inakura, T. Nakatsukasa, and Y. Suzuki, "Systematic analysis of total reaction cross sections of unstable nuclei with Glauber theory", JPS Conf. Proc. 6 (2015) 030079 (4 pages).

K. Sato, J. Dobaczewski, T. Nakatsukasa, W. Satula,"Mean-Field Calculation Based on Proton-Neutron Mixed Energy Density Functionals", Proceedings of the Conference on Advances in Radioactive Isotope Science (ARIS2014), Tokyo, Jun. 1-6, 2014, JPS Conference Proceedings 6, 020051 (2015).*

A. Makinaga, S. Ebata, M. Aikawa, N. Furutachi, D. Ichinkholoo, K. Kato, M. Odsuren, V. Devi, N. Otuka, A. Kohama, H. Otsu, and H. Sakurai, “Compilation of Nuclear Reaction Data from RIBF”, Proceedings of the Conference on Advances in Radioactive Isotope Science (ARIS2014), Tokyo, Jun. 1-6, 2014, JPS Conference Proceedings 6, 030135 (2015).

[Book]

(Original Papers) *Subject to Peer Review

海老原充、他多数（中務孝）、朝倉書店、放射化学の事典、2015.

Oral Presentations

[International Conference etc.]

T. Nakatsukasa, "Recent activities in the time-dependent density-fucntional theory", 9th Japan-China Joint Nuclear Physics Symposium (JCNP2015)", November 7-12, 2015, RCNP（大阪府茨木市）.

T. Nakatsukasa, "Isospin invariant energy density functional and its applications", 2015 SKLTP-BLTP Joing Workshop on Physics of Strong Interaction, October 29-November 3, 2015, Guilin, China.

T. Nakatsukasa, "TDDFT studies of nuclear quantum dynamics in small and large amplitudes", XXII Nuclear Physics Workshop “Marie & Pierre Curie”, September 22-27, 2015, Kazimierz-Dolny, Poland.

T. Nakatsukasa, "Problems associated with the symmetry breaking", Progress in and beyond Theoretical Nuclear Physics Laboratory, RIKEN Wako Campus, Wako, Saitama, March 28th, 2016.

A. Kohama, "Systematic studies of total reaction cross sections", Progress in and beyond Theoretical Nuclear Physics Laboratory, RIKEN Wako Campus, Wako, Saitama, March 28th, 2016.

N. Dinh Dang, *Pairing reentrance in hot rotating nuclei*, invited lecture at the XXII Nuclear Physics Workshop “Marie & Pierre Curie”, September 22 – 27, 2015, Kazimierz Dolny, Poland.

N. Dinh Dang, *Effect of thermal fluctuations in the pairing field on the width of giant dipole resonance*, invited lecture at the 5th International conference on “*Collective Motion in Nuclei Under Extreme Conditions*” (COMEX5), September 14 – 18, 2015, Krakow, Poland.

K. Sato, "Proton-neutron mixed density functional calculation with isospin breaking interaction", 2nd International Workshop & 12th RIBF Discussion on Neutron-Proton Correlations. The University of Hong Kong, Jul. 6-9, 2015.

[Domestic Conference]

中務孝、「原子核構造における自発的対称性の破れ」、日本物理学会年会シンポジウム、2016.3.19-22、東北学院大学（宮城県仙台市）.
Kai Wen, 中務孝、「8Be の崩壊経路と集団質量」、日本物理学会年会、2016.3.19-22、東北学院大学（宮城県仙台市）.
佐藤弘一,「超流動原子核の大振幅集団運動におけるゲージ対称性」『日本物理学会第 71 回年次大会』、東北学院大学、2016 年 3 月
佐藤弘一,「Gauge symmetry in the large-amplitude collective motion of superfluid nuclei」『理研セミナー』、理化学研究所初田量子ハドロン物理学研究室、2016 年 2 月.
佐藤弘一, Jacek Dobaczewski、中務孝、Wojciech Satula,「Isospin breaking term を入れた陽子-中性子混合密度汎関数計算 II」『日本物理学会 2015 年秋季大会』、大阪市立大学、2015 年 9 月.
Koichi Sato, “Gauge symmetry in the large-amplitude collective motion of superfluid nuclei”,『Workshop on many-body correlations in microscopic nuclear model』 尖閣荘(新潟県佐渡市), 2015 年 8 月.

Posters Presentations

[Domestic Conference]

佐藤俊輔, 飯田圭, 小濱洋央, 親松和浩,「反応断面積から探る核構造の質量数依存性」『日本物理学会第 71 回年次大会』学部学生ポスターセッション（合同）、東北学院大学、2016 年 3 月.

Theoretical Research Division
Strangeness Nuclear Physics Laboratory

1. Abstract

We proposed accurate calculation method called 'Gaussian Expansion Method using infinitesimally shifted Gaussian lobe basis function'. When one proceeds to four-body systems, calculation of the Hamiltonian matrix elements becomes much laborious. In order to make the four-body calculation tractable even for complicated interactions, the infinitesimally-shifted Gaussian lobe basis function has been proposed. The GEM with the technique of infinitesimally-shifted Gaussians has been applied to various three-, four- and five-body calculations in hypernuclei, the four-nucleon systems, and cold-atom systems. As results, we succeeded in extracting new understandings in various fields.

2. Major Research Subjects

(1) Hypernuclear structure from the view point of few-body problem
(2) Structure of exotic hadron system
(3) Baryon-baryon interaction based on lattice QCD
(4) Structure of three- and four-body ^{4}He atom systems

3. Summary of Research Activity

(1) Recently, we observed of neutron-rich system nnΛ as a bound state. To investigate this system, we performed nnΛ+Nn Σ three-body coupled channel calculation. Using YN interaction to reproduce observed binding energies for $^4_\Lambda$H, $^4_\Lambda$He, and $^3_\Lambda$H, we do not find any bound state for nnΛ system which is inconsistent with the data. Now, we propose the experimentalists to perform a search experiment of nnΛ system again.
(2) It is interesting to study the structure of Ar isotope, since we have some superdeformed states (SD) in this Isotope. Within the framework of AMD method, we investigate the structure of SD states. In addition, we study the structure of Ar Λ hypernuclei. Then, we found that Λ-separation energy was dependent on the degree of deformation of core nuclei.
(3) Using several realistic 4He atomic potential, we calculate Efimov spectra of trimer and tetramer systems of 4He. Our result shows an extension of the universality in Efimov trimers that the appearance of the repulsive barrier at the three-body hyperradius $R_3 \approx 2\ W_{rvd}$ makes the critical scattering lengths independent of the short-range details of the interactions as reported in the literature and also in the present work for the 4He trimer with the realistic potentials.

Members

Associate Chief Scientist (Lab. Head)
Emiko HIYAMA

Research Scientists
Hiroya SUNO (Research Scientist, concurrent : Strangeness Nuclear Physics Laboratory, Main: Field Theory Research Team)

Contract Researcher
Yasuro FUNAKI
Hyun-Chul KIM (Jan. 4, 2016 – Feb. 20, 2016)

Special Postdoctoral Researcher
Masahiro ISAKA

Postdoctoral Researcher
Hajime TOGASHI (Apr. 1, 2014 –)
Tingting SUN (Oct. 1, 2015 – Mar. 31, 2016)

Research Consultants
Yoshikazu FUJIWARA (Apr. 1, 2014 – Mar. 31, 2015)

Junior Research Associates
Tetsuya YOSHIDA (Apr. 1, 2014 –)
Saori MAEDA (Apr. 1, 2014 –)
Shota OHNISHI (– Mar. 31, 2015)

International Program Associate
Christiane SCHMICKLER (Oct. 1, 2015 – Jan. 20, 2016)
Kaiwen LI (Jul. 1, 2015 – Oct. 1, 2015)
Jehee LEE (Jun. 1, 2015 – Aug. 31, 2015)

Visiting Researchers

Naoyuki Sakumichi (JSPS Fellow, – Apr. 30, 2015)
Christiane SCHMICKLER (Studienstiftung des deutschen Volkes, Apr. 1, 2014 – Mar. 31, 2015)

Visiting Scientists

Masayuki ASAKAWA (Osaka Univ.)
Takayuki MYO (Osaka Inst. of Tech.)
Hidekatsu NEMURA (Univ. of Tsukuba)
Masakiyo KITAZAWA (Osaka Univ.)
Taiichi YAMADA (Kanto Gakuin Univ.)
Takenori FURUMOTO (Ichinoseki Nat'l College of Tech.)
Yasuo YAMAMOTO (Tsuru Univ.)
Makoto OKA (Tokyo Tech.)
Atsushi UMEYA (Nihon Inst. of Tech.)
Tetsuo HYODO (Kyoto Univ.)
Daisuke JIDO (Tokyo Met. Univ.)
Soichi ISHIKAWA (Hosei Univ.)
Thomas Adriaan RIJKEN (Radboud Univ. Nijmegen)
Atsushi HOSAKA (Osaka Univ.)
Shoji SHINMURA (Gifu Univ.)
Akinobu DOTE (KEK)
Kazuma NAKAZAWA (Gifu Univ.)
Toru SATO (Osaka Univ.)
Jinniu HU (Peking Univ.)
Philipp GUBLER (ECT*)
Wolfram WEISE (TUM)
Toshio MOTOBA (Osaka Elec.-Com. Univ.)
Shuichi GOJUKI (SGI Japan Ltd.)
Javier ROCAMAZA (Univ. of Milan)
Hyun-Chul KIM (Inha Univ.)
Xian-Rong ZHOU (Xiamen Univ.)
Satoshi NAKAMURA (Tohoku Univ.)
Satoru HIRENZAKI (Nara Women's Univ.)
Tomokazu FUKUDA (Osaka Elec.-Com. Univ.)
Kiyomi IKEDA (Niigata Univ.)
Ying ZHANG (Tianjin University)
Petr VESELY (Academy of Science of the Czech Republic Institute of the Nuclear Physcis)
Kei KOTAKE (Fukuoka Univ.)
Hans-Josef SCHULZE (Istituto Nazionale di Fisica Nucleare (INFN)
Jean-Marc RICHARD (Lyon University)

Student Trainees

Akira YOKOTA (Tokyo Tech.)
Yongwoo CHOI (Kyungpook Nat'l Univ.)
Hana Gil (Kyungpook Nat'l Univ.)
Karl SALLMEN (TIT)

Part-time Worker

Karl SALLMEN (Dec. 1, 2015 – Feb. 29, 2016)

List of Publications & Presentations

Publications

[Journal]

(Original Papers) *Subject to Peer Review

E. Hiyama, M. Isaka, M. Kimura, T. Myo., T. Motoba, "Resonant states of the neutron-rich Λhypernucleus $^{7}_{\Lambda}$He ", Physical Review C, 91, 054316 (2015).*

M. Isaka, M. Kimura, "Impurity effects of the Λ particle on the 2α cluster states of ^{9}Be and ^{10}Be", Physical Review C, 92, 044326 (2015).*

M. Isaka, M. Kimura, E. Hiyama, H. Sagawa, "Superdeformation of Ar hypernuclei", Progress of Theoretical and Experimental Physics, 103D02(9pages) (2015).*

S. Maeda, M. Oka, A. Yokota, E. Hiyama, Yan-Rui Liu, "A model of charmed baryon–nucleon potential and two- and three-body bound states with charmed baryon", Progress of Theoretical and Experimental Physics, 023D02 (29pages), (2016).*

M. Yoshida, E. Hiyama, A. Hosaka, M. Oka, K. Sadato, "Spectrum of heavy baryons in the quark model", Physical Review D, 92, 114029, (2015).*

E. Hikota, Y. Funaki, E. Hiyama, M. Oka, "Radiative capture reaction rate from ΛΛ to H dibaryon in the imaginary time method", Physical Review C, 92, 015205, (2015).*

N. Yamanaka, E. Hiyama, "Enhancement of the CP-odd effect in the nuclear electric dipole moment of 6Li ". Physical Review C, 91, 054005 (2015).*

Oral Presentations

[International Conference etc.]

E. Hiyama, "Recent progress of hypernuclear physics", 21st International Conference on Few-body Problems in Physics, Chicago, USA, May (2015).

E. Hiyama, "Strangeness and NS", Neutrinos and Dark Matter in Nuclear Physics 2015, Jyväskylä, Finland, June (2015).

E. Hiyama, "Gaussian Expansion Method for quantum few-body problem and its application to atomic and nuclear physics", colloquium at the Physics department of Nanjing University, Nanjing, China, June (2015).

E. Hiyama, "Structure of neutron-rich Λ hypernuclei", 1st Hadron Spanish Network Days and Spanish-Japanese JSPS Workshop, Valencia, Spain, June (2015).

E. Hiyama, "Structure of Neutron Rich Lambda Hypernuclei", The 9th APCTP-BLTP JINR Joint Workshop in Kazakhstan Modern Problems in Nuclear and Elementary Particle Physics, Almaty, Kazakhstan, July (2015).

E. Hiyama, "Few-body view of hypernuclei", EMMI Workshop: Anti-matter, hyper-matter and exotica production ad the LHC, Geneva, Switzerland, July (2015).

E. Hiyama, "Structure of neutron-rich $¥Lambda$ hypernucleus, $^7_¥Lambda ¥mathrm{He}$", CKorJPARC Workshop, Waikoloa, Busan, Korea, Aug. (2015).

E. Hiyama, "Structure of few-body light Λ hypernuclei", HYP2015: 12th International Conference on Hypernuclear and Strange Particle Physics, Sendai, Japan, Sep. (2015).

E. Hiyama, "Hypernuclei: An Overview", XVI International Conference on Hadron Spectroscopy, Newport News, VA, USA, Sep. (2015).

E. Hiyama, "Structure of light Lambda hypernuclei", International Conference on Nuclear Fragmentation 2015 (NUFRA2015), Kemer (Antalya), Turkey, Oct. (2015).
E. Hiyama, "Structure of light Λ few-body hypernuclei", Korea Physics meeting, Gyeongju, Korea, Oct. (2015).
E. Hiyama, "Structure of neutron-rich Λ hypernucleus $^{7}_{\Lambda}$He", Japan-China Joint Symposium on Nuclear physics, Ibaraki, Osaka, Nov. (2015).
E. Hiyama, "Significance of Studies on Light Hypernuclei", The 2nd JLab Hypernuclar Workshop, Newport News, VA, USA, Mar. (2016).
M. Isaka, "Structure of p-sd shell Lambda hypernuclei with AMD", International workshop on strangeness nuclear physics-Future prospect and challenging-, Wako, Japan, Aug. (2015).
M. Isaka, M. Kimura, "Structure of single Lambda Hypernuclei", International workshop on 'Future prospect in nuclear physics with strangeness at J-PARC', Wako, Japan, June(2015)
M. Isaka, K. Fukukawa, M. Kimura, E. Hiyama, H. Sagawa, Y. Yamamoto, "Impurity effects in deformed/clustering hypernuclei with antisymmetric molecular dynamics", Symposium on 'Quarks to Universe in Computatinal Science (QUCS2015),Nara, Japan, Nov.(2015).
M. Isaka., "Effects of LNN three-body force in B_Lam,bda values of hypernuclei", The 31st Reimei Workshop on Hadron Physics in Extreme Conditions at J-PARC, Tokai, Ibaraki, Jan.(2016).
M. Isaka, "Hypernuclear structure with antisymmetrized Molecular dynamics", The 8th Japan-Italy Symposium, Wako, Saitama, Mar.(2016).
M. Isaka, "AMD Calculations of Medium/Heavy Hypernulei with, the ΛNN Three-Body Force in the Nijmegen Potential", Hypernuclear 2016, Newport News, USA, Mar.(2016).
S. Maeda, M. Oka, E. Hiyama, A. Yokota, RL. Yan, "YcN and Lambda_cNN bound states in the potential model", The 12th International conference on Hypernuclear and Strange Particle Physics(HYP2015), Sendai, Japan, Sep.(2015).
H. Togashi, E. Hiyama, Y. Yamamoto, M. Takano, "Variational study of the equation of state for hyperonic neutron stars", Neutrinos and Dark Matter in Nuclear Physics 2015, Jyvaskyla, Finland, June(2015).
H. Togashi, Y. Takehara, S. Yamamuro, K. Nakazato, H. Suzuki, M. Takano, "Equation of state for nuclear matter in core-collapse supernovae with realistic nuclear forces", International Symposium on "Physics and Astonomy of Neutron Satrs and Supernovae", Mitaka, Japan, June(2015).
H. Togashi, E. Hiyama, Y. Yamamoto, M. Takano, "Variational approach to hyperonic nuclear matter", International workshop on strangeness nuclear physics, Wako, Saitama, Aug.(2015).

[Domestic Conference]

井坂政裕, "Structure of Lambda hypernuclei modified and probed by Lambda particle with antisymmetrized molecular dynamics", RCNP 理論セミナー, 茨木, 大阪, 4 月 (2015).
井坂政裕, "Structure of sd shell Lambda hypernuclei with antisymmetrized molecular dynamic", KEK 理論センター JPARC 分室、JAEA 先端基礎研究センター共催研究会 「ストレンジネス核物理の発展方向」, 東海村, 茨城, 8 月 (2015).
前田沙織, 岡眞, 肥山詠美子, 横田朗, Yan Rui-Liu, "YcN interaction and YcNN charm nuclei", チャームハドロンの構造と相互作用, 東海, 茨城, 8 月(2015).
肥山詠美子: "Few-body Problem in Physics –individual and Group behavior--", RIKEN summer School Program, 熊谷, 9 月(2015).
井坂政裕, ""AMD によるハイパー核構造研究と B_{Λ}の質量依存性", ストレンジネスを含む原子核とバリオン間相互作用の将来を考える研究会, 岐阜市, 岐阜, 9 月(2015).
前田沙織, 岡眞, 肥山詠美子, 横田朗, Yan Rui-Liu, "複素スケーリング法による YcN 共鳴状態の探索", 日本物理学会第 71 回秋季大会, 大阪, 9 月(2015)
井坂政裕, "パイパー核の不純物効果とハイペロン・プローブで探る原子核構造研究 ", 第 24 回「核物理×物性セミナー」, 船橋市, 千葉, 10 月(2015).
井坂政裕, "Hypernuclear structure with antisymmetrized molecular dynamics", KEK 理論センター研究会「原子核・ハドロン物理の課題と将来」, つくば市, 茨城, 11 月(2015).
前田沙織, 岡眞, 肥山詠美子, 横田朗, Yan Rui-Liu, "YcN2 体束縛状態と共鳴状態", KEK 理論センター研究会「原子核・ハドロン物理の課題と将来」, つくば市, 11 月(2015).
肥山詠美子: "ミクロの世界の個々と集団", 理化学研究所 と親しむ会, 東京, 2 月 (2016).
富樫甫、肥山詠美子、鷹野正利: "クラスター変分法による有限温度ハイペロン物質状態方程式の研究", 日本物理学会 第 71 回年次大会, 仙台, 3 月(2016).
山中長閑、肥山詠美子: "Standard model contribution to the deuteron EDM with NN-ΛN coupling", 日本物理学会 第 71 回年次大会, 仙台, 3 月(2016).
肥山詠美子, LAZAUSKAS Rimantas, CARBONELL Jaume, 上村正康: "テトラニュートロンの共鳴状態の研究", 日本物理学会 第 71 回年次大会, 仙台, 3 月(2016).
SUN Tingting, 肥山詠美子, SCHULZE Hans-Josef, 佐川弘幸, MENG Jie,: "Relativistic mean field description for cascade- hypernuclei", 日本物理学会 第 71 回年次大会, 仙台, 3 月(2016).
井坂政裕, "ハイパー核束縛エネルギーにおける ΛNN 三体力の効果", 日本物理学会第 71 回年次大会, 仙台市, 宮城, 3 月(2016)
前田沙織, 岡眞, 肥山詠美子, 横田朗, Yan Rui-Liu, "ヘビークォーク極限における Y_c_N 共鳴状態", 日本物理学会第 71 回年次大会, 仙台市, 3 月(2016)
前田沙織, 岡眞, 肥山詠美子, 横田朗, Yan Rui-Liu, "The charm baryon-nucleon interaction and Lambda_c-NN nuclei",Exotic hadrons from high energy collisions, 京都, 3 月(2016).

Sub Nuclear System Research Division
Radiation Laboratory

1. Abstract

Nucleons, such as protons and neutrons, are a bound state of constituent quarks glued together with gluons. The detail structure of nucleons, however, is not well understood yet. Especially the mechanism to build up the spin of proton, which is 1/2, is a major problem in physics of the strong force. The research goal of Radiation Laboratory is to solve this fundamental question using the world first polarized-proton collider, realized at RHIC in Brookhaven National Laboratory (BNL) in USA. RHIC stands for Relativistic Heavy Ion Collider, aiming also to create Quark Gluon Plasma, the state of Universe just after the Big Bang, and study its property. RIKEN-BNL Research Center (RBRC) directed by S. Aronson carries our core team at BNL for those exciting researches using the PHENIX detector. We have observed that the proton spin carried by gluons is finite and indeed sizable. We also identified W bosons in the electron/positron decay channel and in the muon decay channel, with which we are about to conclude how much anti-quarks carry the proton spin. Other than the activities at RHIC we are preparing and starting new experiments at J-PARC and Fermilab to study the nature of hadron. We are also performing technical developments such as novel ion sources, fine-pitch silicon pixel detectors and high-performance trigger electronics.

2. Major Research Subjects

1) Spin physics with relativistic polarized-proton collisions at RHIC
2) Study of nuclear matter at high temperature and/or at high density
3) Technical developments on radiation detectors and accelerators

3. Summary of Research Activity

(1) Experimental study of spin structure of proton using RHIC polarized proton collider

[See also RIKEN-BNL Research Center Experimental Group for the activities at BNL]

In 2015 the final neutral pion double spin asymmetry results at central rapidity and the highest collisions energies of 510 GeV have been successfully published for the PHENIX experiment. They very strongly confirm earlier global fits that the gluon spin contribution to the proton spin is substantial and likely the dominating contribution. The increased collision energy extends the accessed gluon momentum fraction down to previously inaccessible regions. Ongoing measurements of more forward hadrons will extend it to the lowest values accessible before an eventual electron-ion collider. With the valence quark spin contribution already reasonably well known, the contributions from sea quarks and orbital angular momenta remain to be understood. PHENIX has collected data to access the sea quark polarizations via leptonic decays of W bosons. Preliminary results have been obtained using all the data taken so far. The central rapidity electron decay channel results have been published while the forward muon decay channel results are being prepared for publication.

While orbital angular momentum cannot be directly accessed at RHIC, several transverse spin phenomena have been observed which relate to orbital angular momentum and the overall three-dimensional structure of the nucleon. These phenomena in itself have become a major field of research as the dynamics of the strong interaction is being probed. One recent surprise was the behavior of very forward neutron asymmetries when colliding transversely polarized protons with protons, Al and Au ions as happened during the 2015 RHIC running period.

To further investigate these effects the PHENIX experiment proposes substantial detector upgrades to go along the expected accelerator improvements. The proposed upgrade replaces the present magnet with the Babar solenoid, and we are considering to build an open-geometry forward spectrometer which can measure hadrons, photons, electrons, muons and jets. Especially forward jet and Drell-Yan (quark-antiquark annihilation into lepton pairs) transverse single spin asymmetries are the main goal of these upgrades. As a pilot measurement, some of us are participating in the Fermilab Sea Quest experiment which has been collecting muon pairs using a 120-GeV unpolarized proton at Fermilab. By measuring the unpolarized Drell-Yan process, we can study quark spin-orbit effects which supplement what can be learned in the polarized Drell-Yan process. For many jet related measurements fragmentation functions are necessary to gain spin and or flavor sensitivity. Those are currently extracted by some of us using the Belle data.

(2) Experimental study of quark-gluon plasma using RHIC heavy ion collider

[See also RIKEN-BNL Research Center Experimental Group for the activities at BNL]

We have completed several key measurements in the study of quark-gluon plasma at RHIC. As the top of them, we lead the analysis of the first thermal photon measurement in heavy ion collisions. The measurement indicates that the initial temperature reached in the central Au+Au collision at 200 GeV is about 350MeV, far above the expected transition temperature Tc~170MeV, from hadronic phase to quark-gluon plasma. This work was rewarded by Nishina Memorial Prize given to Y. Akiba in 2011. We also measured direct photons in d+Au and direct photon flow strength v2 and v3. Using the same “virtual photon” method used in the thermal photon measurement, measurement of direct photons in Cu+Cu collision is on-going by a JRA student.

We lead measurement of heavy quark (charm and bottom) using VTX, a 4 layer silicon vertex tracker which we jointly constructed with US DOE. The detector was installed in PHENIX in 2011. Analysis of heavy quark using the silicon vertex detector is ongoing. The final results of the 2011 run was published in Physical Review C (PRC93, 034904 (2016). This is the first publication from VTX. The result showed that the electrons from bottom quark decay is suppressed for $pT>4$ GeV/c, but the suppression factor is smaller than that of charm decay electrons for $3<pT<4$ GeV/c. This is the first observation of bottom electron suppression in heavy ion collisions, and the first result that shows the bottom and charm suppression is different. PHENIX recorded approximately 10 times more data of Au+Au collisions in the 2014 run than the 2011 run. The analysis of

this large dataset is on-going.

In Wako we are operating a cluster computer system specialized to analyze huge data sets taken with the PHENIX detector. It consists of 28 nodes (18 old nodes and 10 new nodes) each of which has two CPUs and 10 sets of local disk for data repository (old node: quad-core CPU, 1TB disk, new node: six-core CPU, 2TB disk). There are 264 CPU cores and 380 TB disks in total. This configuration ensures the fastest disk I/O when each job is assigned to the node where the required data sets are stored. It is also important that this scheme doesn't require an expensive RAID system and network. Through this development we have established a fast and cost-effective solution in analyzing massive data.

The 1.7 PB of data produced by the PHENIX experiment was reduced to 0.9PB and relocated to the new Hierarchical Storage system (HSM) which is a part of HOKUSAI-GreateWave supercomputer system operated by the Advanced Center for Computing and Communication (ACCC).

(3) Study of properties of mesons and exotic hadrons with domestic accelerators

Preparation of the experiment E16 at J-PARC 50-GeV PS is underway with several Grant-in-Aids. This experiment aims to perform a systematic study of the spectral modification of low-mass vector mesons in nuclei to explore the chiral symmetry breaking in dense nuclear matter, namely, the mechanism proposed by Nambu to generate the major part of hadron mass.

Gas Electron Multiplier (GEM) technology is adopted for the two key detectors, GEM Tracker (GTR) and Hadron-blind Cherenkov detector (HBD). With a cooperation with Japanese industries, large GEM foils (30cm x 30cm, the world-largest size at that time) were newly developed. Through the beam tests at ELPH, J-PARC, LEPS, and RIKEN RIBF, the followings are achieved and proven; 1) required position resolution of 0.1 mm, and 2) stable operation under the hadron-background environment, typically 30 times higher rate than that expected in the J-PARC experimental area. The design parameters of the GTR and HBD were finalized and the mass-production of GEM is started. A beam-test result on the small-pad readout of HBD, which brings higher pion-rejection performance, is published. For the electron ID, lead-glass calorimeter (LG) is also used. The lead-glass blocks are recycled from the TOPAZ experiment.

For the readout electronics of GEM, a preamp using the APV25 ASIC chip is developed, tested, and mass production is performed. For the digitization and the data transfer, the SRS system developed by CERN is also tested and adopted. Another preamp-ASIC for the trigger signal from GEM foils is also developed in cooperation with the KEK e-sys group, and test is still on-going. Trigger logic boards, which are developed by Belle II collaboration, are tested with the firmware customized for this experiment. We have joined the CERN-RD51 collaboration for the joint-development of the GEM & readout technology.

The development phase of the detectors is over and we are in the production phase. The parts for six modules of GTR and two modules of HBD are delivered and ready to construction. For the readout/trigger electronics modules, the mass production will start after some remained tests. Due to the budgetary limitation, we aim to install a part of detectors, eight modules of GTR/HBD/LG out of 26 modules in full installation, at the beginning of experiment. The construction of the beam line is finally funded in KEK and started at J-PARC in 2013. However, original completion date (March 2016) has been extended. Only the spectrometer magnet is re-assembled and located at the proper position in the planned beam line in October 2015, which uses new pole pieces and some additional parts fabricated in 2011-12 using a Grant-in-Aid.

(4) Detector development for PHENIX experiment

After 7 years of hard work, we installed the silicon vertex tracker (VTX) into the PHENIX detector at RHIC in December 2010. VTX is a 4-layer silicon tracker to measure heavy quark (charm and bottom) production in p+p and heavy ion collisions at RHIC. The detector was funded by RIKEN and the US DOE. We and RIKEN BNL Research Center were responsible for construction and operation of the inner two pixel detectors.

Sea quark polarization measurement via W-boson production is one of the highlight of PHENIX spin program. In order to detect high momentum muons from W-decay, we developed the momentum-sensitive trigger system for the PHENIX forward muon arms with collaborators from KEK, Kyoto and Rikkyo University. Together with new hadron absorber, W-boson measurement was successfully carried out using the new high momentum trigger. We accumulated high-integrated luminosity of about $250pb^{-1}$ in Run13 and almost achieved our goal. The intensive analysis is underway towards the publication. Preliminary results were released in October 2014 and the analysis is at the final stage towards the publication. Besides W detection, the trigger system has been also operated for heavy flavor meson detection in conjunction with a forward vertex (FVTX) detector.

A silicon strip tracker R&D project for sPHENIX was launched in 2014. The high momentum resolution tracker system is the essential component of the temperature measurements using upsilon 3 states. This is one of 3 physics high-lighted goals of sPHENIX. Prototyping silicon sensors and their readout high-density integrated circuits are currently ongoing. The readout chip is to be employed FPHX chip, which was developed for PHENIX-FVTX detector. The low power consumption of the chip, i.e. 1/5th of SVX4 chip used for pixel detector is the advantage so that the cooling system can be designed rather simple to reduce the material budget. The major technical challenge of the silicon strip tracker is to minimize the material budget in order to achieve the good momentum resolution.

(5) Development of beam source

Under the collaboration with Brookhaven National Laboratory, we are developing various techniques for a laser ion source (LIS) to provide high quality heavy-ion beams to the accelerators at present or in the future. In 2014, we installed a new LIS which provides various species of singly charged ions to the RHIC-AGS complex. The commissioning was very successful and we have delivered C, Al, Ti, Si, Ta and Au ions. We also demonstrated fast switching of ion species within one second. Last year we upgraded this LIS to provide gold beam and other lighter ion beams simultaneously by installing another laser system. At the moment, all the ion beams except proton, neon and uranium are being supplied by the LIS and the capability of the fast switching species contributes enhanced versatility and uniqueness of the at the RHIC-AGS. Besides, we are studying the highly charged ionization and magnetic field confinement of laser ablation plasma, and

testing a linear accelerator model which selectively accelerates charge states.

Members

Chief Scientist (Lab. Head)
Hideto EN'YO (Director, RNC)

Vice Chief Scientist
Yasuyuki AKIBA

Research & Technical Scientists
Yasushi WATANABE (Senior Research Scientist)
Yuji GOTO (Senior Research Scientist)
Itaru NAKAGAWA (Senior Research Scientist)
Satoshi YOKKAICHI (Senior Research Scientist)
Ralf SEIDL (Senior Research Scientist)
Hiroaki ONISHI (Senior Research Scientist, concurrent; Advanced Meson Science Lab.)

Contract Researchers
Takashi HACHIYA (– Mar. 31, 2015)
Maki KUROSAWA (Jun.1, 2015 – Oct. 31, 2015)

Foreign Postdoctoral Researchers
Sanghwa PARK (Apr. 1, 2015 – Jan. 31, 2016)

Postdoctoral Researchers
Takayuki SUMITA (May 1, 2013 – Dec. 31, 2015)

Junior Research Associates
Shinichi HAYASHI (Univ. of Tokyo, –Mar. 31, 2015)
Yuko SEKIGUCHI (Univ. of Tokyo)
Koki KANNO (Univ. of Tokyo)
Wataru NAKAI (Univ. of Tokyo)
Sanshiro MIZUNO (Univ. of Tsukuba, –Mar. 31, 2015)
Tomoya TSUJI (Univ. of Tokyo, – Mar. 31, 2015)
Tomoya HOSHINO (Hiroshima Univ.)
Shunsuke IKEDA (Tokyo Tech.)
Masafumi KUMAKI (Waseda Univ.)
Hiroshi NAKAGOMI (Univ. of Tsukuba)
Yasuhiro FUWA (Kyoto Univ., – Mar. 31, 2015)
Satoshi YANO (Hiroshima Univ.)
Daisuke WATANABE (Univ. of Tsukuba)
Kohei TERASAKI (Univ. of Tokyo)
Kazuya NAGASHIMA (Hiroshima Univ.)
Hikari MURAKAMI (Univ. of Tokyo)

International Program Associates
Sanghwa PARK (Seoul Nat'l Univ., – Feb. 26, 2015)
Inseok YOON (Seoul Nat'l Univ. – Feb. 22, 2016)
Minjung KIM (Seoul Nat'l Univ.)
Taebong MOON (Yonsei Univ.)
Se Young HAN (Ewha Womans Univ., Oct. 1, 2014 –)

Senior Visiting Scientists
Toshiaki SHIBATA (Tokyo Tech.)
Takashi NAKANO (Osaka Univ.)

Visiting Scientists
Kyoichiro OZAWA (KEK)
Susumu SATO (JAEA)
Megumi NARUKI (KEK)
Akitomo ENOKIZONO (Rikkyo Univ.)
Yoshinori FUKAO (KEK)
Michiko SEKIMOTO (KEK)
Kiyoshi TANIDA (Seoul Nat'l Univ.)
Hirotsugu KASHIWAGI (JAEA)
Taku GUNJI (Univ. of Tokyo)
Junpei TAKANO (KEK)
Kazuya AOKI (KEK)
Masashi KANETA (Tohoku Univ.)
Munehisa OHTANI (Kyorin Univ.)
Yorito YAMAGUCHI (Univ. of Tokyo)
Youngil KWON (Yonsei Univ.)
Kenichi NAKANO (Tokyo Tech.)
Maya SHIMOMURA (Iowa State Univ.)
Noriyosu HAYASHIZAKI (Tokyo Tech.)
Yuhei MORINO (KEK)
Kenji FUKUSHIMA (Keio Univ.)
Atsushi NAKAMURA (Hiroshima Univ.)
Ryo ICHIMIYA (KEK)
Tomohiro NISHITANI (Nagoya Univ.)
Tomonori TAKAHASHI (Osaka Univ.)
Tsutomu MIBE (KEK)
Makoto KUWAHARA (Nagoya Univ.)
Masahiro OKAMURA (BNL)
Shunzo KUMANO (KEK)
Bentz WOLFGANG (Tokai Univ.)
Alexander BAZILEVSKY (BNL)
Shin-ya SAWADA (KEK)
Ryotaro MUTO (KEK)
Masanori HIRAI (Tokyo Univ. of Sci.)
Kenta SHIGAKI (Hiroshima Univ.)
Sanghwa PARK (Seoul National University, Stony Brook University)
Robert JAMESON (Goethe Universitat Frankfurt)

Student Trainees

Yusuke KOMATSU (Univ. of Tokyo)
Shoichiro NISHIMURA (Univ. of Tokyo)
Yuki OBARA (Univ. of Tokyo)
Yusuke OYA (Hiroshima Univ.)
Kazuya NAGASHIMA (Hiroshima Univ.)
Yosuke UEDA (Hiroshima Univ.)
Key NAGAI (Tokyo Tech.)

Interns

Hidemitsu ASANO (Kyoto Univ.)
Chong KIM (Korea Univ.)
Kotoko SHUKUTANI (Rikkyo Univ.)
Yomei FUKUSHIMA (Rikkyo Univ.)
Junsang PARK (Seoul Nat'l Univ.)
Jaehee YOO (Korea University)
Hidekazu MASUDA (Rikkyo Univ.)
Naoki FUJIYAMA (Rikkyo Univ.)

Part-time Workers

Maki KUROSAWA
Toru NAGASHIMA
Hikari MURAKAMI (Univ. of Tokyo)
Hidemitsu ASANO
Yusuke KOMATSU

Assistant

Keiko SUZUKI

List of Publications & Presentations

Publications

[Journal]

(Original Papers) *Subject to Peer Review

Precision study of the η→μμγ and ω→μ+μμπ^0 line shape in NA60. By NA60 Collaboration (R. Arnaldi et al.). Phys.Lett. B757 (2016) 437-444

Inclusive cross section and double-helicity asymmetry for π0 production at midrapidity in p+p collisions at √s=510 GeV. By PHENIX Collaboration (A. Adare et al.). Phys.Rev. D93 (2016) no.1, 011501

Scaling properties of fractional momentum loss of high-pT hadrons in nucleus-nucleus collisions at $\sqrt{s_{NN}}$ from 62.4 GeV to 2.76 TeV. By PHENIX Collaboration (A. Adare et al.). Phys.Rev. C93 (2016) no.2, 024911

Transverse energy production and charged-particle multiplicity at midrapidity in various systems from $\sqrt{s_{NN}}$ =7.7 to 200 GeV. By PHENIX Collaboration (A. Adare et al.). Phys.Rev. C93 (2016) no.2, 024901

ϕ meson production in the forward/backward rapidity region in Cu+Au collisions at $\sqrt{s_{NN}}$ =200 GeV. By PHENIX Collaboration (A. Adare et al.). Phys.Rev. C93 (2016) no.2, 024904

Centrality-dependent modification of jet-production rates in deuteron-gold collisions at $\sqrt{s_{NN}}$ =200 GeV. By PHENIX Collaboration (A. Adare et al.). Phys.Rev.Lett. 116 (2016) no.12, 122301

Measurements of elliptic and triangular flow in high-multiplicity 3He+Au collisions at $\sqrt{s_{NN}}$ =200GeV. By PHENIX Collaboration (A. Adare et al.). Phys.Rev.Lett. 115 (2015) no.14, 142301

ϕ meson production in d+Au collisions at $\sqrt{s_{NN}}$ =200GeV. By PHENIX Collaboration (A. Adare et al.). Phys.Rev. C92 (2015) no.4, 044909

Measurement of higher cumulants of net-charge multiplicity distributions in Au+Au collisions at $\sqrt{s_{NN}}$ 7.7−200GeV. By PHENIX Collaboration (A. Adare et al.). Phys.Rev. C93 (2016) no.1, 011901

Measurement of parity-violating spin asymmetries in W±production at midrapidity in longitudinally polarized p+p collisions. By PHENIX Collaboration (A. Adare et al.). Phys.Rev. D93 (2016) no.5, 05110313

Systematic study of charged-pion and kaon femtoscopy in Au + Au collisions at $\sqrt{s_{NN}}$ =200 GeV. By PHENIX Collaboration (A. Adare et al.). Phys.Rev. C92 (2015) no.3, 034914

Charged-pion cross sections and double-helicity asymmetries in polarized p+p collisions at √s =200 GeV. By PHENIX Collaboration (A. Adare et al.). Phys.Rev. D91 (2015) no.3, 032001

Search for dark photons from neutral meson decays in p+pand d + Au collisions at $\sqrt{s_{NN}}$ =200 GeV. By PHENIX Collaboration (A. Adare et al.). Phys.Rev. C91 (2015) no.3, 03190117

Low-mass vector-meson production at forward rapidity in p+p collisions at √s=200GeV. By PHENIX Collaboration (A. Adare et al.). Phys.Rev. D90 (2014) no.5, 052002

Cross section for *bbbar* production via dielectrons in d+Au collisions at $\sqrt{s_{NN}}$=200GeV. By PHENIX Collaboration (A. Adare et al.). Phys.Rev. C91 (2015) no.1, 014907

Centrality dependence of low-momentum direct-photon production in Au+Au collisions at $\sqrt{s_{NN}}$ =200GeV. By PHENIX Collaboration (A. Adare et al.). Phys.Rev. C91 (2015) no.6, 064904

Measurement of long-range angular correlation and quadrupole anisotropy of pions and (anti)protons in central d+Au collisions at $\sqrt{s_{NN}}$ =200 GeV. By PHENIX Collaboration (A. Adare et al.). Phys.Rev.Lett. 114 (2015) no.19, 192301

Comparison of the space-time extent of the emission source in d+Au and Au+Au collisions at $\sqrt{s_{NN}}$ =200GeV. By PHENIX Collaboration (N.N. Ajitanand et al.). Nucl.Phys. A931 (2014) 1082-1087

Measurement of Υ(1S+2S+3S) production in *p*+*p* and Au + Au collisions at $\sqrt{s_{NN}}$=200 GeV. By PHENIX Collaboration (A. Adare et al.). Phys.Rev. C91 (2015) no.2, 024913

Preliminary result of rapid solenoid for controlling heavy-ion beam parameters of laser ion source. By Masahiro Okamura, Megumi Sekine, Shunsuke Ikeda, Takeshi Kanesue, Masafumi Kumaki, Yasuhiro Fuwa. Laser Part. Beams 33 (2015) no.02, 137-141

Plasma shape control by pulsed solenoid on laser ion source. By M. Sekine et al., Nuclear Instruments and Methods in Physics Research A, A795 (2015) 151-155

Inclusive cross sections for pairs of identified light charged hadrons and for single protons in e+e- at √s= 10.58 GeV. By R. Seidl et al., Physical Review D, D92 (2015) 9, 092007

Investigation of the Tail of a Fe Plasma Plume Passing Through Solenoidal Magnetic Field for a Laser Ion Source. By S. Ikeda, et al., IEEE Transactions on Plasma Science, 43, 10, 3456-3460

Effect of the solenoid in various conditions of the laser ion source at Brookhaven National Laboratory. By S. Ikeda et al., Review of Scientific Instruments, 87, 2, 02A915

Behavior of moving plasma in solenoidal magnetic field in a laser ion source. By S. Ikeda et al., Review of Scientific Instruments, 87, 2, 02A912

Heavy-quark production and elliptic flow in Au + Au collisions at $\sqrt{s_{NN}}$ =62.4 GeV. By PHENIX Collaboration (A. Adare et al.), Phys. Rev. C, 91, 044907, 2015

Systematic study of azimuthal anisotropy in Cu + Cu and Au + Au collisions at $\sqrt{s_{NN}}$ =62.4 and 200 GeV. By PHENIX Collaboration (A. Adare et al.), Phys. Rev. C, 92, 034913, 2015

Dielectrons production in Au + Au collisions at $\sqrt{s_{NN}}$ =200 GeV. By PHENIX Collaboration (A. Adare et al.), Phys. Rev. C, 93, 014904, 2015

Measurement of higher cumulants of net-charge multiplicity distributions in Au+Au collisions at $\sqrt{s_{NN}}$ =7.7-200GeV. By PHENIX Collaboration (A. Adare et al.), Phys. Rev. C, 93, 011901(R), 2015

Forward J/$¥psi$ production in U + U collisions at $\sqrt{s_{NN}}$ =193 GeV. By PHENIX Collaboration (A. Adare et al.), Phys. Rev. C, 93, 034903, 2015

Single electron yields from semileptonic charm and bottom hadron decays in Au+Au collisions at $\sqrt{s_{NN}}$ =200 GeV. By PHENIX Collaboration (A. Adare et al.), Phys. Rev. C, 93, 034904, 2015

[Proceedings]

(Original Papers) *Subject to Peer Review

RF Acceleration of Ions Produced by Short Pulse Laser. By Yasuhiro Fuwa, Masaki Hashida, Yoshihisa Iwashita, Masahiro Okamura, Shuji Sakabe, Hiromu Tongu and Atsushi Yamazaki. Proceedings, 6th International Particle Accelerator Conference (IPAC 2015) : Richmond, Virginia, USA, May 3-8, 2015

Measurement of Vector Meson Decays in Nuclei at J-PARC. By Y. Morino, K. Aoki, Y. Aramaki, H. En'yo, H. Hamagaki, J Kanaya, K. Kanno, D. Kawama, A. Kiyomichi, Y. Komatsu, S. Masumoto, H. Murakami, R. Muto, W. Nakai, M. Naruki, Y. Obara, K. Ozawa, F. Sakuma, S. Sawada, M. Sekimoto, T. Shibukawa, K. Shigaki, T. N. Takahashi, Y. S. Watanabe, S. Yokkaichi (J-PARC E16 Collaboration). JPS Conf. Proc. 8, 022009 (2015)

The electronics, online trigger system and data acquisition system of the J-PARC E16 experiment. By T N Takahashi, E Hamada, M Ikeno, D Kawama, Y Morino, W Nakai, Y Obara, K Ozawa, H Sendai, M M Tanaka, T Uchida and S Yokkaichi. J. Phys.: Conf. Ser. (JPCS), 664, 082053 (2015)

The Application of DAQ-Middleware to the J-PARC E16 Experiment. By E Hamada, M Ikeno, D Kawama, Y Morino, W Nakai, Y Obara, K Ozawa, H Sendai, T N Takahashi, M M Tanaka and S Yokkaichi. J. Phys.: Conf. Ser. (JPCS), 664, 082016 (2015)

Development of GEM trigger electronics for the J-PARC E16 experiment. By Y. Obara, E. Hamada, M. Ikeno, D. Kawama, Y. Morino, W. Nakai, K. Ozawa, H. Sendai, T. N. Takahashi, M. M. Tanaka, T. Uchida and S. Yokkaichi. J. Phys.: Conf. Ser. (JPCS), 664, 082043 (2015)

Cross Section and Asymmetry Measurement of Very Forward Neutral Particle Production at RHIC. By Yuji Goto for the RHICf Collaboration. Int. J. Mod. Phys. Conf. Ser. 40, 1660110 (2016).

Oral Presentations

[International Conference etc.]

H. Asano, “Latest results of heavy flavor measurements from the PHENIX Experiment at RHIC” in 6th Internalitioanl Workshop on High Energy Physics in the LHC Era, at Universidad Técnica Federico Santa María in Valparaíso, Chili. 2016/1/7

R. Seidl, “Fragmentation measurements in Belle and Babar and impact on RHIC” in Resummation, Evolution and Factorization workshop 2015, REF2015. Hamburg, Germany, 2015/11/02

R. Seidl, “Forward spin + Cold nuclear matter measurements and forward Calorimetry” in Korea-Japan PHENIX meeting. Seoul, Korea, 2015/10/20.

R. Seidl, “Spin physics results from PHENIX” in International conference on New Frontiers in Physics 2015. Kolymbary, Greece, 2015/08/25.

R. Seidl, “fragmentation measurements in Belle” in PHENIX spinfest workshop. Tokai, Japan, 2015/07/22.

R. Seidl, “Fragmentation measurements in Belle” in High energy QCD - Nucleon structure meeting. Wako,Japan, 2015/06/30.

J. Yoo, “SMD gain calibration for local polarimeter at PHENIX” in J4th Japan-Korea PHENIX Collaboration Meeting. Hanyang University, Seoul, Rep. of Korea, 2015/10/19-20.

Y. Goto, “Studies on transverse spin properties of nucleons at PHENIX” in 10th Circum-Pan-Pacific Spin Symposium on High Energy Spin Physics (PacSpin 2015). Academia Sinica, Taipai, Taiwan. 2015/10/8.

Y. Goto, « RHIC-Spin Forward Physics” in Workshop on Forward Physics and High-Energy Scattering at Zero Degrees (HESZ 2015). Nagoya University, Nagoya, Japan, 2015/09/10.

[Domestic Conference]

R. Seidl, “fsPHENIX and eRHIC” in RHIC/PHENIX introductory meeting. Kyoto, Japan, 2015/12/02.

R. Seidl, “W measurements at PHENIX” in JPS Fall meeting. Osaka, Japan, 2015/9/26.

R. Seidl, “Fragmentation measurements in Belle” in JPS Fall meeting. Osaka, Japan, 2015/9/26.

R. Seidl, “di-hadron fragmentation in Belle” in JPS Spring meeting. Tokyo, Japan, 2015/03/24.

池田峻輔, レーザーアブレーションプラズマに対するパルス磁場の影響, 日本物理学会第 70 回年次大会, 早稲田大学,新宿、日本. 2015/3/21

四日市悟、原子核中の vector meson 測定 @ J-PARC, 研究会 「原子核媒質中のハドロン研究 III」, 高エネルギー加速器研究機構, 茨城県東海村, 日本, 2015/10/20

後藤雄二他 RHICf Collaboration, RHIC における超前方生成粒子測定, 日本物理学会第７１回年次大会, 東北学院大学、仙台、日本、2016/03/20.

Posters Presentations

[International Conference etc.]

S. Ikeda, ' Influence of Plasma Properties on Extracted Beam in Laser Ion Source Controlled by Mangetic Field' in The 16th International Conference on Ion Sources at Brookhaven National Laboratory in New York, USA. 2015/8/27

S. Ikeda, 'Effect of Solenoidal Magnetic Field on Moving Plasma Used for Laser Ion Source'in The 16th International Conference on Ion Sources at Brookhaven National Laboratory, New York, USA, 2015/8/27

S. Ikeda, 'Control of Laser Ablation Plasma by Pulsed Magnetic Field for Heavy Ion Beam' in 13th International Conference on Heavy Ion Accelerator Technology, at Yokohama, Japan. 2015/9/9

Sub Nuclear System Research Division
Advanced Meson Science Laboratory

1. Abstract

Particles like muons, pions, and kaons have finite life times, so they do not exist in natural nuclei or matters. By implanting these particles into nuclei/matters, exotic phenomena in various objects can be studied from new point of view.

Kaon is the second lightest meson, which has strange quark as a constituent quark. It is expected that if one embed mesons into nuclei, the sizes of the nuclei become smaller and one can form a high-density object beyond the normal nuclear density. Study of this object could lead to better understanding of the origin of the mass of the matter, and may reveal the quark degree of freedom beyond the quark-confinement. The other example is the weak interaction in nuclear matter. It can only be studied by the weak decay of hypernuclei, which have Lambda particle in the nuclei.

Muon provides even wider scope of studies, covering condensed matter physics as well as nuclear and atomic physics, and we are trying to extend the application field further into chemical and biological studies. For instance, stopping positively charged muon in a material, we obtain information on the magnetic properties or the local field at the muon trapped site (μSR). Injecting negatively charged muon to hydrogen gas, muonic hydrogen atom (μp) is formed. We are planning to measure μp hyperfine splitting energy to measure proton magnetic radius, which is complementary quantity to the proton charge radius and its puzzle lately attracts strong interest. We are also interested in precision measurement of muon property itself, such as muon anomalous magnetic moment (g-2).

In our research, we introduce different kind of impurities into nuclei / matters, and study new states of matter, new phenomena, or the object properties.

2. Major Research Subjects

(1) Study of meson property and interaction in nuclei
(2) Origin of matter mass / quark degree of freedom in nuclei
(3) Condensed matter and material studies with muon
(4) Nuclear and particle physics studies via muonic hydrogen
(5) Development of ultra cold muon beam, and its application from material science to particle physics

3. Summary of Research Activity

(1) Hadron physics at J-PARC, RIKEN-RIBF, GSI and SPring-8

Kaon and pion will shed a new insight to the nuclear physics. The recent discovery of deeply bound pionic atom enables us to investigate the properties of mesons in nuclear matter. At RIKEN-RIBF, we are preparing precise experimental study of the pionic atom. We have also started next generation kaon experiments (E15 and E31) at J-PARC. In these experiments, we are aiming to determine the $K^{bar}N$ interaction precisely, clarify the nature of kaon in nuclei, and Λ(1405) that could be K^-p bound state. At Spring-8 and at GSI, we are also aiming to study omega and eta' nuclei. By these experiments, we aim to be a world-leading scientific research group using these light meta-stable particles.

(1-A) Deeply bound kaonic nuclei

We have performed experimental exploration of theoretically predicted deeply bound kaonic nuclear states, such as the $<K^-pp>$ bound state. One of the most interesting features of the kaonic nucleus is the strong attraction of the $K^{bar}N$ interaction. Because of this strong attraction, the kaon in nucleus will attract surrounding nucleons resulting in extremely high-density object, which is several times larger than normal nuclear density. Measurement of the kaon properties at such high energy density will provide precious information on the origin of hadron masses and the chiral symmetry breaking and its partial restoration.

The experiment J-PARC E15 aims to identify the nature of the $<K^-pp>$ bound state by the in-flight $^3He(K^-, n)$ reaction, which allows us to investigate such state both in the formation via the missing-mass spectroscopy using the emitted neutron, and in its decay via the invariant-mass spectroscopy by detecting decay particles from $<K^-pp>$. For the experiment, we constructed a dedicated spectrometer system at the secondary beam-line, K1.8BR, in the hadron hall of J-PARC.

The first physics data-taking was carried out in March and May, 2013 with $6x10^9$ kaons on ^3He target, corresponding to a ~1% of the approved proposal. We successfully obtained semi-inclusive $^3He(K^-, n)$ X missing-mass spectrum, and found a tail structure just below the mass threshold of $(K^- + p + p)$ which cannot be explained by well-known processes and backgrounds. We also demonstrated an exclusive analysis by reconstructing $^3He(K^-, \Lambda p)$ n events. To derive more information on the $K^{bar}N$ interaction by the exclusive measurement, we carried out the second physics data-taking in November-December, 2015 with $43x10^9$ kaon ^3He target, in which 7 times more data was accumulated. We have been analyzing the new data set, especially focusing on the $^3He(K^-, \Lambda p)n$ channel. This analysis would give us the new insight of the $K^{bar}N$ interaction below the mass threshold.

(1-B) Precision X-ray measurement of kaonic atom

Simultaneously with the above experiment (1), we have performed an X-ray spectroscopy of atomic $3d \rightarrow 2p$ transition of negatively charged K-mesons captured by helium atoms. However, the energy resolution of the conventional semiconductor spectrometers is insufficient to see the K^- - nucleus potential observed by atomic levels at zero energy. This is closely related to the problem on the existence of deeply bound kaonic states in nuclei, well below the atomic levels, and this is one of the biggest problems in strangeness nuclear physics. Aiming to provide a breakthrough from atomic level observation, we will perform high-resolution X-ray spectroscopy of kaonic atoms at a J-PARC hadron beam line using a novel cryogenic X-ray spectrometer: an array of superconducting transition-edge-sensor (TES) micro-calorimeters. The spectrometer offers unprecedented energy resolution, which is about two orders of magnitude better than that of conventional semiconductor detectors. A spectrometer array of 240 pixels will have an effective area of about 20 mm^2. Very recently, we

have performed a proof-of-principle experiment by measuring pionic-atom X rays with a TES array at the PiM1 beam line at the Paul Scherrer Institut (PSI), and successfully demonstrated the feasibility of TES-based exotic-atom x-ray spectroscopy in a hadron-beam environment. Based on the results, we are preparing for the kaonic-atom experiment at J-PARC.

Another important X-ray measurement of kaonic atom would be $2p \rightarrow 1s$ transition of kaonic deuteron. We have measured same transition of kaonic hydrogen, but the width and shift from electro-magnetic (EM) value reflect only isospin average of the $K^{bar}N$ interaction. We can resolve isospin dependence of the strong interaction by the measurement. We are presently preparing a proposal to J-PARC PAC to measure kaonic deuteron X-ray.

(1-C) Deeply bound pionic atoms and η' mesonic nuclei

We have been working on precision spectroscopy of pionic atoms systematically, that leads to understanding of the origin of hadron mass. The precision data set stringent constraints on the chiral condensate at nuclear medium. We are presently preparing for the precision measurement at RIBF. The first measurement is aiming at ^{121}Sn as the first step for the systematic spectroscopy. A pilot experiment was performed in 2010, and showed a very good performance of the system. We have been analyzing the data to improve experimental setup of the pionic atom spectroscopy at the RIBF in RIKEN. We expect to achieve better experimental resolution with much reduced systematic errors.

We are also working on spectroscopy of η' mesonic nuclei in GSI/FAIR. Theoretically, peculiarly large mass of η' is attributed to UA(1) symmetry and chiral symmetry breaking. As a result, large binding energy is expected for η' meson bound states in nuclei (η'-mesonic nuclei). From this measurement, we can access information about partial restoration of chiral symmetry in nuclear media via the binding energy and decay width of η'-nuclear bound state.

(1-D) Hadron physics at SPring-8/LEPS2

Photo production of meson in nuclei is known to be a powerful tool to investigate property of the hadron in nuclear media. For this study, we started a new experimental project named LEPS2 (Laser Electron Photon at SPring-8 II) in this RIKEN Mid-term. The experimental hutch for LEPS2 at SPring-8 was constructed in March 2011, lead by RIKEN. The Large solenoid spectrometer magnet (2.96 m inner diameter x 2.22 m length) was successfully transported from BNL (US) to SPring-8 and installed into LEPS2 hutch in 2011.

One of the first physics programs is photo-production of η' in nuclei. Especially (γ, p) is most important reaction channel, where we can perform missing mass spectroscopy by detecting forward going proton. One of the big advantages of photo-production reaction is that the initial reaction is expected to be much cleaner than the hadron channel.

Detector construction for the first physics program is in progress. The 4π Electro-Magnetic calorimeter has been constructed and proton counter to detect forward going proton produced via (γ,p) reaction was partially installed in November 2013. Engineering run for the first experiment was performed in December 2013 to confirm performance of our detector system. Detector construction have been completed and 1st physics data taking was starting since 2014. Based on data collected, detail analysis to extract signal of η'-mesic nucleus, photoproduction of η etc are in progress.

(2) Muon science at RIKEN-RAL branch

The research area ranges over particle physics, condensed matter studies, chemistry and life science. Our core activities are based on the RIKEN-RAL Muon Facility located at the Rutherford-Appleton Laboratory (UK), which provides intense pulsed-muon beams. We have variety of important research activities such as particle / nuclear physics studies with muon's spin and condensed matter physics by muon spin rotation / relaxation / resonance (μSR).

(2-A) Condensed matter/materials studies with μSR

We have opened the new μSR spectrometer named CHRONUS to collaborative experiments from the May-June cycle in 2014. To have higher affinity on μSR studies with the ISIS muon facility, common data acquisition (DAQ) system with the ISIS standard DAQ (DAEII) and the front-end control system (SECI) have been installed and optimized along with other equipment in Port-4. The same DAQ and control systems will be installed in Port-2 as well. Thus, we can perform two independent μSR experiments in Port-2 and 4 at the same time, switching double-pulse to share beam between the two.

Among our scientific activities on μSR studies from year 2014 to 2016, following six subjects of material sciences are most important achievements at the RIKEN-RAL muon facility:

1) Novel superconducting state having partial nodal gaps in the one-dimensional organic superconductor λ-$[BETS]_2GaCl_4$.
2) Tiny magnetic moments and spin structures of Ir^{4+}, Nd^{3+} and Sm^{3+} in pyrochlore iridates $Nd_2Ir_2O_7$ and $Sm_2Ir_2O_7$.
3) Magnetism and spin structure in superoxide CsO_2 and NaO_2.
4) Magnetic properties of the nano-cluster gold in the border of macro- and micro- scale
5) Coexistence of short-range ordered state and superconductive state in high-T_C superconducting cuprate with the T' structure.
6) Effects of the spatial distributions of magnetic moments and muon positions estimated from density functional theory (DFT) and dipole-field calculations.

(2-B) Nuclear and particle physics studies via ultra cold muon beam and muonic atoms

If we can improve muon beam emittance, timing and energy dispersion (*so-called* "ultra-slow muon"), then the capability of μSR study will be drastically improved. The ultra-slow muon beam can stop in thin foil, multi-layered materials and artificial lattices, so one can apply the μSR techniques to surface and interface science. The development of ultra-slow muon beam is also very important as the source of ultra-cold (pencil-like small emittance) muon beam for muon g-2 measurement. Therefore, we have been working on R&D study.

We had been working on the "ultra-slow muon" generation based on the following technique, namely, positive muon beam with thermal energy has been produced by laser ionization of muoniums in vacuum (bound system of μ^+ and electron) emitted from the hot tungsten surface by stopping "surface muon beam" at Port-3. However, the muon yield and obtained emittance was far from satisfactory,

and remained to be far from any kind of realistic application.

Therefore, in this mid-term, we are developing two key components first, namely high efficiency muonium generator at room temperature and high intensity ionization laser. The study of muonium generator has been done in collaboration with TRIUMF. In 2013, we demonstrated at least 10 times increase of the muonium emission efficiency by fabricating fine laser drill-holes on the surface of silica aerogel. We also developed a high power Lyman-α laser in collaboration with laser group at RIKEN. In this laser development, we succeeded to synthesize novel laser crystal Nd:YGAG, which has an ideal wavelength property for laser amplification to generate Lyman-α by four-wave mixing in Kr gas cell. We already achieved 5 times increase of Lyman-α generation than before. Once the large-size crystal for the main amplifier is completed, the new laser will ionize muoniums 100 times more efficiently for slow muon beam generation. In order to fully apply these new developments to slow muon generation, we designed and manufactured a new ultra-slow muon source chamber dedicated for silica aerogel with new features such as spin manipulation. The beam test started on Sep 2015.

Concerning the muonic atom, we are planning a new precise measurement of proton radius. A large discrepancy was found recently in the proton charge radius between the new precise value from muonic hydrogen atom at PSI and those from normal hydrogen spectroscopy and e-p scattering. We propose a precise measurement of Zemach radius (with charge and magnetic distributions combined) using the laser spectroscopy of hyperfine splitting energy in the muonic hydrogen atom**.** Preparation of the hydrogen target, mid-infrared laser and muon spin polarization detectors is in progress. Port-1, previously used for muon catalysed fusion, is now being converted for the dedicated use by the proton radius measurement involving laser.

Members

Chief Scientist (Lab. Head)
Masahiko IWASAKI

Vice Chief Scientist
Katsuhiko ISHIDA

Research & Technical Scientists
Isao WATANABE (Senior Research Scientist)
Kenta ITAHASHI (Senior Research Scientist)
Haruhiko OUTA (Senior Research Scientist)
Hiroaki OHNISHI (Senior Research Scientist)
Fuminori SAKUMA (Senior Research Scientist)
Yue MA (Research Scientist)

Contract Researchers
Yu OISHI (– May 5, 2015)
Shinji OKADA (– Dec. 31, 2015)
Masaharu SATO
Teiichiro MATSUZAKI (Main; Team Leader, Muon Data Team, Dec. 1, 2014 – Mar. 30, 2015)

Special Postdoctoral Researchers
Tadashi HASHIMOTO (Apr. 1, 2014 –)
Takahiro NISHI (Apr. 1, 2015 –)

Research Consultants
Yoshinori AKAISHI (– Mar. 31, 2015)
Hironari MIYAZAWA
Masayasu KAMIMURA
Eiichi YAGI (Apr. 1, 2015 –)

Junior Research Associates
Kazuo TANAKA (Univ. of Tokyo) (Apr. 1, 2014 –)
Yuki NOZAWA (Kyoto Univ) (– Mar. 31, 2015)
Takuya SHIBUKAWA (Univ. of Tokyo) (Apr. 1, 2014 –)
Hirotomo HAMANO (Osaka Univ.)
Nam TRAN (Osaka Univ.) (Apr. 1, 2014-)
Ryo KITAMURA (Univ. of Tokyo, Apr. 1, 2015 –)
Dita PUSPITA SARI (Osaka Univ., Apr. 1, 2015 –)
Retno ASIH (Osaka Univ., Apr. 1, 2015 –)

International Program Associates
Edi SUPRAYOGA (Bandung Inst. Tech.)
Zhang QI (Lanzhou Univ.)
Noraina ADAM (USM, Feb. 15, 2014 –)
Sungwon YOON (Catholic Univ. of Korea, Nov. 25, 2014 –)
Saidah Sakinah Mohd Tajudin (Universiti Sains Malaysia, Oct. 1, 2015 –)

Senior Visiting Scientist
Kazuhiro TANAKA (KEK)

Visiting Scientists
Toshimitsu YAMAZAKI (Univ. of Tokyo)
Mototsugu MIHARA (Osaka Univ.)
Donald George FLEMING (Univ. of British Columbia/TRIUMF)
Yasuo NOZUE (Osaka Univ.)
Takehito NAKANO (Osaka Univ.)
Tadashi ADACHI (Tohoku Univ.)
Zyun Francis EZAWA (Tohoku Univ.)
Yasuyuki ISHII (Tokyo Med. Univ.)
Johann ZMESKAL (SMI)
Risdiana (UNPAD)
Norimichi KOJIMA (Univ. of Tokyo)
Takao SUZUKI (Shibaura Inst. of Tech.)
Masami IIO (KEK)
Georg Peter BERG (Univ. of Notre Dame)

Takayuki GOTO (Sophia Univ.)
Masaya ENOMOTO (Tokyo Univ. of Sci.)
Hiroyuki FUJIOKA (Kyoto Univ.)
Takayuki KAWAMATA (Tohoku Univ.)
Lee CHOW (UCF)
Helmut WEICK (GSI)
Harry W. K. TOM (UC Riverside)
Agustinus NUGROHO (ITB)
Kawakami Kenji ROLAND (Univ. of California, Riverside)
Ichiro SHIRAKI (Univ. of Yamanashi)
Kensuke SUZUKI (Tohoku Univ.)
Kyosuke ISODA (Tokyo Univ. of Sci.)
Ken SUZUKI (SMI)
Irwan DHARMAWAN (UNPAD)
Koji YOKOYAMA (Queen Marry Univ.)
Kazuki UENO (KEK)
Lusy SAFRIANI (UNPAD)
Hiroyuki NOUMI (Osaka Univ.)
Zhuan XU (Zhejiang Univ.)
Hiroshi TANIDA (Hiroshima Univ.)
Kenji KOJIMA (KEK)
Atsushi OKAZAWA (Univ. of Tokyo)
Tobat Parasian Irianto SARAGI (Univ. of Kassel)
Katsuhiko NISHIMURA (Univ. of Toyama)
Kenji MATSUDA (Univ. of Toyama)
Hexi SHI (Univ. of Tokyo)
Mohamed Ismail MOHAMED IBRAHIM (USM)
Shukri SULAIMAN (USM)
Kenji KAWASHIMA (Aoyama Gakuin Univ.)
Ayi BAHTIAR (UNPAD)
Koichi ICHIMURA (Hokkaido Univ.)
Youichi IGARASHI (KEK)
Makoto YOKOYAMA (Ibaraki Univ.)
Ichihiro YAMAUCHI (KEK)
KwangYong CHOI (Chung-Ang Univ.)
Peklan TOH (Univ. Sains Malaysia)
Emma HAETTNER (GSI)
Andrea VACCHI (INFN)
Eiichi YAGI (Waseda Univ.)
Naohito SAITO (KEK)
Kouichirou SHIMOMURA (KEK)
Eiko TORIKAI (Univ. of Yamanashi)
Wataru HIGEMOTO (JAEA)
Yoji KOIKE (Tohoku Univ.)
Kazuhiko SATO (Saitama Univ.)
Masaru YOSOI (Osaka Univ.)
Dai TOMONO (Kyoto Univ.)
Kazuki OHISHI (Comprehensive Res. Org. for Sci. and Soc.)
Yasuhiro MIYAKE (KEK)
Prasad Tara DAS (SUNY)
Tsutomu MIBE (KEK)
Hiroko ARIGA (Hokkaido Univ.)
Satoru HIRENZAKI (Nara Women's Univ.)
Ryousuke KADONO (KEK)
Hideyuki TATSUNO (Lund Univ.)

Visiting Technicians

Kazuo OOYAMA (JOHO com.)
Dita PUSPITA SARI (Inst. Teknologi Sepuluh Nopember)
Retno ASIH (Insti. Teknologi Sepuluh Nopember)

Research Fellows

Yuta SADA (Kyoto Univ.)
Shun ENOMOTO (Osaka Univ.)
Natsuki HIROE (RCNP)

Student Trainees

Takahiro NISHI (Univ. of Tokyo)
Natsuki TOMIDA (Kyoto Univ.)
Sohtaro KANDA (Univ. of Tokyo)
Kentaro INOUE (Osaka Univ.)
Yoshiki TANAKA (Univ. of Tokyo)
Hiroyuki YAMADA (Univ. of Tokyo)
Anba Datt PANT (Yamanashi Univ.)
Yuni WATANABE (Univ. of Tokyo)
Xingliang Xu (Saga Univ.)
Malik Anjelh BAQIYA (Tohoku Univ.)
Hiroki YAMAKAMI (Kyoto Univ.)
Shingo KAWASAKI (Osaka Univ.)
Ryo KITAMURA (Univ. of Tokyo)
Kazuki MATSUI (Sophia Univ.)
Ainul Fauzeeha Binti ROZLAN (Univ. Saints Malaysia)
Saidah Sakinah Binti MOHD TAJUDIN (Univ. Saints Malaysia)
Kazuhiro KATONO (Hokkaido Univ.)
Shu AIKAWA (Tokyo Tech.)
Hiroshi HORII (Univ. of Tokyo)
Kenji TANIBE (Osaka Univ.)
Kien LUU (Osaka Univ.)
Kazuya KATAYAMA (Tokyo Tech.)
Koshi KURASHIMA (Tohoku Univ.)
Tomotaka UEHARA (Saitama Univ.)
Takuro FUJIMAKI (Yamanashi Univ.)
Govinda KHANAL (Yamanashi Univ.)
Akane SAKAUE (Kyoto Univ.)
Isao YANAGIHARA (Kitasato Univ.)
Muhamad UMAR (Hokkaido Univ.)
Fahmi ASTUTI (Hokkaido Univ.)

Part-time Workers

Makoto TOKUDA (Tokyo Tech.)
Majed ABDEL JAWAD (Waseda Univ.)
Taehyung KIM (Tokyo Tech.)
Yuki NOZAWA (Kyoto Univ.)
Saidah Sakinah MOHD TAJUDIN (Universiti Sains Malaysia)
Fahmi ASTUTI (Hokkaido Univ.)

Assistants

Yoko FUJITA
Mitsue YAMAMOTO (May 1, 2014 –)

List of Publications & Presentations

Publications

[Journal]

(Original Papers) *Subject to Peer Review

A.D. Hillier, D.McK. Paul, K. Ishida, “Probing beneath the surface without a scratch — Bulk non-destructive elemental analysis using negative muons”, Microchemical Journal, 125, 203-207 (2016). *

P. Bakule, O. Sukhorukov, K. Ishida, F.L. Pratt, D. Fleming, T. Momose, Y. Matsuda, and E. Torikai, "First Accurate Experimental Study of Mu Reactivity from a State-Selected Reactant in the Gas Phase: the Mu + H2{1} Reaction Rate at 300 K", J. Phys. B (At. Mol. Opt.) 48, 045204 (2015). *

T. Matsuzaki, K. Ishida, M. Iwasaki, “High-pressure solid hydrogen target for muon catalyzed fusion”, Journal of Radioanalytical and Nuclear Chemistry, DOI 10.1007/s10967-015-4080-y *

Rakesh Mohan Das, Souvik Chatterjee, Masahiko Iwasaki, and Takashi Nakajima, “Ionization efficiencies of Doppler-broadened atoms by transform-limited and broadband nanosecond pulses: one-photon resonant two-photon ionization of muoniums”, J. Opt. Soc. Am. B 32, 1237-1244 (2015). *

T.Hashimoto et al., “Search for the deeply bound K-pp state from the semi-inclusive forward-neutron spectrum in the in-flight K- reaction on helium-3”, Prog. Theor. Exp. Phys., 061D01 (2015). DOI 10.1093/ptep/ptv076 *

[Proceedings]

(Original Papers) *Subject to Peer Review

Masaharu Sato, Katsuhiko Ishida, Masahiko Iwasaki, Sohtaro Kanda, Yue Ma, Yasuyuki Matsuda, Teiichiro Matsuzaki, Katsumi Midorikawa, Yu Oishi, Shinji Okada, Norihito Saito, Kazuo Tanaka and Satoshi Wada, “Laser Spectroscopy of Ground State Hyperfine Splitting Energy of Muonic Hydrogen”,Proc. 2nd Int. Symp. Science at J-PARC, JPS Conf. Proc.8 , 025005 (2015). *

R.Kitamura, G.Beer, K.Ishida, M.Iwasaki, S.Kanda, H.Kawai, N.Kawamura, W.Lee, S.Lee, G.M.Marshall, Y.Matsuda, T.Mibe, Y.Miyake, S.Nishimura, Y.Oishi, S.Okada, A.Olin, M.Otani, N.Saito, K.Shimomura, P.Strasser, M.Tabata, D.Tomono, K.Ueno, E.Won and J-PARC muon g-2/EDM collaboration, “Studies on Muonium Production from Silica Aerogel with Substructure for the Muon g-2/EDM Experiment”, Proc. 2nd Int. Symp. Science at J-PARC, JPS Conf. Proc. 8, 025016 (2015).*

H. A. Torii, M. Aoki, Y. Fukao, Y. Higashi, T. Higuchi, H. Iinuma, Y. Ikedo, K. Ishida, M. Iwasaki, R. Kadono, O. Kamigaito. S. Kanda, D. Kawall, N. Kawamura, A. Koda, K. M. Kojima, K. Kubo, Y. Matsuda, T. Mibe, Y. Miyake, T. Mizutani, K. Nagamine, K. Nishiyama, T. Ogitsu, R. Okubo, N. Saito, K. Sasaki, K. Shimomura, P. Strasser, M. Sugano, M. Tajima, K. S. Tanaka, D. Tomono, “Precise Measurement of Muonium HFS at J-PARC MUSE”, Proc. 2nd Int. Symp. Science at J-PARC, JPS Conf. Proc. 8, 025018 (2015).*

K. Ninomiya, M. K. Kubo, P. Strasser, T. Nagatomo, Y. Kobayashi, K. Ishida, W. Higemoto, N. Kawamura, K. Shimomura, Y. Miyake, T. Suzuki, A. Shinohara, T. Saito, “Elemental Analysis of Bronze Artifacts by Muonic X-ray Spectroscopy”, Proc. 2nd Int. Symp. Science at J-PARC, JPS Conf. Proc., 8, 033005 (2015).*

Oral Presentations

[International Conference etc.]

K. Ishida, "Development of ultra-slow muon source based on room temperature muonium production target and its application to muon g-2/EDM measurement", International USMM & CMSI Workshop: Fronties of Materials and Correlated Electron Science - from Bulk to Thin Films and Interface, Tokyo, Jan 2016.

Y.Sada (J-PARC E15 collaboration), “Exclusive Analysis of the in-flight 3He(K-, Λp)n_missing reaction to search for the KbarNN bound state”, 21st International Conference on Few-Body Problems in Physics (FB21), Chicago, Illinois, USA, May 2015.

F.Sakuma (J-PARC E15 collaboration), “Recent results of the KbarNN search via the in-flight 3He(K-,n) reaction at J-PARC”, The 12th International Conference on Hypernuclear and Strange Particle Physics (HYP2015), Sendai, Japan, Sep 2015

T.Hashimoto (J-PARC E15 collaboration), “Kaonic nuclei searchvia the in-flight (K-, n) reaction on helium-3”, ELPH workshop C013, Meson Production and Meson-Baryon Interaction (MPMBI), Sendai, Sep 2015

H.Ohnishi (J-PARC E15 collaboration), “Recent results of the experiment to search for KbarNN bound state via the in-fight 3He(K-,N) reactions at J-PARC”, ECT*, Frontiers in hadron and nuclear physics with strangeness and charm, Oct 2015

F.Sakuma (J-PARC E15 collaboration), “Experimental Investigations of the KbarN Interaction at J-PARC K1.8BR”, The 31st Reimei WorkShop on Hadron Physics in Extreme Conditions at J-PARC, Tokai, Jan 2016

T.Yamaga (J-PARC E15 collaboration), “Recent result of an exclusive 3He(K-,Lp)n analysis to search for KbarNN bound state”, International workshop on "Progress on J-PARC hadron physics in 2016", Mar 2016

S.Okada (HEATES and J-PARC E17 collaborations), “High-resolution Exotic-Atom x-ray spectroscopy with Transition-Edge-Sensor microcalorimeters”, Jagiellonian Symposium on Fundamental and Applied Subatomic Physics, June 2015

S.Okada (HEATES collaboration), “Hadronic-atom X-ray spectroscopy with cryogenic detectors”, ECT*, Frontiers in hadron and nuclear physics with strangeness and charm, Oct 2015

S.Okada, “Kaonic atom factory at J-PARC”, International workshop on physics at the extended hadron experimental facility of J-PARC, Mar 2016

T.Hashimoto (HEATES and J-PARC E62 collaborations), “Kaonic atom x-ray spectroscopy with superconducting microcalorimeters”, The 12th International Conference on Hypernuclear and Strange Particle Physics (HYP2015), Sendai, Japan, Sep 2015

[Domestic Conference]

北村遼, 深尾祥紀, 石田勝彦, 河村成肇, 近藤恭弘, 三部勉, 三宅康博, 大谷将士, Patrick Strasser, 齊藤直人, 下村浩一郎 他 J-PARC muon g-2/EDM コラボレーション: ″J-PARC ミューオン g-2/EDM 精密測定実験のためのミューオン再加速試験に向けた低速ミューオン源開発の準備状況″, 日本物理学会第 70 回年次大会、早稲田大学、東京、3 月(2015)

山我拓巳(J-PARC E15 collaboration), ”3He(in-flight K-,n)反応を用いた反 K 中間子束縛状態探索のための水素・重水素標的を用いた素過程解析”, 日本物理学会秋季大会, 大阪市立大学, 大阪 9 月(2015)

山我拓巳(J-PARC E15 collaboration), ”J-PARC K1.8BR ビームラインに於ける 3He(K-,n)反応を用いた KbarNN 縛状態の探索”, 日本物理学会第 71 回年次大会, 東北学院大学, 3 月(2016)

橋本直(HEATES and J-PARC E62 collaboration), ”超伝導遷移端マイクロカロリメータを用いた K 中間子原子 X 線精密分光実験 (2)”, 日本物理学会秋季大会, 大阪市立大学, 大阪 9 月(2015)
橋本直(J-PARC E15/E62 collaboration), “J-PARC K1.8BR における K-ビームを用いた KbarN 相互作用の研究”, 滞在型研究会@JPARC「原子核媒質中のハドロン研究 III」, J-PARC, 10 月(2015)

Posters Presentations

[International Conference etc.]

S. Okada, P. Bakule, G. Beer, J. Brewer, Y. Fujiwara, K. Ishida, M. Iwasaki, S. Kanda, H. Kawai, N. Kawamura, R. Kitamura, W. Lee, Y. Ma, G. Marshall, Y. Matsuda, T. Mibe, Y. Miyake, S. Nishimura, Y. Oishi, A. Olin, M. Otani, N. Saito, M. Sato, K. Shimomura, P. Strasser, M. Tabata, D. Tomono, K. Ueno, E. Won, K. Yokoyama, "Ultra-slow muon production with room-temperature thermal-muonium-emitting material", The international workshop on future potential of high intensity proton accelerator for particle and nuclear physics (HINT2015), Oct 2015

Sub Nuclear System Research Division
RIKEN-BNL Research Center

1. Abstract

The RIKEN BNL Research Center was established in April 1997 at Brookhaven National Laboratory with Professor T. D. Lee of Columbia University as its initial Director. It is funded by the Rikagaku Kenkyusho (RIKEN, The Institute of Physical and Chemical Research) of Japan. The Center is dedicated to the study of strong interactions, including spin physics, lattice QCD and RHIC physics through the nurturing of a new generation of young physicists. Professor Lee was succeeded by BNL Distinguished Scientist, N. P. Samios, who served until 2013. The current director is Dr. S. H. Aronson. Support for RBRC was initially for five years and has been renewed three times, and presently extends to 2018. The Center is located in the BNL Physics Department. The RBRC Theory Group activities are closely and intimately related to those of the Nuclear Theory, High Energy Theory, and Lattice Gauge Theory Groups at BNL. The RBRC Experimental Group works closely with the DOE RHIC Spin Group, the RIKEN Spin Group at BNL, and the PHENIX heavy ion groups. BNL provides office space, management, and administrative support. In addition, the Computational Science Center (CSC) and Information Technology Division (ITD) at BNL provide support for computing, particularly the operation and technical support for the RBRC 400 Teraflop QCDCQ (QCD Chiral Quark) lattice gauge theory computer. The Deputy Director of RBRC is R. Pisarski (BNL). D. Kharzeev (Stony Brook/BNL) is leader of the Theory Group. Y. Akiba (RIKEN) is Experimental Group leader with A. Deshpande (Stony Brook) deputy. T. Izubuchi (BNL) is Computing Group leader.

2. Major Research Subjects

Major research subjects of the theory group are
(1) Heavy Ion Collision
(2) Perturbative QCD
(3) Phenomenological QCD

Major research subjects of the computing group are
(1) Search for new law of physics through tests for Standard Model of particle and nuclear physics
(2) Dynamics of QCD and related theories
(3) Theoretical and algorithmic development for lattice field theories, QCD machine design

Major research subject of the experimental group are
(1) Experimental Studies of the Spin Structure of the Nucleon
(2) Study of Quark-Gluon Plasma at RHIC
(3) PHENIX detector upgrades

3. Summary of Research Activity

Summary of Research Activities of the three groups of the Center are given in the sections of each group.

Members

Director
Samuel H. ARONSON

Deputy Director
Robert PISARSKI

Administrative Staff
Mituru KISHIMOTO (Administration Manager, Nishina Center Planning Office)
Yasutaka AKAI (Deputy Administration Manager, Nishina Center Planning Office, Jan. 1, 2015 –)
Colleen MICHAEL (Administrative Assistant)
Pamela ESPOSITO (Administrative Assistant)
Taeko ITO (Administrative Assistant, – Apr.30, 2015)
Tammy STEIN (Sep. 8, 2015 – Jan. 31, 2016)

Sub Nuclear System Research Division
RIKEN-BNL Research Center
Theory Group

1. Abstract

The efforts of the RBRC theory group are concentrated on the major topics of interest in High Energy Nuclear Physics. This includes: understanding of the Quark-Gluon Plasma; the nature of dense quark matter; the initial state in high energy collisions, the Color Glass Condensate; its evolution through a Glasma; spin physics, as is relevant for polarized hadronic collisions; physics relevant to electron-hadron collisions.

Theory Group hosted many joint tenure track positions with universities in U.S. and Japan.

2. Major Research Subjects

(1) Heavy Ion Collision
(2) Perturbative QCD
(3) Phenomenological QCD

3. Summary of Research Activity

(1) Spin Physics

The experimental program at RBRC is strongly focused on determining the origin of spin in the proton and neutron. To extract the spin content of nucleon requires both precise data and precise computation. Dr. Jianwei Qiu of the Nuclear Theory group is one of the world's leading theorists in perturbative QCD, and leading the effort at BNL in spin physics. Their effort will continue to concentrate on computing perturbative QCD effects to sufficient precision that one can reliably extract information from the evolving experimental program. In addition they are developing ideas which might be tested in an electron-hadron collider, such as the one proposed to be built by adding an electron ring to RHIC.

(2) Matter at High Energy Density

The RHIC experimental heavy ion program is designed to study the properties of matter at energy densities much greater than that of atomic nuclei. This includes the initial state of nucleus-nucleus collisions, the Color Glass Condensate, the intermediate state to which it evolves, the Glasma, and lastly the thermal state to which it evolves, the Quark-Gluon Plasma. Theorists at the RBRC have made important contributions to all of these subjects.

Matter at high temperature has been studied by a variety of techniques involving both numerical and analytic methods. Much of the high precision work on numerical simulations of lattice QCD at nonzero temperature and density such matter have been done by members of the Lattice Gauge Theory Group at BNL, including Frithjof Karsch, Peter Petreczsky, Swagato Mukherjee, and postdoctoral assistants. These groups, along with collaborators at Columbia University, the University of Bielefeld, and other groups, have computed numerous properties of QCD in thermodynamic equilibrium. This includes the equation of state for physical quark masses, susceptibilies with respect to quark chemical potentials, and transport coefficients.

Phenomenological theories of the Quark-Gluon Plasma, based upon results from lattice simulations, have been developed by R. Pisarski of the Nuclear Theory Group, in collaboration with Dr. Y. Hidaka (previously of RBRC/BNL, and now a permanent member at RIKEN in Waco), Shu Lin, Daisuke Sato, and other postdoctoral research assistants at RBRC/BNL.

The theory of the Color Glass Condensate and Glasma was largely developed by RBRC scientists. This theory has been successfully applied to a wide variety of experimental results involving high energy collisions of hadrons, electrons and nuclei. There is recent data on heavy ion collisions that are naturally explained by such matter, including data on proton (or deuteron) nucleus collisions. Much of the effort here will be aimed towards excluding or verifying the Color Glass Condensate and Glasma hypothesis in RHIC and LHC experiments.

Thermal matter at high temperature and baryon density has been traditionally conjectured to be of two phases: confined and deconfined, with a direct correlation between deconfinement and the restoration of chiral symmetry. RBRC scientists have recently conjectured a third phase, of quarkyonic matter. This is baryonic matter at energy densities very high compared to the QCD scale. It has a pressure and energy density typical of quarks, yet it is confined. The name arises because it shares properties of confined baryonic matter with unconfined quark matter. This hypothesis is new and predicts new classes of phenomena that might be observed in collisions of nuclei of relatively low energy at RHIC. There are a number of first principle theoretical issues also to be understood.

Efforts on RHIC phenomenology proceed on a broad front. Recent efforts include improving hydrodynamic computations using state of the art equations of state derived from lattice gauge theory. Understanding the nature of matter at high baryon number density has generated the idea of Quarkyonic Matter, that may have implications for an upcoming low energy run at RHIC and eventual experiments in the future at FAIR and NICA. An issue being studied is the nature of mass generation and the breaking of translational invariance. A central focus of work at RBRC, the Color Glass Condensate and the Glasma, matter that controls the high energy limit of QCD, is being realized in experiments at RHIC. Much activity focuses on the relation between observations at LHC and the implications made at RHIC.

Members

Group Leader (Lab. Head)

Larry McLERRAN (– Oct. 30, 2015)
Dmitri KHARZEEV (Nov. 1, 2015 –)

Deputy Group Leader

Robert PISARSKI (concurrent : Deputy Director, RBRC)

RBRC Researchers

Jinfeng LIAO (RHIC Physics Fellow)
Fedor BEZRUKOV ((RHIC Physics Fellow, – Dec. 31, 2015)
Ho-Ung YEE (RHIC Physics Fellow)
Akihiko MONNAI (Special Postdoctoral Researcher)
Lin SHU (Foreign Postdoctoral Researcher, – Aug. 28, 2015)
Sergey SYRITSYN (Foreign Postdoctoral Researchers, - Aug. 28, 2015)
Daniel PITONYAK (Research Associates)
Vladimir SKOKOV

Visiting Scientists

Thomas BLUM (Univ. of Connecticut)
Taku IZUBUCHI (concurrent; Computing Gr.)

List of Publications & Presentations

Publications

[Journal]

(Original Papers) *Subject to Peer Review

Yoshitaka Hatta, Akihiko Monnai, Bo-Wen Xiaoc ”Elliptic flow difference of charged pions in heavy-ion collisions” Nuclear Physics A Volume 947, March 2016, Pages 155–160*

Y. Koike, D. Pitonyak, Y. Takagi, S. Yoshida ” Twist-3 fragmentation effects for ALT in light hadron production from proton–proton collisions” Physics Letters B, Volume 752, 10 January 2016, Pages 95–101*

Larry McLerran, Vladimir V. Skokov ”The Eccentric Collective BFKL Pomeron” arXiv:1407.2651 *

A Monnai, B Schenke ”Pseudorapicity correlations in heavy ion collisions from viscous fluid dynamics”- Physics Letters B, Volume 752, 10 January 2016, Pages 317–321 *

K Fukushima, K Hattori, HU Yee, Y Yin ”Heavy Quark Diffusion in Strong Magnetic Fields at Weak Coupling and Implication to Elliptic Flow” arXiv:1512.03689v2 [hep-ph] 20 Apr 2016

KA Mamo, HU Yee ”Spin Polarized Photons from Axially Charged Plasma at Weak Coupling: Complete Leading Order ” arXiv:1512.01316v3 [hep-ph] 11 Apr 2016

Yuri V. Kovchegov, Daniel Pitonyak, Matthew D. Sievert ”Helicity Evolution at Small-x” arXiv:1511.06737v2 [hep-ph] 12 Jan 2016

Philipp Gubler, Koichi Hattori, Su Houng Lee, Makoto Oka, Sho Ozaki, Kei Suzuki ”D mesons in a magnetic field”arXiv:1512.08864v2 [hep-ph] 28 Mar 2016

Koichi Kanazawa, Yuji Koike, Andreas Metz, Daniel Pitonyak, Marc Schlegel ”Operator constraints for twist-3 functions and Lorentz invariance properties of twist-3 observables” arXiv: 1512.07233v2 [hep-ph] 16 Mar 2016

A Bzdak, V Skokov ”Multi-particle eccentricities in collisions dominated by fluctuations” Nuclear Physics A Volume 943, November 2015, Pages 1–8*

Dmitri E. Kharzeev ”Topology, magnetic field, and strongly interacting matter” arXiv:1501.01336v1 [hep-ph] 6 Jan 2015

Fedor Bezrukov, Dmitry Levkov, Sergey Sibiryakov ”Semiclassical S-matrix for black holes”arXiv:1503.07181v3 [hep-th] 12 Nov 2015

Y Koike, D Pitonyak, S Yoshida ”Twist-3 effect from the longitudinally polarized proton for ALT in hadron production from pp collisions “Physics Letters B Volume 759, 10 August 2016, Pages 75–81 *

Gustavo M. Monteiro, Alexander G. Abanov, and Dmitri E. Kharzeev ”Magneto transport in Dirac metals: chiral magnetic effect and quantum oscillations” Phys. Rev. B 92, 165109 – Published 8 October 2015*

Robert D. Pisarski, Vladimir V. Skokov ”A chiral matrix model of the semi-Quark Gluon Plasma in QCD” arXiv:1604.00022v1 [hep-ph] 31 Mar 2016

Fedor Bezrukov, Dmitry Gorbunov “On the applicability of approximations used in calculation of spectrum of Dark Matter particles produced in particle decays” arXiv:1412.1341v2 [hep-ph] 6 Dec 2015

Xu, Jiechen; Liao, Jinfeng; Gyulassy, Miklos ”Bridging soft-hard transport properties of quark-gluon plasmas with CUJET3.0”Journal of High Energy Physics, Volume 2016, article id.169, 50 pp.*

L McLerran, VV Skokov ”Finite numbers of sources, particle correlations and the Color Glass Condensate” Nuclear Physics A Volume 947, March 2016, Pages 142–154*

Larry McLerran, Vladimir V. Skokov ”The MV Model of the Color Glass Condensate for a Finite Number of Sources Including Coulomb Interactions”arXiv:1604.05286v1 [hep-ph] 18 Apr 2016

Shiyong Li, Kiminad A. Mamo, Ho-Ung Yee ”Jet quenching parameter of quark-gluon plasma in strong magnetic field: perturbative AdS/CFT correspondence”arXiv:1605.00188v2 [hep-ph] 31 May 2016

É. Aubourg and others "Cosmological implications of baryon acoustic oscillation measurements" Phys. Rev. D92, 123516 (2015).

F. Bezrukov and M. Shaposhnikov "Why should we care about the top quark Yukawa coupling?" J. Exp. Theor. Phys. 120, 335-343 (2015).

F. Bezrukov and M. Shaposhnikov "Inflation, LHC and the Higgs boson" Int. J. Mod. Phys. A30, 1545001 (2015).

A. Bzdak and V. Koch "Local Efficiency Corrections to Higher Order Cumulants" Phys. Rev. C91, 027901 (2015).

A. Dumitru, L. McLerran and V. Skokov "Azimuthal asymmetries and the emergence of “collectivity” from multi-particle correlations in high-energy pA collisions" Phys. Lett. B743, 134-137 (2015).

C. Gale, Y. Hidaka, S. Jeon, S. Lin, J.-F. Paquet, R. D. Pisarski, D. Satow, V. V. Skokov and G. Vujanovic "Production and Elliptic Flow of Dileptons and Photons in a Matrix Model of the Quark-Gluon Plasma" Phys. Rev. Lett. 114, 072301 (2015).

Y. Hatta, A. Monnai and B.-W. Xiao "Flow harmonics v_n at finite density" Phys. Rev. D92, 114010 (2015).
K. Hattori, K. Itakura, S. Ozaki and S. Yasui "QCD Kondo effect: quark matter with heavy-flavor impurities" Phys. Rev. D92, 065003 (2015).
Y. Hidaka, S. Lin, R. D. Pisarski and D. Satow "Dilepton and photon production in the presence of a nontrivial Polyakov loop" JHEP 10, 005 (2015).
Y. Hirono, D. Kharzeev and Y. Yin "Self-similar inverse cascade of magnetic helicity driven by the chiral anomaly" Phys. Rev. D92, 125031 (2015).
X.-G. Huang and J. Liao "Glasma Evolution and Bose-Einstein Condensation with Elastic and Inelastic Collisions" Phys. Rev. D91, 116012 (2015).
I. Iatrakis, S. Lin and Y. Yin "Axial current generation by P-odd domains in QCD matter" Phys. Rev. Lett. 114, 252301 (2015).
I. Iatrakis, S. Lin and Y. Yin "The anomalous transport of axial charge: topological vs non-topological fluctuations" JHEP 09, 030 (2015).
K. Jiang, Y. Zhu, W. Liu, H. Chen, C. Li, L. Ruan, Z. Tang, Z. Xu and Z. Xu "Onset of radial flow in p+p collisions" Phys. Rev. C91, 024910 (2015).
Y. Jiang, X.-G. Huang and J. Liao "Chiral vortical wave and induced flavor charge transport in a rotating quark-gluon plasma" Phys. Rev. D92, 071501 (2015).
A. Jimenez-Alba and H.-U. Yee "Second order transport coefficient from the chiral anomaly at weak coupling: Diagrammatic resummation" Phys. Rev. D92, 014023 (2015).
K. Kanazawa, Y. Koike, A. Metz and D. Pitonyak "Transverse single-spin asymmetries in p^↑ p to γ X from quark-gluon-quark correlations in the proton" Phys. Rev. D91, 014013 (2015).
K. Kanazawa, A. Metz, D. Pitonyak and M. Schlegel "Longitudinal–transverse double-spin asymmetries in single-inclusive leptoproduction of hadrons" Phys. Lett. B742, 340-346 (2015).
K. Kanazawa, Y. Koike, A. Metz and D. Pitonyak "Transverse single-spin asymmetries in proton-proton collisions at the AFTER@LHC experiment" Adv. High Energy Phys. 2015, 257934 (2015).
K. Kanazawa, A. Metz, D. Pitonyak and M. Schlegel "Single-spin asymmetries in the leptoproduction of transversely polarized Λ hyperons" Phys. Lett. B744, 385-390 (2015).
D. E. Kharzeev, R. D. Pisarski and H.-U. Yee "Universality of plasmon excitations in Dirac semimetals" Phys. Rev. Lett. 115, 236402 (2015).
K. A. Mamo and H.-U. Yee "Gradient Correction to Photon Emission Rate at Strong Coupling" Phys. Rev. D91, 086011 (2015).
K. A. Mamo and H.-U. Yee "Thermalization of Quark-Gluon Plasma in Magnetic Field at Strong Coupling" Phys. Rev. D92, 105005 (2015).
L. McLerran and M. Praszalowicz "Geometrical Scaling and the Dependence of the Average Transverse Momentum on the Multiplicity and Energy for the ALICE Experiment" Phys. Lett. B741, 246-251 (2015).
L. McLerran "The Electroweak Axion, Dark Energy, Inflation and Baryonic Matter" J. Exp. Theor. Phys. 120, 376-379 (2015).
L. McLerran "Lessons learned and ideas formed from early studies of pA collisions" Annals Phys. 352, 52-58 (2015).
A. Monnai "Effective distributions of quasiparticles for thermal photons" Phys. Rev. C92, 014905 (2015).
S. Ozaki, T. Arai, K. Hattori and K. Itakura "Euler-Heisenberg-Weiss action for QCD+QED" Phys. Rev. D92, 016002 (2015).
M. Stephanov, H.-U. Yee and Y. Yin "Collective modes of chiral kinetic theory in a magnetic field" Phys. Rev. D91, 125014 (2015).
A. Bialas and A. Bzdak "Short-range two-particle correlations from statistical clusters" Phys. Rev. D93, 094015 (2016).
J.-P. Blaizot, Y. Jiang and J. Liao "Gluon transport equation with effective mass and dynamical onset of Bose–Einstein condensation" Nucl. Phys. A949, 48-70 (2016).
J.-P. Blaizot and J. Liao "Gluon Transport Equations with Condensate in the Small Angle Approximation" Nucl. Phys. A949, 35-47 (2016).
G. Denicol, A. Monnai and B. Schenke "Moving forward to constrain the shear viscosity of QCD matter" Phys. Rev. Lett. 116, 212301 (2016).
K. Hattori, T. Kojo and N. Su "Mesons in strong magnetic fields: (I) General analyses" Nucl. Phys. A951, 1-30 (2016).
I. Iatrakis and D. E. Kharzeev "Holographic entropy and real-time dynamics of quarkonium dissociation in non-Abelian plasma" Phys. Rev. D93, 086009 (2016).
S. Lin "Holographic thermalization with initial long range correlation" Phys. Rev. D93, 026007 (2016).
M. A. Stephanov and H.-U. Yee "No-Drag Frame for Anomalous Chiral Fluid" Phys. Rev. Lett. 116, 122302 (2016).
Y. Yin and J. Liao "Hydrodynamics with chiral anomaly and charge separation in relativistic heavy ion collisions" Phys. Lett. B756, 42-46 (2016).
(Review)
Larry McLerran, Vladimir V. Skokov ”The Eccentric Collective BFKL Pomeron” arXiv:1407.2651
Adrian Dumitru, Tuomas Lappi, and Vladimir Skokov ”Distribution of Linearly Polarized Gluons and Elliptic Azimuthal Anisotropy in Deep Inelastic Scattering Dijet Production at High Energy” Phys. Rev. Lett. 115, 252301 – Published 17 December 2015
Fedor Bezrukov, Javier Rubio, and Mikhail Shaposhnikov ”Living beyond the edge: Higgs inflation and vacuum metastability” Phys. Rev. D 92, 083512 – Published 13 October 2015
Dmitri E. Kharzeev and Eugene M. Levin ”Color Confinement and Screening in the θ Vacuum of QCD”Phys. Rev. Lett. 114, 242001 – Published 16 June 2015
[Proceedings]
(Original Papers) *Subject to Peer Review
Koichi Kanazawa, Yuji Koike, Andreas Metz, Daniel Pitonyak ”New Collinear Twist-3 Analysis of Transverse SSA: Toward a Solution for the Sign-Mismatch Problem” Few-Body Systems September 2015, Volume 56, Issue 6, pp 343–348 *
Andreas Metz, Daniel Pitonyak, Andreas Schäfer, Marc Schlegel, Werner Vogelsang ,Jian Zhou ”Transverse Single-Spin Asymmetries: Challenges and Recent Progress” Few-Body Systems September 2015, Volume 56, Issue 6, pp 331-336 *
DE Kharzeev, J Liao, SA Voloshin, G Wang ”Chiral magnetic and vortical effects in high-energy nuclear collisions-A status report”Progress in Particle and Nuclear Physics Volume 88, May 2016, Pages 1–28
D Pitonyak, K Kanazawa, Y Koike, A Metz ”AN in single-inclusive particle production from proton-proton collisions”QCD Evolution Workshop Newport News, VA May 26, 2015
Hattori, K Itakura ”Photon and dilepton spectra from nonlinear QED effects in supercritical magnetic fields induced by heavy-ion collisions”arXiv:1509.03217v1 [hep-ph] 10 Sep 2015
L. Gamberg, K. Kanazawa, Z. Kang, A. Metz, D. Pitonyak, A. Prokudin and M. Schlegel "Twist-3 Spin Observables for Single-Hadron Production in DIS" PoS DIS2015, 208 (2015).

K. Kanazawa, Y. Koike, A. Metz and D. Pitonyak "New Collinear Twist-3 Analysis of Transverse SSA: Toward a Solution for the Sign-Mismatch Problem" Few Body Syst. 56, 343-348 (2015).
L. Mclerran "Inhomogeneous and Quarkyonic phases of High Density QCD" PoS CPOD2014, 046 (2015).
A. Metz, L. Gamberg, K. Kanazawa, Z. Kang, D. Pitonyak, A. Prokudin and M. Schlegel "Twist-3 spin Asymmetries in ℓ N to h X Studied in Collinear Factorization" PoS QCDEV2015, 020 (2015).
A. Monnai "Effects of quark chemical equilibration on thermal photon elliptic flow" J. Phys. Conf. Ser. 612, 012026 (2015).
D. Pitonyak, Y. Koike, K. Kanazawa and A. Metz "A_N in Single-Inclusive Particle Production from Proton-Proton Collisions" PoS QCDEV2015, 011 (2015).
D. Pitonyak, K. Kanazawa, Y. Koike and A. Metz "Transverse Single-Spin Asymmetries in Pion and Photon Production from Proton-Proton Collisions" PoS DIS2015, 211 (2015).
D. Pitonyak, K. Kanazawa, Y. Koike and A. Metz "Transverse Single-Spin Asymmetries in Proton-Proton Collisions Within Collinear Factorization" Int. J. Mod. Phys. Conf. Ser. 37, 1560033 (2015).
D. Pitonyak, K. Kanazawa, Y. Koike and A. Metz "A_N in proton-proton collisions and the role of twist-3 fragmentation" EPJ Web Conf. 85, 02013 (2015).

Sub Nuclear System Research Division
RIKEN-BNL Research Center
Computing Group

1. Abstract

The computing group founded in 2011 as a part of the RIKEN BNL Research Center established at Brookhaven National Laboratory in New York, USA, and dedicated to conduct researches and developments for large-scale physics computations important for particle and nuclear physics. The group was forked from the RBRC Theory Group.

The main mission of the group is to provide important numerical information that is indispensable for theoretical interpretation of experimental data using the theories of particle and nuclear physics. Their primary area of research is lattice quantum chromodynamics (QCD), which describes the sub-atomic structures of hadrons, which allow us the ab-initio investigation for strongly interacting quantum field theories beyond pertrubative analysis.

The RBRC group and its collaborators have emphasized the necessity and importance of precision calculations, which will precisely check the current understandings of nature, and will have a potential to find a physics beyond the current standard model of fundamental physics. We have therefore adopted techniques that aim to control and reduce any systematic errors. This approach has yielded many reliable results.

The areas of the major activities are R&D for high performance computers, developments for computing algorithms, and researches of particle, nuclear, and lattice theories. Since the inception of RBRC, many breakthroughs and pioneering works has carried out in computational forefronts. These are the use of the domain-wall fermions, which preserve chiral symmetry, a key symmetry for understanding nature of particle nuclear physics, the three generations of QCD devoted supercomputers, pioneering works for QCD calculation for Cabibbo-Kobayashi-Maskawa theory, QCD+QED simulation for isospin breaking, novel algorithm for error reduction in general lattice calculation. Now the chiral quark simulation is performed at the physical up, down quark mass, the precision for many basic quantities reached to accuracy of sub-percent, and the group is aiming for further important and challenging calculations, such as the full and complete calaution for $K \to \pi\pi$ decay, ε'/ε, or hadronic contributions go muon's anomalous magnetic moment, or Nucleon's shape and structures related to physics for future Electron Ion Collider (EIC).

2. Major Research Subjects

(1) Search for new law of physics through tests for Standard Model of particle and nuclear physics, especially in the framework of the Cabibbo–Kobayashi–Maskawa (CKM), hadronic contributions to the muon's anomalous magnetic moment (g-2).
(2) Dynamics of QCD and related theories, including study for the structures of nucleons related to physics for Electron Ion Collider (EIC or eRHIC).
(3) Theoretical and algorithmic development for lattice field theories, QCD machine design.

3. Summary of Research Activity

In 2011, QCD with Chiral Quarks (QCDCQ), a third-generation lattice QCD computer that is a pre-commercial version of IBM's Blue Gene/Q, was installed as an in-house computing resource at the RBRC. The computer was developed by collaboration among RBRC, Columbia University, the University of Edinburgh, and IBM. Two racks of QCDCQ having a peak computing power of 2 × 200 TFLOPS are in operation at the RBRC. In addition to the RBRC machine, one rack of QCDCQ is owned by BNL for wider use for scientific computing. In 2013, 1/2 rack of Blue Gene/Q is also installed by US-wide lattice QCD collaboration, USQCD. The group has also used the IBM Blue Gene supercomputers located at Argonne National Laboratory and BNL (NY Blue), and Hokusai and RICC, the super computers at RIKEN (Japan), Fermi National Accelerator Laboratory, the Jefferson Lab, and others.

Such computing power enables the group to perform precise calculations using up, down, and strange quark flavors with proper handling of the important symmetry, called chiral symmetry, that quarks have. The group and its collaborators carried out the first calculation for the direct breaking of CP (Charge Parity) symmetry in the hadronic K meson decay ($K \to \pi\pi$) amplitudes, ε'/ε which provide a new information to CKM paradigm and its beyond. They also provide the hadronic contribution in muon's anomalous magnetic moment $(g\text{-}2)_\mu$ These calculation for ε'/ε hadronic light-by-light of (g-2), are long waited calculation in theoretical physics delivered for the first time by the group. The $K \to \pi\pi$ result in terms of ε'/ε currently has a large error, and deviates from experimental results by 2.1 σ. Hadronic Light-by-light contribution to $(g\text{-}2)_\mu$ is improved by more than two order of magnitudes compared to our previous results. Other projects including flavor physics in the framework of the CKM theory for kaons and B mesons that include the new calculation of b-baryon decay, $\Lambda_b \to p$; the electromagnetic properties of hadrons; the proton's and neutron's formfactors and structure function including electric dipole moments; proton decay; nucleon form factors, which are related to the proton spin problem; Neutron-antineutron oscillations; nonperturbative studies for beyond standard model such composite Higgs or dark matter models from strong strongly interacting gauge theories; a few-body nuclear physics and their electromagnetic properties; and QCD thermodynamics in finite temperature/density systems such as those produced in heavy-ion collisions at the Relativistic Heavy Ion Collider.

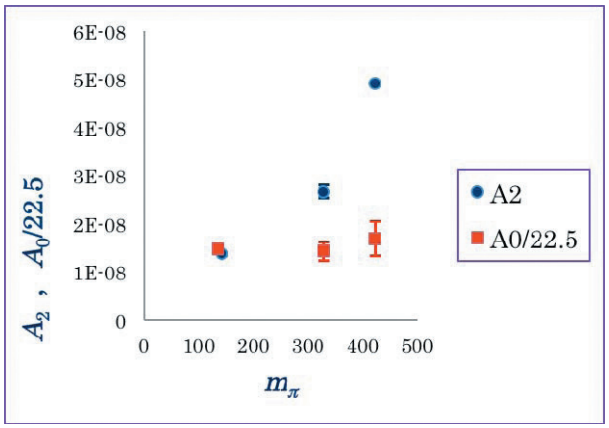

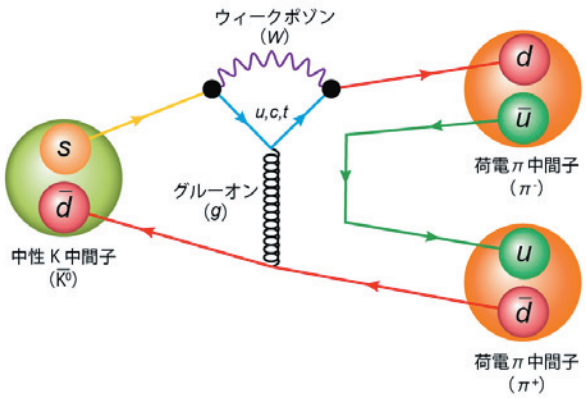

Figure : Computed results of K→ππ decay amplitudes, isospin two, A_2, and isospin zero A_0 divided by 22.5 (left), the schematic diagram of the decay (left).

Theme	Significant Outcomes	Expected Impacts & Extensions
(a) DWF QCD ensemble generation and measurements of basic quantities.	hadron spectrum, f_π, f_K, K_{13}, B_K, and ChPT LECs, with smaller systematic errors	Basis of physical observables such as below
(b) Operator Renormalization	Precise matrix elements, bag parameters quark masses, and coupling constants	Reduced systematic error in *e.g.* $K \to \pi\pi$ amplitudes
(c) Computational Algorithms, Software, and Machines	Fast and Cost-Effective Computing All-Mode Averaging (AMA) PhySyHCAl	Unprecedented precision and new physical quantities (see below)
(d) K physics	K_{13},$\Delta I = 1/2, 3/2, K \to \pi\pi$ amplitudes, ϵ'/ϵ $K_L - K_S$ Mass Difference	New constraints *e.g.* on CKM from rare Kaon decay $K \to \pi\nu\bar{\nu}$
(e) B physics	Matrix elements for (semi-)leptonic decays and $B^0 - \overline{B^0}$ oscillations	CKM matrix, e.g., V_{ub}, V_{ts}, V_{td}.
(f) QED and Isospin breaking effects	Better determination of quark masses Proton-Neutron Mass Difference	A step towards sub-% precision groundwork for $(g-2)_\mu$
(g) Muon Anomalous Magnetic Moment $(g-2)_\mu$	Hadronic Vacuum Polarization contribution Light-by-Light contribution	$(g-2)_\mu$ experiments at BNL, FNAL, J-PARC
(h) Proton/Neutron Physics Electric Dipole Moments, ProtonDecay	Nucleon structure, Parton Distribution Functions (PDF) EM properties, Electric Dipole Moment (EDM)	Electron-Ion Collider (eRHIC) Spin Physics, Kamiokande Origin of matter in Universe

Table: Summery of current physics program and their impacts

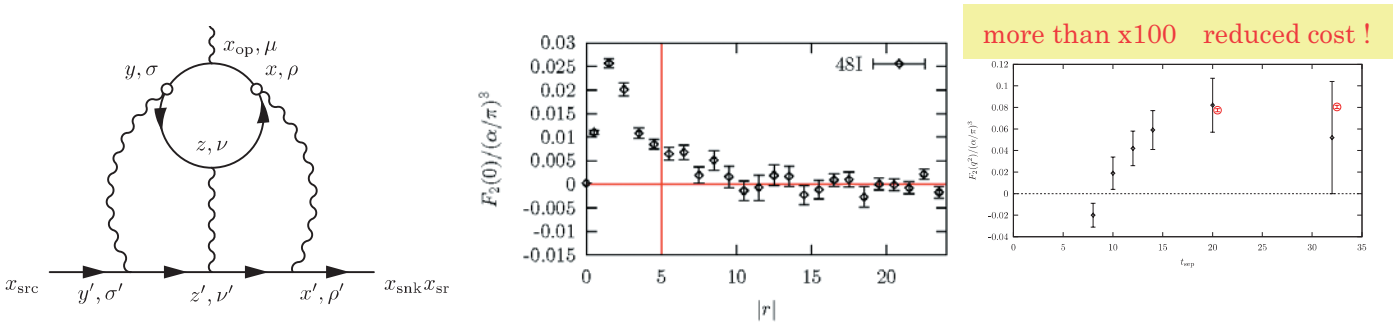

Figure: Hadronic Light-by-light contribution to muon's anomalous moment, diagram, integrand, results, which is improved by more than two order of magnitudes compared to previous calculation.

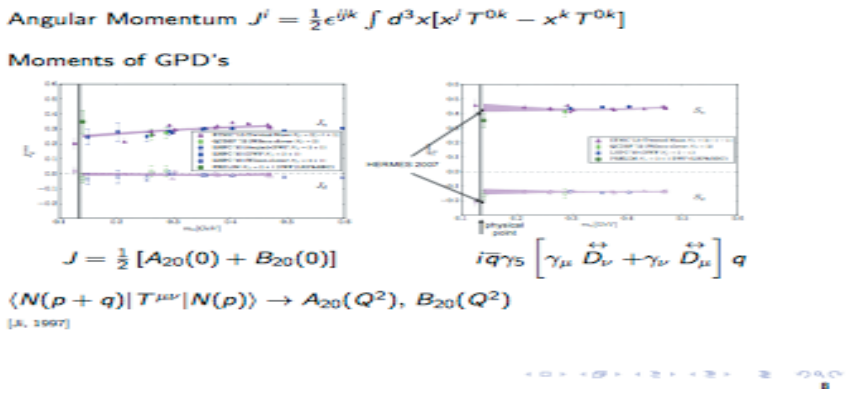

Figure: Preliminary results for Nucleon's Angular momentum (Moments of Generalized Parton Distributions)

The RBRC group and its collaborators have emphasized the necessity and importance of precision calculations, which will precisely check the current understandings of nature, and will have a potential to find physics beyond the current standard model of fundamental physics. We have therefore adopted techniques that aim to control and reduce any systematic errors. This approach has yielded many reliable results, many of basic quantities are now computed within sub-percent accuracies.

The group also delivers an algorithmic breakthrough, which speed up generic lattice gauge theory computation. In this novel technique called All Mode Averaging (AMA), the whole calculation is divided into frequent approximated calculations, and infrequent expensive and accurate calculation using lattice symmetries. Together with another formalism, zMobius fermion, which approximate chiral lattice quark action efficiently, the typical calculation is now improved by a couple of orders of magnitudes compared to the traditional methods.

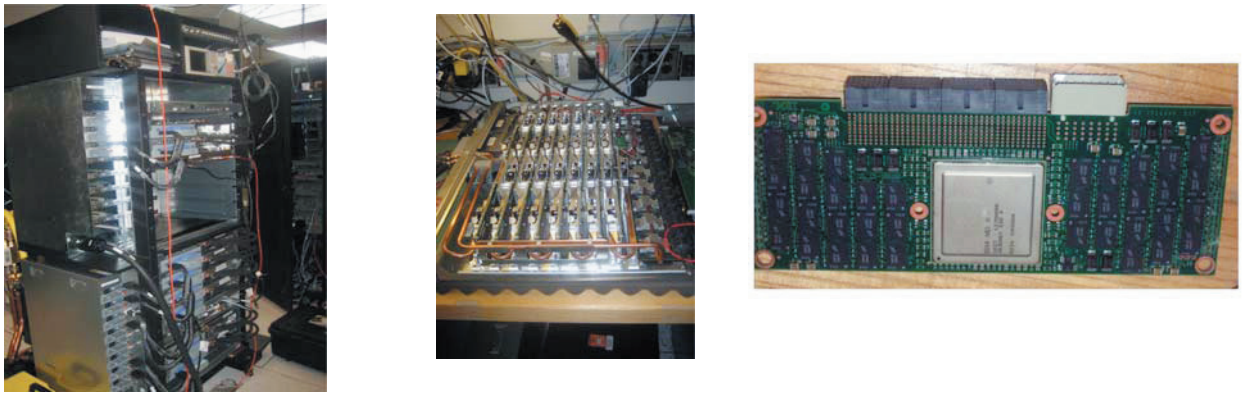

Fig. The rack, motherboard, and chip of QCDCQ

Members

Group Leader (Lab. Head)
Taku IZUBUCHI

RBRC Researcher
Tomomi ISHIKAWA (RIKEN BNL Fellow)
Brian TIBURZI (RHIC Physics Fellow)
Ethan NEIL (RHIC Physics Fellow)
Stefan MEINEL (RHIC Physics Fellow)
Christopher KELLY (Foreign Postdoctoral Researcher)
Hiroshi OKI (Special Postdoctoral Researcher)

Visiting Scientists
Yasumichi AOKI (Nagoya Univ.)
Thomas BLUM (Univ. of Connecticut)
Chulwoo JUNG (BNL)
Christoph LEHNER (BNL)
Meifeng LIN (Yale Univ.)
Robert MAWHINNEY (Columbia)
Shigemi OHTA
Eigo SHINTANI (concurrent, Jul. 1, 2015 -, RIKEN AICS)
Sergey SYRITSYN (Thomas Jefferson National Laboratory)

List of Publications & Presentations

Publications

[Journal]

(Original Papers) *Subject to Peer Review

T. Blum, P.A. Boyle, L. Del Debbio, R.J. Hudspith, T. Izubuchi, A. Jüttner, C. Lehner, R. Lewis, K. Maltman, M. Krstić Marinković, A. Portelli, M. Spraggs (RBC and UKQCD Collaborations), "Lattice calculation of the leading strange quark-connected contribution to the muon g−2", Journal of High Energy Physics, April 2016, 2016 :63, 2016/4/11*

T. Blum, P. A. Boyle, T. Izubuchi, L. Jin, A. Jüttner, C. Lehner, K. Maltman, M. Marinkovic, A. Portelli, and M. Spraggs (RBC and UKQCD Collaborations), "Calculation of the Hadronic Vacuum Polarization Disconnected Contribution to the Muon Anomalous Magnetic Moment", Physical Review Letters Volume 116, Article 232002, 2016/6/8*

Eigo Shintani, Thomas Blum, Taku Izubuchi, and Amarjit Soni (RBC and UKQCD collaborations), "Neutron and proton electric dipole moments from Nf=2+1 domain-wall fermion lattice QCD", Physical Review D Volume 93, Article 094503, 2016/5/5*

Thomas Blum, Norman Christ, Masashi Hayakawa, Taku Izubuchi, Luchang Jin, Christoph Lehner, "Lattice Calculation of Hadronic Light-by-Light Contribution to the Muon Anomalous Magnetic Moment", Physical Review D Volume 93, Article 014503, 2016/1/12*

Z. Bai, T. Blum, P. A. Boyle, N. H. Christ, J. Frison, N. Garron, T. Izubuchi, C. Jung, C. Kelly, C. Lehner, R. D. Mawhinney, C. T. Sachrajda, A. Soni, and D. Zhang (RBC and UKQCD Collaborations), "Standard Model Prediction for Direct CP Violation in K→ππ Decay", Physical Review Letters Volume 115, Article 212001, 2015/11/17*

J. M. Flynn, T. Izubuchi, T. Kawanai, C. Lehner, A. Soni, R. S. Van de Water, and O. Witzel (RBC and UKQCD Collaborations), "B→πℓν and Bs→Kℓν form factors and |Vub| from 2+1-flavor lattice QCD with domain-wall light quarks and relativistic heavy quarks", Physical Review D Volume 91, Article 074510, 2015/4/14*

Matthew E. Matzelle and Brian C. Tiburzi "Low-energy QCD in the delta regime", Physical Review D Volume 93, Article 034506, 2016/2/23*

William Detmold, Kostas Orginos, Assumpta Parreño, Martin J. Savage, Brian C. Tiburzi, Silas R. Beane, and Emmanuel Chang (NPLQCD Collaboration), "Unitary Limit of Two-Nucleon Interactions in Strong Magnetic Fields", Physical Review Letters Volume 116, Article 112301, 2016/3/14*

Jong-Wan Lee and Brian C. Tiburzi "Finite volume corrections to the electromagnetic mass of composite particles", Physical Review D Volume 93, Article 034012, 2016/2/8*

Michael G. Endres, Andrea Shindler, Brian C. Tiburzi, Andre Walker-Loud "Massive photons: an infrared regularization scheme for lattice QCD+QED", arXiv:1507.08916.

Emmanuel Chang, William Detmold, Kostas Orginos, Assumpta Parreño, Martin J. Savage, Brian C. Tiburzi, and Silas R. Beane (NPLQCD Collaboration), "Magnetic structure of light nuclei from lattice QCD", Physical Review D Volume 92, Article 114502, 2015/12/9*

Silas R. Beane, Emmanuel Chang, William Detmold, Kostas Orginos, Assumpta Parreño, Martin J. Savage, and Brian C. Tiburzi (NPLQCD Collaboration), "Ab initio Calculation of the np→dγ Radiative Capture Process", Physical Review Letters Volume 115, Article132001, 2015/9/24*

Brian C. Tiburzi, "Chiral corrections to nucleon two- and three-point correlation functions", Physical Review D Volume 91, Article 094510, 2015/5/19*

Thomas Appelquist, Richard C. Brower, George T. Fleming, Anna Hasenfratz, Xiao-Yong Jin, Joe Kiskis, Ethan T. Neil, James C. Osborn, Claudio Rebbi, Enrico Rinaldi, David Schaich, Pavlos Vranas, Evan Weinberg, Oliver Witzel "Strongly interacting dynamics and the search for new physics at the LHC"arXiv:1601.04027v2 [hep-lat] 28 Jan 2016

Jon A. Bailey, A. Bazavov, C. Bernard, C. M. Bouchard, C. DeTar, Daping Du, A. X. El-Khadra, J. Foley, E. D. Freeland, E. Gámiz, Steven Gottlieb, U. M. Heller, R. D. Jain, J. Komijani, A. S. Kronfeld, J. Laiho, L. Levkova, Yuzhi Liu, P. B. Mackenzie, Y. Meurice, E. T. Neil, Si-Wei Qiu, J. N. Simone, R. Sugar, D. Toussaint, R. S. Van de Water, Ran Zhou, (Fermilab Lattice and MILC Collaborations), "B→Kl+l− decay form factors from three-flavor lattice QCD" Phys. Rev. D 93, 025026 – Published 27 January 2016*

Jon A. Bailey, A. Bazavov, C. Bernard, C. M. Bouchard, C. DeTar, Daping Du, A. X. El-Khadra, J. Foley, E. D. Freeland, E. Gámiz, Steven Gottlieb, U. M. Heller, J. Komijani, A. S. Kronfeld, J. Laiho, L. Levkova, Yuzhi Liu , P. B. Mackenzie, Y. Meurice, E. T. Neil, Si-Wei Qiu, J. Simone, R. Sugar, D. Toussaint, R. S. Van de Water, Ran Zhou, Fermilab Lattice and MILC Collaborations), "|Vub| from B→πℓν decays and (2+1)-flavor lattice QCD" Phys. Rev. D 92, 014024 – Published 23 July 2015*

Jon A. Bailey, A. Bazavov, C. Bernard, C. M. Bouchard, C. DeTar, Daping Du, A. X. El-Khadra, J. Foley, E. D. Freeland, E. Gámiz, Steven Gottlieb, U. M. Heller, J. Komijani, A. S. Kronfeld, J. Laiho, L. Levkova, Yuzhi Liu , P. B. Mackenzie, Y. Meurice, E. T. Neil, Si-Wei Qiu, J. Simone, R. Sugar, D. Toussaint, R. S. Van de Water, Ran Zhou, Fermilab Lattice and MILC Collaborations), "The B→Dℓν form factors

at nonzero recoil and |Vcb| from 2+1-flavor lattice QCD", Phys. Rev. D 92, 034506 – Published 10 August 2015*

T. Appelquist, E. Berkowitz, R. C. Brower, M. I. Buchoff, G. T. Fleming, X.-Y. Jin, J. Kiskis, G. D. Kribs, E. T. Neil, J. C. Osborn, C. Rebbi, E. Rinaldi, D. Schaich, C. Schroeder, S. Syritsyn, P. Vranas, E. Weinberg, and O. Witzel (Lattice Strong Dynamics (LSD) Collaboration) "Detecting Stealth Dark Matter Directly through Electromagnetic Polarizability", Phys. Rev. Lett. 115, 171803 – Published 23 October 2015*

T. Appelquist, R. C. Brower, M. I. Buchoff, G. T. Fleming, X.-Y. Jin, J. Kiskis, G. D. Kribs, E. T. Neil, J. C. Osborn, C. Rebbi, E. Rinaldi, D. Schaich, C. Schroeder, S. Syritsyn, P. Vranas, E. Weinberg, and O. Witzel (Lattice Strong Dynamics (LSD) Collaboration) "Stealth dark matter: Dark scalar baryons through the Higgs portal", Phys. Rev. D 92, 075030 – Published 23 October 2015*

Thomas DeGrand, Yuzhi Liu, Ethan T. Neil, Yigal Shamir, and Benjamin Svetitsky "Spectroscopy of SU(4) gauge theory with two flavors of sextet fermions", Phys. Rev. D 91, 114502 – Published 10 June 2015*

Stefan Meinel, Danny van Dyk "Using Λb→Λ μ +μ− data within a Bayesian analysis of |ΔB|=|ΔS|=1 decays" arXiv:1603.02974v1 [hep-ph] 9 Mar 2016

William Detmold and Stefan Meinel "Λb→Λℓ+ℓ− form factors, differential branching fraction, and angular observables from lattice QCD with relativistic b quarks" Phys. Rev. D 93, 074501 – Published 1 April 2016*

William Detmold, Christoph Lehner, and Stefan Meinel "Λb→pℓ− ν ¯ℓ and Λb→Λcℓ− ν ¯ℓ form factors from lattice QCD with relativistic heavy quarks" Phys. Rev. D 92, 034503 – Published 4 August 2015*

P.A. Boyle, N.H. Christ, N. Garron, C. Jung, A. Jüttner, C. Kelly, R.D. Mawhinney, G. McGlynn, D.J. Murphy, S. Ohta, A. Portelli, C.T. Sachrajda, "The Low Energy Constants of SU(2) Partially Quenched Chiral Perturbation Theory from Nf = 2+1 Domain Wall QCD" Phys. Rev. D 93, 054502 – Published 9 March 2016*

T. Blum, P. A. Boyle, N. H. Christ, J. Frison, N. Garron, T. Janowski, C. Jung, C. Kelly, C. Lehner, A. Lytle, R. D. Mawhinney, C. T. Sachrajda, A. Soni, H. Yin, and D. Zhang (RBC and UKQCD Collaborations) "K→π π ΔI=3/2 decay amplitude in the continuum limit" Phys. Rev. D 91, 074502 – Published 6 April 2015*

[Proceedings]

(Original Papers) *Subject to Peer Review

Meifeng Lin, Eric Papenhausen, M. Harper Langston, Benoit Meister, Muthu Baskaran, Taku Izubuchi, Chulwoo Jung "Optimizing the domain wall fermion Dirac operator using the R-Stream source-to-source compiler", Proceedings of the 33rd International Symposium on Lattice Field Theory, PoS(Lattice 2015) 022.

Luchang Jin, Thomas Blum, Norman Christ, Masashi Hayakawa, Taku Izubuchi, Christoph Lehner, "Hadronic Light by Light Contributions to the Muon Anomalous Magnetic Moment With Physical Pions", Proceedings of the 33rd International Symposium on Lattice Field Theory, arXiv:1511.05198.

Masashi Hayakawa, Thomas Blum, Norman Christ, Taku Izubuchi, Luchang Jin, Christoph Lehner, "On calculating disconnected-type hadronic light-by-light scattering diagrams from lattice QCD", Proceedings of the 33rd International Symposium on Lattice Field Theory, arXiv:1511.01493.

Salman Habib, Robert Roser, Tom LeCompte, Zach Marshall, Anders Borgland, Brett Viren, Peter Nugent, Makoto Asai, Lothar Bauerdick, Hal Finkel, Steve Gottlieb, Stefan Hoeche, Paul Sheldon, Jean-Luc Vay, Peter Elmer, Michael Kirby, Simon Patton, Maxim Potekhin, Brian Yanny, Paolo Calafiura, Eli Dart, Oliver Gutsche, Taku Izubuchi, Adam Lyon, Don Petravick, "High Energy Physics Forum for Computational Excellence: Working Group Reports (I. Applications Software II. Software Libraries and Tools III. Systems)", arXiv:1510.08545 , Oct 28, 2015. 76 pp.

Luchang Jin, Thomas Blum, Norman Christ, Masashi Hayakawa, Taku Izubuchi, Christoph Lehner, "Lattice Calculation of the Connected Hadronic Light-by-Light Contribution to the Muon Anomalous Magnetic Moment", Proceedings of the 33rd International Symposium on Lattice Field Theory, arXiv:1509.08372.

Christoph Lehner, Taku Izubuchi, "Towards the large volume limit - A method for lattice QCD + QED simulations", Proceedings of the 32nd International Symposium on Lattice Field Theory, arXiv:1503.04395

Tomomi Ishikawa, Yasumichi Aoki , Taku Izubuchi , Christoph Lehner, Amarjit Soni "B meson decay constants and ΔB=2ΔB=2 matrix elements with static heavy and doma in-wall light quarks", Proceedings of the 32nd International Symposium on Lattice Field Theory, PoS LATTICE2014 (2015) 376

Michael G. Endres, Andrea Shindler, Brian C. Tiburzi, Andre Walker-Loud, "Photon mass term as an IR regularization for QCD+QED on the lattice", Proceedings of the 33rd International Symposium on Lattice Field Theory, arXiv:1512.08983.

Brian C. Tiburzi, "Excited-state contamination in nucleon correlators from chiral perturbation theory", Proceedings of the 8th International Workshop on Chiral Dynamics, arXiv:1508.00163.

Piotr Korcyl, Christoph Lehner, Tomomi Ishikawa "Non-perturbative renormalization of the static quark theory in a large volume", Proceedings of the 33rd International Symposium on Lattice Field Theory, PoS(LATTICE2015) 254.

Tomomi Ishikawa, Yasumichi Aoki, Taku Izubuchi, Christoph Lehner, Amarjit Soni "B meson decay constants and ΔB=2ΔB=2 matrix elements with static heavy and doma in-wall light quarks", Proceedings of the 32nd International Symposium on Lattice Field Theory, , PoS LATTICE2014 (2015) 376

Yasumichi Aoki, Tatsumi Aoyama, Ed Bennett, Masafumi Kurachi, Toshihide Maskawa, Kohtaroh Miura, Kohtaroh Miura, Kei-ichi Nagai, Hiroshi Ohki, Enrico Rinaldi, Akihiro Shibata, Koichi Yamawaki, Takeshi Yamazaki "Lattice Studies on 8-Flavor QCD in The Light of Physics Beyond The Standard Model" 18th Montpellier International Conference on Quantum Chromodynamics (QCD 15), Nucl.Part.Phys.Proc. 270-272 (2016) 242-246

Yasumichi Aoki, Tatsumi Aoyama, Ed Bennett, Masafumi Kurachi, Toshihide Maskawa, Kohtaroh Miura, Kei-ichi Nagai, Hiroshi Ohki, Enrico Rinaldi, Akihiro Shibata, Koichi Yamawaki, Takeshi Yamazaki "Lattice study of the scalar and baryon spectra in many-flav" Contribution to Sakata Memorial KMI Workshop on "Origin of Mass and Strong Coupling Gauge Theories (SCGT15)", 3-6 March 2015, Nagoya University, arXiv:1510.07373

Cynthia Y.-H. Huang, Issaku Kanamori, C.-J. David Lin, Kenji Ogawa, Hiroshi Ohki, Alberto Ramos, Enrico Rinaldi "Lattice study for conformal windows of SU(2) and SU(3) gauge theories with fundamental fermions" Proceedings of the 33rd International Symposium on Lattice Field Theory, arXiv:1511.01968

N. Yamanaka, H. Ohki, S. Hashimoto, T. Kaneko "Nucleon axial and tensor charges with dynamical overlap quarks" Proceedings of the 33rd International Symposium on Lattice Field Theory, arXiv:1511.04589

Yasumichi Aoki, Tatsumi Aoyama, Ed Bennett, Masafumi Kurachi, Toshihide Maskawa, Kohtaroh Miura, Kei-ichi Nagai, Hiroshi Ohki, Enrico Rinaldi, Akihito Shibata, Koichi Yamawaki, Takeshi Yamazaki "Walking and conformal dynamics in many-flavor QCD" Proceedings of the 33rd International Symposium on Lattice Field Theory, arXiv:1601.02287

Shigemi Ohta "Some nucleon isovector observables from 2+1-flavor domain-wall QCD at the physical pion mass" The 33rd International Symposium on Lattice Field Theory 14 -18 July 2015 Kobe International Conference Center, Kobe, Japan

Sergey Syritsyn "Nucleon Structure on a Lattice at the Physical Point" Journal of Physics: Conference Series, Volume 640, conference 1

[Book]

(Original Papers) *Subject to Peer Review

Brian C. Tiburzi "Chiral Perturbation Theory", Lattice QCD for Nuclear Physics, Volume 889 of the series Lecture Notes in Physics pp 107-152, 2014/9/18

Oral Presentations

[International Conference etc.]

T. Blum "Progress on the muon anomalous magnetic momen from lattice QCD" Plenary talk (ChiralDynamics15)

T. Blum "Precision EW calculations for future experiments" Invited talk (Aspen Winter Conference on Particle Physics 2016)

T. Blum "hadronic contributions to the muon g-2" Invited talk (DPF-APS April Meeting 2016)

N. Christ, "Lattice QCD calculation of direct CP violation and long distance effects in kaon mixing and rare decays" Plenary talk (Flavor Physics & CP Violation, Nagoya, May 2015)

N. Christ, "Using high performance computing to relate asymmetries in particle decays and Physics at the highest energies", Invited talk, (Higgs Symposium, Edinburgh, Jan 2015)

T. Izubuchi, "Recent results of Lattice QCD using chiral quarks" Invited talk, Symposium on Quarks to Universe in Computational Science (QUCS 2015) November 4 -8 (talk November 4) 2015 , Nara, Japan

T. Izubuchi, "Inclusive tau decay and Lattice QCD" Invited talk, Kavli Institute for Theoretical Physics, "Lattice Gauge Theory for the LHC and Beyond" September 7 - 27 (talk on Sep 23), 2015

T. Izubuchi, "Anomalous magnetic moment of the muon" Plenary talk, Mainz Institute for Theoretical Physics workshop "Fundamental Parameters from Lattice QCD" August 29 - September 5 (talk on Sep 1), 2015

T. Izubuchi, "g-2 LbL" Invited talk, Benasque workshop "High Precision QCD at low energy" August 2-12 (talk on Aug 5), 2015

T. Izubuchi, "Latice QCD moments - g-2 and nEDM-" Plenary talk, The 33rd International Symposium on Lattice Field Theory, Kobe, Japan July 14-18, 2015 (talk on July 14)

T. Izubuchi, "Nucleon Structures using Lattice QCD" Invited talk, April 8-10 (talk on April 9), 2015, The 6th workshop of topical group on hadronic physics, APS, Baltimore, MD

T. Izubuchi, "Introduction to forefront research topics at zero temperature Lattice Gauge Theory" Six 1.5-hours-long invited lectures Mar 16-20, 2015, The 4th Huada QCD school on Lattice QCD

1. General Introduction
2. Chiral Fermion 1
3. Chiral Fermion 2
4. Chiral Fermion 3
5. Algorithm
6. Particle Physics applications

T. Izubuchi, "All-mode averaging, zMobius, and their possible applications including DWF measurements on GPU" Invited talk, CCS-BNL LGT2015 workshop, Mar 12-13, 2015, Tsukuba Univ, Tsukuba, Japan

T. Izubuchi, "Nucleon's Electric Dipole Moment from quark's chromo EDM operator" Invited talk, May 1-2 (talk on May 1), 2015, USQCD All hands meeting, FNAL, IL

E. Neil, "New Ideas for the Composition of Dark Matter" Plenary, KITP Blackboard Talk (Lattice Gauge Theory for LHC and Beyond), August 2015

S. Meinel, "Lattice progress for semileptonic b decays", Invited talk (Implications of LHCb measurements and future prospects, CERN, 2015)

S. Meinel, "Hints for physics beyond the Standard Model in decays of beauty quarks", Colloquium (University of Utah, 2015)

S. Meinel, "Determination of $|V_{ub}/V_{cb}|$ using baryonic decays", Invited talk (Brookhaven Forum 2015)

S. Meinel, "Rare b decays", Invited talk (LHP V, 2015)

S. Meinel, "Determination of $|V_{ub}/V_{cb}|$ using baryonic decays", Plenary talk (Lattice 2015)

S. Meinel, "Rare b decays and lattice QCD", Invited talk (CIPANP 2015)

S. Meinel, "Lattice QCD and the search for new physics using beauty quarks", Invited talk (APS Four Corners Meeting, 2014)

C. Kelly, "Kaon decays on the lattice", Plenary talk (5th KEK Flavor Factory Workshop [KEK-FF2015]", Tokyo, Japan 10/2015)

C. Kelly, "CP violation in the kaon sector on the lattice", Plenary talk (MITP workshop: Fundamental Parameters in Lattice QCD", Johannes Gutenberg University Mainz, Germany 09/2015)

C. Kelly, "Standard model prediction for direct CP-violation in K→ππ decay", Plenary talk (Lattice 2015, Kobe, Japan 07/2015)

H. Ohki, (Invited talk) "Composite Scalar Spectrum in many-flavor QCD", KITP Program: Lattice Gauge Theory for the LHC and Beyond, The Kavli Institute for Theoretical Physics, University of California, Santa Barbara, USA, September 18, 2015.

S. Syritsyn " Nucleon structure results from LQCD using Wilson fermions ", April 8-10 (talk on April 9), 2015, The 6th workshop of topical group on hadronic physics, APS, Baltimore, MD

C. Kelly, "Standard model prediction for direct CP-violation in K→ππ decay", Seminar (Los Alamos National Laboratory, USA 12/2015)

C. Kelly, "Standard model prediction for direct CP-violation in K→ππ decay", Seminar (High Energy Accelerator Research Organization [KEK], Tsukuba, Japan 10/2015)

C. Kelly, "Lattice measurement of the Δ I = 1/2 contribution to Standard Model direct CP-violation in $K¥to¥pi¥pi$ decays at physical kinematics", Seminar (University of Edinburgh, UK 09/2014)

Meifeng Lin, Eric Papenhausen, M. Harper Langston, Benoit Meister, Muthu Baskaran, Taku Izubuchi, Chulwoo Jung "Optimizing the domain wall fermion Dirac operator using the R-Stream source-to-source compiler", Proceedings of the 33rd International Symposium on

Lattice Field Theory.
Hiroshi Ohki, “Walking and conformal dynamics in many-flavor QCD” Proceedings of the 33rd International Symposium on Lattice Field Theory
Hiroshi Ohki, “Lattice Study of Walking Dynamics in Many-flavor QCD”, Brookhaven Forum 2015: Great Expectations, a New Chapter, Brookhaven National Laboratory, October 7, 2015.
Shigemi Ohta ”Some nucleon isovector observables from 2+1-flavor domain-wall QCD at the physical pion mass” The 33rd International Symposium on Lattice Field Theory 14 -18 July 2015 Kobe International Conference Center, Kobe, Japan
[Domestic Conference]
Hiroshi Ohki, Lattice study of the scalar and baryon spectra in many-flav” Contribution to Sakata Memorial KMI Workshop on "Origin of Mass and Strong Coupling Gauge Theories (SCGT15)", 3-6 March 2015, Nagoya University,

Sub Nuclear System Research Division
RIKEN-BNL Research Center
Experimental Group

1. Abstract

RIKEN BNL Research Center (RBRC) Experimental Group studies the strong interactions (QCD) using RHIC accelerator at Brookhaven National Laboratory, the world first heavy ion collider and polarized p+p collider. We have three major activities: Spin Physics at RHIC, Heavy ion physics at RHIC, and detector upgrades of PHENIX experiment at RHIC.

We study the spin structure of the proton using the polarized proton-proton collisions at RHIC. This program has been promoted by RIKEN's leadership. The first focus of the research is to measure the gluon spin contribution to the proton spin. Recent results from PHENIX pi0 measurement and STAR jet measurement has shown that gluons in the proton carry about 30% of the proton spin. This is a major milestone of RHIC spin program. The second goal of the spin program is to measure the polarization of anti-quarks in the proton using W→e and W→μ decays. The results of W->e measurement was published.

The aim of Heavy ion physics at RHIC is to re-create Quark Gluon Plasma (QGP), the state of Universe just after the Big Bang. Two important discoveries, jet quenching effect and strong elliptic flows, have established that new state of dense matter is indeed produced in heavy ion collisions at RHIC. We are now studying the property of the matter. Recently, we have measured direct photons in Au+Au collisions for $1<p_T<3$ GeV/c, where thermal radiation from hot QGP is expected to dominate. The comparison between the data and theory calculations indicates that the initial temperature of 300 MeV to 600 MeV is achieved. These values are well above the transition temperature to QGP, which is calculated to be approximately 160 MeV by lattice QCD calculations.

We have major roles in detector upgrades of PHENIX experiment, namely, the silicon vertex tracker (VTX) and muon trigger upgrades. Both of the upgrade is now complete. The VTX is the main device to measure heavy quark (charm and bottom) production and the muon trigger is essential for W→μ measurement. The results from the first run with VTX detector in 2011 was published. The results show that electrons from bottom quark decay is strongly suppressed at high pT, but the suppression is weaker than that of charm decay electron for 3<pT<4 GeV/c. This is the first observation of bottom decay electron suppression as well as the first observation that energy loss of bottom quark is different from that of charm. We have recorded 10 times as much Au+Au collisions data in each of the 2014 run and 2016 run. The large dataset will produce definitive results on heavy quark production at RHIC.

2. Major Research Subjects

(1) Experimental Studies of the Spin Structure of the Nucleon
(2) Study of Quark-Gluon Plasma at RHIC
(3) PHENIX detector upgrades

3. Summary of Research Activity

We study the strong interactions (QCD) using the RHIC accelerator at Brookhaven National Laboratory, the world first heavy ion collider and polarized p+p collider. We have three major activities: Spin Physics at RHIC, Heavy ion physics at RHIC, and detector upgrades of PHENIX experiment.

(1) Experimental study of spin structure of proton using RHIC polarized proton collider

How is the spin of proton formed with 3 quarks and gluons? This is a very fundamental question in Quantum Chromodynamics (QCD), the theory of the strong nuclear forces. The RHIC Spin Project has been established as an international collaboration between RIKEN and Brookhaven National Laboratory (BNL) to solve this problem by colliding two polarized protons for the first time in history. This project also has extended the physics capabilities of RHIC.

The first goal of the Spin Physics program at RHIC is to determine the gluon contribution to proton spin. It is known that the spin of quark accounts for only 25% of proton spin. The remaining 75% should be carried either by the spin of gluons or the orbital angular momentum of quarks and gluons. One of the main goals of the RHIC spin program has been to determine the gluon spin contribution. Before the start of RHIC, there was little experimental constraint on the gluon polarization, ΔG.

PHENIX measures the double helicity asymmetry (A_{LL}) of π^0 production to determine the gluon polarization. Our most recent publication of pi0 ALL measurement at 510 GeV shows non-zero value of ALL, indicating that gluons in the proton is polarized. Global analysis shows that approximately 30% of proton spin is carried by gluons.

RHIC achieved polarized p+p collisions at 500 GeV in 2009. The collision energy increased to 510 GeV in 2012 and 2013. The main goal of these high energy p+p run is to measure anti-quark polarization via single spin asymmetry A_L of the W production. We upgraded the muon trigger system to measure W→m decays in the forward direction. With the measurement of W→ e and W→μ, we can cover a wide kinematic range in anti-quark polarization measurement. The 2013 run is the main spin run at 510 GeV. PHENIX has recorded more than 150/pb of data in the run. The final results of the A_L measurement in W→e channel in combined data of 2011 to 2013 was published. The high statistics results give strong constraints on the polarization of anti-quarks in the proton. The analysis of W→μ is in progress.

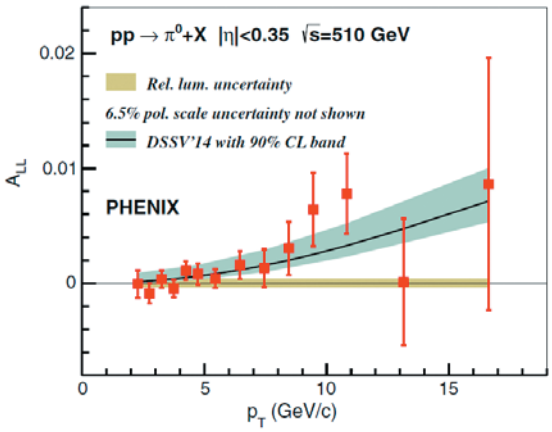

Figure 1 Double spin asymmetry ALL in π^0 production as function of transverse momentum pT. The non-zero ALL indicates that gluons in the proton is polarized. Published in Physical Review D93,011501 (2016)

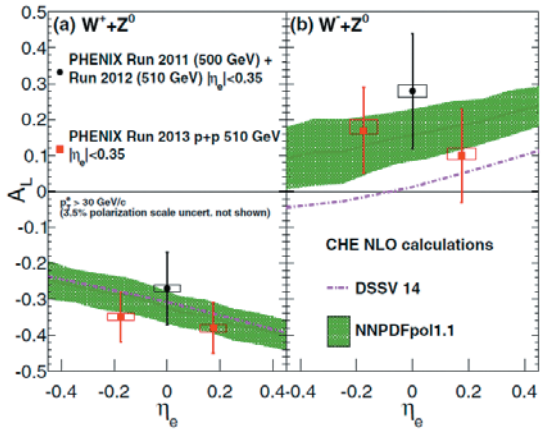

Figure 2 Single spin asymmetry AL of electrons from W and Z decays. The AL is sensitive to the polarization of anti-quarks in the proton. The curves and green shaded region show theoretical calculations based on various polarized parton distribution (PDF) sets. Published in Physical Review D93, 051103(R) (2016)

(2) Experimental study of Quark-Gluon Plasma using RHIC heavy-ion collider

The goal of high energy heavy ion physics at RHIC is study of QCD in extreme conditions i.e. at very high temperature and at very high energy density. Experimental results from RHIC have established that dense partonic matter is formed in Au+Au collisions at RHIC. The matter is very dense and opaque, and it has almost no viscosity and behaves like a perfect fluid. These conclusions are primarily based on the following two discoveries:

- Strong suppression of high transverse momentum hadrons in central Au+Au collisions (jet quenching)
- Strong elliptic flow

These results are summarized in PHENIX White paper, which has approximately 2200 citations to date.

The focus of the research in heavy ion physics at RHIC is now to investigate the properties of the matter. RBRC have played the leading roles in some of the most important results from PHENIX in the study of the matter properties. These include (1) measurements of heavy quark production from the single electrons from heavy flavor decay (2) measurements of J/Psi production (3) measurements of di-electron continuum and (4) measurements of direct photons.

The most important recent result is the measurement of direct photons for $1<p_T<5$ GeV/c in p+p and Au+Au through their internal conversion to e+e- pairs. If the dense partonic matter formed at RHIC is thermalized, it should emit thermal photons. Observation of thermal photon is direct evidence of early thermalization, and we can determine the initial temperature of the matter. It is predicted that thermal photons from QGP phase is the dominant source of direct photons for $1<p_T<3$ GeV/c at the RHIC energy. We measured the direct photon in this p_T region from measurements of quasi-real virtual photons that decays into low-mass e+e- pairs. Strong enhancement of direct photon yield in Au+Au over the scaled p+p data has been observed. Several hydrodynamical models can reproduce the central Au+A data within a factor of two. These models assume formation of a hot system with initial temperature of Tinit = 300 MeV to 600 MeV. This is the first measurement of initial temperature of quark gluon plasma formed at RHIC. These results are recently published in Physical Review Letters. Y. Akiba is the leading person of the analysis and the main author of the paper. **He received 2011 Nishina memorial Prize mainly based on this work.**

(3) PHENIX detector upgrade

The group has major roles in several PHENIX detector upgrades, namely, the silicon vertex tracker (VTX) and muon trigger upgrades. VTX is a high precision charged particle tracker made of 4 layers of silicon detectors. It is jointly funded by RIKEN and the US DOE. The inner two layers are silicon pixel detectors and the outer two layers are silicon strip detectors. Y. Akiba is the project manager and A. Deshpande is the strip system manager. The VTX detector was completed in November 2010 and subsequently installed in PHENIX. The detector started taking data in the 2011 run. With the new detector, we measure heavy quark (charm and bottom) production in p+p, A+A collisions to study the properties of quark-gluon plasma. The final result of the 2011 run was published. The result show that single electrons from bottom quark decay is suppressed, but not as strong as that from charm decay in low pT region (3<pT<4 GeV/c). This is the first measurement of suppression of bottom decay electrons at RHIC and the first observation that bottom suppression is smaller than charm. We have recorded 10 times as much Au+Au collisions data in each of the 2014 run and 2016 run. The large dataset will produce definitive results on heavy quark production at RHIC.

Muon trigger upgrades are needed for W→μ measurement at 500 GeV. New trigger electronics (Muon Trigger FEE) and new Muon trigger detectors using RPC technology were installed in PHENIX muon arms. Additional hadron absorbers were installed in front of the muon arms to reduce the background. These upgrades were essential for the high statistic W→μ measurement in 2013 run. Over 150/pb of data was recorded in the run.

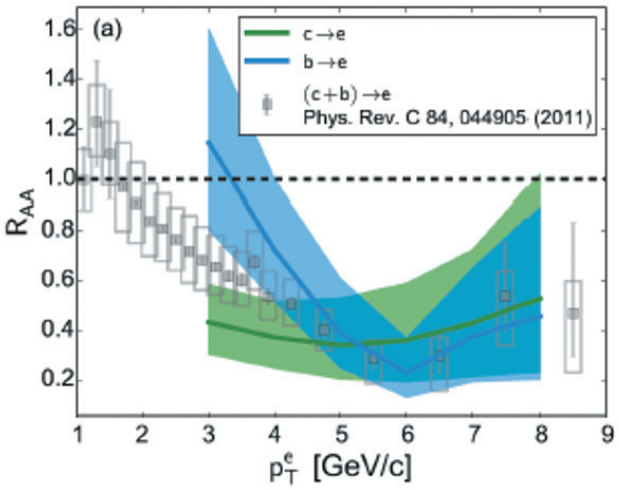

Figure 3. Nuclear modification factor RAA for single electrons from charm (green band) and bottom (blue band) decays. Published in Physical Review C93, 034904 (2016)

Members

Group Leader (Lab. Head)

Yasuyuki AKIBA (Deputy Chief Scientist)

Deputy Group Leader

Abhay DESHPANDE

RBRC Researcher

Zheng LI (– Mar. 31, 2015)
Kieran BOYLE (RIKEN BNL Fellow － Mar. 27, 2015)
Xiaorong WANG (RHIC Physics Fellows)
Takashi HACHIYA (Oct.1 2015 –)
Yorito YAMAGUCHI (Nov. 15, 2015 –)
Gaku MITSUKA (Jun. 1, 2015 –)
Yasushi WATANABE (RIKEN Spin Program Researcher, concurrent: Radiation Lab.)
Yuji GOTO (RIKEN Spin Program Researcher, concurrent: Radiation Lab.)
Itaru NAKAGAWA (RIKEN Spin Program Researcher, concurrent: Radiation Lab.)
Takashi ICHIHARA (RIKEN Spin Program Researcher, concurrent: RI Physics Lab.)
Atsushi TAKETANI (RIKEN Spin Program Researcher, concurrent: Neutoron Beam Technology Team, Advanced Photonics Technology development Group, RAP)
Satoshi YOKKAICHI (RIKEN Spin Program Researcher, concurrent: Radiation Lab.)
Ralf SEIDL (RIKEN Spin Program Researcher, concurrent: Radiation Lab.)

Visiting Scientists

Stefan BATHE (Baruch College University of New York)
Ady HERSHCOVITCH (RBRC Collaborating Scientist, BNL)
Akio OGAWA (BNL)
Rachid NOUICER (RBRC Collaborating Scientist)
Masahiro OKAMURA (concurrent: BNL)
Takao SAKAGUCHI (BNL)
Stefan BATHE ((RHIC Physics Fellows – Jan. 31, 2015)

List of Publications & Presentations

Publications

[Journal]

(Original Papers)

G Mitsuka ”Forward hadron production in ultra-peripheral proton–heavy-ion collisions at the LHC and RHIC” The European Physical Journal C, 2015*

Oral Presentations

[International Conference etc.]

Takashi Hachiya, ”Non-prompt "J"/ψ measurement with the PHENIX VTX detector at RHIC” , 32nd Winter Workshop of Nuclear Dynamics - WWND2016

[Domestic Conference]

Takashi Hachiya, ”Non-prompt "J"/ψ measurement with the PHENIX VTX detector at RHIC” , 日本物理学会　第７１回年次大会

Posters Presentations

[International Conference etc.]

Takashi Hachiya, ”Non-prompt "J"/ψ measurement with the PHENIX VTX detector at RHIC” , Quark Matter 2015

Gaku Mitsuka　”Silicon strip detector R&D for the sPHENIX tracker”　Quark Matter 2015

Sub Nuclear System Research Division
RIKEN Facility Office at RAL

1. Abstract

Our core activities are based on the RIKEN-RAL Muon Facility located at the Rutherford Appleton Laboratory (UK), which provides intense pulsed-muon beams. Muons have their own spins with 100% polarization, and can detect local magnetic fields and their fluctuations at muon stopping sites very precisely. The method to study characteristic of materials by observing time dependent changes of muon spin polarization is called "Muon Spin Rotation, Relaxation and Resonance (μSR method), and is applied to study electro-magnetic properties of insulating, metallic, magnetic, superconducting systems. Muons reveal static and dynamic properties of electronic state of materials in the zero-field condition, which is the ideal magnetic condition for researches on the magnetism. We have carried out μSR investigations on frustrated pyrochlore systems, which have variety of exotic ground state of magnetic spins, so the magnetism study of this system using muon is quite unique.

The ultra-slow muon beam can be stopped in thin foil, multi-layered materials and artificial lattices, which enables us to apply the μSR techniques to surface and interface science. The development of ultra-slow muon beam is also very important as a source of ultra-cold (pencil-like small emittance) muon beam for muon g-2/EDM measurement. We have been developing muonium generators to create more muoniums in vacuum even at room temperature to improve beam quality than the conventional hot-tungsten muonium generator. Very recently, we demonstrated tremendous increase of the muonium emission efficiency by fabricating fine laser drill-holes on the surface of silica aerogel. We also developed a high power Lyman-alpha laser in collaboration with the Advanced Photonics group at RIKEN. The new laser will ionize muoniums 100 times more efficiently for slow muon beam generation.

2. Major Research Subjects

(1) Materials science by muon-spin-relaxation method
(2) Hyperfine interactions at muon sites studied by the computation science
(3) Nuclear and particle physics studies via muonic atoms and ultra-cold muon beam

3. Summary of Research Activity

(1) Material Science at the RIKEN-RAL Muon Facility

Muons have their own spins with 100% polarization, and can detect local magnetic fields and their fluctuations at muon stopping sites very precisely. The μSR method is applied to studies of newly fabricated materials. Muons enable us to conduct (1) material studies under external zero-field condition, (2) magnetism studies with samples without nuclear spins, and (3) measurements of muon spin relaxation changes at wide temperature range with same detection sensitivity. The detection time range of local field fluctuations by μSR is 10^{-6} to 10^{-11} second, which is an intermediate region between neutron scattering method (10^{-10}-10^{-12} second) and Nuclear Magnetic Resonance (NMR) (longer than 10^{-6} second). At Port-2 and 4 of the RIKEN-RAL Muon Facility, we have been performing μSR researches on strong correlated-electron systems, organic molecules and biological samples to study electron structures, superconductivity, magnetism, molecular structures and crystal structures.

In the period from 2012 to 2015, we have obtained excellent results, and the highlights are listed in the following,

1) A static ordering of small Ir moments in the pyrochlore iridate; $Nd_2Ir_2O_7$ is close to a quantum critical point.
2) A static ordering of Yb moment on the corner of the pyrochlore structure of $Yb_2Ti_2O_7$ can be explained by the Higgs mechanism.
3) Spontaneous small static internal fields in the superconducting state of URu_2Si_2 is an evidence of the appearance of an exotic superconducting state.
4) Universality class of the Mott transition is confirmed in $EtMe_3P[Pd(dmit)_2]_2$.
5) Finding new muon sites in La_2CuO_4 which can be explained taking into account an effect of the spatial distribution of Cu spin.
6) A novel coexisting state between Fe spin-glass and Cu stripe ordered states in the overdoped regime of $La_{2-x}Sr_xCu_{1-y}Fe_yO_4$.

Result-1 and 2) Solid observations of a statically magnetic-ordered state of corner-shared magnetic moments on pyrochlore systems gave us new interpretations to understand exotic phenomena, like the quantum criticality of magnetic moments and a quasi-magnetic monopole state. Result-3) We measured an increase of static internal fields at the muon site in the zero-field condition just below the superconducting transition temperature of URu_2Si_2. This could shed a light on the mechanism of the superconductivity, which has been a long-standing problem of this system. Result-4) We have been developing gas-pressurized high-pressure apparatus, which can be used not only for μSR but also for other purposes. We have applied this pressure system to $EtMe_3P[Pd(dmit)_2]_2$, and have found that pressure dependent resistivity and thermoelectric coefficient measurements have shown that the Mott transition belongs to the Ising universality class even in two-dimensional states. Result-5) Well known and deeply investigated La_2CuO_4 has opened a new scheme of the Cu spin. Taking into account the effect of the spatial distribution of Cu spin, we have succeeded to explain newly found muon sites and hyperfine fields at those sites. Result-6) Fe spins form a spin glass state through the RKKY interaction in the over-doped regime in $La_{2-x}Sr_xCu_{1-y}Fe_yO_4$. This spin glass state is expected to co-exist with the stripe ordered state at lower temperatures.

We have been developing muon activities in Asian countries. We enhanced international collaborations to organize new μSR experimental groups and to develop muon-site calculation groups using computational method. We have formed MOU with Universiti Sains Malaysia (USM) in order to develop activities on the muon-site calculation. We have newly started collaboration in μSR experiments on strongly correlated systems with researchers from Taiwan and Korea including graduate student.

As for the facility upgrade, we start operating new μSR spectrometer "Chronus", multi-segmented counter arrays of 608 channels, in Port-4, in parallel with ARGUS in Port-2. Software system, for data acquisition and experimental condition control, is unified to the ISIS

standard system (DAE with SECI), which can handle muon signals more than 100 million events per hour, in both Port-2 and 4.

(2) Ultra Slow (low energy) Muon Beam Generation and Applications

Positive muon beam with thermal energy has been produced by laser ionization of muoniums (bound system of μ^+ and electron) emitted from hot tungsten surface with stopping surface muon beam at Port-3. The method generates positive muon beam with acceleration energy from several 100 eV to several 10 keV, small beam size (a few mm) and good time resolution (less than 8 nsec). By stopping the ultra-slow muon beam in thin foil, multi-layered materials and artificial lattices, we can precisely measure local magnetic field in the materials, and apply the μSR techniques to surface and interface science. Since there has been no appropriate probe to study magnetism at surface and interface, the ultra-slow muon beam will open a new area of these research fields. In addition, the development of ultra-slow muon beam is very important as the source of ultra-cold (pencil-like small emittance) muon beam for muon g-2/EDM measurement. It is essential to increase the slow muon beam production efficiency by 100 times for these applications. There are three key techniques in ultra-slow muon generation: production of thermal muonium, high intensity Lyman-alpha laser and the ultra-slow muon beam line.

In the period from 2011 to 2015, we developed a high power Lyman-alpha laser in collaboration with the Advanced Photonics group at RIKEN. The new laser will ionize muoniums 100 times more efficiently for slow muon beam generation. This development was funded mostly by the Grant-in-Aid for Scientific Research on Innovative Areas “Frontier in Materials, Life and Particle Science Explored by Ultra Slow Muon Microscope”. This Grant-in-Aid research group is a complex of research institutions from universities together with J-PARC muon group and RIKEN. The new laser system was installed to J-PARC slow muon beam line and is being used for the generation of ultra-slow muons. In this development, we succeeded to synthesize novel ceramic-based Nd:YGAG crystal, and this crystal can also be applicable to the flash-lamp based Lyman-alpha laser system of RIKEN-RAL to realize substantial improvement of the laser power at a much reduced cost based on the experiences.

We also aimed to realize drastic improvements on the ultra-slow muon source with much reduced emittance. We have been developing muonium generators to create more muoniums in vacuum even at room temperature. In 2013, we demonstrated at least 10 times increase of the muonium emission efficiency by fabricating fine laser drill-holes on the surface of silica aerogel. The measurement was carried out at TRIUMF in collaboration with J-PARC muon g-2/EDM group. We believe that the better efficiency and beam quality can be achieved in ultra-slow muon generation by using this new muonium source.

We are planning to feed these new techniques to RIKEN-RAL ultra-slow muon beam line to realize further development of ultra-slow muon technology. The muonium production target section, which had been designed with hot tungsten, was completely redesigned and rebuilt to use advantage of the new room temperature silica aerogel target, such as no need of thermal shielding and spin control by applying weak magnetic field, etc. Also, we adopted an all-cylindrical beam-transport design, because of its simpler optics and better manufacture precision, which will contribute to the ultimate cold muon source required for muon g-2/EDM. The test experiment with the muon beam started in Sep 2015.

(3) New Proposal for Fundamental Physics

We proposed the measurement of the proton radius by using the hyperfine splitting of the 1S states of muonic hydrogen. Recent measurement of the proton radius using muonic hydrogen at PSI revealed the proton radius is surprisingly smaller than the radius so far measured using normal hydrogen spectroscopy and e-p scattering by more than 5 times their experimental precision. In contrast to the conventional measurement by means of electron, PSI experiment utilized muonic hydrogen atom, and measured two different allowed transitions from one of the 2S levels to one of the 2P levels. The muonic atom has larger sensitivity to the proton radius because the negative muon orbits closer to the proton, although there is no reason why these measurements can yield inconsistent results if there exists no exotic physics or unidentified phenomenon behind. The cause of the discrepancy is not understood yet, thus a new measurement with independent method is much anticipated.

There are two independent experimental proposals to RIKEN-RAL PAC to measure the hyperfine splitting energy of the 1S energy levels by laser excitation from singlet ground state to triplet state. This energy splitting is sensitive to the Zemach radius, which is a convolution of charge and magnetic distributions inside proton. Both are common to search resonant excitation from singlet 1S (F=0) to triplet 1S (F=1) using high intensity 6.7 μm excitation laser, but different scheme are proposed to detect the resonance. One is to detect muon transfer to the surrounding impurity atom by x-ray (European group), and the other is to detect the muon decay asymmetry recovery along the circularly polarized excitation laser, which selectively excites one of the F=1 states and regenerates the muon spin polarization (RIKEN group). RIKEN-RAL PAC accepted both proposals for their feasibility studies.

RIKEN laser group made basic design of the laser system, based on their recent success on mid-infared (6 μm) high-power pulse laser system. There is no direct way to produce 6.7 μm lasers, so we started to test the wavelength conversion efficiency of the laser key components. Other important progress is the background measurement. Since we need to stop muons in extremely low-density hydrogen target to substantially reduce the polarization quenching effect due to the atomic collision, all the muons stopped in the material other than the target can be a background source. Thus, we plan to use high Z materials for the target cell construction, so as all the muons stopping in surrounding materials quickly die out before the laser is introduced. We have started the measurement of long-life background level, and got a reasonably small value. A further study is planned. Refurbishment of the RIKEN-RAL Port 1 experimental area, following removal of muon catalyzed fusion equipment, is in progress for the proton radius experiment.

(4) Other topics

Muon catalyzed fusion has been one of the main subject of studies since the start of the RIKEN-RAL Muon Facility. It has produced many new results by using the advantage of the high-intensity pulsed muon beam and the advanced tritium handling facility as was reported in previous RIKEN-RAL IACs. Even though, huge increase of the catalysis rate that is enough for energy production is yet difficult to achieve. Considering the limited budget and human resources maintaining the tritium facility, we decided the safe closure of the tritium facility. The safe removal of the tritium handling facility was completed in March 2015 – the tritium handling system was transferred to the UK Atomic Energy Authority, a nice partnership activity between RIKEN, STFC and UKAEA.

New demand is emerging utilizing the muon beam for electronic chip radiation effect studies. Recent progress of semiconductor

devices has produced electronics chips with very fine structure. It is anticipated that the single memory upset by the ionization effect of single muon may result in malfunction or errors of advanced electronics. Muon is the main component of the cosmic ray in our ordinal life and difficult to be removed. Measurements are being performed at RIKEN-RAL to measure such an error rate. Already several groups carried out measurements on several different electronics. Although the sensitivity differs from chips to chips, in most cases, the error rate increases when the muon beam momentum is chosen so that the muon nearly stops in the chip itself (Bragg peak effect).

There were also demands for the use of **negative muons for the non-destructive elements analysis** using muonic x-rays. Especially its good depth sensitivity was clearly demonstrated. The applied objects so far are archaeological coins, sword, and oxygen concentration measurement in levers, etc. The first paper on this work has recently been published (‘Probing beneath the surface without a scratch — bulk non-destructive elemental analysis using negative muons’, AD Hillier et al., Microchemical Journal 125 (2016) 203) which describes the technique’s development and potential capabilities. A project has been initiated with STFC’s Technology Department to develop detectors for this application.

Members

Director
Philip KING

Research & Technical Scientist
Isao WATANABE (concurrent: Advanced Meson Science Lab.)

Administration Manager
Mitsuru KISHIMOTO (concurrent: Nishina Center Planning Office)

List of Publications & Presentations

Publications

[Journal]

(Original Papers) *Subject to Peer Review

A.D. Hillier, D.McK. Paul, K. Ishida, “Probing beneath the surface without a scratch — Bulk non-destructive elemental analysis using negative muons”, Microchemical Journal, 125, 203-207 (2016).＊

P. Bakule, O. Sukhorukov, K. Ishida, F.L. Pratt, D. Fleming, T. Momose, Y. Matsuda, and E. Torikai, "First Accurate Experimental Study of Mu Reactivity from a State-Selected Reactant in the Gas Phase: the Mu + $H_{2(1)}$ Reaction Rate at 300 K", Journal of Physics B (At. Mol. Opt.) 48, 045204 (2015).＊

T. Matsuzaki, K. Ishida, M. Iwasaki, “High-pressure solid hydrogen target for muon catalyzed fusion”, Journal of Radioanalytical and Nuclear Chemistry, DOI 10.1007/s10967-015-4080-y＊

Rakesh Mohan Das, Souvik Chatterjee, Masahiko Iwasaki, and Takashi Nakajima, “Ionization efficiencies of Doppler-broadened atoms by transform-limited and broadband nanosecond pulses: one-photon resonant two-photon ionization of muoniums”, Journal of Optical Society of America B 32, 1237-1244 (2015).＊

M. Enomoto, I. Watanabe, and N. Kojima, "Dynamical Behavior of the Charge Transfer Phase Transition in Dithiooxalato-Bridged Iron Mixed-Valence System", Current Inorganic Chemistry **6**, 49-60 (2016).＊

Sunaryono, Ahmad Taufiq, Edy Giri Rahman Putra, A. Okazawa, I. Watanabe, N. Kojima, Supagorn Rugmai, Siriwat Soontaranon, Mohammad Zainuri, Triwikantoro, Suminar Pratapa, and Darminto, "Small-Angle X-Ray Scattering Study on PVA/Fe_3O_4 Magnetic Hdrogels" NANO **11**, 1650027-1-12 (2016).＊

I. Kawasaki, K. Fujimura, I. Watanabe, M. Avdeev, K. Tenya, and M. Yokoyama, "Muon Spin Relaxation and Neutron Diffraction Studies of Cluster-Glass State in $Sr_{1-x}La_xRuO_3$" Journal of Physical Society of Japan **85**, 054701-1-8 (2016).＊

T. Uehara, M. Ito, J. Angel, J. Shimada, N. Komakine, T. Tsuchiya, H. Taniguchi, K. Satoh, K. Triyana, Y. Ishii, and I. Watanabe, “Studies on Magnetism of the Layered Organic Antiferromagnet Bordered on a Superconducting Phase by Muon Spin Rotation and Magnetization Measurements” Journal of Phyical. Society of Japan **85**, 024710-1-6 (2016).＊

Sungwon Yoon, S.-H. Baek, W.-J. Lee, K.-Y. Choi, I. Watanabe, J.S. Lord, B. Büchner, A. Balodhi, Y. Singh, and B.J. Suh, "Spin Dynamics in $Na_{4-x}Ir_3O_8$ Investigated by ^{23}Na NMR and μSR" Joural of Physics: Condensed Matter. **27**, 485603-1-6 (2015).＊

Ahmad Taufiq, Sunaryono, Edy Giri Rachman Putra, A. Okazawa, I. Watanabe, N. Kojima, Suminar Pratapa, and Darminto, "Nanoscale Clustering and Magnetic Properties of $Mn_xFe_{3-x}O_4$ ParSuticles Prepared from Natural Magnetite" Journal of Superconductors and Novel Magnets **28**, 1649-1874 (2015). DOI 10.1007/s10948-015-3111-9.＊

M. Ito, T. Uehara, H. Taniguchi, K. Satoh, Y. Ishii, and I. Watanabe, " Zero-Field Magnetism of a Two-Dimensional Antiferromagnet, κ-$(BEDT\text{-}TTF)_2Cu[N(CN)_2]Cl$, Determined by Muon Spin Rotation and Magnetization Measurements" Journal of Physical Society of Japan **84**, 053703-1-5 (2015).＊

N. Funamori, K.M. Kojima, D. Wakabayashi, T. Sato, T. Taniguchi, N. Nishiyama, T. Irifune, D. Tomono, T. Matsuzaki, M. Miyazaki, M. Hiraishi, A. Koda, and R. Kadono, “Muonium in Stishovite: Implications for the Possible Existence of Neutral Atomic Hydrogen in the Earth’s Deep Mantle”, Scientific Report **5**, 8437-1-5 (2015).＊

M. Abdel-Jawad, I. Watanabe, N. Tajima, Y. Ishii, and R. Kato, “Universality Class of the Mott-Hubbard Transition”, Physical Review Letters **114**, 106401-1-5 (2015).＊

[Proceedings]

(Original Papers) *Subject to Peer Review

Masaharu Sato, Katsuhiko Ishida, Masahiko Iwasaki, Sohtaro Kanda, Yue Ma, Yasuyuki Matsuda, Teiichiro Matsuzaki, Katsumi Midorikawa, Yu Oishi, Shinji Okada, Norihito Saito, Kazuo Tanaka and Satoshi Wada, "Laser Spectroscopy of Ground State Hyperfine Splitting Energy of Muonic Hydrogen",Proc. 2nd Int. Symp. Science at J-PARC, JPS Conf. Proc.8 , 025005 (2015). *

R.Kitamura, G.Beer, K.Ishida, M.Iwasaki, S.Kanda, H.Kawai, N.Kawamura, W.Lee, S.Lee, G.M.Marshall, Y.Matsuda, T.Mibe, Y.Miyake, S.Nishimura, Y.Oishi, S.Okada, A.Olin, M.Otani, N.Saito, K.Shimomura, P.Strasser, M.Tabata, D.Tomono, K.Ueno, E.Won and J-PARC muon g-2/EDM collaboration, "Studies on Muonium Production from Silica Aerogel with Substructure for the Muon g-2/EDM Experiment", Proc. 2nd Int. Symp. Science at J-PARC, JPS Conf. Proc. 8, 025016 (2015).*

H. A. Torii, M. Aoki, Y. Fukao, Y. Higashi, T. Higuchi, H. Iinuma, Y. Ikedo, K. Ishida, M. Iwasaki, R. Kadono, O. Kamigaito. S. Kanda, D. Kawall, N. Kawamura, A. Koda, K. M. Kojima, K. Kubo, Y. Matsuda, T. Mibe, Y. Miyake, T. Mizutani, K. Nagamine, K. Nishiyama, T. Ogitsu, R. Okubo, N. Saito, K. Sasaki, K. Shimomura, P. Strasser, M. Sugano, M. Tajima, K. S. Tanaka, D. Tomono, "Precise Measurement of Muonium HFS at J-PARC MUSE", Proc. 2nd Int. Symp. Science at J-PARC, JPS Conf. Proc. 8, 025018 (2015).*

K. Ninomiya, M. K. Kubo, P. Strasser, T. Nagatomo, Y. Kobayashi, K. Ishida, W. Higemoto, N. Kawamura, K. Shimomura, Y. Miyake, T. Suzuki, A. Shinohara, T. Saito, "Elemental Analysis of Bronze Artifacts by Muonic X-ray Spectroscopy", Proc. 2nd Int. Symp. Science at J-PARC, JPS Conf. Proc., 8, 033005 (2015).*

H. Kuroe, H. Kuwahara, T. Sekine, I. Watanabe, Andrea-Raeto Raselli, Matthias Elender, Pabitra Kumar Biswas, M. Hase, K. Oka, T. Ito, and H. Eisaki, "Muon-Spin Rotation in Multiferroic $Cu_3Mo_2O_9$ under Electric Fields" Physics Procedia **75**,221-229 (2015). ＊

Goto, K. Matsui, T. Adachi, T. Ohtsuki, Ngoc Han Tu, Y. Tanabe, I. Watanabe, Z. Salman, A. Suter, and T. Prokscha, "Low-energy μSR study on the tetradymite Topological Insulator $Bi_{1.5}Sb_{0.5}TeSe_2$" Physics Procedia **75**,100-105 (2015). ＊

L. Safriani, Risdiana, A. Bahtiar, A. Aprilia, I. Kawasaki, and I. Watanabe, "μSR Study of Charge Carrier Motion in Active Layer P3HT:ZnO:PCBM Hybrid Solar Cells" Mater. Sci. Forum **827**, 131-134 (2015). ＊

L. Safriani, Risdiana, A. Bahtiar, A. Aprilia, R.E. Siregar, R. Hidayat, T.P.I. Saragi, I. Kawasaki, and I. Watanabe, "Charge Carrier Dynamics of Active Material Solar Cell P3HT:ZnO Nanoparticles Sudied by Muon Spin Relaxation (μSR)" Mater. Sci. Forum **827**, 477-480 (2015). ＊

Ayi Bahtiar, Lusi Safriani, Annisa Aprilia, Risdiana, Harsojo, Triwikantoro, Darminto, Agustinus Agung Nugroho, Hanjie Guo, Ikuto Kawasaki, and Isao Watanabe, "Study of Charge Carrier Dynamics of P3HT:PCBM Blend for Active Material Solar Cell Using Muon Spin Relaxation" Mater. Sci. Forum **827**, 168-173 (2015). ＊

Ayi Bahtiar, Siti Halimah Tusaddiah, Wendy Paramandhita, S. Mustikasari, Lusi Safriani, Mariah Kartawidjaja, Kei Kanazawa, Ippei Enokida, Yukio Furukawa, and Isao Watanabe, "Optical, Structural and Morphological Properties of Ternary Thin Film Blend of P3HT:PCBM:ZnO Nanoparticles" Mater. Sci. Forum **827**, 119-124 (2015). ＊

S. Sulaiman, S.N.A. Ahmad, M.I. Mohamed-Ibrahim, and I. Watanabe, "Electronic Structure of Muoniated $Me_4P[Pd(dmit)_2]_2$" Mater. Sci. Forum **827**, 355-359 (2015). ＊

A.F. Rozlan, S. Sulaiman, M.I. Mohamed-Ibrahim, and I. Watanabe, "Electronic Structure of Muonated La_2CuO_4" Mater. Sci. Forum **827**, 240-242 (2015). ＊

I. Watanabe, E. Suprayoga, N. Adam, Mohm-Tajudin S.S., Rozlan A.F., D. Puspita, R. Asih, F. Astuti, M.D. Umar, J. Angel, S. Sulaiman, and M.I. Mohamed-Ibrahim, "Muon Site Estimations by DFT Calculations in Metal and Insulating Systems" Mater. Sci. Forum **827**, 347-454 (2015). ＊

A.D. Pant, Y. Sugawara, I. Yanagihara, G.P. Khanal, I. Shiraki, W. Higemoto, K. Shimomura, K. Ishida, F.L. Pratt, E. Torikai, and K. Nagamine, "Hydration Effect on Electron Transfer in Cytochrome c Monitored by μSR" JPS Conf. Proc. **8**, 033007-1-5 (2015). ＊

K. Matsui, A. Oosawa, K. Yoshizawa, T. Goto, I. Watanabe, T. Suzuki, M. Fujisawa, H. Tanaka, P.K. Biswas, and A. Amato, "μSR Study on Quantum Spin System NH_4CuCl_3" J. Phys. Conf. Ser. **551**, 012007-1-6 (2014). ＊

M. Miyazaki, R. Kadono, M. Hiraishi, I. Yamauchi, A. Koda, K.M. Kojima, I. Kawasaki, I. Watanabe, Y. Okamoto, and Z. Hiroi, "Spin Dynamics of Mn Pyrochlore Lattice in $YMn_2Zn_{20-x}In_x$" J. Phys. Conf. Ser. **551**, 012019-1-6 (2014). ＊

H. Nozaki, S. Ohta, M. Harada, M. Månsson, D. Sheptyakov, V. Pomjakushin, I. Wanabe, Y. Ikedo, Y. Miyake, and J. Sugiyama, "Li-Ion Dynamics in $Li_{5+x}La_3Zr_xNb_{2-x}O_{12}$ " JPS Conf. Proc. **2**, 010303-1-6 (2014). ＊

H. Ariga, K. Shimomura, K. Ishida, F.L. Pratt, K. Yoshizawa, W. Higemoto, E. Torikai, and K. Asakura, "Detection of Oxygen Vacancy in Rutile TiO_2 Single Crystal by μSR Measurement" JPS Conf. Proc. **2**, 010303-1-4 (2014). ＊

Oral Presentations

[International Conference etc.]

K. Ishida, "Development of ultra-slow muon source based on room temperature muonium production target and its application to muon g-2/EDM measurement", International USMM & CMSI Workshop: Fronties of Materials and Correlated Electron Science - from Bulk to Thin Films and Interface, Tokyo, Jan 2016.

T. Kurahashi, T. Adachi, K. Suzuki, Y. Fukunaga, T. Kawamata, H. Noji, H. Miyasaka, I. Watanabe, M. Miyazaki, A. Koda, R. Kadono, andY.Koike, "Possible Ferromagnetic Fluctuations in the Heavily Overdoped Bi -2201 Cuprat" International Workshop on Superconductivity and Related Functional Materials 2016、IMR, Tohoku University, Sendai, Miyagi, March 2016.

T. Adachi, A. Takahashi, K. Suzki, M.A. Baqiya, T. Konno, T.Ohgi, T. Takamatsu, T. Kawamata, M. Kato, I. Watanabe, A. Koda, M. Miyazaki, R. Kadono, H. Oguro, T. Awaji, and Y. Koike, "μSR Study of the Cu-Spin Correlation in the Overdoped Regime of Electron-Doped High-T_C T'-Cuprates" 7th MFL Symposium、Tsukuba、Ibaraki、March 2016.

T. Adachi, A. Takahashi, K. Suzki, M.A. Baqiya, T. Konno, T.Ohgi, T. Takamatsu, T. Kawamata, M. Kato, I. Watanabe, A. Koda, M. Miyazaki, R. Kadono, H. Oguro, T. Awaji, and Y. Koike, "μSR and transport studies in the electron-doped High-T_C T'-superconductors revealing the novel electronic state" International USMM & CMSI Workshop: Frontiers of Materials and Correlated Electron Science : from Bulk to Thin Films and Interfaces, Univeristy of Tokyo, Tokyo, Jan. 2016.

Y. Koike, K. Suzuki, T. Adachi, K. Sato, and I. Watanabe, "Novel Fe-induced magnetism in the overdoped regime of the La-214 High-T_C cuprate: Implication to stripes" International USMM & CMSI Workshop: Frontiers of Materials and Correlated Electron Science : from Bulk to Thin Films and Interfaces, Univeristy of Tokyo, Tokyo, Jan. 2016.

T. Kurahashi, T. Adachi, T. Kawamata, H. Noji, I. Watanabe, M. Miyazaki, A. Koda, R. Kadono, and Y. Koike, "Possible Ferromagnetic Fluctuations in the Heavily Overdoped Bi-2201 Cuprate" 28th International Symposium on Superconductivity (ISS 2015), Tokyo, Nov. 2015.

K. Takao, 劉鐘昇, K. Uji, T. Waki, Y. Tabata, I. Watanabe, and H. Nakamura, "Paramagnetic-to-Nonmagnetic Transition in Antiperovskite Nitride Cr_3GeN Studied by ^{14}N-NMR and μSR" International Workshop on Itinerant-Electron Magnetism, Kyoto University, Kyoto, Sep. 2015.

I. Watanabe, H. Guo, K. Matsuhira, I. Kawasai, R. Wakeshima, Y. Honatsu, and Zhu-an Xu, "μSR Studies of Spin Ground States in the Pyrochlore Iridate $Nd_2Ir_2O_7$" 4th Annual World Congress of Advanced Materials-2015 (WCAM2015), Chingqing, China, May 2015.

I. Watanabe, "Current Status of Muon-Site Estimations in Strongly Correlated Systems" Workshop to Discuss Techniques for Calculation of the Muon Site, Hinckly, UK, May 2015.

I. Watanabe, "Applications of Pulsed Muon Beam to Material Science at the RIKEN-RAL Muon Facility" University Seminar, Fudan University, Shanghai, China, March 2015.

T. Uehara, M. Ito, H. Taniguchi, K. Sato, Y. Ishii, and I. Watanabe, "mSR Study of κ-(h8-BEDT-TTF)$_2$Cu[N(CN)$_2$]Cl and Discussion of Muon Site Using Relaxation Signal from Deuterated κ-(d8-BEDT-TTF)$_2$Cu[N(CN)$_2$]Br" RIKEN Symposium: 1st RIKEN-Sophia Joint Syposium ==Recent Progresses on the Muon-Site Estimation==, Sophia University, Yotsuya, Tokyo, Dec. 2014.

E. Suprayoga, A.A. Nugroho, A.O. Polyakov, T.T.M. Palstra, I. Watanabe, "Search for Muon Stopping Positions in Organic-Inorganic Hybrids Based on Density Functional Theory" RIKEN Symposium: 1st RIKEN-Sophia Joint Syposium ==Recent Progresses on the Muon-Site Estimation==, Sophia University, Yotsuya, Tokyo, Dec. 2014.

S.S. Mohd-Tajudin, S.N.A. Ahmad, D.F. Hasan-Baseri, E. Suprayoga, N. Adam, A.F. Rozlan, S. Sulaiman, M.I. Mohamed-Ibrahim, I. Watanabe, "Investigation of Muon Sites in $YBa_2Cu_3O_6$ by Using Density Functional Theory" RIKEN Symposium: 1st RIKEN-Sophia Joint Syposium ==Recent Progresses on the Muon-Site Estimation==, Sophia University, Yotsuya, Tokyo, Dec. 2014.

A.F. Rozlan, S. Sulaiman, M.I. Mohamed-Ibrahim, I. Watanabe, " Electronic Structure and Hyperfine Interaction of Muonated La_2CuO_4" RIKEN Symposium: 1st RIKEN-Sophia Joint Syposium ==Recent Progresses on the Muon-Site Estimation==, Sophia University, Yotsuya, Tokyo, Dec. 2014.

N. Adam, S. Sulaiman, M.I. Mohamed-Ibrahim, I. Watanabe, "Electronic Structure of $CeRu_2Al_{10}$ based on LSDA+U Calculation" RIKEN Symposium: 1st RIKEN-Sophia Joint Syposium ==Recent Progresses on the Muon-Site Estimation==, Sophia University, Yotsuya, Tokyo, Dec. 2014.

Y. Koike, K. Suzuki, T. Adachi, T. Sato, and I. Watanabe, "Novel Fe-Induced Magnetism in the Overdoped Regime of the La-214 High-T_C Curate: Implication for Dtripe Fluctuation" 27th International Conference on Low Temperature Physics (LT27), Buenos Aires, Argentina, Aug. 2014.

I. Watanabe, "Highlights of μSR at the RIKEN-RAL" Depatment Seminar, Institut Teknologi Sepruluh Nopember, Indonesia, July 2014.

[Domestic Conference]

北村遼, 深尾祥紀, 石田勝彦, 河村成肇, 近藤恭弘, 三部勉, 三宅康博, 大谷将士, Patrick Strasser, 齊藤直人, 下村浩一郎 他 J-PARC muon g-2/EDM コラボレーション: ″J-PARC ミューオン g-2/EDM 精密測定実験のためのミューオン再加速試験に向けた低速ミューオン源開発の準備状況″, 日本物理学会第 70 回年次大会、早稲田大学、東京、3 月(2015)

倉嶋晃士、足立匡、川股隆行、野地尚、宮坂等、渡邊功雄、宮崎正範、 幸田章宏、門野良典、小池洋二、 "銅酸化物超伝導体の極過剰ドープ領域における強磁性ゆらぎ" 日本物理学会春の大会・ 東北学院大学泉キャンパス、宮城県仙台市、3 月 (2016)

Fahmi Astuti、Retno Asih、Dita Puspita Sari、Graeme Blake、中野岳人、野末泰夫、渡邊功雄、"μSR による CsO_2 中の長距離磁気秩序状態の検出" 日本物理学会春の大会・ 東北学院大学泉キャンパス、宮城県仙台市、3 月 (2016)

鈴木栄男、片山和哉、川崎郁斗、渡邊功雄、田中秀数、 "S = 1/2 カゴメ格子磁性体 $(Rb_{1-x}Cs_x)_2Cu_3SnF_{12}$ の量子臨界点近傍における縦磁場中ミュオンスピン緩和測定" 日本物理学会春の大会・ 東北学院大学泉キャンパス、宮城県仙台市、3 月 (2016)

Retno Asih、Noraina Adam、Saidah Sakinah Mohd-Tajudin、松平和之、前田悟、分島亮、日夏幸雄、三宅厚志、徳永将史、渡邊功雄、中野岳仁、野末泰夫、"Effect of Ca-substitution on the magnetic ordered state of $(Nd_{1-x}Ca_x)_2Ir_2O_7$ studied by μSR" 日本物理学会春の大会・ 東北学院大学泉キャンパス、宮城県仙台市、3 月 (2016)

E.Suprayoga、A.A. Nugroho、A.O. Polyakov、T.T.M. Palstra、渡邊功雄、"Muon Sites Estimation on Organic-Inorganic Hybrids of $(C_6H_5CH_2CH_2NH_3)_2CuCl_4$ and $(C_2H_5NH_3)_2CuCl_4$ using DFT and Dipole Fields Calculation" 日本物理学会春の大会・ 東北学院大学泉キャンパス、宮城県仙台市、3 月 (2016)

D.P.Sari、R.Asih、開康一、石井康明、熊谷浩也、河本充司、高橋利宏、渡邊功雄、中野岳仁、野末泰夫、"Probing the Superconducting Ground State Organic Superconductor λ-$(BETS)_2GaCl_4$ by μSR" 日本物理学会春の大会・ 東北学院大学泉キャンパス、宮城県仙台市、3 月 (2016)

Saidah Sakinah Mohd-Tajudin、西嵜照和、吉川明子、Noraina Adam、Edi Suprayoga、Shukri Sulaiman、Mohamed Ismail Mohamed-Ibrahim、"Computational and Experimental Studies of Muon Sites in $YBa_2Cu_3O_6$" 日本物理学会春の大会・ 東北学院大学泉キャンパス、宮城県仙台市、3 月 (2016)

N. Adam、E. Suprayoga、S.S Mohd-Tajudin、谷田博司、D.T. Adroja、高畠敏郎、世良正文、S.Sulaiman、M.I.Mohamed Ismail、渡邊功雄、"Magnetic Ground State of CeT_2Al_{10} (T = Ru,Os)" 日本物理学会春の大会・ 東北学院大学泉キャンパス、宮城県仙台市、3 月 (2016)

足立匡、高橋晶、鈴木謙介、M.A. Baqiya、今野巧也、扇太郎、川股隆行、加藤雅恒、渡邊功雄、幸田章宏、宮崎正範、門野良典、小黒英俊、淡路智、小池洋二、"輸送特性とミュオンスピン緩和から見た電子ドープ型 T'-214 高温超伝導体における磁性と超伝導" 東大物性研短期研究会「低次元電子系におけるエキシトニック相の新展開」千葉県柏市、東京大学物性研、2015 年 11 月.

倉嶋晃士、足立匡、 鈴木謙介、福永泰、川股隆行、野地尚、渡邊功雄、宮崎正範、幸田章宏、門野良典、小池洋二、"Bi-2201 銅酸化物の極過剰ドープ領域における強磁性ゆらぎ" 第 9 回物性科学領域横断研究会、東京都、東京大学、2015 年 11 月.

渡邊功雄、"μSR で磁性体中の微小スピンを見る" 原研先端基礎研究センター・基礎科学セミナー、茨城県東海村、原研先端基礎研究センター、2015 年 10 月.

田邉洋一、足立匡、鈴木謙介、阿子島めぐみ、平郡諭、川股隆行、石井康之、鈴木栄男、渡邊功雄、小池洋二、日本物理学会秋の大会、関西大学千里山キャンパス、大阪府吹田市、2015 年 9 月.

岸本亮三、中野岳仁、Gayan Prasad Hettiarachchi、石井康之、渡邊功雄、野末泰夫、"ゼオライト LSX 中の Na-K 合金クラスターが示すフェリ磁性の He による圧力効果Ⅲ" 日本物理学会秋の大会、関西大学千里山キャンパス、大阪府吹田市、2015 年 9 月.

Sungwon Yoon、新堀佳紀、前川珠理、榎本真哉、根岸雄一、Byoung Jin Suh、渡邊功雄、"金のナノ粒子を用いた μSR 研究" 日本物理学会秋の大会、関西大学千里山キャンパス、大阪府吹田市、2015 年 9 月.

Sungwon Yoon、S.-H. Do、Y.S. Kwon、K.-Y. Choi、渡邊功雄、B.J. Suh、"μSR Investigations of a Kitaev Honeycomb Compound α-RuCl3" 日本物理学会秋の大会、関西大学千里山キャンパス、大阪府吹田市、2015 年 9 月.

Retno Asih、Noraina Adam、Saidah Sakinah Mohd-Tajudin、松平和之、分島亮、日夏幸雄、三宅厚志、徳永将史、渡邊功雄、中野岳仁、 野末泰夫、"Investigation of Magnetic Ordered State in the Pyrochlore Iridates $R_2Ir_2O_7$ (R= Nd,Sm) probed by μSR" 日本物理学会秋の大会、

関西大学千里山キャンパス、大阪府吹田市、2015 年 9 月.

D.P. Sari、R. Asih、開康一、石井康明、熊谷浩也、河本充司、高橋利宏、渡邊功雄、中野岳仁、野末泰夫、“Superconducting Properties of Non-magnetic Anion Based Organic Superconductor λ-$(BETS)_2GaCl_4$ Studied by μSR” 日本物理学会秋の大会、関西大学千里山キャンパス、大阪府吹田市、2015 年 9 月.

Saidah Sakinah Mohd-Tajudin、西嵜照和、吉川明子、Noraina Adam、Edi Suprayoga、Shukri Sulaiman、Mohamed Ismail Mohamed-Ibrahim、渡邊功雄、“μSR and Density Functional Theory Studies on $YBa_2Cu_3O_6$” 日本物理学会秋の大会、関西大学千里山キャンパス、大阪府吹田市、2015 年 9 月.

N. Adam、E. Suprayoga、S.S Mohd-Tajudin、谷田博司、世良正文、S.Sulaiman、M.I.Mohamed Ismail、渡邊功雄、μSR Investigations On The Ground State of $(Ce_{1-x}La_x)Ru_2Al_{10}$“日本物理学会秋の大会、関西大学千里山キャンパス、大阪府吹田市、2015 年 9 月.

Majed Abdel-Jawad、加藤礼三、渡邊功雄、田嶋尚也、石井康之、“Detailed Study of the Mott Transition in $EtMe_3P[Pd(dmit)_2]_2$” 日本物理学会秋の大会、関西大学千里山キャンパス、大阪府吹田市、2015 年 9 月.

石井康之、Majed Abdel-Jawad、渡邊功雄、加藤礼三、“圧力誘起超伝導体 $EtMe_3P[Pd(dmit)_2]_2$ のモット転移と温度ー圧力相図” 日本物理学会秋の大会、関西大学千里山キャンパス、大阪府吹田市、2015 年 9 月.

渡邊功雄“RIKEN-RAL と PSI の現状 RCNP に期待すること”RCNP 研究会「RCNP-MuSIC におけるミューオン科学の展開」大阪大学 RCNP、大阪府豊中市、2015 年 9 月.

濱地紀彰、安井幸夫、河野洋平、橘高俊一郎、榊原俊郎、L.J.Chang、小野田繁樹、渡邊功雄、“量子スピンアイ系 量子スピンアイ系 Yb2T2O7 の μSR 測定”日本物理学会春の大会、早稲田大学、東京都、2015 年 3 月

今野巧也、足立匡、扇太郎、高橋晶、加藤雅恒、渡邊功雄、小黒英俊、淡路智、小池洋二、“電子ドープ型超伝導体 $Pr_{1.3-x}La_{0.7}Ce_xCuO_{4+\delta}$ ($x \leqq 0.10$) 単結晶における還元アニール効果と電子状態” 日本物理学会春の大会、早稲田大学、東京都、2015 年 3 月

松井一樹、渡邊功雄、Sungwon Yoon、星野侑宏、細谷陽介、後藤貴行、長谷正司、佐々木孝彦、“擬一次元競合鎖 $A_2Cu_2Mo_3O_{12}$ (A=Rb or Cs) における NMR/μSR” 日本物理学会春の大会、早稲田大学、東京都、2015 年 3 月

中野岳仁、谷辺健志、Luu Manh Kien、Sungwon Yoon、Majed Abdel-Jawad、Francis L.Pratt、渡邊功雄、野末泰夫、“ソーダライト中の K-Rb 合金および Rb クラスターの μSR” 日本物理学会春の大会、早稲田大学、東京都、2015 年 3 月

高尾健太、劉鐘昇、宇治克俊、太田寛人、和氣剛、田畑吉計、渡邊功雄、中村裕之、“Cr 系逆ペロフスカイト型窒化物の磁性” 日本物理学会春の大会、早稲田大学、東京都、2015 年 3 月

E.Suprayoga、A.A. Nugroho、A.O. Polyakov、T.T.M. Palstra、渡邊功雄、“Electronic Structure of $(C_6H_5CH_2CH_2NH_3)_2CuCl_4$ and $(C_2H_5NH_3)_2CuCl_4$ Organic-Inorganic Hybrid Materials” 日本物理学会春の大会、早稲田大学、東京都、2015 年 3 月

Saidah Sakinah Mohd-Tajudin、Noraina Adam、E.Suprayoga、Shukri Sulaiman、Mohamed Ismail Mohamed-Ibrahim、渡邊功雄、“First-Principles Calculation of Electronic Structure and Muon Sites in $YBa_2Cu_3O_6$” 日本物理学会春の大会、早稲田大学、東京都、2015 年 3 月

N.Adam、E. Suprayoga、S.S. Mohd Tajudin、谷田博司、世良正文、S.Sulaiman、M.I.Mohamed Ismail、渡邊功雄、“The Electronic Structures of $CeRu_2Al_{10}$ and Muon Sites Studied by DFT” 日本物理学会春の大会、早稲田大学、東京都、2015 年 3 月

渡邊功雄、“ミュオン位置計算法の最近の進展”第 8 回 三機関連携「量子複雑現象」研究会、SPring-8、西播磨、兵庫県、2015 年 1 月.

渡邊功雄、“Applications of Pulsed Muon Beam to Material Science at the RIKEN-RAL Muon Facility”NIMS Seminar、NIMS、並木、つくば市、2014 年 10 月.

高尾健太、劉鐘升、宇治克俊、和氣剛、田畑吉計、渡邊功雄、中村裕之、“^{14}N-NMR による逆ペロブスカイト型窒化物 Cr_3GeN の常磁性-非磁性転移の研究”日本物理学会秋の大会、中部大学、名古屋市、2014 年 9 月.

Posters Presentations

[International Conference etc.]

S. Okada, P. Bakule, G. Beer, J. Brewer, Y. Fujiwara, K. Ishida, M. Iwasaki, S. Kanda, H. Kawai, N. Kawamura, R. Kitamura, W. Lee, Y. Ma, G. Marshall, Y. Matsuda, T. Mibe, Y. Miyake, S. Nishimura, Y. Oishi, A. Olin, M. Otani, N. Saito, M. Sato, K. Shimomura, P. Strasser, M. Tabata, D. Tomono, K. Ueno, E. Won, K. Yokoyama, "Ultra-slow muon production with room-temperature thermal-muonium-emitting material", The international workshop on future potential of high intensity proton accelerator for particle and nuclear physics (HINT2015), Oct 2015

S. Kawamura, K. Tomiyasu, A. Koda,K. Nakajima, and I. Watanabe, “Magnetic Properties of One-Dimensional Quantum Spin System $Rb_2Cu_2Mo_3O_{12}$ Studied by μSR “ 7th MFL Symposium、Tsukuba、Ibaraki、March 2016.

Sungwon Yoon, Seung-Hwan Do, Yong Sung Kwon, Kwang-Yong Choi, I. Watanabe, and Byoung Jin Suh, “Study of the magnetic property of a Kitaev Honecyomb material $RuCl_3$ using spin polarized muons” APW-CEMS joint Workshop: Highlights of Modern Condensed Matter Physics, CEMS, RIKEN, Saitama, Jan. 2016。

D.P.Sari、R.Asih、K. Hiraki, H. Kumagai, A. Kawamoto, T. Takahashi, I. Watanabe, T. Nakano, and Y. Nozue, “μSR Study of Non-magnetic Anion Based Superconductors λ-$(BETS)_2GaCl_4$ Studied by μSR “ International Symposium on Present and Future of Material Sciences” Osaka University, Toyonaka, Osaka, Nov. 2015.

R. Asih, Noraina Adam, Saidah Sakinah Mohd-Tajudin, K. Matsuhidra, R. Wakeshima, Y. Hinatsu, A. Miyake, and M. Tokunaga, “μSR Study on the Pyrochlore Iridates $R_2Ir_2O_7$ (R= Nd,Sm)” International Symposium on Present and Future of Material Sciences” Osaka University, Toyonaka, Osaka, Nov. 2015.

T. Adachi, A. Takahashi, K. Suzuki, M.A. Baqiya, T. Konnno, T. Takamatsu, M. Kato, I. Watanabe, A. Koda, M. Miyazaki, R. Kadono, and Y. Koike, “Novel Coexistence of Superconduxtivity with Short-Range Magnetic Order in Electron-Doped High-T_C T'-Cuprate” 27th International Conference on Low Temperature Physics (LT27), Buenos Aires, Argentina, Aug. 2018.

A. Takahashi, K. Susuki, T. Adachi, M.A. Baqiya, H. Guo, I. Kawasaki, I. Watanabe, and Y. Koike, “Coincident Disappearance of The Stripe Order and The Superconductivity in $La_{2-x}Sr_xCu_{1-y}M_yO_4$ (M = Fe, Al)” The 2nd International Symposium on Science at J-APRC, J-PARC, Tokai, Ibaraki, July 2014.

T. Adachi, T. Inabe, K. Suzuki, T. Kawamata, H. Koji, H. Guo, I. Watanabe, and Y. Koike, “Impurity-Induced Development of the Spin Correlation in Iron-Chalcogenide Superconductors Observed by μSR” The 2nd International Symposium on Science at J-APRC, J-PARC, Tokai, Ibaraki, July 2014.

[Domestic Conference]

Sungwon Yoon、新堀佳紀、前川珠理、榎本真哉、根岸雄一、Byoung Jin Suh、渡邊功雄、“μSR Studies of Magnetic Property of Gold Nanoparticle” 日本物理学会春の大会・ 東北学院大学泉キャンパス、宮城県仙台市、3 月（2016）

Retno Asih、Noraina Adam、Saidah Sakinah Mohd-Tajudin、松平和之、分島亮、日夏幸雄、三宅厚志、徳永将史、渡邊功雄、中野岳仁、野末泰夫、“μSR Study on the Pyrochlore Iridates $R_2Ir_2O_7$ (R= Nd,Sm)”東大物性研短期研究会「スピン系物理の深化と最前線」千葉県柏市、東京大学物性研、2015 年 11 月.

黒江晴彦、平田芳規、関根智幸、渡邊功雄、R.A.-Raeto、B.E.Matthias、B.P. Kumar、長谷正司、岡邦彦、伊藤利充、永崎洋、“Cu3Mo2O9 の電場中 μSR 測定” 日本物理学会春の大会、早稲田大学、東京都、2015 年 3 月

渡邊功雄、Budi Adiperdana、Edi Suprayoga、 Noraina Adam、Irwan A. Dharmawan、Rustam Siregr、Saidah Sakinah Mohd-Tajudin、Ainul Fauzeeha Rozlan、Shukri Sulaiman、Mohamad Ismail Mohamed-Ibraham、川股隆行、足立匡、小池洋二、Pabitra Kumar、Alex Amato、“La_2CuO_4におけるミュオン位置計算の進展” 日本物理学会春の大会、早稲田大学、東京都、2015 年 3 月

後藤貴行、松井一樹、足立匡、大槻東巳、田邉洋一、渡邊功雄、“トポロジカル絶縁体におけるスピンロック現象の μSR 検出”新学術領域「超低速ミュオン顕微鏡」第 3 回領域会議、東北大学、仙台市、2014 年 9 月.

足立匡、高橋晶、鈴木謙介、M.A.Baqiya、今野巧也、高松智寿、加藤雅恒、渡邊功雄、幸田章宏、宮崎正範、門野良典、小池洋二、“電子型 T'高温超伝導体における超伝導と短距離磁気秩序の新奇な共存” “トポロジカル絶縁体におけるスピンロック現象の μSR 検出”新学術領域「超低速ミュオン顕微鏡」第 3 回領域会議、東北大学、仙台市、2014 年 9 月.

RIBF Research Division
Radioactive Isotope Physics Laboratory

1. Abstract

This laboratory explores exotic nuclear structures and dynamics in exotic nuclei that have never been investigated before, such as those with largely imbalanced proton and neutron numbers. Our aim is to develop new experimental techniques utilizing fast RI beams to discover new phenomena and properties in exotic nuclei. Another important subject is the equation-of-state in asymmetric nuclear matter, and its association with the origin of elements and with neutron stars. For instance, we are making attempts to the better understand underlying mechanism for exotic stability-enhancements of very neutron-rich fluorine isotopes, the large deformation of the nucleus Mg-34 with N=22 in spite of its vicinity to the N=20 magic neutron number and anomalous collectivity in C-16. We are further extending these studies to medium- and heavy-mass regions by developing facilities, detectors and unique methods at RIBF, thereby leading on the challenging task to find new exotic phenomena. We also perform numerical simulations of nucleosynthesis under the environment of core-collapse supernovae, and moreover quest for footprints of supernovae and solar activities in the past, embedded in Antarctic ice core.

2. Major Research Subjects

(1) Study of structure and dynamics of exotic nuclei through developments of new tools in terms of reaction- and technique-based methodology
(2) Research on EOS in asymmetric nuclear matter via heavy-ion induced reactions
(3) Detector developments for spectroscopy and reaction studies

3. Summary of Research Activity

(1) In-beam gamma spectroscopy

In the medium and heavy mass region explored at RIBF, collective natures of nuclei are one of important subjects, which are obtained through production and observation of high excited and high spin states. To populate such states, heavy-ion induced reactions such as fragmentation, fission are useful. So far, we have developed two-step fragmentation method as an efficient method to identify and populate excited states, and lifetime measurements to deduce transition strength.

Devices utilized for the in-beam gamma spectroscopy are ZeroDegree Spectrometer (ZDS) and a NaI array DALI2. Since the end of 2008, the first spectroscopy on nuclei island-of-inversion region was performed, we have explored step-by-step new and unknown regions in the nuclear chart. The second campaign in 2009 was organized to study background components originating from atomic processes in a heavy target. Neutron-rich nuclei at N=20 to 28 were studied in 2010. In 2011-2013, we conducted experiment programs for Ca-54, Ni-78, neutron-rich nuclei at N=82 and neutron-deficient nuclei at Z=50.

A multitude of data obtained with inelastic, nucleon knock-out, fragmentation channels have been analyzed and published. In 2011-2013, collective natures of Mg-36, 38 and Si-42 were both published in PRL. Excited states firstly observed in Ca-54 were reported in Nature to demonstrate a new nuclear magic number of 34. Fragmentation reaction has been found efficient for nuclei with A>100 and low-lying excited state in Pd-126 has been successfully observed and reported in PRC.

To further strengthen the in-beam gamma spectroscopy at RIBF, we have proposed a new setup of MINOS + DALI2 to search for the 1st excited states in even-even neutron-rich nuclei with Z~20 to 40. The program was submitted to the PAC 2013 as a new category “proposal for scientific program” and was S-ranked. A dedicated collaboration “SEASTAR” has been established as a subset of in-beam gamma collaboration “SUNFLOWER”. The two campaigns were organized in 2014 and 2015 to study very neutron-rich isotopes.

Concerning a next generation detector, a construction proposal of a LaBr3 array “SHOGUN”, was submitted to the PAC 2009, and an international workshop was organized in Feb. 2011 to form the SHOGUN collaboration. An international collaboration is being formed to construct the SHOGUN array.

(2) Decay spectroscopy

Beta- and isomer-spectroscopy is an efficient method for studying nuclear structure, especially for non-yrast levels. We had accumulated experimental techniques at the RIPS facility to investigate nuclear structure in light mass region via beta-gamma and beta-p coincidence. Concerning the medium and heavy mass region available at RIBF, we have developed two position-sensitive active-stoppers, strip-silicon detectors and a cylindrical active stopper called CAITEN, to achieve a low-background measurement by taking correlation between heavy ion stop position and beta-ray emission position. A site of decay-spectroscopy at the new facility of RIBF is the final focal plane of ZDS, where high precision of TOF in particle identification is obtained due to a long flight path from BigRIPS to ZDS.

At the end of 2009, the first decay spectroscopy was organized with a minimum setup of four clover gamma detectors and silicon strip detectors, to study neutron-rich nuclei with A~110. The first campaign was found successful and efficient to publish four letter articles in 2011, two PRL’s and two PLB’s. One of the PRL papers is associated to the r-process path where half-lives for 18 neutron-rich nuclei were determined for the first time. The other PRL paper reported a finding of deformed magic number 64 in the Zr isotopes.

The success of the first decay-spectroscopy campaign stimulated to form a new large-scale collaboration “EURICA”, where a twelve Euroball cluster array is coupled with the silicon-strip detectors to enhance gamma efficiency by a factor of 10. A construction proposal of “EURICA” was approved in the PAC 2011, and the commissioning was successfully organized in spring 2012. Since then, physics runs have been conducted for programs approved to survey nuclei of interest as many as possible, such as Ni-78, Pd-128, Sn-100. So far, 21 papers including 8 PRL’s and 4 PLB’s were published. One of the highlights is discovery of a seniority isomer in Pd-128, of which cascade gamma decay gives the energy of 1st excited state and robustness of N=82 magic number, and the other is a half-life measurement for 110 neutron-rich nuclei across the N=82 shell gap, which shows implications for the mechanism and universality of the r-process path.

Beta-delayed neutron emission probability of medium and heavy neutron-rich nuclei is important to understand nuclear structure and

the r-process path. In 2013, a new collaboration "BRIKEN" has been established to form a He-3 detector array. A present design of the array has neutron efficiency as high as 70% up to 3 MeV. The array will be coupled with the AIDA silicon strip system. A construction proposal was approved at the PAC 2013 and three physics proposals have been approved. The commissioning and physics run will start in autumn 2016.

The CAITEN detector was successfully tested with fragments produced with a Ca-48 beam in 2010.

(3) Equation-of-state via heavy-ion central collisions

Equation-of-state in asymmetric nuclear matter is one of major subjects in physics of exotic nuclei. Pi-plus and pi-minus yields in central heavy ion collisions at the RIBF energy are considered as one of EOS sensitive observables at the RIBF energy. To observe charged pions, a TPC for the SAMURAI spectrometer is being constructed under an international collaboration "SπRIT". Construction proposal was submitted at the PAC 2012, and physics proposals were approved at the PAC 2012 and 2013. The physics runs were successfully conducted in spring 2016.

An international symposium "NuSYM" on nuclear symmetry energy was organized at RIKEN July 2010 to invite researchers in three sub-fields, nuclear structure, nuclear reaction and nuclear astrophysics, and to discuss nuclear symmetry energy together. Since then, the symposium series have been held every year and been useful to encourage theoretical works and to strengthen the collaboration.

(4) Nucleon correlation and cluster in nuclei

Nucleon correlation and cluster in nuclei are matters of central focus in a "beyond mean-field" picture. The relevant programs with in-beam gamma and missing-mass techniques are to depict nucleon condensations and correlations in nuclear media as a function of density as well as temperature. Neutron-halo and –skin nuclei are objects to study dilute neutron matter at the surface. By changing excitation energies in neutron-rich nuclei, clustering phenomena and role of neutrons are to be investigated.

In 2013, two programs were conducted at the SAMURAI spectrometer. One is related to proton-neutron correlation in the C-12 nucleus via p-n knockout reaction with a carbon target. The other is to search for a cluster state in C-16, which was populated via inelastic alpha scattering. The data is being analyzed.

(5) Nuclear data for nuclear waste of long-lived fission products

The nuclear waste problem is an inevitable subject in nuclear physics and nuclear engineering communities. Since the Chicago Pile was established in 1942, nuclear energy has become one of major sources of energy. However, nowadays the nuclear waste produced at nuclear power plants has caused social problems. Minor actinide components of the waste have been studied well as a fuel in fast breeder reactors or ADS. Long-lived fission products in waste, on the other hand, have not been studied extensively. A deep geological disposal has been a policy of several governments, but it is difficult to find out location of the disposal station in terms of security, sociology and politics. To solve the social problem, a scientific effort is necessary for nuclear physics community to find out efficient methods for reduction of nuclear waste radioactivity.

In 2013, we have started up a new project to take nuclear data for transmutation of long-lived fission products to obtain cross section data needed for designing a nuclear waste treatment system. In 2014, we made the first attempt to obtain fragmentation reaction data with Cs-137 and Sr-90 beams at 200A MeV and published the data at PLB in 2016.

Since 2014, this activity has been intensively organized as one of the ImPACT projects by the Nuclear Transmutation Data Research Group.

Members

Chief Scientist (Lab. Head)

Hiroyoshi SAKURAI (Deputy Director, RNC)

Vice Chief Scientist

Takashi ICHIHARA

Research & Technical Scientists

Yoichi NAKAI (Senior Research Scientist)
Takashi KISHIDA (Senior Research Scientist)
Shunji NISHIMURA (Senior Research Scientist)
Tadaaki ISOBE (Research Scientist)
Pieter Christiaan DOORNENBAL (Research Scientist)
Daisuke SUZUKI (Research Scientist, Aug. 1, 2015 –)

Contract Researchers

Satoshi TAKEUCHI (– Mar. 31, 2015)
Mizuki NISHIMURA (Part-time)

Postdoctoral Researchers

He WANG (– Mar. 31, 2015)

Foreign Postdoctoral Researchers

Paer-Anders SOEDERSTROEM
He WANG (Apr. 1, 2015 –)

Research Consultants

Masayasu ISHIHARA
Hiroyuki MURAKAMI

Junior Research Associate

Yoshiaki SHIGA (Rikkyo Univ.)
Noritsugu NAKATSUKA (Kyoto Univ.)

Keishi MATSUI (Univ. of Tokyo)

International Program Associates

Jin WU (Peking Univ. – Sep. 30, 2015)
Sidong CHEN (Peking Univ.)
Phong VI (Hanoi University of Science, Apr. 1, 2015 –)
Longchun TAO (Peking University)

Visiting Researchers

Gabor KISS (JSPS Fellow)
David STEPPENBECK (JSPS Fellow)

Senior Visiting Scientists

Kengo OGAWA (Chiba Univ.)
Shigeru KUBONO (Univ. of Tokyo)

Visiting Scientists

Toshiyuki SUMIKAMA (Tohoku Univ.)
Hooi Jing ONG (RCNP)
Megumi NIIKURA (Univ. of Tokyo)
Silivio CHERUBINI (Univ. of Catania)
Hyo Soon JUNG (Univ. of Notre Dame)
Daiki NISHIMURA (Tokyo Univ. of Sci.)
Nobuyuki KOBAYASHI (Univ. of Tokyo)
Naohiko OTSUKA (Intl. Atomic Energy Agency, Austria)
Giuseppe LORUSSO (National Physics Lab., UK)
Hiu Ching LEE (Univ. of Hong Kong)
Zhengyu XU (Univ. of Hong Kong)
Indranil MAZUMDAR (GSI)
Byungsik HONG (Korea Univ.)
Prabhakar PALNI (MSU)
Rebecca SHANE (MSU)
Alan MCINTOSH (Texas A & M Univ.)
Michael YOUNG (Texas A & M Univ.)
Thomas DAVINSON (Univ. of Edinburgh)
Yassid AYYAD (Osaka Univ.)
Kathrin WIMMER (Univ. of Tokyo)
Tetsuya MURAKAMI (Kyoto Univ.)
Kazuo IEKI (Rikkyo Univ.)
Mitsunori FUKUDA (Osaka Univ.)
Nori AOI (RCNP)
Khiem Hong LE (Vietnam Academy of Sci. and Tech.)
Evgueni NIKOLSKI (RRC Kurchatov Inst.)
Alexey OGLOBLIN (RRC Kurchatov Inst.)
Hiroshi WATANABE (Beihang Univ.)
Akira ONO (Tohoku UNIv.)
Jianjun HE (Institute of Moderan Physics Chinese Academy of Science)
Clementine Angelique SANTAMARIA (Michigan State University)
Hui JIANg (Shanghai Maritime University)
Natsumi IKENO (Tottori Univ.)
Yont Jin KIM(Institute for Basic Science)
Pawlowski PIOTR (Institute of Nuclear Physics PAN)
Giordano CERIZZA (National Superconducting Cyclotron Laboratory)
Marisa GULINO (Universita di Enna Kore Italy)
Satoshi TAKEUCHI (TIT)

Visiting Technicians

Ivan KOJOUHAROV (GSI)

Student Trainees

Jongwon HWANG (Seoul Nat'l Univ.)
Sunji KIM (Seoul Nat'l Univ.)
Junichi OHNO (Osaka Univ.)
Hiroki NISHIBATA (Osaka Univ.)
Tetsuya YAMAMOTO (Osaka Univ.)
Ayumi YAGI (Osaka Univ.)
Kazuma KOBAYASHI (Rikkyo Univ.)
Ryo TANIUCHI (Univ. of Tokyo)
Shunpei KINNO (Tokyo Univ. of Sci.)
Daisuke WATANABE (Univ. of Tsukuba)
Jin-hee CHANG (Korea Univ.)
Tomoki ISHIGAKI (Osaka Univ.)
Rie DAIDO (Osaka Univ.)
Shouta MORIMOTO (Osaka Univ.)
Daiki MUROOKA (Niigata Univ.)
Tadashi TAKO (Tohoku Univ.)
Ippei NISHIZUKA (Tohoku Univ.)
Takuya MIYAZAKI (Univ. of Tokyo)
Satoru MOMIYAMA (Univ. of Tokyo)
Mana TANAKA (Osaka Univ.)
Shintaro YAMAOKA (Osaka Univ.)
Kouta WATANABE (Osaka Univ.)
Justin Brian ESTEE (MSU)
Masanori KANEKO (Kyoto Univ.)
Hideyuki MATSUZAWA (Rikkyo Univ.)
Hirotaka SUZUKI (Osaka Univ.)
Suwat TANGWANCHAROEN (MSU)
JungWoo LEE (Korea Univ.)
Takashi ANDO (Univ. of Tokyo)
Shunpei KOYAMA (Univ. of Tokyo)
Yuki YAMAGUCHI (Rikkyo Univ.)
Hiroyasu NAGAKURA (Rikkyo Univ.)
Hang DU (Osaka Univ.)
Yutaro TANAKA (Osaka Univ.)
Jiro SHIMAYA (Osaka Univ.)
Jonathan BARNEY (MSU)
Hiroyuki OIKAWA (Tokyo Univ. of Sci.)
Yoshimasa TAGUCHI (Tokyo Univ. of Sci.)
Naoya KAMBARA (Tokyo Univ. of Sci.)
Toshiki YOSHINOBU (Tokyo Univ. of Sci.)
Atsushi MIZUKAMI (Tokyo Univ. of Sci.)
Yuki KANKE (Tokyo Univ. of Sci.)
Junya NAGUMO (Tokyo Univ. of Sci.)
Phong VI (Hanoi Univ. of Sci.)
Jiajian LIU (Univ. of Hong Kong)
Shinnosuke KANAYA (Osaka Univ.)
Hiroshi KANAOKA (Osaka Univ.)
Shoichiro MASUOKA (Rikkyo Univ.)
Yan ZHANG (Tsinghua Univ.)
Shiwei XU (University of Chinese Academy of Sciences)
Simon JEANNE (Universite Paris Sud Xi)
Shunnsuke NAGAMINE (Univ. of Tokyo)
Takeshi SAITO (Univ. of Tokyo)
Eri MIYATA (Niigata Univ.)
Vaquero VICTOR (Universidad de Salamanca)
Linh BUI (Institute for Nuclear Science and Technology)
Chung LE (Institute for Nuclear Science and Technology)
Yuta KUNIMOTO (Rikkyo Univ.)

Yohei TANAKA (Rikkyo Univ.)
Sean SWEANY (Michigan state University)
Shoichi YAGI (Tokyo Univ. of Science)
Yuki Takei (Tokyo Univ. of Science)
Shaobo MA (University of Chinese Academy of Sciences)
Pawel LASKO (Jagiellonian University)
Krzysztof PELCZAR (Jagiellonian University)
Ryo HIGUCHI (Univ. of Tokyo)
Riku TAMURA (Univ. of Tokyo)
Masashi USAMI ((Univ. of Tokyo)

Interns

Justin Brian ESTEE (Michigan State University)
Simon JEANNE (Universite Paris Sud Xi)

List of Publications & Presentations

Publications

[Journal]

(Original Papers) *Subject to Peer Review

Y. Shiga, K. Yoneda, D. Steppenbeck, N. Aoi, P. Doornenbal, J. Lee, H. Liu, M. Matsushita, S. Takeuchi, H. Wang, H. Baba, P. Bednarczyk, Zs. Dombradi, Zs. Fulop, S. Go, T. Hashimoto, M. Honma, E. Ideguchi, K. Ieki, K. Kobayashi, Y. Kondo, R. Minakata, T. Motobayashi, D. Nishimura, T. Otsuka, H. Otsu, H. Sakurai, N. Shimizu, D. Sohler, Y. Sun, A. Tamii, R. Tanaka, Z. Tian, Y. Tsunoda, Zs. Vajta, T. Yamamoto, X. Yang, Z. Yang, Y. Ye, R. Yokoyama, and J. Zenihiro., “Investigating nuclear shell structure in the vicinity of 78Ni: Low-lying excited states in the neutron-rich isotopes 80,82Zn”, Physical Review C 93, 024320 (2016). *

N. Kobayashi, T. Nakamura, Y. Kondo, J. A. Tostevin, N. Aoi, H. Baba, R. Barthelemy, M. A. Famiano, N. Fukuda, N. Inabe, M. Ishihara, R. Kanungo, S. Kim, T. Kubo, G. S. Lee, H. S. Lee, M. Matsushita, T. Motobayashi, T. Ohnishi, N. A. Orr, H. Otsu, T. Sako, H. Sakurai, Y. Satou, T. Sumikama, H. Takeda, S. Takeuchi, R. Tanaka, Y. Togano, and K. Yoneda, “One-neutron removal from ^{29}Ne : Defining the lower limits of the island of inversion”, Physical Review C, 93:014613, 2016 *

C.Santamaria, C.Louchart, A.Obertelli, V.Werner, P.Doornenbal, F.Nowacki, G.Authelet, H.Baba, D.Calvet, F.Chateau, A.Corsi, A.Delbart, J.-M.Gheller, A.Gillibert, T.Isobe, V.Lapoux, M.Matsushita, S.Momiyama, T.Motobayashi, M.Niikura, H.Otsu, C.Peron, A.Peyaud,E.C.Pollacco, J.-Y.Rousse, H.Sakurai, M.Sasano, Y.Shiga, S.Takeuchi, R.Taniuchi, T.Uesaka, H.Wang, K.Yoneda, F.Browne, L.X.Chung, Zs.Dombradi, S.Franchoo, F.Giacoppo, A.Gottardo, K.Hadynska-Klek, Z.Korkulu, S.Koyama, Y.Kubota, J.Lee, M.Lettmann, R.Lozeva, K.Matsui, T.Miyazaki, S.Nishimura, L.Olivier, S.Ota, Z.Patel, N.Pietralla, E.Sahin, C.Shand, P.-A.Soderstrom, I.Stefan, D.Steppenbeck, T.Sumikama, D.Suzuki, Zs.Vajta, J.Wu, Z.Xu, “Extension of the N = 40 Island of Inversion towards N = 50: Spectroscopy of 66Cr, 70, 72Fe”, Physical Review Letters 115, 192501 (2015) *

K. Li, Y. Ye, T. Motobayashi, H. Scheit, P. Doornenbal, S. Takeuchi, N. Aoi, M. Matsushita, E. Takeshita, D. Pang, and H. Sakurai. “Relativistic Coulomb excitation in ^{32}Mg near 200 MeV / nucleon with a thick target”, Physical Review C, 92:014608, 2015. *

Zs. Vajta, Zs. Dombradi, Z. Elekes, T. Aiba, N. Aoi, H. Baba, D. Bemmerer, Zs. Fulop, N. Iwasa, A. Kiss, T. Kobayashi, Y. Kondo, T. Motobayashi, T. Nakabayashi, T. Nannichi, H. Sakurai, D. Sohler, S. Takeuchi, K. Tanaka, Y. Togano, K. Yamada, M. Yamaguchi, and K. Yoneda., “γ-ray spectroscopy of ^{19}C via the single-neutron knock-out reaction”, Physical Review C, 91:064315, 2015. *

D. Steppenbeck, S. Takeuchi, N. Aoi, P. Doornenbal, M. Matsushita, H. Wang, Y. Utsuno, H. Baba, S. Go, J. Lee, K. Matsui, S. Michimasa, T. Motobayashi, D. Nishimura, T. Otsuka, H. Sakurai, Y. Shiga, N. Shimizu, P.-A. Soderstrom, T. Sumikama, R. Taniuchi, J. J. Valiente-Dobon, and K. Yoneda., “Low-lying structure of 50Ar and the N=32 subshell closure”, Physical Review Letters 114, 252501 (2015). *

P.-A.Soderstrom, S.Nishimura, Z.Y.Xu, K.Sieja, V.Werner, P.Doornenbal, G.Lorusso, F.Browne, G.Gey, H.S.Jung, T.Sumikama, J.Taprogge, Zs.Vajta, H.Watanabe, J.Wu, H.Baba, Zs.Dombradi, S.Franchoo, T.Isobe, P.R.John, Y.-K.Kim, I.Kojouharov, N.Kurz, Y.K.Kwon, Z.Li, I.Matea, K.Matsui, G.Martinez-Pinedo, D.Mengoni, P.Morfouace, D.R.Napoli, M.Niikura, H.Nishibata, A.Odahara, K.Ogawa, N.Pietralla, E.Sahin, H.Sakurai, H.Schaffner, D.Sohler, I.G.Stefan, D.Suzuki, R.Taniuchi, A.Yagi, K.Yoshinaga, “Two-hole structure outside 78Ni: Existence of a μs isomer of 76Co and β decay into 76Ni”, Physical Review C 92, 051305 (2015) *

D.Suzuki, H.Iwasaki, D.Beaumel, M.Assie, H.Baba, Y.Blumenfeld, F.de Oliveira Santos, N.de Sereville, A.Drouart, S.Franchoo, J.Gibelin, A.Gillibert, S.Giron, S.Grevy, J.Guillot, M.Hackstein, F.Hammache, N.Keeley, V.Lapoux, F.Marechal, A.Matta, S.Michimasa, L.Nalpas, F.Naqvi, H.Okamura, H.Otsu, J.Pancin, D.Y.Pang, L.Perrot, C.M.Petrache, E.Pollacco, A.Ramus, W.Rother, P.Roussel-Chomaz, H.Sakurai, J.-A.Scarpaci, O.Sorlin, P.C.Srivastava, I.Stefan, C.Stodel, Y.Tanimura, S.Terashima, “Second 0+ state of unbound 12O: Scaling of mirror asymmetry”, Physical Review C 93, 024316 (2016) *

A.Fritsch, S.Beceiro Novo, D.Suzuki, W.Mittig, J.J.Kolata, T.Ahn, D.Bazin, F.D.Becchetti, B.Bucher, Z.Chajecki, X.Fang, M.Febbraro, A.M.Howard, Y.Kanada-En'yo, W.G.Lynch, A.J.Mitchell, M.Ojaruega, A.M.Rogers, A.Shore, T.Suhara, X.D.Tang, R.Torres-Isea, H.Wang, “One-dimensionality in atomic nuclei: A candidate for linear-chain α clustering in 14C”, Physical Review C 93, 014321 (2016) *

A.Matta, D.Beaumel, H.Otsu, V.Lapoux, N.K.Timofeyuk, N.Aoi, M.Assie, H.Baba, S.Boissinot, R.J.Chen, F.Delaunay, N.de Sereville, S.Franchoo, P.Gangnant, J.Gibelin, F.Hammache, Ch.Houarner, N.Imai, N.Kobayashi, T.Kubo, Y.Kondo, Y.Kawada, L.H.Khiem, M.Kurata-Nishimura, E.A.Kuzmin, J.Lee, J.F.Libin, T.Motobayashi, T.Nakamura, L.Nalpas, E.Yu.Nikolskii, A.Obertelli, E.C.Pollacco, E.Rindel, Ph.Rosier, F.Saillant, T.Sako, H.Sakurai, A.M.Sanchez-Benitez, J-A.Scarpaci, I.Stefan, D.Suzuki, K.Takahashi, M.Takechi, S.Takeuchi, H.Wang, R.Wolski, K.Yoneda, “New findings on structure and production of 10He from 11Li with the (d, 3He) reaction”, Physical Review C 92, 041302 (2015) *

M.Vandebrouck, J.Gibelin, E.Khan, N.L.Achouri, H.Baba, D.Beaumel, Y.Blumenfeld, M.Caamano, L.Caceres, G.Colo, F.Delaunay, B.Fernandez-Dominguez, U.Garg, G.F.Grinyer, M.N.Harakeh, N.Kalantar-Nayestanaki, N.Keeley, W.Mittig, J.Pancin, R.Raabe, T.Roger, P.Roussel-Chomaz, H.Savajols, O.Sorlin, C.Stodel, D.Suzuki, J.C.Thomas, “Isoscalar response of 68Ni to α-particle and deuteron probes”, Physical Review C 92, 024316 (2015) *

Y.X.Watanabe, Y.H.Kim, S.C.Jeong, Y.Hirayama, N.Imai, H.Ishiyama, H.S.Jung, H.Miyatake, S.Choi, J.S.Song, E.Clement, G.de France, A.Navin, M.Rejmund, C.Schmitt, G.Pollarolo, L.Corradi, E.Fioretto, D.Montanari, M.Niikura, D.Suzuki, H.Nishibata, J.Takatsu, “Pathway for the Production of Neutron-Rich Isotopes around the N=126 Shell Closure”, Physical Review Letters 115, 172503 (2015) *

S. Q. Hou, J. J. He, S. Kubono, and Y. S. Chen, “Revised thermonuclear rate of ^{7}Be(n,α)^{4}He relevant to Big-Bang nucleosynthesis”, Physical Review C 91 (2015) 055802 *

S. Cherubini, M. Gulino, C. Spitaleri, G. G. Rapisarda, M. La Cognata, L. Lamia, R. G. Pizzone, S. Romano, S. Kubono, H. Yamaguchi, S.

Hayakawa, Y. Wakabayashi, N. Iwasa, S. Kato, T. Komatsubara, T. Teranishi, A. Coc, N. de S´er´eville, F. Hammache, G. Kiss, S. Bishop, and D. N. Binh, “First application of the Trojan horse method with a radioactive ion beam: Study of the ^{18}F(p,α)^{15}O reaction at astrophysical energies”, Physical Review C 92 (2015) 015805 *

A. Kim, N.H. Lee, M.H. Han, J.S. Yoo, K.I. Hahn, H. Yamaguchi, D.N. Binh, T. Hashimoto, S. Hayakawa, D. Kahl, T. Kawabata, Y. Kurihara, Y. Wakabayashi, S. Kubono, S. Choi, Y.K. Kwon, J.Y. Moon, H.S. Jung, C.S. Lee, T. Teranishi, S. Kato, T. Komatsubara, B. Guo, W.P. Liu, B. Wang, and Y. Wang, “Measurement of the ^{14}O(a, p)^{17}F cross section at Ecm = 2.1 - 5.3 MeV”, Physical Review C 92 (2015) 035801 *

H. Wang, H. Otsu, H. Sakurai, D.S. Ahn, M. Aikawa, P. Doornenbal, N. Fukuda, T. Isobe, S. Kawakami, S. Koyama, T. Kubo, S. Kubono, G. Lorusso, Y. Maeda, A. Makinaga, S. Momiyama, K. Nakano, M. Niikura, Y. Shiga, P.-A. Söderström, H. Suzuki, H. Takeda, S. Takeuchi, R. Taniuchi, Ya. Watanabe, Yu. Watanabe, H. Yamasaki, and K. Yoshida, “Spallation reaction study for fission products in nuclear waste: Cross section measurements for ^{137}Cs and ^{90}Sr on proton and deuteron”, Physics Letters B 754 (2016) 104-108 *

A. I. Morales, G. Benzoni, H. Watanabe, S. Nishimura, F. Browne, R. Daido, P. Doornenbal, Y. Fang, G. Lorusso, Z. Patel, S. Rice, L. Sinclair, P.-A. Söderström, T. Sumikama, J. Wu, Z. Y. Xu, A. Yagi, R. Yokoyama, H. Baba, R. Avigo, F. L. Bello Garrote, N. Blasi, A. Bracco, F. Camera, S. Ceruti, F. C. L. Crespi, G. de Angelis, M.-C. Delattre, Zs. Dombradi, A. Gottardo, T. Isobe, I. Kojouharov, N. Kurz, I. Kuti, K. Matsui, B. Melon, D. Mengoni, T. Miyazaki, V. Modamio-Hoyborg, S. Momiyama, D. R. Napoli, M. Niikura, R. Orlandi, H. Sakurai, E. Sahin, D. Sohler, H. Shaffner, R. Taniuchi, J. Taprogge, Zs. Vajta, J. J. Valiente-Dobón, O. Wieland, and M. Yalcinkaya, "Low-lying excitations in ^{72}Ni", Physical Review C 93, 034328 (2016) *

S. Shibagaki, T. Kajino, G.J. Mathews, S. Chiba, S. Nishimura, G. Lorusso, "RELATIVE CONTRIBUTIONS OF THE WEAK, MAIN, AND FISSION-RECYCLYING r-PROCESS", Astrophysical. Journal. 816, 79 (2016) *

R. Lozeva, H. Naïdja, F. Nowacki, J. Dudek, A. Odahara, C.-B. Moon, S. Nishimura, P. Doornenbal, J.-M. Daugas, P.-A. Söderström, T. Sumikama, G. Lorusso, J. Wu, Z. Y. Xu, H. Baba, F. Browne, R. Daido, Y. Fang, T. Isobe, I. Kojouharov, N. Kurz, Z. Patel, S. Rice, H. Sakurai, H. Schaffner, L. Sinclair, H. Watanabe, A. Yagi, R. Yokoyama, T. Kubo, N. Inabe, H. Suzuki, N. Fukuda, D. Kameda, H. Takeda, D. S. Ahn, D. Murai, F. L. Bello Garrote, F. Didierjean, E. Ideguchi, T. Ishigaki, H. S. Jung, T. Komatsubara, Y. K. Kwon, P. Lee, C. S. Lee, S. Morimoto, M. Niikura, H. Nishibata, and I. Nishizuka, "New isomer found in $^{140}_{52}$Sb^{89}: Sphericity and shell evolution between N = 82 and N = 90", Physical Review C 93, 014316 (2016) *

Z. Patel, ..., S. Nishimura, …, H. Sakurai et al., "Decay spectroscopy of ^{160}Sm: The lightest four-quasiparticle K isomer", Physics Letters B 753, (2016) 182-186. *

R. Lozeva, ... S. Nishimura, …, H. Sakurai et al., "New decay scheme of the $^{136}_{51}$Sb$_{85}$ 6$^-$ isomer", Physical Review C 92, 024304 (2015) *

G. Benzoni, A.I. Morales, H. Watanabe, S. Nishimura, …, H. Sakurai et al., "Decay properties of ^{68,69,70}Mn: Probing collectivity up to N = 44 in Fe isotopic chain", Physics Letters B 751, (2015) 107-112. *

P. Lee, ..., S. Nishimura, …, H. Sakurai et al., "β-delayed γ-ray spectroscopy of non-yrast statein ^{138}Te near the neutron drip line", Physical Review Letters 115, 192591 (2015) *

F. Browne, ..., S. Nishimura, …, H. Sakurai et al., "Lifetime measurement of the first 2$^+$ states in ^{104,106}Zr: Evolution of ground-state deformations", Physics Letters B 750 (2015) 448-452. *

J. Taprogge, A. Jungclaus, H. Grawe, S. Nishimura, …, H. Sakurai et al., "β decay of ^{129}Cd and excited states in ^{129}In", Physical Review C 91, 054324 (2015) *

K. Steiger, S. Nishimura et al., "Nuclear structure of ^{37,38}Si investigated by decay spectroscopy of ^{37,38}Al", Eur. Phys. J. A 51, 117 (2015) *

G. Lorusso, S. Nishimura, …, H. Sakurai et al., "β-Decay Half-Lives of 110 Neutron-Rich Nuclei across the N = 82 Shell Gap: Implications for the Mechanism and Universality of the Astrophysical r Process", Physical Review Letters 114, 192501 (2015) *

H. Nishibata, ..., S. Nishimura et al., "High-spin states in ^{136}La and possible structure change in the N = 79 region", Physical Review C 91, 054305 (2015) *

S. Tomita, Y. Nakai, S. Funada, H. Tanikawa, I. Harayama, H. Kobara, K. Sasa, J. O. P. Pedersen, P. Hvelplund, “Oxidation of SO_2 and formation of water droplets under irradiation of 20 MeV protons in $N_2/H_2O/SO_2$”, Nuclear Instrumentation and Methods B 365, 616-621 (2015). *

Y. Nakano, A. A. Sokolik, A.V. Stysin, Y. Nakai, K. Komaki, E. Takada, T. Murakami and T. Azuma, “Metastable Ar^{17+}(2s) production by Stark-assisted resonant coherent excitation”, Journal of Physics B: Atom Molecule Optical Physics 48, 144026-1-7 (2015). *

[Proceedings]

(Original Papers) *Subject to Peer Review

S.Benamara, N.de Sereville, P.Adsley, A.M.Laird, F.Hammache, I.Stefan, P.Roussel, S.Ancelin, M.Assie, C.Barton, A.Coc, C.Diget, I.Deloncle, S.Fox, J.Guillot, C.Hamadache, J.Kiener, B.Le Crom, L.Lefebvre, A.Lefebvre-Schuhl, G.Marquinez-Duran, G.Mavilla, P.Morfouace, A.Mutschler, C.T.Nsangu, L.Perrot, N.Oulebsir, A.-M.Sanchez-Benitez, D.Suzuki, V.Tatischeff, M.Vandebrouck, Study of the 26Al(n, p)26Mg and 26Al(n, α))23Na reactions using the 26Al(p, p')27Al inelastic scattering reaction, Nuclear Physics in Astrophysics VI, Lisbon, Portugal, May 19-24, 2013 p.012018 (2016); J.Phys.:Conf.Ser. 665

E.Sahin, F.L.Bello Garrote, A.Gorgen, G.de Angelis, M.Niikura, S.Nishimura, D.Mengoni, Z.Xu, H.Baba, F.Browne, P.Doornenbal, S.Franchoo, G.Guillaume, T.Isobe, P.R.John, H.S.Jung, K.K.Hadynska-Klek, Z.Li, G.Lorusso, I.Matea, K.Matsui, P.Morfouace, D.R.Napoli, H.Nishibata, A.Odahara, H.Sakurai, P.-A.Soderstrom, D.Sohler, I.Stefan, T.Sumikama, D.Suzuki, R.Taniuchi, J.Taprogge, Z.Vajta, H.Watanabe, V.Werner, J.Wu, A.Yagi, K.Yoshinaga, First Results on the Excited States in 77Cu, Acta Physica Polonica B47, 889 (2016)

H. Wang, In-beam gamma-ray spectroscopy and cross section measurement strategy for long-lived fission products at RIBF, Proceedings of the 2014 Symposium on Nuclear Data, 69 (2015).

G. Jhang et al., Study of the Nuclear Symmetry Energy at ρ ~ 2ρ0 with SπRIT-TPC, JPS Conference Proceedings 6, 030136 (2015)

D. Steppenbeck, S. Takeuchi, N. Aoi, P. Doornenbal, M. Matsushita, H. Wang, H. Baba, N. Fukuda, S. Go, M. Honma, J. Lee, K. Matsui, S. Michimasa, T. Motobayashi, D. Nishimura, T. Otsuka, H. Sakurai, Y. Shiga, N. Shimizu, P.-A. Soderstrom, T. Sumikama, H. Suzuki, R. Taniuchi, Y. Utsuno, J. J. Valiente-Dobon, and K. Yoneda., In-beam γ-ray spectroscopy of very neutron-rich N=32 and 34 nuclei., JPS Conf. Proc. **6,** 020019 (2015)

H. Wang, N. Aoi, S. Takeuchi, M. Matsushita, P. Doornenbal, T. Motobayashi, D. Steppenbeck, K. Yoneda, H. Baba, L. Cáceres, Zs. Dombrádi, Y. Kondo, J. Lee, K. Li, H. Liu, R. Minakata, D. Nishimura, H. Otsu, S. Sakaguchi, H. Sakurai, H. Scheit, D. Sohler, Y. Sun, Z. Tian, R. Tanaka, Y. Yogano, Zs. Vajta, Z. Yang, T. Yamamoto, Y. Ye, and R. Yokoyama, Collectivity in the Neutron-Rich Pd Isotopes Toward *N* = 82, Proc. Conf. Advances in Radioactive Isotope Science (ARIS2014), JPS Conf. Proc. 6, 030010 (2015).

J. Wu, S. Nishimura, G. Lorusso, Z.Y. Xu, E Ideguchi, *et al.*:, “β-decay half-lives of neutron-rich nuclei around 158Nd, relevant to the

formation of the A≈165 rare-earth element peak", EPJ Web Conf. 109, 08003 (2016)
P.-A. Söderström, P. H. Regan, P. M. Walker, H. Watanabe, P. Doornenbal, *et al.*, "Heavy rotation – evolution of quadrupole collectivity centred at the neutron-rich doubly mid-shell nucleus 170Dy", AIP Conf. Proc. 1681, 030009 (2015)
H. Watanabe, "Decay spectroscopy of neutron-rich rare-earth isotopes and collectivity around double midshell", AIP Conf. Proc. 1681, 030010 (2015)
A.I. Morales, G. Benzoni, H. Watanabe, D. Sohler, E. Sahin, *et al.*:, "β-decay studies around 78Ni: Investigation of neutron-rich Ni isotopes", In Yu E Penionzhkevich and Yu G Sobolev (editors): *Proceedings of the International Symposium on Exotic Nuclei*, page 429. World Scientific Publishing (2015).
J. Wu, S. Nishimura, G. Lorusso, Z. Y. Xu, E. Ideguchi, *et al.,* "β-Decay of Neutron-Rich Nuclei around 158Nd and the Origin of Rare-Earth Elements, JPS Conf. Proc. 6, 030064 (2015)
I. Nishizuka, T. Sumikama, F. Browne, A. M. Bruce, S. Nishimura, *et al.*:, "β Decay Half-Lives of A ~ 110 Nuclei on the r-Process Path", JPS Conf. Proc. 6, 030062 (2015)
Z.Y. Xu, S. Nishimura, G. Lorusso, P. Doornenbal, M. Niikura, *et al.*:, "Systematic Study of β-Decay Properties in the Vicinity of ^{78}Ni", JPS Conf. Proc. 6, 030048 (2015)
R. Yokoyama, E. Ideguchi, G. Simpson, M. Tanaka, S. Nishimura, *et al.,* "Isomers of Pm Isotopes on the Neutron-Rich Frontier of the Deformed Z ~ 60 Region", JPS Conf. Proc. 6, 030021 (2015)
J. Taprogge, A. Jungclaus, H. Grawe, S. Nishimura, P. Doornenbal, *et al.*:, "Isomer and Beta Decay Spectroscopy in the ^{132}Sn Region with EURICA", JPS Conf. Proc. 6, 030020 (2015)
A. Yagi, A. Odahara, R. Daido, Y. Fang, H. Nishibata, *et al.*:, "New Isomers in Neutron-Rich Cs Isotopes", JPS Conf. Proc. 6, 030019 (2015)
P.-A. Söderström, G. Lorusso, H. Watanabe, S. Nishimura, P. Doornenbal, *et al.*:, "Shape Evolution in Neutron-Rich Ru Nuclei", JPS Conf. Proc. 6, 030013 (2015)
F. Browne, A. M. Bruce, T. Sumikama, I. Nishizuka, S. Nishimura, *et al.*:, "Half-Life Measurements of 2^+_1 States in the Vicinity of ^{108}Zr and their Implications for Ground-State Deformations", JPS Conf. Proc. 6, 030012 (2015)
G. Benzoni, H. Watanabe, A. I. Morales, S. Nishimura, R. Avigo, *et al.*:, "β-Decay Measurements in the Vicinity of ^{78}Ni with the EURICA Setup", JPS Conf. Proc. 6, 020021 (2015)
H. Watanabe:, "The Nature of a Shell Closure at N = 82 Explored with Seniority and Spin-Gap Isomers in Neutron-Rich Palladium and Silver Isotopes", JPS Conf. Proc. 6, 020008 (2015)
K. Moschner, A. Blazhev, N. Warr, P. Boutachkov, P Davies, *et al.*:, "Study of ground and excited state decays in N ≈ Z Ag nuclei", EPJ Web Conf. 93, 01024 (2015)

[Others]
西村俊二、「重元素合成の鍵を握る中性子過剰核の研究: r 過程研究の幕開け」, パリティー 2016 年 1 月号
S. Takeuchi, D. Steppenbeck, and Y. Utsuno, "Discovery of new magic number via in-beam γ-ray spectroscopy", Butsuri **70,** 535–539 (2015).
岸田隆、「『科学コミュニケーション』の著者（物理学者）が影響を受けたフィクション本【特別編】」、サイエンスコミュニケーション vol.4, No. 1, (2015) 16-17

Oral Presentations

[International Conference etc.]

H. Sakurai, "Overview of physics experiments at RIPS/BigRIPS", International Symposium on Physics with Fragment Separators -25th Anniversary of RIKEN-Projectile Fragment Separator (RIPS25), Hayama, Japan, Dec., 2015
H. Sakurai, "Scientific programs with exotic nuclei at RIBF", 27th ASRC International Workshop "Nuclear Fission and Exotic Nuclei", Tokai, Japan, Dec., 2015
H. Sakurai, "Overview of RIBF", RISP Workshop, Daejeon, Korea, Nov., 2015
H. Sakurai, "Current and future programs at RIBF", 2015 ANPhA Symposium, Gyeongju, Korea, Oct., 2015
H. Sakurai, "Recent progress on exotic nuclei at RIBF", Mazurian Lakes Conference on Physics Frontiers in Nuclear Physics, Piaski, Poland, Sept., 2015
H. Sakurai, "New results on the structure of exotic nuclei", APS Spring Meeting, Baltimore, USA, April, 2015
H. Sakurai, "Present Status of and Plans for RIBF", Physics Division Seminar, Oak Ridge, USA, Dec., 2015
H. Sakurai, "New Magicity and Magicity Loss of Nuclei", Dept.-of-Physics Seminar, Knoxville, USA, Dec., 2015
S. Nishimura, "Properties of Exotic Nuclei Identified at RIBF", XXXIV Mazurian Lakes Conference on Physics, September 6 – 13 (2015), Piaski, Poland.
S. Nishimura, "Decay Spectroscopy and Future perspectives at RIBF", ARIEL Science Workshop, July 8 – 9 (2015), Vancouver, Canada.
S. Nishimura, "Decay Spectroscopy of Neutron-Rich Nuclei Relevant to Astrophysical R-Process", The 5th Symposium 'Neutrinos and Dark Matter in Nuclear Physics (NDM15)', June 1 – 5, (2015), Jyväskylä Finland.
P. Doornenbal, "Overview of In-Beam Gamma-ray Spectroscopy at the RIBF", The 3rd Topical Workshop on Nuclear Structure, Bormio, Colombia, February 22-- 28, 2016
P. Doornenbal, "Overview of In-Beam Gamma-ray Spectroscopy at the RIBF", The XI Latin American Symposium on Nuclear Physics and Applications, Medellin, Colombia, November 30 -- December 4, 2015
P. Doornenbal, "In-Beam Gamma-ray Spectroscopy at the RIBF", Nuclear Structure and Dynamics III, Portoroz, Slovenia, June 14-- June 19, 2015
P. Doornenbal, "First Results from SEASTAR and Shell Structure towards 100Sn", The Gordon Research Conference on Nuclear Chemistry, New London, USA, May 31-- June 5, 2015
T. Isobe, "Integration of GET electronics on TPC for HIC program at RIBF", Workshop on Active Targets and Time Projection Chambers for Nuclear Physics Experiments, 18-20 May 2015, Michigan State University
T. Isobe, "Current status of the SπRIT TPC project", NuSYM15, 29 Jun - 2 Jul 2015, Auditorium Maximum, Krakow, Poland
T. Isobe, "SAMURAI-SPiRIT experiment for the study of density dependent nuclear symmetry energy by using heavy RI collision", 8th Japan-Italy symposium, 7-10 Mar 2016, RIKEN
D. Suzuki, "Study of the proton drip-line nuclei using (p,t) reactions", 2nd LISE Workshop from December 16 through 18 at GANIL, Caen, France

D. Suzuki, “Revisit of unbound 12O via the (p, t) reaction”, MUST2 workshop 2015 from June 4 through 6 at CEA-Saclay, Orme des Merisiers, France
S. Kubono, “Explosive Nuclear Burning in the pp-Chain Region and the Breakout Processes”, The 13th International Symposium on Origin of Matter and Evolution of Galaxies, Beijing, China, June 24-27, 2015
S. Kubono, “Neutron and Alpha Structure in Neutron Deficient Nuclei in Astrophysics”, The 5th International Conference on Proton-Emitting Nuclei (PROCON2015), Lanzhou, China, July 6 – 10, 2015
S. Kubono, “Experimental Challenge to the ap-Process in Type II Supernovae”, The 8th European Summer School on Experimental Nuclear Astrophysics, Santa Tecla, Italy, September 13-20, 2015
S. Kubono, “Dynamically Deformed Resonances in Nuclear Astrophysics -Cluster and Molecular Resonances in astrophysics-“, The 27th ASRC International Workshop on Nuclear Fission and Eotic Nuclei, Tokai, Japan, Dec. 1 – 2, 2015
E. Nikolskii, “Missing mass spectroscopy and experiments at RIPS”, International symposium on “Physics with Fragment Separators-25th Anniversary of RIKEN-Projectile Fragment Separator (RIPS25)”, Shonan Village Center on Dec. 6-7, 2015
G.G. Kiss, "Status report on the preparation of the Briken project", 3rd BRIKEN workshop, Valencia, Spain, 22-24, July 2015
D. Steppenbeck et al., “Intermediate-energy Coulomb excitation of neutron-rich Si isotopes: Proposal to be submitted to the 16th PAC Meeting for Nuclear Physics Experiments at the RIBF”, The 4th SUNFLOWER Workshop, Osaka, Japan (September 30, 2015).
G. Jhang et al., “Performance Evaluation of GET Electronics for SπRIT-TPC at HIMAC”, 2015 Spring KPS Conference

[Domestic Conference]

櫻井博儀, "科学するこころ -対象、思索、実行-", 不動岡高校、加須市、2015 年 6 月
S. Nishimura, "Experimental Challenges: Study of R-process Nucleosynthesis at RIBF", The 9th Japan-China Nuclear Physics Symposium (JCNP2015), November 7 - 12 (2015), Osaka, Japan.
S. Nishimura, "Survey of Decay Properties for Exotic Nuclei at RIBF", International symposium on the "Frontier of γ-ray spectroscopy" (Gamma15),September 30 – October 3 (2015), Osaka, Japan.
T. Isobe, “HOKUSAI GreatWave を用いた RIBF 原子核物理実験データ解析”, ペタスケールシステム HOKUSAI GreatWave とアプリケーションの研究開発への針路, 19-Jun-15, RIKEN
T. Isobe, “SAMURAI TPC の読み出しシステム”, 「高密度核物質に挑む実験の将来－施設・装置の観点から」, 5-Dec-15, RIKEN
S. Kubono, “A special series of lectures on nuclear astrophysics”, Hokkaido Nuclear Theory Group Autumn School, Nov. 25 – 27, 2015, Hokkaido University
Y. Nakai, H. Hidaka, N. Watanabe, T. M. Kojima, “Measurements of reaction equilibrium distribution for $H^+(H_2O)_n$ generated in an ion drift tube”, 4th meeting of Ion Mobility Research (Invited talk), Sendai, April 2015.
N. Watanabe, Y. Nakai, T. Hama, H. Hidaka, “Ion-induced nucleation experiment III: Approach to reaction kinetics”, Japan Geoscience Union Meeting 2015, Chiba, May 2015.
Y. Nakai, Y. Motizuki, M. Maruyama, H. Akiyoshi, T. Imamura, “Variation of trace chemical species induced by solar energetic particles in the middle atmosphere: ozone and nitric acid”, Japan Geoscience Union Meeting 2015 (International session), Chiba, May 2015.
Y. Nakai, N. Watanabe, “Current status of experiments for hydrogenation of C_{60} at temperatures of interstellar molecular clouds”, 3rd meeting of Research Project on Evolution of Molecules in Space Grant-in-Aid for Scientific Research on Innovative Areas, Sapporo, October 2015.
岸田隆, 「着眼大局・着手小局 一文明論的視座からのバックキャスティングー」, 第３期イノベーション・デザイン研究会（日本生産性本部・経営アカデミー）、東京 (2015, April)
岸田隆, 「よりよき地方のあり方に関する長期的視野からの提言」, 那須塩原市執行部懇談会、那須塩原 (2015, May)
岸田隆, 「原子力関連情報の科学コミュニケーション」, 研究会「東京と南洋を往還する帝国の残映とゴジラ映画史５０年の比較文化史」、新潟 (2015, May)
岸田隆, 「Preparation for Zero-growth Economy」, Reexamining Japan in Global Context: 8th Forum "Zero-Growth Economy", Suntory Foundation, サントリー文化財団講演会、東京 (2015, May)

Posters Presentations

[International Conference etc.]

S. Tomita, Y. Nakai, S. Funada, H. Tanikawa, I. Harayama, H. Kobara, K. Sasa, J. O. P. Pedersen, P. Hvelplund, “Formation of nanodroplets in N2/H2O/SO2 under irradiation of fast proton beam”, Swift Heavy Ion in Matter 2015, Darmstadt, May 2015.
Y. Nakai, H. Hidaka, N. Watanabe, T. M. Kojima, “Reaction equilibrium for stepwise attachment/detachment of a water molecule to/from $H_3O^+(H_2O)_n$ in electric field of an ion drift tube”, 31st Symposium on Chemical Kinetics and Dynamics, Sapporo, June 2015.
Y. Nakai, H. Hidaka, N. Watanabe, T. M. Kojima, “Reaction equilibrium in electric field of an ion drift tube: stepwise formation of $H_3O^+(H_2O)_n$ cluster ions”, XIX International Symposium on Electron-Molecule Collisions and Swarms, Lisbon, July 2015.
K. Takahashi, Y. Motizuki, Y. Nakai, K. Suzuki, Y. Iizuka, and H. Motoyama, “Overview of chemical composition and the characteristics of the distributions of Na+ and Cl- in shallow ice core samples from DF01 core (Antarctica) drilled in 2001”, The 6th Symposium on Polar Science, Tachikawa, Japan, November 2015. *
Y. Hasebe, Y. Motizuki, Y. Nakai, K. Takahashi, “Diagnose oscillation properties observed in an annual ice-core oxygen isotope record obtained from Dronning Maud Land, Antarctica”, The 6th Symposium on Polar Science, Tachikawa, Japan, November 2015.

RIBF Research Division
Spin isospin Laboratory

1. Abstract

The Spin Isospin Laboratory pursues research activities putting primary focus on interplay of spin and isospin in exotic nuclei. Understanding nucleosyntheses in the universe, especially those in r- and rp-processes is another big goal of our laboratory.

Investigations on isospin dependences of nuclear equation of state, spin-isospin responses of exotic nuclei, occurrence of various correlations at low-densities, evolution of spin-orbit coupling are main subjects along the line. We are leading a mass measurement project with the Rare RI Ring project, too. Through the experimental studies, we will be able to elucidate a variety of nuclear phenomena in terms of interplay of spin and isospin, which will in turn, lead us to better understanding of our universe.

2. Major Research Subjects

(1) Direct reaction studies of neutron-matter equation of state
(2) Study of spin-isospin responses with RI-beams
(3) R-process nucleosynthesis study with heavy-ion storage ring
(4) Application of spin-polarization technique to RI-beam experiments and other fields
(5) Development of special targets for RI-beam experiments

3. Summary of Research Activity

(1) Direct reaction studies of neutron matter equation of state

Direct reactions induced by light-ions serve as powerful tools to investigate various aspects of nuclei. We are advancing experimental programs to explore equation of state of neutron matter, via light-ion induced reactions with RI-beams.

(1-a) Determination of a neutron skin thickness by proton elastic scattering

A neutron skin thickness is known to have strong relevance to asymmetry terms of nuclear equation of state, especially to a term proportional to density. The ESPRI project aims at determining density distributions in exotic nuclei precisely by proton elastic scattering at 200−300 MeV/nucleon. An experiment for ^{132}Sn that is a flagship in this project is planned to be performed in 2015. Prior to the ^{132}Sn experiment, we have applied the ESPRI setup that consists of a solid hydrogen target and recoil proton detectors to ^{16}C in 2012.

(1-b) Asymmetry terms in nuclear incompressibility

Nuclear incompressibility represents stiffness of nuclear matter. Incompressibility of symmetric nuclear matter is determined to be 230±20 MeV, but its isospin dependence still has a large uncertainty at present. A direct approach to the incompressibility of asymmetric nuclear matter is an experimental determination of energies of isoscalar giant monopole resonances (GMR) in heavy nuclei. We have developed, in close collaboration with Center for Nuclear Study (CNS) of University of Tokyo, an active gas target for deuteron inelastic scattering experiments to determine GMR energies. The active gas target has been already tested with oxygen and xenon beams at HIMAC and will be applied to a ^{132}Sn experiment in 2015.

(1-c) Multi-neutron andα-cluster correlations at low densities

Occurrences of multi-neutron andα-cluster correlations are other interesting aspects of nuclear matter and define its low-density behavior. The multi-neutron andα-cluster correlations can be investigated with the large-acceptance SAMURAI spectrometer. The SAMURAI has been already applied to experiments to explore light neutron-rich nuclei close to the dripline. We plan to reinforce experimental capabilities of the SAMURAI by introducing advanced devices such as MINOS (Saclay) and NeuLAND (GSI).

(1-d) Fission barrier heights in neutron-rich heavy nuclei

The symmetry energy has a strong influence on fission barrier heights in neutron-rich nuclei. Knowledge on the fission barrier heights, which is quite poor at present, is quite important for our proper understanding on termination of the r-process. We are planning to perform, in collaboration with the TU Munich group, (p,2p)-delayed fission experiments at the SAMURAI to determine the fission barrier heights in neutron-rich nuclei in Pb region.

(2) Study of spin-isospin responses with RI-beams

The study of spin-isospin responses in nuclei forms one of the important cores of nuclear physics. A variety of collective states, for example isovector giant dipole resonances, isobaric analogue states, Gamow-Teller resonances, have been extensively studied by use of electromagnetic and hadronic reactions from stable targets.

The research opportunities can be largely enhanced with light of availabilities of radioactive isotope (RI) beams and of physics of unstable nuclei. There are three possible directions to proceed. The first direction is studies of spin-isospin responses of unstable nuclei via inverse-kinematics charge exchange reactions. A neutron-detector array WINDS has been constructed, under a collaboration of CNS, Tokyo and RIKEN, for inverse kinematics (p,n) experiments at the RI Beam Factory. We have already applied WINDS to the (p,n) experiments for ^{12}Be, ^{132}Sn and plan to extend this kind of study to other exotic nuclei.

The second direction is studies with RI-beam induced charge exchange reaction. RI-beam induced reactions have unique properties which are missing in stable-beam induced reactions and can be used to reach the yet-to-be-discovered states. We have constructed the

SHARAQ spectrometer and the high-resolution beam-line at the RI Beam Factory to pursue the capabilities of RI-beam induced reactions as new probes to nuclei. One of the highlights is an observation of β^+ type isovector spin monopole resonances (IVSMR) in ^{208}Pb and ^{90}Zr via the (t, ^{3}He) reaction at 300 MeV/nucleon.

The third direction is studies of neutron- and proton-rich nuclei via stable-beam induced charge exchange reactions, which is conducted under collaboration with Research Center for Nuclear Physics (RCNP), Osaka University. We have performed the double charge exchange ^{12}C(^{18}O, ^{18}Ne)^{12}Be reaction at 80 MeV/nucleon to investigate structure of a neutron-rich ^{12}Be nucleus. Peaks corresponding to ground and excited levels in ^{12}Be have been clearly observed. Another double charge exchange reaction, (^{12}C, ^{12}Be(0_2^+)) are being used to search for double Gamow-Teller resonances.

(3) R-process nucleosynthesis study with heavy-ion storage ring

Most of the r-process nuclei become within reach of experimental studies for the first time at RI Beam Factory at RIKEN. The Rare RI Ring at RIBF is the unique facility with which we can perform mass measurements of r-process nuclei. Construction of the Rare RI Ring started in FY2012 in collaboration with Tsukuba and Saitama Universities. A major part of the ring has been completed and the commissioning run is planned in FY2014.

We are planning to start precise mass measurements of r-process nuclei in 2015. A series of experiments will start with nuclei in the A=80 region and will be extended to heavier region.

(4) Application of spin-polarization technique to RI-beam experiments and other fields

A technique to produce nuclear polarization by means of electron polarization in photo-excited triplet states of aromatic molecules can open new applications. The technique is called “Tripletd-DNP”. A distinguished feature of Triplet-DNP is that it works under a low magnetic field of 0.1—0.7 T and temperature higher than 100 K, which exhibits a striking contrast to standard dynamic nuclear polarization (DNP) techniques working in extreme conditions of several Tesla and sub-Kelvin.

We have constructed a polarized proton target system for use in RI-beam experiments. Recent experimental and theoretical studies have revealed that spin degrees of freedom play a vital role in exotic nuclei. Tensor force effects on the evolution of shell and possible occurrence of p-n pairing in the proton-rich region are good examples of manifestations of spin degrees of freedom. Experiments with the target system allow us to explore the spin effects in exotic nuclei. It should be noted that we have recently achieved a proton polarization of 40% at room temperature in a pentacene-d_{14} doped p-terphenyl crystal.

Another interesting application of Triplet-DNP is sensitivity enhancement in NMR spectroscopy of biomolecules. We will start a new project in 2016 to apply the Triplet-DNP technique to study protein-protein interaction via two-dimensional NMR spectroscopy, in close collaboration with biologists and chemists.

(5) Development of special targets for RI-beam experiments

For the research activities shown above, we are developing and hosting special targets for RI-beam experiments listed below:

a) Polarized proton target (described in (4))
b) Thin solid hydrogen target
c) MINOS (developed at Saclay and hosted by the Spin Isospin Laboratory)

Members

Chief Scientist (Lab. Head)

Tomohiro UESAKA

Research & Technical Scientists

Ken-ichiro YONEDA (Senior Research Scientist, concurrent ; Team Leader, User Support Office)
Masaki SASANO (Research Scientist)
Juzo ZENIHIRO (Research Scientist)
Sarah NAIMI (Research Scientist)

Contract Researcher

Daisuke NAGAE

Special Postdoctoral Researchers

Masami SAKO (– Mar. 31, 2015)
Kenichiro TATEISHI
Yuma KIKUCHI

Foreign Postdoctoral Researchers

Zaihong YANG

Postdoctoral Researchers

Masanori DOZONO (– Mar. 31, 2014)
Kenichiro TATEISHI (Apr. 1, 2014 –)
Valerii PANIN

Research Associate

Masami SAKO (Apr. 1, 2015 –)
Kenichiro TATEISHI (– Mar. 31, 2014)

Junior Research Associates

CheongSoo LEE (Univ. of Tokyo)
Fumi SUZAKI (Saitama Univ.)
Keiichi KISAMORI (Univ. of Tokyo, – Mar. 31, 2015)
Yuki KUBOTA (Univ. of Tokyo)

International Program Associates

Chao WEN (Peking Univ. – Mar. 31, 2015)
Sergey CHEBOTARYOV (Kyungpook Nat'l Univ.)
Evgeniy Vladimirovich MILMAN (Kyungpook Nat'l Univ.)
Dahee KIM (Ewha Womans Univ., Oct. 1, 2014 – Sep. 29, 2015)
Zhuang GE (Institute of Modern Physics Chinese Academy of Sciences, Sep. 28, 2015 –)
Julian KAHLBOW (Technical University Darmstadt, Oct. 1, 2015 –)

Research Consultant

Harutaka SAKAGUCHI

Visiting Researchers

Stuhl LASZLO (JSPS Fellow, Apr. 15, 2014 –)
Keiichi KISAMORI (JSPS Fellow, Apr. 1, 2015 –)

Senior Visiting Scientists

Hiroyuki SAGAWA (Aizu Univ.)

Visiting Scientists

Didier BEAUMEL (IPN)
Yosuke KONDO (Tokyo Tech.)
Zoltan ELEKES (Atomki)
Hidetoshi AKIMUNE (Konan Univ.)
Yohei MATSUDA (Osaka Univ.)
Yasuhiro TOGANO (Tokyo Tech.)
Satoshi SAKAGUCHI (Kyusyu Univ.)
Kenjiro MIKI (TU Darmstadt)
Valerie LAPOUX (CEA Saclay)
Alexandre OBERTELLI (CEA Saclay)
Alain GILLIBERT (CEA Saclay)
Emanuel POLLACCO (CEA Saclay)
Anna CORSI (CEA Saclay)
Dennis MUECHER (TUM)
Yury LITVINOV (GSI)
Yuhu ZHANG (CAS)
Igor GASPARIC (Ruder Boskovic Inst. Zagreb Croatia)
Hans Toshihide TOERNQVIST (TU Darmstadt)
Christoph CAESAR (GSI)
Haik SIMON (GSI)
Matthias HOLL (TU Darmstadt)
Takayuki YAMAGUCHI (Saitama Univ.)
Takashi NAKAMURA (Tokyo Tech.)
Atsushi TAMII (Osaka Univ.)
Attila KRASZNAHORKAY (ATOMKI)
Takashi WAKUI (Tohoku Univ.)
Kimiko SAKAGUCHI (Tohoku Univ.)
Dorottya KUNNE SOHLER (Institute of Nuclear Research Hungarian Academy of Sciences (ATOMKI))
Satoru TERASHIMA (Beihang University)
Valdir GUIMARAES (Instituto de Fisica da Universidade de Sao Paulo)
Yasutaka TANIGUCHI (Nihon Institute of Medical Science)
Tetsuaki MORIGUCHI (Univ. of Tsukuba)
Kazuyuki OGATA (Osaka Univ.)
Shinji SUZUKI (Univ. of Tsukuba)
Zsolt VAJTA (Institute of Nuclear Research Hungarian Academy of Sciences (ATOMKI))
Istvan KUTI (Institute of Nuclear Research Hungarian Academy of Sciences (ATOMKI))
Makoto NEGORO (Osaka Univ.)
Konstanze BORETZKY (GSI)
Zsolt FULOP (Institute of Nuclear Research Hungarian Academy of Sciences (ATOMKI))
Zsolt DOMBRADI (Institute of Nuclear Research Hungarian Academy of Sciences (ATOMKI))
Akinori KAGAWA (Osaka Univ.)

Visiting Technicians

Tomomi KAWAHARA (Toho Univ.)
Gilles AUTHELET (CEA Saclay)
Jean-Marc GHELLER (CEA Saclay)
Cedric PERON (CEA Saclay)
Jean-Yves ROUSSE (CEA Saclay)
Denis CALVET (CEA Saclay)
Alan PEYAUD (CEA Saclay)
Alain DELBART (CEA Saclay)
Frederic CHATEAU (CEA Saclay)
Caroline LAHONDE-HAMDOUN (CEA Saclay)
Arnaud GIGANON (CEA Saclay)
Daniel KOERPER (GSI)
Clement HILAIRE (CEA Saclay)

Student Trainees

Shota FUKUOKA (Univ. of Tsukuba)
Zhengyang TIAN (Peking Univ.)
Ryogo MINAKATA (Tokyo Tech.)
Yasunori WADA (Tohoku Univ.)
Tatsuya FURUNO (Kyoto Univ.)
Miho TSUMURA (Kyoto Univ.)
Jumpei YASUDA (Kyushu Univ.)
Taku FUKUNAGA (Kyushu Univ.)
Yuuta SHIOKAWA (Tohoku Univ.)
Shuhei GOTANDA (Univ. of Miyazaki)
Yoshihisa KANAYA (Univ. of Miyazaki)
Satoshi MATSUNAGA (Saitama Univ.)
Yuki ISHII (Kyoto Univ.)
Mizuki SHIKATA (Tokyo Tech.)
Junichi TSUBOTA (Tokyo Tech.)
Yuuki TAKEUCHI (Saitama Univ.)
Syunichirou OHMIKA (Saitama Univ.)
Hiroshi MIURA (Saitama Univ.)
Takuma NISHIMURA (Saitama Univ.)
Motoki MURATA (Kyoto Univ.)

Kazuki SAWAHATA (Tokyo Tech.)
Clementine Angelique Marie SANTAMARIA (Univ.Paris Sud XI)
Syunsuke KAWAKAMI (Miyazaki Univ.)
Daijiro ETO (Tohoku Univ.)
Junki TANAKA (Osaka Univ.)
Sebastian Benedikt REICHERT (TU Munchen)
Tomoyuki OZAKI (Tokyo Tech.)
Atsumi SAITO (Tokyo Tech.)
Yasutaka NISHIO (Kyushu Univ.)
Yusuke SHINDO (Kyushu Univ.)
Munemi TABATA (Kyushu Univ.)
Atomu WATANABE (Tohoku Univ.)
Ayaka OHKURA (Kyushu Univ.)
Yukina ICHIKAWA (Univ. of Tsukuba)
Xiangcheng CHEN (Univ. of Heidelberg)
Kotaro YAMADA (Toho Univ.)
Tomoaki KANEKO (Toho Univ.)
Julian KAHLBOW (TU Darmstadt)
Robert KISSEL (TU Darmstadt)
Gregor DENTINGER (TU Darmstadt)
Taras LOKOTKO (Univ. of Hong Kong)
Dahee KIM (Ewha Womans Univ.)
Natsuki TADANO (Saitama Univ.)
Ikuma KATO (Saitama Univ.)
Tomomi AKIEDA (Tohoku Univ.)
Hiroshi KON (Tohoku Univ.)
Nancy Anne Paul HUPIN (University of Notre Dome)
Tomoyuki MUKAI (Tohoku Univ.)
Shinnosuke NAKAI (Tohoku Univ.)
Takato TOMAI (Tokyo Tech.)
Akihiro HIRAYAMA (Tokyo Tech.)
Yoshiyuki TAJIRI (Univ. of Tsukuba)
Kentaro HIRAISHI (Univ. of Tsukuba)
Simon LINDBERG (Chalmers University of Technology)
Akane SAKAUE (Kyoto Univ.)
Daisuke SAKAE (Kyushu Univ.)
Yasuaki NORIMATSU (Kyushu Univ.)
Takahiro FUKUTA (Kyushu Univ.)
Youhei AKIYAMA (Kyushu Univ.)
Kiyoshi WAKAYAMA (Saitama Univ.)
Han Hagen MAYER (University of Cologne)
Takahiro MORIMOTO (Kyoto Univ.)
Katsuyoshi HEGURI (Konan Univ.)
Takuya MATSUMOTO (Univ. of Tsukuba)
Tomoya HARADA (Toho Univ.)

Interns

Zhuang GE (IMP, CAS)
Lily SIEGENBERG (Univ. of Surrey)
David HEGEDUES (Eotvos Lorand University Budapest Hungary)

Assistants

Emiko ISOGAI
Yu NAYA
Yuri TSUBURAI

List of Publications & Presentations

Publications

[Journal]

(Original Papers) *Subject to Peer Review

L.G. Cao, X. Roca-Maza, G. Colo, H. Sagawa, Constraints on the neutron skin and symmetry energy from the anti-analog giant dipole resonance in Pb-208, Physical Review C **92**, 034308 (2015).

Y. Fujita, H. Fujita, T. Adachi, G. Susoy, A. Algora, C.L. Bai, G. Colo, M. Csatlos, J.M. Deaven, E. Estevez-Aguado, C.J. Guess, J. Gulyas, K. Hatanaka, K. Hirota, M. Honma, D. Ishikawa, A. Krasznahorkay, H. Matsubara, R. Meharchand, F. Molina, H. Nakada, H. Okamura, H.J. Ong, T. Otsuka, G. Perdikakis, B. Rubio, H. Sagawa, P. Sarriguren, C. Scholl, Y. Shimbara, E.J. Stephenson, T. Suzuki, A. Tamii, J.H. Thies, K. Yoshida, R.G.T. Zegers, J. Zenihiro, High-resolution study of Gamow-Teller excitations in the Ca-42(He-3,t)Sc-42 reaction and the observation of a "low-energy super-Gamow-Teller state", Physical Review C **91** 034308 (2015).

T. Hashimoto, A.M. Krumbholz, P.G. Reinhard, A. Tamii, P. von Neumann-Cosel, T. Adachi, N. Aoi, C.A. Bertulani, H. Fujita, Y. Fujita, E. Ganioglu, K. Hatanaka, E. Ideguchi, C. Iwamoto, T. Kawabata, N.T. Khai, A. Krugmann, D. Martin, H. Matsubara, K. Miki, R. Neveling, H. Okamura, H.J. Ong, I. Poltoratska, V.Y. Ponomarev, A. Richter, H. Sakaguchi, Y. Shimbara, Y. Shimizu, J. Simonis, F.D. Smit, G. Susoy, T. Suzuki, J.H. Thies, M. Yosoi, J. Zenihiro, Dipole polarizability of Sn-120 and nuclear energy density functionals, Physical Review C **92**, 031305 (2015).

M. Isaka, M. Kimura, E. Hiyama, H. Sagawa, Superdeformation of Ar hypernuclei, Progress of Theoretical and Experimental Physics **2015** 103d02 (2015).

T. Kawahara, S. Sakaguchi, K. Tateishi, T.L. Tang, T. Uesaka, Kinetic Parameters of Photo-Excited Triplet State of Pentacene Determined by Dynamic Nuclear Polarization, Journal of the Physical Society of Japan **84** 044005 (2015).

M. Krumbholz, P. von Neumann-Cosel, T. Hashimoto, A. Tamii, T. Adachi, C.A. Bertulani, H. Fujita, Y. Fujita, E. Ganioglu, K. Hatanaka, C. Iwamoto, T. Kawabata, N.T. Khai, A. Krugmann, D. Martin, H. Matsubara, R. Neveling, H. Okamura, H.J. Ong, I. Poltoratska, V.Y. Ponomarev, A. Richter, H. Sakaguchi, Y. Shimbara, Y. Shimizu, J. Simonis, F.D. Smit, G. Susoy, J.H. Thies, T. Suzuki, M. Yosoi, J. Zenihiro, Low-energy electric dipole response in Sn-120, Physics Letters B **744**, 7 (2015).

A.K. Kurilkin, T. Saito, V.P. Ladygin, T. Uesaka, M. Hatano, A.Y. Isupov, M. Janek, H. Kato, N.B. Ladygina, Y. Maeda, A.I. Malakhov, J. Nishikawa, T. Ohnishi, H. Okamura, S.G. Reznikov, H. Sakai, N. Sakamoto, S. Sakoda, Y. Satou, K. Sekiguchi, K. Suda, A. Tamii, N. Uchigashima, T.A. Vasiliev, K. Yako, Vector analyzing power A (y) and tensor analyzing powers A (yy) , A (xx) , and A (xz) in the reaction d -> H-3 (p) at the energy of 200 MeV, Physics of Atomic Nuclei **78**, 918 (2015).

J. Marganiec, F. Wamers, F. Aksouh, Y. Aksyutina, H. Alvarez-Pol, T. Aumann, S. Beceiro-Novo, K. Boretzky, M.J.G. Borge, M. Chartier, A. Chatillon, L.V. Chulkov, D. Cortina-Gil, H. Emling, O. Ershova, L.M. Fraile, H.O.U. Fynbo, D. Galaviz, H. Geissel, M. Heil, D.H.H. Hoffmann, J. Hoffmann, H.T. Johansson, B. Jonson, C. Karagiannis, O.A. Kiselev, J.V. Kratz, R. Kulessa, N. Kurz, C. Langer, M. Lantz, T. Le Bleis, R. Lemmon, Y.A. Litvinov, K. Mahata, C. Muntz, T. Nilsson, C. Nociforo, G. Nyman, W. Ott, V. Panin, S. Paschalis, A. Perea, R. Plag, R. Reifarth, A. Richter, C. Rodriguez-Tajes, D. Rossi, K. Riisager, D. Savran, G. Schrieder, H. Simon, J. Stroth, K. Summerer, O. Tengblad, H. Weick, M.

Wiescher, C. Wimmer, M.V. Zhukov, Studies of continuum states in (16) Ne using three-body correlation techniques, European Physical Journal A **51**, 9 (2015).
H. Matsubara, A. Tamii, H. Nakada, T. Adachi, J. Carter, M. Dozono, H. Fujita, K. Fujita, Y. Fujita, K. Hatanaka, W. Horiuchi, M. Itoh, T. Kawabata, S. Kuroita, Y. Maeda, P. Navratil, P. von Neumann-Cosel, R. Neveling, H. Okamura, L. Popescu, I. Poltoratska, A. Richter, B. Rubio, H. Sakaguchi, S. Sakaguchi, Y. Sakemi, Y. Sasamoto, Y. Shimbara, Y. Shimizu, F.D. Smit, K. Suda, Y. Tameshige, H. Tokieda, Y. Yamada, M. Yosoi, J. Zenihiro, Nonquenched Isoscalar Spin-M1 Excitations in sd-Shell Nuclei, Physical Review Letters **115**, 102501 (2015).
S. Omika, T. Yamaguchi, M. Fukuda, A. Kitagawa, S. Matsunaga, D. Nagae, D. Nishimura, T. Nishimura, A. Ozawa, S. Sato, K. Sawahata, T. Suzuki, Y. Takeuchi, Spatial distributions of photons in plastic scintillator detected by multi-anode photomultiplier for heavy-ion position determination, Nuclear Instruments & Methods in Physics Research Section a-Accelerators Spectrometers Detectors and Associated Equipment **797**, 247 (2015).
H. Sagawa, K. Hagino, Theoretical models for exotic nuclei, European Physical Journal A **51**, 102 (2015).
C. Santamaria, C. Louchart, A. Obertelli, V. Werner, P. Doornenbal, F. Nowacki, G. Authelet, H. Baba, D. Calvet, F. Chateau, A. Corsi, A. Delbart, J.M. Gheller, A. Gillibert, T. Isobe, V. Lapoux, M. Matsushita, S. Momiyama, T. Motobayashi, M. Niikura, H. Otsu, C. Peron, A. Peyaud, E.C. Pollacco, J.Y. Rousse, H. Sakurai, M. Sasano, Y. Shiga, S. Takeuchi, R. Taniuchi, T. Uesaka, H. Wang, K. Yoneda, F. Browne, L.X. Chung, Z. Dombradi, S. Franchoo, F. Giacoppo, A. Gottardo, K. Hadynska-Klek, Z. Korkulu, S. Koyama, Y. Kubota, J. Lee, M. Lettmann, R. Lozeva, K. Matsui, T. Miyazaki, S. Nishimura, L. Olivier, S. Ota, Z. Patel, N. Pietralla, E. Sahin, C. Shand, P.A. Soderstrom, I. Stefan, D. Steppenbeck, T. Sumikama, D. Suzuki, Z. Vajta, J. Wu, Z. Xu, Extension of the N=40 Island of Inversion towards N=50: Spectroscopy of Cr-66, Fe-70,Fe-72, Physical Review Letters **115**, 192501 (2015).
X. Xu, M. Wang, Y.H. Zhang, H.S. Xu, P. Shuai, X.L. Tu, Y.A. Litvinov, X.H. Zhou, B.H. Sun, Y.J. Yuan, J.W. Xia, J.C. Yang, K. Blaum, R.J. Chen, X.C. Chen, C.Y. Fu, Z. Ge, Z.G. Hu, W.J. Huang, D.W. Liu, Y.H. Lam, X.W. Ma, R.S. Mao, T. Uesaka, G.Q. Xiao, Y.M. Xing, T. Yamaguchi, Y. Yamaguchi, Q. Zeng, X.L. Yan, H.W. Zhao, T.C. Zhao, W. Zhang, W.L. Zhan, Direct mass measurements of neutron-rich Kr-86 projectile fragments and the persistence of neutron magic number N=32 in Sc isotopes, Chinese Physics C **39**, 104001 (2015).
K. Kisamori, S. Shimoura, H. Miya, S. Michimasa, S. Ota, M. Assie, H. Baba, T. Baba, D. Beaumel, M. Dozono, T. Fujii, N. Fukuda, S. Go, F. Hammache, E. Ideguchi, N. Inabe, M. Itoh, D. Kameda, S. Kawase, T. Kawabata, M. Kobayashi, Y. Kondo, T. Kubo, Y. Kubota, M. Kurata-Nishimura, C.S. Lee, Y. Maeda, H. Matsubara, K. Miki, T. Nishi, S. Noji, S. Sakaguchi, H. Sakai, Y. Sasamoto, M. Sasano, H. Sato, Y. Shimizu, A. Stolz, H. Suzuki, M. Takaki, H. Takeda, S. Takeuchi, A. Tamii, L. Tang, H. Tokieda, M. Tsumura, T. Uesaka, K. Yako, Y. Yanagisawa, R. Yokoyama, K. Yoshida, Candidate Resonant Tetraneutron State Populated by the He-4 (He-8, Be-8) Reaction, Physical Review Letters **116** 052501 (2016).
Y. Kondo, T.Nakamura, R.Tanaka, R.Minakata, S.Ogoshi, N.A.Orr, N.L.Achouri, T.Aumann, H.Baba, F.Delaunay, P.Doornenbal, N.Fukuda, J.Gibelin, J.W.Hwang, N.Inabe, T.Isobe, D.Kameda, D.Kanno, S.Kim, N.Kobayashi, T.Kobayashi, T.Kubo, S.Leblond, J.Lee, F.M.Marques, T.Motobayashi, D.Murai, T.Murakami, K.Muto, T.Nakashima, N.Nakatsuka, A.Navin, S.Nishi, H.Otsu, H.Sato, Y.Satou, Y.Shimizu, H.Suzuki, K.Takahashi, H.Takeda, S.Takeuchi, Y.Togano, A.G.Tuff, M.Vandebrouck, K.Yoneda, " Nucleus 26O: A Barely Unbound System beyond the Drip Line", Physical Review Letters **116**, 102503 (2016).
J. Yasuda, M. Sasano, R.G.T. Zegers, H. Baba, W. Chao, M. Dozono, N. Fukuda, N. Inabe, T. Isobe, G. Jhang, D. Kameda, T. Kubo, M. Kurata-Nishimura, E. Milman, T. Motobayashi, H. Otsu, V. Panin, W. Powell, H. Sakai, M. Sako, H. Sato, Y. Shimizu, L. Stuhl, H. Suzuki, S. Tangwancharoen, H. Takeda, T. Uesaka, K. Yoneda, J. Zenihiro, T. Kobayashi, T. Sumikama, T. Tako, T. Nakamura, Y. Kondo, Y. Togano, M. Shikata, J. Tsubota, K. Yako, S. Shimoura, S. Ota, S. Kawase, Y. Kubota, M. Takaki, S. Michimasa, K. Kisamori, C.S. Lee, H. Tokieda, M. Kobayashi, S. Koyama, N. Kobayashi, T. Wakasa, S. Sakaguchi, A. Krasznahorkay, T. Murakami, N. Nakatsuka, M. Kaneko, Y. Matsuda, D. Mucher, S. Reichert, D. Bazin, J.W. Lee, Nuclear Instruments and Methods in Physics Research B **376**, 393 (2016) .
H. Otsu, S. Koyama, N. Chiga, T. Isobe, T. Kobayashi, Y. Kondo, M. Kurokawa, W.G. Lynch, T. Motobayashi, T. Murakami, T. Nakamura, M. Kurata-Nishimura, V. Panin, H. Sato, Y. Shimizu, H. Sakurai, M.B. Tsang, K. Yoneda, H. Wang, SAMURAI in its operation phase for RIBF users, Nuclear Instruments and Methods in Physics Research B **376**, 175 (2016).

[Proceedings]

(Original Papers) *Subject to Peer Review

Y. Abe, Y. Yamaguchi, M. Wakasugi, T. Uesaka, A. Ozawa, F. Suzaki, D. Nagae, H. Miura, T. Yamaguchi, Y. Yano, Isochronous field study of the Rare-RI Ring, Physica Scripta, **T166** 014047 (2015).
F. Suzaki, Y. Abe, A. Ozawa, T. Suzuki, T. Uesaka, M. Wakasugi, K. Yamada, T. Yamaguchi, Y. Yamaguchi, J. Zenihiro, R.I.R.C. Rare, A resonant Schottky pick-up for Rare-RI Ring at RIKEN, Physica Scripta **T166**, 014059 (2015).
M. von Schmid, S. Bagchi, S. Bonig, M. Csatlos, I. Dillmann, C. Dimopoulou, P. Egelhof, V. Eremin, T. Furuno, H. Geissel, R. Gernhauser, M.N. Harakeh, A.L. Hartig, S. Ilieva, N. Kalantar-Nayestanaki, O. Kiselev, H. Kollmus, C. Kozhuharov, A. Krasznahorkay, T. Kroll, M. Kuilman, S. Litvinov, Y.A. Litvinov, M. Mahjour-Shafiei, M. Mutterer, D. Nagae, M.A. Najafi, C. Nociforo, F. Nolden, U. Popp, C. Rigollet, S. Roy, C. Scheidenberger, M. Steck, B. Streicher, L. Stuhl, M. Thurauf, T. Uesaka, H. Weick, J.S. Winfield, D. Winters, P.J. Woods, T. Yamaguchi, K. Yue, J.C. Zamora, J. Zenihiro, E.X.L. Collaboration, Investigation of the nuclear matter distribution of Ni-56 by elastic proton scattering in inverse kinematics, Physica Scripta, **T166**, 014005 (2015).
Y. Yamaguchi, H. Miura, M. Wakasugi, Y. Abe, A. Ozawa, F. Suzaki, A. Tokuchi, T. Uesaka, T. Yamaguchi, Y. Yano, Fast-kicker system for rare-RI ring, Physica Scripta, **T166**, 014056 (2015).
J.C. Zamora, S. Bagchi, S. Bonig, M. Csatlos, I. Dillmann, C. Dimopoulou, P. Egelhof, V. Eremin, T. Furuno, H. Geissel, R. Gernhauser, M.N. Harakeh, A.L. Hartig, S. Ilieva, N. Kalantar-Nayestanaki, O. Kiselev, K. Kollmus, C. Kozhuharov, A. Krasznahorkay, T. Kroll, M. Kuilman, S. Litvinov, Y.A. Litvinov, M. Mahjour-Shafiei, M. Mutterer, D. Nagae, M.A. Najafi, C. Nociforo, F. Nolden, U. Popp, C. Rigollet, S. Roy, C. Scheidenberger, M. von Schmid, M. Steck, B. Streicher, L. Stuhl, M. Thurauf, T. Uesaka, H. Weick, J.S. Winfield, D. Winters, P.J. Woods, T. Yamaguchi, K. Yue, J. Zenihiro, E.X.L. Collaboration, Isoscalar giant resonance studies in a stored-beam experiment within EXL, Physica Scripta, **T166**, 014006 (2015).

Oral Presentations

[International Conference etc.]

T. Uesaka, ``Double Gamow-Teller Resonances – the other side of ββ-decay'', Neutrino and Dark Matter in Nuclear Physics 2015, Jyvaskyla, Finland, 1—5 June 2015. (invited)
T. Uesaka, ``Rare RI Ring at RIBF – Yet Another Storage Device in RIKEN --'', 6th Interenational Workshop on Electrostatic Storage Devices,

Tokyo, Japan, 8—11 June 2015. (invited)
T. Uesaka, ``New Aspects of Nuclear Spin-Isospin Responses probed with Heavy-Ion Charge Exchange Reactions'', 12th International Coference on Nucleaus-Nucleus Collisions, Catania, Italy, 21—26 June 2015. (invited)
T. Uesaka, ``Probing two-neutron correlations via knockout-delayed particle emission'', 2nd International Wrokshop on Neutron-Proton Correlations, Hong Kong, China, 6—9 July 2015. (invited)
T. Uesaka, ``Experimental methods and measured observables with polarized proton targets : Understanding Spin-Orbit'', Rewriting Nuclear Physics textbooks - 30 years with Radioactive Ion Beam Physics -, Pisa, Italy, 20—24 July 2015. (invited lecture)
T. Uesaka, ``Research Programs at RI Beam Factory'', 9th International Physics Conference of the Balkan Physical Union, Istanbul, Turkey, 24—27 August 2015. (invited)
T. Uesaka, ``Nuclear Astrophysics at RIBF'', 8th European Summer School on Experimental Nuclear Astrophysics, Catania, Italy, 13—20 September 2015. (invited lecture)
T. Uesaka, ``Physics with exotic nuclei at RIKEN and in Asia'', 19th Colloque GANIL, Anglet, France, 11—16 October 2015. (invited)
T. Uesaka, ``New Aspects of Nuclear Spin-Isospin Responses probed with Heavy-Ion Charge Exchange Reactions'', High Resolution Spectrometer Workshop, Darmstadt, Germany, 4—6 November 2015. (invited)
T. Uesaka, ``New Aspects of Nuclear Spin-Isospin Responses probed with Heavy-Ion Charge Exchange Reactions'', International Symposium on High-Resolution Spectroscopy and Tensor Interactions, Osaka, Japan, 16—19 November 2015. (invi1ted)
T. Uesaka, ``Mass Measurements at RIBF'', NUSTAR Annual Meeting 2016, Darmstadt, Germany, 29 February—4 March 2016. (invi1ted)
V. Panin, “New generation of the experiments for the investigation of the stellar (p,γ) reaction rates using SAMURAI”, Fifth International Conference on Proton-emitting Nuclei (PROCON2015), Lanzhou, China, 6-10 July 2015.
V. Panin, “Progress report on Heavy-Ion-Proton project”, SAMURAI International Collaboration Workshop 2015, Wako, Saitama, 7-8 September 2015.
Z. Yang, “Study on the cluster structure of light neutron-rich nuclei”, SINAP-CUSTIPEN Workshop on Clusters and Correlations in Nuclei, Nuclear Reactions and Neutron Stars, Shanghai China, 14-18 Dec (2015).
Z. Yang, “Cluster structure in light neutron-rich nuclei”, International Mini-Workshop on alpha-condensates and monopole excitations, Osaka Japan, 2-3 Sep (2015).
M. Sasano, “Study of Gamow-Teller transitions in 132Sn”, International Conference, Nuclear Structure and Related Topics, Dubna, Russia, 14-18th July (2015). (invited).
M. Sasano, “Gamow-Teller transitions from 132Sn”, Collective motion in nuclei under extreme conditions, Krakow, Poland, 14-18th September (2015). (invited).
M. Sasano, “Status of fission experiments at RIKEN RIBF”, 27th ASRC International Workshop " Nuclear Fission and Exotic Nuclei ", Ibraraki Quantum Beam Research Center, Tokai, Japan, 1-2nd.December (2015). (invited).
M. Sasano, ``Gamow-Teller transitions from ^{56}Ni'', International Symposium on High-Resolution Spectroscopy and Tensor Interactions, Osaka, Japan, 16—19 November 2015. (invited)
L. Stuhl, “Investigation of spin-isospin collectivity in asymmetric nuclear matter”, 14th CNS International Summer School (CNSS15), Wako, Saitama, Japan, 26th August – 1st September (2015).
J. Yasuda, “Slow neutron detector WINDS for (p,n) reaction in inverse kinematics with SAMURAI spectrometer”, International Conference on Electromagnetic Isotope Separator and Related Topics (EMIS 2015), Grand Raipids, MI, US, 11-15th May (2015).
J. Zenihiro, ``Proton elastic scattering and neutron density distributions'', International Symposium on High-Resolution Spectroscopy and Tensor Interactions, Osaka, Japan, 16—19 November 2015. (invited)
Y. Kubota, “Probing multi-neutron correlation via knockout reaction”, Critical Stability in Few-Body Systems, Saitama, Japan, 26–30th January (2015).
S. Reichert, "Study of fission barriers in neutron-rich nuclei using the (p,2p) reaction: Status of SAMURAI Experiment NP1306 SAMURAI14" at DPG Fruehjahrstagung, March 23-27, Heidelberg
S. Reichert, "Fission barrier in n-rich nuclei: Status of SAMURAI Experiment NP1306 SAMURAI14" at RA G Science Day at Max Planck Institute for Extraterrestic Physics, July 9, Munich
H. Sagawa, "Three-body model for exotic nuclei", Gordon conference of nuclear chemistry, New Hampshire, USA, May 31-June 5th, (2015).
H. Sagawa, "Isoscalar spin-triplet pairing interaction and Spin-Isospin excitations", International workshop on Nucleon-nucleon interaction in 2015, Catania, Italy June 18-20 (2015).
H. Sagawa, "Three-body model for unbound nucleus ^{26}O", Nucleus-nucleus collision 2015, Catania, Italy, June 22-26 (2015).
H. Sagawa, "Does monopole pigmy resonance exist in ^{68}Ni?" Nucleus-nucleus collision 2015, Catania, Italy, June 22-26 (2015).
H. Sagawa, "Isoscalar spin-triplet pairing correlations and Spin-Isospin response", 2nd International workshop on neutron-proton correlations, HongKong, China, July 6-9 (2015).
H. Sagawa, " Isoscalar spin-triplet pairing and tensor correlations on Spin-Isospin response", Kyoto CANHP2015 Workshop 5th week “Energy density functionals”, Kyoto, Japan, October 19-23 (2015).
H. Sagawa, " Isoscalar spin-triplet pairing and tensor correlations on Spin-Isospin response", International Workshop on tensor correlations and nuclear structure, Osaka, Japan, Nov 16-19 (2015).

[Domestic Conference]

V. Panin, “Investigation of key nuclear reactions in the astrophysical rp-process using SAMURAI”, 70th JPS Annual meeting, Tokyo, Japan, 21-24 March 2015.
Z. Yang, “Strong Monopole Transition and Clustering in ^{12}Be”, アイソスカラー型単極遷移で探る原子核の励起状態とクラスター構造, Osaka Japan, 16-17 July (2015).
笹野　匡紀, 「ノックアウト(p,2p)反応を用いた核分裂閾値エネルギーの測定」、日本物理学会2015年秋季大会、シンポジウム「重イオン深部非弾性散乱の基礎と応用」、大阪市立大学、2015年9月25日 (招待・シンポジウム講演)
L. Stuhl, “Around the Nucleus”, JSPS Science Dialogue, Tochigi Prefectural Utsunomiya Girl’s Senior High School, Utsunomiya, Japan, 2nd October (2015).
Y. Kubota, "ボロミアン核(p,pn)反応を用いた二中性子運動量相関の研究", 70th JPS meeting, Tokyo, Japan, 25-–28th March (2015).
洲崎ふみ, “稀少 RI リングのための共鳴ショットキーピックアップのオフライン性能試験”, 第 70 回日本物理学会 年次大会, 早稲田大学, 20150321-0324

E. Milman “Experimental Plan for Resonant Scattering of 9C off Polarized Proton at 5.6 MeV/A”, JPS 70th Annual Meeting（2015）, Mar. 21-24, 2015.
T. Uesaka, ``We are at the epoch !'', Workshop on ``Nuclear Physics with Triplet-DNP technique and its application'', Fukuoka, Japan, 8th January (2016).
K. Tateishi, ``What is the important parameter for Triplet-DNP and chemical/medical applications'', Workshop on ``Nuclear Physics with Triplet-DNP technique and its application'', Fukuoka, Japan, 8th January (2016).
S. Chebotaryov, ``Experiments on Elastic Scattering of Polarized Protons from $^{6}$He'', Workshop on ``Nuclear Physics with Triplet-DNP technique and its application'', Fukuoka, Japan, 8th January (2016).
E. Milman, `` Search for $^{10}$N resonances with $^{9}$C + p resonant scattering'', Workshop on ``Nuclear Physics with Triplet-DNP technique and its application'', Fukuoka, Japan, 8th January (2016).
T. Kaneko, `` Polarization transfer from electron to $^{13}$C via $^{1}$H spins'', Workshop on ``Nuclear Physics with Triplet-DNP technique and its application'', Fukuoka, Japan, 8th January (2016).
K. Yamada, ``Hyperpolarization of flowing water with Overhauser DNP'', Workshop on ``Nuclear Physics with Triplet-DNP technique and its application'', Fukuoka, Japan, 8th January (2016).
上坂友洋, “サイクロトロン型蓄積リングによる稀少不安定核の質量測定”, 第 71 回日本物理学会年次大会シンポジウム「イオン蓄積リングが切り拓く多彩な物理」, 仙台, 日本, 2016 年 3 月 19—22 日

Posters Presentations
[International Conference etc.]
L. Stuhl, “A new low-energy neutron detector for (p,n) experiments with pulse shape discrimination properties”, Collective motion in nuclei under extreme conditions, Krakow, Poland, 14-18th September (2015).
Z. Ge, “Rare RI Ring at RIKEN -Isochronous Mass Spectrometry for the r-process nuclei”, The 13th international symposium on Origin of Matter and Evolution of Galaxies (OMEG2015), Beijing, China, June 24-27 (2015).
F. Suzaki, “Performance of a resonant Schottky pick-up in the commissioning of Rare-RI Ring”, 13th International Conference on Heavy Ion Accelerator Technology (HIAT2015), Yokohama, Japan, 201509

RIBF Research Division
Nuclear Spectroscopy Laboratory

1. Abstract

The research group has conducted nuclear-physics studies utilizing stopped/slowed-down radioactive-isotope (RI) beams mainly at the RIBF facility. These studies are based on the technique of nuclear spectroscopy such as β-ray-detected NMR, γ-PAD (Perturbed Angular Distribution), laser, and Mössbauer among other methods that takes advantage of intrinsic nuclear properties such as nuclear spins, electromagnetic moments, and decay modes. In particular, techniques and devices for the production of spin-controlled RI beams have been developed and combined to the spectroscopic studies, which enable high-sensitivity measurements of spin precessions/resonances through a change in the angular distribution of radiations. Anomalous nuclear structures and properties of far unstable nuclei are investigated from thus determined spin-related observables. The group also aims to apply such techniques to interdisciplinary fields such as fundamental physics and materials science by exploiting nuclear probes..

2. Major Research Subjects

(1) Nuclear spectroscopy with stopped/slowed-down RI beams
(2) R&D studies on the production of spin-oriented RI beam
(3) Application of RI probes
(4) Fundamental physics: Study of symmetry

3. Summary of Research Activity

(1) Nuclear spectroscopy with stopped/slowed-down RI beams

Measurements of static electromagnetic nuclear moments over a substantial region of the nuclear chart have been conducted for structure studies on the nuclei far from the β-decay stability. Utilizing nuclear spin orientation phenomena of RIs created in the projectile-fragmentation reaction, ground- and excited-state nuclear moments of nuclei far from the stability have been determined by means of the β-ray-detected nuclear magnetic resonance (β-NMR) and the γ-ray time differential perturbed angular distribution (γ-TDPAD) methods. To extend these observations to extremely rare RIs, a new method has been developed based on the laser spectroscopy which makes use of characteristic atomic properties of RIs surrounded by liquid helium.

(2) R&D studies on the production of spin-oriented RI beams

A new method has been developed for controlling spin in a system of rare RIs, taking advantage of the mechanism of the two-step projectile fragmentation reaction combined with the momentum-dispersion matching technique. This success allows us to utilize spin-controlled world's highest intensity rare RIBs delivered from BigRIPS for researches on the nuclear structure of species situated outside the traditional region of the nuclear chart. In parallel with this work, the development of a new apparatus to produce highly spin-polarized RI beams will be conducted by extending the atomic beam resonance method to fragmentation-based RI beams.

(3) Application of RI probes

The application of RI and heavy ion beams as a probe for condensed matter studies is also conducted by the group. The microscopic material dynamics and properties have been investigated through the deduced internal local fields and the spin relaxation of RI probes based on various spectroscopies utilizing RI probes such as the β-NMR/nuclear quadrupole resonance (NQR) methods, in-beam Mössbauer spectroscopy and the γ-ray time differential perturbed angular correlation (γ-TDPAC) spectroscopy.

(4) Fundamental physics: Study of symmetry

The nuclear spins of stable and unstable isotopes sometimes play important roles in fundamental physics research. New experimental methods and devices have been developed for studies of the violation of time reversal symmetry (T-violation) using spin-polarized nuclei. These experiments aim to detect the small frequency shift in the spin precession arising from new mechanisms beyond the Standard Model.

Members

Chief Scientist (Lab. Head)
Hideki UENO

Research & Technical Scientist
Aiko NAKAO (Senior Research Scientist, – May 31, 2015)
Hiroki YAMAZAKI (Senior Research Scientist)
Yuichi ICHIKAWA (Research Scientist)
Aiko TAKAMINE (Research Scientist)

Research Consultant
Takuya OKADA

Junior Research Associate
Kei IMAMURA (Meiji Univ.)
Yuichi OHTOMO (TIT, – Feb. 28, 2015)

International Program Associate
Ian MURRAY (Univ. Paris Sud, Nov. 5, 2015 –)
Aleksey GLADKOV (Kyungpook National Univ., Jan. 12, 2016 –)

Part-time Worker

Yoko ISHIBASHI (Univ. of Tsukuba, Sep. 1, 2014 –)
Tomomi FUJITA (Osaka Univ., May 1, 2015 –)

Senior Visiting Scientist

Yukari MATSUO (Hosei Univ.)

Visiting Scientists

Wataru SATO (Kanazawa Univ.)
Kensaku MATSUTA (Osaka Univ.)
Jin NAKAMURA (Univ. of Elec.-Com.)
Atsushi HATAKEYAMA (Tokyo Univ. of Agric. and Tech.)
Takeshi FURUKAWA (Tokyo Met. Univ.)
Satoshi TSUTSUI (JASRI)
Takamasa MOMOSE (Univ. of British Columbia)
Jean-Michel DAUGAS (CEA)
Yoshio KOBAYASHI (Univ. of Elec.-Com.)
Jiro MURATA (Rikkyo Univ.)
Koichiro ASAHI (TIT)
Jun MIYAZAKI (Tokyo Univ. of Agric. and Tech.)
Yasuhiro YAMADA (Tokyo Univ. of Sci.)
Kenya KUBO (ICU)
Akihiro YOSHIMI (Okayama Univ.)
Shuangquan ZHANG (Peking University)
Dimiter Loukanov BALABANSKI (IHIN)
Naoki NISHIDA (Tokyo Univ. of Science)
Boulay FLORENT (CNRS GANIL)
Yasuaki EINAGA (Keio Univ.)

Student Trainees

Yoko ISHIBASHI (Univ. of Tsukuba)
Masato TSUCHIYA (Tokyo Tech.)
Miki HAYASAKA (Tokyo Gakugei Univ.)
Ryo MIYATANI (Tokyo Univ. of Sci.)
Kazuma SHIGA (Tokyo Univ. of Sci.)
Tomomi FUJITA (Osaka Univ.)
Yuichi OHTOMO (Tokyo Tech)
Takahiro SUZUKI (Tokyo Tech)
Masaomi TANAKA (Osaka Univ.)
Ryosuke KANBE (Osaka Univ.)
Yu SAKAMOTO (Tokyo Tech)
Yukiko SATO (Univ. of Elec.-Com.)
Shotaro TANIGAWA (Univ. of Elec.-Com.)
Daiki NATORI (Univ. of Elec.-Com.)
Kenichi TANABE (Tokyo Univ. of Sci.)
Miho SATO (Tokyo Univ. of Sci.)
Takafumi TABATA (Tokyo Univ. of Sci.)
Shuichiro KOJIMA (Tokyo Tech.)
Tomoya SATO (Tokyo Tech.)
Aleksey GLADKOV (Kyungpook Nat'l Univ.)
Yonggeun SEON (Kyungpook Nat'l Univ.)
Daiki TOMINAGA (Hosei Univ.)
Syouhei OOSIRO (Tokyo Gakugei Univ.)
Miku MATSUMOTO (Tokyo Gakugei Univ.)
Ryo OGAWA (Univ. of Elec.-Com.)
Yusuke HAMABE (Univ. of Elec.-Com.)
Ippei KUBONO (Tokyo Univ. of Sci.)
Shota AMAGASA (Tokyo Univ. of Sci.)
Chikako FUNAYAMA (Tokyo Tech)
Chika HIRAO (Tokyo Tech)
Taro KOMINE (Tokyo Tech)
Tsuyoshi EGAMI (Hosei Univ.)
Takafumi KAWAGUCHI (Hosei Univ.)
Yuka KOBAYASHI (Tokyo Univ. of Science)
Masanari SEKI (Tokyo Univ. of Science)
Taishi NISHIZAKA (Hosei Univ.)
Takaya KOIZUMI (Univ. of Electro-Communications)
Kenya TAKAHASHI (Univ. of Electro-Communications)
Yuki MINATO (Univ. of Electro-Communications)
Ryouhei KOZU (Univ. of Electro-Communications)
Takayuki KAWAMURA (Osaka Univ.)
Makoto SANJO (Hosei Univ.)
Wataru KOBAYASHI (Hosei Univ.)

Interns

Yan JIANG (Peking University)
Wei LIU (Peking University)
Jian GAO (Peking University)
Zhiyi XU (Peking University)
Hanzhou YU (Peking University)
Haeun WEE (Seoul National University)
Taehun KIM (Seoul National University)
Chang Jun LEE (Seoul National University)
Deokhwa HONG (Seoul National University)
Han Sol SONG (Seoul National University)

List of Publications & Presentations

Publications

[Journal]

(Original Papers) *Subject to Peer Review

T. Sato, Y. Ichikawa, Y. Ohtomo, Y. Sakamoto, S. Kojima, C. Funayama, T. Suzuki, M. Chikamori, E. Hikota, M. Tsuchiya, T. Furukawa, A. Yoshimi, C. P. Bidinosti, T. Ino, H. Ueno, Y. Matsuo, T. Fukuyama, K. Asahi, "EDM measurement in ^{129}Xe atom using dual active feedback nuclear spin maser", Hyperfine Interactions 230, 147-153 (2015).*

Y. Sakamoto, C. P. Bidinosti, Y. Ichikawa, T. Sato, Y. Ohtomo, S. Kojima, C. Funayama, T. Suzuki, M. Tsuchiya, T. Furukawa, A. Yoshimi, T. Ino, H. Ueno, Y. Matsuo, T. Fukuyama, K. Asahi, "Development of high-homogeneity magnetic field coil for ^{129}Xe EDM experiment", Hyperfine Interactions 230, 141-146 (2015).*

K. Imamura, T. Furukawa, X. F. Yang, Y. Mitsuya, T. Fujita, M. Hayasaka, T. Kobayashi, A. Hatakeyama, H. Ueno, H. Odashima, Y. Matsuo, "Measurement of hyperfine splitting of ^{133}Cs atoms in superfluid helium", Hyperfine Interactions 230, 73-77 (2015).*

T. Fujita, T. Furukawa, K. Imamura, X. F. Yang, T. Wakui, Y. Mitsuya, M. Hayasaka, Y. Ichikawa, Y. Ishibashi, H. Shirai, T. Suzuki, T. Sato, Y. Ohtomo, S. Kojima, Y. Ebara, S. Kishi, T. Sagayama, A. Hatakeyama, T. Kobayashi, H. Ueno, K. Asahi, T. Shimoda, Y. Matsuo, "Laser spectroscopy of atoms in superfluid helium for the measurement of nuclear spins and electromagnetic moments of radioisotope atoms", Hyperfine Interact. 236, 95-100 (2015).*

C. Funayama, T. Furukawa, T. Sato, Y. Ichikawa, Y. Ohtomo, Y. Sakamoto, S. Kojima, C. Hirao, T. Suzuki, M. Chikamori, E. Hikota, M. Tsuchiya, A. Yoshimi, C. P. Bidinosti, T. Ino, H. Ueno, Y. Matsuo, T. Fukuyama, K. Asahi, "Performance assessment of a new laser system for efficient spin exchange optical pumping in a spin maser measurement of ^{129}Xe EDM", Hyperfine Interactions 236, 59-64 (2015).*

(Review)

H. Ueno and Y. Ichikawa, "Spin-Aligned Radioactive Isotope Beams via Two-Step Fragmentation Reaction", Nuclear Physics News International, Volume 25, Issue 2, 12-16 (2015).*

[Proceedings]

(Original Papers) *Subject to Peer Review

Y. Ichikawa, H. Ueno, Y. Ishii, T. Furukawa, A. Yoshimi, D. Kameda, H. Watanabe, N. Aoi, K. Asahi, D. L. Balabanski, R. Chevrier, J. M. Daugas, N. Fukuda, G. Georgiev, H. Hayashi, H. Iijima, N. Inabe, M. Ishihara, T. Inoue, T. Kubo, T. Nanao, T. Ohnishi, M. M. Rajabali, K. Suzuki, H. Takeda, M. Tsuchiya, "Spin-aligned RI beams and g-factor measurements", JPS Conference Proceedings 6, 030004 (2015).*

T. Sato, Y. Ichikawa, Y. Ohtomo, Y. Sakamoto, S. Kojima, T. Suzuki, H. Shirai, M. Chikamori, E. Hikota, H. Miyatake, T. Nanao, K. Suzuki, M. Tsuchiya, T. Inoue, T. Furukawa, A. Yoshimi, C. P. Bidinosti, T. Ino, H. Ueno, Y. Mastuo, T. Fukuyama, K. Asahi, "^{129}Xe EDM Search Experiment Using Active Nuclear Spin Maser", JPS Conference Proceedings 6, 020031 (2015).*

Y. Ohtomo, Y. Ichikawa, T. Sato, Y. Sakamoto, S. Kojima, T. Suzuki, H. Shirai, M. Chikamori, E. Hikota, H. Miyatake, T. Nanao, K. Suzuki, M. Tsuchiya, T. Inoue, T. Furukawa, A. Yoshimi, C. P. Bidinosti, T. Ino, H. Ueno, Y. Mastuo, T. Fukuyama, K. Asahi, "^{129}Xe/^{3}He co-magnetometery", JPS Conference Proceedings 6, 030067 (2015).*

H. Ueno, "Nuclear Moments and Structure of Unstable Nuclei", JPS Conference Proceedings 6, 010009 (2015).*

K. Imamura, T. Furukawa, T. Wakui, X. F. Yang, Y. Mitsuya, T. Fujita, Y. Ebara, M. Hayasaka, Y. Ichikawa, H. Shirai, T. Suzuki, T. Sato, Y. Ohtomo, S. Kojima, A. Hatakeyama, H. Odashima, T. Kobayashi, H. Ueno, K. Asahi, Y. Matsuo, "Measurement of hyperfine splitting of alkali atoms in superfluid helium for a laser spectroscopy of atoms with unstable nuclei", JPS Conference Proceedings 6, 030115 (2015).

T. Fujita, T. Furukawa, K. Imamura, X. F. Yang, Y. Mitsuya, M. Hayasaka, T. Sagayama, S. Kishi, T. Kobayashi, T. Shimoda, Y. Matsuo, "Measurement of hyperfine structure of Au atom in superfluid helium", JPS Conference Proceedings 6, 030116 (2015).*

M. Mihara, Y. Ishibashi, Y. Abe, Y. Kamisho, Y. Morita, J. Ohno, M. Tanaka, S. Shinozaki, R. Kanbe, M. Fukuda, K. Matsuta, A. Ozawa, D. Nagae, S. Inaba, S. Okada, Y. Saito, H. Ueno, K. Yamada, T. Izumikawa, T. Ohtsubo, S. Momota, D. Nishimura, T. Suzuki, T. Yamaguchi, Y. Kobayashi, K. Imamura, X.F. Yang, T. Nagatomo, T. Minamisono, M. Takechi, M. Ogura, K. Matsukawa, K. Shirai, T. Fujimura, "Production of Spin Polarized ^{58}Cu and its Magnetic Moment", JPS Conference Proceedings 6, 030114 (2015).*

Oral Presentations

[International Conference etc.]

S. Kinbara, K. Nakazawa, H. Ueno, Y. Ichikawa, J. Yoshida, K. T. Tint, M. K. Soe, A. M. M. Theint, H. Itoh, H. Kobaayashi, S. Hwang, H. Ekawa, S. Hayakawa, "Development of PIS method in nuclear emulsion", The 12th International Conference on Hypernuclear and Strange Particle Physics (HYP2015), Sendai, Japan, September 7-11, 2015.

A. Takamine, "Super-deformation in the ground states of N=Z nuclei", 2015 SSRI-PNS collaboration meeting, Wako, Saitama, September 3-4, 2015.

H. Ueno, "Spin-polarized RI beams utilizing the OEDO-SHARAQ system", OEDO-SHARAQ International Collaboration Workshop, Wako, Saitama, Japan, September 8-19, 2015.

H. Ueno, "Research programs at RIKEN RIBF", The 9th Japan-China Nuclear Physics Symposium (JCNP2015), Suita, Osaka, Japan, November 7-12, 2015.

K. Asahi, "Isotope differential measurement of Xe atomic EDM with a double-species spin maser", 8th International Workshop on "Fundamental Physics Using Atoms" (FPUA2015) –Towards better understanding of our matter universe-, Wako, Saitama, November 30 – December 1, 2015.

H. Ueno, "g-factor measurement with polarized beam", Physics with Fragment Separators – 25th Anniversary of RIKEN-Projectile Fragment Separator (RIPS25)", Hayama, Kanagawa, Japan, December 6-7, 2015.

H. Ueno, "RIBF overview", 8th Japan-Italy Symposium, Wako, Saitama, Japan, March 7-10, 2016.

[Domestic Conference]

金原慎二, 仲澤和馬, 上野秀樹, 市川雄一, 吉田純也, Khin Than Tint, Myint Kyaw Soe, Aye Moh Moh Thient, 伊藤宏紀, 小林秀隆, 中島大輔, 村井李奈, 江川弘行, 早川修平, Sanghoon Hwang, 「原子核乾板中の電離損失による粒子識別法の確立」, 日本物理学会 2015 年秋季大会, 大阪, 2015 年 9 月 25-28 日

佐藤智哉, 市川雄一, 小島修一郎, 舟山智歌子, 坂本雄, 大友祐一, 平尾千佳, 近森正敏, 彦田絵里, 古川武, 吉見彰洋, C. P. Bidinosti, 猪野隆, 上野秀樹, 松尾由賀利, 福山武志, 旭耕一郎, 「^{129}Xe/^{3}He 二核種スピンメーザーを用いた周波数精密測定における周波数不定性」, 日本物理学会 2015 年秋季大会, 大阪, 2015 年 9 月 25-28 日

相川脩, 石田勝彦, 岩崎雅彦, 上野秀樹, 大石裕, 岡田信二, 斎藤徳人, 佐藤将春, 高峰愛子, 馬越, 松崎禎市郎, 緑川克美, 湯本正樹, 和田智之, 神田聡太郎, 田中香津生, 松田恭幸, 「ミュオン水素原子超微細構造エネルギー測定のための中赤外レーザーの開発(I)」, 日本物理学会 2015 年秋季大会, 大阪, 2015 年 9 月 25-28 日

佐藤将春, 石田勝彦, 岩崎雅彦, 上野秀樹, 大石裕, 岡田信二, 斎藤徳人, 高峰愛子, 松崎禎市郎, 馬越, 緑川克美, 湯本正樹, 和田智之, 相川脩, 神田聡太郎, 田中香津生, 松田恭幸, 「ミュオン水素原子超微細構造レーザー分光による陽子半径の測定実験」, 日本物理学会 2015 年秋季大会, 大阪, 2015 年 9 月 25-28 日

山崎展樹, 「The film characterization using RI – What I want to do」, 第 8 回停止・低速 RI ビームを用いた核分光研究会(SSRI), 埼玉県和光市, 2016 年 3 月 4-5 日

市川雄一, 高峰愛子, 西畑洸希, 今村慧, 藤田朋美, 佐藤智哉, 籾山悟至, 清水陽平, D. S. Ahn, 旭耕一郎, 馬場秀忠, D. L. Balabanski, F. Boulay, J. M. Daugas, 江上魁, 福田直樹, 舟山智歌子, 古川武, G. Georgiev, A. Gladkov, 稲辺尚人, 石橋陽子, 小林義男, 小島修一郎, A. Kusoglu, 川口高史, 河村嵩之, I. Mukul, 新倉潤, 西坂太志, 小田原厚子, 大友祐一, D. Ralet, 下田正, G. S. Simpson, 炭竈聡之, 鈴木宏, 竹田浩之, L. C. Tao, 栂野泰宏, 富永大樹, 上野秀樹, 山崎展樹, X. F. Yang, 「中性子過剰核 ^{75}Cu のアイソマー状態の核磁気モーメント」, 日本物理学会第 71 回年次大会, 仙台, 2016 年 3 月 19-22 日

石橋陽子, 市川雄一, 高峰愛子, 今村慧, 藤田朋美, 佐藤智哉, 旭耕一郎, 江上魁, 舟山智歌子, 川口高史, 小島修一郎, 西坂太志, 大友祐一, 小沢顕, 富永大樹, 山崎展樹, 吉見彰洋, 上野秀樹, 「中性子過剰核 ^{39}S の核磁気モーメント」, 日本物理学会第 71 回年次大会, 仙台, 2016 年 3 月 19-22 日

E. Milman, T. Teranishi, S. Sakaguchi, S. Chebotaryov, T. Uesaka, K. Tateishi, Y. Ichikawa, M. Sasano, W. Kim, R. Kaku, Y. Norimatsu, Y. Akiyama, T. Fukuta, D. Sakae, N. Imai, H. Yamaguchi, S. Hayakawa, D. M. Kahl, Y. Sakaguchi, K. Abe, N. Kitamura, T. Kaneko, K. Yamada, S. H. Hwang, D. H. Kim, Al.Galindo-Uribarri, E. Romero-Romero, D. Beaumel, “Search for ^{10}N resonances with ^{9}C + p resonant scattering”, 日本物理学会第 71 回年次大会, 仙台, 2016 年 3 月 19-22 日

早坂美希, 今村慧, 富田英生, 高松峻英, 山口康広, 藤田朋美, 小林徹, 植松晴子, 古川武, 上野秀樹, 松尾由賀利, 「パルス Ti:S レーザーによる超流動ヘリウム中原子のスピン偏極生成」, 日本物理学会第 71 回年次大会, 仙台, 2016 年 3 月 19-22 日

藤田朋美, 今村慧, 富永大樹, 川口高史, 江上魁, 西坂太志, 小林徹, 高峰愛子, 古川武, 上野秀樹, 下田正, 松尾由賀利,「超流動ヘリウム環境下における 11 族原子の超微細構造間遷移」, 日本物理学会第 71 回年次大会, 仙台, 2016 年 3 月 19-22 日

江上魁, 今村慧, 西坂太志, 高峰愛子, 藤田朋美, 富永大樹, 川口高史, 涌井崇志, 古川武, 上野秀樹, 松尾由賀利, 「低収量原子核の核構造研究へ向けたレーザー・MW 二重共鳴信号の強度評価」, 日本物理学会第 71 回年次大会, 仙台, 2016 年 3 月 19-22 日

舟山智歌子, 佐藤智哉, 市川雄一, 小島修一郎, 田中俊也, 坂本雄, 大友祐一, 平尾千佳, 古川武, 吉見彰洋, C. P. Bidinosti, 猪野隆, 上野秀樹, 松尾由賀利, 福山武志, 旭耕一郎,「異核種共存セルにおけるスピン偏極生成・緩和機構」, 日本物理学会第 71 回年次大会, 仙台, 2016 年 3 月 19-22 日

小島修一郎, 佐藤智哉, 市川雄一, 田中俊也, 舟山智歌子, 坂本雄, 大友祐一, 平尾千佳, 古川武, 吉見彰洋, C. P. Bidinosti, 猪野隆, 上野秀樹, 松尾由賀利, 福山武志, 旭耕一郎, 「^{129}Xe/^{131}Xe 共存核スピンメーザーの周波数特性」, 日本物理学会第 71 回年次大会, 仙台, 2016 年 3 月 19-22 日

佐藤智哉, 市川雄一, 小島修一郎, 舟山智歌子, 田中俊也, 坂本雄, 大友祐一, 平尾千佳, 近森正敏, 彦田絵里, 古川武, 吉見彰洋, C. P. Bidinosti, 猪野隆, 上野秀樹, 松尾由賀利, 福山武志, 旭耕一郎, 「異核種共存核スピンメーザーを用いた EDM 測定実験」, 日本物理学会第 71 回年次大会, 仙台, 2016 年 3 月 19-22 日

Posters Presentations

[International Conference etc.]

A. Takamine, M. Wada, Y. Ito, F. Arai, P. Schury, I. Katayama, K. Imamura, Y. Ichikawa, H. Ueno, H. Wollnik, H. A. Schuessler, "Towards high precision measurements of nulear g-factors for Be isotopes”, The 17th International Conference on Electromagnetic Isotope Separators and Related Topics (EMIS2015)

A. Takamine, M. Wada, Y. Ito, F. Arai, P. Schury, I. Katayama, K. Imamura, Y. Ichikawa, H. Ueno, H. Wollnik, H. A. Schuessler, "Towards a hyperfine anomaly measurement of the one-neutron halo nucleus ^{11}Be”, Physics with Fragment Separators -25th Anniversary of RIKEN-Projectile Fragment Separator (RIPS25), Hayama, Kanagawa, Japan, December 5-7, 2015

A. Takamine, R. Shiozuka, H. Maeda, "Population redistribution of cold Rydberg atoms”, 12th International Conference on Low Energy Physics (LEAP2016)

[Domestic Conference]

藤田朋美, 「OROCHI: 超流動ヘリウム中原子のレーザー分光 –低収量 RI の核構造研究に向けて-」, 国際光年シンポジウム, 東京, 2015 年 4 月 21 日

西坂太志, 今村慧, 江上魁, 涌井崇志, 松本未来, 藤田朋美, 富永大樹, 川口高史, 高峰愛子, 古川武, 上野秀樹, 松尾由賀利,「低収量不安定核の核構造研究へ向けた超流動ヘリウム中原子のレーザー誘起蛍光検出系の性能評価」, 日本物理学会第 71 回年次大会, 仙台, 2016 年 3 月 19-22 日

RIBF Research Division
High Energy Astrophysics Laboratory

1. Abstract

In the immediate aftermath of the Big Bang, the beginning of our universe, only hydrogen and helium existed. However, nuclear fusion in the interior of stars and the explosion of supernovae in the universe over the course of 13.8 billion years led to the evolution of a world brimming with the many different elements we have today. By using man-made satellites to observe X-rays and gamma-rays emitted from celestial objects, we are observing the synthesis of the elements at their actual source. Our goal is to comprehensively elucidate the scenarios for the formation of the elements in the universe, together with our research on sub-atomic physics through the use of an accelerator.

2. Major Research Subjects

(1) Nucleosynthesis in Stars and Supernovae
(2) Particle Acceleration Mechanism in Astronomical Objects
(3) Physics in Extremely Strong Magnetism and Gravity
(4) Research and Development of Innovative X-ray and Gamma-ray detectors

3. Summary of Research Activity

High Energy Astrophysics Laboratory started in April 2010. The goal of our research is to reveal the mechanism of nucleosynthesis and the evolution of elements in the universe, and to observe/discover exotic physical phenomena in extremely strong magnetic and/or gravitational fields. We have observed supernova remnants, strongly magnetized neutron stars, pulsars, black holes and galaxies with X-ray astronomical satellites and/or ground-based telescopes.

We are running an X-ray polarimetry satellite mission PRAXyS (Polarimeter for Relativistic Astrophysical X-ray Sources) in collaboration with NASA Goddard Space Flight Center. This is the heritage mission of the canceled GEMS. The mission proposal was submitted to NASA in December 2014, and selected for Phase A (conceptual design) study in July 2015. We are now in step forward to Phase B (flight design) and the expected launch in August 2020. For the PRAXyS project, we have developed gas electron multiplier foils for flights and analyzed calibration data of semi-flight polarimeter to evaluate the systematic uncertainty of the detectors.

We contributed to the 6th Japanese X-ray astronomical satellite ASTRO-H which was launched on February 17, 2016 from JAXA's Tanegashima Space Center (TNSC) by the H-IIA launch vehicle F-30. The JAXA's ASTRO-H mission is constructed by all the Japanese institutes related to the X-ray astrophysics including RIKEN in collaboration with US and Europe. The total mass of the satellite is 2.7 ton and the length is 14 m after deploying the optical boom. ASTRO-H carries four X-ray and gamma-ray detectors covering the 0.3-600 keV energy range. We, in collaboration with JAXA, Tokyo Metropolitan University, Kanazawa University, Saitama University, NASA/GSFC etc., is contributing to the soft X-ray spectrometer (SXS), which achieves unprecedented energy resolution (< 7 eV) in the 0.3-12 keV energy band with a low temperature micro calorimeter. Although ASTRO-H was successfully launched in Low Earth Orbit, the satellite was unfortunately lost by an accident. We are analyzing a small amount of scientific data taken just before the accident, and preparing to publish calibration and scientific papers.

Besides the missions described above, we are partially contributing to the following missions.

- Hisaki: A Japanese small satellite dedicated for planetary science, observing EUV photons. (Contributors: Tomoki Kimura)
- NuSTAR: A NASA's small explorer mission for hard X-ray imaging in the 5–80 keV band. World first imaging capability in hard X-ray band opened a new field in observation: nuclear astrophysics. (Contributors: Takao Kitaguchi)
- NICER and MAXI: Both are the detectors onboard International Space Station (ISS). NICER is a mission of NASA/GSFC for exploring the interior of neutron stars which will be launch in fall 2016. MAXI is the RIKEN-led all sky X-ray monitor mission. (Contributors: Teruaki Enoto, Wataru Iwakiri, Toru Tamagawa)
- Large Synoptic Survey Telescope (LSST): All sky survey telescope in the optical band being constructed by US community. The telescope surveys all sky of the southern hemisphere with ~24 mag sensitivity every three days. It is under construction and expected first light in 2019. This telescope has good synergy with all sky X-ray monitor mission such as MAXI in astrophysics. (Contributors: Yuki Okura, Toru Tamagawa through RIKEN Brookhaven Research Center)
- Future X-ray spectrometry missions, DIOS and Athena: DIOS is a Japanese small satellite exploring the missing baryon in the universe in 2020's, and Athena is the ESA's large class mission for observing the evolution of galaxies/clusters in late 2020's. (Contributors: Noda Hirofumi, Toru Tamagawa)

Members

Associate Chief Scientist (Lab. Head)
Toru TAMAGAWA

Contract Researcher
Yuki OKURA (Jun. 1, 2014 –)
Asami HAYATO (Dec. 1, 2015 –)

Special Postdoctoral Researchers

Asami HAYATO (– Nov. 30, 2015)
Kumi ISHIKAWA (– Mar. 31, 2016)
Hirofumi NODA (– Mar. 31, 2016)
Takayuki YUASA (– Mar. 31, 2016)
Tomoki KIMURA (Apr. 1, 2015 –)

Part-time Workers

Megu KUBOTA (Aug. 17, 2015 – Feb. 29, 2016)
Kazuki NISHIDA (Aug. 17, 2015 – Feb. 29, 2016)
Sonoe ODA (Sep. 14, 2015 – Feb. 29, 2016)
Tatsuya YOSHIDA (Jan. 7, 2016 – Jan. 28, 2016)

Visiting Researchers

Wataru IWAKIRI (JSPS Fellow, Saitama Univ. – Mar. 31, 2016)
Teruaki ENOTO (JSPS Fellow, Stanford Univ. – Mar. 31, 2015)

Visiting Scientists

Yukikatsu TERADA (Saitama Univ.)
Yujin NAKAGAWA (Waseda Univ.)
Masaki WAKABAYASHI (Jakulin Commercial Company LC)
Aya BAMBA (Aoyama Gakuin Univ.)
Naohisa INADA (National Institute of Tech., Nara College)
Rohta TAKAHASHI (Tomakomai Nat'l College of Tech.)
Toru MISAWA (Shinshu Univ.)
Hiroya YAMAGUCHI (Harvard Univ.)
Satoru KATSUDA (JAXA)
Shin'ya YAMADA (Tokyo Met. Univ.)
Takao KITAGUCHI (Hiroshima Univ.)
Harufumi TSUCHIYA (JAEA)
Teruaki ENOTO (Kyoto Univ.)
Yuzuru TAWARA (Nagoya Univ.)

Student Trainees

Akifumi YOSHIKAWA (Tokyo Univ. of Sci.)
Yoko TAKEUCHI (Tokyo Univ. of Sci.)
Kenta KANEKO (Kogakuin Univ.)
Megu KUBOTA (Tokyo Univ. of Sci.)
Kazuki NISHIDA (Tokyo Univ. of Sci.)
Ryouta MICHIGAMI (Nagasaki Institute of Applied Science)

List of Publications & Presentations

Publications

[Journal]

(Original Papers) *Subject to Peer Review

Grefenstette, B. W., Harrison, F. A., Boggs, S. E., Reynolds, S. P., Fryer, C. L., Madsen, K. K., Wik, D. R., Zoglauer, A., Ellinger, C. I., Alexander, D. M., An, H., Barret, D., Christensen, F. E, Craig, W. W., Forster, K., Giommi, P., Hailey, C. J., Hornstrup, A., Kaspi, V. M., Kitaguchi, T., Koglin, J. E., Mao, P. H., Miyasaka, H., Mori, K., Perri, M., Pivovaroff, M. J., Puccetti, S., Rana, V., Stern, D., Westergaard, N. J., Zhang, W. W.: "Asymmetries in core-collapse supernovae from maps of radioactive 44Ti in Cassiopeia A" Nature 506, 339-342 (2014).*

Yasuda, Tetsuya; Iwakiri, Wataru B.; Tashiro, Makoto S.; Terada, Yukikatsu; Kouzu, Tomomi; Enoto, Teruaki; Nakagawa, Yujin E.; Bamba, Aya; Urata, Yuji; Yamaoka, Kazutaka; Ohno, Masanori; Shibata, Shinpei; Makishima, Kazuo: "Sub-MeV band observation of a hard burst from AXP 1E 1547.0-5408 with the Suzaku Wide-band All-sky Monitor" Publications of the Astronomical Society of Japan, 67, 4112 (2015).*

Katsuda, Satoru; Acero, Fabio; Tominaga, Nozomu; Fukui, Yasuo; Hiraga, Junko S.; Koyama, Kat- suji; Lee, Shiu-Hang; Mori, Koji; Nagataki, Shigehiro; Ohira, Yutaka; Petre, Robert; Sano, Hidetoshi; Takeuchi, Yoko; Tamagawa, Toru; Tsuji, Naomi; Tsunemi, Hiroshi; Uchiyama, Yasunobu: "Evidence for Thermal X-Ray Line Emission from the Synchrotron-dominated Supernova Remnant RX J1713.7-3946" The Astrophysical Journal, 814, 29 (2015).*

Okura, Y.; Plazas, A. A.; May, M.; Tamagawa, T.: "Spurious shear induced by the tree rings of the LSST CCDs" Journal of Instrumentation, 10, C08010 (2015).*

Okura, Yuki; Futamase, Toshifumi: "A new weak lensing shear analysis method using ellipticity defined by 0th order moments" Astronomy & Astrophysics, 576, A63 (2015).*

Marcu-Cheatham, Diana M.; Pottschmidt, Katja; Khnel, Matthias; Mller, Sebastian; Falkner, Sebastian; Caballero, Isabel; Finger, Mark H.; Jenke, Peter J.; Wilson-Hodge, Colleen A.; Frst, Felix; Grinberg, Victoria; Hemphill, Paul B.; Kreykenbohm, Ingo; Klochkov, Dmitry; Rothschild, Richard E.; Terada, Yukikatsu; Enoto, Teruaki; Iwakiri, Wataru; Wolff, Michael T.; Becker, Peter A.; Wood, Kent S.; Wilms, Jrn: "The Transient Accreting X-Ray Pulsar XTE J1946+274: Stability of X-Ray Properties at Low Flux and Updated Orbital Solution" The Astrophysical Journal, 815, 44 (2015).*

K. Masunaga, K. Seki, N. Terada, F. Tsuchiya, T. Kimura, K. Yoshioka, G. Murakami, A. Yamazaki, M. Kagitani, C. Tao, A. Fedorov, Y. Futaana, T. L. Zhang, D. Shiota, F. Leblanc, J.-Y. Chaufray, and I. Yoshikawa "Periodic variations of oxygen EUV dayglow in the upper atmosphere of Venus: Hisaki/EXCEED observations" J. Geophys. Res. Planets, 120, 004849 (2015).*

Ichinohe, Yuto; Uchida, Yuusuke; Watanabe, Shin; Edahiro, Ikumi; Hayashi, Katsuhiro; Kawano, Taka- fumi; Ohno, Masanori; Ohta, Masayuki; Takeda, Shin'ichiro; Fukazawa, Yasushi; Katsuragawa, Miho; Nakazawa, Kazuhiro; Odaka, Hirokazu; Tajima, Hiroyasu; Takahashi, Hiromitsu; Takahashi, Tadayuki; Yuasa, Takayuki: "The first demonstration of the concept of "narrow-FOV Si/CdTe semiconductor Comp- ton camera" Nuclear Inst. and Methods in Physics Research, A, 806 (2016).*

Chihiro Tao, Tomoki Kimura, Sarah V. Badman, Nicolas Andr, Fuminori Tsuchiya, Go Murakami, Kazuo Yoshioka, Ichiro Yoshikawa, Atsushi Yamazaki and Masaki Fujimoto, "Variation of Jupiter's Aurora Observed by Hisaki/EXCEED: 2. Estimations of Auroral Parameters and Magnetospheric Dynamics" J. Geophys. Res., (in press).*

Takeuchi, Yoko; Yamaguchi, Hiroya; Tamagawa, Toru: "A systematic study of evolved supernova rem- nants in the large and small Magellanic Clouds with Suzaku" Publications of the Astronomical Society of Japan, (in press).*

Oral Presentations

[International Conference etc.]

Tamagawa, Toru: “X-ray generator: an application of micro pattern gas detector” 4th Interna- tional Micro Pattern Gaseouse Detector Conference, Trieste, Italy, October (2015).
Kitaguchi, Takao: “Development of the GEM-TPC X-ray polarimeter with the Scalable Readout System” RD51 Collaboration Meeting, Trieste, Italy, October (2015).
Kimura Tomoki: “Hisaki science team, Dynamics of Jupiter’s auroral acceleration investigated by multiwavelength plasma remote sensing with space telescopes”, Japan Geoscience Union Meeting 2015, Makuhari, Japan (2015).

[Domestic Conference]
武内陽子, 山口弘悦, 玉川徹: “「すざく」によるマゼラン星雲の古い超新星残骸の系統解析” 日本天文学会, 2015 年秋季年会, (日本天文学会), 神戸, 9 月, (2015)
野田博文, 林佑, 山崎典子, 満田和久: “有限要素熱解析による Cu/Bi 多層膜吸収体を用いた超電導遷移端 型マイ クロカロリメータのパルス波形の検証” 日本天文学会 2015 年秋季年会, (日本天文学会), 神戸, 9 月, (2015)
早藤麻美, 北口貴雄, 岩切渉, 玉川徹, 窪田恵, 西田和樹, 武内陽子榎戸輝揚, 武井大, 高山裕貴: “SPring-8 に おけるマイクロパターンガス偏光計の性能評価” 日本天文学会 2015 年秋季年会, (日本天文学会), 神戸, 9 月, (2015)
芹野素子, 岩切渉, 玉川徹, 中平聡志, 松岡勝, 三原建弘: “全天 X 線監視装置 MAXI が観測した superburst”, 日本物理学会 2015 年秋季大会, (日本物理学会), 大阪, 9 月, (2015)
西田和樹, 玉川徹, 岩切渉, 鈴木良一, 加藤英俊, 志岐成友, 武内陽子, 北口貴雄, 早藤麻美, 榎戸輝陽, 窪田 恵: “電気パルスで変調駆動できる可搬型 X 線発生装置の開発” 日本物理学会 2015 年秋季大会, (日本物理 学会), 大阪, 9 月, (2015)
湯浅孝行, 榎戸輝揚, 土屋晴文, 米徳大輔, 澤野達哉, 中澤知洋, 牧島一夫, 楳本大悟, 古田禄大, 山田真也: “GROWTH 実験:雷雲起源ガンマ線放射の石川県での 2014 年度冬季観測結果と検出器小型化に向けた開 発状況” 日本物理学会 2015 年秋季大会, (日本物理学会), 大阪, 9 月, (2015)
湯浅孝行, 曽田康広, 大竹優, 山地光久, 川口実, 檜原弘樹, 藤城巌, 程島文夫: “SpaceWire 高速化研究のス テータス報告” 宇宙科学技術連合会, 鹿児島, 10 月 (2015).
湯浅孝行: “雷雲ガンマ線プロジェクト×市民科学” 日本科学未来館, 東京, 11 月 (2015).
木村智樹: “JUNO, HISAKI による木星探査・観測に期待されるサイエンス” Symposium on Planetary Science 2016, 東北大学, 2 月 (2016).
木村智樹: “回転惑星磁気圏が駆動するオーロラの物理と中性子星磁気圏への応用” 中性子星の観測と理論〜研究活性化ワークショップ, 京都大学, 12 月 (2015).
木村智樹: “多波長遠隔観測でみる回転惑星磁気圏のオーロラ加速” 国立天文台理論天文学研究会 2015, 伊豆, 10 月 (2015).
木村智樹: “衛星周囲のプラズマ環境と惑星-衛星電磁相互作用” 衛星系研究会, 北大低温研, 7 月 (2015).
木村智樹: “その場観測と多波長遠隔観測に基づく高エネルギー磁気圏物理” 巨大惑星系研究会, 東工大学 地球生命研究所 4 月 (2015).
Kimura, T., R. Kraft, R. Elsner, G. Branduardi-Raymont, R. Gladstone, C. Tao, K. Yoshioka, G. Murakami, A. Yamazaki, F. Tsuchiya, M. F. Vogt, A. Masters, H. Hasegawa, S. V. Badman, E. Roediger, Y. Ezoe, I. Yoshikawa, M. Fujimoto, and S. S. Murray: “宇宙望遠鏡群による木星オーロラの多波長観測:極冠領域における X 線発光”, 地球電磁気・地球惑星圏学会 第 138 回総会・講演会, 東京, 11 月 (2015).
玉川徹: “宇宙の進化とブラックホールの謎” 長崎総合科学 大学大学院・新技術創成研究所公開講演会「21 世紀の科学技術」 〜みんなで学ぼう!宇宙の最前線〜, 長崎, 12 月 (2015)

Posters Presentations

[International Conference etc.]
Kubota, Megu: “Measurement of the GEM gain uniformity for the PRAXyS mission” 4th International Micro Pattern Gaseouse Detector Conference, Trieste, Italy, October (2015).
Kitaguchi, Takao: “Development of the GEM-TPC X-ray Polarimeter with the Scalable Readout System” 4th International Micro Pattern Gaseouse Detector Conference, Trieste, Italy, October (2015).

RIBF Research Division
Astro-Glaciology Research Unit

Summary of Research Activities

Our Astro-Glaciology Research Unit promotes both experimental and theoretical studies to open up the new interdisciplinary research field of astro-glaciology, which combines astrophysics and glaciology.

On the experimental side, we analyze ice cores drilled at the Dome Fuji station, in Antarctica, in collaboration with the National Institute of Polar Research (NIPR, Tokyo). These ice cores are time capsules. In particular, the ice cores obtained at Dome Fuji are known to be unique because they contain much more information on conditions in the stratosphere than any other ice cores recovered from other locations in either hemisphere. This means that there are significant advantages in using Dome Fuji ice cores if we wish to study astronomical phenomena of the past. Since gamma-rays and high-energy protons that are emitted in certain astronomical processes affect the chemical and isotopic compositions in the stratosphere but not those in the troposphere, we have been measuring:

(1) Variations in the nitrate ion (NO_3-) concentrations in the ice cores, in an effort to establish a new proxy for supernova explosions in our own galaxy as well as past solar activity.
(2) Variations in the water isotopes (^{18}O and ^{2}H) in the ice cores, in order to construct in more detail records of past changes in the temperature of the surface of the earth; and
(3) Variations in the nitrogen isotope (^{15}N) in the nitrates contained in the ice cores, in order to investigate the possibility of utilizing ^{15}N as a new and more stable proxy for galactic supernovae explosions and past solar activity.

In the case of items (1), (2), and (3), our analyses of Dome Fuji ice cores cover the most recent 2000 years. The temporal resolution of the results of our research is currently 12 months. We intend to compare the results obtained in item (1) with those in item (2), in order to understand better the relationships between solar activity and long-term changes in the temperature of the earth. The underlying assumptions in item (2) are already well accepted in glaciology. Item (3) refers to one of the very first measurements of ^{15}N concentrations in ice cores.

On the theoretical side, we are simulating numerically:

(4) Changes in the chemical composition of the stratosphere induced by gamma-rays and/or high-energy particles emitted from explosive astronomical phenomena, such as galactic supernovae and solar proton events; and
(5) The explosive nucleosynthesis (including the r-process, the rapid neutron capture process, which creates elements heavier than iron) that arises in the environment of core-collapse supernova explosions.

Items (4) and (5) in our list, the chemical composition of the stratosphere and explosive nucleosynthesis, are very important in solar–terrestrial research and nuclear astrophysics; furthermore, these simulations provide a theoretical support when considering the characteristics of supernova explosions and solar activity, as seen in our ice core data. These studies are also important because it is necessary to discount the effects of the meteorological noise.

It is noteworthy that the as yet not fully understood frequency of supernova explosions in our galaxy is crucial to an understanding of the r-process nucleosynthesis. The results obtained from items (1) and (3) are expected to reveal the average rate of supernova explosions in our galaxy during the past million years of ice deposition.

Members

Research Unit Leader (Lab. Head)
Yuko MOTIZUKI

Research & Technical Scientists
Kazuya TAKAHASHI (Concurrent: RI Application Team, Senior Research Scientist)
Yoichi NAKAI (Concurrent: RI Physics Lab., Senior Research Scientist)

Part-time Workers
Manami MARUYAMA (Oct. 10, 2012 – Mar. 31, 2016)
Yuma HASEBE (Saitama Univ., Nov. 1, 2014 –)
Sachiko MIYAZAKI (Aug. 1, 2015 – Mar. 31, 2016)
Yoko HOSHINO (Jan. 5, 2016 - Mar. 31, 2016)

Visiting Scientists
Yasushige YANO (Concurrent)
Akira HORI (Kitami Inst. of Tech.)
Hideharu AKIYOSHI (Nat ʻl Inst. for Environ. Studies)
Hideki MADOKORO (Mitsubishi Heavy Ind., Ltd.)

Student Trainees
Yuma HASEBE (Saitama Univ.)

List of Publications & Presentations

Publications

[Journal]

(Original Papers) *Subject to Peer Review

Shuji Fujita, Kumiko Goto-Azuma, Motohiro Hirabayashi, Akira Hori, Yoshinori Iizuka, Yuko Motizuki, Hideaki Motoyama, Kazuya Takahashi: “Densification of layered firn of the ice sheet at Dome Fuji, Antarctica”, Journal of Glaciology (2016), 21 pages, Available on CJO2016 doi:10.1017/jog.2016.16*

Michael Sigl, J.R. McConnell, M. Toohey, G. Plunkett, F. Ludlow, M. Winstrup, S. Kipfstuhl, Y. Motizuki: “The history of volcanic eruptions since Roman times”, PAGES MAGAZINE, 23, 48-49, 2015.*

Fusa Miyake, Asami Suzuki, Kimiaki Masuda, Kazuho Horiuchi, Hideaki Motoyama, Hiroyuki Matsuzaki, Yuko Motizuki, Kazuya Takahashi, Yoichi Nakai: “Cosmic ray event of AD 774-775 shown in quasi-annual ^{10}Be data from the Antarctic Dome Fuji ice core”, Geophysical Research Letters, 42, 84-89, 2015.*

望月優子: 「南極の氷床コアから太陽活動と気候変動の関係を探る」、理研環境報告書2015、pp.17-20、2015.

Y. Nakai, Y. Motizuki, M. Maruyama, H. Akiyoshi, T. Imamura : “Variation of chemical composition induced by solar energetic particle events in the middle atmosphere”, RIKEN Accel. Prog. Rep. 48, 168, 2015.*

Y. Motizuki, S. Okamoto, K. Takahashi, Y. Nakai, A. Makabe, K. Koba, H. Motoyama : “Measurements of nitrogen isotope ratios in samples with very low nitrate concentrations from the Dome Fuji ice core (Antarctica) drilled in 2010”, RIKEN Accel. Prog. Rep. 48, 169, 2015.*

M. Sigl, J. McConnell, M. Toohey, M. Curran, S. Das, R. Edwards, E. Isaksson, K. Kawamura, S. Kipfstuhl, K. Krüger, L. Layman, O. Maselli, Y. Motizuki, H. Motoyama, D. Pasteris, M. Severi: “Insights from Antarctica on volcanic forcing during the Common Era”, RIKEN Accel. Prog. Rep. 48, 167, 2015.*

[Book]

(Original Papers) *Subject to Peer Review

望月優子：『放射化学の事典』（共同執筆）、日本放射化学会編、pp. 274-277（「軽い元素の原子核合成」「重い元素の原子核合成」）、朝倉書店、2015.＊

Oral Presentations

[International Conference etc.]

(Invited talk) Yuko Motizuki: “Astronomical signatures embedded in ice cores", Baymfest in Tokyo -Exploring Extreme Forms of Matter-, Tokyo, Japan, Mar. 14, 2016.

Kenji Tanabe and Yuko Motiziuki: “Possible geologial records of symbiotic binary R Aquarii’s historical outbursts”, XXIX IAU General Assembly, Honolulu, USA, Aug. 3-14, 2015.

Y. Nakai, Y. Motizuki, M. Maruyama, H. Akiyoshi, T. Imamura: “Variation of trace chemical species induced by solar energetic particles in the middle atmosphere: ozone and nitric acid”, Japan Geoscience Union Meeting, Chiba, May 24-28, 2015.

[Domestic Conference]

（招待講演）望月優子：「アイスコアからさぐる天文・宇宙のサイエンスー過去の超新星の爆発から宇宙のリズムまでー」、大阪大学理学部講義「理学への招待」、豊中、2015年11月30日.

（招待講演）望月優子：「浅層コア詳細化学解析ーこれまでのまとめと第9期の研究提案、IPICS 2kへの貢献を見据えてー」極地研研究集会「南極雪氷科学の展開による新たな古環境復元とメカニズム理解にむけて」、立川、2015年9月24-25日.

長谷部憂磨、望月優子：「南極ドローニングモードランドアイスコアの酸素同位体比からわかる気温変動と太陽活動周期との関係」、日本天文学会2015年秋季年会、神戸、2015年9月9-11日.

（招待講演）望月優子：「宇宙と生命とのつながりー生命と元素、星、宇宙のリズムー」、平成２７年度スーパーサイエンスハイスクール生徒研究発表会研究者ミニライブ、大阪、2015年8月6日.

（招待講演）望月優子：「南極アイスコアから探る環境変動」、文部科学省科学技術・学術政策研究所主催「近未来への招待状～ナイスステップな研究者2014からのメッセージ」、東京、2015年7月27日.

Posters Presentations

[International Conference etc.]

Kazuya Takahashi, Yuko Motizuki, Yoichi Nakai, Keisuke Suzuki, Yoshinori Iizuka, and Hideaki Motoyama: “Overview of chemical composition and the characteristics of the distributions of Na^+ and Cl^- in shallow ice core samples from DF01 core (Antarctica) drilled in 2001” (A poster paper), The 6th Symposium on Polar Science, Tachikawa, Japan, Nov. 16-19, 2015.

Yuma Hasebe, Yuko Motizuki, Yoichi Nakai, Kazuya Takahashi: “Diagnose oscillation properties observed in an annual ice-core oxygen isotope record obtained from Dronning Maud Land, Antarctica” (A poster paper), The 6th Symposium on Polar Science, Tachikawa, Japan, Nov. 16-19, 2015.

[Domestic Conference]

（招待講演）望月優子：「地球規模の気候に影響を与えた火山噴火に関する南極アイスコア科学の推進」（パネル発表）、第56回（2015年度）文部科学省科学技術週間展示、東京、2015年4月13日-19日.

RIBF Research Division
Research Group for Superheavy Element

1. Abstract

The elements with their atomic number Z>103 are called as trans-actinide or superheavy elements. The chemical properties of those elements have not yet been studied in detail. Those elements do not exist in nature. Therefore, they must be produced by artificially for the scientific study of those elements. In our laboratory, we have been studying the physical and chemical properties of the superheavy elements utilizing the accelerators in RIKEN and various methods of efficient production of the superheavy elements.

2. Major Research Subjects

(1) Search for new superheavy elements
(2) Decay spectroscopy of the heaviest nuclei
(3) Study of the chemical properties of the heaviest elements
(4) Study of the reaction mechanism of the fusion process (theory)

3. Summary of Research Activity

(1) Searching for new elements

To expand the periodic table of elements and the nuclear chart, we will search for new elements.

(2) Spectroscopic study of the nucleus of heavy elements

Using the high sensitivity system for detecting the heaviest element, we plan to perform a spectroscopic study of nuclei of the heavy elements.

(3) Chemistry of superheavy elements

Study of chemistry of the trans-actinide (superheavy element) has just started world-wide, making it a new frontier in the field of chemistry. Relativistic effects in chemical property are predicted by many theoretical studies. We will try to develop this new field.

(4) Study of a reaction mechanism for fusion process

Superheavy elements have been produced by complete fusion reaction of two heavy nuclei. However, the reaction mechanism of the fusion process is still not well understood theoretically. When we design an experiment to synthesize nuclei of the superheavy elements, we need to determine a beam-target combination and the most appropriate reaction energy. This is when the theory becomes important. We will try to develop a reaction theory useful in designing an experiment by collaborating with the theorists.

(5) Research Highlight

The discovery of a new element is one of the exciting topics both for nuclear physicists and nuclear chemists. The elements with their atomic number Z>103 are called as trans-actinides or superheavy elements. The chemical properties of those elements have not yet been studied in detail. Since those elements do not exist in nature, they must be produced by artificially, by using nuclear reactions for the study of those elements. Because the production rate of atoms of those elements is extremely small, an efficient production and collection are key issues of the superheavy research. In our laboratory, we have been trying to produce new elements, studying the physical and chemical properties of the superheavy elements utilizing the accelerators in RIKEN.

Although the Research Group for Superheavy element has started at April 2013, the Group is a renewal of the Superheay Element Laboratory started at April 2006, based on a research group which belonged to the RIKEN accelerator research facility (RARF), and had studied the productions of the heaviest elements. The main experimental apparatus is a gas-filled recoil ion separator GARIS. The heaviest elements with their atomic numbers, 107 (Bohrium), 108 (Hassium), 109 (Meitnerium), 110 (Darmstadtium), 111 (Roentogenium), and 112 (not yet named) were discovered as new elements at Helmholtzzentrum für Schwerionenforschung GmbH (GSI), Germany by using ^{208}Pb or ^{209}Bi based complete fusion reactions, so called “cold fusion” reactions. We have made independent confirmations of the productions of isotopes of 108th, 110th, 111th, and 112th elements by using the same reactions performed at GSI. After these work, we observed an isotope of the 113th element, ^{278}113, in July 2004, in April, 2005, and in August 2012. The isotope, ^{278}113, has both the largest atomic number, (Z = 113) and atomic mass number (A = 278) which have determined experimentally among the isotopes which have been produced by cold fusion reactions. We could show the world highest sensitivity for production and detection of the superheavy elements by these observations. Finally, our results that related to ^{278}113 has been recognized as a discovery of new element by a Joint Working Party of the International Union of Pure and Applied Chemistry (IUPAC) and International Union of Pure and Applied Physics (IUPAP).

We decided to make one more recoil separator GARIS-II, which has an acceptance twice as large as existing GARIS, in order to realize higher sensitivity. The design of GARIS-II has finished in 2008. All fabrication of the separator will be finished at the end of fiscal year 2008. It will be ready for operation in fiscal year 2009 after some commissioning works.

Preparatory work for the study of the chemical properties of the superheavy elements has started by using the gas-jet transport system coupled to GARIS. The experiment was quite successful. The background radioactivity of unwanted reaction products has been highly suppressed. Without using the recoil separator upstream the gas-jet transport system, large amount of unwanted radioactivity strongly prevents the unique identification of the event of our interest. This new technique makes clean and clear studies of chemistry of the heaviest elements promising.

The spectroscopic study of the heaviest elements has started by using alpha spectrometry. New isotope, ^{263}Hs (Z=108), which has the smallest atomic mass number ever observed among the Hassium isotopes, had discovered in the study. New spectroscopic information for ^{264}Hs and its daughters have obtained also. The spectroscopic study of Rutherfordium isotope ^{261}Rf (Z=104) has done and 1.9-s isomeric state has directly produced for the first time.

Preparatory works for the study of the new superheavy elements with atomic number 119 and 120 have started in 2013. We measured

the reaction products of the ^{248}Cm(^{48}Ca, xn)$^{296-x}$Lv(Z=116) previously studied by Frelov Laboratory of Nuclear Reaction, Russia, and GSI. We observed 5 isotopes in total which tentatively assigned to ^{293}Lv, and ^{292}Lv.

Members

Group Director
Kosuke MORITA

Visiting Scientist
Kunihiro FUJITA (Kyushu Univ.)

Student Trainees
Taiki TANAKA (Kyushu Univ.)
Kenyu WATANABE (Kyushu Univ.)
Yuki YAMANO (Kyushu Univ.)

List of Publications & Presentations

Publications

[Journal]

(Original Papers) *Subject to Peer Review

D. Kaji, K. Morimoto, H. Haba, E. Ideguchi, H. Koura, K. Morita "Decay Properties of New Isotopes 234Bk and 230Am, and Even–Even Nuclides 234Cm and 230Pu", Journal of the Physical Society of Japan, 85, 015002 (2016) *

D. Kaji, K. Morimoto, Double-layered target and identification method of individual target correlated with evaporation residues, Nuclear Instruments & Methods in Physics Research A792 (2015) 11-14*

[解説、和文]

K. Morimoto 113 番新元素の合成 "Synthesis of 113th new element", 放射化学 The Japan Society of Nuclear and Radiochemical Sciences, Vol.33, pp. 10-16

Oral Presentations

[International Conference etc.]

D. Kaji, K. Morimoto, Y. Wakabayashi, M. Takeyama, S. Yamaki, K. Tanaka, K. Morita, H. Haba, M. Murakami, S. Goto, H. Kikunaga, and M. Asai "GARIS-II: New Gas-filled Recoil Ion Separator at RIKEN", 超アクチノイド元素の化学と物理国際会議 2015（TAN15）, Aizu Fukushima Japan, May 29 2015"

S. Wakabayashi, K. Morita, K. Morimoto, D. Kaji, H. Haba, M. Takeyama, S. Yamaki, K. Tanaka, T. Tanaka, M. Murakami, Y. Komori, K. Nishio, H. Koura, M. Asai, Y. Aritomo, A. Yoneda "Production of new isotopes, ^{215}U and ^{216}U close to N = 126", The 5th International Conference on the Chemistry and Physics of the Transactinide Elements (TAN15), Aizu Fukushima Japan, May 29 2015

K. Morimoto "Superheavy element research at RIKEN", The International Conference on Nuclear Structure and Related Topics, Dubna Russia, July 17 2015

K. Morimoto "Synthesis of superheavy elements at RIKEN", The International Chemical Congress of PACIFIC BASIN SOCIETIES（PACIFICHEM 2015), Hawaii USA, December 19 2015

D. Kaji "Heavy element study using a new separator GARIS-II", The International Chemical Congress of PACIFIC BASIN SOCIETIES（PACIFICHEM 2015), Hawaii USA, December 19 2015

K. Morita, "SHE research at RIKEN/GARIS", The 9th Japan-China Joint Nuclear Physcs Symposium(JCNP2015), Osaka University Japan, Novermber 7-12 2015

K. Morita, "SHE research at RIKEN/GARIS", TAN15 Fukushima Japan, May 25-29 2015

K. Morita, "Research of superheavy element at RIKEN", LEAP2016, Kanazawa Japan, March 6-11 2016

[Domestic Conference]

D. Kaji, K. Morimoto, M. Haba, Y. Wakabayashi, M. Takeyama, S. Yamamoto, K. Tanaka, M. Huang, Y. Komori, J. Kanaya, M. Murakami, K. Katori, H. Hasebe, A. Yoneda, A. Yoshida, F. Tokanai, T. Yoshida, T. Yamaguchi, M. Asai, Z.Gan, L. Ma, H. Geissel, S. Hofmann, J. Maurer, K. Fujita, Y. Narikiyo, T. Tanaka, S. Yamamoto, K. Morita "GARIS を用いたホットフュージョン反応 ^{248}Cm+^{48}Ca→^{296}Lv*に関する研究", 第 59 回放射化学討論会, Tohoku University Japan, September 26 2015

T. Tanaka, K. Morita, K. Morimoto, D. Kaji, H. Haba, Y. Wakabayashi, Y. Komori, M. Takeyama, S. Yamaki, K. Tanaka, H. Hasebe, M. Huang, J. Kanaya, M. Murakami, A. Yoneda, A. Yoshida, T. Yamaguchi, F. Tokanai, Y. Yoshida, Z.Gan, L. Ma, H. Geissel, S. Hofmann, Y. Maurer, K. Fujita, Y. Narikiyo, S. Yamamoto, M. Asai, K. Katori "The reaction 48Ca+248Cm→296Lv* studied at the RIKEN-GARIS", JPS 2015 Autumn Meeting, Kansai University Japan, Septmeber 27 2015

T. Tanaka, Y. Narikiyo, K. Morita, K. Fujita, D. Kaji, K. Morimoto, S. Yamaki, Y. Wakabayashi, K. Tanaka, M. Takeyama, A. Yoneyama, H. Haba, Y. Komori, S. Yanou, B. J. P. Gall, Z. Asfari, H. Faure, H. Hasebe, M. Huang, J. Kanaya, M. Murakami, A. Yoshida, T. Yamaguchi, T. Tokanai, T. Yoshida, Z. Gan, L. Ma, H. Geissel, S. Hofmann, Y. Maurer, S. Yamamoto, Y. Yamano, K. Watanabe, S. Ishizawa, M. Asai, R. Aono, S. Goto, K. Katori "Study of barrier distribution in heavy reaction system at the RIKEN-GARIS", JPS 71th Annual Meeting (2016), Tohoku Gakuin University Japan, March 21 2016

R. Aono, S. Goto, D. Kaji, K. Morimoto, H. Haba, M. Murakami, K. Ooe, H. Kudo "Production of neutron-deficient rutherfordium isotopes in the Pb-208 + Ti-48,50 reactions", 2015 日本放射化学会年会・第 59 回放射化学討論会, Tohoku Univercity Japan, Septmeber 26 2015

Posters Presentations

[International Conference etc.]

M. Takeyama, D. Kaji, K. Morimoto, Y. Wakabayashi, F. Tokanai, K. Morita "Detector calibration to spontaneous fission for the study of superheavy elements using gas-filled recoil ion separator", International Symposium on Radiation Detectors and Their Uses (ISRD2016), Tsukuba Japan December 19 2015

RIBF Research Division
Research Group for Superheavy Element
Superheavy Element Production Team

1. Abstract

The elements with their atomic number Z>103 are called as trans-actinide or superheavy elements. The chemical properties of those elements have not yet been studied in detail. Those elements do not exist in nature. Therefore, they must be produced by artificially for the scientific study of those elements. In our laboratory, we have been studying the physical and chemical properties of the superheavy elements utilizing the accelerators in RIKEN and various methods of efficient production of the superheavy elements.

2. Major Research Subjects

(1) Search for new supreheavy elements
(2) Decay spectroscopy of the heaviest nuclei
(3) Study of the chemical properties of the heaviest elements
(4) Study of the reaction mechanism of the fusion process (theory)

Summary of Research Activity

(1) Searching for new elements

To expand the periodic table of elements and the nuclear chart, we will search for new elements.

(2) Spectroscopic study of the nucleus of heavy elements

Using the high sensitivity system for detecting the heaviest element, we plan to perform a spectroscopic study of nuclei of the heavy elements.

(3) Chemistry of superheavy elements

Study of chemistry of the trans-actinide (superheavy element) has just started world-wide, making it a new frontier in the field of chemistry. Relativistic effects in chemical property are predicted by many theoretical studies. We will try to develop this new field.

(4) Study of a reaction mechanism for fusion process

Superheavy elements have been produced by complete fusion reaction of two heavy nuclei. However, the reaction mechanism of the fusion process is still not well understood theoretically. When we design an experiment to synthesize nuclei of the superheavy elements, we need to determine a beam-target combination and the most appropriate reaction energy. This is when the theory becomes important. We will try to develop a reaction theory useful in designing an experiment by collaborating with the theorists.

Members

Team Leader
Kosuke MORITA (concurrent; Group Director, Research Group for Superheavy Element)

Research & Technical Scientist
Kouji MORIMOTO (Senior Research Scientist, concurrent; Team Leader, Superheavy Element Device Development Team)

Nishina Center Research Scientist
Daiya KAJI (concurrent; Superheavy Element Device Development Team)

Nishina Center Technical Scientist
Akira YONEDA

Contract Researcher
Yasuo WAKABAYASHI (Apr. 1, 2015 – June 30, 2015)

Special Postdoctoral Researcher
Yasuo WAKABAYASHI (Apr. 2012 – Mar. 31, 2015)

Research Consultant
Kenji KATORI

Junior Research Associate
Mirei TAKEYAMA (Yamagata Univ., – Mar. 31, 2015)

Part-time Worker
Kengo TANAKA (Tokyo Univ. of Sci., – Mar. 31, 2015)

Visiting Scientists

Hiroyuki KOURA (JAEA)
Benoit Jean-Paul GALL (Strasbourg Univ.)
Marc ASFARI (Institut Pluridisciplinaire Hubert Curien)
Mirei TAKEYAMA (Yamagata Univ.)

Student Trainees

Takuya YOKOKITA (Osaka Univ.)
Kengo TANAKA (Tokyo Univ. of Sci.)
Christian Stefan BERNER (Technische Universitat Munchen)
Hugo FAURE (Strasbourg University)

List of Publications & Presentations

Publications

[Journal]

(Original Papers) *Subject to Peer Review

D. Kaji, K. Morimoto, H. Haba, E. Ideguchi, H. Koura, K. Morita "Decay Properties of New Isotopes 234Bk and 230Am, and Even–Even Nuclides 234Cm and 230Pu", Journal of the Physical Society of Japan, 85, 015002 (2016) *

(Review)

[解説、和文]

K. Morimoto 113 番新元素の合成 "Synthesis of 113th new element", 放射化学 The Japan Society of Nuclear and Radiochemical Sciences, Vol.33, pp. 10-16

Oral Presentations

[International Conference etc.]

D. Kaji, K. Morimoto, Y. Wakabayashi, M. Takeyama, S. Yamaki, K. Tanaka, K. Morita, H. Haba, M. Murakami, S. Goto, H. Kikunaga, and M. Asai "GARIS-II: New Gas-filled Recoil Ion Separator at RIKEN"", 超アクチノイド元素の化学と物理国際会議 2015（TAN15）, Aizu Fukushima Japan, May 29 2015"

S. Wakabayashi, K. Morita, K. Morimoto, D. Kaji, H. Haba, M. Takeyama, S. Yamaki, K. Tanaka, T. Tanaka, M. Murakami, Y. Komori, K. Nishio, H. Koura, M. Asai, Y. Aritomo, A. Yoneda "Production of new isotopes, ^{215}U and ^{216}U close to N = 126", The 5th International Conference on the Chemistry and Physics of the Transactinide Elements (TAN15), Aizu Fukushima Japan, May 29 2015

K. Morimoto "Superheavy element research at RIKEN", The International Conference on Nuclear Structure and Related Topics, Dubna Russia, July 17 2015

K. Morimoto "Synthesis of superheavy elements at RIKEN", The International Chemical Congress of PACIFIC BASIN SOCIETIES （PACIFICHEM 2015), Hawaii USA, December 19 2015

D. Kaji "Heavy element study using a new separator GARIS-II", The International Chemical Congress of PACIFIC BASIN SOCIETIES （PACIFICHEM 2015), Hawaii USA, December 19 2015

K. Morita, "SHE research at RIKEN/GARIS", The 9th Japan-China Joint Nuclear Physcs Symposium(JCNP2015), Osaka University Japan, Novermber 7-12 2015

K. Morita, "SHE research at RIKEN/GARIS", TAN15 Fukushima Japan, May 25-29 2015

K. Morita, "Research of superheavy element at RIKEN", LEAP2016, Kanazawa Japan, March 6-11 2016

[Domestic Conference]

D. Kaji, K. Morimoto, M. Haba, Y. Wakabayashi, M. Takeyama, S. Yamamoto, K. Tanaka, M. Huang, Y. Komori, J. Kanaya, M. Murakami, K. Katori, H. Hasebe, A. Yoneda, A. Yoshida, F. Tokanai, T. Yoshida, T. Yamaguchi, M. Asai, Z.Gan, L. Ma, H. Geissel, S. Hofmann, J. Maurer, K. Fujita, Y. Narikiyo, T. Tanaka, S. Yamamoto, K. Morita "GARIS を用いたホットフュージョン反応 ^{248}Cm+^{48}Ca→^{296}Lv*に関する研究 ", 第 59 回放射化学討論会, Tohoku University Japan, September 26 2015

T. Tanaka, K. Morita, K. Morimoto, D. Kaji, H. Haba, Y. Wakabayashi, Y. Komori, M. Takeyama, S. Yamaki, K. Tanaka, H. Hasebe, M. Huang, J. Kanaya, M. Murakami, A. Yoneda, A. Yoshida, T. Yamaguchi, F. Tokanai, Y. Yoshida, Z.Gan, L. Ma, H. Geissel, S. Hofmann, Y. Maurer, K. Fujita, Y. Narikiyo, S. Yamamoto, M. Asai, K. Katori "The reaction 48Ca+248Cm→296Lv* studied at the RIKEN-GARIS", JPS 2015 Autumn Meeting, Kansai University Japan, Septmeber 27 2015

T. Tanaka, Y. Narikiyo, K. Morita, K. Fujita, D. Kaji, K. Morimoto, S. Yamaki, Y. Wakabayashi, K. Tanaka, M. Takeyama, A. Yoneyama, H. Haba, Y. Komori, S. Yanou, B. J. P. Gall, Z. Asfari, H. Faure, H. Hasebe, M. Huang, J. Kanaya, M. Murakami, A. Yoshida, T. Yamaguchi, T. Tokanai, T. Yoshida, Z. Gan, L. Ma, H. Geissel, S. Hofmann, Y. Maurer, S. Yamamoto, Y. Yamano, K. Watanabe, S. Ishizawa, M. Asai, R. Aono, S. Goto, K. Katori "Study of barrier distribution in heavy reaction system at the RIKEN-GARIS", JPS 71th Annual Meeting (2016), Tohoku Gakuin University Japan, March 21 2016

R. Aono, S. Goto, D. Kaji, K. Morimoto, H. Haba, M. Murakami, K. Ooe, H. Kudo "Production of neutron-deficient rutherfordium isotopes in the Pb-208 + Ti-48,50 reactions", 2015 日本放射化学会年会・第 59 回放射化学討論会, Tohoku Univercity Japan, Septmeber 26 2015

Posters Presentations

[International Conference etc.]

M. Takeyama, D. Kaji, K. Morimoto, Y. Wakabayashi, F. Tokanai, K. Morita "Detector calibration to spontaneous fission for the study of superheavy elements using gas-filled recoil ion separator", International Symposium on Radiation Detectors and Their Uses (ISRD2016), Tsukuba Japan December 19 2015

RIBF Research Division
Research Group for Superheavy Element
Superheavy Element Device Development Team

1. Abstract

A gas-filled recoil ion separator has been used as a main experimental device for the study of superheavy elements. This team is in charge of maintain, improve, develop and operate the separators and related devices. There are two gas-filled recoil ion separators installed at RILAC experimental hall. One is GARIS that is designed for symmetric reaction such as cold-fusion reaction, and the other is newly developed GARIS-II that is designed for an asymmetric reaction such as hot-fusion reaction. New elements ^{278}113 were produced by ^{70}Zn + ^{209}Bi reaction using GARIS. Further the new element search Z > 118 are preparing by using GARIS-II.

2. Major Research Subjects

(1) Maintenance of GARIS and development of new gas-filled recoil ion separator GARIS-II.
(2) Maintenance and development of detector and DAQ system for GARIS and GARIS-II.
(3) Maintenance and development of target system for GARIS and GARIS-II.

3. Summary of Research Activity

The GARIS-II is newly developed which has an acceptance twice as large as existing GARIS, in order to realize higher sensitivity. It will be ready for operation in fiscal year 2014 after some commissioning works. We will also offer user-support if a researcher wishes to use the devices for his/her own research program.

Members

Team Leader
Kouji MORIMOTO

Nishina Center Research Scientist
Daiya KAJI

Nishina Center Technical Scientist
Akira YONEDA (concurrent: Superheavy Element Production Team)

Junior Research Associate
Sayaka YAMAKI (Saitama Univ., Apr. 1, 2014 –)

Part-time Worker
Sayaka YAMAKI (– Mar. 31, 2014)

Visiting Scientists
Fuyuki TOKANAI (Yamagata Univ.)

Student Trainee
Satoshi ISHIZAWA (Yamagata Univ.)

List of Publications & Presentations

Publications

[Journal]
(Original Papers) *Subject to Peer Review

D. Kaji, K. Morimoto, H. Haba, E. Ideguchi, H. Koura, K. Morita "Decay Properties of New Isotopes 234Bk and 230Am, and Even–Even Nuclides 234Cm and 230Pu", Journal of the Physical Society of Japan, 85, 015002 (2016) *

D. Kaji, K. Morimoto, Double-layered target and identification method of individual target correlated with evaporation residues, Nuclear Instruments & Methods in Physics Research A792 (2015) 11-14*

(Review)
[解説、和文]

K. Morimoto 113 番新元素の合成 "Synthesis of 113th new element", 放射化学 The Japan Society of Nuclear and Radiochemical Sciences, Vol.33, pp. 10-16

Oral Presentations

[International Conference etc.]

D. Kaji, K. Morimoto, Y. Wakabayashi, M. Takeyama, S. Yamaki, K. Tanaka, K. Morita, H. Haba, M. Murakami, S. Goto, H. Kikunaga, and

M. Asai "GARIS-II: New Gas-filled Recoil Ion Separator at RIKEN"", 超アクチノイド元素の化学と物理国際会議 2015（TAN15）, Aizu Fukushima Japan, May 29 2015"

S. Wakabayashi, K. Morita, K. Morimoto, D. Kaji, H. Haba, M. Takeyama, S. Yamaki, K. Tanaka, T. Tanaka, M. Murakami, Y. Komori, K. Nishio, H. Koura, M. Asai, Y. Aritomo, A. Yoneda "Production of new isotopes, ^{215}U and ^{216}U close to N = 126", The 5th International Conference on the Chemistry and Physics of the Transactinide Elements (TAN15), Aizu Fukushima Japan, May 29 2015

K. Morimoto "Superheavy element research at RIKEN", The International Conference on Nuclear Structure and Related Topics, Dubna Russia, July 17 2015

K. Morimoto "Synthesis of superheavy elements at RIKEN", The International Chemical Congress of PACIFIC BASIN SOCIETIES（PACIFICHEM 2015), Hawaii USA, December 19 2015

D. Kaji "Heavy element study using a new separator GARIS-II", The International Chemical Congress of PACIFIC BASIN SOCIETIES（PACIFICHEM 2015), Hawaii USA, December 19 2015

K. Morita, "SHE research at RIKEN/GARIS", The 9th Japan-China Joint Nuclear Physcs Symposium(JCNP2015), Osaka University Japan, Novermber 7-12 2015

K. Morita, "SHE research at RIKEN/GARIS", TAN15 Fukushima Japan, May 25-29 2015

K. Morita, "Research of superheavy element at RIKEN", LEAP2016, Kanazawa Japan, March 6-11 2016

[Domestic Conference]

D. Kaji, K. Morimoto, M. Haba, Y. Wakabayashi, M. Takeyama, S. Yamamoto, K. Tanaka, M. Huang, Y. Komori, J. Kanaya, M. Murakami, K. Katori, H. Hasebe, A. Yoneda, A. Yoshida, F. Tokanai, T. Yoshida, T. Yamaguchi, M. Asai, Z.Gan, L. Ma, H. Geissel, S. Hofmann, J. Maurer, K. Fujita, Y. Narikiyo, T. Tanaka, S. Yamamoto, K. Morita "GARIS を用いたホットフュージョン反応 ^{248}Cm+^{48}Ca→^{296}Lv*に関する研究", 第 59 回放射化学討論会, Tohoku University Japan, September 26 2015

T. Tanaka, K. Morita, K. Morimoto, D. Kaji, H. Haba, Y. Wakabayashi, Y. Komori, M. Takeyama, S. Yamaki, K. Tanaka, H. Hasebe, M. Huang, J. Kanaya, M. Murakami, A. Yoneda, A. Yoshida, T. Yamaguchi, F. Tokanai, Y. Yoshida, Z.Gan, L. Ma, H. Geissel, S. Hofmann, Y. Maurer, K. Fujita, Y. Narikiyo, S. Yamamoto, M. Asai, K. Katori "The reaction 48Ca+248Cm→296Lv* studied at the RIKEN-GARIS", JPS 2015 Autumn Meeting, Kansai University Japan, Septmeber 27 2015

T. Tanaka, Y. Narikiyo, K. Morita, K. Fujita, D. Kaji, K. Morimoto, S. Yamaki, Y. Wakabayashi, K. Tanaka, M. Takeyama, A. Yoneyama, H. Haba, Y. Komori, S. Yanou, B. J. P. Gall, Z. Asfari, H. Faure, H. Hasebe, M. Huang, J. Kanaya, M. Murakami, A. Yoshida, T. Yamaguchi, T. Tokanai, T. Yoshida, Z. Gan, L. Ma, H. Geissel, S. Hofmann, Y. Maurer, S. Yamamoto, Y. Yamano, K. Watanabe, S. Ishizawa, M. Asai, R. Aono, S. Goto, K. Katori "Study of barrier distribution in heavy reaction system at the RIKEN-GARIS", JPS 71th Annual Meeting (2016), Tohoku Gakuin University Japan, March 21 2016

R. Aono, S. Goto, D. Kaji, K. Morimoto, H. Haba, M. Murakami, K. Ooe, H. Kudo "Production of neutron-deficient rutherfordium isotopes in the Pb-208 + Ti-48,50 reactions", 2015 日本放射化学会年会・第 59 回放射化学討論会, Tohoku Univercity Japan, Septmeber 26 2015

Posters Presentations

[International Conference etc.]

M. Takeyama, D. Kaji, K. Morimoto, Y. Wakabayashi, F. Tokanai, K. Morita "Detector calibration to spontaneous fission for the study of superheavy elements using gas-filled recoil ion separator", International Symposium on Radiation Detectors and Their Uses (ISRD2016), Tsukuba Japan December 19 2015

RIBF Research Division
Nuclear Transmutation Data Research Group

1. Abstract

The disposal of high-level radioactive wastes from nuclear power plants is a problem considered to be one of the most important issues at both national and international levels. As a fundamental solution to the problem, the establishment of nuclear transmutation technology where long-lived nuclides can be changed to short-lived or stable ones will be vital. Progress in R & D in the transmutation of long-lived fission products (LLFP) in the nuclear wastes however, has been slow. Our group aims to obtain reaction data of LLFP at RIBF and other facilities which may lead to a new discovery and invention for peaceful use of nuclear power and the welfare of humanity.

2. Major Research Subjects

The Group is formed by three research teams. The first two Teams, “Fast RI Data Team” and “Slow RI Data Team”, are in charge of proton- and deuteron-induced reaction data of LLFP in inverse kinematics at RIBF. The third Team “Muon Data Team” is to obtain muon capture data of LLFP at muon facilities. All of the teams are focusing to obtain high-quality data which are essentially necessary to establish reliable reaction models. Each team has its own subjects and promotes LLFP reaction programs based on their large experiences, techniques and skills.

3. Summary of Research Activity

In 2014, all the teams polished up experimental strategies, formed collaboration and prepared experiments. Physics runs for spallation reaction were successfully organized at RIBF in 2015. The muon program started at J-PARC and RCNP, Osaka University in spring 2016.

Members

Group Director

Hiroyoshi SAKURAI (concurrent: Chief Scientist, RI Physics Lab.)

Assitant

Izumi YOSHIDA (Apr. 1, 2015 –)
Asako TAKAHASHI (Apr. 1, 2015 –)

RIBF Research Division
Nuclear Transmutation Data Research Group
Fast RI Data Team

1. Abstract

Fast RI team aims at obtaining and accumulating the cross section data for long lived fission products (LLFPs) in order to explore the possibility of using accelerator for nuclear transmutation.

LLFPs as nuclear waste have been generated continuously in nuclear power plants for wealth for human lives, while people noticed the way of disposal has not necessarily been established, especially after the Fukushima Daiichi power plant disaster. One of the ways to reduce the amount of LLFP or to recover them as recycled resources is nuclear transmutation technique.

RIBF facility has a property to generate such LLFP as a secondary beam and the beam species are identified by event by event. Utilizing the property, absolute values of the cross section of various reactions on LLFPs are measured and accumulated as database.

2. Major Research Subjects

1) Measurement of reaction products by the interaction of LLFPs with proton, deuteron, and photon to explore candidate reactions for transmutation of LLFPs.
2) Evaluation of the cross section data for the neutron induced reactions from the obtained data.

3. Summary of Research Activity

1) Acting as collaboration hub on many groups which plan to take data using fast RI beam in RIBF facility.
2) Concentrating on take data for proton and deuteron induced spallation reactions with inverse kinematics.
3) Accumulating the cross section data and evaluating them as evaluated nuclear data.
4) Evaluating cross section of neutron induced reaction on LLFP by collaborating with the nuclear model calculation and evaluation group.

Members

Team Leader

Hideaki OTSU (Oct. 1, 2014–, concurrent: Team Leader, SAMURAI Team)

Technical Staff I

Nobuyuki CHIGA (Jan. 1, 2015–)

Part-time Worker

Meiko Kurokara UESAKA (Apr. 1, 2015 – Jul. 26, 2015)

Student Trainees

Shouhei ARAKI (Kyushu Univ.)
Tatsuya YAMAMOTO (Miyazaki Univ.)
Keita NAKANO (Kyushu Univ.)
Ayaka IKEDA (Niigata Univ.)
Kazuya CHIKAATO (Niigata Univ.)
Hiroki TAKAHASHI (Niigata Univ.)
Kenji NISHIZUKA (Niigata Univ.)
Junki SUWA (Kyushu Univ.)
Masamichi AMANO (Rikkyo Univ.)
Junki AMANO (Rikkyo Univ.)

List of Publications & Presentations

Publications

[Journal]

(Original Papers)

H. Wang[a,*], H. Otsu[a], H. Sakurai[a], D.S. Ahn[a], M. Aikawa[b], P. Doornenbal[a], N. Fukuda[a], T. Isobe[a], S. Kawakami[c], S. Koyama[d], T. Kubo[a], S. Kubono[a], G. Lorusso[a], Y. Maeda[c], A. Makinaga[e], S. Momiyama[d], K. Nakano[f], M. Niikura[d], Y. Shiga[g,a], P.-A. Söderström[a], H. Suzuki[a], H. Takeda[a], S. Takeuchi[a], R. Taniuchi[d,a], Ya. Watanabe[a], Yu. Watanabe[f], H. Yamasaki[d], K. Yoshida[a], "Spallation reaction study for fission products in nuclear waste: Cross section measurements for ^{137}Cs and ^{90}Sr on proton and deuteron", Phys. Lett. B 754 (2016), 104-108.

Oral Presentations

[Domestic Conference]

川瀬頌一郎、陽子・重陽子に対する 100MeV/u ^{93}Zr 入射核破砕反応による同位体生成断面積の測定、日本物理学会秋季大会、大阪市立大学、2015 年 9 月 28 日

武内聡、107,108Pd のクーロン分解反応による光吸収断面積の測定、日本物理学会秋季大会、大阪市立大学、2015 年 9 月 28 日

四方瑞紀、93,94Zr のクーロン分解反応による光吸収断面積の測定、日本物理学会秋季大会、大阪市立大学、2015 年 9 月 28 日

尾崎友志、飛行核分裂によって生成された 107Pd のアイソマー比の測定、日本物理学会秋季大会、大阪市立大学、2015 年 9 月 28 日

川上駿介, 前田幸重, 王赫, 大津秀暁, 櫻井博義 他 22 名、"90Sr 近傍核種における荷電交換反応測定"、日本物理学会 2015 年秋季大会、

大阪市立大学、2015 年 9 月 28 日
中野敬太、水素・重水素に対する 100MeV/u ^{93}Zr 及び ^{93}Nb 入射核破砕反応の残留核生成断面積測定、日本原子力学会九州支部研究発表会、九州大学、2015 年 12 月 5 日
川上駿介, 前田幸重, 王赫, 大津秀暁, 櫻井博義　他 22 名、"90Sr 近傍の核分裂生成核種ビームによる荷電交換反応測定"、日本物理学会 2015 年九州支部例会、九州工業大学、2015 年 12 月 5 日
千賀信幸、相関陽子検出器の開発、平成 27 年度高エネルギー加速器研究機構技術研究会、KEK つくばキャンパス、平成 28 年 3 月 17 日
渡辺幸信、逆運動学手法を用いた陽子・重陽子による核破砕反応の残留核生成断面積測定 (1) 実験目的と概要、日本原子力学会春の大会、東北大学、2016 年 3 月 27 日
川瀬頌一郎、逆運動学手法を用いた陽子・重陽子による核破砕反応の残留核生成断面積測定 (2) 100 MeV/u ^{93}Zr入射反応、日本原子力学会春の大会、東北大学、2016 年 3 月 27 日
中野敬太、逆運動学手法を用いた陽子・重陽子による核破砕反応の残留核生成断面積測定 (3) 100 MeV/u ^{93}Nb 入射反応、日本原子力学会春の大会、東北大学、2016 年 3 月 27 日
武内聡、クーロン分解反応による 107,108Pd および 93,94Zr の光吸収断面積、日本物理学会年次大会、東北学院大学、2016 年 3 月 19 日
尾崎友志、238U の飛行核分裂によって生成される 107Pd,79Se のアイソマー比、日本物理学会年次大会、東北学院大学、2016 年 3 月 20 日

Posters Presentations

[Domestic Conference]

中野敬太、逆運動学的手法を用いた陽子･重陽子による核破砕反応の残留核生成断面積測定、日本原子力学会春の大会、東北大学、2016 年 3 月 27 日

RIBF Research Division
Nuclear Transmutation Data Research Group
Slow RI Data Team

1. Abstract

This team is in charge of the development of low-energy RI beams of long-lived fission fragments (LLFP) from the ^{238}U by means of degrading the energy of beams produced by the BigRIPS fragment separator.

2. Major Research Subjects

Studies of the energy degradation and purification of RI beams are the main subjects of the team. Developments of devices used for the energy degradation of RI beams are also an important subject.

3. Summary of Research Activity

1) Study and development of the energy degradation methods for LLFP.
2) Development of the devices used for the energy degradation.
3) Operation of the BigRIPS separator and supply the low energy LLFP beam to the experiment in which the cross sections of LLFP are measured at the low energy.

Members

Team Leader

Koichi YOSHIDA (concurrent: BigRIPS Team)

RIBF Research Division
Nuclear Transmutation Data Research Group
Muon Data Team

1. Abstract

Dr. Yoshio Nishina observed muons in cosmic rays in 1937. The muon is an elementary particle belonging to electron group, and is 207 times as heavy as electron. The muon has positive or negative electric charge, and the lifetime is 2.2 μsec. The negative muon is caught by a nucleus (atomic number: Z) in materials to form a muonic atom, and is then captured by the nucleus. The negative muon is combined with a proton to form a neutron and a neutrino to create an excited state of the nucleus with the atomic number of Z-1, followed by emissions of neutrons and gamma rays. The muon nuclear capture reaction produces the isotopes of the (Z-1) nucleus. However, the reaction mechanism is not yet well clarified. The research team aims at obtaining the experimental data to understand the mechanism of muon nuclear capture reactions as well as at establishing the reaction theory.

2. Major Research Subjects

(1) Experimental clarification on reaction mechanism of nuclear muon-capture
(2) Establishment of reaction theory on nuclear muon-capture
(3) Interdisciplinary applications of nuclear muon-capture reactions

3. Summary of Research Activity

Clarification of muon nuclear capture reaction and the application

Members

Team Leader
Teiichiro MATSUZAKI

RIBF Research Division
High-Intensity Accelerator R&D Group

1. Abstract

The R&D group, consisting of two teams, develops elemental technology of high-power accelerators and high-power targets, aiming at future applications to nuclear transmutations of long-lived fission product into short-lived nuclides. The research subjects are superconducting rf cavities for low-velocity ions, design of high-power accelerators, high-power target systems and related technologies.

2. Major Research Subjects

(1) R&D of elemental technology of high-power accelerators and high-power targets

3. Summary of Research Activity

(1) Based on the discussion with other research groups, R&D study of various accelerator components and elements is under progress.

Members

Group Director

Osamu KAMIGAITO (concurrent: Chief Scientist, Group Director, Accelerator Gr.)

RIBF Research Division
High-Intensity Accelerator R&D Group
High-Gradient Cavity R&D Team

Abstract

We develop new components for accelerators dedicated for low-beta-ions with very high intensity. Specifically, we are designing and constructing a cryomodule for superconducting linac efficient for acceleration of low-beta-ions. In parallel, we try to optimize an rf acceleration system by making computer simulations for acceleration of very high intensity beams.

Major Research Subjects

-Development of high-gradient cavites for low beta ions
-Development of power saving cryomodules

Summary of Research Activity

Development of highly efficient superconducting accelerator modules

Members

Team Leader

Naruhiko SAKAMOTO (concurrent: Cyclotron Team)

Research & Technical Scientists

Kazunari YAMADA (concurrent: Senior Technical Scientist, Beam Dynamics & Diagnostics Team)
Kazutaka OHZEKI (concurrent: Technical Scientist, Cyclotron Team)
Yutaka WATANABE (concurrent: Senior Technical Scientist, RILAC team)

Nishina Center Research Scientist

Kenji SUDA (concurrent: Cyclotron Team)

List of Publications & Presentations

Publications

[Proceedings]

Naruhiko Sakamoto et al., Design Studies for Quarter-Wave Resonators and Cryomodules for the RIKEN SC-LINAC, Proceedings of the 17th International Conference on RF Superconductivity, Whistler, September 16 2015.
Kazutaka Ozeki et al., Design of Input Coupler for RIKEN Superconducting Quarter-Wave Resonator, Proceedings of the 17th International Conference on RF Superconductivity, Whistler, September 16 2015.
Kazutaka Ozeki et al., Heat flow estimation of the cryomodule for superconducting quarter-wavelength resonator, Proceedings of the 12th Annual Meeting of Particle Accelerator Society of Japan, Suruga, 6 August 2015.

Oral Presentations

[International Conference etc.]

Naruhiko Sakamoto et al., Design Studies for Quarter-Wave Resonators and Cryomodules for the RIKEN SC-LINAC, 17th International Conference on RF Superconductivity, Whistler, September 16 2015.
Kazutaka Ozeki et al., Design of Input Coupler for RIKEN Superconducting Quarter-Wave Resonator , TESLA Technology Collaboration Meeting, Menlo Park, USA, December 2, 2015.

Posters Presentations

[International Conference etc.]

Kazutaka Ozeki et al., Design of Input Coupler for RIKEN Superconducting Quarter-Wave Resonator, 17th International Conference on RF Superconductivity, Whistler, September 16 2015.

[Domestic Conference]

Kazutaka Ozeki et al., Heat flow estimation of the cryomodule for superconducting quarter-wavelength resonator, 12th Annual Meeting of Particle Accelerator Society of Japan, Suruga, 6 August 2015.

RIBF Research Division
High-Intensity Accelerator R&D Group
High-Power Target R&D Team

1. Abstract

The subjects of this team cover R&D studies with respect to target technology for the transmutation of the LLFPs.

2. Major Research Subjects

(1) Liquid lithium target for production of neutron or muon
(2) beam window without solid structure

3. Summary of Research Activity

(1) Liquid lithium target for production of neutron or muon
(H. Okuno, N. Ikoma)
(2) beam window with solid structure
(H. Imao, N. Ikoma)

Members

Team Leader

Hiroki OKUNO (concurrent: Deputy Group Director, Accelerator Gr.)

Research and Technical Scientist

Kanenobu TANAKA (concurrent: Deputy Group Director, Safety Management Group)
Hiroshi IMAO (concurrent: Senior Research Scientist,Accelerator R&D Team)
Takashi NAGATOMO (concurrent: Technical Scientist, Ion Source Team)

Part-time Worker

Noya IKOMA (Sep. 1, 2015 -)

RIBF Research Division
Accelerator Group

1. Abstract

The accelerator group, consisting of seven teams, pursues various upgrade programs of the world-leading heavy-ion accelerator facility, RI-Beam Factory (RIBF), to enhance the accelerator performance and operation efficiency. The programs include the R&D of superconducting ECR ion source, charge stripping systems, beam diagnostic devices, radiofrequency systems, control systems, and beam simulation studies. We are also maintaining the large infrastructure to realize effective operation of the RIBF, and are actively promoting the applications of the facility to a variety of research fields.

Our primary mission is to supply intense, stable heavy-ion beams for the users through effective operation, maintenance, and upgrade of the RIBF accelerators and related infrastructure. The director members shown below govern the development programs that are not dealt with by a single group, such as intensity upgrade and effective operation. We also promote the future plans of the RIBF accelerators along with other laboratories belonging to the RIBF research division.

2. Major Research Subjects

(1) Intensity upgrade of RIBF accelerators (Okuno)
(2) Effective and stable operation of RIBF accelerators (Fukunishi)
(3) Operation and maintenance of infrastructures for RIBF (Kase)
(4) Promotion of the future plan (Kamigaito, Fukunishi, Okuno)

3. Summary of Activity

(1) The maximum intensity of the calcium beam reached 689 pnA at 345 MeV/u, which corresponds to 10.4 kW. That of the krypton beam reached 486 pnA, corresponding to 13.4 kW.
(2) The maximum intensities of the uranium and xenon beams reached 49 and 102 pnA, respectively, at 345 MeV/u.
(3) The overall beam availability for the RIBF experiments in 2015 reached 92 %. It has been kept above 90 % since 2014.
(4) The large infrastructure was properly maintained based on a well-organized cooperation among the related sections.
(5) An intensity-upgrade plan of the RIBF has been further investigated, mainly on the design of a new superconducting linac.

Members

Group Director
Osamu KAMIGAITO

Deputy Group Directors
Hiroki OKUNO (Intensity upgrade)
Nobuhisa FUKUNISHI (Stable and efficient operation)
Masayuki KASE (Energy-efficiency management)

Research Consultant
Tadashi FUJINAWA

International Program Associate
Vasileios TZOGANIS (Univ. of Liverpool, – Jan. 15, 2016)

Visiting Researchers
Akira GOTO (Yamagata Univ.)
Toshiyuki HATTORI (TIT)
Kensei UMEMORI (KEK)
Hirotaka NAKAI (KEK)
Eiji KAKO (KEK)

Assistant
Karen SAKUMA

RIBF Research Division
Accelerator Group
Accelerator R&D Team

1. Abstract

We are developing the key hardware in upgrading the RIBF accelerator complex. Our primary focus and research is charge stripper which plays an essential role in the RIBF accelerator complex. Charge strippers remove many electrons in ions and realize efficient acceleration of heavy ions by greatly enhancing charge state. The intensity of uranium beams is limited by the lifetime of the carbon foil stripper conventionally installed in the acceleration chain. The improvement of stripper lifetimes is essential to increase beam power towards the final goal of RIBF in the future. We are developing the low-Z gas stripper. In general gas stripper is free from the lifetime related problems but gives low equilibrium charge state because of the lack of density effect. Low-Z gas stripper, however, can give as high equilibrium charge state as that in carbon foil because of the suppression of the electron capture process. Another our focus is the upgrade of the world's first superconducting ring cyclotron.

2. Major Research Subjects

(1) Development of charge strippers for high power beams (foil, low-Z gas)
(2) Upgrade of the superconducting ring cyclotron
(3) Maintenance and R&D of the electrostatic deflection/inflection channels for the beam extraction/injection

3. Summary of Research Activity

(1) Development of charge strippers for high power beams (foil, low-Z gas)

(Hasebe, H., Imao, H. Okuno., H.)

We are developing the charge strippers for high intensity heavy ion beams. We are focusing on the developments on carbon or berrilium foils and gas strippers including He gas stripper.

(2) Upgrade of the superconducting ring cyclotron

(Ohnishi, J., Okuno, H.)

We are focusing on the upgrade of the superconducting ring cyclotron.

(3) Maintenance and R&D of the electrostatic deflection/inflection channels for the beam extraction/injection

(Ohnishi, J., Okuno, H.)

We are developing high-performance electrostatic channels for high power beam injection and extraction.

Members

Team Leader

Hiroki OKUNO (concurrent: Deputy Group Director, Accelerator Gr.)

Research & Technical Scientists

Hiroshi IMAO (Senior Research Scientist)
Jun-ichi OHNISHI (Senior Technical Scientist)

Nishina Center Technical Scientist

Hiroo HASEBE

Visiting Scientists

Andreas ADELMANN (PSI)
Noriyosu HAYASHIZAKI (TIT.)
Hironori KUBOKI (KEK)

Student Trainee

Naoya IKOMA (Nagaoka Univ. of Technology)

List of Publications & Presentations

Publications

[Journal]

(Original Papers) *Subject to Peer Review

H. Hasebe, H. Okuno, H. Kuboki, H. Imao, N. Fukunishi, M. Kase, O. Kamigaito, “Development of rotating beryllium disk stripper”, Journal of .Radioanalytical and Nuclear Chemistry, 305, 825 (2015).

[Proceedings]

(Original Papers) *Subject to Peer Review

H. Hasebe, H. Okuno, H. Kuboki, H. Imao, N. Fukunishi, M. Kase, O. Kamigaito, “History of Solid Disk Improvement for Rotating Charge Stripper”, Proceeding of HIAT2015, Yokohama, Japan (2015) MOA1C01.

Oral Presentations

[International Conference etc.]

H. Hasebe, H. Okuno, H. Kuboki, H. Imao, N. Fukunishi, M. Kase, O. Kamigaito, “History of Solid Disk Improvement for Rotating Charge Stripper”, HIAT2015, Yokohama, Japan (2015) MOA1C01.

Posters Presentations

[International Conference etc.]

H. Imao, H. Kuboki, H. Hasebe, O. Kamigaito, M. Kase, H. Okuno, “Operation of Gas Strippers at RIBF ; Thining Effect of High-Intensity Very Heavy Ion Beams“ , HIAT2015, Yokohama, Japan (2015) MOPA32.

RIBF Research Division
Accelerator Group
Ion Source Team

1. Abstract

Our aim is to operate and develop the ECR ion sources for the accelerator-complex system of the RI Beam Factory. We focus on further upgrading the performance of the RI Beam Factory through the design and fabrication of a superconducting ECR ion source for production of high-intensity uranium ions.

2. Major Research Subjects

(1) Operation and development of the ECR ion sources
(2) Development of a superconducting ECR heavy-ion source for production of high-intensity uranium ion beams

3. Summary of Research Activity

(1) Operation and development of ECR ion sources

(T. Nakagawa, M. Kidera, Y. Higurashi, T. Nagatomo, and H. Haba)

We routinely produce and supply various kinds of heavy ions such as zinc and calcium ions for the super-heavy element search experiment as well as uranium ions for RIBF experiments. We also perform R&D's to meet the requirements for stable supply of high-intensity heavy ion beams.

(2) Development of a superconducting ECR ion source for use in production of a high-intensity uranium ion beam

(T. Nakagawa, J. Ohnishi, M. Kidera, Y. Higurashi, and T. Nagatomo)

The RIBF is required to supply uranium ion beams with very high intensity so as to produce RI's. We have designed and are fabricating an ECR ion source with high magnetic field and high microwave- frequency, since the existing ECR ion sources have their limits in beam intensity. The coils of this ion source are designed to be superconducting for the production of high magnetic field. We are also designing the low-energy beam transport line of the superconducting ECR ion source.

Members

Team Leader
Takahide NAKAGAWA

Research & Technical Scientist
Takashi NAGATOMO (Technical Scientist)

Nishina Center Research Scientists
Masanori KIDERA, Yoshihide HIGURASHI

Special Postdoctoral Researcher
Tatsuya URABE (Apr. 1, 2014 –)

Research Consultant
Tadashi KAGEYAMA (Apr. 1, 2014 – Mar. 31, 2015)

Part-time Worker
Yumi KURAMITSU (–Jun. 30, 2015)

List of Publications & Presentations

Publications

[Journal]

(Original Papers) *Subject to Peer Review

K. Ozeki, Y. Higurashi, M. Kidera and T. Nakagawa, 'Effect of hot liner in producing ^{40,48}Ca beam from RIKEN 18-GHz electron cyclotron resonance ion source', Rev. Sci. Instrum. 86(2015)016114*

[Proceedings]

(Original Papers) *Subject to Peer Review

A.Uchiyama, K. Ozeki, Y. Higurashi, M. Kidera, M. Komiyama, and T. Nakagawa, 'Control system renewal for efficient operation in RIKEN 18 GHz electron cyclotron resonance ion source', Rev. Sci. Instrum. 87(2016)02A722*

J. Ohnishi, Y. Higurashi, T. Nakagawa, 'Progress in high-temperature oven development for 28 GHz electron cyclotron resonance ion source', Rev. Sci. Instrum. 87(2016)02A709*

Oral Presentations

[International Conference etc.]

T. Nakagawa, 'Recent developments of RIKEN 28GHz SC-ECRIS', 21st Int. Workshop on ECR ion sources, August 24-28, 2014, Nizhny Novgorod, Russia

Y. Higurashi, 'Emittance measurement for RIKEN 28 GHz SC-ECRIS', 21st Int. Workshop on ECR ion sources, August 24-28, 2014, Nizhny Novgorod, Russia

T. Nakagawa, 'Further improvement of RIKEN 28GHz SC-ECRIS for production of intense U beam', ICIS2015, Aug. 23-28, 2015, New York, USA

Y. Higurashi, 'Emittance measurement for RIKEN 28GHz SC-ECRIS' ICIS2015, Aug. 23-28, 2015, New York, USA

[Domestic Conference]

T. Nakagawa, 'Development of ECR ion sources for production of the intense beam of highly charged heavy ions', 12th Annual Meeting of PASJ, Aug. 5-8, 2015, Tsuruga,

Posters Presentations

[International Conference etc.]

T. Nagatomo, 'Development of an in-situ emittance meter installed in LEBT following 18-GHz Superconducting ECR Ion Source', 21st Int. Workshop on ECR ion sources, August 24-28, 2014, Nizhny Novgorod, Russia

[Domestic Conference]

K. Ozeki, 'Installation of new 18-GHz ECR ion source for the RIKEN RILAC', 11th Annual Meeting of PASJ, Aug. 9-11, 2014, Aomori,

T. Nagatomo, 'Development of the on-line beam monitor based on the pepper-pot method for high-brightness low-energy multi-charged ion beams extracted from ECR ion source', 12th Annual Meeting of PASJ, Aug. 5-8, 2015, Tsuruga,

RIBF Research Division
Accelerator Group
RILAC Team

1. Abstract

The operation and maintenance of the RIKEN Heavy-ion Linac (RILAC) have been carried out. There are two operation modes: one is the stand-alone mode operation and the other is the injection mode operation. The RILAC has been used especially as an injector for the RIKEN RI- Beam Factory accelerator complex. The RILAC is composed of the ECR ion source, the frequency-variable RFQ linac, six frequency-variable main linac cavities, and six energy booster cavities (CSM).

2. Major Research Subjects

(1) The long term high stability of the RILAC operation.
(2) Improvement of high efficiency of the RILAC operation.

3. Summary of Research Activity

The RILAC was started to supply ion beams for experiments in 1981. Thousands hours are spent in a year for delivering many kinds of heavy-ion beams to various experiments.

The RILAC has two operation modes: one is the stand-alone mode operation delivering low-energy beams directly to experiments and the other is the injection mode operation injecting beams into the RRC. In the first mode, the RILAC supplies a very important beam to the nuclear physics experiment of “the research of super heavy elements”. In the second mode, the RILAC plays a very important role as upstream end of the RIBF accelerator complex.

The maintenance of these devices is extremely important in order to keep the log-term high stability and high efficiency of the RILAC beams. Therefore, improvements are always carried out for the purpose of more stable and more efficient operation.

Members

Team Leader
Eiji IKEZAWA

Research & Technical Scientist
Yutaka WATANABE (Senior Technical Scientist)

Research Consultants
Masatake HEMMI
Toshiya CHIBA

RIBF Research Division
Accelerator Group
Cyclotron Team

1. Abstract

Together with other teams of Nishina Center accelerator division, maintaining and improving the RIBF cyclotron complex. The accelerator provides high intensity heavy ions. Our mission is to have stable operation of cyclotrons for high power beam operation. Recently stabilization of the rf system is a key issue to provide 10 kW heavy ion beam.

2. Major Research Subjects

(1) RF technology for Cyclotrons
(2) Operation of RIBF cyclotron complex
(3) Maintenance and improvement of RIBF cyclotrons
(4) Single turn operation for polarized deuteron beams
(5) Development of superconducting cavity

3. Summary of Research Activity

・Development of the rf system for a reliable operation
・Development of highly stabilized low level rf system
・Development of superconducting rebuncher cavity
・Development of the intermediate-energy polarized deuteron beams.

Members

Team Leader
Naruhiko SAKAMOTO

Research & Technical Scientist
Kazutaka OHZEKI (Technical Scientist)

Nishina Center Research Scientist
Kenji SUDA

List of Publications & Presentations

Publications

[Journal]

(Original Papers) *Subject to Peer Review

R. Koyama, N. Sakamoto, M. Fujimaki, N. Fukunishi, A. Goto, M. Hemmi, M. Kase, K. Suda, T. Watanabe, K. Yamada, O. Kamigaito, “Online monitoring of beam phase and intensity using lock-in amplifiers”, Nuclear Instruments and Methods A729(2013)p788-799.

K. Suda, N. Sakamoto, K. Yamada, S. Arai, Y. Chiba, M. Kase, H. Okuno, Y. Watanabe, O. Kamigaito, “Design and construction of drift tube linac cavities for RIKEN RI-Beam Factory”, Nuclear Instruments and Methods A722(2013)p55-64.

K. Sekiguchi, H. Okamura, N. Sakamoto, H. Suzuki, M. Dozono, Y. Maeda, T. Saito, S. Sakaguchi, H. Sakai, M. Sasano, Y. Shimizu, T. Wakasa, K. Yako, H. Witala, W. Glockle, J. Golak, H. Kamada, and A. Nogga, “Three Nucleon Force Effects in Intermediate Energy Deuteron Analyzing Powers for dp Elastic Scattering”, Physical Review C **83**, 061001(R) (2011).

[Proceedings]

(Original Papers) *Subject to Peer Review

N. Sakamoto, O. Kamigaito, H. Okuno, K. Ozeki, K. Suda, Y. Watanabe, K. Yamada, H. Hara, K.Okihira, K. Sennyu, T. Yanagisawa, E. Kako, H. Nakai, K. Umemori, “Design Studies for Quarter-Wave Resonators and Cryomodules for the RIKEN SC-LINAC”, Proceedings of the 17th International Conference on RF Superconductivity, Whistler(2015)p976, WEBA06.

K. Suda, M. Nishida, S. Fukuzawa, M. Hamanaka, S. Ishikawa, K. Kobayashi, R. Koyama, T. Nakamura, M. Nishimura, J. Shibata, N. Tsukiori, K. Yadomi, Y. Kotaka, T. Dantsuka, M. Fujimaki, N. Fukunishi, T. Fujinawa, H. Hasebe, Y. Higurashi, E. Ikezawa, H. Imao, M. Kase, T. Kageyama, O. Kamigaito, M. Kidera, K. Kumagai, M. Komiyama, T. Maie, M. Nagase, T. Nakagawa, M. Nakamura, J. Ohnishi, H. Okuno, K. Ozeki, N. Sakamoto, A. Uchiyama, T. Watanabe, Y. Watanabe, S. Watanabe, K. Yamada, H. Yamasawa, “Status Report of the Operation of the RIKEN Ring Cyclotrons”, Proceedings of the 13th International Conference on Heavy Ion Accelerator Technology, Yokohama(2015)p65, MOPA12.

K. Ozeki, T. Nakamura, S. Ishikawa, K. Kobayashi, R. Koyama, J. Shibata, N. Tsukiori, M. Nishida, M. Nishimura, M. Hamanaka, S. Fukuzawa, K. Yadomi, K. Suda, A. Uchiyama, H. Okuno, T. Kageyama, M. Kase, O. Kamigaito, K. Kumagai, M. Komiyama, N. Sakamoto, T. Nakagawa, M. Nagase, T. Nagatomo, N. Fukunishi, M. Fujimaki, T. Maie, K. Yamada, T. Watanabe, Y. Watanabe, S. Yamaka, Y. Ohshiro, and Y. Kotaka, “Status Report of the Operation of RIKEN AVF Cyclotron”, Proceedings of the 13th International Conference on Heavy Ion Accelerator Technology, Yokohama(2015)p191, WEPB01.

M. Nishida, S. Fukuzawa, M. Hamanaka, S. Ishikawa, K. Kobayashi, R. Koyama, T. Nakamura, M. Nishimura, J. Shibata, N. Tsukiori, K. Yadomi, Y. Kotaka, T. Dantsuka, M. Fujimaki, N. Fukunishi, T. Fujinawa, H. Hasebe, Y. Higurashi, E. Ikezawa, H. Imao, M. Kase, T. Kageyama, O. Kamigaito, M. Kidera, K. Kumagai, M. Komiyama, T. Maie, M. Nagase, T. Nakagawa, M. Nakamura, J. Ohnishi, H. Okuno, K. Ozeki, N. Sakamoto, K. Suda, A. Uchiyama, T. Watanabe, Y. Watanabe, S. Watanabe, K. Yamada, H. Yamasawa, “Status Report of the Operation of the RIKEN Ring Cyclotrons”, Proceedings of the 12th annual meeting of Particle Accelerator Society of Japan, Suruga(2015)p276, FSP003.

K. Suda, E. Ikezawa, O. Kamigaito, N. Sakamoto, K. Yamada, Y. Touchi, “Construction of the New Amplifieres for the RIKEN-LINAC”, Proceedings of the 27th International Linear Accelerator Conference, Geneva(2014)p339, MOPP122.

N. Sakamoto, M. Fujimaki, N. Fukunishi, Y. Higurashi, O. Kamigaito, H. Okuno, K. Suda, T. Watanabe, Y. Watanabe, K. Yamada, R. Koyama, “Performance of New Injector RILAC2 for RIKEN RI-Beam Factory”, Proceedings of the 27th International Linear Accelerator Conference, Geneva(2014)p1123, THPP116.

T. Nakamura, S. Ishikawa, K. Kobayashi, R. Koyama, J. Shibata, N. Tsukiori, M. Nishida, M. Nishimura, M. Hamanaka, S. Fukuzawa, K. Yadomi, K. Suda, A. Uchiyama, K. Ozeki, H. Okuno, T. Kageyama, M. Kase, O. Kamigaito, K. Kumagai, M. Komiyama, N. Sakamoto, T. Nakagawa, M. Nagase, T. Nagatomo, N. Fukunishi, M. Fujimaki, T. Maie, K. Yamada, T. Watanabe, Y. Watanabe, S. Yamaka, Y. Ohshiro, and Y. Kotaka, “Status Report of the Operation of RIKEN AVF Cyclotron”, Proceedings of the 12th annual meeting of Particle Accelerator Society of Japan, Suruga(2015)p305, FSP011.

L. Lu, O. Kamigaito, N. Sakamoto, K. Suda, and K. Yamada, “Design of a Triple-Spoke Cavity as a Rebuncher for RIKEN RI-Beam Factory”, Proc the 16th International Conference on RF Superconductivity, Paris (2013).

N. Sakamoto, M. Fujimaki, H. Hasebe, Y. Higurashi, O. Kamigaito, H. Okuno, K. Suda, T. Watanabe, and K. Yamada, “Commissioning of a New Injector for the RIKEN RI-Beam Factory”, the XXVI Linear Accelerator Conference, Tel-Aviv(2012)p125-129.

N. Sakamoto, T. Dantsuka, T. Fujinawa, N. Fukunishik H. Hasebe, Y. Higurashi, K. Ikegami, E. Ikezawa, H. Imao, T. Kageyama, O. Kamigaito, M. Kase, M. Kidera, M. Komiyama, H. Kuboki, K. Kumagai, T. Maie, M. Nagase, T. Nakagawa, M. Nakamura, H. Okuno, J. Ohnishi, K. Suda, H. Watanabe, T. Watanabe, Y. Watanabe, K. Yamada, L. Lu, H. Yamasawa, K. Ozeki, “High intensity heavy-ion-beam operation of RIKEN RIBF”, Proc. the 9th Annual Meeting of Particle Accelerator Society Japan, Toyonaka (2012)p7-11.

K. Suda, M. Fujimaki, N. Fukunishi, H. Hemmi, O. Kamigaito, M. Kase, R. Koyama, K. Kumagai, N. Sakamoto, T. Watanabe, and K. Yamada, “Stable Operation of RF Systems for RIBF”, Proc. the 19th International Conference on Cyclotrons and Their Applications, Lanzhou, China (2010).

N. Sakamoto, M. Fujimaki, A. Goto, O. Kamigaito, M. Kase, R. Koyama, K.Suda, K. Yamada, and S. Yokouchi, “Operating Experience with the RF System for Superconducting Ring Cyclotron of RIBF”, Proc. the 19th International Conference on Cyclotrons and Their Applications, Lanzhou, China (2010)p338-340.

N. Sakamoto, M. Fujimaki, A. Goto, M. Kase, O. Kamigaito, K. Suda, K. Yamada, and S. Yokouchi, “RF system for Heavy Ion Cyclotrons at RIKEN RIBF”, Proc. the 11th International Conference on Heavy Ion Accelerator Technology, Venezia, Italy (2009)p69-73.

N. Sakamoto, O. Kamigaito, S. Kohara, H. Okuno, M. Kase, A. Goto, and Y. Yano, “RF system for the RIBF Superconducting Ring Cyclotron”, Proc. the 18th International Conference on Cyclotrons and Their Applications, Giardini-Naxos, Italy (2007), p455-457.

Oral Presentations

[International Conference etc.]

N. Sakamoto, O. Kamigaito, H. Okuno, K. Ozeki, K. Suda, Y. Watanabe, K. Yamada, H. Hara, K.Okihira, K. Sennyu, T. Yanagisawa, E. Kako, H. Nakai, K. Umemori, “Design Studies for Quarter-Wave Resonators and Cryomodules for the RIKEN SC-LINAC”, Proceedings of the 17th International Conference on RF Superconductivity, Whistler(2015)p976, WEBA06.

N. Sakamoto, “Present Performance of the RF Systems fo the RIBF Accelerator Complex and their Upgrade plans”, Workshop on Science with Rare Ion Beams (SCRIBE-2014), Kolkata(2014).

N. Sakamoto, M. Fujimaki, H. Hasebe, Y. Higurashi, O. Kamigaito, H. Okuno, K. Suda, T. Watanabe, and K. Yamada, “Commissioning of a New Injector for the RIKEN RI-Beam Factory”, the XXVI Linear Accelerator Conference, Tel-Aviv(2012)p125-129.

K. Suda, M. Fujimaki, N. Fukunishi, H. Hemmi, O. Kamigaito, M. Kase, R. Koyama, K. Kumagai, N. Sakamoto, T. Watanabe, and K. Yamada, “Stable Operation of RF Systems for RIBF”, Proc. the 19th International Conference on Cyclotrons and Their Applications, Lanzhou, China (2010).

N. Sakamoto, M. Fujimaki, A. Goto, O. Kamigaito, M. Kase, R. Koyama, K.Suda, K. Yamada, and S. Yokouchi, “Operating Experience with the RF System for Superconducting Ring Cyclotron of RIBF”, Proc. the 19th International Conference on Cyclotrons and Their Applications, Lanzhou, China (2010)p338-340.

N. Sakamoto, M. Fujimaki, A. Goto, M. Kase, O. Kamigaito, K. Suda, K. Yamada, and S. Yokouchi, “RF system for Heavy Ion Cyclotrons at RIKEN RIBF”, Proc. the 11th International Conference on Heavy Ion Accelerator Technology, Venezia, Italy (2009)p69-73.

[Domestic Conference]

N. Sakamoto, T. Dantsuka, T. Fujinawa, N. Fukunishik H. Hasebe, Y. Higurashi, K. Ikegami, E. Ikezawa, H. Imao, T. Kageyama, O. Kamigaito, M. Kase, M. Kidera, M. Komiyama, H. Kuboki, K. Kumagai, T. Maie, M. Nagase, T. Nakagawa, M. Nakamura, H. Okuno, J. Ohnishi, K. Suda, H. Watanabe, T. Watanabe, Y. Watanabe, K. Yamada, L. Lu, H. Yamasawa, K. Ozeki, “High intensity heavy-ion-beam operation of RIKEN RIBF”, Proc. the 9th Annual Meeting of Particle Accelerator Society Japan, Toyonaka (2012)p7-11.

Posters Presentations

[International Conference etc.]

K. Suda, M. Nishida, S. Fukuzawa, M. Hamanaka, S. Ishikawa, K. Kobayashi, R. Koyama, T. Nakamura, M. Nishimura, J. Shibata, N. Tsukiori, K. Yadomi, Y. Kotaka, T. Dantsuka, M. Fujimaki, N. Fukunishi, T. Fujinawa, H. Hasebe, Y. Higurashi, E. Ikezawa, H. Imao, M. Kase, T. Kageyama, O. Kamigaito, M. Kidera, K. Kumagai, M. Komiyama, T. Maie, M. Nagase, T. Nakagawa, M. Nakamura, J. Ohnishi, H. Okuno, K. Ozeki, N. Sakamoto, A. Uchiyama, T. Watanabe, Y. Watanabe, S. Watanabe, K. Yamada, H. Yamasawa, “Status Report of the Operation of the RIKEN Ring Cyclotrons”, 13th International Conference on Heavy Ion Accelerator Technology, Yokohama(2015)p65, MOPA12.

K. Ozeki, T. Nakamura, S. Ishikawa, K. Kobayashi, R. Koyama, J. Shibata, N. Tsukiori, M. Nishida, M. Nishimura, M. Hamanaka, S. Fukuzawa, K. Yadomi, K. Suda, A. Uchiyama, H. Okuno, T. Kageyama, M. Kase, O. Kamigaito, K. Kumagai, M. Komiyama, N. Sakamoto,

T. Nakagawa, M. Nagase, T. Nagatomo, N. Fukunishi, M. Fujimaki, T. Maie, K. Yamada, T. Watanabe, Y. Watanabe, S. Yamaka, Y. Ohshiro, and Y. Kotaka, “Status Report of the Operation of RIKEN AVF Cyclotron”, 13th International Conference on Heavy Ion Accelerator Technology, Yokohama(2015)p191, WEPB01.

L. Lu, O. Kamigaito, N. Sakamoto, K. Suda, and K. Yamada, “Design of a Triple-Spoke Cavity as a Rebuncher for RIKEN RI-Beam Factory”, Proc the 16th International Conference on RF Superconductivity, Paris (2013).

K. Suda, M. Fujimaki, N. Fukunishi, H. Hemmi, O. Kamigaito, M. Kase, R. Koyama, K. Kumagai, N. Sakamoto, T. Watanabe, and K. Yamada, “Stable Operation of RF Systems for RIBF”, 19th International Conference on Cyclotrons and Their Applications, Lanzhou, China (2010).

N. Sakamoto, O. Kamigaito, S. Kohara, H. Okuno, M. Kase, A. Goto, and Y. Yano, “RF system for the RIBF Superconducting Ring Cyclotron”, 18th International Conference on Cyclotrons and Their Applications, Giardini-Naxos, Italy (2007), p455-457.

[Domestic Conference]

M. Nishida, S. Fukuzawa, M. Hamanaka, S. Ishikawa, K. Kobayashi, R. Koyama, T. Nakamura, M. Nishimura, J. Shibata, N. Tsukiori, K. Yadomi, Y. Kotaka, T. Dantsuka, M. Fujimaki, N. Fukunishi, T. Fujinawa, H. Hasebe, Y. Higurashi, E. Ikezawa, H. Imao, M. Kase, T. Kageyama, O. Kamigaito, M. Kidera, K. Kumagai, M. Komiyama, T. Maie, M. Nagase, T. Nakagawa, M. Nakamura, J. Ohnishi, H. Okuno, K. Ozeki, N. Sakamoto, K. Suda, A. Uchiyama, T. Watanabe, Y. Watanabe, S. Watanabe, K. Yamada, H. Yamasawa, “Status Report of the Operation of the RIKEN Ring Cyclotrons”, 12th annual meeting of Particle Accelerator Society of Japan, Suruga(2015)p276, FSP003.

T. Nakamura, S. Ishikawa, K. Kobayashi, R. Koyama, J. Shibata, N. Tsukiori, M. Nishida, M. Nishimura, M. Hamanaka, S. Fukuzawa, K. Yadomi, K. Suda, A. Uchiyama, K. Ozeki, H. Okuno, T. Kageyama, M. Kase, O. Kamigaito, K. Kumagai, M. Komiyama, N. Sakamoto, T. Nakagawa, M. Nagase, T. Nagatomo, N. Fukunishi, M. Fujimaki, T. Maie, K. Yamada, T. Watanabe, Y. Watanabe, S. Yamaka, Y. Ohshiro, and Y. Kotaka, “Status Report of the Operation of RIKEN AVF Cyclotron”, 12th annual meeting of Particle Accelerator Society of Japan, Suruga(2015)p305, FSP011.

S. Fukuzawa, M. Hamanaka, S. Ishikawa, Y. Kotaka, K. Kobayashi, R. Koyama, T. Nakamura, M. Nishida, M. Nishimura, J. Shibata, N. Tsukiori, K. Yadomi, K. Suda, T. Dantsuka, M. Fujimaki, N. Fukunishi, T. Fujinawa, H. Hasebe, Y. Higurashi, E. Ikezawa, H. Imao, M. Kase, T. Kageyama, O. Kamigaito, M. Kidara, K. Kumagai, H. Kuboki, M. Komiyama, T. Maie, M. Nagase, T. Nakagawa, M. Nakamura, J. Ohnishi, H. Okuno, K. Ozeki, N. Sakamoto, A. Uchiyama, T. Watanabe, Y. Watanabe, S. Watanabe, K. Yamada, and H. Yamasawa, “Status Report of the Operation of the RIBF Ring Cyclotrons”, 11th annual meeting of Particle Accelerator Society of Japan, Aomori(2014)p401, FSP024.

Y. Kotaka, S. Ishikawa, K. Kobayashi, R. Koyama, J. Shibata, N. Tsukiori, T. Nakamura, M. Nishida, M. Nishimura, M. Hamanaka, S. Fukuzawa, K. Yadomi, N. Sakamoto, A. Uchiyama, H. Okuno, T. Kageyama, M. Kase, O. Kamigaito, K. Kumagai, M. Komiyama, K. Suda, T. Nakagawa, M. Nagase, T. Nagatomo, N. Fukunishi, M. Fujimaki, T. Maie, K. Yamada, T. Watanabe, Y. Watanabe, S. Yamaga, and Y. Oshiro, “Status Report of the Operation of the RIKEN AVF Cyclotron”, 11th annual meeting of Particle Accelerator Society of Japan, Aomori(2015)p364, FSP015.

RIBF Research Division
Accelerator Group
Beam Dynamics & Diagnostics Team

1. Abstract

The cascaded cyclotron system at RIKEN RI Beam Factory (RIBF) requires not only strict matching of operation parameters but also high stability of all the accelerator components in order to establish stable operation of the world's most intense heavy-ion beams. Beam Dynamics and Diagnostics Team is responsible for power supplies, beam instrumentation, computer control and beam dynamic of the RIBF accelerator complex and strongly contributes to the performance upgrade of the RIBF.

2. Major Research Subjects

(1) Extracting the best performance of the RIBF accelerator complex based on the precise beam dynamics study.
(2) Maintenance and developments of the beam instrumentation, especially non-destructive monitors.
(3) Upgrade of the computer control system of the RIBF accelerator complex.
(4) Maintenance and improvements of the magnets and power supplies.
(5) Upgrade of the existing beam interlock system for higher intensity beams.

3. Summary of Research Activity

(1) High-intensity heavy-ion beams including 49-pnA uranium, 102-pnA xenon, 486-pnA krypton, and 689-pnA calcium beams have been obtained.
(2) The world-first high-Tc SQUID beam current monitor has been developed.
(3) The bending power of the fixed-frequency Ring Cyclotron has been upgraded to 700 MeV. It enables us to accelerate $^{238}U^{64+}$ ions obtained by the helium gas stripper.
(4) An EPICS-based control system and a homemade beam interlock system have been stably operated. Replacements of the existing legacy control system used in the old half of our facility is ongoing. Construction of the new control system for the new injector RILAC2 was successfully completed, where the embedded EPICS system running on F3RP61-2L CPU module, developed by KEK and RIKEN control group, was used.
(5) We replaced some dated power supplies of RIKEN Ring Cyclotron by new ones, which have better long-term stability than the old ones. The other existing power supplies (~900) are stably operated owing to elaborate maintenance work.
(6) We have contributed to RILAC2 construction, especially in its beam diagnosis, control system, magnet power supplies, vacuum system, high-energy beam transport system etc.

Members

Team Leader
Nobuhisa FUKUNISHI (concurrent; Deputy Group Director, Accelerator Gr.)

Research & Technical Scientists
Masaki FUJIMAKI (Senior Technical Scientist)
Keiko KUMAGAI (Senior Technical Scientist)
Tamaki WATANABE (Senior Technical Scientist)
Kazunari YAMADA (Senior Technical Scientist)

Nishina Center Technical Scientists
Misaki KOMIYAMA
Akito UCHIYAMA

Special Postdoctoral Researcher
Takuya MAEYAMA

Part-time Workers
Yuki SHIRAISHI
Makoto NAGASE

Visiting Scientists
Kenichi ISHIKAWA (Univ. of Tokyo)
Shin-ichiro Hayashi (Hiroshima Int'l Univ.)
Hiromichi RYUTO (Kyoto Univ.)

Visiting Technician
Jun-ichi ODAGIRI (KEK)

List of Publications & Presentations

Publications

[Journal]

(Original Papers) *Subject to Peer Review

Maeyama T., Fukunishi N., Ishikawa K.L., Furuta T., Fukasaku K., Takagi S., Noda S., Himeno R., and Fukuda S., “Radiological characteristics of MRI-based VIP polymer gel under carbon beam irradiation”, Radiation Physics and Chemistry **107**, pp. 7–11 (2015)*.

Furuta T., Maeyama T., Ishikawa K. L., Fukunishi N., Fukasaku K., Takagi S., Noda S., Himeno R., Hayashi S., “Comparison between Monte Carlo Simulation and Measurement with a 3D Polymer Gel Dosimeter for Dose Distributions in Biological Samples”, Physics in Medicine and Biology Vol. 60, No. 16, pp. 6531-6546 (2015)*.

Oral Presentations

[International Conference etc.]

Maeyama T., Fukunishi N., Ishikawa K. L., Fukasaku K., Fukuda S., “Radiological Properties of the Nanocomposite Fricke Gel Dosimeter for Heavy Ion Beams”, 15th International Congress of Radiation Research (ICRR2015), Kyoto, Japan, May 2015.

Fukunishi N., “Review of Heavy-ion Cyclotrons”, 13th International Conference on Heavy Ion Accelerator Technology (HIAT2015), Yokohama, Japan, September 2015, M0A1I01 (2015).

Watanabe T., Fukunishi N., Kase M., Inamori S., Kon K., “HTC-Squid Beam Current Monitor at the RIBF”, International Beam Instrumentation Conference 2015 (IBIC2015), Melbourne, Australia, September 2015, WECLA03 (2015).

[Domestic Conference]

前山拓哉、福西暢尚、石川顕一、深作和明、福田茂一、「化学線量計による重粒子線線量分布測定」、先端放射線化学シンポジウム(日本放射線化学会)、東京、日本、2015 年 3 月

前山拓哉、福西暢尚、石川顕一、深作和明、福田茂一、「有機ゲル化剤を含まないナノコンポジットフリッケゲル線量計」、先端放射線化学シンポジウム(日本放射線化学会)、浜松 静岡 日本、2015 年 10 月

Posters Presentations

[International Conference etc.]

Fukunishi N., Fujimaki M., Komiyama M., Kumagai K., Maie T., Watanabe Y., Hirano T., and Abe T., “New High-Energy Beam Transport Line Dedicated to Biological Applications in RIKEN RI Beam Factory”, 13th International Conference on Heavy Ion Accelerator Technology (HIAT2015), Yokohama, Japan, September 2015, MOPA04 (2015).

Komiyama M., Fujimaki M., Fukunishi N., Kumagai K., Uchiyama A., Nakamura T., “Recent Updates on the RIKEN RI Beam Factory Control System”, 13th International Conference on Heavy Ion Accelerator Technology (HIAT2015), Yokohama, Japan, September 2015, MOPA27 (2015).

Uchiyama A., Komiyama M., Fukunishi N., “EPICS PV Management and Method for RIBF Control System”, International Conference on Accelerator and Large Experimental Physics Control System 2015 (ICALEPCS2015), Melbourne, Australia, October 2015, WEPGF032 (2015).

[Domestic Conference]

Watanabe T., Fujimaki M., Fukunishi N., “Development of Beam Energy Measurement System by Using Electrostatic Pickups at the RIBF”, 12th Annual Meeting of Particle Accelerator Society of Japan, August 2015, Tsuruga, Japan, pp. 1198-1201 (2015).

RIBF Research Division
Accelerator Group
Cryogenic Technology Team

1. Abstract

We are operating the cryogenic system for the superconducting ring cyclotron in RIBF. We are operating the helium cryogenic system in the south area of RIKEN Wako campus and delivering the liquid helium to users in RIKEN. We are trying to collect efficiently gas helium after usage of liquid helium.

2. Major Research Subjects

(1) Operation of the cryogenic system for the superconducting ring cyclotron in RIBF
(2) Operation of the helium cryogenic plant in the south area of Wako campus and delivering the liquid helium to users in Wako campus.

3. Summary of Research Activity

(1) Operation of the cryogenic system for the superconducting ring cyclotron in RIBF
(Okuno, H., Dantsuka, T., Nakamura, M., Maie, T.)
(2) Operation of the helium cryogenic plant in the south area of Wako campus and delivering the liquid helium to users in Wako campus.
(Dantsuka, T., Tsuruma, S., Okuno, H.).

Members

Team Leader
Hiroki OKUNO (concurrent: Deputy Group Director, Accelerator Gr.)

Research & Technical Scientist
Masato NAKAMURA (Senior Technical Scientist)

Nishina Center Technical Scientist
Takeshi MAIE

Technical Staff I
Tomoyuki DANTSUKA

Research Consultant
Kumio IKEGAMI (Apr. 1, 2014 –)

Part-time Worker
Shizuho TSURUMA

RIBF Research Division
Accelerator Group
Infrastructure Management Team

1. Abstract

The RIBF facility is consisting of many accelerators and its infrastructure is very important in order to make an efficient operation of RIBF project. We are maintaining the infrastructure of the whole system and to support the accelerator operation with high performance. We are also concerning the contracts of gas- and electricity-supply companies according to the annual operation plan. The contracts should be reasonable and also flexible against a possible change of operations. And we are searching the sources of inefficiency in the operation and trying to solve them for the high-stable machine operation.

2. Major Research Subjects

(1) Operation and maintenance of infrastructure for RIBF accelerators.
(2) Renewal of the old equipment for the efficient operation.
(3) Support of accelerator operations.

Members

Team Leader

Masayuki KASE (concurrent; Deputy Group Director, Accelerator Gr.)

Research & Technical Scientists

Shu WATANABE (Senior Technical Scientist)
Hideyuki YAMASAWA (Manager)

Visiting Scientist

Hideshi MUTO (Tokyo Univ. of Sci. Suwa)

List of Publications & Presentations

Posters Presentations

[International Conference etc.]

E. Ikezawa, M. Fujimaki, Y. Higurashi, O. Kamigaito, M. Kase, M. Komiyama, T. Nakagawa, K. Ozeki, N. Sakamoto, K. Suda, A. Uchiyama, K. Yamada, K. Kaneko, T. Ohki, K. Oyamada, M. Tamura, H. Yamauchi, A. Yusa.”HEAVY-ION BEAM ACCELERATION AT RIKEN FOR SUPER-HEAVY ELEMENT SEARCH”, Proceedings of HIAT2015, Yokohama, Japan, pp222-224.

Yutaka Watanabe, Masayuki Kase, Masaki Fujimaki, Nobuhisa Fukunishi, Eiji Ikezawa, Osamu Kamigaito, Keiko Kumagai, Takeshi Maie, Jun-ichi Ohnishi, Kazutaka Ohzeki, Hiroki Okuno, Naruhiko Sakamoto, Kenji Suda, Shu Watanabe, Kazunari Yamada, Seiji Fukuzawa, Makoto Hamanaka, Shigeru Ishikawa, Kiyoshi Kobayashi, Ryo Koyama, Takeshi Nakamura, Minoru Nishida, Makoto Nishimura, Junsho Shibata, Noritoshi Tsukiori, Kazuyoshi Yadomi. “RIKEN RING CYCLOTRON (RRC) “, Proceedings of HIAT2015, Yokohama, Japan, 54-57.

K. Ozeki, T. Dantsuka, M. Fujimaki, T. Fujinawa, N. Fukunishi, H. Hasebe, Y. Higurashi, E. Ikezawa, H. Imao, T. Kageyama, O. Kamigaito, M. Kase, M. Kidera, M. Komiyama, K. Kumagai, T. Maie, M. Nagase, T. Nagatomo, T. Nakagawa, M. Nakamura, J. Ohnishi, H. Okuno, N. Sakamoto, K. Suda, A. Uchiyama, S. Watanabe, T. Watanabe, Y. Watanabe, K. Yamada, H. Yamasawa, RIKEN Nishina Center, Wako, JapanS. Fukuzawa, M. Hamanaka, S. Ishikawa, K. Kobayashi, R. Koyama, T. Nakamura, M. Nishida, M. Nishimura, J. Shibata, N. Tsukiori, K. Yadomi, Y. Kotaka. ”STATUS REPORT ON THE OPERATION OF THE RIBF RING CYCLOTRONS”, Proceedings of HIAT2015, Yokohama, Japan, pp191-193.

K. Suda, M. Fujimaki, N. Fukunishi, T. Kageyama, O. Kamigaito, M. Kase, M. Komiyama, K. Kumagai, T. Maie, M. Nagase, T. Nagatomo, T. Nakagawa, H. Okuno, N. Sakamoto, A. Uchiyama, T. Watanabe, Y. Watanabe, K. Yamada,T. Nakamura, S. Fukuzawa, M. Hamanaka, S. Ishikawa, K. Kobayashi, R. Koyama, M. Nishida, M. Nishimura, J. Shibata, N. Tsukiori, K. Yadomi, Y. Kotaka, Y. Ohshiro, S. Yamaka, ”STATUS REPORT OF THE OPERATION OF THE RIKEN AVF CYCLOTRON”, Proceedings of HIAT2015, Yokohama, Japan, pp65-67.

V Tzoganis, T. Nagatomo, M. Kase, O. Kamigaito, T. Nakagawa, C.P. Welsch, “DEVELOPMENT OF AN ONLINE EMITTANCE MONITOR FOR LOW ENERGY HEAVY ION BEAMS“, Proceedings of HIAT2015, Yokohama, Japan, pp250-252.

[Domestic Conference]

Minoru Nishida, Kazutaka Ozeki, Tomoyuki Dantsuka, Masaki Fujimaki, Tadashi Fujinawa, Nobuhisa Fukunishi, Seiji Fukuzawa, Makoto Hamanaka, Hiroo Hasebe, Yoshihide Higurashi, Eiji Ikezawa, Hiroshi Imao, Shigeru Ishikawa, Masayuki Kase, Tadashi Kageyama, Osamu Kamigaito, Masanori Kidera, Kiyoshi Kobayashi, Misaki Komiyama, Yasuteru Kotaka, Ryo Koyama, Keiko Kumagai, Takeshi Maie, Makoto Nagase, Takashi Nagatomo, Takahide Nakagawa, Masato Nakamura, Takeshi Nakamura, Makoto Nishimura, Jun-ichi Ohnishi, Hiroki Okuno, Naruhiko Sakamoto, Junsho Shibata, Kenji Suda, Noritoshi Tsukiori, Akito Uchiyama, Tamaki Watanabe, Yutaka Watanabe, Shu Watanabe, Kazuyoshi Yadomi, Kazunari Yamada, Hideyuki Yamasawa. “STATUS REPORT OF THE OPERATION OF THE RIBF RING CYCLOTRONS“, Proceedings of the 12th Annual Meeting of Particle Accelerator Society of Japan, August 5-7, 2015, Tsuruga,

Japan pp276-280.
Takeshi Nakamura, Shigeru Ishikawa, Kiyoshi Kobayashi, Ryo Koyama, Junsho Shibata, Noritoshi Tsukiori, Minoru Nishida, Makoto Nishimura, Makoto Hamanaka, Seiji Fukuzawa, Kazuyoshi Yadomi, Kenji Suda, Akito Uchiyama, Kazutaka Ozeki, Hiroki Okuno, Tadashi Kageyama, Masayuki Kase, Osamu Kamigaito, Keiko Kumagai, Misaki Komiyama, Naruhiko Sakamoto, Takahide Nakagawa, Makoto Nagase, Takashi Nagatomo,Nobuhisa Fukunishi, Masaki Fujimaki, Takeshi Maie, Kazunari Yamada, Tamaki Watanabe, Yutaka Watanabe, Shoichi Yamaka, Yukimitsu Ohshiro, Yasuteru Kotaka. “STATUS REPORT OF THE OPERATION OF THE RIKEN AVF CYCLOTRON“, Proceedings of the 12th Annual Meeting of Particle Accelerator Society of Japan, August 5-7, 2015, Tsuruga, Japan pp305-308.
Tomonori Ohki, Eiji Ikezawa, Hiromoto Yamauchi, Kazuyuki Oyamada, Masashi Tamura, Akira Yusa, Kenta Kaneko, Yutaka Watanabe, Uchiyama Akito, Masayuki Kase, Osamu Kamigaito. “PRESENT STATUS OF RILAC”, Proceedings of the 12th Annual Meeting of Particle Accelerator Society of Japan, August 5-7, 2015, Tsuruga, Japan pp309-311.

RIBF Research Division
Instrumentation Development Group

1. Abstract

This group develops core experimental installations at the RI Beam factory. Experimental installations currently under testing include common elements enabling multiple-use (SLOWRI), as well as others that are highly program specific (SCRIT and Rare-RI Ring). All were designed to maximize the research potential of the world's most intense RI beams, made possible by the exclusive equipment available at the RI Beam Factory. Beam manipulation techniques, such as a beam accumulation and a beam cooling, will be able to provide opportunities of new experimental challenges and the foundation for future developments of RIBF.

2. Major Research Subjects

(1) SCRIT Project
(2) SLOWRI Project
(3) Rear RI Ring Project

3. Summary of Research Activity

We are developing beam manipulation technology in carrying out above listed project. They are the high-quality slow RI beam production (SCRIT and SLOWRI), the beam cooling and stopping (SCRIT and SLOWRI), and the beam accumulation technology (Rare RI Ring). The technological knowhow accumulated in our projects will play a significant role in the next generation RIBF. Status and future plan for each project is described in subsections. SCRIT is now under test experimental phase in which the angular distribution of scattered electrons from ^{132}Xe isotopes has been successfully measured and the nuclear charge density distribution has been obtained. Electron scattering off unstable nuclei is now under preparation for the first experiment in 2016. Rare RI Ring construction has been commissioned in two-times machine-study experiments, and we have demonstrated that the ring has an ability for precision mass measurement with the accuracy of the order of 10 ppm. We will be able to try to measure masses of nuclei around ^{78}Ni region and continuously make improvement in the accuracy in 2016. Construction of the SLOWRI system has been completed in 2014. PALIS device was commissioned in 2015, and basic functions such as the RI-beam stopping in Ar gas cell and the extraction with the gas flow were confirmed. Other devices are now under setting up for the first commissioning.

Members

Group Director
Masanori WAKASUGI

Visiting Scientist
Akira OZAWA (Univ. of Tsukuba)

Student Trainees
Kohei YAMADA (Rikkyo Univ.)
Kousuke ADACHI (Rikkyo Univ.)
Takahiro FUJITA (Rikkyo Univ.)
Mitsuki HORI (Rikkyo Univ.)
Nobuaki UCHIDA (Rikkyo Univ.)
Shin-nosuke SASAMURA (Rikkyo Univ.)

List of Publications & Presentations

Publications and presentations for each project team are listed in subsections.

RIBF Research Division
Instrumentation Development Group
SLOWRI Team

1. Abstract

Construction of a next-generation stopped and low-energy radioactive ion beam facility (SLOWRI) which will provide low-energy, high-purity and small emittance ion beams of all elements has been started in FY2013 as one of the principal facilities at the RIKEN RI-beam factory (RIBF). High-energy radioactive ion beams from the projectile fragment separator BigRIPS are thermalized in a large He gas catcher cell (RFC cell) or in a small Ar gas catcher cell (PALIS cell). In the RFC cell, thermalized ions in buffer gas are guided and extracted to a vacuum environment by a combination of dc electric fields and inhomogeneous rf fields (rf carpet ion guide). The PALIS cell will be placed in the vicinity of the second focal plane slits of BigRIPS and can be used continuously during other experiments. From these gas cells, the low-energy ion beams will be delivered via mass separators and switchyards to various devices: such as an ion trap, a collinear fast beam apparatus, and a multi-reflection time of flight mass spectrograph. In the R&D works at the present ring cyclotron facility, an extraction efficiency of 33% for a 100A MeV ^{8}Li ion beam from the projectile fragment separator RIPS was achieved and the dependence of the efficiency on the ion beam intensity was investigated.

First spectroscopy experiment at the prototype SLOWI was performed on Be isotopes. Energetic ions of ^{7,10,11}Be from the RIPS were trapped and laser cooled in a linear rf trap and precision spectroscopy was performed. The evaluated ion temperature of <10 mK demonstrates that a reduction of more than 15 orders of magnitude for the kinetic energy of radioactive Be was achieved online. The ground state hyperfine constants of all Be isotopes have been measured precisely by laser and microwave. These precision measurements will be used to confirm the anomalous mean radius of the valence neutron of the so called neutron halo nucleus. Other laser spectroscopy experiments using the slow RI-beams are also under progress in off-line setups.

A multi-reflection time-of-flight mass spectrograph (MRTOF) has been developed and tested online for radioactive lithium isotope, ^{8}Li at RIPS. A high mass resolving power of 170,000 has been obtained for an isobaric doublet of ^{40}K and ^{40}Ca with a very short flight time of 2 ms. This performance allowed accurate mass determination of $<10^{-7}$ accuracy by a single isobaric reference. Two mass measurement projects using MRTOF mass spectrographs have been started: one is for trans uranium elements at the GARIS facility and the other is for r-process nuclides at SLOWRI facility. At GARIS-II, we performed mass measurements of ^{206}Fr, ^{205}Fr, ^{201}At and their isobars simultaneously.

Resonance ionization spectroscopy has been tested during the offline development of PALIS gas cell. Stable isotopes of Co, Cu, Fe, Ni, Ti, Nb, Sn, In, and Pd were resonantly ionized by excimer pumped dye lasers or Nd:YAG laser pumped Ti:Sapphire lasers with the prototype gas cell setup. The resonance spectra are in many cases sufficient to resolve the hyperfine structures. Nuclear spins and magnetic moments will be determined for various isotopes obtained during other experiments. An online commissioning experiment of parasitic low-energy production facility (PALIS) was performed and confirmed that the PALIS setup can coexist with other BigRIPS experiments and obtained radioactive Cu isotopes from the gas cell.

2. Major Research Subjects

(1) Construction of stopped and low-energy RI-beam facility, SLOWRI.
(2) Laser spectroscopy of trapped radioactive Beryllium isotopes.
(3) Development of a multi-reflection time-of-flight mass spectrograph for precision mass measurements of short-lived nuclei.
(4) Development of collinear laser spectroscopy apparatus.
(5) Development of parasitic slow RI-beam production method using resonance laser ionization.

3. Summary of Research Activity

(1) Construction of stopped and low-energy RI-beam facility (SLOWRI)

(WADA, Michiharu, SONODA, Tetsu, KATAYAMA, Ichiro, KOJIMA, Takao, SCHURY, Peter, ITO, Yuta, ARAI, Fumiya, ARAI, Shigeaki, KUBO, Toshiyuki, KUSAKA, Kensuke, FUJINAWA Tadashi, MAIE Takeshi, YAMASAWA Hideyuki, WOLLNIK, Hermann,)

Installation of SLOWRI has been started in FY2013. It consists of two gas catchers (RF Carpet gas cell and PALIS gas cell), mass separators a 50-m beam transport line, a beam cooler-buncher, an isobar separator, and a laser system. The RFCarpet gas cell will be installed at the exit of the D5 dipole magnet of BigRIPS. The gas catcher contains a large cryogenic He gas cell with a large traveling wave rf-carpet. It will convert main beams of BigRIPS to low-energy, low-emittance beams without any restrictions on the chemical properties of the elements. The PALIS gas cell will be installed in the vicinity of the second focal plane slit of BigRIPS. It will provide parasitic RI-beams from those ions lost in the slits during other experiments. In this gas catcher, thermalized RI ions quickly become neutral and will be re-ionized by resonant laser radiations. These gas catchers will be tested off-line in FY2014. The 50 m beam transport line consists of four dipole magnets (SD1 to SD4), two focal plane chambers, 62 electrostatic quadrupole singlets, 11 electrostatic quadrupole quartets (EQQ1 to EQQ11) and 7 beam profile monitors (BPM). SD1 and SD2, located right after the gas catchers will be used for isotope separation. After eliminating contaminant ions at the focal plane chamber, the low energy beam will be transported by FODO lattice structure with phase space matching using EQQs. The EQQs have multipole elements made of 16 rods on which various potentials can be applied to produce 6-pole and 8 pole fields, simultaneously, for compensation of ion optical aberrations. This multipole element can also produce dipole fields for steering and scanning the beam. The BPM have a classical cross-wire beam monitor as well as a channel electron multiplier with a pinhole collimator. Combining the scanning capability of the EQQs and the pinhole detector, we can observe a

beam profile even for a very low-intensity RI-beams. Off- and on-line commissioning are underway.

(2) Laser spectroscopy of trapped radioactive beryllium isotope ions

(WADA, Michiharu, TAKAMINE, Aiko, SCHURY Peter, SONODA Tetsu, OKADA, Kunihiro, KANAI, Yasuyuki, YOSHIDA, Atsushi, KUBO, Toshiyuki, WOLLNIK, Hermann, SCHUESSLER, Hans, KATAYAMA Ichiro)

As a first application of the prototype SLOWRI setup, we applied hyperfine structure spectroscopy to the beryllium isotopes to determine in particular the anomalous radius of the valence neutron of the neutron halo nucleus ^{11}Be, and to determine the charge radii of these beryllium isotopes through laser-laser double resonance spectroscopy of laser-cooled ions. Laser cooling is an essential prerequisite for these planned experiments. The first laser spectroscopy experiments for beryllium isotopes were performed to measure the resonance frequencies of 2s $^2S_{1/2}$ - 2p $^2P_{3/2}$ transition of ^{7}Be+, ^{9}Be+, ^{10}Be$^+$ and ^{10}Be+ ions and the nuclear charge radii of these isotopes were determined. The hyperfine structures of ^{11}Be$^+$ and ^{7}Be$^+$ ions using the laser-microwave double resonance spectroscopy were also performed and the magnetic hyperfine constants of ^{7}Be$^+$ and ^{11}Be$^+$ ions were determined with accuracies of better than10^{-7}.

(3) Development of a multi-reflection TOF mass spectrograph for short-lived nuclei

(WADA, Michiharu, SCHURY Peter, ITO, Yuta, ARAI, Fumiya, MUARRY, Ian, SONODA Tetsu, WOLLNIK, Hermann, MORIMOTO, Koji, KAJI, Daiya, HABA, Hiromitsu, KOURA, Hiroyuki)

The atomic mass is one of the most important quantities of a nucleus and has been studied in various methods since the early days of physics. Among many methods we chose a multi-reflection time-of-flight (MR-TOF) mass spectrometer. Slow RI beams extracted from the RF ion-guide are bunch injected into the spectrometer with a repetition rate of ~100 Hz. The spectrometer consists of two electrostatic mirrors between which the ions travel back and forth repeatedly. These mirrors are designed such that energy-isochrononicity in the flight time is guaranteed during the multiple reflections while the flight time varies with the masses of ions. A mass-resolving power of 170,000 has been obtained with a 2 ms flight time for 40K and 40Ca isobaric doublet. This mass-resolving power should allow us to determine ion masses with an accuracy of 10^{-7}. An online mass measurement for radioactive lithium isotope has been carried out at the prototype SLOWRI setup.

The MR-TOF mass spectrograph has been placed under the GARIS-II separator aiming at direct mass measurements of trans-uranium elements. A small cryogenic gas catcher cell was placed at the focal plane box of GARIS-II and a bunched low-energy heavy ion beam were transported to the trap of MR-TOF. In online commissioning experiments, we achieved more than 30% of extraction efficiency from the cryogenic gas cell. We measured masses of ^{206}Fr, ^{205}Fr, ^{201}At and some of their isobars simultaneously. Further measurements towards trans-uranium isotopes is planned in FY2016.

(4) Development of collinear fast beam apparatus for nuclear charge radii measurements

(WADA, Michiharu, SCHUESSLER, Hans, IIMURA, Hideki, SONODA, Tetsu, SCHURY, Peter, TAKAMINE, Aiko, OKADA, Kunihiro, WOLLNIK, Hermann)

The root-mean-square charge radii of unstable nuclei have been determined exclusively by isotope shift measurements of the optical transitions of singly-charged ions or neutral atoms by laser spectroscopy. Many isotopes of alkaline, alkaline-earth, noble-gases and several other elements have been measured by collinear laser spectroscopy since these ions have all good optical transitions and are available at conventional ISOL facilities. However, isotopes of other elements especially refractory and short-lived ones have not been investigated so far.

In SLOWRI, isotopes of all atomic elements will be provided as well collimated mono-energetic beams. This should expand the range of applicable nuclides of laser spectroscopy. In the first years of the RIBF project, Ni and its vicinities, such as Ni, Co, Fe, Cr, Cu, Ga, Ge are planned to be investigated. They all have possible optical transitions in the ground states of neutral atoms with presently available laser systems. Some of them have so called recycle transitions which enhance the detection probabilities noticeably. Also the multistep resonance ionization (RIS) method can be applied to the isotopes of Ni as well as those of some other elements. The required minimum intensity for this method can be as low as 10 atoms per second.

We have built an off-line mass separator and a collinear fast beam apparatus with a large solid-angle fluorescence detector. A 617 nm transition of the metastable Ar+ ion at 20 keV was measured with both collinear and anti-collinear geometry that allowed us to determine the absolute resonant frequency of the transition at rest with more than 10^{-8} accuracy. Such high accuracy measurements for Ti and Ni isotopes are in progress.

(5) Development of parasitic slow RI-beam production scheme using resonance laser ionization

(SONODA Tetsu, IIMURA Hideki, REPONEN, Mikael, WADA Michiharu, KATAYAMA Ichiou, KOJIMA, Takao, ADACHI Yoshitaka, NOTO Takuma, TAKATSUKA Takaaki, TOMITA Hideki, WENDT Klaus, ARAI Fumiya, ITOU Yuta, SCHURY Peter, FUKUDA Naoki, INABE Naohito, KUBO Toshiyuki, KUSAKA Kensuke, TAKEDA Hiroyuki, SUZUKI H., WAKASUGI Masanori, YOSHIDA Koichi)

More than 99.9% of RI ions produced in projectile fission or fragmentation are simply dumped in the first dipole magnet and the slits. A new scheme, named PALIS, to rescue such dumped precious RI using a compact gas catcher cell and resonance laser ionization was proposed as a part of SLOWRI. The thermalized RI ions in a cell filled with Ar gas can be quickly neutralized and transported to the exit of the cell by gas flow. Irradiation of resonance lasers at the exit ionizes neutral RI atoms efficiently and selectively. The ionized RI ions can be further selected by a magnetic mass separator and transported to SLOWRI experimental area for various experiment. The resonance ionization scheme itself can also be a useful method to perform hyperfine structure spectroscopy of RI of many elements.

A prototype setup has been tested for resonance ionization scheme of several elements, extraction from the cell, and transport to a high vacuum chamber. An online setup, has been fabricated in FY2013 and the first online commissioning took place in Fy2015. We confirmed that the PALIS gas cell doesn't harm BigRIPS experiment, and a reasonable amount of radioactive Cu isotopes were extracted from the cell by gas flow. A second online commissioning is scheduled in FY2016 and we are going to provide parasitic low-energy RI-beams for various experiments at the SLOWRI experimental area.

Members

Team Leader
Michiharu WADA

Research & Technical Scientist
Takao KOJIMA (Senior Research Scientist, Apr. 1, 2015)
Hideyuki YAMASAWA (concurrent; Infrastructure Management Team)

Nishina Center Research Scientists
Tetsu SONODA
Kensuke KUSAKA (concurrent; BigRIPS Team)

Nishina Center Technical Scientist
Takeshi MAIE (concurrent; Cryogenic Technology Team)

Contract Researcher
Peter Henry SCHURY (– Mar. 31, 2015)

Special Postdoctoral Researcher
Yuta ITO (Apr. 1, 2014 –)

Part-time Workers
Shigeaki ARAI
Ichiro KATAYAMA
Sota KIMURA (Feb. 1, 2016 –)

Research Consultant
Hirokane KAWAKAMI

Visiting Researcher
Mikael REPONEN (JSPS, Aug. 4, 2014 –)

Visiting Scientists
Hans A SCHUESSLER (Texas A&M Univ.)
Hermann WOLLNIK (Univ. of Giessen)
Aiko TAKAMINE (Aoyama Gakuin Univ.)
Hideki IIMURA (JAEA)
Hideki TOMITA (Nagoya Univ.)
Klaus WENDT (Johannes Gutenberg Univ. Mainz)
Kunihiro OKADA (Sophia Univ.)
Peter Henry SCHURY (Univ. of Tsukuba)
Volker SONNENSCHEIN (Nagoya Univ.)

Student Trainees
Takuma NOTO (Nagoya Univ.)
Fumiya ARAI (Univ. of Tsukuba)
Yoshitaka ADACHI (Nagoya Univ.)
Takahide TAKAMATSU (Nagoya Univ.)
Daiki MATSUI (Nagoya Univ.)

List of Publications & Presentations

Publications

[Proceedings]

(Original Papers) *Subject to Peer Review

K. Okada, M. Ichikawa, M. Wada, « Characterization of ion crystals for fundamental science », Hyp. Int. DOI 10.1007/s10751-015-1188-y, 2015*

Y. Hirayama, Y.X. Watanabe, N. Imai, H. Ishiyama, S.C. Jeong, H.S. Jung, H. Miyatake, M. Oyaizu, S. Kimura, M. Mukai, Y.H. Kim, T. Sonoda, M. Wada, M. Huyse, Yu. Kudryavtsev,P. van Duppen, « On-line experimental results of an argon gas cell-based laser ion source (KEK Isotope Separation System) », Nucl. Inst. Meth. B376 (2016) 52-56.*

M. Mukai, Y. Hirayama, H. Ishiyama, H.S. Jung, H. Miyatake, M. Oyaizu, Y.X. Watanabe, S. Kimura, A. Ozawa, S.C. Jeong, T. Sonoda, « Search for efficient laser resonance ionization schemes of tantalum using a newly developed time-of-flight mass spectrometer in KISS », Nucl. Inst. Meth B376 (2016) 73-76.*

S. Kimura, H. Ishiyama, H. Miyatake, Y. Hirayama, Y.X. Watanabe, H.S. Jung, M. Oyaizu, M. Mukai, S.C. Jeong, A. Ozawa, « Development of the detector system for image-decay spectroscopy at the KEK Isotope Sepaator System », Nucl. Inst. Meth. B376 (2016) 338-340.*

Y. Hirayama, H. Miyatake, Y.X. Watanabe, N. Imai, H. Ishiyama, S.C. Jeong, H.S. Jung, M. Oyaizu, M. Mukai, S. Kimura, T. Sonoda, M. Wada, Y.H. Kim, M. Huyse, Yu Kudryavtsev, P. van Duppen, « Deta-decay spectroscopy of r-process nuclei around N=126 », EPJ Web Conf. 109 (2016) 08001, 1-6.*

Y. Hirayama, Y.X. Watanabe, N. Imai, H. Ishiyama, S.C. Jeong, H. Miyatake, M. Oyaizu, S. Kimura, M. Mukai, Y.H. Kim, T. Sonoda, M. Wada, M. Huyse, Yu. Kudryavtsev, P. van Duppen, « Laser ion source for multi-nucleon transfer products », Nucl. Inst. Meth B353 (2015) 4-15.*

Oral Presentations

[International Conference etc.]

P. Schury et al., « Status of the low-energy Super-Heavy Element Facility at RIKEN », May 11-15, 2015, EMIS2015, Grand Rapids, MI, USA

M. Wada et al., « SHE-mass project at RIKEN RIBF », May 25-29, 2015, TAN2015, Urabandai, Fukushima, Japan
T. Sonoda et al., « Development of the parasitic production of low-energy RI-beam and gas-ject nuclear spectroscopy at RIKEN BigRIPS « , June 7-10, 2015, LAP2015, Michigan State Univ. East Lancing, MI, USA
M. Wada, « Laser spectroscopy and mass measurements at RIKEN SLOWRI », Aug. 24-27, ECT* Workshop, TRENTO, Italy
M. Wada et al, « Towards high precision nuclear spectroscopy at SLOWRI, RIKEN RIBF », Nov. 07-12, JCNP2015, RCNP, Osaka, Japan.

Posters Presentations

[International Conference etc.]

Y. Ito et al., « Development of a gas cell system for SHE-mass project at RIKEN », May 25-29, 2015, TAN2015, Urabandai, Fukushima, Japan
M. Reponen, et al., « Resonance ionization spectroscopy data-analysis software for PALIS-facility », June 7-10, 2015, LAP2015, Michigan State Univ., East Lancing, MI, USA

RIBF Research Division
Instrumentation Development Group
Rare RI-ring Team

1. Abstract

Mass measurement is one of the most important contributions to a nuclear property research especially for short-lived unstable nuclei far from the beta-stability line. In particular, a high-precision mass measurement for nuclei located around the r-process pass (rare-RI) is required in nucleosynthesis point of view. We chose a method of isochronous mass spectrometry (IMS) to make a measurement time shorter than 1 ms. Heavy-ion storage ring named "Rare-RI Ring (R3)" has been constructed until end of 2013 and commissioning experiments were successfully performed in last year. Our target performance in the mass determination is to achieve accuracy of the order of 1 ppm (~100 keV) even if we get only one event. Since an isochronism in R3 is established over a wide range of the momentum, rare-RIs with a large momentum spread, $\Delta p/p=\pm 0.5$ %, are acceptable. Another significant feature of the R3 system is an individual injection scheme in which a produced rare-RI itself triggers the injection kicker. In the first commissioning experiment using primary ^{78}Kr beam, we could demonstrated a high ability of R3 as a storage ring and succeed in establishing the individual injection scheme for the first time. In the second experiment using secondary beams of ^{36}Ar and ^{25}Cl, we successfully demonstrated mass determination by measuring revolution time for both isotopes with the accuracy of ~20 ppm. We are going to try to measure masses for isotopes around ^{78}Ni region in 2016.

2. Major Research Subjects

(1) Developments of heavy-ion storage ring
(2) Precision mass measurement for rarely produced isotopes related to r-process.

3. Summary of Research Activity

Since the lattice design of R3 is based on the cyclotron motion, it can provide an isochronism in a wide range of the momentum. We expect a great improvement in mass resolution in IMS as long as the isochronous field is precisely formed in R3. Therefore, IMS using R3 is capable of both a high-precision measurement and a fast measurement. All the devices in R3 was designed under the assumption that an incoming beam has an energy of less than 200 MeV/u and a charge to mass ratio, m/q, of less than 3. The ring structure was designed with a similar concept of a separate-sector ring cyclotron. It consists of six sectors and 4.02-m straight sections, and each sector consists of four rectangular bending magnets. A radially homogeneous magnetic field is produced in the magnet, and a magnetic rigidity is 6.5 Tm at maximum, for instance, ^{78}Ni with the magnetic rigidity of 5.96 Tm. Two magnets at both ends of each sector are additionally equipped with ten trim coils to form a precise isochronous magnetic field. For $\Delta p=0$ particle, the circumference is 60.35 m and the betatron tunes are $\nu x=1.21$ and $\nu y=0.84$ in horizontal and vertical directions, respectively. The momentum acceptance is $\Delta p/p=\pm 0.5$ %, and the transverse acceptances are 20π mmmrad and 10π mmmrad in horizontal and vertical directions, respectively.

Another performance required for R3 is to efficiently seize hold of an opportunity of the measurement for rare-RIs produced unpredictably. We adopted an individual injection scheme in which the produced rare-RI itself triggers the injection kicker magnets. Full activation of the kicker magnetic field has to be completed within the flight time of the rare-RI from an originating point (F3 focal point in BigRIPS) of the trigger signal to the kicker position in R3. We successfully developed an ultra-fast response kicker system working with the repetition rate of 100 Hz.

Since R3 accumulates, in principle, only single ion, we need high-sensitive beam diagnostic devices in the ring, and they should be applicable even for a single particle circulation. One of them is a cavity type of Schottky pick-up installed for tuning of isochronous field. A resonance frequency is 171 MHz, a measured quality factor is about 1945, and shunt impedance is 190 kΩ. Another is a timing monitor, which detects secondary electrons emitted from thin carbon foil placed on the accumulation orbit. The thickness of the foil will be 50 μg/cm^2. The rare-RI with the energy of 200 MeV/u survives only for first 100 turns because of an energy loss at the foil.

In last year, we had two times of commissioning experiments. In the first experiment, we use primary ^{78}Kr^{36+} beam with the energy of 168 MeV/u. We succeeded in beam injection particle by particle in individual injection scheme, beam extraction after 700-μs accumulation (~1860 turns), and measurements of the TOF from the injection to the extraction. It was demonstrated that R3 works well as a storage ring and a single particle is certainly manipulated in this storage ring system. The individual injection scheme was established for the first time in the world. In addition, the Schottky pick-up monitored a single ^{78}Kr^{36+} particle circulation with the measuring time of less than 10 ms. That demonstrated that our pick-up is world most sensitive non-destructive monitor. In this experiment, we could tune completely the first order isochronism, but higher order components was remained, consequently, the 10-ppm accuracy of the isochronism was obtained. More precise tuning is possible with reference the Schottky data. In the second commissioning experiment, we injected two isotopes, ^{36}Ar and ^{35}Cl, selected in the secondary beams into the ring, in which the isochronism is tuned for ^{36}Ar. It was obviously demonstrated that the mass of ^{35}Cl relative to ^{36}Ar is determined by comparing the TOF values for both isotopes, and the accuracy was ~20 ppm, which is one-order less than our target value of a few ppm. We found that the imperfection of isochronism significantly contributes to the time resolution of measured TOF values and the magnetic field fluctuation (less than 10 ppm) is also considerable. These inexpediencies will be improved in next time. In this year, we will be able to try mass measurements for isotopes related r-process pass around ^{78}Ni region.

Members

Team Leader

Masanori WAKASUGI (concurrent; Group Director, Instrumentations Development Gr.)

Research & Technical Scientists

Yoshiyuki YANAGISAWA (Senior Research Scientist, concurrent; BigRIPS Team)
Tamaki WATANABE (Senior Technical Scientist, concurrent; Beam Dynamics and Diagnostics Team)
Yutaka WATANABE (Senior Technical Scientist, concurrent; RILAC team)
Naohito INABE (Senior Technical Scientist, concurrent; BigRIPS Team)
Hideyuki YAMASAWA (concurrent; Infrastructure Management Team)

Nishina Center Research Scientist

Yoshitaka YAMAGUCHI
Daisuke NAGAE (Spin-Isospin Lab.)
Fumi SUZAKU (Spin-Isospin Lab.)

Nishina Center Technical Scientists

Takeshi MAIE (concurrent; Cryogenic Technology Team)
Misaki KOMIYAMA (concurrent; Beam Dynamics and Diagnostics Team)

Special Postdoctoral Researcher

Yasushi ABE (Apr. 1, 2015 –)

Research Consultant

Akira NODA (– Mar. 31, 2014)

Student Trainees

Ayano ENOMOTO (Saitama Univ.)

List of Publications & Presentations

Publications

[Journal]

(Review)

Y. Yamaguchi, M. Wakasugi, Y. Abe, F. Suzaki, D. Nagae, S. Omika, H. Miura, S. Naimi, Z. Ge, T. Yamaguchi, A. Ozawa, T. Uesaka, J. Ohnishi, T. Kikuchi, M. Komiyama, K. Kumagai, A. Tokuchi, T. Fujinawa, T. Maie, H. Yamasawa, Y. Yanagisawa, T. Watanabe, Y. Watanabe, and Y. Yano, “Construction of the rare-RI ring at RIKEN RI Beam Factory” , Journal of Particle Accelerator of Japan, Vol.12, No.3, 132-141 (2015).

[Proceedings]

(Original Papers) *Subject to Peer Review

F. Suzaki, J. Zenihiro, Y. Abe, A. Ozawa, T. Suzuki, T. Uesaka, M. Wakasugi, K. Yamada, T. Yamaguchi, and Y. Yamaguchi, “Performance of a resonant Schottky pick-up for the Rare-RI Ring project”, JPS Conference Proceedings Vol.6 (2015) 030119.*

T. Yamaguchi, “Present status of Rare-RI Ring facility at RIBF”, Physica Scripta T166 (2015) 014039.*

Y. Abe, Y. Yamaguchi, M. Wakasugi, T. Uesaka, A. Ozawa, F. Suzaki, D. Nagae, H. Miura, and T. Yamaguchi, “Isochronous field study of the Rare-RI Ring”, Physica Scripta T166 (2015) 014039.*

F. Suzaki, J. Zenihiro, A. Ozawa, T. Suzuki, T. Uesaka, M. Wakasugi, K. Yamada, T. Yamaguchi, Y. Abe, and Y. Yamaguchi, “A resonant Schottky pick-up for Rare-RI Ring at RIKEN”, Physica Scripta T166 (2015) 014059.*

Y. Yamaguchi, H. Miura, M. Wakasugi, Y. Abe, A. Ozawa, F. Suzaki, A. Tokuchi, T. Uesaka, T. Yamaguchi, and Y. Yano, “Fast-kicker system for rare-RI ring” Physica Scripta T166 (2015) 014056.*

H. Miura, Y. Abe, Z. Ge, K. Hiraishi, Y. Ishikawa, I. Kato, T. Moriguchi, D. Nagae, S. Naimi, T. Nishimura, S. Omika, A. Ozawa, F. Suzaki, S. Suzuki, “Performance of a fast kicker magnet for rare-RI ring”, Proceedings of the HIAT2015 (2015) 95-97.

F. Suzaki, Y. Abe, Z. Ge, D. Nagae, S. Naimi, T. Uesaka, T. Watanabe, M. Wakasugi, K. Yamada, Y. Yamaguchi, J. Zenihiro, Y. Yano, I. Kato, H. Miura, T. Nishimura, S. Omika, T. Suzuki, N. Tadano, Y. Takeuchi, T. Yamaguchi, K. Hiraishi, Y. Ichikawa, T. Moriguchi, A. Ozawa, S. Suzuki, and Y. Tajiri, “Performance of a resonant Schottky pick-up in the commissioning of rare-RI ring”, Proceedings of the HIAT2015 (2015) 98-100.

Y. Yamaguchi, Y. Abe, and rare-RI ring collaborators, “The rare-RI ring at RIKEN RI Beam Factory”, Proceedings of the HIAT2015 (2015) 121-123.

T. Yamaguchi, T. Izumikawa, S. Miyazawa, T. Suzuki, F. Tokanai, H. Furuki, N. Ichihashi, C. Ichikawa, A. Kitagawa, T. Kuboki, S. Momota, D. Nagae, M. Nagashima, Y. Nakamura, R. Nishikiori, T. Ohtsubo, A. Ozawa, K. Sato, S. Sato, and S. Suzuki, “Performance of high-resolution position-sensitive detectors developed for storage-ring decay experiments”, Nuclear Instruments and Methods in Physics Research Section B 317 (2013) 697-700.*

F. Suzaki, J. Zenihiro, T. Yamaguchi, A. Ozawa, T. Uesaka, M. Wakasugi, K. Yamada, Y. Yamaguchi, and rare-RI ring collaboration, “Design study of a resonant Schottky pick-up for the Rare-RI Ring project”, Nuclear Instruments and Methods in Physics Research Section B317 (2013) 636-639.*

D. Nagae, S. Okada, A. Ozawa, T. Yamaguchi, H. Suzuki, T. Moriguchi, Y. Ishibashi, S. Fukuoka, R. Nishikiori, T. Niwa, T. Suzuki, K. Sato, H.

Furuki, N. Ichihashi, S. Miyazawa, Y. Yamaguchi, T. Uesaka, and M. Wakasugi, “Time-of-flight detector applied to mass measurements in Rare-RI Ring”, Nuclear Instruments and Methods in Physics Research Section B 317 (2013) 640-643.*

Y. Yamaguchi, M. Wakasugi, T. Uesaka, A. Ozawa, Y. Abe, T. Fujinawa, M. Kase, M. Komiyama, T. Kubo, K. Kumagai, T. Maie, D. Nagae, J. Ohnishi, F. Suzaki, A. Tokuchi, Y. Watanabe, K. Yoshida, K. Yamada, T. Yamaguchi, H. Yamasawa, Y. Yanagisawa, J. Zenihiro, and Y. Yano, “Construction of rare-RI ring at RIKEN RI Beam Factory”, Nuclear Instruments and Methods in Physics Research Section B 317 (2013) 629-635.*

Yu.A. Litvinov, S. Bishop, K. Blaum, F. Bosch, C. Brandau, L.X. Chen, I. Dillmann, P. Egelhof, H. Geissel, R.E. Grisenti, S. Hagmann, M. Heil, A. Heinz, N. Kalantar-Nayestanaki, R. Knoebel, C. Kozhuharov, M. Lestinsky, X.W. Ma, T. Nilsson, F. Nolden, A. Ozawa, R. Raabe, M.W. Reed, R. Reifarth, M.S. Sanjari, D. Schneider, H. Simon, M. Steck, T. Stoehlker, B.H. Sun, X.L. Tu, T. Uesaka, P.M. Walker, M. Wakasugi, H. Weick, N. Winckler, P.J. Woods, H.S. Xu, T. Yamaguchi, Y. Yamaguchi, and Y.H. Zhang, “Nuclear physics experiments with ion storage rings”, Nuclear Instruments and Methods in Physics Research Section B 317 (2013) 603-616.*

T. Yamaguchi, Y. Yamaguchi, and A. Ozawa “The challenge of precision mass measurements of short-lived exotic nuclei: Development of a new storage-ring mass spectrometry”, Journal of Mass Spectrometry 349-350 (2013) 240-246.*

M. Wakasugi, and rare-RI ring collaborators, “Construction of the rare-RI ring at the RIKEN RI beam factory”, Proceedings of Cyclotron2013 (2013) 477-481.

Y. Abe, D. Nagae, and rare-RI ring collaboration, “Developments of time-of-flight detectors for Rare-RI Ring”, Proceedings of the 12th Asia Pacific Physics Conference 1 (2013) 013059.*

F. Suzaki, T. Yamaguchi, and rare-RI ring collaboration, “Storage-ring mass spectrometry in Japan”, Proceedings of the 12th Asia Pacific Physics Conference 1 (2013) 013058.*

M. Komiyama, A. Uchiyama, N. Fukunishi, M. Wakasugi, M. Hamanaka, and M. Nishimura, “Status of the RIKE RI Beam Factory Control System”, Proceedings of ICALEPCS2013 (2013) 348-351.

Oral Presentations

[International Conference etc.]

Y. Yamaguchi, “The Rare RI Ring at RI Beam Factory”, 13th International Conference on Heavy Ion Accelerator Technology, Yokohama, Japan, September (2015).

Y. Yamaguchi, “Commissioning of the Rare-RI Ring at RI Beam Factory”, International Workshop on Beam Cooling and Related Topics, Newport News, USA, October (2015).

Y. Yamaguchi, “Commissioning of the Rare-RI Ring at RI Beam Factory”, The 9th Japan-China Joint Nuclear Physics Symposium, Osaka, Japan, November (2015).

Ozawa, and rare-RI ring collaboration, “Mass measurement with Rare-RI Ring at RIKEN”, SKLTP-BLTP Joint Workshop on Physics of Strong Interaction, Guangxi, China, November (2015).

Y. Yamaguchi, and rare-RI ring collaboration, “Present status of Rare-RI Ring”, RIBF Users Meeting 2015, Wako, Japan, September (2015).

M. Wakasugi, and rare-RI ring collaboration, “The Rare-RI Ring Facility at RIKEN RI Beam Factory”, 2nd Conference on Advances in Radioactive Isotope Science, Tokyo, Japan, June (2014).

Y. Yamaguchi, and rare-RI ring collaboration, “Rare-RI Ring at RIKEN RI Beam Factory”, The 6th International Conference on Trapped Charged Particles and Fundamental Physics, Takamatsu, Japan, Desember (2014).

Y. Abe, Y. Yamaguchi, M. Wakasugi, T. Uesaka, A. Ozawa, F. Suzaki, H. Miura, T. Yamaguchi, and Y. Yano, “Isochronous study of the Rare-RI Ring”, 9th International Conference on Nuclear Physics at Storage Rings, St. Goar, Germany, September (2014).

Ozawa, “Mass measurement with Rare-RI Ring”, Science and Next Generation Experiments at FRIB and RIBF, Hawaii, USA, October (2014).

Y. Abe, “Mass measurement of RI with Rare-RI Ring at RIKEN”, Post-TCP PMM Workshop, Wako, Japan, December (2014).

M. Wakasugi, and rare-RI ring collaborators, “Construction of the Rare RI Ring (R3) at the RIKEN RI Beam Factory”, The 20th International Conference on Cyclotrons and Their Applications, Vancouver, Canada, September (2013).

T. Yamaguchi, “Rare-RI Ring project in RIKEN”, Sino-German Symposium on (High precision experiments with stored exotic and stable nuclei), Lanzhou, China, November (2013).

Y. Yamaguchi, and rare-RI ring collaboration, “Construction status of the Rare-RI Ring”, RIBF Users Meeting 2013, Wako, Japan, June (2013).

Ozawa, and rare-RI ring collaboration, “Rare-RI Ring for Mass measurements at RIBF”, The 12th International Symposium on Origin of Matter and Evolution of Galaxies, Tsukuba, Japan, November (2013).

[Domestic Conference]

大甕舜一朗、山口貴之、若杉昌徳、山口由高、阿部康志、上坂友洋、小沢顕、洲嵜ふみ、鈴木健、長江大輔、三浦宙、柳澤善行、 「稀少 RI リング個別入射方式のための同軸菅の開発」日本物理学会 2015 年秋季大会、大阪市、9 月 (2015).

鈴木伸司、市川ゆきな、長江大輔、小沢顕、阿部康志、森口哲朗、岡田俊祐、石橋陽子、松本拓也、田尻芳之、斎藤祐多、稲葉成紀、沢畑克樹、山口貴之、鈴木健、河野準平、山木さやか、松本達、榎本彩乃、大甕舜一朗、竹内勇貴、加藤郁磨、只野奈津生、西村拓真、北川敦志、佐藤眞二、「RI ビーム飛行時間検出器の開発」日本物理学会 2015 年秋季大会、大阪市、9 月 (2015).

阿部康志、山口由高、上坂友洋、小沢顕、洲嵜ふみ、山口貴之、若杉昌徳、稀少 RI リングコラボレーション、「稀少 RI リングの性能評価」日本物理学会第 71 回年次大会、仙台市、3 月 (2016).

洲嵜ふみ、阿部康志、Ge Zhuang、平石健太郎、市川ゆきな、加藤郁磨、三浦宙、森口哲朗、長江大輔、Naimi Sarah、西村拓真、大甕舜一朗、小沢顕、鈴木伸司、鈴木健、只野奈津生、田尻芳之、竹内勇貴、上坂友洋、若杉昌徳、渡邊環、山田一成、山口貴之、山口由高、銭廣十三、矢野安重、「稀少 RI リングのための共鳴ショットキーピックアップのオンライン性能評価」日本物理学会第 71 回年次大会、仙台市、3 月 (2016).

鈴木伸司、小沢顕、市川ゆきな、森口哲朗、田尻芳之、平石健太郎、松本拓也、長江大輔、阿部康志、Naimi Sarah、Ge Zhuang、山口貴之、松本達、鈴木健、大甕舜一朗、竹内勇貴、加藤郁磨、只野奈津生、西村拓真、北川敦志、佐藤眞二、「質量測定用飛行時間検出器の開発」日本物理学会第 71 回年次大会、仙台市、3 月 (2016).

小沢顕、「Present status of Rare-RI Ring project at RIBF」実験と観測で解き明かす中性子星の核物質 第 4 回研究会、葉山、9 月 (2015).

山口貴之、「稀少 RI リングによる r プロセス核の測定計画」宇宙核物理連絡協議会 研究会、三鷹市、2 月 (2016).

Naimi Sarah、「Mass measurement in connection to the nuclear astrophysics」宇宙核物理連絡協議会 研究会、三鷹市、2 月 (2016).

洲嵜ふみ、阿部康志、Naimi Sarah、三浦宙、小沢顕、鈴木健、上坂友洋、若杉昌徳、山田一成、山口貴之、山口由高、銭廣十三、Chen Xiangcheng、「稀少 RI リングの共鳴ショットキーピックアップのオフライン性能試験」日本物理学会第 70 回年次大会、東京、3 月 (2015).
三浦宙、山口由高、若杉昌徳、阿部康志、小沢顕、洲嵜ふみ、徳地明、上坂友洋、山口貴之、長江大輔、柳澤善行、鈴木健、「稀少 RI リングのためのキッカーマグネットの開発」日本物理学会第 70 回年次大会、東京、3 月 (2015).
阿部康志、長江大輔、岡田俊祐、小沢顕、山口貴之、石橋陽子、斎藤祐多、沢畑克樹、鈴木健、河野準平、山木さやか、山口由高、上坂友洋、若杉昌徳、「稀少 RI リングのビームモニターの開発」日本物理学会 2013 年秋季大会、高知市、9 月 (2013).
洲嵜ふみ、銭廣十三、小沢顕、鈴木健、上坂友洋、若杉昌徳、山田一成、山口貴之、山口由高、「稀少 RI リングの共鳴ショットキーピックアップ設計のための電磁場シミュレーション」日本物理学会 2013 年秋季大会、高知市、9 月 (2013).
洲嵜ふみ、銭廣十三、小沢顕、鈴木健、上坂友洋、若杉昌徳、山田一成、山口貴之、山口由高、「稀少 RI リングの共鳴ショットキーピックアップの性能試験」日本物理学会第 69 回年次大会、平塚市、3 月 (2014).

Posters Presentations

[International Conference etc.]

H. Miura and rare-RI ring collaborators, “Development of a Fast Kicker System for Rare-RI RIng”, 13th International Conference on Heavy Ion Accelerator Technology, Yokohama, Japan, September (2015).
F. Suzaki and rare-RI ring collaborators, “Performance of a resonant Schottky pick-up in the commissioning of Rare-RI Ring”, 13th International Conference on Heavy Ion Accelerator Technology, Yokohama, Japan, September (2015).
Z. Ge and rare-RI ring collaborators, “Rare-RI Ring at RIKEN”, The 13th International Symposium on Origin of Matter and Evolution of Galaxies, Beijing, China, June (2015).
Y. Yamaguchi, H. Miura, M. Wakasugi, Y. Abe, A. Ozawa, F. Suzaki, A. Tokuchi, T. Uesaka, T. Yamaguchi, and Y. Yano, “Fast-kicker system for Rare-RI Ring”, 9th International Conference on Nuclear Physics at Storage Rings, St. Goar, Germary, September (2014).
F. Suzaki, J. Zenihiro, A. Ozawa, T. Suzuki, T. Uesaka, M. Wakasugi, K. Yamada, T. Yamaguchi, Y. Abe, and Y. Yamaguchi, “A resonant Schottky pick-up for Rare-RI Ring at RIKEN”, 9th International Conference on Nuclear Physics at Storage Rings, St. Goar, Germany, September (2014).
F. Suzaki, J. Zenihiro, A. Ozawa, T. Suzuki, T. Uesaka, M. Wakasugi, K. Yamada, T. Yamaguchi, Y. Abe, and Y. Yamaguchi, “Performance of a resonant Schottky pick-up for Rare-RI Ring project”, 2nd Conference on Advances in Radioactive Isotope Science, Tokyo, Japan, June (2014).
Y. Abe, and D. Nagae, “Developments of time-of-flight detectors for Rare-RI Ring”, The 12th Asia Pacific Physics Conference, Chiba, Japan, July (2013).
T. Yamaguchi, F. Suzaki, and rare-RI ring collaborators, “Storage-ring mass spectrometry in Japan”, The 12th Asia Pacific Physics Conference, Chiba, Japan, July (2013).
T. Yamaguchi, “Cherenkov light detection as a velocity selector for uranium fission products at intermediate energies”, 8th International workshop on Ring imaging Cherenkov Detectors, Hayama, Japan, Desember (2013).

[Domestic Conference]

山口由高、若杉昌徳、阿部康志、洲嵜ふみ、藤縄雅、加瀬昌之、込山美咲、熊谷桂子、眞家武士、長江大輔、大西純一、小沢顕、上坂友洋、渡邉裕、山口貴之、山澤秀行、柳澤善行、銭廣十三、矢野安重、「理研 RIBF における稀少 RI リングの現状」第 11 回日本加速器学会年会、青森市、8 月 (2014).

RIBF Research Division
Instrumentation Development Group
SCRIT Team

1. Abstract

The SCRIT Electron Scattering Facility has been constructed at RIKEN RIBF. This aims at investigation of internal nuclear structure for short-lived unstable nuclei by means of electron scattering. SCRIT (Self-Confining RI Ion Target) is a novel method to form internal targets in an electron storage ring. This is a unique method for making electron scattering experiments for unstable nuclei possible. Construction of the facility has been started in 2009. This facility consists of an electron accelerator (RTM), a SCRIT-equipped electron storage ring (SR2), an electron-beam-driven RI separator (ERIS), and a detector system consisting of a high-resolution magnetic spectrometer, drift chambers and trigger scintillators. Installation of all components in the facility was completed in 2015, and it is now under comprehensive test experiment phase. In the test experiments, the luminosity was reached to 3×10^{27} /(cm^2s) with the number of injected ions of 3×10^8, and we successfully measured a diffraction pattern in the angular distribution of scattered electrons from ^{132}Xe isotope and determined the charge density distribution for the first time. The facility is now under setting up to move the first experiment for unstable nuclei.

2. Major Research Subjects

Development of SCRIT electron scattering technique and measurement of the nuclear charge density distributions of unstable nuclei.

3. Summary of Research Activity

SCRIT is a novel technique to form internal target in an electron storage ring. Positive ions are three dimensionally confined in the electron beam axis by transverse focusing force given by the circulating electron beam and applied electrostatic longitudinal mirror potential. The created ion cloud composed of RI ions injected from outside works as a target for electron scattering. Construction of the SCRIT electron scattering facility has been started in 2009. The electron accelerators RTM and the storage ring SR2 were successfully commissioned in 2010. Typical accumulation current in SR2 is 250-300 mA at the energy range of 100-300 MeV that is required energy range in electron scattering experiment. The SCRIT device was inserted in the straight section of SR2 and connected to an ISOL named ERIS (Electron-beam-driven RI separator for SCRIT) by 20-m long low energy ion transport line. A buncher system based on RFQ linear trap was inserted in the transport line to convert the continuous beam from ERIS to pulsed beam, which is acceptable for SCRIT. A detector system consisting of a high-resolution magnetic spectrometer, drift chambers and trigger schintillators was constructed, and this has a solid angle of 100 msr, energy resolution of 10^{-3}, and the scattering angle coverage of 25-55 degrees. A wide range of momentum transfer, 80-300 MeV/c, is covered by changing the electron beam energy from 150 to 300 MeV. Installation of all the components in the facility has been completed in last year, and we are now under comprehensive test experiments.

We successfully measured a diffraction pattern in the angular distribution of scattered electron from ^{132}Xe isotope at the electron beam energy of 150MeV, 200MeV, and 300MeV, and derived the nuclear charge distribution by assuming two-parameters Fermi model for the first time. At this time luminosity was reached to 3×10^{27}/(cm^2s) at maximum and the averaged value was 1.2×10^{27}/(cm^2s) with the number of injected target ions of 3×10^8.

We are now under preparation for going to the experiments for unstable nuclei. There are some key issues for that. They are increasing the intensity of the RI beams from ERIS, efficient DC-to-pulse conversion at the buncher, and effective suppression of the background in measurement of scattered electrons. RI beam intensity will be improved by upgrading the electron beam power from 10W to 60W, increasing the contained amount of U in the target ion source, and some modifications in mechanical structure in the ion source. For efficient DC-to-pulse conversion, we will innovate two-step bunching method, which is time compression at the buncher in combination with pre-bunching at the ion source using grid action, and was already demonstrated in off-line test. Since one of significant contribution to the background for scattered electron is scattering from massive structural objects around the trapping region originated from halo components of the electron beam, we will remodel the SCRIT electrodes. Luminosity for radioactive Xe isotopes is expected to be more than 10^{26}/(cm^2s) after these improvements. Then, we will be able to start experiments for unstable nuclei. When further upgrading in the RTM power planed to be 3kW will be achieved, we can extend the measurements to more exotic nuclei.

Members

Team Leader

Masanori WAKASUGI (concurrent; Group Director, Instrumentations Development Gr.)

Research & Technical Scientists

Masamitsu WATANABE (Senior Research Scientist)
Tetsuya OHNISHI (Senior Technical Scientist)

Research Consultants

Tadaaki TAMAE
Shin-ichi ICHIKAWA
Masahiro HARA
Takashi EMOTO

Senior Visiting Scientist
Toshitada HORI (Hiroshima Univ.)

Visiting Scientists
Shuo WANG (Tohoku Univ.)
Kyo TSUKADA (Tohoku Univ.)
Toshimi SUDA (Tohoku Univ.)
Akitomo ENOKIZONO (Rikkyo Univ.)
Kazuyoshi KURITA (Rikkyo Univ.)

Student Trainees
Kohei YAMADA (Rikkyo Univ.)
Takahiro FUJITA (Rikkyo Univ.)
Nobuaki UCHIDA (Rikkyo Univ.)
Kousuke ADACHI (Rikkyo Univ.)
Mitsuki HORI (Rikkyo Univ.)
Shin-nosuke SASAMURA (Rikkyo Univ.)

List of Publications & Presentations

Publications

[Proceedings]

(Original Papers) *Subject to Peer Review

M. Togasaki, K. Kurita, K. Yamada, R. Toba, M. Hara, T. Ohnishi, and M. Wakasugi, “Development of a buffer-gas-free buncher for low energy RI ion beam”, HIAT2015 proceedings, 253 (2015).

T. Ohnishi, S. Ichikawa, and M. Wakasugi, “Electron-beam-driven RI separator for SCRIT at RIKEN RI Beam Factory”, HIAT2015 proceedings, 194 (2015).

T. Ohnishi, A. Enokizono, M. Hara, T. Hori, S. Ichikawa, K. Kurita, S. Matsuo, T. Suda, T. Tamae, M. Togasaki, K. Tsukada, T. Tsuru, S. Wang, S. Yoneyama, and M. Wakasugi, “The SCRIT electron scattering facility project at RI Beam Factory”, Physca Scripta, T166 , 014071 (2015).*

T. Suda, A. Enokizono, M. Hara, Y. Haraguchi, S. Ichikawa, K. Kurita, S. Matsuo, T. Ohnishi, T. Tamae, M. Togasaki, K. Tsukada, T. Tsuru, S. Wang, S. Yoneyama, and M. Wakasugi, “SCRIT Electron Scattering Facility”, JPS Conf. Proc. 6, 030100 (2015).*

T. Suda, “Electron Scattering for Exotic Nuclei”, Pramana Journal of Physics 83, 739-747 (2014).

若杉昌徳、大西哲哉、須田利美、栗田和好、”不安定核構造を映す電子顕微鏡をつくる”、日本物理学会誌、68, 810 (2013).*

M. Wakasugi, T. Ohnishi, S. Wang, Y. Miyashita, T. Adachi, T. Amagai, A. Enokizono, A. Enomoto, Y. Haraguchi, M. Hara, T. Hori, S. Ichikawa, T. Kikuchi, R. Kitazawa, K. Koizumi, K. Kurita, T. Miyamoto, R. Ogawara, Y. Shimakura, H. Takehara, T. Tamae, S. Tamaki, M. Togasaki, T. Yamaguchi, K. Yanagi, and T. Suda, “Construction of the SCRIT electron scattering facility at the RIKEN RI Beam Factory”, Nucl. Instrum. Meth., B317, 668-673 (2013).*

T. Ohnishi, S. Ichikawa, K. Koizumi, K. Kurita, Y. Miyashita, R. Ogawara, S. Tamaki, M. Togasaki, and M. Wakasugi, “Electron-beam-driven RI separator for SCRIT (ERIS) at RIKEN RI beam factory”, Nucl. Instrum. Meth., B317, 357-360 (2013).*

R. Ogawara, T. Ohnishi, M. Togasaki, S. Tamaki, Y. Miyashita, H. Takehara, K. Koizumi, K. Kurita, and M. Wakasugi “Ion-trapping properties of SCRIT”, Nucl. Instrum. Meth., B317, 674-678 (2013).*

Oral Presentations

[International Conference etc.]

M. Wakasugi, “The SCRIT Facility at RIKEN”, Int. Workshop on Electron Radioactive Collision, Apr. 25-27, CEA Saclay, France (2016).

M. Wakasugi, T. Ohnishi, W. Watanabe, S. Ichikawa, M. Hara, T. Hori, M. Togasaki, K. Yamada, T. Fujita, K. Adachi, M. Hori, A, Enokizono, K. Kurita, K. Tsukada, T. Tamae, and T. Suda, “Current status of electron-RI collision project at RIKEN“, Int. Workshop on Beem Cooling and Related Topics COOL15, Sep.28-Oct.2, JLab Newport News, Virginia, USA (2015).

T. Ohnishi, A. Enokizono, M. Hara, T. Hori, S. Ichikawa, K. Kurita, S. Matsuo, T. Suda, T. Tamae, M. Togasaki, K. Tsukada, T. Tsuru, S. Wang, S. Yoneyama, and M. Wakasugi, “The SCRIT electron scattering facility project at RI Beam Factory”, 9th Int. Conf. on Nuclear Physics at Storage Ring, Sep.28-Oct.2, Schloss Rheinfels, St. Goar, Germany (2015).

M. Wakasugi, “The SCRIT Electron Scattering Facility at RIKEN RI Beam Factory”, 5th EURISOL User Group Topical Meeting, Jun.15-17, York, UK (2014).

M. Wakasugi, T. Ohnishi, W. Watanabe, S. Ichikawa, M. Hara, T. Hori, M. Togasaki, Y, Matsuo, K. Yamada, A, Enokizono, K. Kurita, S, Yoneyama, T. Tsuru, Y. Moriya, K. Tsukada, T. Tamae, and T. Suda, R. Toba, and T. Kikuchi, “The SCRIT Electron Scattering Facility“, 6th Int. Conf. on Trapped Charged Particles and Fundamental Phtsics, Takamatsu, Japan (2014).

T. Suda, “Electron Scattering for Exotic Nuclei”, Int. DAE Symposium on Nuclear Physics, Dec. 4, Munbaim India (2013).

T. Suda, “Electron Scattering and Photonuclear Reaction for Short-Lived Nuclei”, JUSTIPEN-JUSEIPEN Int. Workshop, Dec. 9, Wako, Japan (2013).

M. Wakasugi, T. Ohnishi, S. Wang, Y. Miyashita, T. Adachi, T. Amagai, A. Enokizono, A. Enomoto, Y. Haraguchi, M. Hara, T. Hori, S. Ichikawa, T. Kikuchi, R. Kitazawa, K. Koizumi, K. Kurita, T. Miyamoto, R. Ogawara, Y. Shimakura, H. Takehara, T. Tamae, S. Tamaki, M. Togasaki, T. Yamaguchi, K. Yanagi, and T. Suda, “Construction of the SCRIT electron scattering facility at the RIKEN RI Beam Factory”, Dec. 2-7, Matsue, Japan (2012).

[Domestic Conference]

塚田暁、足立江介、市川進一、榎園昭智、大西哲哉、栗田和好、須田利美、玉江忠明、水流輝明、戸ケ崎衛、原雅弘、藤田峻広、堀利匡、堀充希、松田一衛、山田耕平、若杉昌徳、渡邊正満、”SCRIT 法を用いたXe 同位体標的における電子散乱の角度分布測定“、日本物理学会、3月、東北学院大、仙台(2016).

榎園昭智、足立江介、市川進一、大西哲哉、栗田和好、須田利美、玉江忠明、塚田暁、水流輝明、戸ケ崎衛、原雅弘、藤田峻広、堀利匡、堀充希、松田一衛、山田耕平、若杉昌徳、渡邊正満、”SCRIT 法を用いた電子・不安定Xe 核散乱実験におけるルミノシティの測定“、日本物理学会、3月、東北学院大、仙台(2016).

塚田暁、市川進一、榎園昭智、大西哲哉、栗田和好、須田利美、玉江忠明、水流輝明、戸ケ崎衛、原雅弘、藤田峻広、堀利匡、松田一衛、山

田耕平、若杉昌徳、渡邊正満、”SCRIT 法を用いた電子・不安定核散乱実験に向けた電子スペクトロメータのアクセプタンス評価“、日本物理学会、9月、大阪市立大、大阪(2015).

榎園昭智、足立江介、市川進一、大西哲哉、栗田和好、須田利美、玉江忠明、塚田暁、水流輝明、戸ケ崎衛、原雅弘、藤田峻広、堀利匡、松田一衛、山田耕平、若杉昌徳、渡邊正満、”SCRIT 法を用いた電子・不安定核散乱実験に向けたルミノシティ決定精度の評価“、日本物理学会、9月、大坂市立大、大坂(2015).

戸ケ崎衛、大西哲哉、栗田和好、鳥羽瞭太、原雅弘、山田耕平、若杉昌徳、“イオンビームクーラー・バンチャーの開発”、日本物理学会、9月、大坂市立大、大坂(2015).

塚田暁、市川進一、榎園昭智、大西哲哉、栗田和好、須田利美、玉江忠明、水流輝明、戸ケ崎衛、堀利匡、原雅弘、松尾咲希、松田一衛、森谷洋祐、米山俊平、若杉昌徳、”SCRIT 電子スペクトロメータの運動量分解能とアクセプタンス評価“、日本物理学会、3月、早稲田大、東京(2015).

米山俊平、榎園昭智、大西哲哉、栗田和好、須田利美、玉江忠明、塚田暁、水流輝明、戸ケ崎衛、松尾咲希、松田一衛、森谷洋祐、若杉昌徳、”SCRIT 実験用ルミノシティーモニタ“、日本物理学会、3月、早稲田大、東京(2015).

松尾咲希、市川進一、榎園昭智、大西哲哉、栗田和好、須田利美、玉江忠明、塚田暁、水流輝明、戸ケ崎衛、原雅弘、堀利匡、松田一衛、森谷洋祐、米山俊平、若杉昌徳、”SCRIT 実験における散乱電子スペクトロメータの開発“、日本物理学会、3月、早稲田大、東京(2015).

K. Tukada, T. Miyamoto, T. Suda, T. Tsuru, S. Yoneyama, M. Hara, T. Hori, S. Ichikawa, T. Ohnishi, M. Wakasugi, A. Enokizono, K. Kurita, S. Matsuo, Y. Shimakura, M. Togasaki, Y. Haraguchi, and S. Wang, “SCRIT Electron Scattering Facility”, Japan-US joint Phys. Soc. Meeting, Sep. Hawai, USA (2014).

Posters Presentations

[International Conference etc.]

M. Togasaki, K. Kurita, K. Yamada, R. Toba, M. Hara, T. Ohnishi, and M. Wakasugi, “Development of a buffer-gas-free buncher for low energy RI ion beam”, 13th Int. Conf. on Heavy Ion Accelerator Technorogy HIAT2015, Sep. 7-11, Yokohama, Japan (2015).

T. Ohnishi, S. Ichikawa, and M. Wakasugi, “Electron-beam-driven RI separator for SCRIT at RIKEN RI Beam Factory”, 13th Int. Conf. on Heavy Ion Accelerator Technorogy HIAT2015, Sep. 7-11, Yokohama, Japan (2015).

T. Suda, A. Enokizono, M. Hara, Y. Haraguchi, S. Ichikawa, K. Kurita, S. Matsuo, T. Ohnishi, T. Tamae, M. Togasaki, K. Tsukada, T. Tsuru, S. Wang, S. Yoneyama, and M. Wakasugi, “SCRIT Electron Scattering Facility”, 2nd Int. Conf. on Advances in Radioactive Isotope Science, Jun. 1-6, Tokyo, Japan (2014).

T. Ohnishi, S. Ichikawa, K. Koizumi, K. Kurita, Y. Miyashita, R. Ogawara, S. Tamaki, M. Togasaki, and M. Wakasugi, “Electron-beam-driven RI separator for SCRIT (ERIS) at RIKEN RI beam factory”, 16th IUPAP Int. Conf. on Electromagnetic Isotope Separators and Techniques Related to Their Applications, Dec. 2-7, Matsue, Japan (2012).

R. Ogawara, T. Ohnishi, M. Togasaki, S. Tamaki, Y. Miyashita, H. Takehara, K. Koizumi, K. Kurita, and M. Wakasugi “Ion-trapping properties of SCRIT”, 16th IUPAP Int. Conf. on Electromagnetic Isotope Separators and Techniques Related to Their Applications, Dec. 2-7, Matsue, Japan (2012).

RIBF Research Division
Research Instruments Group

1. Abstract

The research instruments group is the driving force at RI Beam Factory (RIBF) for continuous enhancement of activities and competitiveness of experimental research. Consisting of four teams, we are in charge of the construction, operation and improvement of the core research instruments at RIBF, such as BigRIPS in-flight separator, ZeroDegree spectrometer and SAMURAI spectrometer, and the related infrastructure and equipment. We are also in charge of the production and delivery of RI beams using the BigRIPS separator. The group also conducts related experimental research as well as R&D studies on the research instruments.

2. Major Research Subjects

Design, construction, operation and improvement of the core research instruments at RIBF and related R&D studies. Experimental studies on exotic nuclei.

3. Summary of Research Activity

The current research subjects are summarized as follows:
(1) Production and delivery of RI beams and related research
(2) Design, construction, operation and improvement of the core research instruments at RIBF and their related infrastructure and equipment
(3) R&D studies on the core research instruments and their related equipment at RIBF
(4) Experimental research on exotic nuclei using the core research instruments at RIBF

Members

Group Director
Toshiyuki KUBO

Junior Research Associates
Daichi MURAI (Rikkyo Univ.)
Momo MUKAI (Tsukuba Univ.)

Part-time Worker
Meiko UESAKA (– Mar. 31, 2015)

Senior Visiting Scientist
Toshio KOBAYASHI (Tohoku Univ.)

Student Trainee
Katrina Elizabeth KOEHLER (West Michigan University)

RIBF Research Division
Research Instruments Group
BigRIPS Team

1. Abstract

This team is in charge of design, construction, development and operation of BigRIPS in-flight separator and its related research instruments at RI beam factory (RIBF). They are employed not only for the production of RI beams but also the experimental studies using RI beams.

2. Major Research Subjects

Design, construction, development and operation of BigRIPS in-flight separator, RI-beam transport lines, and their related research instruments

3. Summary of Research Activity

This team is in charge of design, construction, development and operation of BigRIPS in-flight separator, RI-beam transport lines, and their related research instruments such as ZeroDegree spectrometer at RI beam factory (RIBF). They are employed not only for the production of RI beams but also various kinds of experimental studies using RI beams.
The research subjects may be summarized as follows:
(1) General studies on RI-beam production using in-flight scheme.
(2) Studies on ion-optics of in-flight separators, including particle identification of RI beams
(3) Simulation and optimization of RI-beam production.
(4) Development of beam-line detectors and their data acquisition system.
(5) Experimental studies on production reactions and unstable nuclei.
(6) Experimental studies of the limits of nuclear binding.
(7) Development of superconducting magnets and their helium cryogenic systems.
(8) Development of a high-power production target system.
(9) Development of a high-power beam dump system.
(10) Development of a remote maintenance and remote handling systems.
(11) Operation, maintenance and improvement of BigRIPS separator system, RI-beam transport lines, and their related research instruments such as ZeroDegree spectrometer and so on.
(12) Experimental research using RI beams.

Members

Team Leader
Koichi YOSHIDA

Research & Technical Scientists
Yoshiyuki YANAGISAWA (Senior Research Scientist)
Naohito INABE (Senior Technical Scientist)
Masao OHTAKE (Senior Technical Scientist)
Kanenobu TANAKA (Senior Technical Scientist, concurrent; Deputy Group Director, Safety Management Gr.)

Nishina Center Research Scientists
Hiroyuki TAKEDA
Kensuke KUSAKA
Naoki FUKUDA

Contract Researcher
Toshiyuki SUMIKAMA (Apr. 1, 2015 –)
Yohei SHIMIZU (Jan. 1, 2015 –)

Postdoctoral Researchers
Hiroshi SUZUKI
Deuk Soon AHN
Zeren KORKULU (May 1, 2015 –)

International Program Associate
Ha JEONGSU (Seoul National University, Apr. 1, 2015 – Aug. 30, 2015)

Part-time Worker
Tetsuro KOMATSUBARA (Jun. 1, 2015 –)

Research Consultant
Hidekazu KUMAGAI (Apr. 1, 2014 –)

Senior Visiting Scientist
Jerry NOLEN (Argonne National Lab.)

Visiting Scientists
Daisuke KAMEDA (TOSHIBA Corp.)
Michael A. FAMIANO (Western Michigan Univ.)
Daniel Pierre BAZIN (NSCL, MSU)
Oleg Borisovich TARASOV (NSCL, MSU)
Hans GEISSEL (GSI)
David Joseph MORRISSEY (NSCL, MSU)
Bradley Marc SHERRILL (NSCL, MSU)
Martin Alfred WINKLER (GSI)
Mauricio PORTILLO (NSCL, MSU)
Dogyun KIM (IBS)
Eunhee KIM (IBS)
Alan Matthew AMTHOR (Bucknell Univ.)
Yutaka MIZOI (Osaka Elec.-Com. Univ.)
Naohito IWASA (Tohoku Univ.)
Sadao MOMOTA (Kochi Univ. of Tech.)
Kazuo IEKI (Rikkyo Univ.)

Student Trainees
Kousei ASADA (Tohoku Univ.)
Ha JEONGSU (Seoul National University)

List of Publications & Presentations

Publications

[Journal]

(Original Papers) *Subject to Peer Review

G. Lorusso, S. Nishimura, Z. Y. Xu, A. Jungclaus, Y. Shimizu, G. S. Simpson, P.-A. Söderström, H. Watanabe, F. Browne, P. Doornenbal, G. Gey, H. S. Jung, B. Meyer, T. Sumikama, J. Taprogge, Zs. Vajta, J. Wu,H. Baba, G. Benzoni, K. Y. Chae, F. C. L. Crespi, N. Fukuda, R. Gernhäuser, N. Inabe, T. Isobe, T. Kajino, D. Kameda, G. D. Kim, Y.-K. Kim, I. Kojouharov, F. G. Kondev, T. Kubo, N. Kurz,Y. K. Kwon, G. J. Lane, Z. Li, A. Montaner-Pizá, K. Moschner, F. Naqvi, M. Niikura, H. Nishibata, A. Odahara, R. Orlandi, Z. Patel, Zs. Podolyák, H. Sakurai, H. Schaffner, P. Schury, S. Shibagaki, K. Steiger,H. Suzuki, H. Takeda, A. Wendt, A. Yagi, and K. Yoshinaga, "β-Decay Half-Lives of 110 Neutron-Rich Nuclei across the N = 82 Shell Gap: Implications for the Mechanism and Universality of the Astrophysical r Process", Physical Review Letter 114, 192501, (2015).*

J. Taprogge, A. Jungclaus, H. Grawe, S. Nishimura, P. Doornenbal, G. Lorusso, G. S. Simpson, P.-A. Söderström, T. Sumikama, Z. Y. Xu, H. Baba, F. Browne, N. Fukuda, R. Gernhäuser, G. Gey, N. Inabe, T. Isobe, H. S. Jung, D. Kameda, G. D. Kim, Y.-K. Kim, I. Kojouharov, T. Kubo, N. Kurz, Y. K. Kwon, Z. Li, H. Sakurai, H. Schaffner, K. Steiger, H. Suzuki, H. Takeda, Zs. Vajta, H. Watanabe, J. Wu, A. Yagi, K. Yoshinaga, G. Benzoni, S. Bönig, K. Y. Chae, L. Coraggio, A. Covello, J.-M. Daugas, F. Drouet, A. Gadea, A. Gargano, S. Ilieva, F. G. Kondev, T. Kröll, G. J. Lane, A. Montaner-Pizá, K. Moschner, D. Mücher, F. Naqvi, M. Niikura, H. Nishibata, A. Odahara, R. Orlandi, Z. Patel, Zs. Podolyák, and A. Wendt, "β decay of ^{129}Cd and excited states in ^{129}In", Physical Review C 91, 054324 (2015).*

P.Lee, C.-B.Moon, C.S.Lee, A.Odahara, R.Lozeva, A.Yagi, S.Nishimura, P.Doornenbal, G.Lorusso, P-A.Söderström, T, Sumikama, H.Watanabe, T.Isobe, H.Baba, H.Sakurai, F.Browne, R.Daido, Y.Fang, H.Nishibata, Z.Patel, S.Rice, L.Sinclair, J.Wu, Z.Y.Xu, R.Yokoyama. T.Kubo, N.Inabe, H.Suzuki, N.Fukuda, D.Kameda, H.Takeda, D.S.Ahn, D.Murai, F.L.Bello Garrote, J.M.Daugas, F.Didierjean, E.Ideguchi, T.Ishigaki, H.S.Jung, T.Komatsubara, Y.K.Kwon, S.Morimoto, M.Niikura, I.Nishizuka, and K.Tshoo, "β-delayed γ-ray spectroscopy on non-yrast states in ^{138}Te near the neutron drip line", Physical Review C92, 044320 (2015).*

R. Lozeva, A. Odahara, C.-B. Moon, S. Nishimura, P. Doornenbal, H. Naïdja, F. Nowacki, P.-A. Söderström, T. Sumikama, G. Lorusso, J. Wu, Z. Y. Xu, H. Baba, F. Browne, R. Daido, J.-M. Daugas, F. Didierjean, Y. Fang, T. Isobe, I. Kojouharov, N. Kurz, Z. Patel, S. Rice, H. Sakurai, H. Schaffner, L. Sinclair, H. Watanabe, A. Yagi, R. Yokoyama, T. Kubo, N. Inabe, H. Suzuki, N. Fukuda, D. Kameda, H. Takeda, D. S. Ahn, D. Murai, F. L. Bello Garrote, E. Ideguchi, T. Ishigaki, H. S. Jung, T. Komatsubara, Y. K. Kwon, S. Morimoto, M. Niikura, H. Nishibata, I. Nishizuka, T. Shimoda, and K. Tshoo, "New decay scheme of the $^{136}_{51}Sb_{85}$ 6$^-$ isomer", Physical Review C92, 024304(2015).*

F.Browne, A.M.Bruce, T.Sumikama, I.Nishizuka, S.Nishimura, P.Doornenbal, G.Lorusso, P.-A.Söderström, H.Watanabe, R.Daido, Z.Patel, S.Rice, L.Sinclair, J.Wu, Z.Y.Xu, A.Yagi, H.Baba, N.Chiga, R.Carroll, F.Didierjean, Y.Fang, N.Fukuda, G.Gey|, E.Ideguchi, N.Inabe, T.Isobe, D.Kameda, I.Kojouharov, N.Kurz, T.Kubo, S.Lalkovski, Z.Li, R.Lozeva, H.Nishibata, A.Odahara, Zs.Podolyák, P.H.Regan, O.J.Roberts, H.Sakurai, H.Schaffner, G.S.Simpson, H.Suzuki, H.Takeda, M.Tanaka, J.Taprogge, V.Werner, O.Wieland, "Lifetime measurements of the first 2+states in 104,106Zr: Evolution of ground-state deformation", Physics Letter B750, 448, (2015).*

[Proceedings]

(Original Papers) *Subject to Peer Review

K. Kusaka, M. Ohtake, K. Tanaka, K. Yoshida, and, T. Kubo, "Beam heat loads to superconducting quadrupoles for BigRIPS In-flight separator at RIKEN", IEEE Transactions on Applied Superconductivity, Vol. 25, 4100404, (2015).*

Yuki SATO, Naoki FUKUDA, Hiroyuki TAKEDA, Daisuke KAMEDA, Hiroshi SUZUKI , Yohei SHIMIZU, DeukSoon AHN, Daichi MURAI, Naohito INABE, Takehiro SHIMAOKA, Masakatsu TSUBOTA, Junichi H. KANEKO, Akiyoshi CHAYAHARA, Hitoshi UMEZAWA, Shinichi SHIKATA, Hidekazu KUMAGAI, Hiroyuki MURAKAMI, Hiromi SATO, Koichi YOSHIDA, and Toshiyuki KUBO, "Status of beam line detectors for the BigRIPS fragment separator at RIKEN RI Beam Factory: issues on high rates and resolution", JPS Conference Proceedings 6, 030124 (2015).*

Oral Presentations

[International Conference etc.]

T. Kubo, "Recent Progress of in-flight separators and rare isotope production", International Conference on Electromagnetic Isotope Separators and Related Topics (EMIS 2015) at Grand Rapids, USA, May 11 - 15, 2015.*

D.S.Ahn, N. Fukuda, T. Kubo, H. Geissel, H. Suzuki, Y. Shimizu, H. Takeda, D. Murai, N. Inabe K. Yoshida, O. Tarasov, "Operational

Experiences in Particle Identification and Isotope Separation with BigRIPS In-flight Separator", International Conference on Electromagnetic Isotope Separators and Related Topics (EMIS 2015) at Grand Rapids, USA, May 11 - 15, 2015.*

T. Sumikama, D.S. Ahn,, N. Fukuda, N. Inabe, T. Kubo, Y. Shimizu, H. Suzuki, H. Takeda, N. Aoi, D. Beaumel, K. Hasegawa, E. Ideguchi, N. Imai, T. Kobayashi, S. Michimasa, M. Matsushita, H. Otsu, T. Teranishi, "First production test of slowed-down RI beam at RIBF", International Conference on Electromagnetic Isotope Separators and Related Topics (EMIS 2015), Grand Rapids, MI, USA, May 11 - 15, 2015.*

[Domestic Conference]

横山輪, 井手口栄治, G. Simpson, 田中まな, 西村俊二, P. Doornenbal, P-A Söderström, G. Lorusso, Z. Y. Xu, J. Wu, 炭竈聡之, 青井考, 馬場秀忠, F. Bello, F. Browne, 大道理恵, Y. Fang, 福田直樹, G. Gey, 郷慎太郎, 稲辺尚人, 磯部忠昭, 亀田大輔, 小林和馬, 小林幹, 小松原哲郎, 久保敏幸, I. Kuti, Z. Li, 松下昌史, 道正新一郎, C.-B. Moon, 西畑洸希, 西塚一平, 小田原厚子, Z. Patel, S. Rice, Sahin, L. Sinclair, 鈴木宏, 竹田浩之, J. Taprogge, E. Z. Vajta, 渡邉寛, 八木彩祐未**, "Investigation of the octupole correlation of neutron-rich Z〜56 isotopes by □-□ spectroscopy", 日本物理学会 第 70 回年次大会(2015), 早稲田大学、東京都、3/21 – 24, 2015.**

田中まな, 井手口栄治, G. Simpson, 横山輪, 西村俊二, P. Doornenbal, G. Lorusso, P.-A. Soderstrom, Z. Xu, J. Wu, 青井考, 馬場秀忠, F. Bello, F. Browne, 大道理恵, Y. Fang, 福田直樹, G. Gey, 郷慎太郎, 稲辺尚人, 磯辺忠昭, 亀田大輔, 小林和馬, 小林幹, 小松原哲郎, 久保敏幸, I. Kuti, Z. Li, 松下昌史, 道正新一郎, C.-B. Moon, 西畑洸希, 西塚一平, 小田原厚子, Z. Patel, S. Rice, E. Sahin, L. Sinclair, 炭竈聡之, 鈴木宏, 竹田浩之, J. Taprogge, Zs. Vajta, 渡邉寛, 八木彩祐未**,「中性子過剰 Z〜60 同位体の β-γ 分光」, 日本物理学会 第 70 回年次大会(2015), 早稲田大学、東京都、3/21 – 24, 2015.**

齊藤敦美, 近藤洋介, 中村隆司, Nadia Lynda Achouri, Thomas Aumann, 馬場秀忠, Franck Delaunay, Pieter Doornenbal, 福田直樹, Julien Gibelin, Jongwon Huang, 稲辺尚人, 磯部忠昭, 亀田大輔, 簡野大輝, Sunji Kim, 小林信之, 小林俊雄, 久保敏幸, Sylvain Leblond, Jenny Lee, Miguel Marques, 南方亮吾, 本林透, 村井大地, 村上哲也, 武藤琴美, 中嶋丈嘉, 中塚徳継, Alahari Navin, 西征爾郎, 生越駿, Nigel AndrewOrr, 大津秀暁, 佐藤広海, 佐藤義輝, 清水陽平, 鈴木宏, 高橋賢人, 竹田浩之, 武内聡, 田中隆己, 栂野泰宏, Adam Garry Tuff, Marine Vandebrouck, 米田健一郎**,「中性子過剰 ^{19}B の相互作用断面積」, 日本物理学会 第 70 回年次大会(2015), 早稲田大学、東京都、3/21 – 24, 2015.**

栂野泰宏, 南方亮吾, 生越駿, 中村隆司, 磯部忠昭, 稲辺尚人, 大津秀暁, 亀田大輔, 簡野大輝, 久保敏幸, 小林俊雄, 小林信之, 近藤洋介, 佐藤広海, 佐藤義輝, 清水陽平, 鈴木宏, 高橋賢人, 武内聡, 竹田浩之, 田中隆己, 中嶋丈嘉, 中塚徳継, 西征爾郎, 福田直樹, 馬場秀忠, 武藤琴美, 村井大地, 村上哲也, 本林透, 米田健一郎, N. L. Achouri, A. G. Tuff, T. Aumann, F. Delaunay, J. Gibelin, J. Hwang, S. Kim, J. Lee, M. Marques, A.Navin, N. A. Orr, P. Doornenbal, S. Leblond, M. Vandebrouck,**「^{19,20,22}C の反応断面積」, 日本物理学会 第 70 回年次大会(2015), 早稲田大学、東京都、3/21 – 24, 2015.**

小林幹, 道正新一郎, 清川裕, 馬場秀忠, G.P.A. Berg, 堂園昌伯, 福田直樹, 古野達也, 井手口栄治, 稲辺尚人, 川畑貴裕, 川瀬頌一郎, 木佐森慶一, 小林和馬, 久保敏幸, 久保田悠樹, 李清秀, 松下昌史, 宮裕之, 水上淳, 永倉弘康, 西村太樹, 笈川浩之, 大田晋輔, 酒井英行, 下浦享, A. Stolz, 鈴木宏, 高木基伸, 竹田浩之, 武内聡, 時枝紘史, 上坂友洋, 矢向謙太郎, 山口勇貴, 柳澤善行, 横山輪, 吉田光一,**「中性子数 34 近傍カルシウム同位体の直接質量測定」,** 日本物理学会 2015 年秋季大会、大阪市立大学、大阪市、9/25 - 28, 2015

村井大地, 家城和夫, 久保敏幸, 稲辺尚人, 福田直樹, 竹田浩之, 鈴木宏, 安得順, 清水陽平, 佐藤広海, 佐藤優樹, 日下健祐, 柳澤善行, 大竹政雄, 吉田光一, 大津秀暁, 岩佐直仁, 中村隆司, Oleg B. Tarasov, Brad M. Sherrill, Dave J. Morrissey, Hans Geissel,**「大強度 ^{48}Ca ビームを用いた F 中性子ドリップラインの探索」,** 日本物理学会 2015 年秋季大会、大阪市立大学、大阪市、9/25 - 28, 2015

近藤洋介, 中村隆司, Nadia Lynda Achouri, Thomas Aumann, 馬場秀忠, Franck Delaunay, Pieter Doornenbal, 福田直樹, Julien Gibelin, Jongwon Hwang, 稲辺尚人, 磯部忠昭, 亀田大輔, 簡野大輝, Sunji Kim, 小林信之, 小林俊雄, 久保敏幸, Sylvain Leblond, Jenny Lee, Miguel Marques, 南方亮吾, 本林透, 村井大地, 村上哲也, 武藤琴美, 中嶋丈嘉, 中塚徳継, Alahari Navin, 西征爾郎, 生越駿, Nigel Andrew Orr, 大津秀暁, 佐藤広海, 佐藤義輝, 清水陽平, 鈴木宏, 高橋賢人, 竹田浩之, 武内聡, 田中隆己, 栂野泰宏, Adam Garry Tuff, Marine Vandebrouck, 米田健一郎,**「非束縛酸素同位体 ^{26}O の不変質量核分光」**, 日本物理学会 2015 年秋季大会、大阪市立大学、大阪市、9/25 - 28, 2015

清川裕, 道正新一郎, 小林幹, 西村太樹, 横山輪, 小林和馬, 水上淳, 笈川浩之, 馬場秀忠, G.P.A. Berg, 堂園昌伯, 福田直樹, 古野達也, 井手口栄治, 稲辺尚人, 川畑貴裕, 川瀬頌一郎, 木佐森慶一, 久保敏幸, 久保田悠樹, 李清秀, 松下昌史, 宮裕之, 永倉弘康, 大田晋輔, 酒井英行, 下浦享, A. Stolz, 鈴木宏, 高木基伸, 竹田浩之, 武内聡, 時枝紘史, 上坂友洋, 矢向謙太郎, 山口勇貴, 柳澤善行, 吉田光一,**「SHARAQ におけるアイソマー同定システムの開発」**, 日本物理学会 2015 年秋季大会、大阪市立大学、大阪市、9/25 - 28, 2015

横山輪, 井手口栄治, G. Simpson, 田中まな, 西村俊二, P. Doornenbal, P-A Söderström, G. Lorusso, Z. Y. Xu, J. Wu, 炭竈聡之, 青井考, 馬場秀忠, F. Bello, F. Browne, 大道理恵, Y. Fang, 福田直樹, G. Gey, 郷慎太郎, 稲辺尚人, 磯部忠昭, 亀田大輔, 小林和馬, 小林幹, 小松原哲郎, 久保敏幸, I. Kuti, Z. Li, 松下昌史, 道正新一郎, C.-B. Moon, 西畑洸希, 西塚一平, 小田原厚子, Z. Patel, S. Rice, Sahin, L. Sinclair, 鈴木宏, 竹田浩之, J. Taprogge, E. Z. Vajta, 渡邉寛, 八木彩祐未,「β-γ 核分光を用いた中性子過剰 La 同位体の変形」, 日本物理学会 2015 年秋季大会、大阪市立大学、大阪市、9/25 - 28, 2015

金岡裕志, 小田原厚子, R. Lozeva, C. Moon, 八木彩祐未, 方一帆, 大道理恵, 西畑洸希, P. Lee, 下田正, 西村俊二, P. Doornenbal, G. Lorusso, 炭竈聡之, 渡辺寛, P. Söderström, J. Wu, F. Brown, Z.Y. Xu, 横山輪, 磯部忠昭, 馬場秀忠, 櫻井博儀, 鈴木宏, 稲辺尚人, 亀田大輔, 福田直樹, 竹田浩之, 安得順, 清水陽平, 佐藤広海, 久保敏幸, 石垣知樹, 森本翔太, 井手口栄治, 小松原哲郎, 新倉潤, 西塚一平, C.S. Lee, and the EURICA collaborators,**「中性子過剰な親核 I の β 崩壊による中性子過剰な娘核 Xe の研究」,** 日本物理学会 2015 年秋季大会、大阪市立大学、大阪市、9/25 - 28, 2015

八木彩祐未, 小田原厚子, R. Lozeva, C. Moon, 方一帆, 大道理恵, 西畑洸希, 金岡裕志, P. Lee, 下田正, 西村俊二, P. Doornenbal, G. Lorusso, 炭竈聡之, 渡辺寛, P. Söderström, J. Wu, F. Brown, Z.Y. Xu, 横山輪, 磯部忠昭, 馬場秀忠, 櫻井博儀, 鈴木宏, 稲辺尚人, 亀田大輔, 福田直樹, 竹田浩之, 安得順, 清水陽平, 佐藤広海, 久保敏幸, 石垣知樹, 森本翔太, 井手口栄治, 小松原哲郎, 新倉潤, 西塚一平, C.S. Lee, and the EURICA collaborators,「*N*=90 近傍の中性子過剰な Xe と Cs 同位体の研究」, 日本物理学会 2015 年秋季大会、大阪市立大学、大阪市、9/25 - 28, 2015

園田哲, 和田道治, 飯村秀紀, 片山一郎, Reponen.M, 小島隆夫, Sonnenschein.V, 富田英生, 久保敏幸, 吉田光一, 稲辺尚人, 福田直樹, 竹田浩之, 鈴木宏, 日下健祐, 若杉昌徳, 新井重昭, 新井郁也, Schury.P, 伊藤由太, 宮武宇也, 石山博恒, 今井伸明, 平山賀一, 渡辺裕, 岡田邦宏,「RIBF におけるパラサイト低速 RI ビーム生成とガスジェットレーザー核分光の開発」, 日本物理学会 2015 年秋季大会、大阪市立大学、大阪市、9/25 - 28, 2015

Posters Presentations

[International Conference etc.]

Y. Shimizu, N. Fukuda, H. takeda, H. Suzuki, D.S. Ahn, T. Sumikama, D. Murai, N. Inabe, K. Yoshida, T. Kubo, "Status and overview of RI

beam production at BigRIPS separator", Physics with Fragment Separators – 25th anniversary of RIKEN Projectile Fragment Separator (RIPS25), December 6, 2015, Shonan Village Center, Kanagawa, Japan

RIBF Research Division
Research Instruments Group
SAMURAI Team

1. Abstract

In collaboration with research groups in and outside RIKEN, the team designs, develops and constructs the SAMURAI spectrometer and relevant equipment that are and will be used for reaction experiments using RI beams at RI Beam Factory. The SAMURAI spectrometer consists of a large superconducting dipole magnet and a variety of detectors to measure charged particles and neutrons. After the commissioning experiment in March 2012, the team prepared and conducted, in collaboration with researchers in individual experimental groups, the first series of experiments with SAMURAI in May 2012. Then, several numbers of experiments were well performed until now utilizing the property of SAMURAI. The team also provides basis for research activities by, for example, organizing collaboration workshops by researchers who are interested in studies or plan to perform experiments with the SAMURAI spectrometer.

2. Major Research Subjects

Design, operation, maintenance and improvement of the SAMURAI spectrometer and its related research instruments. Help and management for SAMURAI-based research programs.

3. Summary of Research Activity

The current research subjects are summarized as follows:

(1) Operation, maintenance and improvement of a large superconducting dipole magnet that is the main component of the SAMURAI spectrometer
(2) Design, development and construction of various detectors that are used for nuclear reaction experiments using the SAMURAI spectrometer.
(3) Preparation for planning experiments using SAMURAI spectrometer.
(4) Maintenance and improvement of the SAMURAI beam line.
(5) Formation of a collaboration platform called "SAMURAI collaboration"

Members

Team Leader
Hideaki OTSU

Visiting Scientist
Bertis Charles RASCO (Louisiana State Univ.)

List of Publications & Presentations

Publications

[Journal]

(Original Papers)

Y. Kondo, T.Nakamura, R.Tanaka, R.Minakata, S.Ogoshi, N.A.Orr, N.L.Achouri, T.Aumann, H.Baba, F.Delaunay, P.Doornenbal, N.Fukuda, J.Gibelin, J.W.Hwang, N.Inabe, T.Isobe, D.Kameda, D.Kanno, S.Kim, N.Kobayashi, T.Kobayashi, T.Kubo, S.Leblond, J.Lee, F.M.Marques, T.Motobayashi, D.Murai, T.Murakami, K.Muto, T.Nakashima, N.Nakatsuka, A.Navin, S.Nishi, H.Otsu, H.Sato, Y.Satou, Y.Shimizu, H.Suzuki, K.Takahashi, H.Takeda, S.Takeuchi, Y.Togano, A.G.Tuff, M.Vandebrouck, K.Yoneda, " Nucleus 26O: A Barely Unbound System beyond the Drip Line", Phys. Rev. Lett 116, 102503 (6pages) (2016).

H. Otsu, S. Koyama, N. Chiga, T. Isobe, T. Kobayashi, Y. Kondo, M. Kurokawa, W.G. Lynch, T. Motobayashi, T. Murakami, T. Nakamura, M. Kurata-Nishimura, V. Panin, H. Sato, Y. Shimizu, H. Sakurai, M.B. Tsang, K. Yoneda, H. Wang, "SAMURAI in its operation phase for RIBF", NIMB 376, (2016), 175-179.

J. Yasuda, M. Sasano, R.G.T. Zegers, H. Baba, W. Chao, M. Dozono, N. Fukuda, N. Inabe, T. Isobe, G. Jhang, D. Kameda, T. Kubo, M. Kurata-Nishimura, E. Milman, T. Motobayashi, H. Otsu, V. Panin, W. Powell, H. Sakai, M. Sako, H. Sato, et al., "Inverse kinematics (p,n) reactions studies using the WINDS slow neutron detector and the SAMURAI spectrometer",NIMB 376 (2016), 393-396.

T. Nakamura, Y. Kondo, "Large acceptance spectrometers for invariant mass spectroscopy of exotic nuclei and future developments", NIMB 376 (2016), 156-161.

(Review)

T. Motobayashi, "Study of weakly bound nuclei at RIKEN RIBF" , Few-Body Systems 57, 337-341 (2016).

Oral Presentations

[International Conference etc.]

T. Motobayashi, "Summary" , 12th International Conference on Nucleus-Nucleus Collisions (NN2015), June 21-26, 2015, Catania, Italy

V. Panin, "New generation of the experiments for the investigation of the stellar (p,γ) reaction rates using SAMURAI", Fifth International Conference on Proton-emitting Nuclei (PROCON2015), , Lanzhou, China, 6-10 July 2015.

V. Panin, “Progress report on Heavy-Ion-Proton project”, SAMURAI International Collaboration Workshop 2015, Wako, Saitama, 7-8 September 2015.
S. Koyama, “Study of cluster degree of freedom in neutron-rich sd-shell nuclei via alpha inelastic scattering”, SAMURAI International Collaboration Workshop 2015, Wako, Saitama, 7-8 September 2015.
H. Otsu, “Report on Day-two experiments”, SAMURAI International Collaboration Workshop 2015, Wako, Saitama, 7-8 September 2015.
M. Sasano, “Study of Gamow-Teller transitions in 132Sn”, International Conference, Nuclear Structure and Related Topics, Dubna, Russia, 14-18th July (2015). An invited talk.
M. Sasano, “Gamow-Teller transitions from 132Sn”, Collective motion in nuclei under extreme conditions, Krakow, Poland, 14-18th September (2015). An invited talk.
H. Otsu, “SAMURAI in its operation phase for RIBF”, International Conference on Electromagnetic Isotope Separator and Related Topics (EMIS 2015), Grand Raipids, MI, US, 11-15th May (2015).
J. Yasuda, “Slow neutron detector WINDS for (p,n) reaction in inverse kinematics with SAMURAI spectrometer”, International Conference on Electromagnetic Isotope Separator and Related Topics (EMIS 2015), Grand Raipids, MI, US, 11-15th May (2015).
Y. Kubota, “Probing multi-neutron correlation via knockout reaction”, Critical Stability in Few-Body Systems, Saitama, Japan, 26–30th January (2015).
Y. Kubota, “Direct measurement of two neutron correlation in 11Li via the (p,pn) reaction”, Critical Stability in Few-Body Systems, Saitama, Japan, 1–5th February (2016).
S. Reichert, "Study of fission barriers in neutron-rich nuclei using the (p,2p) reaction: Status of SAMURAI Experiment NP1306 SAMURAI14" at DPG Fruehjahrstagung, March 23-27, Heidelberg
S. Reichert, "Fission barrier in n-rich nuclei: Status of SAMURAI Experiment NP1306 SAMURAI14" at RA G Science Day at Max Planck Institute for Extraterrestic Physics, July 9, Munich
L. Stuhl, “Investigation of spin-isospin collectivity in asymmetric nuclear matter”, 14th CNS International Summer School (CNSS15), Wako, Saitama, Japan, 26th August – 1st September (2015).

[Domestic Conference]

大津　秀暁、”Particle/Gamma detectors in RIBF”, ELPH 研究会 C10、「素粒子・原子核実験における全吸収型カロリメーターの実例と応用」、東北大学 ELPH、2015 年 3 月 10 日
V. Panin, “Investigation of key nuclear reactions in the astrophysical rp-process using SAMURAI”, 70th JPS Annual meeting, Tokyo, Japan, 21-24 March 2015.
Y. Kondo, “Recent experimental studies using SAMURAI at RIBF”, Current Activities and Future Prospects on Unstable Nuclei: Japan-Korea Exchange Program (JPS meeting), Tohoku gakuin University, 21, March, 2016 (Invited)
笹野　匡紀, 「ノックアウト(p,2p)反応を用いた核分裂閾値エネルギーの測定」、日本物理学会 2015 年秋季大会、シンポジウム「重イオン深部非弾性散乱の基礎と応用」、大阪市立大学、2015 年 9 月 25 日 (招待・シンポジウム講演)
大津　秀暁, “Unbound states in neutron rich nuclei studied at SAMURAI”, 日本物理学会 2015 年秋季大会、シンポジウム「ドリップライン近傍のハイパー核と不安定核」、大阪市立大学、2015 年 9 月 27 日 (シンポジウム講演)
Y. Kondo, “Experimental study of unbound oxygen isotopes beyond the drip line”, International Workshop on "Critical Stability in Few-Body Systems", RIKEN, 4 Feb, 2016 (Invited)
Y. Kondo, “Invariant spectroscopy at RIPS and RIBF”, Physics with Fragment Separators - 25th Anniversary of RIKEN-Projectile Fragment Separator (RIPS25), Shonan Village center, December 6-7, 2015 (Invited)
近藤洋介, “Island of Inversion の南側”, 九大研究会　-中性子過剰領域における弱束縛系の物理- , 九州大学箱崎キャンパス, 2015 年 3 月 9, 10 日 (招待講演)
L. Stuhl, “Around the Nucleus”, JSPS Science Dialogue, Tochigi Prefectural Utsunomiya Girl’s Senior High School, Utsunomiya, Japan, 2nd October (2015).
Y. Kubota, "ボロミアン核(p,pn)反応を用いた二中性子運動量相関の研究", 70th JPS meeting, Tokyo, Japan, 25 - 28th March (2015).
Y. Kubota, "ボロミアン核(p,pn)反応を用いた二中性子運動量相関の研究", 71th JPS meeting, Miyagi, Japan, 19 - 22nd March (2016).
Y. Kondo, “Experimental study of unbound oxygen isotopes”, 「実験と観測で解き明かす中性子星の核物質」第 4 回研究会, 湘南国際村センター, 17-18, September, 2015
Y. Kondo, “Report on Day one experiments”, SAMURAI International Collaboration Workshop 2015, RIKEN, 7-8, September, 2015
近藤洋介, 中村隆司, Nadia Lynda Achouri, Thomas Aumann, 馬場秀忠, Franck Delaunay, Pieter Doornenbal, 福田直樹, Julien Gibelin, Jongwon Hwang, 稲辺尚人, 磯部忠昭, 亀田大輔, 簡野大輝, Sunji Kim, 小林信之, 小林俊雄, 久保敏幸, Sylvain Leblond, Jenny Lee, Miguel Marques, 南方亮吾, 本林透, 村井大地, 村上哲也, 武藤琴美, 中嶋丈嘉, 中塚徳継, Alahari Navin, 西征爾郎, 生越駿, Nigel Andrew Orr, 大津秀暁, 佐藤広海, 佐藤義輝, 清水陽平, 鈴木宏, 高橋賢人, 竹田浩之, 武内聡, 田中隆己, 栂野泰宏, Adam Garry Tuff, Marine Vandebrouck, 米田健一郎, “非束縛酸素同位体 26O の不変質量核分光”, 日本物理学会 2015 年秋季大会 大阪市立大学杉本キャンパス, 9 月 25 日- 29 日, 2015

Posters Presentations

[International Conference etc.]

L. Stuhl, “A new low-energy neutron detector for (p,n) experiments with pulse shape discrimination properties”, Collective motion in nuclei under extreme conditions, Krakow, Poland, 14-18th September (2015).

RIBF Research Division
Research Instruments Group
Computing and Network Team

1. Abstract

This team is in charge of development, management and operation of the computing and network environment, mail and information servers and data acquisition system and management of the information security of the RIKEN Nishina Center.

2. Major Research Subjects

(1) Development, management and operation of the general computing servers
(2) Development, management and operation of the mail and information servers
(3) Development, management and operation of the data acquisition system
(4) Development, management and operation of the network environment
(5) Management of the information security

3. Summary of Research Activity

This team is in charge of development, management and operation of the computing and network environment, mail and information servers and data acquisition system and management of the information security. The details are described elsewhere in this progress report.

(1) Development, management and operation of the general computing servers

We are operating Linux/Unix NIS/NFS cluster system for the data analysis of the experiments and general computing. This cluster system consists of eight computing servers with 64 CPU cores and totally 200 TB RAID of highly-reliable Fibre-channel interconnection. Approximately 600 user accounts are registered on this cluster system. We are adopting the latest version of the Scientific Linux (X86_64) as the primary operating system, which is widely used in the accelerator research facilities, nuclear physics and high-energy physics communities in the world. We have added a 52 TB RAID for the data analysis in the autumn of 2014 and replaced the ssh login server (RIBF00) in the winter of 2015.

(2) Development, management and operation of the mail and information servers

We are operating RIBF.RIKEN.JP server as a mail/NFS/NIS server. This server is a core server of RIBF Linux cluster system. Postfix has been used for mail transport software and dovecot has been used for imap and pop services. These software packages enable secure and reliable mail delivery. Sophos Email Security and Control (PMX) installed on the mail front-end servers tags spam mails and isolates virus-infected mails. The probability to identify the spam is approximately 95-99%. We are operating several information servers such as Web servers, Integrated Digital Conference (INDICO) server, Wiki servers, Groupware servers, Wowza streaming servers, and an anonymous FTP server (FTP.RIKEN.JP). A new Web server has been installed in April 2014 as an official Web server of RNC to replace the old Web server installed in 2005. A new 72 TB RAID was installed to replace the old RAID to the anonymous FTP server in August 2014. A research record server (RIBFDBOX) was installed, and is started operation in April 2015. This server consists of an HP DL-320e server, a 52 TB SAS RAID6 system, and Proself 4 software.

(3) Development, management and operation of the data acquisition system

We have developed the standard data-acquisition system named as RIBFDAQ. This system can process up to 40 MB/s data. By using parallel readout from front-end systems, the dead time could be small. To synchronize the independent DAQ systems, the time stamping system has been developed. The resolution and depth of the time stamp are 10 ns and 48 bit, respectively. This time stamping system is very useful for beta decay experiments such as EURICA and BRIKEN projects. The current main task is the DAQ coupling, because detector systems with dedicated DAQ systems are transported to RIBF from foreign facilities. In case of SAMURAI Silicon (NSCL/TUM/WUSTL), the readout system is integrated into RIBFDAQ. The projects of MUST2 (GANIL), MINOS (CEA Saclay), and NeuLAND (GSI) cases, data taken by their DAQ systems are transferred to RIBFDAQ. For SPIRIT (RIKEN/GANIL/CEA Saclay/NSCL), RIBFDAQ is controlled from the NARVAL-GET system that is a large-scale signal processing system for the time projection chamber. EURICA (GSI) and BRIKEN (GSI/Univ. Liverpool/IFIC) projects, we adopt the time stamping system to use individual trigger for each detector system. In this case, data are merged in offline. In addition to the development DAQ system, we are developing intelligent circuits based on FPGA. Mountable Controller (MOCO) is a very fast readout controller for VME modules. General Trigger Operator (GTO) is an intelligent triggering NIM module. Functions of “common trigger management”, “gate and delay generator”, “scaler” are successfully implemented on GTO.

(4) Development, management and operation of the network environment

We have been managing the network environment collaborating with Advanced Center for Computing and Communications (ACCC). All the Ethernet ports of the information wall sockets are capable of the Gigabit Ethernet connection (10/100/1000BT). In addition, a 10 Gbps network port has been introduced to the RIBF Experimental area in for the high speed data transfer of RIBF experiment to ACCC in near future. Approximately 60 units of wireless LAN access points have been installed to cover the almost entire area of Nishina Center.

(5) Management of the information security

It is essential to take proper information security measures for information assets.

We are managing the information security of Nishina Center collaborating with ACCC.

Members

Team Leader
Takashi ICHIHARA (concurrent; Vice Chief Scientist, RI Physics Lab.)

Research & Technical Scientist
Yasushi WATANABE (concurrent; Senior Research Scientist, Radiation Lab.)

Nishina Center Research Scientist
Hidetada BABA

Junior Research Associate
Ryousuke TANUMA (Rikkyo Univ.)

RIBF Research Division
Research Instruments Group
Detector Team

1. Abstract

This team is in charge of development, fabrication, and operation of various detectors used for nuclear physics experiments at RIBF. Our current main mission is maintenance and improvement of detectors which are used at BigRIPS separator and its succeeding beam lines for beam diagnosis and particle identification of RI beams. We are also engaged in R&D of new detectors that can be used for higher-intensity RI beams. In addition, we are doing the R&D which uses the pelletron accelerator together with other groups.

2. Major Research Subjects

Development, fabrication, and operation of various detectors for nuclear physics experiments, including beam-line detectors which are used for the production and delivery of RI beams (beam diagnosis and particle identification). R&D which uses the pelletron accelerator.

3. Summary of Research Activity

The current research subjects are summarized as follows:

(1) Maintenance and improvement of the beam-line detectors which are used at BigRIPS separator and its succeeding beam lines.
(2) Development of new beam-line detectors with radiation hardness and tolerance for higher counting rates
(3) Management of the pelletron accelerator and R&D which uses the pelletron

Members

Team Leader
Hiromi SATO (Apr. 1, 2014 –)

Research and Technical Scientist
Tokihiro IKEDA (Senior Research Scientist, Oct. 1, 2015 –)

Special Postdoctoral Researcher
Yuki SATO (– Jun. 30, 2015)

Research Consultant
Hiroyuki MURAKAMI

Visiting Scientist
Kohei FUJIWARA (Tokyo Met. Ind. Tech. Res. Inst.)

List of Publications & Presentations

Publications

[Journal]

(Original Papers) *Subject to Peer Review

Y. Sato, H. Murakami, “Pulse height decrease in a single-crystal CVD diamond detector”, Japanese Journal of Applied Physics 54, 096401 (2015). *

Y. Sato, T. Shimaoka, J.H. Kaneko, H. Murakami, M. Isobe, M. Osakabe, M. Tsubota, K. Ochiai, A. Chayahara, H. Umezawa, S. Shikata, “Radiation hardness of a single crystal CVD diamond detector for MeV energy protons”, Nuclear Instruments and Methods in Physics Research Section A, 784, 147 (2015). *

K. Kisamori, S. Shimoura, H. Miya, S. Michimasa, S. Ota, M. Assie, H. Baba, T. Baba, D. Beaumel, M. Dozono, T. Fujii, N. Fukuda, S. Go,F. Hammache, E. Ideguchi, N. Inabe, M. Itoh, D. Kameda, S. Kawase, T. Kawabata, M. Kobayashi, Y. Kondo, T. Kubo, Y. Kubota, M. Kurata-Nishimura, C.S. Lee, Y. Maeda, H. Matsubara, K. Miki, T. Nishi, S. Noji, S. Sakaguchi, H. Sakai, Y. Sasamoto, M. Sasano, H. Sato, Y. Shimizu, A. Stolz, H. Suzuki, M. Takaki, H. Takeda, S. Takeuchi, A. Tamii, L. Tang, H. Tokieda, M. Tsumura, T. Uesaka, K. Yako, Y. Yanagisawa, R. Yokoyama, and K. Yoshida, “Candidate Resonant Tetraneutron State Populated by the He-4 (He-8, Be-8) Reaction”, Physical Review Letters 116, 052501 (2016). *

Y. Kondo, T. Nakamura, R. Tanaka, R. Minakata, S. Ogoshi, N. A. Orr, N. L. Achouri, T. Aumann, H. Baba, F. Delaunay, P. Doornenbal, N. Fukuda, J. Gibelin, J. W. Hwang, N. Inabe, T. Isobe, D. Kameda, D. Kanno, S. Kim, N. Kobayashi, T. Kobayashi, T. Kubo, S. Leblond, J. Lee, F. M. Marqués, T. Motobayashi, D. Murai, T. Murakami, K. Muto, T. Nakashima, N. Nakatsuka, A. Navin, S. Nishi, H. Otsu, H. Sato, Y. Satou, Y. Shimizu, H. Suzuki, K. Takahashi, H. Takeda, S. Takeuchi, Y. Togano, A. G. Tuff, M. Vandebrouck, and K. Yoneda, “Nucleus O^{26}: A Barely Unbound System beyond the Drip Line”, Physical Review Letters 116, 102503 (2016). *

F. Hespeels, R. Tonneau, T. Ikeda, and S. Lucas, “Comparison of experimental and Monte-Carlo simulation of MeV particle transport through tapered/straight glass capillaries and circular collimators”, Nuclear Instruments and Methods in Physics Research Section B 362, 72-79 (2015). *

W.-G. Jin, T. Minowa, and T. Ikeda, “Transmission of Laser Beam Through Tapered Glass Capillaries for Light Microbeams”, Journal of the Physical Society of Japan 84, 114301 (2015). *

[Proceedings]

(Original Papers) *Subject to Peer Review

Y. Sato, N. Fukuda, H. Takeda, D. Kameda, H. Suzuki, Y. Shimizu, D.S. Ahn, D. Murai, N. Inabe, T. Shimaoka, M. Tsubota, J.H. Kaneko, A. Chayahara, H. Umezawa, S. Shikata, H. Kumagai, H. Murakami, H. Sato, K. Yoshida, and T. Kubo, “Status of beam line detectors for the BigRIPS fragment separator at RIKEN RI Beam Factory: issues on high rates and resolution”, JPS Conference Proceedings 6, 030124 (2015). *

J. Yasuda, M. Sasano, R.G.T. Zegers, H. Baba, W. Chao, M. Dozono, N. Fukuda, N. Inabe, T. Isobe, G. Jhang, D. Kameda, T. Kubo, M. Kurata-Nishimura, E. Milman, T. Motobayashi, H. Otsu, V. Panin, W. Powell, H. Sakai, M. Sako, H. Sato, Y. Shimizu, L. Stuhl, H. Suzuki, S. Tangwancharoen, H. Takeda, T. Uesaka, K. Yoneda, J. Zenihiro, T. Kobayashi, T. Sumikama, T. Tako, T. Nakamura, Y. Kondo, Y. Togano, M. Shikata, J. Tsubota, K. Yako, S. Shimoura, S. Ota, S. Kawase, Y. Kubota, M. Takaki, S. Michimasa, K. Kisamori, C.S. Lee, H. Tokieda, M. Kobayashi, S. Koyama, N. Kobayashi, T. Wakasa, S. Sakaguchi, A. Krasznahorkay, T. Murakami, N. Nakatsuka, M. Kaneko, Y. Matsuda, D. Mucher, S. Reichert, D. Bazin, J.W. Lee, “Inverse kinematics (p,n) reactions studies using the WINDS slow neutron detector and the SAMURAI spectrometer”, Nuclear Instruments and Methods in Physics Research Section B, 376, 393-396 (2016). *

H. Otsu, S. Koyama, N. Chiga, T. Isobe, T. Kobayashi, Y. Kondo, M. Kurokawa, W.G. Lynch, T. Motobayashi, T. Murakami, T. Nakamura, M. Kurata-Nishimura, V. Panin, H. Sato, Y. Shimizu, H. Sakurai, M.B. Tsang, K. Yoneda, H. Wang, "SAMURAI in its operation phase for RIBF users", Nuclear Instruments and Methods in Physics Research Section B, 376, 175-179 (2016). *

Oral Presentations

[International Conference etc.]

Y. Sato, H. Murakami, T. Shimaoka, M. Tsubota, J.H. Kaneko :“Single-crystal CVD Diamond Detector for Low-Energy Charged Particles with Energies Ranging from 100 keV to 2 MeV", Advancements in Nuclear Instrumentation Measurement Methods and their Applications, (Lisbon Congress Center), Lisbon, Portugal, April (2015).

[Domestic Conference]

H. Sato, and H. Kumagai: “Present status of the PPAC development”, RIBF Users Meeting, (RIKEN Nishina Center), Wako, Japan, September (2015).

村井大地, 家城和夫, 久保敏幸, 稲辺尚人, 福田直樹, 竹田浩之, 鈴木宏, 安得順, 清水陽平, 佐藤広海, 佐藤優樹, 日下健祐, 柳澤善行, 大竹政雄, 吉田光一, 大津秀暁, 岩佐直仁, 中村隆, Oleg B. Tarasov, Brad M. Sherrill, Dave J. Morrissey, Hans Geissel: “大強度 ^{48}Ca ビームを用いた F 中性子ドリップラインの探索”, 日本物理学会 2015 年秋季大会, （大阪大学）, 大阪, 9 月 (2015).

近藤洋介, 中村隆司, Nadia Lynda Achouri, Thomas Aumann, 馬場秀忠, Franck Delaunay, Pieter Doornenbal, 福田直樹, Julien Gibelin, Jongwon Hwang, 稲辺尚人, 磯部忠昭, 亀田大輔, 簡野大輝, Sunji Kim, 小林信之, 小林俊雄, 久保敏幸, Sylvain Leblond, Jenny Lee, Miguel Marques, 南方亮吾, 本林透, 村井大地, 村上哲也, 武藤琴美, 中嶋丈嘉, 中塚徳継, Alahari Navin, 西征爾郎, 生越駿, Nigel Andrew Orr, 大津秀暁, 佐藤広海, 佐藤義輝, 清水陽平, 鈴木宏, 高橋賢人, 竹田浩之, 武内聡, 田中隆己, 梅野泰宏, Adam Garry Tuff, Marine Vandebrouck, 米田健一郎 :“非束縛酸素同位体 ^{26}O の不変質量核分光”, 日本物理学会 2015 年秋季大会, （大阪大学）, 大阪, 9 月 (2015).

坪田潤一, 中村隆司, 近藤洋介, Nadia Lynda Achouri, Thomas Aumann, 馬場秀忠, Franck Delaunay, Pieter Doornenbal, 福田直樹, JulienGibelin, Jongwon Hwang, 稲辺尚人, 磯部忠昭, 亀田大輔, 簡野大輝, Sunji Kim, 小林信之, 小林俊雄, 久保敏幸, SylvainLeblond, Jenny Lee, Miguel Marques, 南方亮吾, 本林透, 村井大地, 村上哲也, 武藤琴美, 中嶋丈嘉, 中塚徳継, Alahari Navin, 西征爾郎, 生越駿, Nigel Andrew Orr, 大津秀暁, 佐藤広海, 佐藤義輝, 清水陽平, 鈴木宏, 高橋賢人, 竹田浩之, 武内聡, 田中隆己, 梅野泰宏, Adam Garry Tuff, Marine Vandebrouck, 米田健一郎: “^{26}F の不変質量核分光”, 日本物理学会 2015 年秋季大会, （大阪大学）, 大阪, 9 月 (2015).

大田晋輔, 銭廣十三, 竹田浩之, 堂園昌伯, 今井伸明, 木佐森慶一, 清川裕, 小林幹, 松下昌史, 増岡翔一朗, 道正新一郎, 下浦享, 渡辺珠以, 矢向謙太郎, 山口勇貴, AHN DeukSoon, 馬場秀忠, 福田直樹, 稲辺尚人, 久保敏幸, 村井大地, 大津秀暁, 佐藤広海, 佐藤優樹, 鈴木宏, 上坂友洋, 吉田光一:“理研 RIBF BigRIPS における大強度不安定核ビームの粒子識別の開発”, 日本物理学会 2015 年秋季大会, （大阪大学）, 大阪, 9 月 (2015).

金岡裕志, 小田原厚子, R. Lozeva, C. Moon, 八木彩祐未, 方一帆, 大道理恵, 西畑洸希, P. Lee, 下田正, 西村俊二, P. Doornenbal, G. Lorusso, 炭竈聡之, 渡辺寛, P. S derstr m, J. Wu, F. Brown, Z.Y. Xu, 横山輪, 磯部忠昭, 馬場秀忠, 櫻井博儀, 鈴木宏, 稲辺尚人, 亀田大輔, 福田直樹, 竹田浩之, 安得順, 清水陽平, 佐藤広海, 久保敏幸, 石垣知樹, 森本翔太, 井手口栄治, 小松原哲郎, 新倉潤, 西塚一平, C.S. Lee, and the EURICA collaborators: “中性子過剰な親核 I の β 崩壊による中性子過剰な娘核 Xe の研究”, 日本物理学会 2015 年秋季大会, （大阪大学）, 大阪, 9 月 (2015).

八木彩祐未, 小田原厚子, R. Lozeva, C. Moon, 方一帆, 大道理恵, 西畑洸希, 金岡裕志, P. Lee, 下田正, 西村俊二, P. Doornenbal, G. Lorusso, 炭竈聡之, 渡辺寛, P. S derstrm, J. Wu, F, F. Brown, Z.Y. Xu, 横山輪, 磯部忠昭, 馬場秀忠, 櫻井博儀, 鈴木宏, 稲辺尚人, 亀田大輔, 福田直樹, 竹田浩之, 安得順, 清水陽平, 佐藤広海, 久保敏幸, 石垣知樹, 森本翔太, 井手口栄治, 小松原哲郎, 新倉潤, 西塚一平, C.S. Lee, and the EURICA collaborators: “N=90 近傍の中性子過剰な Xe と Cs 同位体の研究”, 日本物理学会 2015 年秋季大会, （大阪大学）, 大阪, 9 月 (2015).

小山俊平, 大津秀暁, 清水陽平, 米田健一郎, 佐藤広海, 本林透, 西村美月, 銭廣十三, 櫻井博儀, 武内聡, 磯部忠昭, 馬場秀忠, 日下健祐, 大西純一, 笹野匡紀, P. Doornenbal, 福田直樹, 小林俊雄, 炭竈聡之, 松田洋平, 佐藤義輝, J. Hwang, 近藤洋介, 中村隆司, 梅野泰宏, 南方亮吾, 生越駿, 村上哲也, 中塚徳継, J. Gibelin, L. Sylvain, 新倉潤, 小林信之, H. Liu, J. Lee, E. Nikolskii, 坂口聡志, D. Beaumel: “不変質量法を用いた 16C のクラスター状態の研究”, 日本物理学会第 71 回年次大会, （東北学院大学）, 仙台, 3 月 (2016).

久保田悠樹, Anna Corsi, 笹野匡紀, 上坂友洋, Alexandre Obertelli, Clementine Santamaria, Emanuel Pollacco, 銭廣十三, 堂園昌伯, 大田晋輔, 時枝紘史, 川瀬頌一郎, Tang Tsz Leung, 高木基伸, 木佐森慶一, 李清秀, 矢向謙太郎, 小林幹, 小林俊雄, 長谷川邦彦, 中村隆司, 近藤洋介, 梅野泰宏, 四方瑞紀, 坪田潤一, 齊藤敦美, 米田健一郎, 佐藤広海, 大津秀暁, 清水陽平, 本林透, Pieter Doornenbal, 馬場秀忠, 磯部忠昭, 松下昌史, 安田淳平, 坂口聡, 小林信之, Valerie Lapoux, Alain Gillibert, 酒向正己, 進藤佑輔, 田端心海, 大倉綾華, Laszlo Stuhl, Zeren Korkulu, 清川裕, 鈴木大介, Freddy Flavigny, Julien Gibelin, Nigel Orr, Marques Miguel, Zaihong Yang, 金谷佳尚, 川上駿介: “ボロミアン核(p,pn)反応を用いた二中性子運動量相関の研究”, 日本物理学会第 71 回年次大会, （東北学院大学）, 仙台, 3 月 (2016).

村井大地, 家城和夫, 久保敏幸, 稲辺尚人, 福田直樹, 竹田浩之, 鈴木宏, 安得順, 清水陽平, 佐藤広海, 佐藤優樹, 日下健祐, 柳澤善行, 大竹政雄, 吉田光一, 大津秀暁, 岩佐直仁, 中村隆司, Oleg B. Tarasov, Brad M. Sherrill, Dave J. Morrissey, Hans Geissel: “大強度 ^{48}Ca ビー

ムを用いた中性子ドリップライン探索 II”，日本物理学会第 71 回年次大会，（東北学院大学），仙台, 3 月 (2016).
安田淳平，笹野匡紀，R.G.T. Zegars，馬場秀明，W. Chao，福田直樹，稲辺尚人，磯部忠明，G. Jhang，亀田大輔，久保敏幸，西村美月，E. Milman，本林透，大津秀暁，V. Panin，W. Powell，酒井英行，酒向正巳，佐藤広海，清水陽平，L. Stuhl，鈴木宏，S. Tangwancharoen，竹田浩之，上坂友洋，米田健一郎，銭廣十三，小林俊雄，炭竈聡之，田高義，中村隆司，近藤洋介，栂野泰宏，四方瑞紀，坪田潤一，矢向謙太郎，下浦享，大田晋輔，川瀬頌一郎，久保田悠樹，高木基伸，道正新一郎，木佐森慶一，李清秀，時枝紘史，堂園昌伯，小林幹，小山俊平，小林信之，若狭智嗣，坂口聡，A. Krasznahorkay，村上哲也，中塚徳継，金子雅紀，松田洋平，D. Mucher，S. Reichert，D. Bazin，J.W. Lee: “^{132}Sn(p,n)反応によるガモフテラー遷移の研究”，日本物理学会第 71 回年次大会，（東北学院大学），仙台, 3 月 (2016).

RIBF Research Division
Accelerator Applications Research Group

1. Abstract

This group promotes various applications of ion beams from RI Beam Factory (RIBF). Radiation Biology Team studies various biological effects of fast heavy ions and develops new technology to breed plants and microbes by heavy-ion irradiations. RI Applications Team studies production and application of radioisotopes for various research fields, development of trace element analysis and its application, and development of chemical materials for ECR ion sources of RIBF accelerators.

2. Major Research Subjects

Research and development in biology, chemistry and materials science utilizing heavy-ion beams from RI Beam Factory.

3. Summary of Research Activity

(1) Biological effects of fast heavy ions.
(2) Research and development of heavy-ion breeding.
(3) Research and development of RI production technology at RIBF.
(4) Developments of trace elements analyses.
(5) Development of chemical materials for ECR ion sources of RIBF accelerators.

Members

Group Director
Tomoko ABE

RIBF Research Division
Accelerator Applications Research Group
Ion Beam Breeding Team

1. Abstract

Ion beam breeding team studies various biological effects of fast heavy ions. It also develops new technique to breed plants and microbes by heavy-ion irradiations. Fast heavy ions can produce dense and localized ionizations in matters along their tracks, in contrast to photons (X rays and gamma rays) which produce randomly distributed isolated ionizations. These localized and dense ionization can cause double-strand breaks of DNA which are not easily repaired and result in mutation more effectively than single-strand breaks. A unique feature of our experimental facility at the RIKEN Ring Cyclotron (RRC) is that we can irradiate living tissues in atmosphere since the delivered heavy-ion beams have energies high enough to penetrate deep in matter. This team utilizes a dedicated beam line (E5B) of the RRC to irradiate microbes, plants and animals with beams ranging from carbon to iron. Its research subjects cover physiological study of DNA repair, genome analyses of mutation, and development of mutation breeding of plants by heavy-ion irradiation. Some new cultivars have already been brought to the market.

2. Major Research Subjects

(1) Study on the biological effects by heavy-ion irradiation
(2) Study on the molecular nature of DNA alterations induced by heavy-ion irradiation
(3) Innovative applications of heavy-ion beams

3. Summary of Research Activity

We study biological effects of fast heavy ions from the RIKEN Ring Cyclotron using 135A MeV C, N, Ne ions, 95A MeV Ar ions and 90A MeV Fe ions. We also develop breeding technology of microbes and plants. Main subjects are:

(1) Study on the biological effects by heavy-ion irradiation

Heavy-ion beam deposits a concentrated amount of dose at just before stop with severely changing the linear energy transfer (LET). The peak of LET is achieved at the stopping point and known at the Bragg peak (BP). It is well known to be good for cancer therapy to adjust the BP to target malignant cells. On the other hand, a uniform dose distribution is a key to the systematic study for heavy-ion mutagenesis, and thus to the improvement of the mutation efficiency. Therefore plants and microbes are treated using ions with stable LET. We investigated the effect of LET ranging from 23 to 640 keV/μm, on mutation induction using dry seeds of the model plants *Arabidopsis thaliana*. The most effective LET (LETmax) was 30 keV/μm. LETmax irradiations showed the same mutation rate as that by chemical mutagens, which typically cause high mutation rate. The LETmax of imbibed rice (*Oryza sativa* L.) seeds and dry wheat (*Triticum monococcum*) seeds were shown to be 50-63 keV/μm and 50 keV/μm, respectively. In the case of microbe (*Mesorhizobium lothi*), the results showed a higher incidence of deletion mutations for Fe ions at 640 KeV/μm than for C ions at 23-40 keV/μm. Thus, the LET is an important factor to be considered in heavy-ion mutagenesis.

(2) Study on the molecular nature of DNA alterations induced by heavy-ion irradiation

Detailed analyses on the molecular nature of DNA alterations have been reported as an LET-dependent effect for induced mutation. The most mutations were deletions ranging from a few to several tens of base pairs (bp) in the *Arabidpsis* mutants induced by irradiation with C ions at 30 keV/μm and rice mutants induced by irradiation with C ions at 50 keV/μm or Ne ions at 63 keV/μm. LETmax is effective for breeding because of its very high mutation frequency. Since most mutations are small deletions, these are sufficient to disrupt a single gene. Thus, irradiation can efficiently generate knockout mutants of a target gene, and can be applied to reverse genetics. On the other hand, irradiation with Ar ions at 290 keV/μm showed a mutation spectrum different from that at LETmax: the proportion of small deletions (<1 kbp) was low, while that of large deletions ranging from several to several tens of kbp, and rearrangements was high. Many genes in the genome (> 10%) are composed of tandem duplicated genes that share functions. For knockout of the tandem duplicated genes, large deletions are required, and the appropriate deletion size is estimated to be around 5-10 kbp and 10-20 kbp based on the gene density in *Arabidpsis* and rice, respectively. No method is currently available to efficiently generate deletion mutants of this size. As such, higher LET irradiation is promising as a new mutagen suitable for the functional analysis of tandem duplicated genes.

(3) Innovative application of heavy-ion beams

We have formed a consortium for ion-beam breeding. It consisted of 24 groups in 1999, in 2015, it consisted of 158 groups from Japan and 8 from overseas. Breeding was performed previously using mainly flowers and ornamental plants. We have recently put a new Japanese barnyard millet cultivar with low amylose content and short culm, 'Nebarikko No. 2' on the market. Beneficial variants have been grown for various plant species, such as high yield rice, semi-dwarf early rice, semi-dwarf buckwheat, semi-dwarf barley, hypoallergenic peanut, spineless oranges, non-flowering Eucalyptus and lipids-hyperaccumulating unicellular alga. We collaborate with Miyagi prefecture and Tohoku University to breed salt-resistant lines in the more delicious commercial rice varieties, 'Hitomebore' and 'Manamusume'. Imbibed seeds were irradiated with the LETmax (C-ions) on 16 April, 2011. We isolated 73 candidate lines of salt-resistant mutants from 719 M_2 progenies grown in the saline paddy field in Tohoku University in 2012. From these, we selected 12 salt-resistant M_3 lines in 2013 and 4 M_4 lines in 2014. The target of heavy-ion breeding is extended from flowers to crops like grains so that it will contribute to solve the global problems of food and environment.

Members

Team Leader
Tomoko ABE (concurrent: Group Director, Accelerator Applications Research Gr.)

Research & Technical Scientist
Kazuhide TSUNEIZUMI (Senior Research Scientist)
Masako IZUMI (Senior Research Scientist)
Teruyo TSUKADA (Senior Research Scientist)
Katsunori ICHINOSE (Senior Technical Scientist)
Hiroshi ABE (Senior Technical Scientist)
Ryouhei MORITA (Technical Scientist)
Tokihiro IKEDA (Senior Research Scientist, – Sep. 30, 2015: concurrent, Oct. 1, 2015 –)

Contract Researchers
Hiroyuki ICHIDA (Feb. 1, 2015 –)
Yusuke KAZAMA

Postdoctoral Researcher
Kotaro ISHII

Technical Staff I
Yoriko HAYASHI
Motoko MURAKAMI (Apr. 1, 2014 – Mar. 31, 2016)
Yuki SHIRAKAWA (May 1, 2015 –)

Technical Staff II
Sumie OHBU

Foreign Postdoctoral Researcher
Reka BERECZKY (– Mar. 31, 2016)

Research Consultants
Tadashi SATO (– Mar. 31, 2015)
Masahiro MII

Part-time Workers
Hideo TOKAIRIN
Yuki SHIRAKAWA (– Apr. 30, 2015)
Sachiko KOGURE (Apr. 15, 2014 –)
Taeko WAKANA
Mieko YAMADA
Satoko YASUDA (– Mar. 31, 2015)
Haruka WATANABE (– Sep. 18, 2015)

Visiting Scientist
Makoto FUJIWARA (Univ. of Tokyo)
Masao WATANABE (Tohoku Univ.)
Hisashi TSUJIMOTO (Tottori Univ.)
Yutaka MIYAZAWA (Tohoku Univ.)
Toshinari GODO (Botanic Gardens Toyama)
Masanori TOMITA (CRIEPI)
Toshikazu MORISHITA (Nat'l. Inst. Agric. Res.)
Hiroyuki ICHIDA (Stanford Univ.)
Koji MURAI (Fukui Pref. Univ.)
Hinako TAKEHISA (Nat'l. Inst. Agric. Sci.)
Akiko HOKURA (Tokyo Denki Univ.)
Norihiro OHTSUBO (Natl. Inst. Floricult. Sci.)
Eitaro FUKATSU (Forestry and Forest Products Res. Inst.)
Tomonari HIRANO (Univ. of Miyazaki)
Yoichi SATO (Riken Food Co., Ltd.)
Ali FERJANI (Tokyo Gakugei Univ.)
In-Ja SONG (Jeju Nat'l University)
Katsutomo SASAKI (Nat'l Agric. and Food Res. Org.)
Kunio SUZUKI (Technoflora, Co., Ltd.)
Kazumitsu MIYOSHI (Akita Pref. Univ.)
Makoto UBUKATA (Hokkaido Univ.)
Akihiro IWASE (Osaka Pref. Univ.)
Tadashi SATO (Tohoku Univ.)

Visiting Technicians
Takuji YOSHIDA (Takii Seed Co., Ltd.)
Tomojirou KOIDE (Riken Vitamin Co., Ltd.)
Yutaka ITOH (Riken Food Co., Ltd.)
Keiji IKEDA (KK SeaAct)

Research Fellows
Naoji WAKITA (Wadomari Cho Agr. Exp. Station)
Kyousuke NIWA (Hyogo Pref. Res. Inst.)
Miyuki NISHI (Saga Agric. Experiment Station)
Tadahito OOTUBO (Wadomari Cho Agr. Exp. Station)
Shunsuke IMANISHI (Natl. Inst.Veg. and Tea Sci.)
Tomihiro TAKESHITA (Wadomari Cho)
Humio SUGAMURA (Wadomari Cho)
Hiroshi ASATO (Wadomari Cho)
Kenji OOYOSHI (Wadomari Cho)
Yoshiharu TAKE (Wadomari Cho)

Student Trainees
Fumitaka YAMAGISHI (Tokyo Denki Univ.)
Fumitaka TAMEZAWA (Tokyo Denki Univ.)
Kentaro FUJITA (Tokyo Denki Univ.)
Kana MIYOSHI (Tokyo Univ. of Sci.)
Takuto TAKAHASHI (Tokyo Denki Univ.)
Yu IMAMURA (Tokyo Denki Univ.)
Hiroki ISHIKAWA (Sophia Univ.)
Mao SUZUKI (Sophia Univ.)
Shun SASAKI (Sophia Univ.)
Kazuki TAKANASHI (Tokyo Denki Univ.)
Koichi NAMBU (Tokyo Denki Univ.)
Naoko HIROSE (Tokyo Denki Univ.)

Takuya NISHINOBO (Tokyo Denki Univ.) Junki SHIRAKAWA (Chiba Univ.)

List of Publications & Presentations

Publications

[Journal]

(Original Papers) *Subject to Peer Review

Kojima T., Ikeda T., Kanai Y., Yamazaki Y.: “Ion guiding in curved glass capillaries”, Nuclear Instruments and Methods in Physics Research B **354**, 16-19 (2015). *

JimW.G., Minowa T., Ikeda T.: “Transmission of Laser Beam Through Tapered Glass Capillaries for Light Microbeams”, Journal of the Physical Society of Japan **84**, 114301/1-5 (2015). *

Hespeels F., Tonneau R., Ikeda T., Lucas S.: “Comparison of experimental and Monte-Carlo simulation of MeV particle transport through tapered/straight glass capillaries and circular collimators”, Nuclear Instruments and Methods in Physics Research Section B: Beam Interactions with Materials and Atoms **362**, 72-79 (2015). *

Fujiwara M.T., Kojo K.H., Kazama Y., Sasaki S., Abe T., Itoh R.D.: “The Arabidopsis *minE* mutation causes new plastid and FtsZ1 localization phenotypes in the leaf epidermis”, Front. Plant Sci. **6**, Article 823 (2015).*

Fitzgerald T. L., Powell J. J., Stiller J., Weese T. L., Abe T., Zhao G., Jia J., McIntyre C. L., Li Z.i, Manners J. M., Kazan K.,: ”An assessment of heavy ion irradiation mutagenesis for reverse genetics in wheat (*Triticum aestivum* L.)”, PLoS ONE **10**, e0117369 (2015).*

本田真央, 北島信行, 阿部知子, 梅村知也, 保倉明子: “放射光蛍光 X 線分析を用いるモエジマシダ(*Pteris vittata L.*)におけるクロム蓄積機構の解明”, 分析化学 **64**, 801-810 (2015). *

内海好規, 櫻井哲也, 石谷学, 内海稚佳子, 阿部知子, 平野智也, 武井良郎, Ha V. T., Le H. H., Nguyen D. V., Nguyen V. A., Triwitayakorn K., Narangajavana J., 関原明: “熱帯の塊根モデル植物キャッサバ”, 植物の生長調節 **50**, 118-124(2015). *

Kazama Y., Ishii K., Aonuma W., Ikeda T., Kawamoto H., Koizumi A., D. A. Filatov, M. Chibalina, R. Bergero, D. Charlesworth, Abe T., Kawano S.: “A new physical mapping approach refines the sex-determining gene positions on the Silene latifolia Y-chromosome”, Sci.Rep. **6**, Article No.18917 (2016). *

Katano M., Takahashi K., Hirano T., Kazama Y., Abe T., Tsukaya H., Ferjani A.: “Suppressor Screen and Phenotype Analyses Revealed an Emerging Role of the Monofunctional Peroxisomal Enoyl-CoA Hydratase 2 in Compensated Cell Enlargement”, Front. Plant Sci. **7**, Article 132 (2016). *

(Review)

阿部知子: “重イオンビームを用いた生物研究の新領域開拓—Mutagenesis から Mutagenomics へ—”, Isotope News **733**, 2-6 (2015).

内藤健, 高橋有, 山内卓樹, 福島健児, 風間裕介, 江崎文一, 友岡憲彦: “ワイルドはセクシーだ！”, 育種学研究 **17**, 64-70 (2015).

Abe T., Kazama Y., Hirano T.: “Ion beam breeding and gene discovery for function analyses using mutants”, Nuclear Physics News **25**, 30-35 (2015).

[Proceedings]

(Original Papers) *Subject to Peer Review

Nishiura A., Kazama Y., Abe T., Mizuno N., Nasuda S., Murai K.: “*Extra Early-Flowering(exe)* Mutants in Einkorn Wheat Generated by Heavy-Ion Beam Irradiation”, Advances in Wheat Genetics: From Genome to Field:Proceedings of the 12th International Wheat Genetics Symposium, p.175-180 (2015). *

Fukunishi N., Fujimaki M., Komiyama M., Kumagai K., Maie T., Watanabe Y., Hirano T. and Abe T.: "New High-Energy Beam Transport Line Dedicated to Biological Applications in RIKEN RI Beam Factory", 13th International Conference on Heavy Ion Accelerator Technology, ISBN 978-3-95450-131-1(2015).

[Book]

阿部知子: “イオンビーム育種”, 放射化学の事典 p.312 朝倉書店 (2015).

[Others]

泉雅子: “Radiation Quantities and Units” Effects of Radiation on Human Body, Chapter 1, 2, 公益社団法人 日本アイソトープ協会 (2015).

Oral Presentations

(Domestic Conference)

遠藤幸子, 齋藤裕太郎, 島貫源基, 阿部篤智, 阿部知子: “食用ぎく新品種「山園 K４号」の特性”, 第 58 回東北農業試験研究発表会, 山形, 7 月 (2015).

風間裕介, 石井公太郎, 池田時浩, Filatov D., Chibalina M. , Bergero R., Charlesworth D., 河野重行, 阿部知子: “ヒロハノマンテマ Y 染色体の構造解析と組換え抑制領域の欠失マッピングプログラム DelMapper の開発”, 日本植物学会第 79 回大会, 新潟, 9 月 (2015).

風間裕介, 平野智也, 石井公太郎, 大部澄江, 白川侑希, 阿部知子: “シロイヌナズナで明らかにした重イオンビームのＬＥＴ効果～変異率と変異スペクトラムについて～”, ＳＩＰ新しい育種技術２系／３系突然変異グループ合同ワークショップ, 新潟, 9 月 (2015).

林依子, 森田竜平, 一瀬勝紀, 臼田祥子, 佐藤雅志, 阿部知子: “イネにおける重イオンビーム変異誘発の最適化”, ＳＩＰ新しい育種技術２系／３系突然変異グループ合同ワークショップ, 新潟, 9 月 (2015).

森田竜平, 市田裕之, 石井公太郎, 一瀬勝紀, 林依子, 白川侑希, 齊藤大樹, 奥本裕, 佐藤雅志, 阿部知子: “放射線照射で誘発したイネ変異遺伝子同定の迅速化”, ＳＩＰ新しい育種技術２系／３系突然変異グループ合同ワークショップ, 新潟, 9 月 (2015).

平野智也, 高城啓一, 星野洋一郎, 阿部知子: “雄性配偶子における重イオンビーム誘発 DNA 損傷応答”, ＳＩＰ新しい育種技術２系／３系突然変異グループ合同ワークショップ, 新潟, 9 月 (2015).

市田裕之, 阿部知子: “超並列 PC クラスタを利用したイネエキソーム情報解析と全ゲノムを対象とした変異検出への応用”, ＳＩＰ新しい育種技術２系／３系突然変異グループ合同ワークショップ, 新潟, 9 月 (2015).

石井公太郎, 風間裕介, 池田時浩, 川元寛章, 河野重行, 阿部知子: “重イオンビーム照射による巨大欠失を利用して組換え抑制領域をマッピングする”, ＳＩＰ新しい育種技術２系／３系突然変異グループ合同ワークショップ, 新潟, 9 月 (2015).

岡本充智, 古谷雅司, 中村茂和, 濱崎櫻, 山家一哲, 永嶋友香, 渡村加奈子, 阿部知子: “ブラッドオレンジにおける重イオンビーム照射個体の変異比較”, ＳＩＰ新しい育種技術２系／３系突然変異グループ合同ワークショップ, 新潟, 9 月 (2015).

小林康志, 二宮泰造, 奥定丈博, 阿部知子: “温州みかんにおける重イオンビーム照射が果実品質と接ぎ木活着に及ぼす影響”, ＳＩＰ新しい

育種技術２系／３系突然変異グループ合同ワークショップ, 新潟, 9 月 (2015).
村井耕二, 北川哲, 黒坂真素美, 風間裕介, 阿部知子: “2 倍体コムギにおける重イオンビーム処理条件と早生性変異の関係”, ＳＩＰ新しい育種技術２系／３系突然変異グループ合同ワークショップ, 新潟, 9 月 (2015).
森田竜平, 中川繭, 臼田祥子, 一瀬勝紀, 林依子, 東海林英夫, 竹久妃奈子, 佐藤雅志, 阿部知子: “重イオンビーム照射で誘発したイネ virescent 変異体の原因遺伝子同定”, 日本育種学会第 128 回講演会, 新潟, 9 月 (2015).
北川哲, 西浦愛子, 水野信之, 那須田周平, 風間裕介, 阿部知子, 村井耕二: “イオンビーム照射による超極早生変異体 (exe2) の日長反応性関連遺伝子の発現解析”, 日本育種学会第 128 回講演会, 新潟, 9 月 (2015).
福西暢尚, 佐藤陽一, 市田裕之, 阿部知子, 平野智也: “三陸における特産海藻類の品種改良技術開発と新品種育成に関する拠点形成”, 東日本大震災からの復興・再生に向けた新たな水産業の創成につながる新技術開発, 仙台, 9 月 (2015).
風間裕介, 石井公太郎, 阿部知子, 河野重行: “巡回セールスマン問題を用いた植物型巨大Ｙ染色体のマッピング”, 日本遺伝学会第 87 回大会, 仙台, 9 月 (2015).
加藤雅博, 正村典也, 正野仁慈, 岡本大作, 上山雅恵, 阿部知子, 今井真介: “涙の出ない、辛みのないタマネギの作出と特性解析”, 第 30 回日本香辛料研究会学術講演会, 京都, 12 月 (2015).
風間裕介, 平野智也, 大田修平, 佐藤陽一, 村井耕二, 河野重行, 小野克徳, 阿部知子: “重イオンビームによるグリーンイノベーションの創出”, 近畿作物・育種研究会公開シンポジウム　変異創成技術の現状と未来, 京都, 12 月 (2015).
山崎誠和, 鴻巣絵梨香, 武田行平, 竹下毅, 平田愛子, 大田修平, 風間裕介, 阿部知子, 河野重行: “硫黄飢餓におけるクロレラの脂質とデンプンの蓄積動態”, 第 57 回日本植物生理学会年会, 盛岡, 3 月 (2016).
北川哲, Mo L.T., 水野信之, 那須田周平, 藤田直子, 風間裕介, 阿部知子, 村井耕二: “一粒系コムギの新規極早生突然変異体 *extra early-flowering 5 (exe5)* の RNA-seq 解析”, 日本育種学会 第 129 回講演会, 横浜, 3 月 (2016).

Posters Presentations

(International Conference etc.)

Ishii K., Kazama Y., Hirano T., Hamada M., Ono Y., Abe T.: “Pipeline for whole-genome analysis of heavy-ion-induced mutants in *Arabidopsis thaliana*”, The 26th International Conference on Arabidopsis Research (ICAR 2015), Paris, France, July (2015).

Kazama Y., Hirano T., Ishii K., Ohbu S., Shirakawa Y., Abe T.: “Comprehensive characterization of genomic rearrangement in heavy-ion induced *Arabidopsis* mutants by wholegenome resequencing”, The 26th International Conference on Arabidopsis Research (ICAR 2015), Paris, France, July (2015).

(Domestic Conference)

石井公太郎, 風間裕介, 平野智也, 白川侑希, 大部澄江, 山田美恵子, 若菜妙子, 阿部知子: “重イオンビーム誘発欠失変異体集団を用いたシロイヌナズナ必須染色体領域のマッピング”, 日本育種学会第 128 回講演会, 新潟, 9 月 (2015).
林依子, 森田竜平, 一瀬勝紀, 臼田祥子, 東海林英夫, 佐藤雅志, 阿部知子: “高 LET イオンビーム照射によるイネの突然変異誘発効果”, 日本育種学会第 128 回講演会, 新潟, 9 月 (2015).
佐々木駿, 石川浩樹, 加賀谷奨, 風間裕介, 阿部知子, 伊藤竜一, 藤原誠: “シロイヌナズナ花粉色素体の増殖制御機構の解析”, 日本農芸化学会関東支部 2015 年度支部大会, 東京, 9 月 (2015).
石川浩樹, 佐々木駿, 鈴木麻央, 平野智也, 風間裕介, 阿部知子, 伊藤竜一, 藤原誠: “シロイヌナズナ花粉発生過程における色素体増殖の解析”, 日本農芸化学会関東支部 2015 年度支部大会, 東京, 9 月 (2015).
山崎誠和, 鴻巣絵梨香, 竹下毅, 大田修平, 平田愛子, 風間 裕介, 阿部知子, 河野重行: “微細緑藻 *Parachlorella kessleri* のシステイン要求性変異体はオイルとデンプンの蓄積動態に異常を示す”, 第 67 回日本生物工学会大会, 鹿児島, 10 月 (2015).
北川哲, 西浦愛子, 水野信之, 那須田周平, 風間裕介, 阿部知子, 村井耕二: “イオンビーム照射による超極早生変異体(*exe2*)の日長反応性関連遺伝子の発現解析”, 第 8 回　北陸合同バイオシンポジウム, 石川, 10 月 (2015).
遠藤貴司, 佐伯研一, 佐藤浩子, 中込佑介, 阿部知子, 佐藤雅志, 鳥山欽也: “重イオンビーム照射による塩害耐性イネの開発”, 第 10 回東北育種研究集会, 仙台, 11 月 (2015).
佐藤雅志, 阿部知子, 鳥山欽哉: “重イオンビーム照射処理によるインドネシア在来イネの早生化変異体作出へのアプローチ”, 第 10 回東北育種研究集会, 仙台, 11 月 (2015).
風間智彦, 阿部知子, 鳥山欽哉: “細胞質雄性不稔イネへの変異原処理による稔性回復復帰変異体スクリーニングの試み”, 第 10 回東北育種研究集会, 仙台, 11 月 (2015).
北川哲, 西浦愛子, 水野信之, 那須田周平, 風間裕介, 阿部知子, 村井耕二: “イオンビーム照射による一粒系コムギ超極早生変異体 (*exe2*) の花成関連遺伝子の発現パターン解析”, 第 10 回ムギ類研究会, 伊勢, 12 月 (2015).
Mo L.T., 北川哲, 風間裕介, 阿部知子, 水野信之, 那須田周平, 藤田直子, 村井耕二: “イオンビーム照射による一粒系コムギの新規極早生突然変異体 *extra early-flowering 5 (exe 5)* の解析”, 第 10 回ムギ類研究会, 伊勢, 12 月 (2015).
佐藤陽一, 平野智也, 村上素子, 伊藤泰, 最上谷美穂, 佐々木直子, 菅原美加, 市田裕之, 福西暢尚, 阿部知子, 河野重行: “重イオンビーム育種技術を用いた三陸産ワカメの優良系統開発”, 日本藻類学会第 40 回大会, 東京, 3 月 (2016).
澤田倫平, 平野智也, 飯牟禮和彦, 阿部知子, 尾崎行生: “レタス(*Lactuca sativa* L.)プロトプラストへのイオンビーム照射によって出現した低ポリフェノールオキシターゼ活性を示す突然変異体”, 園芸学会 平成 28 年度春季大会, 厚木, 3 月 (2016).
石川浩樹, 佐々木駿, 平野智也, 風間裕介, 阿部知子, 伊藤竜一, 藤原誠: “シロイヌナズナ花粉体細胞分裂時における色素体の増殖”, 日本農芸化学会 2016 年度大会, 札幌, 3 月 (2016).
佐々木駿, 石川浩樹, 鈴木麻央, 風間裕介, 阿部知子, 伊藤竜一, 藤原誠: “シロイヌナズナにおける花粉色素体増殖の遺伝的制御解析”, 日本農芸化学会 2016 年度大会, 札幌, 3 月 (2016).

RIBF Research Division
Accelerator Applications Research Group
RI Applications Team

1. Abstract

The RI Applications Team develops production technologies of radioisotopes (RIs) at RIKEN RI Beam Factory (RIBF) for application studies in the fields of physics, chemistry, biology, engineering, medicine, pharmaceutical and environmental sciences. We use the RIs mainly for nuclear and radiochemical studies such as RI production and superheavy element chemistry. The purified RIs such as ^{65}Zn and ^{109}Cd are delivered to universities and institutes through Japan Radioisotope Association. We also develop new technologies of mass spectrometry for the trace-element analyses using accelerator technology and apply them to the research fields such as cosmochemistry, environmental science, archaeology and so on. We also develop chemical materials for ECR ion sources of heavy-ion accelerators in RIBF.

2. Major Research Subjects

(1) Research and development of RI production technology at RIBF
(2) RI application researches
(3) Development of trace element and isotope analyses using accelerator techniques and its applications to geoscience and environmental science
(4) Development of chemical materials for ECR ion sources of heavy-ion accelerators in RIBF

3. Summary of Research Activity

(1) Research and development of RI production technology at RIBF and RI application studies

Due to its high sensitivity, the radioactive tracer technique has been successfully applied for investigations of the behavior of elements in the fields of chemistry, biology, engineering, medicine, pharmaceutical and environmental sciences. We have been developing production technologies of useful radiotracers at RIBF and conducted their application studies in collaboration with many researchers in various fields. With 14-MeV proton, 24-MeV deuteron, and 50-MeV alpha beams from the AVF cyclotron, we presently produce about 30 radiotracers from ^{7}Be to ^{211}At. Among them, ^{65}Zn, ^{85}Sr, ^{88}Y, and ^{109}Cd are delivered to Japan Radioisotope Association for fee-based distribution to the general public in Japan. On the other hand, radionuclides of a large number of elements are simultaneously produced from metallic targets such as ^{nat}Ti, ^{nat}Ag, ^{nat}Hf, and ^{197}Au irradiated with a 135-MeV nucl.$^{-1}$ ^{14}N beam from the RIKEN Ring Cyclotron. These multitracers are also supplied to universities and institutes as collaborative researches.

In 2014–2015, we developed production technologies of radioisotopes such as ^{28}Mg, ^{48,51}Cr, ^{44}Ti, ^{67}Cu, ^{75}Se, ^{95m}Tc, ^{121m}Te, ^{181}W, ^{182}Ta, ^{183,184m,184g}Re, ^{191}Pt, and ^{211}At which were strongly demanded but lack supply sources in Japan. We also investigated the excitation functions for the ^{27}Al(α,x), ^{nat}Ti(α,x), ^{nat}Cu(α,x), ^{nat}Ge(α,x), ^{nat}Zr(α,x), ^{nat}Mo(d,x), ^{nat}Cd(α,x), ^{116}Cd(α,x), ^{nat}Pd(α,x), ^{nat}Ce(d,x), ^{nat}Sm(d,x), ^{159}Tb(d,x), ^{nat}Ho(α,x), ^{169}Tm(d,x), ^{nat}Lu(p,x), ^{nat}Lu(d,x), ^{nat}Ta(p,x), ^{nat}Ta(d,x), ^{nat}W(d,x), and ^{nat}Pt(d,x) reactions to quantitatively produce useful RIs. We used radiotracers of ^{139}Ce for application studies in chemistry, ^{65}Zn, ^{67}Cu, ^{88}Y, ^{191}Pt, and ^{211}At in nuclear medicine, ^{88,89}Zr, ^{95}Nb, ^{175}Hf, and ^{177}Ta in geochemistry, and ^{85}Sr and ^{121m}Te in environmental science. We also produced ^{65}Zn, ^{85}Sr, ^{88}Y, and ^{109}Cd for our scientific researches on a regular schedule and supplied the surpluses through Japan Radioisotope Association to the general public. In 2014–2015, we have accepted 10 orders of ^{65}Zn with a total activity of 59 MBq, 1 order of ^{85}Sr with 1 MBq, 2 orders of ^{88}Y with 2 MBq, and 6 orders of ^{109}Cd with 26 MBq.

(2) Superheavy element chemistry

Chemical characterization of newly-discovered superheavy elements (SHEs, atomic numbers $Z \geq 104$) is an extremely interesting and challenging subject in modern nuclear and radiochemistry. We are developing SHE production systems as well as rapid single-atom chemistry apparatuses at RIBF. Using heavy-ion beams from RILAC and AVF, ^{261}Rf ($Z = 104$), ^{262}Db ($Z = 105$), and ^{265}Sg ($Z = 106$) are produced in the ^{248}Cm(^{18}O,5n)^{261}Rf, ^{248}Cm(^{19}F,5n)^{262}Db, and ^{248}Cm(^{22}Ne,5n)^{265}Sg reactions, respectively, and their chemical properties are investigated.

We have been developing a gas-jet transport system at the focal plane of the gas-filled recoil ion separator GARIS at RILAC. This system is a promising approach for exploring new frontiers in SHE chemistry: (i) the background radioactivities of unwanted reaction products are strongly suppressed, (ii) the intense beam is absent in the gas-jet chamber and hence high gas-jet efficiency is achieved, and (iii) the beam-free condition also allows for investigations of new chemical systems. In 2014–2015, the isotope of element 107 ^{266}Bh was produced in the ^{248}Cm(^{23}Na,5n)^{266}Bh reaction, and its decay properties were investigated using the rotating wheel apparatus MANON for α/SF spectrometry. Toward the SHE chemistry behind GARIS, we developed a gas-chromatograph apparatus directly coupled to GARIS, which enabled in-situ complexation and gas-chromatographic separation of a large variety of volatile compounds of SHEs. Toward aqueous chemistry of the heaviest elements such as Sg and Bh, we have started to develop a new rapid chemistry apparatus which consists of a continuous dissolution apparatus Membrane DeGasser (MDG), a Flow Solvent Extractor (FSE), and a flow liquid scintillation detector for α/SF-spectrometry. The performance of MDG and FSE were investigated using ^{92,94m}Tc and ^{181}Re produced in the ^{nat}Mo(d,xn) and ^{nat}W(d,xn) reactions, respectively, at AVF.

At AVF, the distribution coefficients (K_d) of ^{261}Rf on the Aliquat 336 resin were measured in HCl with the AutoMated Batch-type solid-liquid Extraction apparatus for Repetitive experiments of transactinides (AMBER) in collaboration with Osaka Univ. The extraction behavior of ^{89m}Zr and ^{173}Hf in the Aliquat 336/HCl system was investigated for Rf chemistry with the flow-type liquid-liquid extraction apparatus. The reversed-phase TTA extraction chromatography of ^{261}Rf and its homologues ^{85}Zr and ^{169}Hf was conducted in HF/HNO_3 using the Automated Rapid Chemistry Apparatus (ARCA) in collaboration with Niigata Univ. and JAEA. The reversed-phase extraction

chromatography of ^{90g}Nb and ^{178a}Ta in Aliquat 336/HF and the anion-exchange chromatography of ^{90g}Nb and ^{178a}Ta in HF/HNO_3 were also conducted with ARCA for chemical studies of Db. We also used radiotracers of ^{88,89m}Zr, ^{95}Nb, ^{93m}Mo, ^{95m}Tc, ^{173,175}Hf, ^{178a,179}Ta, ^{177,179m,181}W, and ^{183}Re for model experiments of SHEs.

(3) Development of trace element analysis using accelerator techniques and its application to geoscience and archaeological research fields

We developed a new mass spectrometry technology for trace element analyses as an application of accelerator technology to various fields such as cosmochemistry, environmental science, and archaeology. ECRIS-AMS is a new type of accelerator mass spectrometry at RILAC equipped with an ECR ion source. This system is available for measuring trace elements (10^{-14}–10^{-15} level) and is expected to be especially effective for measurements of low-electron-affinity elements such as ^{26}Al, ^{41}Ca, and ^{53}Mn. In 2014–2015, we have renovated the detection system and examined the sensitivity and mass resolution power. We also attempted to develop another technology by customizing a mass spectrometer equipped with a stand-alone ECR ion source for analyses of elemental and isotopic abundances. Especially, we equipped a laser-ablation system with an ion source to achieve high-resolution analysis.

Using the conventional ICP-MS, TIMS, IRMS and so on, we also examined the origin of burials from ancient tombs and ruins. We are challenging two issues. One is the analyses of sulfur and lead isotope ratios for cinnabar samples from ancient tombs in Japan to elucidate the establishment of Yamato dynasty around 3rd and 4th centuries. We showed that the lead isotopes in cinnabar ore exhibited clear local characteristics and the origin of the cinnabar ore could be distinguished from the lead isotope compositions. The other issue is to elucidate the market of oil and asphalt in Jomon Period in the North Japan based on the sulfur isotopes. We started a feasibility study to analyze the sulfur isotope ratios to distinguish the origin of oil samples.

(4) Development of chemical materials for ECR ion sources of RIBF

In 2014–2015, we developed a chemical procedure to recover an enriched $^{48}CaCO_3$ from the ^{48}CaO/Al mixture used in the 18-GHz ECR ion source of RILAC. We prepared metallic ^{238}U rods and $^{238}UO_2$ on a regular schedule for ^{238}U-ion accelerations with the 28-GHz ECR of RILAC II.

Members

Team Leader
Hiromitsu HABA

Research & Technical Scientist
Kazuya TAKAHASHI (Senior Research Scientist)

Postdoctoral Researchers
Yukiko KOMORI

Technical Staff I
Shinya YANOU (Apr. 1, 2015 –)

Research Consultant
Seiichi SHIBATA

Junior Research Associate
Masashi MURAKAMI (Niigata Univ., – Mar. 31, 2015)

Part-time Workers
Michiko KITAGAWA
Yu Vin SAHOO
Nozomi SATO
Keiko WATANABE

Visiting Scientists
Akihiko YOKOYAMA (Kanazawa Univ.)
Kazuhiko AKIYAMA (Tokyo Met. Univ.)
Kazuhiro OOE (Niigata Univ.)
Hidetoshi KIKUNAGA (Tohoku Univ.)
Masayoshi TODA (Tokyo Univ. Marine Sci. and Tech.)
Mayeen Uddin KHANDAKER (Univ. Malaya)
Takahiro YAMADA (Japan Rad. Assoc.)
Miho TAKAHASHI (Tokyo Univ. Marine Sci. and Tech.)
Hiroshi SHIMIZU (Rissho Univ.)
Atsushi TOYOSHIMA (JAEA)
Aya SAKAGUCHI (Univ. of Tsukuba)
Masayuki AIKAWA (Hokkaido Univ.)
Takumi KUBOTA (Kyoto Univ.)

Visiting Technicians
Yuichiro WAKITANI (Japan Rad. Assoc.)
Shinya YANOU (Japan Rad. Assoc.)

Student Trainees
Junichi HIRATA (Tokyo Univ. Marine Sci. and Tech.)
Yuuta KITAYAMA (Kanazawa Univ.)
Kouhei NAKAMURA (Osaka Univ.)
Yoshiki FUKUDA (Kanazawa Univ.)
Yudai SHIGEKAWA (Osaka Univ.)
Shingo UENO (Kanazawa Univ.)
Kazunori HAYASHI (Kanazawa Univ.)
Takumi TANIGUCHI (Kanazawa Univ.)
Naoya GOTO (Niigata Univ.)
Takumi KOYAMA (Niigata Univ.)

Shohei TSUTO (Niigata Univ.)
Ryuji AONO (Niigata Univ.)
Daisuke SATO (Niigata Univ.)
Akira TANAKA (Niigata Univ.)
Tetuya NAGAOKA (Niigata Univ.)
Iori CHIYONISHIO (Kanazawa Univ.)
Ahmed USMAN (Univ. of Malaya)
Kento MURAKAMI (Kanazawa Univ.)
Teruyoshi FUJISAWA (Kanazawa Univ.)
Yukari YATSU (Kanazawa Univ.)
Yuki YASUDA (Osaka Univ.)
Yoshihiko HAYASHI (Osaka Univ.)
Risa MOTOYAMA (Niigata Univ.)
Tomihiro TOMITSUKA (Niigata Univ.)
Kaori SHIRAI (Niigata Univ.)
Yu NAMBA (Niigata Univ.)
Kouki MORIYA (Kanazawa Univ.)
Shuta OE (Kanazawa Univ.)
Kouki OUCHI (Osaka Univ.)
Narumi KONDO (Osaka Univ.)
Moemi SAITOH (Hokkaido Univ.)
Junpei INAGAKI (Univ. of Tsukuba)

List of Publications & Presentations

Publications

[Journal]

(Original Papers) *Subject to Peer Review

A. Toyoshima, K. Ooe, S. Miyashita, M. Asai, M. F. Attallah, N. Goto, N. S. Gupta, H. Haba, M. Huang, J. Kanaya, Y. Kaneya, Y. Kasamatsu, Y. Kitatsuji, Y. Kitayama, K. Koga, Y. Komori, T. Koyama, J. V. Kratz, H. V. Lerum, Y. Oshimi, V. Pershina, D. Sato, T. K. Sato, Y. Shigekawa, A. Shinohara, A. Tanaka, K. Tsukada, S. Tsuto, T. Yokokita, A. Yokoyama, J. P. Omtvedt, Y. Nagame, and M. Schädel, “Chemical studies of Mo and W in preparation of a seaborgium (Sg) reduction experiment using MDG, FEC, and SISAK”, Journal of Radioanalytical and Nuclear Chemistry **303**, 1169–1172 (2015).*

K. Ooe, M. F. Attallah, M. Asai, N. Goto, N. S. Gupta, H. Haba, M. Huang, J. Kanaya, Y. Kaneya, Y. Kasamatsu, Y. Kitatsuji, Y. Kitayama, K. Koga, Y. Komori, T. Koyama, J. V. Kratz, H. V. Lerum, S. Miyashita, Y. Oshimi, V. Pershina, D. Sato, T. K. Sato, Y. Shigekawa, A. Shinohara, A. Tanaka, A. Toyoshima, K. Tsukada, S. Tsuto, T. Yokokita, A. Yokoyama, J. P. Omtvedt, Y. Nagame, and M. Schädel, “Development of a new continuous dissolution apparatus with a hydrophobic membrane for superheavy element chemistry”, Journal of Radioanalytical and Nuclear Chemistry **303**, 1317–1320 (2015).*

Y. Komori, T. Yokokita, Y. Kasamatsu, H. Haba, A. Toyoshima, K. Toyomura, K. Nakamura, J. Kanaya, M. Huang, Y. Kudou, N. Takahashi, and A. Shinohara, “Solid-liquid extraction of Mo and W by Aliquat 336 from HCl solutions toward extraction chromatography experiments of Sg”, Journal of Radioanalytical and Nuclear Chemistry **303**, 1385–1388 (2015).*

D. Kaji, K. Morimoto, H. Haba, Y. Wakabayashi, Y. Kudou, M. Huang, S. Goto, M. Murakami, N. Goto, T. Koyama, N. Tamura, S. Tsuto, T. Sumita, K. Tanaka, M. Takeyama, S. Yamaki, and K. Morita, “Startup of a new gas-filled recoil separator GARIS-II”, Journal of Radioanalytical and Nuclear Chemistry **303**, 1523–1525 (2015).*

J. Even, D. Ackermann, M. Asai, M. Block, H. Brand, A. Di Nitto, Ch. E. Düllmann, R. Eichler, F. Fan, H. Haba, W. Hartmann, A. Hübner, F. P. Heßberger, M. Huang, E. Jäger, D. Kaji, J. Kanaya, Y. Kaneya, J. Khuyagbaatar, B. Kindler, J. V. Kratz, J. Krier, Y. Kudou, N. Kurz, M. Laatiaoui, B. Lommel, J. Maurer, S. Miyashita, K. Morimoto, K. Morita, M. Murakami, Y. Nagame, H. Nitsche, K. Ooe, Z. Qin, T. K. Sato, M. Schädel, J. Steiner, T. Sumita, M. Takeyama, K. Tanaka, A. Toyoshima, K. Tsukada, A. Türler, I. Usoltsev, Y. Wakabayashi, Y. Wang, N. Wiehl, A. Yakushev, and S. Yamaki, “In-situ synthesis of volatile carbonyl complexes with short-lived nuclides”, Journal of Radioanalytical and Nuclear Chemistry **303**, 2457–2466 (2015).*

M. U. Khandaker, H. Haba, M. Murakami, and N. Otuka, “Production cross-sections of long-lived radionuclides in deuteron-Induced reactions on natural zinc up to 23 MeV”, Nuclear Instruments and Methods in Physics Research Section B **346**, 8–16 (2015).*

M. Huang, H. Haba, M. Murakami, M. Asai, D. Kaji, J. Kanaya, Y. Kasamatsu, H. Kikunaga, Y. Kikutani, Y. Komori, H. Kudo, Y. Kudou, K. Morimoto, K. Morita, K. Nakamura, K. Ozeki, R. Sakai, A. Shinohara, T. Sumita, K. Tanaka, A. Toyoshima, K. Tsukada, Y. Wakabayashi, and A. Yoneda, “Production of ^{88}Nb and ^{170}Ta for chemical studies of element 105, Db, using the GARIS gas-jet system”, Journal of Radioanalytical and Nuclear Chemistry **304**, 845–859 (2015).*

Y. Wang, Z. Qin, F. L. Fan, H. Haba, Y. Komori, S. W. Cao, X.-L. Wu, and C.-M. Tan, “Gas-phase chemistry of technetium carbonyl complexes”, Physical Chemistry Chemical Physics **17**, 13228–13234 (2015).*

S. Sekimoto, S. Okumura, H. Yashima, Y. Matsushi, H. Matsuzaki, H. Matsumura, A. Toyoda, K. Oishi, N. Matsuda, Y. Kasugai, Y. Sakamoto, H. Nakashima, D. Boehnlein, R. Coleman, G. Lauten, A. Leveling, N. Mokhov, E. Ramberg, A. Soha, K. Vaziri, K. Ninomiya, T. Omoto, T. Shima, N. Takahashi, A. Shinohara, M.W. Caffee, K.C. Welten, K. Nishiizumi, S. Shibat, and T. Ohtsuki, “Measurements of production cross sections of ^{10}Be and ^{26}Al by 120 GeV and 392 MeV proton bombardment of ^{89}Y, ^{159}Tb, and ^{nat}Cu targets”, Nuclear Instruments and Methods in Physics Research Section B **361** 685–688 (2015).*

M. U. Khandaker, H. Haba, M. Murakami, N. Otuka, and H. A. Kassim, “Excitation functions of deuteron-induced nuclear reactions on natural platinum up to 24 MeV”, Nuclear Instruments and Methods in Physics Research Section B **362** 151–162 (2015).*

Y. Kasamatsu, A. Kino, T. Yokokita, K. Nakamura, Y. Komori, K. Toyomura, T. Yoshimura, H. Haba, J. Kanaya, M. Huang, Y. Kudou, N. Takahashi, and A. Shinohara, “Development of an automated batch-type solid-liquid extraction apparatus and extraction of Zr, Hf, and Th by triisooctylamine from HCl solutions for chemistry of element 104, Rf”, Radiochimica Acta **103**, 513–521 (2015).*

I. Usoltsev, R. Eichler, Y. Wang, J. Even, A. Yakushev, H. Haba, M. Asai, H. Brand, A. Di Nitto, Ch.E. Düllmann, F. Fangli, W. Hartmann, M. Huang, E. Jäger, D. Kaji, J. Kanaya, Y. Kaneya, J. Khuyagbaatar, B. Kindler, J.V. Kratz, J. Krier, Y. Kudou, N. Kurz, B. Lommel, S. Miyashita, K. Morimoto, K. Morita, M. Murakami, Y. Nagame, H. Nitsche, K. Ooe, T.K. Sato, M. Schädel, J. Steiner, P. Steinegger, T. Sumita, M. Takeyama, K. Tanaka, A. Toyoshima, K. Tsukada, A. Türler, Y. Wakabayashi, N. Wiehl, S. Yamaki, and Z. Qin, “Decomposition studies of group 6 hexacarbonyl complexes. Part 1: Production and decomposition of $Mo(CO)_6$ and $W(CO)_6$”, Radiochimica Acta **104**, 141–151 (2015).*

A. Kino, Y. Kasamatsu, T. Yokokita, T. Yoshimura, Y. Komori, Y. Kikutani, N. Takahashi, and A. Shinohara, “Solvent extraction of zirconium and hafnium as homologues of rutherfordium by triisooctylamine from HCl solutions”, Solvent Extraction Research and Development, Japan **22**, 127–134 (2015).*

A. R. Usman, M. U. Khandaker, H. Haba, M. Murakami, and N. Otuka, "Measurements of deuteron-induced reaction cross-sections on natural nickel up to 24 MeV", Nuclear Instruments and Methods in Physics Research Section B **368**, 112–119 (2016).*

D. Kaji, K. Morimoto, H. Haba, E. Ideguchi, H. Koura, and K. Morita, "Decay properties of new isotopes ^{234}Bk and ^{230}Am, and even–even Nuclides ^{234}Cm and ^{230}Pu", Journal of the Physical Society of Japan **85**, 015002 (2016).*

S. Cao, Y. Wang, Z. Qin, F. Fan, H. Haba, Y. Komori, X. Wu, C. Tan, and X. Zhang, "Gas-phase chemistry of ruthenium and rhodium carbonyl complexes", Physical Chemistry Chemical Physics **18**, 119–125 (2016).*

J. Hirata, K. Takahashi, Yu Vin Sahoo, and M. Tanaka, "Laser ablation inductively coupled plasma mass spectrometry for quantitative imaging of elements in ferromanganese nodule", Chemical Geology **427**, 65–72 (2016).*

S. Sekimoto, T. Kobayashi, K. Takamiya, M. Ebihara, and S. Shibata, "Origin of spherule samples recovered from Antarctic ice sheet - Terrestrial or extraterrestrial?", Nuclear Engineering and Technology **48**, 293–298 (2016).*

A. R. Usman, M. U. Khandaker, H. Haba, N. Otuka, M. Murakami, and Y. Komori, "Production cross-sections of radionuclides from α-induced reactions on natural copper up to 50 MeV", Applied Radiation and Isotopes (in press).*

S. Fujita, K. Goto-Azuma, M. Hirabayashi, A. Hori, Y. Iizuka, Y. Motizuki, H. Motoyama, and K. Takahashi, "Densification of layered firn of the ice sheet at Dome Fuji Antarctica", J. Glaciology (in press).*

(Review)

H. Haba, "Productions of radioisotopes for application studies at RIKEN RI Beam Factory", Journal of the Particle Accelerator Society of Japan **12**, 206–212 (2015) (in Japanese).

[Book]

(Original Papers)

K. Takahashi, "Frequently used evaluations for aerial and solid pollution" in *Corrosion control and surface finishing* edited by H. Kanematsu and D. M. Barry, pp. 141–151, Springer (2016).

Oral Presentations

[International Conference etc.]

H. Haba, "Productions and decay studies of transactinide elements for superheavy element chemistry", DAE-BRNS 12th National Symposium on Nuclear and Radiochemistry (NUCAR-2015), (Board of Research in Nuclear Sciences, Department of Atomic Energy; Indian Association of Nuclear Chemists and Allied Scientists), Mumbai, India, Feb. (2015).

H. Haba, "Production and decay studies of ^{265}Sg for chemical studies of seaborgium using the gas-filled recoil ion separator GARIS at RIKEN", 249th American Chemical Society National Meeting & Exposition, (American Chemical Society), Denver, USA, Mar. (2015).

H. Yashima, S. Sekimoto, K. Ninomiya, Y. Kasamatsu, T. Shima, N. Takahashi, A. Shinohara, H. Matsumura, D. Satoh Y. Iwamoto, M. Hagiwara, K. Nishiizumi, M. W. Caffee, and S. Shibata, "Measurements of the neutron activation cross sections for Bi and Co at 134 MeV", Tenth International Conference on Methods and Applications of Radioanalytical Chemistry (MARC X), (Los Alamos National Laboratory), Kailua-Kona, USA, Apr. (2015).

Y. Kasamatsu, K. Toyomura, T. Yokokita, Y. Shigekawa, H. Haba, Y. Komori, J. Kanaya, M. Huang, K. Morita, N. Takahashi, M. Murakami, H. Kikunaga, T. Mitsugashira, T. Yoshimura, T. Ohtsuki, K. Takamiya, and A. Shinohara, "Coprecipitation behavior of Rf with Sm hydroxide", 5th International Conference on the Chemistry and Physics of the Transactinide Elements (TAN15), (Advanced Science Research Center, Japan Atomic Energy Agency; Nishina Center for Accelerator-Based Science, RIKEN), Urabandai, Japan, May (2015).

T. Yokokita, Y. Kasamatsu, Y. Shigekawa, Y. Yasuda, K. Nakamura, A. Kino, K. Toyomura, N. Takahashi, H. Haba, Y. Komori, M. Murakami, T. Yoshimura, and A. Shinohara, "Solid-liquid extraction of Rf with Aliquat 336 from HCl", 5th International Conference on the Chemistry and Physics of the Transactinide Elements (TAN15), (Advanced Science Research Center, Japan Atomic Energy Agency; Nishina Center for Accelerator-Based Science, RIKEN), Urabandai, Japan, May (2015).

A. Toyoshima, K. Ooe, M. Asai, M.F. Attallah, N. Goto, N.S. Gupta, H. Haba, M. Kaneko, Y. Kaneya, Y. Kasamatsu, Y. Kitatsuji, Y. Kitayama, K. Koga, Y. Komori, T. Koyama, J.V. Kratz, H.V. Lerum, A. Mitsukai, S. Miyashita, Y. Oshimi, V. Pershina, D. Sato, T.K. Sato, Y. Shigekawa, A. Shinohara, A. Tanaka, K. Tsukada, S. Tsuto, A. Vascon, T. Yokokita, A. Yokoyama, J. P. Omtvedt, Y. Nagame, and M. Schädel, "Developments towards aqueous phase chemistry of transactinide elements", 5th International Conference on the Chemistry and Physics of the Transactinide Elements (TAN15), (Advanced Science Research Center, Japan Atomic Energy Agency; Nishina Center for Accelerator-Based Science, RIKEN), Urabandai, Japan, May (2015).

H. Haba, R. Aono, D. Kaji, Y. Kasamatsu, H. Kikunaga, Y. Komori, H. Kudo, K. Morimoto, K. Morita, M. Murakami, K. Nishio, K. Ooe, A. Shinohara, M. Takeyama, T. Tanaka, A. Toyoshima, K. Tsukada, S. Tsuto, Y. Wakabayashi, S. Yamaki, T. Yokokita, and A. Yoneda, "Production of radioisotopes of ^{261}Rf, ^{262}Db, ^{265}Sg, and ^{266,267}Bh for superheavy element chemistry using GARIS at RIKEN", 5th International Conference on the Chemistry and Physics of the Transactinide Elements (TAN15), (Advanced Science Research Center, Japan Atomic Energy Agency; Nishina Center for Accelerator-Based Science, RIKEN), Urabandai, Japan, May (2015).

Y. Wakabayashi, K. Morimoto, D. Kaji, H. Haba, K. Nishio, H. Koura, M. Takeyama, S. Yamaki, K. Tanaka, M. Asai, Y. Komori, M. Murakami, T. Tanaka, A. Yoneda, and K. Morita, "Production of new isotopes, ^{215}U and ^{216}U close to N = 126", 5th International Conference on the Chemistry and Physics of the Transactinide Elements (TAN15), (Advanced Science Research Center, Japan Atomic Energy Agency; Nishina Center for Accelerator-Based Science, RIKEN), Urabandai, Japan, May (2015).

D. Kaji, K. Morimoto, Y. Wakabayashi, M. Takeyama, S. Yamaki, K. Tanaka, and K. Morita, H. Haba, M. Murakami, S. Goto, H. Kikunaga, and M. Asai, "GARIS-II: new gas-filled recoil ion separator at RIKEN", 5th International Conference on the Chemistry and Physics of the Transactinide Elements (TAN15), (Advanced Science Research Center, Japan Atomic Energy Agency; Nishina Center for Accelerator-Based Science, RIKEN), Urabandai, Japan, May (2015).

H. Haba, "Status and perspectives of SHE syntheses at RIKEN GARIS", 14th Workshop on Recoil Separator for Superheavy Element Chemistry (TASCA15), (GSI Helmholtzzentrum für Schwerionenforschung GmbH), Darmstadt, Germany, Oct. (2015).

Y. Komori, "Development of a rapid solvent extraction apparatus for aqueous chemistry of the heaviest elements", 14th Workshop on Recoil Separator for Superheavy Element Chemistry (TASCA15), (GSI Helmholtzzentrum für Schwerionenforschung GmbH), Darmstadt, Germany, Oct. (2015).

Y. Komori, H. Haba, K. Ooe, and A. Toyoshima, "Development of a rapid solvent extraction apparatus for aqueous chemistry of the heaviest elements", International Chemical Congress of Pacific Basin Societies 2015 (Pacifichem 2015), (American Chemical Society; Canadian Society for Chemistry; Chemical Society of Japan; New Zealand Institute of Chemistry; Royal Australian Chemical Institute; Korean

Chemical Society; Chinese Chemical Society), Hawaii, USA, Dec. (2015).

A. Yokoyama, Y. Kitayama, Y. Fukuda, H. Kikunaga, M. Murakami, Y. Komori, H. Haba, K. Tsukada, and A. Toyoshima, "Extraction behavior of a cationic fluoride complex of rutherfordium with a TTA chelate extractant from HF/HNO_3 acidic solutions", International Chemical Congress of Pacific Basin Societies 2015 (Pacifichem 2015), (American Chemical Society; Canadian Society for Chemistry; Chemical Society of Japan; New Zealand Institute of Chemistry; Royal Australian Chemical Institute; Korean Chemical Society; Chinese Chemical Society), Hawaii, USA, Dec. (2015).

Y. Komori, M. Murakami, and H. Haba, "Measurement of production cross sections of Tc and Re isotopes in deuteron-induced reactions on ^{nat}Mo and ^{nat}W up to 24 MeV", International Chemical Congress of Pacific Basin Societies 2015 (Pacifichem 2015), (American Chemical Society; Canadian Society for Chemistry; Chemical Society of Japan; New Zealand Institute of Chemistry; Royal Australian Chemical Institute; Korean Chemical Society; Chinese Chemical Society), Hawaii, USA, Dec. (2015).

H. Haba, "Production and decay studies of ^{261}Rf, ^{262}Db, ^{265}Sg, and ^{266,267}Bh for superheavy element chemistry using GARIS at RIKEN", International Chemical Congress of Pacific Basin Societies 2015 (Pacifichem 2015), (American Chemical Society; Canadian Society for Chemistry; Chemical Society of Japan; New Zealand Institute of Chemistry; Royal Australian Chemical Institute; Korean Chemical Society; Chinese Chemical Society), Hawaii, USA, Dec. (2015).

Y. Kasamatsu, T. Yokokita, Y. Shigekawa, A. Kino, K. Nakamura, Y. Yasuda, K. Toyomura, N. Takahashi, H. Haba, Y. Komori, M. Murakami, Y. Kuboki, T. Yoshimura, and A. Shinohara, "Solid-liquid and liquid-liquid extractions of Zr, Hf, Th and element 104, Rf, in an Aliquat 336/HCl system", International Chemical Congress of Pacific Basin Societies 2015 (Pacifichem 2015), (American Chemical Society; Canadian Society for Chemistry; Chemical Society of Japan; New Zealand Institute of Chemistry; Royal Australian Chemical Institute; Korean Chemical Society; Chinese Chemical Society), Hawaii, USA, Dec. (2015).

[Domestic Conference]

羽場宏光, "理研における RI 製造応用", 東北大学電子光理学研究センター研究会「大強度電子ビームとその応用利用」, (東北大学電子光理学研究センター), 仙台市, 3 月 (2015).

横北卓也, 中村宏平, 重河優大, 安田勇輝, 笠松良崇, 高橋成人, 吉村崇, 羽場宏光, 小森有希子, 村上昌史, 篠原厚, "104 番元素 Rf の抽出挙動の時間依存性:バッチ型固液抽出装置を用いた Rf の Aliquat336/HCl 系の固液抽出", 日本化学会第 95 春季年会, (日本化学会), 船橋市, 3 月 (2015).

北山雄太, 福田芳樹, 羽場宏光, 塚田和明, 豊嶋厚史, 菊永英寿, 小森有希子, 村上昌史, 上野慎吾, 谷口拓海, 林和憲, 谷津由香里, 千代西尾伊織, 村上拳冬, 横山明彦, "TTA 逆相クロマトグラフィーによる超重元素ラザホージウム(Rf)フッ化物錯体逐次形成の評価", 日本化学会第 95 春季年会, (日本化学会), 船橋市, 3 月 (2015).

矢納慎也, 羽場宏光, 柴田誠一, 脇谷雄一郎, 山田崇裕, "^{70}Zn(d,αn)^{67}Cu 反応による ^{67}Cu の試験的製造", 第 52 回アイソトープ・放射線研究発表会, (日本アイソトープ協会),文京区, 7 月 (2015).

豊嶋厚史, 水飼秋菜, 村上昌史, 佐藤大輔, 本山李沙, 大江一弘, 小森有希子, 羽場宏光, 浅井雅人, 塚田和明, 佐藤哲也, 金谷佑亮, 永目諭一郎, "ドブニウム（Db）フッ化物錯体の同定に向けた HF/HNO_3 水溶液中における Nb, Ta の陰イオン交換実験", 2015 日本放射化学会年会・第 59 回放射化学討論会, (日本放射化学会), 仙台市, 9 月 (2015).

横北卓也, 笠松良崇, 重河優大, 安田勇輝, 中村宏平, 木野愛子, 豊村恵悟, 高橋成人, 羽場宏光, 小森有希子, 村上昌史, 吉村 崇, 篠原 厚, "ラザホージウムの陰イオン塩化物錯体の抽出における分配係数の決定", 2015 日本放射化学会年会・第 59 回放射化学討論会, (日本放射化学会), 仙台市, 9 月 (2015).

小森有希子, 羽場宏光, 大江一弘, 豊嶋厚史, 水飼秋菜, 村上昌史, 佐藤大輔, 本山李沙, 矢納慎也, 渡邉慶子, 坂口 綾, 菊永英寿, Jon Petter Omtvedt, "超重元素の溶液化学研究に向けた GARIS ガスジェット直結型フロー溶媒抽出装置の開発", 2015 日本放射化学会年会・第 59 回放射化学討論会, (日本放射化学会), 仙台市, 9 月 (2015).

福田芳樹, 北山雄太, 羽場宏光, 豊嶋厚史, 塚田和明, 小森有希子, 村上昌史, 菊永英寿, MingHui Huang, 大江一弘, 水飼秋菜, 上野慎吾, 谷口拓海, 林 和憲, 谷津由香里, 千代西尾伊織, 村上拳冬, 大江崇太, 森谷紘基, 横山明彦, "TTA 逆相クロマトグラフィー測定による超重元素 Rf の陽イオンフッ化物錯形成の F^-濃度依存性", 2015 日本放射化学会年会・第 59 回放射化学討論会, (日本放射化学会), 仙台市, 9 月 (2015).

水飼秋菜, 豊嶋厚史, 金谷佑亮, 大江一弘, 佐藤大輔, 村上昌史, 小森有希子, 羽場宏光, 浅井雅人, 塚田和明, 佐藤哲也, 永目諭一郎, "硫酸-Aliquat336 系における Mo ならびに W の溶媒抽出挙動：超重元素 Sg の硫酸錯体形成に向けたモデル実験", 2015 日本放射化学会年会・第 59 回放射化学討論会, (日本放射化学会), 仙台市, 9 月 (2015).

矢納慎也, 羽場宏光, 柴田誠一, 小森有希子, 高橋和也, 脇谷雄一郎, 山田崇裕, 松本幹雄, "^{70}Zn(d,αn)^{67}Cu 反応による ^{67}Cu の製造", 2015 日本放射化学会年会・第 59 回放射化学討論会, (日本放射化学会), 仙台市, 9 月 (2015).

青野竜士, 後藤真一, 加治大哉, 森本幸司, 羽場宏光, 村上昌史, 大江一弘, 工藤久昭, "^{208}Pb + ^{48,50}Ti 反応における中性子欠損 Rf 同位体の合成", 2015 日本放射化学会年会・第 59 回放射化学討論会, (日本放射化学会), 仙台市, 9 月 (2015).

加治大哉, 森本幸司, 羽場宏光, 若林泰生, 武山美麗, 山木さやか, 田中謙伍, M. Huang, 小森有希子, 金谷淳平, 村上昌史, 鹿取謙二, 長谷部裕雄, 米田 晃, 吉田 敦, 門叶冬樹, 吉田友美, 山口貴之, 浅井雅人, Z. Gan, L. Ma, H. Geissel, S. Hofmann, J. Maurer, 藤田訓裕, 成清義博, 田中泰貴, 山本翔也, 森田浩介, "GARIS を用いたホットフュージョン反応 ^{248}Cm+^{48}Ca→^{296}Lv*に関する研究②", 2015 日本放射化学会年会・第 59 回放射化学討論会, (日本放射化学会), 仙台市, 9 月 (2015).

羽場宏光, "理研 RI ビームファクトリーにおける RI 製造応用", 日本放射性医薬品協会講演会, (日本放射性医薬品協会), 千代田区, 1 月 (2016).

羽場宏光, "理研における RI 製造", 東北大学電子光理学研究センター研究会 「放射性同位元素（RI）製造計画と多分野における RI 利用の現状」, (東北大学電子光理学研究センター研究会), 仙台市, 2 月 (2016).

羽場宏光, "理研 RI ビームファクトリーにおけるアルファ放射体利用", 第 7 回アルファ放射体実験室利用研究会, (東北大学金属材料研究所), 仙台市, 2 月 (2016).

羽場宏光, "加速器を用いた応用研究用ラジオアイソトープの製造", 日本物理学会第 71 回年次大会, (日本物理学会), 仙台市, 3 月 (2016).

Posters Presentations

[International Conference etc.]

M. Murakami, S. Goto, K. Ooe, D. Sato, S. Tsuto, N. Goto, T. Koyama, R. Aono, H. Haba, M Huang, and H. Kudo, "Excitation functions of Db isotopes produced in ^{248}Cm(^{19}F,xn) reaction", 5th International Conference on the Chemistry and Physics of the Transactinide Elements (TAN15), (Advanced Science Research Center, Japan Atomic Energy Agency; Nishina Center for Accelerator-Based Science, RIKEN), Urabandai, Japan, May (2015).

Y. Ito, P. Schury, M. Wada, F. Arai, I. Katayama, K. Okada, T. Sonoda, A. Takamine, H. Wollnik, H. Haba, D. Kaji, K. Morimoto, K. Morita, H. Koura, S. Jeong, H. Miyatake, and A. Ozawa, "Development of a gas cell system for SHE-mass project at RIKEN", 5th International Conference on the Chemistry and Physics of the Transactinide Elements (TAN15), (Advanced Science Research Center, Japan Atomic Energy Agency; Nishina Center for Accelerator-Based Science, RIKEN), Urabandai, Japan, May (2015).

Y. Wang, Z. Qin, F.L. Fan, H. Haba, Y. Komori, S.-W. Cao, X.-L. Wu, and C.-M. Tan, "Gas-phase chemistry of short-lived technetium carbonyl complexes", 5th International Conference on the Chemistry and Physics of the Transactinide Elements (TAN15), (Advanced Science Research Center, Japan Atomic Energy Agency; Nishina Center for Accelerator-Based Science, RIKEN), Urabandai, Japan, May (2015).

A. Mitsukai, A. Toyoshima, A. Vascon, Y. Kaneya, M. Murakami, K. Ooe, N. Goto, D. Sato, Y. Komori, H. Haba, K. Tsukada, M. Asai, T.K. Sato, Y. Nagame, and M. Schädel, "Extraction behavior of Mo and W from H_2SO_4 with Aliquat336 as homologs of seaborgium (Sg)", 5th International Conference on the Chemistry and Physics of the Transactinide Elements (TAN15), (Advanced Science Research Center, Japan Atomic Energy Agency; Nishina Center for Accelerator-Based Science, RIKEN), Urabandai, Japan, May (2015).

D. Sato, M. Murakami, H. Haba, H. Kikunaga, K. Ooe, S. Goto, and H. Kudo, "Liquid-liquid extraction studies of Nb and Ta as homologs of Db with Aliquat 336 from HF solutions", 5th International Conference on the Chemistry and Physics of the Transactinide Elements (TAN15), (Advanced Science Research Center, Japan Atomic Energy Agency; Nishina Center for Accelerator-Based Science, RIKEN), Urabandai, Japan, May (2015).

Y. Kitayama, Y. Fukuda, H. Haba, K. Tsukada, A. Toyoshima, H. Kikunaga, M. Murakami, Y. Komori, M.H. Huang, T. Taniguchi, S. Ueno, K. Hayashi, Y. Yatsu, I. Chiyonishio, K. Murakami, and A. Yokoyama, "Extraction behavior of rutherfordium as a cationic fluoride complex with a TTA chelate extractant from HF/HNO_3 acidic solutions", 5th International Conference on the Chemistry and Physics of the Transactinide Elements (TAN15), (Advanced Science Research Center, Japan Atomic Energy Agency; Nishina Center for Accelerator-Based Science, RIKEN), Urabandai, Japan, May (2015).

Y. Fukuda, Y. Kitayama, H. Haba, K. Tsukada, A. Toyoshima, H. Kikunaga, M.H. Huang, M. Murakami, Y. Komori, I. Chiyonishio, and A. Yokoyama, "Adsorption behavior of Zr and Hf by TTA-reversed-phase chromatography for aqueous chemistry of a super-heavy element, Rf", 5th International Conference on the Chemistry and Physics of the Transactinide Elements (TAN15), (Advanced Science Research Center, Japan Atomic Energy Agency; Nishina Center for Accelerator-Based Science, RIKEN), Urabandai, Japan, May (2015).

Y. Kasamatsu, K. Nakamura, T. Yokokita, Y. Shigekawa, Y. Yasuda, N. Takahashi, Y. Kuboki, H. Haba, M. Murakami, T. Yoshimura, and A. Shinohara, "Development of a rapid flow-type solvent extraction apparatus for extraction of Rf", 5th International Conference on the Chemistry and Physics of the Transactinide Elements (TAN15), (Advanced Science Research Center, Japan Atomic Energy Agency; Nishina Center for Accelerator-Based Science, RIKEN), Urabandai, Japan, May (2015).

K. Ooe, A. Tanaka, R. Yamada, R. Yamada, H. Kikunaga, M. Murakami, Y. Komori, H. Haba, S. Goto, and H. Kudo, "Solvent extraction behavior of Zr and Hf with chelate extractants for aqueous chemical studies of Rf ", 5th International Conference on the Chemistry and Physics of the Transactinide Elements (TAN15), (Advanced Science Research Center, Japan Atomic Energy Agency; Nishina Center for Accelerator-Based Science, RIKEN), Urabandai, Japan, May (2015).

Y. Komori, H. Haba, K. Ooe, and A. Toyoshima for the Aqueous Chemistry Collaboration with GARIS, "Development of a rapid solvent extraction apparatus for aqueous chemistry of the heaviest elements", 5th International Conference on the Chemistry and Physics of the Transactinide Elements (TAN15), (Advanced Science Research Center, Japan Atomic Energy Agency; Nishina Center for Accelerator-Based Science, RIKEN), Urabandai, Japan, May (2015).

A. Mitsukai, A. Toyoshima, M. Asai, K. Tsukada, T. Sato, Y. Kaneya, S. Takeda, Y. Nagame, M. Schädel, Y. Komori, M. Murakami, H. Haba, K. Ooe, D. Sato, N. Goto, and S. Tsuto, "Extraction behavior of Mo and W from H_2SO_4 with Aliquat336 as homologues of seaborgium (Sg)", International Chemical Congress of Pacific Basin Societies 2015 (Pacifichem 2015), (American Chemical Society; Canadian Society for Chemistry; Chemical Society of Japan; New Zealand Institute of Chemistry; Royal Australian Chemical Institute; Korean Chemical Society; Chinese Chemical Society), Hawaii, USA, Dec. (2015).

K. Ooe, A. Tanaka, R. Yamada, H. Kikunaga, M. Murakami, Y. Komori, H. Haba, S. Goto, and H. Kudo, "Liquid-liquid extraction behavior of zirconium and hafnium as homologs of element 104, rutherfordium using chelate extractants", International Chemical Congress of Pacific Basin Societies 2015 (Pacifichem 2015), (American Chemical Society; Canadian Society for Chemistry; Chemical Society of Japan; New Zealand Institute of Chemistry; Royal Australian Chemical Institute; Korean Chemical Society; Chinese Chemical Society), Hawaii, USA, Dec. (2015).

H. Kikunaga, M. Murakami, Y. Komori, and H. Haba, "Measurement of alpha-induced reaction cross sections of Cr isotopes on natural Ti", International Chemical Congress of Pacific Basin Societies 2015 (Pacifichem 2015), (American Chemical Society; Canadian Society for Chemistry; Chemical Society of Japan; New Zealand Institute of Chemistry; Royal Australian Chemical Institute; Korean Chemical Society; Chinese Chemical Society), Hawaii, USA, Dec. (2015).

K. Takahashi, T. Minami, S. Imazu, Y.-V. Sahoo, M. Kitagawa, and M. Kidera, "Sources of vermilion collected from ancient Japanese tombs, based on the trace elements and lead isotopes", International Chemical Congress of Pacific Basin Societies 2015 (Pacifichem 2015), (American Chemical Society; Canadian Society for Chemistry; Chemical Society of Japan; New Zealand Institute of Chemistry; Royal Australian Chemical Institute; Korean Chemical Society; Chinese Chemical Society), Hawaii, USA, Dec. (2015).

[Domestic Conference]

山田亮平, 大江一弘, 村上昌史, 羽場宏光, 小森有希子, 菊永英寿, 後藤真一, 工藤久昭, "Rf の溶液化学実験に向けた同族元素 Zr, Hf の HDEHP による溶媒抽出挙動", 2015 日本放射化学会年会・第 59 回放射化学討論会, (日本放射化学会), 仙台市, 9 月 (2015).

本山李沙, 大江一弘, 村上昌史, 羽場宏光, 後藤真一, 工藤久昭, "ドブニウム（Db）の化学実験に向けた 5 族元素 Nb, Ta の塩化物錯体のトリイソオクチルアミンによる抽出挙動", 2015 日本放射化学会年会・第 59 回放射化学討論会, (日本放射化学会), 仙台市, 9 月 (2015).

佐藤大輔, 村上昌史, 大江一弘, 本山李沙, 羽場宏光, 小森有希子, 豊嶋厚史, 水飼秋菜, 菊永英寿, 後藤真一, 工藤久昭, "105 番元素 Db の化学実験のための Aliquat 336 樹脂を用いた Nb, Ta のフッ化水素酸中からの固液抽出", 2015 日本放射化学会年会・第 59 回放射化学討論会, (日本放射化学会), 仙台市, 9 月 (2015).

二宮和彦, 南部明弘, 重河優大, 高橋成人, 篠原厚, 関本俊, 八島浩, 嶋達志, 萩原雅之, 岩元洋介, 柴田誠一, M. W. Caffee, 西泉邦彦, "隕石構成元素に対する 80 MeV 単色中性子による核反応生成物の測定", 2015 日本放射化学会年会・第 59 回放射化学討論会, (日本放射化学会), 仙台市, 9 月 (2015).

RIBF Research Division
User Liaison and Industrial Cooperation Group

1. Abstract

The essential mission of the “User Liaison and Industrial Cooperation (ULIC) Group” is to maximize the research activities of RIBF by attracting users in various fields with a wide scope.

The ULIC Group consists of two teams.

The RIBF User Liaison Team provides various supports to visiting RIBF users through the User’s Office. The Industrial Cooperation Team supports potential users in industries who use the beams for application purposes or for accelerator related technologies other than basic research. Production of various radioisotopes by the AVF cyclotron is also one of the important mission. The produced radioisotopes are distributed to researchers in Japan for a charge through the Japan Radioisotope Association.

In addition the ULIC Group takes care of laboratory tours for RIBF visitors from public. The numbers of visitors amounts to 2,300 per year.

Members

Group Director
Hideyuki SAKAI

Deputy Group Director
Hideki UENO (concurrent: Chief Scientist, Nuclear Spectroscopy Lab.)

Special Temporary Employee
Tadashi KAMBARA

Senior Visiting Scientists
Ikuko HAMAMOTO (Lund Univ.)
Munetake ICHIMURA (Univ. of Tokyo)

Assistants
Katsura IWAI
Noriko KIYAMA
Tomoko IWANAMI
Tomomi OKAYASU

RIBF Research Division
User Liaison and Industrial Cooperation Group
RIBF User Liaison Team (User Support Office)

1. Abstract

To enhance synergetic common use of the world-class accelerator facility, the Radioisotope Beam Factory (RIBF), it is necessary to promote a broad range of applications and to maximize the facility's importance. The facilitation and promotion of the RIBF are important missions charged to the team. Important operational activities of the team include: i) the organization of international Program Advisory Committee (PAC) meetings to review experimental proposals submitted by RIBF users, ii) RIBF beam-time operation management, and iii) promotion of facility use by hosting outside users through the RIBF Independent Users program, which is a new-user registration program begun in FY2010 at the RIKEN Nishina Center (RNC) to enhance the synergetic common use of the RIBF. The team opened the RIBF Users Office in the RIBF building in 2010, which is the main point of contact for Independent Users and provides a wide range of services and information.

2. Major Research Subjects

(1) Facilitation of the use of the RIBF
(2) Promotion of the RIBF to interested researchers

3. Summary of Research Activity

(1) Facilitation of the use of the RIBF

The RIBF Users Office, formed by the team in 2010, is a point of contact for user registration through the RIBF Independent User program. This activity includes:

- registration of users as RIBF Independent Users,
- registration of radiation workers at the RIKEN Wako Institute,
- provision of an RIBF User Card (a regular entry permit) and an optically stimulated luminescence dosimeter for each RIBF Independent User, and
- provision of safety training for new registrants regarding working around radiation, accelerator use at the RIBF facility, and information security, which must be completed before they begin RIBF research.

The RIBF Users Office is also a point of contact for users regarding RIBF beam-time-related paperwork, which includes:

- contact for beam-time scheduling and safety review of experiments by the In-House Safety Committee,
- preparation of annual Accelerator Progress Reports, and
- maintaining the above information in a beam-time record database.

In addition, the RIBF Users Office assists RIBF Independent Users with matters related to their visit, such as invitation procedures, visa applications, and the reservation of on-campus accommodation.

(2) Promotion of the RIBF to interested researchers

- The team has organized an international PAC for RIBF experiments; it consists of leading scientists worldwide and reviews proposals in the field of nuclear physics (NP) purely on the basis of their scientific merit and feasibility. The team also assists another PAC meeting for material and life sciences (ML) organized by the RNC Advanced Meson Laboratory. The NP and ML PAC meetings are organized twice a year.
- The team coordinates beam times for PAC-approved experiments and other development activities. It manages the operating schedule of the RIBF accelerator complex according to the decisions arrived at by the RIBF Machine Time Committee.
- To promote research activities at RIBF, proposals for User Liaison and Industrial Cooperation Group symposia/mini-workshops are solicited broadly both inside and outside of the RNC. The RIBF Users Office assists in the related paperwork.
- The team is the point of contact for the RIBF users' association. It arranges meetings at RNC headquarters for the RIBF User Executive Committee of the users' association.
- The Team conducts publicity activities, such as arranging for RIBF tours, development and improvement of the RNC official web site, and delivery of RNC news via email and the web.

Members

Team Leader
Ken-ichiro YONEDA

Deputy Team Leader
Yasushi WATANABE (concurrent: Senior Research Scientist, Radiation Lab.)

Technical Staff I
Narumasa MIYAUCHI

RIBF Research Division
User Liaison and Industrial Cooperation Group
Industrial Cooperation Team

1. Abstract

Industrial cooperation team handles non-academic activities at RIBF corresponding to industries and to general public.

2. Major Research Subjects

(1) Fee-based distribution of radioisotopes produced at RIKEN AVF Cyclotron
(2) Support of industrial application using the RIBF accelerator beam and its related technologies including novel industrial applications.
(3) Development of real-time wear diagnostics of industrial material using RI beams

3. Summary of Research Activity

(1) Fee-based distribution of radioisotopes

This team handles fee-based distribution of radioisotopes Zn-65, Y-88 and Cd-109 from 2007, which are produced by the RI application team at the AVF cyclotron, to nonaffiliated users under a Material Transfer Agreement (MTA) between Japan Radioisotope Association and RIKEN. In 2015, the MTA was amended to newly list Sr-85. We delivered 3 shipments of Cd-109 with a total activity of 4 MBq, 2 shipments of Zn-65 with a total activity of 10 MBq and one shipment of Y-88 with an activity of 1 MBq. The final recipients of the RIs were five universities and one hospital.

(2) Support of Industrial application using RIBF

In 2009, RNC started a new project “Promotion of applications of high-energy heavy ions and RI beams” as a grant-in-aid program of MEXT “Sharing Advanced Facilities for Common Use Program”. In this project, RNC opens the old part of the RIBF facility, which includes the AVF cyclotron, RILAC, RIKEN Ring Cyclotron and experimental instruments like RIPS, to non-academic proposals from users including private companies. This MEXT program was terminated in 2010, but RNC succeed and promote this facility-sharing program after that. The proposals are reviewed by a program advisory committee, industrial PAC (InPAC). The proposals which have been approved by the InPAC are allocated with beam times and the users pay RIKEN the beam time fee. The intellectual properties obtained by the use of RIBF belong to the users. In order to encourage the use of RIBF by those who are not familiar with utilization of ion beams, the first two beam times of each proposal can be assigned to trial uses which are free of beam time fee.

The fifth InPAC meeting held in January 2016 reviewed two fee-based proposals from private companies and approved them. Until now, three proposals of fee-based utilization have been performed. Private companies used heavy-ion beams of Ar-40 (95 MeV/A) and Kr-84 (70 MeV/A) at the E5A beamline for an irradiation test of space-use semi-conductors.

(3) Development of real-time wear diagnostics using RI beams

We are promoting a method for real-time wear diagnostics of industrial materials using RI beams as tracers. For that purpose, very intense RI beams of Be-7 (T1/2=52 days) at 4.1 MeV/A and Na-22 (T1/2=2.6 years) at 3.7 MeV/A were produced via the (p,n) reaction at the CRIB separator using beams from the AVF cyclotron. As we can provide RI beams of different nuclides and control the implantation depth, we have developed a novel method of wear diagnostics.

In 2014, under a collaborative research agreement between RIKEN, University of Tokyo and two private companies, we had two beam-times to produce RI beams of Be-7 and Na-22 and implanted them near surface of metallic machine parts, whose wear-loss rate was evaluated through measurements of the radio-activities. Until now, one proposal of fee-based utilization using Be-7 beam have been accepted, but it is not completed yet.

We are also developing a new method to determine the spatial distribution of positron-emitting RIs on periodically-moving objects in a closed system, named “GIRO” (Gamma-ray Inspection of Rotating Object). This is based on the same principle as the medical PET systems but is simpler and less expensive. We have constructed a test bench and performed measurements with Na-22 sources to verify the principle and evaluate the resolution. In future this method can be used for real-time evaluation of wear loss in a running machine.

Members

Team Leader
Atsushi YOSHIDA

Technical Staff I
Shinya YANOU (concurrent: RI Application Team)

List of Publications & Presentations

Publications

[Journal]

(Original Papers) *Subject to Peer Review

A.Yoshida, T.Kambara, A.Nakao, R.Uemoto, H.Uno, A.Nagano, H.Yamaguchi, T.Nakao, D.Kahl, Y.Yanagisawa, D.Kameda, T.Ohnishi , N.Fukuda, T.Kubo, “Wear diagnostics of industrial material using RI beams of 7Be and 22Na”, Nuclear Instruments and Methods in Physics Research Section B 317, 785-788 (2013) *

T. Kambara, A. Yoshida, H. Takeichi, "Gamma-ray inspection of rotating object", Nuclear Instruments and Methods in Physics Research B-A 797, 1-7 (2015) *.

[Proceedings]

(Original Papers) *Subject to Peer Review

T. Kambara, A. Yoshida, Y. Yanagisawa, D. Kameda, N. Fukuda, T. Ohnishi, T. Kubo, R. Uemoto, A. Nagano, and H. Uno, ”Industrial Application of Radioactive Ion Beams at the RIKEN RI Beam Factory”, AIP Conference Proceedings 1412 (2011), American Institute of Physics *

[Book]

(Original Papers) *Subject to Peer Review

A. Yoshida, T. Kambara, R. Uemoto, “RI ビーム打込み法を用いた摩耗検査法の開発“, 月刊トライボロジー2014-08 No324 pg.16-18,新樹社(2014)

A. Yoshida, T. Kambara, “研究室紹介 No.43 理化学研究所仁科加速器研究センター産業連携チーム“, 月刊トライボロジー2015-02 No330 pg.66,新樹社(2014)

T. Kambara, "RI ビーム照射を用いた摩耗試験", 加速器 Vol. 12, No. 4(2015)

Oral Presentations

[International Conference etc.]

T. Kambara, et al., “Industrial Application of Radioactive Ion Beams at the RIKEN RI Beam Factory”, 11th International Conference on Applications of Nuclear Techniques, Crete, Greece, Jun (2011)

A.Yoshida, et al., “Wear diagnostics of industrial material using RI beams of 7Be and 22Na”, 16th International Conference on Electromagnetic Iso-tope Separators and Techniques Related to their Applications (EMIS2012), Matsue, Dec.(2012)

[Domestic Conference]

A.Yoshida, “RI ビームの工業応用ー 表面摩耗量検査法開発“, 理研シンポジウム第 16 回「トライボコーティングの現状と将来」, (トライボコーティング技術研究会主催), 和光, 2 月 (2014).

A.Yoshida, “理研 RI ビームバラエティ（産業利用まで）“, 第 54 回放射線科学研究会(エキゾチックビームシリーズ<12>), 大阪ニュークリアサイエンス協会, 大阪, 7 月(2014).

T. Kambara, "イオン照射による材料改質と摩耗試験", 日本物理学会 年次大会, 東北学院大学 仙台, 03/19-22 (2016)

Posters Presentations

[Domestic Conference]

A. Yoshida, T. Kambara, “ＲＩビームでオンライン精密摩耗量測定～摩耗のイメージング～“, nano tech 2016 第 15 回国際ナノテクノロジー総合展・技術会議, 01/27-29, 東京ビッグサイト, (2016)

RIBF Research Division
Safety Management Group

1. Abstract

The RIKEN Nishina Center for Accelerator-Based Science possesses one of the largest accelerator facilities in the world, which consists of two heavy-ion linear accelerators and five cyclotrons. This is the only site in Japan where uranium ions are accelerated. The center also has electron accelerators of microtron and synchrotron storage ring. Our function is to keep the radiation level in and around the facility below the allowable limit and to keep the exposure of workers as low as reasonably achievable. We are also involved in the safety management of the Radioisotope Center, where many types of experiments are performed with sealed and unsealed radioisotopes.

2. Major Research Subjects

(1) Safety management at radiation facilities of Nishina Center for Accelerator-Based Science
(2) Safety management at Radioisotope Center
(3) Radiation shielding design and development of accelerator safety systems

3. Summary of Research Activity

Our most important task is to keep the personnel exposure as low as reasonably achievable, and to prevent an accident. Therefore, we daily patrol the facility, measure the ambient dose rates, maintain the survey meters, shield doors and facilities of exhaust air and wastewater, replenish the protective supplies, and manage the radioactive waste. Advice, supervision and assistance at major accelerator maintenance works are also our task.

Training is very important for safety, and we started annual retraining to all the RIBF users by using an e-learning system. The users can take the training anywhere in the world. Unless the users finish it, their entry is refused at the gate of radiation area.

The radiation monitor system at the Nishina building were installed in 1986. While the central control unit was replaced about 10 years ago, repair of the detector heads became difficult recently, and their replacement was started in 2015.

According to the change of guideline issued by Nuclear Regulation Authority, we must measure the radionuclides concentrations of exhaust air from all the facilities where nuclear fuel materials are used. The exhaust lines of the linac building and the Nishina building were modified, and we could meet the requirement without increase the online concentration monitors which were very expensive.

Minor improvements of the radiation safety systems were also done, for example, the warning sirens of irradiation rooms in the RIBF building were replaced by voice alarms, which made clear what place became dangerous.

Members

Group Director
Yoshitomo UWAMINO

Deputy Group Director
Kanenobu TANAKA

Nishina Center Technical Scientists
Rieko HIGURASHI
Hisao SAKAMOTO
Takeshi MAIE (concurrent; Cryogenic Technology Team)

Technical Staff I
Atsuko AKASHIO
Tomoyuki DANTSUKA (concurrent; Cryogenic Technology Team)

Research Consultant
Masaharu OKANO (Japan Radiation Res. Soc.)

Visiting Scientists
Hee Seock LEE (POSTECH)
Joo-Hee OH (POSTECH))
Nam-Suk JUNG (POSTECH)
Takashi NAKAMURA (Shimizu Corp.)
Noriaki NAKAO (Shimizu Corp.)
Koji OHISHI (Shimizu Corp.)
Arim LEE (Pohang Accelerator Laboratory POSTECH)

Assigned Employee
Hiroki MUKAI

Temporary Staffing
Ryuji SUZUKI

Part-time Workers
Hiroshi KATO
Satomi IIZUKA

Kimie IGARASHI
Hiroko AISO
Naoko USUDATE
Shin FUJITA

Assistant
Tomomi OKAYASU (concurrent: User Liaison and Industrial Cooperation Group)

List of Publications & Presentations

Publications

[Journal]

(Original Papers)

Mikami, S., Maeyama, T., Hoshide, Y., Sakamoto, R., Sato, S., Okuda, N., Demongeot, S., Gurriaran, R., Uwamino, Y., Kato, H., Fujiwara, M., Sato, T., Takemiya, H. and Saito, K.: "Spatial distributions of radionuclides deposited onto ground soil around the Fukushima Dai-ichi Nuclear Power Plant and their temporal change until December 2012", Journal of Environmental Radioactivity, 139, 320-343 (2015). *

[Book]

遮蔽ハンドブック研究専門委員会編: "放射線遮蔽ハンドブックー基礎編ー", 日本原子力学会 (2015).

Oral Presentations

[International Conference etc.]

Oh, J., Jung, N., Lee, H., Oranj, L., Nakao, N., Uwamino, Y. and Ko S.: "Measurements of secondary neutrons spectra from 50 MeV/u 238U beams with the beryllium stripper", 8th International Symposium on Radiation Safety and Detection Technology (ISORD-8), Jeju, Korea, July (2015).

[Domestic Conference]

田中鐘信: "理化学研究所 RI ビームファクトリー加速器施設の放射線安全", 第３回加速器施設安全シンポジウム, 東海村, 1 月,(2016).

赤塩敦子, 田中鐘信, 今尾 浩士: "RIBF 加速器におけるヘリウムガスへのウランビーム 11MeV/u 照射による放射化評価", 日本原子力学会 2016 年春の年会, 仙台, 3 月 (2016).

中尾徳晶, 上蓑義朋, 田中鐘信: "345 MeV/u ウランビームによるターゲットからの前方生成中性子の測定" 日本原子力学会 2015 年秋の大会, 静岡, 9 月 (2015).

Partner Institution

The Nishina Center established the research partnership system in 2008. This system permits an external institute to develop its own projects at the RIKEN Wako campus in equal partnership with the Nishina Center. At present, three institutes, Center for Nuclear Study of the University of Tokyo (CNS), Institute of Particle and Nuclear Studies of KEK (KEK), and Department of Physics, Niigata University (Niigata) are conducting research activities under the research partnership system.

CNS and the Nishina Center signed the partnership agreement in 2008. Until then, CNS had collaborated in joint programs with RIKEN under the "Research Collaboration Agreement on Heavy Ion Physics" (collaboration agreement) signed in 1998. The partnership agreement redefines procedures related to the joint programs while keeping the spirit of the collaboration agreement. The joint programs include experimental nuclear physics activities using CRIB, SHARAQ, GRAPE at RIBF, theoretical nuclear physics activities with ALPHLEET, accelerator development, and activities at RHIC PHENIX.

The partnership agreement with the Niigata University was signed in 2010. The activity includes theoretical and experimental nuclear physics, and nuclear chemistry.

KEK started low-energy nuclear physics activity at RIBF in 2011 under the research partnership system. The newly constructed isotope separator KISS will be available for the users in near future.

The activities of CNS, Niigata, and KEK are reported in the following pages.

Partner Institution
Center for Nuclear Study, Graduate School of Science
The University of Tokyo

1. Abstract

The Center for Nuclear Study (CNS) aims to elucidate the nature of nuclear system by producing the characteristic states where the Isospin, Spin and Quark degrees of freedom play central roles. These researches in CNS lead to the understanding of the matter based on common natures of many-body systems in various phases. We also aim at elucidating the explosion phenomena and the evolution of the universe by the direct measurements simulating nuclear reactions in the universe. In order to advance the nuclear science with heavy-ion reactions, we develop AVF upgrade, CRIB and SHARAQ facilities in the large-scale accelerators laboratories RIBF. We started a new project OEDO for a new energy-degrading scheme, where a RF deflector system is introduced to obtain a good quality of low-energy beam. We promote collaboration programs at RIBF as well as RHIC-PHENIX and ALICE-LHC with scientists in the world, and host international meetings and conferences. We also provide educational opportunities to young scientists in the heavy-ion science through the graduate course as a member of the department of physics in the University of Tokyo and through hosting the international summer school.

2. Major Research Subjects

(1) Accelerator Physics
(2) Nuclear Astrophysics
(3) Nuclear spectroscopy of exotic nuclei
(4) Quark physics
(5) Nuclear Theory
(6) OEDO/SHARAQ project
(7) Exotic Nuclear Reaction
(8) Low Energy Nuclear Reaction Group
(9) Active Target Development

3. Summary of Research Activity

(1) Accelerator Physics

One of the major tasks of the accelerator group is the AVF upgrade project that includes development of ion sources, upgrading the AVF cyclotron of RIKEN and the beam line to CRIB. Development of ECR heavy ion sources is to provide new HI beams, higher and stable beams of metallic ions, and to improve the control system. The Hyper ECR and the Super ECR sources provide all the beams for the AVF cyclotron and support not only CRIB experiments but also a large number of RIBF experiments. Injection beam monitoring and control are being developed and studied. Detailed study of the optics from the ion sources are expected to improve transmission and qualities of beams for the RIBF facility.

(2) Nuclear Astrophysics

The nuclear astrophysics group in CNS is working for experimental researches using the low-energy RI beam separator CRIB. In 2015, experiments on the alpha-cluster structure in ^{14}C and ^{19}Ne nuclei, ^{18}F(p, α) astrophysical reaction using the Trojan Horse method with a improved precision, and the ^{17}F+Ni scattering near the Coulomb barrier were performed at CRIB under international collaborations including Korean, Italian, and Chinese groups. The call for CRIB proposals at the NP-PAC has been resumed in 2014, and 3 new proposals were approved in 2015.

(3) Nuclear structure of exotic nuclei

The NUSPEQ (NUclear SPectroscopy for Extreme Quantum system) group studies exotic structures in high-isospin and/or high-spin states in nuclei. The CNS GRAPE (Gamma-Ray detector Array with Position and Energy sensitivity) is a major apparatus for high-resolution in-beam gamma-ray spectroscopy. Missing mass spectroscopy using the SHARAQ is used for another approach on exotic nuclei. In 2015, the following progress has been made.

Experimental data taken in 2013 under the EURICA collaboration has been analyzed for studying octupole deformation in neutron-rich Ba isotopes and preparing publication. Exothemic charge exchange reaction (^{8}He,^{8}Li*(1+)) on ^{4}He has been analyzed for studying spin-dipole response of few-body system on the photon line. The tetra-neutron studied by the ^{4}He(^{8}He,^{8}Be)4n reaction, showing a candidate of the ground state of the tetra neutrons just above the 4n threshold as well as continuum at higher excitation energy, has been published. We plan to measure the reaction with better statistics and more accuracy in missing mass.

The readout system of 14 detectors of the CNS GRAPE was upgraded, where digital pulse data taken by sampling ADCs are analyzed by FPGAs on boards.

(4) Quark Physics

Main goal of the quark physics group is to understand the properties of hot and dense nuclear matter created by colliding heavy nuclei at relativistic energies. The group has been involved in the PHENIX experiment at Relativistic Heavy Ion Collider (RHIC) at Brookhaven National Laboratory, and the ALICE experiment at Large Hadron Collider (LHC) at CERN. As for PHENIX, the group has been concentrating on the physics analysis involving dielectron measurement in Au+Au collisions. As for ALICE, the group has involved in the

data analyses, which include the measurement of low-mass lepton pairs in Pb-Pb and p-Pb collisions, heavy flavor baryon measurements in pp and p-Pb collisions, particle correlations with large rapidity gap in p-Pb collisions, and searches for dibaryons in Pb-Pb collisions. The group has involved in the ALICE-TPC upgrade using a Gas Electron Multiplier (GEM). Performance evaluation of the MicroMegas + GEM systems for the upgrade has been performed. R&D of GEM and related techniques has been continuing. Development of Teflon GEM has been progressing in collaboration with the Tamagawa group of RIKEN.

(5) Nuclear Theory

The nuclear theory group has been promoting the CNS-RIKEN collaboration project on large-scale nuclear structure calculations and performed shell-model calculations under various collaborations with many experimentalists for investigating the exotic structure of neutron-rich nuclei, such as ^{37,38}Si, ^{50}Ar and ^{80,82}Zn. We also participated in activities of HPCI Strategic Programs, which was finished at the end of FY2015. Since FY2015, we joined a new project "Priority Issue 9 to be tackled by using the Post-K Computer" and promotes computational nuclear physics utilizing supercomputers.

(6) OEDO/SHARAQ project

The OEDO/SHARAQ group promotes high-resolution experimental studies of RI beams by using the high-resolution beamline and SHARAQ spectrometer. A mass measurement by TOF-Bρ technique was performed for very neutron-rich calcium isotopes around N=34. For the experiment, we introduced new detector devices. A set of diamond detectors, developed as timing counters with excellent resolution, were installed as time-of- flight counters at the first and final foci of the beam line. Clover-type Ge detectors were installed at the final focal plane of the SHARAQ spectrometer for the first time, enabling particle identification of RI beams by probing delayed gamma rays from known isomeric states of specific nuclei. The OEDO project, which is a major upgrade of the high-resolution beamline for high-quality RI beams with energies lower than 100 MeV/u, is ongoing. The basic magnet arrangement and ion optics was fixed. We will finish the construction of the new beamline before March, 2017.

(7) Exotic Nuclear Reaction

The Exotic Nuclear Reaction group studies various exotic reactions induced by beams of unstable nuclei. In 2015, analyses of experiments performed in 2014 showed progress: (1) parity transfer probe of the (^{16}O, ^{16} F(g.s)) reaction on ^{12}C gave an enhancement on 0 - states in ^{12}B near zero degrees demonstrating the effectiveness of this reaction, (2) the spectrum of two-neutron relative momentum in knockout reactions from Borromean nucleus ^{11}Li was successfully decomposed into each angular momentum and a candidate of a d-wave resonance was found.

(8) Low Energy Nuclear Reaction Group

We measured the proton resonance elastic scattering with the energy degraded ^{34}Si beam at RIPS facility. This experiment aims to get the excitation function with higher statistics and better energy resolution than the previous experiment. Though the beam intensity was less than expected, we successfully observed the excitation function.

We're also developing two types of the exotic targets, Ti-3H and high-spin isomeric state of ^{178m2}Hf. For the first target, we tested vulnerability with Ti-D which has an atomic ratio of 1:0.2 as the first step. We're going to test the uniformity and impurity in the target with ^{20}Ne beam of 8.2 MeV/u. For the second target, we measured the production cross section of natYb(a,2n) reaction and conducted the chemical separation. Although the activities of other short-lived isotopes are around 10MBq, we successfully identified the cascade decay from ^{178m2}Hf of about 100 Bq by employing EURICA. We obtained the condition for mass production of ^{178m2}Hf at RIBF.

(9) Active Target Development

Two types of gaseous active target TPCs called GEM-MSTPC and CAT are developed and used for the missing mass spectroscopy in inverse kinematics. The common remarkable features of these detectors are the capabilities of the high intensity beam injection and the low energy recoil measurement. The astrophysical reactions of (α,p) on ^{18}Ne, ^{22}Mg and ^{30}S were measured by using the GEM-MSTPC. The alpha emission following the beta decay of ^{16}N was measured with the GEM-MSTPC in combination with the gating grid. The present topic of the CAT is the monopole transition strength distribution in nuclei extracted via deuteron inelastic scattering.
We measured the deuteron scattering off ^{132}Xe and ^{16}O to study the equation of state of nuclear matter and the cluster structure, respectively, at the HIMAC in Chiba. The measurement of deuteron inelastic scattering off ^{132}Sn will be performed in RIBF soon.

Members

Director

Takaharu OTSUKA

Scientific Staff

Susumu SHIMOURA (Professor)
Hideki HAMAGAKI (Professor)
Kentaro YAKO (Associate Professor)
Nobuaki IMAI (Associate Professor)
Noritaka SHIMIZU (Project Associate Professor)
Hidetoshi YAMAGUCHI (Lecturer)
Shin'ichiro MICHIMASA (Assistant Professor)
Taku GUNJI (Assistant Professor)
Shinsuke OTA (Assistant Professor)

Guest Scientists
Hiroaki UTSUNOMIYA (Guest Professor)
Yutaka UTSUNO (Guest Associate Professor)

Technical Staff
Yasuteru KOTAKA

Techinical Assistants
Yukimitsu OHSHIRO
Yukio YAMANAKA
Shoichi YAMAKA
Kazuyuki YOSHIMURA
Mamoru KATAYANAGI

Project Research Associates
Tooru YOSHIDA
Yoritaka IWATA

Post Doctoral Associates
Masanori DOZONO
Tomoaki TOGASHI
Naofumi TSUNODA
Masafumi MATSUSHITA
Yusuke TSUNODA
Yosuke WATANABE
Seiya HAYAKAWA

Graduate Students
David. M KAHL
Hiroyuki MIYA
Motonobu TAKAKI
Motoki KOBAYASHI
Shoichiro MASUOKA
Yuko SEKIGUCHI
Yuki KUBOTA
Yu KIYOKAWA
Keita KAWATA
Keijiro ABE
Shoichiro KAWASE
Hiroshi TOKIEDA
Rin YOKOYAMA
Yuki YAMAGUCHI
ShinIchi HAYASHI
Kohei TERASAKI
CheongSoo LEE
Noritaka KITAMURA
Yuji SAKAGUCHI

Administration Staff
Hiroshi YOSHIMURA (–2015.6)
Ikuko YAMAMOTO
Takako ENDO
Sashiko DOHI
Mikio Oki (2015.7–)
Yukino KISHI
Yuko SOMA

List of Publications & Presentations

Publications

[Journal]

(Original Papers) *Subject to Peer Review

A. Pakou, N. Keeley, D. Pierroutsakou, M. Mazzocco, L. Acosta, X. Aslanoglou, A. Boiano, C. Boiano, D. Carbone, M. Cavallaro, J.Grebosz, M. La Commara, C. Manea, G. Marquinez-Duran, I. Martel, C. Parascandolo, K. Rusek, A.M. Sanchez-Benitez, O. Sgouros, C. Signorini, F. Soramel,V.Soukeras, E. Stiliaris, E. Strano, D. Torresi, A. Trzcinska, Y.X. Watanabe, and H. Yamaguchi:``Total reaction cross sections for ^{8}Li+^{90}Zr at near barrier energies",Eur. Phys. J. A 51, 55 (2015)*

S. Cherubini, M. Gulino, C. Spitaleri, G. G. Rapisarda, M. La Cognata, L. Lamia, R. G. Pizzone, S. Romano, S. Kubono, H. Yamaguchi, S. Hayakawa, Y. Wakabayashi, N. Iwasa, S. Kato, T. Komatsubara, T. Teranishi, A. Coc, N. De Sereville, F. Hammache, G. Kiss, S. Bishop, D. N. Binh:``First application of the trojan horse method with a radioactive ion beam: Study of the ^{18}F (p, alpha)^{15}O reaction at astrophysical energies", Phys. Rev. C 92, 015805 (2015)*

A. Kim, N.H. Lee, M. H. Han, J.S. Yoo, K.I. Hahn, H. Yamaguchi,D. Binh, T. Hashimoto, S. Hayakawa, D. Kahl, T. Kawabata, Y. Kurihara, Y. Wakabayashi, S. Kubono, S. Choi, Y. K. Kwon, J. Y. Moon, H. S. Jung, C.S. Lee, T. Teranishi, S. Kato, T. Komatsubara, B. Guo, W. P. Liu, B. Wang, and Y. Wang:``Measurement of the ^{14}O(alpha, p)^{17}F cross section at Ec.m .=2.1.-5.3 MeV", Phys. Rev. C 92, 035801 (2015) *

H. Utsunomiya, S. Katayama, I. Gheorghe, S. Imai, H. Yamaguchi, D. Kahl, Y. Sakaguchi, T. Shima, K. Takahisa, and S. Miyamoto:``Photodisintegration of ^{9}Be through the 1/2+ state and cluster dipole resonance", Phys. Rev. C 92, 064323 (2015)*

A. Adare et al. [PHENIX Collaboration],``Inclusive cross section and double-helicity asymmetry for pi^{0} production at midrapidity in p + p collisions at √s=510 GeV", Phys. Rev. D 93, no. 1, 011501 (2016) *

J. Adam et al. [ALICE Collaboration],``Pseudorapidity and transverse-momentum distributions of charged particles in proton–proton collisions at √s = 13 TeV", Phys. Lett. B753, 319 (2016) *

J. Adam et al. [ALICE Collaboration],``Inclusive quarkonium production at forward rapidity in pp collisions at √s = 8 TeV", Eur. Phys. J. C76, no. 4, 184 (2016) *

J. Adam et al. [ALICE Collaboration],``Measurement of electrons from heavy-flavour hadron decays in p-Pb collisions at √s_{NN} = 5.02 TeV", Phys. Lett. B754, 81 (2016) *

J. Adam et al. [ALICE Collaboration],``Azimuthal anisotropy of charged jet production in √s_{NN} = 2.76 TeV Pb-Pb collisions", Phys. Lett. B753, 511 (2016) *

J. Adam et al. [ALICE Collaboration],``Direct photon production in Pb-Pb collisions at √s_{NN} = 2.76 TeV", Phys. Lett. B754, 235 (2016) *

J. Adam et al. [ALICE Collaboration],``Centrality evolution of the charged-particle pseudorapidity density over a broad pseudorapidity range in Pb-Pb collisions at $\sqrt{s_{NN}}$ = 2.76 TeV'', Phys. Lett. B754, 373 (2016) *
J. Adam et al.[ALICE Collaboration],``Measurement of D_s^+ production and nuclear modification factor in Pb-Pb collisions at $\sqrt{s_{NN}}$ = 2.76 TeV'',JHEP 1603, 082 (2016) *
J. Adam et al. [ALICE Collaboration],``Multiplicity and transverse momentum evolution of charge-dependent correlations in pp, p–Pb, and Pb–Pb collisions at the LHC'', Eur. Phys. J. C76, no. 2, 86 (2016) *
J. Adam et al. [ALICE Collaboration],``Transverse momentum dependence of D-meson production in Pb-Pb collisions at $\sqrt{s_{NN}}$= 2.76 TeV'',JHEP1603, 081 (2016) *
A. Adare et al. [PHENIX Collaboration],``Scaling properties of fractional momentum loss of high- p_T hadrons in nucleus-nucleus collisions at $\sqrt{s_{NN}}$ from 62.4 GeV to 2.76 TeV'', Phys. Rev. C93, no. 2, 024911 (2016) *
A. Adare et al. [PHENIX Collaboration],``Transverse energy production and charged-particle multiplicity at midrapidity in various systems from $\sqrt{s_{NN}}$=7.7 to 200 GeV'', Phys. Rev. C93, no. 2, 024901 (2016) *
A. Adare et al. [PHENIX Collaboration],`` Φ meson production in the forward/backward rapidity region in Cu + Au collisions at $\sqrt{s_{NN}}$=200 GeV'',Phys. Rev. C93, no. 2, 024904 (2016) *
A. Adare et al. [PHENIX Collaboration],``Forward J/ψ production in U + U collisions at $\sqrt{s_{NN}}$=193 GeV'', Phys. Rev. C93, no. 3, 034903 (2016) *
A. Adare et al. [PHENIX Collaboration],``Dielectron production in Au + Au collisions at $\sqrt{s_{NN}}$ =200 GeV'', Phys. Rev. C93, no. 1, 014904 (2016) *
A. Adare et al. [PHENIX Collaboration],``Single electron yields from semileptonic charm and bottom hadron decays in Au + Au collisions at $\sqrt{s_{NN}}$=200 GeV'', Phys. Rev. C93, no. 3, 034904 (2016) *
A. Adare et al. [PHENIX Collaboration],``Centrality-dependent modification of jet-production rates in deuteron-gold collisions at $\sqrt{s_{NN}}$ =200 GeV'', Phys. Rev. Lett. 116, no. 12, 122301 (2016) *
J. Adam et al. [ALICE Collaboration],``Coherent psi (2S) photo-production in ultra-peripheral Pb-Pb collisions at $\sqrt{s_{NN}}$ = 2.76 TeV'', Phys. Lett. B 751, 358 (2015) *
J. Adam et al. [ALICE Collaboration],``Precision measurement of the mass difference between light nuclei and anti-nuclei'', Nature Phys. 11, no. 10, 811 (2015) *
J. Adam et al. [ALICE Collaboration],``Study of cosmic ray events with high muon multiplicity using the ALICE detector at the CERN Large Hadron Collider'', JCAP 1601, no. 01, 032 (2016) *
J. Adam et al. [ALICE Collaboration],``Centrality dependence of pion freeze-out radii in Pb-Pb collisions at $\sqrt{s_{NN}}$ = 2.76 TeV'', Phys. Rev. C 93, no. 2, 024905 (2016) *
A. Adare et al. [PHENIX Collaboration],``Measurements of elliptic and triangular flow in high-multiplicity ^{3}He + Au collisions at $\sqrt{s_{NN}}$ = 200 GeV'', Phys. Rev. Lett. 115, no. 14, 142301 (2015) *
J. Adam et al. [ALICE Collaboration],``Event shape engineering for inclusive spectra and elliptic flow in Pb-Pb collisions at $\sqrt{s_{NN}}$ = 2.76 TeV'', Phys. Rev. C93, no. 3, 034916 (2016) *
J. Adam et al. [ALICE Collaboration],``Elliptic flow of muons from heavy-flavour hadron decays at forward rapidity in Pb–Pb collisions at $\sqrt{s_{NN}}$ = 2.76 TeV'', Phys. Lett. B753, 41 (2016) *
J. Adam et al. [ALICE Collaboration],``Production of light nuclei and anti-nuclei in pp and Pb-Pb collisions at energies available at the CERN Large Hadron Collider'', Phys. Rev. C93, no. 2, 024917 (2016) *
J. Adam et al. [ALICE Collaboration],``Centrality dependence of inclusive J/ψ production in p-Pb collisions at $\sqrt{s_{NN}}$ = 5.02 TeV'', JHEP 1511, 127 (2015) *
J. Adam et al. [ALICE Collaboration],`` $^3_{\Lambda}$H and $^3_{\Lambda bar}$H production in Pb-Pb collisions at $\sqrt{s_{NN}}$ = 2.76 TeV'', Phys. Lett. B754, 360 (2016) *
A. Adare et al. [PHENIX Collaboration],`` phi meson production in d+Au collisions at $\sqrt{s_{NN}}$ = 200 GeV'', Phys. Rev. C92, no. 4, 044909 (2015) *
J. Adam et al. [ALICE Collaboration],``Forward-central two-particle correlations in p-Pb collisions at $\sqrt{s_{NN}}$ = 5.02 TeV'', Phys. Lett. B753, 126 (2016) *
J. Adam et al. [ALICE Collaboration],``One-dimensional pion, kaon, and proton femtoscopy in Pb-Pb collisions at $\sqrt{s_{NN}}$ = 2.76 TeV'', Phys. Rev. C92, no. 5, 054908 (2015) *
A. Adare et al. [PHENIX Collaboration],``Measurement of higher cumulants of net-charge multiplicity distributions in Au + Au collisions at $\sqrt{s_{NN}}$=7.7-200 GeV'', Phys. Rev. C93, no. 1, 011901 (2016) *
J. Adam et al. [ALICE Collaboration],``Search for weakly decaying bar{Λn}} and Λ-Λ exotic bound states in central Pb-Pb collisions at $\sqrt{s_{NN}}$ = 2.76 TeV'', Phys. Lett. B752, 267 (2016) *
J. Adam et al. [ALICE Collaboration],``Centrality dependence of the nuclear modification factor of charged pions, kaons, and protons in Pb-Pb collisions at $\sqrt{s_{NN}}$ =2.76 TeV'',Phys. Rev. C93, no. 3, 034913 (2016) *
J. Adam et al. [ALICE Collaboration],``Centrality dependence of high-p_T D meson suppression in Pb-Pb collisions at $\sqrt{s_{NN}}$ = 2.76 TeV'', JHEP1511, 205 (2015) *
J. Adam et al. [ALICE Collaboration],``Measurement of jet quenching with semi-inclusive hadron-jet distributions in central Pb-Pb collisions at $\sqrt{s_{NN}}$=2.76 TeV'', JHEP1509, 170 (2015) *
J. Adam et al. [ALICE Collaboration],``Measurement of charm and beauty production at central rapidity versus charged-particle multiplicity in proton-proton collisions at √s=7 TeV'', JHEP1509, 148 (2015) *
A. Adare et al. [PHENIX Collaboration],``Measurement of parity-violating spin asymmetries in W production at midrapidity in longitudinally polarized p + p collisions'', Phys. Rev. D 93, no. 5, 051103 (2016) *
J. Adam et al. [ALICE Collaboration],``Inclusive, prompt and non-prompt J/ psi production at mid-rapidity in Pb-Pb collisions at $\sqrt{s_{NN}}$ = 2.76 TeV'', JHEP 1507, 051 (2015) *
A. Adare et al. [PHENIX Collaboration], ``Systematic study of charged-pion and kaon femtoscopy in Au + Au collisions at $\sqrt{s_{NN}}$ =200 GeV'', Phys. Rev. C92, no. 3, 034914 (2015) *
J. Adam et al. [ALICE Collaboration],``Measurement of pion, kaon and proton production in proton–proton collisions at √s = 7 TeV'', Eur. Phys. J. C 75, no. 5, 226 (2015) *
J. Adam et al. [ALICE Collaboration],``Coherent ρ^0 photoproduction in ultra-peripheral Pb-Pb collisions at $\sqrt{s_{NN}}$ =2.76 TeV'', JHEP 1509, 095

(2015) *
J. Adam et al. [ALICE Collaboration],``Rapidity and transverse-momentum dependence of the inclusive J/psi nuclear modification factor in p-Pb collisions at √s_{NN} = 5.02 TeV'', JHEP 1506, 055 (2015) *
J. Adam et al. [ALICE Collaboration],``Measurement of dijet k_T in p–Pb collisions at √s_{NN} = 5.02 TeV'', Phys. Lett. B 746, 385 (2015) *
J. Adam et al. [ALICE Collaboration],``Measurement of charged jet production cross sections and nuclear modification in p-Pb collisions at √s_{NN} = 5.02 TeV'', Phys. Lett. B 749, 68 (2015) *
J. Adam et al. [ALICE Collaboration],``Measurement of jet suppression in central Pb-Pb collisions at √s_{NN} = 2.76 TeV'', Phys. Lett. B 746, 1 (2015) *
J. Adam et al. [ALICE Collaboration],``Two-pion femtoscopy in p-Pb collisions at √s_{NN} = 5.02 TeV'', Phys. Rev. C 91, 034906 (2015) *
J. Adam et al. [ALICE Collaboration],``Forward-backward multiplicity correlations in pp collisions at √s = 0.9, 2.76 and 7 TeV'', JHEP 1505, 097 (2015) *
J. Adam et al. [ALICE Collaboration],``Centrality dependence of particle production in p-Pb collisions at √s_{NN} = 5.02 TeV'', Phys. Rev. C91, no. 6, 064905 (2015) *
A. Adare et al. [PHENIX Collaboration],``Systematic Study of Azimuthal Anisotropy in Cu+Cu and Au+Au Collisions at √s_{NN} = 62.4 and 200 GeV'', Phys.Rev. C 92, no. 3, 034913 (2015) *
B. B. Abelev et al. [ALICE Collaboration],``Inclusive photon production at forward rapidities in proton-proton collisions at √s = 0.9, 2.76 and 7 TeV'', Eur. Phys. J. C 75, no. 4, 146 (2015) *
B. B. Abelev et al. [ALICE Collaboration],``Charged jet cross sections and properties in proton-proton collisions at √s = 7 TeV'', Phys. Rev. D 91, no. 11, 112012 (2015) *
B. B. Abelev et al. [ALICE Collaboration],``Production of inclusive ¥Upsilon (1S) and Upsilon (2S) in p-Pb collisions at √s_{NN} = 5.02} TeV'', Phys. Lett. B 740, 105 (2015) *
A. Adare et al. [PHENIX Collaboration],``Charged-pion cross sections and double-helicity asymmetries in polarized p+p collisions at √s = 200 GeV'', Phys. Rev. D 91, no. 3, 032001 (2015) *
A. Adare et al. [PHENIX Collaboration],``Search for dark photons from neutral meson decays in p+p and d+Au collisions at √s_{NN} = 200 GeV'', Phys. Rev. C 91, no. 3, 031901 (2015) *
B. B. Abelev et al. [ALICE Collaboration],``Multiplicity dependence of jet-like two-particle correlation structures in p–Pb collisions at √s_{NN} =5.02 TeV'', Phys. Lett. B 741, 38 (2015) *
B. B. Abelev et al. [ALICE Collaboration],``Production of Sigma(1385)$^{\pm}$ and Xi(1530)^0 in proton-proton collisions at √s = 7 TeV'', Eur. Phys. J. C 75, no. 1, 1 (2015) *
B. B. Abelev et al. [ALICE Collaboration],``Elliptic flow of identified hadrons in Pb-Pb collisions at √s_{NN} = 2.76 TeV'', JHEP 1506, 190 (2015) *
B. B. Abelev et al. [ALICE Collaboration],``Measurement of electrons from semileptonic heavy-flavor hadron decays in pp collisions at √s = 2.76 TeV'', Phys. Rev. D 91, no. 1, 012001 (2015) *
A. Adare et al. [PHENIX Collaboration],``Cross section for b¥bar{b} production via dielectrons in d + Au collisions at √s_{NN} = 200 GeV'', Phys. Rev. C 91, no. 1, 014907 (2015) *
A. Adare et al. [PHENIX Collaboration],``Centrality dependence of low-momentum direct-photon production in Au + Au collisions at √s_{NN} = 200 GeV'', Phys. Rev. C 91, no. 6, 064904 (2015) *
A. Adare et al. [PHENIX Collaboration],``Heavy-quark production and elliptic flow in Au + Au collisions at √s_{NN} = 62.4 GeV'', Phys. Rev. C 91, no. 4, 044907 (2015) *
A. Adare et al. [PHENIX Collaboration],``Measurement of long-range angular correlation and quadrupole anisotropy of pions and (anti)protons in central d + Au collisions at √s_{NN} =200 GeV'', Phys. Rev. Lett. 114, no. 19, 192301 (2015) *
A. Adare et al. [PHENIX Collaboration],``Measurement of ¥Upsilon(1S+2S+3S) production in p+p and Au+Au collisions at √s_{NN} = 200 GeV'', Phys.Rev.C 91, no. 2, 024913 (2015) *
B. B. Abelev et al. [ALICE Collaboration],`` K^(892)^0 and ϕ(1020) production in Pb-Pb collisions at √s_{NN} = 2.76 TeV'', Phys. Rev. C 91, 024609 (2015) *
Y.G. Ma, D.Q. Fang, X.Y. Sun, P. Zhou, Y. Togano, N. Aoi, H. Baba, X.Z. Cai, X.G. Cao, J.G. Chen, Y. Fu, W. Guo, Y. Hara, T. Honda, Z.G. Hu, K. Ieki, Y. Ishibashi, Y. Ito, N. Iwasa, S. Kanno, T. Kawabata, H. Kimura, Y. Kondo, K. Kurita, M. Kurokawa, T. Moriguchi, H. Murakami, H. Ooishi, K. Okada, S. Ota, A. Ozawa, H. Sakurai, S. Shimoura, R. Shioda, E. Takeshita, S. Takeuchi, W.D. Tian, H.W. Wang, J.S. Wang, M. Wang, K. Yamada, Y. Yamada, Y. Yasuda, K. Yoneda, G.Q. Zhang, T. Motobayashi:{``Different mechanism of two-proton emission from proton-rich nuclei ^{23}Al and ^{22} Mg''}, Phys. Lett. B 743, 306--309 (2015) *
K. Kisamori, S. Shimoura, H. Miya, S. Michimasa, S. Ota, M. Assie, H. Baba, T. Baba, D. Beaumel, M. Dozono, T. Fujii, N. Fukuda, S. Go, F. Hammache, E. Ideguchi, N. Inabe, M. Itoh, D. Kameda, S. Kawase, T. Kawabata, M. Kobayashi, Y. Kondo, T. Kubo, Y. Kubota, M. Kurata-Nishimura, C.S. Lee, Y. Maeda, H. Matsubara, K. Miki, T. Nishi, S. Noji, S. Sakaguchi, H. Sakai, Y. Sasamoto, M. Sasano, H. Sato, Y. Shimizu, A. Stolz, H. Suzuki, M. Takaki, H. Takeda, S. Takeuchi, A. Tamii, L. Tang, H. Tokieda, M. Tsumura, T. Uesaka, K. Yako, Y. Yanagisawa, R. Yokoyama, K. Yoshida:``Candidate Resonant Tetraneutron State Populated by the ^{4}He(^{8}He, ^{8}Be) Reaction'', Phys. Rev. Lett. 116, 052501 (2016) *
D. Steppenbeck, S. Takeuchi, N. Aoi, P. Doornenbal, M. Matsushita, H. Wang, Y. Utsuno, H. Baba, S. Go, J. Lee, K. Matsui, S. Michimasa, T. Motobayashi, D. Nishimura, T. Otsuka, H. Sakurai, Y. Shiga, N. Shimizu, P.-A. Soderstrom, T. Sumikama, R. Taniuchi, J. J. Valiente-Dobon, and K. Yoneda: ``Low-Lying Structure of ^{50}Ar and the N=32 Subshell Closure'',Phys. Rev. Lett. 114, 252501 (2015) *
D. Suzuki, H. Iwasaki, D. Beaumel, M. Assie, H. Baba, Y. Blumenfeld, F. de Oliveira Santos, N. de Sereville, A. Drouart, S. Franchoo, J. Gibelin, A. Gillibert, S. Giron, S. Grevy, J. Guillot, M. Hackstein, F. Hammache, N. Keeley, V. Lapoux, F. Marechal, A. Matta, S. Michimasa, L. Nalpas, F. Naqvi, H. Okamura, H. Otsu, J. Pancin, D.Y. Pang, L. Perrot, C.M. Petrache, E. Pollacco, A. Ramus, W. Rother, P. Roussel-Chomaz, H. Sakurai, J.-A. Scarpaci, O. Sorlin, P.C. Srivastava, I. Stefan, C. Stodel, Y. Tanimura, S. Terashima:``Second 0^+ state of unbound ^{12}O: Scaling of mirror asymmetry'',Phys. Rev. C 93, 024316 (2016) *
Z. Patela, Zs. Podolyak, P.M. Walker, P.H. Regan, P.-A. Soderstrom, H. Watanabe, E. Ideguchi, G.S. Simpson, S. Nishimura, F. Browne, P. Doornenbal, G. Lorusso, S. Rice, L. Sinclair, T. Sumikama, J. Wu, Z.Y. Xu, N. Aoi, H. Baba, F.L. Bello Garrote, G. Benzoni, R. Daido, Zs. Dombradi, Y. Fang, N. Fukuda, G. Gey, S. Go, A. Gottardo, N. Inabe, T. Isobe, D. Kameda, K. Kobayashi, M. Kobayashi, T. Komatsubara, I. Kojouharov, T. Kubo, N. Kurz, I. Kuti, Z. Li, H.L. Liu, M. Matsushita, S. Michimasa, C.-B. Moon, H. Nishibata, I. Nishizuka, A. Odahara, E. Sahin, H. Sakurai, H. Schaffner, H. Suzuki, H. Takeda, M. Tanaka, J. Taprogge, Zs. Vajta, F.R. Xu, A. Yagi, R. Yokoyama:``Decay

spectroscopy of ^{160}Sm: The lightest four-quasiparticle K isomer", Phys. Lett. B 753, 182--186 (2016) *

C. Santamaria, C. Louchart, A. Obertelli,V. Werner,P. Doornenbal, F. Nowacki, G. Authelet, H Baba, D. Calvet,F. Chateau, A. Corsi, A. Delbart, J.-M. Gheller, A. Gillibert, T. Isobe, V. Lapoux, M. Matsushita,S. Momiyama, T. Motobayashi, M. Niikura, H. Otsu, C. Peron,A. Peyaud, E.C. Pollacco, J.-Y. Rousse, H. Sakurai,M Sasano, Y. Shiga, S. Takeuchi, R. Taniuchi,T. Uesaka, H. Wang, K. Yoneda, F. Browne, L.X. Chung, Zs. Dombradi, S. Franchoo, F. Giacoppo, A. Gottardo, K. Hadynska-Klek, Z. Korkulu, S. Koyama, Y. Kubota, J Lee, M. Lettmann, R. Lozeva, K. Matsui, T. Miyazaki, S. Nishimura, L. Olivier, S. Ota, Z. Patel, N. Pietralla, E. Sahin, C. Shand, P.-A. Soderstrom, I. Stefan, D. Steppenbeck, T. Sumikama, D. Suzuki, Zs. Vajta, J. Wu, Z. Xu:``Extension of the N=40 Island of Inversion towards N=50: Spectroscopy of ^{66}Cr, ^{70}Fe, ^{72}Fe", Phys. Rev. Lett. 115, 192501 (2016) *

A. Corsi, S. Boissinot, A. Obertelli, P. Doornenbal, M. Dupuis, F. Lechaftois, M. Matsushita, S. Peru, S. Takeuchi, H. Wang, N. Aoi, H. Baba, P. Bednarczyk, M. Ciemala, A. Gillibert, T. Isobe, A. Jungclaus, V. Lapoux, J. Lee, M. Martini, K. Matsui, T. Motobayashi, D. Nishimura, S. Ota, E. Pollacco, H. Sakurai, C. Santamaria, Y. Shiga, D. Sohler, D. Steppenbeck, R. Taniuchi, ``Neutron-driven collectivity in light tin isotopes: Proton inelastic scattering from ^{104}Sn", Phys. Lett. B 743, 451-455 (2016) *

D.A. Finl, T.E. Cocolios, A.N. Andreyev, S. Antalic, A.E. Bazarkh, B. Bastin, D.V. Fedorov, V.N. Fedosseev, K.T. Flanagan, L.Ghys, A. Gottberg, M. Huyse, N. Imai, T. Kron, N. Lecesne, K. M. Lynch, B.A. Marsh, D. Pauwels, E. Rapisarda, S.D. Richter, R.E. Rossel, S. Rothe, M.D. Seliverstov, A.M. Sjordin, C.Van Beveren, P. Van Duppen, K.D.A. Wendt: ``In-Source Laser Spectroscopy with the Laser Ion Source and Trap: First Direct Study of the Ground-State Properties of 217,219Po", Phys. Rev. X5, 011018 (2015) *

A. Matta, D. Beaumel, H. Otsu, V. Lapoux, N.K. Timofeyuk, N. Aoi, N. Assie, H. Baba, S. Boissinot, R.J. Chen, F. Delaunay, N. de Sereville, S. Franchoo, P. Gangnant, J. Gibelin, F. Hammache, Ch. Houarner, N. Imai, N. Kobayashi, T. Kubo, Y. Kondo, Y. Kawada, L.H. Khiem, M. Kurata-Nishimura, E.A. Kuzmin, J. Lee, J.F. Libin, T. Motobayashi, T. Nakamura, L. Nalpas, E.Yu. Nikoslkii, A. Obertelli, E.C. Pollacco, E. Rindel, Ph. Rosier, F. Saillant, T. Sako, H. Sakurai, A.M. Sanchez-Benitez, J-A. Scarpaci, I. Stefan, D. Suuki, K. Takahashi, M. Takechi, H. Wang, R. Wolski, and K. Yoneda:``New findings on structure and production of ^{10}He from ^{11}Li with the (d, ^{3}He) reaction", Phys.Rev. C 92, 041302 (2015), Pub.Note Phys.Rev. C 92, 044903 (2015) *

Y.X. Watanabe, Y. H. Kim, S.C. Jeong, Y. Hirayama, N. Imai, H. Ishiyama, H.S. Jung, H. Miyatake, S. Choi, J.S. Song, E. Clement, G. de France, A. Navin, M. Rejmund, C. Shmitt, G. Pollarolo, L. Corradi, E. Fioretto, D. Montanari, M. Niikura,, D. Suzuki, H. Nishibata, J. Takatsu,``Pathway for the Production of Neutron-Rich Isotopes around the N=126 Shell Closur", Phys.Rev.Lett. 115, 172503 (2015) *

T. Miyagi, T. Abe, R. Okamoto, and T. Otsuka:``Ground-state energies and charge radii of ^{4}He, ^{16}O, ^{40}Ca, and ^{56}Ni in the unitary-model-operator approach", Prog. Theor. Exp. Phys. 2015, no. 4, 041D01 (2015)*

Y. Iwata: ``Energy-dependent existence of soliton in the synthesis of chemical elements", Mod. Phys. Lett. A 30, No. 16, 155008 (2015)*

D. Steppenbeck, S. Takeuchi, N. Aoi, P. Doornenbal, M. Matsushita, H. Wang, Y. Utsuno, H. Baba, S. Go, J. Lee, K. Matsui, S. Michimasa, T. Motobayashi, D. Nishimura, T. Otsuka, H. Sakurai, Y. Shiga, N. Shimizu, P.-A. Soderstrom, T. Sumikama, R. Taniuchi, J.J. Valiente-Dobon, and K. Yoneda:``Low-Lying Structure of ^{50}Ar and the N=32 Subshell Closure", Phys. Rev. Lett. 114 252501 (2015) *

Y. Iwata, T. Ichikawa, N. Itagaki, J.A. Maruhn, and T. Otsuka: ``Examination of the stability of a rod-shaped structure in ^{24}Mg", Phys. Rev. C 92 011303(R) (2015). *

K. Steiger, S. Nishimura, Z. Li, R. Gernhauser, Y. Utsuno, R. Chen, T. Faestermann, C. Hinke, R. Krucken, M. Kurata-Nishimura, G. Lorusso, Y. Miyashita, N. Shimizu, K. Sugimoto, T. Sumikama, H. Watanabe, and K. Yoshinaga: ``Nuclear structure of ^{37,38}Si investigated by decay spectroscopy of $^{37, 38}$Al", Eur. Phys. J. A 51 117 (2015)*

T. Otsuka, and Y. Tsunoda: “The role of shell evolution in shape coexistence", J. Phys. G: Nucl. Part. Phys. 43 024009 (2016).

T. Suzuki, T. Otsuka, C. Yuan, and N. Alfari: ``Two-neutron “halo” from the low-energy limit of neutron–neutron interaction: Applications to drip-line nuclei ^{22}C and ^{24}O", Phys. Lett. B 753 199-203 (2016) *

Y. Shiga, K. Yoneda, D. Steppenbeck, N. Aoi, P. Doornenbal, M. Matsushita, S. Takeuchi, H. Wang, H. Baba, P. Bednarczyk, Zs. Dombradi, Zs. Fulop, S. Go, T. Hashimoto, M. Honma, E. Ideguchi, K. Ieki, K. Kobayashi, Y. Kondo, R. Minakata, T. Motobayashi, D. Nishimura, T. Otsuka, H. Otsu, H. Sakurai, N. Shimizu, D. Sohler, Y. Sun, A. Tamii, R. Tanaka, Z. Tian, Y. Tsunoda, Zs. Vajta, T. Yamamoto, X. Yang, Z. Yang, Y. Ye, R. Yokoyama, and J. Zenihiro: ``Investigateing nuclear structure in the vicinity of ^{78}Ni: Low-lying excited states in the neutron-rich isotopes ^{80,82}Zn", Phys. Rev. C 93 024320 (2016) *

A. Gade, J.A. Tostevin, V. Bader, T. Baugher, D. Bazin, J.S. Berryman, B.A. Brown, D.J. Hartley, E. Lunderberg, F. Recchia, S.R. Stroberg, Y. Utsuno, D. Weisshaar, and K. Wimmer: ``One-neutron pickup into ^{49}Ca: Bound neutron $g_{9/2}$ spectroscopic strength at N=29 ",Phys. Rev. C 93 031601 (2016) *

Y. Iwata, N. Shimizu, T. Otsuka, Y. Utsuno, J. Menendez, M. Honma, and T. Abe: ``Large-scale shell-model analysis of the neutrinoless $\beta\beta$ decay of ^{48}Ca", Phys. Rev. Lett. 116 112502 (2016) *

[Proceedings]

(Original Papers) *Subject to Peer Review

S. Sanfilippo, S. Cherubini, S. Hayakawa, A. Di Pietro, P. Figuera, M. Gulino, M. La Cognata, M. Lattuada, C. Spitaleri, H. Yamaguchi, D. Kahl, T. Nakao, S. Kubono, Y. Wakabayashi, T. Hashimoto, N. Iwasa, Y. Okoda, K. Ushio, T. Teranishi, M. Mazzocco, C. Signorini, D. Torresi, J.Y. Moon, T. Komatsubara, P.S. Lee, K.Y. Chae, M.S. Gwak: “ β delayed α decay of ^{16}N and the ^{12}C (α, γ)^{16}O cross section at astrophysical energies: A new experimental approach", American Institute of Physics Conference Series 1645 387--391 (2015).

Pilsoo Lee, Chun Sik Lee, Jun Young Moon, Kyung Yuk Chae, Soo Mi Cha, Hidetoshi Yamaguchi, Taro Nakao, David M. Kahl, Shigeru Kubono, Silvio Cherubini, Seiya Hayakawa, Cosimo Signorini: ``Development and performance test of the analysis software for the CRIB active target", Journal of the Korean Physical Society 66 459--464 (2015).

H. Yamaguchi, D. Kahl, S. Hayakawa, Y. Sakaguchi, T. Nakao, Y. Wakabayashi, T. Hashimoto, T. Teranishi, S. Kubono, S. Cherubini, M. Mazzocco, C. Signorini, M. Gulino, A. Di Pietro, P. Figuera, M. La Cognata, M. Lattuada, C. Spitaleri, D. Torresi, P.S. Lee, C.S. Lee, T. Komatsubara, N. Iwasa, Y. Okoda, D. Pierroutsakou, C. Parascandolo, M. La Commara, E. Strano, C. Boiano, A. Boiano, C. Manea, A.M. Sanchez-Benitez, H. Miyatake, Y.X. Watanabe, H. Ishiyama, S.C. Jeong, N. Imai, Y. Hirayama, S. Kimura, M. Mukai, Y.H. Kim, C.J. Lin, H.M. Jia, L. Yan, Y.Y. Yang, T. Kawabata, Y.K. Kwon, D.N. Binh, L.H. Khiem, and N.N. Duy: ``Studies on Nuclear Astrophysics and Exotic Structure at the Low-Energy RI Beam Facility CRIB", The Physical Society of Japan Conference Proceedings 6 010011 (2015).

K. Roed, T. Gunji et al. [ALICE TPC Collaboration], ``Upgrade of the ALICE TPC FEE online radiation monitoring system”, JINST 10, no. 12, P12019 (2015).

Shoichiro Kawase, Tsz Leung Tang, Tomohiro Uesaka, Didier Beaumel, Masanori Dozono, Toshihiko Fujii, Taku Fukunaga, Naoki Fukuda, Alfredo Galindo-Uribarri, SangHoon Hwang, Naohito Inabe, Daisuke Kameda, Tomomi Kawahara, Wooyoung Kim, Keiichi Kisamori, Motoki Kobayashi, Toshiyuki Kubo, Yuki Kubota, Kensuke Kusaka, CheongSoo Lee, Yukie Maeda, Hiroaki Matsubara, Shin'ichiro Michimasa, Hiroyuki Miya, Tetsuo Noro, Alexandre Obertelli, Shinsuke Ota, Elizabeth Padilla-Rodal, Satoshi Sakaguchi, Hideyuki Sakai, Masaki Sasano, Susumu Shimoura, Samvel Stepanyan, Hiroshi Suzuki, Motonobu Takaki, Hiroyuki Takeda, Hiroshi Tokieda, Tomotsugu Wakasa4 Takashi Wakui, Kentaro Yako, Yoshiyuki Yanagisawa, Jumpei Yasuda, Rin Yokoyama, Koichi Yoshida, Juzo Zenihiro: ``Spectroscopy of Single-Particle States in Oxygen Isotopes via (p,2p) Reaction'', Proceedings of the Conference on Advances in Radioactive Isotope Science (ARIS2014), JPS Conf. Proc. 6, 020003 (2015)

Motonobu Takaki, Hiroaki Matsubara, Tomohiro Uesaka, Nori Aoi, Masanori Dozono, Takashi Hashimoto, Takahiro Kawabata, Shoichiro Kawase, Keiichi Kisamori, Yuki Kubota, Cheng Soo Lee, Jenny Lee, Yukie Maeda, Shin'ichiro Michimasa, Kenjiro Miki, Shinsuke Ota, Masaki Sasano, Susumu Shimoura, Tomokazu Suzuki, Keiji Takahisa, Tsz Leung Tang, Atsushi Tamii, Hiroshi Tokieda, Kentaro Yako, Rin Yokoyama, Juzo Zenihiro: ``Heavy-Ion Double-Charge Exchange Study via a ^{12}C(^{18}O, ^{18}Ne)^{12}Be Reaction'', Proceedings of the Conference on Advances in Radioactive Isotope Science (ARIS2014), JPS Conf. Proc. 6, 020038 (2015)

Yasuhiro Togano, Yusuke Yamada, Naohito Iwasa, Kazunari Yamada, Tohru Motobayashi, Nori Aoi, Hidetada Baba, Shawn Bishop, Xiangzhou Cai, Pieter Doornenbal, Deqing Fang, Takeshi Furukawa, Kazuo Ieki, Takahiro Kawabata, Shoko Kanno, Nobuyuki Kobayashi, Yosuke Kondo, Takamasa Kuboki, Naoto Kume, Kazuyoshi Kurita, Meiko Kurokawa, Yu-Gang Ma, Yukari Matsuo, Hiroshi Murakami, Masafumi Matsushita, Takashi Nakamura, Kensuke Okada, Shinsuke Ota, Yoshiteru Satou, Susumu Shimoura, Ryota Shioda, Kana Tanaka, Satoshi Takeuchi, Wendong Tian, Hongwei Wang, Jiansong Wang, Ken-ichiro Yoneda: ``Hindered Proton Collectivity in the Proton-Rich Nucleus ^{28}S: Possible Magic Number Z = 16 at Proton-Rich Side'', Proceedings of the Conference on Advances in Radioactive Isotope Science (ARIS2014), JPS Conf. Proc. 6, 030002 (2015)

Shintaro Go, Eiji Ideguchi, Rin Yokoyama, Motoki Kobayashi, Keiichi Kisamori, Motonobu Takaki, Hiroyuki Miya, Shinsuke Ota, Shinichiro Michimasa, Susumu Shimoura, Megumi Niikura, Takeshi Koike, Takeshi Yamamoto, Yosuke Ito, Jun Takatsu, Ayumi Yagi, Hiroki Nishibata, Tomokazu Suzuki, Kotaro Shirotori, Yutaka Watanabe, Yoshikazu Hirayama, Masahiko Sugawara, Mitsuo Koizumi, Yosuke Toh, Toshiyuki Shizuma, Atsushi Kimura, Hideo Harada, Kazuyoshi Furutaka, Shoji Nakamura, Fumito Kitatani, Yuichi Hatsukawa, Masumi Oshima, Iolanda Matea, Daisuke Suzuki, David Verney, Faiccal Azaiez: ``Superdeformation in ^{35}S'', Proceedings of the Conference on Advances in Radioactive Isotope Science (ARIS2014), JPS Conf. Proc. 6, 030005 (2015)

Yoshiteru Satou, Jongwon Hwang, Sunji Kim, Kyoungho Tshoo, Seonho Choi, Takashi Nakamura, Takashi Sugimoto, Yosuke Kondo, Nobuyuki Matsui, Yoshiko Hashimoto, Takumi Nakabayashi, Toshifumi Okumura, Mayuko Shinohara, Naoki Fukuda, Toru Motobayashi, Yoshiyuki Yanagisawa, Nori Aoi, Satoshi Takeuchi, Tomoko Gomi, Hiroyoshi Sakurai, Hideaki Otsu, Masayasu Ishihara, Yasuhiro Togano, Shoko Kawai, Hooi Ong, Takeo Onishi, Susumu Shimoura, Mitsuru Tamaki, Toshio Kobayashi, Yohei Matsuda, Natsumi Endo, Mitsuhisa Kitayama: ``Hole States in ^{16}C Observed via One-Neutron Knockout of ^{17}C'', Proceedings of the Conference on Advances in Radioactive Isotope Science (ARIS2014), JPS Conf. Proc. 6, 030029 (2015)

Keiichi Kisamori, Susumu Shimoura, Hiroyuki Miya, Marlene Assie, Hidetada Baba, Tatsuo Baba, Didier Beaumel, Masanori Dozono, Toshihiko Fujii, Naoki Fukuda, Shintaro Go, Fariouz Hammache, Eiji Ideguchi, Naohiro Inabe, Masatoshi Itoh, Daisuke Kameda, Shoichiro Kawase, Takahiro Kawabata, Motoki Kobayashi, Yosuke Kondo, Toshiyuki Kubo, Yuki Kubota, Mizuki Kurata-Nishimura, CheongSoo Lee, Yukie Maeda, Hiroaki Matsubara, Shin'ichiro Michimasa, Kenjiro Miki, Takahiro Nishi, Shumpei Noji, Shinsuke Ota, Satoshi Sakaguchi, Hideyuki Sakai, Yoshiko Sasamoto, Masaki Sasano, Hiromi Sato, Yohei Shimizu, Andreas Stolz, Hiroshi Suzuki, Motonobu Takaki, Hiroyuki Takeda, Satoshi Takeuchi, Atsushi Tamii, Leung Tang, Hiroshi Tokieda, Miho Tsumura, Tomohiro Uesaka, Kentaro Yako, Yoshiyuki Yanagisawa, Rin Yokoyama: ``Missing-Mass Spectroscopy of the 4-Neutron System by Exothermic Double-Charge Exchange Reaction ^{4}He(^{8}He,^{8}Be)4n'', Proceedings of the Conference on Advances in Radioactive Isotope Science (ARIS2014), JPS Conf. Proc. 6, 030075 (2015)

Tsz Leung Tang, Shoichiro Kawase, Tomohiro Uesaka, Didier Beaumel, Masanori Dozono, Naoki Fukuda, Taku Fukunaga, Toshihiko Fujii, Alfredo Galindo-uribarri, SangHoon Hwang, Daisuke Kameda, Tomomi Kawahara, Wooyoung Kim, Keiichi Kisamori, Motoki Kobayashi, Yuki Kubota, Kensuke Kusaka, CheongSoo Lee, Yukie Maeda, Hiroaki Matsubara, Shin'ichiro Michimasa, Hiroyuki Miya, Tetsuo Noro, Alexandre Obertelli, Shinsuke Ota, Elizabeth Padilla-Rodal, Satoshi Sakaguchi, Masaki Sasano, Susumu Shimoura, Samvel Stepanyan, Hiroshi Suzuki, Motonobu Takaki, Hiroyuki Takeda, Hiroshi Tokieda, Tomotsugu Wakasa, Takashi Wakui, Kentaro Yako, Jumpei Yasuda, Rin Yokoyama, Juzo Zenihiro: ``Proton Single-Particle Energy of ^{23}F by Quasi-Free (p ,2p) Scattering and Operation of Polarized Proton Target'', Proceedings of the Conference on Advances in Radioactive Isotope Science (ARIS2014), JPS Conf. Proc. 6, 030077 (2015)

Motoki Kobayashi, Kentaro Yako, Susumu Shimoura, Masanori Dozono, Naoki Fukuda, Naohito Inabe, Daisuke Kameda, Shoichiro Kawase, Keiichi Kisamori, Toshiyuki Kubo, Yuki Kubota, CheongSoo Lee, Shin'ichiro Michimasa, Hiroyuki Miya, Shinsuke Ota, Hideyuki Sakai, Masaki Sasano, Hiroshi Suzuki, Motonobu Takaki, Hiroyuki Takeda, Yoshiyuki Yanagisawa: ``Spin-Isospin Response of the Neutron-Rich Nucleus ^{8}He via the (p,n) Reaction in Inverse Kinematics'', Proceedings of the Conference on Advances in Radioactive Isotope Science (ARIS2014), JPS Conf. Proc. 6, 030089 (2015)

Shin'ichiro Michimasa, Yoshiyuki Yanagisawa, Kiyohiko Inafuku, Nori Aoi, Zolton Elekes, Zsolt Fulop, Yuichi Ichikawa, Naohito Iwasa, Kazuyoshi Kurita, Meiko Kurokawa, Tomohiro Machida, Tohru Motobayashi, Takashi Nakamura, Takumi Nakabayashi, Masahiro Notani, Hooi Jin Ong, Takeo Onishi, Hideaki Otsu, Hiroyoshi Sakurai, Mayuko Shinohara, Toshiyuki Sumikama, Satoshi Takeuchi, Kanenobu Tanaka, Yasuhiro Togano, Kazunari Yamada, Mitsutaka Yamaguchi, Ken-ichiro Yoneda: ``Proton Inelastic Scattering on Island-of-Inversion Nuclei'', Proceedings of the Conference on Advances in Radioactive Isotope Science (ARIS2014), JPS Conf. Proc. 6, 020007 (2015)

David Steppenbeck, Satoshi Takeuchi, Nori Aoi, Pieter Doornenbal, Masafumi Matsushita, He Wang, Hidetada Baba, Naoki Fukuda, Shintaro Go, Michio Honma, Jenny Lee, Keishi Matsui, Shin'ichiro Michimasa, Tohru Motobayashi, Daiki Nishimura, Takaharu Otsuka, Hiroyoshi Sakurai, Yoshiaki Shiga, Noritaka Shimizu, Par-Anders Soderstrom, Toshiyuki Sumikama, Hiroshi Suzuki, Ryo Taniuchi, Yutaka Utsuno, Jose Javier Valiente-Dobón, Ken'ichiro Yoneda: ``In-Beam γ-Ray Spectroscopy of Very Neutron-Rich N = 32 and 34 Nuclei'', Proceedings of the Conference on Advances in Radioactive Isotope Science (ARIS2014), JPS Conf. Proc. 6, 020019 (2015)

H. Liu, J. Lee, P. Doornenbal, H. Scheit, S. Takeuchi, N. Aoi, K. Li, M. Matsushita, D. Steppenbeck, H. Wang, H. Baba, E. Ideguchi, N. Kobayashi, Y. Kondo, G. Lee, S. Michimasa, T. Motobayashi, H. Sakurai, M. Takechi, Y. Togano, J.A. Tostevin, Y. Utsuno: ``Single-Neutron Knockout Reaction from ^{30}Ne'', Proceedings of the Conference on Advances in Radioactive Isotope Science (ARIS2014), JPS Conf. Proc. 6, 030003 (2015)

Rin Yokoyama, Eiji Ideguchi, Gary Simpson, Mana Tanaka, Shunji Nishimura, Pieter Doornnbal, Par-Anders Soderstrom, Giuseppe Lorusso, Zhengyu Xu, Jin Wu, Toshiyuki Sumikama, Nori Aoi, Hidetada Baba, Frank Bello, Frank Browne, Rie Daido, Yifan Fang, Naoki Fukuda, Guillaume Gey, Shintaro Go, Naohiro Inabe, Tadaaki Isobe, Daisuke Kameda, Kazuma Kobayashi, Motoki Kobayashi, Tetsuro Komatsubara, Toshiyuki Kubo, Istvan Kuti, Zhihuan Li, Masafumi Matsushita, Shin'ichiro Michimasa, Chang-Bum Moon, Hiroki Nishibata, Ippei Nishizuka, Atsuko Odahara, Zena Patel, Simon Rice, Eda Sahin, Laura Sinclair, Hiroshi Suzuki, Hiroyuki Takeda, Jan Taprogge, Zsolt Vajta, Hiroshi Watanabe, Ayumi Yagi: ``Isomers of Pm Isotopes on the Neutron-Rich Frontier of the Deformed Z 60 Region'', Proceedings of the Conference on Advances in Radioactive Isotope Science (ARIS2014), JPS Conf. Proc. 6, 030021 (2015)

Yuki Kubota, Masaki Sasano, Tomohiro Uesaka, Masanori Dozono, Masatoshi Itoh, Shoichiro Kawase, Motoki Kobayashi, CheongSoo Lee, Hiroaki Matsubara, Kenjiro Miki, Hiroyuki Miya, Shinsuke Ota, Kimiko Sekiguchi, Tatsushi Shima, Takahiro Taguchi, Atsushi Tamii, Tsz Leung Tang, Hiroshi Tokieda, Tomotsugu Wakasa, Takashi Wakui, Jumpei Yasuda, Juzo Zenihiro: ``A Segmented Neutron Detector with a High Position Resolution for the (p,pn) Reactions'', Proceedings of the Conference on Advances in Radioactive Isotope Science (ARIS2014), JPS Conf. Proc. 6, 030118 (2015)

Clementine Santamaria, Alexandre Obertelli, Shinsuke Ota, Masaki Sasano, Eichi Takada, Laurent Audirac, Hidetada Baba, Denis Calvet, Fr¥'ed¥'eric Ch¥^ateau, Anna Corsi, Alain Delbart, Pieter Doornenbal, Arnaud Giganon, Alain Gillibert, Yosuke Kondo, Yuki Kubota, Caroline Lahonde-Hamdoun, Val¥'erie Lapoux, Cheong Soo Lee, Hideaki Otsu, Alan Peyaud, Emanuel C. Pollacco, Hiroshi Tokieda, Tomohiro Uesaka, Juzo Zenihiro: ``In-Beam Performances of the MINOS TPC for the Spectroscopy of Very Exotic Nuclei'', Proceedings of the Conference on Advances in Radioactive Isotope Science (ARIS2014), JPS Conf. Proc. 6, 030130 (2015)

CheongSoo Lee, Shinsuke Ota, Hiroshi Tokieda, Reiko Kojima, Yuni Watanabe, Raphael Saiseau, Tomohiro Uesaka: ”Property of THGEM in Low-Pressure Deuterium for a Low-Pressure Gaseous Active Target'', Proceedings of the Conference on Advances in Radioactive Isotope Science (ARIS2014), JPS Conf. Proc. 6, 030140 (2015)

Shinsuke Ota, H. Tokieda, C.S. Lee, R. Kojima, Y.N. Watanabe, A. Corsi, M. Dozono, J. Gibelin, T. Hashimoto, T. Kawabata, S. Kawase, S. Kubono, Y. Kubota, Y. Maeda, H. Matsubara, Y. Matsuda, S. Michimasa, T. Nakao, T. Nishi, A. Obertelli, H. Otsu, C. Santamaria, M. Sasano, M. Takaki, Y. Tanaka, T. Leung, T. Uesaka, K. Yako, H. Yamaguchi, J. Zenihiro, E. Takada: ``Development of CNS Active Target for Deuteron Induced Reactions with High Intensity Exotic Beam'', Proceedings of the Conference on Advances in Radioactive Isotope Science (ARIS2014), JPS Conf. Proc. 6, 030117 (2015)

G. Benzoni, H. Watanabe, A.I. Morales, S. Nishimura, R. Avigo, H. Baba, F.L. Bello Garrote, N. Blasi, A. Bracco, F. Browne, S. Ceruti, F.C.L. Crespi, R. Daido, G. de Angelis, M.C. Delattre, Zs. Dombradi, P. Doornenbal, Y. Fang, A. Gottardo, T. Isobe, I. Kuti, G. Lorusso, K. Matsui, B. Melon, D. Mengoni, T. Miyazaki, V. Modamio-Hoybjor, S. Momiyama, D.R. Napoli, M. Niikura, R. Orlandi, Z. Patel, S. Rice, E. Sahin, H. Sakurai, L. Sinclair, P. A. Soderstrom, D. Sohler, T. Sumikama, R. Taniuchi, J. Taprogge, Zs. Vajta, J. J. Valiente-Dob`on, O. Wieland, J. Wu, Z.Y. Xu, A. Yagi, M. Yalcinkaya, R. Yokoyama: ``β 4-Decay Measurements in the Vicinity of ^{78}Ni with the EURICA Setup'', Proceedings of the Conference on Advances in Radioactive Isotope Science (ARIS2014), JPS Conf. Proc. 6, 020021 (2015)

Yoshiaki Shiga, Ken-ichiro Yoneda, David Steppenbeck, Nori Aoi, Pieter Doornenbal, Jenny Lee, Hongna Liu, Masafumi Matushita, Satoshi Takeuchi, He Wang, Hidetada Baba, Piotr Bednarczyk, Zsolt Dombradi, Zsolt Fulop, Shintaro Go, Takashi Hashimoto, Eiji Ideguchi, Kazuo Ieki, Kota Kobayashi, Yosuke Kondo, Ryogo Minakata, Tohru Motobayashi, Daiki Nisimura, Hideaki Otsu, Hiroyoshi Sakurai, Dora Sohler, Yelei Sun, Atsushi Tamii, Ryuki Tanaka, Zhengyang Tian, Zsolt Vajta, Tetsuya Yamamoto, Xiaofei Yang, Zaihong Yang, Yanlin Ye, Rin Yokoyama, Juzo Zenihiro: ``Persistence of N = 50 Shell Closure in the Vicinity of ^{78}Ni Studied by In-Beam γ-Ray Spectroscopy'', Proceedings of the Conference on Advances in Radioactive Isotope Science (ARIS2014), JPS Conf. Proc. 6, 030008 (2015)

He Wang, Nori Aoi, Satoshi Takeuchi, Masafumi Matsushita, Pieter Doornenbal, Tohru Motobayashi, David Steppenbeck, Kenichiro Yoneda, Hidetaba Baba, Lucia Caceres, Zsolt Dombrádi, Yosuke Kondo, Jenny Lee, Kuo-ang Li, Hong-Na Liu, Ryogo Minakata, Daiki Nishimura, Hideaki Otsu, Satoshi Sakaguchi, Hiroyoshi Sakurai, Heiko Scheit, Dora Sohler, Ye-Lei Sun, Zheng-Yang Tian, Ryuki Tanaka, Yasuhiro Togano, Zsolt Vajta, Zai-Hong Yang, Tetsuya Yamamoto, Yan-Lin Ye, Rin Yokoyama: ``Collectivity in the Neutron-Rich Pd Isotopes Towards N = 82'', Proceedings of the Conference on Advances in Radioactive Isotope Science (ARIS2014), JPS Conf. Proc. 6, 030010 (2015)

A. Yagi, A. Odahara, R. Daido, Y. Fang, H. Nishibata, R. Lozeva, C.-B. Moon, S. Nishimura, P. Doornenbal, G. Lorusso, P.A. S¥"oderstr¥"om, T. Sumikama, H. Watanabe, T. Isobe, H. Baba, H. Sakurai, F. Browne, Z. Patel, S. Rice, L. Sinclair, J. Wu, Z.Y. Xu, R. Yokoyama, T. Kubo, N. Inabe, H. Suzuki, N. Fukuda, D. Kameda, H. Takeda, D.S. Ahn, D. Murai, F.L. Bello Garrote, J.M. Daugas, F. Didierjean, E. Ideguchi, T. Ishigaki, H.S. Jung, T. Komatsubara, Y. K. Kwon, C.S. Lee, P.S. Lee, S. Morimoto, M. Niikura, I. Nishizuka, T. Shimoda, K. Tshoo: ``New Isomers in Neutron-Rich Cs Isotopes'', Proceedings of the Conference on Advances in Radioactive Isotope Science (ARIS2014), JPS Conf. Proc. 6, 030019 (2015)

J. Wu, S. Nishimura, G. Lorusso, Z.Y. Xu, E. Ideguchi, G. S. Simpson, H. Baba, F. Browne, R. Daido, P. Doornenbal, Y. F. Fang, T. Isobe, Z. Li, Z. Patel, S. Rice, L. Sinclair, P. A. Soderstrom, T. Sumikama, H. Watanabe, A. Yagi, R. Yokoyama, N. Aoi, F.L. Bello Garrote, G. Benzoni, G. Gey, A. Gottardo, H. Nishibata, A. Odahara, H. Sakurai, M. Tanaka, J. Taprogge, T. Yamamoto, and the EURICA collaboration: ``β-Decay of Neutron-Rich Nuclei around ^{158}Nd and the Origin of Rare-Earth Elements'', Proceedings of the Conference on Advances in Radioactive Isotope Science (ARIS2014), JPS Conf. Proc. 6, 030064 (2015)

K. Sekiguchi, Y. Wada, J. Miyazaki, T. Taguchi, U. Gebauer, M. Dozono, S. Kawase, Y. Kubota, C.S. Lee, Y. Maeda, T. Mashiko, K. Miki, H. Okamura, S. Sakaguchi, H. Sakai, N. Sakamoto, M. Sasano, Y. Shimizu, K. Takahashi, T.L. Tang, T. Uesaka, T. Wakasa, K. Yako: ``Complete Set of Deuteron Analyzing Powers for dp Elastic Scattering at Intermediate Energies and Three Nucleon Forces'', Proceedings of the Conference on Advances in Radioactive Isotope Science (ARIS2014), JPS Conf. Proc. 6, 030087 (2015)

H. Yamaguchi, D. Kahl, S. Hayakawa, Y. Sakaguchi, T. Nakao, Y. Wakabayashi, T. Hashimoto, T. Teranishi, S. Kubono, S. Cherubini, M. Mazzocco, C. Signorini, M. Gulino, A. Di Pietro, P. Figuera, M. La Cognata, M. Lattuada, C. Spitaleri, D. Torresi, P.S. Lee, C.S. Lee, T. Komatsubara, N. Iwasa, Y. Okoda, D. Pierroutsakou, C. Parascandolo, M. La Commara, E. Strano, C. Boiano, A. Boiano, C. Manea, A. M. Sanchez-Benítez, H. Miyatake, Y.X. Watanabe, H. Ishiyama, S. C. Jeong, N. Imai, Y. Hirayama, S. Kimura, M. Mukai, Y.H. Kim, C. J. Lin, H.M. Jia, L. Yan, Y.Y. Yang, T. Kawabata, Y.K. Kwon, D.N. Binh, L.H. Khiem, N.N. Duy: ``Studies on Nuclear Astrophysics and Exotic Structure at the Low-Energy RI Beam Facility CRIB'', Proceedings of the Conference on Advances in Radioactive Isotope Science (ARIS2014), JPS Conf. Proc. 6, 010011 (2015)

N. Imai, M. Mukai, J. Cederkall, H. Aghai, P. Golubev, H. T. Johansson, D. Kahl, T. Teranishi, Y.X. Watanabe: ``Quenched Spectroscopic Factors for Low-Lying Positive Parity States in ^{31}Mg'', Proceedings of the Conference on Advances in Radioactive Isotope Science (ARIS2014), JPS Conf. Proc. 6, 020005 (2015)

A. Matta, D. Beaumel, H. Otsu, V. Lapoux, N.K. Timofeyuk, N. Aoi, M. Assie, H. Baba, S. Boissinot, R. Chen, F. Delaunay, N. de Sereville, S. Franchoo, P. Gangnant, J. Gibelin, F. Hammache, C. Houarner, N. Imai, N. Kobayashi, T. Kubo, Y. Kondo, Y. Kawada, L.H. Khiem, M. Kurata-Nishimura, E.A. Kuzmin, J. Lee, J.F. Libin, T. Motobayashi, T. Nakamura, L. Nalpas, E. Yu. Nikolskii, A. Obertelli, E.C. Pollacco, E. Rindel, Ph. Rosier, F. Saillant, T. Sako, H. Sakurai, A. Sanchez-Benitez, J. A. Scarpaci, I. Stefan, D. Suzuki, K. Takahashi, M. Takechi, S. Takeuchi, H. Wang, R. Wolski, K. Yoneda: ``Missing Mass Spectroscopy of ^{8}He and ^{10}He by (d, ^{3}He) Reaction'', Proceedings of the Conference on Advances in Radioactive Isotope Science (ARIS2014), JPS Conf. Proc. 6, 030026 (2015)

Y. Hirayama, Y.X. Watanabe, N. Imai, H. Ishiyama, S.C. Jeong, H. Miyatake, M. Oyaizu, M. Mukai, S. Kimura, Y. H. Kim, T. Sonoda, M. Wada, M. Huyse, Yu. Kudryavtsev, P. Van Duppen: ``Beta-Decay Spectroscopy of r-Process Nuclei with N = 126 at KEK Isotope Separation System'', Proceedings of the Conference on Advances in Radioactive Isotope Science (ARIS2014), JPS Conf. Proc. 6, 030125 (2015)

M. Mukai, Y. Hirayama, N. Imai, H. Ishiyama, S.C. Jeong, H. Miyatake, M. Oyaizu, Y.X. Watanabe, Y.H. Kim, S. Kimura: ``Search for Efficient Laser Resonance Ionization Schemes of Refractory Elements for KISS'', Proceedings of the Conference on Advances in Radioactive Isotope Science (ARIS2014), JPS Conf. Proc. 6, 030127 (2015)

T. Sumikama, D.S. Ahn, N. Fukuda, N. Inabe, T. Kubo, Y. Shimizu, H. Suzuki, H. Takeda, N. Aoi, D. Beaumel, K. Hasegawa, E. Ideguchi, N. Imai, T. Kobayashi, M. Matsushita, S. Michimasa, H. Otsu, S. Shimoura, T. Teranishi: ``First test experiment to produce the slowed-down RI beam with the momentum-compression mode at RIBF'', Proceedings of 17th International Conference on Electromagnetic Isotope Separators and Related Topics (EMIS2015), Nucl. Instr. Meth. Phys. Res. B (2016), in press

J. Yasuda, M. Sasano, R.G.T. Zegers, H. Baba, W. Chao, M. Dozono, N. Fukuda, N. Inabe, T. Isobe, G. Jhang, D. Kameda, T. Kubo, M. Kurata-Nishimura, E. Milman, T. Motobayashi, H. Otsu, V. Panin, W. Powell, H. Sakai, M. Sako, H. Sato, Y. Shimizu, L. Stuhl, H. Suzuki, S. Tangwancharoen, H. Takeda, T. Uesaka, K. Yoneda, J. Zenihiro, T. Kobayashi, T. Sumikama, T. Tako, T. Nakamura, Y. Kondo, Y. Togano, M. Shikata, J. Tsubota, K. Yako, S. Shimouraf, S. Otaf, S. Kawasef, Y. Kubotaf, M. Takakif, S. Michimasaf, K. Kisamorif, C.S. Leef, H. Tokieda, M. Kobayashi, S. Koyama, N. Kobayashi, T. Wakasa, S. Sakaguchi, A. Krasznahorkay, T. Murakami, N. Nakatsuka, M. Kaneko, Y. Matsuda, D. Mucher, S. Reichert, D. Bazin, J.W. Lee: ``Inverse kinematics (p,n) reactions studies using the WINDS slow neutron detector and the SAMURAI spectrometer'', Proceedings of 17th International Conference on Electromagnetic Isotope Separators and Related Topics (EMIS2015), Nucl. Instr. Meth. Phys. Res. B (2016), in press

M. Sasano, J. Yasuda, R.G.T. Zegers, H. Baba, W. Chao, M. Dozono, N. Fukuda, N. Inabe, T. Isobe, G. Jhang, D. Kamaeda, T. Kubo, M. Kurata-Nishimura, E. Milman, T. Motobayashi, H. Otsu, V. Panin, W. Powell, H. Sakai, M. Sako, H. Sato, Y. Shimizu, L. Stuhl, H. Suzuki, S. Tangwancharoen, H. Takeda, T. Uesaka, K. Yoneda, J. Zenihiro, T. Kobayashi, T. Sumikama, T. Tako, T. Nakamura, Y. Kondo, Y. Togano, M. Shikata, J. Tsubota, K. Yako, S. Shimoura, S. Ota, S. Kawase, Y. Kubota, M. Takaki, S. Michimasa, K. Kisamori, C.S. Lee, H. Tokieda, M. Kobayashi, S. Koyama, N. Kobayashi, T. Wakasa, S. Sakaguchi, A. Krasznahorkay, T. Murakami, N. Nakatsuka, M. Kaneko, Y. Matsuda, D. Mucher, S. Reichert, D. Bazin J.W. Lee: ``Study of Gamow-Teller transitions from ^{132}Sn via the (p,n) reaction at 220 MeV/u in inverse kinematics'', Proceedings of International Conference on Nuclear Structure and Related Topics (NSRT15), EPJ Web of Conferences, 107 (2016) 06003

Hideshi Mutoa, Yukimitsu Ohshiro, Shoichi Yamaka, Shin-ichi Watanabe, Michihiro Oyaizu, Shigeru Kubono, Hidetoshi Yamaguchi, Masayuki Kase, Toshiyuki Hattori, Susumu Shimoura: ``Status of Plasma Spectroscopy Method for CNS Hyper-ECR Ion Source at RIKEN'', Proceedings of 23rd International Conference on the Application of Accelerators in Research and Industry (CAARI 2014), Physics Procedia, 66, 140--147 (2015)

Y. Kotaka, Y. Ohshiro, S. Watanabe, H. Yamaguchi, N. Imai, S. Shimoura, M. Kase, S. Kubono, K. Hatanaka, A. Goto, H. Muto: ``Development of low-energy heavy-ion beams by the Riken AVF cyclotron and Hyper ECR ion source of CNS'', Proceedings of the 13th International Conference on Heavy Ion Accelerator Technology, 58--61 (2016)

H. Muto, Y. Oshiro, Y. Kotaka, S. Yamaka, S. Watanabe, H. Yamaguchi, S. Shimoura, M. Kase, S. Kubono, K. Kobayashi, M. Nishimura, M. Oyaizu, T. Hattori: ``Observation of sublimation effect of Mg and Ti ions at the Hyper-electron cyclotron resonance ion source'', Proceedings of the 13th International Conference on Heavy Ion Accelerator Technology, 262--264 (2016)

S. Ota, H. Tokieda, C.S. Lee, Y.N. Watanabe: “CNS active target (CAT) for missing mass spectroscopy with intense beams'', Proceedings of the 27th world conference of the international nuclear target, J. Radioanalytical and Nuclear Chemistry,

Y. Utsuno, T. Otsuka, Y. Tsunoda, N. Shimizu, M. Honma, T. Togashi, T. Mizusaki, ``Recent Advances in Shell Evolution with Shell-Model Calculations'', JPS Conf. Proc. 6 010007 (2015).

N. Shimizu, T. Abe, M. Honma, T. Otsuka, Y. Tsunoda, Y. Utsuno, and T. Yoshida: ``Frontier of nuclear shell-model calculations and high performance computing'', JPS Conf. Proc. 6 010021 (2015).

T. Yoshida, N. Shimizu, T. Abe, T. Otsuka: ``Cluster structure of Be isotopes based on Monte Carlo shell model'', JPS Conf. Proc. 6 030028 (2015).

T. Miyagi, T. Abe, R. Okamoto and T. Otsuka: ``Many-Body Calculations for Medium-Mass Nuclei by the Unitary Transformation Method'', JPS Conf. Proc. 6 030037 (2015).

T. Togashi, N. Shimizu, Y. Utsuno, T. Otsuka, M. Honma: ``Shell-Model Calculation of High-Spin States in Neutron-Rich Cr and Fe Isotopes'', JPS Conf. Proc. 6 030046 (2015).

Y. Iwata, N. Shimizu, Y. Utsuno, M. Honma, T. Abe, T. Otsuka: ``Ingredients of nuclear matrix element for two-neutrino double-beta decay of 48Ca'', JPS Conf. Proc. 6 030057 (2015).

[Others]

大塚孝治、阿部喬: ``原子核物理における大規模数値計算の進展'' パリティ Vol.30 (2015年6月号) p.24-28(丸善出版社).

Oral Presentations

[International Conference etc.]

H. Yamaguchi for the CRIB collaboration (oral, invited): ``Nuclear astophysics projects with low-energy RI beams at CRIB'': Pioneering Symposium: ``Nuclear physics at the RIB facilities'' in Korean Physical Society Meeting, Apr 22--24, 2015, Daejeon Convention Center, Daejeon, Korea.

H. Yamaguchi (oral, invited): ``Studying astrophysical reactions with low-energy RI beams at CRIB'', The 12th International Conference on Nucleus-Nucleus Collisions (NN2015), June 21--26 2015, Department of Physics and Astronomy, Catania University.

H. Yamaguchi (oral): ``Experimental study on astrophysical reactions with low-energy RI beams'', The 13th Russbach School on Nuclear

Astrophysics, Mar. 6--11, 2016, Russbach am Pass Gschutt, Austria.
S. Hayakawa (oral): ``Trojan horse method at CRIB for RI+n reactions'', The 8th Japan-Italy symposium, Mar. 7--10 2016, RIKEN, Saitama, Japan.
T. Gunji for the ALICE Collaboration (oral): ``Overview of Recent ALICE Results'', XXV International Conference on Ultrarelativistic Nucleus-Nucleus Collisions (QM2015), Sept. 19 - Oct. 3, 2015, Kobe, Japan
T. Gunji (oral, invited): ``Quarkonia and heavy flavour production in heavy-ion collisions - an experimental overview'', 6th Asian Triangle Heavy-Ion Conference, Feb. 15-19, India International Center, New Delhi, India
T. Gunji (oral, invited): ``Dark photon search in heavy ion experiments at RHIC and LHC'', International workshop on Light Dark Matter at Accelerator, June 24 - 26, 2015, Camogli, Italy
Y. Watanabe (oral, invited): ``Experimental overview on EM observables'', XXV International Conference on Ultrarelativistic Nucleus-Nucleus Collisions (QM2015), Sept. 19 - Oct. 3, 2015, Kobe, Japan
Y. Watanabe (oral, invited): ``Dilepton production in heavy ion collisions'', 6th Asian Triangle Heavy-Ion Conference, Feb. 15-19, India International Center, New Delhi, India
Y. Watanabe for the PHENIX Collaboration (oral): ``Dielectron measurements by PHENIX'', ECT* workshop on New perspectives on Photons and Dileptons in Ultrarelativistic Heavy-Ion Collisions at RHIC and LHC, Nov. 30 - Dec. 11, Trento, Italy
Y. Watanabe (oral, invited): ``Charmed and exotic hadron measurements with ALICE at the LHC'', ExHIC2016 workshop, Mar. 24, 2016, Kyoto, Japan
S. Hayashi on behalf of the ALICE Collaboration (oral): ``Dielectron measurement in pp, p-Pb, and Pb-Pb collisions with the ALICE detector'', Hard Probes 2015, June 29 -July 3, 2015, McGill University, Montreal, Canada
Y.Sekiguchi for the ALICE collaboration (oral): ``Two particle correlations in p-Pb collisions at $\sqrt{s_{NN}}$ = 5.02 TeV with the ALICE detector'', 6th Asian Triangle Heavy-Ion Conference, Feb. 15-19, India International Center, New Delhi, India
M. Matsushita (Oral): ``New energy-degrading scheme for low-energy reaction measurements of rare isotope beams'', Advances in Nuclear Structure at Extreme Conditions, Feb. 19--22, 2014, Bormio, Italy.
S. Shimoura (invited): ``Nucleon-nucleon correlation in neutron-rich nuclei'', International Workshop & the 12th RIBF Discussion on Neutron-Proton Correlations, July 6--9, 2015, Hong Kong.
S. Ota (invited):”On pn-pair transfer/pick-up reactions'', International Workshop & the 12th RIBF Discussion on Neutron-Proton Correlations, July 6--9, 2015, Hong Kong.
S. Ota (invited): ``Using TPC to study ISGMR/ISGDR'', Science with SpRIT TPC Workshop, June, 5--6, 2015, RIKEN, Japan.
S. Ota (invited): ``Active Target Development in Japan'', Workshop on Active Targets and Time Projection Chambers for Nuclear Physics Experiments, May 18--20, 2015, MSU
S. Michimasa (Oral): ``Construction of OEDO beamline'', OEDO-SHARAQ International Collaboration Workshop, September 8--9, 2015, CNS Wako, Saitama, Japan
M. Matsushita (Oral): ``Simulation of OEDO beam line'', OEDO-SHARAQ International Collaboration Workshop, September 8--9, 2015, CNS Wako, Saitama, Japan
S. Shimoura (Oral): ``Present status of GRAPE'', OEDO-SHARAQ International Collaboration Workshop, September 8--9, 2015, CNS Wako, Saitama, Japan
K. Yako (Oral): ``Spin-isospin studies at SHARAQ'', OEDO-SHARAQ International Collaboration Workshop, September 8--9, 2015, CNS Wako, Saitama, Japan
M. Kobayashi (Oral): ``Direct mass measurements of neutron-rich Ca isotopes beyond N=34”, OEDO-SHARAQ International Collaboration Workshop, September 8--9, 2015, CNS Wako, Saitama, Japan
M. Dozono (Oral): ``The parity-transfer (^{16}O,^{16}F) reaction for studies of the spin-dipole 0^- mode'', OEDO-SHARAQ International Collaboration Workshop, September 8--9, 2015, CNS Wako, Saitama, Japan
M. Takaki (Oral): ``Investigation of Double Gamow-Teller Giant Resonances via heavy-ion double charge exchange reactions'', OEDO-SHARAQ International Collaboration Workshop, September 8--9, 2015, CNS Wako, Saitama, Japan
S. Ota (Oral): ``Transfer Reaction and Active Target'', OEDO-SHARAQ International Collaboration Workshop, September 8--9, 2015, CNS Wako, Saitama, Japan
N. Imai (Oral): ``Two experimental proposals using the energy-degraded beams'', OEDO-SHARAQ International Collaboration Workshop, September 8--9, 2015, CNS Wako, Saitama, Japan
M. Dozono (Oral): ``Parity-transfer reaction for study of spin-dipole 0^- mode'', 5th International Conference on Collective Motion in Nuclei under Extreme Conditions (COMEX5), September 14--18, 2015, Krakow, Poland
S. Ota (Oral): ``Towards the first observation of isoscalar giant monopole resonance in unstable Tin isotopes with CNS active target'', 5th International Conference on Collective Motion in Nuclei under Extreme Conditions (COMEX5), September 14--18, 2015, Krakow, Poland
M. Takaki (Oral): ``Search for double Gamow-Teller resonance via heavy-ion double charge exchange reaction'', 5th International Conference on Collective Motion in Nuclei under Extreme Conditions (COMEX5), September 14--18, 2015, Krakow, Poland
R. Yokoyama (Oral): ``Investigation of the octupole correlation of neutron-rich Z 56 isotopes by beta-gamma spectroscopy'', 5th International Conference on Collective Motion in Nuclei under Extreme Conditions (COMEX5), September 14--18, 2015, Krakow, Poland
S. Shimoura (invited): ``OEDO project -- New energy degraded beam line at RIBF'', International symposium on the Frontier of γ-ray spectroscopy (Gamma15), October 1--3, 2015, Osaka University, Japan
R. Yokoyama (Oral): ``Investigation of the octupole correlation of neutron-rich Z ~ 56 isotopes by beta-gamma spectroscopy'', International symposium on the Frontier γ-ray spectroscopy (Gamma15), October 1--3, 2015, Osaka University, Japan
S. Michimasa (invited): ``Dispersion-matching of RI-beams and its applications to nuclear structure studies'', HRS-Workshop on high-resolution magnetic spectrometers and experiments with them, November 4--6, 2015, GSI, Darmstadt, Germany.
S. Shimoura (invited): ``OEDO Project: EXTENDED dispersion-matching technique for production of low-energy RI beams'', HRS-Workshop on high-resolution magnetic spectrometers and experiments with them, November 4--6, 2015, GSI, Darmstadt, Germany.
M. Takaki (invited): ``Challenges with heavy-ion double charge exchange reactions at RCNP and RIBF'', NUMEN2015 workshop, December 1--2, 2015, Catania, Italy
S. Shimoura (invited): ``Tetraneutron at SHARAQ'', International Workshop on Critical Stability in Few-Body Systems, Feb. 1--5 2016, RIKEN, Wako, Japan

M. Takaki (invited): ``Recent Activities with Heavy-Ion Double Charge Exchange Reactions at RCNP and RIBF'', 8th Japan-Italy symposium on Nuclear Physics, March 7--10, 2016, RIKEN, Japan

Y. Utsuno(Oral, Invited): ``Shell and shape evolution in exotic nuclei'', Korean Physical Society (KPS) Spring Meeting 2015, Apr. 22-24, 2015, Daejeon, Korea.

Y. Utsuno(Oral, Invited), T. Otsuka, N. Shimizu, and T. Togashi: ``Probing shell evolution with large-scale shell-model calculation'', International Collaborations in Nuclear Theory: Theory for open-shell nuclei near the limits of stability, May 11-29, 2015, East Lansing, Michigan, USA.

N. Tsunoda: ``Neutron-rich nuclei from the nuclear force'', International Collaborations in Nuclear Theory (ICNT) workshop, May 24-30, 2015, Michigan State University, Michigan, USA.

Y. Tsunoda(Oral, Invited):``Structure of Exotic Ni and Neighboring Nuclei'', The 2015 Gordon Research Conference on Nuclear Chemistry, June 2, 2015, Colby-Sawyer College, New Hampshire, USA.

Y. Iwata, N. Shimizu, T. Otsuka, Y. Utsuno, J. Menendez, M. Honma, and T. Abe: `` Large-scale shell model calculation project for neutrinoless double-beta decay of Ca48'', June 1-5, 2015, Neutrinos and Dark Matter in Nuclear Physics 2015 (NDM15), Jyvaskyla, Finland.

T. Otsuka: ``Dual quantum liquid picture of nuclei and its implication to reflection asymmetry'', ``Reflections on the atomic nucleus'', July 30, 2015, University of Liverpool, U.K.

Y. Tsunoda: ``Large-scale shell model calculations for structure of nuclei around Z=28'', The 14th CNS International Summer School (CNSSS15), Aug. 28, 2015, RIKEN, Wako, Saitama, Japan.

N. Tsunoda: ``Construction of Effective interaction for shell model calculation and its appli- cation to island of inversion”, The 14th CNS International Summer School (CNSSS15), Aug. 26- Sep. 1, 2015, RIKEN, Wako, Saitama, Japan.

N. Shimizu(Oral, Invited): ``Large-scale shell model calculations on E1 spectra in medium-heavy nuclei'', The 5th international conference on ``Collective Motion in Nuclei under Extreme Conditions (COMEX5)'', Sep. 15, 2015, Krakow, Poland.

Y. Tsunoda(Oral, Invited): ``Monte Carlo shell model calculations for structure of Ni isotope'', the international symposium on the ``Frontier of γ-ray spectroscopy'' (Gamma15), Oct. 1, 2015, Osaka University, Toyonaka campus, Osaka, Japan.

T. Otsuka(Oral, Invited): ``Dual quantum liquid picture of atomic nuclei'', the international symposium on the ``Frontier of γ-ray spectroscopy'' (Gamma15), Oct. 1-3, 2015, Osaka University, Toyonaka campus, Osaka, Japan.

T. Otsuka: ``Quantum chaos and symmetry'', YIPQS Long-term workshop Computational Advances in Nuclear and Hadron Physics (CANHP 2015), Sep. 30, 2015, Yukawa Institute, Kyoto University, Kyoto, Japan.

N. Shimizu: ``Shell model study of nuclei around N=80'', YIPQS Long-term workshop Computational Advances in Nuclear and Hadron Physics (CANHP 2015), Oct. 2, 2015, Yukawa Institute, Kyoto University, Kyoto, Japan.

Y. Tsunoda: ``Monte Carlo shell model calculations for structure of nuclei around Z=28'', YIPQS Long-term and Nishinomiya-Yukawa Memorial International workshop Computational Advances in Nuclear and Hadron Physics (CANHP 2015), Sep. 29, 2015, Kyoto, Japan.

T. Togashi, N. Shimizu, Y. Utsuno, T. Otsuka, and M. Honma: ``Electric dipole transitions in medium-heavy nuclei described with Monte Carlo shell model'', YIPQS Long-term and Nishinomiya-Yukawa Memorial International workshop Computational Advances in Nuclear and Hadron Physics (CANHP 2015), Oct. 2, 2015, Kyoto, Japan.

Y. Utsuno, N. Shimizu, T. Otsuka, M. Honma, S. Yoshida, and S. Ebata: ``Shell-model study of strength function in the sd-pf shell region'', YIPQS Long-term and Nishinomiya-Yukawa Memorial International workshop Computational Advances in Nuclear and Hadron Physics (CANHP 2015), Sep. 28-Oct. 2, 2015, Kyoto, Japan.

Y. Iwata:``Two-neutrino and neutrinoless double beta decay of Ca48'', YIPQS Long-term and Nishinomiya-Yukawa Memorial International workshop Computational Advances in Nuclear and Hadron Physics (CANHP 2015), Sep. 28-Oct. 2, 2015, Kyoto, Japan.

Y. Iwata: ``Heavy Neutrino-Exchange Potential for the Large-Scale Shell Model Calculations of Double-Beta Decay'', YIPQS Long-term and Nishinomiya-Yukawa Memorial International workshop Computational Advances in Nuclear and Hadron Physics (CANHP 2015), Sep. 28-Oct. 2, 2015, Kyoto, Japan.

T. Yoshida, N. Shimizu, T. Abe, and T. Otsuka: ``Study of shell and cluster configurations of 12Be based on Monte Carlo shell model'', YIPQS Long-term and Nishinomiya-Yukawa Memorial International workshop Computational Advances in Nuclear and Hadron Physics (CANHP 2015), Sep. 28-Oct. 2, 2015, Kyoto, Japan.

N. Tsunoda: ``Construction of Effective interaction for shell model calculation and its appli- cation to island of inversion”, YIPQS Long-term and Nishinomiya-Yukawa Memorial International workshop Computational Advances in Nuclear and Hadron Physics (CANHP 2015), Sep. 21-Oct. 30, 2015, Kyoto, Japan.

T. Otsuka, K. Tsukiyama and R. Fujimoto: ``Feshbash's doorway-state resonances, heavy-ion induced nucleon transfer reactions and exotic nuclei”, YIPQS Long-term workshop Computational Advances in Nuclear and Hadron Physics (CANHP 2015), Oct. 28, 2015, Yukawa Institute, Kyoto University, Kyoto, Japan.

T. Togashi(Oral, Invited), N. Shimizu, Y. Utsuno, T. Otsuka, and M. Honma: ``Photoabsorption cross sections in medium-heavy nuclei calculated with Monte Carlo shell model'', The 5th International Workshop on Compound-Nuclear Reactions and Related Topics (CNR*15), Oct. 19, 2015, Tokyo, Japan.

N. Shimizu: ``Stochastic estimation of level density in nuclear shell-model calculations'', The 5th International Workshop on Compound-Nuclear Reactions and Related Topics (CNR*15),Oct. 20, 2015, Tokyo Institute of Techinology, Ookayama, Tokyo, Japan.

Y. Utsuno(Poster), N. Shimizu, and T. Otsuka: ``Large-scale shell-model calculation for γ-ray strength function'', The 5th International Workshop on Compound-Nuclear Reactions and Related Topics, Oct. 19-23, 2015, Tokyo, Japan.

T. Otsuka: ``Report on Large-scale Quantum Many-body Calculation on Nuclear Properties and its Applications'', International symposium on ``Quarks to Universe in Computational Science (QUCS 2015)'', Nov. 4, 2015, Nara Kasugano International Forum IRAKA, Nara, Japan.

N. Tsunoda (Oral, Invited): ``Nuclear force to Neutron-rich nuclei'', ``Quark to Universe in Computational Science 2015 (QUCS2015)'', Nov. 4-8, 2015, Nara Kasugano International Forum IRAKA, Nara, Japan.

N. Shimizu (Oral, Invited): ``Nuclear structure and excitations clarified by Monte Carlo Shell Model calculation on K computer'', International symposium on ``Quarks to Universe in Computational Science (QUCS 2015)'', Nov. 4-8, 2015, Nara Kasugano International Forum IRAKA, Nara, Japan.

Y. Tsunoda: ``Monte Carlo shell model calculations for structure of nuclei around Z=28'', International symposium on ``Quarks to Universe in Computational Science (QUCS 2015)'', Nov. 4-8, 2015, Nara Kasugano International Forum IRAKA, Nara, Japan.

T. Togashi, N. Shimizu, Y. Utsuno, T. Otsuka, and M. Honma: ``Monte Carlo shell model for electric dipole strength distribution in medium-heavy nuclei'', Nov. 5, 2015, Symposium on Quarks to Universe in Computational Science (QUCS 2015), Nara, Japan.

Y. Iwata:``The nuclear matrix element of double beta decay'', Nov. 4-8, 2015. Symposium on Quarks to Universe in Computational Science (QUCS 2015), Nara, Japan.

Y. Utsuno (Oral, Invited), S. Yoshida, N. Shimizu, and T. Otsuka: ``Shell model calculations for Gamow-Teller strength function in the neutron-rich sd-pf shell region'', Dec. 1-2, 2015, 27th ASRC International Workshop ``Nuclear Fission and Exotic Nuclei“, Tokai, Japan.

[Domestic Conference]

坂口裕司 (oral): ``CRIB による 14C の linear-chain cluster states の探索'', RCNP 研究会「アイソスカラー型単極遷移で探る原子核の励起状態とクラスター構造」, 2015 年 7 月 16--17 日, 阪大 RCNP

S. Ota (invited): ``アクティブ標的を用いた錫１３２近傍原子核の巨大単極共鳴測定'', RCNP 研究会「アイソスカラー型単極遷移で探る原子核の励起状態とクラスター構造」, 2015 年 7 月 16–17 日, 阪大 RCNP

H. Yamaguchi (oral): ``Recent activities at the low-energy RI beam separator CRIB'', RIBF Users Meeting 2015, Sep. 10--11, 2015, RIKEN Nishina Center, Wako, Saitama, Japan.

早川勢也(oral):「CRIB における Trojan horse method の応用による Big Bang 元素合成反応の測定計画」, 宇宙核物理連絡協議会研究会 2016 年 2 月 22-24 日, 国立天文台 三鷹キャンパス

T. Gunji (invited),``高エネルギー重イオン衝突実験の面白さと今後の課題'', QCD Club, Dec. 18, 2015, the University of Tokyo, Hongo, Japan

T. Gunji (invited),``高エネルギー重イオン衝突実験の今後の展望'', 高密度核物質に挑む実験の将来－施設装置の観点から, Dec. 5, 2015, RIKEN, Japan

K. Terasaki, T. Gunji, H. Hamagaki (oral): ``LHC-ALICE 実験 TPC 高度化の為の研究開発と量産準備状況'', 第 12 回 MPDG 研究会, Dec.4-5, Hiroshima University, Higashi-hiroshima, Japan

S. Ota (invited): ``GMR で探る状態方程式'', 宇宙核物理連絡協議会研究会, February 22--24, 2016, Mitaka campus, National Astronomical Observatory of Japan.

岩田順敬: ``ニュートリノレス二重ベータ崩壊の核行列要素の大規模殻模型計算'', 新学術領域 「宇宙の歴史をひもとく地下素粒子原子核研究」2015 年領域研究会、 2015 年 5 月 15 日、神戸大学百年記念館、神戸市.

Y. Iwata: ``TDDFT による超重核合成反応の計算'', 2015 年 8 月, SI 研究会, 近畿大学, 大阪.

T. Otsuka: ``Shell-model perspectives for quantities of astrophysical interests in medium and heavy nuclei'', Numazu Workshop 2015: ``Challenges of modeling supernovae with nuclear data'', Sep. 2, 2015, Mishima, Numazu, Japan.

Y. Utsuno (Oral, Invited), N. Shimizu, and T. Otsuka: ``Current frontiers and perspectives in large-scale shell-model study'', RIBF Users Meeting 2015, Sep. 10-11, 2015, Wako, Japan.

岩田順敬: ``ニュートリノレス二重ベータ崩壊の核行列要素の成分分析'', 第 7 回「学際計算科学による新たな知の発見・統合・創出」シンポジウム, 筑波大学, つくば市 2015 年 10 月.

Y. Utsuno (Oral, Invited), N. Shimizu, T. Otsuka, M. Honma, S. Ebata, T. Mizusaki, Y. Futamura, and T. Sakurai: ``Large-scale shell-model study of E1 strength function and level density'', Nov. 16-19, 2015, “High-resolution Spectroscopy and Tensor interactions” (HST15), Osaka, Japan.

Y. Tsunoda:``「モンテカルロ殻模型計算による Z=28 近傍の核構造の研究」'', KEK 理論センター研究会「原子核・ハドロン物理の課題と将来」、2015 年 11 月 25 日、高エネルギー加速器研究機構研究本館、つくば市.

Y. Watanabe for the ALICE Collaboration, ``LHC-ALICE 実験におけるチャームバリオン生成の測定'', 71th JPS annual meeting, Mar.19-22, Tohoku Gakuin University, Sendai, Japan

Y. Sekiguchi for the ALICE collaboration, ``Long-range correlations in p-Pb collisions at $\sqrt{s_{NN}}$ = 5.02 TeV with the ALICE detector'', 71th JPS annual meeting, Mar.19-22, Tohoku Gakuin University, Sendai, Japan

K. Terasaki for the ALICE Collaboration, ``Search for exotic strange dibaryon at LHC-ALICE'', 71th JPS annual meeting, Mar.19-22, Tohoku Gakuin University, Sendai, Japan

H. Murakami for the ALICE collaboration, ``Status of direct photon measurements via external conversions in high multiplicity pp collisions at 13 TeV with ALICE'', 71th JPS annual meeting, Mar.19-22, Tohoku Gakuin University, Sendai, Japan

S. Shimoura (invited): ``Experimental studies of the tetra-neutron system by using RI-beam'',「ドリップライン近傍のハイパー核と不安定核」シンポジウム, JPS Fall meeting, September 25--28, 2015, Osaka City University, Osaka, Japan

K. Yako (invited): ``荷電交換反応による新モード探索'' 「スピン・アイソスピン応答研究の新たな地平」シンポジウム, JPS Fall meeting, September 25--28, 2015, Osaka City University, Osaka, Japan

S. Ota et al.: ``理研 RIBF BigRIPS における大強度不安定核ビームの粒子識別の開発'', JPS Fall meeting, September 25--28, 2015, Osaka City University, Osaka, Japan

M. Takaki et al.: ``重イオン二重荷電交換反応による ^{48}Ti の二重ガモフテラー共鳴探索'', JPS Fall meeting, September 25--28, 2015, Osaka City University, Osaka, Japan

R. Yokoyama et al.: ``β-γ核分光を用いた中性子過剰 La 同位体の変形'', JPS Fall meeting, September 25--28, 2015, Osaka City University, Osaka, Japan

M. Kobayashi et al.: ``中性子数 34 近傍カルシウム同位体の直接質量測定'', JPS Fall meeting, September 25--28, 2015, Osaka City University, Osaka, Japan

Y. Kiyokawa et al.:``SHARAQ におけるアイソマー同定システムの開発'', JPS Fall meeting, September 25--28, 2015, Osaka City University, Osaka, Japan

M. Dozono et al.: ``パリティ移行核反応による原子核の 0$^-$状態の研究 II'', JPS Fall meeting, September 25--28, 2015, Osaka City University, Osaka, Japan

S. Michimasa, M. Kobayashi, Y. Kiyokawa, M. Takaki, M. Dozono, S. Go, H. Baba, E. Ideguchi, K. Kisamori, T. Matsubara, M. Matsushita, H. Miya, S. Ota, H. Sakai, S. Shimoura, A. Stolz, T.L. Tang, H. Tokieda, T. Uesaka, R.G.T. Zegers: ``多結晶ダイヤモンド検出器の開発'', JPS Spring meeting, March 19--22, 2016, Tohoku Gakuin Unversity, Sendai, Japan

Y. Kubota et al.: ``ボロミアン核(p,pn)反応を用いた二中性子運動量相関の研究'', JPS Spring meeting, March 19--22, 2016, Tohoku Gakuin Unversity, Sendai, Japan

Y. Kiyokawa et al.:``SHARAQ における中性子過剰 Sc 近傍核の核異性体γ線分光'',JPS Spring meeting, March 19--22, 2016, Tohoku Gakuin Unversity, Sendai, Japan

S. Masuoka, S. Shimoura, K. Kobayashi, Y. Kunimoto: ``複数中性子識別のための反跳陽子飛跡検出器の開発'', JPS Spring meeting, March

19--22, 2016, Tohoku Gakuin Unversity, Sendai, Japan
Y. Yamaguchi, S. Shimoura, N. Imai, K. Wimmer, T. Kitamura: ``DSP を用いた多重ガンマ線検出用 Ge 検出器アレイの為のデータ収集系の開発'', JPS Spring meeting, March 19--22, 2016, Tohoku Gakuin Unversity, Sendai, Japan
T. Kitamura, N. Imai, Y. Yamaguchi, H. Haba: ``高スピンアイソマー^{178m2}Hf 標的開発のためのアイソマー生成および純化手法の検討'', JPS Spring meeting, March 19--22, 2016, Tohoku Gakuin Unversity, Sendai, Japan
Y. Iwata(Oral, Invited): ``TDHF で見た fission'', the JPS Autumn Meeting, Sep. 25-28, 2015, Osaka City University, Osaka, Japan.
N. Shimizu, Y. Futamura, T. Sakurai, T. Mizusaki, Y. Utsuno, and T. Otsuka:``殻模型計算における確率論的な準位密度計算法'', the JPS Autumn Meeting, Sep. 27, 2015, Osaka City University, Osaka, Japan.
Y. Utsuno, N. Shimizu, T. Togashi, T. Otsuka, T. Suzuki, and M. Honma: ``第一禁止ベータ崩壊データによる中性子過剰カルシウム同位体の殻進化の解析'', the JPS Autumn Meeting, Sep. 25-28, 2015, Osaka City University, Osaka, Japan.
Y. Iwata, N. Shimizu, T. Otsuka, Y. Utsuno, J. Menendez, M. Honma, and T. Abe:``48Ca の二重ベータ崩壊の 殻模型計算による記述 III'', the JPS Autumn Meeting, Sep. 25-28, 2015, Osaka City University, Osaka, Japan.
T. Togashi, T. Otsuka, N. Shimizu, and Y. Utsuno: ``モンテカルロ殻模型によるセレン 79 の光吸収断面積の計算'', the JPS Autumn Meeting, Sep. 25-28, 2015, Osaka City University, Osaka, Japan.
T. Yoshida, N. Shimizu, T. Abe, and T. Otsuka:``12Be における殻構造と クラスター構造のモンテカルロ殻模型による研究'', the JPS Autumn Meeting, Sep. 26, 2015, Osaka City University, Osaka, Japan.
N. Tsunoda:``核力に基づいた中性子過剰 Ca 同位体の構造'', the JPS Autumn Meeting, Sep. 25-28, 2015, Osaka City University, Osaka, Japan.
Y. Tsunoda:``大規模殻模型計算による Z=28 近傍の核構造の研究'', the JPS Autumn Meeting, Sep. 27, 2015, Osaka City University, Osaka, Japan.
Y. Utsuno(Oral, Invited):``中性子過剰な原子核の物理'', the JPS Spring Meeting, Mar. 19-22, 2016, Tohoku Gakuin University, Sendai, Japan.
Y. Tsunoda:``大規模殻模型計算による Z=28 近傍の核構造の研究'', the JPS Spring Meeting, Mar. 22, 2016, Tohoku Gakuin University, Sendai, Japan.
T. Yoshida, N. Shimizu, T. Abe, and T. Otsuka: ``Be 同位体における intrinsic 状態の研究'', the JPS Spring Meeting, Mar. 19, 2016, Tohoku Gakuin University, Sendai, Japan.
T. Togashi, T. Otsuka, N. Shimizu, and Y. Utsuno:``モンテカルロ殻模型による 79Se,90Sr,93Zr の光吸収断面積の計算'', the JPS Spring Meeting, Mar. 22, 2016, Tohoku Gakuin University, Sendai, Japan.
Y. Iwata, N. Shimizu, T. Otsuka, J. Menendez, Y. Utsuno, M. Honma, and T. Abe: `` Ca48 のニュートリノレス二重ベータ 崩壊に対するステライル・ニュートリノの影響'', the JPS Spring Meeting, Mar. 19-22, 2016, Tohoku Gakuin University, Sendai, Japan.
N. Tsunoda: ``核力に基づいた pf-shell 原子核の構造'', the JPS Spring Meeting, Mar. 19-22, 2016, Tohoku Gakuin University, Sendai, Japan.

Posters Presentations

[International Conference etc.]

S. Hayashi on behalf of the ALICE Collaboration (poster): ``Dielectron measurement from charm and bottom quark decays in p-Pb collisions with the ALICE detector'', XXV International Conference on Ultrarelativistic Nucleus-Nucleus Collisions (QM2015), Sept. 27 - Oct. 3, Kobe, Japan
M. Dozono (poster): ``The parity-transfer (^{16}O,^{16}F) reaction for studies of the spin-dipole 0$^-$ mode'', International symposium on Physics with Fragment Separators --25th Anniversary of RIKEN-Projectile Fragment Separator (RIPS25), December 6--7, 2015, Hayama, Kanagawa, Japan
M. Kobayashi (poster):``Time-of-flight mass measurements of neutron-rich Ca isotopes beyond N = 34'', International symposium on Physics with Fragment Separators --25th Anniversary of RIKEN-Projectile Fragment Separator (RIPS25), December 6--7, 2015, Hayama, Kanagawa, Japan
S. Michimasa (poster): ``OEDO beamline for high-quality slow-down RI beams'', International symposium on Physics with Fragment Separators --25th Anniversary of RIKEN-Projectile Fragment Separator (RIPS25), December 6--7, 2015, Hayama, Kanagawa, Japan
Y. Kotaka, Y. Ohshiro, S. Watanabe, H. Yamaguchi, N. Imai, S. Shimoura, M. Kase, S. Kubono, K. Hatanaka, A. Goto, H. Muto (poster): ``Development of low-energy heavy-ion beams by the Riken AVF cyclotron and Hyper ECR ion source of CNS'', 13th International Conference on Heavy Ion Accelerator Technology (HIAT2015), September 7-11, 2015, Yokohama, Japan
H. Muto, Y. Oshiro, Y. Kotaka, S. Yamaka, S. Watanabe, H. Yamaguchi, S. Shimoura, M. Kase, S. Kubono, K. Kobayashi, M. Nishimura, M. Oyaizu, T. Hattori (poster): ``Observation of sublimation effect of Mg and Ti ions at the Hyper-electron cyclotron resonance ion source'', 13th International Conference on Heavy Ion Accelerator Technology (HIAT2015), September 7-11, 2015, Yokohama, Japan
N. Tsunoda(Poster): ``Neutron-rich nuclei from the nuclear force'', Gordon Research Conference, May 31- June 5, 2015, Colby-Sawyer college, NH, USA.
T. Yoshida(Poster), N. Shimizu, T. Abe, and T. Otsuka:``Alpha-cluster structure for Be isotopes appeared in the wave function of Monte Carlo shell model'', Nov. 4-8, 2015, Symposium on Quarks to Universe in Computational Science (QUCS 2015), Nara, Japan.

Partner Institution
Center for Radioactive Ion Beam Sciences
Institute of Natural Science and Technology, Niigata University

1. Abstract

The Center for Radioactive Ion Beam Sciences, Niigata University, aims at uncovering the properties of atomic nuclei and heavy elements and their roles in the synthesis of elements, with use of the advanced techniques of heavy ion and radioactive ion beam experiments as well as the theoretical methods. Main research subjects include the measurements of various reaction cross sections and moments of neutron- or proton-rich nuclei, synthesis of super-heavy elements and radio-chemical studies of heavy nuclei, and theoretical studies of exotic nuclei based on quantum many-body methods and various nuclear models. In addition, we promote interdisciplinary researches related to the radioactive ion beam sciences, such as applications of radioactive isotopes and radiation techniques to material sciences, nuclear engineering and medicine. Many of them are performed in collaboration with RIKEN Nishina Center and with use of the RIBF facilities. The center emphasizes also its function of graduate education in corporation with the Graduate School of Science and Technology, Niigata University, which invites three researchers in RIKEN Nishina Center as visiting professors.

2. Major Research Subjects

(1) Reaction cross section and radii of neutron-rich nuclei
(2) Production of superheavy nuclei and radiochemistry of heavy elements
(3) Nuclear theory

3. Summary of Research Activity

(1) Reaction cross section and radii of neutron-rich nuclei

The experimental nuclear physics group has studied nuclear structure with the RI beam. One of our main interests is the interaction/reaction cross section measurements. They are good probes to investigate nuclear matter radii and nuclear matter distributions including halo or skin structure. Recently we have measured the interaction sections of Ne, Na, Mg and Al isotopes from stable region to neutron drip line with BigRIPS in RIBF. We found a large enhancement of cross section at ^{31}Ne. It suggests that ^{31}Ne nucleus has a neutron halo. It is consistent with the soft E1 excitation measurement. We also found an enhancement at ^{37}Mg. For odd-Z nuclei, Na and Al, we did not find such a large enhancement from neighbor isotopes. The systematics of observed interaction/reaction cross sections shows the changing of nuclear structure from stable region to neutron drip line via island of inversion.

(2) Production of superheavy nuclei and radiochemistry of heavy elements

The nuclear chemistry group has been investigating decay properties of super-heavy nuclei, measured the excitation functions of rutherfordium isotopes, and clarified the ambiguity of the assignment of a few-second spontaneously fissioning isotope of ^{261}Rf. The new equipment designed for measurement of short-lived alpha emitters is under development.
For the chemistry research of super-heavy elements, preparatory experiments, such as solvent extraction for the group 4, 5, and 6th elements and gaseous phase chemistry for group-4 elements, have been performed using radioisotopes of corresponding homolog elements.

(4) Nuclear theory

One of the main activities of the nuclear theory group concerns with developments of the nuclear density functional theory and exploration of novel correlations and excitations in exotic nuclei. A fully selfconsistent scheme of the quasiparticle random phase approximation (QRPA) on top of the Skyrme-Hartree-Fock-Bogoliubov mean-field for deformed nuclei has been developed in the group. The versatility of this method to describe the deformation splitting of the giant resonances associated with the onset of deformation has been demonstrated for the first time by the intensive numerical calculation performed for the light nuclei such as ^{24}Mg and ^{28}Si. The same method is further extended to describe the spin-isospin modes of excitation. A successful description of the Gamow-Teller transition strengths in ^{42}Ca is achieved with this method, which implies an important role of proton-neutron pair correlation in the $N = Z$ nucleus ^{42}Sc. Another correlation of interest in neutron-rich nuclei is the neutron-pair correlation, for which the spatial di-neutron correlation has been a key topic. Applying the continuum QRPA to the pairing modes of excitation in neutron-rich Sn isotopes, we predict the emergence of an anomalous pair vibration for isotopes with $A > 132$. Furthermore the new mode is predicted to exhibits the di-neutron character. In addition to these studies, the di-neutron correlation in the asymptotic tail in drip-line nuclei, the quasiparticle resonances in unbound odd-N nuclei are under way. As an application of the continuum QRPA, a microscopic theory of the direct neutron capture reaction has been developed recently. Cluster structure and the ab initio studies of light nuclei are also important research subjects of the theory group.

Members

Director

Masayuki MATSUO (Professor)

Scientific Staff

Hisaaki KUDO (Professor)
Takashi OHTSUBO (Associate Professor)
Shin-ichi GOTO (Associate Professor)
Shigeyoshi AOYAMA (Associate Professor)

Takuji IZUMIKAWA (Associate Professor)
Kenichi YOSHIDA (Assistant Professor)
Kazuhiro OOE (Assistant Professor)
Jun GOTO (Assistant Professor)
Maya TAKECHI (Assistant Professor)

Post Doctoral Associates
Tsunenori INAKURA
Fumiharu KOBAYASHI

Graduate Students
Kazuya HIROKAWA
Yoshihiko KOBAYASHI

List of Publications & Presentations

Publications

[Journal]

(Original Papers) *Subject to Peer Review

T. K. Sato, M. Asai, A. Borschevsky, T. Stora, N. Sato, Y. Kaneya, K. Tsukada, Ch. E. Düllmann, K. Eberhardt, E. Eliav, S. Ichikawa, U. Kaldor, J. V. Kratz, S. Miyashita, Y. Nagame, K. Ooe, A. Osa, D. Renisch, J. Runke, M. Schädel, P. Thörle-Pospiech, A. Toyoshima and N. Trautmann, “Measurement of the first ionization potential of lawrencium, element 103”, Nature **520**, 209 (2015).*

D. Kaji, K. Morimoto, H. Haba, Y. Wakabayashi, Y. Kudou, M. Huang, S. Goto, M. Murakami, N. Goto, T. Koyama, N. Tamura, S. Tsuto, T. Sumita, K. Tanaka, M. Takeyama, S. Yamaki, and K. Morita, Startup of a new gas-filled recoil separator GARIS-II, J. Radioanal. Nucl. Chem. **303**, 1523 (2015).*

I. Usoltsev, R. Eichler, Y. Wang, J. Even, A. Yakushev, H. Haba, M. Asai, H. Brand, A. Di Nitto, Ch. E. Düllmann, F. Fangli, W. Hartmann, M. Huang, E. Jäger, D. Kaji, J. Kanaya, Y. Kaneya, J. Khuyagbaatar, B. Kindler, J.V. Kratz, J. Krier, Y. Kudou, N. Kurz, B. Lommel, S. Miyashita, K. Morimoto, K. Morita, M. Murakami, Y. Nagame, H. Nitsche, K. Ooe, T.K. Sato, M. Schädel, J. Steiner, P. Steinegger, T. Sumita, M. Takeyama, K. Tanaka, A. Toyoshima, K. Tsukada, A. Türler, Y. Wakabayashi, N. Wiehl, S. Yamaki, and Z. Qin, “Decomposition studies of group 6 hexacarbonyl complexes. Part 1: Production and decomposition of $Mo(CO)_6$ and $W(CO)_6$”, Radiochimica Acta **104**, 141, (2016).*

Y. K. Gupta, U. Garg, J. T. Matta, D. Patel, T. Peach, J. Hoffman, K. Yoshida, M. Itoh, M. Fujiwara, K. Hara, H. Hashimoto, K. Nakanishi, M. Yosoi, H. Sakaguchi, S. Terashima, S. Kishi, T. Murakami, M. Uchida, Y. Yasuda, H. Akimune, T. Kawabata, and M. N. Harakeh, “Splitting of ISGMR strength in the light-mass nucleus ^{24}Mg due to ground-state deformation”, Physics Letters B **748**, 343 (2015)*.

Y. Fujita, H. Fujita, T. Adachi, G. Susoy, A. Algora, C. L. Bai, G. Colo, M. Csatllos, J. M. Deaven, E. Estevez-Aguado, C. J. Guess, J. Gulyas, K. Hatanaka, K. Hirota, M. Honma, D. Ishikawa, A. Krasznahorkay, H. Matsubara, R. Meharchand, F. Molina, H. Nakada, H. Okamura, H. J. Ong, T. Otsuka, G. Perdikakis, B. Rubio, H. Sagawa, P. Sarriguren, C. Scholl, Y. Shimbara, E. J. Stephenson, T. Suzuki, A. Tamii, J. H. Thies, K. Yoshida, R. G. T. Zegers, and J. Zenihiro, “High-resolution study of Gamow-Teller excitations in the ^{42}Ca(^{3}He,t)^{42}Sc reaction and the observation of a ’low-energy super-Gamow-Teller state’”, Physical Review C **91**, 064316 (2015)*.

Y. Kobayashi, M. Matsuo, “Effects of pairing correlation on the low-lying quasiparticle resonance in neutron drip-line nuclei”, Progress of Theoretical and Experimental Physics **2016**, 013D01 (2016)*.

T. Inakura, H. Nakada, “Constraining the slope parameter of the symmetry energy from nuclear structure”, Physical Review C **92**, 064302 (2016)*.

Y. Kanada-En’yo, F. Kobayashi, “Proton and neutron correlations in ^{10}B”, Physical Review C **91**, 054323 (2016)*.

F. Kobayashi, Y. Kanada-En’yo, “Analysis of the effect of core structure upon dineutron correlation using antisymmetrized molecular dynamics”, Physical Review C **93**, 024310 (2016)*.

A. Matta, D. Beaumel, H. Otsu, V. Lapoux, N.K. Timofeyuk, N. Aoi, M. Assie, H. Baba, S. Boissinot, R.J. Chen, F. Delaunay, N. de Sereville, S. Franchoo, P. Gangnant, J. Gibelin, F. Hammache, Ch. Houarner, N. Imai, N. Kobayashi, T. Kubo, Y. Kondo, Y. Kawada, L.H. Khiem, M. Kurata-Nishimura, E.A. Kuzmin, J. Lee, J.F. Libin, T. Motobayashi, T. Nakamura, L. Nalpas, E. Yu. Nikolskii, A. Obertelli, E.C. Pollacco, E. Rindel, Ph. Rosier, F. Saillant, T. Sako, H. Sakurai, A.M. Sanchez-Benitez, J-A. Scarpaci, I. Stefan, D. Suzuki, K. Takahashi, M. Takechi, S. Takeuchi, H. Wang, R. Wolski, K. Yoneda, “New findings on structure and production of He-10 from Li-11 with the (d,He-3) reaction”, Physical Review C **92**, 041302, (2015).*

I. Mukha, L.V. Grigorenko, X. Xu, L. Acosta, E. Casarejos, A.A. Ciemny, W. Dominik, J. Duenas-Diaz, V. Dunin, J.M. Espino, A. Estrade, F. Farinon, A. Fomichev, H. Geissel, T.A. Golubkova, A. Gorshkov, Z. Janas, G. Kaminski, O. Kiselev, R. Knoebel, S. Krupko, M. Kuich, Yu A. Litvinov, G. Marquinez-Duran, I. Martel, C. Mazzocchi, C. Nociforo, A.K. Orduz, M. Pfuetzner, S. Pietri, M. Pomorski, A. Prochazka, S. Rymzhanova, A.M. Sanchez-Benitez, C. Scheidenberger, P. Sharov, H. Simon, B. Sitar, R. Slepnev, M. Stanoiu, P. Strmen, I. Szarka, M. Takechi, Y.K. Tanaka, H. Weick, M. Winkler, J.S. Winfield, M.V. Zhukov, “Observation and Spectroscopy of New Proton-Unbound Isotopes Ar-30 and Cl-29: An Interplay of Prompt Two-Proton and Sequential Decay”, Physical Review Letters **115**, 202501, (2015).*

D. Atanasov, K. Blaum, F. Bosch, C. Brandau, P. Buhler, X. Chen, I. Dillmann, T. Faestermann, B. Gao, H. Geissel, R. Gernhauser, S. Hagmann, T. Izumikawa, P.-M. Hillenbrand, C. Kozhuharov, J. Kurcewicz, S. A Litvinov, Y. A Litvinov, X. Ma, G. Munzenberg, M. A. Najafi, F. Nolden, T. Ohtsubo, A. Ozawa, F. C. Ozturk, Z. Patyk, M. Reed, R. Reifarth, M. S. Sanjari, D. Schneider, M. Steck, T. Stohlker, B. Sun, F. Suzaki, T. Suzuki, C. Trageser, X. Tu, T. Uesaka, P. Walker, M. Wang, H. Weick, N. Winck- ler, P. Woods, H. Xu, T. Yamaguchi, X. Yan, and Y. Zhang, “Between atomic and nuclear physics: radioactive decays of highly-charged ions”, Journal of Physics B **48**, 144024 (2015).

Y. Shimbara, T. Matsuzaki, K. Abe, Y. Fujita, J. Goto, T. Itoh, N. Kikukawa, M. Nagashima, Y. Nakamura, T. Ogura, T. Ohtsubo, S. Ohya, T. Sakai, D. Sera, S. Suzuki, K. Takeda, A. Yajima, T. Yoshikawa, “Observation of Muonic X-rays of Cosmic-Ray Muons Stopped in Al and Fe Targets“, Journal of the Physical Society of Japan **84**, 023401, (2015).*

(Review)

K. Matsuyanagi, M. Matsuo, T. Nakatsukasa, K. Yoshida, N. Hinohara, K. Sato, “Microscopic derivation of the quadrupole collective Hamiltonian for shape coexistence/mixing dynamics”, Journal of Physics G: Nuclear and Particle Physics **43**, 024006 (2016)*.

[Proceedings]

(Original Papers) *Subject to Peer Review

K. Yoshida, “Charge-exchange modes of excitation in deformed neutron-rich nuclei”, AIP Conference Proceedings **1681**, 050006 (2015).
K. Yoshida, “Low-Lying Gamow-Teller Excitations and Beta-Decay Properties of Neutron-Rich Even-N Zr Isotopes”, JPS Conference Proceedings **6**, 020017 (2015)*.
W. Horiuchi, T. Inakura, T. Nakatsukasa, and Y. Suzuki,“Systematic analysis of total reaction cross section of unstable nuclei with Glauber theory”, JPS Conference Proceedings **6**, 030079 (2015)
W. Horiuchi, Y. Suzuki, and T. Inakura,“Probing neutron-skin thickness of unstable nuclei with total reaction cross section”, JPS Conference Proceedings **6**, 030080 (2015)

Oral Presentations

[International Conference etc.]

K. Shirai, Y. Oshimi, S. Goto, K. Ooe and H. Kudo, “Gas chromatographic behavior of chloride compounds of group 4 elements”, The 4th International Congress on Natural Science, Changhua, Taiwan, September 10–12, 2015.
K. Yoshida, Charge-exchange modes of excitation in deformed neutron-rich nuclei, 3rd International Conference on Nuclear Structure and Dynamics, Portrose, Slovenia, June 14–19, 2015.
K. Yoshida, Proton-neutron pairing vibrations, 2nd International Workshop & 12th RIBF Discussion on Neutron-Proton Correlation, University of Hong Kong, China, July 6–9, 2015.
K. Yoshida, Pairing in spin-isospin responses, YIPQS Long-term and Nishinomiya-Yukawa Memorial International workshop ‘Computational Advances in Nuclear and Hadron Physics’, YITP, Kyoto University, September 21–October 30, 2015.
K. Yoshida, Skyrme energy-density-functional method for large-scale linear-response calculations, Symposium on ‘Quarks to Universe in Computational Science’, Nara Kasugano International Forum IRAKA, Nara, November 4–8, 2015.
S. Tamaki, M. Matsuo, Monopole pair transfer on the neutron-rich N=84 isotopes : a characteristic pair-vibrational state, The 14th CNS International Summer School, CNS, Wako, August 26–September 1, 2015.
T. Inakura, “Low-lying E1 mode and constraint on nuclear equation of state”, RIBF Users Meeting 2015, RIKEN, September 10–11, 2015
T. Inakura, “Low-energy E1 mode and constraint on nuclear equation of state”, International symposium on High-resolution Spectroscopy & Tensor interaction (HST15), Osaka University Nakanoshima Center, November. 16–19, 2015

[Domestic Conference]

R. Aono, S. Goto, D. Kaji, K. Morimoto, H. Haba, M. Murakami, K. Ooe and H. Kudo, “^{208}Pb + ^{48,50}Ti 反応における中性子欠損 Rf 同位体の合成”, 第 59 回放射化学討論会, 東北大学川内キャンパス, 9 月 (2015).
K. Shirai, Y. Oshimi, S. Goto, K. Ooe and H. Kudo, “超重元素の気相化学実験における吸着エンタルピー導出法の検討”, 日本化学会 第 96 春季年会, 同志社大学京田辺キャンパス, 3 月 (2016).
J. Goto, Y. Amaya, T. Izumikawa, R. Endo, T. Shiiya, Y. Shobugawa, T. Takahashi, H. Yoshida, and M. Naito, “指向性があるガンマ線自動車走行サーベイシステムの開発状況”, 日本原子力学会 2015 年秋の年会, 静岡大学静岡キャンパス, 9 月 (2015).
J. Goto, Y. Amaya, T. Izumikawa, R. Endo, T. Shiiya, Y. Shobugawa, T. Takahashi, H. Yoshida, and M. Naito, “指向性があるガンマ線自動車走行サーベイシステムの開発と測定例”, 環境放射能除染学会第 4 回研究発表会, タワーホール船堀, 7 月 (2015).

吉田賢市, “中重不安定核の半径から見る核構造”, RCNP 研究会「全反応断面積及び荷電変化断面積による陽子・中性子半径研究の現状と展望」, 大阪大学核物理研究センター, 1 月 (2016).
坂井新九郎, 吉田賢市, “中性子過剰 Ne 同位体における対相関と変形”, RCNP 研究会「全反応断面積及び荷電変化断面積による陽子・中性子半径研究の現状と展望」, 大阪大学核物理研究センター, 1 月 (2016).
小林良彦, 松尾正之, “中性子過剰核における一中性子共鳴の共鳴幅に対する対相関効果”, KEK 理論センター研究会「原子核・ハドロン物理の課題と将来」, 高エネルギー加速器研究機構, 茨城県つくば市, 11 月 (2015).
稲倉恒法, “*N* = *Z* 安定原子核の超変形状態と八重極モード”, RCNP 研究会「アイソスカラー型単極遷移で探る 原子核の励起状態とクラスター構造」,RCNP, 大阪大学, 7 月 (2015).
T. Inakura and H. Nakada, “Constraint slope parameter of symmetry energy from nuclear structure”,「実験と観測で解き明かす中性子星の核物質」第 4 回研究会, 湘南国際センター, 9 月 (2015).
稲倉恒法, 松尾正之, “中性子星内殻における超流動中性子・原子核系の集団運動”, 低密度研究会, 東京大学, 2 月 (2016).
吉田賢市, “中性子陽子対振動”, 日本物理学会 2015 年秋季大会シンポジウム「スピン・アイソスピン応答研究の新たな地平」, 大阪市立大学, 9 月 (2015).
吉田賢市, “中性子陽子対振動”, KEK 理論センター研究会「原子核・ハドロン物理の課題と将来」, 高エネルギー加速器研究機構, 11 月 (2015).
宮田絵里, “チェレンコフ光を利用した不安定核ビーム高時間分解能検出器の開発”, 日本物理学会秋季大会, 大阪市立大学, 3 月 (2016).

Posters Presentations

[International Conference etc.]

K. Ooe, A. Tanaka, R. Yamada, H. Kikunaga, M. Murakami, Y. Komori, H. Haba, S. Goto and H. Kudo, “Solvent extraction behavior of Zr and Hf with chelate extractants for aqueous chemical studies of Rf”, The 5th International Conference on the Chemistry and Physics of the Transactinide Elements, Fukushima, Japan, May 25–29, 2015.
M. Murakami, S. Goto, K. Ooe, D. Sato, S. Tsuto, N. Goto, T. Koyama, R. Aono, H. Haba, M. Huang, and H. Kudo, “Excitation function of Db isotopes produced in ^{248}Cm(^{19}F, *x*n) reaction”, The 5th International Conference on the Chemistry and Physics of the Transactinide Elements, Fukushima, Japan, May 25–29, 2015.
S. Goto, Y. Oshimi, K. Shirai, K. Ooe, and H. Kudo, “Off-line experiment of isothermal chromatography for Zr and Hf tetrachloride in macro- and tracer-scale”, The 5th International Conference on the Chemistry and Physics of the Transactinide Elements, Fukushima, Japan, May 25–29, 2015.
K. Ooe, A. Tanaka, R. Yamada, H. Kikunaga, M. Murakami, Y. Komori, H. Haba, S. Goto and H. Kudo, “Liquid-liquid extraction behavior of zirconium and hafnium as homologs of element 104, rutherfordium using chelate extractants”, The 2015 International Chemical Congress of Pacific Basin Societies, Hawaii, USA, December 15–20, 2015.
S. Goto, Y. Oshimi, K. Shirai, K. Ooe, and H. Kudo, “Gas chromatographic behaviors of $ZrCl_4$ and $HfCl_4$ in macro- and tracer-scale”, The 2015 International Chemical Congress of Pacific Basin Societies, Hawaii, USA, December 15–20, 2015.
J. Goto, Y. Shobugawa, Y. Kawano, Y. Amaya, T. Izumika, Y. Katsuragi, T. Shiiya, T. Suzuki, T. Takahashi, T. Takahashi, H. Yoshida, and M.

Naito, “Development of a portable gamma-ray survey system for measurements of dose rates in air“, International Symposium on Radiation Detectors and Their Uses, KEK, Japan, January 18–21, 2016.

[Domestic Conference]

R. Yamada, K. Ooe, M. Murakami, H. Haba, Y. Komori, H. Kikunaga, S. Goto and H. Kudo, “Rf の溶液化学実験に向けた同族元素 Zr, Hf の HDEHP による溶媒抽出挙動”,第 59 回放射化学討論会, (日本放射化学会), 東北大学 (川内キャンパス), 9 月 (2015).

K. Shirai, T. Asai, Y. Nanba, R. Aono, S. Goto, K. Ooe and H. Kudo, “超重元素の気相化学実験における標準としての $BiCl_3$ の利用”, 第 59 回放射化学討論会, (日本放射化学会), 東北大学 (川内キャンパス), 9 月 (2015).

R. Motoyama, K. Ooe, M. Murakami, H. Haba, S. Goto and H. Kudo, “ドブニウム(Db)の化学実験に向けた 5 族元素 Nb,Ta の塩化物錯体のトリイソオクチルアミンによる抽出挙動”, 第 59 回放射化学討論会, (日本放射化学会), 東北大学 (川内キャンパス), 9 月 (2015).

D. Sato, M. Murakami, K. Ooe, R. Motoyama, H. Haba, Y. Komori, A. Toyoshima, A. Mitsukai, H. Kikunaga, S. Goto and H. Kudo, “105 番元素 Db の化学実験のための Aliquat 336 樹脂を用いた Nb, Ta のフッ化水素酸中からの固液抽出”, 第 59 回放射化学討論会, (日本放射化学会), 東北大学 (川内キャンパス), 9 月 (2015).

Partner Institution
Wako Nuclear Science Center, IPNS (Institute for Particle and Nuclear Studies)
KEK (High Energy Accelerator Research Organization)

1. Abstract

The KEK Isotope Separation System (KISS) has been constructed to experimentally study the β-decay properties of unknown neutron-rich nuclei with around neutron magic numbers N = 126 for astrophysical interest. In FY2015, a new rotational target system was introduced and higher yields and more stable operational conditions were achieved. Resonance ionization spectroscopy for the hyperfine structure of ^{199}Pt has been performed at KISS. An international collaboration with IBS (Institute of Basic Science), Korea has been organized for development of an array of super-clover germanium detectors and an MRTOF mass spectrograph.

2. Major Research Subjects

(1) Radioactive isotope beam production and manipulation for nuclear experiments.
(2) Explosive nucleosyhnthesis (r- and rp-process).
(3) Heavy ion reaction mechanism for producing heavy neutron-rich nuclei.
(4) Development of MRTOF mass spectrograph for short-lived heavy nuclei.
(5) Development of RNB probes for materials science applications.

3. Summary of Research Activity

The KISS is an element-selective isotope separator using a magnetic mass separator combined with in-gas-cell resonant laser ionization. The gas cell filled with argon gas of 50 kPa is a central component of the KISS for extracting only the element of interest as ion beam for subsequent mass separation. In the cell, the element primarily produced by low-energy heavy ion reactions is stopped (thermalization and neutralization), transported by buffer gas (argon gas-flow of ~50 kPa in the present case), and then re-ionized by laser irradiation just before the exit. The gas cell was fabricated to efficiently correct the reaction products produced by the multi-nucleon transfer reaction of ^{136}Xe +^{198}Pt system. For the first extraction of the reaction products, the ^{136}Xe beam energy and ^{198}Pt target thickness were set at 10.8 MeV/u and 6 mg/cm^2, respectively. In FY2014, half-lives of 199Pt were measured with β-ray telescopes and a tape transport system were installed at the focal point of KISS. The β-ray telescopes were composed of three double-layered thin plastic scintillators; thickness of the first layer and second one were 0.5 and 1 mm, respectively. In order to reduce the background, they were surrounded with low-activity lead blocks and a veto counter system consisting of plastic scintillator bars. The background rate of the present β-ray telescopes was measured to be 0.7 counts per second. In order to drastically reduce the background rate, lower than a few counts per hour, a gas counter based beta-ray telescope is under development in FY2015.

For higher primary beam intensities and higher extraction efficiency, we developed a doughnut-shaped gas cell and a rotating target wheel setup for KISS. With this new setup, resonance ionization spectroscopy of the ground state hyperfine structure of ^{198}Pt was performed. The nuclear g-factor and the charge radius of ^{199}Pt can be deduced from the experimental results.

As a continuing effort for search for effective laser ionization scheme of elements of our interest (Z<82), a reference cell was fabricated, and is currently being used to search for auto ionizing states in Ta, W, and etc…

In order to investigate the feasibility of the multi-nucleon transfer (MNT) in the reaction system of ^{136}Xe on ^{198}Pt for producing heavy neutron-rich isotopes around the mass number of 200 with the neutron magic number of 126, We performed the cross section measurement at GANIL in 2012 and the analysis of the data has been completed. The cross sections of target-like fragments around N =126 were comparable to those estimated using the GRAZING code, and they appear to be mainly contributed by the reactions with low total energy loss with the weak N/Z equilibration and particle evaporation. This suggests the promising use of the MNT reactions with a heavy projectile at the energies above the Coulomb barrier for production of the neutron-rich isotopes around N = 126.

Aiming at direct mass measurements of short-lived heavy nuclei at KISS and other facilities, we worked on a development of a multi-reflection time-of-flight mass spectrograph (MRTOF-MS). In FY2015, we demonstrated mass measurements of Fr and At isotopes at GARIS-II with a collaboration with the SLOWRI team and the Super Heavy Element Synthesis team of RIKEN.

The diffusion coefficient of lithium in solid materials used in secondary Li-ion batteries is one of key parameters that determine how fast a battery can be charged. The reported Li diffusion coefficients in solid battery materials are largely scattered over several order of magnitudes. We have developed an in-situ nanoscale diffusion measurement method using α-emitting radioactive ^{8}Li tracer. In the method, while implanting a pulsed ^{8}Li beam of 8 keV, the alpha particles emitted at a small angle ($\theta = 10 \pm 1^{\circ}$) relative to a sample surface were detected as a function of time. We can obtain Li diffusion coefficient from the time dependent yields of the α particles, whose energy loss can be converted to nanometer-scale position information of diffusing ^{8}Li. The method has been successfully applied to measure the lithium diffusion coefficients for an amorphous Li_4SiO_4 - Li_3VO_4 (LVSO) which was used as a solid electrotype in a solid-state Li thin film battery, well demonstrating that the present method has the sensitivity to the diffusion coefficients down to a value of 10^{-12} cm^2/s, corresponding with nanoscale Li diffusion. In FY2015, we continued measuring Li diffusion coefficients in a spinel type Li compound of $LiMn_2O_4$ (LMO), which is used as a positive electrode of a Li battery in an electric vehicle. We have observed a significant change on the time dependent yields of the α particles at the sample temperature of around 623 K and will continue the measurements to obtain temperature dependency of Li diffusion coefficients in LMO.

Members

Group Leader

Hiroari MIYATAKE

Members

Michiharu WADA
Yoshikazu HIRAYAMA
Yutaka WATANABE
Peter SCHURY
Yutaka KAKIGUCHI
Michihiro OYAIZU
Hyo-Soon Jung
Jun-young Moon
Jin-hyung Park
Yung-Hee KIM (PhD. Student, Seoul National Univ.)
Momo MUKAI (PhD. Student, Tsukuba Univ.)
Sota KIMURA (PhD. Student, Tsukuba Univ.)

List of Publications & Presentations

Publications

[Journal]

(Original Papers) *Subject to Peer Review

Y.X. Watanabe, Y.H. Kim, S.C. Jeong, Y. Hirayama, N. Imai, H. Ishiyama, H.S. Jung, H. Miyatake, S. Choi, J.S. Song, E. Clement, G. de France, A. Navin, M. Rejmund, C. Schmitt, G. Polarolo, L. Corradi, E. Fioretto, D. Montanari, M. Niikura, D. Suzuki, H. Nishibata, J. Takatsu, « Pathway for the production of neutron-rich isotopes around N=126 shell closure », Phys. Rev. Lett. 115 (2015) 172503, 1-5.*

[Proceedings]

(Original Papers) *Subject to Peer Review

Y. Hirayama, Y.X. Watanabe, N. Imai, H. Ishiyama, S.C. Jeong, H.S. Jung, H. Miyatake, M. Oyaizu, S. Kimura, M. Mukai, Y.H. Kim, T. Sonoda, M. Wada, M. Huyse, Yu. Kudryavtsev,P. van Duppen, « On-line experimental results of an argon gas cell-based laser ion source (KEK Isotope Separation System) », Nucl. Inst. Meth. B376 (2016) 52-56.*

M. Mukai, Y. Hirayama, H. Ishiyama, H.S. Jung, H. Miyatake, M. Oyaizu, Y.X. Watanabe, S. Kimura, A. Ozawa, S.C. Jeong, T. Sonoda, « Search for efficient laser resonance ionization schemes of tantalum using a newly developed time-of-flight mass spectrometer in KISS », Nucl. Inst. Meth B376 (2016) 73-76.*

S. Kimura, H. Ishiyama, H. Miyatake, Y. Hirayama, Y.X. Watanabe, H.S. Jung, M. Oyaizu, M. Mukai, S.C. Jeong, A. Ozawa, « Development of the detector system for image-decay spectroscopy at the KEK Isotope Sepaator System », Nucl. Inst. Meth. B376 (2016) 338-340.*

Y. Hirayama, H. Miyatake, Y.X. Watanabe, N. Imai, H. Ishiyama, S.C. Jeong, H.S. Jung, M. Oyaizu, M. Mukai, S. Kimura, T. Sonoda, M. Wada, Y.H. Kim, M. Huyse, Yu Kudryavtsev, P. van Duppen, « Deta-decay spectroscopy of r-process nuclei around N=126 », EPJ Web Conf. 109 (2016) 08001, 1-6.*

Y. Hirayama, Y.X. Watanabe, N. Imai, H. Ishiyama, S.C. Jeong, H. Miyatake, M. Oyaizu, S. Kimura, M. Mukai, Y.H. Kim, T. Sonoda, M. Wada, M. Huyse, Yu. Kudryavtsev, P. van Duppen, « Laser ion source for multi-nucleon transfer products », Nucl. Inst. Meth B353 (2015) 4-15.*

K. Okada, M. Ichikawa, M. Wada, « Characterization of ion crystals for fundamental science », Hyp. Int. DOI 10.1007/s10751-015-1188-y, 2015*

Oral Presentations

[International Conference etc.]

H. Miyatake, « Beta-decay spectroscopy of r-process nuclei around N=126 », OMEG2015, June 24-27, Beijing, China.

Y. Hirayama, « Online experimental results of an argon gas cell based laser ion source (KEK Isotope Separation System), May 11-15, EMIS2015, Grand Rapids, MI, USA.

M. Wada, « Towards high precision nuclear spectroscopy at SLOWRI, RIKEN RIBF », Nov. 07-12, JCNP2015, RCNP, Osaka, Japan.

[Domestic Conference]

Y. Hirayama, « Nuclear spectroscopy of the waiting point nuclides around the third peak in r-process (KISS project) », Feb. 22-24, NAOJ, Mitaka, Japan.

Posters Presentations

[International Conference etc.]

M. Mukai, « Search for efficient laser resonance ionization schemes of tantalum using a newly developed time-of-flight mass spectrometer in KISS », May 11-15, EMIS2015, Grand Rapids, MI, USA.

S. Kimura, « Development of the detector system for image-decay spectroscopy at the KEK Isotope Sepaator System », May 11-15, EMIS2015, Grand Rapids, MI, USA.

[Domestic Conference]

S. Kimura, « Mass measurements of N=Z-2 nuclei in the vicinity of proton drip line », Feb. 22-24, NAOJ, Mitaka, Japan.

M. Mukai, « Development of low background gas-counter for KISS », Feb. 22-24, NAOJ, Mitaka, Japan.

Events (April 2015 - March 2016)

RNC

Apr. 23	Wako Open campus
Jun. 27 - 28	The 14th NP-PAC
Jul. 27 – Aug. 7	Nishina School
Aug. 11	Safety Review Committee for Accelerator Experiments
Sep. 10-11	RIBF Users Meeting 2015
Sep. 18	Effect of MOU between RNC and The University of Hong Kong
Oct. 30	Effect of MOU between RNC and Technishe Universität Darmstadt
Dec. 3-5	The 16th NP-PAC
Dec. 6-7	Physics with Fragment Separators - 25th Anniversary of RIKEN-Projectile Fragment Separator [RIPS25]
Jan. 12	Interim Review of the Chief Scientist, Osamu KAMIGAITO
Jan. 13	The 5th In PAC
Feb. 16-17	The 12th ML-PAC
Mar. 8	Hot-Lab Safety Review Committee Interim Review of Associate Chief Scientist, Toru TAMAGAWA
Mar. 31	End of Theoretical Nuclear Physics Laboratory led by associate chief scientist Takashi Nakatsukasa

CNS

Aug. 26 - Sep. 1	The 14th CNS international Summer School (CNSSS15) http://indico.cns.s.u-tokyo.ac.jp/conferenceDisplay.py?confId=231

Niigata Univ.

	not held in FY2015

KEK

	not held in FY2015

Press Releases (April 2015 - March 2016)

RNC

May 12	For the violent r-process, the devil's in the details. Success in precise measurements of the half-lives of 110 nuclei which hold the key to the synthesis of heavy elements -A major step forward toward providing an experimental ground for models of the mysterious astrophysical "r-process"-	Giuseppe Lorusso, Shunji Nishimura, Hiroyoshi Sakurai; Radioactive Isotope Physics Laboratory, EURICA collaboration
Nov. 4	Supercomputing the Strange Difference between Matter and Antimatter -The first calculation of direct "CP" symmetry violation—how the behavior of subatomic particles (in this case, the decay of kaons) differs when matter is swapped out for antimatter-	Taku Izubuchi, Christopher Kelly,; Computing Group, RBRC
Dec. 22	Discovery of a tetraneutron resonance nucleus—exploring the highway of the study for neutron matter	Susumu Shimoura (CNS),; Joint PR: Released from the Univ. of Tokyo
Dec. 31	It's official! Element 113 was discovered at RIKEN —Element 113 has become the first element on the periodic table found in Asia—	Kosuke Morita, Research Group for Superheavy Element
Jan. 8	Construction of plant Y-chromosome gene map -Application of heavy-ion induced mutants revealing large inversion of Y-chromosome during its evolution-	Tomoko Abe, Yusuke Kazama, Koutaro Ishii; Ion Beam Breeding Team, Univ. of Tokyo, Univ. of Oxford, Univ. of Edinburgh
Jan. 8	Precise measurement of the orientation of gluons in the proton -A major step in solving the puzzle of the proton spin-	Yasuyuki Akiba, Yuji Goto, Yoon Inseok; Experimental Group, RBRC
Feb. 19	The first attempt in the history of nuclear physics to solve the problem of the LLFP transmutation and has triggered the reaction studies for other long-lived fission products. -Spallation reaction study for fission products in nuclear waste: Cross section measurements for 137Cs and 90Sr on proton and deuteron-	He Wong, Hiroyoshi Sakurai, Hideaki Otsu; Radioactive Isotope Physics Laboratory, SAMURAI Team
Mar. 10	"Two neutrons barely unbound to a nucleus – a picture of a nucleus at the limit, depicted by mass measurement for a heavy Oxygen isotope"	SAMURAI Team, Radioactive Isotope Physics Laboratory ; Joint PR: Released from TIT
Mar. 23	Solar Wind Induces Jupiter's X-ray Aurora	High Energy Astrophysics Laboratory; Joint PR: Released from JAXA

CNS

Dec. 22	Candidate Resonant Tetraneutron State Populated by the ^{4}He(^{8}He, ^{8}Be) Reaction	K. Kisamori, S. Shimoura, T. Uesaka et al.
Mar. 17	Large-scale shell-model analysis of the neutorinoless $\beta\beta$ decay of ^{48}Ca	Y. Iwata, N. Shimizu, T. Otsuka, Y. Utsuno, J. Menendez, M. Honma, T. Abe

VII. LIST OF PREPRINTS

List of Preprints (April 2015 - March 2016)

RIKEN NC-NP

151	Effects of thermal shape fluctuations and pairing fluctuations on the giant dipole resonance in warm nuclei	A.K. Rhine Kumar, P. Arumugam et al.
152	Experimental investigation on the temperature dependence of the nuclear level density parameter	B. Dey, D. Pandit et al.
153	Giant dipole resonance built on hot rotating nuclei produced during evaporation of light particles from the 88Mo compound nucleus	M. Ciemała, M. Kmiecik et al.
154	Adiabatic hyperspherical approach to large-scale nuclear dynamics	Y. Suzuki
155	Reentrance phenomenon of superfluid pairing in hot rotating nuclei	N. Quang Hung, N. Dinh Dang et al.
156	A Universal Damping Mechanism of Quantum Vibrations in Deep Sub-Barrier Fusion	T. Ichikawa, K. Matsuyanagi
157	Microscopic derivation of the quadrupole collective Hamiltonian for shape coexistence/mixing dynamics	K. Matsuyanagi, M. Matsuo et al.
158	Pairing reentrance in warm rotating ^{104}Pd nucleus	N. Quang Hung, N. Dinh Dang et al.
159	Time-dependent density functional studies of nuclear quantum dynamics in large amplitudes	K. Wen, K. Washiyama et al.
160	Covariant density functional theory: the structure of superheavy nuclei revisited	S.E. Agbemava, A.V. Afanasjev et al.
161	First Online Mass Measurements of Isobar Chains via Multi-Reflection Time-of-Flight Mass Spectrograph Coupled with GARIS-II	P. Schury, M. Wada et al.
162	Gauge symmetry in the large-amplitude collective motion of superfluid nuclei	K. Sato
163	Interplay between one-particle and collective degrees of freedom in nuclei	I. Hamamoto

RIKEN NC- AC

	Not Applicable	

RIKEN MP

112	Transport Process in Multi-Junctions of Quantum Systems	T. Kimura, M. Murata

RIKEN QHP

187	QCD Kondo effect: quark matter with heavy-flavor impurities	K. Hattori, K. Itakura et al.
188	U(1) axial symmetry and Dirac spectra in QCD at high temperature	T. Kanazawa, N. Yamamoto
189	Euler-Heisenberg-Weiss action for QCD+QED	S. Ozaki, T. Arai et al.
190	Locating phase boundary from net-baryon number multiplicity distribution	K. Morita, A. Nakamura
191	Effective model for in-medium ¥bar{K}N interactions including the L=1 partial wave	A. Cieplý, V. Krejčiřík
192	Functional dependence of axial anomaly via mesonic fluctuations in the three flavor linear sigma model	G. Fejos

193	Chiral symmetry breaking with no bilinear condensate revisited	T. Kanazawa
194	Heavy-tailed chiral random matrix theory	T. Kanazawa
195	Reinterpretation of the Starobinsky model	T. Asaka, S. Iso et al.
196	Hamilton dynamics for the Lefschetz thimble integration akin to the complex Langevin method	K. Fukushima, Y. Tanizaki
197	Relation between the Reducibility Structures and between the Master Actions in the Witten Formulation and the Berkovits Formulation of Open Superstring Field Theory	Y. Iimori, S. Torii
198	Spontaneous symmetry breaking and Nambu-Goldstone modes in dissipative systems	Y. Minami, Y. Hidaka
199	Lefschetz-thimble path integral for solving the mean-field sign problem	Y. Tanizaki, H. Nishimura et al.
200	Lefschetz-thimble analysis of the sign problem in one-site fermion model	Y. Tanizaki, Y. Hidaka et al.
201	Photon and dilepton spectra from nonlinear QED effects in supercritical magnetic fields induced by heavy-ion collisions	K. Hattori, K. Itakura
202	Complex saddle points and the sign problem in complex Langevin simulation	T. Hayata, Y. Hidaka et al.
203	Nonrelativistic Banks-Casher relation and random matrix theory for multi-component fermionic superfuids	T. Kanazawa, A. Yamamoto
204	Interplay between Mach cone and radial expansion and its signal in gamma-jet events	Y. Tachibana, T. Hirano
205	D meson mass increase by restoration of chiral symmetry in nuclear matter	K. Suzuki, P. Gubler et al.
206	Thermodynamics and reference scale of SU(3) gauge theory from gradient flow on fine lattices	M. Kitazawa, M. Asakawa et al.
207	Lifshitz-type SU(N) lattice gauge theory in five dimensions	T. Kanazawa, A. Yamamoto
208	First results of baryon interactions from lattice QCD with physical masses (1) -- General overview and two-nucleon forces --	T. Doi, S. Aoki et al.
209	Towards Lattice QCD Baryon Forces at the Physical Point: First Results	T. Doi, S. Aoki et al.
210	Heavy Quark Diffusion in Strong Magnetic Fields at Weak Coupling and Implication to Elliptic Flow	K. Fukushima, K. Hattori et al.
211	Dipolar quantization and the infinite circumference limit of 2d conformal field theories	N. Ishibashi, T. Tada
212	D mesons in a magnetic field	P. Gubler, K. Hattori et al.
213	Mesons in strong magnetic fields: (I) General analyses	K. Hattori, T. Kojo et al.
214	Cigar-shaped quarkonia under strong magnetic field	K. Suzuki, T. Yoshida
215	Sharing lattice QCD data over a widely distributed file system	T. Amagasa, S. Aoki et al.
216	Fate of the Tetraquark Candidate Zc(3900) in Lattice QCD	Y. Ikeda, S. Aoki et al.
217	Classical Integrability for Three-Point Functions: Cognate Structure at Weak and Strong Couplings	Y. Kazama, S. Komatsu et al.
218	Effective field theory and the scattering process for magnons in the ferromagnet, antiferromagnet, and ferrimagnet	S. Gongyo, Y. Kikuchi et al.

CNS-REP

94	CNS Annual Report 2014	T. Gunji, Y. Kishi

Nishina Center Preprint server (not including Partner Institution) can be found at
http://nishina-preprints.riken.jp/

VIII. LIST OF SYMPOSIA, WORKSHOPS & SEMINARS

List of Symposia & Workshops (April 2015 - March 2016)

RNC

1	21st International Conference on Computing in High Energy and Nuclear Physics CHEP2015 http://chep2015.kek.jp/index.html	OIST	Apr. 13-17
2	RIKEN Symposium (Category C) - Lipids Structure and Dynamics -	Main Bldg. 424/426	May 14
3	Workshop on Science with SpiRIT TPC http://indico2.riken.jp/indico/conferenceDisplay.py?confId=1773	RIBF Conference Hall	Jun. 5-6
4	1st Workshop on Compact Cyclotrons for High Power Ion Beams (CC2015) http://indico2.riken.jp/indico/conferenceDisplay.py?confId=1937	RIBF Conference Hall	Jun. 26, 29
5	RI ビームファクトリー大強度化計画に関するキックオフ・ミーティング http://indico2.riken.jp/indico/conferenceDisplay.py?confId=1985	Nishina Hall	Jul. 29
6	停止低速放射性同位体の精密核分光(SSRI-PNS)のコラボレーションミーティング http://indico2.riken.jp/indico/conferenceDisplay.py?confId=2008	Aoba Science Hall, Tohoku Unviersity	Sep. 3-5
7	SAMURAI International Collaboration Workshop 2015 http://indico2.riken.jp/indico/conferenceDisplay.py?confId=1790	RIBF Conference Hall	Sep. 7-8
8	13th International Conference on Heavy Ion Accelerator Technology (HIAT2015) http://www.rarf.riken.jp/hiat2015/index.html	WORKPIA YOKOHAMA	Sep. 7-11
9	PHENIX pre-QM15 Collaboration Meeting http://indico2.riken.jp/indico/conferenceDisplay.py?confId=1949	Okochi Hall	Sep. 25-27
10	Quark Matter 2015 http://qm2015.riken.jp/index.php?id=0	KOBE Fashion Mart	Sep. 27 - Oct. 3
11	MPGD2015 (4th International Conference on Micro Pattern Gaseous Detectors) https://agenda.infn.it/conferenceDisplay.py?ovw=True&confId=8839	Stazione Marittima Congress Center, Trieste	Oct. 12-17
12	pre-DNP sPHENIX Workshop https://www.panic05.lanl.gov/sphenix/tracking_mtg.html	Hilton Santafe	Oct. 27
13	1st International Conference on Science and Technology (ICST2015) http://icst.ugm.ac.id/	UGM Yogyakarta, Indonesia	Nov. 11-13
14	Comprehensive Studies of Neutron Star http://indico2.riken.jp/indico/conferenceDisplay.py?confId=2078	Nishina Hall	Nov. 24-25
15	Physics at Fragment Separators -- 25th anniversary of RIKEN RI Beam Facility https://indico2.riken.jp/indico/conferenceDisplay.py?confId=1907	Shonan Village Center	Dec. 6-7
16	The 31st Reimei Workshop on Hadron Physics in Extreme Condition http://asrc.jaea.go.jp/soshiki/gr/hadron/workshop/reimei2016/index.html	JAEA	Jan. 18-20
17	変異創成によるグリーンイノベーションの未来 – 花・食・エネルギー	Suzuki Umetaro Hall	Jan. 21-22
18	Frontier of the Muon Science Applications	Main Bldg. 224/226/424/426 , Main Cafeteria	Feb.16-17
19	8th Japan-Italy Symposium https://indico2.riken.jp/indico/confLogin.py?returnURL=http%3A%2F%2Findico2.riken.jp%2Findico%2FconferenceDisplay.py%3FconfId%3D2150&confId=2150	Nishina Hall	Mar. 7-10
20	Measurements of Reaction & Charge Changing Cross Sections for Ni Isotopes and Related Topics http://indico2.riken.jp/indico/conferenceDisplay.py?confId=2171	RIBF building room 401	Mar. 11

CNS

1	OEDO-SHARAQ International Collaboration Workshop http://indico.cns.s.u-tokyo.ac.jp/conferenceDisplay.py?confId=244	CNS	Sept. 8-9
2	第 12 回 AVF サイクロトロン合同打合せ	RIKEN	Oct. 1–2

List of Seminars (April 2015 - March 2016)

Nuclear Physics Monthly Colloquium

1	Kozi Nakai (KEK)	核物理・核化学・核医学 http://indico2.riken.jp/indico/conferenceDisplay.py?confId=1810	Apr. 24
2	Shoji Nagamiya (RIKEN/KEK)	J-PARC 建設から今後へ http://indico2.riken.jp/indico/conferenceDisplay.py?confId=1970	Oct. 6
3	Yoshiko Kanada-En'yo (Kyoto U.)	Clustering in light neutron-rich nuclei http://indico2.riken.jp/indico/conferenceDisplay.py?confId=2152	Feb. 16

RIBF Nuclear Physics Seminar

1	Hirofumi NODA (RNC)	宇宙 X 線衛星「すざく」で迫る活動銀河核エンジンの新たな描像 http://indico2.riken.jp/indico/conferenceDisplay.py?confId=1821	Apr. 14
2	Susumu Shimoura (CNS)	New energy degraded beam project at RIBF - OEDO project – http://indico2.riken.jp/indico/conferenceDisplay.py?confId=1842	May 22
3	Valeria Pershina (GSI)	Relativistic Quantum Chemistry for Chemical Identification of the Superheavy Elements http://indico2.riken.jp/indico/conferenceDisplay.py?confId=1844	Jun. 2
4	Kei Kotake (Fukuoka U.)	Probing Core-Collapse Supernova Physics with Multi-Messenger Observations http://indico2.riken.jp/indico/conferenceDisplay.py?confId=1855	Jun. 23
5	Takaharu Otsuka (CNS)	Structure evolutions in exotic nuclei and nuclear forces http://indico2.riken.jp/indico/conferenceDisplay.py?confId=1905	Jul. 1-2
6	Nami SAKAI (RIKEN)	Astrochemical Approach to Star and Planet Formation http://indico2.riken.jp/indico/conferenceDisplay.py?confId=1938	Jul. 14
7	Fumiharu Kobayashi (Niigata U.)	Investigation of two-nucleon spatial correlation in light unstable nuclei http://indico2.riken.jp/indico/conferenceDisplay.py?confId=1944	Jul. 17
8	Keiichi Kisamori (RNC)	A candidate of a tetra-neutron state populated by 4He(8He,8Be) reaction http://indico2.riken.jp/indico/conferenceDisplay.py?confId=1958	Jul. 21
9	Zaihong Yang (RNC)	The cluster structure in light neutron-rich nuclei http://indico2.riken.jp/indico/conferenceDisplay.py?confId=1988	Sep. 15
10	Hajime Togashi (RNC)	Nuclear equation of state for core-collapse simulations with realistic nuclear forces http://indico2.riken.jp/indico/conferenceDisplay.py?confId=2051	Oct. 27
11	Steven Karataglidis (U. Johannesburg)	Mapping the densities of exotic nuclei http://indico2.riken.jp/indico/conferenceDisplay.py?confId=2056	Nov. 20
12	Hans Werner Hammer (Theory Center, Institute of Nuclear Physics, TU Darmstadt)	Few-body universality and halo nuclei http://indico2.riken.jp/indico/conferenceDisplay.py?confId=2072	Nov. 27
13	Hiroshi Toki (RCNP)	Tensor optimized antisymmetrized molecular dynamics (TOAMD) http://indico2.riken.jp/indico/conferenceDisplay.py?confId=2087	Dec. 11
14	Philipp Schrock (CNS)	The Electric Dipole Response of 132Sn http://indico2.riken.jp/indico/conferenceDisplay.py?confId=2118	Dec. 17
15	Takuya Maeyama (RNC)	Application and development of 3D chemical dosimetry using gel matrix for heavy ion beam http://indico2.riken.jp/indico/conferenceDisplay.py?confId=2135	Dec. 22
16	Peter H. Schury (KEK)	Present status and future plans for MRTOF-MS at RIBF http://indico2.riken.jp/indico/conferenceDisplay.py?confId=2147	Feb. 12

17	Daisuke Suzuki (RNC)	Illuminating alpha clusters in an active target and time projection chamber http://indico2.riken.jp/indico/conferenceDisplay.py?confId=2209	Mar. 29

Lecture Series on Nuclear Physics

	not held in FY2015		

Special Seminar

	not held in FY2015		

Seminar by Each Laboratory

Theoretical Research Division

1	Tilo Wettig (U. Regensburg)	QHP Seminar: Induced QCD with two bosonic flavors	Apr. 3
2	Kanako Yamazaki (RNC)	QHP Seminar: Hadrons in the PNJL model for interacting quarks	Apr. 13
3	Haozhao Liang (RNC)	QHP Seminar: Self-consistent studies on nuclear spin-isospin excitations	Apr. 13
4	Kei Suzuki (RIKEN)	QHP Seminar: Heavy meson properties in extreme environments from QCD sum rules	Apr. 20
5	Hiroshi Ohki (RIKEN)	QHP Seminar: Walking and conformal dynamics in many flavor QCD on the lattice	Apr. 20
6	Tatsuhiro Misumi (Keio U.)	QHP Seminar: Bions and related topics	Apr. 27
7	Akihiko Monnai (RNC)	QHP Seminar: Exploring the shining quark-gluon plasma in nuclear collisions	May 8
8	Hiroaki Sumiyoshi (Kyoto U.)	QHP Seminar: Torsional response and quantum anomaly in Weyl semimetal with dislocation	May 11
9	Satoshi Nagi (Japan Fisheries Research and Education Agency)	珪藻の生活史、生態、ゲノム研究、および研究の将来展望について	May 15
10	Tomoki Otsuki (Kavli Institute for the Physics and Mathematics of the Universe)	QHP Seminar: Bootstrapping controversial phase transitions	May 18
11	Koutarou Kyutoku (RIKEN)	QHP Seminar: Exploring tidal effects in coalescing binary neutron stars in numerical relativity	May 25
12	Shoichi Sasaki (Tohoku U.)	QHP Seminar: Potential description of the charmonium from lattice QCD	Jun. 1
13	Shinya Gongyo (Kyoto U.)	QHP Seminar: Phase structure of SU(2) Higgs model on the lattice	Jun. 8
14	Panagiota Papakonstantinou (RISP, IBS)	QHP Seminar: Beyond the mean-field picture, with realistic nuclear interactions	Jun. 9

15	Kenji Fukushima (U. Tokyo)	QHP Seminar: Chiral Gap Effect	Jun. 15
16	Teruaki Enoto (Kyoto U.)	宇宙X線で見る中性子星の多様性と磁気現象の物理	Jun. 15
17	Gergely Fejos (RNC)	QHP Seminar: Functional renormalization group analysis of the chiral linear sigma model	Jun. 22
18	Tomoya Murata (Osaka U.)	SNP Seminar: Neutrino induced 4He break up reaction	Jun. 22
19	Kengo Kikuchi (Kyoto U.)	QHP Seminar: Generalized Gradient Flow Equation and Its Applications	Jun. 29
20	Shinsei Ryu (U. Illinois)	QHP Seminar: Quantum anomalies in symmetry-protected topological phases	Jul. 6
21	Takahiro Sagawa (U. Tokyo)	QHP Seminar: Thermodynamics of Information Processing	Jul. 6
22	Wolfram Weise (ECT* Trento, Italy and TU Munich)	QHP Seminar: Nuclear Phases, Neutron Stars and the Functional Renormalization Group	Jul. 14
23	Madanagopalan Padmanath (U. Graz)	QHP Seminar: Excited state charm baryon spectroscopy from lattice QCD	Jul. 21
24	Thorsten Kurth (LBNL)	QHP Seminar: Nuclear Physics from Lattice QCD - Higher Partial Waves and Parity Violation	Jul. 21
25	Sayantan Sharma (BNL)	QHP Seminar: The high temperature phase of QCD and axial anomaly	Jul. 21
26	Kei Yamamoto (KEK)	SNP Seminar: Probing high scale SUSY in low energy FCNC	Jul. 22
27	Petr Vesely (Nuclear Physics Institute)	SNP Seminar: Hypernuclear Spectra within Mean Field and Beyond Mean Field Approach	Jul. 27
28	Evan Berkowitz (Lawrence Livermore National Laboratory)	QHP Seminar: Lattice QCD Input to Axion Cosmology	Jul. 27
29	Y. F. Niu (INFN, and China Academy of Engineering Physics)	QHP Seminar: Particle-vibration coupling effects on Gamow-Teller transition and beta-decay of magic nuclei	Jul. 30
30	Jean-Paul Blaizot (Saclay)	QHP Seminar: Heavy quark bound states in a quark-gluon plasma	Aug. 10
31	Di-Lun Yang (RNC)	QHP Seminar: Collective Flow of Photons in Strongly Coupled Gauge Theories	Oct. 5
32	Yang-Ting Chien (Los Alamos National Laboratory)	QHP Seminar: Towards the Understanding of Jet Shapes and Cross Sections in Heavy Ion Collisions Using Soft Collinear Effective Theory	Oct. 7
33	Francesco Becattini (U. Florence)	QHP Seminar: Quantum corrections to the stress energy tensor in thermodynamic	Oct. 9
34	Taro Kimura (Keio U.)	QHP Seminar: Domain-wall/overlap, and topological insulators	Oct. 19
35	Carlo Barbieri (U. Surrey)	SNP Seminar: Medium-mass isotopes from three-nucleon chiral interactions and Lattice QCD forces	Oct. 19
36	Takuo Tanaka (RIKEN)	SNP seminar : 光メタマテリアル	Oct. 19
37	Hiroshi Suzuki (Kyushu U.)	QHP Seminar: Lattice energy-moemtnum tensor from the gradient flow	Nov. 2

38	Nguyen Thanh Phuc (RIKEN)	QHP Seminar: Controlling and probing non-Abelian emergent gauge potentials in spinor Bose-Fermi mixtures	Nov. 9
39	Doerte Blume (Washington State U.)	SNP Seminar: The helium Efimov trimer and larger bosonic droplets	Nov. 12
40	Takuma Yamashita (Tohoku U.)	SNP Seminar: Weakly binding system of positronic alkali atom: relativistic effects and resonance states	Nov. 20
41	Hirotsugu Fujii (U. Tokyo)	QHP Seminar: Lefschetz thimble method applied to 1 dim Thirring model at finite density	Nov. 30
42	Gen Tatara (RIKEN)	QHP Seminar: Thermal vector potential theory of transport induced by temperature gradient	Dec. 7
43	Shin-ichiro Fujimoto (ABB/Kumamoto U.)	Nucleosynthesis in supernova explosions of massive stars http://indico2.riken.jp/indico/conferenceDisplay.py?confId=2119	Dec. 8
44	Yasuro Funaki (RNC)	Triple-alpha reaction http://indico2.riken.jp/indico/conferenceDisplay.py?confId=2119	Dec. 7
45	Kazuo Makishima (RIKEN)	QHP Seminar: Recent Studies of Strongly Magnetized Neutron Stars	Dec. 14
46	Kenta Miyahara (Kyoto U.)	SNP Seminar: Weak decays of charmed baryons for the study of strange baryon resonances	Dec. 18
47	Keitaro Nagata (KEK)	QHP Seminar: A new method for fermionic singular-drift problem in complex Langevin method	Dec. 21
48	Ulugbek Yakhshiev (Inha U.)	SNP Seminar: From nucleons to nucleonic systems (Chiral soliton approach)	Jan. 6
49	Andrey Mishchenko (RIKEN)	Bold diagrammatic Monte Carlo and unbiased analytic continuation methods to get unbiased solutions for many-particle problems http://indico2.riken.jp/indico/conferenceDisplay.py?confId=2137	Jan/ 18
50	Nilakash Sorokhaibam (Tata Institute of Fundamental Research)	QHP Internal Seminar: 2D Critical quench, Thermalization and UV/IR mixing	Jan. 22
51	Yuki Yokokura (RIKEN)	QHP Seminar: Thermodynamic entropy as a Noether invariant	Jan. 25
52	Keiichio Tokita (Nagoya U.)	自己免疫疾患の分子擬態モデル	Jan. 25
53	Hiroshi Isozaki (U. Tsukuba)	QHP Seminar: Mathematical aspects of quantum mechanical many-body problems	Feb. 1
54	Jaeha Lee (U. Tokyo)	QHP Seminar: Weak Value and Uncertainty Relations based on Quasi-probability Distributions of Quantum Observables	Feb. 3
55	Takuya Kanazawa (RIKEN)	QHP Seminar: QCD and nonrelativistic superfluids	Feb. 8
56	Naoki Yamamoto (Keio U.)	トポロジカル輸送現象：物性から宇宙物理まで	Feb. 9
57	Sho Fujibayashi (Kyoto U.)	QHP Seminar: Nucleosynthesis in Neutrino-driven Winds in Hypernovae	Feb. 15
58	Shin Watanabe (Kyushu U.)	QHP Seminar: Dynamic properties of 6Li elastic scattering	Feb. 17
59	Hideaki Obuse (Hokkaido U.)	QHP Seminar: Conformal invariance at the Anderson transition	Feb. 22
60	Koichi Sato (RNC)	QHP Seminar: Gauge symmetry in large-amplitude collective motion of superfluid nuclei	Feb. 29

61	Ryo Yoshiike (Kyoto U.)	QHP Seminar: Magnetic properties of quark matter in the inhomogeneous chiral phase	Feb. 29
62	Yusuke Horinouchi (U. Tokyo)	QHP Seminar: Topological property of a limit cycle and universal four-body bound states in Efimov physics	Mar. 7
63	Shinjiro Ogita (Hiroshima Pref. U.)	タケの高機能化に適した細胞・組織培養系樹立と活用	Mar. 11
64	Shuichiro Ebata (Hokkaido U.) et al.	Progress in and beyond Theoretical Nuclear Physics Laboratory http://indico2.riken.jp/indico/conferenceDisplay.py?confId=2187	Mar. 28-29

QHP Seminar -> http://ribf.riken.jp/QHP/seminar.html
SNP Seminar -> http://snp.riken.jp/seminar.html

Sub Nuclear System Research Division

1	Matt Sievert (BNL)	RIKEN/BNL Lunch Time Talk	Apr. 2
2	Susanta Lahiri (SINP)	A Ride on Time Machine	Apr. 9
3	Yuji Hirono (Stony Brook U.)	RIKEN/BNL Lunch Time Talk	Apr. 16
4	Hongxi Xing (LANL)	RIKEN/BNL Lunch Time Talk	May 7
5	Yan Fen Lee (U. Sains Malaysia)	Liquid-Structure and Dynamics	May 12
6	Michal Praszalowicz (Jagiellonian U.)	RIKEN/BNL Lunch Time Talk	May 14
7	Piotr Warchol (Jagiellonian U.)	RIKEN/BNL Lunch Time Talk	May 21
8	Antonio Vairo (Munich Technical U.)	RIKEN/BNL Lunch Time Talk	Jun. 4
9	Abhay Deshpande (SUNY/RBRC)	Understanding the Glue that Binds Us All — The science of Electron Ion Collider http://indico2.riken.jp/indico/conferenceDisplay.py?confId=1915	Jun. 12
10	Yi Yin (BNL)	RIKEN/BNL Lunch Time Talk	Jun. 18
11	Jacobus Verbaarschot (Stony Brook U.)	RIKEN/BNL Lunch Time Talk	Jun. 25
12	Chia Cheng Chang (U. Illinois at Urbana-Champaign)	RIKEN/BNL Lunch Time Talk	Jul. 2
13	Wen-Chen Chang (Institute of Physics, Academia Sinica)	Study Nucleon Partonic Structure at High-Momentum Beamline at J-PARC http://indico2.riken.jp/indico/conferenceDisplay.py?confId=1904	Jul. 3
14	Ho-Ung Yee (U. Illinois at Chicago)	RIKEN/BNL Lunch Time Talk	Jul. 30
15	Emilio Bagan (GIQ, Physics Dept., UAB, Spain and Hunter College of the CUNY)	RIKEN/BNL Lunch Time Talk	Aug. 13
16	Jorge Noronha (U. Sao Paulo)	RIKEN/BNL Lunch Time Talk	Sep. 3

17	Dmitri Kharzeev (Stony Brook U., BNL)	The Chiral Magnetic Effect: from Quark-gluon Plasma to Dirac Semimetals	Sep. 24
18	Thorben Graf (Institut für Theoretische Physik, Johann Wolfgang Goethe-Universität)	RIKEN/BNL Lunch Time Talk	Oct. 15
19	Hiroshi Ohki (RBRC Computing Group)	RIKEN/BNL Lunch Time Talk	Oct. 22
20	Adam Lichtl (Delta Brain, Inc.)	RIKEN/BNL Lunch Time Talk	Nov. 5
21	Elisabetta Furlan (ETH, Zurich)	RIKEN/BNL Lunch Time Talk	Nov. 12
22	Kiminad Mamo (U. Illinois at Chicago)	RIKEN/BNL Lunch Time Talk	Nov. 19
23	Isao Watanabe (RNC)	Physics Seminar, Department of Physics	Nov. 24
24	Louis Lello (U. Pittsburgh)	RIKEN/BNL Lunch Time Talk	Dec. 3
25	Derek Horkel (U. Washington)	RIKEN/BNL Lunch Time Talk	Dec. 10
26	Takumi Iritani (Stony Brook U.)	RIKEN/BNL Lunch Time Talk	Dec. 17
27	Rasmus Larsen (Stony Brook U.)	RIKEN/BNL Lunch Time Talk	Jan. 14
28	Ralf Seidl (RNC)	Emerging Spin and Transverse Momentum Effects in pp and p+a Collisions https://www.bnl.gov/estm2016/	Feb. 8
29	Niklas Mueller (U. Heidelberg)	RIKEN/BNL Lunch Time Talk	Mar. 3
30	Taku Izubuchi (BNL/ RBRC)	Lattice Gauge theories 2016 https://www.bnl.gov/events/details.php?q=11302	Mar.9
31	Mark Mace (Stony Brook U.)	RIKEN/BNL Lunch Time Talk	Mar. 31

RIKEN/BNL Lunch Time Talk -> https://sites.google.com/site/rikenlunch/talks

RIBF Research Division

1	Tomoki KIMURA (RNC)	High Energy Astrophysics Lab. Seminar: High energy plasma accelerations in rotating planetary magnetospheres probed by multi-wavelength remote sensing and in-situ measurement http://indico2.riken.jp/indico/conferenceDisplay.py?confId=1845	May 14
2	Noboru Sasao (Okayama U.), Motohiko Yoshimura (Okayama U.)	新しいニュートリノビームとガンマ線ビームの生成法について http://indico2.riken.jp/indico/conferenceDisplay.py?confId=1941	Jun. 22
3	Yasuyuki Tanaka (Hiroshima U.)	High Energy Astrophysics Lab. Seminar: フェルミ衛星と多波長データで探る Broad Line Radio Galaxy 3C 120, 3C 111 における相対論的ジェットの散逸領域、散逸機構、超高速アウトフローとの関連性	Jul. 9
4	Gu Liyi (Netherlands Institute for Space Research, SRON)	Charge exchange emission from astrophysical plasmas	Jul. 30
5	Kumiko Nobukawa (Kyoto U.)	High Energy Astrophysics Lab. Seminar: 銀河リッジ X 線放射の中性鉄輝線の起源	Nov. 12

6	Mathias Frey (ETH)	Matched Distributions in Cyclotrons with Higher Order Moments of the Charge Distribution http://indico2.riken.jp/indico/conferenceDisplay.py?confId=2099	Nov. 25
7	Kathrin Wimmer (U. Tokyo), Kazuyuki Ogata (RCNP, Osaka U.)	13th RIBF Discussion http://indico2.riken.jp/indico/conferenceDisplay.py?confId=2079	Nov. 27
8	Hitoshi Nakada (Chiba U.)	Evidence for threenucleon interaction in isotope shifts of Z=magic nuclei	Dec. 21
9	Peter Möller (Los Alamos National Laboratory)	CURRENT STATUS, RESULTS AND FUTURE DIRECTIONS IN THE FRDM/FRLDM FOR NUCLEAR GROUND-STATE AND FISSION PROPERTIES http://indico2.riken.jp/indico/conferenceDisplay.py?confId=2156	Jan. 27
10	Hitoshi Nakada (Chiba U.) et al.	第 8 回　停止・低速 RI ビームを用いた核分光研究会（SSRI） http://indico2.riken.jp/indico/conferenceDisplay.py?confId=2169	Mar. 4-5
11	Ruben de Groote (KU Leuven)	Collinear laser spectroscopy measurements performed by the Leuven nuclear moments group at ISOLDE, CERN http://indico2.riken.jp/indico/conferenceDisplay.py?confId=2205	Mar. 15

High Energy Astrophysics Lab. Seminar -> http://astro.riken.jp/wordpress/?page_id=65

CNS

1	Haozhao Liang (RNC)	Nuclear spin and isospin physics in collective excitations and single-particle spectra	June. 23
2	Andrea Vitturi (U. Padova/INFN)	Pair transfer reactions as a structure spectroscopic tool for the study of pairing interactions	July. 14
3	Andrea Vitturi	Excitation of low-lying (PDR) and high-lying (GDR) dipole modes in neutron-rich nuclei by nuclear and electromagnetic fields	July. 16
4	Anatoli Afanasjev (Mississippi State U.)	The extremes of nuclear landscape in density functional theory	July. 21
5	Prof. Takaharu OTSUKA(UT, CNS)	Structure evolutions in exotic nuclei and nuclear forces	July. 2-3
6	Prof. Olga BELIUSKINA (CNS)	On the synthesis of neutron-rich isotopes along the N=126 shell in multinucleon transfer reactions, Diamond dE-E-ToF telescope for heavy ion reactions at low energies	July. 16
7	Prof. Umesh GARG (Univ. of Notre Dame)	Exotic Quantal Rotation in Nuclei	July. 23
8	Dr. Philipp SCHROCK (CNS)	The Electric Dipole Response of 132Sn	Dec. 17
9	Koichi Hagino (Tohoku Univ.)	Heavy-ion subbarrier fusion: a sensitive tool to probe nuclear structure	Feb. 22

理化学研究所
埼玉県　和光市　広沢
RIKEN 2016-035